SIXTH EDITION

STRUCTURAL ANALYSIS

A UNIFIED CLASSICAL AND MATRIX APPROACH

Spon Press

SPON TEXT

A. GHALI, A.M. NEVILLE and T.G. BROWN

Structural Analysis

This comprehensive textbook, now in its sixth edition, combines classical and matrix-based methods of structural analysis and develops them concurrently. New solved examples and problems have been added, giving over 140 worked examples and more than 400 problems with answers.

The introductory chapter on structural analysis modeling gives a good grounding to the beginner, showing how structures can be modeled as beams, plane or space frames and trusses, plane grids or assemblages of finite elements. Idealization of loads, anticipated deformations, deflected shapes and bending moment diagrams are presented. Readers are also shown how to idealize real three-dimensional structures into simplified models that can be analyzed with little or no calculation, or by more involved calculations using computers. Dynamic analysis, essential for structures subject to seismic ground motion, is further developed in this edition and in a code-neutral manner. The topic of structural reliability analysis is discussed in a new chapter.

Translated into six languages, this textbook is of considerable international renown, and is widely recommended by many civil and structural engineering lecturers to their students because of its clear and thorough style and content.

Amin Ghali is Fellow of the Canadian Academy of Engineering and Professor Emeritus in the Civil Engineering Department of the University of Calgary, Canada.

Adam Neville is former Vice President of the Royal Academy of Engineering and former Principal and Vice Chancellor of the University of Dundee, Scotland.

Tom G. Brown is Professor and Head of the Civil Engineering Department of the University of Calgary, Canada.

Structural Analysis

A unified classical and matrix approach
6th edition

A. Ghali, A. M. Neville
and T. G. Brown

Spon Press
an imprint of Taylor & Francis
LONDON AND NEW YORK

6th edition published 2009
by Taylor & Francis
2 Park Square, Milton Park, Abingdon, Oxon OX14 4RN

Simultaneously published in the USA and Canada
by Taylor & Francis
270 Madison Avenue, New York, NY 10016, USA

Taylor & Francis is an imprint of the Taylor & Francis Group, an informa business

Typeset in Sabon by
Integra Software Services Pvt. Ltd, Pondicherry, India
Printed and bound in Great Britain by
CPI Antony Rowe Ltd, Chippenham, Wiltshire

British Library Cataloguing in Publication Data
A catalogue record for this book is available from the British Library

Library of Congress Cataloging in Publication Data
Ghali, A. (Amin)
Structural analysis : a unified classical and matrix approach /
A. Ghali, A.M. Neville, and T.G. Brown. — 6th ed.
p. cm.
Includes bibliographical references and index.
I. Structural analysis (Engineering) I. Neville, Adam M.
II. Brown, T. G. (Tom G.) III. Title.
TA645.G48 2009
624.1'71—dc22 2008046077

ISBN13: 978–0–415–77432–1 Hardback
ISBN13: 978–0–415–77433–8 Paperback
ISBN10: 0–415–77432–2 Hardback
ISBN10: 0–415–77433–0 Paperback

Contents

Preface to the sixth edition

We are proud that this book now appears in its sixth edition; it exists also in six translations, the most recent being the Japanese (2003) and the Chinese (2008). This new edition is updated and expanded.

The changes from the fifth edition have been guided by developments in knowledge as well as by reviews and comments of teachers, students, and designers who have been using the earlier editions. There are added chapters and sections, an additional appendix, revisions to existing chapters, and more examples and problems. The answers to all problems are given at the end of the book. Throughout the book, great attention is given to the analysis of three-dimensional spatial structures.

The book starts with a chapter on structural analysis modeling by idealizing a structure as a beam, a plane or a space frame, and a plane or a space truss, a plane grid, or as an assemblage of finite elements. There are new sections on the strut-and-tie models for the analysis of reinforced structures after cracking. There is a discussion of the suitability of these models, forces, and deformations, sketching deflected shapes, and bending moment diagrams, and a comparison of internal forces and deflections in beams, arches and trusses.

The chapter on modeling is followed by a chapter on the analysis of statically determinate structures, intended to provide a better preparation for students. To encourage early use of computers, five of the computer programs described in Appendix L, available from a web site, are mentioned in Chapter 1. These are for the linear analysis of plane and space trusses, plane and space frames, and plane grids. Simple matrix algebra programs, which can perform frequently needed matrix operations, can also be downloaded from the web site. The web site address is:

http://www.routledge.com/books/Structural-Analysis-isbn9780415774338

In Chapters 3 to 6 we introduce two distinct general approaches of analysis: the force method and the displacement method. Both methods involve the solution of linear simultaneous equations relating forces to displacements. The emphasis in these four chapters is on the basic ideas in the two methods, without obscuring the procedure by the details of derivation of the coefficients needed to form the equations. Instead, use is made of Appendices B, C, and D, which give, respectively, displacements due to applied unit forces, forces corresponding to unit displacements, and fixed-end forces in straight members due to various loadings. The consideration of the details of the methods of displacement calculation is thus delayed to Chapters 7 to 10, by which time the need for this material in the analysis of statically indeterminate structures is clear. This sequence of presentation of material is particularly suitable when the reader is already acquainted with some of the methods for calculating the deflection of beams. If, however, it is thought preferable first to deal with methods of calculation of displacements, Chapters 7 to 10 should be studied before Chapters 4 to 6; this will not disturb the continuity.

The material presented is both elementary and advanced, covering the whole field of structural analysis. The classical and modern methods of structural analysis are combined in a unified presentation, but some of the techniques not widely used in modern practice have been omitted.

However, the classical methods of column analogy and moment distribution, suitable for hand calculations, continue to be useful for preliminary calculation and for checking computer results; these are presented in Chapter 11. To provide space for new topics needed in modern practice, the coverage of the two methods is shorter compared to the fifth edition. The no-shear moment distribution technique, suitable for frames having many joint translations, has been removed because computers are now commonly employed for such frames.

The methods for obtaining the influence lines for beams, frames, grids and trusses are combined in Chapter 12, which is shorter than the sum of the two chapters in the fifth edition. In Chapter 13, the effects of axial forces on the stiffness characteristics of members of framed structures are discussed and applied in the determination of the critical buckling loads of continuous frames.

Chapter 14 deals with the analysis of shear walls, commonly used in modern buildings. The chapter summarizes the present knowledge, states the simplifying assumptions usually involved, and presents a method of analysis that can be applied in most practical cases.

The provision of outriggers is an effective means of reducing the drift and the bending moments due to lateral loads in high-rise buildings. The analysis of outrigger-braced buildings and the location of the outriggers for optimum effectiveness are discussed in new sections in Chapter 14. The analysis is demonstrated in a solved example of a 50-storey building.

The finite-difference method and, to an even larger extent, the finite-element method are powerful tools, which involve a large amount of computation. Chapter 15 deals with the use of finite differences in the analysis of structures composed of beam elements and extends the procedure to axisymmetrical shells of revolution. The finite-difference method is also used in the analysis of plates. Chapters 16 and 17 are concerned with two- and three-dimensional finite elements. Chapters 21, 22, 16, and 17 can be used, in that order, in a graduate course on the fundamentals of the finite-element method.

Modern design of structures is based on both the elastic and plastic analyses. The plastic analysis cannot replace the elastic analysis but supplements it by giving useful information about the collapse load and the mode of collapse. Chapters 18 and 19 deal with the plastic analysis of framed structures and slabs respectively.

An introduction to structural dynamics is presented in Chapter 20. This is a study of the response of structures to dynamic loading produced by machinery, gusts of wind, blast, or earthquakes. First, free and forced vibrations of a system with one degree of freedom are discussed. This is then extended to multi-degree-of-freedom systems. Several new sections discuss the dynamic analysis of structures subjected to earthquakes.

Some structures, such as cable nets and fabrics, trusses, and frames with slender members, may have large deformations, so that it is necessary to consider equilibrium in the real deformed configurations. This requires the geometric nonlinear analysis treated in Chapter 23, in which the Newton-Raphson's iterative technique is employed. The same chapter also introduces the material-nonlinearity analysis, in which the stress–strain relation of the material used in the structure is nonlinear.

Chapter 24, based on the probability theory, is new in this edition. This chapter represents a practical introductory tool for the reliability analysis of structures. The objective is to provide a measure for the reliability or the probability of satisfactory performance of new or existing structures. The most important probability aspects used in Chapter 24 are presented in Appendix M; previous knowledge of probability and statistics is not required. Chapter 24 and Appendix M were written in collaboration with Professor Andrzej S. Nowak of the University of Nebraska, Lincoln, USA. Professor Marc Maes was the first to include reliability of structures in an undergraduate course on structural analysis at the University of Calgary, Canada; the authors are grateful to him for making his lecture notes available.

The techniques of analysis, which are introduced, are illustrated by many solved examples and a large number of problems at the ends of chapters, with answers given at the end of the

book. In this edition, with new solved examples and problems added, there are more than 140 worked examples and more than 400 problems with answers.

No specific system of units is used in most of the examples and problems. However, there is a small number of examples and problems where it was thought advantageous to use actual dimensions of the structure and to specify the magnitude of forces. These problems are set in the so-called Imperial or British units (still common in the USA) as well as in the SI units. Each problem in which Imperial units are used is followed by a version of the same problem in SI units, so that the reader may choose the system of units he or she prefers.

Data frequently used are presented in the appendices, with Appendix A offering a review of matrix operations usually needed in structural analysis. Matrix notation is extensively used in this book because this makes it possible to present equations in a compact form, helping the reader to concentrate on the overall operations without being distracted by algebraic or arithmetical details.

Several computer programs are briefly described in Appendix L. These include the computer programs available from the web site mentioned above and four nonlinear analysis programs. An order form at the end of the book can be used to obtain the nonlinear analysis programs. The computer programs can be employed in structural engineering practice and also to aid the study of structural analysis. However, understanding the book does not depend upon the availability of these programs.

The text has been developed by the first and principal author in teaching, over a number of years, undergraduate and graduate courses at the University of Calgary, Canada. The third author, who joined in the fifth edition, has also been teaching the subject at Calgary. Teaching and understanding the needs of the students have helped in preparing a better edition, believed to be easier to study.

Chapters 1 to 13, 18, and 19 contain basic material which should be covered in the first courses. From the remainder of the book, a suitable choice can be made to form a more advanced course. The contents have been selected to make the book suitable not only for the student but also for the practicing engineer who wishes to obtain guidance on the most convenient methods of analysis for a variety of types of structures.

Dr. Ramez Gayed, research associate at the University of Calgary, has checked the new material, the solution of the examples, and some of the answers of the problems, and provided the figures for the sixth edition.

Calgary, Alberta, Canada A. Ghali
London, England A. M. Neville
Calgary, Alberta, Canada T. G. Brown
April 2008

Notation

The following is a list of symbols which are common in the various chapters of the text; other symbols are used in individual chapters. All symbols are defined in the text when they first appear.

A	Any action, which may be a reaction or a stress resultant. A stress resultant at a section of a framed structure is an internal force: bending moment, shearing force or axial force.
a	Cross-sectional area.
D_i or D_{ij}	Displacement (rotational or translational) at coordinate i. When a second subscript j is provided it indicates the coordinate at which the force causing the displacement acts.
E	Modulus of elasticity.
EI	Flexural rigidity.
F	A generalized force: a couple or a concentrated load.
FEM	Fixed-end moment.
f_{ij}	Element of flexibility matrix.
G	Modulus of elasticity in shear.
I	Moment of inertia or second moment of area.
i, j, k, m, n, p, r	Integers.
J	Torsion constant (length^4), equal to the polar moment of inertia for a circular cross section.
l	Length.
M	Bending moment at a section, e.g. M_n = bending moment at sections. In beams and grids, a bending moment is positive when it causes tension in bottom fibers.
M_{AB}	Moment at end A of member AB. In plane structures, an end-moment is positive when clockwise. In general, an end-moment is positive when it can be represented by a vector in the positive direction of the axes x, y, or z.
N	Axial force at a section or in a member of a truss.
P, Q	Concentrated loads.
q	Load intensity.
R	Reaction.
S_{ij}	Element of stiffness matrix.
s	Used as a subscript, indicates a statically determinate action.
T	Twisting moment at a section.
u	Used as a subscript, indicates the effect of unit forces or unit displacements.

V	Shearing force at a section.
W	Work of the external applied forces.
ϵ	Strain.
η	Influence ordinate.
ν	Poisson's ratio.
σ	Stress.
τ	Shearing stress.
$\{\ \}$	Braces indicate a vector, i.e. a matrix of one column. To save space, the elements of a vector are sometimes listed in a row between two braces.
$[\ ]$	Brackets indicate a rectangular or square matrix.
$[\mathrm{T}]^{T}_{n\times m}$	Superscript T indicates matrix transpose. $n \times m$ indicates the order of the matrix which is to be transposed resulting in an $m \times n$ matrix.
$\longrightarrow\!\!\!\!\!\rightarrow$	Double-headed arrow indicates a couple or a rotation: its direction is that of the rotation of a right-hand screw progressing in the direction of the arrow.
$\longrightarrow$	Single-headed arrow indicates a load or a translational displacement.
$z \underset{y}{\overset{}{\rightarrow}} x$	Axes: the positive direction of the z axis points away from the reader.

The SI system of units of measurement

Length	meter	m
	millimeter $= 10^{-3}$ m	mm
Area	square meter	m^2
	square millimeter $= 10^{-6}\ m^2$	mm^2
Volume	cubic meter	m^3
Frequency	hertz = 1 cycle per second	Hz
Mass	kilogram	kg
Density	kilogram per cubic meter	kg/m^3
Force	newton	N
	= a force which applied to a mass of one kilogram gives it an acceleration of one meter per second, i.e. $1N = 1\,kgm/s^2$	
Stress	newton per square meter	N/m^2
	newton per square millimeter	N/mm^2
Temperature interval	degree Celsius	deg C; °C

Nomenclature for multiplication factors

10^9	giga	G
10^6	mega	M
10^3	kilo	k
10^{-3}	milli	m
10^{-6}	micro	μ
10^{-9}	nano	n

Chapter 1

Structural analysis modeling

1.1 Introduction

This book may be used by readers familiar with basic structural analysis and also by those with no previous knowledge beyond elementary mechanics. It is mainly for the benefit of people in the second category that Chapter 1 is included. It will present a general picture of the analysis but, inevitably, it will use some concepts that are fully explained only in later chapters. Readers may therefore find it useful, after studying Chapter 2 and possibly even Chapter 3, to reread Chapter 1.

The purpose of structures, other than aircraft, ships and floating structures, is to transfer applied loads to the ground. The structures themselves may be constructed specifically to carry loads (for example, floors or bridges) or their main purpose may be to give protection from the weather (for instance, walls or roofs). Even in this case, there are loads (such as self-weight of the roofs and also wind forces acting on them) that need to be transferred to the ground.

Before a structure can be designed in a rational manner, it is essential to establish the loads on various parts of the structure. These loads will determine the stresses and their resultants (internal forces) at a given section of a structural element. These stresses or internal forces have to be within desired limits in order to ensure safety and to avoid excessive deformations. To determine the stresses (forces/unit area), the geometrical and material properties must be known. These properties influence the self-weight of the structure, which may be more or less than originally assumed. Hence, iteration in analysis may be required during the design process. However, consideration of this is a matter for a book on design.

The usual procedure is to idealize the structure by one-, two-, or three-dimensional elements. The lower the number of dimensions considered, the simpler the analysis. Thus, beams and columns, as well as members of trusses and frames, are considered as one-dimensional; in other words, they are represented by straight lines. The same applies to strips of plates and slabs. One-dimensional analysis can also be used for some curvilinear structures, such as arches or cables, and also certain shells. Idealization of structures by an assemblage of finite elements, considered in Chapter 17, is sometimes necessary.

Idealization is applied not only to members and elements but also to their connections to supports. We assume the structural connection to the supports to be free to rotate, and then treat the supports as hinges, or to be fully restrained, that is, built-in or encastré. In reality, perfect hinges rarely exist, if only because of friction and also because non-structural members such as partitions restrain free rotation. At the other extreme, a fully built-in condition does not recognize imperfections in construction or loosening owing to temperature cycling.

Once the analysis has been completed, members and their connections are designed: the designer must be fully conscious of the difference between the idealized structure and the actual outcome of construction.

The structural idealization transforms the structural analysis problem into a mathematical problem that can be solved by computer or by hand, using a calculator. The model is analyzed

for the effects of loads and applied deformations, including the self-weight of the structure, superimposed stationary loads or machinery, live loads such as rain or snow, moving loads, dynamic forces caused by wind or earthquake, and the effects of temperature as well as volumetric change of the material (e.g. shrinkage of concrete). This chapter explains the type of results that can be obtained by the different types of models.

Other topics discussed in this introductory chapter are: transmission (load path) of forces to the supports and the resulting stresses and deformations; axial forces in truss members; bending moments and shear forces in beams; axial and shear forces, and bending moments in frames; arches; the role of ties in arches; sketching of deflected shapes and bending moment diagrams; and hand checks on computer results.

1.2 Types of structures

Structures come in all shapes and sizes, but their primary function is to carry loads. The form of the structure, and the shape and size of its members are usually selected to suit this load-carrying function, but the structural forces can also be dictated by the function of the system of which the structure is part. In some cases, the form of the structure is dictated by architectural considerations.

The simplest structural form, the beam, is used to bridge a gap. The function of the bridge in Figure 1.1 is to allow traffic and people to cross the river: the load-carrying function is accomplished by transferring the weight applied to the bridge deck to its supports.

A similar function is provided by the arch, one of the oldest structural forms. Roman arches (Figure 1.2a) have existed for some 2000 years and are still in use today. In addition to bridges, the arch is also used in buildings to support roofs. Arches have developed because of confidence in the compressive strength of the material being used, and this material, stone, is plentiful. An arch made of stone remains standing, despite there be no cementing material between the arch blocks, because the main internal forces are compressive. However, this has some serious implications, as we shall see below. The arch allows longer spans than beams with less material: today, some very elegant arch bridges are built in concrete (Figure 1.2b) or in steel.

The third, simple form of structural type, is the cable. The cable relies on the tensile capacity of the material (as opposed to the arch, which uses the compressive capacity of the material) and hence its early use was in areas where natural rope-making materials are plentiful. Some of the earliest uses of cables are in South America where local people used cables to bridge gorges.

Figure 1.1 Highway bridge.

(a)

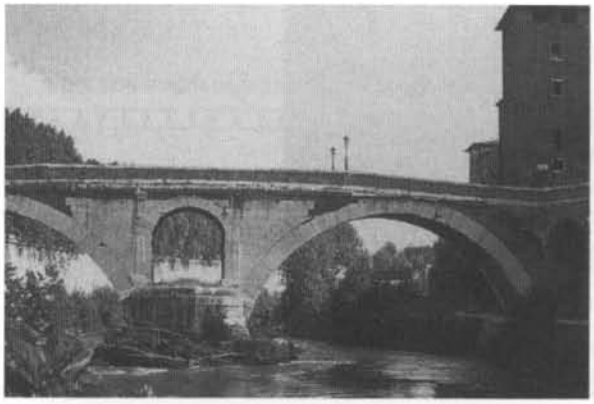

(b)

Figure 1.2 Arch bridges. (a) Stone blocks. (b) Concrete.

Subsequent developments of the chain, the wire and the strand, permit bridges to span great lengths with elegant structures; today, the world's longest bridges are cable supported (Figures 1.3a, b and c).

The shapes of the arch and suspended cable structures show some significant similarities, the one being the mirror-image of the other. Cable systems are also used to support roofs, particularly long-span roofs where the self-weight is the most significant load. In both arches and cables, gravity loads induce inclined reactions at the supports (Figures 1.4a and b). The arch reactions produce compressive forces in the direction (or close to the direction) of the arch axis at the ends. The foundation of the arch receives inclined outward forces equal and opposite to the reactions. Thus, the foundations at the two ends are pushed outwards and downwards; the subgrade must be capable of resisting the horizontal thrust and therefore has to be rock or a concrete block. A tie connecting the two ends of an arch, as in Example 1.1, Figure 1.25d, can eliminate the horizontal forces on the supports. Thus, an arch with a tie subjected to gravity load has only vertical reactions. Figures 1.5a and b show arch bridges with ties, carrying respectively a steel water pipe and a roadway. The weights of the pipe and its contents, the roadway deck and its traffic, hang from the arches by cables. The roadway deck can serve as a tie. Thus, due to gravity loads, the structures have vertical reactions.

The cable in Figure 1.4a, carrying a downward load, is pulled upward in an inclined direction of the tangent at the two ends. Again, the arrows in the figure show the directions of the reactions necessary for equilibrium of the structure. Further discussion on cables and arches is presented in Section 1.2.1.

(a)

(b)

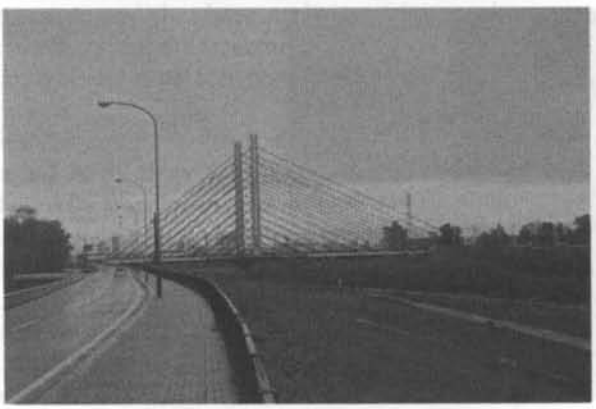

(c)

Figure 1.3 Use of cables. (a) Suspension bridge. (b) and (c) Two types of cable-stayed bridges.

The introduction of the railroad, with its associated heavy loads, has resulted in the need for a different type of structure to span long distances – hence, the development of the truss (Figure 1.6a). In addition to carrying heavy loads, trusses can also be used to span long distances effectively, and are therefore also used to support long-span roofs; wood roof trusses are extensively used in housing. Trusses consist of straight members. Ideally, the members are pin-connected, so that they carry either compressive or tensile forces, depending on the truss configuration and the nature of the loading. In modern trusses, the members are usually nearly-rigidly connected (although assumed pinned in analysis).

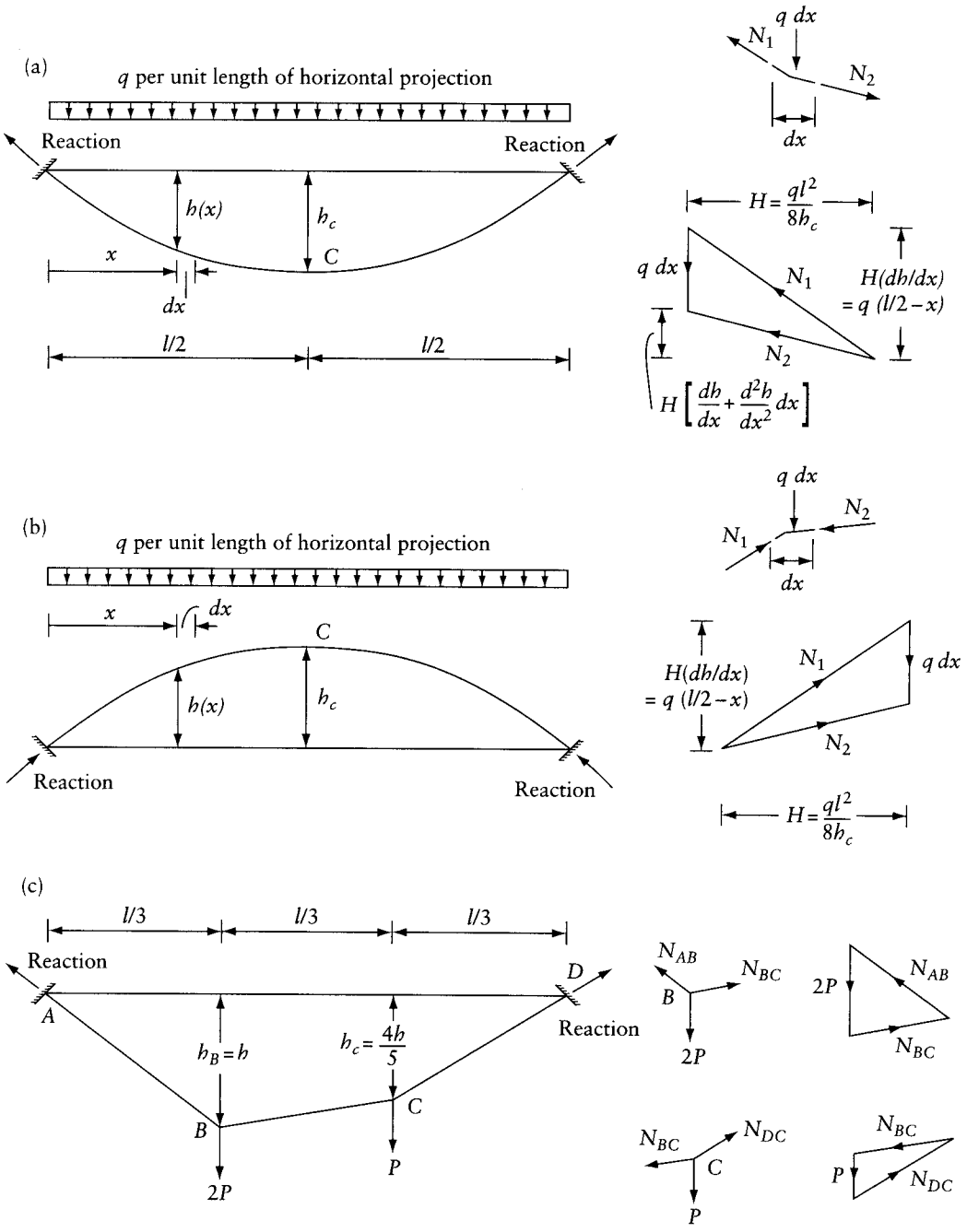

Figure 1.4 Structures carrying gravity loads. (a) Cable – tensile internal force. (b) Arch – compressive internal force. (c) Funicular shape of a cable carrying two concentrated downward loads.

If the members are connected by rigid joints, then the structure is a frame – another very common form of structural system frequently used in high-rise buildings. Similar to trusses, frames come in many different configurations, in two or three dimensions. Figures 1.7a and b show a typical rigid joint connecting two members before and after loading. Because of the rigid

(a)

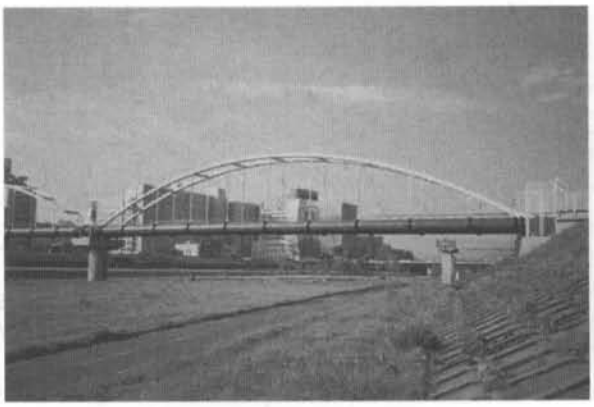

(b)

Figure 1.5 Arches with ties. (a) Bridge carrying a steel pipe. (b) Bridge carrying traffic load.

connection, the angle between the two members remains unchanged, when the joint translates and rotates, as the structure deforms under load.

One other category of structures is plates and shells whose one common attribute is that their thickness is small in comparison to their other dimensions. An example of a plate is a concrete slab, monolithic with supporting columns, which is widely used in office and apartment buildings, and in parking structures. Cylindrical shells are plates curved in one direction. Examples are: storage tanks, silos and pipes. As with arches, the main internal forces in a shell are in the plane of the shell, as opposed to shear force or bending moment.

Axisymmetrical domes, generated by the rotation of a circular or parabolic arc, carrying uniform gravity loads, are mainly subjected to membrane compressive forces in the middle surface of the shell. This is the case when the rim is continuously supported such that the vertical and the radial displacements are prevented; however, the rotation can be free or restrained. Again, similar to an arch or a cable, the reaction at the outer rim of a dome is in the direction or close to the direction of the tangent to the middle surface (Figure 1.8a). A means must be provided to resist the radial horizontal component of the reaction at the lower rim of the dome; most commonly this is done by means of a circular ring subjected to hoop tension (Figure 1.8b).

In Figure 1.8c, the dome is isolated from the ring beam to show the internal force at the connection of the dome to the rim. A membrane force N per unit length is shown in the meridian

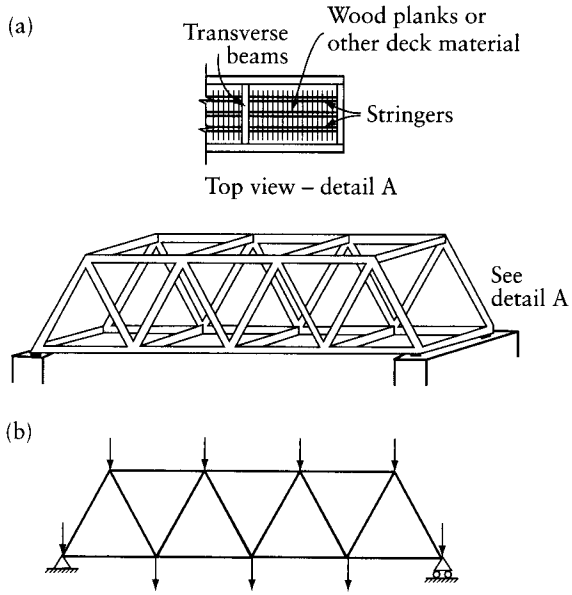

Figure 1.6 Truss supporting a bridge deck. (a) Pictorial view. (b) Plane truss idealization.

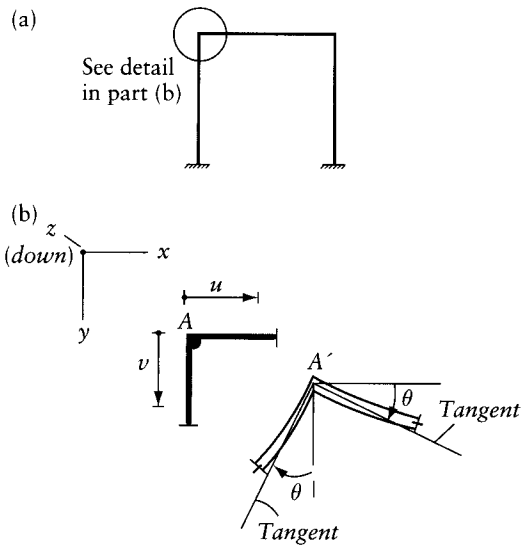

Figure 1.7 Definition of a rigid joint: example joint of a plane frame. (a) Portal frame. (b) Detail of joint before and after deformation.

direction at the rim of the dome (Figure 1.8a). The horizontal component per unit length, $(N\cos\theta)$, acts in the radial direction on the ring beam (Figure 1.8c) and produces a tensile hoop force $= rN\cos\theta$, where r is the radius of the ring and θ is the angle between the meridional tangent at the edge of the dome and the horizontal. The reaction of the structure (the dome with its ring beam) is vertical and of magnitude $(N\sin\theta = qr/2)$ per unit length of the periphery.

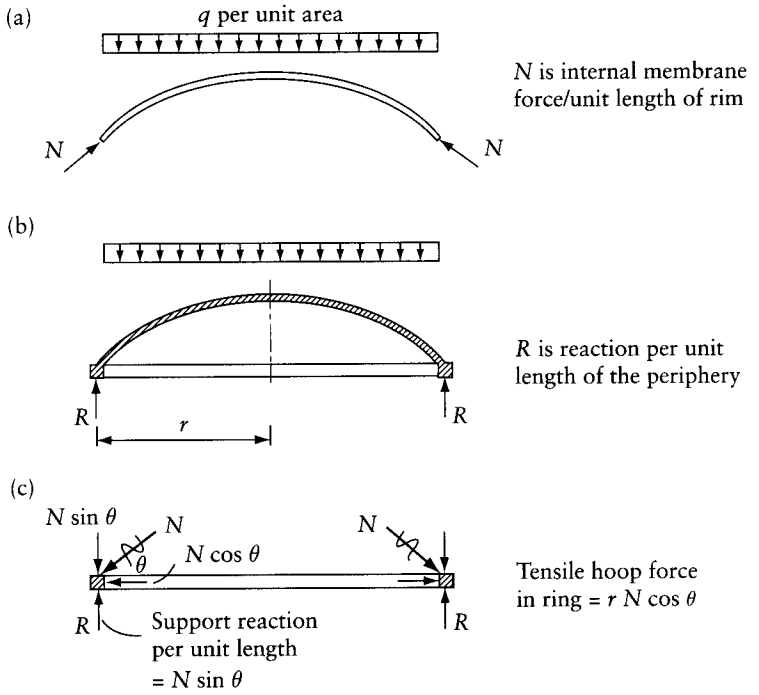

Figure 1.8 Axisymmetrical concrete dome subjected to uniform downward load. (a) Reaction when the dome is hinged or totally fixed at the rim. (b) Dome with a ring beam. (c) The ring beam separated to show internal force components and reaction.

In addition to the membrane force N, the dome is commonly subjected to shear forces and bending moments in the vicinity of the rim (much smaller than would exist in a plate covering the same area). The shear and moment are not shown for simplicity of presentation.

Arches, cables and shells represent a more effective use of construction materials than beams. This is because the main internal forces in arches, cables and shells are axial or membrane forces, as opposed to shear force and bending moment. For this reason, cables, arches or shells are commonly used when it is necessary to enclose large areas without intermediate columns, as in stadiums and sports arenas. Examples are shown in Figures 1.9a and b. The comparisons in Section 1.12 show that to cover the same span and carry the same load, a beam needs to have much larger cross section than arches of the same material.

1.2.1 Cables and arches

A cable can carry loads, with the internal force axial tension, by taking the shape of a curve or a polygon (funicular shape), whose geometry depends upon the load distribution. A cable carrying a uniform gravity load of intensity q/unit length of horizontal projection (Figure 1.4a) takes the shape of a second degree parabola, whose equation is:

$$h(x) = h_C \left[\frac{4x(l-x)}{l^2} \right] \tag{1.1}$$

where h is the absolute value of the distance between the horizontal and the cable (or arch), h_C is the value of h at mid-span.

(a)

(b)

Figure 1.9 Shell structures. (a) The "Saddle dome", Olympic ice stadium, Calgary, Canada. Hyperbolic paraboloid shell consisting of precast concrete elements carried on a cable network (see Prob. 24.9). (b) Sapporo Dome, Japan. Steel roof with stainless steel covering 53000 m^2, housing a natural turf soccer field that can be hovered and wheeled in and out of the stadium.

This can be shown by considering the equilibrium of an elemental segment dx as shown. Sum of the horizontal components or the vertical components of the forces on the segments is zero. Thus, the absolute value, H of the horizontal component of the tensile force at any section of the cable is constant; for the vertical components of the tensile forces N_1 and N_2 on either side of the segment we can write:

$$q dx + H\left[\frac{dh}{dx} + \frac{d^2h}{dx^2}dx\right] = H\left(\frac{dh}{dx}\right) \tag{1.2}$$

$$\frac{d^2h}{dx^2} = -\frac{q}{H} \tag{1.3}$$

Double integration and setting $h = 0$ at $x = 0$ and $x = l$; and setting $h = h_c$ at $x = l/2$ gives Eq. 1.1 and the horizontal component of the tension at any section:

$$H = \frac{ql^2}{8h_C} \tag{1.4}$$

When the load intensity is $\bar{q}$ per unit length of the cable (e.g. the self-weight), the funicular follows the equation of a catenary (differing slightly from a parabola). With concentrated gravity loads, the cable has a polygonal shape. Figure 1.4c shows the funicular polygon of two concentrated loads $2P$ and P at third points. Two force triangles at B and C are drawn to graphically give the tensions N_{AB}, N_{BC} and N_{CD}. From the geometry of these figures, we show below that the ratio of $(h_C/h_B) = 4/5$, and that this ratio depends upon the magnitudes of the applied forces. We can also show that when the cable is subjected to equally-spaced concentrated loads, each equal to P, the funicular polygon is composed of straight segments connecting points on a parabola (see Prob. 1.9).

In the simplified analysis presented here, we assume that the total length of the cable is the same, before and after the loading, and is equal to the sum of the lengths of AB, BC and CD, and after loading, the applied forces $2P$ and P are situated at third points of the span. Thus, h_B and h_C are the unknowns that define the funicular shape in Figure 1.4c.

By considering that for equilibrium the sum of the horizontal components of the forces at B is equal to zero, and doing the same at C, we conclude that the absolute value, H of the horizontal component is the same in all segments of the cable; thus, the vertical components are equal to H multiplied by the slope of the segments. The sum of the vertical components of the forces at B or at C is equal to zero. This gives:

$$2P - H\left(\frac{3h_B}{l}\right) - H\left[\frac{3(h_B - h_C)}{l}\right] = 0$$

$$P + H\left(\frac{3(h_B - h_C)}{l}\right) - H\left[\frac{3h_C}{l}\right] = 0 \tag{1.5}$$

Solution for H and h_C in terms of h_B gives:

$$h_C = \frac{4}{5}h_B \text{ and } H = \frac{Pl}{1.8h_B} \tag{1.6}$$

The value of h_B can be determined by equating the sum of the lengths of the cable segments to the total initial length.

Figure 1.4b shows a parabolic arch (mirror image of the cable in Figure 1.4a) subjected to uniform load q/unit length of horizontal projection. The triangle of the three forces on a segment dx is shown, from which we see that the arch is subjected to axial compression. The horizontal component of the axial compression at any section has a constant absolute value H, given by Eq. 1.4.

Unlike the cable, the arch does not change shape when the distribution of load is varied. Any load other than that shown in Figure 1.4b produces axial force, shear force and bending moment. The most efficient use of material is achieved by avoiding the shear force and the bending moment. Thus, in design of an arch we select its profile such that the major load (usually the dead load) does not produce shear or bending.

It should be mentioned that in the above discussion, we have not considered the shortening of the arch due to axial compression. This shortening has the effect of producing shear and bending of small magnitudes in the arch in Figure 1.4b.

Cables intended to carry gravity loads are frequently prestressed (stretched between two fixed points). Due to the initial tension combined with the self-weight, a cable will have a sag depending upon the magnitudes of the initial tension and the weight. Subsequent application of a downward concentrated load at any position produces displacements u and v at the point of load application, where u and v are translations in the horizontal and vertical directions respectively.

Calculations of these displacements and the associated changes in tension, and in cable lengths, are discussed in Chapter 24.

1.3 Load path

As indicated in the previous section, the primary function of any structure is the transfer of loads, the final support being provided by the ground. Loads are generally categorized as dead or live. Dead loads are fixed or permanent loads – loads that do not vary throughout the life of the structure. Very often, the majority of the dead load derives from the self-weight of the structure. In long-span bridges, the dead load constitutes the larger portion of the total gravity load on the structure. Live loads and other transient loads represent the effects of occupancy or use, traffic weight, environment, earthquakes, and support settlement.

One of the objectives of the analysis of a structure is to determine the internal forces in its various elements. These internal forces result from the transfer of the loads from their points of application to the foundations. Understanding load paths is important for two reasons: providing a basis for the idealization of the structure for analysis purposes, as well as understanding the results of the analysis. Virtually all civil engineering structures involve the transfer of loads, applied to the structure, to the foundations, or some form of support.

A given structure may have different load paths for different applied loads. As an example, consider the water tank supported by a tower that consists of four vertical trusses (Figure 1.10). The weight of the tank and its contents is carried by the columns on the four corners (Figure 1.10b), the arrows illustrating the transfer of the weight by compression in the four columns. However, the wind load on the tank (Figure 1.10b) causes a horizontal force that must be transferred to the supports (equally) by the two vertical trusses that are parallel to the wind direction. This produces forces in the diagonal members, and also increases or decreases the axial forces in the columns. The other two trusses (at right angles) will not contribute simultaneously to this load path, but would become load paths if the wind direction changed 90°.

Figure 1.11a represents a plane-frame idealization of a cable-stayed bridge. The frame is composed of beam *AB*, rigidly connected to towers *CD* and *EF*. The beam is stayed by cables that make it possible to span a greater distance. Figure 1.11c shows the deflected shape of the frame due to traffic load on the main span. A typical cable is isolated in Figure 1.11c as a free body; the arrows shown represent the forces exerted by the beam or the tower on the cable. The cables are commonly pretensioned in construction; the arrows represent an increase in the tension force due to the traffic load. Figure 1.11c shows the deflected shape due to traffic load on the left exterior span.

Understanding load paths allows a considerable simplification in the subsequent analyses. It is also an important component in the determination of the forces to be applied to a structure being analyzed.

Consider the example of a bridge deck supported by two parallel trusses (Figures 1.6a and b). The deck is supported on a series of transverse beams and longitudinal beams (stringers) that eventually transfer the weight of the traffic to the trusses. Here, we want to examine how that transfer occurs, and what it means for the various components of the bridge deck. These components can then be analyzed and designed accordingly.

In a timber bridge deck, the deck beams are only capable of transferring the wheel loads along their lengths to the supports provided by the stringers. The loading on the stringers will come from their self-weight, the weight of the deck, and the wheel loads transferred to it. Each stringer is only supported by the two adjacent floor beams, and can therefore only transfer the load to these floor beams. These are then supported at the joints on the lower chord of the trusses. We have selected here a system with a clear load path. The transfer of the load of the deck to the truss will be less obvious if the wooden deck and stringers are replaced by a concrete slab. The self-weight of the slab and the wheel loads are transferred in two directions to the trusses

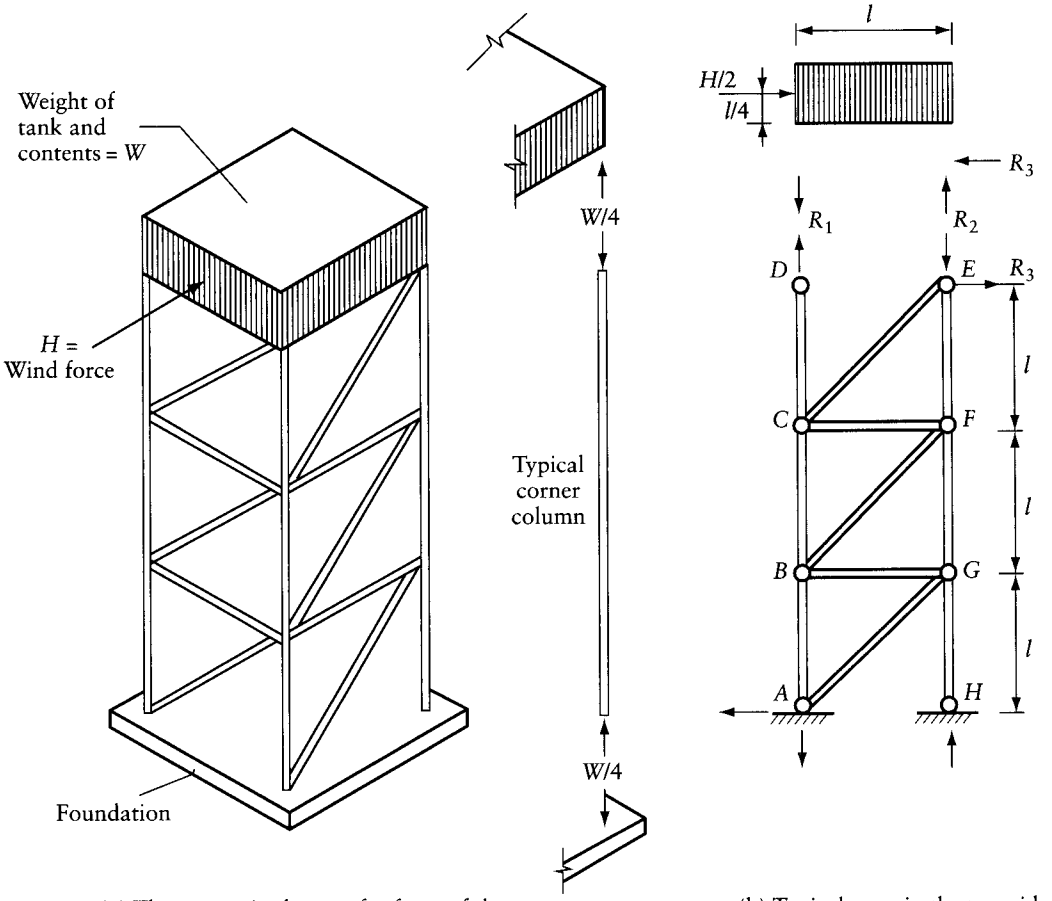

(a) The trusses in the two far faces of the tank are not shown for clarity

(b) Typical truss in the two sides parallel to wind direction

Figure 1.10 Load path example. (a) Water tower. (b) Load paths for gravity force and for wind force.

and the transverse beams (two-way slab action). However, this difference in load path is often ignored in an analysis of the truss.

Understanding the load path is essential in design. As we have seen in the preceding section, the downward load on the arch in Figure 1.4b is transferred as two inclined forces to the supports. The foundation must be capable of resisting the gravity load on the structure and the outward thrust (horizontal component of the reactions in reversed directions). Similarly, the path of the gravity load on the dome in Figure 1.8b induces a horizontal outward thrust and a downward force in the ring beam. The horizontal thrust is resisted by the hoop force in the ring beam, and the structure needs only a vertical reaction component.

Some assessment of the load path is possible without a detailed analysis. One example of this is how lateral loads are resisted in multistorey buildings (Figure 1.12). These buildings can be erected as rigid frames, typically with columns and beams, in steel or concrete, connected in a regular array represented by the skeleton shown in Figure 1.12a. The walls, which may be connected to the columns and/or the floors, are treated as non-structural elements. The beams carry a concrete slab or steel decking covered with concrete; with both systems, the floor can be considered rigid when subjected to loads in its plane (in-plane forces). Thus, the horizontal wind

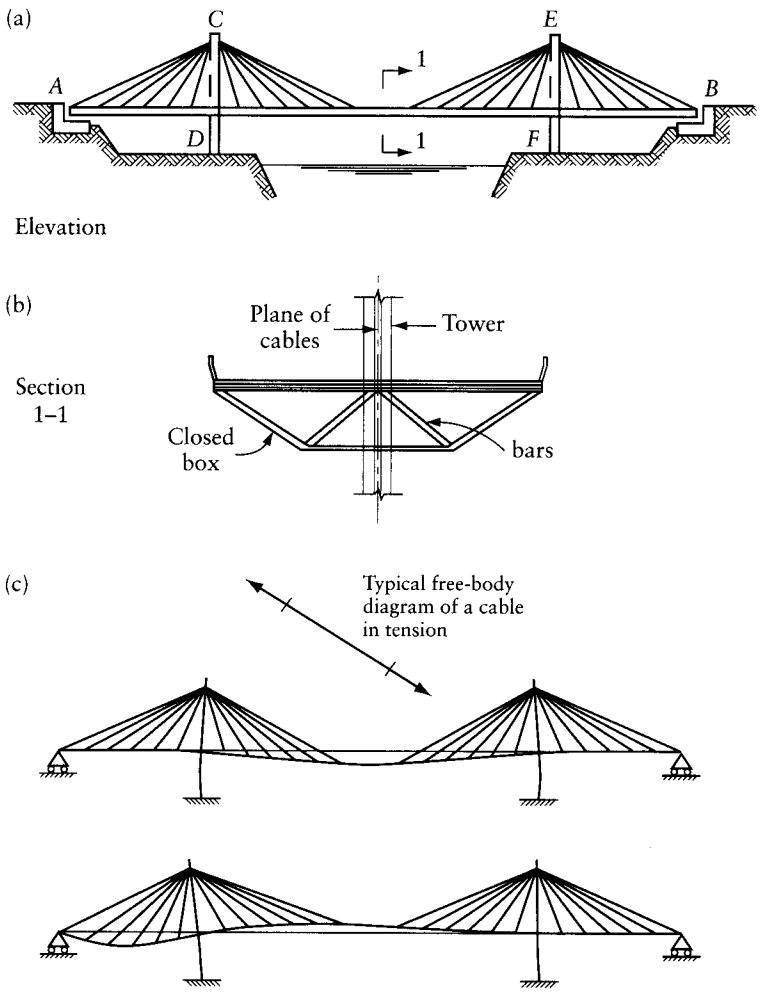

Figure 1.11 Behavior of a cable-stayed bridge. (a) and (b) Elevation of plane frame idealization and bridge cross section. (c) Deflected shape and forces in cables due to traffic load on interior or exterior span.

load on the building will cause the floors to move horizontally as rigid bodies, causing all the columns at each floor level to deflect equally. If the columns and beams in each two-dimensional frame on grid lines *A* to *D* have the same dimensions, then all the frames will have the same stiffness and any lateral wind load will be distributed equally (one quarter) to each frame. The plane frame idealization of one frame shown in Figure 1.12b is all that is required for analysis.

If, however, the frames are different, then the wind load resisted by each frame will depend on its stiffness. For example, consider the same structure with the two outer frames *A* and *D*, containing shear walls (Figure 1.12c). Because plane frames *A* and *D* are much stiffer than plane frames *B* and *C*, the stiffer frames will tend to "attract" or resist the major part of the wind load on the structure (See Chapter 14).

Analysis of the plane frame shown in Figure 1.12b will give the internal forces in all the members and the support reactions. These are the forces exerted by the foundations on the column bases. Typically, at supports built-in (encastré) to the foundation, there will be vertical, horizontal and moment reactions (Figure 1.12b). The horizontal reactions must add up to

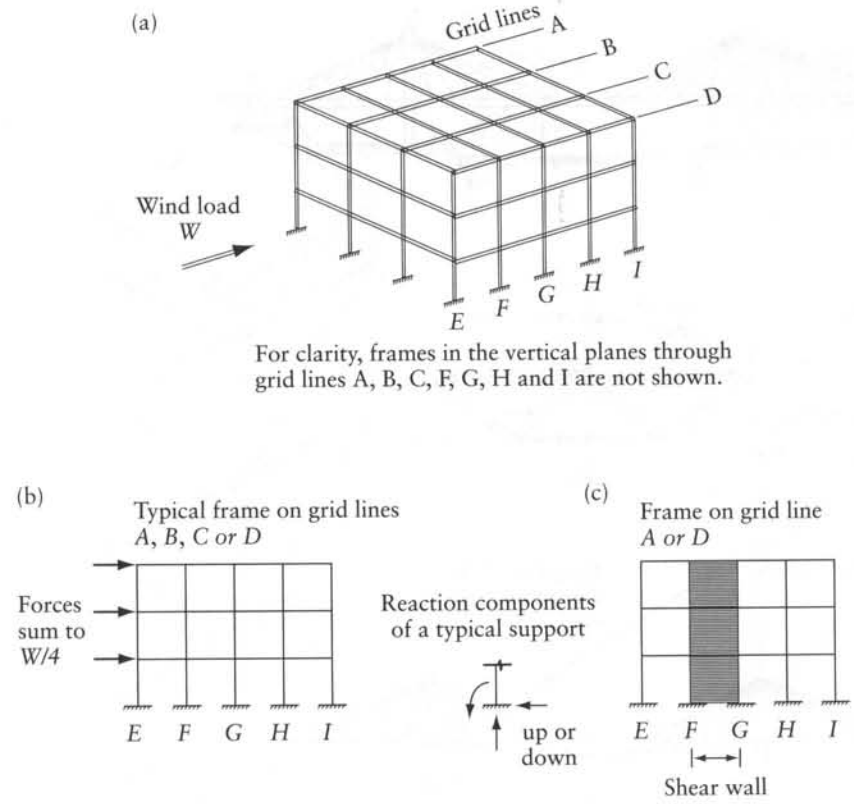

Figure 1.12 Idealization of a building for analysis of the effects of wind load. (a) Space frame. (b) Plane frame idealization. (c) Plane frame containing shear wall.

$W/4$, the wind load applied to this frame in the case considered. Also, the sum of the moments of the applied forces and the reactions about any point must be zero.

However, the individual vertical reactions will not be zero: the vertical reactions at E and I will be downward and upward respectively. We conclude from this discussion that considering the load path helps to decide on the structural analysis model that can be used as an idealization of the actual structure, the type of results that the analysis should give, and the requirements that the answers must satisfy. Structural idealization is further discussed in Section 1.5.

1.4 Deflected shape

As we have noted in the previous section, deflections can play an important part in understanding load paths. Moreover, understanding deflected shapes also aids in the interpretation of the results of our analyses. In the very simplest case, if we walk across a simply-supported wooden plank (Figure 1.13a), our weight will cause the plank to deflect noticeably. What is perhaps less obvious is that the ends of the plank rotate – because of the simple supports at the ends, which provide no restraint to rotation. A simply-supported beam usually has one *hinged* support and one *roller* support. The roller support allows horizontal translation caused by the thermal expansion or contraction of the beam.

If we now extend the beam to become a two-span continuous beam, ABC (Figure 1.13b), then the deflected shape will change. The downward (positive) deflection that we feel under our feet

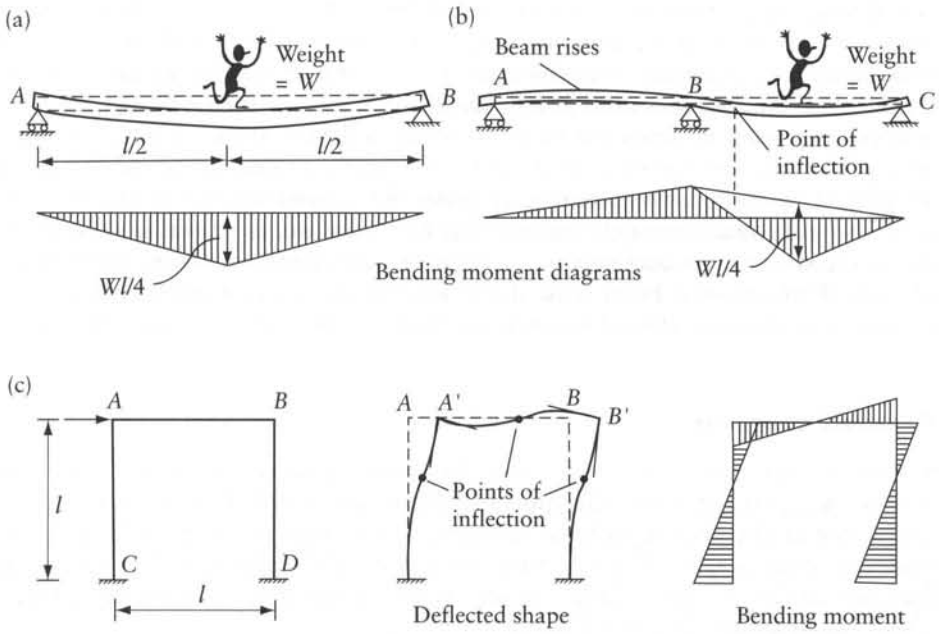

Figure 1.13 Deflected shapes and bending moment diagrams. (a) Simple beam. (b) Continuous beam. (c) Plane frame.

is accompanied by a negative deflection (rise) in the adjacent span. There will be a downward reaction at *A*; so there must be some way of holding down the plank at *A*, or it will lift off the support. The deflected shape has concave and convex parts; the point of inflection at which the curvature changes sign corresponds to a point of zero bending moment. This is further discussed in Sections 1.10 and 1.11.1.

Under the action of a horizontal load, the frame in Figure 1.13c will obviously deflect to the right. The joints at *A* and *B* will also rotate as they translate sideways. Because the joint is rigid, the angle between the column and beam remains a right angle and, therefore, the entire joint must rotate. The beam and the columns must deflect with double curvature – the point between the two curves in each member is a point of inflection. This point corresponds to a point of zero bending moment. Deflected shapes are drawn throughout this book because they aid in the understanding of how a given structure behaves.

It is important to recognize that the displacements experienced by structures are small when compared to the dimensions of the structure, and we therefore exaggerate them when drawing them. The deflected shape and the original shape of the structure are drawn on the same figure, with the deflections drawn to a larger scale than the structure. Design guidelines suggest that the maximum deflection of a simple beam should not exceed (*span*/300). The public would not thank us for beams that deflect more than this. More discussion and examples of deflected shapes are presented in Section 1.10.

1.5 Structural idealization

Structural idealization is the process in which an actual structure is represented by a simpler model that can be analyzed. The model consists of *elements* whose force/displacement relationship is known, or can be generated, that are connected at joints (nodes). For the analysis

of framed structures, the elements are one-dimensional bars, oriented in one-, two-, or three-dimensional space. The joints can be rigid or hinged. For plates, membranes, shells and massive structures (such as gravity dams), the elements are termed *finite elements* and may be one-, two-, or three-dimensional, connected by nodes at the corners and/or at sides (Figure 16.1). In any structural idealization, the loads must also be modeled, as must be the supports.

For analysis purposes, we draw the model as a free body and show by arrows a system of forces in equilibrium. The system consists of the externally applied loads and the reactions. Internal forces at a section can be shown and represented by pairs of opposite arrows; each pair consists of forces of equal magnitude and opposite direction. See, as an example, Figure 1.10b.

Loads on the structural model produce translations and rotations of the nodes: these are referred to as *displacements*. From these displacements, the internal forces and the support reactions can be determined; this information can then be used in the design of the structure.

1.6 Framed structures

All structures are three-dimensional. However, for analysis purposes, we model many types of structures as one-, two-, or three-dimensional skeletons composed of bars. Thus, an idealized *framed* structure can be one-dimensional (a beam), two-dimensional (a plane frame or truss), or three-dimensional (a space frame or truss, or a grid). The skeleton usually represents the *centroidal axes* of the members; the reason for use of centroidal axis is given in Section 1.11. The six types of structures are defined below.

Beam: The idealized structure is a straight line (the centroidal axis). A simple beam covers a single span and has a hinged and a roller support. Commonly, a continuous beam covers more than one span and has one support hinged or one end support built-in (encastré) and the remaining supports are rollers. A straight line can be used to model beams, slabs, and composite beam/slabs. Bridge superstructures are often modeled as straight lines, regardless of the shape

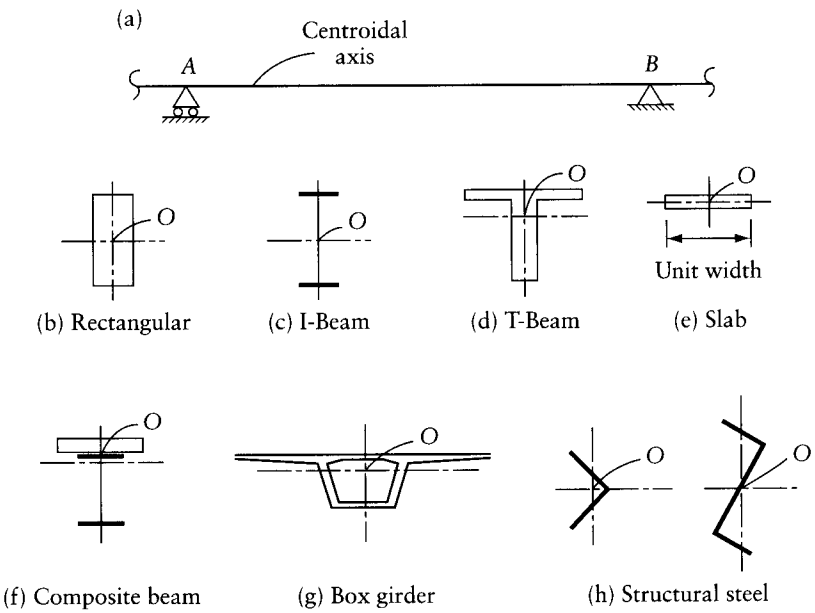

Figure 1.14 Beam idealization. (a) Interior span of a continuous beam. (b) to (h) Possible cross sections.

of their cross sections. Figure 1.14a illustrates beam *AB* that can be an idealization of structures having, as examples, any of the cross sections in Figures 1.14b to h. For each cross section, the centroidal principal axes are shown. All the applied loads, the reactions and the deflected axis of the beam are in one plane through a centroidal principal axis. A structure for which the loads are not applied through the centroidal principal axes must be idealized as a spatial structure.

Plane frame: A plane frame consists of members, connected by rigid joints. Again, the cross section of all members has a centroidal principal axis lying in one plane; all applied loads and reactions are in the same plane. Simple and continuous beams are special cases of plane frames. Thus, the computer program PLANEF (Appendix L) applies to plane frames and beams. Plane frames are widely used as idealizations of structures such as industrial buildings, multistorey buildings, and bridges. Figures 1.11a, b and c show a cable-stayed bridge and its idealization as a plane frame. Figures 1.12a, b and c show a multistorey building and its idealization as a plane frame for analysis of the effects of wind loads. Figure 1.15 shows a concrete bridge and a plane frame idealization.

Plane truss: A plane truss is similar to a plane frame but all joints are assumed pin-connected, and the loads are usually applied at the joints (still in the plane of the truss). Figures 1.6b and 12.20 are examples of plane truss idealizations of bridges; Figure 1.10b of a tower; and Figure 7.7 of a roof truss. Often, we do not draw circles at the joints (e.g. Figure 12.20), but the assumption that the members are pin-connected is implied. Note the triangulated nature of trusses – a requirement for their stability. The two assumptions of pin connections and forces applied at joints mean that truss members are subjected only to axial forces, without shear force or bending moment.

Space frame: Members and loads are now spatial (in three dimensions) with members connected by rigid joints. Most tall buildings are space frames – certainly if constructed in reinforced concrete or steel. However, much simpler structures often have to be modeled as space frames,

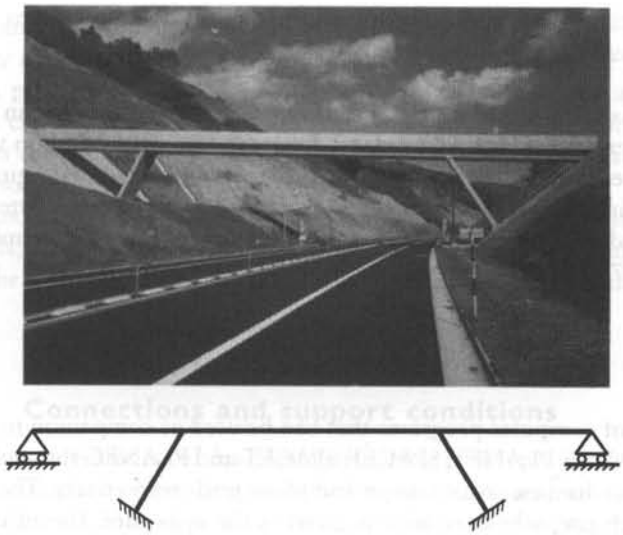

Figure 1.15 Plane frame idealization of a concrete bridge.

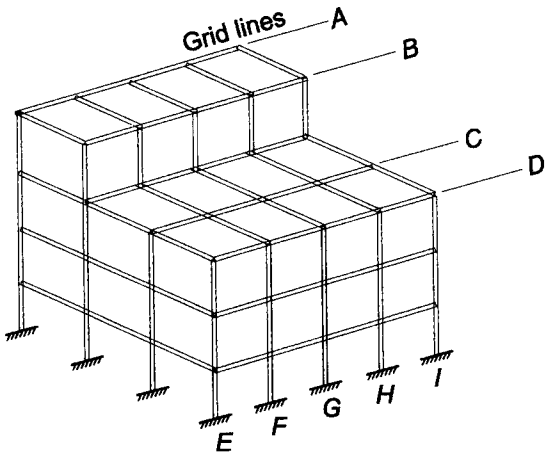

Figure 1.16 Space frame lacking symmetry, when analyzed for the effects of wind load in directions of the shown grid lines.

particularly if the loads are out-of-plane, or the members or the structures lack symmetry. As an example, the box-girder of Figure 1.14g must be idealized as a space frame if the bridge is curved. The same box-girder bridge, even when straight, must be idealized as a space frame when being analyzed for horizontal wind loads, or for load of traffic on a side lane. The building in Figure 1.16, which is of the same type as that shown in Figure 1.12a, should be modeled as a space frame because of the lack of symmetry, when the analysis is for the effect of wind load in the direction of the shown grid lines.

Space Truss: This is like a plane truss, but with members and loads in three dimensions. All joints are pin-connected. Space trusses are most commonly used in long-span roofs.

Grid: A grid is really a special case of a space frame, except that all the members are in one plane and the loads are applied perpendicular to that plane. Figure 1.17a shows the top view and sectional elevation of a concrete bridge deck having three simply-supported main girders monolithically connected to three intermediate cross-girders. Traffic load will be transmitted to the supports of all three main girders. The internal forces in all members can be determined using the grid model of Figure 1.17b.

1.6.1 Computer programs

Appendix L includes descriptions of computer programs that can be used as companion to this book. These include programs PLANEF, PLANET, SPACEF, SPACET and PLANEG for analysis of plane frames, plane trusses, space frames, space trusses and plane grids respectively. The five programs are available from a web site, whose address is given in the appendix. Use of these programs is encouraged at an early stage of study.

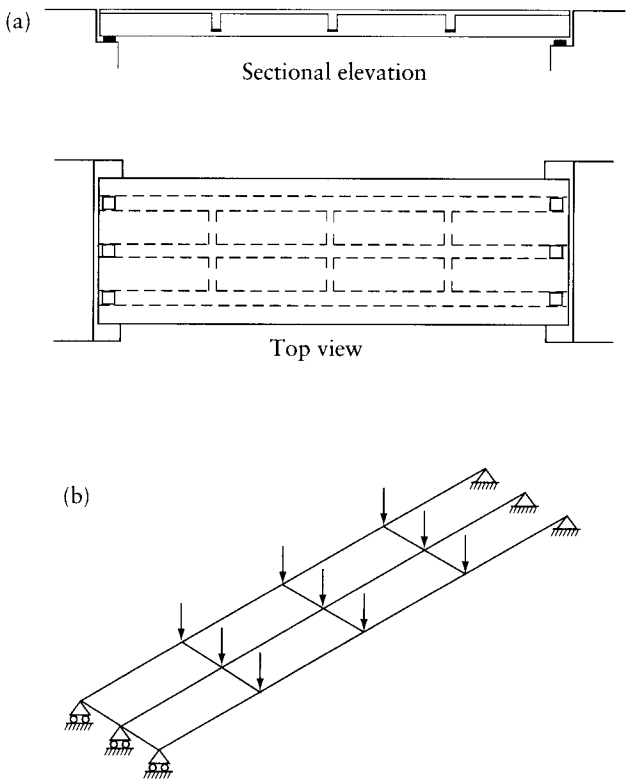

Figure 1.17 Idealization of a bridge deck as a grid. (a) Plan and sectional elevation of concrete bridge deck. (b) Grid idealization.

1.7 Non-framed or continuous structures

Continuous systems, such as walls, slabs, shells and massive structures can be modeled using *finite elements* (Figure 16.1). It is also possible to model the shear walls of Figure 1.12c as part of a plane frame model (Chapter 14). We have seen how a strip or unit width of a one-way slab can be modeled as a beam (Figure 1.14e). Bending moments and shear forces in two-way slabs can also be obtained using a plane grid model. Solid slabs and their supporting columns are sometimes modeled as plane frames.

Another type of modeling is used in Chapter 15 for the analysis of beams, circular cylindrical shells, plates subjected to in-plane forces and plates in bending. This is through approximations to the governing differential equations of equilibrium by *finite differences*.

1.8 Connections and support conditions

Much of the process of developing an appropriate representation of the actual structure relates to the connections between members of the structure, and between the structure and its supports or foundations. Like all of the process of structural modeling, this involves some approximations: the actual connections are seldom as we model them.

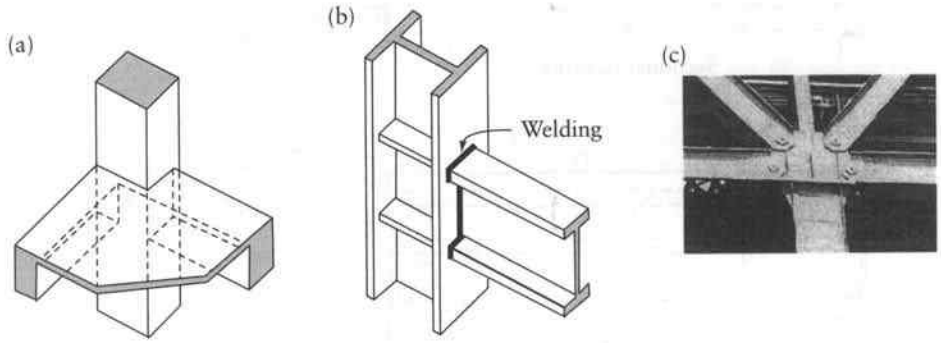

Figure 1.18 Connections. (a) Rigid connection of a corner column with slab and edge beams in a concrete building. (b) Rigid connection of steel column to beam. (c) Pin-connected truss members.

Most connections between frame members are modeled as rigid (Figure 1.7), implying no relative rotation between the ends of members connected at a joint, or as pinned, implying complete freedom of rotation between members connected at a joint. These represent the two extremes of connections; in fact, most connections fall somewhere between these two extremes.

Figures 1.18a and b show two rigid connections, in concrete and in steel construction respectively. Figure 1.18c is a photograph of a pinned connection in an old steel truss. A rigid joint transfers moment between the members connected to the joint, while the pinned joint does not do so. In trusses, we assume in the analysis that the members are pin-connected although in modern practice most are constructed as rigid connections. With rigid joints, the members will be subjected mainly to axial forces; but, in addition, there are bending moments that are frequently ignored. The stress in the cross section of members is no longer uniform. To consider that the members are rigidly connected at the joints, a plane truss or a space truss must be analyzed as a plane frame or a space frame respectively. This will commonly require use of a computer. The answers of Prob. 1.14 show a comparison of the results of analyses of a plane truss and a plane frame having the same configuration.

Connections to foundations, or supports, must also be modeled in structural analysis. The three common forms of supports for beams and plane frames are illustrated in Figure 1.19, with the associated reaction components; the hinge and roller supports (Figures 1.19c and d) are also used for plane trusses. A hinged support is sometimes shown as a pin-connection to a rigid surface (Figure 1.19c). Figure 1.19a shows the displacement components at a typical joint, and Figures 1.19b to d indicate the displacement components that are prevented, and those that are free, at the support. The roller support (Figure 1.19d) is used when the structure must accommodate axial expansion or contraction, usually due to thermal effects, but also due to creep, shrinkage and prestressing effects.

In many cases, the actual form of support is different from the idealizations shown in Figure 1.19. For example, short-span beams and trusses in buildings are often provided with no specific support system at their ends. The absence of specific means of restraining end rotations or axial displacements justifies their analysis as simply-supported ends.

Special supports (bearings) to ensure that translation or rotation can freely occur as assumed in the analysis are commonly provided for longer spans (Figure 1.19e). A wide variety of bridge bearings, which vary in complexity depending on the magnitude of the reactions and the allowed displacements, is commercially available.

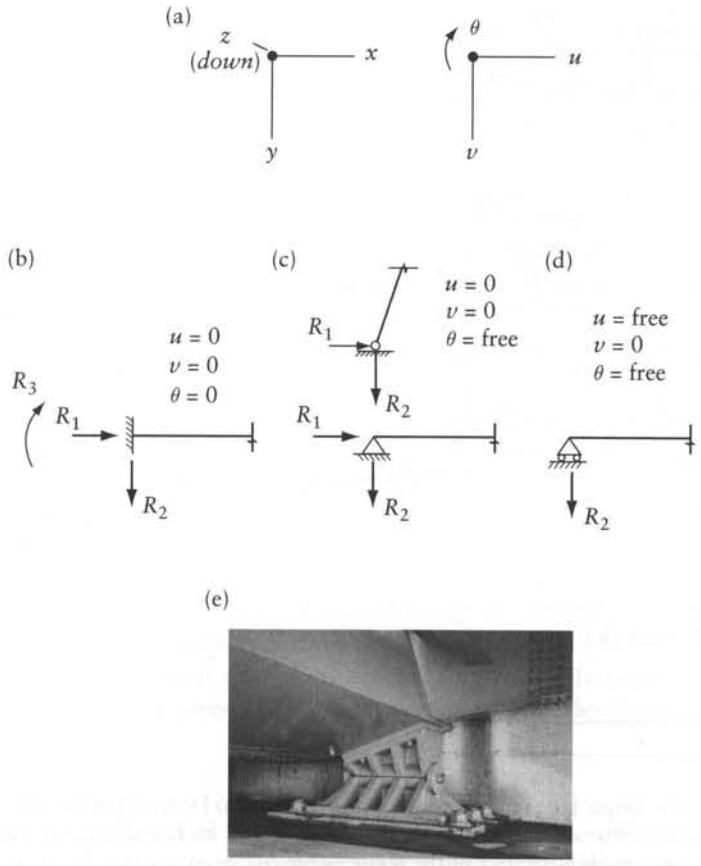

Figure 1.19 Idealized supports for beams and plane frames. (a) Displacement components at a typical joint. (b) Totally fixed (encastré). (c) Hinged (two alternatives). (d) Roller. (e) Hinged bridge bearing.

1.9 Loads and load idealization

Several causes of stresses and deformations need to be considered in structural analysis. Gravity load is the main cause. Examples of gravity loads are the weight of the structure, of non-structural elements such as floor covering and partitions, of occupants, furniture, equipment, as well as traffic and snow. Pressure of liquids, earth, granular materials and wind is another type of load. Prestressing produces forces on concrete structures (see Appendix K).

We can idealize loads as a set of concentrated loads. The arrows shown on the truss nodes in Figure 1.6b can represent the self-weight of the members and the weight of the deck and the traffic load it carries. Alternatively, the analysis may consider load distribution over length or over an area or a volume and defined by the load intensity (force/unit length or force/unit area or force/ unit volume).

In many cases the deformations due to temperature variation cannot occur freely, causing stresses, internal forces and reactions. This is briefly discussed in Section 1.9.1.

If one of the supports of a simple beam (Figure 1.20a) settles downward, the beam rotates as a rigid body and no stress is developed. But if the beam is continuous over two or more spans, a support settlement produces internal forces and reactions (Appendix E). Figure E-1 shows the deflected shape, the reactions and bending moments over the supports due to settlement of an interior support of a beam continuous over three spans.

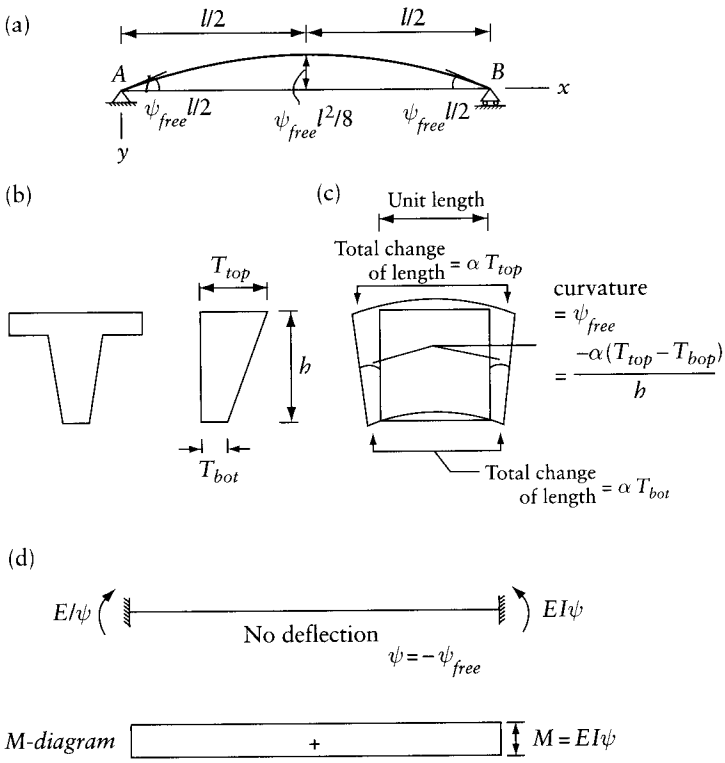

Figure 1.20 Deformation of a simple beam due to temperature change. (a) Deflected shape. (b) Cross section and variation in a rise of temperature over its height. (c) Free change in shape of a segment of unit length. (d) Effect of the temperature rise in part (b) on the beam with ends encastré.

For some materials, such as concrete, a stress increment introduced and sustained thereafter produces not only an immediate strain but also an additional strain developing gradually with time. This additional strain is creep. Similar to thermal expansion or contraction, when creep is restrained, stresses and internal forces develop. Analysis of the effects of creep, shrinkage and temperature including the effect of cracking is discussed elsewhere.[1]

Ground motion in an earthquake produces dynamic motion of the structure causing significant inertial forces. Analysis of the internal forces can be done by a dynamic computer analysis of the idealized structure, subjected to a recorded ground motion. In lieu of the dynamic analysis, codes allow a static analysis using equivalent lateral forces, commonly applied at floor levels. Because these forces represent inertial effect, their values are proportional to the mass of the structure commonly lumped at each floor level.

1.9.1 Thermal effects

Thermal expansion or contraction produces deformation, but no stress, when it can occur freely, without restraint. This is the case of the simple beam in Figure 1.20a, subjected to temperature

1 See Ghali, A., Favre, R. and Elbadry, M., *Concrete Structures: Stresses and Deformations*, 3rd ed., Spon Press, London, 2002, 608pp.

rise varying linearly between T_{top} at top fiber and T_{bot} at bottom fiber (Figure 1.20b). When $T_{top} = T_{bot} = T$, the beam elongates and the roller at B moves outward a distance equal to $\alpha T l$; where α is coefficient of thermal expansion and l is beam length. When $T_{top} \neq T_{bot}$ the beam will have constant free curvature:

$$\psi_{free} = \frac{\alpha(T_{bot} - T_{top})}{h} \tag{1.7}$$

Figure 1.20c shows the change in shape of a segment of unit length (with $T_{top} > T_{bot}$). The two sections at the limits of this length rotate relative to each other, and the angle ψ_{free} is equal to the curvature

$$\psi_{free} = -\frac{d^2y}{dx^2} \tag{1.8}$$

where y is the deflection (positive when downward); x is the distance between the left-hand end of the beam and any section. In the case considered, the beam deflects upwards as shown in Figure 1.20a; the end rotations and the deflection at mid-span given in the figure can be checked by integration of Eq. 1.8. The negative sign in Eq. 1.8 results from the directions chosen for the axes and the common convention that sagging is associated with positive curvature.

When a beam continuous over two spans is subjected to the same rise of temperature as presented in Figure 1.20b, the upward deflection cannot occur freely; a downward reaction develops at the intermediate support and the deflected shape of the beam is as shown in Figure 4.2c.

Restraint of thermal expansion can develop relatively high stresses. A uniform change in temperature of T degrees in a beam with ends encastré develops a stress

$$\sigma = -\alpha E T \tag{1.9}$$

where E is modulus of elasticity. For a concrete beam with $E = 40\,\text{GPa}$ (5.8×10^6 psi), $\alpha = 10 \times 10^{-6}$ per degree centigrade (6×10^{-6} per degree Fahrenheit), $T = -15°\,\text{C}$ ($-27°\,\text{F}$), with the minus sign indicating temperature drop, the stress is $\sigma = 6\,\text{MPa}$ (940 psi). This tensile stress can cause the concrete to crack; the restraint is then partially or fully removed and the thermal stress drops. Analysis of the effect of temperature accounting for cracking requires nonlinear analysis. Linear analysis of the effect of temperature is treated in Chapters 4 and 5. Shrinkage or swelling can be treated in the same way as thermal contraction or expansion respectively.

We conclude the discussion on the effects of temperature and shrinkage (similar to settlement of supports) by stating that these produce stresses and internal forces only in statically indeterminate structures, such as continuous beams; no stresses or internal forces develop in statically determinate structures, such as simple beams.

The topic of statical indeterminacy is discussed in more detail in Section 3.2. We should also mention that a temperature rise that varies nonlinearly over the depth of section of the simple beam in Figure 1.20a produces self-equilibrating stress; this means that the resultant of this stress (the internal force) is nil (Section 6.9).

1.10 Stresses and deformations

Structures deform under the action of forces. The column of Figure 1.21a is acted on by forces P and Q as shown. Figure 1.21b shows the deflected shape of the column. The applied forces cause internal forces that are stress resultants. The resultants of stresses at any section are bending moment, M, shear force, V and axial force, N. To show these internal forces, the structure must be cut (Figure 1.21c). Now we have two free body diagrams, with the internal forces shown at the location of the cut. Note that we must show the internal forces on both sides of the cut as

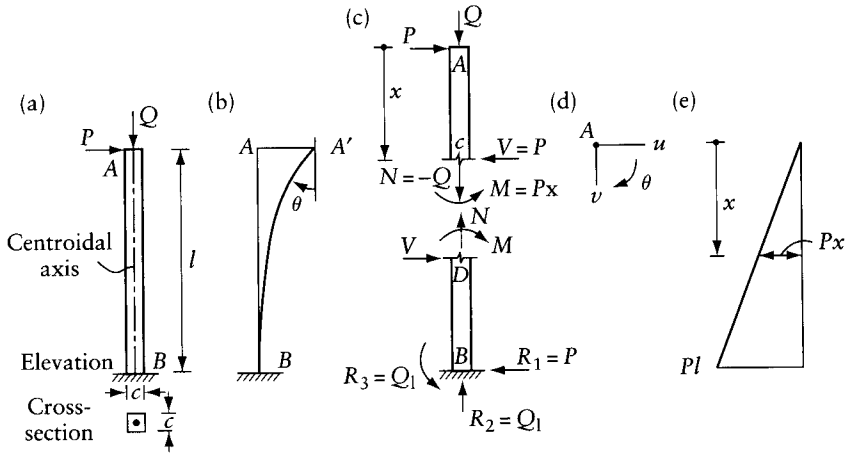

Figure 1.21 Deflected shape and internal forces in a column. (a) Elevation and cross section. (b) Deflected shape. (c) Cut to show internal force at a section. (d) Displacement components at the tip. (e) Bending moment diagram.

pairs of arrows in opposite directions. Applying equilibrium equations to the upper free body diagram (part AC), we get:

$$N = -Q;\ V = P;\ M = Px \tag{1.10}$$

The same answers can be obtained by considering equilibrium of part DB. The sign convention for the internal forces and their calculation is discussed in detail in Section 2.3. The above equations tell us that N and V are constant throughout the height of the column, but M varies linearly from top to bottom (Figure 1.21e). These internal forces are resultants of stresses that produce strains. Each strain results in a form of deformation – in this case, axial, shear, and bending (flexural). Generally, the first two are small in comparison to the flexural deformation. For example, if the column is made of timber, 0.1 m (4 in.) square, and 3 m (10 ft) long, and the two forces, P and Q, are each 1.00 kN (225 lb), then the displacement components at the top of the column are (Figure 1.21d):

$$u = 0.11\,\text{m}\ (4.3\,\text{in.});\ v = 30 \times 10^{-6}\,\text{m}\ (0.0012\,\text{in.});\ \theta = 0.054\,\text{rad}$$

These values are calculated by virtual work (Chapter 8) assuming the modulus of elasticity, $E = 10\,\text{GPa}$ (1.145×10^6 psi) and the shear modulus, $G = 4\,\text{GPa}$ (0.6×10^6 psi). The displacement component v is the axial shortening of the column due to the axial force, N; u is the sidesway at the top due to the shear force, V, and to the moment, M (the latter is generally much larger than the former, in this case by a ratio of 1200 to 1); and θ is the angular rotation due to the moment. A knowledge of deflections and the deflected shape aids us to understand the behavior of the structure.

When we sketch deflected shapes, we generally consider only the bending deformation and, as mentioned in Section 1.4, we show the deflections on a larger scale than the structure itself. Thus, we show the deflected position A' of the tip of the column at its original height A, indicating that the change in length of the column is ignored (Figure 1.21b). For the same reason, we show in the deflected shape in Figure 1.13c A and A' at the same level, and likewise for B and B'. Also, because we ignore the change of length of member AB, the distance $\overline{AA'}$ is shown the

same as $\overline{BB}'$. For the same reason, the length of member AB in Figure 1.21 does not change and A moves on an arc of a circle to A'. But, because the deflections are small compared to the member lengths, the displacement $\overline{AA}'$ is shown perpendicular to AB; in other words, the arc of circle is shown as a straight line $\overline{AA}'$ perpendicular to the original direction of AB. This is explained again in Section 7.2. When drawing the deflected shape of the frame in Prob. 1.1c, the movement of node B should be shown perpendicular to AB (downward) and the movement of C perpendicular to CD (upward).

We often draw diagrams showing the variations of M and V over the length. These are termed *bending moment* and *shear force diagrams*. The sign convention for the bending moment diagram is important. Bending or flexure produces tension on one face of the cross section, and compression on the other. Examining the deflected shape of Figure 1.21b, it is not difficult to imagine the tension on the left-hand side of the column, and, therefore, the bending moment diagram is drawn on that (tension) side (Figure 1.21e). The axial force N and the bending moment M produce a normal stress, tensile or compressive. Calculation of normal stresses is discussed in the following section.

1.11 Normal stress

Figures 1.22a and b represent the elevation and cross section of a column subjected at the top section to a distributed load of intensity p/unit area. The resultant of the load has the components

$$N = \int p\,da \qquad M_x = \int p\,y\,da \qquad M_y = \int p\,x\,da \tag{1.11}$$

where N is normal force at the centroid of the the cross-sectional area; M_x and M_y are moments about the *centroidal axes* x and y respectively. The positive-sign convention for N, M_x, and M_y is shown in Figure 1.22; the reference point O is chosen at the centroid of the cross section. In the deformed configuration, each cross section, originally plane, remains plane and normal to the longitudinal centroidal axis of the member. This assumption, attributed to Bernoulli (17th–18th century), is confirmed by experimental measurements. The stress and the strain are considered positive for tension and elongation respectively.

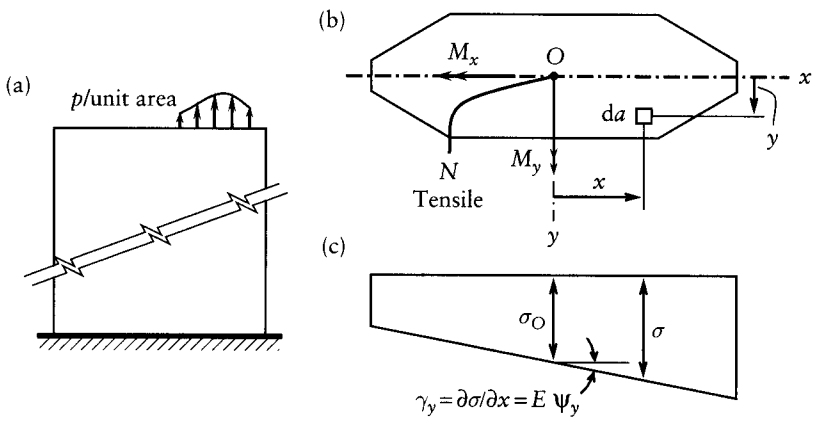

Figure 1.22 Normal stress distribution in a column cross section. Positive sign convention. (a) Elevation. (b) Cross section. (c) Stress variation along the x axis.

It can be assumed that any section away from the top remains plane after deformation. Thus, considering a linearly elastic material with a modulus of elasticity E, the strain ε and the stress σ at any point can be expressed as

$$\varepsilon = \varepsilon_O + \psi_x y + \psi_y x \qquad \sigma = \sigma_O + \gamma_x y + \gamma_y x \tag{1.12}$$

where ε_O is the strain at the centroid O; $\psi_x = \partial\varepsilon/\partial y$ is the curvature about the x axis; $\psi_y = \partial\varepsilon/\partial x$ is the curvature about the y axis; $\sigma_O = E\varepsilon_O$ is the stress at O; $\gamma_x = E\psi_x = \partial\sigma/\partial y$; $\gamma_y = E\psi_y = \partial\sigma/\partial x$ (Figure 1.22c). Tensile stress is considered positive.

The stress resultants are

$$N = \int \sigma \, da \qquad M_x = \int \sigma y \, da \qquad M_y = \int \sigma x \, da \tag{1.13}$$

Substitution of Eq. 1.12 in Eq. 1.13 and solution of the resulting equations gives the parameters σ_O, γ_x, and γ_y:

$$\sigma_o = \frac{N}{a} \qquad \gamma_x = \frac{M_x I_y - M_y I_{xy}}{I_x I_y - {I_{xy}}^2} \qquad \gamma_y = \frac{M_y I_x - M_x I_{xy}}{I_x I_y - {I_{xy}}^2} \tag{1.14}$$

Thus, the stress at any point (x, y) is

$$\sigma = \frac{N}{a} + \left(\frac{M_x I_y - M_y I_{xy}}{I_x I_y - {I_{xy}}^2}\right) y + \left(\frac{M_y I_x - M_x I_{xy}}{I_x I_y - {I_{xy}}^2}\right) x \tag{1.15}$$

where $a = \int da$ is the area of the cross section; $I_x = \int y^2 \, da$ is the second moment of area about the x axis; $I_y = \int x^2 \, da$ is the second moment of area about the y axis; and $I_{xy} = \int xy \, da$ is the product of inertia. When x and y are *centroidal principal axes*, $I_{xy} = 0$ and Eq. 1.15 simply becomes

$$\sigma = \frac{N}{a} + \frac{M_x}{I_x} y + \frac{M_y}{I_y} x \tag{1.16}$$

The derivation of Eq. 1.14 will involve the first moments of area about the x and y axes, $B_x = \int y \, da$ and $B_y = \int x \, da$; however, both terms vanish because the axes x and y are chosen to pass through the centroid O.

1.11.1 Normal stresses in plane frames and beams

A plane frame is a structure whose members have their centroidal axes in one plane; the cross sections of all members have a centroidal principal axis in this plane, in which all the forces and the reactions lie. Figures 1.23a and b show a segment of unit length and the cross section of a plane frame. A reference point O is chosen arbitrarily on a centroidal principal axis of the cross section (in this case, a vertical axis of symmetry). The general case in Figure 1.22b becomes the same as the case in Figure 1.23c when M_y is absent and M is used to mean M_x; the equations in Section 1.11 apply when O is chosen at the centroid of the section and M_y, ψ_y, γ_y, and I_{xy} are set equal to zero. Because the case in Figure 1.23b is of frequent occurrence, we derive below equations for the distributions of strain ε, stress σ and the curvature corresponding to the stress resultants N and M (the internal axial force and bending moment), with the reference point O not necessarily the centroid of the section. The positive sign conventions for N, M, and the coordinate y of any fiber are indicated in Figure 1.23b.

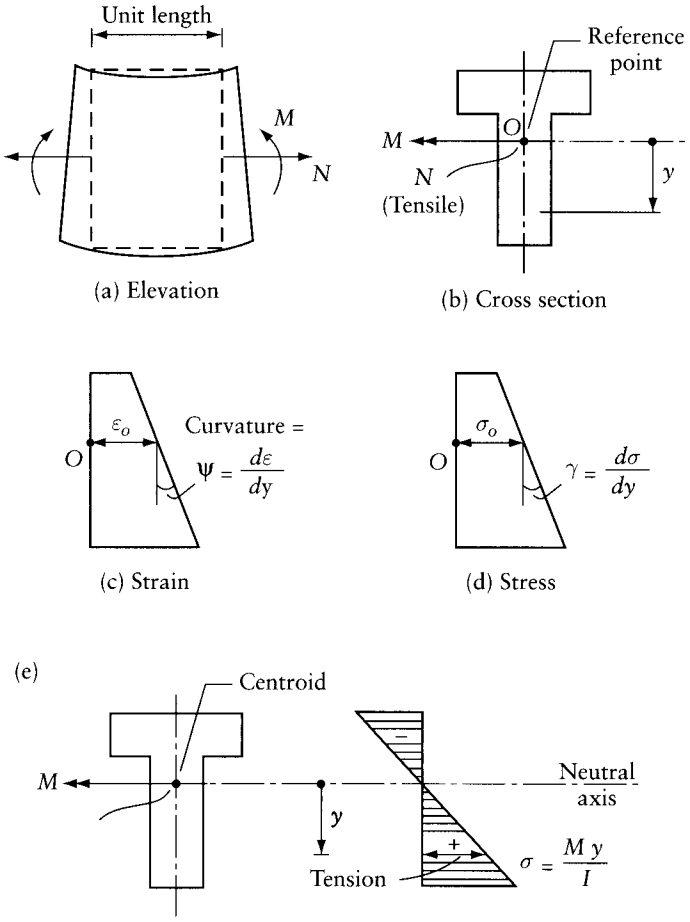

Figure 1.23 Normal stress and strain in a cross section of a beam. (a) Elevation of a segment of unit length. Positive sign convention of N and M. (b) Cross section. (c) Strain diagram. (d) Stress diagram. (e) Stress in a section subjected to M without N.

The two sections of the segment in Figure 1.23a are represented by vertical dashed lines before deformation; after deformation, the sections are represented by the rotated solid straight lines. The variations of the strain ε and the stress σ over the depth of the section shown in Figures 1.23c and d are expressed as:

$$\varepsilon = \varepsilon_O + \psi y \qquad \sigma = \sigma_O + \gamma y \tag{1.17}$$

where ε_O and σ_O are, respectively, the strain and the stress at the reference point O; $\psi = d\varepsilon/dy$ and $\gamma = d\sigma/dy$ are the slopes of the strain and the stress diagrams. Here, the symbols ψ and γ stand for ψ_x and γ_x in Section 1.11; ψ, of unit length^{-1}, is the curvature in the vertical plane.

The resultants N and M of the stress σ can be expressed by integration over the area of the section:

$$N = \int \sigma \, da \qquad M = \int \sigma y \, da \tag{1.18}$$

Substitution of Eq. 1.17 in Eq. 1.18 gives:

$$N = \sigma_O a + \gamma B \qquad M = \sigma_O B + \gamma I \tag{1.19}$$

where

$$a = \int da \qquad B = \int y\,da \qquad I = \int y^2\,da \tag{1.20}$$

a, B, and I are the area and its first and second moment about a horizontal axis through the reference point O. Solution of Eq. 1.19 and substitution of Eq. 1.17 gives the parameters σ_O and γ, ε_O, and ψ that define the stress and the strain diagrams:

$$\sigma_o = \frac{IN - BM}{aI - B^2} \qquad \gamma = \frac{-BN + aM}{aI - B^2} \tag{1.21}$$

$$\varepsilon_o = \frac{IN - BM}{E(aI - B^2)} \qquad \psi = \frac{-BN + aM}{E(aI - B^2)} \tag{1.22}$$

When O is at the centroid of the cross section, $B = 0$ and Eqs. 1.21 to 1.24 simplify to:

$$\sigma_o = \frac{N}{a}; \gamma = \frac{M}{I} \tag{1.23}$$

$$\epsilon_o = \frac{N}{Ea}; \psi = \frac{M}{EI} \tag{1.24}$$

Substitution of Eq. 1.22 in Eq. 1.17 gives the stress at any fiber whose coordinate is y with respect to an axis through the centroid:

$$\sigma = \frac{N}{a} + \frac{My}{I} \tag{1.25}$$

When a section is subjected to bending moment, without a normal force (Figure 1.23e), the normal stress at any fiber is:

$$\sigma = \frac{My}{I} \tag{1.26}$$

with y measured downward from the centroidal axis and I is second moment of area about the same axis. The normal stress is tensile and compressive at the fibers below and above the centroid respectively. Thus, the neutral axis is a centroidal axis, only when N is zero. The bottom fiber is subjected to tension when M is positive; but when M is negative the tension side is at the top fiber.

We note that Eqs. 1.23 to 1.26 apply only with the reference axis through O being at the centroid. We recall that framed structures are analyzed as a skeleton representing the centroidal axes of the members (Section 1.6); this is to make possible use of the simpler Eqs. 1.23 and 1.24 in lieu of Eqs. 1.21 to 1.22, which must be used when O is not at the centroid.

1.11.2 Examples of deflected shapes and bending moment diagrams

The curvature ψ is the change in slope of the deflected shape per unit length. From Eq. 1.24, it is seen that the curvature ψ is proportional to the bending moment M. Figure 1.24a shows

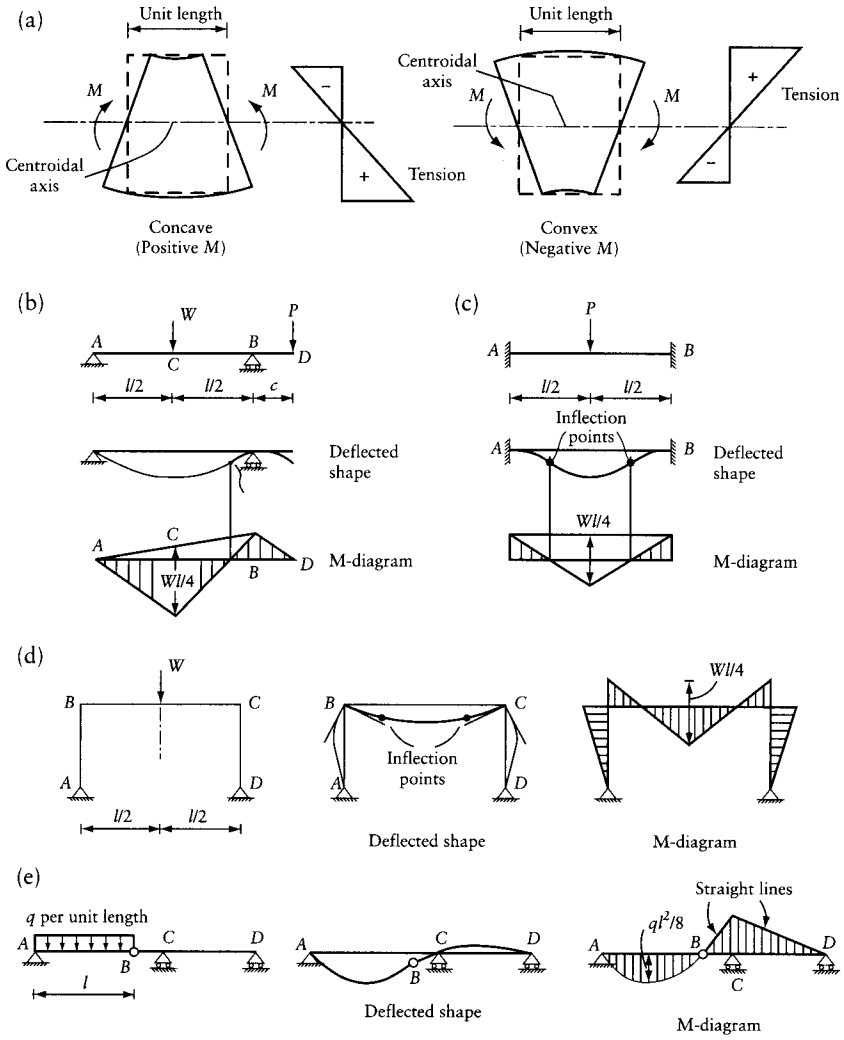

Figure 1.24 Curvature, deflection and bending moment diagrams for beams. (a) Curvature and stress due to bending moment. (b) to (e) Examples of deflected shapes and bending moment diagrams.

segments of unit length subjected to positive and negative bending moments. The corresponding stress distributions are shown in the same figures, from which it is seen that positive M produces a concave curvature and tension at bottom fiber; negative M produces a convex curvature and tension at top fiber.

Figure 1.24b shows the deflected shape and bending moment diagram for a beam. Without calculation, we can sketch the deflected shape by intuition. The bending moment diagram can then be drawn by following simple rules: at a free end, at an end supported by a hinged support or roller and at an intermediate hinge, the bending moment is zero. The bending moment is also zero at points of inflection, where the curvature changes from concave to convex. The bending moment diagram is a straight line for any straight member not subjected to distributed load; see parts *AC*, *CB* and *BD* in Figure 1.24b and parts *BC* and *CD* in Figure 1.24e. The bending moment graph is a second degree parabola for a part of a member carrying a uniform transverse load; see part *AB* in Figure 1.24e.

Throughout this book, we plot the ordinates of the bending moment diagram in a direction perpendicular to the axis of the member and on the tension side. The hatching of the M-diagram indicates the direction in which the ordinates are plotted. We can now verify that the M-diagram in Figures 1.13a to c and 1.24b to e follow these rules.

We recall that in drawing the deflected shapes, we show only the bending deformation. Thus, the members do not change in length. Because neither the columns nor the beam in Figure 1.24d, BC, change length, joints B and C must remain at the same height and at the same horizontal location (because of symmetry) and therefore only rotate. The deflected shape in Figure 1.24e is discontinuous at the intermediate hinge B; thus, the slopes just to the left and just to the right of the hinge are different.

Some of the ordinates that define the M-diagrams in Figures 1.13 and 1.24 are statically indeterminate and thus require calculations. These are not given in the figures, only the statically determinate values, such as $Wl/4$ and $ql^2/8$ being shown; these represent the bending moment of a simply-supported member of length l, carrying a transverse concentrated load W at its middle or a uniformly distributed load of intensity q/unit length.

1.11.3 Deflected shapes and bending moment diagrams due to temperature variation

The simple beam in Figure 1.20a subjected to temperature rise that varies linearly over its depth deflects freely as shown in the figure. A constant curvature (concave), ψ_{free} given by Eq. 1.7 occurs, with the bending moment equal to zero at all sections. When $T_{top} > T_{bot}$, Eq. 1.7 gives negative curvature (convex, Figure 1.20a). The simple beam is a statically determinate structure in which the thermal expansion or contraction is unrestrained. The same temperature rise in a beam with ends encastré produces reactions and a constant bending moment $M = -EI\psi_{free}$ (Figure 1.20d). This bending moment is positive, producing tension at bottom, and compression at top fibers. The corresponding curvature (Eq. 1.26) is: $\psi = M/(EI) = -\psi_{free}$. Thus, the net curvature is zero and the beam does not deflect. The beam with totally fixed ends is a statically indeterminate structure in which the thermal expansion or contraction is restrained.

We conclude from this discussion that the deflected shape due to temperature variation in a statically indeterminate structure is the sum of the free deflection, in which the thermal expansion or contraction is not restrained and the deflection due to restraining forces. The deflected shape of the continuous beam in Figure 4.2c is the sum of the free deflected shape in Figure 4.2b and the deflection of simple beam AC subjected to downward force at B. The net deflected shape due to temperature cannot be used to draw the bending moment diagram; thus, the points of inflection in the deflected shape in Figure 4.2c are not points of zero bending moment.

1.12 Comparisons: beams, arches and trusses

The examples presented below compare the behaviour of different types of plane structures that carry the same load and cover the same span (Figure 1.25). The structures considered are: a simple beam, arches with and without ties and with different support conditions and a simply-supported truss. The discussion will show that we can use a lighter structure by avoiding or reducing bending moments.

Example 1.1: Load path comparisons: beam, arch and truss

Each of the five structures shown in Figures 1.25a to e carries a uniformly distributed load of total value 480 kN (108×10^3 lb). This load is idealized as a set of equally spaced

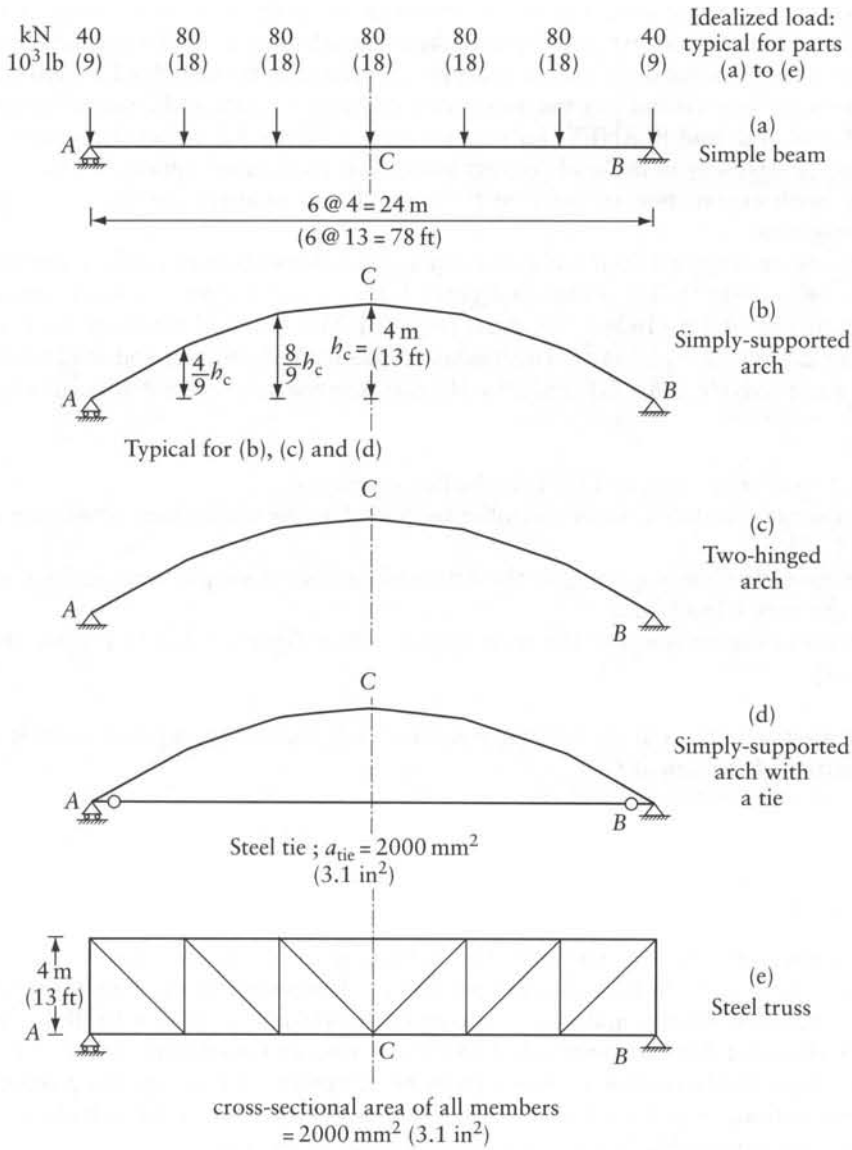

Figure 1.25 Structures covering same span and carrying same load (Example 1.1). (a) Simple beam. (b) Simply-supported arch. (c) Two-hinged arch. (d) Simply-supported arch with a tie. (e) Truss.

concentrated forces as shown. The five structures transmit the same loads to the supports, but produce different internal forces and different reactions. The objective of this example is to study these differences.

The simple beam in Figure 1.25a, the simply-supported arch in Figure 1.25b, and the truss in Figure 1.25e are statically determinate structures. But, the two arches in Figures 1.25c and d are statically indeterminate to the first degree. Chapters 2 and 3 discuss the topic of statical indeterminacy and explain the analysis of determinate and indeterminate structures.

Here, we give and compare some significant results of the analysis, with the objective of understanding the differences in the load paths, the internal forces, and the deformations in the structural systems. Some details of the analyses are presented in Examples 2.11 and 4.5.

The analyses can be performed by the use of computer programs PLANEF (for structures in Figures 1.25a to d) and PLANET (for the structure in Figure 1.25e); see Appendix L. Use of the programs early in the study of this book is an encouraged option. Simple data preparation (with explanation included in the appendix) is required for the use of the computer programs.

The simple beam (Figure 1.25a) has a concrete rectangular section of height 1.2 m and width 0.4 m ($47 \times 16\,\text{in.}^2$). The arches in Figures 1.25b, c and d have a constant square cross section of side 0.4 m (16 in.). The truss (Figure 1.25e) has steel members of cross-sectional area $2 \times 10^{-3}\,\text{m}^2$ ($3.1\,\text{in.}^2$). The moduli of elasticity of concrete and steel are 40 and 200 GPa respectively (5.8×10^6 and 29×10^6 psi). The analysis results discussed below are for:

1. The mid-span deflections at node C in the five structures.
2. The horizontal displacement of the roller support A in the simply-supported arch in Figure 1.25b.
3. The bending moment diagrams for the left-hand half of the simple beam and for the arches (Figures 1.26a to d).
4. The forces in the members of the truss (Figure 1.26e; Figures 1.26a to e show also reactions).

Table 1.1 gives the values of the bending moments at C, the horizontal displacement at A and the vertical deflection at C.

Discussion of results

1. The mid-span bending moment and the deflection at C in the simple beam are 1440 kN-m (1050×10^3 lb-ft) and 0.037 m (1.5 in.) respectively. In the simply-supported arch, the bending moment at mid-span is also equal to 1440 kN-m (1050×10^3 lb-ft). In the same arch, the roller A moves outwards 0.851 m (33.5 in.) and the deflection at C is 1.02 m (40.2 in.). These displacements are too high to be acceptable, indicating that a reduction of the cross section, from $0.4 \times 1.2\,\text{m}^2$ in the beam to $0.4 \times 0.4\,\text{m}^2$ in the arch (16×47 to $16 \times 16\,\text{in.}^2$), is not feasible by only changing the beam to an arch.
2. When the horizontal displacement at A is prevented, by changing the roller to a hinge (Figure 1.26c), the bending moment at C is reduced to almost zero, 2.5 kN-m (1.5×10^3 lb-ft) and the deflection at C to 0.002 m (0.08 in.). At the same time, axial compressive forces are produced in the members of the arch. In addition to the vertical reaction components, the two-hinged arch has horizontal reaction components pointing inwards.
3. The reductions in deflection and in bending moments achieved by replacing the roller at A by a hinge can be partly achieved by a tie connecting the two supports. The amounts of the reduction depend upon the cross-sectional area and the modulus of elasticity of the tie. With the given data, the horizontal displacement at A is 0.021 m (0.83 in.) outwards; the bending moment at C is 38 kN-m (28×10^3 lb-ft) and the deflection at C is 0.027 m (1.1 in.).
4. The forces in the top and bottom chords of the truss are compressive and tensile respectively, with absolute values approximately equal to the bending moment values in the simple beam

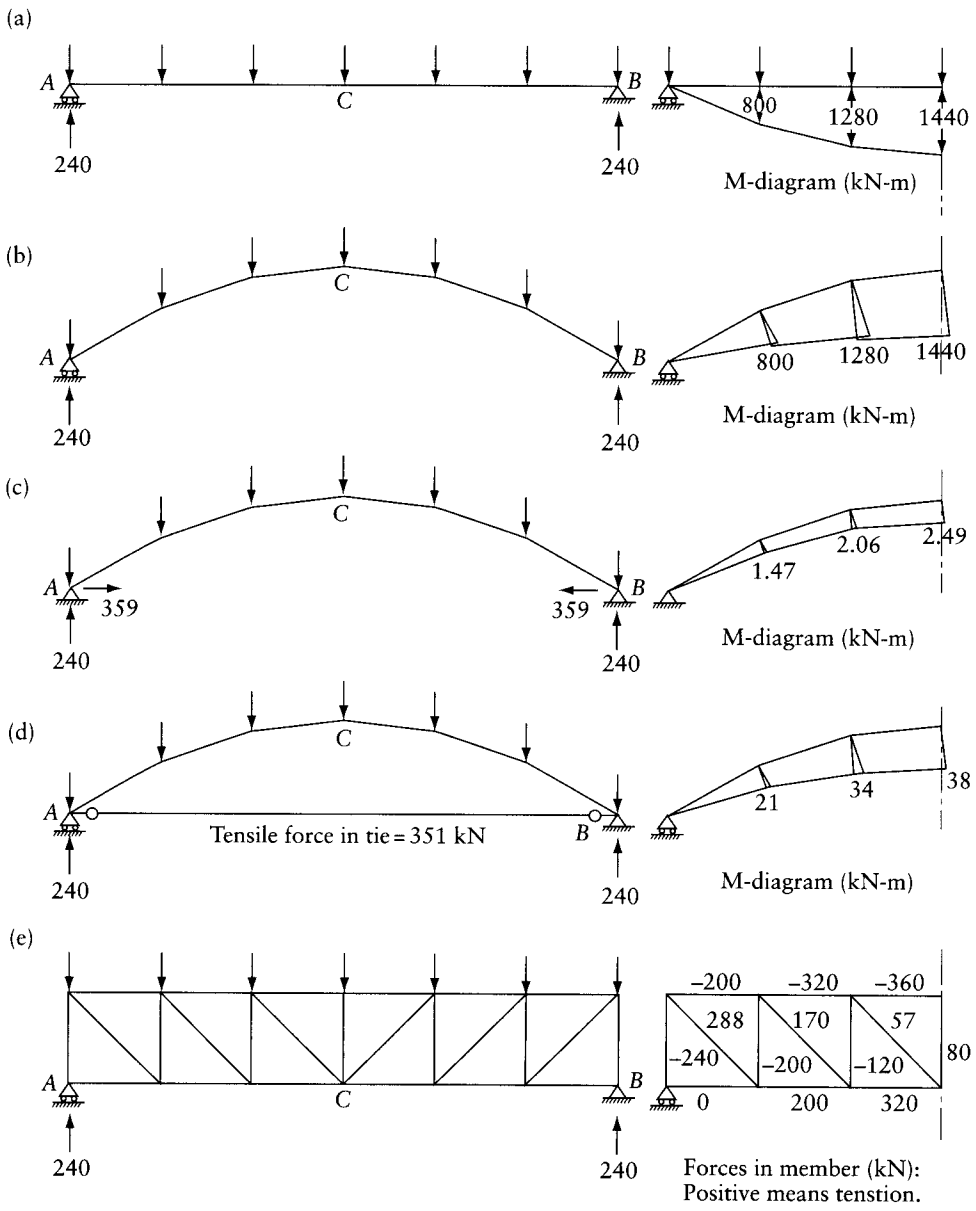

Figure 1.26 Reactions and internal forces in the structures of Figure 1.24. Total load = 480 kN; span = 24 m. (a) Simple beam. (b) Simply-supported arch. (c) Two-hinged arch. (d) Simply-supported arch with a tie. (e) Truss.

(Figure 1.26a) divided by the height of the truss. The absolute value of the force in any vertical member of the truss is almost the same as the absolute value of the shear at the corresponding section of the simple beam.

5. The deflection at C in the truss is also small, 0.043 m (1.7 in.), compared to the structures in Figures 1.25a and b. This is so because of the absence of bending moment, which is generally the largest contributor to deflections in structures.

Table 1.1 Bending Moments, Horizontal Displacements at A and Vertical Deflections at C in the Structures in Figure 1.24.

System	*Figure*	*Bending moment at C kN-m (lb-ft)*	*Horizontal displacement at A m (in.)*	*Vertical deflection at C m (in.)*
Concrete simple beam	1.24a	1440 (1050×10^3)	0	0.037 (1.5)
Concrete simply-supported arch	1.24b	1440 (1050×10^3)	0.851 (33.5)	1.02 (40.2)
Concrete two-hinged arch	1.24c	2.5 (1.5×10^3)	0	0.002 (0.08)
Concrete simply-supported arch with a tie	1.24d	38 (28×10^3)	0.021 (0.83)	0.027 (1.1)
Steel truss	1.24e	–	0.010 (0.41)	0.043 (1.7)

6. In Figure 1.25, a uniformly distributed load $q = 20$ kN-m (1385 lb-ft) is idealized as a system of concentrated loads. To show that this idealization is satisfactory, we compare the deflection and the bending moment at C and the shearing force at a section just to the right of A in the simple beam (Figure 1.25a) when subjected to the actual distributed load or to the idealized concentrated loads:

For the uniform load:

$D_C = 0.037$ m (1.5 in.); $M_C = 1440$ kN-m (1050×10^3 lb-ft);

$V_{Ar} = 240$ kN (54×10^3 lb)

For the concentrated load:

$D_C = 0.037$ m (1.5 in.); $M_C = 1440$ kN-m (1050×10^3 lb-ft);

$V_{Ar} = 200$ kN(45×10^3 lb)

We can see that the differences in results between the actual and the idealized loads are small and would vanish as the spacing between the concentrated forces is reduced to zero. In the values given above, there is no difference in M_c, and the difference in D_c does not appear with two significant figures.

Example 1.2: Three-hinged, two-hinged, and totally fixed arches

Figure 1.24c and Example 1.1 contain data for a two-hinged arch. The reaction components for this arch are given in Figure 1.26c. Figure 1.27a shows the corresponding results for the same arch but with an intermediate hinge inserted at C; similarly, Figure 1.27c represents the case for the same arch but with the hinged ends becoming encastré (totally fixed, i.e. translation and rotations are prevented). The values given in Figure 1.27 are in terms of load intensity q, span length l and the height of the arch at mid-span, $h_C = l/6$.

The three-hinged arch in Figure 1.27a is statically determinate; this is discussed in Chapter 2, Example 2.11. Here, we discuss the results of the analysis shown in the figure. The bending moment at any section is equal to the sum of the moments of the forces situated to the left-hand side of the section about that section. Thus, the bending moments at A, D, E and C are:

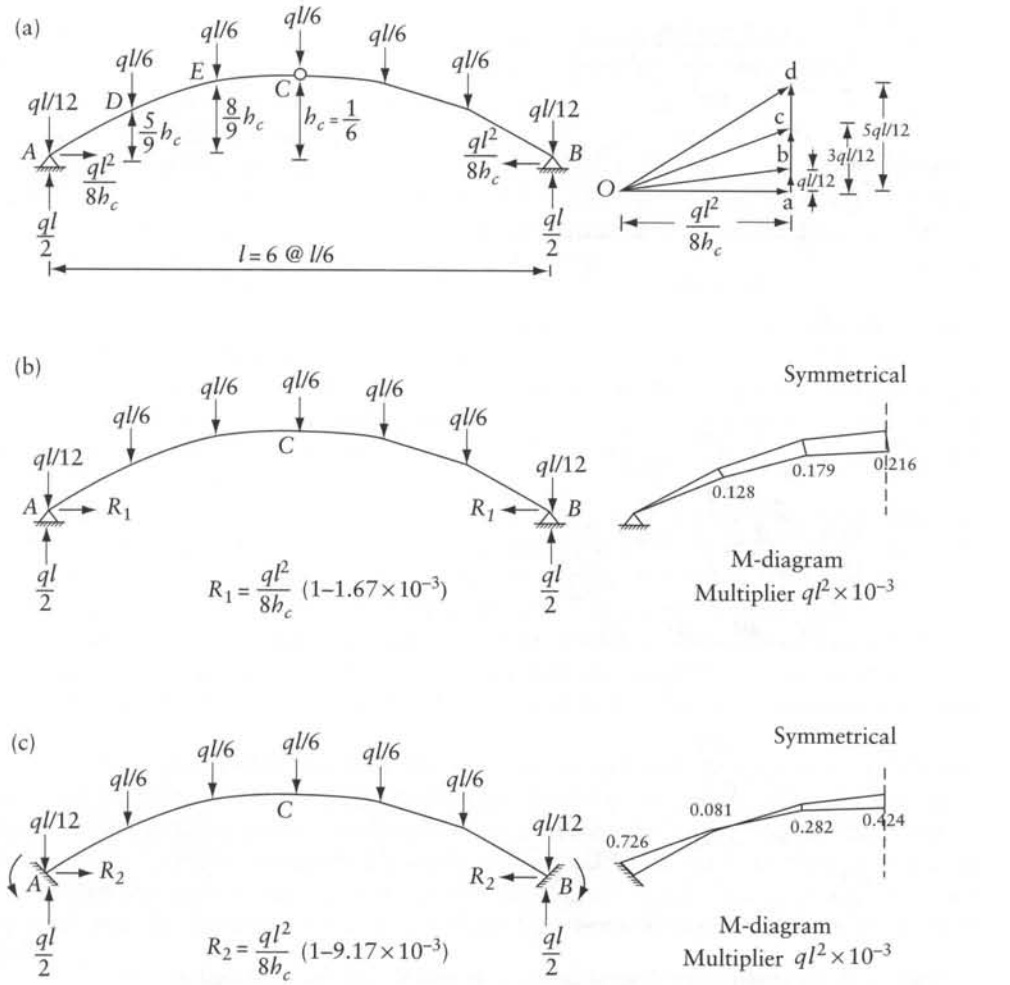

Figure 1.27 Arches with and without an intermediate hinge. Total load = ql (a) The arch in Figure 1.25c with an intermediate hinge introduced at C. (b) Two-hinged arch. (c) Arch with ends encastré.

$$M_A = 0$$

$$M_D = \left(\frac{ql}{2} - \frac{ql}{12}\right)\frac{l}{6} - \frac{ql^2}{8h_C}\left(\frac{5}{9}h_C\right) = 0$$

$$M_E = \left(\frac{ql}{2} - \frac{ql}{12}\right)\frac{l}{3} - \frac{ql}{6}\left(\frac{l}{6}\right) - \frac{ql^2}{8h_C}\left(\frac{8}{9}h_C\right) = 0$$

$$M_C = \left(\frac{ql}{2} - \frac{ql}{12}\right)\frac{l}{2} - \frac{ql}{6}\left(\frac{l}{3}\right) - \frac{ql}{6}\left(\frac{l}{6}\right) - \frac{ql^2}{8h_C}h_C = 0$$

All the calculated M-values are zero and the only internal force in the arch members is an axial force. This can be verified by the graphical construction shown on the right-hand

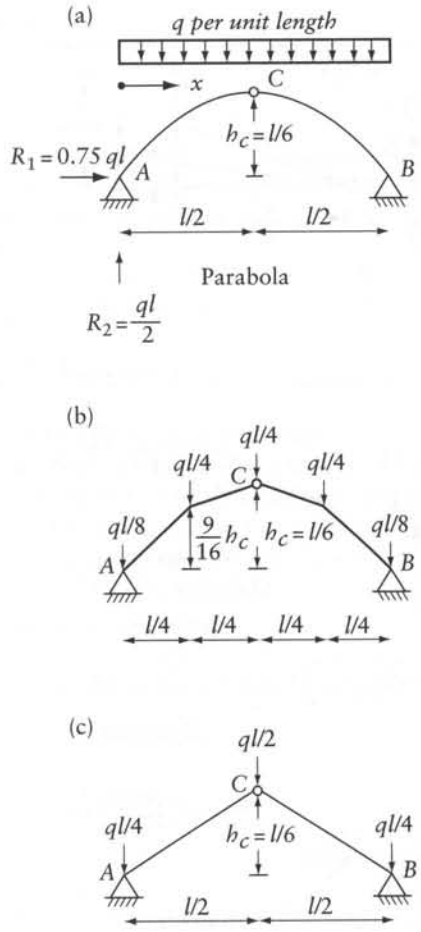

Figure 1.28 Alternative three-hinged arches with zero M, due to a total load ql.

side of Figure 1.27a. This is a force polygon in which $\overline{Oa}[= ql^2/(8h_C)]$ represents the horizontal reaction. $\overline{ad}$ is the resultant of the vertical forces to the left of D; $\overline{ac}$ those to the left of E, and $\overline{ab}$ those to the left of C. The vectors Od, Oc and Ob represent the resultant forces in segments AD, DE and EC respectively. It can be verified that the slopes of the three force resultants are equal to the slopes of the corresponding arch segments. Thus, we conclude that this arch is subjected only to axial compression, with the shear force V, and the bending moment M equal to zero at all sections.

In fact, in setting this example the geometry of the arch axis is chosen such that V and M are zero. This can be achieved by having the nodes of the arch situated on a second-degree parabola, whose equation is:

$$h(x) = \frac{4x(l-x)}{l^2} h_C \tag{1.27}$$

where $h(x)$ is the height at any section; x is the horizontal distance between A and any node; h_C is the height of the parabola at mid-span. We can verify that each of the three-hinged arches in Figure 1.28, carrying a total load $= ql$, has a geometry that satisfies Eq. 1.27 and has V and M equal to zero at all sections. For all the arches, the horizontal components of the reactions are inward and equal to $ql^2/(8h_c)$.

Elimination of the intermediate hinge at C (Figure 1.25c) results in a small change in the horizontal components of the reactions at the ends, and V and M become nonzero. However, the values of V and M in a two-hinged arch are small compared to the values in a simply-supported beam carrying the same load (compare the ordinates of M-diagrams in Figure 1.27b with $ql^2/8$).

Similarly, elimination of the hinge at C, combined with making the ends at A and B encastré, changes slightly the horizontal reaction component and produces moment components of the support reactions (Figure 1.27c). Again, we can see that the ordinates of the M-diagram in Figure 1.27c are small compared to the ordinates for the simply-supported beam (Figure 1.26a). The values given in Figures 1.27b and c are calculated using the same values of E, I, h_C, q and cross-sectional area as in Example 1.1.

From the above discussion, we can see that arches in which the horizontal reactions at the supports are prevented (or restrained) can transfer loads to the supports, developing small or zero bending moments. For this reason, arches are used to cover large spans, requiring smaller cross sections than beams. The geometry of the axis of a three-hinged arch can be selected such that V and M are zero. With the same geometry of the axis, the intermediate hinge can be eliminated (to simplify the construction), resulting in small bending and shear (much smaller than in a beam of the same span and load).

The arches considered in this example are subjected to a uniform gravity load. We have seen that the geometry of the arch axis can be selected such that the values of the shearing force and bending moment are small or zero due to the uniform load, which can be the major load on the structure. However, other load cases, such as wind pressure on one half of the arch combined with suction on the other half, and non-uniform gravity loads produce bending moments and shear forces that may have to be considered in design.

1.13 Strut-and-tie models in reinforced concrete design

Steel bars in concrete resist tensile stresses after cracking while compressive stresses continue to be resisted by concrete. Strut-and-tie models are plane (or occasionally space) trusses whose members resist resultants of compressive and tensile stresses. Figure 1.29a is a strut-and-tie model (a plane truss) idealizing a cracked simple beam, carrying uniformly distributed load, and having rectangular cross section reinforced with longitudinal bars and stirrups (Figure 1.29b). At a typical section n, the stress resultants in the beam are a shearing force V and a bending moment M (Figure 1.29c). The strain and the stress distributions normal to the section are shown in Figure 1.29d. The top horizontal member IJ of the truss carries a compressive force whose absolute value $= M/y_{CT}$, where y_{CT} is the distance between the resultants of compressive and tensile stresses; M is the bending moment at C or I. The vertical member IC carries a tensile force equal to the shearing force V. The layout of a strut-and-tie model applies only for a specified load. A member in which the force is known to be zero is often not drawn (e.g. no member is shown connecting nodes G and H in Figure 1.29a); the struts and the ties are shown as dashed and continuous lines respectively.

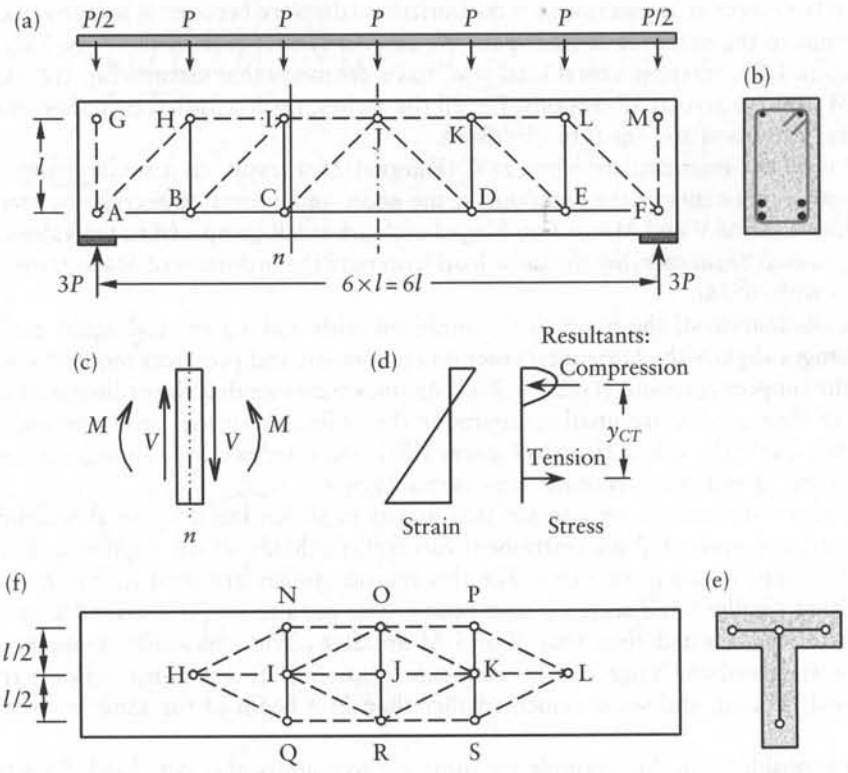

Figure 1.29 Strut-and-tie models for the idealization of a cracked simply-supported beam. (a) Plane truss idealization of the beam with rectangular cross section. Also elevation of a space truss idealization of the beam with T-cross section. (b) Rectangular cross section of beam. (c) Internal forces at section *n*. (d) Strain and stress distribution at *n*. (e) Cross section of spatial truss idealization of a T-beam. (f) Top view of spatial truss.

If the simple beam considered above has a T-section (Figure 1.29e) and is subjected to the same loading, it can be idealized as a space truss, the elevation and top views of which are shown in Figures 1.29e and f respectively. Again, this space truss can become unstable with different loading; e.g. a vertical load at any of nodes *N*, *O*, *P*, *Q*, *R*, or S would cause partial collapse.

1.13.1 B- and D-regions

The design of a reinforced concrete member whose length is large compared to its cross-sectional dimensions is commonly based on Bernoulli's assumption: a plane section before deformation remains plane. The assumption permits the linear strain distribution shown in Figures 1.23c and 1.29d; also, for materials obeying Hooke's law (Eq. 1.11), it permits the linear stress distribution (Eq. 1.12) and the derivation of the remaining equations of Section 1.11. The validity of the assumption for members of any material is proven experimentally at all load levels for their major parts, referred to as B-regions, where B stands for "Bernoulli". The assumption is not valid at D-regions, where D stands for "disturbance" or "discontinuity" regions, e.g. at concentrated loads or reactions, at sudden changes of cross sections, and at openings. The major use of the strut-and-tie models is in the design and the detailing of the reinforcement in the D-regions. The design of the B-regions is mainly done by code equations (some of which are based on truss

idealization), without the need to analyze strut-and-tie models. Figure 1.30 shows examples of strut-and-tie models for D-regions representing: (a) and (b) a wall subjected, respectively, to a uniform load and to a concentrated load; (c) a member end with anchorage of a prestressing tendon; (d) a connection of a column and a beam; (e) a tall wall supporting an eccentric load; (f) a beam with a sudden change in depth adjacent to a support; (g) a corbel; and (h) a pile cap (spatial model).

In each application, the strut-and-tie model is an isolated part of a structure subjected, at its boundaries, to a self-equilibrated set of forces of known magnitudes and distributions. The models in Figure 1.30 are statically determinate; the forces in the members can be determined without the need of knowing the *Ea* values (the axial rigidities) of the members. The analysis gives the forces in the ties and hence determines the cross-sectional area of the steel bars for a

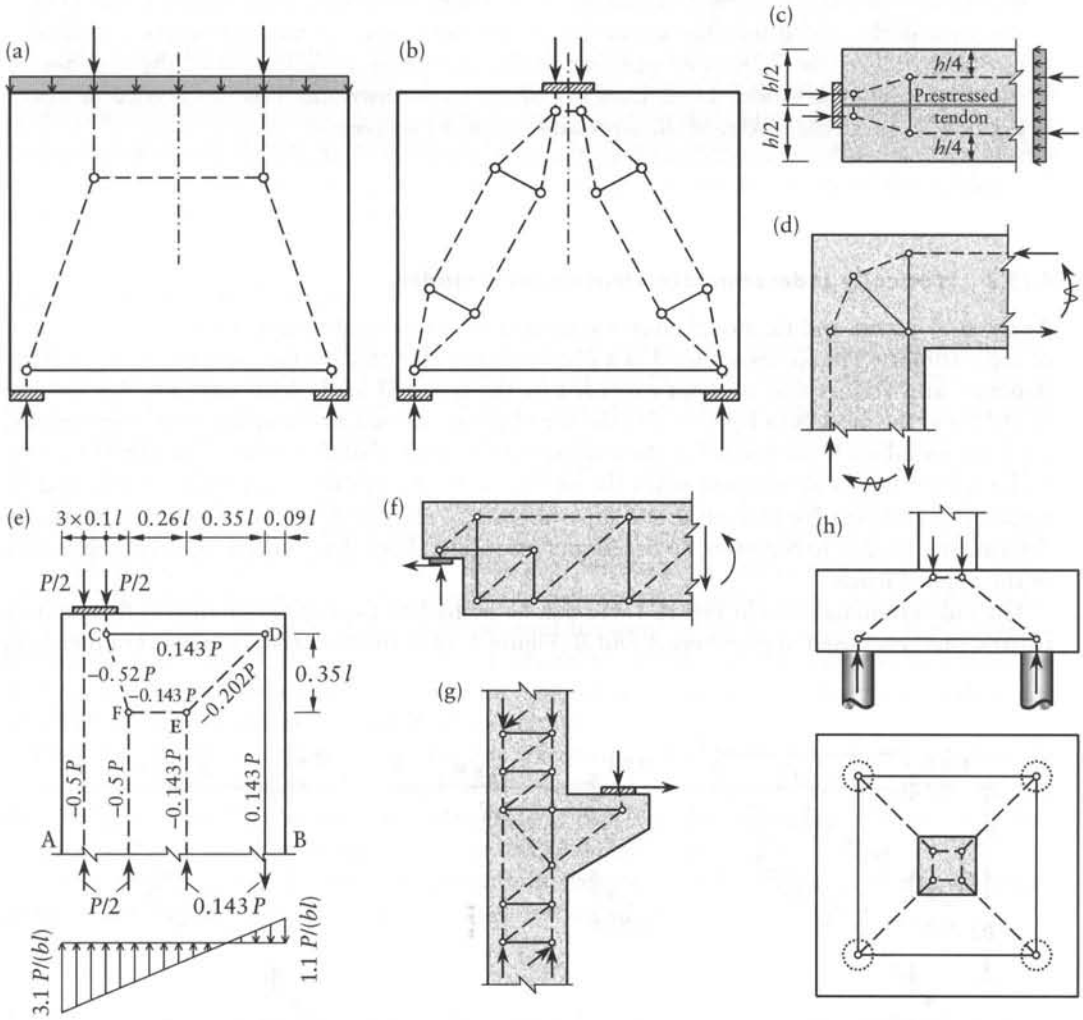

Figure 1.30 Strut-and-tie model applications for: (a) and (b) wall carrying uniform or concentrated load; (c) anchorage of a prestressing tendon; (d) connection of a column with a beam; (e) tall wall supporting a column; (f) sudden change in depth of a beam adjacent to its support; (g) corbel; (h) spatial strut-and-tie model for a pile cap.

specified stress. The struts and ties meet at nodes, whose sizes must satisfy empirical rules to ensure that the forces of the struts and the ties do not produce crushing of concrete or failure of the anchorage of the ties.

Example 1.3: Strut-and-tie model for a wall supporting an eccentric load

The wall in Figure 1.30e, of thickness b, is subjected to the eccentric load P at its top. Find the forces in the members of the strut-and-tie model shown.

The strain and stress distributions at section AB can be assumed linear, because the section is far from the D-region. Equation 1.25 gives the stress distribution shown in Figure 1.30e, which is statically equivalent to the four vertical forces shown at AB. It can be verified that the forces shown on the figure maintain equilibrium of each node.

It is noted that the truss is stable only with the set of forces considered. The trapezoidal part $CDEF$ is a mechanism that can be made stable by adding a member EC (or DF); the force in the added member would be nil and the pattern of member forces would be unchanged. The distribution of stress at section AB helps in the layout of the members of the strut-and-tie model. Determination of the stress distribution is not needed in this example because the layout of the strut-and-tie model is given.

1.13.2 Statically indeterminate strut-and-tie models

Analysis of a strut-and-tie model gives a system of forces in equilibrium, without consideration of compatibility. The forces are used in a plastic design that predicts the ultimate strength of the structure and verifies that it is not exceeded by the factored load. With statically determinate models (e.g. the models in Figure 1.30) the members are drawn as centerlines; the axial rigidity, Ea of the members is not needed in the analyses of the forces that they resist. The value of Ea for each member has to be assumed when the analysis is for a statically indeterminate strut-and-tie model. It is also possible to analyze and superimpose the member forces of two or more statically determinate models to represent an indeterminate model. Each determinate model carries a part of the applied loads.

The indeterminate truss in Figure 1.31a can be treated as a combination of two determinate trusses, one composed of members A and B (Figure 1.31b) and the other composed of members

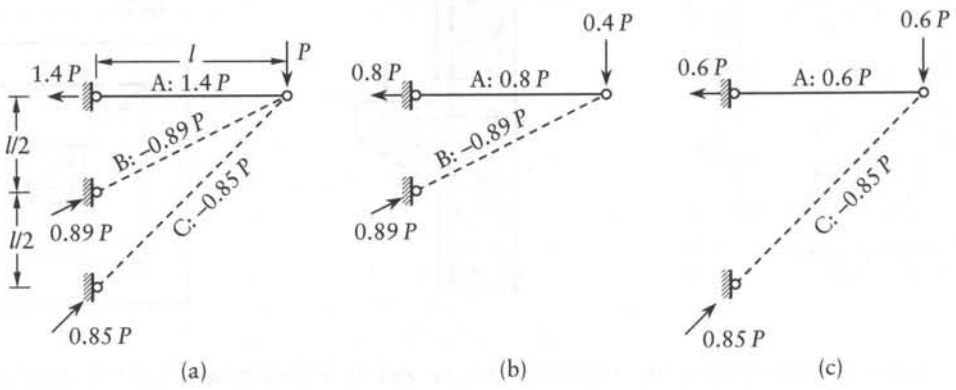

Figure 1.31 Statically indeterminate strut-and-tie model, (a) treated as a combination of two determinate trusses (b) and (c).

A and C (Figure 1.31c). If we assume that the first and the second trusses carry $0.4P$ and $0.6P$ respectively, the forces in the members in the first truss will be $N_A = 0.8P$; $N_B = -0.89P$; in the second truss, $N_A = 0.6P$; $N_C = -0.85P$. Superposition of forces gives: $N_A = 1.4P$; $N_B = -0.89P$; $N_C = -0.85P$ (Figure 1.31a). The solution in Figure 1.31a satisfies equilibrium but does not satisfy the compatibility required in elastic analysis of structures; the loaded node in the trusses in Figures 1.31b and c exhibits non-compatible translations.

The statically indeterminate spatial strut-and-tie model shown in elevation and top view in Figures 1.29e and f respectively can be analyzed by summing up the statically determinate forces in the spatial model in absence of members HI, IJ, JK and KL to the forces in a plane model composed only of the members shown in Figure 1.29a; the applied load has to be partitioned on the two models (see Prob. 1.16).

Plastic analysis of strength of elastic-perfectly plastic materials is permissible without considering compatibility. However, because plastic deformation of concrete is limited, strut-and-tie models that excessively deviate from elastic stress distribution may give overestimation of the strength.

Elastic finite-element analysis (Chapter 16) of a D-region can indicate the directions of principal compressive and principal tensile stresses. These should be the approximate directions of the struts and the ties respectively, in the strut-and-tie models. However, an elastic analysis may be needed only in exceptional cases. The layout of the struts and ties for D-regions of frequent occurrence (e.g. the models in Figure 1.30) and guides on the choice of the models and reinforcement details are available.[2]

1.14 Structural design

Structural analysis gives the deformations, the internal forces, and the reactions that are needed in structural design. The loads that we consider are the probable load specified by codes or assumed by the designer. The members, their connections, and their supports are then designed following code requirements specifying minimum strength or maximum allowable deformations; these components must have a resistance (strength) that exceeds the load effect. Because of the variability of material strength or the differences between the actual dimensions from those specified by the designer, *strength-reduction factors* (also called "resistance factors") less than 1.0 apply to the computed strength. The loads that the structure must carry are also variables. Thus, *load factors* greater than 1.0 are applied to the expected loads. Codes specify values of the strength reduction and the load factors to account for some of the uncertainties; the difference between a factor and 1.0 depends upon the probable variance of the actual values from the design values. The calculations that we use for member resistance and for structural analysis are based on simplifying assumptions that are uncertain.

Thus, because of the uncertainties, it is not possible to achieve zero probability of failure. In design codes, the resistance and the load factors are based on statistical models that assume that the chance of a combination of understrength and overload that produces collapse, or failure that the structure performs as required, is at the predicted target level.

The structural safety, the ability to perform as required, can be measured by the reliability analysis and the reliability index, as discussed in Chapter 24.

2 Schlaich, J., Schäefer, K. and Jennewein, M., "Toward a Consistent Design of Structural Concrete," *J. Prestressed Concrete Inst.*, 32(3) (May–June 1987), pp. 74–150.
Schlaich. J. and Schäefer, K., "Design and Detailing of Structural Concrete Using Strut-and-Tie Models," *Struct. Engineer*, 69(6) (March 1991), 13pp.
MacGregor, J. G. and Wight, J. K., *Reinforced Concrete: Mechanics and Design*, 4th ed., Prentice Hall, Upper Saddle River, New Jersey, 2005, 1132pp.

1.15 General

In presenting some of the concepts, it has been necessary to discuss above, without much detail, some of the subjects covered in the following chapters. These include static indeterminacy of structures and calculation of the reactions and internal forces in statically determinate structures. Chapter 2 deals with the analysis of statically determinate structures. After studying Chapter 2, it may be beneficial to review parts of Chapter 1 and attempt some of its problems, if not done so earlier.

Problems

1.1 Sketch the deflected shape and the bending moment diagram for the structures shown. In the answers at the back of the book, the axial and shear deformations are ignored and the second moment of area, I is considered constant for each structure; the rotations and member end moments are considered positive when clockwise; u and v are translations horizontal to the right and downward respectively.

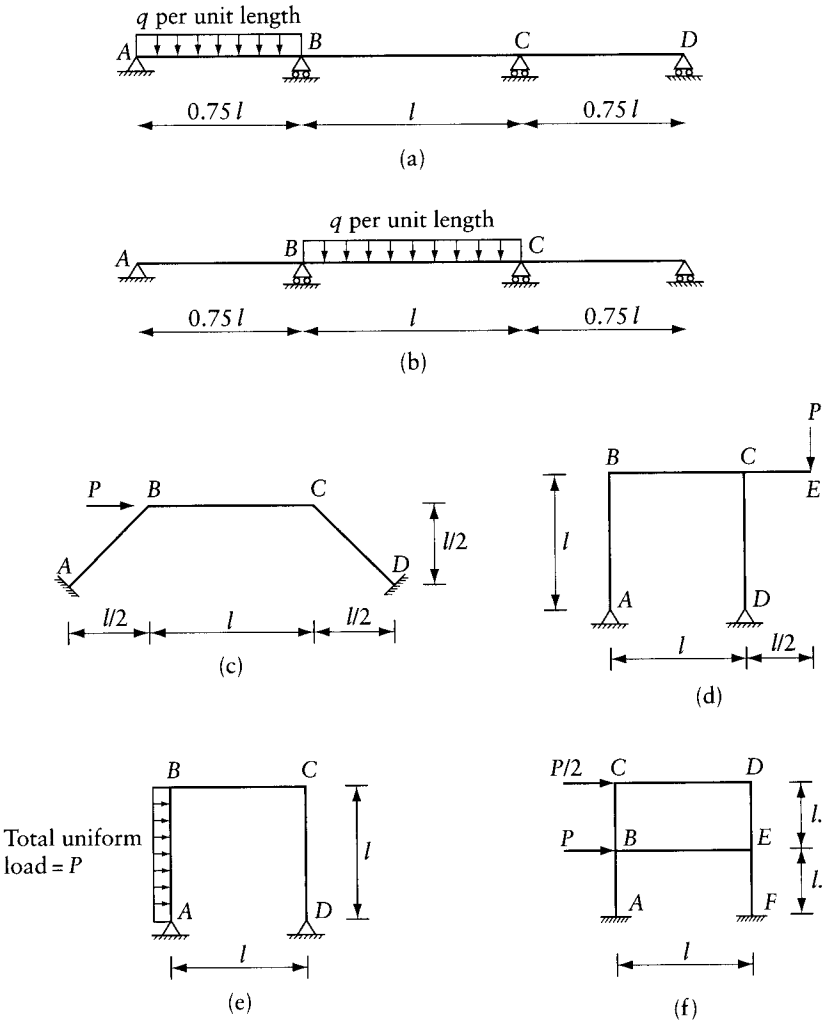

Prob. 1.1

1.2 Apply the requirements of Prob. 1.1 to the frame in Figure 1.13c subjected to a downward settlement δ of support D, with no load applied.

1.3 A rectangular section of width b and height h is subjected to a normal tensile force, N, at the middle of the top side. Find the stress distribution by the use of Eq. 1.13, with the reference point at the top fiber. Verify the answer by changing the reference point to the centroid.

1.4 Find the forces in the members of the water tower shown in Figure 1.10b due to a wind load H.

1.5 For the beam in Figure 1.20a verify that the deflection at mid-span is $y = \psi_{free} l^2/8$ and the rotations at A and B are equal to $(dy/dx)_A = \psi_{free} l/2 = -(dy/dx)_B$; where ψ_{free} is given by Eq. 1.7.

1.6 For the continuous beam in Figure 4.2, what is the interior support reaction due to temperature gradient as shown. Express the answer in terms of the curvature ψ_{free} given by Eq. 1.7. Assume that the total length of the beam is $2l$, the intermediate support is at the middle, and EI = constant.
Hint: The reaction is the force R that will eliminate the deflection at the intermediate support; Appendix B gives the deflection due to R.

1.7 Select the dimensions h_1 and h_2 such that the three-hinged arch shown has no bending moment or shear force at all sections.

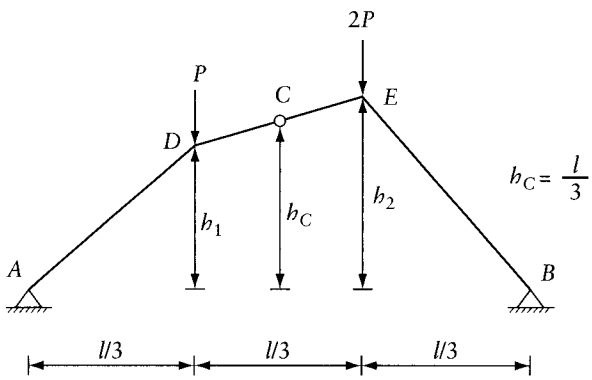

Prob. 1.7

1.8 Consider the parabolic three-hinged arch in Figure 1.27a subjected to a concentrated downward load P at $x = l/4$. Calculate the bending moment at this section and the shearing force just to the right and just to the left of the same section. Also, determine the bending moment value at $x = 3l/4$ and sketch the bending moment diagram.

1.9 The figure shows a cable carrying equally spaced downward loads, P. Verify that the cable takes the shape of a funicular polygon with $h_D/h_C = 0.75$. What are the horizontal and vertical components of the tensile force in each straight part of the cable?

1.10 Show that when the number of equal forces applied on the cable in Prob. 1.9 is n, spaced equally at $l/(n+1)$, the cable will have the shape of a funicular polygon joining points on a parabola (Eq. 1.1). Show that, in any straight part of the cable, the horizontal component of the tension in the cable will be equal to $Pl(n+1)/(8h_C)$; where h_C is the depth of the parabola at the center.

1.11 *Control of drift of a portal frame:* Use the computer program PLANEF (Appendix L) to compare the horizontal displacement at B and the moments at the ends of member AB in the portal frame in (a), without bracing and with bracing as shown in (b) and (c).

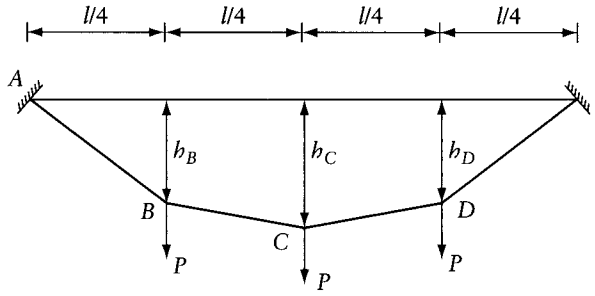

Prob. 1.9

All members have hollow square sections; the section properties for members *AB*, *BC* and *CD* are indicated in (d); the properties of the bracing members are indicated in (e). Enter $l = 1$, $P = 1$ and $E = 1$; give the displacement in terms of $Pl^3/(EI)_{AB}$ and the bending moment in terms of Pl. Alternatively, use SI or Imperial units as indicated in Probs. 1.12 or 1.13 respectively.

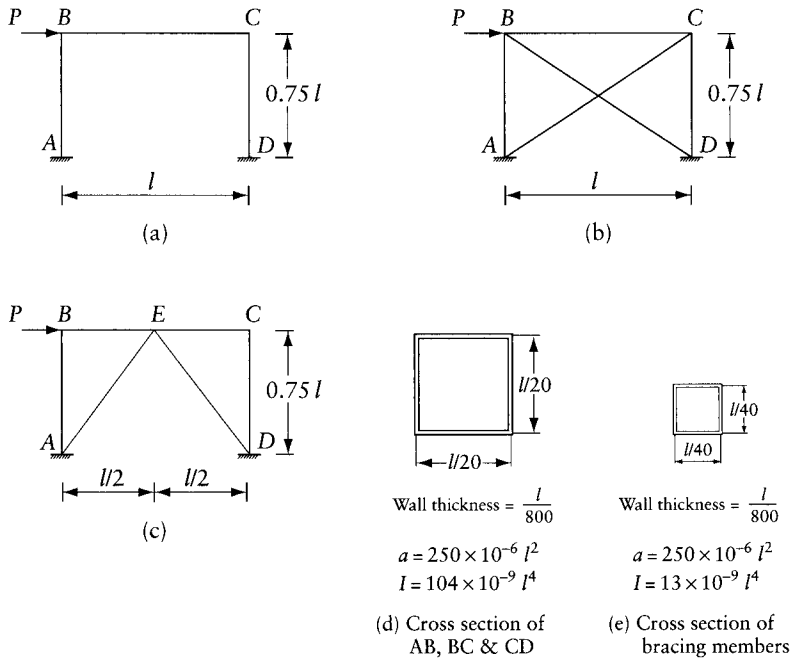

Prob. 1.11 to 14

1.12 SI units. Solve Prob. 1.11 with $l = 8\,\text{m}$, $P = 36 \times 10^3\,\text{N}$ and $E = 200\,\text{GPa}$.

1.13 Imperial units. Solve Prob. 1.11 with $l = 320$ in., $P = 8000\,\text{lb}$ and $E = 30 \times 10^6\,\text{lb/in.}^2$.

1.14 Use the computer program PLANET to find the horizontal displacement at B and the axial forces in the members treating the structure of Prob. 1.11 part (b) as a plane truss. Compare with the following results obtained by treating the structure as a plane frame: Horizontal deflection at $B = 0.968 \times 10^{-3} Pl^3/(\text{EI})_{AB}$; $\{N_{AB}, N_{BC}, N_{CD}, N_{AC}, N_{BD}\} = P\{0.411, -0.447, -0.334, 0.542, -0.671\}$.

1.15 Find the forces in the spatial strut-and-tie model shown in elevation in Figure 1.29a and in top view in Figure 1.29f. Omit or assume to be zero forces in the members *HI*, *IJ*, *JK*, and *KL*.

1.16 Find the forces in the statically indeterminate spatial strut-and-tie model shown in elevation in Figure 1.29a and in top view in Figure 1.29f. Solve the problem by the superposition of the forces in the statically determinate space truss of Prob. 1.15 carrying 50 percent of the load and a statically determinate plane truss shown in Figure 1.29a carrying the remainder of the load.

Chapter 2

Statically determinate structures

2.1 Introduction

A large part of this book is devoted to the modern methods of analysis of framed structures, that is, structures consisting of members which are long in comparison to their cross section. Typical framed structures are beams, grids, plane and space frames or trusses (see Figure 2.1). Other structures, such as walls and slabs, are considered in Chapters 15, 16, 17 and 19.

In all cases, we deal with structures in which displacements – translation or rotation of any section – vary linearly with the applied forces. In other words, any increment in displacement is proportional to the force causing it. All deformations are assumed to be *small*, so that the resulting displacements do not significantly affect the geometry of the structure and hence do not alter the forces in the members. Under such conditions, stresses, strains, and displacements due to different actions can be added using the principle of superposition; this topic is dealt with in Section 3.6. The majority of actual structures are designed so as to undergo only small deformations and they deform linearly. This is the case with metal structures; the material obeys Hooke's law; concrete structures are also usually assumed to deform linearly. We are referring, of course, to behavior under working loads, that is, to elastic analysis; plastic analysis is considered in Chapters 18 and 19.

It is, however, possible for a straight structural member made of a material obeying Hooke's law to deform nonlinearly when the member is subjected to a lateral load and to a large axial force. This topic is dealt with in Chapters 13 and 24. Chapter 24 also discusses nonlinear analysis when the material does not obey Hooke's law.

Although statical indeterminacy will be dealt with extensively in the succeeding chapters, it is important at this stage to recognize the fundamental difference between statically determinate and indeterminate (hyperstatic) structures, in that the forces in the latter cannot be found from the equations of static equilibrium alone: a knowledge of some geometric conditions under load is also required.

The analysis of statically indeterminate structures generally requires the solution of linear simultaneous equations. The number of equations depends on the method of analysis. Some methods avoid simultaneous equations by using iterative or successive correction techniques in order to reduce the amount of computation, and are suitable when the calculations are made by hand or by a hand-held or small desk calculator.

For large and complicated structures hand computation is often impracticable, and a computer has to be used. Its advent has shifted the emphasis from easy problem solution to efficient problem formulation: using matrices and matrix algebra, a large quantity of information can be organized and manipulated in a compact form. For this reason, in many cases, equations in this book are written in matrix form. Review of chosen matrix operations is presented in Appendix A. In the text, the basic computer methods are discussed but details of programming are not given.

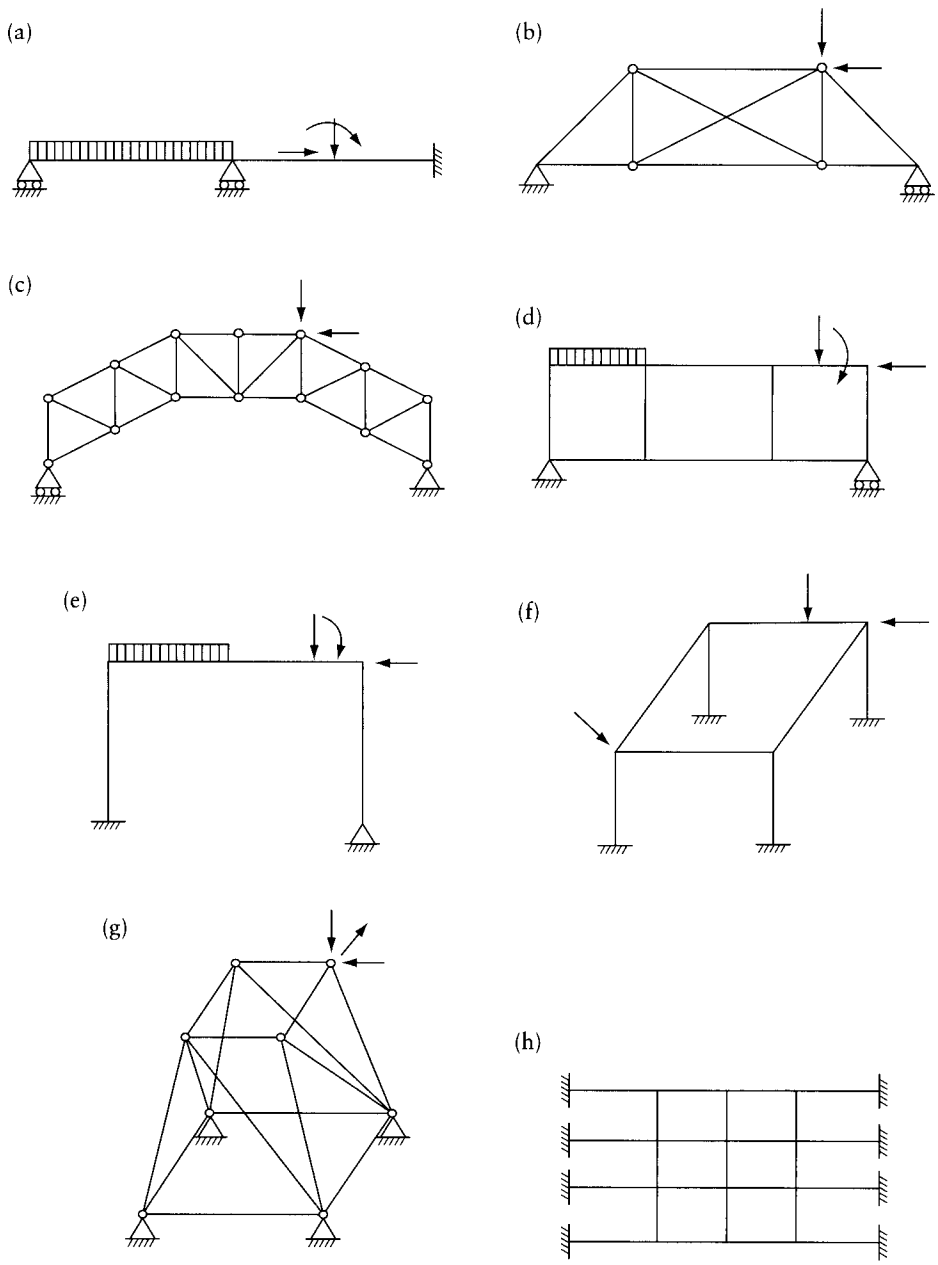

Figure 2.1 Examples of framed structures. (a) Continuous beam. (b) and (c) Plane trusses. (d) and (e) Plane frames. (f) Space frame. (g) Space truss. (h) Horizontal grid subjected to vertical loads.

We should emphasize that the hand methods of solution must not be neglected. They are of value not only when a computer is not available but also for preliminary calculations and for checking of computer results.

The remaining sections of this chapter are concerned with the analysis of statically determinate structures.

2.2 Equilibrium of a body

Figure 2.2a represents a body subjected to forces F_1, F_2, ..., F_n in space. The word *force* in this context means either an action of a concentrated load or a couple (a moment); in the latter case the moment is represented by a double-headed arrow.[1] A typical force F_i acting at point (x_i, y_i, z_i) is shown in Figure 2.2b using a right-handed system[2] of orthogonal axes x, y, and z. Components of F_i in the direction of the force axes are

$$F_{ix} = F_i\lambda_{ix} \quad F_{iy} = F_i\lambda_{iy} \quad F_{iz} = F_i\lambda_{iz} \tag{2.1}$$

where F_i is force magnitude; λ_{ix}, λ_{iy}, and λ_{iz} are called *direction cosines* of the force F_i; they are equal to the cosine of the angles α, β and γ between the force and the positive x, y and z directions respectively. Note that the components F_{ix}, F_{iy} and F_{iz} do not depend upon the position of the point of application of F_i. If the length of $\overline{iD}$ equal to the magnitude of F_i, projections of $\overline{iD}$ on the x, y and z directions represent the magnitudes of the components F_{ix}, F_{iy}, and F_{iz}.

The moment of a concentrated load F_i about axes x, y, and z (Figure 2.2b) is equal to the sum of moments of the components F_{ix}, F_{iy} and F_{iz}; thus

$$M_{ix} = F_{iz}y_i - F_{iy}z_i \quad M_{iy} = F_{ix}z_i - F_{iz}x_i \quad M_{iz} = F_{iy}x_i - F_{ix}y_i \tag{2.2}$$

Note that a component in the direction of one of the axes, say x, produces no moment about that axis (x axis). The positive sign convention for moments used in Eq. 2.2 is shown in Figure 2.2b. Naturally, Eq. 2.2 applies only when F_i represents a concentrated load, not a

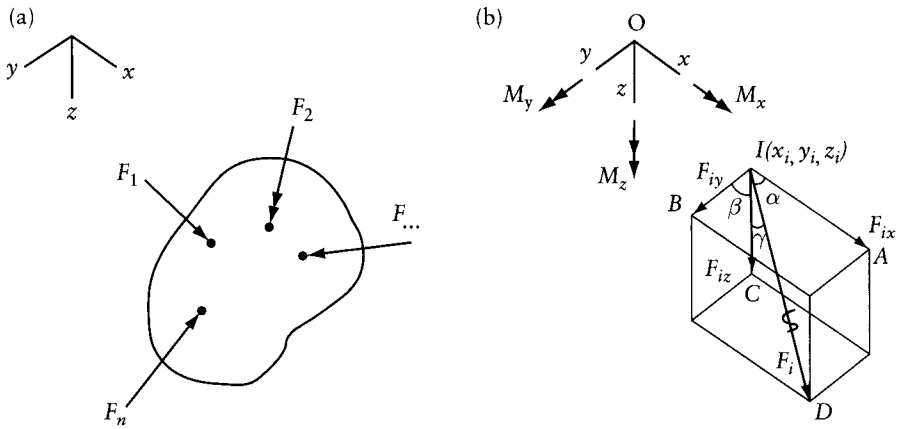

Figure 2.2 Force system and force components. (a) Body subjected to forces in space. (b) Components of a typical force and positive sign convention for M_x, M_y and M_z.

1 All through this text, a couple (or rotation) is indicated in planar structures by an arrow in the form of an arc of a circle (see, for example, Figures 3.1 and 3.3). In three-dimensional structures, a couple (or rotation) is indicated by a double-headed arrow. The direction of the couple is that of the rotation of a right-hand screw progressing in the direction of the arrow. This convention should be well understood at this stage.

2 In a right-handed system, directions of orthogonal axes x and y can be chosen arbitrarily, but the direction of the z axis will be that of the advance of a right-handed screw turned through the angle from x axis to y axis. A right-handed system of axes is used throughout this text, for example, see Figures 2.2a and 2.3a.

moment. When F_i represents a moment (e.g. F_2 in Figure 2.2a), Eq. 2.1 can be used to determine three moment components to be represented by double-headed arrows in the x, y, and z directions (not shown in figure).

The resultant of a system of forces in space has six components, determined by summing the components of individual forces, e.g.

$$F_{x\,\text{resultant}} = \sum_{i=1}^{n} F_{ix} \qquad M_{x\ \text{resultant}} = \sum_{i=1}^{n} M_{ix} \tag{2.3}$$

For a body in equilibrium, components of the resultant in the x, y, and z directions must vanish, so that the following equations apply:

$$\left.\begin{array}{lll} \Sigma F_x = 0 & \Sigma F_y = 0 & \Sigma F_z = 0 \\ \Sigma M_x = 0 & \Sigma M_y = 0 & \Sigma M_z = 0 \end{array}\right\} \tag{2.4}$$

The summation in these equations is for all the components of the forces and of the moments about each of the three axes. Thus, for a body subjected to forces in three dimensions, six equations of static equilibrium can be written. When all the forces acting on the free body are in one plane, only three of the six equations of statics are meaningful. For instance, when the forces act in the x-y plane, these equations are

$$\Sigma F_x = 0 \quad \Sigma F_y = 0 \quad \Sigma M_z = 0 \tag{2.5}$$

When a structure in equilibrium is composed of several members, the equations of statics must be satisfied when applied on the structure as a whole. Each member, joint or portion of the structure is also in equilibrium and the equations of statics must also be satisfied.

The equilibrium Eqs. 2.4 and 2.5 can be used to determine reaction components or internal forces, provided that the number of unknowns does not exceed the number of equations. In trusses with pin-connected members and forces applied only at the joints, the members are subjected to axial forces only; thus, for a truss joint, equations expressing equilibrium of moments included in Eqs. 2.4 and 2.5 are trivial, but they can be applied to a truss part to determine member forces (see Example 2.5).

Example 2.1: Reactions for a spatial body: a cantilever

The prismatic cantilever in Figure 2.3a is subjected, in the plane of cross section at the end, to forces $F_1 = P$, $F_2 = 2Pb$, as shown. Determine components at O of the resultant reaction at the fixed end; point O is center of the cross section.

Assume positive directions of reaction components the same as those of x, y, and z axes. Coordinates of point of application of F_1 are $(3b, 0.5b, -0.75b)$. Direction cosines of F_1 are

$$\{\lambda_{1x}, \lambda_{1y}, \lambda_{1z}\} = \{0, 0.5, 0.866\}$$

Application of Eqs. 2.1 and 2.2 gives

$$\{F_{1x}, F_{1y}, F_{1z}\} = P\{0, 0.5, 0.866\}$$

$$\left\{\begin{array}{l} M_{1x} \\ M_{1y} \\ M_{1z} \end{array}\right\} = Pb \left\{\begin{array}{l} 0.866 \times 0.5 - 0.5 \times (-0.75) \\ -0.866 \times 3 \\ 0.5 \times 3 \end{array}\right\} = Pb \left\{\begin{array}{r} 0.808 \\ -2.598 \\ 1.500 \end{array}\right\}$$

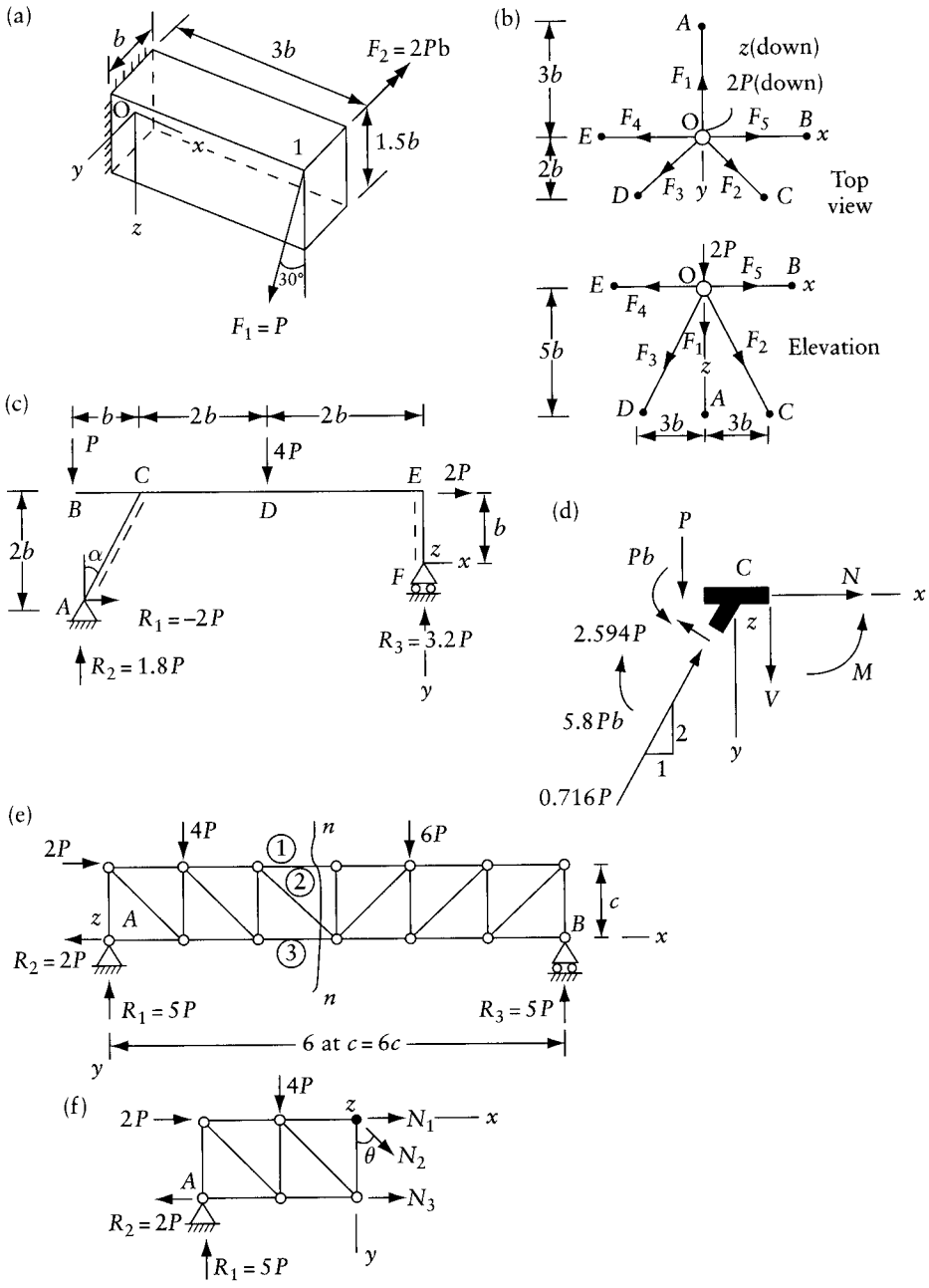

Figure 2.3 Examples 2.1 to 2.5 of uses of equilibrium equations. (a) Space cantilever. (b) Joint of space truss. (c) Plane frame. (d) Joint of a plane frame. (e) Plane truss. (f) Part of plane truss.

The applied moment F_2 has only one component: $M_{2y} = -2Pb$. The equilibrium Eqs. 2.4 give components of the reaction at O:

$$\{F_{ox}, F_{oy}, F_{oz}\} = P\{0, -0.5, -0.866\}$$

$$\{M_{ox}, M_{oy}, M_{oz}\} = Pb\{-0.808, 4.598, -1.5\}$$

Note that the reactions would not change if the double-headed arrow, representing the moment F_2 in Figure 2.3a, is moved to another position without change in direction.

Example 2.2: Equilibrium of a node of a space truss

Figure 2.3b represents the top view and elevation of joint O connecting five members in a space truss. The joint is subjected to a downward force $2P$ as shown. Assuming that the forces in members 4 and 5 are $F_4 = 2P$, $F_5 = -P$, what are the forces in the other members?

An axial force in a member is considered positive when tensile. In Figure 2.3b the forces in the five members are shown in positive directions (pointing away from the joint). The arrows thus represent the effect of members on the joint. Magnitudes and direction cosines of the forces at the joint are

Force number	1	2	3	4	5	External force
Force magnitude	F_1	F_2	F_3	$2P$	$-P$	$2P$
λ_x	0	$\frac{3}{\sqrt{38}}$	$\frac{-3}{\sqrt{38}}$	-1	1	0
λ_y	$\frac{-3}{\sqrt{34}}$	$\frac{2}{\sqrt{38}}$	$\frac{2}{\sqrt{38}}$	0	0	0
λ_z	$\frac{5}{\sqrt{34}}$	$\frac{5}{\sqrt{38}}$	$\frac{5}{\sqrt{38}}$	0	0	1

Direction cosines for any force, say F_3, are equal to the length of projections on x, y, and z directions of an arrow pointing from O to D divided by the length OD. The appropriate sign must be noted; for example, λ_x for F_3 is negative because moving from O to D represents an advance in the negative x direction.

Only three equations of equilibrium can be written for joint O

$$\Sigma F_x = 0 \quad \Sigma F_y = 0 \quad \Sigma F_z = 0$$

Substitution in Eq. 2.1 of the values in the table above gives

$$\begin{bmatrix} 0 & \frac{3}{\sqrt{38}} & -\frac{3}{\sqrt{38}} \\ -\frac{3}{\sqrt{34}} & \frac{2}{\sqrt{38}} & \frac{2}{\sqrt{38}} \\ \frac{5}{\sqrt{34}} & \frac{5}{\sqrt{38}} & \frac{5}{\sqrt{38}} \end{bmatrix} \begin{Bmatrix} F_1 \\ F_2 \\ F_3 \end{Bmatrix} = P \begin{bmatrix} 3 \\ 0 \\ -2 \end{bmatrix}$$

The right-hand side of this equation is equal to minus the sum of the components of the externally applied force at O and the components of the known member forces F_4 and F_5. The solution is

$$\{F_1, F_2, F_3\} = P\{-0.9330, 2.3425, -3.8219\}$$

The member forces or the reactions obtained from any source can be verified by considering joint equilibrium, as done above. As an example, we verify below the equilibrium of node D of the space truss in Prob. 2.2. Given: forces in members DA and DB are: $\{N_{DA}, N_{DB}\} = \{-4.70, -3.14\}P$; reaction components at D are: $\{R_x, R_y, R_z\}_D = \{-1.78, 0.61, -7.39\}P$.

$$\left[\begin{Bmatrix}\lambda_x\\ \lambda_y\\ \lambda_z\end{Bmatrix}_{DA} \begin{Bmatrix}\lambda_x\\ \lambda_y\\ \lambda_z\end{Bmatrix}_{DB}\right] \begin{Bmatrix}N_{DA}\\ N_{DB}\end{Bmatrix} = -\begin{Bmatrix}R_x\\ R_y\\ R_z\end{Bmatrix}_D ; \frac{1}{2.121}\begin{bmatrix}-0.683 & -0.183\\ -0.183 & 0.683\\ -2.000 & -2.000\end{bmatrix}\begin{Bmatrix}-4.70\\ -3.14\end{Bmatrix} P$$

$$= -\begin{Bmatrix}-1.78\\ 0.61\\ -7.39\end{Bmatrix} P$$

Example 2.3: Reactions for a plane frame

Determine the reaction components for the plane frame shown in Figure 2.3c.

Select x, y and z axes as shown and apply Eqs. 2.5:

$$\Sigma F_x = 0 \quad R_1 + 2P = 0$$

$$\Sigma M_z = 0 \quad -R_1 b + R_2(5b) - P(5b) - 4P(2b) + 2P(b) = 0$$

$$\Sigma F_y = 0 \quad -R_2 - R_3 + P + 4P = 0$$

The first of the above three equations gives the value of R_1, which, when substituted in the second equation, allows R_2 to be determined. Substitution of R_2 in the third equation gives R_3. The answers are: $R_1 = -2P$; $R_2 = 1.8P$; $R_3 = 3.2P$.

It is good practice to check the answers before using them in design or in further analysis. In this problem, we can verify that $\Sigma M_z = 0$ with the z axis at a different point, e.g. point A. Note that this does not give a fourth equation which could be used to determine a fourth unknown; this is so because the fourth equation can be derived from the above three.

Example 2.4: Equilibrium of a joint of a plane frame

Figure 2.3d represents a free body diagram of a joint of a plane frame (e.g. joint C of the frame in Figure 2.3c). The arrows represent the forces exerted by the members on the joint. The forces at sections just to the left and just below the joint C are given. Use equilibrium equations to determine unknown internal forces N, V, and M representing normal force, shearing force and bending moment at the section just to the right of C. (Diagrams plotting variation of N, V, and M over the length of members of plane frames are discussed in Section 2.3, but here we determine internal forces in only one section.)

Equilibrium Eqs. 2.5 apply:

$$\Sigma F_x = 0 \quad N + 0.716P\left(\frac{1}{\sqrt{5}}\right) + 2.594P\left(\frac{-2}{\sqrt{5}}\right) = 0$$

$$\Sigma F_y = 0 \quad V + P + 2.594P\left(\frac{-1}{\sqrt{5}}\right) + 0.716P\left(\frac{-2}{\sqrt{5}}\right) = 0$$

$$\Sigma M_z = 0 \quad -M + 5.8Pb - Pb = 0$$

This gives $N = 2P$; $V = 0.8P$; $M = 4.8Pb$.

Example 2.5: Forces in members of a plane truss

Find the forces in members 1, 2 and 3 of the plane truss shown in Figure 2.3e by application of equilibrium Eqs. 2.5 to one part of the structure to the right or to the left of section $n-n$.

First, we determine the reactions by equilibrium Eqs. 2.5 applied to all external forces including the reactions: $\Sigma F_x = 0$ gives $R_2 = 2P$; $\Sigma M_z = 0$ gives $R_3 = 5P$; $\Sigma F_y = 0$ gives $R_1 = 5P$.

The part of the structure situated to the left of section $n-n$ is represented as a free body in equilibrium in Figure 2.3f. The forces N_1, N_2 and N_3 in the cut members, shown in their positive directions, are in equilibrium with the remaining forces in the figure. The unknown member forces N_1, N_2, and N_3 are determined by the equilibrium Eqs. 2.5:

$$\Sigma M_z = 0 \quad -N_3 c + 5P(2c) + 2Pc - 4Pc = 0; \text{ thus } N_3 = 8P$$

$$\Sigma F_y = 0 \quad N_2 \cos\theta - 5P + 4P = 0; \text{ thus } N_2 = \sqrt{2}P$$

$$\Sigma F_x = 0 \quad N_1 + N_2 \sin\theta + N_3 - 2P + 2P = 0; \text{ thus } N_1 = -9P$$

We may wish to verify that the same results will be reached by considering equilibrium of the part of the structure situated to the right of section $n-n$.

2.3 Internal forces: sign convention and diagrams

As mentioned earlier, the purpose of structural analysis is to determine the reactions at the supports and the internal forces (the stress resultants) at any section. In beams and plane frames in which all the forces on the structure lie in one plane, the resultant of stresses at any section has generally three components: an axial force N, a shearing force V, and a bending moment M. The positive directions of N, V, and M are shown in Figure 2.4c, which represents an element (DE) between two closely spaced sections of the horizontal beam in Figure 2.4a. A positive axial force N produces tension; a positive shearing force tends to push the left face of the element upwards and the right face downwards; a positive bending moment produces tensile stresses at the bottom face and bends the element in a concave shape.

In Figure 2.4b, each of the three parts AD, DE, and EC is shown as a free body subjected to a set of forces in equilibrium. To determine the internal forces at any section F (Figure 2.4a) it is sufficient to consider only the equilibrium of the forces on AD; thus N, V, and M at F are the three forces in equilibrium with R_1 and R_2. The same internal forces are the statical equivalents of P_1, P_2, P_3, and R_3. Thus, at any section F the values of N, V, and M are, respectively, equal to the sums of the horizontal and vertical components and of the moments of the forces situated

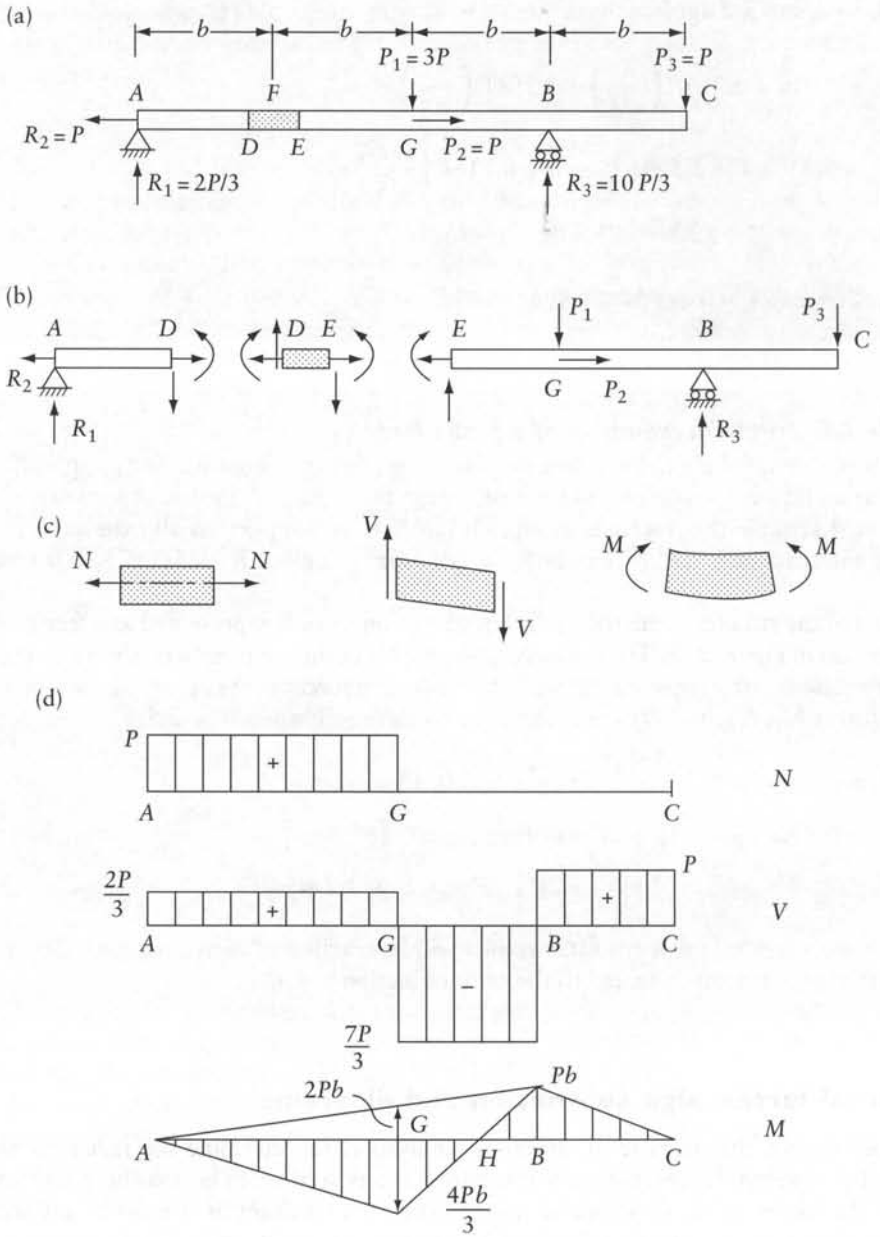

Figure 2.4 Sign convention for internal forces in plane frames and beams. (a) Beam. (b) Free-body diagrams. (c) Positive N, V and M. (d) Axial force, shearing force and bending moment diagrams.

to the left of F. The values of N, V, and M are positive when they are in the directions shown at end E of part EC in Figure 2.4b. The internal forces at section F can also be considered as the statical equivalents of the forces situated to the right of F; in that case the positive directions of N, V, and M will be as shown at end D of part AD.

The variations in N, V, and M over the length of the member are presented graphically by the axial force, shearing force and bending moment diagrams, respectively, in Figure 2.4d. Positive N and V are plotted upwards, while positive M is plotted downwards. Throughout this book,

the bending moment ordinates are plotted on the tension face, that is, the face where the stresses due to M are tensile. If the structure is of reinforced concrete, the reinforcement to resist bending is required near the tension face. Thus, the bending moment diagram indicates to the designer where the reinforcement is required; this is near the bottom face for part AH and near the top face for the remainder of the length (Figure 2.4d). With this convention, it is not necessary to indicate a sign for the ordinates of the bending moment diagram.

Calculation of the values of the internal forces at any section F in the beam of Figure 2.4a requires knowledge of the forces situated to the left or to the right of section F. Thus, when reactions are included, they must be first determined. The values of the reactions and the internal-forces ordinates indicated in Figures 2.4a and d may now be checked.

In the above discussion we considered a horizontal beam. If the member is vertical, as, for example, the column of a frame, the signs of shear and bending will differ when the member is looked at from the left or the right. However, this has no effect on the sign of the axial force or on the significance of the bending moment diagram when the ordinates are plotted on the tension side without indication of a sign. On the other hand, the signs of a shearing force diagram will have no meaning unless we indicate in which direction the member is viewed. This will be discussed further in connection with the frame in Figure 2.5.

Examples of shearing force and bending moment diagrams for a three-hinged plane frame are shown in Figure 2.5. The three equilibrium equations (Eq. 2.5) together with the condition that the bending moment vanishes at the hinge C may be used to determine the reactions. The values indicated for the reactions and the V and M diagrams may now be checked. When determining the signs for the shearing force diagram the nonhorizontal members are viewed with the dashed lines in Figure 2.5 at the bottom face. (See also Figures 2.8, 2.3c and 2.9.)

The ordinates of the shearing force diagram for member BC (Figure 2.5b) may be checked as follows:

$$V_{Br} = R_1 \cos\theta - R_2 \sin\theta$$

$$V_{Cl} = [R_1 - q(2b)]\cos\theta - R_2 \sin\theta$$

where the subscripts r and l refer, respectively, to sections just to the right of B and just to the left of C; θ is the angle defined in Figure 2.5a.

To draw diagrams of internal forces in frames with straight members, it is necessary only to plot the ordinates at member ends and at the sections where external forces are applied, and then to join these ordinates by straight lines. When a part (or the whole) of the length of a member is covered by a uniform load, the ordinates of the bending moment diagram at the two ends of the part are to be joined by a second-degree parabola (see Figure 2.5c). The ordinate of the parabola at the mid-point is $(qc^2/8)$, measured from the straight line joining the ordinates at the ends; q is the load intensity and c is the length of the part considered. A graphical procedure for plotting a second-degree parabola is included in Appendix F.

It is good practice to plot the ordinates perpendicular to the members and to indicate the values calculated and used to plot the diagram.

The internal forces at any section of a member of a framed structure can be easily determined if the end-forces are known. In Figures 3.8a and b, typical members of plane and space frames are shown. The forces shown acting on each member, being the external applied force(s) and the member end-forces, represent a system in equilibrium. Thus, the member may be treated as a separate structure. The internal forces at any section are the statical equivalents of the forces situated to its left or right.

In a space frame, the internal forces generally have six components: a force and a moment in the direction of x^*, y^*, and z^* axes, where x^* is the centroidal axis of the member and y^* and z^* are centroidal principal axes of the cross section (Figure 22.2).

Computer programs for the analysis of framed structures usually give the member end-forces (Figures 3.8a and b) rather than the stress resultants at various sections. The sign convention for

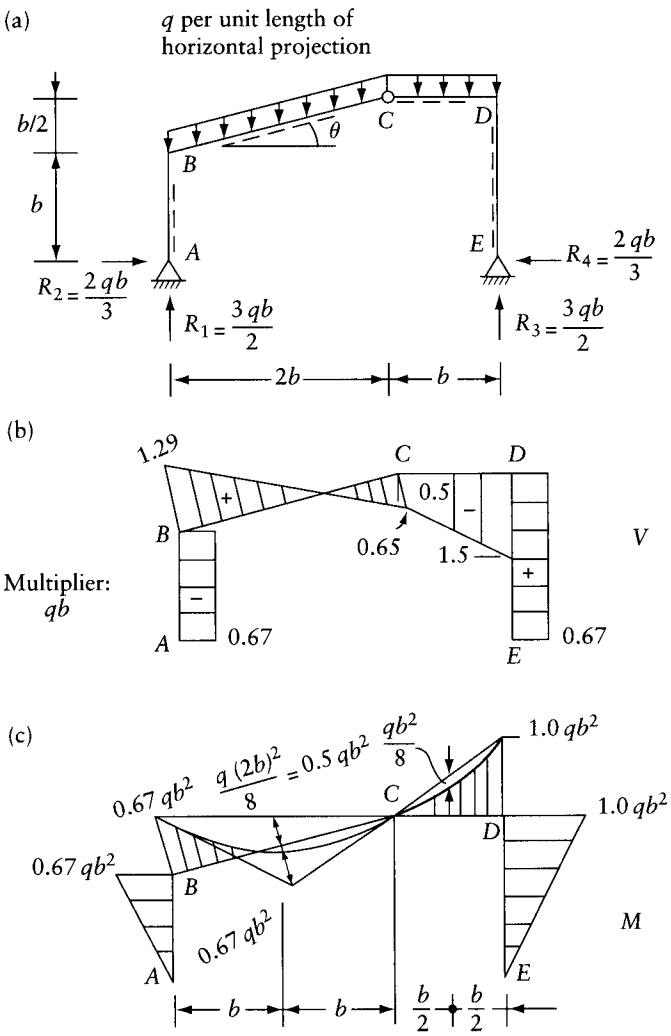

Figure 2.5 A three-hinged plane frame. (a) Dimensions and loading. (b) Shearing force diagram. (c) Bending moment diagram.

the end-forces usually relates to the member local axes, in the direction of the member centroidal axis and centroidal principal axes of the cross section. It is important at this stage to note that the stress resultants at the member ends may have the same magnitude as the member end-forces, but different signs, because of the difference in sign conventions. For example, at the left end of a typical member of a plane frame (Figure 3.8a), the axial force, the shearing force and the bending moment are: $N = -F_1$; $V = -F_2$; $M = F_3$. The stress resultants at the right end are: $N = F_4$; $V = F_5$; $M = -F_6$. Here the member is viewed in a horizontal position and the positive directions of N, V and M are as indicated in Figure 2.4c.

2.4 Verification of internal forces

In this section, we discuss ways of checking the calculations involved in the determination of internal forces in beams and plane frames. For this purpose, we consider the internal forces of the beam in Figure 2.4a. The values of V, N and M at section F can be calculated from the forces

situated to the left of F; the positive directions of the internal forces in this case are shown at E in Figure 2.4b. The same values of V, N and M at section F can also be calculated form the forces situated to the right of F; but in this case, the positive directions of the internal forces would be as shown at D in Figure 2.4b. This alternative calculation is a means of checking the values of the internal forces.

The arrows at D and E in Figure 2.4b are in opposite directions; thus, the values of N, M and V calculated by the two alternatives described above must be equal. This is so because the forces situated to the left of F, combined with the forces situated to the right of F, represent a system in equilibrium, satisfying Eqs. 2.5. When the values of N, M and V calculated by the two alternatives are not equal, the forces on the structure are not in equilibrium; one or more of the forces on the structure (e.g. the reaction components) can be erroneous.

The following relationships can also be employed to verify the calculated values of V and M at any section of a member:

$$\frac{dV}{dx} = -q \tag{2.6}$$

$$\frac{dM}{dx} = V \tag{2.7}$$

where x is the distance measured along the axis of the member (in direction AB); q is the intensity of distributed transverse load acting in the direction of the y axis. For a plane frame, the z axis is perpendicular to the plane of the frame, pointing away from the reader. The three axes x, y and z form a right-handed system (see footnote 2 of this chapter). Thus, for the beam in Figure 2.4a, if the x axis is considered in the direction AB, then the y axis will be vertical downward. For this beam, the slope of the shearing force diagram (dV/dx) is zero at all sections because the beam is subjected to concentrated loads only ($q = 0$). For the same beam, the bending moment diagram is composed of three straight lines, whose slope (dM/dx) can be verified to be equal to the three shearing force values shown in Figure 2.4d.

As a second example, we will use Eqs. 2.6 and 2.7 to verify the V and M-diagrams for member BC of the frame in Figure 2.5. We consider the x axis in the direction BC; thus, the y axis is in the perpendicular direction to BC, pointing towards the bottom of the page. The component of the distributed load in the y direction has an intensity equal to:

$$q_{transverse} = q\cos^2\theta \tag{2.8}$$

This equation can be verified by considering that the resultant of the load on BC is a downward force equal to $2bq$, and the component of the resultant in the y direction is $2bq\cos\theta$. Division of this value by the length of BC ($=2b/\cos\theta$) gives Eq. 2.8. Thus, for member BC, $q_{transverse} = 0.94q$ and we can verify that this is equal to minus the slope of the V-diagram:

$$q_{transverse} = 0.94q = -\left[\frac{(-0.65) - 1.29}{2b/\cos\theta}\right]qb$$

Figure 2.5c shows tangents at the ends of the parabolic bending moment diagram of member BC. The slopes of the two tangents are:

$$\left(\frac{dM}{dx}\right)_B = \left[\frac{0.67 - (-0.67)}{b/\cos\theta}\right]qb^2 = 1.29\,qb; \left(\frac{dM}{dx}\right)_C = \left[\frac{0 - 0.67}{b/\cos\theta}\right]qb^2 = -0.65\,qb$$

As expected (by Eq. 2.7), the two slope values are equal to the shearing force values at B and C (Figure 2.5b). Equation 2.7 also indicates that where $V = 0$, the bending moment diagram has

zero slope and the value of M is either a minimum or a maximum (e.g. the point of zero shear on member BC in Figure 2.5). Under a concentrated force, the shearing force diagram has a sudden change in value and Eq. 2.7 indicates that the M-diagram has a sudden change in slope.

Example 2.6: Member of a plane frame: V and M-diagrams

Figure 2.6a represents a free-body diagram of a member of a plane frame. Three of the member end forces are given: $F_1 = 0.2\,ql$; $F_3 = -0.06\,ql^2$; $F_6 = 0.12\,ql^2$. What is the magnitude of the remaining three end forces necessary for equilibrium? Draw the V and M-diagrams.

The three equilibrium Eqs. 2.5 are applied, by considering the sum of the forces in horizontal direction, the sum of the moments of forces about B, and the sum of the forces in vertical direction:

$$F_1 + F_4 = 0$$

$$-F_2 l + F_3 + F_6 - \frac{ql^2}{2} = 0$$

$$F_2 + F_5 + ql = 0$$

Substitution of the known values and solution gives:

$$F_2 = -0.44\,ql; F_4 = -0.2\,ql; F_5 = -0.56\,ql$$

The values of F_3 and F_6 give the bending moment ordinates at A and B, and their signs indicate that the tension face of the member is at the top fiber at both ends. The M-diagram in Figure 2.6b is drawn by joining the end ordinates by a straight line and *"hanging down"* the bending moment of a simple beam carrying the transverse load (a parabola).

The forces F_2 and F_5 give the ordinates of the V-diagram at the two ends. Joining the two ordinates by a straight line gives the V-diagram shown in Figure 2.6c.

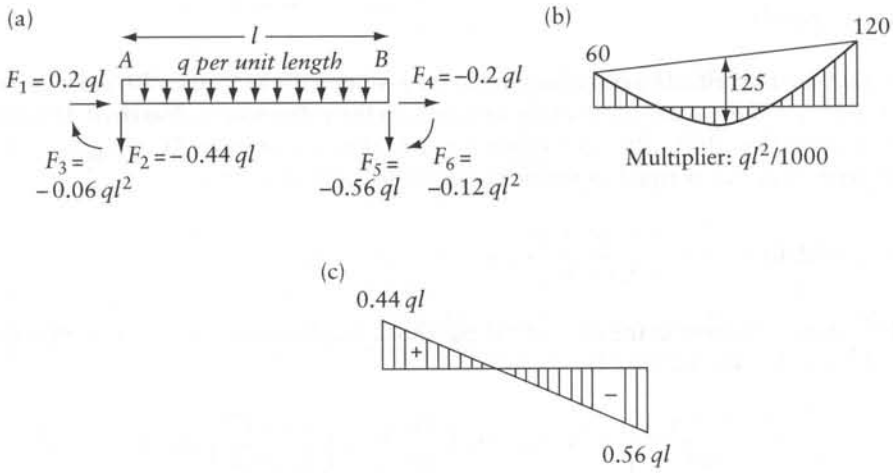

Figure 2.6 Shearing force and bending moment diagrams of a member of a plane frame, Example 2.6. (a) Free-body diagram. (b) M-diagram. (c) Shearing force diagram.

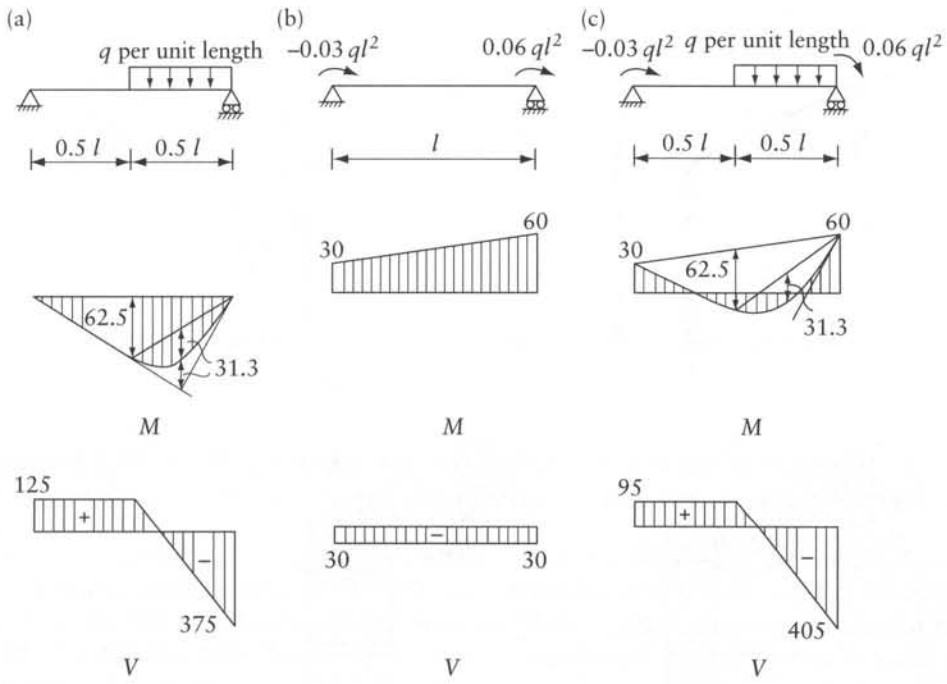

Figure 2.7 Simple beams of Example 2.7. (a) Beam subjected to transverse load. (b) Beam subjected to end moments. (c) Beam subjected to a combination of the loadings in (a) and (b). Multiplier for the M-diagrams: $ql^2/1000$. Multiplier for the V-diagrams: $ql/1000$.

Example 2.7: Simple beams: verification of V and M-diagrams

The simple beams in Figures 2.7a and b are subjected to a transverse distributed load and to end moments respectively. The simple beam in Figure 2.7c is subjected to a combination of the two loadings. Draw the V and M-diagrams for the three beams.

The values of the ordinates may be calculated by the reader and compared with the values given in Figure 2.7. Also, it may be verified that the ordinates satisfy the relationships between q, V and M, Eqs. 2.6 and 2.7. It can also be noted that the ordinates of the V and M-diagrams in part (c) of the figure are equal to the sum of the corresponding ordinates in parts (a) and (b). Thus, the diagrams in part (c) can be derived alternatively by the superposition of the diagrams in parts (a) and (b).

Example 2.8: A cantilever plane frame

Determine the bending moment, the shearing force and the axial force diagrams for the cantilever frame in Figure 2.8.

To find the internal forces at any section of a cantilever, consider the forces situated between that section and the free end. In this way, the reactions are not involved. The ordinates of the M, V and N-diagrams in Figure 2.8 may be verified by the reader. We show

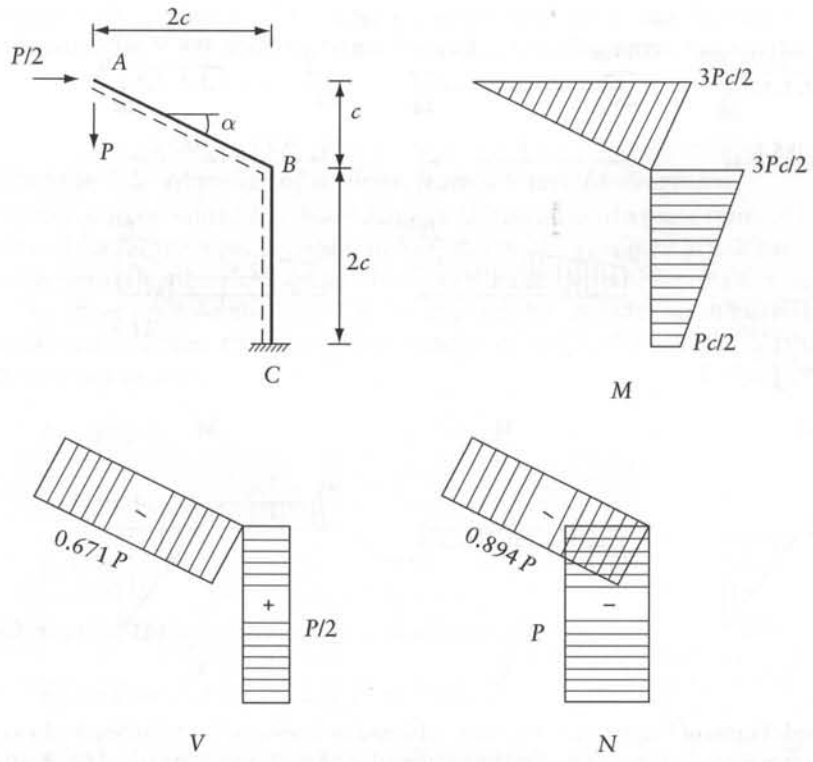

Figure 2.8 Cantilever frame of Example 2.8: bending moment, shearing force and axial force diagrams.

below the calculation of the shearing force and the axial force only for a section anywhere in member AB.

$$V = (P/2)\sin\alpha - P\cos\alpha = -0.671\,P$$

$$N = -(P/2)\cos\alpha - P\sin\alpha = -0.894\,P$$

Example 2.9: A simply-supported plane frame

Determine the bending moment and the shearing force diagrams for the frame in Figure 2.3c. What are the axial forces in the members?

The M and V-diagrams are shown in Figure 2.9. The reader may wish to verify the ordinates given in this figure. See also Example 2.4. The axial forces in the members are:

$$N_{AC} = -R_1\sin\alpha - R_2\cos\alpha = -(-2P)\frac{1}{\sqrt{5}} - 1.8P\left(\frac{2}{\sqrt{5}}\right) = -0.716P$$

$$N_{CE} = -R_1 = -(-2P) = 2P$$

$$N_{EF} = -R_3 = -3.2P;\ N_{BC} = 0$$

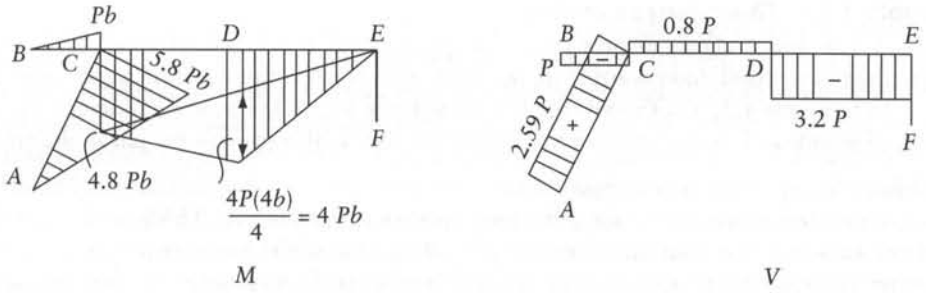

Figure 2.9 Bending moment and shearing force diagrams for the frame in Figure 2.3c.

Example 2.10: M-diagrams determined without calculation of reactions

Draw the *M*-diagrams and sketch the deflected shapes for the beams shown in Figure 2.10.

The ordinates of the bending moment diagrams shown in Figure 2.10 require simple calculations as indicated. Note that the calculation of the reactions is not needed to determine the *M*-diagrams. The sketched deflected shapes show concave and convex parts of the beam. The points of inflection at which the curvature changes sign correspond to points of zero bending moment.

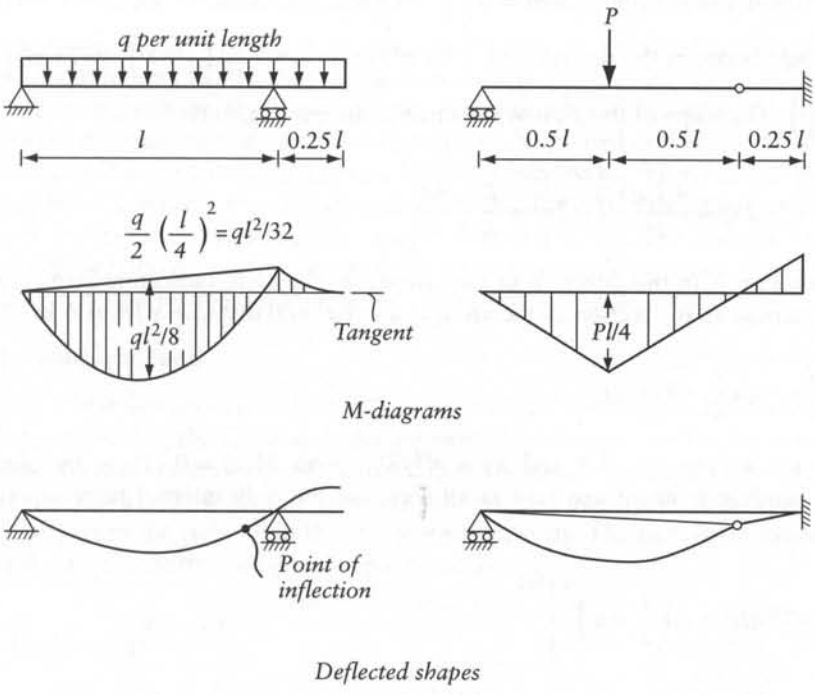

Figure 2.10 Bending moments and deflected shapes for beams of Example 2.10.

Example 2.11: Three-hinged arches

Figures 1.27b and a show, respectively, a polygonal and a parabolic three-hinged arch carrying the same total downward load, ql. Verify that the reactions are the same for both arches. In Example 1.2, it is shown that the shear force V and the bending moment M are zero at all sections of the polygonal arch. Verify that this is also true for the parabolic arch.

Reactions for any of the two arches:

Sum of the moments of all the forces on the structure about B is zero. This gives $R_2 = ql/2$. The same answer is expected from symmetry; R_2 is equal to half the total gravity load on the structure. The reaction R_1 can be determined from the condition that the bending moment M_C is zero at the hinge. Thus, sum of moments of the forces situated to the left of C is zero about C. For the structure in Figure 1.27b,

$$\left(\frac{ql}{2} - \frac{ql}{8}\right)\frac{l}{2} - \frac{ql}{4}\left(\frac{l}{4}\right) - R_1 h_C = 0$$

$$R_1 = 0.75\,ql$$

Similarly for the arch in Figure 1.27a,

$$\left(\frac{ql}{2}\right)\frac{l}{2} - \frac{ql}{2}\left(\frac{l}{4}\right) - R_1 h_C = 0$$

$$R_1 = 0.75\,ql$$

Internal forces in parabolic arch:

The resultant of the forces situated to the left of any section at a horizontal distance x from A has a vertical upward component $= q\left(\frac{l}{2} - x\right)$ and a horizontal component $= R_1 = 0.75\,ql$. The angle between the resultant and the x axis is $\tan^{-1}\left[q\left(\frac{l}{2} - x\right)/(0.75\,ql)\right] = \tan^{-1}\left(\frac{2}{3} - \frac{4x}{3l}\right)$. The slope of the arch at the same section is (Eq. 1.1):

$$\frac{dh}{dx} = \frac{4h_C}{l^2}(l - 2x) = \frac{4(l/6)}{l^2}(l - 2x) = \frac{2}{3} - \frac{4x}{3l}$$

Thus, the resultant is in the direction of the tangent to the arch, indicating zero shear. The bending moment at any section of the arch, at a horizontal distance x from A is:

$$M(x) = \frac{ql}{2}x - qx\frac{x}{2} - R_1 h(x)$$

Substituting for $h(x)$ by Eq. 1.1 and $R_1 = ql^2/8h_C$ gives $M(x) = 0$. Thus, the shear force and the bending moment are zero at all sections; the only internal force is axial of magnitude:

$$N = -\left[(0.75\,ql)^2 + q\left(\frac{l}{2} - x\right)^2\right]^{1/2}$$

The minus sign indicates a compressive axial force.

2.5 Effect of moving loads

In design of structures it is necessary to know the internal forces due to the permanent and the transient service loads. These are referred to as *dead* and *live* loads respectively. Examples of live loads are the weight of snow on a roof, the weight of furniture and of occupants on a floor, and the wheel loads of a truck on a bridge or of a traveling crane on a crane beam. In analysis, the live load is usually represented by a uniformly distributed load or a series of concentrated forces.

Naturally, in design, we are concerned with the maximum values of the internal forces at various sections. Thus, for the maximum value of an action at any section, the live load must be placed on the structure in a position such that the maximum occurs. In many cases, the position of the load which produces a maximum is obvious. In other cases the use of *influence lines*, discussed in Section 2.6 and in Chapters 12 and 13, can help in determining the position of the moving load which results in the maximum value of the action considered.

We shall now consider the effects of moving loads on simple beams; the effects of moving loads on continuous beams are discussed in Section 4.8.

2.5.1 Single load

Consider the effect of a single concentrated downward force P moving on a simple beam shown in Figure 2.11a. At any section n, the bending moment is maximum positive when P is directly above n. The shear at n is maximum positive when P is just to the right of n, and is maximum negative when P is just to the left of n. The maximum values of bending and shear due to a single concentrated load on a simple beam may be expressed as

$$M_{n\max+} = P\frac{x(l-x)}{l} \tag{2.9}$$

$$V_{n\max+} = P\frac{l-x}{l}; \quad V_{n\max-} = -P\frac{x}{l} \tag{2.10}$$

The expression *maximum negative value* is commonly used in structural design and is used here to mean a minimum value in the mathematical sense.

The bending moment and shearing force diagrams when P is at n are shown in Figure 2.11b. If the load changes position, similar diagrams can be plotted and an envelope of the maximum ordinates can be constructed (Figure 2.11c). The envelope for the maximum positive moment in the case considered is a second-degree parabola (Eq. 2.9); for shear, the envelopes for maximum positive and negative ordinates are straight lines (Eq. 2.10). The ordinates of such diagrams, which will be referred to as *maximum bending moment* and *maximum shearing force* diagrams, indicate in design the maximum internal forces that any section must resist.

2.5.2 Uniform load

Figure 2.11d shows the maximum bending moment and shearing force diagrams due to a uniform load q per unit length. The load is placed over the full length of the beam or its part so as to produce the maximum effect. At any section n, the maximum bending moment occurs when q covers the full length; however, the maximum positive or negative shear occurs when q covers only the part to the right or to the left of n respectively. The maximum values of bending and shear due to a uniform load on a simple beam are

$$M_{n\max+} = q\frac{x(l-x)}{2} \tag{2.11}$$

$$V_{n\max+} = q\frac{(l-x)^2}{2l}; \quad V_{n\max-} = -q\frac{x^2}{2l} \tag{2.12}$$

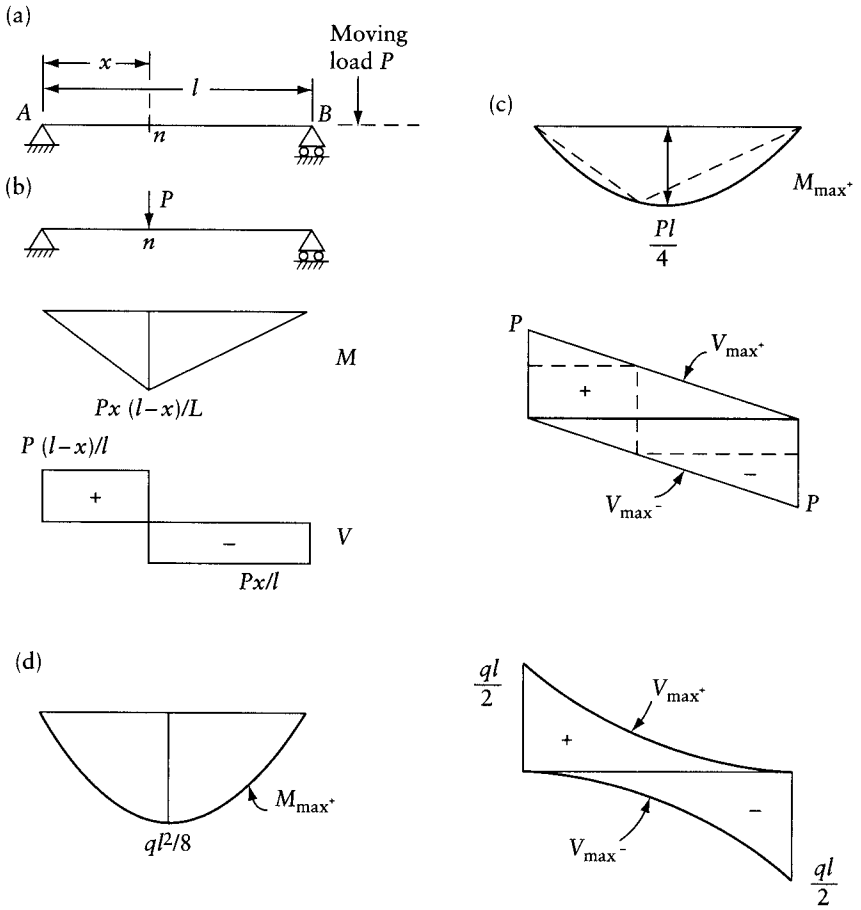

Figure 2.11 Effect of moving loads on a simple beam. (a) Single concentrated load P. (b) Bending moment and shearing force diagrams when P is directly above any section n. (c) Envelopes of the M and V-diagrams in (b): M_{max+}, V_{max+} and V_{max-} due to P. (d) Diagrams for maximum bending moment and shearing force due to uniform load q per unit length.

It can be seen that the maximum bending moment and shearing force diagrams are second-degree parabolas.

2.5.3 Two concentrated loads

Consider the effects of two concentrated loads P_1 and P_2, with $P_1 \geqslant P_2$, moving on a simple beam (Figure 2.12a). At any section n, the maximum bending moment occurs when P_1 or P_2 is directly upon the section (Figure 2.12b or c), producing

$$M_{n\max+} = \frac{x(l-x)}{l}\left(P_1 + P_2\frac{l-x-s}{l-x}\right) \text{ with } 0 \leqslant x \leqslant (l-s) \tag{2.13}$$

or

$$M_{n\max+} = \frac{x(l-x)}{l}\left(P_2 + P_1\frac{x-s}{x}\right) \text{ with } s \leqslant x \leqslant l \tag{2.14}$$

where s is the spacing between the loads and l is the span.

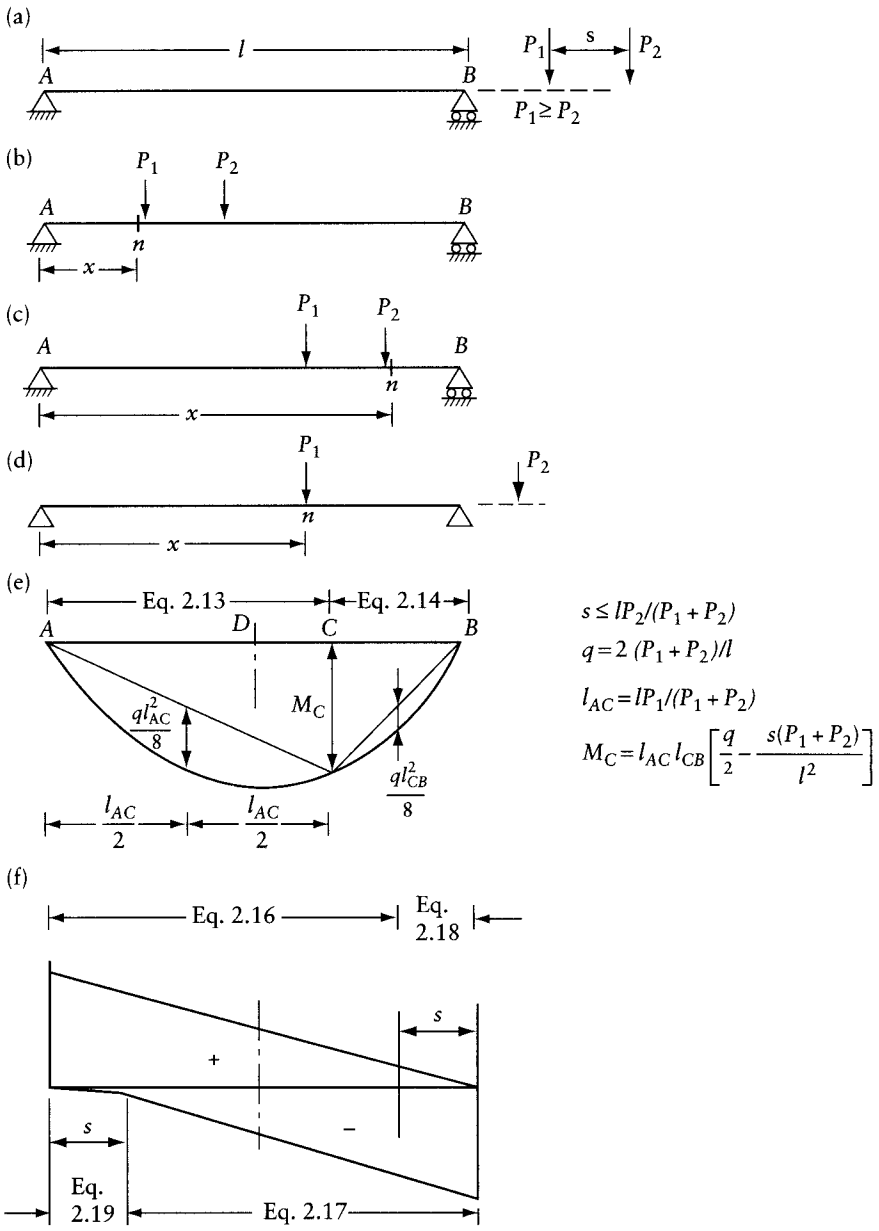

Figure 2.12 Effect of two concentrated moving loads P_1 and P_2 with $P_1 \geqslant P_2$. (a) A simple beam. (b), (c) and (d) Load positions for maximum bending moment or shear at any section n. (e) Maximum bending moment diagram when $s \leqslant lP_2/(P_1+P_2)$. (f) Maximum shearing force diagram.

A third load position to be considered is shown in Figure 2.12d, with P_2 falling outside the beam; the corresponding bending moment at n is

$$M_{n\max+} = P_1 \frac{x(l-x)}{l} \text{ with } (l-s) \leqslant x \leqslant l \tag{2.15}$$

The diagram for the maximum bending moment for any part of the beam is a second-degree parabola represented by one of the above three equations, whichever has the largest ordinate. It can be shown that Eq. 2.15 governs in the central part of the beam only when $s > lP_2/(P_1 + P_2)$. The maximum bending moment diagram in this case is composed of three parabolic parts (see Prob. 2.7). The maximum bending moment diagram when $s \leqslant lP_2/(P_1 + P_2)$ is shown in Figure 2.12e, which indicates the span portions to which Eqs. 2.13 and 2.14 apply. The case when $s > lP_2/(P_1 + P_2)$ is discussed in Prob. 2.7. In that problem it is indicated that the diagram for the maximum bending moment due to specific moving load systems on a simple beam is the same as the bending moment diagram due to virtual (unreal) stationary load systems.

The loads in the positions shown in Figures 2.12b and c produce maximum positive and negative values of shear at section n. These are given by

$$V_{n\max+} = P_1\frac{l-x}{l} + P_2\frac{l-x-s}{l} \text{ with } 0 \leqslant x \leqslant (1-s) \tag{2.16}$$

$$V_{n\max-} = -\left(P_1\frac{x-s}{l} + P_2\frac{x}{l}\right) \text{ with } s \leqslant x \leqslant l \tag{2.17}$$

The maximum shear may also be produced by P_1 or P_2 alone, placed just to the left or just to the right of n, giving (Figure 2.12d)

$$V_{n\max+} = P_1\frac{l-x}{l} \text{ with } (l-s) \leqslant x \leqslant l \tag{2.18}$$

$$V_{n\max-} = -P_2\frac{x}{l} \text{ with } 0 \leqslant x \leqslant s \tag{2.19}$$

where x is the distance between support A and P_1 or P_2.

The maximum shearing force diagram for any part of the beam is a straight line represented by one of the above four equations, whichever has the largest ordinate (Figure 2.12).

The maximum bending moment and shearing force diagrams shown in Figure 2.12 are for the two forces P_1 and P_2, with the larger force P_1 to the left of P_2. If the forces can also be placed on the beam in a reversed order, with P_1 on the right-hand side of P_2, the larger of the two ordinates at any two sections symmetrically placed with respect to the center line must be considered as the maximum ordinate. Thus, assuming that the ordinates in Figure 2.12 are larger for the left-hand half of the beam AD compared with their counterparts in the other half, the maximum bending moment diagram should be a curve as at present shown for AD completed by its mirror image for DB.

Example 2.12: Maximum bending moment diagram

Find the maximum bending moment diagrams for a simple beam of span l, subjected to two moving loads $P_1 = P$ and $P_2 = 0.8P$, spaced at a distance (a) $s = 0.3l$ and (b) $s = 0.6l$.

Assume that P_1 is on the left-hand side of P_2 and that this order is nonreversible. Repeat case (a) assuming that the order of loads can be reversed.

The maximum bending moment ordinates in case (a) are calculated directly, using the equations in Figure 2.12e because $s < lP_2/(P_1 + P_2) = l(0.8/1.8) = 0.44l$. The resulting diagram is shown in Figure 2.13a.

For case (b), we plot three parabolas corresponding to Eqs. 2.13 to 2.15 and use for any part of the beam the curve with the largest ordinate (Figure 2.13b).

With reversible loads in case (a), the maximum bending moment diagram is the curve AD and its mirror image shown dotted in Figure 2.13a. The ordinate at D is $0.330Pl$.

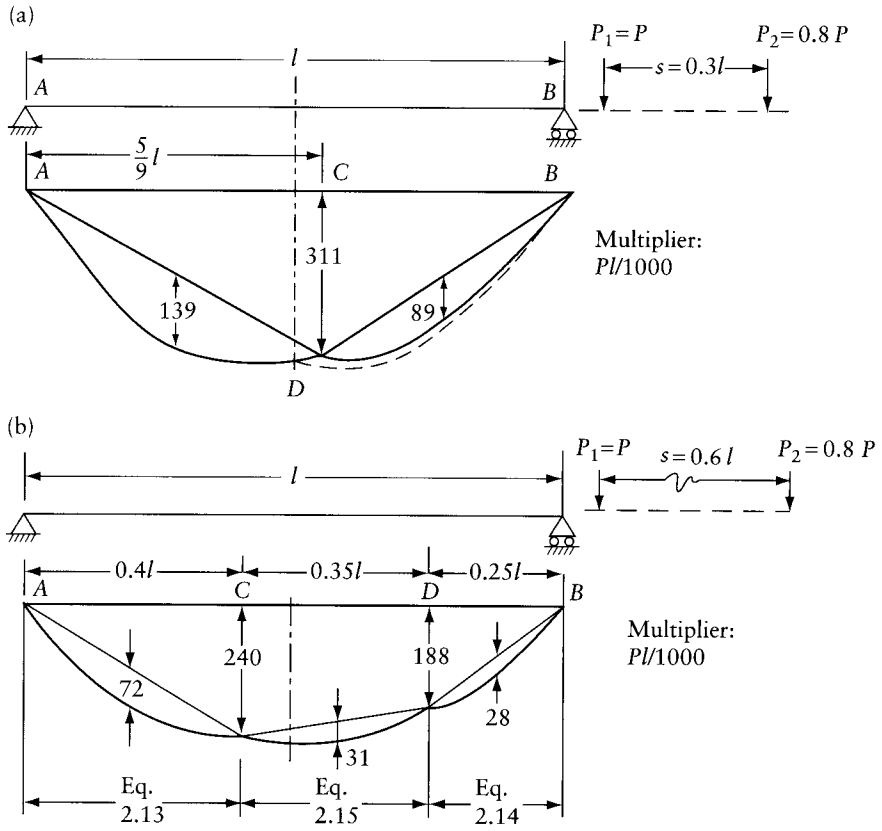

Figure 2.13 Maximum bending moment diagrams due to two moving concentrated loads. Example 2.12. (a) $s = 0.3\,l$. (b) $s = 0.6\,l$.

2.5.4 *Group of concentrated loads*

The maximum bending moment at any section n due to a system of concentrated moving loads on a simple beam (Figure 2.14a) occurs when one of the loads is at n; by trial and error we can find which load should be at n to cause $M_{n\max+}$. The maximum positive shear at n occurs when P_1 is just to the right of n (Figure 2.14b). The maximum negative shear at n occurs when the last load P_m is just to the left of n (Figure 2.14c). It is possible, when the first (or last) load is relatively small, that the maximum shear occurs when another load is situated just to the left or to the right of n. Again, by trial and error we can find which load position produces the maximum effect at the section considered.

2.5.5 *Absolute maximum effect*

In the above we considered the position of moving loads to produce the maximum bending moment or shearing force at a specified section. In design, we also need to know the location and magnitude of the largest ordinate of the diagram of maximum bending moment or maximum shear. The section at which the maximum effect occurs is often identified by inspection. For example, in a simple beam, the absolute maximum shear occurs at the supports. The absolute maximum bending moment is at mid-span due to a single or uniform live load.

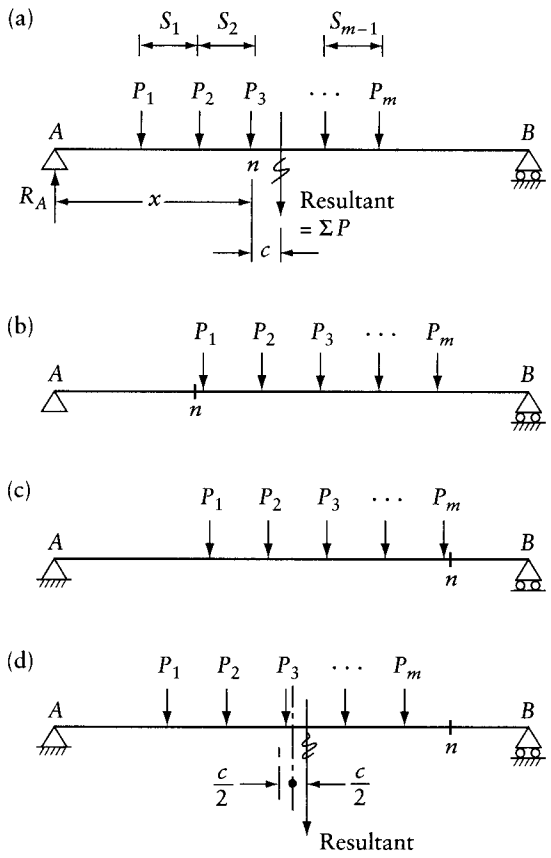

Figure 2.14 Effect of a system of moving loads on a simple beam. (a) Position of load for $M_{n\max+}$. (b) Position of load for $V_{n\max+}$. (c) Position of load for $V_{n\max-}$. (d) Position of load to produce largest bending moment directly beneath P_3.

For a series of concentrated loads, the absolute maximum must occur directly beneath one of the loads, but it is not obvious which one. This is often determined by trial and error; usually, the absolute maximum bending moment occurs below one of the forces close to the resultant.

Assume that, in Figure 2.14a, the absolute maximum moment occurs under load P_3. It is necessary to determine the variable x defining the position of the load system for which the bending moment M_n below P_3 is maximum. The value of M_n may be expressed as

$$M_n = R_A(x) - P_1(s_1 + s_2) - P_2 s_2 \tag{2.20}$$

and

$$R_A = \frac{l - x - c}{l} \Sigma P \tag{2.21}$$

where c is the distance between the resultant of the system and P_3, and R_A is the reaction at A.

The maximum value of M occurs when $(dM_n/dx) = 0$. Substitution of Eq. 2.21 in Eq. 2.20 and differentiation give

$$\frac{dM_n}{dx} = \frac{\Sigma P}{l}(l - 2x - c) = 0$$

whence

$$x = \frac{l}{2} - \frac{c}{2} \tag{2.22}$$

Thus, the absolute maximum bending moment due to a system of concentrated loads on a simple beam occurs under one of the loads. The concentrated loads are to be placed such that the center of the span is mid-way between the resultant and that particular load (Figure 2.14d).

It should be noted that the above rule is derived on the assumption that all the forces are situated on the span. It is possible that the absolute maximum occurs when one or more of the forces are situated outside the beam. In this case the rule of the preceding paragraph may be applied using the resultant of only those forces which are located on the span. As an example of this condition, consider the beam in Figure 2.13b: the absolute maximum is at the center line and its value is $0.25Pl$, occurring when P_1 is at mid-span and P_2 is outside the beam.

In design of cross sections of members it is often necessary to consider the interaction of two or more internal forces. For example, in the design of reinforced concrete beams for shear, we consider at any section the value of the maximum shearing force combined with the corresponding bending moment resulting from the same loading. The value of the moment to be used in this case will obviously be smaller than the ordinate of the maximum bending moment diagram.

In practice, with the wide use of computers, structural designers identify a number of loading cases representing the permanent loads, combined with the moving loads in the positions which are likely to produce maximum bending moment, axial force, shearing force or torsion at selected, critical sections. The designer also specifies the possible combinations of loading cases and the desired multipliers (load factors) of the individual cases. The computer can then be used to scan the internal forces due to the load combinations and give for each section the maximum positive and negative values of one of the internal forces and the values of the other internal forces occurring for the same loading. These are the values to be used in the design of sections.

Example 2.13: Simple beam with two moving loads

Find the absolute maximum bending moment in a simple beam subjected to two concentrated moving loads shown in Figure 2.13a. What is the shearing force at the section of absolute maximum moment when the maximum occurs?

The resultant is of magnitude $1.8P$, situated at a distance $c = 0.133l$ from P_1. Thus, the absolute maximum moment occurs at a section at a distance $c/2 = 0.067l$ to the left of the center line. When P_1 is directly above this section, the reaction $R_A = 0.78P$ and the bending moment at the same section is the absolute maximum:

$$M_{\text{abs max}} = 0.78P(0.433l) = 0.338Pl$$

The corresponding shearing force to the left of P_1 is $R_A = 0.78P$.

2.6 Influence lines for simple beams and trusses

The subject of influence lines is treated in detail in Chapters 12 and 13. In this section we introduce only briefly the derivation of influence lines for shearing force and bending moment at a section of a simple beam and for the axial force in a member of a simply-supported truss.

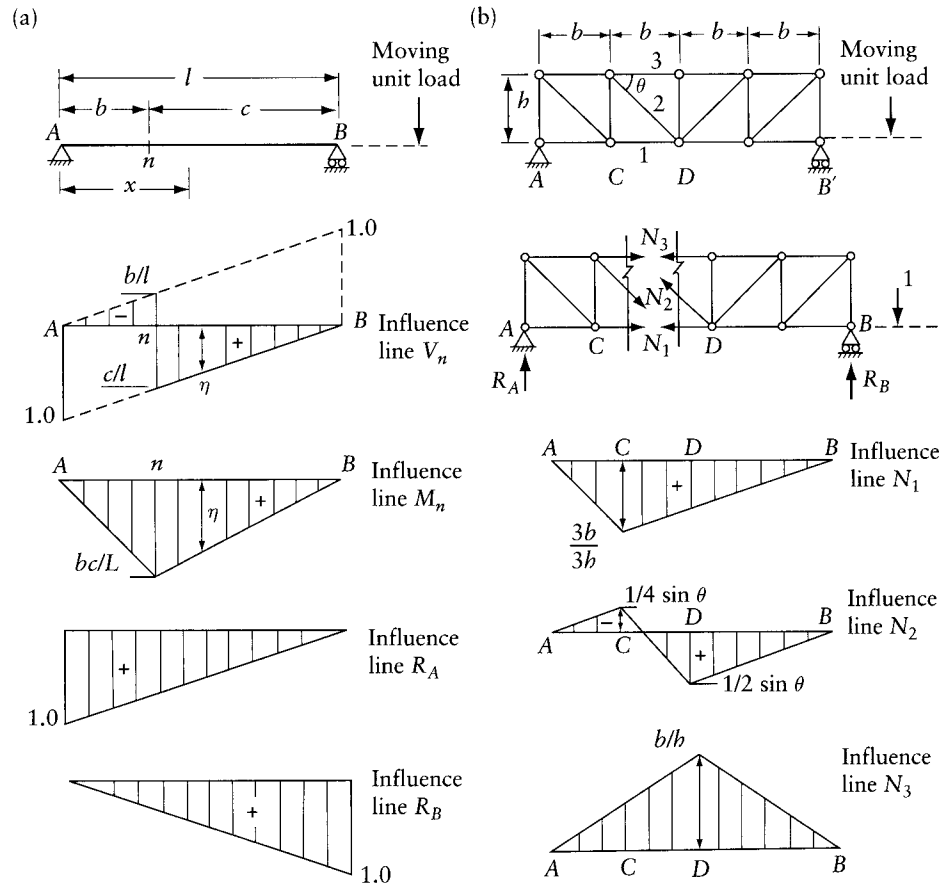

Figure 2.15 Influence lines for simply-supported structures. (a) Beam. (b) Truss.

The influence line for any of these actions is a plot of the value of the action at a given cross section as a unit load traverses the span.

Figure 2.15a shows the influence lines for the shear V_n and the bending moment M_n at any section n of a simple beam. The ordinate η at any section, at a distance x from the left-hand support, is equal to the value of V_n and M_n when the unit load is placed directly above the ordinate. Positive ordinates are plotted downwards.

The most effective method for obtaining an influence line uses Müller-Breslau's principle discussed in Section 12.3. It is based on energy theorems discussed in later chapters. We can also derive the influence lines for the structures considered here using simple statics. For this purpose, consider the influence line for the reaction R_A. When the unit load is at a distance x from support A, the reaction is $R_A = (l - x)/l$. Thus, we can express the ordinate of the influence line of R_A as

$$\eta_{RA} = (l - x)/l$$

Similarly, the ordinate of the influence line of R_B is

$$\eta_{RB} = x/l$$

Thus, the influence lines of the reactions are straight lines as shown in Figure 2.15a. The shear at n is equal to R_A when the unit load is at any section between B and n. We can therefore use the part from B to n of the influence line for R_A to represent the influence line for V_n. Similarly, $V_n = -R_B$ when the unit load is in any position between n and A. Thus, between n and A, the influence line for V_n is the same as the influence line for R_B with reversed sign.

When the unit load is between B and n, the bending moment is $M_n = R_A b$; when the load is between n and A, $M_n = R_B c$. Thus, the ordinates of the influence lines for R_A and R_B, multiplied respectively by b and c, can be used to construct the appropriate parts of the influence line for M_n.

Consider the effect of a unit load moving on the bottom chord of a simply-supported truss (Figure 2.15b). The influence lines for the forces in members 1, 2 and 3 are shown. These are constructed from the influence lines for the reactions R_A and R_B, which are the same as for the beam in Figure 2.15a. Separating the truss into two parts by a vertical section and considering the equilibrium of each part, we can write the following equations. When the unit load is between B and D,

$$N_1 = R_A(b/h) \quad N_2 = R_A(\sin\theta)^{-1} \quad N_3 = R_A(-2b/h)$$

When the unit load is between C and A,

$$N_1 = R_B(3b/h) \quad N_2 = R_B(-\sin\theta)^{-1} \quad N_3 = R_B(-2b/h)$$

Again, the ordinates of the influence line for R_A or R_B multiplied by the quantities in brackets in the above equations give the ordinates of the influence lines for N_1, N_2, and N_3 over the length BD or CA. The influence lines between C and D are simply the straight lines joining the ordinates at C and D. This is justified because we are assuming, as usual, that the members are pin-connected and any external load is applied only at the joints. A unit moving load, when situated between two nodes such as C and D, is replaced by two statically equivalent downward forces at C and D; that is, the unit load is partitioned between C and D in inverse proportion to the distances from the load to C and D (see Section 12.4).

The use of influence lines to determine the effects of a series of concentrated loads is explained by the following example (see also Section 12.3).

Example 2.14: Maximum values of M and V using influence lines

Find the maximum bending moment and shearing force values at section n for the beam in Figure 2.16a due to the given system of three moving forces, representing the axle loads of a truck.

In Figure 2.15, we have seen how to find the influence line for the bending moment and the shear force at any section of a simple beam. The influence line for M_n is shown in Figure 2.16b. The bending moment M_n due to the loads in any position is given by

$$M_n = \sum_{i=1}^{3} P_i \eta_i$$

where η_i is the influence-line ordinate directly beneath P_i. The maximum value of M_n is obtained by trial so that the sum of the products of the value of the individual axle load and the influence ordinate below it is as large as possible. A first trial of the truck position is shown in Figure 2.16b; the corresponding value of M_n is

$$(M_n)_{\text{trial 1}} = Wl[0.2(0.12) + 0.8(0.24) + 0.8(0.16)] = 0.344\,Wl$$

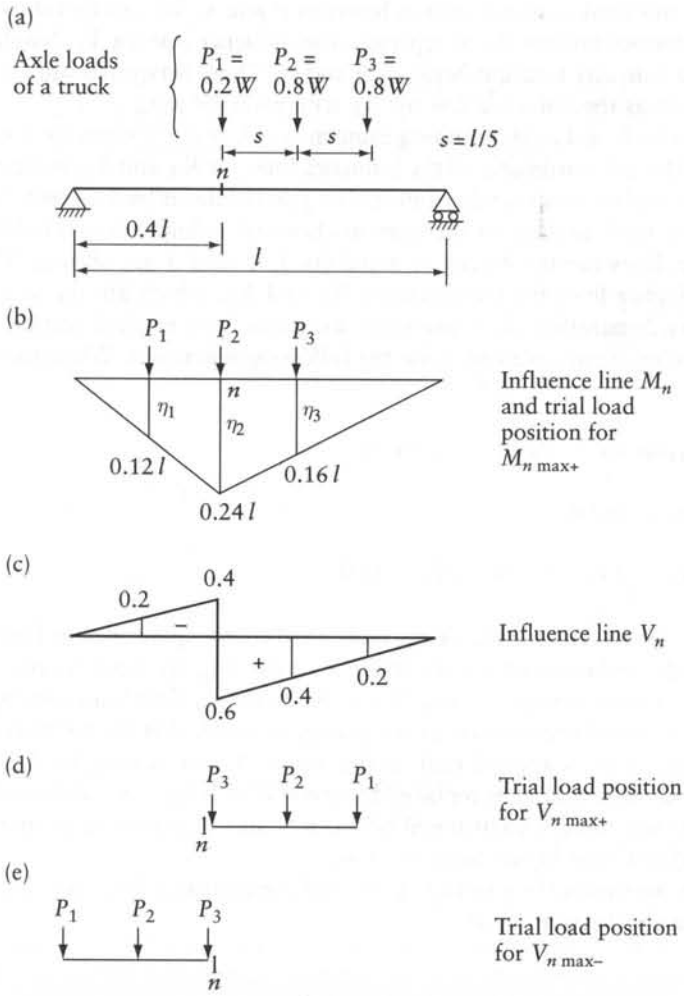

Figure 2.16 Use of influence lines to determine the effects of a moving system of loads, Example 2.14.

In a second trial we place the loads in a reversed order, with P_3 at n and the other two loads to the right; this gives $(M_n)_{\text{trial }2} = 0.336Wl$. In a third trial we place P_2 at n, with P_3 at its left, giving $(M_n)_{\text{trial }3} = 0.320Wl$. The largest value is obtained in trial 1 and hence $M_{\max+} = 0.344Wl$.

The influence line for V_n is shown in Figures 2.16c, d and e, which indicate one trial load position for the maximum positive shearing force and another trial load position for the maximum negative shearing force. These trials give

$$V_{n\max+} = W[0.8(0.6) + 0.8(0.4) + 0.2(0.2)] = 0.84W$$
$$V_{n\max-} = W[0.2(0) + 0.8(-0.2) + 0.8(-0.4)] = -0.48W$$

It is clear in this case that no other trials would give larger values of V_n. Hence, we consider that the above are the maximum shear values.

We should note that influence lines give the maximum value of an action at a specified section but do not give absolute maximum values. However, if the above analysis is performed at a number of sections, a plot of the values obtained gives the maximum diagram and hence the absolute maximum ordinate can be seen.

2.7 General

For statically determinate structures, the equilibrium equations are sufficient to determine the reactions and the internal forces. Indeed, this is why the structures are called statically determinate. Additional equations, considering deformations, are necessary in the analysis of statically indeterminate structures. For all structures, the equilibrium equations apply to the structure as a whole, to an isolated part, and to individual joints. The application of these equations will give unknown components of reactions and internal forces when the number of unknowns does not exceed the number of equilibrium equations.

Problems

2.1 Find member forces and reaction components in x and y or in x, y and z directions for the statically determinate trusses shown.

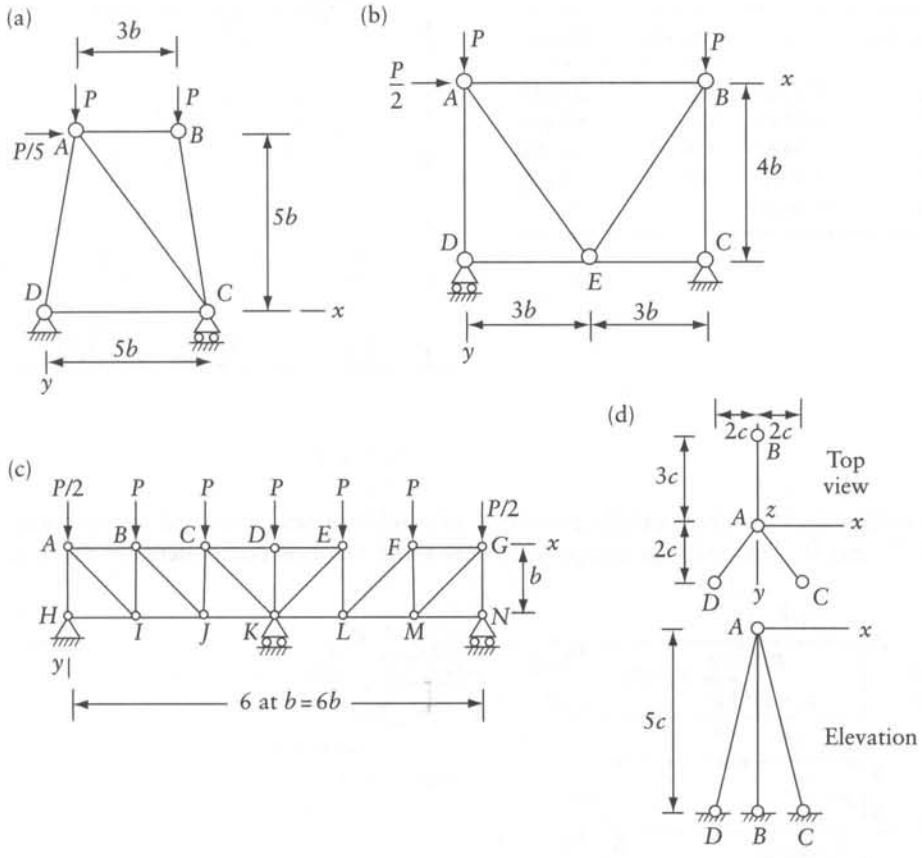

External applied forces at A:
$F_x = 2P$; $F_y = 3P$; $F_z = 5P$

Prob. 2.1

2.2 The space truss shown is composed of three horizontal members AB, BC, and CA and six inclined members connecting A, B and C to the support nodes E, F, and D. The structure is subjected to forces $\{F_x, F_y, F_z\} = P\{1, 0, 3\}$ at each of joints A, B, and C. Write down nine equilibrium equations from which the reaction components in x, y, and z directions can be determined. Verify the equations by substituting the answers given below. Also verify equilibrium of one of joints A, B, or C using the member forces given in the answers.

Table 2.1 Reactions in Terms of P:

	R_x	R_y	R_z
At D	−1.7835	0.6071	−7.3923
At E	−0.7321	−0.7500	−3.0000
At F	−0.4845	0.1430	1.3923

Table 2.2 Forces in members in Terms of P:

Member	Force	Member	Force
AB	1.1585	BE	−0.0381
BC	0.1585	CE	−3.1439
CA	−0.8415	CF	−0.0381
AD	−4.6968	AF	1.5148
BD	−3.1439		

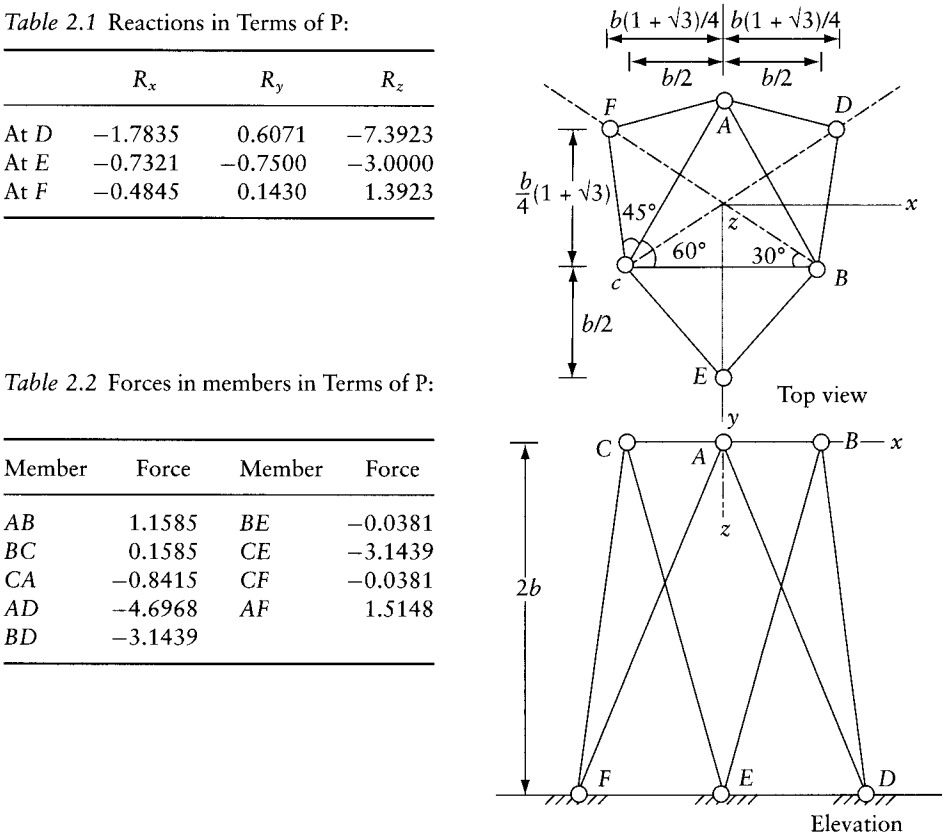

Prob. 2.2

2.3 A bridge deck is schematically presented as a solid prism supported on bearings at A, B, C, and D. The bearings can provide only seven reaction components in the x, y, and

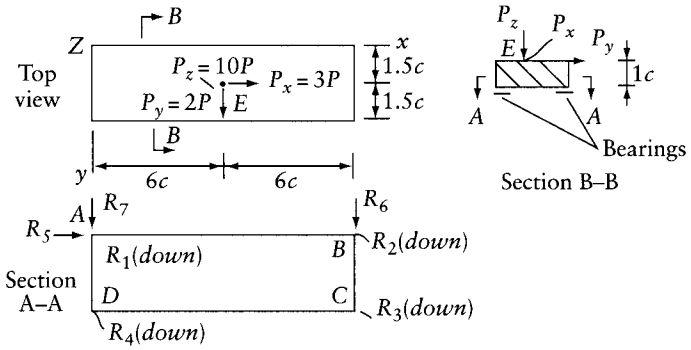

Prob. 2.3

z directions as shown. Given $R_2 = -2.5P$, determine the remaining reactions due to the external applied forces shown at E.

2.4 Obtain the shearing force and bending moment diagrams for the statically determinate beams and frames shown.

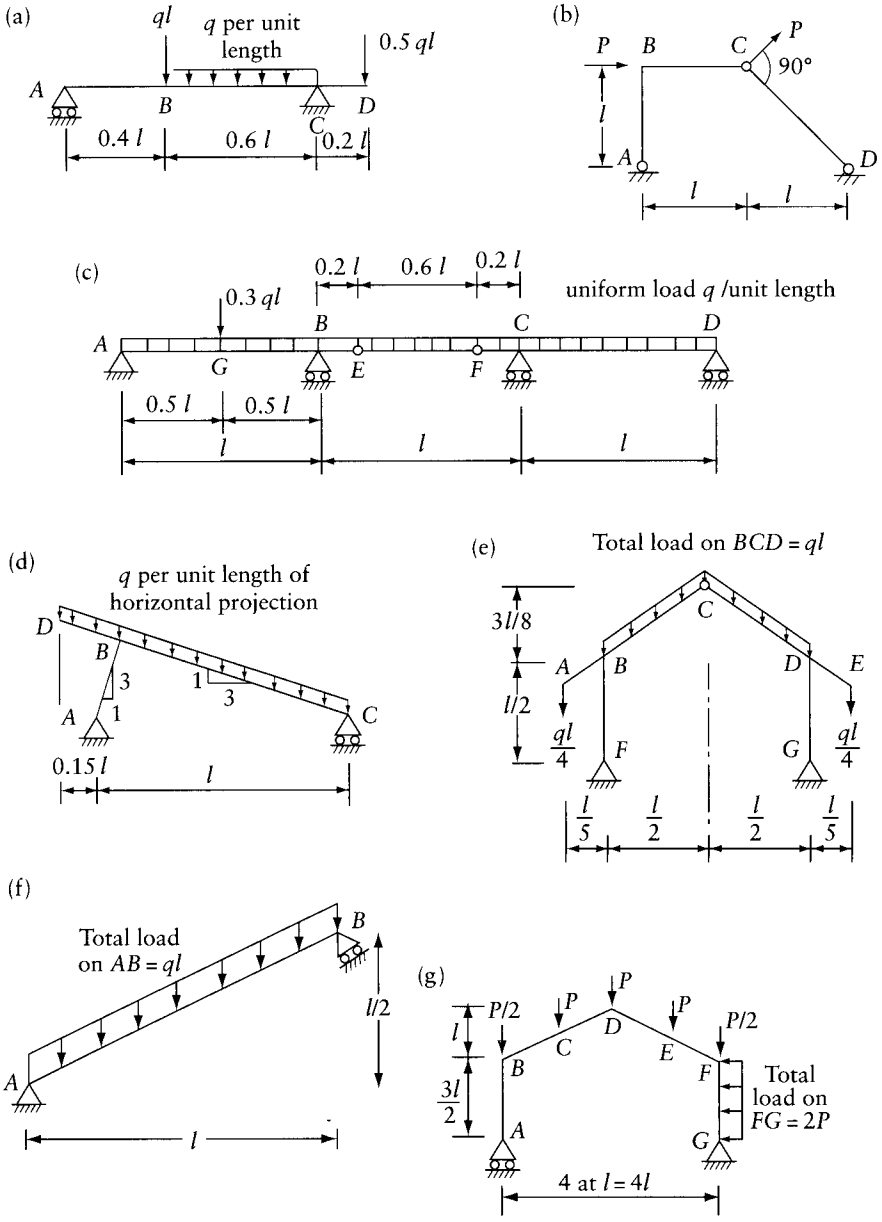

Prob. 2.4

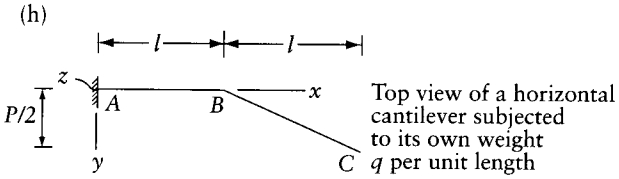

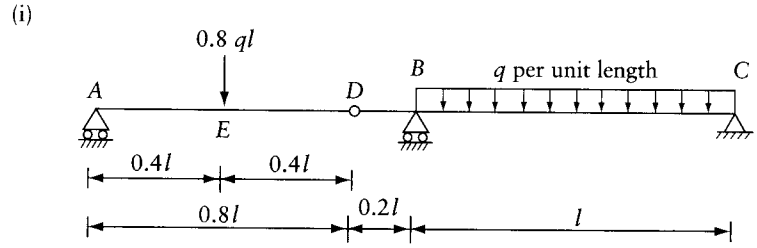

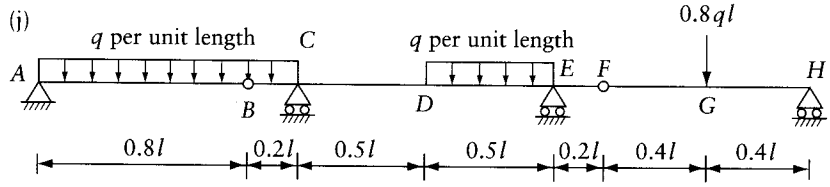

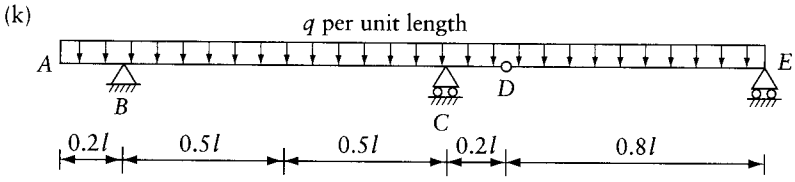

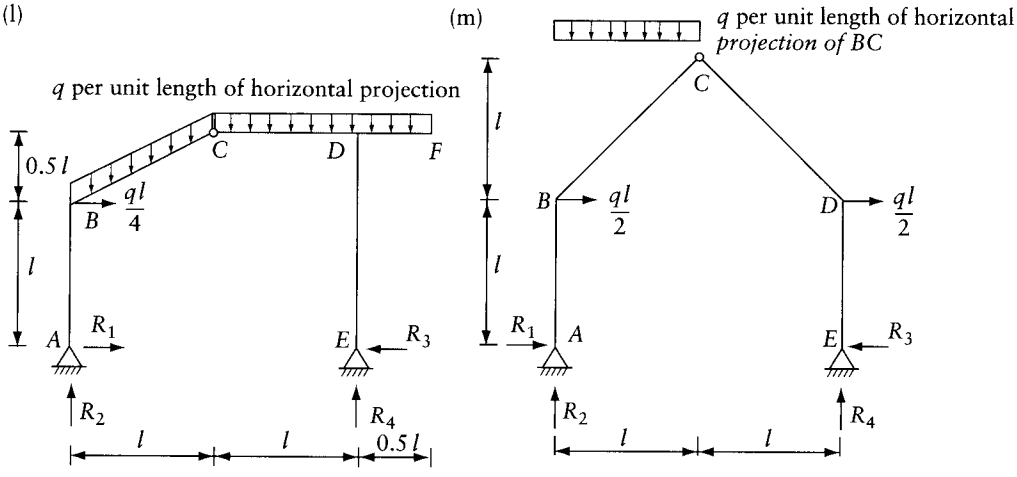

Prob. 2.4 (Continued)

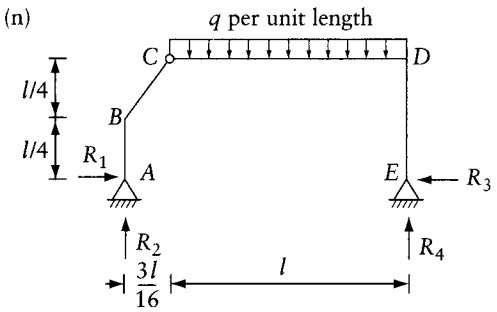

Prob. 2.4 (Continued)

2.5 For a simple beam of span l, determine the maximum bending moment and its location due to the following moving loads:

(a) Two forces $P_1 = P_2 = W$, spaced at $s = 0.2l$.
(b) Three forces $P_1 = W$, $P_2 = W$, $P_3 = W/2$, spaced at $s = 0.2$/between P_1 and P_2 and between P_2 and P_3.
(c) Two forces $P_1 = P_2 = W$, spaced at $s = 0.55l$.

2.6 For the simple beam and the truck axle loads specified in Example 2.13 (Figure 2.16), determine the maximum bending moment and shearing force and their locations.

2.7 Verify that, for each of the simple beams shown, the maximum bending moment diagram due to the moving load system in (a) is the same as the bending moment diagram due to the virtual (unreal) stationary load system in (b).
Hint. For any section n, place the moving load in the position which produces maximum moment and verify that M_n due to the moving load is the same as that due to the stationary load. The derivation of the virtual stationary load system is given in Wechsler, M. B., "Moment Determination for Moving Load Systems," *Journal of Structural Engineering*, American Society of Civil Engineers, 111 (6) (June 1985), pp. 1401–1406.

2.8 Assuming that in Example 2.11 the simple beam is extended by an overhanging part of length $0.35l$ at each end, and assuming that the order of the two loads can be reversed, find the maximum bending moments.

2.9 A simple beam of span l has an overhang of length $0.35l$ at each end; the total length of the beam is thus $1.7l$. Obtain the influence lines for M and V at a section n within the span at $0.25l$ from the left-hand support. Use the influence line to find $M_{n\max+}$, $M_{n\max-}$ and $V_{n\max+}$ due to: (a) two moving loads $P_1 = P$ and $P_2 = 0.8P$, separated by a distance $s = 0.3l$, assuming that the order of the loads can be reversed; and (b) a uniform moving load of q per unit length (use Eq. 12.3).

2.10 Find the maximum positive and negative bending moment values for the beam in Prob. 2.4a due to a moving pair of concentrated gravity loads, P and $0.8P$, spaced at a distance $0.3l$, combined with the self-weight of the beam, $q = P/(2l)$ per unit length. Assume that the moving loads can be placed on the beam: (a) with P on the left-hand side of $0.8P$, or (b) with P on the right-hand side of $0.8P$.

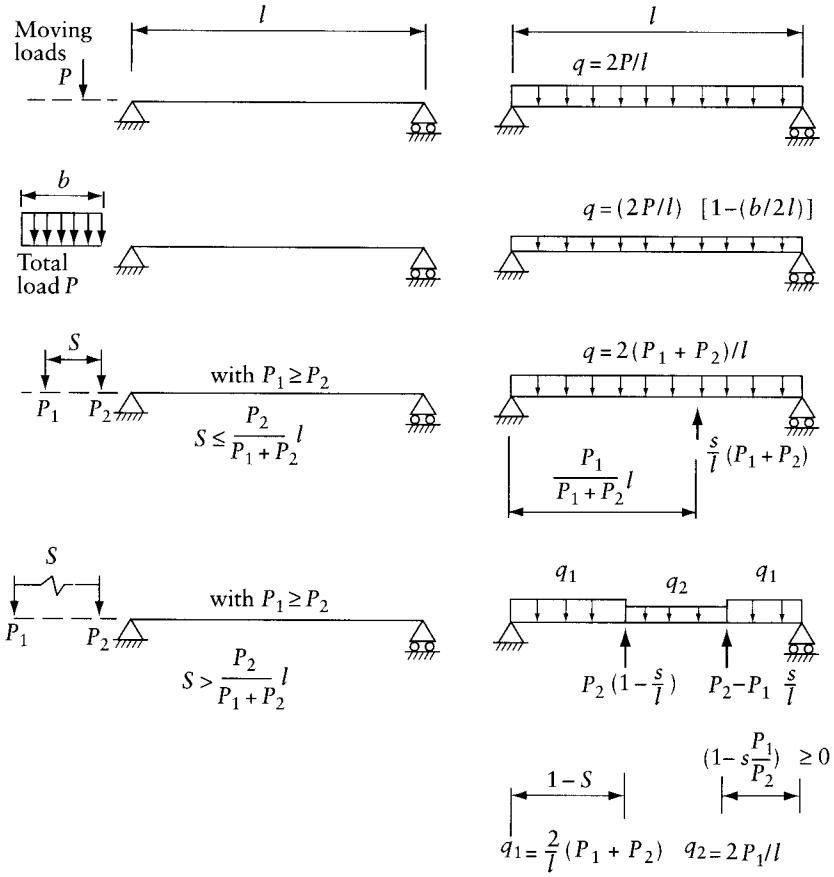

(a) Moving load system

(b) Virtual stationary load system

Prob. 2.7

2.11 The beam in Prob. 2.4i, without the loads shown, is subjected to two moving loads $P_1 = P$ and $P_2 = 0.8P$ spaced at a distance $s = 0.3l$, with P_1 on the left-hand side of P_2. Find:

(a) The maximum positive and the maximum negative bending moment diagrams for part DC.
(b) The influence line of the bending moment at section n at a distance $(17/30)l$ from C.

Use the influence line to check the ordinates at n of the diagrams determined in (a).

2.12 A prismatic reinforced concrete cantilever subjected to an externally applied twisting couple T is shown in cross section in (a). The structure is idealized as a space truss shown in pictorial view in (b) (strut-and-tie model, see Section 1.13). For clarity, the members in the bottom horizontal plane of the truss, not shown in (b), are shown in top view in (c); similarly, the members in the vertical far side of the truss, not shown in (b), are shown in elevation in (d). The applied couple T is represented by component forces, each $= T/(2l)$

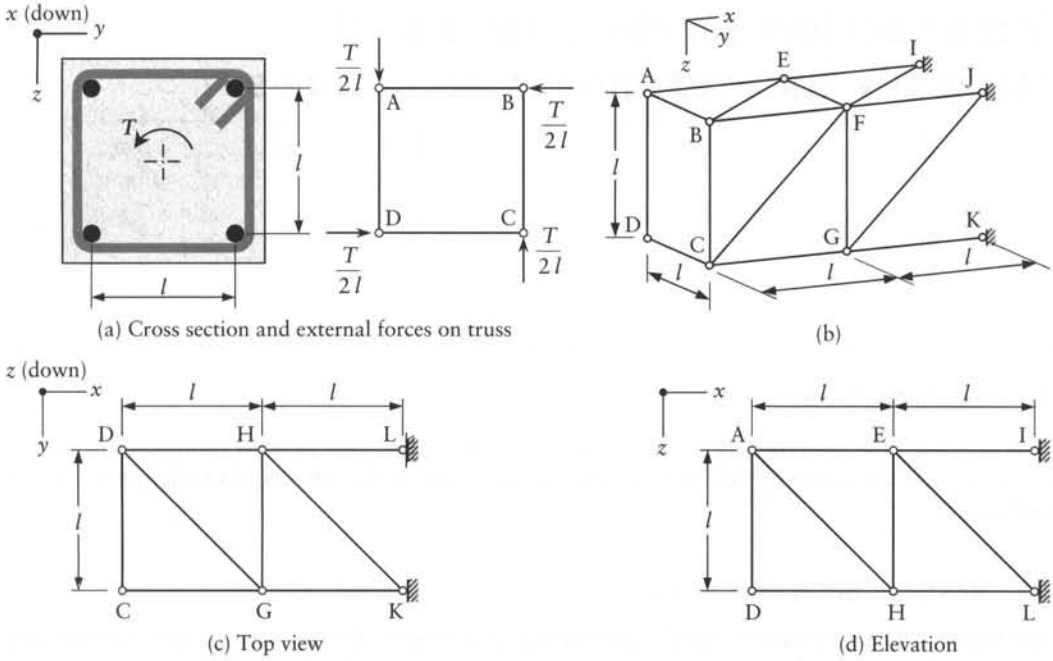

(a) Cross section and external forces on truss

(b)

(c) Top view

(d) Elevation

Prob. 2.12

at nodes A, B, C, and D as shown in (a). Find the forces in the members and the reaction components at I, J, K, and L. The answer will show that the members in the x direction are tensile and resisted by the longitudinal reinforcing bars; the transverse members in the y and z directions are also tensile and resisted by the legs of the stirrups; the diagonal members are in compression and resisted by concrete.

Chapter 3

Introduction to the analysis of statically indeterminate structures

3.1 Introduction

This chapter develops concepts which are necessary for the two general methods of analysis of structures: the force method and the displacement method (considered in Chapters 4 and 5 respectively).

3.2 Statical indeterminacy

The analysis of a structure is usually carried out to determine the reactions at the supports and the internal stress resultants. As mentioned earlier, if these can be determined entirely from the equations of statics alone, then the structure is statically determinate. This book deals mainly with statically indeterminate structures, in which there are more unknown forces than equations. The majority of structures in practice are statically indeterminate.

The indeterminacy of a structure may either be *external, internal*, or both. A structure is said to be externally indeterminate if the number of reaction components exceeds the number of equations of equilibrium. Thus, a space structure is in general externally statically indeterminate when the number of reaction components is more than six. The corresponding number in a plane structure is three. The structures in Figures 2.1a, c, e, f, g and h are examples of external indeterminacy. Each of the beams of Figures 3.1a and b has four reaction components. Since there are only three equations of static equilibrium, there is one unknown force in excess of those that can be found by statics, and the beams are externally statically indeterminate. We define the degree of indeterminacy as the number of unknown forces in excess of the equations of statics. Thus, the beams of Figures 3.1a and b are indeterminate to the first degree.

Some structures are built so that the stress resultant at a certain section is known to be zero. This provides an additional equation of static equilibrium and allows the determination of an additional reaction component. For instance, the three-hinged frame of Figure 3.1c has four reaction components, but the bending moment at the central hinge must vanish. This condition, together with the three equations of equilibrium applied to the structure as a free body, is sufficient to determine the four reaction components. Thus, the frame is statically determinate. The continuous beam of Figure 3.1d has five reaction components and one internal hinge. Four equilibrium equations can therefore be written so that the beam is externally indeterminate to the first degree.

Let us now consider structures which are externally statically determinate but internally indeterminate. For instance, in the truss[1] of Figure 3.2a, the forces in the members cannot be determined by the equations of statics alone. If one of the two diagonal members is removed (or cut) the forces in the members can be calculated from equations of statics. Hence, the truss is

1 A truss is pin-jointed; a frame is rigid-jointed.

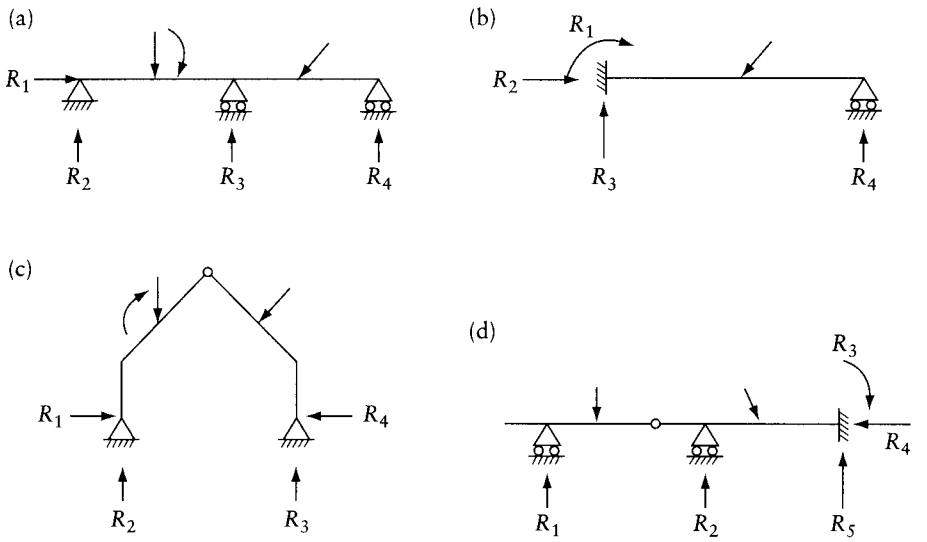

Figure 3.1 (a), (b) and (d) Externally statically indeterminate structures. (c) Statically determinate three-hinged frame.

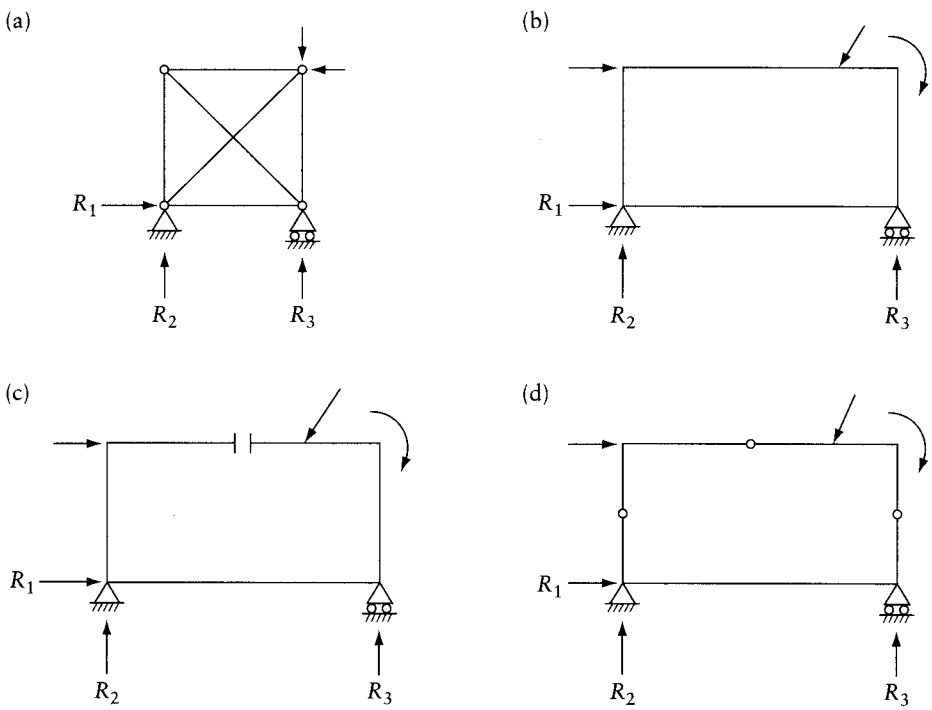

Figure 3.2 Internally statically indeterminate structures.

internally indeterminate to the first degree, although it is externally determinate. The frame in Figure 3.2b is internally indeterminate to the third degree: it becomes determinate if a cut is made in one of the members (Figure 3.2c). The cut represents the removal or *release* of three stress resultants: axial force, shearing force, and bending moment. The number of releases necessary to make a structure statically determinate represents the degree of indeterminacy. The same frame becomes determinate if the releases are made by introducing three hinges as in Figure 3.2d, thus removing the bending moment at three sections.

Structures can be statically indeterminate both internally and externally. The frame of Figure 3.3a is externally indeterminate to the first degree, but the stress resultants cannot be determined by statics even if the reactions are assumed to have been found previously. They can, however, be determined by statics if the frame is cut at two sections, as shown in Figure 3.3b, thus providing six releases. It follows that the frame is internally indeterminate to the sixth degree, and the total degree of indeterminacy is seven.

The space frame of Figure 3.4 has six reaction components at each support: three components X, Y, and Z and three couples M_x, M_y, and M_z. To avoid crowding the figure, the six components are shown at one of the four supports only. The moment vectors are indicated by double-headed arrows.[2] Thus, the number of reaction components of the structure is 24, while the equations of

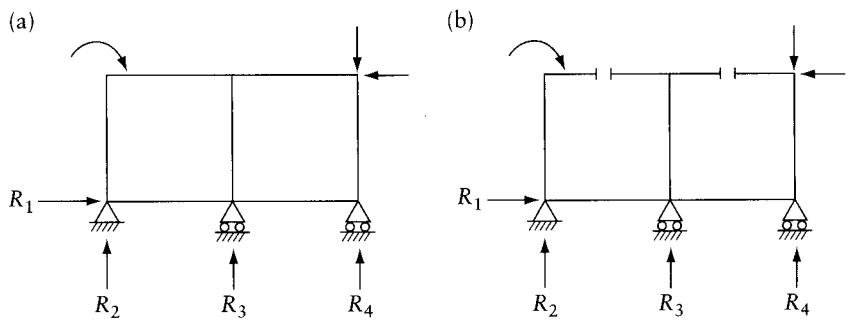

Figure 3.3 Frame that is statically indeterminate both externally and internally.

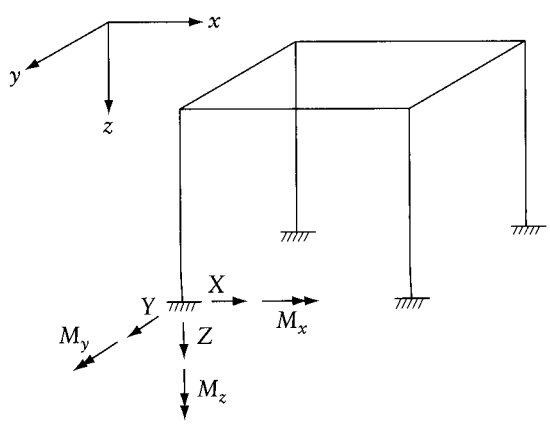

Figure 3.4 Rigid-jointed space frame.

2 All through this text, a moment or a rotation is indicated either by an arrow in the form of an arc of a circle (planar structures) or by a double-headed arrow (space structures): see footnote 1 in Chapter 2.

equilibrium that can be written are six in number (cf. Eq. 2.4). The frame is therefore externally indeterminate to the 18th degree. If the reactions are known, the stress resultants in the four columns can be determined by statics but the beams forming a closed frame cannot be analyzed by statics alone. Cutting one of the beams at one section makes it possible to determine the stress resultants in all the beams. The number of releases in this case is six: axial force, shear in two orthogonal directions, bending moment about two axes and twisting moment. The structure is thus internally indeterminate to the sixth degree, and the total degree of indeterminacy is 24.

The members of the horizontal grid of Figure 3.5a are assumed to be rigidly connected (as shown in Figure 3.5b) and to be subjected to vertical loads only. Thus, both the reaction components X, Z, and M_y and the stress resultants X, Z and M_y, vanish for all members of the grid. Hence, the number of equilibrium equations which can be used is three only. The reaction components at each support are Y, M_x, and M_z, so that the number of reaction components for the whole structure is $8 \times 3 = 24$. Thus, it is externally statically indeterminate to the 21st degree.

If the reactions are known, the stress resultants in the beams of the grid can be determined by statics alone except for the central part $ABCD$, which is internally statically indeterminate. Cutting any of the four beams of this part ($ABCD$) in one location produces three releases and makes it possible for the stress resultants to be determined by the equations of statics alone. Thus, the structure is internally indeterminate to the third degree, and the total degree of indeterminacy is 24.

If the members forming the grid are not subjected to torsion – which is the case if the beams of the grid in one direction cross over the beams in the other direction with hinged connections (Figure 3.5c) or when the torsional rigidity of the section is negligible compared with its bending stiffness – the twisting moment component (M_z in Figure 3.5a) vanishes and the structure

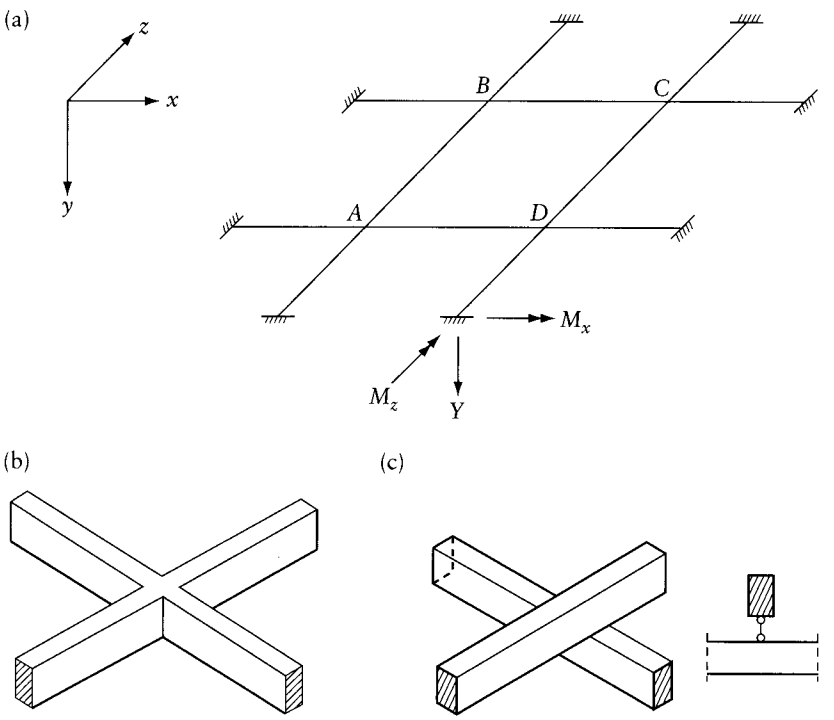

Figure 3.5 Statical indeterminacy of a grid. (a) Grid. (b) Rigid connection of beams. (c) Hinged connection of beams.

becomes indeterminate to the 12th degree. The grid needs at least four simple supports for stability and becomes statically determinate if the fixed supports are removed and only four hinged supports are provided. Each hinged support has one reaction component in the y direction. Since the number of reaction components in the original grid is 16, it is externally indeterminate to the 12th degree. This number is equal to the number of reaction components minus the four reaction components in the y direction mentioned above. There is no internal indeterminacy and, once the reactions have been determined, the internal forces in all the beams of the grid can be found by simple statics.

3.3 Expressions for degree of indeterminacy

In Section 3.2 we found the degree of indeterminacy of various structures by inspection or from the number of releases necessary to render the structure statically determinate. For certain structures, especially those with a great many members, such an approach is difficult, and the use of a formal procedure is preferable.

Let us therefore consider a *plane* truss with three reaction components, m members and j hinged (pinned) joints (including the supports, which are also hinged). The unknown forces are the three reaction components and the force in each member – that is, $3+m$. Now, at each joint two equations of equilibrium can be written:

$$\Sigma F_x = 0 \quad \Sigma F_y = 0 \tag{3.1}$$

the summation being for the components of all the external and internal forces meeting at the joint. Thus, the total number of equations is $2j$.

For statical determinacy, the number of equations of statics is the same as the number of unknowns, that is,

$$2j = m + 3 \tag{3.2}$$

Providing the structure is stable, some interchange between the number of members and the number of reaction components r is possible, so that for overall determinacy the condition

$$2j = m + r \tag{3.3}$$

has to be satisfied. The degree of indeterminacy is then

$$i = (m + r) - 2j \tag{3.4}$$

For the truss shown in Figure 3.6, $r = 4$, $m = 18$, and $j = 10$. Hence, $i = 2$.

In the case of a pin-jointed *space* frame, three equations of equilibrium can be written, viz.

$$\Sigma F_x = 0 \quad \Sigma F_y = 0 \quad \Sigma F_z = 0 \tag{3.5}$$

the summation again being for all the internal and external forces meeting at the joint. The total number of equations is $3j$, and the condition of determinacy is

$$3j = m + r \tag{3.6}$$

The degree of indeterminacy is

$$i = (m + r) - 3j \tag{3.7}$$

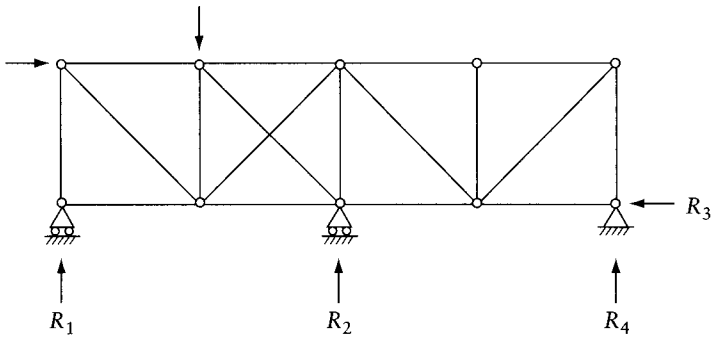

Figure 3.6 Statically indeterminate plane truss.

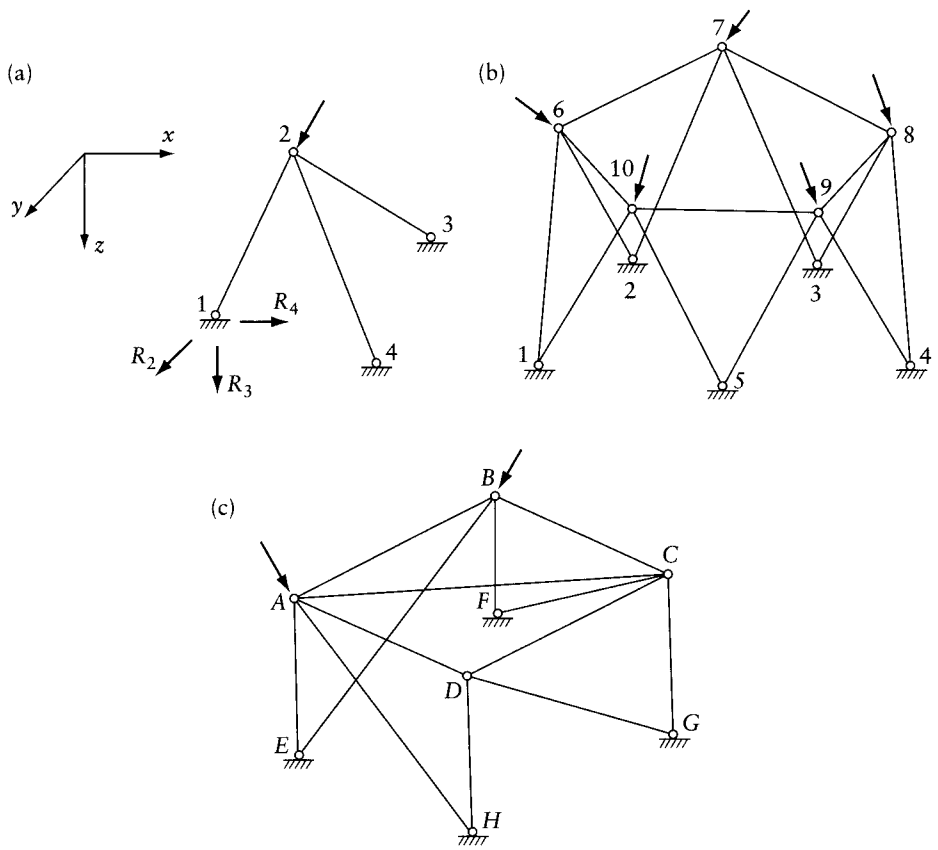

Figure 3.7 Space trusses. (a) and (b) Statically determinate. (c) Statically indeterminate.

The use of these expressions can be illustrated with reference to Figure 3.7. For the truss of Figure 3.7a, $j = 4$, $m = 3$, and $r = 9$, there being three reaction components at each support. Thus, Eq. 3.6 is satisfied and the truss is statically determinate.

In the truss of Figure 3.7b, $j = 10$, $m = 15$, and $r = 15$. Hence, again Eq. 3.6 is satisfied.

However, for the truss of Figure 3.7c, $j = 8$, $m = 13$, and $r = 12$, so that from Eq. 3.7, $i = 1$. Removal of member AC would render the truss determinate.

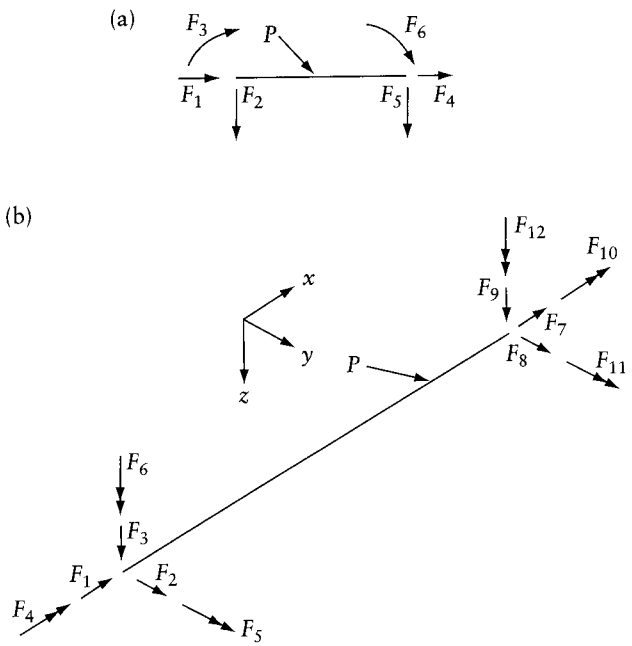

Figure 3.8 End-forces in a member of a rigid-jointed frame. (a) Plane frame. (b) Space frame.

Expressions similar to those of Eqs. 3.4 and 3.7 can be established for frames with rigid joints. At a rigid joint of a *plane* frame, two resolution equations and one moment equation can be written. The stress resultants in any member of a plane frame (Figure 3.8a) can be determined if any three of the six end-forces $F_1, F_2, \ldots, F_6$ are known, so that each member represents three unknown internal forces. The total number of unknowns is equal to the sum of the number of unknown reaction components r and of the unknown internal forces. Thus, a rigid-jointed plane frame is statically determinate if

$$3j = 3m + r \tag{3.8}$$

and the degree of indeterminacy is

$$i = (3m + r) - 3j \tag{3.9}$$

In these equations j is the total number of rigid joints including the supports and m is the number of members.

If a rigid joint within the frame is replaced by a hinge, the number of equilibrium equations is reduced by one but the bending moments at the ends of the members meeting at the joint vanish, so that the number of unknowns is reduced by the number of members meeting at the hinge. This modification has to be observed when applying Eqs. 3.8 and 3.9 to plane frames with mixed type joints. We should note that at a rigid joint where more than two members meet and one of the members is connected to the joint by a hinge, the number of unknowns is reduced by one, without a reduction in the number of equilibrium equations. For example, we can verify that the frame of Prob. 3.5 is four times statically indeterminate, and the degree of indeterminacy becomes three if a hinge is inserted at the left end of member CF (just to the right of C).

As an example of rigid-jointed plane frame, let us consider the frame of Figure 3.3a: $j = 6$, $m = 7$, and $r = 4$. From Eq. 3.9 the degree of indeterminacy $i = (3 \times 7 + 4) - 3 \times 6 = 7$, which is the same result as that obtained in Section 3.2. For the frame of Figure 3.1c, $j = 5$, $m = 4$, and $r = 4$. However, one of the internal joints is a hinge, so that the number of unknowns is $(3m + r - 2) = 14$ and the number of equilibrium equations is $(3j - 1) = 14$. The frame is therefore statically determinate, as found before.

At a rigid joint of a *space* frame, three resolution and three moment equations can be written. The stress resultants in any members can be determined if any six of the twelve end-forces shown in Figure 3.8b are known, so that each member represents six unknown forces. A space frame is statically determinate if

$$6j = 6m + r \tag{3.10}$$

and the degree of indeterminacy is

$$i = (6m + r) - 6j \tag{3.11}$$

Applying Eq. 3.11 to the frame of Figure 3.4, we have $m = 8$, $r = 24$, and $j = 8$. From Eq. 3.11, $i = 24$, which is, of course, the same as the result obtained in Section 3.2.

Consider a grid with rigid connections (Figures 3.5a and b). Three equations of equilibrium can be written at any joint ($\Sigma F_y = 0$; $\Sigma M_x = 0$; $\Sigma M_z = 0$). Member end-forces are three, representing a shearing force in the y direction, a twisting moment, and a bending moment. The internal forces at any section can be determined when three of the six member end-forces are known; thus, each member represents three unknown forces. A grid with rigid joints is statically determinate when

$$3j = 3m + r \tag{3.12}$$

when this condition is not satisfied, the degree of indeterminacy is

$$i = (3m + r) - 3j \tag{3.13}$$

When the connections of grid members are hinged as shown in Figure 3.5c, the members are not subjected to torsion and the degree of indeterminacy is

$$i = (2m + r) - (3j + 2\bar{j}) \tag{3.14}$$

Although torsion is absent, three equations of equilibrium can be applied at a joint connecting two or more members running in different directions, e.g. joints A, B, C, and D in Figure 3.5a when the connections are of the type shown in Figure 3.5c. The three equations are: sum of the end-forces in the y direction equals zero and sum of the components of the end moments in x and z directions equals zero. The symbol j in Eq. 3.14 represents the number of joints for which three equations can be written. But only two equilibrium equations (one resolution and one moment equation) can be written for a joint connected to one member (e.g. at the supports in Figure 3.5a) or to two members running in the same direction. The symbol $\bar{j}$ in Eq. 3.14 represents the number of joints of this type.

We can apply Eq. 3.13 or 3.14 to verify that for the grid in Figure 3.5a, $i = 24$ or 12 respectively when the connections are rigid or hinged (Figure 3.5b or c).

For each type of framed structure, the relation between the numbers of joints, members, and reaction components must apply when the structure is statically determinate (e.g. Eq. 3.3 or 3.6). However, this does not imply that when the appropriate equation is satisfied the structure is stable. For example, in Figure 3.7b, removal of the member connecting nodes 5 and 10 and

addition of a member connecting nodes 5 and 4 will result in an unstable structure even though it satisfies Eq. 3.6.

3.4 General methods of analysis of statically indeterminate structures

The objective of the analysis of structures is to determine the external forces (reaction components) and the internal forces (stress resultants). The forces must satisfy the conditions of equilibrium and produce deformations compatible with the continuity of the structure and the support conditions. As we have already seen, the equilibrium equations are not sufficient to determine the unknown forces in a statically indeterminate structure, and have to be supplemented by simple *geometrical* relations between the deformations of the structure. These relations ensure the *compatibility* of the deformations with the geometry of the structure and are called *geometry conditions* or *compatibility conditions*. An example of such conditions is that at an intermediate support of a continuous beam there can be no deflection and the rotation is the same on both sides of the support.

Two general methods of approach can be used. The first is the *force or flexibility* method, in which sufficient *releases* are provided to render the structure statically determinate. The released structure undergoes inconsistent deformations, and the inconsistency in geometry is then corrected by the application of additional forces.

The second approach is the *displacement* or *stiffness* method. In this method, restraints are added to prevent movement of the joints, and the forces required to produce the restraint are determined. Displacements are then allowed to take place at the joints until the fictitious restraining forces have vanished. With the joint displacements known, the forces on the structure are determined by superposition of the effects of the separate displacements.

Either the force or the displacement method can be used to analyze any structure. Since, in the force method, the solution is carried out for the forces necessary to restore consistency in geometry, the analysis generally involves the solution of a number of simultaneous equations equal to the number of unknown forces, that is, the number of releases required to render the structure statically determinate. The unknowns in the displacement method are the possible joint translations and rotations. The number of the restraining forces to be added to the structure equals the number of possible joint displacements. This represents another type of indeterminacy, which may be referred to as *kinematic indeterminacy*, and is discussed in the next section. The force and displacement methods themselves are considered in more detail in Chapters 4 and 5.

3.5 Kinematic indeterminacy

When a structure composed of several members is subjected to loads, the joints undergo displacements in the form of rotation and translation. In the displacement method of analysis it is the rotation and translation of the joints that are the unknown quantities.

At a support, one or more of the displacement components are known. For instance, the continuous beam in Figure 3.9 is fixed at C and has roller supports at A and B. The fixity at C prevents any displacement at this end while the roller supports at A and B prevent translation

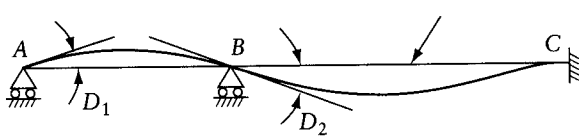

Figure 3.9 Kinematic indeterminacy of a continuous beam.

in the vertical direction but allow rotation. We should note that roller supports are assumed to be capable of resisting both downward and upward forces.

If we assume that the axial stiffness of the beam is so large that the change in its length due to axial forces can be ignored, there will be no horizontal displacements at A or at B. Therefore, the only unknown displacements at the joints are the rotations D_1 and D_2 at A and B respectively (Figure 3.9). The displacements D_1 and D_2 are independent of one another, as either can be given an arbitrary value by the introduction of appropriate forces.

A system of joint displacements is called *independent* if each displacement can be varied arbitrarily and independently of all the others. In the structure in Figure 3.9, for example, the rotations D_1 and D_2 are independent, because any of the two, say, D_1 can be varied while maintaining D_2 unchanged. This can be achieved by applying a couple of appropriate magnitude at A, while preventing the rotation at B by another couple. The number of the independent joint displacements in a structure is called the *degree of kinematic indeterminacy* or the *number of degrees of freedom*. This number is a sum of the degrees of freedom in rotation and in translation. The latter is sometimes called *freedom in sidesway*.

As an example of the determination of the number of degrees of freedom, let us consider the plane frame $ABCD$ of Figure 3.10a. The joints A and D are fixed, and the joints B and C each have three components of displacement $D_1, D_2, \ldots, D_6$, as indicated in the figure. However, if the change in length of the members due to axial forces is ignored, the six displacements are not independent as the translation of the joints B and C is in a direction perpendicular to the original direction of the member. If an arbitrary value is assigned to any one of the translation displacements D_1, D_2, D_4, or D_5, the value of the other three is determined from geometrical relations.

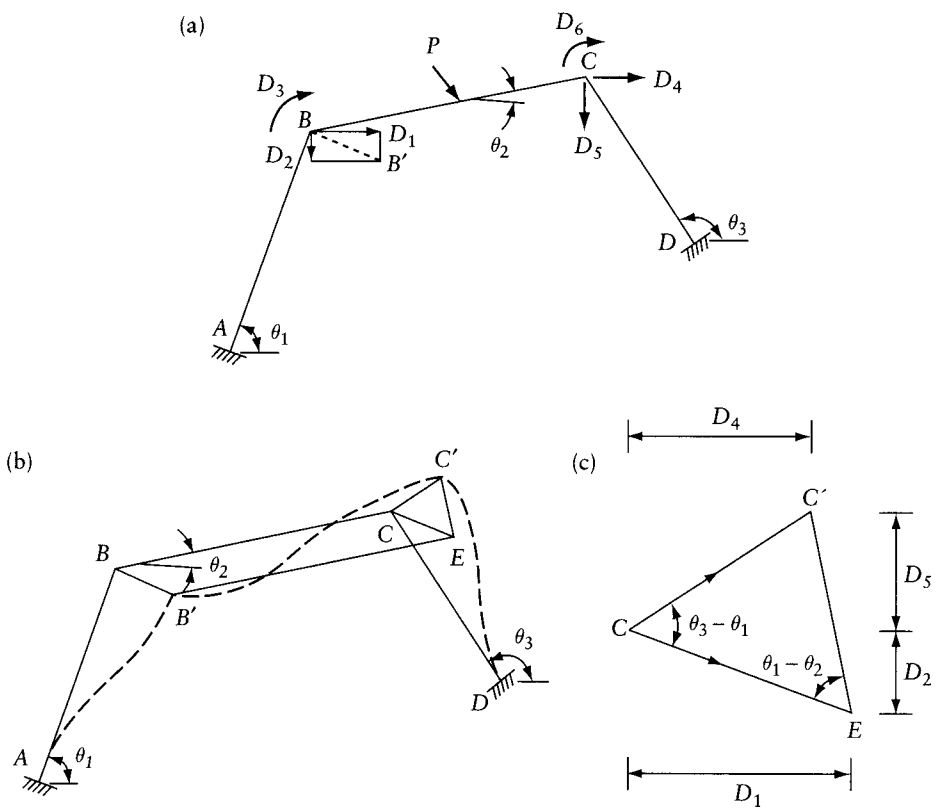

Figure 3.10 (a) Kinematic indeterminacy of a rigid-jointed plane frame. (b) and (c) Displacement diagrams.

For example, if D_1 is assigned a certain value, D_2 is equal to $(D_1 \cot \theta_1)$ to satisfy the condition that the resultant translation at B is perpendicular to AB. Once the position B' (joint B after displacement) is defined, the displaced position C' is defined, since it can have only one location if the lengths BC and CD are to remain unchanged. The joint displacement diagram is shown in Figure 3.10b, in which the displacements D_2, D_4, and D_5 are determined graphically from a given value of D_1. In this figure, BB' is perpendicular to AB, $BCEB'$ is a parallelogram, and EC' and CC' are perpendicular to BC and CD respectively.

From the above discussion, it can be seen that the translation of the joints in the frame considered represents one unknown, or one degree of freedom.

We should note that the translations of the joints are very small compared with the length of the members. For this reason, the translation of the joints is assumed to be along a straight line perpendicular to the original direction of the member rather than along an arc of a circle. The triangle $CC'E$ is drawn to a larger scale in Figure 3.10c, from which the displacements D_2, D_4, and D_5 can be determined. The same displacements can be expressed in terms of D_1 by simple geometrical relations.

Now, the rotations of the joints at B and C are independent of one another. Thus, the frame of Figure 3.10a has one degree of freedom in sidesway and two degrees of freedom in rotation, so that the degree of kinematic indeterminacy for the frame is three. If the axial deformations are not neglected, the four translational displacements are independent and the total degree of kinematic indeterminacy is six.

The plane frame of Figure 3.11 is another example of a kinematically indeterminate structure. If the axial deformation is neglected, the degree of kinematic indeterminacy is two, the unknown joint displacements being rotations at A and at B.

We must emphasize that the kinematic indeterminacy and the statical indeterminacy must not be confused with one another. For instance, the frame of Figure 3.11 has seven reaction components and is statically indeterminate to the fourth degree. If the fixed support at D is replaced by a hinge, the degree of statical indeterminacy will be reduced by one, but at the same time rotation at D becomes possible, thus increasing the kinematic indeterminacy by one. In general, the introduction of a release decreases the degree of statical indeterminacy and increases the degree of kinematic indeterminacy. For this reason, the higher the degree of statical indeterminacy, the more suitable the displacement method for analysis of the structure.

In a pin-jointed truss with all the forces acting at the joints, the members are subjected to an axial load only (without bending moment or shear) and therefore remain straight. The deformed shape of a plane truss is completely defined if the components of the translation in two orthogonal directions are determined for each joint, and each joint – other than a support – has two degrees of freedom.

Thus, the plane structure of Figure 3.12 is kinematically indeterminate to the second degree, as only joint A can have a displacement that can be defined by components in two orthogonal directions. From Eq. 3.4, the degree of statical indeterminacy is three. The addition to the system

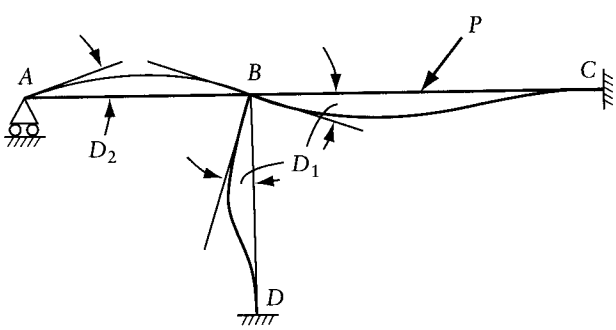

Figure 3.11 Kinematic indeterminacy of a rigid-jointed plane frame.

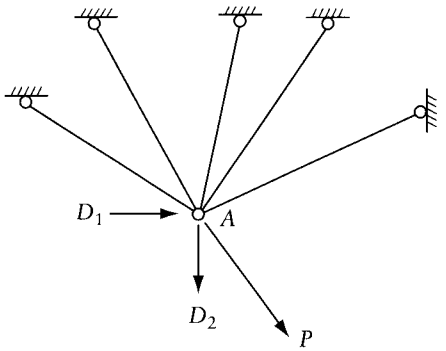

Figure 3.12 Kinematic indeterminacy of a plane truss.

of an extra bar pinned at A at one end and at a support at the other would not change the degree of kinematic indeterminacy, but would increase the degree of statical indeterminacy by one.

In a pin-jointed space truss loaded at the joints only, the translation of the joints can take place in any direction and can therefore be defined by components in three orthogonal directions, so that each joint – other than a support – has three degrees of freedom. It can be easily shown that the degree of kinematic indeterminacy of the truss of Figure 3.7a is 3, that of the truss of Figure 3.7b is 15 and that of the truss in Figure 3.7c is 12.

Each joint of a rigid-jointed space frame can in general have six displacement components: three translations in three orthogonal directions, and three rotations, which can be represented by vectors in each of the three orthogonal directions (double-headed arrows).

Let us consider the frame of Figure 3.13. It has eight joints, of which four are fixed in space. Each of the joints A, B, C, and D can have six displacements such as those shown at A. The degree of kinematic indeterminacy of the frame is therefore $4 \times 6 = 24$.

If the axial deformations are neglected, the lengths of the four columns remain unchanged so that the component D_3 of the translation in the vertical direction vanishes, thus reducing the unknown displacements by four. Also, since the lengths of the horizontal members do not change, the horizontal translations in the x direction of joints A and D are equal; the same applies to the joints B and C. Similarly, the translations in the y direction of joints A and B are equal; again, the same is the case for joints C and D. All this reduces the unknown displacements by four. Therefore, the degree of kinematic indeterminacy of the frame of Figure 3.13, without axial deformation, is 16.

If a rigid-jointed grid is subjected to loads in the perpendicular direction to the plane of the grid only, each joint can have three displacement components: translation perpendicular to

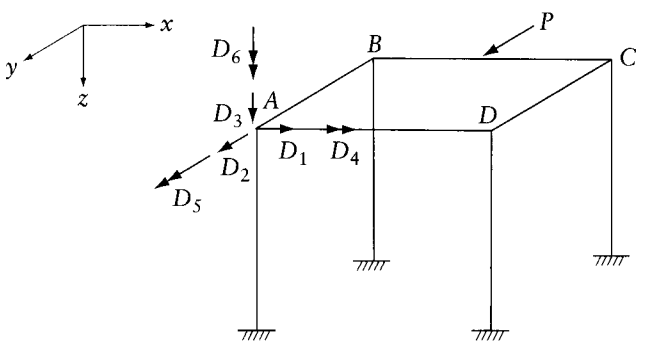

Figure 3.13 Kinematic indeterminacy of a rigid-jointed space frame.

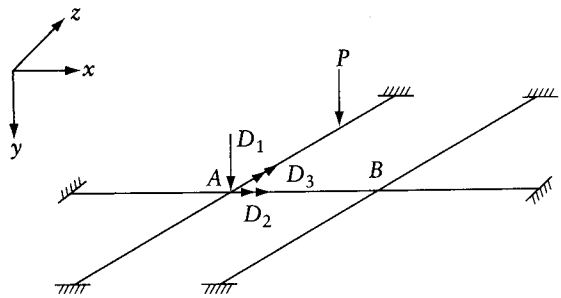

Figure 3.14 Kinematic indeterminacy of a rigid-jointed grid loaded in a direction normal to its plane.

the plane of the grid and rotation about two orthogonal axes in the plane of the grid. Thus, the grid of Figure 3.14 is kinematically indeterminate to the sixth degree. The degree of statical indeterminacy of this grid is 15.

If the beams of a grid in one direction are hinged to the beams in the perpendicular direction in the manner shown in Figure 3.5c, the beams will not be subjected to torsion. Hence, the degree of statical indeterminacy of the grid of Figure 3.14 with hinged connections is eight. On the other hand, the degree of kinematic indeterminacy remains unchanged.

3.6 Principle of superposition

In Section 2.1, we mentioned that when deformations in a structure are proportional to the applied loads the principle of superposition holds. This principle states that the displacement due to a number of forces acting simultaneously is equal to the sum of the displacements due to each force acting separately.

In the analysis of structures it is convenient to use a notation in which a force F_j causes at a point i a displacement D_{ij}. Thus, the first subscript of a displacement describes the position and direction of the displacement, and the second subscript the position and direction of the force causing the displacement. Each subscript refers to a *coordinate* which represents the location and direction of a force or of a displacement. The coordinates are usually indicated by arrows on the diagram of the structure.

This approach is illustrated in Figure 3.15a. If the relation between the force applied and the resultant displacement is linear, we can write

$$D_{i1} = f_{i1}F_1 \tag{3.15}$$

where f_{i1} is the displacement at coordinate i due to a unit force at the location and direction of F_1 (coordinate 1).

If a second force F_2 is applied causing a displacement D_{i2} at i (Figure 3.15b)

$$D_{i2} = f_{i2}F_2 \tag{3.16}$$

where f_{i2} is the displacement at i due to a unit force at coordinate 2.

If several forces $F_1, F_2, \ldots, F_n$ act simultaneously (Fig 3.15c) the total displacement at i is

$$D_i = f_{i1}F_1 + f_{i2}F_2 + \cdots + f_{in}F_n \tag{3.17}$$

Clearly, the total displacement does not depend on the order of the application of the loads. This, of course, does not hold if the stress–strain relation of the material is nonlinear.

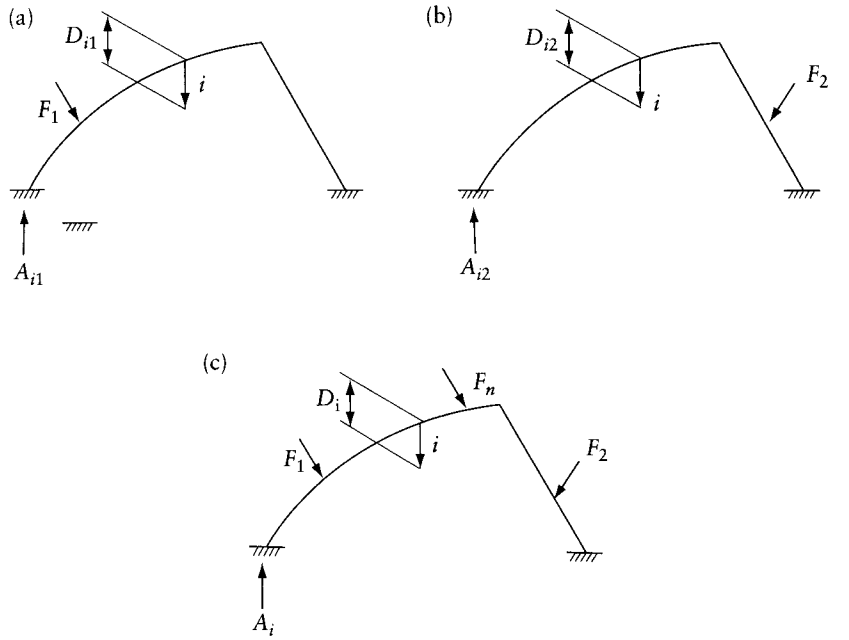

Figure 3.15 Superposition of displacements and forces.

A structure made of material obeying Hooke's law may behave nonlinearly if large changes in the geometry are caused by the applied loads (See Chapter 24). Consider the slender strut in Figure 3.16a subjected to an axial force F_1, not large enough to cause buckling. The strut will, therefore, remain straight, and the lateral displacement at any point A is $D_A = 0$. Now, if the strut is subjected to a lateral load F_2 acting alone, there will be a lateral deflection D_A at points A (Figure 3.16b). If both F_1 and F_2 act (Figure 3.16c), the strut will be subjected to an additional bending moment equal to F_1 multiplied by the deflection at the given section. This additional bending causes additional deflections and the deflection D'_A at A will, in this case, be greater than D_A.

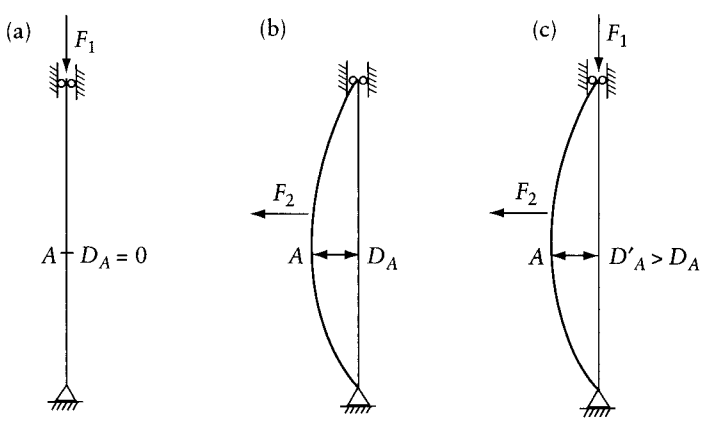

Figure 3.16 Structure to which superposition does not apply.

No such bending moment exists, of course, when the loads F_1 and F_2 act separately, so that the combined effect of F_1 and F_2 is not equal to the sum of their separate effects, and the principle of superposition does not hold.

When a structure behaves linearly, the principle of superposition holds for forces as well as for displacements. Thus, the internal stress resultants at any section or the reaction components of the structure in Figure 3.15c can be determined by adding the effects of the forces $F_1, F_2, \ldots, F_n$ when each acts separately.

Let the symbol A_i indicate a general *action* which may be a reaction, bending moment, shear, or thrust at any section due to the combined effect of all the forces. A general superposition equation of forces can then be written:

$$A_i = A_{ui1}F_1 + A_{ui2}F_2 + \cdots + A_{uin}F_n \tag{3.18}$$

where A_{ui1} is the magnitude of the action A_i when a unit force is applied alone at coordinate 1. Similarly, $A_{ui2}, \ldots, A_{uin}$ are the values of the action A_i when a unit force acts separately at each of the coordinates $2, \ldots, n$.

Equation 3.18 can be written in matrix form:

$$A_i = [A_{ui}]_{1\times n}\{F\}_{n\times 1} \tag{3.19}$$

We should note that the superposition of forces of Eq. 3.18 holds good for statically determinate structures regardless of the shape of the stress–strain relation of the material, provided only that the loads do not cause a distortion large enough to change appreciably the geometry of the structure. In such structures, any action can be determined by equations of statics alone without considering displacements. On the other hand, in statically indeterminate structures the superposition of forces is valid only if Hooke's law is obeyed because the internal forces depend on the deformation of the members.

3.7 General

The majority of modern structures are statically indeterminate, and with the flexibility method it is necessary to establish for a given structure the degree of indeterminacy, which may be external, internal, or both. In simple cases the degree of indeterminacy can be found by simple inspection, but in more complex or multispan and multibay structures it is preferable to establish the degree of indeterminacy with the aid of expressions involving the number of joints, members, and reaction components. These expressions are available for plane and space trusses (pin-jointed) and frames (rigid-jointed).

Two general methods of analysis of structures are available. One is the force (or flexibility) method, in which releases are introduced to render the structure statically determinate; the resulting displacements are computed and the inconsistencies in displacements are corrected by the application of additional forces in the direction of the releases. Hence, a set of compatibility equations is obtained: its solution gives the unknown forces.

In the other method – the displacement (or stiffness) method – restraints at joints are introduced. The restraining forces required to prevent joint displacements are calculated. Displacements are then allowed to take place in the direction of the restraints until the restraints have vanished; hence, a set of equilibrium equations is obtained: its solution gives the unknown displacements. The internal forces on the structure are then determined by superposition of the effects of these displacements and those of the applied loading with the displacements restrained.

The number of restraints in the stiffness method is equal to the number of possible independent joint displacements, which therefore has to be determined prior to the analysis. The number of independent displacements is the degree of kinematic indeterminacy, which has to be

distinguished from the degree of statical indeterminacy. The displacements can be in the form of rotation or translation.

The analysis of structures by the force or the displacement method involves the use of the principle of superposition, which allows a simple addition of displacements (or actions) due to the individual loads (or displacements). This principle can, however, be applied only if Hooke's law is obeyed by the material of which a statically indeterminate structure is made. In all cases, the displacements must be small compared with the dimensions of the members so that no gross distortion of geometry of the structure takes place.

Problems

3.1 to 3.6 What is the degree of statical indeterminacy of the structure shown below? Introduce sufficient releases to render each structure statically determinate.

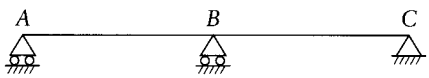

Prob. 3.1

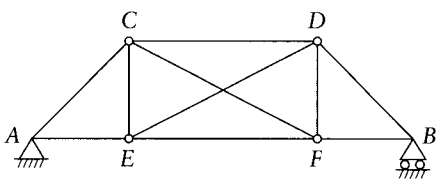

Prob. 3.2

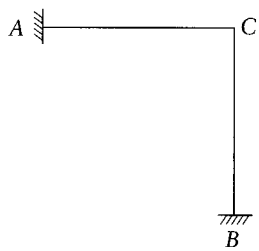

Prob. 3.3

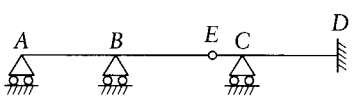

Prob. 3.4

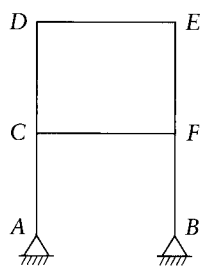

Prob. 3.5

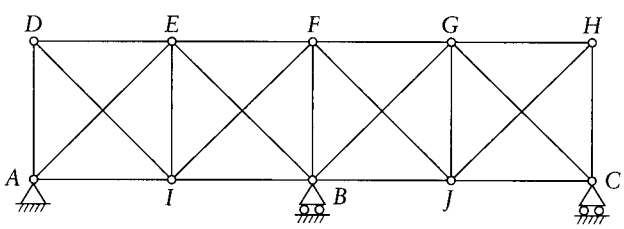

Prob. 3.6

3.7 The bars *AB*, *BC*, and *CD* are rigidly connected and lie in a horizontal plane. They are subjected to vertical loading. What is the degree of statical in determinacy?

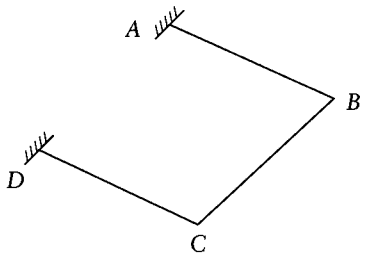

Prob. 3.7

3.8 The horizontal grid shown in the figure is subjected to vertical loads only. What is the degree of statical indeterminacy?

(a) assuming rigid connections at the joints.
(b) assuming connections of the type shown in Figure 3.5c, i.e. a torsionless grid. Introduce sufficient releases in each case to render the structure statically determinate.

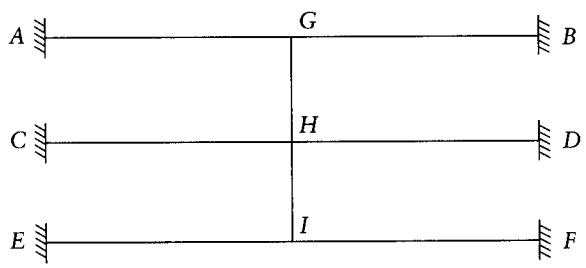

Prob. 3.8

3.9 The figure shows a pictorial view of a space truss pin-jointed to a vertical wall at *A*, *B*, *C*, and *D*. Determine the degree of statical indeterminacy. Introduce sufficient releases to make the structure statically determinate.

3.10 Determine the degree of kinematic indeterminacy of the beam of Prob. 3.1 and indicate a coordinate system of joint displacements. What is the degree of kinematic indeterminacy if the axial deformation is ignored?

3.11 Apply the questions of Prob. 3.10 to the frame of Prob. 3.5.

3.12 What is the degree of kinematic indeterminacy of the rigid-connected grid of Prob. 3.8?

3.13 Introduce sufficient releases to render the structure in the figure statically determinate and draw the corresponding bending moment diagram. Draw the bending moment diagram for another alternative released structure.

3.14 The figure shows a space truss which has two planes of symmetry: *xz* and *yz*. The members are four horizontals, four verticals plus two diagonals in each of five orthogonal planes. Figure (a) is the elevation of one of the four identical sides of the truss. Introduce sufficient releases to make the structure statically determinate, and find the forces in the members of the released structure due to two equal forces *P* at the top node *A*.

3.15 (a) Introduce sufficient releases to make the frame shown statically determinate. Indicate the releases by a set of coordinates.

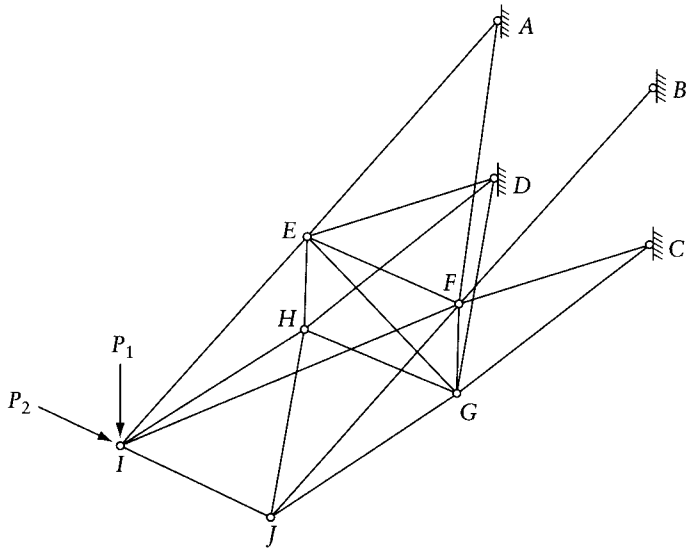

Prob. 3.9

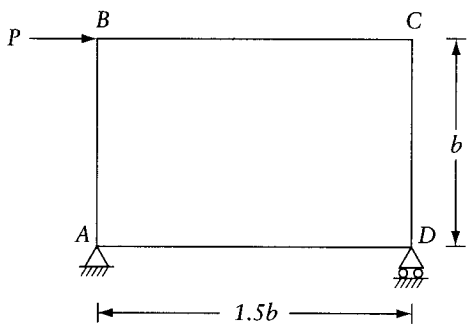

Prob. 3.13

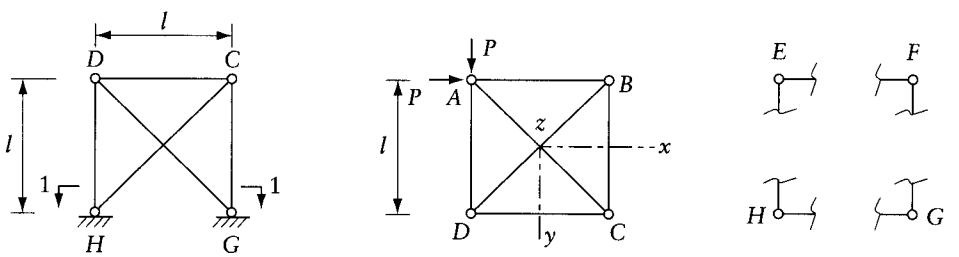

Prob. 3.14

(b) Introduce a hinge at the middle of each member and draw the bending moment diagram for the frame due to two horizontal forces, each equal to P, at E and C. Show by a sketch the magnitude and direction of the reaction components at A.

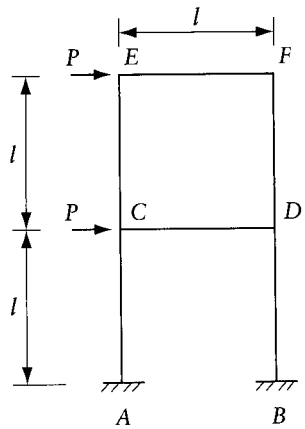

Prob. 3.15

3.16 Verify that the space truss shown is once statically indeterminate. Find the forces in the members and the reaction components with the structure released by the cutting of member BC.

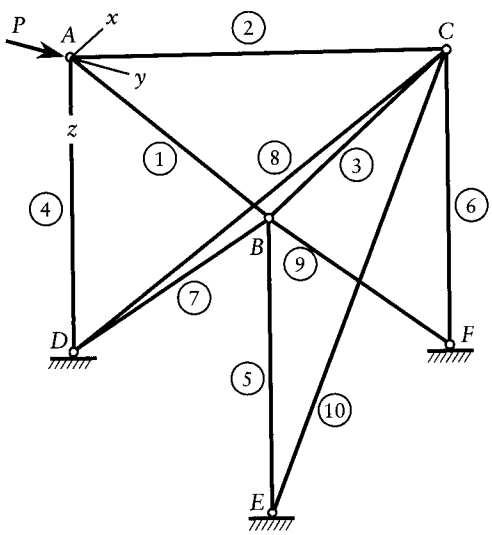

(a) Pictorial view

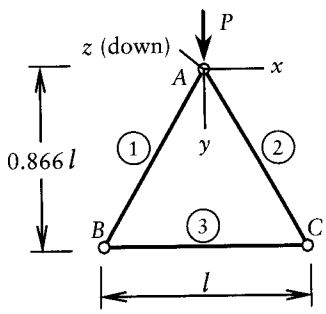

(b) Top view of members: 1, 2 and 3

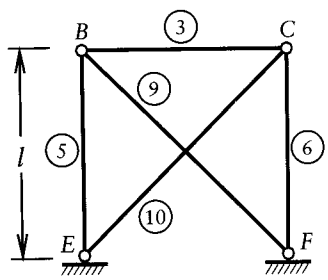

(c) Elevation of members: 3, 5, 6, 9 and 10

Prob. 3.16

Chapter 4

Force method of analysis

4.1 Introduction

As mentioned in Section 3.4, this is one of the basic methods of analysis of structures. It is proposed to outline the procedure in this chapter, and then in Chapter 6 to compare the force and the displacement methods.

4.2 Description of method

The force method involves five steps. They are briefly mentioned here; but they are explained further in examples and in sections below.

1. First of all, the degree of statical indeterminacy is determined. A number of releases equal to the degree of indeterminacy is now introduced, each release being made by the removal of an external or an internal force. The releases must be chosen so that the remaining structure is stable and statically determinate. However, we will learn that in some cases the number of releases can be less than the degree of indeterminacy, provided the remaining statically indeterminate structure is so simple that it can be readily analyzed. In all cases, the released forces, which are also called **redundant forces**, should be carefully chosen so that the released structure is easy to analyze.
2. Application of the given loads on the released structure will produce displacements that are inconsistent with the actual structure, such as a rotation or a translation at a support where this displacement must be zero. In the second step these inconsistencies or "errors" in the released structure are determined. In other words, we calculate the magnitude of the "errors" in the displacements corresponding to the redundant forces. These displacements may be due to external applied loads, settlement of supports, or temperature variation.
3. The third step consists of a determination of the displacements in the released structure due to unit values of the redundants (cf. Figures 4.1d and e). These displacements are required at the same location and in the same direction as the error in displacements determined in step 2.
4. The values of the redundant forces necessary to eliminate the errors in the displacements are now determined. This requires the writing of super position equations in which the effects of the separate redundants are added to the displacements of the released structure.
5. Hence, we find the forces on the original indeterminate structure: they are the sum of the correction forces (redundants) and forces on the released structure.

This brief description of the application of the force method will now be illustrated by examples.

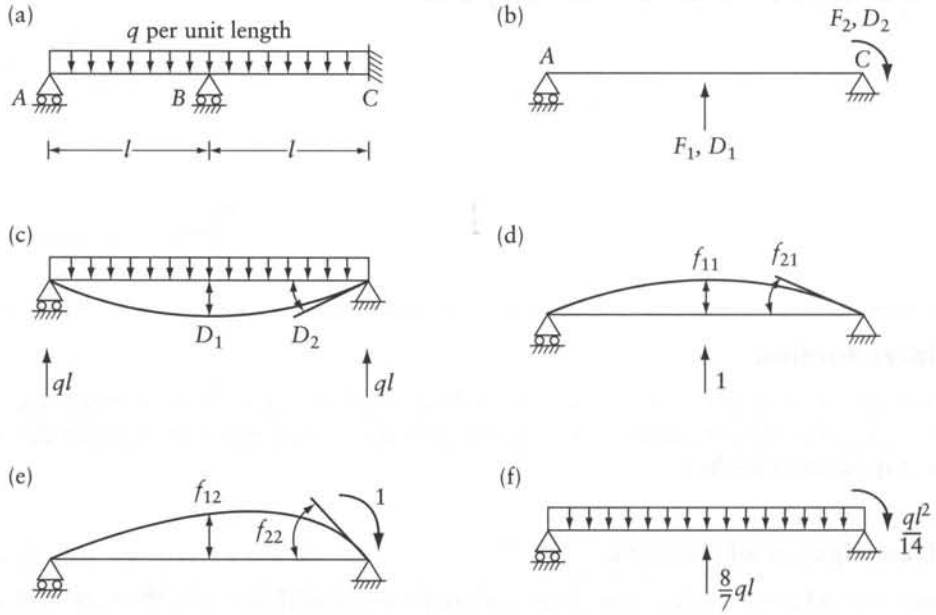

Figure 4.1 Continuous beam considered in Example 4.1. (a) Statically indeterminate beam. (b) Coordinate system. (c) External load on released structure. (d) $F_1 = 1$. (e) $F_2 = 1$. (f) Redundants.

Example 4.1: Structure with degree of indeterminacy = 2

Figure 4.1a shows a beam ABC fixed at C, resting on roller supports at A and B, and carrying a uniform load of q per unit length. The beam has a constant flexural rigidity EI. Find the reactions of the beam.

Coordinate system

Step 1 The structure is statically indeterminate to the second degree, so that two redundant forces have to be removed. Several choices are possible, e.g. the moment and the vertical reaction at C, or the vertical reactions at A and B. For the purposes of this example, we shall remove the vertical reaction at B and the moment at C. The released structure is then a simple beam AC with redundant forces and displacements as shown in Figure 4.1b. The location and direction of the various redundants and displacements are referred to as a coordinate system.

The positive directions of the redundants F_1 and F_2 are chosen arbitrarily but the positive directions of the displacements at the same location must always accord with those of the redundants. The arrows in Figure 4.1b indicate the chosen positive directions in the present case and, since the arrows indicate forces as well as displacements, it is convenient in a general case to label the coordinates by numerals 1, 2, ..., n.

Step 2 Following this system, Figure 4.1c shows the displacements at B and C as D_1 and D_2 respectively. In fact, as shown in Figure 4.1a, the actual displacements at those points are zero, so that D_1 and D_2 represent the inconsistencies in deformation.

The magnitude of D_1 and D_2 can be calculated from the behavior of the simply-supported beam of Figure 4.1c. For the present purposes, we can use Eqs. B.1 and B.3, Appendix B. Thus,

$$D_1 = -\frac{5ql^4}{24EI} \quad \text{and} \quad D_2 = -\frac{ql^3}{3EI}$$

The negative signs show that the displacements are in directions opposite to the positive directions chosen in Figure 4.1b.

It is good practice to show the selected coordinate system in a separate figure, such as Figure 4.1b, rather than adding arrows to Figure 4.1a. The arbitrary directions selected for the arrows establish the force and displacement sign convention which must be adhered to throughout the analysis. Note that when the release is for an internal force, it must be represented in the coordinate system by a pair of arrows in opposite directions (Figure 4.7) and the corresponding displacement will be the relative translation or relative rotation of the two sections on either side of the coordinate.

Step 3 The displacements due to unit values of the redundants are shown in Figures 4.1d and e. These displacements are as follows (Eqs. B.7–9 and B.12, Appendix B):

$$f_{11} = \frac{l^3}{6EI} \qquad f_{12} = \frac{l^2}{4EI}$$

$$f_{21} = \frac{l^2}{4EI} \qquad f_{22} = \frac{2l}{3EI}$$

The general coefficient f_{ij} represents the displacement at the coordinate i due to a unit redundant at the coordinate j.

Geometry relations (compatibility equations)

Step 4 The *geometry relations* express the fact that the final vertical translation at B and the rotation at C vanish. The final displacements are the result of the superposition of the effect of the external loading and of the redundants on the released structure. Thus, the geometry relations can be expressed as

$$\left.\begin{aligned} D_1 + f_{11}F_1 + f_{12}F_2 = 0 \\ D_2 + f_{21}F_1 + f_{22}F_2 = 0 \end{aligned}\right\} \tag{4.1}$$

A more general form of Eq. 4.1 is

$$\left.\begin{aligned} D_1 + f_{11}F_1 + f_{12}F_2 = \Delta_1 \\ D_2 + f_{21}F_1 + f_{22}F_2 = \Delta_2 \end{aligned}\right\} \tag{4.2}$$

where Δ_1 and Δ_2 are prescribed displacements at coordinates 1 and 2 in the actual structure. If, in the example considered, the analysis is required for the combined effects of the given load q and a downward settlement δ_B of support B (Figure 4.1a), we must substitute $\Delta_1 = -\delta_B$, $\Delta_2 = 0$; see Example 4.3, case (2).

Flexibility matrix

The relations of Eq. 4.2 can be written in matrix form:

$$[f]\{F\} = \{\Delta - D\} \tag{4.3}$$

where

$$\{D\} = \begin{Bmatrix} D_1 \\ D_2 \end{Bmatrix} \qquad [f] = \begin{bmatrix} f_{11} & f_{12} \\ f_{21} & f_{22} \end{bmatrix} \qquad \text{and} \qquad \{F\} = \begin{Bmatrix} F_1 \\ F_2 \end{Bmatrix}$$

(The necessary elements of the matrix algebra are given in Appendix A.)

The column vector $\{\Delta - D\}$ depends on the external loading. The elements of the matrix $[f]$ are displacements due to the unit values of the redundants. Therefore, $[f]$ depends on the properties of the structure, and represents the *flexibility* of the released structure. For this reason, $[f]$ is called the flexibility matrix and its elements are called *flexibility coefficients.*

We should note that the elements of a flexibility matrix are not necessarily dimensionally homogeneous as they represent either a translation or a rotation due to a unit load or to a couple. In the above example, f_{11} is a translation due to a unit concentrated load; thus, f_{11} has units (length/force) (e.g. m/N or in./kip). The coefficient f_{22} is a rotation in radians due to a unit couple; thus, its units are (force length)$^{-1}$. Both f_{12} and f_{21} are in (force)$^{-1}$ because f_{12} is a translation due to a unit couple, and f_{21} is a rotation due to a unit load.

The elements of the vector $\{F\}$ are the redundants which can be obtained by solving Eq. 4.3; thus,

$$\{F\} = [f]^{-1}\{\Delta - D\} \tag{4.4}$$

In the example considered, the order of the matrices $\{F\}$, $[f]$, and $\{D\}$ is 2×1, 2×2, 2×1. In general, if the number of releases is n, the order will be $n \times 1$, $n \times n$, $n \times 1$ respectively. We should note that $[f]$ is a square symmetrical matrix. The generality of this property of the flexibility matrix will be proved in Section 6.6.

In the example considered, the flexibility matrix and its inverse are

$$[f] = \begin{bmatrix} \dfrac{l^3}{6EI} & \dfrac{l^2}{4EI} \\ \dfrac{l^2}{4EI} & \dfrac{2l}{3EI} \end{bmatrix} \tag{4.5}$$

and

$$[f]^{-1} = \frac{12EI}{7l^3} \begin{bmatrix} 8 & -3l \\ -3l & 2l^2 \end{bmatrix} \tag{4.6}$$

The displacement vector is

$$\{\Delta - D\} = \frac{ql^3}{24EI} \begin{Bmatrix} 5l \\ 8 \end{Bmatrix}$$

Substituting in Eq. 4.4, or solving Eq. 4.3, we obtain

$$\{F\} = \frac{ql}{14} \begin{Bmatrix} 16 \\ l \end{Bmatrix}$$

Therefore, the redundants are

$$F_1 = \frac{8}{7}ql \qquad \text{and} \qquad F_2 = \frac{ql^2}{14}$$

The positive sign indicates that the redundants act in the positive directions chosen in Figure 4.1b.

It is important to note that the flexibility matrix is dependent on the choice of redundants: with different redundants, the same structure would result in a different flexibility matrix.

Step 5 The final forces acting on the structure are shown in Figure 4.1f, and any stress resultants in the structure can be determined by the ordinary methods of statics.

The reactions and the internal forces can also be determined by the superposition of the effect of the external loads on the released structure and the effect of the redundants. This can be expressed by the superposition equation

$$A_i = A_{si} + (A_{ui1}F_1 + A_{ui2}F_2 + \cdots + A_{uin}F_n) \tag{4.7}$$

where

A_i = any action i, that is, reaction at a support, shearing force, axial force, twisting moment, or bending moment at a section in the actual structure

A_{si} = same action as A_i but in the released structure subjected to the external loads

$A_{ui1}, A_{ui2}, \ldots, A_{uin}$ = corresponding action due to a unit force acting alone on the released structure at the coordinate 1, 2, ..., n, respectively

$F_1, F_2, \ldots, F_n$ = redundants acting on the released structure

From Eq. 3.18, the term in parentheses in Eq. 4.7 represents the action of all the redundants applied simultaneously to the released structure.

Generally, several reactions and internal forces are required. These can be obtained by equations similar to Eq. 4.7. If the number of actions is m, the system of equations needed can be put in the matrix form

$$\{A\}_{m\times 1} = \{A_s\}_{m\times 1} + [A_u]_{m\times n}\{F\}_{n\times 1} \tag{4.8}$$

The order of each matrix is indicated in Eq. 4.8 but it may be helpful to write, on this occasion, the matrices in full. Thus,

$$\{A\} = \begin{Bmatrix} A_1 \\ A_2 \\ \cdots \\ A_m \end{Bmatrix} \qquad \{A_s\} = \begin{Bmatrix} A_{s1} \\ A_{s2} \\ \cdots \\ A_{sm} \end{Bmatrix} \qquad [A_u] = \begin{bmatrix} A_{u11} & A_{u12} & \cdots & A_{u1n} \\ A_{u21} & A_{u22} & \cdots & A_{u2n} \\ \cdots & \cdots & \cdots & \cdots \\ A_{um1} & A_{um2} & \cdots & A_{umn} \end{bmatrix}$$

4.3 Released structure and coordinate system

In the first step of the force method, it is necessary to draw a figure showing the released structure and a system of numbered arrows. The arrows indicate the locations and the positive directions of the statically indeterminate forces removed from the structure. The removed forces (the releases) can be external, such as the reaction components. As an example, see Figure 4.1b which indicates the removal of reaction components represented by arrows (coordinates) 1 and 2. The release can also be achieved by the removal of internal forces, e.g. by cutting a member or by introducing a hinge.

When the released force is external, it is to be represented by a single arrow. But, when the released force is internal, e.g. an axial force, a shearing force or a bending moment, it must be represented by a pair of arrows pointing in opposite directions. Each pair represents a coordinate and thus bears one number (e.g. Figure 4.4b).

The remaining steps of the force method involve the calculation and the use of forces and displacements at the coordinates defined in the first step. Thus, it is impossible to follow or check the calculated forces or displacements (particularly their signs) when the coordinate system is not defined. For this reason, we recommend that the released structure and the coordinate system be represented by a figure that does not show the external applied forces. It should only show a released structure and a set of numbered single arrows, when the released forces are external, or pairs of arrows, when the released forces are internal.

4.3.1 *Use of coordinate represented by a single arrow or a pair of arrows*

A coordinate indicates the location and the direction of a force or a displacement. A single arrow represents an external force (e.g. a reaction component) or a displacement in the direction of the arrow. The force can be a concentrated load or a couple; the displacement will then be a translation or a rotation respectively. Coordinates 1 and 2 in Figure 4.1b represent a vertical reaction at B and a couple (a moment) component of the reaction at C; the same coordinates also represent a vertical translation at B and a rotation at C. The directions of the arrows are arbitrarily chosen; but the choice sets the sign convention that must be followed throughout the analysis.

In Prob. 4.1a, the continuous beam in Figure 4.1a is released by the insertion of a hinge at B and the replacement of the totally fixed support at C by a hinged support. The hinge at B releases an internal force (a bending moment), that must be represented by a pair of opposite arrows, jointly denoted coordinate 1; the release of the reaction component at C (a couple) is represented by a single arrow, coordinate 2. The pair of arrows, coordinate 1, represents also the relative rotation (the angular discontinuity) of the two member ends connected by the hinge inserted at B. Coordinate 2 represents also the rotation of the beam end C.

4.4 Analysis for environmental effects

The force method can be used to analyze a statically indeterminate structure subjected to effects other than applied loads. An example of such an effect which causes internal stresses is the movement of a support. This may be due to the settlement of foundations or to a differential temperature movement of supporting piers.

Internal forces are also developed in any structure if the free movement of a joint is prevented. For example, the temperature change of a beam with two fixed ends develops an axial force. Stresses in a structure may also be caused by a differential change in temperature.

As an example, let us consider the continuous beam ABC of Figure 4.2a when subjected to a rise in temperature varying linearly between the top and bottom faces. If support B is removed, the beam becomes statically determinate, and the rise in temperature causes it to deflect upward (Figure 4.2b). If the beam is to remain attached to the support at B, a downward force F_1 will develop so as to correct for the error in displacement, D_1. The deflected shape of the beam axis is then as shown in Figure 4.2c.

If a member of a truss is manufactured shorter or longer than its theoretical length and then forced to fit during erection, stresses will develop in the truss. This lack of fit has a similar effect to a change in temperature of the member in question. The effect of shrinkage of concrete members on drying is also similar to the effect of a drop in temperature.

Another cause of internal forces in statically indeterminate structures is the prestrain induced in prestressed concrete members. This may be illustrated by reference to Figure 4.3a, which

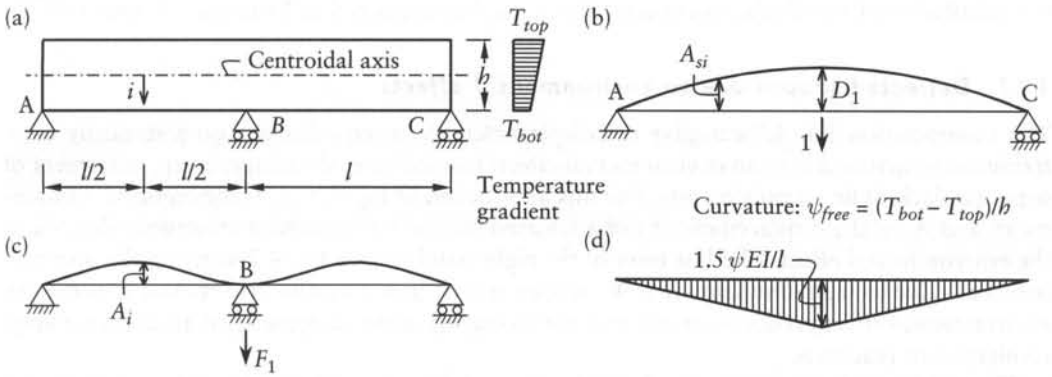

Figure 4.2 Effect of a differential rise in temperature across a continuous beam. (a) Continuous beam subjected to temperature rise. (b) Deflected shape of statically determinate structure. (c) Deflected shape of the statically indeterminate structure in (a). (d) Bending moment diagram.

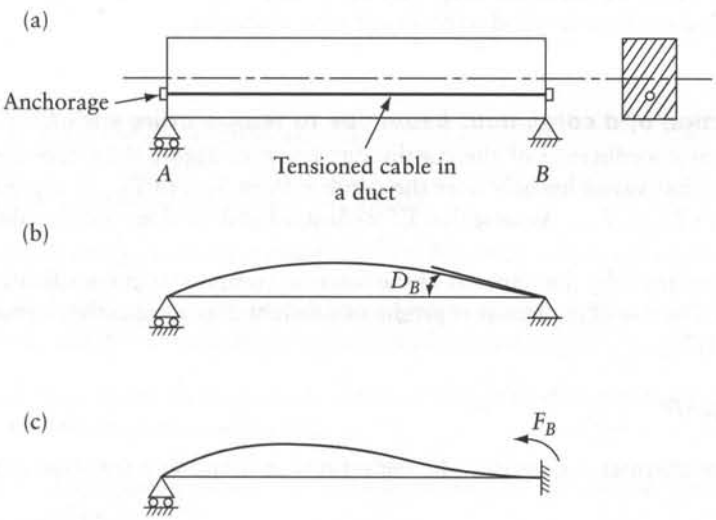

Figure 4.3 Effect of prestrain in a beam.

shows a statically determinate concrete beam of rectangular cross section. A cable is inserted through a duct in the lower part of the cross section. The cable is then tensioned and anchored at the ends. This produces compression in the lower part of the cross section and causes the beam to deflect upward (Figure 4.3b). If the beam is statically indeterminate, for example, if the end B is fixed, the rotation at this end cannot take place freely and a couple will develop at B so as to cause the rotation D_B to vanish (Figure 4.3c).

In all these cases, Eq. 4.4 can be applied to calculate the redundant forces, the elements of the matrix $\{D\}$ being the errors in the displacement of the released structure due to the given effect, or to the various effects combined. The effects of temperature, shrinkage, creep, and prestressing are discussed in more detail in Sections 6.9 to 6.11.

We should note that the matrix $\{\Delta\}$ includes the prescribed displacement of the support if this displacement corresponds to one of the coordinates. Otherwise, the effect of the support

movement on the displacement of the released structure at a coordinate should be included in the calculation of the displacement $\{D\}$. This is further explained in Example 4.4, case (1).

4.4.1 Deflected shapes due to environmental effects

The superposition Eq. 4.7 can give the displacement A_i at coordinate i on a statically indeterminate structure due to an environmental effect: temperature, shrinkage, creep, movement of supports, lack of fit, or prestressing. For this application of Eq. 4.7, A_i is the required displacement, and A_{si} is the displacement at i of a released statically determinate structure subjected to the environmental effect. The last term in the right-hand side of Eq. 4.7 sums up the displacements at i due to the redundants $\{F\}$. We recognize that in a statically determinate structure an environmental effect produces strains and displacements without stresses, internal forces (stress resultants) or reactions.

We refer again to the continuous beam in Figure 4.2a subjected to a rise in temperature, the distribution of which over the depth h is linear as shown in the figure; the deflection A_i of the centroidal axis of the beam is equal to A_{si} of the released structure in Figure 4.2b plus the deflection at i due to the redundant F_1. Note that the released structure deflects while its internal forces and reactions are nil; the bending moment diagram, Figure 4.2d, is not directly related, by Eq. 1.24, to the curvature of the deflected shape in Figure 4.2c; e.g. the points of inflection on both sides of support B do not correspond to points of zero moments.

Example 4.2: Deflection of a continuous beam due to temperature variation

Find the deflection A_i at coordinate i of the continuous beam in Figure 4.2a subjected to a rise in temperature that varies linearly over the depth h from T_{top} to T_{bot} at top and bottom respectively, with $T_{top} > T_{bot}$. Assume that EI = constant and consider only bending deformation.

A released structure obtained by the removal of the reaction component at coordinate 1 is shown in Figure 4.2b. The rise of temperature produces constant curvature in the released structure given by Eq. 1.7:

$$\psi_{free} = \alpha(T_{bot} - T_{top})/h$$

where α is coefficient of thermal expansion. The deflections at B and at i are (Eqs. B.39 and B.40):

$$D_1 = \psi_{free}(2l)^2/8 = 0.5\,\psi_{free} l^2$$

$$A_{si} = \psi_{free}(0.5l)(1.5l)/2 = 0.375\psi_{free} l^2$$

Displacements due to $F_1 = 1$ are (Eqs. B.8 and B.5):

$$f_{11} = (2l)^3/(48EI) = l^3/(6EI)$$

$$A_{u1i} = \frac{l(0.5l)}{6(2l)EI}[2l(2l) - l^2 - (0.5l)^2] = 0.1146 l^3/(EI)$$

Equation 4.4 gives the redundant:

$$F_1 = -f_{11}^{-1} D_1 = -\frac{6EI}{l^3}(0.5\psi_{free} l^2) = -\frac{3EI}{l}\psi_{free}$$

The deflection at i is (Eq. 4.7):

$$A_i = A_{si} + A_{u1i} F_1$$

$$A_i = 0.375\psi_{free} l^2 + 0.1146 \frac{l^3}{EI}\left(-\frac{3EI}{l}\psi_{free}\right) = 31.2 \times 10^{-3}\psi_{free} l^2$$

Because $T_{top} > T_{bot}$, ψ_{free} is negative and the deflection at i is upward.

4.5 Analysis for different loadings

When using Eq. 4.3 to find the redundants in a given structure under a number of different loadings, the calculation of the flexibility matrix (and its inverse) need not be repeated. When the number of loadings is p the solution can be combined into one matrix equation

$$[F]_{n\times p} = [f]^{-1}_{n\times n}\,[\Delta - D]_{n\times p} \tag{4.9}$$

where each column of $[F]$ and $[D]$ corresponds to one loading.

The reactions or the stress resultants in the original structure can be determined from equations similar to Eq. 4.8, viz.

$$[A]_{m\times p} = [A_s]_{m\times p} + [A_u]_{m\times n}[F]_{n\times p} \tag{4.10}$$

4.6 Five steps of force method

The analysis by the force method involves five steps which are summarized as follows:

Step 1 Introduce releases and define a system of coordinates. Also define $[A]_{m\times p}$, the required actions, and define their sign convention (if necessary).

Step 2 Due to the loadings on the released structure, determine $[D]_{n\times p}$, and $[A_s]_{m\times p}$. Also fill-in the prescribed displacements $[\Delta]_{n\times p}$.

Step 3 Apply unit values of the redundants one by one on the released structure and generate $[f]_{n\times n}$ and $[A_u]_{m\times n}$.

Step 4 Solve the geometry equations:

$$[f]_{n\times n}[F]_{n\times p} = [\Delta - D]_{n\times p} \tag{4.11}$$

This gives the redundants $[F]_{n\times p}$.

Step 5 Calculate the required actions by superposition:

$$[A]_{m\times p} = [A_s]_{m\times p} + [A_u]_{m\times n}[F]_{n\times p} \tag{4.12}$$

At the completion of step 3, all the matrices necessary for the analysis have been generated. The last two steps involve merely matrix algebra. Step 5 may be eliminated when no action besides the redundants is required, or when the superposition can be done by inspection after determination of the redundants (see Example 4.5). When this is the case, the matrices $[A]$, $[A_s]$, and $[A_u]$ are not required.

For quick reference, the symbols used in this section are defined again as follows:

n, p, m = number of redundants, number of loading cases, and number of actions required
$[A]$ = the required actions (the answers to the problem)
$[A_s]$ = values of the actions due to the loadings on the released structure
$[A_u]$ = values of the actions in the released structure due to unit forces applied separately at each coordinate
$[D]$ = displacements of the released structure at the coordinates due to the loadings; these displacements represent incompatibilities to be eliminated by the redundants
$[\Delta]$ = prescribed displacements at the coordinates in the actual structure; these represent imposed displacements to be maintained
$[f]$ = flexibility matrix.

Example 4.3: A stayed cantilever

Figure 4.4a shows a cantilever stayed by a link member AC. Determine the reaction components $\{R_1, R_2\}$ at B due to the combined effect of the uniform load shown and a drop of temperature T degrees in AC only. Assume that:

$$a_{AC} = 30I_{AB}/l^2;\ \alpha T = (ql^3/EI_{AB})/40$$

where a_{AC} and I_{AB} are the cross-sectional area and second moment of area of AC and AB respectively; α is coefficient of thermal expansion (degree^{-1}) for AC; E is modulus of elasticity of the structure.

Step 1 Figure 4.4b shows the structure released by cutting AC. The arbitrarily chosen directions of the arrows representing coordinate 1 indicate that F_1 is positive when the force in AC is tensile. The same arrows also indicate that D_1 is positive when the gap at the cut section closes.

The required actions are:

$$\{A\} = \begin{Bmatrix} R_1 \\ R_2 \end{Bmatrix}$$

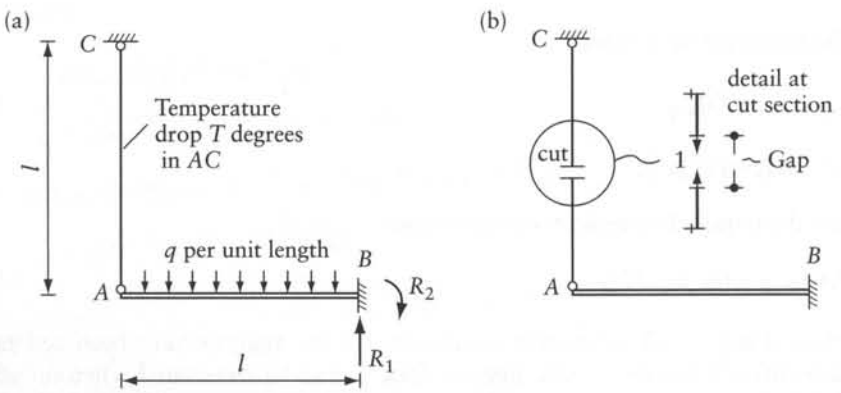

Figure 4.4 A stayed cantilever: Example 4.2. (a) Actual structure. (b) Released structure and coordinate system.

Step 2 Application of the load and the temperature change to the released structure produces the following displacement and reactions:

$$D_1 = -\left(\frac{ql^4}{8EI}\right)_{AB} - (\alpha Tl)_{AC} = -0.15\frac{ql^4}{EI_{AB}}$$

$$\{A_s\} = \begin{Bmatrix} ql \\ ql^2/2 \end{Bmatrix}$$

The load q produces a downward deflection at A (given by Eq. B.27 Appendix B) and opens the gap at the cut section by the same amount. Also, the drop in temperature in AC opens the gap at the cut section. Thus, the two terms in the above equation for D_1 are negative.

Step 3 Application of two equal and opposite unit forces F_1 causes the following displacement and actions in the released structure:

$$f_{11} = \left(\frac{l^3}{3EI}\right)_{AB} + \left(\frac{l}{Ea}\right)_{AC} = \frac{11}{30}\frac{l^3}{EI_{AB}}$$

$$[A_u] = \begin{bmatrix} -1 \\ -l \end{bmatrix}$$

The first term in the above equation for f_{11} is given by Eq. B.19.

Step 4 In this example the compatibility Eq. 4.11 expresses the fact that the actual structure has no gap; thus,

$$f_{11}F_1 = \Delta_1 - D_1$$

with $\Delta_1 = 0$.

The solution gives the force necessary to eliminate the gap:

$$F_1 = f_{11}^{-1}(\Delta_1 - D_1)$$

$$F_1 = \left(\frac{11}{30}\frac{l^3}{EI_{AB}}\right)^{-1}\left[0 - \left(-0.15\frac{ql^4}{EI_{AB}}\right)\right] = 0.409ql$$

Step 5 The superposition Eq. 4.12 gives the required reaction components:

$$\{A\} = \{A_s\} + [A_u]F_1$$

$$\{A\} = \begin{Bmatrix} ql \\ ql^2/2 \end{Bmatrix} + \begin{bmatrix} -1 \\ -l \end{bmatrix} 0.409ql = \begin{Bmatrix} 0.591ql \\ 0.091ql^2 \end{Bmatrix}$$

Example 4.4: A beam with a spring support

Solve Example 4.3, replacing the link member AC in Figure 4.4a by a spring support below A, of stiffness $K = 30(EI)_{AB}/l^3$, where K is the magnitude of the force per unit shortening of the spring. Assume that the spring can produce only a vertical force at the tip A of the cantilever. The loading is q/unit length on AB, as in Example 4.2, combined with a rise in temperature of the spring that would cause it to expand, if it were free, by $[ql^4/(EI)_{AB}]/40$.

Step 1 Release the structure by separating the spring from the cantilever, creating a gap and coordinate 1, represented by a pair of arrows pointing upward on the cantilever and downward on the spring.

Step 2 The displacement D_1 due to the load on AB and the temperature rise of the spring is:

$$D_1 = -\frac{ql^4}{8(EI)_{AB}} - \frac{ql^4}{40(EI)_{AB}}$$

The first term on the right-hand side is given by Eq. B.27; the second term is the given expansion of the spring. Both terms are negative because they are translations in the opposite direction of coordinate 1.

Step 3 A pair of forces $F_1 = 1$ produces relative translations (widening the gap):

$$f_{11} = \frac{l^3}{3(EI)_{AB}} + \frac{1}{K} = \frac{l^3}{3(EI)_{AB}} + \frac{l^3}{30(EI)_{AB}} = \frac{11\,l^3}{30(EI)_{AB}}$$

Steps 4 and 5 The same as in Example 4.3.

Example 4.5: Simply-supported arch with a tie

Figure 4.5a represents a concrete arch with a steel tie. Determine the bending moments at C, D and E due to: (1) the loads shown; (2) the loads shown combined with a rise of temperature, $T = 30\,°C$ only in the tie AB. Consider only the bending deformation of the arch and the axial deformation of the tie. Given data:

For arch AEB: $a = 0.16\,m^2$; $I = 2.133 \times 10^{-3}\,m^4$; $E = 40\,GPa$

For tie AB: $a = 2000\,mm^2$; $E = 200\,GPa$; $\alpha = 10 \times 10^{-6}$ per degree Celsius

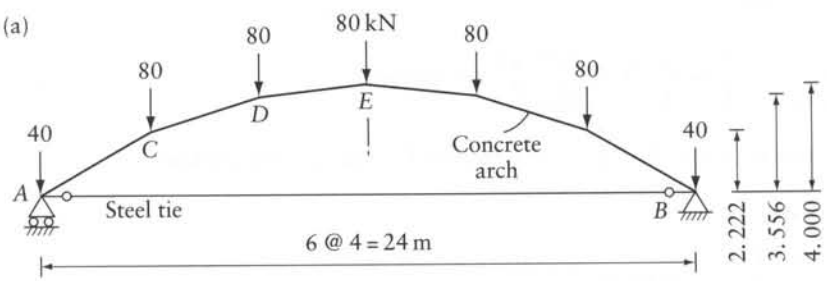

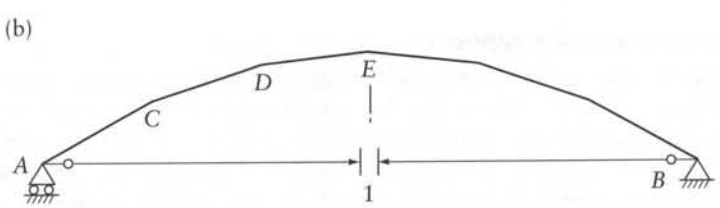

Figure 4.5 Arch with a tie of Example 4.3. (a) Actual structure. (b) Released structure and coordinate system.

where a and I are area and second moment of area of a cross section; E is modulus of elasticity and α is coefficient of thermal expansion.

We follow below the five steps of the force method. The displacements required in Steps 2 and 3 are presented without calculation. Their values can be verified using virtual work, as discussed in Section 8.2 and Example 8.11. We concentrate on understanding the steps of the force method, leaving out the details of displacement calculation. The units used below are N and m.

Step 1 The structure is released by cutting the tie. Since the release is an internal force, it must be represented by a pair of arrows, constituting coordinate 1 (Figure 4.5b). With the directions of the arrows arbitrarily chosen in Figure 4.5b, F_1 and D_1 are considered positive when the force in the tie is tensile and when the gap at the cut section closes. The required actions are:

$$[A] = \left[\begin{Bmatrix} M_C \\ M_D \\ M_E \end{Bmatrix}_{Case\ 1} \quad \begin{Bmatrix} M_C \\ M_D \\ M_E \end{Bmatrix}_{Case\ 2} \right] \tag{a}$$

We consider that positive M produces tension at the inner face of the arch.

Step 2 The following displacements and actions (bending moments) occur when the released structure is subjected to the loading cases (1) and (2):

$$[D_{1\ Case\ 1}\ D_{1\ Case\ 2}] = [-0.85109 \quad -0.84389]\ \text{m} \tag{b}$$

$$[A_s] = [\{A_s\}_{Case\ 1}\ \{A_s\}_{Case\ 2}] = 10^3 \begin{bmatrix} 800 & 800 \\ 1280 & 1280 \\ 1440 & 1440 \end{bmatrix} \text{N-m} \tag{c}$$

We note that with the tie cut, the bending moment values, with or without temperature change, are the same as the values for a simple beam having the same span and carrying the same vertical loads. The downward forces on the arch cause the roller at A to move outwards and the gap at the cut section to open a distance = 0.85109 m. The thermal expansion of the tie reduces the opening of the gap by the value $(\alpha T l)_{tie} = 10 \times 10^{-6}\ (30)\ (24) = 7.2 \times 10^{-3}$ m, where l_{tie} is the length of the tie.

Step 3 Opposite unit forces (1 N) at coordinate 1 produce bending moments at C, D and E equal to $\{-2.222, -3.556, -4.000\}$ N-m; these values are the elements of $[A_u]$. The same unit forces close the gap at the cut section by a distance equal to:

$$[f_{11}] = [2.4242 \times 10^{-6}]\ \text{m/N} \tag{d}$$

This is equal to the sum of an inward movement of the roller at A equal to 2.3642×10^{-6} and an elongation of the tie $= (l/aE)_{tie} = 24/[2000 \times 10^{-6}(200 \times 10^9)] = 0.0600 \times 10^{-6}$.

$$[A_u] = \begin{bmatrix} -2.222 \\ -3.556 \\ -4.000 \end{bmatrix} \text{N-m/N} \tag{e}$$

In calculating the displacements in Steps 2 and 3, the deformations due to shear and axial forces in the arch are ignored because their effect in this type of structure is small. Calculation of the contribution of any internal force in a framed structure can be done by virtual work (Section 8.2 and Example 8.11).

Step 4 The compatibility Eq. 4.11 and its solution in this example are:

$$[f_{11}][(F_1)_{Case\ 1}\ (F_1)_{Case\ 2}] = [(\Delta_1 - D_1)_{Case\ 1}\ (\Delta_1 - D_1)_{Case\ 2}]$$

$$[(F_1)_{Case\ 1}\ (F_1)_{Case\ 2}] = [f_{11}]^{-1}[(\Delta_1 - D_1)_{Case\ 1}\ (\Delta_1 - D_1)_{Case\ 2}]$$

$$[F] = [2.4242 \times 10^{-6}]^{-1}[(0 - (-0.85109))\ (0 - (-0.84389))]$$

$$[F] = [351.08\ \ 348.11]10^3\ \text{N} \qquad \text{(f)}$$

In the two loading cases $\Delta_1 = 0$, because no displacement is prescribed at coordinate 1.

Step 5 The superposition Eq. 4.12 gives the required values of bending moments in the two loading cases:

$$[A] = [A_s] + [A_u][F]$$

Substitution of Eqs. (a), (c), (e) and (f) gives:

$$[A] = \left[\begin{Bmatrix} M_C \\ M_D \\ M_E \end{Bmatrix}_{Case\ 1} \begin{Bmatrix} M_C \\ M_D \\ M_E \end{Bmatrix}_{Case\ 2} \right] = \begin{bmatrix} 19.9 & 26.5 \\ 31.6 & 42.1 \\ 35.7 & 47.6 \end{bmatrix} 10^3\ \text{N-m}$$

These bending moments are much smaller than the moments in a simple beam of the same span carrying the same downward forces. This example shows an advantage of an arch with a tie, that is, covering large spans without developing large bending moments.

Example 4.6: Continuous beam: support settlement and temperature change

Find the bending moments M_B and M_C and the reaction R_A for the continuous beam of Example 4.1 (Figure 4.1) due to the separate effect of: (1) a downward settlement δ_A of support A; (2) a downward settlement δ_B of support B; (3) a rise of temperature varying linearly over the depth h, from T_t to T_b in top and bottom fibers respectively.

Step 1 We choose the releases and the coordinate system as in Example 4.1, Figure 4.1b. The required actions are

$$[A] = \left[\begin{Bmatrix} M_B \\ R_A \end{Bmatrix}_1 \quad \begin{Bmatrix} M_B \\ R_A \end{Bmatrix}_2 \quad \begin{Bmatrix} M_B \\ R_A \end{Bmatrix}_3 \right]$$

Bending moment is considered positive when it produces tensile stress in the bottom fiber. Upward reaction R_A is positive. The required action M_C does not need to be included in $[A]$ because $M_C = -F_2$ and the values of the redundants $\{F\}$ will be calculated in Step 4. The subscripts 1, 2, and 3 in the above equation refer to the three load cases.

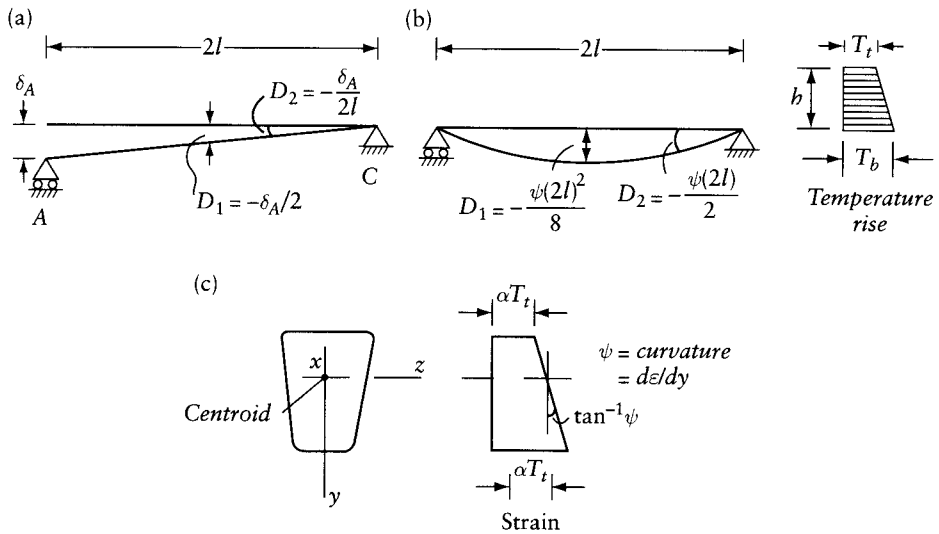

Figure 4.6 Released structure in Example 4.4. (a) Settlement δ_A at support A. (b) Rise of temperature varying linearly over the depth h. (c) Strain due to temperature rise.

Step 2 The released structure is depicted in Figures 4.6a and b for cases (1) and (3) respectively. The displacement vectors $\{\Delta\}$ and $\{D\}$ in the three cases are

$$[\Delta] = \begin{bmatrix} 0 & -\delta_B & 0 \\ 0 & 0 & 0 \end{bmatrix}; \quad [D] = \begin{bmatrix} -\delta_A/2 & 0 & -\psi(2l)^2/8 \\ -\delta_A/(2l) & 0 & -\psi(2l)/2 \end{bmatrix}$$

Here ψ is thermal curvature in the released structure (slope of the strain diagram, Figure 4.6c):

$$\psi = \alpha(T_b - T_t)/h \tag{4.13}$$

where α is the thermal expansion coefficient (degree^{-1}); see Eqs. B.39 and B.41 for values of $\{D\}$ in case (3).

Note that in case (1), $\{\Delta\} = \{0\}$ because the actual structure has zero displacements at coordinates 1 and 2; however, the released structure has displacements to be eliminated at the coordinates: $\{D\} = \{-\delta_A/2, -\delta_A/2l\}$.

The values of the actions in the released structure are zero in all three cases:

$$[A_s] = [0]_{2\times 3}$$

Step 3 Unit forces applied at the coordinates are represented in Figures 4.1d and e. The flexibility matrix $[f]$ and its inverse, determined in Example 4.1, apply (Eqs. 4.5 and 4.6). Values of the actions due to $F_1 = 1$ or $F_2 = 1$ are

$$[A_u] = \begin{bmatrix} -0.5l & -0.5 \\ -0.5 & -1/(2l) \end{bmatrix}$$

Step 4 Substitution in the geometry Eq. 4.11 gives

$$\frac{1}{EI}\begin{bmatrix} l^3/6 & l^2/4 \\ l^2/4 & 2l/3 \end{bmatrix}[F]=\begin{bmatrix} \delta_A/2 & -\delta_B & \psi l^2/2 \\ \delta_A/(2l) & 0 & \psi l \end{bmatrix}$$

The solution is

$$[F]=\frac{12EI}{7l^3}\begin{bmatrix} 2.5\delta_A & -8\delta_B & \psi l^2 \\ -0.5l\delta_A & 3l\delta_B & 0.5\psi l^3 \end{bmatrix}$$

Step 5 Substitution in the superposition Eq. 4.12 gives

$$[A]=\frac{12}{7}EI\begin{bmatrix} -\delta_A/l^2 & 2.5\delta_B/l^2 & -0.75\psi \\ -\delta_A/l^3 & 2.5\delta_B/l^3 & -0.75\psi/l \end{bmatrix}$$

The elements of $[A]$ are the required values of M_B and R_A in the three cases; reversal of sign of F_2 gives the corresponding values of M_C:

$$[M_C]=\frac{12EI}{7l^3}[0.5l\delta_A \; -3l\delta_B \; -0.5\psi l^3]$$

We should note that R_A, M_B, and M_C are proportional to the value of the product EI. In general, the reactions and the internal forces caused by support settlements or temperature variation of statically indeterminate structures are proportional to the value of EI employed in linear analysis.

Design of concrete structures commonly allows cracking to take place, resulting in a substantial reduction in the moment of inertia, I (the second moment of area) at the cracked sections. Ignoring cracking can greatly overestimate the effects of support movements and of temperature.[1] Also, using a modulus of elasticity E, based on the relation between stress and instantaneous strain, will overestimate the effects of settlement and temperature. This is because such an approach ignores creep, that is, the strain which develops gradually with time (months or years) under sustained stress.

Example 4.7: Release of a continuous beam as a series of simple beams

Analyze the continuous beam of Figure 4.7a for (a) a uniformly distributed load of intensity q on all spans; (b) a unit downward movement of support A; (c) a unit downward movement of support B. The beam has a constant flexural rigidity EI.

A statically determinate released structure can be obtained by introducing a hinge over each interior support, that is, by the removal of two equal and opposite forces (moments) acting on either side of the support, so that the released structure is a series of simply-supported beams (Figure 4.7b). The released bending moments are sometimes called *connecting moments*.

The inconsistencies in displacements of the released structure are the relative rotations of the three pairs of adjacent beam ends, that is, the angles between the tangent to the axis

1 Accounting for the effects of cracking and creep is studied in: Ghali, A., Favre, R. and Elbadry, M., *Concrete Structures: Stresses and Deformations*, 3rd ed., E & FN Spon, London and New York, 2002; Chapters 16.20 of Neville, A. M., Dilger, W. H. and Brooks, J. J., *Creep of Plain and Structural Concrete*, Longman, London and New York, 1983, pp. 246–349.

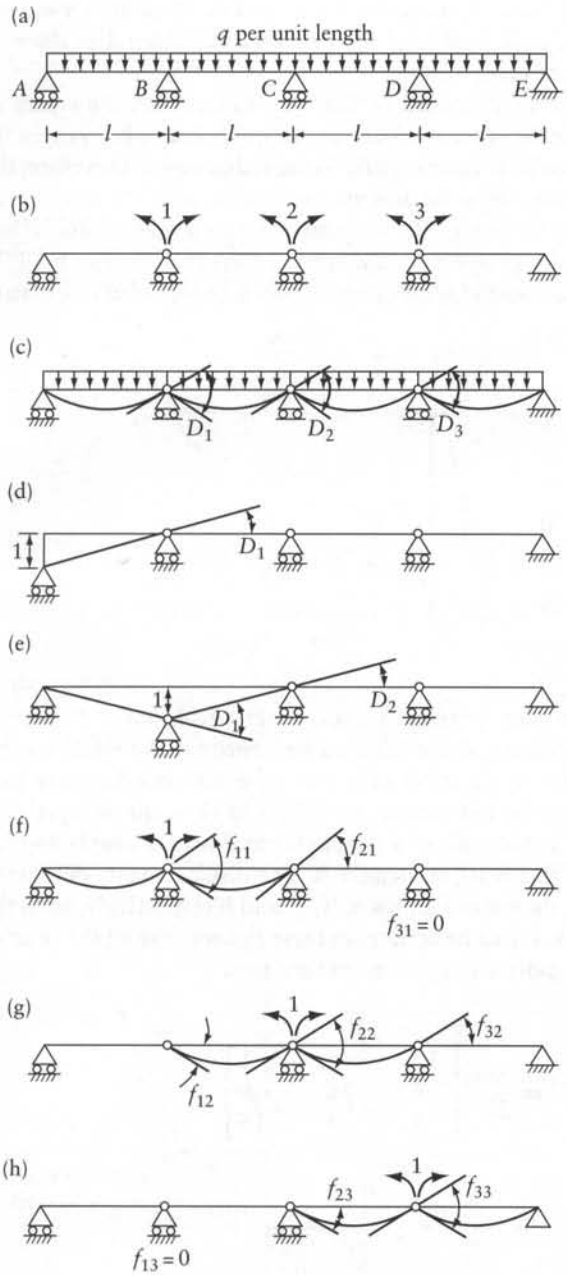

Figure 4.7 Analysis of a continuous beam by the force method (Example 4.5).

of one deflected beam and the corresponding tangent to an adjacent beam (Figure 4.7c). The positive directions of the redundants and therefore of the displacements are shown in Figure 4.7b. These are chosen so that a connecting moment is positive if it produces tension in the fibers at the bottom face of a beam.

The superposition involved in Step 5 can be done by inspection or by relatively simple calculations. Thus, the matrices $[A]$, $[A_s]$, and $[A_u]$ are not required. Step 1 is done in Figure 4.7b, while Steps 2, 3, and 4 are done below.

The solution of the three cases can be obtained by Eq. 4.9. In case (a), the errors in geometry of the released structure can be obtained from Eq. B.3, Appendix B. In cases (b) and (c), the movements of the supports do not correspond to the redundants. Therefore, the relative rotations at B, C, and D resulting from the downward movement of the supports of the released structure are included in the matrix $[D]$, and matrix $[\Delta]$ is a null matrix. These rotations are easily determined from the geometry of the released structure in Figures 4.7d and e. The inconsistency in the displacements for all three cases can be included in a matrix with one column per case:

$$[\Delta - D] = -[D] = -\begin{bmatrix} \frac{ql^3}{12EI} & \frac{1}{l} & -\frac{2}{l} \\ \frac{ql^3}{12EI} & 0 & \frac{1}{l} \\ \frac{ql^3}{12EI} & 0 & 0 \end{bmatrix}$$

(All the relative rotations are positive except D_1 in case (c), see Figure 4.7e.)

Now, the flexibility influence coefficients of the released structure are the relative rotations of the beam ends caused by the application of a pair of equal and opposite unit moments. Separately, apply at each of the redundants at B, C, and D a pair of equal and opposite unit couples. The rotations at the ends of a simple beam due to a couple applied at one end can be found by Eqs. B.9 and B.10, Appendix B. The displacements due to the unit value of each of the redundants, shown in Figures 4.7f, g, and h respectively, form the three columns of the flexibility matrix. It can be seen from these figures that all the relative rotations are positive. The flexibility matrix and its inverse are thus

$$[f] = \frac{1}{6EI}\begin{bmatrix} 4 & 1 & 0 \\ 1 & 4 & 1 \\ 0 & 1 & 4 \end{bmatrix}; \quad [f]^{-1} = \frac{3EI}{28l}\begin{bmatrix} 15 & -4 & 1 \\ -4 & 16 & -4 \\ 1 & -4 & 15 \end{bmatrix}$$

Substituting in Eq. 4.9,

$$[F] = -\frac{3EI}{28l}\begin{bmatrix} 15 & -4 & 1 \\ -4 & 16 & -4 \\ 1 & -4 & 15 \end{bmatrix}\begin{bmatrix} \frac{ql^3}{12EI} & \frac{1}{l} & -\frac{2}{l} \\ \frac{ql^3}{12EI} & 0 & \frac{1}{l} \\ \frac{ql^3}{12EI} & 0 & 0 \end{bmatrix}$$

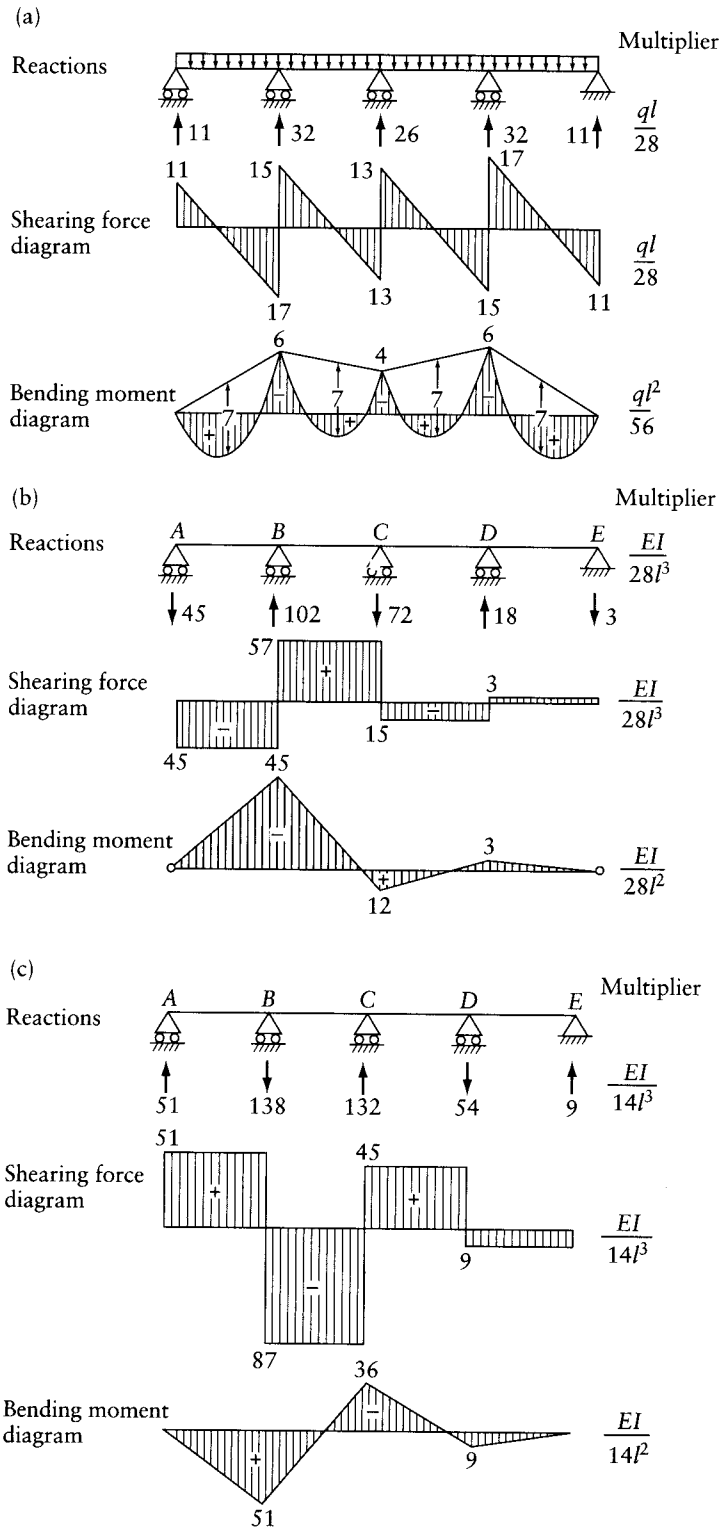

Figure 4.8 Bending moment and shearing force diagrams for the continuous beam of Example 4.5: (a) Uniform load q per unit length. (b) Displacement of support A. (c) Displacement of support B.

whence

$$[F]=\begin{bmatrix} -\frac{3}{28}ql^2 & -\frac{45}{28}\frac{EI}{l^2} & \frac{51}{14}\frac{EI}{l^2} \\ -\frac{ql^2}{14} & \frac{3}{7}\frac{EI}{l^2} & -\frac{18}{7}\frac{EI}{l^2} \\ -\frac{3}{28}ql^2 & -\frac{3}{28}\frac{EI}{l^2} & \frac{9}{14}\frac{EI}{l^2} \end{bmatrix}$$

The columns in this matrix correspond to cases (a), (b), and (c) and the three elements in each column are the bending moments at B, C, and D. Having found the values of the redundants, the bending moment and shearing force at any section can be obtained by simple statics. The reactions, and the bending moment[2] and shearing force diagrams for the three cases, are shown in Figure 4.8.

4.7 Equation of three moments

The analysis of continuous beams subjected to transverse loading and to support settlement is very common in structural design, and it is useful to simplify the general force method approach to this particular case. The resulting expression is known as the equation of three moments. We may note that historically this equation, developed by Clapeyron, precedes the matrix formulation of the force method.

Figure 4.9a represents two typical interior spans of a continuous beam. Let the spans to the left and to the right of an interior support i have, respectively, lengths l_l and l_r and flexural rigidities EI_l and EI_r, assumed to be constant within each span. The supports $i-1$, i, and $i+1$ are assumed to have settled in the direction of the applied loading by δ_{i-1}, δ_i, and δ_{i+1} respectively.

A statically determinate released structure can be obtained by introducing a hinge in the beam at each support (Figure 4.9), so that each span deforms as a simple beam, as in Example 4.5. The same sign convention as in that example will be used, as shown in Figure 4.9d.

As before, the inconsistencies in the displacements of the released structure are the relative rotations of adjacent beam ends, that is, with reference to Figures 4.9b and c,

$$D_i=\alpha_i+\gamma_i \tag{4.14}$$

We should note that D_i is due both to the transverse loading and to the settlement of supports.

In an actual continuous beam, the redundants $\{F\}$ are the *connecting moments* $\{M\}$, which must be of such magnitude that the angular discontinuities vanish. A superposition equation to satisfy the continuity condition at i can be written in the form

$$D_i+f_{i,\,i-1}F_{i-1}+f_{ii}F_i+f_{i,\,i+1}F_{i+1}=0 \tag{4.15}$$

where the terms f represent the flexibility coefficients of the released structure.

At this stage, we should consider the behavior of a beam hinged at each end and subjected to a unit moment at one end. Figure 4.10a shows such a beam and Figure 4.10b gives

2 Throughout this text an ordinate representing a bending moment is plotted on the side of the beam on which it produces tension.

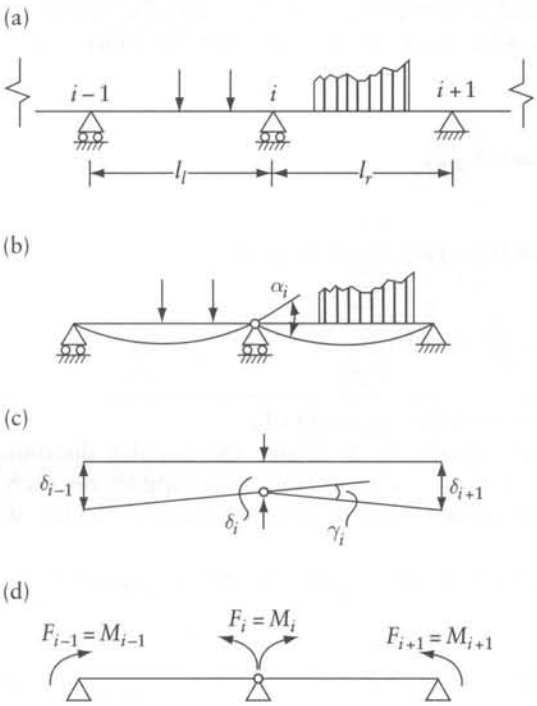

Figure 4.9 Analysis of a continuous beam by the equation of three moments. (a) Continuous beam. (b) Deflection of released structure due to transverse loading. (c) Deflection of released structure due to support settlement. (d) Positive direction of redundants.

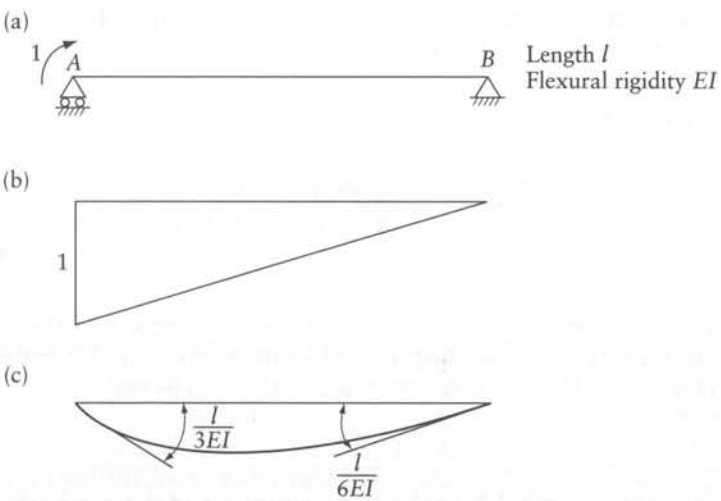

Figure 4.10 Angular displacements in a beam with hinged ends. (a) Beam. (b) Bending moment diagram. (c) Deflection.

the resulting bending moment diagram. Figure 4.10c shows the deflected shape: the angular displacements are $l/3EI$ and $l/6EI$ at A and B respectively (see Appendix B). Applying these results to the released structure of Figure 4.9d, it can be seen that the flexibility coefficients are

$$f_{i,i-1} = \frac{l_l}{6EI_l}; \quad f_{ii} = \frac{l_l}{3EI_l} + \frac{l_r}{3EI_r}; \quad f_{i,i+1} = \frac{l_r}{6EI_r}$$

With these values, and using the fact that $\{F\} = \{M\}$, Eq. 4.15 yields

$$M_{i-1}\frac{l_l}{EI_l} + 2M_i\left[\frac{l_l}{EI_l} + \frac{l_r}{EI_r}\right] + M_{i+1}\frac{l_r}{EI_r} = -6D_i \tag{4.16}$$

where l and r refer to the spans respectively to the left and right of i.

This is known as the equation of three moments. It relates the angular discontinuity at a support i to the connecting moments at this support and at a support on each side of i. The equation is valid only for continuous beams of constant flexural rigidity within each span.

For a continuous beam of constant flexural rigidity EI throughout, the equation of three moments simplifies to

$$M_{i-1}l_l + 2M_i(l_l + l_r) + M_{i+1}l_r = -6EID_i \tag{4.17}$$

Similar equations can be written for each support at which the bending moment is not known, thus forming a system of simultaneous equations, the solution of which gives the unknown moments. These equations can, in fact, be written in the general matrix form of Eq. 4.3. We can note that the particular released structure chosen has the advantage that each row of the flexibility matrix has only three nonzero elements. Also, we note that $\Delta_i = 0$ because the actual structure has no displacement (angular discontinuity) at coordinate i.

The displacement D_i in the equation of three moments can be calculated from Eq. 4.14, with the angle γ_i determined from the geometry of Figure 4.9c:

$$\gamma_i = (\delta_{i-1} - \delta_i)/l_l + (\delta_{i+1} - \delta_i)/l_r \tag{4.18}$$

and the angle α_i calculated by the method of elastic weights (see Section 10.4):

$$\alpha_i = r_{il} + r_{ir} \tag{4.19}$$

where r_{il} and r_{ir} are the reactions of the beams to the left and right of the support i loaded by the simple-beam bending moment due to lateral loading divided by the appropriate EI. For many of the practical cases the value of α_i can also be determined directly from Appendix B.

Example 4.8: The beam of Example 4.7 analyzed by equation of three moments

Use the equation of three moments to determine the connecting moments for the continuous beam of Example 4.7 in each of its three loading cases.

Table 4.1 Displacements D_B, D_C and D_D (Angular Discontinuities) for use in the Three-moment Equations in the Three Cases of Loading of Example 4.6

Support	*Case 1*			*Case 2*			*Case 3*		
	α	γ	D	α	γ	D	α	γ	D
B	$\frac{2ql^3}{24EI}$	0	$\frac{ql^3}{12EI}$	0	$\frac{1}{l}$	$\frac{1}{l}$	0	$-\frac{2}{l}$	$-\frac{2}{l}$
C	$\frac{2ql^3}{24EI}$	0	$\frac{ql^3}{12EI}$	0	0	0	0	$\frac{1}{l}$	$\frac{1}{l}$
D	$\frac{2ql^3}{24EI}$	0	$\frac{ql^3}{12EI}$	0	0	0	0	0	0

At the end supports, $M_A = M_E = 0$. The three-moment Eq. 4.17 needs to be applied at B, C and D:

$$2M_B(l+l) + M_C l = -6EID_B$$
$$M_B l + 2M_C(l+l) + M_D l = -6EID_C$$
$$M_C l + 2M_D(l+l) = -6EID_D$$

The displacements D_B, D_C and D_D in the three cases of loading are determined in Table 4.1 using Eqs. 4.14, 4.18 and 4.19. Appendix B may also be used to give the angles α instead of Eq. 4.19. The three-moment equations and their solutions for the three loading cases can be presented in matrix form:

$$\begin{bmatrix} 4 & 1 & 0 \\ 1 & 4 & 1 \\ 0 & 1 & 4 \end{bmatrix} \left[\begin{Bmatrix} M_B \\ M_C \\ M_D \end{Bmatrix}_{\text{Case 1}} \begin{Bmatrix} M_B \\ M_C \\ M_D \end{Bmatrix}_{\text{Case 2}} \begin{Bmatrix} M_B \\ M_C \\ M_D \end{Bmatrix}_{\text{Case 3}} \right] = \begin{bmatrix} -\frac{ql^2}{2} & -\frac{6EI}{l^2} & -\frac{12EI}{l^2} \\ -\frac{ql^2}{2} & 0 & -\frac{6EI}{l^2} \\ -\frac{ql^2}{2} & 0 & 0 \end{bmatrix}$$

$$\left[\begin{Bmatrix} M_B \\ M_C \\ M_D \end{Bmatrix}_{\text{Case 1}} \begin{Bmatrix} M_B \\ M_C \\ M_D \end{Bmatrix}_{\text{Case 2}} \begin{Bmatrix} M_B \\ M_C \\ M_D \end{Bmatrix}_{\text{Case 3}} \right] = \begin{bmatrix} -3ql^2/28 & -45EI/(28l^2) & 51EI/(14l^2) \\ -ql^2/14 & 3EI/(7l^2) & -18EI/(7l^2) \\ -3ql^2/28 & -3EI/(28l^2) & 9EI/(14l^2) \end{bmatrix}$$

Example 4.9: Continuous beam with overhanging end

Obtain the bending moment diagrams for the beam in Figure 4.11a due to: (a) the given vertical loads; (b) vertical settlement of $b/100$ and $b/200$ at supports B and C respectively. The beam has a constant flexural rigidity EI.

The equation of three moments has to be applied at supports A and B to find the two unknown bending moments M_1 at A and M_2 at B, while the bending moment at C is known from simple statics. When applying the equation at the built-in end A, the beam may be considered to extend

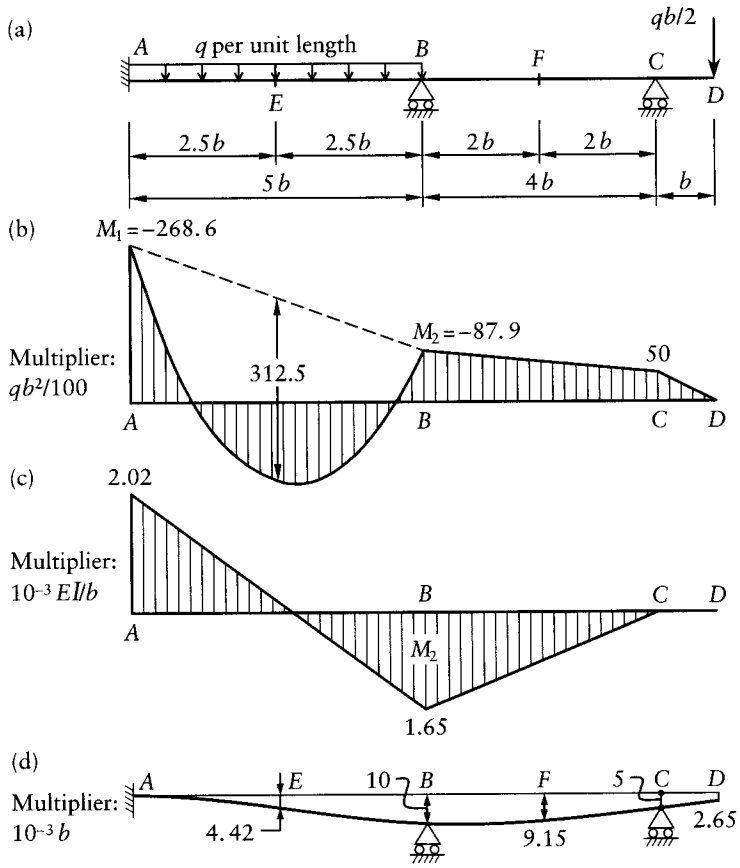

Figure 4.11 Continuous beam with sinking supports considered in Example 4.9. (a) Beam properties and loading. (b) Bending moment diagram due to vertical loading. (c) Bending moment diagram due to settlement of $b/100$ at support B and $b/200$ at support C. (d) Deflected shape due to the support settlement (Example 4.10).

over an imaginary span to the left of A, either of infinitely small length or of infinitely large flexural rigidity.

We find $\{D\}$ from Eq. 4.14, noting that for case (a), $\{\gamma\} = \{0\}$, while for case (b), $\{\alpha\} = \{0\}$. Hence, with the aid of Eq. B.3, Appendix B, it can be shown that for case (a)

$$\{D\}_a = \begin{Bmatrix} 5.208 \dfrac{qb^3}{EI} \\ 5.208 \dfrac{qb^3}{EI} \end{Bmatrix}$$

For case (b), calculating γ from Eq. 4.18, we obtain

$$\{D\}_b = \begin{Bmatrix} +0.00200 \\ -0.00325 \end{Bmatrix}$$

Using Eq. 4.17, we find for case (a)

$$\frac{b}{EI}(10M_1 + 5M_2) = -6 \times 5.208\frac{qb^3}{EI}$$

$$\frac{b}{EI}(5M_1 + 18M_2 - 4\frac{qb^2}{2}) = -6 \times 5.208\frac{qb^3}{EI}$$

and for case (b)

$$\frac{b}{EI}(10M_1 + 5M_2) = -6 \times 0.00200$$

$$\frac{b}{EI}(5M_1 + 18M_2) = +6 \times 0.00325$$

The two systems of equations can be combined in a matrix equation:

$$\frac{b}{EI}\begin{bmatrix}10 & 5\\ 5 & 18\end{bmatrix}[M] = \begin{bmatrix}-31.25\dfrac{qb^3}{EI} & -0.0120\\ -29.25\dfrac{qb^3}{EI} & 0.0195\end{bmatrix}$$

The same equation can be obtained following the more general procedure of the force method, with the released structure formed by introducing hinges at A and B. The square matrix on the left-hand side of the equation represents then the flexibility matrix of the released structure.

Solving for $[M]$, we find

$$[M] = \begin{bmatrix}-2.686qb^2 & -0.00202\dfrac{EI}{b}\\ -0.879qb^2 & 0.00165\dfrac{EI}{b}\end{bmatrix}$$

The bending moment diagrams for the two cases are plotted in Figures 4.11b and c.

Example 4.10: Deflection of a continuous beam due to support settlements

Sketch the deflected shape and calculate the deflections at E and F of the continuous beam of Example 4.9, case (b) (Figure 4.11a).

The bending moment diagram determined in Example 4.9 is shown in Figure 4.11c. Let $\{A_1, A_2\}$ = {deflection at E, deflection at F}; downward deflection is considered positive. Apply Eq. 4.10:

$$\{A\} = \{A_s\} + [A_u]\{F\} \qquad \text{(a)}$$

where $\{A_s\}$ represents the deflections of a released structure, having a hinge at each of A and B, with settlements $b/100$ and $b/200$ at supports B and C respectively; this structure has the shape of two straight segments: AB and BC, extended to D.

$$\{A_s\} = \begin{Bmatrix}0.0050\,b\\ 0.0075\,b\end{Bmatrix} \qquad \text{(b)}$$

The redundants $\{F\}$, the connecting moments at A and B determined in Example 4.9 are:

$$\{F\} = \frac{10^{-3} EI}{b} \begin{Bmatrix} -2.02 \\ 1.65 \end{Bmatrix} \tag{c}$$

The positive directions of the connecting moments are defined in Figure 4.9d. The deflections at E and F due to unit values of the redundants are (Eq. B.12):

$$[A_u] = \frac{b^2}{EI} \begin{bmatrix} (5)^2/16 & (5)^2/16 \\ 0 & (4)^2/16 \end{bmatrix} \tag{d}$$

Substitution of Eqs. (b), (c) and (d) in Eq. (a) gives:

$$\{A\} = 10^{-3} b \begin{Bmatrix} 5.0 \\ 7.5 \end{Bmatrix} + 10^{-3} b \begin{bmatrix} 1.5625 & 1.5625 \\ 0 & 1.0000 \end{bmatrix} \begin{Bmatrix} -2.02 \\ 1.65 \end{Bmatrix} = 10^{-3} b \begin{Bmatrix} 4.422 \\ 9.150 \end{Bmatrix}$$

The deflected shape of the beam is shown in Figure 4.11d.

4.8 Moving loads on continuous beams and frames

The live load on continuous beams and frames is often represented in design by a uniformly distributed load which may occupy any part of the structure so as to produce the maximum value of an internal force at a section or the maximum reaction at a support. We shall now discuss which parts of a continuous beam should be covered by the live load to produce these maxima.

Figures 4.12a and b show the deflected shapes, reactions, and bending moment and shearing force diagrams for a continuous beam due to a uniform live load covering one span only. It can be seen that the deflection is largest in the loaded span and reverses sign, with much smaller values, in adjacent spans. The two reactions at either end of the loaded span are upward; the reactions on either side of the loaded span are reversed in direction and have much smaller magnitude. The values given in the figures are for the case of equal spans l and load p per unit length; EI is constant.

In a loaded span, the bending moment is positive in the central part and negative at the supports. In the adjacent spans, the bending moment is negative over the major part of the length. The points of inflection on the deflected shapes correspond to the points O_1 and O_2 where the bending moment is zero. These points are closer to the supports C and D in case (a) and (b) respectively, than one-third of their respective spans. This is so because a couple applied at a supported end of a beam produces a straight-line bending moment diagram which reverses sign at one-third of the span from the far end when that end is totally fixed. When the far end is hinged (or simply-supported) the bending moment has the same sign over the whole span. The behavior of the unloaded spans BC and CD in Figure 4.12a and of span CD in Figure 4.12b lies between these two extremes.

The maximum absolute value of shear occurs at a section near the supports of the loaded span. Smaller values of shear of constant magnitude occur in the unloaded spans, with sign reversals as indicated.

In Figures 4.12a and b, we have loaded spans AB and BC. From these two figures, and perhaps two more figures corresponding to the uniform load on each of the remaining two spans, we can decide which load patterns produce the maximum values of the deflections, reactions, or internal

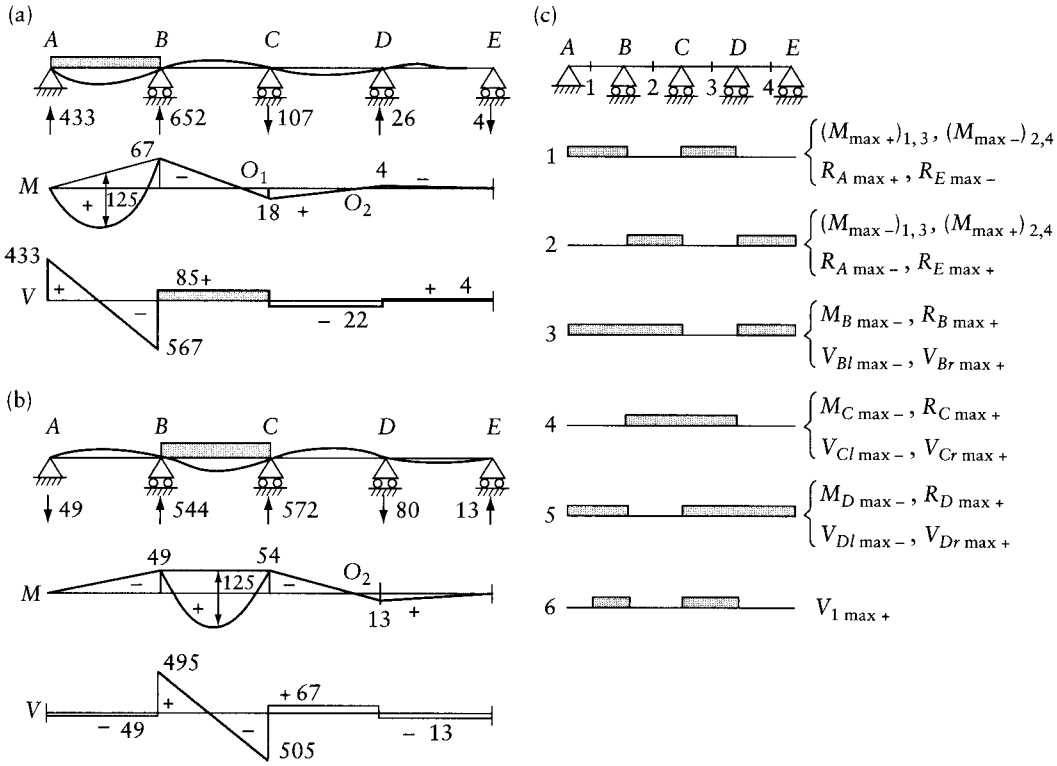

Figure 4.12 Effect of uniform live load on continuous beams. (a) and (b) Deflection, bending moment and shearing force diagrams due to load p per unit length covering one span. The values given are for equal spans l; the multipliers are $10^{-3}\,pl$ for reactions and shears, and $10^{-3}\,pl^2$ for moments. (c) Load patterns to produce maximum actions.

forces at any section. Figure 4.12c shows typical load patterns which produce maximum values of various actions.

It can be seen from this figure that maximum deflection and maximum positive bending moment at a section near the middle of a span occur when the load covers this span as well as alternate spans on either side. The maximum negative bending moment, the maximum positive reaction, and the maximum absolute value of shear near a support occur when the load covers the two adjacent spans and alternate spans thereafter. The loading cases (3), (4), and (5) in Figure 4.12c refer to sections just to the left or right of a support, the subscripts l and r denoting left and right respectively.

Partial loading of a span may produce maximum shear at a section as in case (6) in Figure 4.12c. Also, partial loading may produce maximum bending moments at sections near the interior supports (closer than one-third of the span) but not at the supports. However, in practice, partial span loading is seldom considered when the maximum bending moment values are calculated.

The effect of live load patterns needs to be combined with the effect of the dead load (permanent load) in order to obtain the maximum actions to be used in design. For example, if the beam in Figure 4.12c is designed for uniform dead and live loads of intensities q and p respectively, we can obtain the maximum bending moment diagram by considering q on all spans combined with p according to the loading cases (1) to (5) in Figure 4.12c. The maximum bending moment diagram due to dead and live loads combined is shown in Figure 4.13 for a continuous beam of

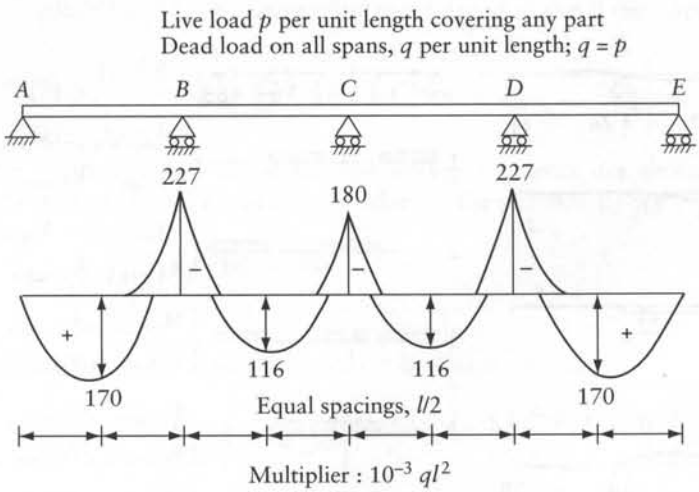

Figure 4.13 Maximum bending moment diagram for a continuous beam due to dead and live loads.

four equal spans l, with $q = p$. The diagram is obtained by plotting on one graph the bending moment due to q combined with p in cases (1) to (5) in Figure 4.12c and using for any part of the beam the curve with the highest absolute values. Additional load cases which produce a maximum positive bending moment due to p may need to be considered when p is large compared with q. For example, $M_{B\max+}$ occurs when p covers CD only, and $M_{C\max+}$ occurs when AB and DE are covered.

In practice, the live load may be ignored on spans far away from the section at which the maximum action is required. For example, the maximum negative moment and the maximum positive reaction at support B may be assumed to occur when the live load covers only the adjacent spans AB and BC, without loading on DE (see case (3), Figure 4.12). This approach may be acceptable because of the small effect of the ignored load, or on the grounds of a low probability of occurrence of the alternate load pattern with the full value of live load.

The alternate load patterns discussed above are typical for continuous beams and are frequently used in structural design. Similar patterns for continuous frames are shown in Figure 4.14. The two loading cases represented produce maximum positive and negative values of the bending moments in the horizontal beams or the end-moments in the columns. As followed throughout this book, the bending moment in beams is considered positive when it produces tension at the bottom face; a clockwise member end-moment is positive.

A sketch of the deflected shape may help to determine whether or not a span should be considered loaded so as to produce a maximum effect. A span should be loaded if this results in accentuating the deflected shape in all members. However, in some cases the deflected shape is not simple to predict in all parts of the frame, particularly when sidesway occurs. Use of influence lines (see Chapters 12 and 13) helps in determining the load position for maximum effect, particularly when the live load is composed of concentrated loads.

Example 4.11: Two-span continuous beam

A continuous beam of two equal spans l and constant EI is subjected to a uniform dead load q per unit length over the whole length, combined with a uniform live load of intensity $p = 0.6q$. Determine the maximum bending moment diagram. What are the values of the

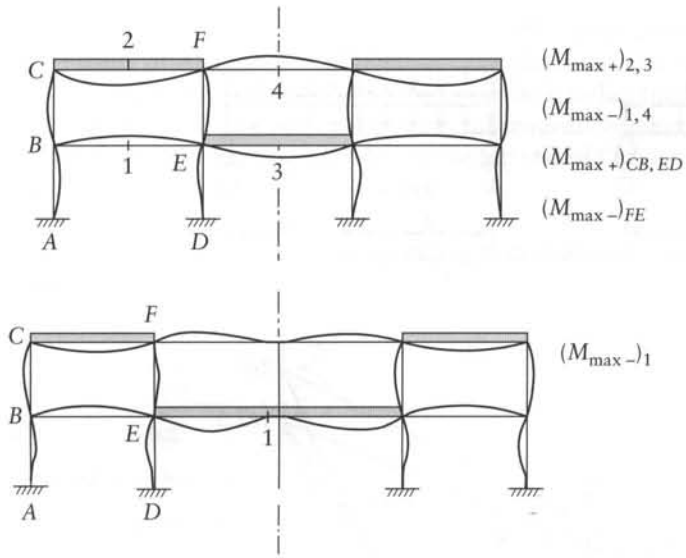

Figure 4.14 Examples of live load patterns to produce maximum bending moments in beams or end-moments in columns of plane frames.

maximum positive shearing force at the left-hand end A and at a section just to the right of the central support B (Figure 4.15)? What is the maximum positive value of the reaction R_B at B?

The bending moment values are $M_A = M_C = 0$. Application of the three-moment Eq. 4.17 at B gives for the two loading cases in Figures 4.15a and b:

$$\text{In case } a\text{: } 2M_B(l+l) = -6EI\left(\frac{1.6ql^3}{24EI} + \frac{ql^3}{24EI}\right)$$

$$\text{In case } b\text{: } 2M_B(l+l) = -6EI\left[2\left(\frac{1.6ql^3}{24EI}\right)\right]$$

$$(M_B)_{Case\ a} = -0.1625ql^2; (M_B)_{Case\ b} = -0.2ql^2$$

The bending moment diagrams for the two cases, as well as for a case represented by a mirror image of Figure 4.15a, are plotted for span AB in Figure 4.15c. The curves with the highest absolute values – shown with solid lines – represent the maximum bending moment diagram. A mirror image of Figure 4.15c gives the maximum bending moment diagram for span BC.

The maximum positive shear V_A occurs in case *(a)* and its value is:

$$V_{A\,max+} = 1.6ql/2 - 0.1625ql^2/l = 0.6375ql$$

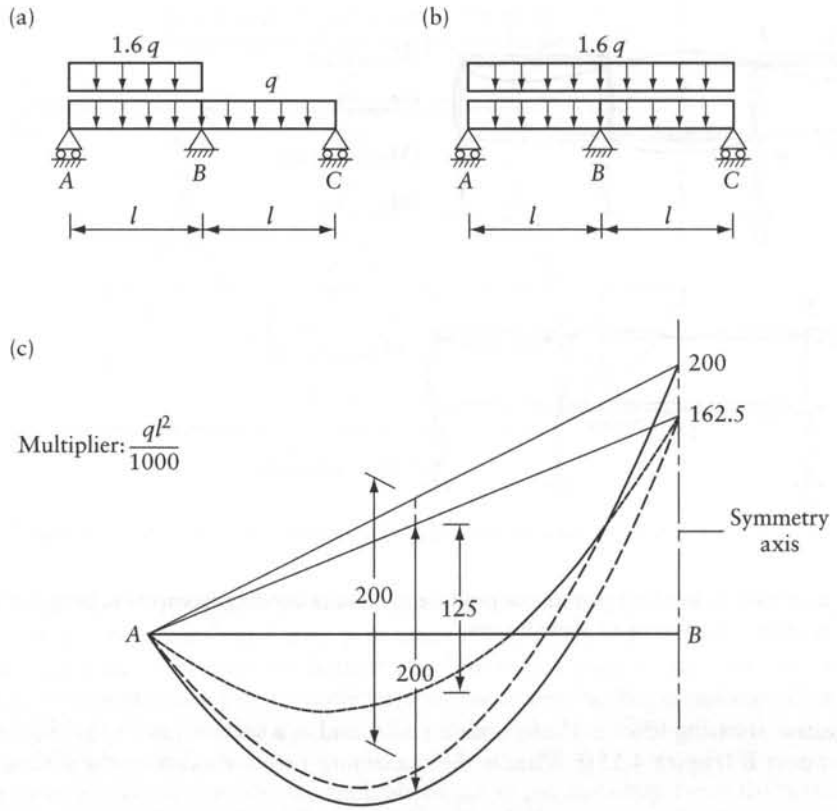

Figure 4.15 Continuous beam of Example 4.8. (a) and (b) Cases of loading that need to be analyzed. (c) Maximum bending moment diagram.

Case of loading (*b*) produces the maximum positive shear just to the right of *B* and the maximum positive reaction at *B*:

$$V_{Br\max+} = 1.6ql/2 + 0.2ql^2/l = 1.0ql$$

$$R_{B\max+} = 2(1.6ql)/2 + 2(0.2ql^2)/l = 2.0ql$$

4.9 General

The force (or flexibility) method of analysis can be applied to any structure subjected to loading or environmental effects. The solution of the compatibility equations directly yields the unknown forces. The number of equations involved is equal to the number of redundants. The force method is not well suited to computer use in the case of highly redundant structures, as will be discussed further in Section 6.3.

Problems

The following are problems on the application of the force method of analysis. At this stage, use can be made of Appendix B to determine the displacements required in the analysis, with attention directed to the procedure of the force method, rather than to the methods of computation of displacements. These will be treated in subsequent chapters. Additional problems on the application of the force method can be found at the end of Chapter 8, which require calculation of displacements by method of virtual work.

4.1 Write the flexibility matrix corresponding to coordinates 1 and 2 for the structures shown below.

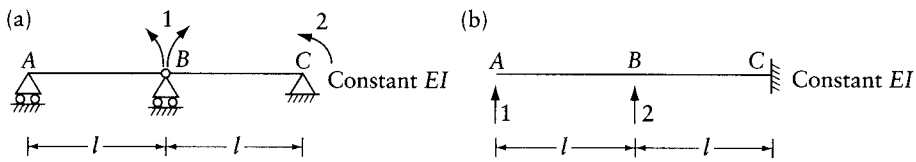

Prob. 4.1

4.2 Use the flexibility matrices derived in Prob. 4.1 to find two sets of redundant forces in two alternative solutions for the continuous beam of Example 4.1.

4.3 Use the force method to find the bending moment at the intermediate supports of the continuous beam shown in the figure.

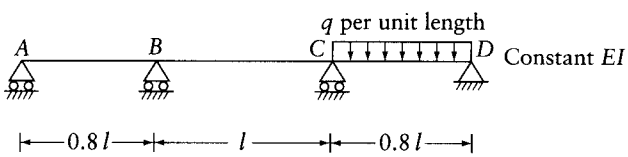

Prob. 4.3

4.4 Obtain the bending moment diagram for the beam of Prob. 4.3 on the assumption that support B settles vertically a distance $l/1200$. (No distributed load acts in this case.)

4.5 Use the force method to find the bending moments at the supports of a continuous beam on elastic (spring) supports. The beam has a constant flexural rigidity EI, and the stiffness of the elastic supports is $K = 20EI/l^3$.

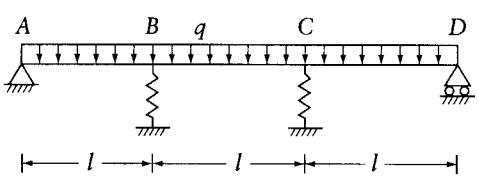

Prob. 4.5

4.6 Use the force method to find the forces in the three springs A, B, and C in the system shown. The beams DE and FG have a constant flexural rigidity EI, and the springs have the same stiffness, $100\ EI/l^3$. (a)What are the values of the vertical reactions at D, E, F, and G?

(b) If the springs A, B and C are replaced by rigid link members, what will be the forces in the links and the reactions?

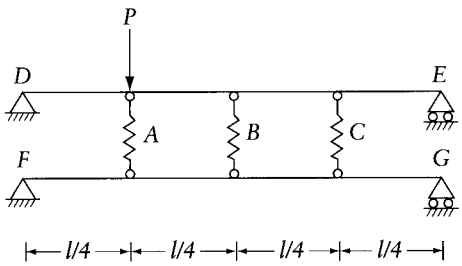

Prob. 4.6

4.7 Find the forces in the springs A and B of the system shown. Assume that the mast EF is rigid, the bars GC and HD have a constant flexural rigidity EI, and the stiffness of the springs A and B is EI/l^3. Note that in the displaced position of the mast EF, the vertical force P tends to rotate the mast about the hinge E. *Hint:* In this problem the displacement of the mast alters the forces acting on it; therefore, the principle of superposition cannot be applied (see Section 3.6). However, if the vertical force P is assumed to be always acting, the superposition of the effects of two transverse loadings on the mast can be made. This idea is further discussed in Chapter 14. For the analysis by the force method, the flexibility is determined for a released structure which has the vertical load P acting, and the inconsistency in displacement of this structure caused by the load Q is also calculated with the load P present.

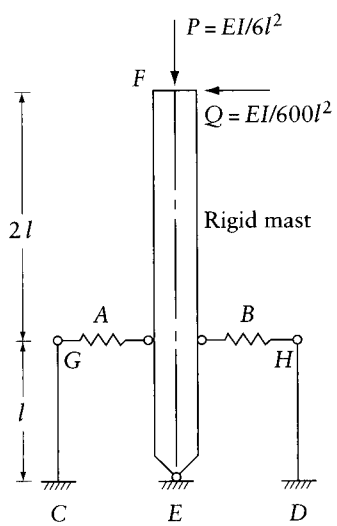

Prob. 4.7

4.8 Imperial units. A steel beam AB is supported by two steel cables at C and D. Using the force method, find the tension in the cables and the bending moment at D due to a load $P = 5$ k and a drop of temperature of 40° Fahrenheit in the two cables. For the beam $I = 40$ in.^{4}, for the cables $a = 0.15$ in.^{2}; the modulus of elasticity for both is $E = 30 \times 10^3$ ksi, and the coefficient of thermal expansion for steel is 6.5×10^{-6} per degree Fahrenheit.

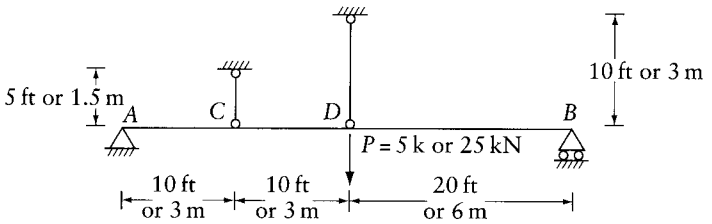

Prob. 4.8 (imperial units) or *Prob. 4.9* (SI units)

4.9 SI units. A steel beam AB is supported by two steel cables at C and D. Using the force method, find the tension in the cables and the bending moment at D due to a load $P = 25$ kN and a drop of temperature of 20 degrees Celsius in the two cables. For the beam $I = 16 \times 10^6$ mm^4, for the cables $a = 100$ mm^2; the modulus of elasticity for both is $E = 200$ GN/m^2, and the coefficient of thermal expansion for steel is 1×10^{-5} per degree Celsius.

4.10 Using the equation of three moments, find the bending moment diagram for the beam shown.

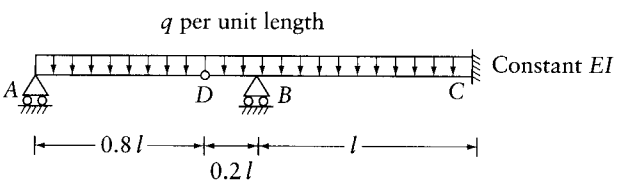

Prob. 4.10

4.11 Using the equation of three moments, obtain the bending moment and shearing force diagrams for the continuous beam shown.

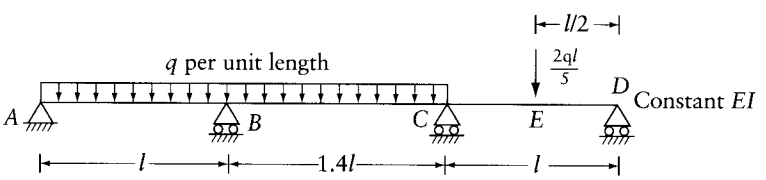

Prob. 4.11

4.12 For the beam in Figure 4.1a, but without the uniform load, find the reactions at the supports and the bending moment diagram due to a rise in temperature varying linearly over the beam depth h. The temperature rise in degrees at top and bottom fibers is T_t and T_b respectively. The coefficient of thermal expansion is α per degree.

4.13 For the beam shown, obtain the bending moment and shearing force diagrams.

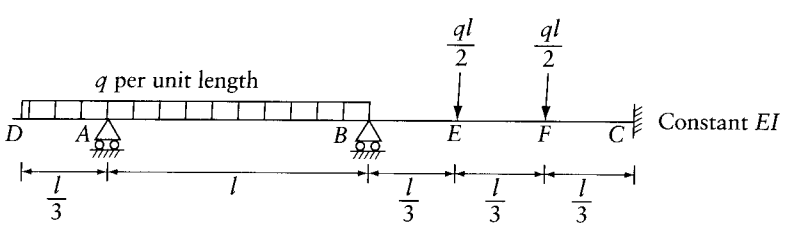

Prob. 4.13

4.14 The reinforced concrete bridge ABC shown in the figure is constructed in two stages. In stage 1, part AD is cast and its forms are removed. In stage 2, part DC is cast and its forms are removed; a monolithic continuous beam is obtained. Obtain the bending moment diagrams and the reactions due to the structure self-weight, q per unit length, immediately at the end of stages 1 and 2.

Hint: At the end of stage 1, we have a simple beam with an overhang, carrying a uniform load. In stage 2, we added a load q per unit length over DC in a continuous beam. Superposition gives the desired answers for the end of stage 2. Creep of concrete tends gradually to make the structure behave as if it were constructed in one stage (see the references mentioned in footnote 1 of Chapter 4).

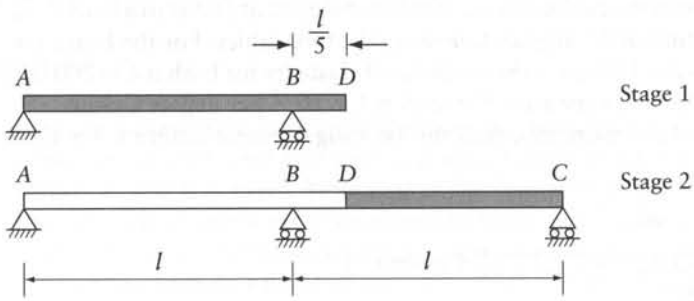

Prob. 4.14

4.15 A continuous beam of four equal spans l and constant EI is subjected to a uniform dead load q per unit length over the whole length, combined with a uniform live load of intensity $p = q$. Determine the maximum bending moment values over the supports and at the centers of spans. The answers to this problem are given in Figure 4.13.

4.16 A continuous beam of three equal spans l and constant EI is subjected to a uniform dead load q per unit length over the whole length, combined with a uniform live load of intensity $p = q$. Determine:

(a) The maximum bending moments at the interior supports and mid-spans.
(b) Diagram of maximum bending moment.
(c) Maximum reaction at an interior support.
(d) Absolute maximum shearing force and its location.

4.17 For the beam of Prob. 4.13, find the reactions, and the bending moment and shearing force diagrams due to a unit downward settlement of support B. (The main answers for this problem are included in Table E-3, Appendix E. Note that the presence of the overhang DA has no effect.)

4.18 For the continuous beam shown, determine: (a) the bending moment diagram, (b) the reaction at B and (c) the deflection at the center of BC.

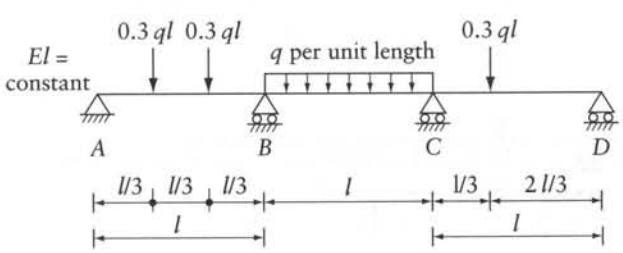

Prob. 4.18

4.19 For the continuous beam shown, determine the bending moment diagram, the reaction at B and the deflection at D due to the given loads. What is the reaction at B due to the downward settlement δ at support B?

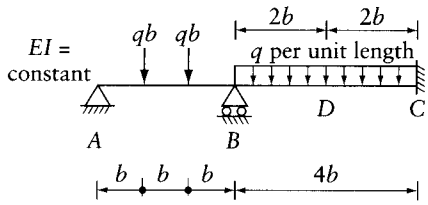

Prob. 4.19

4.20 Consider the beam in Figure 4.11. Due to uniform load q/unit length covering the whole length, combined with a uniform live load $p = q$ per unit length, find: $M_{B\max -}$, $M_{E\max +}$ and $R_{C\max +}$. E is at the middle of AB; EI is constant.

4.21 The beam of Prob. 4.10 is subjected to a rise of temperature that varies linearly over the depth h from T_{top} to T_{bot} at the top and bottom respectively. Sketch the deflected shape assuming that $T_{top} > T_{bot}$. Calculate the deflections at the middle of AD, at D, and at the middle of BC. Consider only bending deformation; EI is constant and the coefficient of thermal expansion is α per degree.

4.22 Find the bending moment diagram for the frame shown. Assume $(Ea)_{\text{Tie BD}} = 130EI/l^2$, where EI is the flexural rigidity of ABCDE. Use the force method cutting the tie BD to release the structure.

Hint: Calculation of the displacements in steps 2 and 3 of the force method has not been covered in earlier chapters. The problem can be solved using given information: the load applied on the released structure would move B and D away from each other a distance $= 0.1258ql^4/(EI)$. Two unit horizontal forces each $= F_1 = 1$ applied inwards at each of B and D of the released structure would move the joints closer to each other by a distance $= 0.1569l^3/(EI)$.

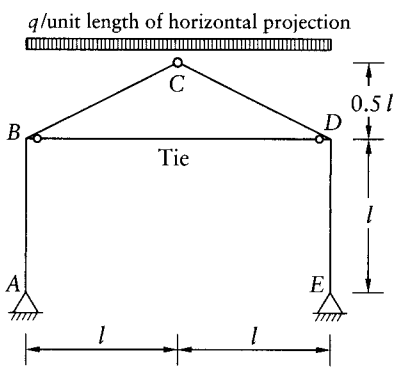

Prob. 4.22

4.23 The continuous beam of Prob. 4.11 is subjected to a uniform dead load of q per unit length combined with a uniform live load of intensity $p = 0.75q$. Determine:

(a) Diagram of maximum bending moment.
(b) Maximum reaction at B.
(c) Absolute maximum shearing force.

4.24 Use the force method to verify the equations relevant to any of the beams shown in Appendix C.

4.25 Use the force method to verify the equations relevant to any of the members shown in Appendix D.

4.26 Use the equation of three moments to verify the values given in Tables E.1, E.2 or E.3 for any number of spans considered in Appendix E.

Chapter 5

Displacement method of analysis

5.1 Introduction

The mathematical formulation of the displacement method and force method is similar, but from the point of view of economy of effort one or the other method may be preferable. This will be considered in detail in Section 6.3.

The displacement method can be applied to statically determinate or indeterminate structures, but it is more useful in the latter, particularly when the degree of statical indeterminacy is high.

5.2 Description of method

The displacement method involves five steps:

1. First of all, the degree of kinematic indeterminacy has to be found. A coordinate system is then established to identify the location and direction of the joint displacements. Restraining forces equal in number to the degree of kinematic indeterminacy are introduced at the coordinates to prevent the displacement of the joints. In some cases, the number of restraints introduced may be smaller than the degree of kinematic indeterminacy, provided that the analysis of the resulting structure is a standard one and is therefore known. (See remarks following Example 5.2.)

   We should note that, unlike the force method, the above procedure requires no choice to be made with respect to the restraining forces. This fact favors the use of the displacement method in general computer programs for the analysis of a structure.
2. The restraining forces are now determined as a sum of the fixed-end forces for the members meeting at a joint. For most practical cases, the fixed-end forces can be calculated with the aid of standard tables (Appendices C and D). An external force at a coordinate is restrained simply by an equal and opposite force that must be added to the sum of the fixed-end forces.

   We should remember that the restraining forces are those required to prevent the displacement at the coordinates due to all effects, such as external loads, temperature variation, or prestrain. These effects may be considered separately or may be combined.

   If the analysis is to be performed for the effect of movement of one of the joints in the structure, for example, the settlement of a support, the forces at the coordinates required to hold the joint in the displaced position are included in the restraining forces.

   The internal forces in the members are also determined at the required locations with the joints in the restrained position.
3. The structure is now assumed to be deformed in such a way that a displacement at one of the coordinates equals unity and all the other displacements are zero, and the forces required to hold the structure in this configuration are determined. These forces are applied

at the coordinates representing the degrees of freedom. The internal forces at the required locations corresponding to this configuration are determined.

The process is repeated for a unit value of displacement at each of the coordinates separately.

4. The values of the displacements necessary to eliminate the restraining forces introduced in (2) are determined. This requires superposition equations in which the effects of separate displacements on the restraining forces are added.
5. Finally, the forces on the original structure are obtained by adding the forces on the restrained structure to the forces caused by the joint displacements determined in (4).

The use of the above procedure is best explained with reference to some specific cases.

Example 5.1: Plane truss

The plane truss in Figure 5.1a consists of m pin-jointed members meeting at joint A. Find the forces in the members due to the combined effect of: (1) an external load P applied at A; (2) a rise of temperature T degrees of the kth bar alone.

The degree of kinematic indeterminacy of the structure is two ($n=2$), because displacement can occur only at joint A, which can undergo a translation with components D_1 and D_2 in the x and y directions. The positive directions for the displacement components, as well as for the restraining forces, are arbitrarily chosen, as indicated in Figure 5.1b. Here, a coordinate system is represented by arrows defining the locations and the positive directions of displacements $\{D\}_{n\times 1}$ and forces $\{F\}_{n\times 1}$. In this first step of the displacement method, we also define the required actions, $\{A\}_{m\times 1}$; in this example, the elements of $\{A\}$ are the forces in the truss members due to the specified loading.

The joint displacements are artificially prevented by introducing at A a force equal and opposite to P plus a force $(Ea\alpha T)_k$ in the direction of the kth member. Here, E, a and α are, respectively, modulus of elasticity, cross-sectional area, and coefficient of thermal expansion of the kth bar. Components of the restraining forces in the directions of the coordinates are

$$F_1 = -P\cos\beta + (Ea\alpha T\cos\theta)_k$$

$$F_2 = -P\sin\beta + (Ea\alpha T\sin\theta)_k$$

where θ_k is the angle between the positive x direction and the kth bar. With the displacements at A prevented, the change in length of any member is zero; thus, the axial force is zero, with the exception of the kth bar. Because the thermal expansion is prevented, an axial force is developed in the kth bar; this is equal to $-(Ea\alpha T)_k$, with the minus sign indicating compression. Denoting by $\{A_r\}$ the axial forces in the bars in the restrained condition, we have

$$\{A_r\} = \{0, 0, \ldots, -(Ea\alpha T)_k, \ldots, 0\}$$

All elements of the vector $\{A_r\}$ are zero except the kth. In this second step, we have determined the forces $\{F\}$ necessary to prevent the displacements at the coordinates when the loading is applied; we have also determined the actions $\{A_r\}$ due to the loading while the displacements are artificially prevented.

Figure 5.1c shows the forces required to hold the structure in a deformed position such that $D_1 = 1$ and $D_2 = 0$. Now, from Figure 5.1d, a unit horizontal displacement of A causes a shortening of any bar i by a distance $\cos\theta_i$ and produces a compressive force of $(a_iE_i/l_i)\cos\theta_i$.

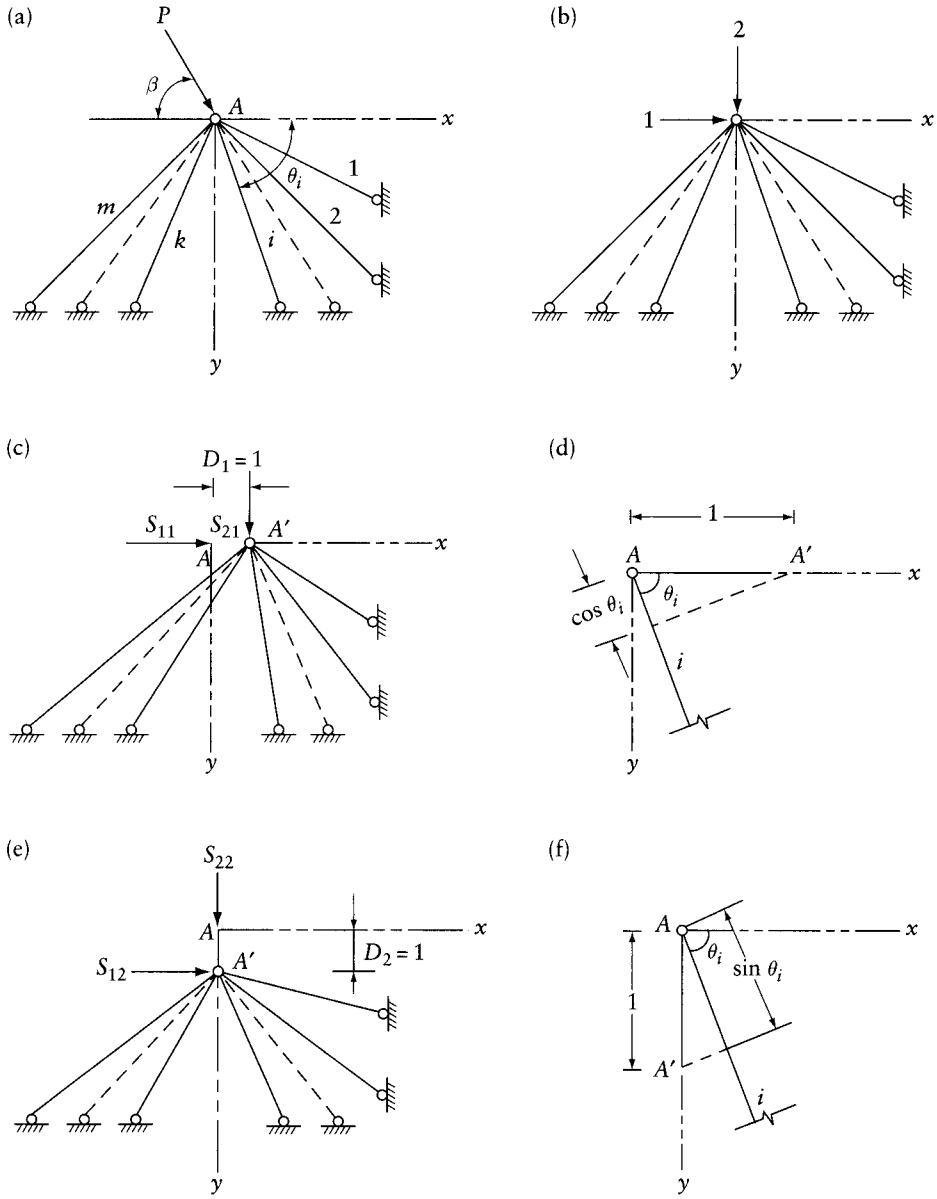

Figure 5.1 Analysis of a plane truss by the displacement method – Example 5.1. (a) Plane truss. (b) Coordinate system. (c) $D_1 = 1$ and $D_2 = 0$. (d) Change in length in the ith member due to $D_1 = 1$. (e) $D_1 = 0$ and $D_2 = 1$. (f) Change in length in the ith member due to $D_2 = 1$.

Therefore, to hold joint A in the displaced position, forces $(a_i E_i / l_i) \cos^2 \theta_i$ and $(a_i E_i / l_i) \cos \theta_i \sin \theta_i$ have to be applied in directions 1 and 2 respectively. The forces required to hold all the bars in the displaced position are

$$S_{11} = \sum_{i=1}^{m} \left(\frac{aE}{l} \cos^2 \theta \right)_i ; \; S_{21} = \sum_{i=1}^{m} \left(\frac{aE}{l} \cos \theta \sin \theta \right)_i$$

By a similar argument, the forces required to hold the joint A in the displaced position such that $D_1 = 0$ and $D_2 = 1$ (Figures 5.1e and f) are

$$S_{12} = \sum_{i=1}^{m} \left(\frac{aE}{l} \sin\theta \cos\theta \right)_i ; \; S_{22} = \sum_{i=1}^{m} \left(\frac{aE}{l} \sin^2\theta \right)_i$$

The first subscript of S in the above equations indicates the coordinate of the restraining force, and the second subscript the component of the displacement which has a unit value.

In the actual structure, joint A undergoes translations D_1 and D_2 and there are no restraining forces. Therefore, the superposition of the fictitious restraints and of the effects of the actual displacements must be equal to zero. Thus, we obtain *statical relations* which express the fact that the restraining forces vanish when the displacements D_1 and D_2 take place. These statical relations can be expressed as

$$\text{and} \quad \left.\begin{aligned} F_1 + S_{11}D_1 + S_{12}D_2 &= 0 \\ F_2 + S_{21}D_1 + S_{22}D_2 &= 0 \end{aligned}\right\} \tag{5.1}$$

Stiffness matrix

The statical relations of Eq. 5.1 can be written in matrix form

$$\text{or} \quad \begin{aligned} \{F\}_{n\times 1} + [S]_{n\times n}\,\{D\}_{n\times 1} &= \{0\} \\ [S]_{n\times n}\,\{D\}_{n\times 1} &= \{-F\}_{n\times 1} \end{aligned} \tag{5.2}$$

(This equation may be compared with Eq. 4.3 for the geometry relations in the force method of analysis.)

The column vector $\{F\}$ depends on the loading on the structure. The elements of the matrix $[S]$ are forces corresponding to unit values of displacements. Therefore, $[S]$ depends on the properties of the structure, and represents its stiffness. For this reason, $[S]$ is called the *stiffness matrix* and its elements are called *stiffness coefficients*. The elements of the vector $\{D\}$ are the unknown displacements and can be determined by solving Eq. 5.2, that is,

$$\{D\} = [S]^{-1}\,\{-F\} \tag{5.3}$$

In a general case, if the number of restraints introduced in the structure is n, the order of the matrices $\{D\}, [S]$, and $\{F\}$ is $n \times 1, n \times n$, and $n \times 1$ respectively. The stiffness matrix $[S]$ is thus a square symmetrical matrix. This can be seen in the above example by comparing the equations for S_{21} and S_{12} but a formal proof will be given in Section 6.6.

In the third step of the displacement method, we determine $[S]_{n\times n}$ and $[A_u]_{m\times n}$. To generate any column, j, of the two matrices, we introduce a unit displacement $D_j = 1$ at coordinate j, while the displacements are prevented at the remaining coordinates. The forces necessary at the n coordinates to hold the structure in this deformed configuration form the jth column of $[S]$; the corresponding m actions form the jth column of $[A_u]$. In the fourth step of the displacement method, we solve the statical Eq. 5.2 (also called *equilibrium equation*). This gives the actual displacements $\{D\}_{n\times 1}$ at the coordinates.

The final force in any member i can be determined by superposition of the restrained condition and of the effect of the joint displacements.

$$A_i = A_{ri} + (A_{ui1}D_1 + A_{ui2}D_2 + \cdots + A_{uin}D_n) \tag{5.4}$$

The *superposition* equation for all the members in matrix form is

$$\{A\}_{m\times 1} = \{A_r\}_{m\times 1} + [A_u]_{m\times n}\,\{D\}_{n\times 1}$$

where the elements of $\{A\}$ are the final forces in the bars, the elements of $\{A_r\}$ are the bar forces in the restrained condition, and the elements of $[A_u]$ are the bar forces corresponding to unit displacements. Specifically, the elements of column j of $[A_u]$ are the forces in the members corresponding to a displacement $D_j = 1$ while all the other displacements are zero.

Since the above equation will be used in the analysis of a variety of structures, it is useful to write it in a general form

$$\{A\} = \{A_r\} + [A_u]\,\{D\} \tag{5.5}$$

where the elements of $\{A\}$ are the final forces in the members, the elements of $\{A_r\}$ are the forces in members in the restrained condition, and the elements of $[A_u]$ are the forces in members corresponding to unit displacements. The fifth step of the displacement method gives the required action $\{A\}$ by substituting in Eq. 5.5 matrices $\{A_r\}, [A_u]$ and $\{D\}$ determined in steps 2, 3 and 4.

In the truss of Example 5.1, with axial tension in a member considered positive, it can be seen that

$$[A_u] = \begin{bmatrix} -\dfrac{a_1E_1}{l_1}\cos\theta_1 & -\dfrac{a_1E_1}{l_1}\sin\theta_1 \\ -\dfrac{a_2E_2}{l_2}\cos\theta_2 & -\dfrac{a_2E_2}{l_2}\sin\theta_2 \\ \cdots & \cdots \\ -\dfrac{a_mE_m}{l_m}\cos\theta_m & -\dfrac{a_mE_m}{l_m}\sin\theta_m \end{bmatrix}$$

In a frame with rigid joints, we may want to find the stress resultants in any section or the reactions at the supports. For this reason, we consider the notation A in the general Eq. 5.5 to represent any action, which may be shearing force, bending moment, twisting moment, or axial force at a section or a reaction at a support.

5.3 Degrees of freedom and coordinate system

In the first step of the displacement method, the number n of the independent joint displacements (the number of degrees of freedom, Section 3.5) is determined. A system of n coordinates is defined. A coordinate is an arrow representing the location and the positive direction of a displacement D or a force F. The coordinate system is indicated in a figure showing the actual structure with n arrows at the joint.

The remaining steps of the displacement method involve generating and use of matrices: $\{F\}, \{D\}$ and $[S]$. The elements of these matrices are either forces or displacements at the coordinates. Thus, it is impossible to follow or check the calculations, particularly the signs of the parameters, when the coordinate system is not clearly defined. For this reason, it is recommended that the coordinate system be shown in a figure depicting only n numbered arrows; the forces applied on the structure should not be shown in this figure.

Example 5.2: Plane frame

The plane frame in Figure 5.2a consists of rigidly connected members of constant flexural rigidity EI. Obtain the bending moment diagram for the frame due to concentrated loads P at E and F, and a couple Pl at joint B. The change in length of the members can be neglected.

The degree of kinematic indeterminacy is three because there are three possible joint displacements, as shown in Figure 5.2b, which shows also the chosen coordinate system. The restraining forces, which are equal to the sum of the end-forces at the joints, are calculated with the aid of Appendix C (Eqs. C.1 and C.2). As always, they are considered positive when their direction accords with that of the coordinates.

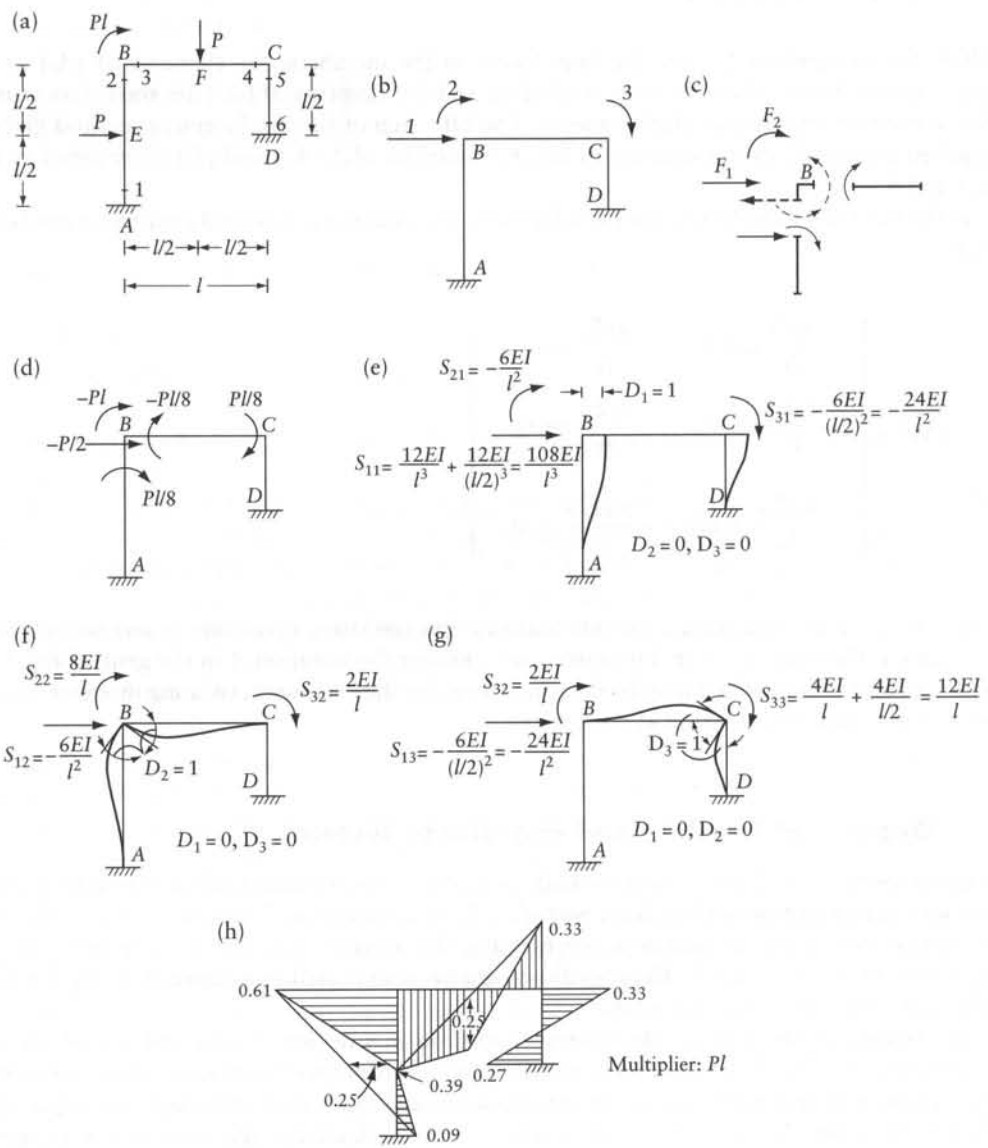

Figure 5.2 Plane frame analyzed in Example 5.2.

To illustrate the relation between the end-forces and the restraining forces, joint B is separated from the members connected to it in Figure 5.2c. The forces acting on the end of the members in the direction of the coordinate system are indicated by full-line arrows. Equal and opposite forces act on the joint, and these are shown by dotted-line arrows. For equilibrium of the joint, forces F_1 and F_2 should be applied in a direction opposite to the dotted arrows. Therefore, to obtain the restraining forces, it is sufficient to add the end-forces at each joint as indicated in Figure 5.2d, and it is not necessary to consider the forces as in Figure 5.2c.

The external applied couple acting at B requires an equal and opposite restraining force. Therefore,

$$\{F\} = \begin{Bmatrix} -\frac{P}{2} \\ \left(\frac{Pl}{8} - \frac{Pl}{8} - Pl\right) \\ \frac{Pl}{8} \end{Bmatrix} = P \begin{Bmatrix} -0.5 \\ -l \\ 0.125l \end{Bmatrix} \tag{a}$$

To draw the bending moment diagram, the values of the moments at the ends of all the members are required, it being assumed that an end-moment is positive if it acts in a clockwise direction. We define the required actions as the member end-moments:

$$\{A\} = \{M_{AB}, M_{BA}, M_{BC}, M_{CB}, M_{CD}, M_{DC}\}$$

Throughout this book, a clockwise end-moment for a member of a plane frame is considered positive. The two clockwise end-moments shown in Figure 3.8a are positive. At the left-hand end of the member, the clockwise moment produces tension at the bottom face; but at the right-hand end, the clockwise moment produces tension at the top face. The member ends 1, 2,..., 6 are identified in Figure 5.2a. Thus, the values of the six end-moments corresponding to the restrained condition are

$$\{A_r\} = \frac{Pl}{8}\{-1, 1, -1, 1, 0, 0\}$$

Now, the elements of the stiffness matrix are the forces necessary at the location in the direction of the coordinates to hold the structure in the deformed shape illustrated in Figures 5.2e, f, and g. These forces are equal to the sum of the end-forces, which are taken from Appendix D (Eqs. D.1 to D.5). We should note that the translation of joint B must be accompanied by an equal translation of joint C in order that the length BC remains unchanged. The stiffness matrix is

$$[S] = \frac{EI}{l} \begin{bmatrix} \frac{108}{1^2} & -\frac{6}{l} & -\frac{24}{l} \\ -\frac{6}{l} & 8 & 2 \\ -\frac{24}{l} & 2 & 12 \end{bmatrix} \tag{b}$$

To write the matrix of end-moments due to the unit displacements, we put the values at the beam ends 1, 2,..., 6 in the first, second, and third column, respectively, for the displacements shown in Figures 5.2e, f, and g. Thus,

$$[A_u] = \frac{EI}{l}\begin{bmatrix} -\frac{6}{l} & 2 & 0 \\ -\frac{6}{l} & 4 & 0 \\ 0 & 4 & 2 \\ 0 & 2 & 4 \\ -\frac{24}{l} & 0 & 8 \\ -\frac{24}{l} & 0 & 4 \end{bmatrix} \tag{c}$$

The deflected shapes of the members in Figures 5.2e, f and g and the corresponding end-moments are presented in Appendix D, which is used to determine the elements of $[A_u]$. For example, with $D_3 = 1$, member BC in Figure 5.2g has the same deflected shape as in the second figure of Appendix D. Thus, the end-moments $2EI/l$ and $4EI/l$ taken from this figure are equal to elements A_{u33} and A_{u43} respectively.

Substituting Eqs. (a) and (b) into Eq. 5.3 and solving for $\{D\}$, we obtain

$$\{D\} = \frac{Pl^2}{EI}\begin{Bmatrix} 0.0087l \\ 0.1355 \\ -0.0156 \end{Bmatrix} \tag{d}$$

The final end-moments are calculated by Eq. 5.5:

$$\{A\} = Pl\begin{Bmatrix} -0.125 \\ 0.125 \\ -0.125 \\ 0.125 \\ 0 \\ 0 \end{Bmatrix} + \frac{EI}{l}\begin{bmatrix} -\frac{6}{l} & 2 & 0 \\ -\frac{6}{l} & 4 & 0 \\ 0 & 4 & 2 \\ 0 & 2 & 4 \\ -\frac{24}{l} & 0 & 8 \\ -\frac{24}{l} & 0 & 4 \end{bmatrix} \frac{Pl^2}{EI}\begin{Bmatrix} 0.0087l \\ 0.1355 \\ -0.0156 \end{Bmatrix} = Pl\begin{Bmatrix} 0.09 \\ 0.61 \\ 0.39 \\ 0.33 \\ -0.33 \\ -0.27 \end{Bmatrix} \tag{e}$$

The bending moment diagram is plotted in Figure 5.2h, the ordinate appearing on the side of the tensile fiber.

The application of the preceding procedure to a frame with inclined members is illustrated in Example 5.3.

Remarks

(1) If, in the above example, the fixed end A is replaced by a hinge, the kinematic indeterminacy is increased by the rotation at A. Nevertheless, the structure can be analyzed using only the three coordinates in Figure 5.2 because the end-forces for a member hinged at one end and fully fixed at the other are readily available (Appendices C and D).

As an exercise, we can verify the following matrices for analyzing the frame in Figure 5.2, with support A changed to a hinge

$$\{F\} = (P/16)\{-11,\ -15l,\ 2l\};\quad \{A_r\} = (Pl/16)\{0, 3, -2, 2, 0, 0\}$$

$$[S] = \frac{EI}{l}\begin{bmatrix} 99/l^2 & & \text{sym.} \\ -3/l & 7 & \\ -24/l & 2 & 12 \end{bmatrix}$$

$$[A_u]^T = \frac{EI}{l}\begin{bmatrix} 0 & -3/l & 0 & 0 & -24/l & -24/l \\ 0 & 3 & 4 & 2 & 0 & 0 \\ 0 & 0 & 2 & 4 & 8 & 4 \end{bmatrix}$$

$$\{D\} = \frac{Pl^2}{EI}\{0.0058l,\ 0.1429,\ -0.0227\}$$

$$\{A\} = Pl\{0,\ 0.60,\ 0.40,\ 0.32,\ -0.32,\ -0.23\}$$

(2) When a computer is used for the analysis of a plane frame, axial deformations are commonly not ignored and the unknown displacements are two translations and a rotation at a general joint. Three forces are usually determined at each member end (Figure 22.2). These can be used to give the axial force, the shearing force, and the bending moment at any section. The superposition Eq. 5.5 is applied separately to give six end-forces for each member, using the six displacements at its ends. This is discussed in detail in Chapter 22 for all types of framed structures.

5.4 Analysis for different loadings

We have already made it clear that the stiffness matrix (and its inverse) are properties of a structure and do not depend on the system of the load applied. Therefore, if a number of different loadings are to be considered, Eq. 5.2 can be used for all of them. If the number of cases of loading is p and the number of degrees of freedom is n, the solution can be combined into one matrix equation:

$$[D]_{n\times p} = [S]^{-1}_{n\times n}\,[-F]_{n\times p} \tag{5.6}$$

with each column of $[D]$ and $[-F]$ corresponding to one loading.

The third step of the displacement method involves generation of $[A_u]_{m\times n}$ in addition to $[S]_{n\times n}$. The elements of any column of $[A_u]$ are values of the required m actions when a unit displacement is introduced at one coordinate, while the displacements are prevented at the remaining coordinates. Thus, similar to $[S]$, the elements of $[A_u]$ do not depend on the applied load. Therefore, the same matrix $[A_u]$ can be used for all loading cases. With p loading cases, the superposition Eq. 5.5 applies with the sizes of matrices: $[A]_{m\times p}, [A_r]_{m\times p}, [A_u]_{m\times n}$ and $[D]_{n\times p}$.

5.5 Analysis for environmental effects

In Section 4.4 we used the force method to analyze the separate or combined effects of temperature change, lack of fit, shrinkage, or prestrain. We shall now show how the displacement method can be used for the same purpose. Equation 5.3 is directly applicable but in this case $\{F\}$ represents the forces necessary to prevent the joint displacements due to the given effects.

When the analysis is carried out for the effect of movement of support, Eq. 5.3 can also be applied, provided the movement of the support does not correspond with one of the unknown displacements forming the kinematic indeterminacy. When the movement of the support does so correspond, a modification of Eq. 5.3 is necessary. This is explained with reference to Example 5.5.

5.6 Five steps of displacement method

The analysis by the displacement method involves five steps which are summarized as follows:

Step 1 Define a system of coordinates representing the joint displacements to be found. Also, define $[A]_{m\times p}$, the required actions as well as their sign convention (if necessary).

Step 2 With the loadings applied, calculate the restraining forces $[F]_{n\times p}$ and $[A_r]_{m\times p}$.

Step 3 Introduce unit displacements at the coordinates, one by one, and generate $[S]_{n\times n}$ and $[A_u]_{m\times n}$.

Step 4 Solve the equilibrium equations:

$$[S]_{n\times n}\,[D]_{n\times p} = -[F]_{n\times p} \tag{5.7}$$

This gives the displacements $[D]$.

Step 5 Calculate the required actions by superposition:

$$[A]_{m\times p} = [A_r]_{m\times p} + [A_u]_{m\times n}\,[D]_{n\times p} \tag{5.8}$$

In a manner similar to the force method (Section 4.6), when Step 3 above is completed all the matrices necessary for the analysis have been generated. The last two steps involve merely matrix algebra.

For quick reference, the symbols used in this section are defined again as follows:

n, p, m = number of degrees of freedom, number of loading cases and number of actions required
$[A]$ = required actions (the answers to the problem)
$[A_r]$ = values of the actions due to loadings on the structure while the displacements are prevented
$[A_u]$ = values of the actions due to unit displacements introduced separately at each coordinate
$[F]$ = forces at the coordinates necessary to prevent the displacements due to the loadings
$[S]$ = stiffness matrix

Example 5.3: Plane frame with inclined member

Obtain the bending moment diagrams for the plane frame in Figure 5.3a due to the separate effects of: (1) the loads shown; (2) a downward settlement δ_D at support D. Consider EI = constant and neglect the change in length of members.

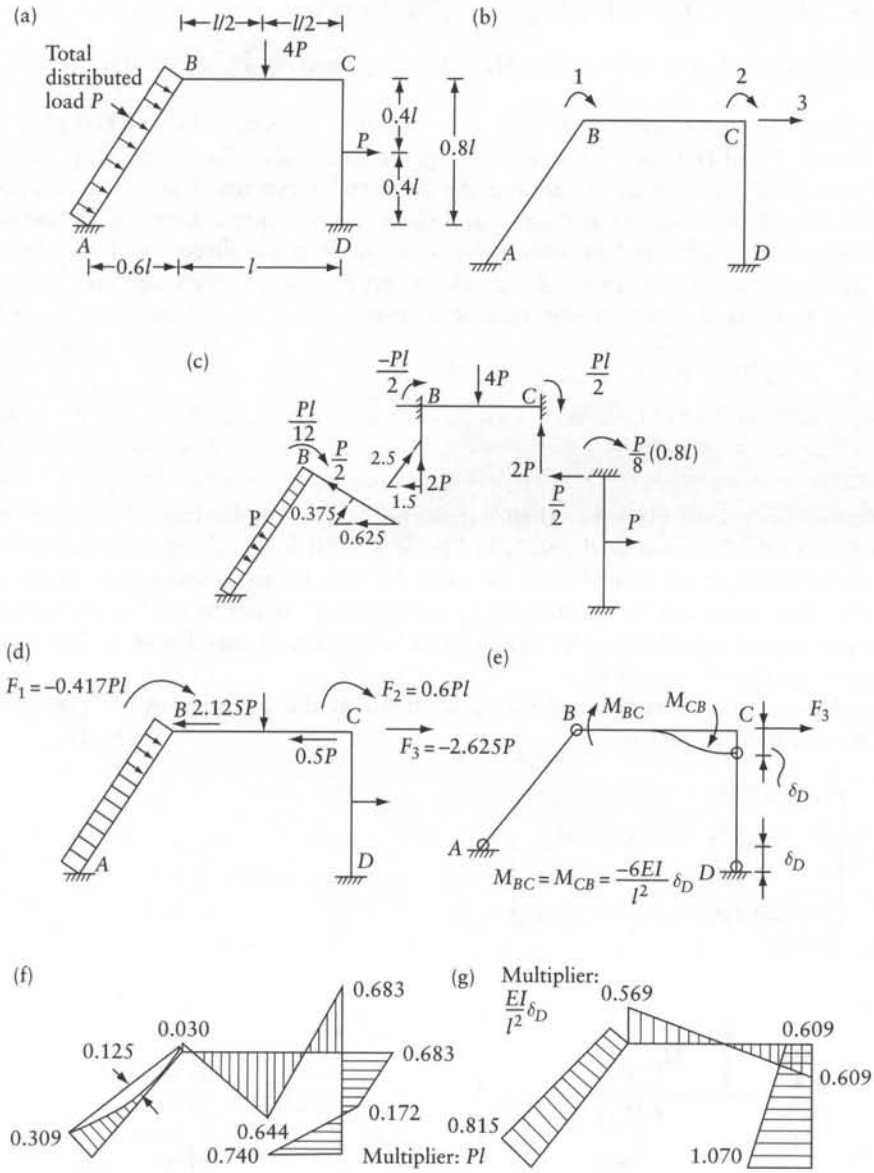

Figure 5.3 Frame analyzed in Example 5.3. (a) Frame dimensions and loading. (b) Coordinate system. (c) Fixed-end forces in case (1). (d) Restraining forces $\{F\}$ in case (1). (e) Member-end moments with the displacements restrained at the coordinates in case (2). (f) Bending moment diagram in case (1). (g) Bending moment diagram in case (2).

Step 1 Figure 5.3b defines a coordinate system corresponding to three independent joint displacements (the kinematic indeterminacy; see Section 3.5). The required bending moment diagrams can be drawn from the member-end moments (considered positive when clockwise):

$$[A] = \left[\begin{Bmatrix} M_{AB} \\ M_{BC} \\ M_{CD} \\ M_{DC} \end{Bmatrix}_1 \quad \begin{Bmatrix} M_{AB} \\ M_{BC} \\ M_{CD} \\ M_{DC} \end{Bmatrix}_2 \right] \tag{a}$$

$M_{BA} = -M_{BC}$ and $M_{CB} = -M_{CD}$; thus M_{BA} and M_{CB} need not be included in $[A]$.

Step 2 The fixed-end forces for the members are found from Appendices C and D (Eqs. C.1, C.2, C.7, C.8, D.1 and D.2) and are shown in Figures 5.3c and e. The restraining couples F_1 and F_2 are obtained directly by adding the fixed-end moments. For the calculation of F_3, the shearing forces meeting at joints B and C are resolved into components along the member axes, and F_3 is obtained by adding the components in the direction of coordinate 3 (Figure 5.3d). An alternative method for calculating F_3 using a work equation will be explained below. Now, we write the restraining forces:

$$[F] = \begin{bmatrix} -0.417Pl & -6(EI/l^2)\delta_D \\ 0.6Pl & -6(EI/l^2)\delta_D \\ -2.625P & -9(EI/l^2)\delta_D \end{bmatrix} \tag{b}$$

The value of F_3 in case (1) is equal to minus the sum of the horizontal components $0.625P, 1.5P$ and $0.5P$ shown at B and C in Figure 5.3c. If a similar figure is drawn for case (2), the shearing force at end B of member BC will be an upward force equal to $(12EI\delta_D/l^3)$. This force can be substituted by a component equal to $(15EI\delta_D/l^3)$ along AB and a component equal to $(-9EI\delta_D/l^3)$ in the direction of coordinate 3. The latter component is equal to F_3 in case (2).

The member-end moments when the displacements at the coordinates are prevented (Figure 5.4a and Figure 5.3e) are

$$[A_r] = \begin{bmatrix} -0.0833Pl & 0 \\ -0.5Pl & -6(EI/l^2)\delta_D \\ 0.1Pl & 0 \\ -0.1Pl & 0 \end{bmatrix} \tag{c}$$

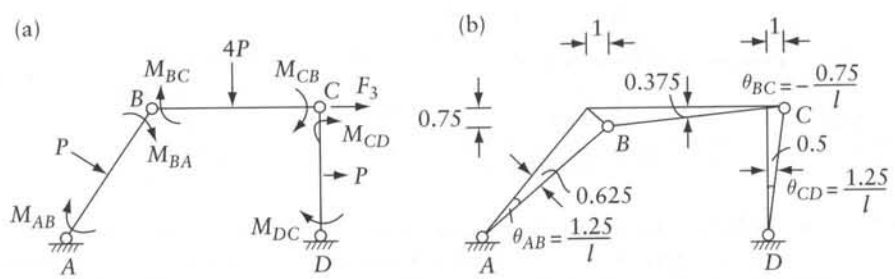

Figure 5.4 Calculation of restraining force F_3 in Example 5.3 using work equation. (a) Fixed-end moments shown as external forces on a mechanism, case (1). (b) Virtual displacement of the mechanism in (a).

The work equation which can give F_3-values in Eq. b will be applied to a mechanism (Figure 5.4b), in which hinges are introduced at the joints. The members of the mechanism are subjected to the same external forces as in Figure 5.4a, in which the end-moments are represented as external applied forces. The forces in Figure 5.4a, including F_3 and the reactions (not shown) at A and D, constitute a system in equilibrium. Introducing a unit virtual (fictitious) displacement at coordinate 3 (Figure 5.4b) will cause members of the mechanism to rotate and translate, without deformation, as shown in Figure 5.4b. No work is required for the virtual displacement; thus, the sum of the forces (concentrated loads or couples) in Figure 5.4a multiplied by the corresponding virtual displacements in Figure 5.4b is equal to zero:

$$\theta_{AB}(M_{AB}+M_{BA})+\theta_{BC}(M_{BC}+M_{CB})+\theta_{CD}(M_{CD}+M_{DC})$$
$$+F_3\times 1+[P(0.625)+4P(0.375)+P(0.5)]=0 \qquad (5.9)$$

The values of member-end moments are (Appendix C, Eqs. C.1 and C.7): $M_{AB}=-M_{BA}=-Pl/12; M_{BC}=-M_{CB}=-Pl/2; M_{CD}=-M_{DC}=Pl/10; \theta_{AB}=1.25/l; \theta_{BC}=-0.75/l; \theta_{CD}=1.25/l$; substitution in Eq. 5.9 gives $F_3=-2.625P$. Similarly, the sum of the forces in Figure 5.3e multiplied by the displacement in Figure 5.4b is equal to zero; for case (2) this gives $F_3=-9EI\delta_D/l^3$.

Step 3 Separate displacements $D_1=1$, $D_2=1$, and $D_3=1$ produce the member-end moments shown in Figures 5.5a, b, and c respectively (Appendix D, Eqs. D.1 to D.5). Summing up the member-end moments at joints B and C gives the elements of the first two rows of the stiffness matrix [S], given below. Work equations summing the product of the

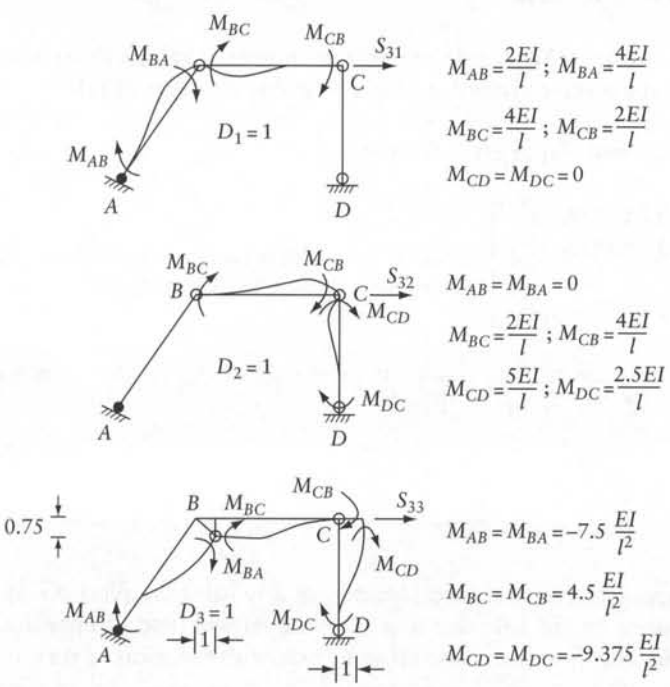

Figure 5.5 Generation of stiffness matrix for the frame of Example 5.3 (Figure 5.3b). (a), (b) and (c) Member-end moments represented as external forces on a mechanism when $D_1=1, D_2=1$, and $D_3=1$, respectively.

forces in each of Figures 5.5a, b, and c multiplied by the displacements in Figure 5.4b give S_{31}, S_{32}, and S_{33}. The work equation will be the same as Eq. 5.9, but without the last term in square brackets; the values of the member-end moments are given in Figures 5.5a, b, and c. The same figures are also used to generate $[A_u]$:

$$[S] = EI \begin{bmatrix} 8/l & 2/l & -3/l^2 \\ 2/l & 9/l & -4.875/l^2 \\ -3/l^2 & -4.875/l^2 & 48.938/l^3 \end{bmatrix} \tag{d}$$

$$[A_u] = \begin{bmatrix} 2EI/l & 0 & -7.5EI/l^2 \\ 4EI/l & 2EI/l & 4.5EI/l^2 \\ 0 & 5EI/l & -9.375EI/l^2 \\ 0 & 2.5EI/l & -9.375EI/l^2 \end{bmatrix} \tag{e}$$

Step 4 Substitution of $[S]$ and $[F]$ in Eq. 5.7 and solution or inversion of $[S]$ and substitution in Eq. 5.6 give

$$[D] = \frac{10^{-3}}{EI} \begin{bmatrix} 133.75l & -26.72l & 5.54l^2 \\ -26.72l & 122.79l & 10.59l^2 \\ 5.54l^2 & 10.59l^2 & 21.83l^3 \end{bmatrix} \begin{bmatrix} 0.417Pl \dfrac{6EI}{l^2}\delta_D \\ -0.6Pl \dfrac{6EI}{l^2}\delta_D \\ 2.625P \dfrac{9EI}{l^3}\delta_D \end{bmatrix}$$

$$= \begin{bmatrix} 0.0863Pl^2/EI & 0.6920\delta_D/l \\ -0.0570Pl^2/EI & 0.6717\delta_D/l \\ 0.0532Pl^2/EI & 0.2932\delta_D \end{bmatrix} \tag{f}$$

A calculator may be used to invert $[S]$ considering only the numerial values; the symbols for any element of $[S]^{-1}$ are the inverse symbols in corresponding elements of $[S]$.

Step 5 Substituting $[A_r], [A_u]$, and $[D]$ in Eq. 5.8 gives

$$[A] = \begin{bmatrix} -0.309Pl & -0.815EI\delta_D/l^2 \\ -0.030Pl & -0.569EI\delta_D/l^2 \\ -0.683Pl & 0.609EI\delta_D/l^2 \\ -0.740Pl & -1.070EI\delta_D/l^2 \end{bmatrix}$$

The elements of $[A]$ are the member-end moments used to plot the bending moment diagrams for load cases (1) and (2), Figures 5.3f and g.

Example 5.4: A grid

Find the three reaction components (vertical force, bending and twisting couples) at end A of the horizontal grid shown in Figure 5.6a due to a uniform vertical load of intensity q acting on AC. All bars of the grid have the same cross section with the ratio of torsional and flexural rigidities $GJ/EI = 0.5$.

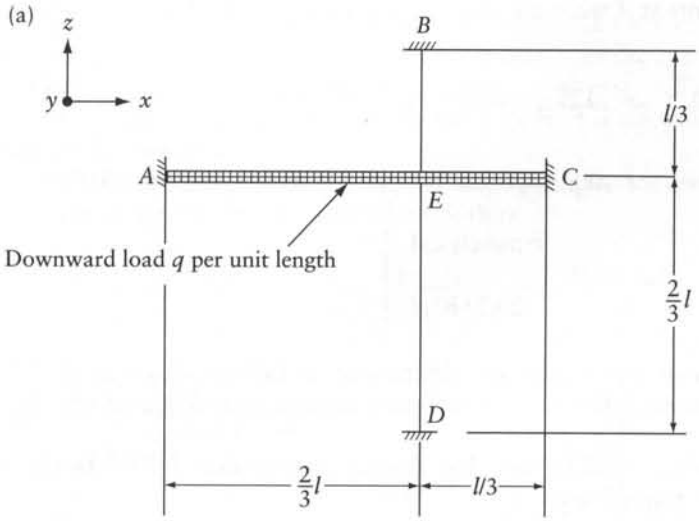

(b)
Reaction components at A

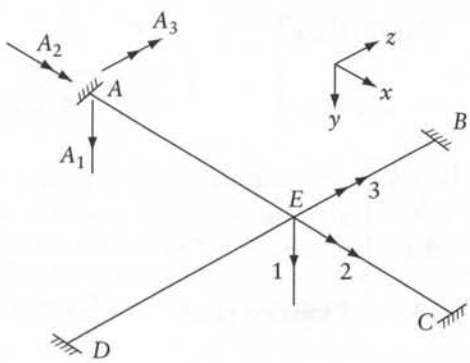

Figure 5.6 Grid analyzed in Example 5.4. (a) Grid plan. (b) Pictorial view showing chosen coordinates 1, 2, and 3 and positive directions of the reaction components at A.

Step 1 There are three independent joint displacements represented by the three coordinates in Figure 5.6b. The required actions and their positive directions are defined in the same figure.

Step 2 The restraining forces at the three coordinates are (using Appendix C, Eqs. C.7 and C.8)

$$\{F\} = \begin{Bmatrix} (-ql/2)_{AE} - (ql/2)_{EC} \\ 0 \\ (ql^2/12)_{AE} - (ql^2/12)_{EC} \end{Bmatrix} = q \begin{Bmatrix} -l/2 \\ 0 \\ l^2/36 \end{Bmatrix}$$

The reaction components at A while the displacements are prevented at the coordinates are

$$\{A_r\} = \{(-ql/2)_{AE},\ 0,\ (-ql^2/12)_{AE}\} = q\{-l/3,\ 0,\ -l^2/27\}$$

Step 3 The stiffness matrix is (using Appendix D, Eqs. D.1 to D.5, D.10 and D.11)

$$[S] = EI\begin{bmatrix} 729/l^3 & & \text{symmetrical} \\ -40.5/l^2 & 20.25EI/l & \\ 40.5/l^2 & 0 & 20.25EI/l \end{bmatrix}$$

The nonzero elements of this matrix are determined as follows: $S_{11} = \Sigma(12EI/l^3)$, with the summation performed for the four members meeting at E (Figure 5.6b). $S_{21} = (6EI/l^2)_{ED} - (6EI/l^2)_{EB}$.

Similarly, $S_{31} = (6EI/l^2)_{EC} - (6EI/l^2)_{EA}$. The angular displacement $D_2 = 1$ bends and twists beams BD and AC respectively;

$$S_{22} = (4EI/l)_{EB} + 4(EI/l)_{ED} + (GJ/l)_{EC} + (GJ/l)_{EA}$$

Because of symmetry of the structure, S_{33} is the same as S_{22}.

Values of the reactions at A due to separate unit displacements are

$$[A_u] = \begin{bmatrix} (-12EI/l^3)_{AE} & 0 & (6EI/l^2)_{AE} \\ 0 & (-GJ/l)_{AE} & 0 \\ (-6EI/l^2)_{AE} & 0 & (2EI/l)_{AE} \end{bmatrix}$$

$$= EI\begin{bmatrix} -40.5/l^3 & 0 & 13.5/l^2 \\ 0 & -0.75/l & 0 \\ -13.5/l^2 & 0 & 3/l \end{bmatrix}$$

Step 4 Substitution of $[S]$ and $\{F\}$ in Eq. 5.7 and solution gives

$$\{D\} = \frac{10^{-3}q}{EI}\{0.9798l^4,\ 1.960l^3,\ -3.331l^3\}$$

Step 5 Substitution of $[A_r]$, $[A_u]$, and $\{D\}$ in Eq. 5.8 gives the required reaction components:

$$\{A\} = \begin{Bmatrix} -\frac{ql}{3} \\ 0 \\ -\frac{ql^2}{27} \end{Bmatrix} + 10^{-3}q\begin{bmatrix} -\frac{40.5}{l^3} & 0 & \frac{13.5}{l^2} \\ 0 & \frac{-0.75}{l} & 0 \\ -\frac{13.5}{l^2} & 0 & \frac{3}{l} \end{bmatrix}\begin{Bmatrix} 0.9798l^4 \\ 1.960l^3 \\ -3.331l^3 \end{Bmatrix}$$

$$= \begin{Bmatrix} -0.4180ql \\ -1.470(10^{-3}\ ql^2) \\ -60.26(10^{-3}\ ql^2) \end{Bmatrix}$$

5.7 Analysis of effects of displacements at the coordinates

Consider a structure whose degree of kinematic indeterminacy is n, corresponding to a system of n coordinates. Our objective is to analyze the structure for the effect of forced displacements of prescribed values $\{\Delta\}_{m\times 1}$ at the first m coordinates (with $m < n$). The structure will be subjected to unknown forces $\{F^*\}_{m\times 1}$ at the coordinates 1 to m. It is assumed that no external forces are applied on the members.

We write the stiffness matrix so that the coordinates corresponding to the known displacements occur in the first m rows and columns, thus

$$[S] = \left[\begin{array}{cccc:ccc} S_{11} & S_{12} & \dots & S_{1m} & S_{1(m+1)} & \dots & S_{1n} \\ S_{21} & S_{22} & \dots & & \dots & & \dots \\ \dots & & & & \dots & & \dots \\ S_{m1} & S_{m2} & \dots & S_{mm} & S_{m(m+1)} & \dots & S_{mn} \\ \hdashline S_{(m+1)l} & \dots & & & \dots & & \dots \\ \dots & & & & \dots & & \dots \\ S_{n1} & S_{n2} & \dots & & \dots & & S_{mn} \end{array}\right] \tag{5.10}$$

This matrix can be partitioned along the dashed lines shown above and can therefore be written in the form

$$[S] = \begin{bmatrix} [S_{11}] & [S_{12}] \\ [S_{21}] & [S_{22}] \end{bmatrix} \tag{5.11}$$

where $[S_{ij}]$ are the partitional matrices or submatrices. By inspection of Eq. 5.10, the order of submatrices is $[S_{11}]_{m\times m}, [S_{12}]_{m\times(n-m)}, [S_{21}]_{(n-m)\times m}, [S_{22}]_{(n-m)\times(n-m)}$.

To produce the displacements $\Delta_1, \Delta_2, \dots, \Delta_m$, external forces $F_1^*, F_2^*, \dots, F_m^*$ must be applied at the coordinates 1 to m with no forces applied at the remaining coordinates, thus allowing displacements $\overline{D}_{m+1}, \overline{D}_{m+2}, \dots, \overline{D}_n$ to occur. The forces and the displacements can be related by

$$\begin{bmatrix} [S_{11}] & [S_{12}] \\ [S_{21}] & [S_{22}] \end{bmatrix} \begin{Bmatrix} \{D^*\} \\ \{\overline{D}\} \end{Bmatrix} = \begin{Bmatrix} \{F^*\} \\ \{0\} \end{Bmatrix} \tag{5.12}$$

where $\{D^*\} = \{\Delta\}$, that is, the prescribed displacements; $\{\overline{D}\}_{m-n\times 1}$ is the vector of unknown displacements at the coordinates $m+1, m+2, \dots, n$; and $\{F^*\}_{m\times 1}$ is the vector of unknown forces at the first m coordinates.

From the second row of the above matrix equation, we find

$$\{\overline{D}\} = -[S_{22}]^{-1}\,[S_{21}]\,\{D^*\} \tag{5.13}$$

With the displacements at all the n coordinates known, the stress resultants at any section can be determined by the equation

$$\{A\} = [A_u]\,\{D\} \tag{5.14}$$

where $\{A\}$ is any action, and $[A_u]$ is the same action corresponding to a unit displacement at the given coordinate only. This equation is the same as Eq. 5.5 with $\{A_r\} = \{0\}$, since the actions required are due to the effect of the displacements $\{D\}$ only.

If the forces $\{F^*\}$ are required, they can be obtained from the first row of Eq. 5.12 and Eq. 5.13, as follows:

$$\{F^*\} = [[S_{11}] - [S_{12}][S_{22}]^{-1}[S_{21}]]\{D^*\} \tag{5.15}$$

Equation 5.15 can be rewritten in the form

$$\{F^*\} = [S^*]\{D^*\} \tag{5.16}$$

where $[S^*]$ is a condensed stiffness matrix of the structure corresponding to the first m coordinates, with the remaining coordinates omitted. The condensed stiffness matrix is

$$[S^*] = [S_{11}] - [S_{12}][S_{22}]^{-1}[S_{21}] \tag{5.17}$$

Example 5.5: A plane frame: condensation of stiffness matrix

Determine the force required at coordinate 1* to produce a displacement $D_1^* = \Delta$ for the frame in Figure 5.7a. What are the corresponding rotations at joints B and C? Ignore the change in length of members and consider $EI =$ constant.

In Example 5.3, we derived the stiffness matrix for the same frame corresponding to the coordinate system in Figure 5.3b. The numbering of the coordinates is changed in Figure 5.7b so that the coordinate with prescribed displacement is counted first; the stiffness matrix corresponding to the coordinates in Figure 5.7b is

$$[S] = EI \left[\begin{array}{c|cc} 48.938/l^3 & -4.875/l^2 & -3/l^2 \\ \hline -4.875/l^2 & 9/l & 2/l \\ -3/l^2 & 2/l & 8/l \end{array}\right] \tag{a}$$

This is the same as $[S]$ derived in Example 5.3, after interchanging rows 1 and 3, followed by interchanging columns 1 and 3.

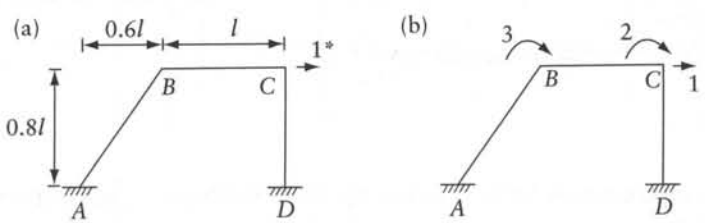

Figure 5.7 Plane frame analyzed in Example 5.5. (a) Single-coordinate system. (b) Three-coordinate system.

The stiffness corresponding to the single coordinate in Figure 5.7a (Eq. 5.17) is

$$[S^*] = \left[\frac{48.938EI}{l^3}\right] - \left[-\frac{4.875EI}{l^2} \quad -\frac{3EI}{l^2}\right] \begin{bmatrix} \frac{9EI}{l} & \frac{2EI}{l} \\ \frac{2EI}{l} & \frac{8EI}{l} \end{bmatrix}^{-1} \begin{bmatrix} \frac{-4.875EI}{l^2} \\ \frac{-3EI}{l^2} \end{bmatrix}$$

$$= [45.81EI/l^3] \tag{b}$$

Substituting $[S^*]$ and $\{D^*\} = \{\Delta\}$ in Eq. 5.16 gives the force F_1^* necessary to produce the displacement $D_1^* = \Delta$ (Figure 5.7a):

$$[F^*] = [45.811(EI/l^3)\Delta] \tag{c}$$

The corresponding rotations at C and B are respectively equal to $\overline{D}_1$ and $\overline{D}_2$, determined by Eq. 5.13:

$$\{\overline{D}\} = -\begin{bmatrix} \frac{9EI}{l} & \frac{2EI}{l} \\ \frac{2EI}{l} & \frac{8EI}{l} \end{bmatrix}^{-1} \begin{bmatrix} \frac{-4.875EI}{l^2} \\ \frac{-3EI}{l^2} \end{bmatrix} \{\Delta\} = \begin{Bmatrix} 0.485\frac{\Delta}{l} \\ 0.254\frac{\Delta}{l} \end{Bmatrix}$$

5.8 General

The displacement (or stiffness) method of analysis can be applied to any structure but the largest economy of effort arises when the order of statical indeterminacy is high. The procedure is standardized and can be applied without difficulty to trusses, frames, grids, and other structures subjected to external loading or to prescribed deformation, e.g. settlement of supports or temperature change. The displacement method is extremely well suited to computer solutions (see Chapters 22 and 23).

Problems

5.1 Use the displacement method to find the forces in the members of the truss shown. Assume the value l/aE to be the same for all members.

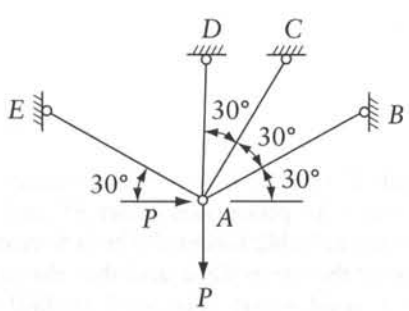

Prob. 5.1

5.2 A rigid mast AB is hinged at A, free at B and is pin-jointed to n bars of which a typical one is shown. Using the displacement method, find the force A in the ith bar if $l/aE =$ constant for each bar. Assume that the mast and all the bars are in one plane.

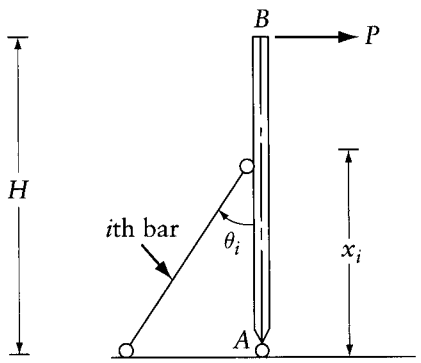

Prob. 5.2

5.3 Solve Prob. 4.7 by the displacement method.

5.4 For the truss shown in the figure, write the stiffness matrix corresponding to the four coordinates indicated. Assume a and E to be the same for all members.

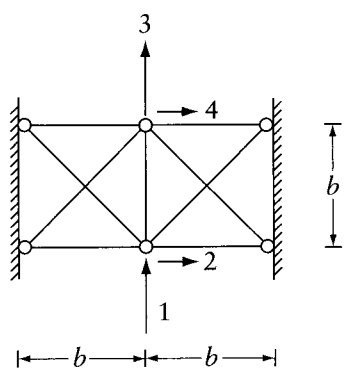

Prob. 5.4

5.5 Find the forces in the members of the truss of Prob. 5.4 due to $F_1 = -P$ at coordinate 1.

5.6 Member AB represents a chimney fixed at B and stayed by prestressed cables AC and AD. Find the bending moment at B and the changes in the cable forces due to a horizontal force P at A. Assume that AB, AC and AD are in the same plane and that the cables continue to be in tension after application of P. Consider that: $(Ea)_{\text{cable}} = 10(EI/l^2)_{AB}$. Only bending deformation of AB and axial deformation of the cables need to be considered.

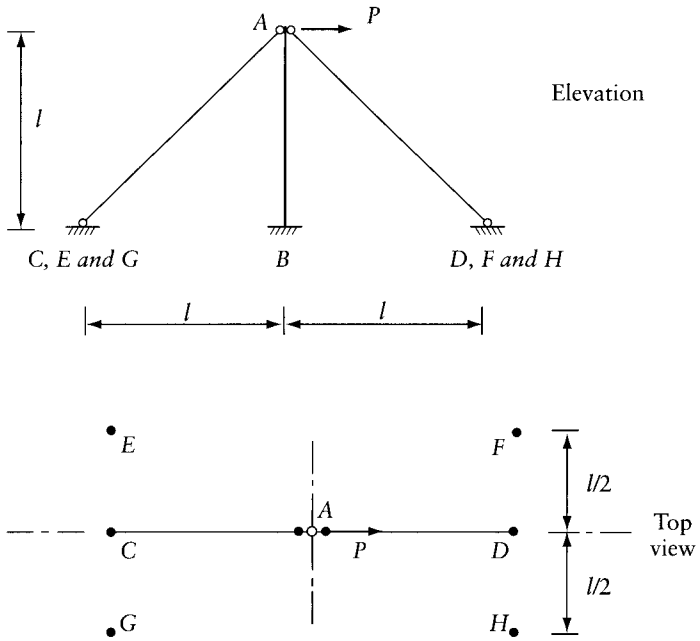

Prob. 5.6 and 5.7

5.7 Solve Prob. 5.6 with cables AC and AD replaced by four cables joining A to each of E, F, G and H. Consider that $(Ea)_{\text{cable}}$ is the same as in Prob. 5.6.

5.8 Neglecting axial deformations, find the end-moments M_{BC} and M_{CF} for the frame shown. Consider an end-moment to be positive when it acts in a clockwise direction on the member end.

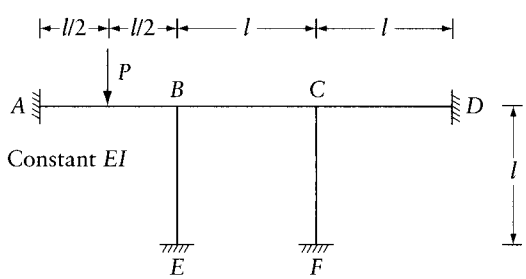

Prob. 5.8

5.9 Solve Prob. 5.8 if support E moves downward a distance Δ and the load P is not acting.

5.10 Write the stiffness matrix corresponding to the coordinates 1 and 2 of the frame in the figure. What are the values of the end-moments M_{BC} and M_{CB} due to uniform load q per unit length on BC and what are the reaction components at A? Neglect axial deformations.

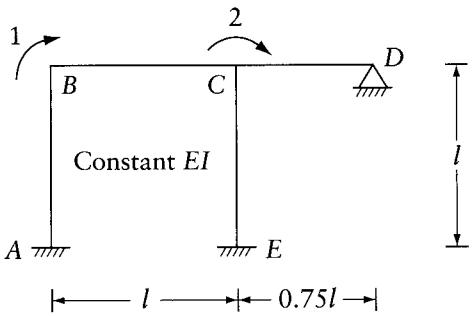

Prob. 5.10

5.11 Imperial units. Find the end-moments M_{BC} and M_{CB} in the frame of Prob. 5.10 due to a rise in temperature of 40° Fahrenheit in part BD only. Assume the coefficient of thermal expansion to be $\alpha = 6.5 \times 10^{-6}$ per degree Fahrenheit, and take $EI = 10^4 \text{k ft}^2$. The load q is not acting in this case. The members are assumed to have infinite axial rigidity; $l = 20$ ft.

5.12 SI units. Find the end-moments M_{BC} and M_{CB} in the frame of Prob. 5.11 due to a rise in temperature of 20 °C in part BD only. Assume the coefficient of thermal expansion to be $\alpha = 1 \times 10^{-5}$ per degree Celsius, take $EI = 4000 \text{ kN m}^2$ and $l = 6$ m. The members are assumed to have infinite axial rigidity. The load q is not acting in this case.

5.13 For the frame in the figure, write the first three columns of the stiffness matrix corresponding to the six coordinates indicated. The moment of inertia and the area of the cross section are shown alongside the members.

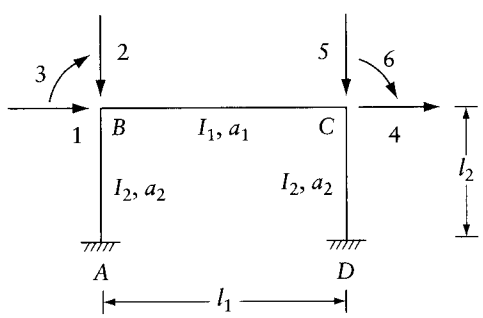

Prob. 5.13

5.14 Write the stiffness matrix for the frame of Prob. 5.13, neglecting the axial deformations. Number the coordinates in the following order: clockwise rotation at B, clockwise rotation at C, horizontal translation to the right at C.

5.15 Using the results of Prob. 5.14, obtain the bending moment diagram for the frame due to a horizontal load P to the right at B and a downward vertical load $4P$ at the middle of BC. Take $l_1 = 2l_2$ and $I_1 = 4I_2$.

5.16 Use the displacement method to find the bending moment and shearing force diagrams for the frame in the figure. Neglect axial deformations.

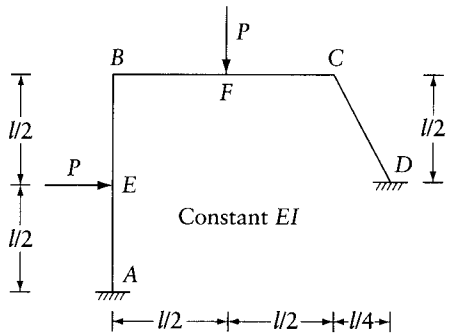

Prob. 5.16

5.17 For the grid shown in plan in the figure, calculate the displacements corresponding to the three degrees of freedom at joint B. Assume $GJ/EI = 0.8$ for AB and BC. Draw the bending moment diagram for BC.

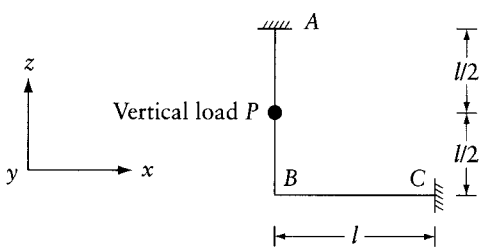

Prob. 5.17

5.18 Considering three degrees of freedom: a downward deflection, and rotations represented by vectors in the x and z directions at each of the joints I, J, K, and L of the grid in the figure,

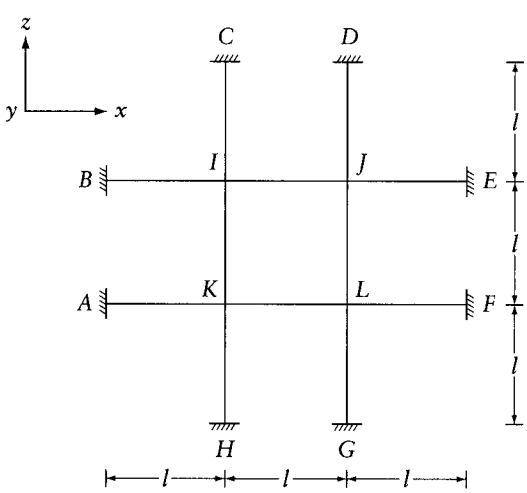

Prob. 5.18

write the first three columns of the corresponding stiffness matrix. Number the twelve coordinates in the order in which they are mentioned above, that is, the first three at I followed by three at J, and so on. Take $GJ/EI = 0.5$ for all members.

5.19 Solve Prob. 4.5 by the displacement method. Consider the vertical deflections at B and C as the unknown displacements and use Appendix E.

5.20 Neglecting torsion, find the bending moment in girders BE and AF of the grid of Prob. 5.18 subjected to a vertical load P at joint I. Consider the vertical deflections at the joints as the unknown displacements and use Appendix E.

5.21 A horizontal grid is composed of n members meeting at one joint A of which a typical member i is shown in the figure. Write the stiffness matrix corresponding to the coordinates 1, 2, and 3 indicated, with coordinate 1 representing a downward deflection, and 2 and 3 being rotations. The length of the ith member, its torsional rigidity, and its flexural rigidity in the vertical plane through its axis are l_i, GJ_i, and EI_i respectively. *Hint:* The stiffness matrix of the grid can be obtained by the summation of the stiffness matrices of individual members. To obtain the first column of the stiffness matrix of the ith member, a unit downward displacement is introduced and the end-forces are taken from Appendix D. These forces are resolved into components at the three coordinates. For the second and third columns, a unit rotation at coordinate 2 and 3 is resolved into two rotations represented by vectors along and normal to the beam axis and the corresponding end-forces are taken from Appendix D. These forces are then resolved into components at the coordinates to obtain elements of the stiffness matrix.

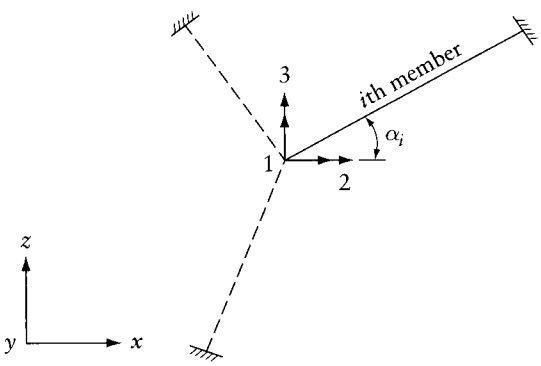

Prob. 5.21

5.22 Figure E-1, Appendix E shows a prismatic continuous beam of three equal spans l with a unit settlement at one of the interior supports. Using the displacement method, verify the bending moments and the reactions given in the figure. Two coordinates only need be used, representing the rotation at each of the interior supports.

5.23 Solve Example 5.2 with the supports at A and D changed to hinges (Figure 5.2a).

5.24 Solve Example 5.3 with the support at A changed to a hinge (Figure 5.3a). Consider case (1) loading only.

Chapter 6

Use of force and displacement methods

6.1 Introduction

The preceding two chapters outlined two basic methods of analysis, and obviously either can be used to analyze any structure. It is worthwhile, however, to see clearly the advantages of each method so as to choose the one more economical in terms of effort in any particular case.

6.2 Relation between flexibility and stiffness matrices

Consider a system of n coordinates defined on a structure to which the principle of superposition applies (see Section 3.6). In the preceding chapters, we have defined the flexibility matrix, $[f]$ and its elements, the flexibility coefficients. We have also defined the stiffness matrix, $[S]$ and its elements, the stiffness coefficients. A typical flexibility coefficient, f_{ij} is the displacement at coordinate i due to a force $F_j = 1$ at coordinate j, with no forces applied at the remaining coordinates. A typical stiffness coefficient, S_{ij} is the force at coordinate i when the structure is deformed such that $D_j = 1$, while the displacements are zero at the remaining coordinates. We will show below that the flexibility and the stiffness matrices, *corresponding to the same coordinate system*, are related:

$$[S] = [f]^{-1} \tag{6.1}$$

$$[f] = [S]^{-1} \tag{6.2}$$

Equations 6.1 to 6.5 apply with any number of coordinates. For simplicity of presentation, we consider a system of two coordinates ($n = 2$) shown in Figure 6.1a. The displacements $\{D_1, D_2\}$ can be expressed as the sum of the displacements due to each of forces F_1 and F_2 acting separately (see the superposition Eq. 3.17):

$$D_1 = f_{11}F_1 + f_{12}F_2$$

$$D_2 = f_{21}F_1 + f_{22}F_2$$

These equations can be put in matrix form:

$$\{D\} = [f]\{F\} \tag{6.3}$$

The forces $\{F\}$ can be expressed in terms of the displacements by solving Eq. 6.3:

$$\{F\} = [f]^{-1}\{D\} \tag{6.4}$$

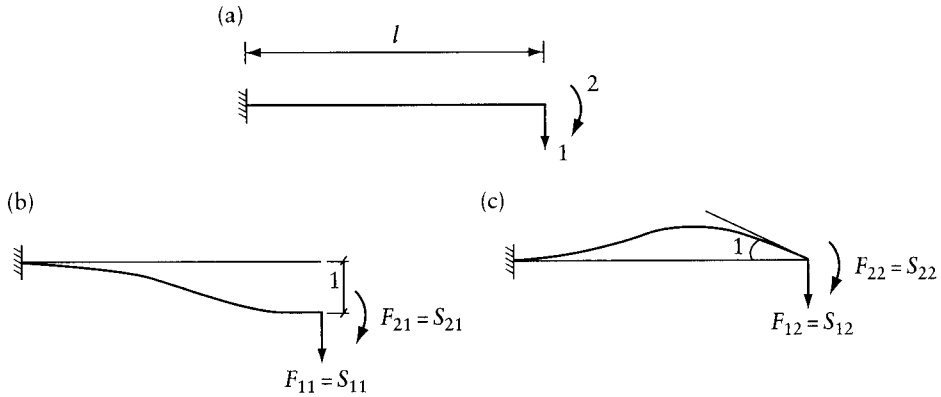

Figure 6.1 A structure with two coordinates, Example 6.1. (a) Coordinate system. (b) Forces holding the structure in a deformed configuration with $D_1 = 1$, while $D_2 = 0$. (c) Forces holding the structure in a deformed configuration with $D_1 = 0$, while $D_2 = 1$.

Consider the structure in two deformed configurations: $D_1 = 1$ while $D_2 = 0$ (Figure 6.1b), and $D_1 = 0$ while $D_2 = 1$ (Figure 6.1c).

Application of Eq. 6.4 gives:

$$\begin{bmatrix} F_{11} & F_{12} \\ F_{21} & F_{22} \end{bmatrix} = [f]^{-1} \begin{bmatrix} 1 & 0 \\ 0 & 1 \end{bmatrix}$$

The elements of the matrix on the left-hand side of this equation are in fact the stiffness coefficients, as defined above. The last matrix on the right-hand side of the equation is a unit matrix (identity matrix defined in Section A.2). Thus, the equation can be written in the same form as Eq. 6.1. Inversion of both sides of Eq. 6.1 gives Eq. 6.2. Substitution of Eq. 6.1 in Eq. 6.4 gives:

$$\{F\} = [S]\{D\} \tag{6.5}$$

Equations 6.1 and 6.2 show that the stiffness matrix is the inverse of the flexibility matrix, and vice versa, provided the same coordinate system of forces and displacements is used in the formation of the two matrices.

We may recall that in the force method of analysis, releases are introduced to render the structure statically determinate. The coordinate system represents the location and direction of these released forces. Now, in the displacement method of analysis, restraining forces are added to prevent joint displacements. The coordinate system in this case represents the location and direction of the unknown displacements. It follows that the two coordinate systems cannot be the same for the same structure. Therefore, the inverse of the flexibility matrix used in the force method is a matrix, whose elements are stiffness coefficients, but not those used in the displacement method of analysis. Furthermore, we note that the flexibility matrix determined in the force method is that of a released structure, whereas in the displacement method we use the stiffness matrix of the actual structure.

Equation 6.3 must not be confused with the equation: $[f]\{F\} = \{-D\}$ used in the force method of analysis, where we apply unknown redundants $\{F\}$ of such a magnitude as will produce displacements $\{-D\}$ to correct for inconsistencies $\{D\}$ of the released structure.

Similarly, Eq. 6.5 must not be confused with the equation: $[S]\{D\} = \{-F\}$ used in the displacement method of analysis, where we seek unknown displacements $\{D\}$ of such a magnitude as will eliminate the artificial restraining forces $\{F\}$.

Example 6.1: Generation of stiffness matrix of a prismatic member

Assume that the cantilever shown in Figure 6.1a has a constant flexural rigidity EI and use Appendix B to generate the flexibility matrix $[f]$ corresponding to the indicated coordinate system. Invert $[f]$ to obtain the stiffness matrix $[S]$. The elements of $[S]$ may be compared with the member-end forces given in Appendix D (Eqs. D.1 to D.5).

Due to $F_1 = 1$, Appendix B gives the displacements at coordinates 1 and 2; these are respectively equal to f_{11} and f_{21}. Similarly, due to $F_2 = 1$, the appendix gives f_{12} and f_{22}.

$$[f] = \begin{bmatrix} \frac{l^3}{3EI} & \frac{l^2}{2EI} \\ \frac{l^2}{2EI} & \frac{l}{EI} \end{bmatrix}$$

$$[S] = [f]^{-1} = \begin{bmatrix} \frac{12EI}{l^3} & \frac{6EI}{l^2} \\ \frac{6EI}{l^2} & \frac{4EI}{l} \end{bmatrix}$$

6.3 Choice of force or displacement method

In the force method, the choice of the released structure may affect the amount of calculation. For example, in the analysis of a continuous beam, the introduction of hinges above intermediate supports produces a released structure consisting of a series of simple beams (see Example 4.5), so that the application of a unit value of the redundants has a local effect on the two adjacent spans only. In structures other than continuous beams, it may not be possible to find a released structure for which the redundants have a local effect only, and usually a redundant acting separately produces displacements at all the coordinates.

In the displacement method, generally all joint displacements are prevented regardless of the choice of the unknown displacements. Generation of the stiffness matrix is usually not difficult because of the localized effect discussed earlier. A displacement of a joint affects only the members meeting at the given joint. These two properties generally make the displacement method easy to formulate, and it is for these two reasons that the displacement method is more suitable for computer programming.

When the analysis is performed by hand, it is important to reduce the number of simultaneous equations to be solved, and thus the choice of the force or displacement method may depend on which is smaller: the degree of static or kinematic indeterminacy. No general rule can be established, so that, when a structure is statically as well as kinematically indeterminate to a low degree, either method may involve about the same amount of computation.

When the computation is done by hand, it is possible in the displacement method to reduce the number of simultaneous equations by preventing only some of the joint displacements, provided that the resulting structure can be readily analyzed. This is illustrated in Example 6.2.

Example 6.2: Reactions due to unit settlement of a support of a continuous beam

Generate the flexibility matrix $[f]$ for the beam and the coordinate system indicated in Figure 6.2a. Invert $[f]$ to obtain the stiffness matrix $[S]$. The elements of $[S]$ may be compared with minus the values of the reactions due to a settlement of a support in a continuous beam (Figure 6.2c); see Table E.1 of Appendix E.

To write the flexibility matrix, we obtain displacements such as those shown in Figure 6.2b (for the first column of the matrix), their values being taken from Appendix B. Thus,

$$[f] = \frac{l^3}{12EI}\begin{bmatrix} 9 & 11 & 7 \\ 11 & 16 & 11 \\ 7 & 11 & 9 \end{bmatrix}$$

To generate directly the stiffness matrix requires the analysis of a statically indeterminate structure for each column of $[S]$. For example, the elements of the first column of $[S]$ are the forces necessary to hold the structure in the deformed shape illustrated in Figure 6.2c, and this requires the solution of a structure statically indeterminate to the third degree. This exercise is left to the reader; its solution will provide a check on the stiffness matrix[1] obtained by the inversion of the flexibility matrix.

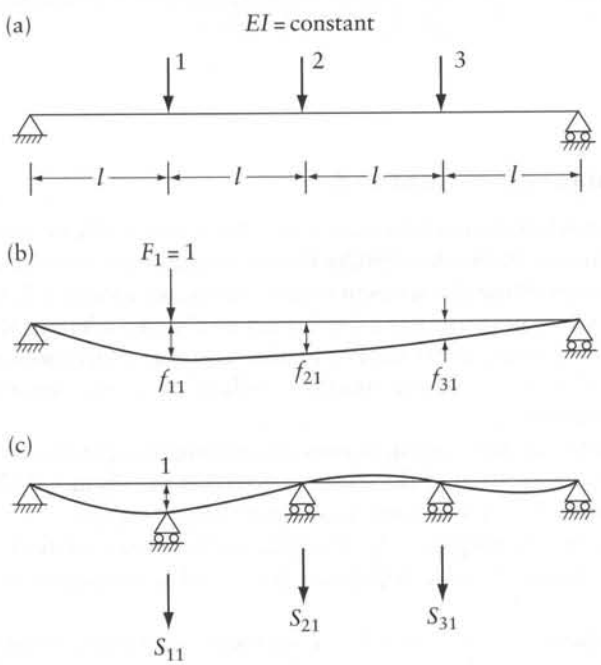

Figure 6.2 Deflected configuration to generate the first column of $[f]$ and $[S]$ in Example 6.2.

1 The elements of the stiffness matrix corresponding to the coordinates chosen in this example can be used in the analysis of continuous beams with equal spans on elastic supports or for the analysis of grids with hinged connections (torsionless grids). These elements are equal to minus the reactions at the supports caused by the vertical translation of one support only. Appendix E gives the values of the reactions and bending moments at the supports for continuous beams of 2 to 5 equal spans.

$$[S]=[f]^{-1}=\frac{EI}{l^3}\begin{bmatrix} 9.857 & -9.429 & 3.857 \\ -9.429 & 13.714 & -9.429 \\ 3.857 & -9.429 & 9.857 \end{bmatrix}$$

Example 6.3: Analysis of a grid ignoring torsion

The grid in Figure 6.3a is formed by four simply-supported main girders (m) and one cross-girder (c) of a bridge deck, with a flexural rigidity in the ratio $EI_m : EI_c = 3:1$. The torsional rigidity is neglected. Find the bending moment diagram for a cross-girder due to a concentrated vertical load P acting at joint 1.

There are three degrees of freedom at any joint of the grid: vertical translation, and rotation about two perpendicular axes in the plane of the grid. However, if the vertical translation of the joints is prevented, while the rotations are allowed, the grid becomes a system of continuous beams, and, using Appendix E, we can analyze the effect of downward movement of one joint without the necessity of knowing the rotations.

Let the coordinate system be the four vertical deflections at 1, 2, 3, and 4, considered positive downward. The stiffness matrix can be generated by using the tabulated values of the reactions in Appendix E for the case of two equal spans for the main girders, and three equal spans for the cross-girder. The elements of the first row of the stiffness matrix of the grid are calculated as follows. The required actions are the bending moments in the cross girders at 2 and 3.

$$\{A\}=\{M_2, M_3\}$$

The displacements $D_1 = 1$ and $D_2 = D_3 = D_4 = 0$ deform the main girder A and the cross-girder, but girders B, C, and D are not deflected. The rotations at the joints are allowed to take place freely. Then, adding the vertical forces required to hold the girder A and the cross-girder in this deflected shape, we obtain

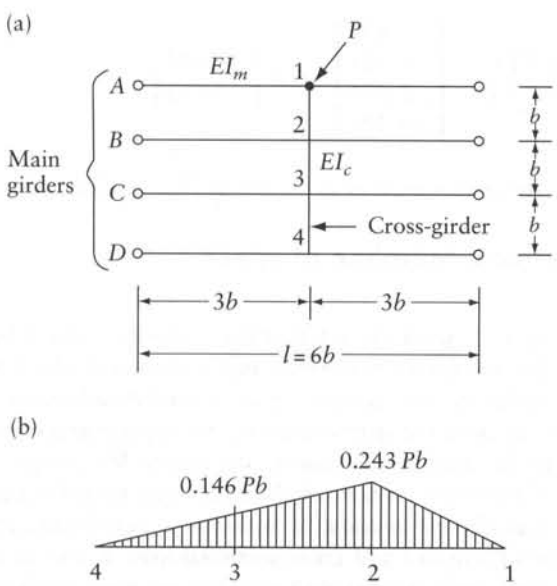

Figure 6.3 Grid considered in Example 6.3.

$$S_{11} = 6.0\frac{EI_m}{(3b)^3} + 1.6\frac{EI_c}{b^3} = 2.267\frac{EI_c}{b^3}$$

$$S_{21} = -3.6\frac{EI_c}{b^3}; \quad S_{31} = 2.4\frac{EI_c}{b^3}; \quad S_{41} = -0.4\frac{EI_c}{b^3}$$

The elements of other columns of the stiffness matrix are determined in a similar way, so that finally

$$[S] = \frac{EI_c}{b^3}\begin{bmatrix} 2.267 & -3.600 & 2.400 & -0.400 \\ -3.600 & 10.267 & -8.400 & 2.400 \\ 2.400 & -8.400 & 10.267 & -3.600 \\ -0.400 & 2.400 & -3.600 & 2.267 \end{bmatrix}$$

With the load P at coordinate 1, we need only an equal and opposite force at this coordinate to prevent the joint displacements. Thus, $\{F\} = \{-P, 0, 0, 0\}$. Substituting in Eq. 5.2: $[S]\{D\} = -\{F\}$ and solving for the displacements, we find

$$\{D\} = \frac{Pb^3}{EI_c}\begin{Bmatrix} 1.133 \\ 0.511 \\ 0.076 \\ -0.221 \end{Bmatrix}$$

The bending moment in the cross-girder is zero at the ends 1 and 4, so that only moments at 2 and 3 have to be determined. Considering the bending moment positive if it causes tension in the bottom fiber, we find the moment from Eq. 5.5. In the present case, the bending moment in the restrained structure $\{A_r\} = \{0\}$ because the load P is applied at a coordinate.

The elements of $[A_u]$ are obtained from Appendix E. We find

$$[A_u] = \frac{EI_c}{b^2}\begin{bmatrix} -1.6 & 3.6 & -2.4 & 0.4 \\ 0.4 & -2.4 & 3.6 & -1.6 \end{bmatrix}$$

and

$$\{A\} = \frac{EI_c}{b^2}\begin{bmatrix} -1.6 & 3.6 & -2.4 & 0.4 \\ 0.4 & -2.4 & 3.6 & -1.6 \end{bmatrix}\frac{Pb^3}{EI_c}\begin{Bmatrix} 1.133 \\ 0.511 \\ 0.076 \\ -0.221 \end{Bmatrix} = Pb\begin{Bmatrix} -0.243 \\ -0.146 \end{Bmatrix}$$

Hence, the bending moment diagram for the cross-girder is as shown in Figure 6.3b.

6.4 Stiffness matrix for a prismatic member of space and plane frames

In the examples in this chapter and in Chapter 5, we have seen that the elements of the stiffness matrix of a structure are obtained by adding the forces at the ends of the members which meet at a joint. These end-forces are elements of the stiffness matrix for individual members and are derived by the use of Appendix D. In this section, the stiffness matrix for a prismatic member is generated because it is often needed in the analysis of framed structures. We consider 12 coordinates at the ends, representing translations and rotations about three rectangular axes x, y, and z (Figure 6.4a), with the y and z axes chosen to coincide with the principal axes of the cross section. The beam is assumed to be of length l and cross-sectional area a, and to have second moments of area I_z and I_y about the z and y axes respectively; the modulus of elasticity of the material is E, and the torsional rigidity GJ.

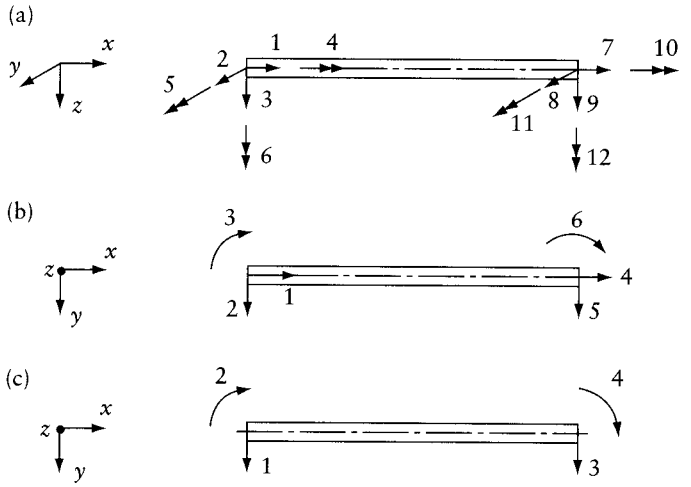

Figure 6.4 Coordinate systems corresponding to stiffness matrices: (a) Eq. 6.6, (b) Eq. 6.7, and (c) Eq. 6.8.

If we neglect shear deformations and warping caused by twisting, all the elements of the stiffness matrix can be taken from Appendix D. The elements in any column j are equal to the forces at the coordinates produced by a displacement $D_j = 1$ at coordinate j only. The resulting stiffness matrix is given below:

$$[S] = \begin{array}{c|cccccc:cccccc} & 1 & 2 & 3 & 4 & 5 & 6 & 7 & 8 & 9 & 10 & 11 & 12 \\ \hline 1 & \frac{Ea}{l} & & & & & & & & & & & \\ 2 & & \frac{12EI_z}{l^3} & & & & \frac{4EI_z}{l} & & & & & & \\ 3 & & & \frac{12EI_y}{l^3} & & -\frac{6EI_y}{l^2} & & & & & & & \\ 4 & & & & \frac{GJ}{l} & & & & & & & & \\ 5 & & & -\frac{6EI_y}{l^2} & & \frac{4EI_y}{l} & & & & & & & \\ 6 & & \frac{6EI_z}{l^2} & & & & \frac{4EI_z}{l} & & & & & & \\ \hdashline 7 & -\frac{Ea}{l} & & & & & & \frac{Ea}{l} & & & & & \\ 8 & & -\frac{12EI_z}{l^3} & & & & -\frac{6EI_z}{l^2} & & \frac{12EI_z}{l^3} & & & & \\ 9 & & & -\frac{12EI_y}{l^3} & & \frac{6EI_y}{l^2} & & & & \frac{12EI_y}{l^3} & & & \\ 10 & & & & -\frac{GJ}{l} & & & & & & \frac{GJ}{l} & & \\ 11 & & & -\frac{6EI_y}{l^2} & & \frac{2EI_y}{l} & & & & \frac{6EI_y}{l^2} & & \frac{4EI_y}{l} & \\ 12 & & \frac{6EI_z}{l^2} & & & & \frac{2EI_z}{l} & & -\frac{6EI_z}{l^2} & & & & \frac{4EI_z}{l} \end{array}$$

Symmetrical elements not shown are zero

(6.6)

For two-dimensional problems of a frame in the x-y plane, the stiffness matrix needs to be considered for six coordinates only: 1, 2, 6, 7, 8, and 12 (Figure 6.4a). Deletion of the columns and rows numbered 3, 4, 5, 9, 10, and 11 from the matrix in Eq. 6.6 results in the following stiffness matrix of a prismatic member corresponding to the six coordinates in Figure 6.4b to be used in the analysis of plane frames:

$$[S] = \begin{array}{c} \\ 1 \\ 2 \\ 3 \\ 4 \\ 5 \\ 6 \end{array} \begin{array}{c} \begin{array}{cccccc} 1 & 2 & 3 & 4 & 5 & 6 \end{array} \\ \begin{bmatrix} \frac{Ea}{l} & & & & & \\ & \frac{12EI}{l^3} & \text{Symmetrical} & & & \\ & & \text{elements not} & & & \\ & & \text{shown are zero} & & & \\ & \frac{6EI}{l^2} & \frac{4EI}{l} & & & \\ -\frac{Ea}{l} & & & \frac{Ea}{l} & & \\ & -\frac{12EI}{l^3} & -\frac{6EI}{l^2} & & \frac{12EI}{l^3} & \\ & \frac{6EI}{l^2} & \frac{2EI}{l} & & -\frac{6EI}{l^2} & \frac{4EI}{l} \end{bmatrix} \end{array} \tag{6.7}$$

where $I = I_z$.

If, in a plane frame, the axial deformations are ignored, the coordinates 1 and 4 in Figure 6.4b need not be considered, and the stiffness matrix of a prismatic member corresponding to the four coordinates in Figure 6.4c becomes

$$[S] = \begin{array}{c} \\ 1 \\ 2 \\ 3 \\ 4 \end{array} \begin{array}{c} \begin{array}{cccc} 1 & 2 & 3 & 4 \end{array} \\ \begin{bmatrix} \frac{12EI}{l^3} & \text{Symmetrical} & & \\ \frac{6EI}{l^2} & \frac{4EI}{l} & & \\ -\frac{12EI}{l^3} & -\frac{6EI}{l^2} & \frac{12EI}{l^3} & \\ \frac{6EI}{l^2} & \frac{2EI}{l} & -\frac{6EI}{l^2} & \frac{4EI}{l} \end{bmatrix} \end{array} \tag{6.8}$$

The stiffness matrix for members in which the shear deformations are not ignored is derived in Section 15.2. The presence of a high axial force in a deflected member causes an additional bending moment, and if this effect is to be taken into account, the above stiffness matrices must be modified. This is discussed in Chapter 13.

The stiffness matrices derived above correspond to coordinates which coincide with the beam axis or with the principal axes of its cross section. However, in the analysis of structures composed of a number of members running in arbitrary directions, the coordinates may be taken parallel to a set of *global axes* and thus the coordinates may not coincide with the principal axes of a given member. In such a case, the stiffness matrices given above (corresponding to the coordinates coinciding with the principal axes of the members) will have to be transformed to stiffness matrices corresponding to another set of coordinates by the use of transformation matrices formed by geometrical relations between the two sets of coordinates. This will be further discussed in Section 9.4.

6.5 Condensation of stiffness matrices

We recall that a stiffness matrix relates displacements $\{D\}$ at a number of coordinates to the forces $\{F\}$ applied at the same coordinates by the equation:

$$[S]\{D\} = \{F\} \tag{6.9}$$

If the displacement at a number of coordinates is prevented by the introduction of supports, and the matrices in the above equations are arranged in such a way that the equations corresponding to these coordinates appear at the end, we can write Eq. 6.9 in the partitioned form:

$$\begin{bmatrix} [S_{11}] & [S_{12}] \\ [S_{21}] & [S_{22}] \end{bmatrix} \begin{Bmatrix} \{D_1\} \\ \{D_2\} \end{Bmatrix} = \begin{Bmatrix} \{F_1\} \\ \{F_2\} \end{Bmatrix} \tag{6.10}$$

where $\{D_2\} = \{0\}$ represents the prevented displacements. From this equation, we write

$$[S_{11}]\{D_1\} = \{F_1\} \tag{6.11}$$

and

$$[S_{21}]\{D_1\} = \{F_2\} \tag{6.12}$$

It is apparent from Eq. 6.11 that, if a support is introduced at a number of coordinates, the stiffness matrix of the resulting structure can be obtained simply by deleting the columns and the rows corresponding to these coordinates, resulting in a matrix of a lower order. If the displacements $\{D_1\}$ are known, Eq. 6.12 can be used to calculate the reactions at the supports preventing the displacements $\{D_2\}$.

As a simple example, consider the beam in Figure 6.4c and assume that the vertical displacements at coordinates 1 and 3 are prevented, as in the case of a simple beam; the stiffness matrix corresponding to the remaining two coordinates (2 and 4) is obtained by deletion of columns and rows numbered 1 and 3 in the matrix Eq. 6.8:

$$[S^*] = \begin{bmatrix} \dfrac{4EI}{l} & \text{symmetrical} \\ \dfrac{2EI}{l} & \dfrac{4EI}{l} \end{bmatrix} \tag{6.13}$$

The vertical reactions $\{F_1, F_3\}$ at coordinates 1 and 3 can be calculated from Eq. 6.12 by rearrangement of the elements in Eq. 6.8 as described for Eq. 6.10. Thus,

$$\begin{bmatrix} \dfrac{6EI}{l^2} & \dfrac{6EI}{l^2} \\ -\dfrac{6EI}{l^2} & -\dfrac{6EI}{l^2} \end{bmatrix} \begin{Bmatrix} D_2 \\ D_4 \end{Bmatrix} = \begin{Bmatrix} F_1 \\ F_3 \end{Bmatrix} \tag{6.14}$$

where the subscripts of D and F refer to the coordinates in Figure 6.4c.

If the forces are known to be zero at some of the coordinates, that is, the displacements at these coordinates can take place freely, the stiffness matrix corresponding to the remaining coordinates can be derived from the partitioned matrix Eq. 6.10. In this case, we consider that the equations below the horizontal dashed line relate forces $\{F_2\}$, assumed to be zero, to the

displacements $\{D_2\} \neq \{0\}$ at the corresponding coordinates. Substituting $\{F_2\} = \{0\}$ in Eq. 6.10, we write

$$\left.\begin{aligned} &[S_{11}]\{D_1\} + [S_{12}]\{D_2\} = \{F_1\} \\ \text{and} \quad &[S_{21}]\{D_1\} + [S_{22}]\{D_2\} = \{0\} \end{aligned}\right\} \tag{6.15}$$

Using the second equation to eliminate $\{D_2\}$ from the first, we obtain

$$[[S_{11}] - [S_{12}][S_{22}]^{-1}[S_{21}]]\{D_1\} = \{F_1\} \tag{6.16}$$

which is the same as Eq. 5.15. Equation 6.16 can be written in the form

$$[S^*]\{D_1\} = \{F_1\} \tag{6.17}$$

where $[S^*]$ is a condensed stiffness matrix relating forces $\{F_1\}$ to displacements $\{D_1\}$, and is given by

$$[S^*] = [S_{11}] - [S_{12}][S_{22}]^{-1}[S_{21}] \tag{6.18}$$

The condensed stiffness matrix $[S^*]$ corresponds to a reduced system of coordinates $1^*, 2^*, \ldots$, eliminating the coordinates corresponding to the second row of the partitioned matrix Eq. 6.10. Using the symbols $\{F^*\} \equiv \{F_1\}$ and $\{D^*\} \equiv \{D_1\}$, Eq. 6.17 becomes $[S^*]\{D^*\} = \{F^*\}$, which is the same as Eq. 5.16. Similarly, Eq. 6.18 is the same as Eq. 5.17.

The stiffness matrix of a structure composed of a number of members is usually derived from the stiffness matrix of the individual members, and relates the forces at all the degrees of freedom to the corresponding displacements. In many cases, however, the external forces on the actual structure are limited to a small number of coordinates, and it may therefore be useful to derive a matrix of a lower order $[S^*]$ corresponding to these coordinates only, using Eq. 6.18. A simple example of the application of Eq. 6.18 is given as a problem on matrix algebra in Prob. A.7 of Appendix A.

Example 6.4: End-rotational stiffness of a simple beam

With the displacements at coordinates 1 and 3 prevented for the beam in Figure 6.4c, as in a simple beam, what is the moment necessary to produce a unit rotation at coordinate 4, while the rotation is free to occur at coordinate 2? See the fourth figure in Appendix D (Eq. D.8).

Consider the beam in Figure 6.4c with simple supports at the ends. Define new coordinates $\overline{1}$ and $\overline{2}$ (not shown) in the same direction and locations as coordinates 2 and 4 respectively. The stiffness matrix for the new system is given in Eq. 6.13. We now condense this stiffness matrix (using Eq. 6.18) to obtain a 1×1 stiffness matrix corresponding to a single coordinate:

$$S_{\overline{1}\,\overline{1}} = \frac{4EI}{l} - \frac{2EI}{l}\left(\frac{4EI}{l}\right)^{-1}\left(\frac{2EI}{l}\right) = \frac{3EI}{l}$$

$S_{\overline{1}\,\overline{1}}$ is the end-rotational stiffness of a simple beam; it is equal to the moment necessary to introduce a unit rotation at one end while the rotation at the other end is free to occur.

6.6 Properties of flexibility and stiffness matrices

Consider a force F_i applied gradually to a structure, so that the kinetic energy of the mass of the structure is zero. Let the resulting displacement at the location and in the direction of F_i be D_i. If the structure is elastic the force-displacement curve follows the same path on loading and unloading, as shown in Figure 6.5a.

Assume now that at some stage of loading, the force F_i is increased by ΔF_i, and the corresponding increase in the displacement D_i is ΔD_i. The work done by this load increment is

$$\Delta W \simeq F_i \Delta D_i$$

This is shown as the hatched rectangle in Figure 6.5a. If the increments are sufficiently small, it can be seen that the total external work done by F_i during the displacement D_i is the area below the curve between 0 and D_i.

When the material in the structure obeys Hooke's law, the curve in Figure 6.5a is replaced by a straight line (Figure 6.5b), and the work done by the force F_i becomes

$$W = \frac{1}{2} F_i D_i$$

If the structure is subjected to a system of forces $F_1, F_2, \ldots, F_n$, increased gradually from zero to their final value, causing displacements $D_1, D_2, \ldots, D_n$ at the location and in the direction of the forces, then the total external work is

$$W = \frac{1}{2}(F_1 D_1 + F_2 D_2 + \cdots + F_n D_n) = \frac{1}{2} \sum_{i=1}^{n} F_i D_i \tag{6.19}$$

This equation can be written in the form

$$[W]_{1\times 1} = \frac{1}{2} \{F\}^T_{n\times 1} \{D\}_{n\times 1} \tag{6.20}$$

where $\{F\}^T$ is the transpose of the column vector $\{F\}$ representing the forces.

Work done is a scalar quantity whose dimensions are (force × length).

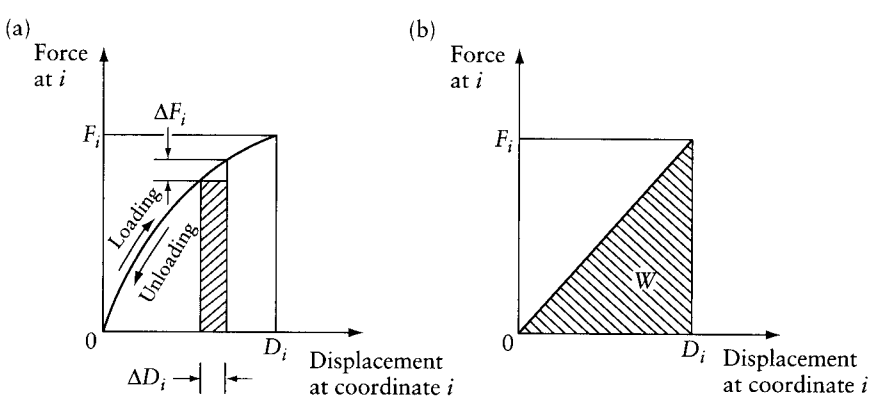

Figure 6.5 Force-displacement relations.

The displacements and the forces are related by Eq. 6.3. Substituting in Eq. 6.20,

$$[W]_{1\times1} = \frac{1}{2}\{F\}^T_{n\times1}[f]_{n\times n}\{F\}_{n\times1} \tag{6.21}$$

Taking the transpose of both sides does not change the left-hand side of the equation. The right-hand side becomes the product of the transpose of the matrices on this side but in reverse order. Therefore,

$$[W]_{1\times1} = \frac{1}{2}\{F\}^T_{n\times1}[f]^T_{n\times n}\{F\}_{n\times1} \tag{6.22}$$

From Eqs. 6.21 and 6.22, it follows that the flexibility matrix and its transpose are equal, that is,

$$[f]^T = [f] \tag{6.23}$$

This means that for a general element of the flexibility matrix

$$f_{ij} = f_{ji} \tag{6.24}$$

and is known as *Maxwell's reciprocal relation*. In other words, the flexibility matrix is a symmetrical matrix. This property is useful in forming the flexibility matrix because some of the coefficients need not be calculated or, if they are, a check is obtained. The property of symmetry can also be used to save a part of the computational effort required for matrix inversion or for a solution of equations.

Equation 6.1 tells us that the stiffness matrix is the inverse of the flexibility matrix. Since the inverse of a symmetrical matrix is also symmetrical, the stiffness matrix [*S*] is a symmetrical matrix. Thus, for a general stiffness coefficient

$$S_{ij} = S_{ji} \tag{6.25}$$

This property can be used in the same way as in the case of the flexibility matrix.

Another important property of the flexibility and the stiffness matrices is that the elements on the main diagonal, f_{ii} or S_{ii} must be positive as demonstrated below. The element f_{ii} is the deflection at coordinate i due to a unit force at i. Obviously, the force and the displacement must be in the same direction: f_{ii} is therefore positive. The element S_{ii} is the force required at coordinate i to cause a unit displacement at i. Here again, the force and the displacement must be in the same direction so that the stiffness coefficient S_{ii} is positive.

We should note, however, that in unstable structures, for example, a strut subjected to an axial force reaching the buckling load, the stiffness coefficient S_{ii} can be negative. This is discussed further in Chapter 13.

Let us now revert to Eq. 6.21, which expresses the external work in terms of the force vector and the flexibility matrix. If we substitute the force vector from Eq. 6.9 in Eq. 6.20, the work can also be expressed in terms of the displacement vector and the stiffness matrix, thus

$$W = \frac{1}{2}\{F\}^T[f]\{F\} \tag{6.26}$$

or

$$W = \frac{1}{2}\{D\}^T[S]\{D\} \tag{6.27}$$

The quantity on the right-hand side of these equations is referred to as the *quadratic form* in variable F or D. A quadratic form is said to be *positive definite* if it assumes positive values for any nonzero vector of the variable, and moreover is zero only when the vector of the variables is zero ($\{F\}$ or $\{D\} = \{0\}$). It can also be proved that the determinant of a positive definite symmetrical matrix is greater than zero.

From the above discussion, we can see that the quadratic forms in Eqs. 6.26 and 6.27 represent the external work of a system of forces producing a system of displacements, and this quantity must be positive in a stable structure. Physically, this means that work is required to produce any set of displacements $\{D\}$ by the application of a set of forces $\{F\}$. Thus, the quadratic forms $\left(\frac{1}{2}\right)\{F\}^T[f]\{F\}$ and $\left(\frac{1}{2}\right)\{D\}^T[S]\{D\}$ are positive definite and the matrices $[f]$ and $[S]$ are said to be *positive definite matrices*. It follows therefore that, for a stable structure, the stiffness and flexibility matrices must be positive definite and the systems of linear equations

$$[S]\{D\} = \{F\}$$

and

$$[f]\{F\} = \{D\}$$

are positive definite. Further, since the determinants $|S|$ or $|f|$ must be greater than zero, for any nonzero vector on the right-hand side of the equations, each system has a single unique solution, i.e. there is only one set of D_i or F_i values which satisfies the first and second sets of equations respectively.

The stiffness matrix of a free (unsupported) structure can be readily generated, as, for example, Eqs. 6.6 to 6.8 for the beams in Figure 6.4. However, such a matrix is singular and cannot be inverted. Thus, no flexibility matrix can be found unless sufficient restraining forces are introduced for equilibrium.

The criterion of nonsingularity of stiffness matrices for stable structures can be used for the determination of buckling loads, as will be discussed in Chapter 13. We shall see that the stiffness of members of a frame is affected by the presence of high axial forces and the frame is stable only if its stiffness matrix is positive definite and thus its determinant is greater than zero. If the determinant is put equal to zero, a condition is obtained from which the buckling load can be calculated.

If a symmetrical matrix is positive definite, the determinants of all its minors are also positive. This has a physical significance relevant to the stiffness matrix of a stable structure. If the displacement D_i is prevented at a coordinate i, for example, by introduction of a support, the stiffness matrix of the resulting structure can be obtained simply by deletion of ith row and column from the stiffness matrix of the original structure. Addition of a support to a stable structure results in a structure which is also stable and thus the determinant of its stiffness matrix is positive. This determinant is that of a minor of the original stiffness matrix.

6.7 Analysis of symmetrical structures by force method

In practice, many structures have one or more axes or planes of symmetry, which divide the structure into identical parts. If, in addition, the forces applied to the structure are symmetrical, the reactions and internal forces are also symmetrical. This symmetry can be used to reduce the number of unknown redundants or displacements when the analysis is by the force or the displacement method. The analysis by the force method of several symmetrical structures is discussed below.

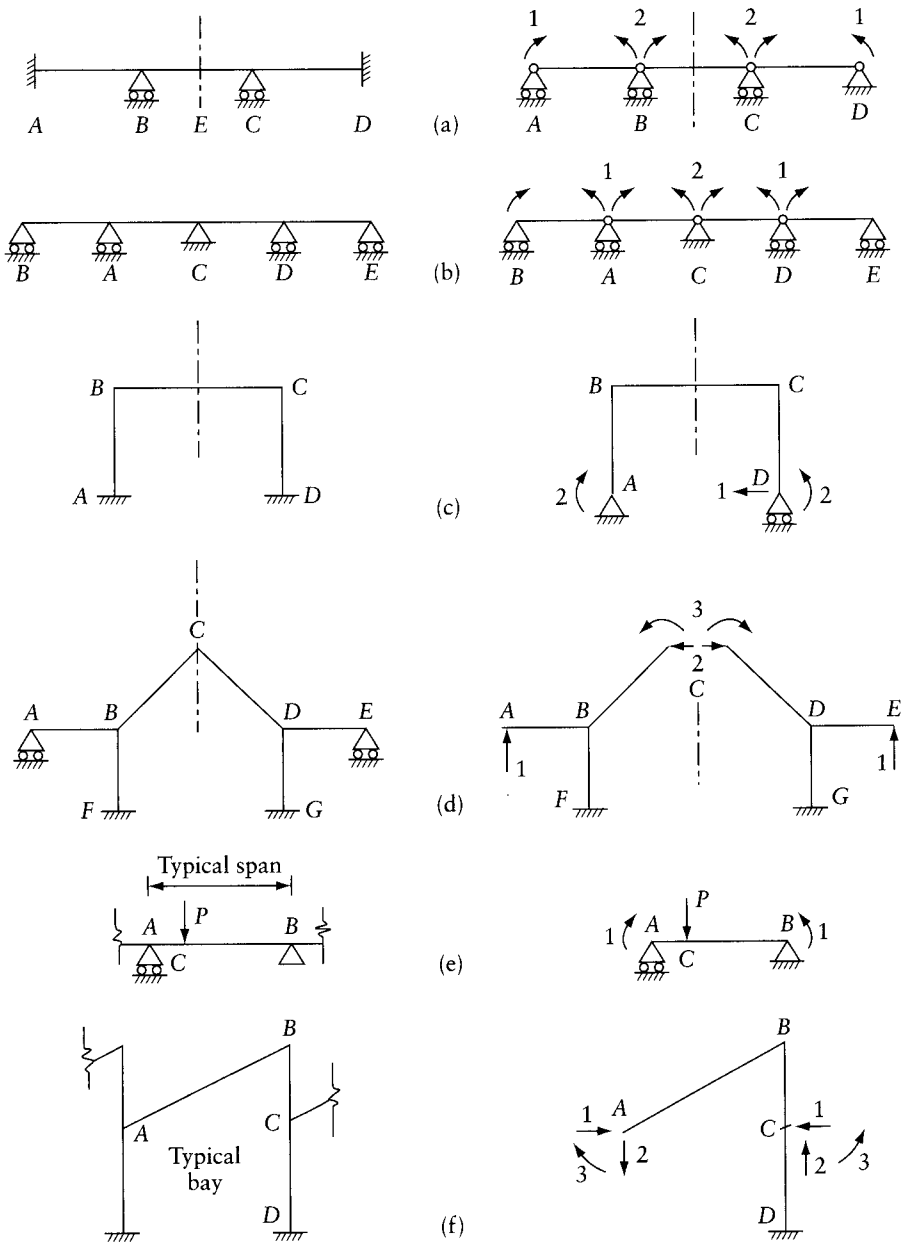

Figure 6.6 Examples of releases for analysis by the force method of symmetrical continuous beams and frames subjected to symmetrical loading.

When the structure to be analyzed is symmetrical and symmetrically loaded, it is logical to select the releases so that the released structure is also symmetrical. In Figures 6.6a to d, releases are suggested for a number of plane structures with a vertical axis of symmetry. Equal redundants on opposite sides of the axis of symmetry are given the same number; see, for example, the coordinates at *A* and *D* in Figures 6.6a and b. Coordinate 1 in these figures represents the

redundant force or the displacement at A (and at D). The flexibility coefficients f_{11} and f_{21} represent, respectively, displacements at coordinate 1 (at A and at D) and at coordinate 2 due to unit forces applied simultaneously at A and at D. The flexibility matrices for the two released structures in Figures 6.6a and b are (Appendix B)

$$[f]_{\text{Figure6.6a}} = \begin{bmatrix} \left(\frac{l}{3EI}\right)_{AB} & \left(\frac{l}{6EI}\right)_{AB} \\ \left(\frac{l}{6EI}\right)_{AB} & \left(\frac{l}{3EI}\right)_{AB} + \left(\frac{l}{2EI}\right)_{BC} \end{bmatrix}$$

$$[f]_{\text{Figure6.6b}} = \begin{bmatrix} \left(\frac{l}{3EI}\right)_{BA} + \left(\frac{l}{3EI}\right)_{AC} & \left(\frac{l}{6EI}\right)_{AC} \\ 2\left(\frac{l}{6EI}\right)_{AC} & 2\left(\frac{l}{3EI}\right)_{AC} \end{bmatrix}$$

In the released structure in Figure 6.6b, there are two coordinates with the number 1 but only one coordinate with the number 2. This causes f_{21} to be equal to $2f_{12}$ and thus the flexibility matrix is not symmetrical. However, symmetry of the geometry equations $[f]\{F\} = -\{D\}$ may be restored by division of the second row by 2.

The released structure in Figure 6.6a has a roller support at A and a hinge support at D, but this does not disturb the symmetry because under symmetrical loading the horizontal reaction at D must be zero.

Because of symmetry, the slope of the deflected shape of the beam at C in Figure 6.6b must be horizontal. Thus, no rotation or deflection can occur at C; hence, the analysis can be done for half the beam only, say BAC, with end C encastré. However, this cannot be done for the beam in Figure 6.6a because, at the center line, the rotation is zero but the deflection is not.

The frame in Figure 6.6c may be released by cutting BC at its middle, thus separating the structure into two identical cantilevers. Cutting a member of a plane frame generally releases an axial force, a shearing force, and a bending moment. Moreover, because of symmetry, the shear at the middle of BC must be zero; hence, the analysis needs to determine two unknown redundants instead of three. The same frame may also be released by changing A into a hinge and D into a roller. This does not disturb the symmetry of forces because, when symmetrical loads are applied on the released structure, the horizontal reaction at A is zero and any force introduced at coordinate 1 must produce a symmetrical force at A.

The frame in Figure 6.6d is released by removal of the roller supports at A and E and by cutting the frame at C. Because of symmetry, only two components represent the internal forces at C, with the vertical component being zero. It may be noted that the released structure will again have the flexibility coefficient f_{21} equal to $2f_{12}$.

Figure 6.6e represents a typical span of a continuous beam having many spans of the same length and the same loading. One span only needs to be analyzed, using the released structure as a simple beam with one unknown redundant representing the connecting moments which must be equal and opposite at the two ends. Here, the displacement D_1 and the flexibility coefficient f_{11} represent relative rotations of the two ends of the simple beam AB.

The frame in Figure 6.6f has an infinite number of identical bays. The analysis may be done for one bay, using the released structure and the three unknown redundants as shown. Here again, the displacements and the flexibility coefficients represent relative translations and rotations of A and C in the released structure.

6.8 Analysis of symmetrical structures by displacement method

Advantage can be taken of symmetry to reduce the number of unknown displacement components when the analysis is done by the displacement method. Because of symmetry, the displacement magnitude at a coordinate is zero or is equal to the value at one (or more) coordinate(s). For a zero displacement, the coordinate may be omitted; any two coordinates where the displacement magnitudes are equal may be given the same number. Figure 6.7 shows examples of coordinate systems which may be used in the analysis by the displacement method of symmetrical structures subjected to symmetrical loading.

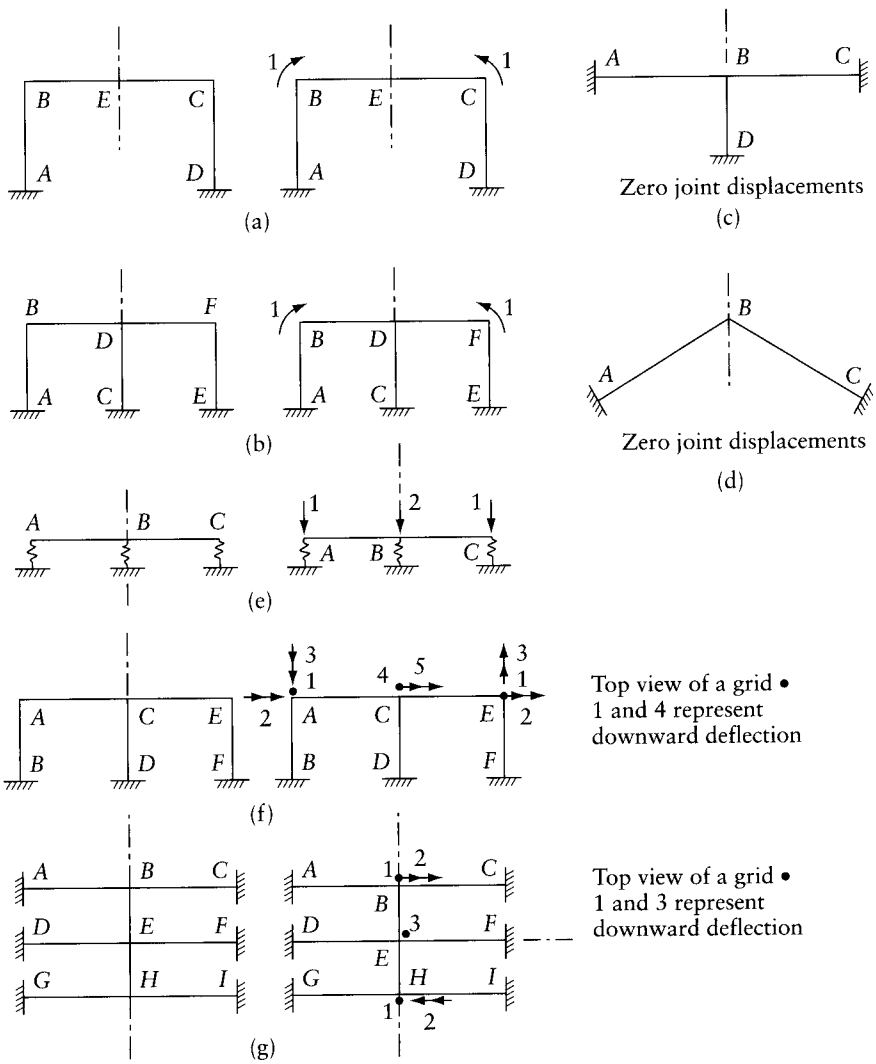

Figure 6.7 Examples of degrees of freedom for analysis and the displacement method of symmetrical plane frames and grids subjected to symmetrical loading.

Figures 6.7a to d represent plane frames in which axial deformations are ignored. In Figure 6.7a the rotations at B and C are equal and are therefore given the same coordinate number, 1. Because sidesway cannot occur under a symmetrical load, the corresponding coordinate is omitted. In Figure 6.7b the rotations at B and F are equal, while the rotation at D and the sidesway are zero; hence, this frame has only one unknown displacement component. No coordinate systems are shown for the structures in Figures 6.7c and d, because the displacement components are zero at all nodes. Thus, no analysis is needed; the member end-forces are readily available from Appendix C.

The beam over spring supports in Figure 6.7e has only two unknown displacement components representing the vertical translation at the top of the springs. Because of symmetry, no rotation occurs at B. Also, no coordinates are shown for the rotations at A and C because the end-forces are readily available for a member with one end hinged and the other fixed (Appendix D, Eqs. D.8 and D.9). The stiffness matrix for the structure (assuming equal spans l and EI = constant) is

$$[S] = \begin{bmatrix} \frac{3EI}{l^3} + K & -\frac{3EI}{l^3} \\ -2\left(\frac{3EI}{l^3}\right) & 2\left(\frac{3EI}{l^3}\right) + K \end{bmatrix}$$

where K is the spring stiffness (assumed the same for the three springs). The element S_{11} represents the force at coordinate 1 (at A and C) when unit downward displacement is introduced simultaneously at A and at C; S_{21} is the corresponding force at 2. We should note that $S_{21} = 2S_{12}$ so that the stiffness matrix is not symmetrical. This is so because the system has two coordinates numbered 1 but only one coordinate numbered 2. The symmetry of the equilibrium equations, $[S]\{D\} = -\{F\}$, can be restored by division of the second row by 2.

If axial deformations are considered, additional coordinates must be used. In Figure 6.7a, a horizontal and a vertical arrow will have to be added at B and at C. Because of symmetry, each of the two corresponding arrows takes the same number, bringing the number of unknown displacements to three. Each of the frames in Figures 6.7c and d will have one unknown displacement: a vertical translation at B.

The horizontal grids shown in Figures 6.7f and g have one or more vertical planes of symmetry. The coordinate systems shown may be used for the analysis of the effects of symmetrical loads.

Each of the structures in Figures 6.7a to g may be analyzed by considering only one-half (or one-quarter) of the structure through separating it at the axis or plane of symmetry. The members situated on the axis or plane of symmetry for the part analyzed should have properties such as a, I, J, or K equal to half the values in the actual structure. The same coordinate systems shown on one-half (or one-quarter) of the structure may be used. An exception is the frame in Figure 6.7a: separation at E will result in a new node at which the vertical translation is unknown, requiring an additional coordinate.

When the analysis of small structures is done by hand or by a calculator, with the matrices generated by the analyst, consideration of one-half or one-quarter of the structure may represent no advantage. However, in large structures with many members and nodes, the analysis is usually performed entirely by computer, considering as small a part of the structure as possible and taking full advantage of symmetry. This is further discussed in Sections 22.4 to 22.6.

The structure shown in Figure 6.6f, representing a typical bay of a frame with an infinite number of bays, may be analyzed by the displacement method, using three degrees of freedom at each of A, B, and C: a translation in the horizontal and vertical directions, and a rotation. The corresponding three displacements at A and C have the same magnitude and direction; hence, there are only six unknown displacements.

Example 6.5: Single-bay symmetrical plane frame

For the frame shown in Figure 6.8a find the bending moment diagram and the reactions R_1 and R_2 at support A. Ignore axial deformations and consider only bending deformations.

We apply the five steps of the displacement method (Section 5.6):

Step 1 Because axial deformations are ignored, only rotations can occur at B and C. A system with a single coordinate is defined in Figure 6.8b. The rotation at A and D will be allowed to occur freely in the analysis steps; thus, no coordinate to represent the rotations is needed. Also, the overhangs EB and FC produce statically determinate forces at B and C. Thus, by taking these forces into account, the analysis can be done for a frame without the cantilevers. The end-moment $M_{BE} = q\frac{l}{2}(0.4l) = 0.2ql^2$. We define the unknown actions as:

$$\{A\} = \{M_{BA},\ M_{BC}\}$$

The values of the three end-moments will be sufficient to draw the bending moment diagram for the left-hand half of the frame. From symmetry, the reaction $R_1 = 1.5ql$ (half the total downward load). The reaction R_2 will be calculated by statics from M_{BA}.

Step 2 $\{F\} = \{0.2ql^2 - q(2l)^2/12\} = \{-0.1333\,ql^2\}$

The first term is the moment to prevent the rotation due to the load on the cantilever. The second term is the fixed-end moment for BC (Appendix C).

$$\{A_r\} = \{0, -q(2l)^2/12\} = \{0, -0.333\,ql^2\}$$

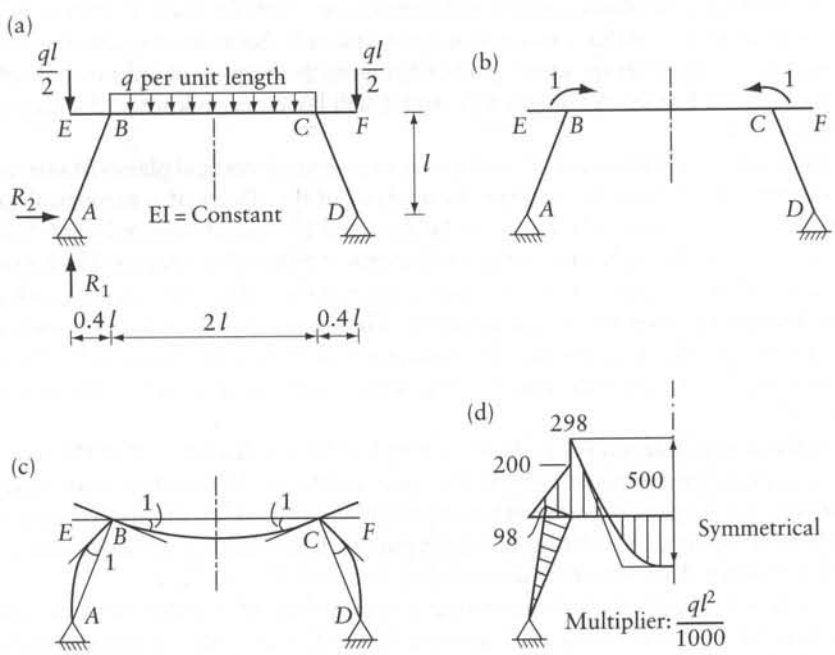

Figure 6.8 Symmetrical plane frame of Example 6.5 (a) Frame dimensions and loading. (b) Coordinate system. (c) Deflected shape with $D_1 = 1$. (d) Bending moment diagram.

Step 3 $$[S]=\left[\left(\frac{3EI}{l}\right)_{BA}+\left(\frac{2EI}{l}\right)_{BC}\right]=\left[\left(\frac{3}{1.077l}+\frac{2}{2l}\right)EI\right]=\left[3.785\frac{EI}{l}\right]$$

$$[A_u]=\begin{bmatrix}(3EI/l)_{BA}\\(2EI/l)_{BC}\end{bmatrix}=\begin{bmatrix}2.785EI/l\\1.0EI/l\end{bmatrix}$$

With $D_1=1$, the deflected shape of the frame will be as shown in Figure 6.8c; the terms $(3EI/l)_{BA}$ and $(2EI/l)_{BC}$ in the above calculations are taken from Appendix D. (See the fourth and the last figures in the appendix.)

Step 4 $$\{D\}=[S]^{-1}\{-F\}=[3.785EI/l]^{-1}\{0.1333\,ql^2\}=\left\{35.22\times10^{-3}\frac{ql^3}{EI}\right\}$$

Step 5 $$\{A\}=\{A_r\}+[A_u]\{D\}=\begin{Bmatrix}0\\-0.333ql^2\end{Bmatrix}+\begin{bmatrix}2.785EI/l\\1.0EI/l\end{bmatrix}\left\{35.22\times10^{-3}\frac{ql^3}{EI}\right\}$$

$$\{A\}=\begin{Bmatrix}98\\-298\end{Bmatrix}\frac{ql^2}{1000}$$

These are the values of the end-moments used to draw the bending moment diagram in Figure 6.8d. The reaction R_2 is given by:

$$M_{BA}=-R_1(0.4l)+R_2l$$

Substitution of $M_{BA}=0.098\,ql^2$ and $R_1=1.5\,ql$ gives $R_2=0.698\,ql$.

Example 6.6: A horizontal grid subjected to gravity load

Figure 6.9a shows a horizontal grid subjected to a uniformly distributed gravity load q per unit length on AB. Find the bending moment diagram for member AB. All members have the same cross section, with $GJ/EI=0.8$.

We apply the five steps of the displacement method (Section 5.6):

Step 1 Three coordinates define the symmetrical displacement components at A and B (Figure 6.9b). To draw the bending moment diagram for AB, we need the value of M_A (or M_B). We consider the bending moment to be positive when it produces tension at the bottom face of the member. Thus, we define the required action:

$$\{A\}=\{M_A\}$$

Step 2 $$\{F\}=\begin{Bmatrix}-ql/2\\0\\-ql^2/12\end{Bmatrix};\quad\{A_r\}=\left\{-\frac{ql^2}{12}\right\}$$

The elements of these vectors are fixed-end forces taken from Appendix C (Eqs. C.7 and C.8).

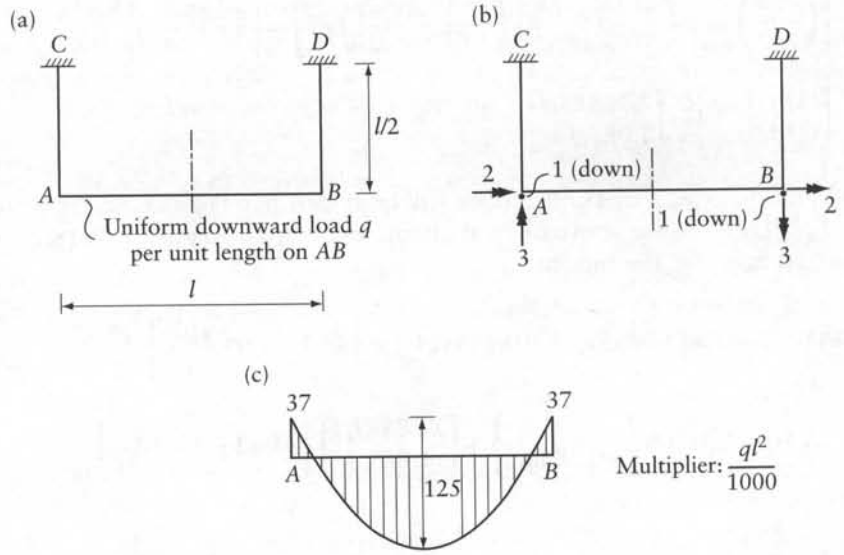

Figure 6.9 Symmetrical horizontal grid of Example 6.6. (a) Top view. (b) Coordinate system. (c) Bending moment diagram for member AB.

Step 3

$$[S] = \begin{bmatrix} \left(\frac{12EI}{l^3}\right)_{AC} & & \text{Symmetrical} \\ -\left(\frac{6EI}{l^2}\right)_{AC} & \left(\frac{4EI}{l}\right)_{AC} & \\ 0 & 0 & \left(\frac{2EI}{l}\right)_{AB} + \left(\frac{GJ}{l}\right)_{AC} \end{bmatrix}$$

$$[A_u] = \begin{bmatrix} 0 & 0 & \left(\frac{2EI}{l}\right)_{AB} \end{bmatrix}$$

For the elements of the first columns of $[S]$ and $[A_u]$ a unit downward deflection, $D_1 = 1$ is introduced at each of A and B. Members AC and BD take the deflected shape shown in the first figure of Appendix D (Eqs. D.1 and D.2), while AB will translate downward as a rigid body (without deformation or end forces). With $D_2 = 1$, members AC and BD will take the deflected shape shown in the second figure of Appendix D (Eqs. D.3 and D.4), while again, member AB will rotate as a rigid body. For the third columns of $[S]$ and $[A_u]$, rotations $D_3 = 1$ are introduced at A and B, causing AB to deflect as shown in the last figure in Appendix D (Eq. D.11); members AC and BD are twisted without bending. The member end-forces given in Appendix D can be used to determine the elements of $[S]$ and $[A_u]$.

Step 4 $\{D\} = [S]^{-1}\{-F\}$

Substituting $[S]$ and $\{F\}$ determined above and performing the matrix inversion and multiplication gives:

$$\{D\} = \frac{ql^3}{1000EI}\{20.8l,\ 62.5,\ 23.2\}$$

Step 5 $\{A\} = \{A_r\} + [A_u]\{D\}$

Substitution of the matrices determined in Steps 2, 3 and 4 gives:

$$\{A\} = -0.037ql^2$$

The bending moment diagram for AB is shown in Figure 6.9c.

6.9 Effect of nonlinear temperature variation

Analysis of changes in stresses and internal forces in structures due to a variation in temperature or due to shrinkage or creep can be done in the same way. The distribution of temperature over the cross section of members is generally nonlinear, as shown in Figure 6.10b for a bridge girder (Figure 6.10a) exposed to the radiation of the sun. In a cross section composed of different

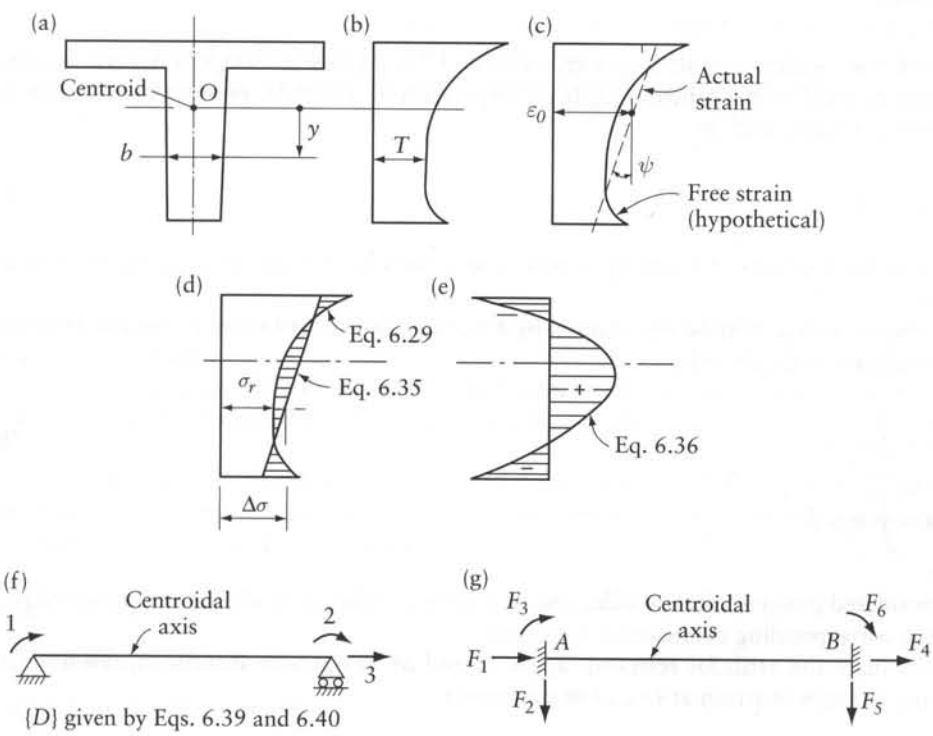

Figure 6.10 Analysis of the effects of nonlinear temperature variation. (a) Cross section of a member. (b) Distribution of temperature rise. (c) Strain distribution. (d) Stresses σ_r and $\Delta\sigma$. (e) Self-equilibrating stresses. (f) Displacements due to a temperature rise in a simple beam. (g) Fixed-end forces due to a temperature rise.

materials such as concrete and steel, the components tend to contract or expand differently because of shrinkage and creep. However, contraction and expansion cannot occur freely and changes in stresses occur. In the following, we consider the effect of temperature rise varying nonlinearly over the cross section of members of a framed structure. The temperature rise is assumed constant over the length of individual members.

In a statically determinate frame, no stresses are produced when the temperature variation is linear; in this case the thermal expansion occurs freely, without restraint. This results in changes in length or in curvature of the members, but produces no changes in the reactions or in the internal forces. However, when the temperature variation is nonlinear, each fiber, being attached to adjacent fibers, is not free to undergo the full expansion, and this induces stresses. These stresses must be self-equilibrating in an individual cross section as long as the structure is statically determinate. The *self-equilibrating stresses* caused by nonlinear temperature (or shrinkage) variation over the cross section of a statically determinate frame are sometimes referred to as the *eigenstresses*.

If the structure is statically indeterminate, the elongations and the rotations at the member ends may be restrained or prevented. This results in changes in the reactions and in the internal forces which can be determined by an analysis using the force or the displacement method. We should note that the reactions produced by temperature must represent a set of forces in equilibrium.

Let us now analyze the self-equilibrating stresses in a statically determinate member, e.g. a simple beam of homogeneous material, subjected to a nonlinear rise in temperature (Figure 6.10a). The hypothetical strain which would occur in each fiber if it were free to expand is

$$\epsilon_f = \alpha T \tag{6.28}$$

where α is the coefficient of thermal expansion and $T = T(y)$ is the temperature rise in any fiber at a distance y below the centroid O. If the expansion is artificially prevented, the stress in the restrained condition will be

$$\sigma_r = -E\epsilon_f \tag{6.29}$$

where E is the modulus of elasticity. Tensile stress and the corresponding strain are considered positive.

The resultant of σ_r may be represented by a normal force N at O and a moment M about the horizontal axis at O, given by

$$N = \int \sigma_r \, da \tag{6.30}$$

$$M = \int \sigma_r y \, da \tag{6.31}$$

N is considered positive when tensile, and M is positive when it produces tension in the bottom fiber; the corresponding curvature ψ is positive.

To eliminate the artificial restraint, apply N and M in opposite directions, resulting in the following changes in strain at O and in curvature:

$$\epsilon_o = -\frac{N}{Ea} \tag{6.32}$$

$$\psi = -\frac{M}{EI} \tag{6.33}$$

where a and I are the area of the cross section and its second moment about a horizontal axis through O respectively. The corresponding strain and stress at any fiber are

$$\epsilon = \epsilon_o + y\psi \tag{6.34}$$

$$\Delta\sigma = E(\epsilon_o + y\psi) \tag{6.35}$$

The addition of σ_r to $\Delta\sigma$ gives the self-equilibrating stress due to temperature:

$$\sigma_s = E(-\alpha T + \epsilon_o + y\psi) \tag{6.36}$$

The stress σ_s must have a zero resultant because its components σ_r and $\Delta\sigma$ have equal and opposite resultants. The distribution of the self-equilibrating stress is shown in Figure 6.10e; the ordinates of this graph are equal to the ordinates between the curve σ_r and the straight line $\Delta\sigma$ in Figure 6.10d.

The changes in axial strain and curvature due to temperature are derived from Eqs. 6.28 to 6.33:

$$\epsilon_o = \frac{\alpha}{a}\int T b\, dy \tag{6.37}$$

$$\psi = \frac{\alpha}{I}\int T b y\, dy \tag{6.38}$$

where $b = b(y)$ is the width of the section. The actual strain distribution over the depth of the section is presented in Figure 6.10c by a dashed line defined by the values ϵ_o and ψ. The two values may be used to calculate the displacements at the coordinates in Figure 6.10f (see Appendix B):

$$D_1 = -D_2 = \psi\frac{l}{2} \tag{6.39}$$

$$D_3 = \epsilon_o l \tag{6.40}$$

When using Eq. 6.39 we should note that, according to the sign convention adopted, ψ in Figure 6.10c is negative.

If the structure is statically indeterminate, the displacements $\{D\}$, such as those given above, may be used in the force method for the analysis of statically indeterminate reactions and internal forces.

When the analysis is by the displacement method, the values ϵ_o and ψ (Eqs. 6.37 and 6.38) can be used to determine the internal forces in a member in the restrained condition and the corresponding member end-forces (Figure 6.10g):

$$N = -Ea\epsilon_o \tag{6.41}$$

$$M = -EI\psi \tag{6.42}$$

$$\{F\} = E\{a\epsilon_o 0, -I\psi, -a\epsilon_o, 0, I\psi\} \tag{6.43}$$

In the special case when the rise in temperature varies linearly from T_{top} to T_{bot} at top and bottom fibers in a member of constant cross section, the fixed-end forces (Figure 6.10g) may be calculated by Eq. 6.43, with $\epsilon_o = \alpha T_o$ and $\psi = \alpha(T_{bot} - T_{top})/h$; here, T_o is the temperature at the cross-section centroid and h is the section depth.

The forces F_1 and F_3 are along the centroidal axis, and the other forces are along centroidal principal axes of the member cross section. The six forces are self-equilibrating. The restraining forces at the ends of individual members meeting at a joint should be transformed in the directions of the global axes and summed to give the external restraining forces which will artificially prevent the joint displacements of the structure. (The assemblage of end-forces is discussed further in Section 22.9.) In the restrained condition, the stress in any fiber may be calculated by Eq. 6.29.

When the temperature rise varies from section to section or when the member has a variable cross section, ϵ_o and ψ will vary over the length of the member. Equations 6.41 and 6.42 may be applied at any section to give the variables N and M in the restrained condition; the member forces are given by

$$\{F\} = E\{\{a\epsilon_o, 0, -I\psi\}_A, \{-a\epsilon_o, 0, I\psi\}_B\} \tag{6.44}$$

The subscripts A and B refer to the member ends (Figure 6.10g). For equilibrium, a distributed axial load p and a transverse load q must exist. The load intensities (force per length) are given by

$$p = E\frac{d(a\epsilon_o)}{dx} \tag{6.45}$$

$$q = E\frac{d^2(I\psi)}{dx^2} \tag{6.46}$$

Positive p is in the direction A to B, and positive q is downwards; x is the distance from A to any section. Equations 6.45 and 6.46 can be derived by considering the equilibrium of a small length of the beam separated by two sections dx apart.

The restraining forces given by Eqs. 6.44 to 6.46 represent a system in equilibrium. The displacements due to temperature can be analyzed by considering the effect of these restraining forces applied in reversed directions. In the restrained condition, the displacement at *all* sections is zero and the internal forces are given by Eqs. 6.41 and 6.42. These internal forces must be superimposed on the internal forces resulting from the application of the reversed self-equilibrating restraining forces in order to give the total internal forces due to temperature.

The self-equilibrating stresses and the statically indeterminate forces caused by temperature change are proportional to the modulus of elasticity, E. Some materials, such as concrete, exhibit creep (increase in strain), when subjected to sustained stress. The thermal effects will be overestimated when the value of E used in the analysis is based on the relation of stress to instantaneous strain, ignoring creep (see Section 6.10).

Inevitable cracking of reinforced concrete members reduces the effective values of a and I. If cracking is ignored in the values of a and I used in analysis of thermal effects, the results can be greatly overestimated.[2]

Example 6.7: Thermal stresses in a continuous beam

The continuous concrete beam in Figure 6.11a is subjected to a rise of temperature which is constant over the beam length but varies over the depth as follows:

$$T = T_o + 4.21T_{top}\left(\frac{7}{16} - \frac{y}{h}\right)^5 \quad \text{for } -\frac{5h}{16} \leq y \leq \frac{7h}{16}$$

$$T = T_o \quad \text{for } \frac{7h}{16} \leq y \leq \frac{11h}{16}$$

2 See footnote 1, Chapter 4.

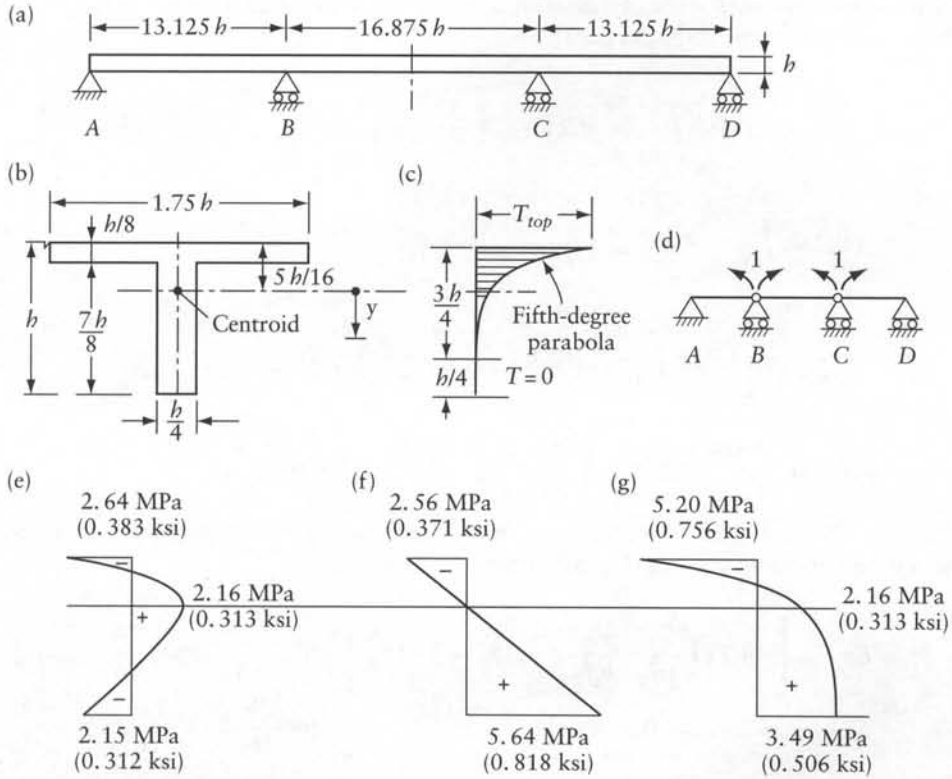

Figure 6.11 Stresses due to a temperature rise in a continuous beam, Example 6.7. (a) Beam elevation. (b) Beam cross section. (c) Temperature rise. (d) Released structure and coordinate system. (e) Self-equilibrating stresses. (f) Continuity stresses. (g) Total stresses.

where T is the temperature rise in degrees, T_{top} is the temperature rise in the top fiber, and $T_0 =$ constant. The beam has a cross section as shown in Figure 6.11b, with an area $a = 0.4375h^2$ and the second moment of area about the centroidal axis is $I = 0.0416h^4$. Find the stress distribution due to the temperature rise in the section at support B.

Consider $h = 1.6$ m(63in.), $E = 30$ GPa (4350 ksi), $\alpha = 1 \times 10^{-5}$ per degree Celsius $(5/9) \times 10^{-5}$ per degree Fahrenheit) and $T_{top} = 25°$ Celsius (45° Fahrenheit).

The above equations represent the temperature distribution which can occur in a bridge girder on a hot summer's day. When the temperature rise is constant, the length of the beam will increase freely, without inducing any stress or deflection. Hence, to solve the problem, we may put $T_o = 0$; the temperature rise will then vary as shown in Figure 6.11c.

Application of Eqs. 6.28 and 6.29 gives the artificial stress which would prevent thermal expansion:

$$\sigma_r = -4.21E\alpha T_{top}\left(\frac{7}{16} - \frac{y}{h}\right)^5 \qquad \text{for } -\frac{5}{16} \le \frac{y}{h} \le \frac{7}{16}$$

This equation applies for the upper three-quarters of the beam depth, while $\sigma_r = 0$ for the remainder.

If the structure were statically determinate, the axial strain and the curvature at any section would be (Eqs. 6.37 and 6.38)

$$\epsilon_o = \frac{\alpha}{0.437h^2}\left[1.75h\int_{-5h/16}^{-3h/16} 4.21\,T_{top}\left(\frac{7}{16}-\frac{y}{h}\right)^5 dy\right.$$

$$\left.+0.25h\int_{-3h/16}^{7h/16} 4.21 T_{top}\left(\frac{7}{16}-\frac{y}{h}\right)^5 dy\right] = 0.356\alpha\, T_{top}$$

$$\psi = \frac{\alpha}{0.0416h^4}\left[1.75h\int_{-5h/16}^{-3h/16} 4.21\,T_{top}\left(\frac{7}{16}-\frac{y}{h}\right)^5 y\,dy\right.$$

$$\left.+0.25h\int_{-3h/16}^{7h/16} 4.21\,T_{top}\left(\frac{7}{16}-\frac{y}{h}\right)^5 y\,dy\right] = -0.931\alpha\, T_{top}h^{-1}$$

The self-equilibrating stresses (Eq. 6.36) are

$$\sigma_s = E\alpha T_{top}\left[-4.21\left(\frac{7}{16}-\frac{y}{h}\right)^5 + 0.356 - 0.931\frac{y}{h}\right] \quad \text{for } -\frac{5h}{16} \leqslant y \leqslant \frac{7h}{16}$$

$$\sigma_s = E\alpha T_{top}\left(0.356 - 0.931\frac{y}{h}\right) \quad \text{for } \frac{7h}{16} \leqslant y \leqslant \frac{11h}{16}$$

Substitution of E, α, T, and the y values at the top fiber, the centroid, and at the bottom fiber gives the values of the self-equilibrating stresses shown in Figure 6.11e. This stress diagram is valid for all sections.

Because the structure is statically indeterminate, the temperature rise produces reactions, internal forces, and stresses. The stresses due to the indeterminate forces are referred to as *continuity stresses*. We apply the five steps of the force method (see Section 4.6) to determine the continuity stresses:

Step 1 A released structure and a coordinate system are selected in Figure 6.11d, taking advantage of symmetry (see Section 6.7). The required action is $A = \sigma$, the stress at any fiber of the cross section at B.

Step 2 The displacement of the released structure is the relative rotation of the beam ends at B (or at C). Using Eq. 6.39 or Appendix B,

$$D_1 = \frac{\psi l_{AB}}{2} + \frac{\psi l_{BC}}{2} = -\frac{0.931}{2}\alpha\, T_{top}(13.125 + 16.875) = -13.97\alpha T_{top}$$

The value of the required action in the released structure is the self-equilibrating stress in Figure 6.11e; hence,

$$A_s = \sigma_s$$

Step 3 Applying $F_1 = 1$ at the coordinates in Figure 6.11d gives the flexibility (see Appendix B)

$$f_{11} = \left(\frac{l}{3EI}\right)_{AB} + \left(\frac{l}{2EI}\right)_{BC} = \frac{1}{E(0.0416h^4)}\left(\frac{13.125h}{3} + \frac{16.875h}{2}\right) = \frac{308}{Eh^3}$$

In this problem, A_u is the stress at any fiber of the cross section at B due to $F_1 = 1$, that is, the stress due to unit bending moment:

$$A_u = \frac{y}{I} = \frac{y}{0.0416h^4} = 24\frac{y}{h^4}$$

Step 4 The redundant (the connecting moment at B or C) is

$$F_1 = -f_{11}^{-1}D_1 = -\left(\frac{308}{Eh^3}\right)^{-1}(-13.97\alpha T_{top}) = 0.0454\alpha T_{top}Eh^3$$

Step 5 The stress at any fiber is obtained by the superposition equation:

$$A = A_s + A_u F_1$$

Substitution gives

$$\sigma = \sigma_s + 1.09\alpha T_{top}Ey/h$$

The second term in this equation represents the continuity stress plotted in Figure 6.11f. The total stress at section B is plotted in Figure 6.11g, which is a superposition of Figures 6.11e and f.

Example 6.8: Thermal stresses in a portal frame

Member BC of the frame in Figure 6.12a is subjected to a rise of temperature which is constant over the beam length but varies over its depth following a fifth-degree parabola, as shown in Figure 6.11c. The cross section of member BC of the frame is the same as in Figure 6.11b. Assuming that the columns AB and CD have a rectangular cross section (Figure 6.12c) and that the rise of temperature is limited to member BC, find the corresponding stress distribution at any cross section of this member. Consider bending and axial deformations. Other data needed for the solution are the same as in Example 6.7.

The five steps of the displacement method (Section 5.6) are followed:

Step 1 A coordinate system is defined in Figure 6.12c. Taking advantage of symmetry, the number of unknown joint displacements is three. The stress distribution is the same at any section of BC and the stress at any fiber is the action required; thus, $A = \sigma$.

Step 2 The values $\epsilon_o = 0.356\alpha T_{top}$ and $\psi = -0.931\alpha T_{top}h^{-1}$ determined in Example 6.7 apply here to member BC. The first three elements of the vector in Eq. 6.43 are the restraining forces at the left-hand end of BC. Because AB and CD are not subjected to temperature

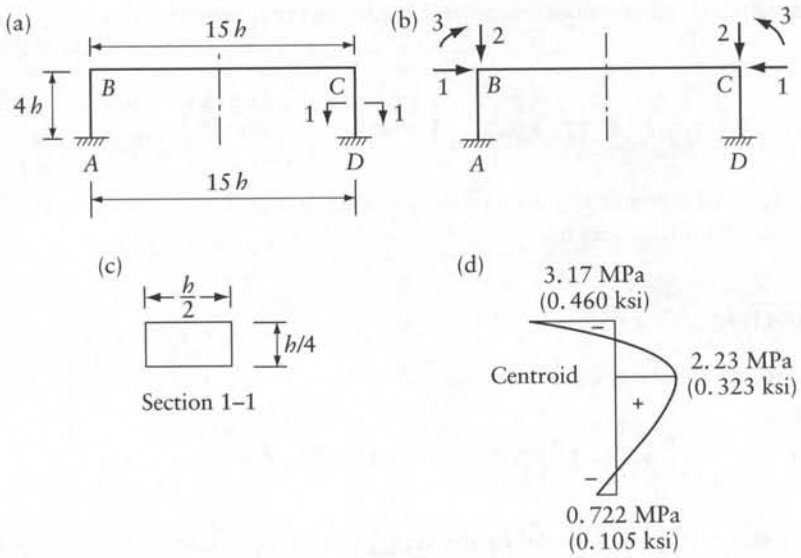

Figure 6.12 Analysis of stresses due to a temperature rise by the displacement method, Example 6.8. (a) Plane frame with a cross section of member BC and a temperature rise as in Figures 6.11b and c. (b) Cross section of columns AB and CD. (c) Coordinate system. (d) Stress distribution at any cross section of BC.

change, no restraining forces need to be determined for these two members. The restraining forces at the three coordinates at B or C are

$$\{F\} = E\begin{Bmatrix} 0.4375h^2(0.356\alpha T_{top}) \\ 0 \\ -0.0416h^4(-0.931\alpha T_{top}h^{-1}) \end{Bmatrix} = E\alpha T_{top}h^2\begin{Bmatrix} 0.156 \\ 0 \\ 0.0387h \end{Bmatrix}$$

The stress at any fiber of member BC with the joint displacement prevented is the same as determined in Example 6.7. Thus,

$$A_r = \sigma_r = -4.21E\alpha T_{top}\left(\frac{7}{16} - \frac{y}{h}\right)^5 \qquad \text{for } -\frac{5h}{16} \le y \le \frac{7h}{16}$$

$$A_r = 0 \qquad \text{for remainder for depth}$$

Step 3 The stiffness matrix of the structure (using Appendix D) is

$$[S] = \begin{bmatrix} \left(\frac{12EI}{l^3}\right)_{AB} + \left(2\frac{Ea}{l}\right)_{BC} & & \text{symmetrical} \\ 0 & \left(\frac{Ea}{l}\right)_{AB} & \\ -\left(\frac{6EI}{l^2}\right)_{AB} & 0 & \left(\frac{4EI}{l}\right)_{AB} + \left(\frac{2EI}{l}\right)_{BC} \end{bmatrix}$$

Substitute: for $AB, l = 4h$, $a = 0.125h^2$, and $I = 2.60 \times 10^{-3}h^4$; for BC, $l = 15h$, $a = 0.4375h^2$, and $I = 0.0416h^4$.

Hence,

$$[S] = E\begin{bmatrix} 58.82 \times 10^{-3}h & & \text{symmetrical} \\ 0 & 31.25 \times 10^{-3}h & \\ -975.0 \times 10^{-6}h^2 & 0 & 8.147 \times 10^{-3}h^3 \end{bmatrix}$$

The stress at any fiber due to unit displacements at the coordinates is

$$[A_u] = E\left[-\left(\frac{2}{l}\right)_{BC} \quad 0 \quad \left(\frac{2I}{l}\right)_{BC}\frac{y}{I_{BC}}\right]$$

$$[A_u] = E\left[-\frac{2}{25h} \quad 0 \quad \frac{2y}{15h}\right]$$

Step 4 Substitution for $[S]$ and $\{F\}$ and solution of the equilibrium equation $[S]\{D\} = -\{F\}$ gives

$$\{D\} = \alpha T_{top}\begin{Bmatrix} -2.736h \\ 0 \\ -5.078 \end{Bmatrix}$$

Step 5 By superposition, the stress at any fiber is

$$A = A_r + [A_u]\{D\}$$

Substitution for $A_r, [A_u]$, and $\{D\}$ gives

$$\sigma = \sigma_r + E\alpha T_{top}\left(0.365 - 0.677\frac{y}{h}\right)$$

$$\sigma = E\alpha T_{top}\left[-4.21\left(\frac{7}{16} - \frac{y}{h}\right)^5 + 0.365 - 0.677\frac{y}{h}\right] \quad \text{for } -\frac{5h}{16} \leqslant y \leqslant \frac{7h}{16}$$

$$\sigma = E\alpha T_{top}\left(0.365 - 0.677\frac{y}{h}\right) \quad \text{for } \frac{7h}{16} \leqslant y \frac{11h}{16}$$

Substituting for y the values $-5h/16$, 0, and $11h/16$ and using the values of E, α, and T_{top} from the data for Example 6.7 gives the stress values indicated in Figure 6.12d.

6.10 Effect of shrinkage and creep

The phenomena of shrinkage and creep occur in various materials, but in the following discussion we shall refer mainly to concrete because it is so widely used in structures.

Shrinkage of concrete is a reduction in volume associated with drying in air. As with a temperature drop, if the change in volume is restrained by the difference in shrinkage of various parts of the structure or by the supports or by the reinforcing steel, stresses develop.

If we imagine a material which shrinks without creep, the analysis for the effect of shrinkage can be performed using the equations of Section 6.9, but replacing the term αT by ϵ_f, where ϵ_f is the free (unrestrained) shrinkage. The effect of swelling can be treated in the same manner as shrinkage but with a reversed sign. Swelling occurs in concrete under water.

The strain which occurs during the application of stress, or within a few seconds thereafter, may be referred to as the *instantaneous strain*. For some materials, the strain continues to increase gradually when the stress is sustained without a change in magnitude. The increase in strain with time, under a sustained stress, is referred to as *creep*. For concrete, creep is two to four times larger than the instantaneous strain, depending upon the composition of concrete, the ambient humidity and temperature, the size of the element considered, the age of concrete when the stress is applied, and the length of the period during which the stress is sustained.

If creep is assumed to be equal to the instantaneous strain multiplied by a constant coefficient, creep will have no effect on the internal forces or stresses in a structure made of a homogeneous material. Creep will cause larger displacements, which can be accounted for by the use of a reduced (effective) E, but this has no effect on the reactions even when the structure is statically indeterminate.

When a concrete structure is constructed and loaded in stages, or when member cross sections contain reinforcement, or when the section is composed of a concrete part connected to structural steel, the creep which is different in various components cannot occur freely. Similarly to temperature expansion, restrained creep induces stresses. In statically determinate structures, creep changes the distribution of stresses within a section without changing the reactions or the stress resultants. This is not so in statically indeterminate structures, where creep influences also the reactions and the internal forces.

In concrete structures, shrinkage and creep occur simultaneously. The stress changes caused by these two phenomena develop gradually over long periods, and with these changes there is associated additional creep. Hence, the analysis must account also for the creep effect of the stress which is gradually introduced. Analysis of the time-dependent stresses and deformations in reinforced and prestressed concrete structures is treated in more detail in books devoted to this subject.[3]

When a change in temperature in a concrete structure develops gradually over a period of time (hours or days), the resulting stresses are reduced by creep which occurs during the same period. Ignoring creep overestimates the effects of temperature variations.

6.11 Effect of prestressing

In Section 4.4, we discussed the effect of prestressing a concrete beam by a cable inserted through a duct and then anchored at the ends. This method is referred to as post-tensioning. In this section, we shall discuss the effects of a post-tensioned tendon which has a nonlinear profile. For simplicity of presentation, we ignore the friction which commonly exists between the tendon and the inner wall of the duct; thus, we assume that the tensile force in the tendon is constant over its length. Let P represent the absolute value of the force in the tendon.

A straight tendon as in Figure 4.3a produces two inward horizontal forces on the end sections, each equal to P. The two forces represent a system in equilibrium, and the reactions in the statically determinate beam are zero. The internal forces at any section are an axial force $-P$ and a bending moment $-Pe$. The sign convention used here is indicated in Figure 2.4c. The eccentricity e is measured downward from the centroidal axis. The ordinates between the centroidal axis and the tendon profile represent the bending moment diagram with a multiplier $-P$.

Usually, the tendon profile is selected so that the prestressing partly counteracts the effects of forces which the structure has to carry. Whenever a tendon changes direction, a transverse force is exerted by the tendon on the member. The tendon shown in Figure 6.13a produces, at the end anchorages, two inward forces of magnitude P along the tangents to the tendon profile.

3 See footnote 1, Chapter 4.

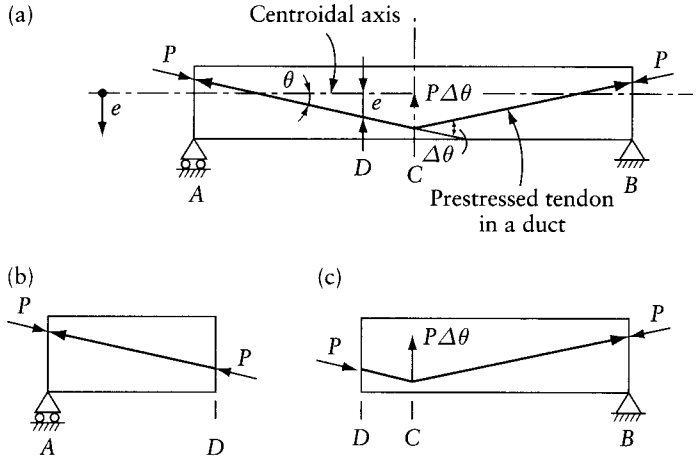

Figure 6.13 Forces due to prestressing in a statically determinate beam. (a) Representation of prestressing by a system of forces in equilibrium. (b) and (c) Free-body diagrams showing the stress resultant at section D.

In addition, an upward force is produced at point C. Thus, the profile in Figure 6.13a may be used in a simple beam carrying a large downward concentrated load.

The three forces shown in Figure 6.13a represent a set of forces in equilibrium. In most practical cases, the angle θ between the centroidal axis and the tangent to the tendon is small, so that we need to consider only the axial component of the prestressing force, P, and the perpendicular component, $P\theta$. It follows that the force at C is equal to $P\Delta\theta$, where $\Delta\theta$ is the absolute value of the change in slope.

A parabolic tendon produces a uniform transverse load and is thus suitable to counteract the effect of the self-weight and other distributed gravity loads. Appendix K gives the magnitude and direction of the forces produced by tendons having profiles commonly used in practice. The forces shown represent the effect of the prestressing tendon on the other components of the member. The forces produced by a prestressed tendon must constitute a system in equilibrium.

Prestressing of a statically determinate structure produces no reactions. It can be shown that the resultant of the internal forces at any section is a force P along the tangent of the tendon profile. This can be seen in Figure 6.13b, where the beam is separated into two parts in order to show the internal forces at an arbitrary section D. The ordinate e between the centroidal axis and the tendon profile represents the bending moment ordinate with a multiplier $-P$. The axial force is $-P$ and the shear is $-P\theta$.

The internal forces, determined as outlined in the preceding paragraph, are referred to as *primary forces*. Prestressing of statically indeterminate structures produces reactions and hence induces additional internal forces referred to as *secondary forces*. The reactions also represent a system of forces in equilibrium. When the structure is statically determinate, the force in the prestressed steel at any section is equal and opposite to the resultant of stresses in other components of the section, and thus the total stress resultant on the whole section is zero. This is not so in a statically indeterminate structure.

In the analysis of the effects of prestressing it is not necessary to separate the primary and secondary effects. The total effect of prestressing may be directly determined by representing the prestressing by a system of external applied self-equilibrating forces (see Appendix K). The analysis is then performed in the usual way by either the force or the displacement method.

Example 6.9: Post-tensioning of a continuous beam

Find the reactions and the bending moment diagram due to prestressing for the continuous beam shown in Figure 6.14a. The prestressing tendon profile for each span of the beam is composed of two second-degree parabolas, *ACD* and *DB*, with a common tangent at *D* (Figure 6.14b). The parabolas have horizontal tangents at *B* and *C*. Assume a constant prestressing force *P*.

The profile shown in Figure 6.14b is often used in practice for the end span of a continuous beam. The condition that the two parabolas have a common tangent at *D* is required to avoid a sudden change in slope, which would produce an undesired concentrated transverse force at *D*. In design, the geometry of the profile can be obtained by choosing α, c_A, and c_B arbitrarily and determining β and c_D so that

$$\beta = \gamma \frac{c_D}{c_B - c_D} \quad \text{and} \quad c_D = c_A \frac{\beta^2}{\alpha^2}$$

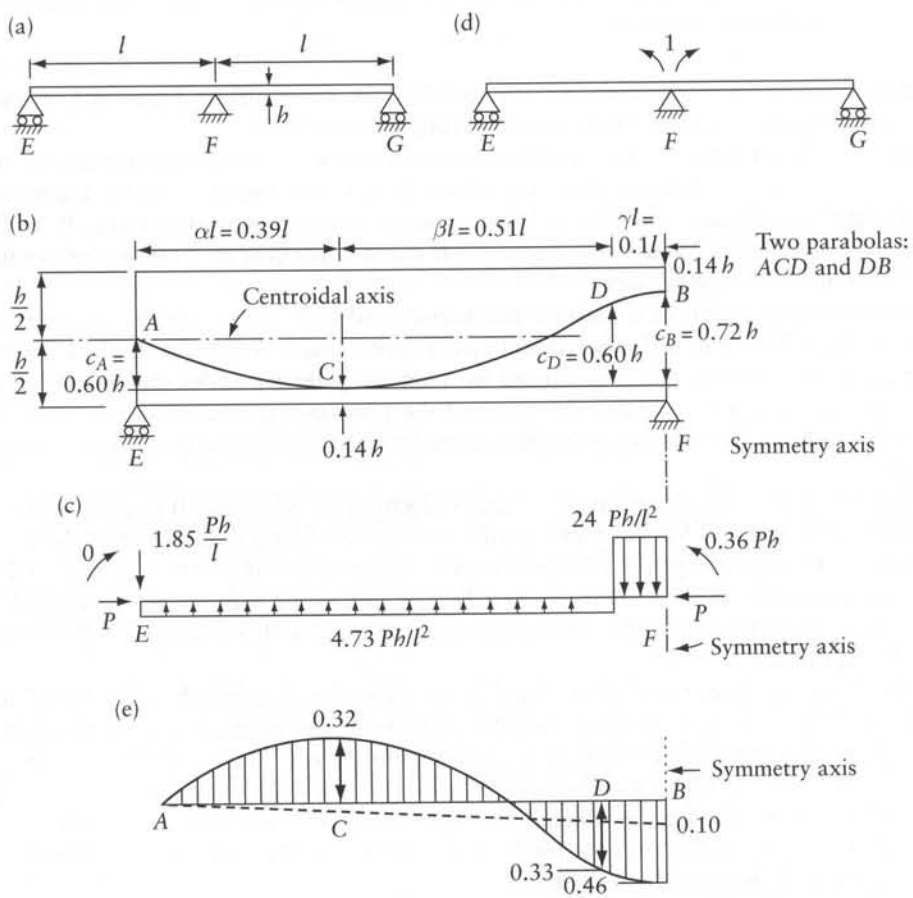

Figure 6.14 Effect of prestressing on a continuous beam, Example 6.9. (a) Beam elevation. (b) Prestressing tendon profile in one-half of the structure. (c) Self-equilibrating forces produced by prestressing. (d) Released structure and coordinate system. (e) Bending moment diagram.

These two geometrical relations ensure that the slope of the tangents to the two parabolas at D is the same and that ACD is one parabola with a horizontal tangent at C. Solution of the two equations for the unknowns β and c_D may be obtained by trial and error, noting that $\alpha+\beta+\gamma=1$ (Newton-Raphson's technique).

The forces produced by the tendon are calculated by the equations of Appendix K and are shown in Figure 6.14c for the left-hand half of the beam.

The five steps of the force method (Section 4.6) are applied to determine the statically indeterminate reactions:

Step 1 The released structure and the coordinate system are shown in Figure 6.14d. The actions required are

$$\{A\}=\{R_E, R_F, R_G\}$$

A positive reaction is upwards.

Step 2 The forces in Figure 6.14c when applied on the released structure give the following displacement (Appendix B):

$$D_1=2\frac{Phl}{24EI}\{24(0.1)^2[4-4(0.1)+(0.1)^2]$$

$$-4.73(0.9)^2[2-(0.9)^2]\}+2(0.36Ph)\frac{l}{3EI}=-0.068\frac{Phl}{EI}$$

The applied forces are self-equilibrating and hence produce zero reactions in the released structure; thus,

$$\{A_s\}=\{0\}$$

Step 3 The flexibility coefficient (Appendix B) is

$$f_{11}=\frac{2l}{3EI}$$

A unit redundant, $F_1=1$, produces the following reactions:

$$[A_u]=\frac{1}{l}\begin{bmatrix}1\\-2\\1\end{bmatrix}$$

Step 4

$$f_{11}F_1=-D_1$$

$$F_1=-\left(\frac{2l}{3EI}\right)^{-1}\left(-0.068\frac{Phl}{EI}\right)=0.102\,Ph$$

Step 5 Superposition gives the required reactions:

$$\{A\} = \{A_s\} + [A_u]\{F\}$$

$$\begin{Bmatrix} R_E \\ R_F \\ R_G \end{Bmatrix} = \{0\} + \frac{0.102\,Ph}{l} \begin{Bmatrix} 1 \\ -2 \\ 1 \end{Bmatrix} = \frac{Ph}{l} \begin{Bmatrix} 0.102 \\ -0.203 \\ 0.102 \end{Bmatrix}$$

The bending moment diagram is plotted in Figure 6.14e. Its ordinate at any section of span EF may be expressed as

$$M = -Pe + 0.102\frac{Phx}{l}$$

where x is the horizontal distance from E to the section and e is the vertical distance from the centroidal axis to the tendon profile; e is positive where the tendon is below the centroid. Following the convention used throughout this book, the bending moment ordinates are plotted on the tension side of the beam. The dashed line in Figure 6.14e is the statically indeterminate bending moment due to prestressing, called the *secondary bending moment*.

6.12 General

The stiffness and flexibility matrices are related by the fact that one is the inverse of the other, provided the same coordinate system of forces and displacements is used in their formation. However, because the coordinate systems chosen in the displacement and force methods of analysis are not the same, the relation is not valid between the stiffness and flexibility matrices involved in the analyses.

The choice of the method of analysis depends on the problem in hand and also on whether a computer is to be used. The displacement method is generally more suitable for computer programming.

Stiffness matrices for a prismatic member in a three- and two-dimensional frame, given in this chapter, are of value in standardizing the operations. Some other properties discussed are also of use in various respects, including the calculations of buckling loads, considered in Chapter 14.

Problems

6.1 Ignoring torsion, find by the use of Appendix E the stiffness matrix for the horizontal grid in Prob. 5.18 corresponding to four downward coordinates at I, J, K, and L in this order. Use this matrix to find the deflection at the coordinates due to downward equal forces P at I and J. Take advantage of the symmetry of the structure and of the loading. Draw the bending moment diagram for beam DG.

6.2 Write the stiffness matrix corresponding to the four downward coordinates at A, B, C, and D in the horizontal grid shown in the figure. Ignore torsion and make use of Appendix E (cf. Prob. 6.5). Find the bending moment in beams AD and BF due to a pair of equal

downward loads P at B and C. Take advantage of the symmetry of the structure and of the loading to reduce the number of equations to be solved.

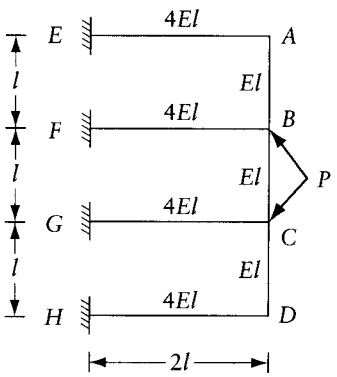

Prob. 6.2

6.3 The figure shows three coordinate systems for a beam of constant flexural rigidity EI. Write the stiffness matrix corresponding to the four coordinates in (a). Condense this stiffness matrix to obtain the stiffness matrices corresponding to the three coordinates in (b) and to the two coordinates in (c).

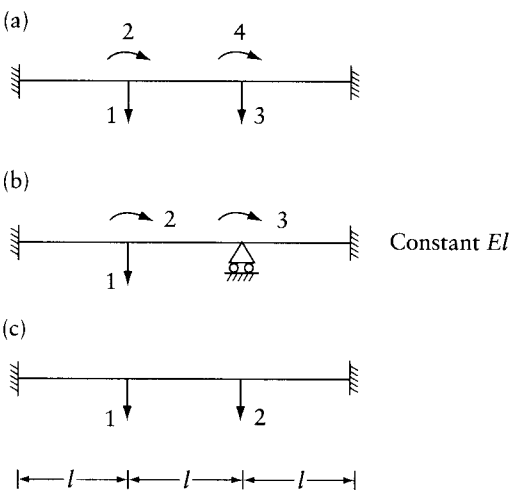

Prob. 6.3

6.4 Apply the requirements of Prob. 6.3 to the member shown in the figure.

6.5 The figure represents a beam on three spring supports of stiffness $K_1 = K_2 = K_3 = EI/l^3$. Using Appendix E, derive the stiffness matrix corresponding to the three coordinates in the figure. Use this matrix to find the deflection at the three coordinates due to loads $\{F\} = \{3P, P, 0\}$.

6.6 If the stiffness of any two of the spring supports in Prob. 6.5 is made equal to zero, the stiffness matrix becomes singular. Verify this and explain why.

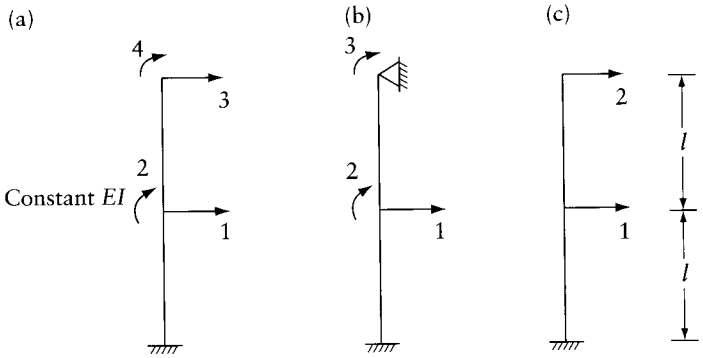

Prob. 6.4

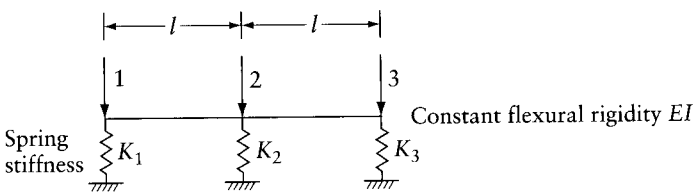

Prob. 6.5

6.7 Neglecting axial deformations and using Appendix D, write the stiffness matrix for the frame in the figure corresponding to the four coordinates in (a). Condense this matrix to find the 2×2 stiffness matrix corresponding to the coordinates in (b).

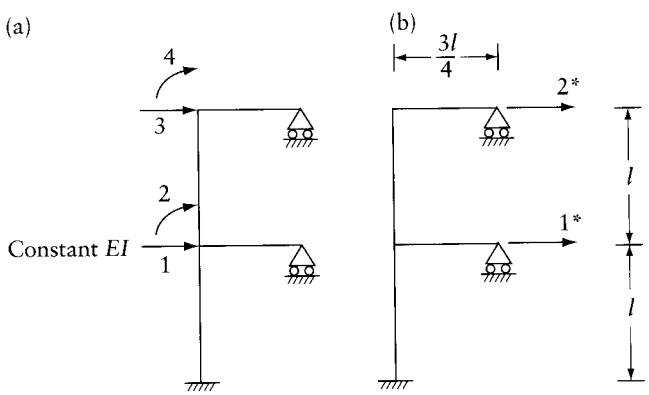

Prob. 6.7

6.8 In Prob. 5.14 we derived the stiffness matrix $[S]_{3\times3}$ for a portal frame. Use this stiffness matrix to derive the stiffness coefficient S^*_{11} corresponding to the one-coordinate system shown in the figure. Express the answer in terms of the elements S_{ij} of the matrix $[S]$.

6.9 What is the value of the force P which makes the structure in Prob. 4.7 unstable? *Hint*: Write the stiffness matrix in terms of P; then find the value of P which makes the determinant vanish.

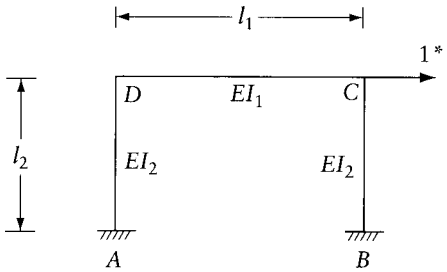

Prob. 6.8

6.10 Find the smallest value of P (in terms of Kl) which will make the system in the figure unstable. The bars AB, BC, and CD are rigid. See hints to Probs. 4.7 and 6.9.

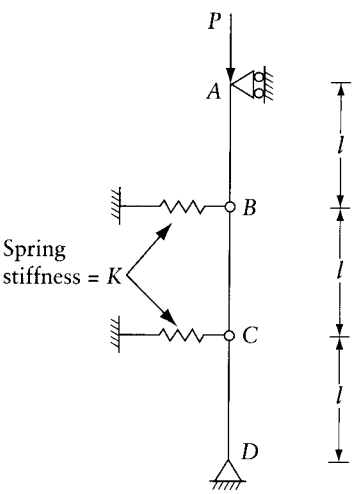

Prob. 6.10

6.11 Find the bending moment and shearing force diagrams for the beam in Figure 6.6a due to a concentrated downward force P at E, the middle of BC. Assume all spans have the same length l, and EI = constant.

6.12 Find the bending moments at A, C, and D in the beam of Figure 6.6b due to a uniform load q per unit length over the whole length, taking advantage of symmetry. The answers to this problem are given in Figure 4.8.

6.13 Figure 6.6e represents a typical span of a continuous beam having an infinite number of spans. Obtain the bending moment and shearing force diagrams and the reactions. Assume the lengths of members are $AB = l$, $AC = l/3$, $CB = 2l/3$, and EI = constant.

6.14 Solve Prob. 6.13 assuming that the load shown is applied only on alternate spans.

6.15 Solve Prob. 6.13 assuming that alternate spans are subjected to uniform load q per unit length, while the remaining spans have no load.

6.16 Obtain the bending moment diagram and the reaction components at A for the frame of Figure 6.7a due to a uniform downward load q per unit length on BC. Assume the lengths of members are $AB = b$ and $BC = 1.5b$, with EI constant. Consider bending deformations only.

6.17 Obtain the bending moment diagram and the reaction components at A and C for the frame in Figure 6.7b due to a uniform downward load q per unit length on BF. Consider bending deformations only. Assume that all members have the same length l, and $EI =$ constant.

6.18 Obtain the bending moment and shearing force diagrams for member AB of the frame in Figure 6.7d, ignoring axial deformations. The frame is subjected to a uniform downward load covering ABC of total magnitude $2ql$, where $2l$ is the length AC. Assume that the inclination of AB to the horizontal is θ.

6.19 The horizontal grid in Figure 6.7f is subjected to a downward concentrated load P at C. Write the equations of equilibrium at the five coordinates shown. Use the values of $\{D\}$ given in the Answers to check the equations. Consider that all members have the same length l and the same cross section, with $GJ/EI = 0.5$.

6.20 The horizontal grid in Figure 6.7g is subjected to a uniform downward load q per unit length on DF only. Write the equations of equilibrium at the three coordinates shown. Use the values of $\{D\}$ given in the Answers to check the equations. Consider that all members have the same cross section, with $GJ/EI = 0.5$. Assume the lengths of members are: $AB = BC = l$, $BE = EH = l/2$.

6.21 A simple beam of length l and rectangular cross section of width b and depth d is subjected to a rise of temperature which is constant over the length of the beam but varies over the depth of the section. The temperature rise at the top is T and varies linearly to zero at mid-depth; the rise of temperature is zero for the lower half of the section. Determine the stress distribution at any section, the change in length of the centroidal axis and the deflection at mid-span. Modulus of elasticity is E and coefficient of thermal expansion is α.

6.22 If the beam of Prob. 6.21 is continuous over two spans, each of length l, with one support hinged and the other two on rollers, obtain the bending moment diagrams, the reactions, and the stress distribution at the central support due to the same rise of temperature.

6.23 Member BC of the frame in Figure 6.7a is subjected to a rise of temperature which is constant over the length of the beam but varies linearly over the depth d, from T at the top to zero at the bottom. Obtain the bending moment diagram and the reaction components at A. Ignore deformations due to axial and shear forces. Assume the lengths of members are $AB = 10d$ and $BC = 15d$, and all members have a constant rectangular cross section. The second moment of area is I, and the coefficient of thermal expansion is α.
Hint: Because of symmetry and because the deformation due to the axial force is ignored, the translation of B and C is horizontal outward, each with a magnitude of $\alpha T(15d)/4$ (half the elongation of the centroidal axis BC). Thus, the structure has only one unknown joint displacement: the rotation at B or C.

6.24 Find the bending moment diagram, the reactions, and the deflection at the middle of span AB due to prestressing of the continuous beam shown. Assume the prestressing force P

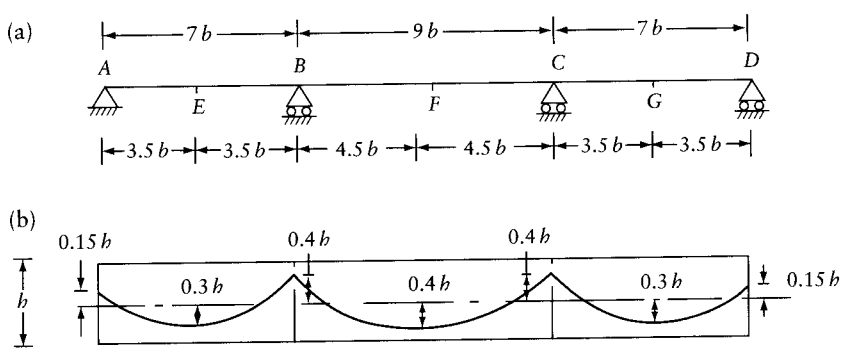

Prob. 6.24

is constant and the tendon profile is a second-degree parabola in each span. Draw the shearing force diagram.

6.25 Solve Prob. 6.24 assuming that the tendon has a profile composed of straight lines with the eccentricities:

$$\{e_A, e_E, e_B, e_F, e_C, e_G, e_D\} = h\{0, 0.3, -0.4, 0.4, -0.4, 0.3, 0\}$$

6.26 Determine the stress distribution at a cross section over the interior support of a continuous beam of two equal spans. The beam has a rectangular cross section subjected to a rise of temperature, T, varying over the height of the section, h, according to the equation: $T = T_{top}(0.5 - \mu)^5$, where T_{top} is the temperature rise at the top fiber; $\mu = y/h$, with y being the distance measured downward from the centroid to any fiber. Give the answer in terms of E, α, T_{top} and μ, where E and α are the modulus of elasticity and the thermal expansion coefficient of the material. What is the value of stress at the extreme tension fiber? Using SI units, assume $E = 30$ GPa, $\alpha = 10^{-5}$ per degree Celsius and $T_{top} = 30$ degrees Celsius; or using Imperial units, assume $E = 4300$ ksi; $\alpha = 0.6 \times 10^{-5}$; $T_{top} = 50$ degrees Fahrenheit. The answers will show that the stress is high enough to reach or exceed the tensile strength of concrete; thus, cracking could occur.

6.27 Find the bending moment diagram and the force in the tie in the frame of Prob. 4.22, replacing the hinge at C by a rigid joint. Use the displacement method and take advantage of symmetry. Assume that the tie is rigid. Consider only bending deformation.

6.28 Solve Prob. 6.27, assuming $(Ea)_{Tie} = 130EI/l^2$; where EI is the flexural rigidity of $ABCDE$.

6.29 For the space truss shown, find the forces in the members and the reaction components due to an external force at O having the components $\{P_x, P_y, P_z\} = P\{1.0, 2.0, 3.0\}$.
Hint. Although the truss is statically indeterminate, it can be analyzed using the equations of equilibrium by taking advantage of symmetry; e.g. P_x produces tensile forces in OA and OD and compressive forces in OB and OC having equal absolute value. As an exercise, check the forces in the members using the displacement method.

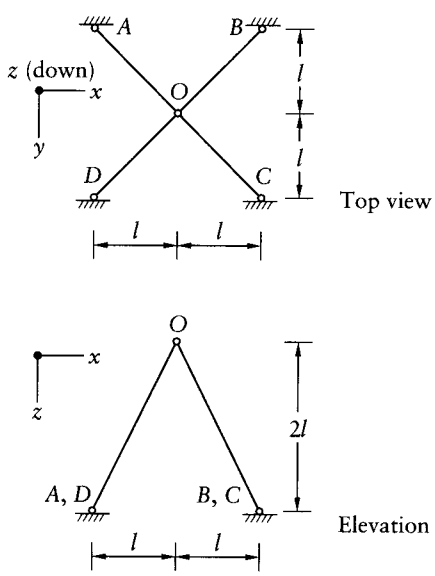

Prob. 6.29

Chapter 7

Strain energy and virtual work

7.1 Introduction

We have already seen that the knowledge of the magnitude of displacements in a structure is necessary in the analysis of statically indeterminate structures, and in the preceding two chapters we used, for the purpose, either the displacements due to forces or the forces induced by imposed displacements. Displacements are, of course, also of interest in design, and, in fact, in some cases the consideration of deflections under design loads may be the controlling factor in proportioning of members.

Calculation of displacements of structures made of materials obeying Hooke's law requires the knowledge of the modulus of elasticity in tension and compression (usually identical) E, and of the shear modulus G. When the stress–strain relation is nonlinear, it is necessary to develop an expression relating forces and deformations, in terms of stress and strain, axial load and extension, or moment and curvature. In this book, we deal mainly with linear structures as these are most common.

When the displacements are required solely for the solution of statically indeterminate linear structures, we need to know only the relative values of Ea, EI, and GJ at all cross sections and for all members of the structures, where a is the area of the cross section, I its second moment of area, and J a torsional constant, with a dimension (length)^4, equal to the polar moment of inertia in the case of a solid or a hollow circular bar. (For other cross sections, see Appendix G.)

If the actual values of the displacements are required or if the structure is to be analyzed for the effect of settlement of supports or for a temperature variation, it becomes necessary to know the values of E or G, or both. For some materials, such as metals, these moduli have standard values, given in a handbook or guaranteed by the manufacturer to vary within fixed limits. In the case of concrete,[1] the elastic properties are a function of many variables in the material itself and in its ambient conditions; in reinforced concrete, the amount and type of reinforcement also affect the apparent overall cross-section properties. When cracking occurs, the rigidity of a reinforced concrete member is greatly reduced.[2] It is obvious that, under such circumstances, the accuracy of the structural analysis depends on the reliability of the assumed values of E, G, and cross-section properties.

Several methods are available for the determination of displacements, of which the most versatile is the method of virtual work. It is particularly suitable when the displacements at

1 See, for example, Neville, A.M., *Properties of Concrete*, 4th ed., Longman, London, and John Wiley, New York, 1996.

2 See Ghali, A., Favre, R. and Elbadry, M., *Concrete Structures: Stresses and Deformations*, 3rd ed., Spon Press, London, 2002.

only a few locations are required. However, when the complete deformed shape of a structure is required,[3] other methods discussed in Chapter 10 are more advantageous to use.

7.2 Geometry of displacements

In most cases, we deal with structures in which the deflections are small compared with the length of the members and the angular rotations result in small translation of the joints. This assumption is essential for much of what follows, but for clarity the displacements will be sketched to a much larger scale than the structure itself. Thus, the distortion in the geometry of the deformed structure will be exaggerated.

Consider the frame ABC of Figure 7.1a, in which the members are connected at B by a rigid joint. This means that the angle ABC between the tangents to BA and BC at B is unaffected by loading, even though the position, direction, and shape of the members AB and BC change. The assumption that the displacements are small leads to a simplification in the calculation of the magnitude of translation of the joints. For example, suppose that we want to determine the displaced location of joints B and C in the frame of Figure 7.1a caused by an angular displacement of θ radians at A in the plane of the frame. Joint B will move through an arc BB_1 of length $l_1\theta$, where l_1 is the length of AB. Since q and BB_1 are small, the arc BB_1 can be replaced by BB_2, perpendicular to AB and of the same length as BB_1. Thus, while member AB undergoes a rotation only, member BC undergoes a translation and a rotation. The translation means that C moves to C_1, such that $CC_1 = BB_2 = l_1\theta$. The rotation – which must be equal to θ since the angle ABC is unchanged – causes a further translation $C_1C_2 = l_2\theta$, where l_2 is the length of BC.

The total displacement of joint C can also be determined directly by drawing CC_2 perpendicular to the line joining A and C, with a length $CC_2 = l_3\theta$ (see Figure 7.1b). In other words, the rotation at A is considered to cause a rotation of the whole frame as a rigid body. This is correct if the members of the frame are not subjected to bending deformation, but, even if they are and the axes of members assume a deflected shape, the translation of joints B and C due to the rotation θ at A alone can still be determined in the same manner.

It is often convenient to express the displacements in terms of components in the direction of rectangular axes. From Figure 7.1b we can see that the horizontal and vertical components of the displacement CC_2 are

$$D_1 = l_4\theta \text{ and } D_2 = l_5\theta$$

where l_4 and l_5 are as defined in the figure. The two equations may be rewritten:

$$D_x = -y\theta; D_y = x\theta \tag{7.1}$$

where D_x and D_y are displacement components in the positive x and y directions respectively; x and y are coordinates of orthogonal axes with origin at the rotation center, A; θ is rotation in the clockwise direction (Figure 7.1b).

As stated before, this type of calculation of displacements caused by a rotation θ at A is valid for a small θ only. In the presence of axial forces, the contribution of the rotation θ at A to the displacement of C can still be determined by the expressions given above with l_4 and l_5 equal to the original lengths.

From the above discussion we conclude that in a plane frame, a small angular rotation θ at a section causes a relative displacement at any other section equal to $l\theta$, where l is the original

3 In Chapter 12 it will be shown that the deflected shape caused by a specific loading represents an influence line for the structure.

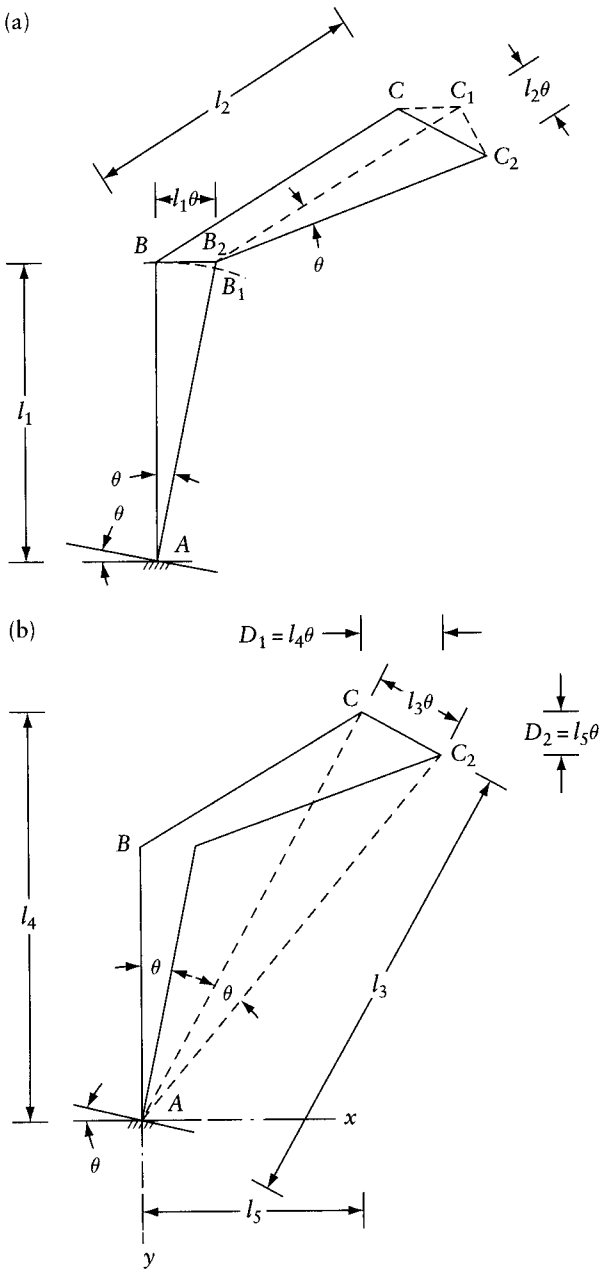

Figure 7.1 Displacements caused by rotation through a small angle.

length of the line joining the centers of the two sections considered. This displacement is a translation in a direction perpendicular to the line joining the two points.

Because the displacements are small, they can be assumed not to cause gross distortions of the geometry of the structure so that the equilibrium equations can be based on the original directions and relative position of the external forces and of the members. This is a reasonable assumption in the majority of structures but, in some cases, the distorted structure is appreciably

changed in geometry so that the equilibrium conditions based on the original geometry of the structure no longer hold. As a result, the structure behaves nonlinearly even if the stress–strain relation of the material is linear. This means that equal increments of external load will not always produce equal increments of displacement: any additional displacement depends upon the total load already acting. (See Chapter 24).

7.3 Strain energy

In Section 6.6 we derived an expression for the work done on a structure subjected to a system of loads $\{F\}$. This work will be completely stored in the elastic structure in the form of strain energy, provided that no work is lost in the form of kinetic energy causing vibration of the structure, or of heat energy causing a rise in its temperature. In other words, the load must be applied gradually, and the stresses must not exceed the elastic limit of the material. When the structure is gradually unloaded, the internal energy is recovered, causing the structure to regain its original shape. Therefore, the external work W and the internal energy U are equal to one another:

$$W = U \tag{7.2}$$

This relation can be used to calculate deflections or forces, but we must first consider the method of calculating the internal strain energy.

Consider a small element of a linear elastic structure in the form of a prism of cross-sectional area da and length dl. The area da can be subjected to either a normal stress σ (Figure 7.2a), or to a shear stress τ (Figure 7.2b). Assume that the left-hand end B of the element is fixed while the right-hand end C is free. The displacement of C under the two types of stress is then

$$\Delta_1 = \frac{\sigma}{E} dl \text{ and } \Delta_2 = \frac{\tau}{G} dl$$

where E is the modulus of elasticity in tension or compression, and G is the modulus of elasticity in shear. When the forces $\sigma\ da$ and $\tau\ da$, which cause the above displacements, are applied gradually, the energy stored in the two elements is

$$dU_1 = \frac{1}{2}(\sigma\ da)\Delta_1 = \frac{1}{2}\frac{\sigma^2}{E} dl\, da$$

$$dU_2 = \frac{1}{2}(\tau\ da)\Delta_2 = \frac{1}{2}\frac{\tau^2}{G} dl\, da$$

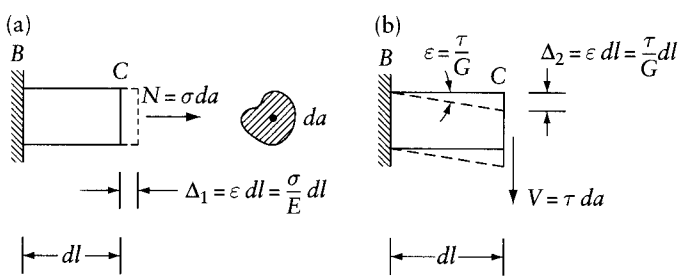

Figure 7.2 Deformation of an element due to (a) normal stress, and (b) shearing stress.

Using ϵ as a general symbol for strain, the above equations can be put in the general form

$$dU = \frac{1}{2}\sigma\epsilon \, dv \tag{7.3}$$

where $dv = dl\, da$ = volume of the element, and σ represents a generalized stress, that is, either a normal or a shearing stress.

The strain ϵ in Eq. 7.3 is either due to a normal stress and has magnitude $\epsilon = \sigma/E$, or due to a shearing stress, in which case $\epsilon = \tau/G$. But G and E are related by

$$G = \frac{E}{2(1+\nu)} \tag{7.4}$$

where ν is Poisson's ratio, so that the strain due to the shearing stress can be written $\epsilon = 2(\tau/E)(1+\nu)$.

The increase in strain energy in any elastic element of volume dv due to a change in strain from $\epsilon = 0$ to $\epsilon = \epsilon_f$ is

$$dU = dv \int_0^{\epsilon_f} \sigma \, d\epsilon \tag{7.5}$$

where the integral $\int_0^{\epsilon_f} \sigma \, d\epsilon$ is called the *strain energy density* and is equal to the area under the stress–strain curve for the material (Figure 7.3a). If the material obeys Hooke's law, the stress–strain curve is a straight line (Figure 7.3b), and the strain energy density is $(\frac{1}{2})\sigma_f\epsilon_f$.

Any structure can be considered to consist of small elements of the type shown in Figure 7.4 subjected to normal stresses σ_x, σ_y, σ_z and to shearing stresses τ_{xy}, τ_{xz}, and τ_{yz}, with resulting strains ϵ_x, ϵ_y, ϵ_z, γ_{xy}, γ_{xz} and γ_{yz}, where the subscripts x, y, and z refer to rectangular cartesian coordinate axes. The total strain energy in a linear structure is then

$$U = \frac{1}{2}\sum_{m=1}^{6} \int_v \sigma_m \epsilon_m dv \tag{7.6}$$

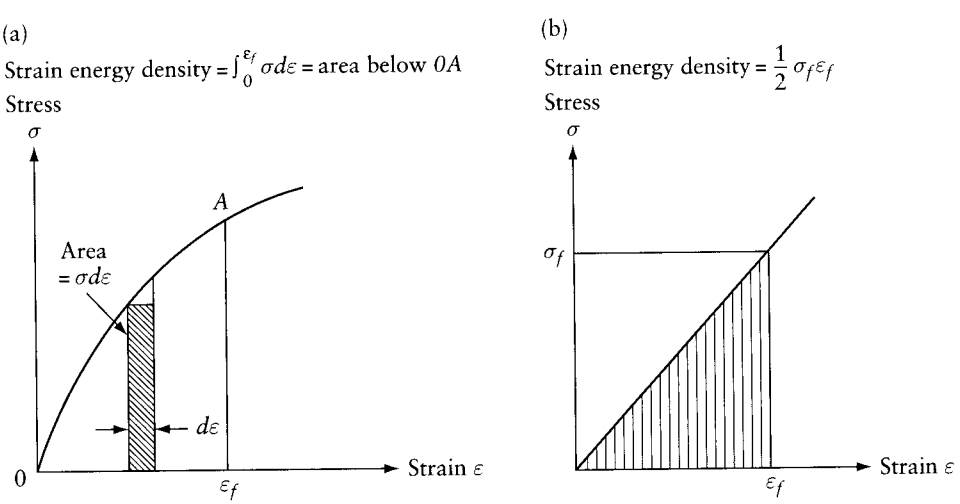

Figure 7.3 Stress–strain relations: (a) nonlinear, and (b) linear.

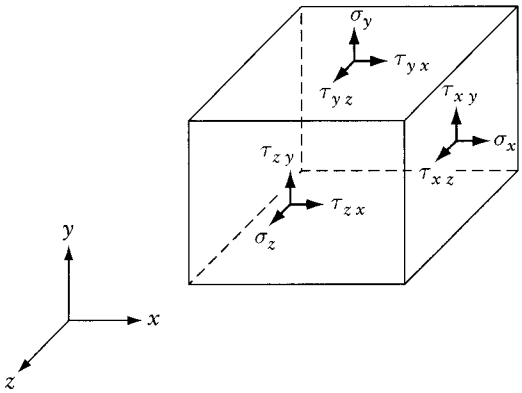

Figure 7.4 Stress components on an element (stresses on the hidden faces act in the opposite directions).

where m refers to the type of stress and to the corresponding strain. This means that the integration has to be carried out over the volume of the structure for each type of stress separately.

In the case of a nonlinear structure, the strain energy equation corresponding to Eq. 7.6 is obtained by integration of Eq. 7.5 for the six stress and strain components:

$$U = \sum_{m=1}^{6} \int_v \int_0^{\epsilon_{fm}} \sigma_m \, d\epsilon_m \, dv \tag{7.7}$$

where ϵ_{fm} is the final value of each strain component.

The expression $\epsilon_{fm} = (\sigma/E)$ for a linear material applies when the stress is applied normal to one plane only. In the more general case, when six types of stress act (Figure 7.4), the stress–strain relation for a homogeneous and isotropic material obeying Hooke's law can be written in matrix form:

$$\{\epsilon\} = [e]\{\sigma\} \tag{7.8}$$

where $\{\epsilon\}$ is a column vector of the six types of strain, that is,

$$\{\epsilon\} = \{\epsilon_x, \epsilon_y, \epsilon_z, \gamma_{xy}, \gamma_{xz}, \gamma_{yz}\} \tag{7.9}$$

$\{\sigma\}$ is the stress vector, that is,

$$\{\sigma\} = \{\sigma_x, \sigma_y, \sigma_z, \tau_{xy}, \tau_{xz}, \tau_{yz}\} \tag{7.10}$$

and $[e]$ is a square symmetrical matrix representing the flexibility of the element:

$$[e] = \frac{1}{E} \begin{bmatrix} 1 & -\nu & -\nu & 0 & 0 & 0 \\ -\nu & 1 & -\nu & 0 & 0 & 0 \\ -\nu & -\nu & 1 & 0 & 0 & 0 \\ 0 & 0 & 0 & 2(1+\nu) & 0 & 0 \\ 0 & 0 & 0 & 0 & 2(1+\nu) & 0 \\ 0 & 0 & 0 & 0 & 0 & 2(1+\nu) \end{bmatrix} \tag{7.11}$$

Equation 7.8 does no more than write in a succinct form the well-known equations of elasticity. For instance, the first equation represented by Eq. 7.8 is

$$\epsilon_x = \frac{\sigma_x}{E} - \frac{\nu(\sigma_y + \sigma_z)}{E}$$

Likewise, the fourth equation is

$$\gamma_{xy} = \tau_{xy}\frac{2(1+\nu)}{E}$$

Inversion of Eq. 7.8 enables us to express stress in terms of strain thus:

$$\{\sigma\} = [d]\{\epsilon\} \tag{7.12}$$

where $[d] = [e]^{-1}$ is a square symmetrical matrix representing the rigidity of the element. The matrix $[d]$ is referred to as the *elasticity matrix;* for a three-dimensional isotropic solid

$$[d] = \frac{E}{(1+\nu)(1-2\nu)}\begin{bmatrix} (1-\nu) & \nu & \nu & 0 & 0 & 0 \\ \nu & (1-\nu) & \nu & 0 & 0 & 0 \\ \nu & \nu & (1-\nu) & 0 & 0 & 0 \\ 0 & 0 & 0 & \frac{(1-2\nu)}{2} & 0 & 0 \\ 0 & 0 & 0 & 0 & \frac{(1-2\nu)}{2} & 0 \\ 0 & 0 & 0 & 0 & 0 & \frac{(1-2\nu)}{2} \end{bmatrix} \tag{7.13}$$

Using the notation of Eqs. 7.9 and 7.10, Eq. 7.6 can be written in the form

$$U = \frac{1}{2}\int_v \{\sigma\}^T\{\epsilon\}dv \tag{7.14}$$

or

$$U = \frac{1}{2}\int_v \{\epsilon\}^T\{\sigma\}\,dv \tag{7.15}$$

Substituting Eq. 7.8 or Eq. 7.12 into Eqs. 7.14 and 7.15, we obtain respectively

$$U = \frac{1}{2}\int_v \{\sigma\}^T[e]\{\sigma\}\,dv \tag{7.16}$$

and

$$U = \frac{1}{2}\int_v \{\epsilon\}^T[d]\{\epsilon\}\,dv \tag{7.17}$$

These equations are general for a linear elastic structure of any type. However, in framed structures the strain energy due to different types of stress resultants is best determined separately – in the manner discussed below.

7.3.1 Strain energy due to axial force

Consider a segment dl of a member of cross-sectional area a and length l subjected to an axial force N (Figure 7.5a). The normal stress is $\sigma = N/a$, the strain is $\epsilon = N/Ea$, and there is no shear. From Eq. 7.3, the total strain energy is

$$U = \frac{1}{2}\int_l \frac{N^2}{Ea} dl \tag{7.18}$$

For a prismatic member this becomes

$$U = \frac{1}{2}\frac{N^2 l}{Ea} \tag{7.19}$$

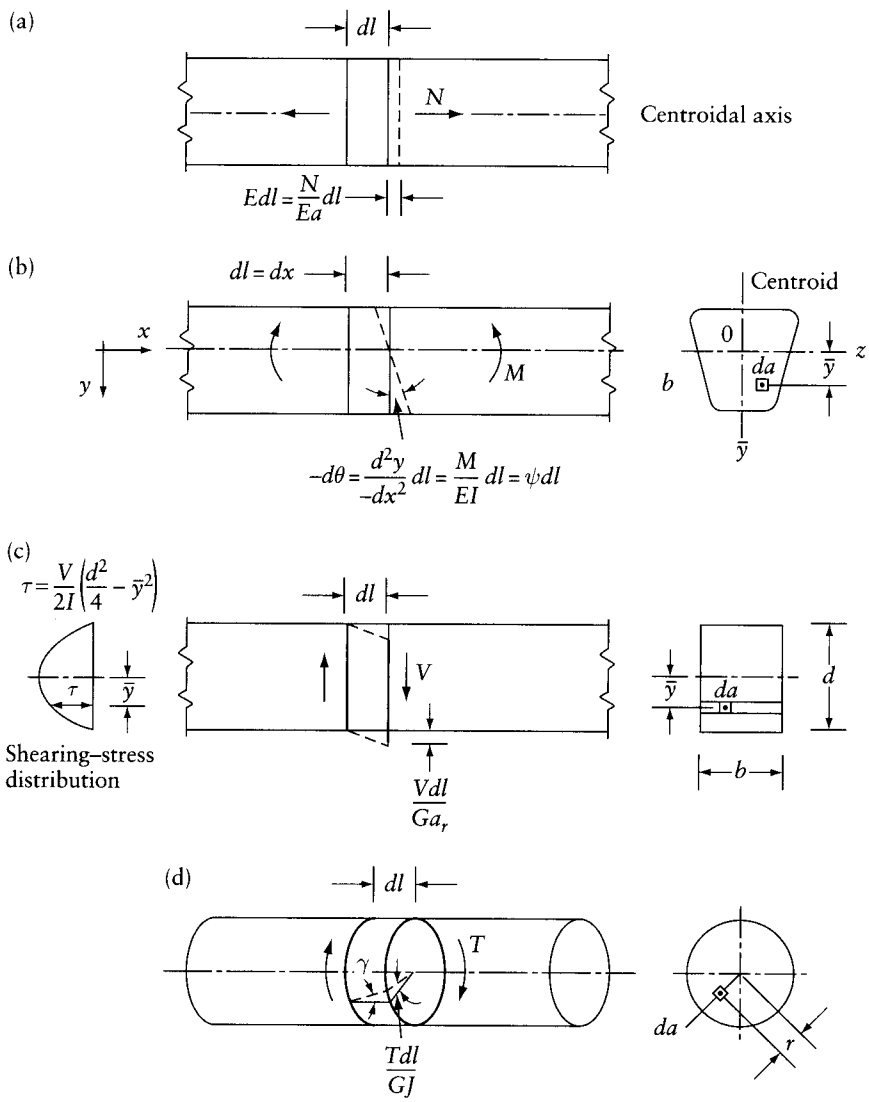

Figure 7.5 Deformation of a segment of a member due to internal forces. (a) Axial force. (b) Bending moment. (c) Shearing force. (d) Twisting moment.

7.3.2 Strain energy due to bending moment

Consider a segment dl subjected to a bending moment M about the z axis – one of the principal axes of the cross section (Figure 7.5b). The normal stress on an element da at a distance $\bar{y}$ from the z axis is $\sigma = M\bar{y}/I$ where I is the second moment of area about the z axis. The corresponding strain is $\epsilon = \sigma/E = M\bar{y}/EI$. From Eq 7.3, the strain energy of the element is

$$dU = \frac{1}{2}\frac{M^2\bar{y}^2}{EI^2}dv = \frac{1}{2}\frac{M^2\bar{y}^2}{EI^2}da\,dl$$

Integrating over the cross section of the segment dl, we find the strain energy to be

$$\Delta U = \frac{1}{2}\frac{M^2}{EI^2}dl\int_a \bar{y}^2\,da$$

The integral in the above equation is equal to I, so that

$$\Delta U = \frac{1}{2}\frac{M^2}{EI}dl \tag{7.20}$$

Hence, for the whole structure the strain energy due to bending is

$$U = \frac{1}{2}\int \frac{M^2 dl}{EI} \tag{7.21}$$

the integration being carried out over the entire length of each member of the structure.

Referring to Figure 7.5b, we can see that the two sections limiting the segment dl rotate relative to one another by an angle $-d\theta = -(d^2y/dx^2)\,dl$ where y is the downward deflection. The external work done by a couple M moving through $-d\theta$ is

$$\Delta W = -\frac{1}{2}M\,d\theta \tag{7.22}$$

The minus sign is included in this equation because a positive bending moment M (causing tensile stress at bottom fibers) produces a decrease of the slope $\theta = dy/dx$ of the deflected axis of the beam. The difference in slope of the tangent of the deflected beam axis at the right-hand and left-hand ends of the segment dx is $-d\theta = -(d^2y/dx^2)dl = \psi\,dl$; where ψ is the curvature.

Since the internal and external work on the segment are equal to one another, that is, $\Delta W = \Delta U$, we find from Eqs. 7.20 and 7.22

$$d\theta = -\frac{M}{EI}dl \tag{7.23}$$

Substituting in Eq. 7.21, the strain energy due to bending for the whole structure can also be given in the form

$$U = -\frac{1}{2}\int M\,d\theta \tag{7.24}$$

7.3.3 Strain energy due to shear

Consider the segment dl of Figure 7.5c, subjected to a shearing force V. If the shearing stress induced is τ, the shearing strain ϵ in an element of area da is given by τ/G. Then the strain energy for the segment dl is (from Eq. 7.3)

$$\Delta U = \frac{1}{2}\int \frac{\tau^2}{G} dl\, da \tag{7.25}$$

The integration is carried out over the whole cross section.

For any cross section (Figure 7.5c), the shearing stress at any fiber at a distance $\bar{y}$ below the centroidal principal axis z is

$$\tau = \frac{VQ}{Ib} \tag{7.26}$$

where I is the second moment of area of cross section about the z axis, b is the width of the cross section at the fiber considered, and Q is the first moment about the z axis of the area of the part of the section below the fiber considered.

Substituting Eq. 7.26 into Eq. 7.25 and noting that $da = b\, d\bar{y}$, we obtain

$$\Delta U = \frac{1}{2}\frac{V^2}{Ga_r} dl \tag{7.27}$$

where

$$a_r = I^2 \left(\int \frac{Q_2}{b_2} da\right)^{-1} \tag{7.28}$$

From Eq. 7.27 we can write the strain energy due to shear for the whole structure as

$$U = \frac{1}{2}\int \frac{V^2}{Ga_r} dl \tag{7.29}$$

where the integration is carried out over the entire length of each member of the structure.

The term a_r in units (length)^2, is called the reduced cross-sectional area. It can be expressed as $a_r = a/\beta$, where a is the actual area and β is a coefficient greater than 1.0, depending upon the geometrical shape of the cross section.[4] Values of β are 1.2 and 10/9 for rectangular and circular cross sections respectively. For a rolled steel I section, $a_r \simeq$ area of the web. For a thin-walled hollow circular cross section, $a_r \simeq a/2$. For a thin-walled hollow rectangular section subjected to vertical shearing force, $a_r \simeq$ area of the two vertical sides of the section.

We may wish to verify the value of a_r for a rectangular section of width b and depth d (Figure 7.5c). The value of Q at any fiber is

$$Q = \frac{b}{2}\left(\frac{d^2}{4} - \bar{y}^2\right) \tag{7.30}$$

The shearing stress distribution is parabolic (Figure 7.5c). Substituting this equation in Eq. 7.28, with $I = bd^3/12$ and $da = b\, d\bar{y}$, and evaluating the integral between $\bar{y} = -d/2$ and $d/2$, gives $a_r = 5bd/6 = a/1.2$.

4 See Timoshenko, S. P. and Gere, J. M., *Mechanics of Materials*, Van Nostrand, New York, 1972, 372pp.

7.3.4 Strain energy due to torsion

Figure 7.5d shows a segment dl of a circular bar subjected to a twisting moment T. The shearing stress at any point distance r from the center is $\tau = (Tr/J)$, where J is the polar moment of inertia. The corresponding strain is $\epsilon = (\tau/G)$. From Eq. 7.3, the strain energy in the segment dl is

$$\Delta U = \frac{1}{2}\int \frac{T^2 r^2}{GJ^2}\,da\,dl = \frac{1}{2}\frac{T^2 dl}{GJ^2}\int r^2\,da$$

The integral $\int r^2\,da = J$ is the polar moment of inertia. Therefore, $\Delta U = (\frac{1}{2})(T^2\,dl/GJ)$. Thus, for the whole structure the strain energy due to torsion is

$$U = \frac{1}{2}\int \frac{T^2 dl}{GJ} \tag{7.31}$$

This equation can be used for members with cross sections other than circular, but in this case J is a torsion constant [in units (length)^4] which depends on the shape of the cross section.[5] Expressions for J for some structural sections are given in Appendix G.

7.3.5 Total strain energy

In a structure in which all the four types of internal forces discussed above are present, the values of energy obtained by Eqs. 7.18, 7.21, 7.29, and 7.31 are added to give the total strain energy

$$U = \frac{1}{2}\int \frac{N^2\,dl}{Ea} + \frac{1}{2}\int \frac{M^2\,dl}{EI} + \frac{1}{2}\int \frac{V^2\,dl}{Ga_r} + \frac{1}{2}\int \frac{T^2\,dl}{GJ} \tag{7.32}$$

The integration is carried out along the whole length of each member of the structure. We should note that each integral involves a product of an internal force N, M, V, or T acting on a segment dl and of the relative displacement of the cross section at the two ends of the segment. These displacements are $Ndl/(Ea)$, $Mdl/(EI)$, $Vdl/(Ga_r)$, and $Tdl/(GJ)$ (see Figure 7.5).

7.4 Complementary energy and complementary work

The concept of complementary energy is general and, like strain energy, can be applied to any type of structure. Here, complementary energy will be considered first with reference to a bar of a pin-jointed truss subjected to an axial force. Assume that the bar undergoes an extension e due to an axial tension N, and an extension e_t due to other environmental changes such as temperature, shrinkage, etc. Let $\Delta = e_t + e$. Assume further a relation between the tension N and the extension Δ as shown in Figure 7.6. Then, for a gradually applied force reaching a final value N_f and causing a final extension e_f, so that $\Delta_f = e_t + e_f$, the strain energy is $U = \int_0^{e_f} N\,de$, which is equal to the area shaded horizontally in Figure 7.6.

We can now define the complementary energy as

$$U^* = \int_0^{N_f} \Delta\,dN \tag{7.33}$$

5 For the theory of torsion of noncircular sections, see Timoshenko, S. P., *Strength of Materials*, Part II, 3rd ed., Van Nostrand, New York, 1956.

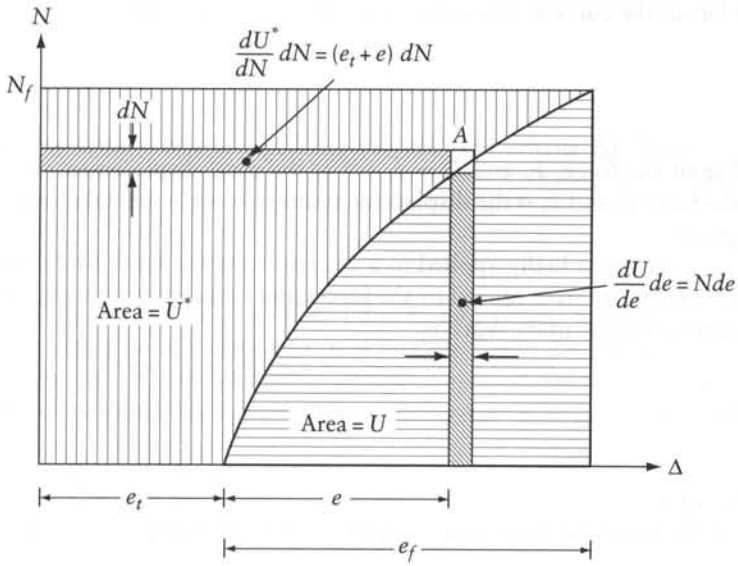

Figure 7.6 Force-extension relation.

or

$$U^* = N_f e_t + \int_0^{N_f} e\, dN \tag{7.34}$$

which is the area shaded vertically in Figure 7.6. The complementary energy has no physical meaning and the concept is used only because of its convenience in structural analysis.

From Figure 7.6 it is apparent that the sum of complementary energy and strain energy is equal to the area of the rectangle $N_f(e_t + e_f) = U + U^*$.

From the same figure, it can also be seen that if the extension is increased from e to $(e + de)$, U increases by an amount $N\, de$, so that

$$\frac{dU}{de} = N \tag{7.35}$$

The corresponding derivative of U^* with respect to N is equal to the extension Δ, that is,

$$\frac{dU^*}{dN} = e_t + e = \Delta \tag{7.36}$$

If a stress–strain $(\sigma - \epsilon)$ diagram similar to Figure 7.6 is drawn, the area to the left of the curve is the complementary energy density. The complementary energy can be expressed for any structure in terms of σ and ϵ:

$$U^* = \sum_{m=1}^{6} \int_{vol} \int_0^{\sigma_{fm}} \epsilon_m d\sigma_m\, dv \tag{7.37}$$

where m refers to the six types of stress and strain defined in Eqs. 7.9 and 7.10.

If a force-displacement *(F-D)* diagram (similar to the force-extension diagram of Figure 7.6) is drawn, the area to the left of the curve is defined as complementary work W^*. Thus,

$$W^* = \int_0^{F_f} D\, dF \tag{7.38}$$

where F_f is the final value of the force, F, and $D = d_t + d$ is the total displacement, d is the displacement caused by the force F, and d_t is the displacement due to environmental effects such as temperature, shrinkage, etc.

If a set of forces $F_1, F_2, \ldots, F_n$ is gradually applied to a structure and the total displacements at the location and direction of these forces caused by the forces and other environmental effects are $D_1, D_2, \ldots, D_n$ then the complementary work is

$$W^* = \sum_{i=1}^{n} \int_0^{F_{if}} D_i\, dF_i \tag{7.39}$$

where F_{if} is the final value of F_i.

If only one final value of the forces increases from F_j to $(F_j + \partial F_j)$, W^* increases by an amount $D_j\, \partial F_j$, so that

$$\frac{\partial W^*}{\partial F_j} = D_j \tag{7.40}$$

where D_j is the final value of the displacement at the location and in the direction of the jth force. Here, and in the presentation below, the subscript f indicating a final value will be omitted. All symbols, such as N, F and D will mean final value of force or displacement.

Similarly to Eq. 7.2, the complementary work and complementary energy are equal:

$$W^* = U^* \tag{7.41}$$

The forces $\{F\}$ and the displacements $\{D\}$ considered above may be referred to as real forces and real displacements. If, before application of the real forces, the structure has been subjected, at any coordinate j, to a virtual force Q_j, it would cause additional virtual complementary work of $Q_j D_j$, where D_j is real displacement at coordinate j due to the $\{F\}$ system. No integral is required for the virtual complementary work, because Q_j acts at its full value along the displacement D_j. The concept of virtual work will be further discussed in the following section.

Below, we will use Eq. 7.40 to give the displacement D_j at any coordinate for a linear or nonlinear truss composed of m members, assuming that the elongations $\{\Delta\}$ are known for all members. The cause of the elongations can be external applied forces combined with temperature variation, shrinkage, etc.

If a force ∂F_j is added to the system, W^* and U^* will increase such that (Eq. 7.41)

$$\frac{\partial W^*}{\partial F_j} = \frac{\partial U^*}{\partial F_j} \tag{7.42}$$

The complementary energy U^* for the truss is equal to the sum of the values of the complementary energy U^*_i for individual members (each given by Eq. 7.33). Thus, we can write:

$$\frac{\partial U^*}{\partial F_j} = \sum_{i=1}^{m} \frac{\partial U^*}{\partial N_i} \frac{\partial N_i}{\partial F_j} \tag{7.43}$$

Substitution of Eqs. 7.36 and 7.40 in 7.42 gives

$$D_j = \sum_{i=1}^{m} \frac{\partial N_i}{\partial F_j} \Delta_i \tag{7.44}$$

Define the symbol N_{uij} as equal to $(\partial N_i/\partial F_j)$ and rewrite Eq. 7.44:

$$D_j = \sum_{i=1}^{m} N_{uij}\, \Delta_i \tag{7.45}$$

N_{uij} is the force in any member i due to unit virtual force at coordinate j. Equation 7.45 is the *unit load theory* applied to a truss (see Eq. 7.47). The theory is presented in a general form in Section 7.6. When the truss is linearly elastic and the axial forces $\{N\}$ are caused only by external loads (without temperature or shrinkage etc.), $\Delta_i = (Nl/Ea)_i$ and Eq. 7.45 becomes:

$$D_j = \sum_{i=1}^{m} N_{uij} \left(\frac{Nl}{Ea}\right)_i \tag{7.45a}$$

where l, E and a are the length, the modulus of elasticity and the cross-sectional area of member respectively.

7.5 Principle of virtual work

This principle relates a system of forces in equilibrium to a compatible system of displacements in a linear or nonlinear structure. The name of the principle is derived from the fact that a fictitious (virtual) system of forces in equilibrium or of small virtual displacements is applied to the structure and related to the actual displacements or actual forces respectively. Any system of virtual forces or displacements can be used, but it is necessary that the condition of equilibrium of the virtual forces or of compatibility of the virtual displacements be satisfied. This means that the virtual displacements can be any geometrically possible infinitesimal displacements: they must be continuous within the structure boundary and must satisfy the boundary conditions. With an appropriate choice of virtual forces or displacements, the principle of virtual work can be used to compute displacements or forces.

Let us consider a structure deformed by the effect of external applied forces and of environmental causes such as temperature variation or shrinkage. Let the *actual* total strain at any point be ϵ, and the corresponding (actual) displacements at n chosen coordinates be $D_1, D_2 \ldots, D_n$. Suppose now that before these actual loads and deformations have been introduced, the structure was subjected to a system of *virtual* forces $F_1, F_2, \ldots, F_n$ at the coordinates $1, 2, \ldots, n$ causing a stress σ at any point. The system of virtual forces is in equilibrium but it need not correspond to the actual displacements $\{D\}$. The principle of virtual work states that the product of the actual displacements and the corresponding virtual forces (which is the virtual complementary work) is equal to the product of the actual internal displacements and the corresponding virtual internal forces (which is the virtual complementary energy). Thus,

Virtual complementary work = Virtual complementary energy

This can be expressed in a general form

$$\sum_{i=1}^{n} F_i D_i = \int_v \{\sigma\}^T \{\epsilon\}\, dv \tag{7.46}$$

where σ is a stress corresponding to virtual forces F, and ϵ is a real strain compatible with the real displacements $\{D\}$. The integration is carried out over the volume of the structure and the summation is for all the virtual forces $\{F\}$. Equation 7.46 states that the values of the complementary work of the virtual external forces and of the complementary energy of the virtual internal forces while *moving* along the real displacements are equal. In other words,

$$\sum_{i=1}^{n}\left(\begin{array}{c}\text{virtual force}\\ \text{at } i\end{array}\right)\left(\begin{array}{c}\text{actual displacement}\\ \text{at } i\end{array}\right)$$
$$=\int_v\left(\begin{array}{c}\text{virtual internal}\\ \text{forces}\end{array}\right)\left(\begin{array}{c}\text{actual internal}\\ \text{displacements}\end{array}\right)dv$$

The principle of virtual work in this form is used in Section 7.6 to calculate the displacement at any coordinate from the strains due to known actual internal forces. The principle can also be used to determine the external force at a coordinate from the internal forces. In the latter case, the structure is assumed to acquire virtual displacements $\{D\}$ compatible with virtual strain pattern ϵ at any point. The product of the actual external forces $\{F\}$ and the virtual displacements $\{D\}$ is equal to the product of the actual internal forces and the virtual internal displacements compatible with $\{D\}$. This relation can be written

Virtual work = Virtual strain energy

which is also expressed by Eq. 7.46:

$$\sum_{i=1}^{n}F_iD_i=\int_v\{\sigma\}^T\{\epsilon\}\,dv$$

but with σ being the actual stress corresponding to the actual forces $\{F\}$ and ϵ being the virtual strain compatible with the virtual displacements $\{D\}$. In this case, Eq. 7.46 states that the external and internal virtual work of the real forces while moving along the virtual displacements is the same. The same equation can be written in words as follows:

$$\sum_{i=1}^{n}\left(\begin{array}{c}\text{real force}\\ \text{at } i\end{array}\right)\left(\begin{array}{c}\text{virtual displacement}\\ \text{at } i\end{array}\right)$$
$$=\int_v\left(\begin{array}{c}\text{real internal}\\ \text{forces}\end{array}\right)\left(\begin{array}{c}\text{virtual internal}\\ \text{displacements}\end{array}\right)dv$$

When the principle of virtual work is used for the calculation of a displacement (or a force) the virtual loads (or the virtual displacements) are chosen in such a manner that the right-hand side of Eq. 7.46 directly gives the desired quantity. This is achieved by the so-called unit-load theorem or unit-displacement theorem for the calculation of displacement and force respectively.

Equation 5.9 is application of Eq. 7.46 for the real forces and the virtual displacements in Figures 5.4a and b respectively. In this application, the right-hand side of Eq. 7.46 is zero, because the virtual strain is zero; in Figure 5.4b the members rotate or/and translate as rigid bodies.

7.6 Unit-load and unit-displacement theorems

When the principle of virtual work is used to calculate the displacement D_j at a coordinate j, the system of virtual forces $\{F\}$ is chosen so as to consist only of a unit force at the coordinate j. Equation 7.46 becomes

$$1 \times D_j = \int_v \{\sigma_{uj}\}^T \{\epsilon\}\, dv$$

or

$$D_j = \int_v \{\sigma_{uj}\}^T \{\epsilon\}\, dv \tag{7.47}$$

where σ_{uj} is the virtual stress corresponding to a unit virtual force at j, and ϵ is the real strain due to the actual loading. This equation is known as the *unit-load theorem*, and is the general form (not limited by linearity) of Eq. 8.4 developed later for linear elastic framed structures.

We should observe that the principle of virtual work as used in the unit-load theorem achieves a transformation of an actual geometrical problem into a fictitious equilibrium problem. Advantages of this will be considered with reference to examples in Section 7.7.

The principle of virtual work can also be used to determine the force at a coordinate j if the distribution of the real stresses or of the internal forces is known. The structure is assumed to acquire a virtual displacement D_j at the coordinate j, but the displacement at the points of application of all the other forces remains unaltered. The corresponding compatible internal displacements are now determined. The external and internal virtual work of the real forces while moving along the virtual displacements is the same, that is, we can write from Eq. 7.46:

$$F_j \times D_j = \int_v \{\sigma\}^T \{\epsilon\}\, dv \tag{7.48}$$

Thus, $\{\sigma\}$ are the actual stress components due to the system of real loads, and $\{\epsilon\}$ are the virtual strain components compatible with the configuration of the virtual displacements.

In a linear elastic structure, the strain component ϵ at any point is proportional to the magnitude of displacement at j, so that

$$\epsilon = \epsilon_{uj} D_j \tag{7.49}$$

where ϵ_{uj} is the strain compatible with a unit displacement at j, there being no other displacement at the points of application of other forces. Equation 7.48 becomes

$$F_j = \int_v \{\sigma\}^T \{\epsilon_{uj}\}\, dv \tag{7.50}$$

This equation is known as the *unit-displacement theorem*.

The unit-displacement theorem is valid for linear elastic structures only, owing to the limitation of Eq. 7.49. No such limitation is imposed on the unit-load theorem because it is always possible to find a statically determinate virtual system of forces in equilibrium which results in linear relations between virtual external and internal forces, even though the material does not obey Hooke's law.

The unit-displacement theorem is the basis of calculation of the stiffness properties of structural elements used in the finite element method of analysis (see Chapter 17), where a continuous structure (e.g. a plate or a three-dimensional body) is idealized into elements with fictitious boundaries (e.g. triangles or tetrahedra). In one of the procedures used to obtain the stiffness of an element, a stress or displacement distribution within the element is assumed. The unit-displacement theorem is then used to determine the forces corresponding to a unit displacement at specified coordinates on the element.

Although the unit-displacement theorem is valid strictly only for linear elastic structures, it is used in nonlinear finite-element analysis, which usually involves a series of linear analyses, resulting in errors corrected by iterations.

7.7 Virtual-work transformations

From the preceding discussion it can be seen that the principle of virtual work can be used to transform an actual geometrical problem into a fictitious equilibrium problem or an actual equilibrium problem into a fictitious geometrical problem.

The first type of transformation can be considered by reference to the plane truss in Figure 7.7 composed of m pin-jointed members, subjected to external applied forces $\{P\}$ and to a change in temperature of T degrees in some of the members; we want to find the displacement at a coordinate j. By equations of statics, the force in any member N_i can be determined and the total extension can be calculated: $\Delta_i = \alpha T_i l_i + N_i l_i/(Ea_i)$, where α is coefficient of thermal expansion, and l_i and a_i are respectively the length and cross-sectional area of the member.

Once the elongation of all the members is determined, the displacements of the joints can be found from consideration of geometry alone, for instance graphically, but this procedure is laborious and, of course, not suitable for computer work. By the unit-load theorem it is possible to transform the actual geometrical problem into a fictitious equilibrium problem, which is easier to solve. The procedure is to apply a unit virtual load at j, causing virtual internal forces N_{uij} in any member i. The virtual work Eq. 7.47 can be applied in this case in the form

$$D_j = \sum_{i=1}^{m} N_{uij}\,\Delta_i \tag{7.51}$$

or in matrix form

$$D_j = \{N_u\}_j^T \{\Delta\} \tag{7.52}$$

where $\{N_u\}_j = \{N_{u1j}, N_{u2j}, \ldots, N_{umj}\}$ and $\{\Delta\} = \{\Delta_1, \Delta_2, \ldots, \Delta_m\}$. Equation 7.51 is the same as Eq. 7.45, for which the proof is included in Section 7.4.

As the second type of transformation, let us consider the bridge structure shown in Figure 7.8a, in which it is required to determine the variation in a reaction component A_j, e.g. the horizontal reaction at E when a moving vertical force P crosses the deck from F to G. We apply a unit virtual

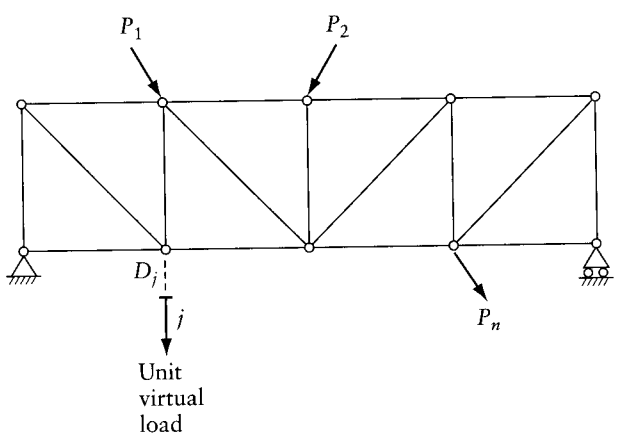

Figure 7.7 Application of the unit-load theorem to determine displacement at coordinate j of a plane truss.

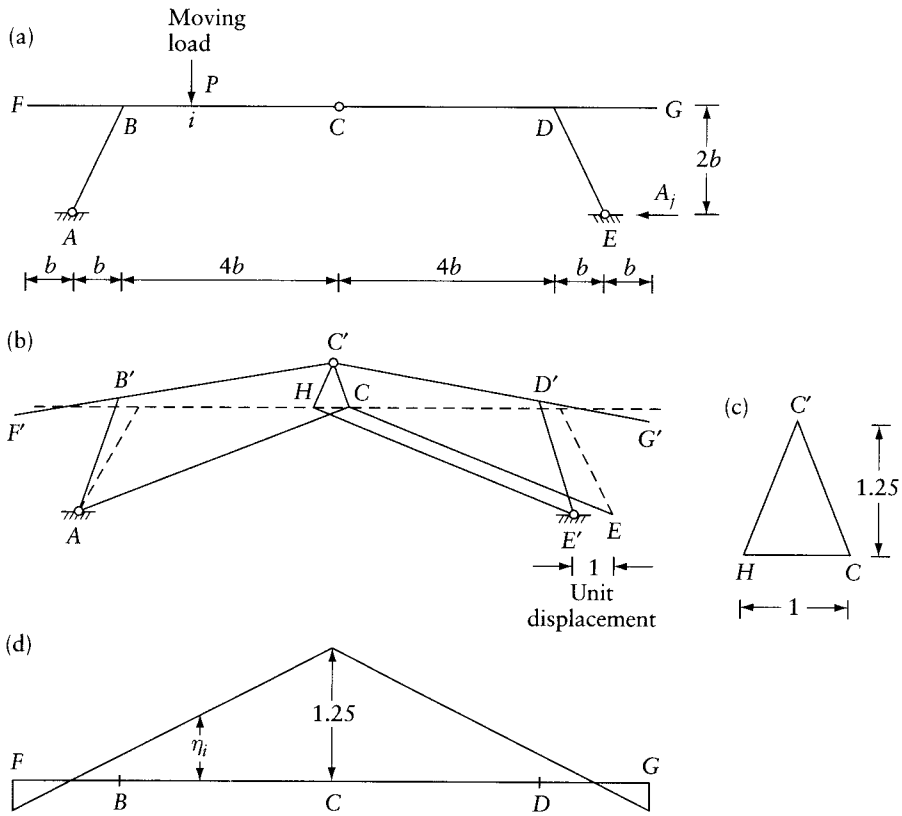

Figure 7.8 Application of the principle of virtual work. (a) Statically determinate frame. (b) Virtual displacements. (c) Displacement diagram for joint C. (d) Influence line for A_j.

displacement at the coordinate j and draw the corresponding shape of the frame, as shown in Figure 7.8b. (In constructing this figure we should note that the movement of C to C' takes place along the perpendicular to AC: a displacement diagram for joint C is shown in Figure 7.8c.) It is obvious that, in this statically determinate structure, the members of the frame will move to their new positions as rigid bodies without strain. The vertical displacement of FG is replotted to a larger scale in Figure 7.8d.

Consider now the unit vertical force P in any position i (Figure 7.8a) in equilibrium with the reaction components at A and E, including A_j. Applying the principle of virtual work (Eq. 7.46) to the real system of forces in Figure 7.8a and the virtual displacements in Figure 7.8b, we obtain

$$A_j \times 1 - P\eta_i = 0 \tag{7.53}$$

where η_i is the displacement at i.

This equation can be easily checked by noting that only A_j and P do work because the displacements along all the other reactions are zero. The right-hand side of the equation is zero because no strain is induced by the virtual displacement. Specifically, the right-hand side of Eq. 7.53 is $\int_v \{\sigma\}^T \{\epsilon_{uj}\}\, dv$, where $\{\epsilon_{uj}\}$ is the strain corresponding to a unit virtual displacement at j, and $\{\sigma\}$ is the stress in the actual structure due to real loading, that is, due to the load P acting at i.

This integral is zero even if the structure is statically indeterminate, e.g. if the hinges at A and C are replaced by rigid joints.

The condition that the displacement D_j of the actual structure is zero can be written with the aid of the unit-load theorem (Eq. 7.47):

$$D_j = \int_v \{\sigma_{uj}\}^T \{\epsilon\}\, dv = 0$$

where $\{\sigma_{uj}\}$ is the stress due to a unit force at j and $\{\epsilon\}$ is the strain in the actual structure due to the load P. But in a linear elastic structure, the stress and strain components σ_{uj} and ϵ_{uj} are proportional to one another at all points of the structure. Therefore, the integral $\int_v \{\sigma\}^T \{\epsilon_{uj}\}\, dv$ vanishes also in the case of a statically indeterminate structure.

From Eq. 7.53, $A_j = P\eta_i$, it follows that the coordinate η_i at any point i is equal to the value of the reaction component A_j due to a unit vertical load at i. The plot of η_i is called the *influence line* of the reaction component A_j. The frame dimensions and the values of A_j are given in Figure 7.8 so that the result can be checked by considerations of statics.

Further applications of the principle of virtual work in transformation of an actual equilibrium problem to a fictitious geometrical problem will be made in the derivation of influence lines (Chapter 12) and in the analysis of the collapse mechanism of frames and slabs (Chapters 18 and 19).

Example 7.1: Transformation of a geometry problem

Find the downward displacement at D (at coordinate 1) for the truss shown in Figure 7.9a due to a drop of temperature T degrees in members AB and BC only. Assume $\alpha T = 0.003$, where α is coefficient of thermal expansion. Use the unit-load theorem, then check the answer by geometry.

In a statically determinate truss, a change in temperature produces elongation or shortening of members, but induces no forces. Thus, only members AB and BC change length by the amounts

$$\Delta_{AB} = \Delta_{BC} = -\alpha T(\sqrt{2}\, l)$$

A unit force introduced at coordinate 1 produces the axial forces $\{N_{u1}\}$ given in Figure 7.9b; *in* AB and BC, the axial forces are:

$$N_{uAB1} = N_{uBC1} = -1/\sqrt{2}$$

The deflection at coordinate 1 (Eq. 7.51)

$$D_1 = \sum N_{ui1}\, \Delta_i$$

$$D_1 = 2\left(-\frac{1}{\sqrt{2}}\right)(-\alpha T \sqrt{2}\, l) = 2\alpha T l = 0.0060\, l$$

The deflected shape of the truss is shown in Figure 7.9c. The length of members AD or $BD = l$ (unchanged), while the length of AB is changed to $(0.997\ \sqrt{2}\, l)$. The angle $ADB = 2\sin^{-1}[AB/(2\ AD)] = [(\pi/2) - 0.0060]$. Thus, AD or DC makes an angle 0.0060 with the horizontal and the deflection D_1 is equal to the vertical distance between D and line $AC = l \sin 0.0060 = 0.0060l$.

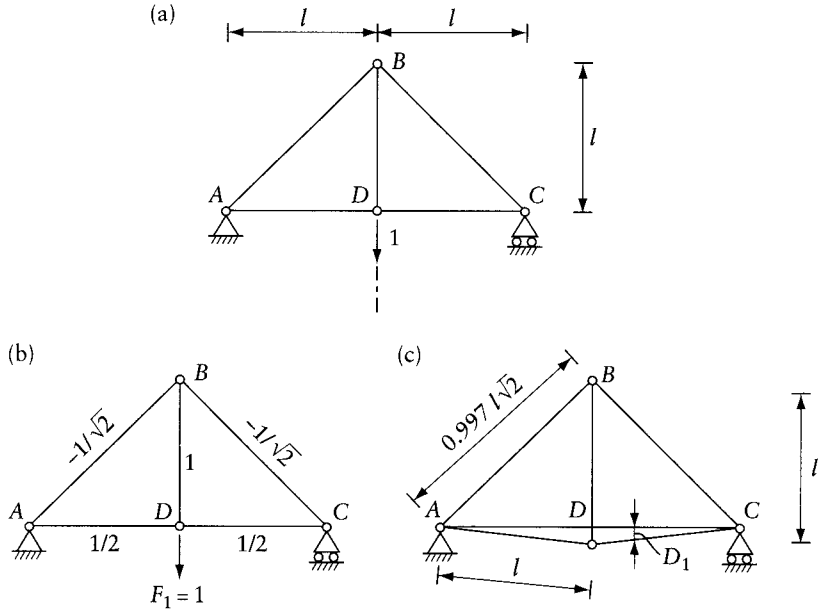

Figure 7.9 Deflection of a plane truss due to drop of temperature of members AB and BC, Example 7.1 (a) Truss dimensions. (b) Axial forces $\{N_{u1}\}$ due to $F_1 = 1$. (c) Deflected shape of the truss.

7.8 Castigliano's theorems

Castigliano published in 1879 a book on the analyses of statically indeterminate structures, including two well-known theorems, presented briefly in Sections 7.8.1 and 7.8.2. The theorems are not used beyond these two sections because what they can achieve can be done more conveniently by the unit-load or the unit-displacement theorem or by the force or the displacement method as presented in other sections of this book. Both Castigliano's theorems are for linear elastic structures and deformations caused by external forces only.

7.8.1 *Castigliano's first theorem*

Castigliano's first theorem states that if, in any structure with independent displacements $\{D_1, D_2, \ldots, D_n\}$ corresponding to external applied forces $\{F_1, F_2, \ldots, F_n\}$ along their lines of action, the strain energy U is expressed in terms of the displacements D, then n equilibrium equations can be written in the form

$$\frac{\partial U}{\partial D_j} = F_j \tag{7.54}$$

The theorem is proved by virtual work, as follows. Let the structure acquire a virtual displacement δD_j at j, while all the other displacements remain zero and environmental conditions are unchanged. The only force which does work is F_j, so that the work done during this virtual displacement is

$$\delta W = F_j \, \delta D_j$$

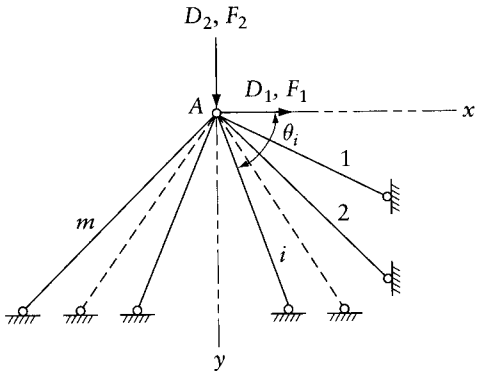

Figure 7.10 Plane truss considered in the derivation of Castigliano's first theorem.

This is equal to the gain in the strain energy of the structure

$$\delta U = F_j \, \delta D_j \tag{7.55}$$

In the limit, when $\delta D_j \to 0$, Eq. 7.55 gives Eq. 7.54.

Castigliano's theorem, Part I is applicable to both linear and nonlinear *elastic* structures. Referring to the truss of Figure 7.10 which has m members and two unknown displacements D_1 and D_2 at joint A, we can express the extension of any member i in terms of D_1 and D_2 as

$$\Delta_i = -(D_1 \cos\theta_i + D_2 \sin\theta_i) \tag{7.56}$$

where θ_i is the angle of the ith member with the horizontal. Assuming that the material obeys Hooke's law, the force in the member is

$$N_i = \frac{a_i E_i}{l_i} \Delta_i \tag{7.57}$$

where a_i is the cross-sectional area of the member and l_i its length. The strain energy of the structure is

$$U = \frac{1}{2} \sum_{i=1}^{m} N_i \, \Delta_i = \frac{1}{2} \sum_{i=1}^{m} \frac{a_i E_i}{l_i} \Delta_i^2 \tag{7.58}$$

Substituting Eqs. 7.56 and 7.57 into Eq. 7.58,

$$U = \frac{1}{2} \sum_{i=1}^{m} \frac{a_i E_i}{l_i} (D_1 \cos\theta_i + D_2 \sin\theta_i)^2$$

whence

$$\frac{\partial U}{\partial D_1} = \sum_{i=1}^{m} \frac{a_i E_i}{l_i} \cos\theta_i (D_1 \cos\theta_i + D_2 \sin\theta_i) \tag{7.59}$$

Applying Eq. 7.54, we obtain:

$$F_1 = \left(\sum_{i=1}^{m} \frac{a_i E_i}{l_i} \cos^2 \theta_i\right) D_1 + \left(\sum_{i=1}^{m} \frac{a_i E_i}{l_i} \cos\theta_i \sin\theta_i\right) D_2 \tag{7.60}$$

and

$$F_2 = \left(\sum_{i=1}^{m} \frac{a_i E_i}{l_i} \cos\theta_i \sin\theta_i\right) D_1 + \left(\sum_{i=1}^{m} \frac{a_i E_i}{l_i} \sin^2 \theta_i\right) D_2 \tag{7.61}$$

The last two equations express the fact that the sum of the horizontal components of the bar forces at joint A is equal to the external force F_1; the same applies to the vertical components and to F_2. In Section 5.2, the same problem was treated by the displacement method of analysis, and it can be easily seen that Eqs. 7.60 and 7.61 are identical with the statical relations used in that method to find the unknown displacements. We should also recognize that the terms in brackets in Eqs. 7.60 and 7.61 are the stiffness coefficients of the structure.

The stiffness coefficients S_{jr} can, in general, be obtained by taking the partial derivative with respect to any displacement in Eq. 7.54. Thus,

$$\frac{\partial^2 U}{\partial D_r \partial D_j} = \frac{\partial F_j}{\partial D_r} \tag{7.62}$$

In a linear structure, $\partial F_j / \partial D_r$ is the force at j due to a unit displacement at r. Therefore,

$$S_{jr} = \frac{\partial^2 U}{\partial D_j \partial D_r} \tag{7.63}$$

For example, the stiffness coefficient S_{11} for the structure of Figure 7.10 can be obtained by taking the partial derivative of Eq. 7.59

$$S_{11} = \frac{\partial^2 U}{\partial D_1^2} = \sum_{i=1}^{m} \frac{a_i E_i}{l_i} \cos^2 \theta_i \tag{7.64}$$

which is the same as the value obtained in Section 5.2.

7.8.2 *Castigliano's second theorem*

When the deformations of a linear elastic structure are caused by external forces only, without temperature or shrinkage etc., the complementary energy U^* is equal to the strain energy U (Figure 7.6) and the following equations apply:

$$\frac{\partial U^*}{\partial F_j} = \frac{\partial U}{\partial F_j} \tag{7.65}$$

$$D_j = \frac{\partial U}{\partial F_j} \tag{7.66}$$

$$D_j = \sum_{i=1}^{m} N_{uij}\, \Delta_i \tag{7.67}$$

$$D_j = \sum_{i=1}^{m} N_{uij} \left(\frac{Nl}{Ea}\right)_i \tag{7.68}$$

Equation 7.66, obtained by substitution of Eqs. 7.65 and 7.42 in 7.40, gives the displacement at coordinate j subjected to forces $F_1, F_2, \ldots, F_n$. For this purpose, U has to be expressed in terms of the forces $\{F\}$. Equation 7.66 is known as Castigliano's second theorem; its use is equivalent to the unit-load theory. Equations 7.67 and 7.68 are applications of Eq. 7.66 to a truss; here, N, l, E and a are the axial force, the length, the modulus of elasticity and the cross-sectional area of a typical ith member; m is the number of members; $\Delta_i = (Nl/Ea)_i$ is the elongation of the member; N_{uij} is the force in the member due to $F_j = 1$; that is,

$$N_{uij} = \frac{\partial N_i}{\partial F_j} \tag{7.69}$$

Equation 7.68 can be derived from Eq. 7.66, with U expressed as the sum of the strain energy of individual members (Eq. 7.19):

$$U = \frac{1}{2} \sum_{i=1}^{m} \left(\frac{N^2\, l}{a\, E}\right)_i \tag{7.70}$$

Figure 7.11 shows a structure subjected to external applied loads, together with statically indeterminate redundants $F_1, F_2, \ldots, F_n$; the effects of temperature, shrinkage, etc. are not considered. The redundant forces $\{F\}$ are of the magnitudes that result in $D_j = 0$ for $j = 1, 2 \ldots, n$. Expressing D_j by Eq. 7.66 gives *Castigliano's equations of compatibility:*

$$\frac{\partial U}{\partial F_j} = 0 \text{ for } j = 1, 2, \ldots\ldots, n \tag{7.71}$$

where U is the strain energy due to the external applied load and the redundants.

Equation 7.71 indicates that the strain energy has a stationary value and this value, as will be proved below, is a minimum. This is referred to as *the principle of least work*, which may

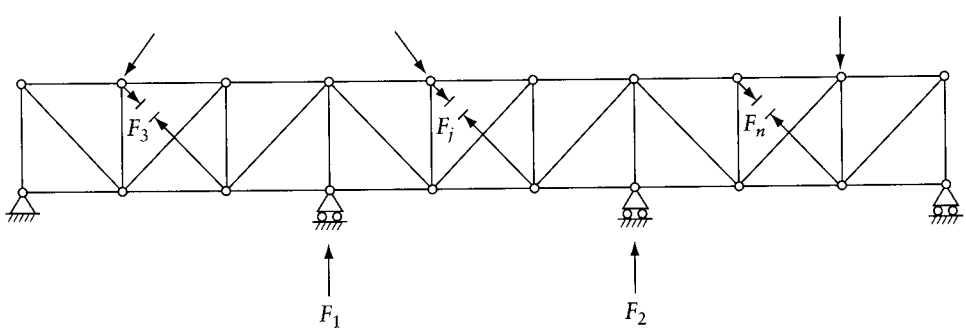

Figure 7.11 Statically indeterminate truss used in derivation of Castigliano's compatibility equations and principle of least work.

be stated as follows: in a linear statically indeterminate structure, the redundants, caused by externally applied forces, are of such a magnitude that the internal strain energy is minimum.

To show that the value of U is a minimum, we differentiate Eq. 7.70 with respect to a redundant F_j and another time with respect to redundant F_r.

$$\frac{\partial U}{\partial F_i} = \sum_{i=1}^{m} \frac{\partial N_i}{\partial F_j} \left(\frac{Nl}{aE}\right)_i \tag{7.72}$$

Substitution of Eq. 7.69 in 7.72 gives:

$$\frac{\partial U}{\partial F_i} = \sum_{i=1}^{m} N_{uij} \left(\frac{Nl}{aE}\right)_i \tag{7.73}$$

$$\frac{\partial^2 U}{\partial F_j \, \partial F_r} = \sum_{i=1}^{m} N_{uij} N_{uir} \left(\frac{l}{aE}\right)_i \tag{7.74}$$

The term on the right-hand side of this equation is the flexibility coefficient

$$f_{jr} = \sum_{i=1}^{m} N_{uij} N_{uir} \left(\frac{l}{Ea}\right)_i \tag{7.75}$$

By setting $r = j$, Eq. 7.75 gives element f_{jj} on the diagonal of the flexibility matrix, which is a positive value. Thus,

$$\frac{\partial^2 U}{\partial F_j^2} = \sum_{i=1}^{m} N_{uij}^2 \left(\frac{l}{Ea}\right)_i = f_{jj} \tag{7.76}$$

This proves that U has a minimum value because the second derivative is positive.

7.9 General

The concept of strain energy is important in structural analysis, and it is useful to express the strain energy due to any type of stress in a general form amenable to matrix treatment. It is possible then to consider at the same time components of strain energy due to axial force, bending moment, shear, and torsion.

Complementary energy has no physical meaning, but it is of value in helping to understand some of the energy equations. The same applies to the analogous concept of complementary work.

The principle of virtual work relates a system of forces in equilibrium to a compatible system of displacements in any structure, linear or nonlinear. In analysis, we apply virtual forces or virtual displacements and use the equality of the complementary work of virtual external forces and the complementary energy of the virtual internal forces moving along the real displacements. Alternatively, we utilize the equality of external and internal virtual work of the real forces moving along the virtual displacements. Unit-load and unit-displacement theorems offer a convenient formulation. It should be noted that the latter theorem is applicable only to linear structures.

We should note that the principle of virtual work makes it possible to transform an actual geometrical problem into a fictitious equilibrium problem or an actual equilibrium problem into a fictitious geometrical problem, and there exist circumstances when either transformation is desirable. Chapter 8 discusses further the applications of virtual work for calculation of displacements. The problems at the end of Chapter 8 are related to the material presented in both Chapters 7 and 8.

Chapter 8

Determination of displacements by virtual work

8.1 Introduction

In Chapter 7, we adopted the principle of virtual work and used it (in Section 7.6) to derive the unit-load theorem, which is applicable to linear or nonlinear structures of any shape. In this chapter and in the succeeding one, we shall consider the method of virtual work further, first with reference to trusses and later to beams and frames. The present chapter will also deal with evaluation of integrals for calculation of displacements by the method of virtual work.

To begin with, we shall use the unit-load theorem to calculate displacements due to external applied loading on linear framed structures and we shall also present the theory for this particular application.

8.2 Calculation of displacement by virtual work

Consider the linear elastic structure shown in Figure 8.1 subjected to a system of forces F_1, $F_2, \ldots, F_n$, causing the stress resultants N, M, V, and T at any section. The magnitude of external and internal work is the same, so that from Eq. 7.2 and 7.32,

$$\frac{1}{2}\sum_{i=1}^{n} F_i D_i = \frac{1}{2}\int \frac{N^2\,dl}{Ea} + \frac{1}{2}\int \frac{M^2\,dl}{EI} + \frac{1}{2}\int \frac{V^2\,dl}{Ga_r} + \frac{1}{2}\int \frac{T^2\,dl}{GJ} \tag{8.1}$$

where D_i is the displacement at the location and in the direction of F_i, and N, M, V, and T are the stress resultants at any section due to the $\{F\}$ system.

Suppose that at the time when the forces $\{F\}$ are applied to the structure, there is already a virtual force Q_j acting at the location and in the direction of a coordinate j (Figure 8.1). This

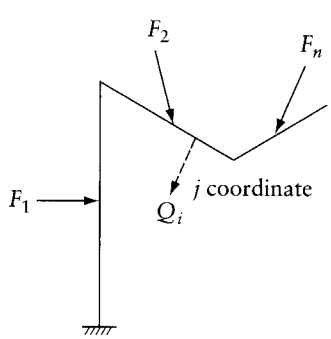

Figure 8.1 Linear elastic structure used to illustrate the calculation of displacement by virtual work.

force induces at any section internal forces N_{Qj}, M_{Qj}, V_{Qj}, and T_{Qj}. The magnitude of internal and external work during the application of the {F} system of loads is again the same, so that

$$\frac{1}{2}\sum_{i=1}^{n} F_i D_i + Q_j D_j = \frac{1}{2}\left[\int \frac{N^2}{Ea}\,dl + \int \frac{M^2}{EI}\,dl + \int \frac{V^2}{Ga_r}\,dl + \int \frac{T^2}{GJ}\,dl\right] + \left[\int \frac{N_{Qj}N}{Ea}\,dl + \int \frac{M_{Qj}M}{EI}\,dl + \int \frac{V_{Qj}V}{Ga_r}\,dl + \int \frac{T_{Qj}T}{GJ}\,dl\right] \tag{8.2}$$

where D_j is the displacement at j due to the {F} system in the direction of the virtual force Q_j. The second term on each side of Eq. 8.2 represents the work due to the force Q_j while moving along the displacement by the {F} system. As explained in Section 7.4, the coefficient 1/2 does not appear in these terms because the load Q_j and the corresponding internal forces act at their full value along the entire displacement by the {F} system.

Subtracting Eq. 8.1 from Eq. 8.2, we find

$$Q_j D_j = \int \frac{N_{Qj}N}{aE}\,dl + \int \frac{M_{Qj}M}{EI}\,dl + \int \frac{V_{Qj}V}{Ga_r}\,dl + \int \frac{T_{Qj}T}{GJ}\,dl \tag{8.3}$$

To determine the deflection at any location and in any direction due to the {F} system, we divide Eq. 8.3 by Q_j. Hence, the displacement at j is

$$D_j = \int \frac{N_{uj}N}{Ea}\,dl + \int \frac{M_{uj}M}{EI}\,dl + \int \frac{V_{uj}V}{Ga_r}\,dl + \int \frac{T_{uj}T}{GJ}\,dl \tag{8.4}$$

where

$$N_{uj} = \frac{N_{Qj}}{Q_j};\ M_{uj} = \frac{M_{Qj}}{Q_j};\ V_{uj} = \frac{V_{Qj}}{Q_j};\ \text{and } T_{uj} = \frac{T_{Qj}}{Q_j}$$

These are the values of the internal forces at any section due to a unit virtual force ($Q_j = 1$) applied at the coordinate j where the displacement is required.

Referring back to Eq. 7.47, we can see that Eq. 8.4 is, in fact, a particular case of the unit-load theorem applicable to linear framed structures, subjected to external loads only (that is, with no environmental effects). The only internal force in a truss member is an axial force, which is constant at all its sections. Thus, Eq. 8.4 becomes the same as Eq. 7.45a, by replacing the first integral by a summation and dropping the remaining integrals. Hence, the displacement at coordinate j in a truss (Eq. 7.45a repeated)

$$D_j = \Sigma\, N_{uj}\frac{Nl}{Ea}$$

where the summation is for all members of the truss; l, E and a are length, modulus of elasticity and cross-sectional area of a typical member.

In order to use Eq. 8.4 for the determination of the displacement at any section, the internal forces at all sections of the structure must be determined due to: (i) the actual loads, and (ii) a unit virtual force. The latter is a fictitious force or a *dummy load* introduced solely for the purpose of the analysis. Specifically, if the required displacement is a translation, the fictitious load is a concentrated unit force acting at the point and in the direction of the required deflection. If the required displacement is a rotation, the unit force is a couple acting in the same direction and at the same location as the rotation. If the relative translation of two points is to be found,

two unit loads are applied in opposite directions at the given points along the line joining them. Similarly, if a relative rotation is required, two unit couples are applied in opposite directions at the two points.

The internal forces N_{uj}, M_{uj}, V_{uj}, and T_{uj} are forces per unit virtual force. If the displacement to be calculated is a translation, and the Newton, meter system is used, then N_{uj}, M_{uj}, V_{uj}, and T_{uj} have respectively, the dimensions: N/N, N m/N, N/N and N m/N. When the virtual force is a couple, N_{uj}, M_{uj}, V_{uj}, and T_{uj} have, respectively, the dimensions: N/N m, N m/N m, N/N m, N m/N m. A check on the units in Eq. 8.4, when used to determine translation or rotation, should easily verify the above statements.

Each of the four terms on the right-hand side of Eq. 8.4 represents the contribution of one type of internal forces to the displacement D_j. In the majority of practical cases, not all the four types of the internal forces are present, so that some of the j terms in Eq. 8.4 may not be required. Furthermore, some of the terms may contribute very little compared to the others and may therefore be neglected. For example, in frames in which members are subjected to lateral loads, the effect of axial forces and shear is very small compared to bending. This is, however, not the case in members with a high depth-to-length ratio or with a certain shape of cross sections, when the displacement due to shear represents a significant percentage of the total. This will be illustrated in Example 8.4.

The internal forces at a section of a space frame are generally composed of six components: N, V_{y^*}, V_{z^*}, M_{y^*}, M_{z^*}, and T, shown in Figure 8.2 in the directions of local orthogonal axes x^*, y^*, and z^* of a typical member. The x^* axis is normal to the cross section through the centroid; y^* and z^* are centroidal principal axes in the plane of the section.

When Eq. 8.4 is applied to a space frame, the second term, representing the contribution of bending deformation, is to be replaced by two terms:

$$\int (M_{uj}\, M/EI)_{y^*} \quad \text{and} \quad \int (M_{uj}\, M/EI)_{z^*}$$

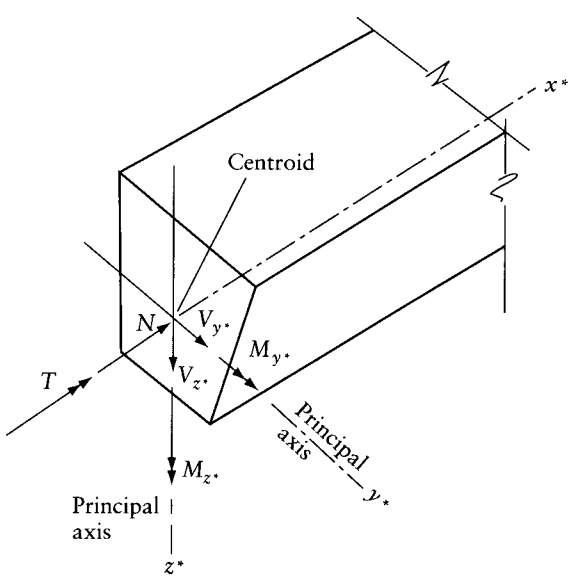

Figure 8.2 Internal forces in a section in a member of a space frame: a normal force N, two shearing forces V_{y^*} and V_{v^*}, two bending moments M_{y^*} and M_{z^*}, and a twisting moment T.

The subscripts y^* or z^* indicate that the M and I values inside the brackets are about the principal axis y^* or z^* respectively. Similarly, the third term in Eq. 8.4, representing the contribution of shear deformation, is to be replaced by two terms:

$$\int (V_{uj}\ V/Ga_r)_{y^*} \text{ and } \int (V_{uj}\ V/Ga_r)_{z^*}$$

In Eq. 8.4, the terms $(N/Ea) = \epsilon_o$ and $(M/EI) = \psi$, represent respectively the centroidal normal strain and the curvature due to N and M on a cross section (Figure 7.5). When D_j is required for the combined effects of N and M together with thermal expansion, the terms (N/Ea) and (M/EI) are to be replaced, respectively, by $[(N/Ea) + \epsilon_{OT}]$ and $[(M/EI) + \psi_T]$, where ϵ_{OT} and ψ_T are the centroidal strain and curvature due to thermal expansion (Eqs. 6.37 and 6.38). When the structure is statically indeterminate, N and M must include the statically indeterminate axial force and moment due to temperature (Section 6.9).

8.3 Displacements required in the force method

The five steps in the analysis of statically indeterminate structures by the force method (Section 4.6) include calculation of displacements of the released structure due to the specified loads (step 2) and displacements of the released structure due to unit values of the redundant forces (flexibility coefficients, step 3). Virtual work can be used to determine these displacements.

Consider the linear analysis of a statically indeterminate framed structure by the force method (Section 4.6). When the number of the statically indeterminate forces is n, the displacements $\{D\}_{n\times 1}$ can be determined by Eq. 8.4, with $j = 1, 2, \ldots, n$; N_{uj}, M_{uj}, V_{uj}, and T_{uj} are internal forces in the released structure due to a force $F_j = 1$; N, M, V, and T are internal forces in the released structure subjected to the specified loads. When thermal effects are included, the terms (N/Ea) and (M/EI) in Eq. 8.4 are to be replaced by $[(N/Ea) + \epsilon_{OT}]$ and $[(M/EI) + \psi_T]$ where ϵ_{OT} and ψ_T are thermal centroidal strain and curvature at a section of the released structure (Eqs. 6.37 and 6.38).

Any coefficient, f_{ij}, required to generate the flexibility matrix $[f]_{n\times n}$, can be determined by application of Eq. 8.4. In this application, f_{ij} is the displacement at coordinate i due to a real load $F_j = 1$ on the released structure; the corresponding internal forces at any section are N_{uj}, M_{uj}, V_{uj}, and T_{uj}. Apply a unit virtual load, $F_i = 1$ at coordinate i on the released structure, producing at any section the internal forces N_{ui}, M_{ui}, V_{ui}, and T_{ui}. Application of Eq. 8.4 gives the flexibility coefficient

$$f_{ij} = \int \frac{N_{ui}\ N_{uj}}{Ea}\, dl + \int \frac{M_{ui}\ M_{uj}}{EI}\, dl + \int \frac{V_{ui}\ V_{uj}}{Ga_r}\, dl + \int \frac{T_{ui}\ T_{uj}}{GJ}\, dl \tag{8.5}$$

For a plane or a space truss, the flexibility coefficient

$$f_{ij} = \Sigma N_{ui}\, N_{uj} \frac{l}{Ea} \tag{8.6}$$

where the summation is for all members of the truss; l, E and a are, respectively, the length, the modulus of elasticity and the cross-sectional area of a typical member.

8.4 Displacement of statically indeterminate structures

As shown in Chapter 7, the principle of virtual work is applicable to any structure, whether determinate or indeterminate. However, in the latter case, the internal forces induced by the real loading in all parts of the structure must be known. This requires the solution of the statically indeterminate structure by any of the methods discussed in Chapters 4 and 5.

Furthermore, we require the internal forces N_{uj}, M_{uj}, V_{uj}, and T_{uj} due to a unit virtual load applied at j. These forces can be determined for any released structure satisfying the requirement of equilibrium with the unit virtual load at j. Thus, it is generally sufficient to determine the internal forces due to a unit virtual load at j acting on a released stable statically determinate structure obtained by the removal of arbitrarily chosen redundants. This is so because the principle of virtual work relates a compatible system of deformations of the actual structure to a virtual system of forces in equilibrium which need not correspond to the actual system of forces (see Section 7.5).

As an example, we can apply the above procedure to the frame of Figure 8.3a in order to find the horizontal displacement at C, D_4. Bending deformations only need be considered. The frame has a constant flexural rigidity EI.

The bending moment diagram was obtained in Example 5.2 and is shown again in Figure 8.3b.

A unit virtual load is now applied at coordinate 4 to a statically determinate system obtained by cutting the frame just to the left of C (thus forming two cantilevers), Figure 8.3c. The bending moment diagram for M_{u4} is shown in Figure 8.3d.

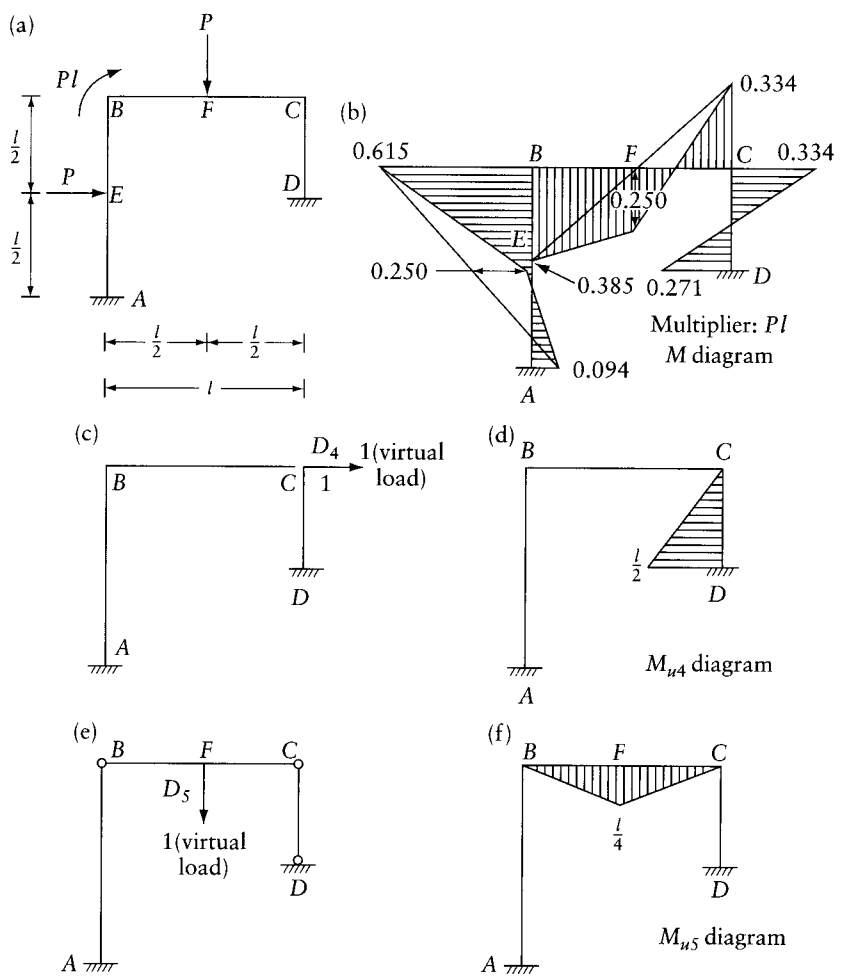

Figure 8.3 Displacement of a statically indeterminate plane frame by virtual work.

Applying Eq. 8.4 and considering bending only,

$$D_4 = \int \frac{M_{u4} M}{EI}\, dl \qquad (a)$$

This integral needs to be evaluated for the part CD only because M_{u4} is zero in the remainder of the frame. Using Appendix H, we find

$$D_4 = \frac{1}{EI}\left[\frac{l}{2}\frac{(l/2)}{6}(2 \times 0.271Pl - 0.334Pl)\right] = 0.0087\frac{Pl^3}{EI}$$

Suppose now that we want to find the vertical deflection at F, denoted by D_5. We assume that the virtual unit load acts on the three-hinged frame of Figure 8.3e. The corresponding bending moment diagram M_{u5} is shown in Figure 8.3f. By the same argument as used for D_4, we obtain

$$D_5 = \int \frac{M_{u5} M}{EI}\, dl \qquad (b)$$

The integral has to be evaluated for the part BC only because M_{u5} is zero elsewhere. Using the table in Appendix H, we find

$$D_5 = 0.0240\frac{Pl^3}{EI}$$

It may be instructive to calculate D_4 and D_5 using some other choice of the virtual system of forces.

Application of the unit load on a released structure, instead of the actual structure, does not change the results, but greatly simplifies the calculations. To prove this, assume that $F_5 = 1$ is applied on the actual structure to obtain $(M_{u5})_{alternative}$ to replace $(M_{u5})_s$ when Eq. (b) is used to calculate D_5 where $(M_{u5})_s$ is the statically determinate bending moment depicted in Figure 8.3f and used in the above calculation. We will show that

$$D_5 = \int (M_{u5})_s \frac{M}{EI}\, dl \qquad (c)$$

or

$$D_5 = \int (M_{u5})_{alternative} \frac{M}{EI}\, dl \qquad (d)$$

Any ordinate of the diagram of $(M_{u5})_{alternative}$ (not shown) may be expressed as:

$$(M_{u5})_{alternative} = (M_{u5})_s + F_6 M_{u6} + F_7 M_{u7} + F_8 M_{u8} \qquad (e)$$

where F_6, F_7 and F_8 are, respectively, the ordinates of $(M_{u5})_{alternative}$ at B, C and D; M_{u6}, M_{u7} or M_{u8} is the value of the bending moment at any section due to a pair of opposite unit couples applied on the released structure (Figure 8.3e) at B, C or D respectively. Substitution of Eq. (e) in Eq. (d) gives:

$$D_5 = \int (M_{u5})_s \frac{M}{EI}\, dl + F_6 \int M_{u6} \frac{M}{EI}\, dl + F_7 \int M_{u7} \frac{M}{EI}\, dl + F_8 \int M_{u8} \frac{M}{EI}\, dl \qquad (f)$$

Any of the last three integrals in this equation is zero because it represents the relative rotation of the two sections adjacent to B, C or D in the actual structure (subjected to M in Figure 8.3b). Since the actual structure is continuous at these locations, the relative rotations are zero. Thus, calculations of D_5 by Eq. (*c*) or Eq. (*d*) must give the same result.

8.5 Evaluation of integrals for calculation of displacement by method of virtual work

In the preceding section we have seen that integrals of the type

$$\int \frac{M_{uj}M}{EI}\,dl$$

often occur in the equations of virtual work. We shall consider here how this particular integral can be evaluated but other integrals of this type can, of course, be treated in a similar manner.

If a structure consists of m members, the integral can be replaced by a summation

$$\int \frac{M_{uj}M}{EI}\,dl = \sum_{\text{members}} \int_l M_{uj}\frac{M}{EI}\,dl \tag{8.7}$$

so that the problem really lies in the evaluation of the integral for one member.

Let us consider, therefore, a straight member AB of length l and of variable cross section, subjected to bending (Figure 8.4a). Figure 8.4b shows the bending moment diagram due to an arbitrary loading. If we divide each ordinate of this diagram by the value of EI at the given section, we obtain the $M/(EI)$ diagram shown in Figure 8.4c.

Since the member AB is straight, the plot of the bending moment, M_{uj} between A and B due to a unit virtual force applied at any coordinate j (not located between A and B) must be a straight line (Figure 8.4d). Let the ordinates of this diagram at A and B be M_{uAj} and M_{uBj} respectively. The ordinate at any section distance x from A is then

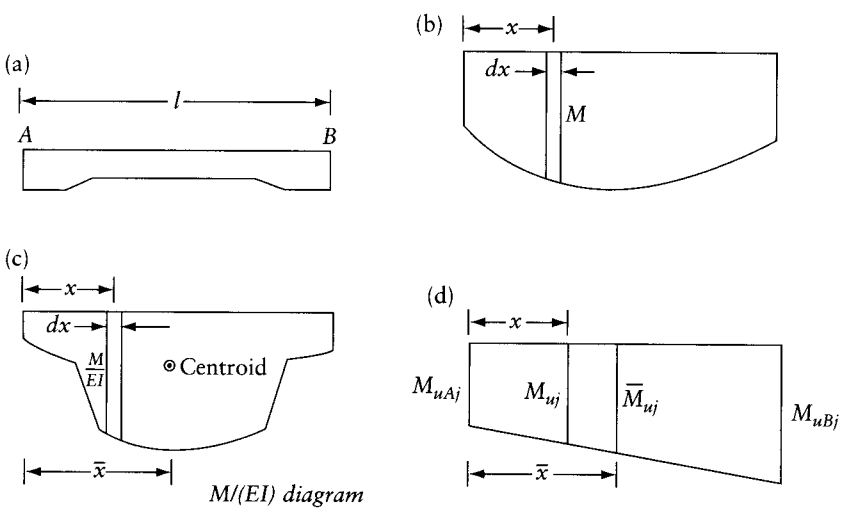

Figure 8.4 Evaluation of integral $\int_l M_{uj}(M/EI)dl$. (a) Member AB. (b) Bending moment diagram due to any real loading. (c) $M/(EI)$ diagram. (d) Bending moment diagram due to a unit virtual load.

$$M_{uj} = M_{uAj} + (M_{uBj} - M_{uAj})\frac{x}{l} \tag{8.8}$$

Substituting this value of M_{uj} in the integral, we obtain

$$\int_l M_{uj}\frac{M}{EI}\,dl = M_{uAj}\int_0^l \frac{M}{EI}\,dx + \left(\frac{M_{uBj} - M_{uAj}}{l}\right)\int_0^l \frac{M}{EI}x\,dx \tag{8.9}$$

Let us denote the area of the $M/(EI)$ diagram by $a_M = \int_0^l (M/EI)\,dx$. If $\bar{x}$ is the distance of the centroid of the $M/(EI)$ diagram from the left-hand end A, then the first moment of the area a_M about A is $\int_0^l (M/EI)x\,dx = a_M\bar{x}$.

Substituting for the integrals in Eq. 8.9,

$$\int_l \frac{M_{uj}M}{EI}\,dl = a_M\left[M_{uAj} + (M_{uBj} - M_{uAj})\frac{\bar{x}}{l}\right]$$

The term in square brackets in this equation is equal to the ordinate $\overline{M}_{uj}$ of the M_{uj} diagram (Figure 8.4d) at the section through the centroid of the $M/(EI)$ diagram. Therefore,

$$\int_l \frac{M_{uj}M}{EI}\,dl = a_M\overline{M}_{uj} \tag{8.10}$$

By parallel argument, the other integrals of similar type (see, for instance, Eq. 8.4) can be evaluated thus:

$$\int_0^l \frac{V_{uj}V}{Ga_r}\,dx = a_v\overline{V}_{uj} \tag{8.11}$$

$$\int_0^l \frac{T_{uj}T}{GJ}\,dx = a_T\overline{T}_{uj} \tag{8.12}$$

$$\int_0^l \frac{N_{uj}N}{Ea}\,dx = a_N\overline{N}_{uj} \tag{8.13}$$

The notation used on the right-hand side of Eqs. 8.10 to 8.13 can be summarized as follows:

a_M, a_V, a_T, and a_N	are the areas of the $M/(EI)$, $V/(Ga_r)$, $T/(GJ)$, and $N/(Ea)$ diagrams respectively
$\overline{M}_{uj}$, $\overline{V}_{uj}$, $\overline{T}_{uj}$, and $\overline{N}_{uj}$	are the values respectively of M_{uj}, V_{uj}, T_{uj}, and N_{uj} at the centroid of each of the areas a considered above

The areas and the location of the centroid for some geometrical figures frequently needed for the application of Eqs. 8.10 to 8.13 are listed in Appendix F. For members with a constant EI, the values of the integral $\int M_u M\,dl$ for geometrical figures which commonly form bending moment diagrams are given in Appendix H.

We should note that the value of the integral does not depend on the sign convention used for the internal forces, provided that the same convention is used for the forces due to the real and virtual loadings.

In the majority of cases, the plots of M_{uj}, V_{uj}, T_{uj}, and N_{uj} are straight lines or can be divided into parts such that the plot of the ordinate is one straight line; under these circumstances,

Eqs. 8.10 to 8.13 can be applied. However, in structures with curved members, these plots are not rectilinear, but it is possible to approximate a curved member by a number of straight parts over which the diagram of the internal forces due to virtual loading can be considered straight.

8.5.1 Definite integral of product of two functions

Equations 8.10 to 8.13 may be presented in one general mathematical equation that evaluates the integral of the product of two functions, $y_1(x)$ and $y_2(x)$ in the range between x_1 and x_2 (Figure 8.5a). The first function, y_1 is an arbitrary function while the second function, y_2 is one straight line between x_1 and x_2.

$$\int_{x_1}^{x_2} y_1 y_2 \, dx = a_{y1}\overline{y_2} \tag{8.14}$$

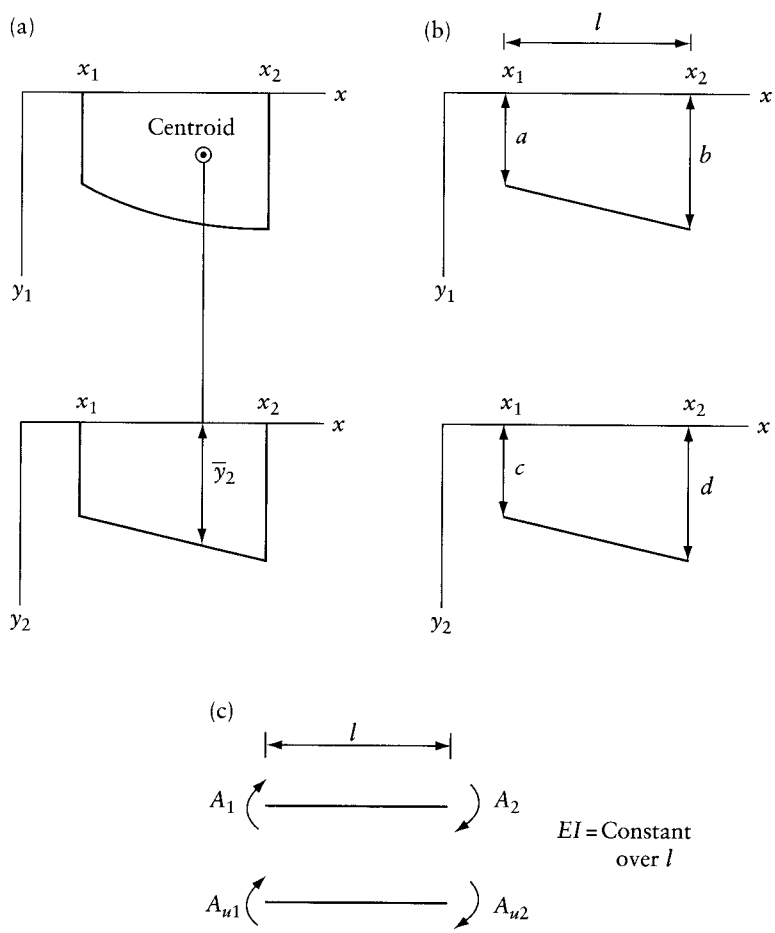

Figure 8.5 Evaluation of the integral of the product of two functions $y_1(x)$ and $y_2(x)$. (a) General case: y_1 is arbitary function and y_2 is one straight line between x_1 and x_2. (b) Special case: each of y_1 and y_2 is a straight line between x_1 and x_2. (c) Positive end moments for a member of a plane frame.

where a_{y1} is the area of the graph of y_1 between x_1 and x_2; $\overline{y_2}$ is the ordinate of y_2 opposite to the centroid of a_{y1}. In the special case when each of the two functions is one straight line between x_1 and x_2 (Figure 8.5b), the value of the integral is

$$\int_{x_1}^{x_2} y_1\, y_2\, dx = \frac{l}{6}(2ac + 2bd + ad + bc) \tag{8.15}$$

where $l = x_2 - x_1$; a to d are ordinates defined in Figure 8.5b.

8.5.2 Displacements in plane frames in terms of member end moments

Application of the unit-load theorem to calculate the displacement at a coordinate in a plane frame, accounting for bending deformations only, involves evaluation of the integral

$$D = \int \frac{MM_u}{EI}\, dl \tag{8.16}$$

When the members are straight prismatic and both M and M_u vary linearly over the length of each member (e.g. when equivalent joint loads are used, Section 8.7), D can be expressed as the sum of contributions of individual members

$$D = \sum \left(\frac{1}{EI}\int M M_u\, dl\right)_{member} \tag{8.17}$$

$$\left(\frac{1}{EI}\int M M_u\, dl\right)_{member} = \left[\frac{l}{6EI}(2A_1A_{u1} + 2A_2A_{u2} - A_1A_{u2} - A_2A_{u1})\right]_{member} \tag{8.18}$$

The sum in Eq. 8.17 is for all members; l and EI are the length and the flexural rigidity of a typical member, respectively; A_1 and A_2 are member end moments due to the actual load; A_{u1} and A_{u2} are member end moments due to the unit virtual load. Throughout this book, a clockwise end moment for a member of a plane frame is considered positive (Figure 8.5c). Equation 8.18 is derived by Eq. 8.15 substituting $A_1, -A_2, A_{u1}$ and $-A_{u2}$ for a, b, c and d respectively. Note that a clockwise end moment produces positive bending moment at the left-hand end of the member, but produces negative bending moment at the right-hand end.

8.6 Truss deflection

In a plane or space truss composed of m pin-jointed members, with loads applied solely at joints, the only internal forces present are axial, so that Eq. 8.4 can be written

$$D_j = \sum_{i=1}^{m} \int_l \frac{N_{uj}N_i}{Ea}\, dl \tag{8.19}$$

Generally, the cross section of any member is constant along its length. Equation 8.19 can therefore be written

$$D_j = \sum_{i=1}^{m} \frac{N_{uij}N_i}{E_i a_i} l_i \tag{8.20}$$

where m is the number of members, N_{uij} is the axial force in member i due to a virtual unit load at j, and $N_i l_i/(E_i a_i)$ is the change in length of a member caused by the real loads, assuming that the material obeys Hooke's law.

Equation 8.20 can also be written in the form

$$D_j = \sum_{i=1}^{m} N_{uij}\, \Delta_i \tag{8.21}$$

where Δ_i is the real change in length of the ith member. This form is used when the deflection due to causes other than applied loading is required, for example, in the case of a change in temperature of some members.

When the material obeys Hooke's law,

$$\Delta_i = \Delta_{ij} + \left(\frac{Nl}{aE}\right)_i \tag{8.22}$$

where Δ_i is the free (unrestrained) elongation of the member due to temperature; N_i is the axial force in the member due to all effects (including the effect of temperature when the truss is statically indeterminate). The unrestrained elongation of the member due to a rise of temperature T degrees is

$$\Delta_{it} = \alpha T l_i \tag{8.23}$$

where l_i is the length of the member and α is the coefficient of thermal expansion. Equations 8.20 and 8.21 are the same as Eqs. 8.5 and 7.51 respectively. Equation 8.21 is valid for linear and nonlinear trusses.

Example 8.1: Plane truss

The *plane truss* of Figure 8.6a is subjected to two equal loads P at E and D. The cross-sectional area of the members labeled 1, 2, 3, 4, and 5 is a, and that of members 6 and 7 is $1.25a$. Determine the horizontal displacement D_1, at joint C, and the relative movement, D_2, of joints B and E.

The internal forces in the members due to the actual loading are calculated by simple statics and are given in Figure 8.6b.

The internal forces due to a unit virtual load at the coordinates D_1 and D_2 are then determined (Figures 8.6c and d). The values obtained can be checked by considering the equilibrium of the joints.

We have taken axial forces as positive when tensile, which is the common practice. However, the final result is not affected by the sign convention used.

The displacements D_1 and D_2 are calculated by Eq. 8.20. It is convenient to use a tabular form, as shown in Table 8.1. The table is self-explanatory, the displacement D_1 or D_2 being equal to the sum of the appropriate column of $N_u Nl/(Ea)$. Thus, $D_1 = -2.334\, Pl/(Ea)$ and $D_2 = -0.341\, Pl/(Ea)$.

The negative sign of D_1 indicates that the displacement is in a direction opposite to the direction of the virtual load in Figure 8.6c. This means that the horizontal translation of joint C is to the right. Likewise, the negative sign of D_2 means that the relative movement of B and E is opposite to the directions of the virtual forces assumed, that is, separation.

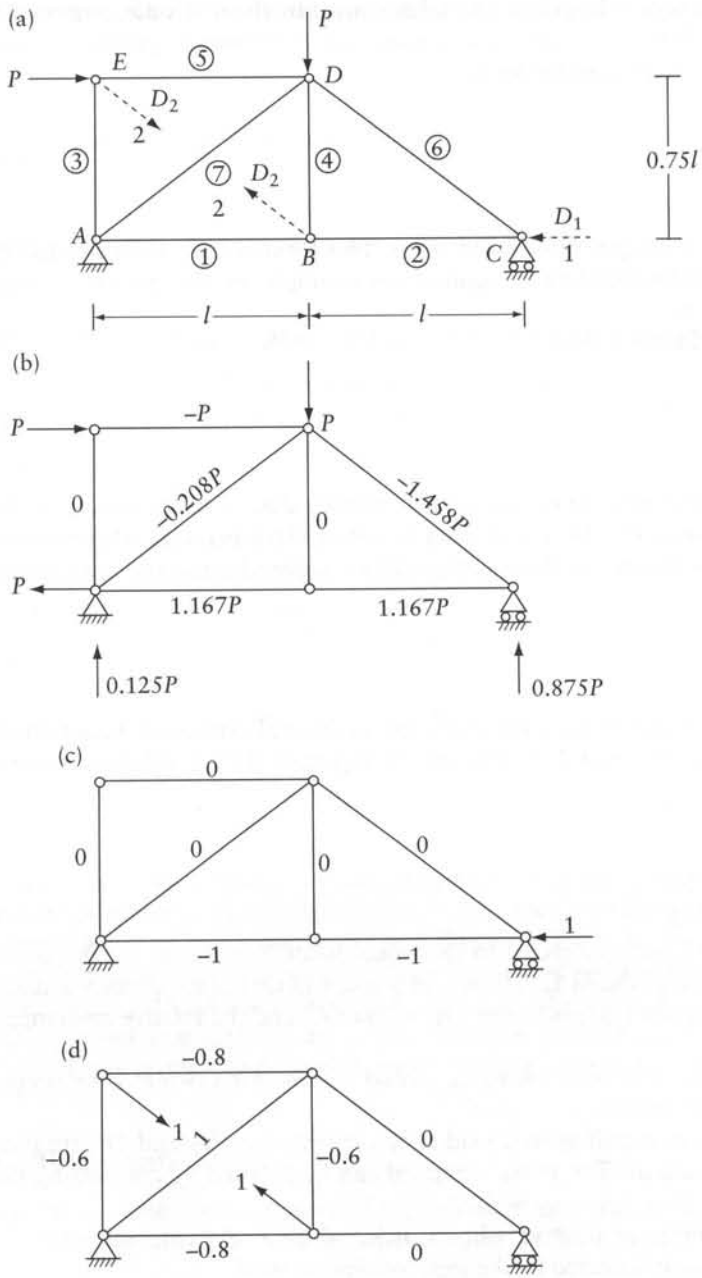

Figure 8.6 Plane truss considered in Examples 8.1 and 8.2.

Example 8.2: Deflection due to temperature: statically determinate truss

For the same truss of Figure 8.6a, find the displacement D_2 due to a rise in temperature of members 5 and 6 by 30 degrees. (The loads P are not acting in this case.) Assume the coefficient of thermal expansion $\alpha = 0.6 \times 10^{-5}$ per degree.

Table 8.1 Example 8.1: Calculation of Displacements D_1 and D_2.

Member	*Properties of member*			*Actual loading*	*Calculation of* D_1		*Calculation of* D_2	
	Length l	*Area of cross section* a	$\frac{l}{Ea}$	N	N_u	$\frac{N_u N l}{Ea}$	N_u	$\frac{N_u N l}{Ea}$
1	1	1	1	1.167	−1	−1.167	−0.8	−0.933
2	1	1	1	1.167	−1	−1.167	0	0
3	0.75	1	0.75	0	0	0	−0.6	0
4	0.75	1	0.75	0	0	0	−0.6	0
5	1	1	1	−1	0	0	−0.8	+0.800
6	1.25	1.25	1	−1.458	0	0	0	0
7	1.25	1.25	1	−0.208	0	0	1	−0.208
Multiplier	l	a	$l/(Ea)$	P	–	$Pl/(Ea)$ −2.334	–	$Pl/(Ea)$ −0.341

A unit virtual force is applied in the same manner as in Figure 8.6d, so that the forces in the members, indicated on the figure, can be used again.

The real change in length occurs in two members only, so that from Eq. 8.23:

$$\Delta_5 = 0.6 \times 10^{-5} \times 30 \times l = 18 \times 10^{-5} l$$

and

$$\Delta_6 = 0.6 \times 10^{-5} \times 30 \times 1.25l = 22.5 \times 10^{-5} l$$

Applying Eq. 8.21 with the summation carried out for members 5 and 6 only

$$D_2 = \sum_{i=5,6} N_{ui2}\, \Delta_i$$

or

$$D_2 = -0.8(18 \times 10^{-5} l) + 0 \times (22.5 \times 10^{-5} l) = -14.4 \times 10^{-5} l$$

It is clear that the same method of calculation can be used if Δ_i is due to any other cause, for example, lack of fit (see Section 4.4).

8.7 Equivalent joint loading

In the analysis of structures by the force method we have to know the displacements at a number of coordinates usually chosen at the joints due to several loading arrangements. This requires that the loads be applied at joints only, but any loads acting between joints can be replaced by equivalent loads acting at the joints. The equivalent loads are chosen so that the resulting displacements at the joints are the same as the displacements due to the actual loading. The displacements at points other than the joints will not necessarily be equal to the displacements due to the actual loading.

Consider the beam in Figure 8.7a for which the displacements at the coordinates 1 and 2 at B (Figure 8.7b) are required. We consider B as a joint between members AB and BC. In Figure 8.7c, the displacements at joints B and C are restrained and the fixed-end forces due to the actual loading on the restrained members are determined. The formulas in Appendix C may be used for this purpose. The fixed-end forces at each joint are then totaled and reversed on the actual structure, as in Figure 8.7d. These reversed forces are statically equivalent to the actual loading on the structure and produce the same displacement at the coordinates 1 and 2 as the actual loading. The rotation at C is also equal to the rotation due to the actual loading, but this is not true for the displacements at the other joints A and D. This statement can be proved as follows.

The displacements at 1 and 2 and the rotation at C can be obtained by superposition of the displacements due to the loadings under the conditions shown in Figures 8.7c and d. However, the forces in Figure 8.7c produce no displacements at the restrained joints B and C. Removal of the three restraining forces is equivalent to the application of the forces in Figure 8.7d, and it follows that due to these forces the structure will undergo displacements at joints B and C equal to the displacements due to the actual loading.

From the above, we can see that restraints have to be introduced only at the coordinates where the deflection is required. Sometimes, additional restraints may be introduced at other convenient locations (such as C in the structure considered above) in order to facilitate the calculation of the fixed-end forces on the structure.

It is apparent that the use of the equivalent joint loading results in the same reactions at supports as the actual loading. The internal forces at the ends of the members caused by the equivalent joint loading, when added to the fixed-end forces caused by the actual loading, give the end-forces in the actual condition.

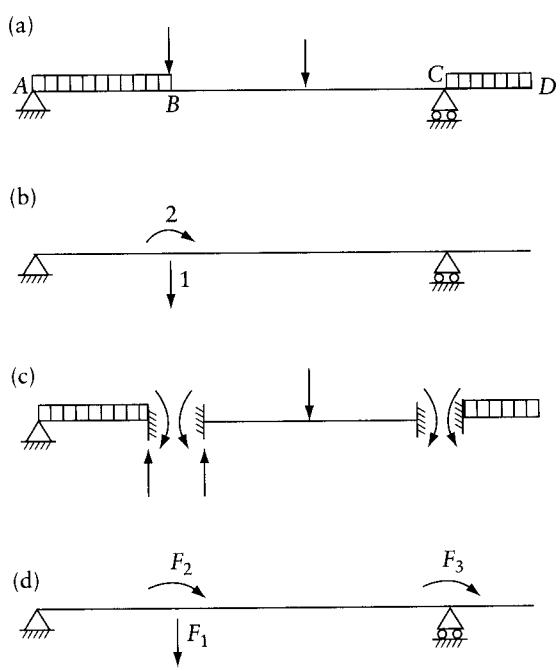

Figure 8.7 Equivalent joint loading. (a) Beam. (b) Coordinate system. (c) Restrained condition. (d) Restraining forces reversed on actual structure.

The advantage of the use of equivalent loads concentrated at the joints instead of the actual loading is that the diagrams of the stress resultants become straight lines. As a result, the evaluation of the integrals of the type involved in Eq. 8.4 can be done by Eq. 8.15. This is illustrated in Example 8.5.

8.8 Deflection of beams and frames

The main internal forces in beams and frames are bending moments and shearing forces. Axial forces and twisting moments are either absent or they make little contribution to the lateral deflections and rotations. For this reason, in most cases, the terms in Eq. 8.4 representing the contribution of the axial force and torsion can be omitted when lateral deflections or rotations are calculated. It follows that the displacement in beams subjected to bending moment and shear is given by

$$D_j = \int \frac{M_{uj}M}{EI}\,dl + \int \frac{V_{uj}V}{Ga_r}\,dl \tag{8.24}$$

Furthermore, the cross section of beams generally used in practice is such that contribution of shear to deflection is small and can be neglected. Thus, the deflection is given by

$$D_j = \int \frac{M_{uj}M}{EI}\,dl \tag{8.25}$$

From Eq. 7.23 the change in slope of the deflected axis of a beam along an element of length dl is $d\theta = -(M/EI)\,dl$. Substituting in Eq. 8.25,

$$D_j = -\int M_{uj}d\theta \text{ or } D_j = \int M_{uj}\,\psi\,dl \tag{8.26}$$

where $\psi = M/EI =$ the curvature.

The angle $\theta = dy/dx$ and $d\theta/dx = d^2y/dx^2$, where y is the deflection. With the positive directions of x and y defined in Figure 7.5b, the angle change and the bending moment indicated in Figure 7.5b are negative and positive respectively.

Equation 8.26 can be used when we want to find displacements due to causes other than external loading, for instance, a temperature differential between the top and bottom surfaces of a beam. The use of Eq. 8.26 will be illustrated by Example 8.6.

Example 8.3: Simply-supported beam with overhanging end

Figure 8.8a shows a beam ABC with an overhanging end. Find the vertical deflection D_1 at C and the angular rotation D_2 at A. The beam has a constant flexural rigidity EI. Only the deformation caused by bending is required.

The bending moment diagram is shown in Figure 8.8c with the ordinates plotted on the tension side of the beam. Figures 8.8e and f show the bending moments due to a unit force at the coordinates 1 and 2 respectively. Because the second moment of area of the beam is constant, the calculation of the areas and the location of the centroid can be carried out for the M diagram instead of the $M/(EI)$ diagram, the resulting values being divided by EI. The M diagram is divided into parts for which the areas and the centroids are easily determined, with the additional provision that the M_{uj} diagram corresponding to each part

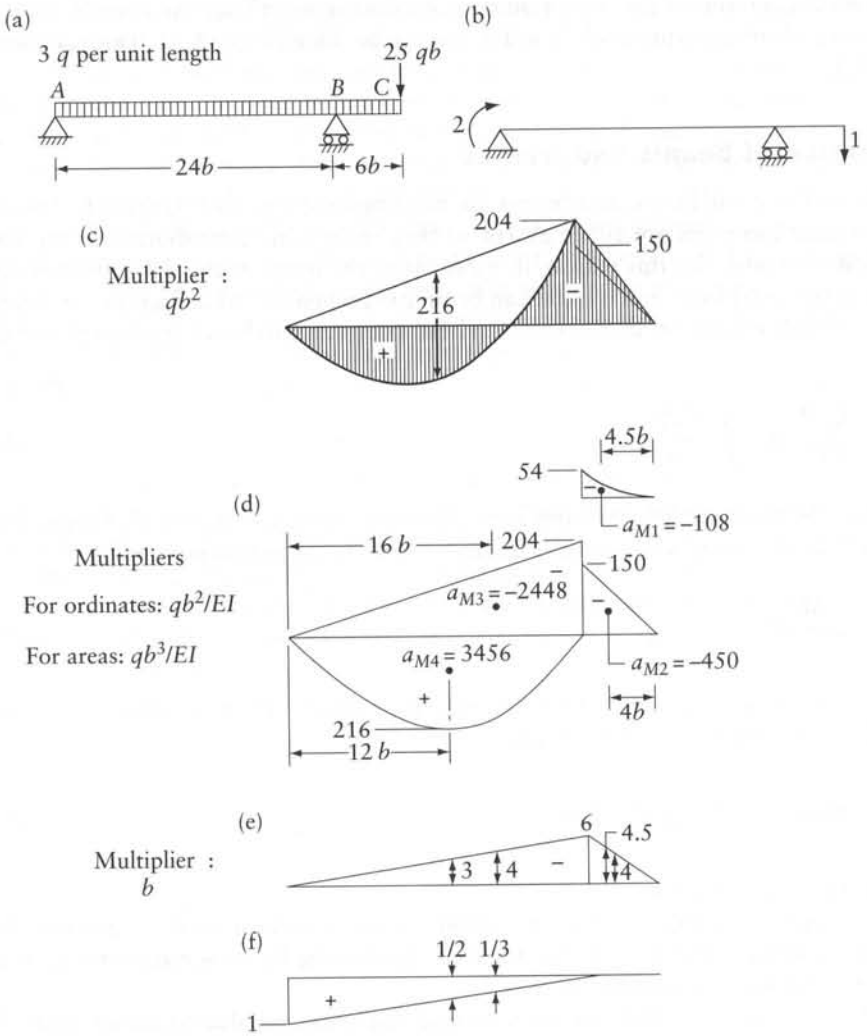

Figure 8.8 Beam analyzed in Example 8.3. (a) Beam. (b) Coordinate system. (c) M diagram. (d) Areas and centroids of M/EI diagram. (e) M_{u1} diagram. (f) M_{u2} diagram.

is a straight line. These areas and their centroids are shown in Figure 8.8d (see Appendix F). Note that the area of a positive bending moment diagram is given a positive sign, and that only the location of the centroid along the beam need be determined.

As a next step, we require the ordinates of the M_{uj} diagrams corresponding to the centroid of each area (see Figures 8.8e and f).

The displacements D_1 and D_2 are given by Eq. 8.8 but the integral can be evaluated with the help of Eq. 8.10 for the different parts of the M diagram.

Thus,

$$D_j = \sum a_M \overline{M}_{uj}$$

where $\overline{M}_{uj}$ denotes the ordinate at the centroid of the bending moment M-diagram. Hence,

$$D_1 = \frac{qb^4}{EI}(108 \times 4.5 + 450 \times 4 + 2,448 \times 4 - 3,456 \times 3) = \frac{1,710}{EI} qb^4$$

and

$$D2 = \frac{qb^3}{EI}\left(-2,448 \times \frac{1}{3} + 3,456 \times \frac{1}{2}\right) = \frac{912}{EI} qb^3$$

The positive sign of D_1 and D_2 indicates that the vertical deflection at C and the rotation at A are in the directions indicated by the coordinates in Figure 8.8b.

Example 8.4: Deflection due to shear in deep and shallow beams

Find the ratio of the contribution of shear to the contribution of bending moment in the total deflection at the center of a steel beam of I cross section, carrying a uniformly distributed load over a simple span (Figure 8.9a). Other conditions of the problem are: the second moment of area $= I$; $a_r \simeq a_w =$ area of web; $G/E = 0.4$; span $= l$; and intensity of loading $= q$ per unit length.

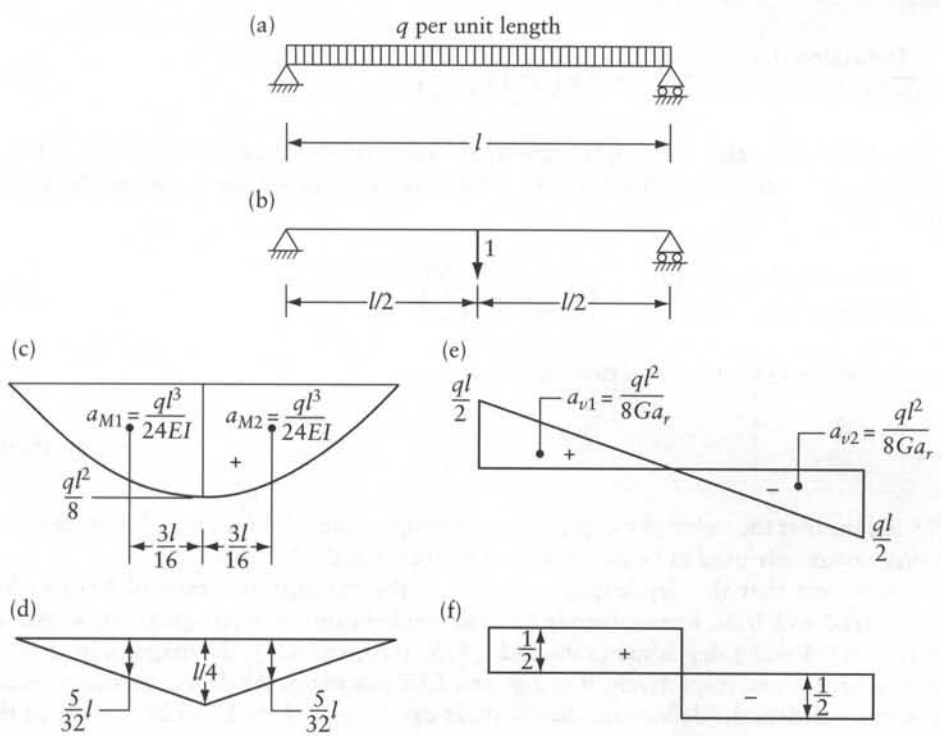

Figure 8.9 Beam considered in Example 8.4. (a) Beam. (b) Coordinate system. (c) M diagram. (d) M_{u1} diagram. (e) V diagram. (f) V_{u1} diagram.

Figures 8.9c and e show the bending moment and shearing force diagrams due to the real loading. A unit virtual load is applied at coordinate 1 (Figure 8.9b) where the deflection is required. The corresponding plots of the bending moment M_{u1} and the shearing force V_{u1} are shown in Figures 8.9d and f.

The M and V diagrams are now divided into two parts such that the corresponding portions of the M_{u1} and V_{u1} diagrams are straight lines. The ordinates $\overline{M}_{u1}$ and $\overline{V}_{u1}$ corresponding to the centroids of the two parts of the M and V diagrams are then determined.

The total deflection at the center is

$$D_1 = \int \frac{M_{u1} M\, dl}{EI} + \int \frac{V_{u1} V\, dl}{Ga_r} \tag{8.27}$$

Of this, the deflection due to bending is

$$\int \frac{M_{u1} M\, dl}{EI} = \sum a_M \overline{M}_{u1} = 2\left(\frac{ql^3}{24EI}\right)\left(\frac{5l}{32}\right) = \frac{5}{384}\frac{ql^4}{EI}$$

and the deflection due to shear is

$$\int \frac{V_{u1} V\, dl}{Ga_r} = \sum a_V \overline{V}_{u1} = 2\left(\frac{ql^2}{8Ga_r}\right)\left(\frac{1}{2}\right) = \frac{ql^2}{8Ga_r}$$

Hence,

$$\frac{\text{Deflection due to shear}}{\text{Deflection due to bending}} = 9.6\left(\frac{E}{G}\right)\left(\frac{I}{l^2 a_r}\right) \tag{8.28}$$

This equation is valid for simply-supported beams of any cross section subjected to a uniform load. In our case, substituting $G = 0.4E$ and $a_r = a_w$, we find for a steel beam of I section

$$\frac{\text{Deflection due to shear}}{\text{Deflection due to bending}} = 24\frac{I}{l^2 a_w} = c\left(\frac{h}{l}\right)^2 \tag{8.29}$$

where h is the height of the I section, and

$$c = \frac{24I}{a_w h^2} \tag{8.30}$$

We can see that the value of c depends on the proportions of the section. For rolled steel sections, commonly used in beams, c varies between 7 and 20.

We may note that the depth/span ratio h/l in the majority of practical I-beams lies between 1/10 and 1/20. For uniformly loaded simple beams of rectangular cross section, with $G/E = 0.4$ and a depth/span ratio $h/l = 1/5$, 1/10, and 1/15, the magnitude of shear deflection represents, respectively, 9.6, 2.4, and 1.07 percent of the deflection due to bending. In plate girders the deflections due to shear can be as high as 15 to 25 percent of the deflection due to bending.

Example 8.5: Deflection calculation using equivalent joint loading

Consider a uniformly loaded simply-supported beam AB, shown in Figure 8.10a. In Example 8.4 we found the deflection at the center using the actual loading. In this example the equivalent joint loading will be used to determine the deflection at the center and the rotation at a support. The deflection due to shear is neglected.

The coordinate system for the required displacements is shown in Figure 8.10b, and Figure 8.10c gives the fixed-end forces due to the actual loading on the restrained beam. The resultants of these forces are reversed and applied to the actual structure, as shown in Figure 8.10d. The bending moment diagram due to the reversed loading is given in Figure 8.10e, and the bending moment diagrams due to a unit force at coordinates 1 and 2 are plotted in Figures 8.10f and g.

The displacements D_1 and D_2 can then be calculated from Eq. 8.10 or 8.15 or using the data of Appendix H. Thus,

$$D_1 = \int \frac{M_{u1} M \, dl}{EI} = 2\left(\frac{ql^3}{96EI} \times \frac{l}{8} + \frac{ql^3}{32EI} \times \frac{l}{6}\right) = \frac{5ql^4}{384EI}$$

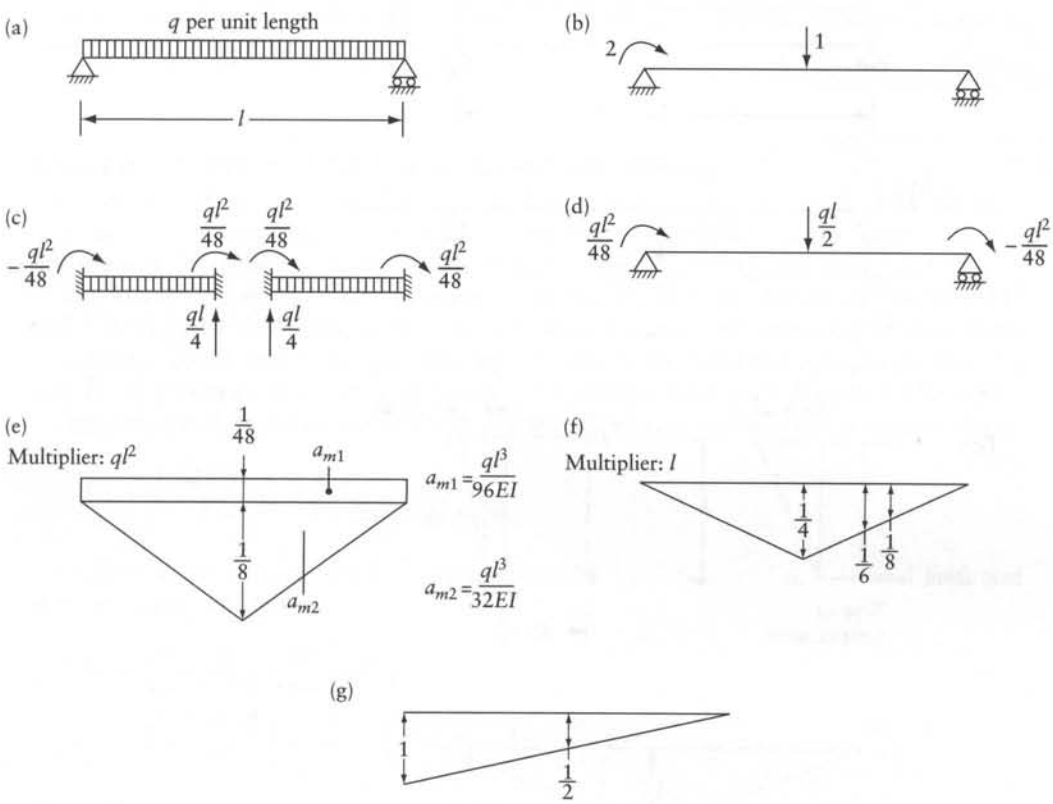

Figure 8.10 Beam considered in Example 8.9. (a) Beam loading. (b) Coordinate system. (c) Restraint conditions. (d) Restraining forces reversed on actual structure. (e) M diagram. (f) M_{u1} diagram. (g) M_{u2} diagram.

and

$$D_2 = \int \frac{M_{u2} M\, dl}{EI} = 2\left(\frac{ql^3}{96EI} + \frac{ql^3}{32EI}\right)\frac{1}{2} = \frac{ql^3}{24EI}$$

These values are, of course, the same as the values listed in Appendix B.

Example 8.6: Deflection due to temperature gradient

Find the deflection at the center of a simply-supported beam of length l and depth h (Figure 8.11a) caused by a rise in temperature which varies linearly between the top and bottom of the beam (Figure 8.11c). The coefficient of thermal expansion is α per degree.

Consider an element $ABCD$ of length dl, shown in Figure 8.11c. It is convenient to assume AB to be fixed in position. The rise of temperature will then cause a displacement of CD to $C'D'$. The angular rotation of CD with respect to AB is

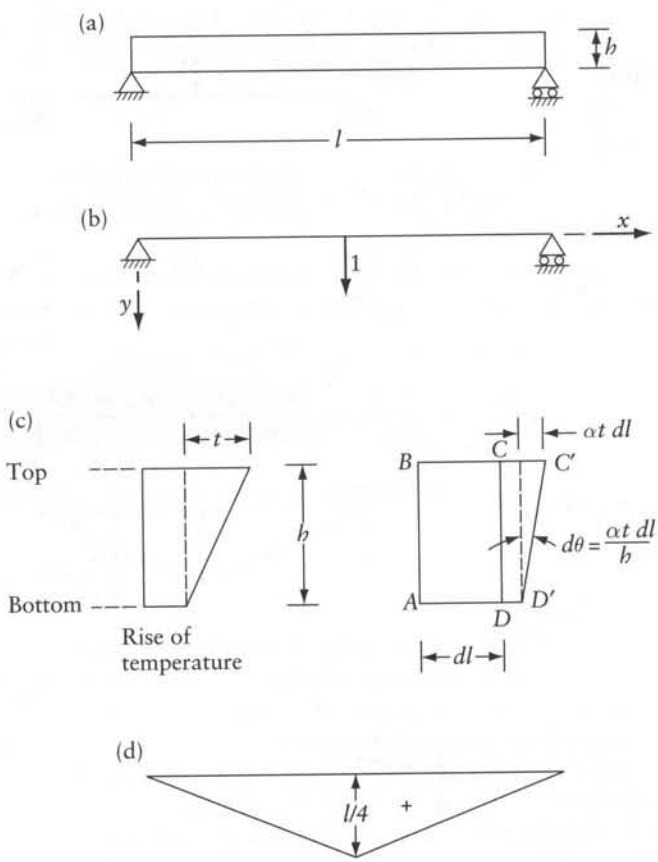

Figure 8.11 Beam considered in Example 8.10. (a) Beam. (b) Coordinate system. (c) Deformation of an element of length dl. (d) M_u^1 diagram.

$$d\theta = \frac{\alpha t\, dl}{h} \tag{8.31}$$

Figure 8.11d shows the plot of the bending moment M_{u1} due to a unit virtual load at coordinate 1 (Figure 8.11b), corresponding to the vertical deflection at the center of the span.

Substituting Eq. 8.31 in Eq. 8.26,

$$D_1 = -\frac{\alpha t}{h}\int M_{u1}\, dl$$

The integral $\int M_{u1}\, dl$ is the area under the M_{u1}, diagram, that is,

$$\int M_{u1}\, dl = \frac{l^2}{8}$$

whence

$$D_1 = \frac{\alpha t l^2}{8h}$$

The minus sign indicates that the deflection is in a direction opposite to the coordinate 1, that is, upward (as expected).

Example 8.7: Effect of twisting combined with bending

The tube ABC shown in Figure 8.12a is cantilevered with AB and BC in a horizontal plane. A vertical load is applied at the free end C. Find the vertical deflection at C due to bending and torsion. The tube has a constant cross section. Take $G = 0.4E$ and note that $J = 2I$.

The M and T diagrams corresponding to the real loadings are shown in Figures 8.11c and d, in which the areas and the location of their centroids are indicated. A unit virtual load is applied at coordinate 1, that is, vertically at C, where the deflection is required. The M_{u1} and T_{u1} diagrams corresponding to the virtual loading are shown in Figures 8.12e and f.

Applying Eq. 8.4, but including the bending and twisting moment terms only, we have

$$D_1 = \int \frac{M_{u1}M}{EI}\, dl + \int \frac{T_{u1}T}{GJ}\, dl$$

Evaluating the integrals for the parts AB and BC by the use of Eq. 8.10 and 8.12 and then summing, we obtain

$$\begin{aligned} D_1 &= \sum a_M \overline{M}_{u1} + \sum a_T \overline{T}_{u1} \\ &= \left(-\frac{4.5Pb^2}{EI}\right)(-2b) + \left(-\frac{0.5Pb^2}{EI}\right)\left(-\frac{2b}{3}\right) + \left(-\frac{3.0Pb^2}{GJ}\right)(-b) \end{aligned}$$

or

$$D_1 = 9.33\frac{Pb^3}{EI} + \frac{3.00Pb^3}{GJ}$$

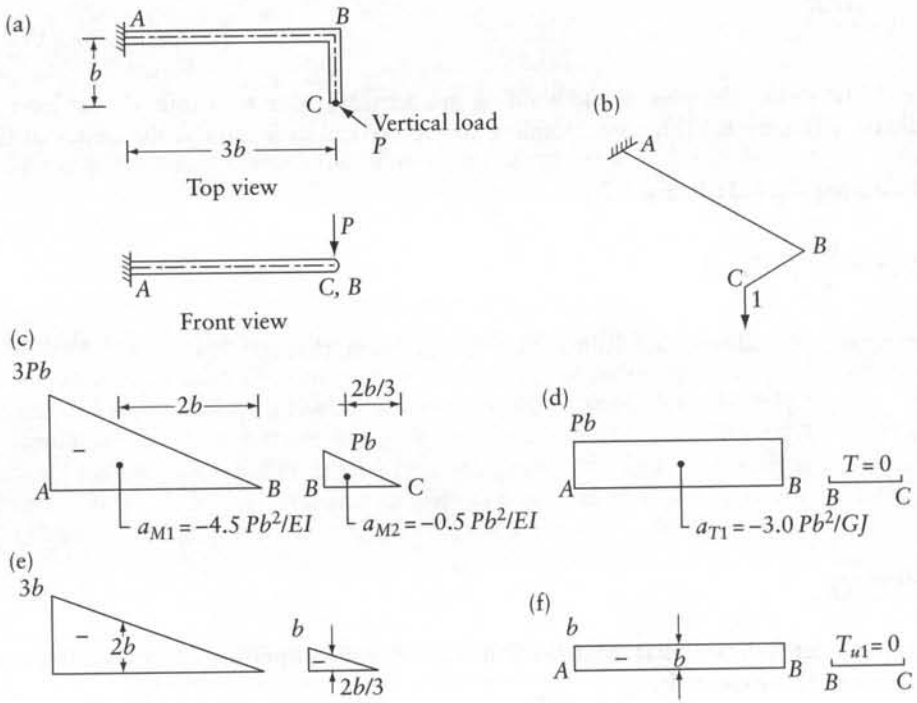

Figure 8.12 Tube considered in Example 8.11. (a) Tube. (b) Coordinate system. (c) M diagram. (d) T diagram. (e) M_{u1} diagram. (f) T_{u1} diagram.

Now,

$$GJ = 0.8EI$$

Substituting,

$$D_1 = 13.08\frac{Pb^3}{EI}$$

Example 8.8: Plane frame: displacements due to bending, axial and shear deformations

The rigid frame of Figure 8.13a is made of a steel I section which has the following properties: $a = 134 \times 10^{-6} l^2$, $a_r = a_{web} = 65 \times 10^{-6} l^2$, and $I = 53 \times 10^{-9} l^4$. Also, $G = 0.4E$.

Determine the contribution of bending, axial force, and shear deformations to the displacement at the three coordinates in Figure 8.13b.

First, we replace the actual forces by equivalent loads at the joints A, B, C, and D. To do this, the joints are restrained (Figure 8.13c), and the fixed-end forces are determined by

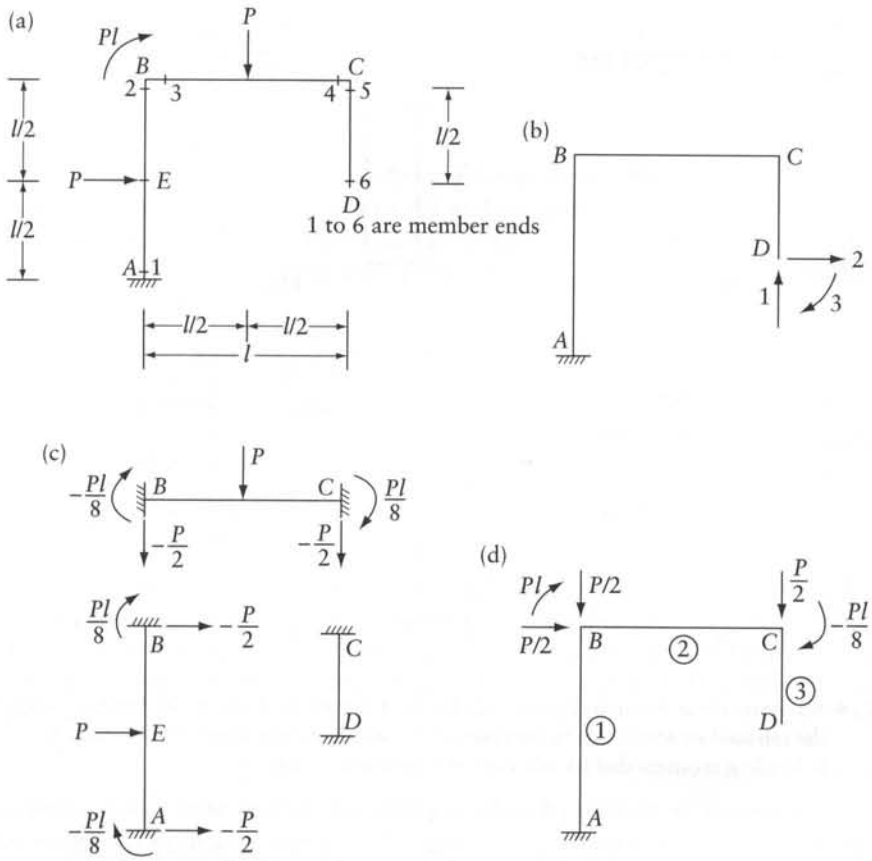

Figure 8.13 Frame considered in Example 8.8. (a) Frame geometry and loading. (b) Coordinate system. (c) Fixed-end forces. (d) Equivalent joint loading.

the use of the formulas in Appendix C. These forces are reversed and added to the actual forces acting at the joints (only the couple Pl, in this example) to obtain the equivalent joint loading shown in Figure 8.13d. We then proceed to find the displacements due to the equivalent loading.

The contribution of the three types of deformation is now determined by Eqs. 8.10, 8.11 and 8.13. We will work with the equivalent joint loading; alternatively, the actual loads can, of course, be used.

(a) *BENDING DEFORMATION.* Figure 8.14 shows diagrams for the bending moment M_s due to the equivalent joint loads, and the bending moments M_{u1}, M_{u2} and M_{u3} due to unit load applied separately at the coordinates. We use Eq. 8.10:

$$D_j = \int M_{uj} \frac{M_s}{EI}\, dl \quad \text{with } j = 1,\ 2,\ 3$$

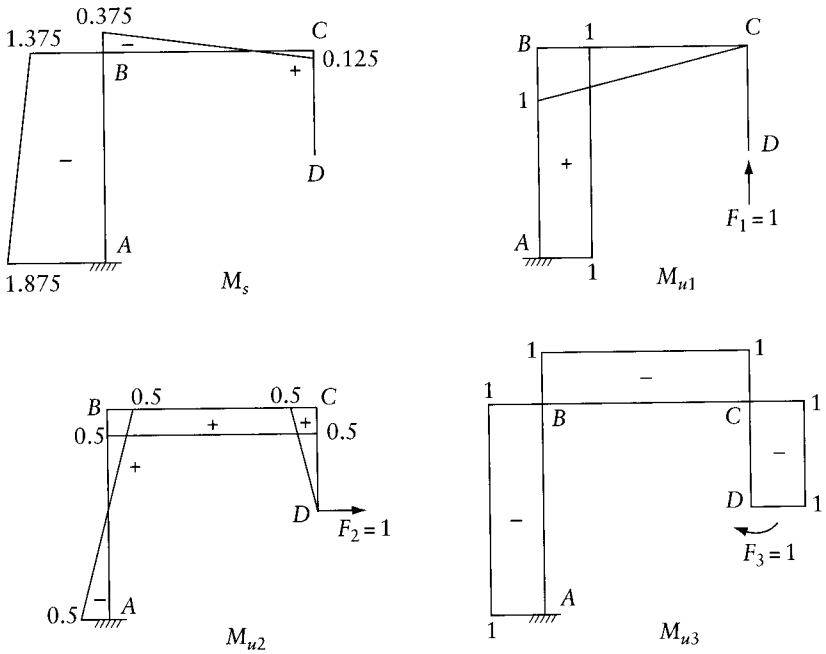

Figure 8.14 Analysis of the frame in Figure 5.2a by the force method. M_s is the bending moment of the released structure due to the equivalent joint loading in Figure 8.13d; M_{u1}, M_{u2} or M_{u3} is bending moment due to unit load at coordinate 1, 2 or 3.

We evaluate the integrals by applying Eq. 8.15 to members *AB*, *BC* and *CD*:

$$D_1 = \frac{Pl^3}{EI}\left[\frac{1}{6}(-2\times 1.875\times 1 - 2\times 1.375 - 1.375\times 1 - 1.875\times 1) + \frac{1}{6}(-2\times 0.375\times 1 + 0.125\times 1)\right] = -1.729\frac{Pl^3}{EI} = -32.63\times 10^6\frac{P}{El}$$

$$D_2 = \frac{Pl^3}{EI}\left[\begin{array}{l}\frac{1}{6}(2\times 1.875\times 0.5 - 2\times 1.375\times 0.5 + 1.375\times 0.5 - 1.875\times 0.5) \\ +\frac{1}{6}(-2\times 0.375\times 0.5 + 2\times 0.125\times 0.5 - 0.375\times 0.5 + 0.125\times 0.5)\end{array}\right]$$

$$= -20.83\times 10^{-3}\frac{Pl^3}{EI} = -393.1\times 10^3\frac{P}{El}$$

$$D_3 = 1.75\frac{Pl^2}{EI} = 33.02\times 10^6\frac{P}{El^2}$$

Because M_{u3} is constant, the integral for D_3 is simply equal to minus the area of M_s divided by *EI*.

(b) *DEFORMATION DUE TO AXIAL FORCES.* The axial forces in the members due to the equivalent joint loading are equal to $-P$ for *AB* and zero for the other members. A unit load $F_1 = 1$ produces an axial force equal to $+1$ in *AB* and zero in other members. Thus, Eq. 8.13 gives

$$D_1 = -\frac{Pl}{Ea} = -7.463 \times 10^3 \frac{P}{El}$$

$$D_2 = 0$$

$$D_3 = 0$$

(c) *SHEAR DEFORMATION.* The shearing forces in the members due to the equivalent joint loading are equal to $P/2$ in each of AB and BC and equal to zero in CD. $F_1 = 1$ produces shearing force equal to -1 in BC and zero in the other members. $F_2 = 1$ produces shearing force equal to $+1$ in AB, zero in BC, and -1 in DC; $F_3 = 1$ produces no shear. Application of Eq. 8.11 gives:

$$D_1 = -0.5\frac{Pl}{Ga_r} = -19.23 \times 10^3 \frac{P}{El}$$

$$D_2 = 0.5\frac{Pl}{Ga_r} = 19.23 \times 10^3 \frac{P}{El}$$

$$D_3 = 0$$

A comparison of the contributions to the displacement made by the three types of deformation shows that, in the present example, the displacement caused by bending is much greater than that due to the axial forces and shear. This is true in most practical cases and, for this reason, the displacements caused by the axial and shear deformations are often neglected.

Example 8.9: Plane frame: flexibility matrix by unit-load theorem

Determine the flexibility matrix of the frame of Example 8.8 corresponding to the three coordinates in Figure 8.13b. Consider the bending deformation only.

In Example 5.2, we have used the displacement method to analyze a frame, which is the same as the frame in Figure 8.13a, but with end D totally fixed (Figure 5.2a). The calculations in Example 8.8 and the present example complete Steps 1 to 3 to solve the same problem by the force method (see Section 4.6). Solve the geometry (compatibility) Eq. 4.11 to obtain the forces $\{F\}$, the reaction components at D, that will eliminate the displacements at the three coordinates.

When only bending deformation is considered, the elements of the flexibility matrix are given by Eq. 8.5 as:

$$f_{ij} = \int \frac{M_{ui} M_{uj}}{EI}\, dl \tag{8.32}$$

The bending moment diagrams due to unit forces at the coordinates are shown in Figures 8.14b, c and d. We apply Eq. 8.32 to generate the elements of the lower triangle of a 3×3 flexibility matrix, evaluating the integrals by either Eq. 8.10, Eq. 8.15 or Appendix H. This gives:

$$[f] = \frac{l}{EI}\begin{bmatrix} (4/3)l^2 & 0.25l^2 & -1.5l \\ 0.25l^2 & 0.375l^2 & -0.625l \\ -1.5l & -0.625l & 2.5 \end{bmatrix}$$

We show below, as an example, the calculation of f_{22} using M_{u2} (Figure 8.14), Eq. 8.15 for member AB and Eq. 8.10 for BC and CD:

$$f_{22}=\frac{l^3}{EI}\left[\frac{1}{6}(2\times 0.5\times 0.5+2\times 0.5\times 0.5-2\times 0.5\times 0.5)+0.5\times 0.5+\frac{1}{6}\right.$$

$$\left.\times 0.5\times 0.5\right]=0.375\frac{l^3}{EI}$$

Application of the geometry Eq. 4.11 and its solution gives (using the values of $\{D\}$ determined in Example 8.8):

$$[f]\{F\}=-\{D\}$$

$$\frac{l}{EI}\begin{bmatrix}(4/3)l^2 & 0.25l^2 & -1.5l\\ 0.25l^2 & 0.375l^2 & -0.625l\\ -1.5l & -0.625l & 2.5\end{bmatrix}\{F\}=-\begin{Bmatrix}-1.729l\\ -20.83\times 10^{-3}l\\ 1.75\end{Bmatrix}\frac{Pl^2}{EI}$$

$$\{F\}=P\,\{1.219,-1.208,-0.2708L\}$$

We may now wish to use these reaction components to verify the ordinates of the bending moment diagram determined by the displacement method in Example 5.2 (Figure 5.2h). Note that for this purpose the actual loads, not the equivalent joint loads, must be used.

Example 8.10: Plane truss: analysis by the force method

Find the forces in the members of the truss shown in Figure 8.15a due to: (*i*) the force P, and (*ii*) a rise of temperature T degrees in all members. The modulus of elasticity E, the cross-sectional area a, and the thermal expansion coefficient α are the same for all members.

We follow the five steps of the force method (Section 4.6). In Step 1, the structure is released by cutting a member; the two arrows in Figure 8.15b define a system of one coordinate. In Step 2, we calculate the displacement D_1 at the coordinate for each load case using Eq. 8.20 or 8.21.

$$(D_1)_{Case\ i}=\sum\left(\frac{N_{u1}N_s}{Ea}l\right)_i$$

$$=\frac{1}{Ea}\left[P\sqrt{2}(1)l\sqrt{2}-P\left(-\frac{1}{\sqrt{2}}\right)l\right]=2.707\frac{Pl}{Ea}$$

$$(D_1)_{Case\ ii}=\sum(N_{u1}\,\Delta_t)_i \text{ with } \Delta_{ti}=\alpha\,T\,l_i$$

$$=\alpha\,T\left[3\left(-\frac{1}{\sqrt{2}}\right)l+2(1)\,\sqrt{2}\,l\right]=0.7071\,\alpha\,T\,l$$

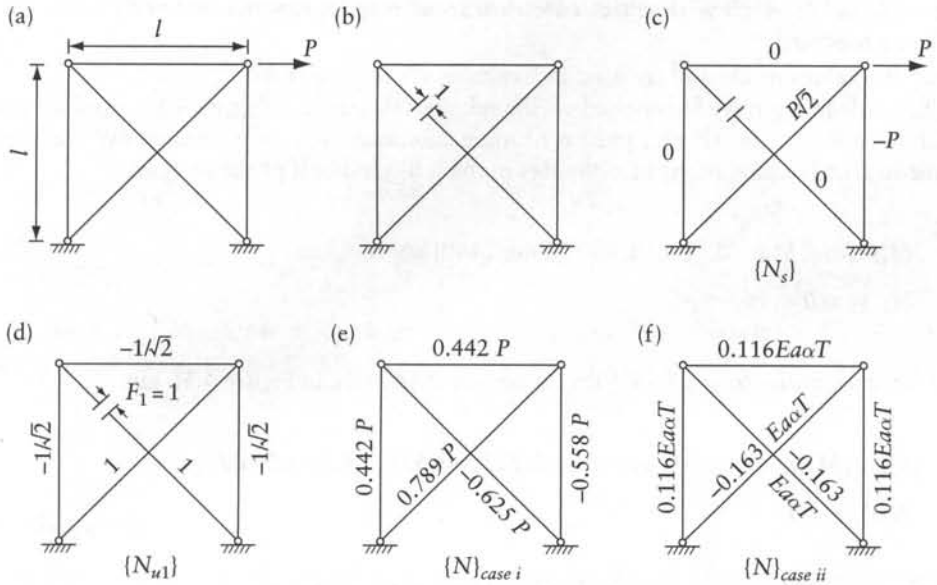

Figure 8.15 Analysis of a plane truss by force method, Example 8.10. (a) Dimensions and applied load. (b) Released structure and coordinate system. (c) Forces in members due to the given load on the released stucture. (d) Forces in members due to $F_1 = 1$ on the released structure. (e) and (f) Axial forces in the actual structure in cases i and ii respectively.

The subscript i refers to any member and the summations are for all members.

In Step 3 we determine the flexibility matrix $[f]_{1\times 1}$ (Eq. 8.6):

$$f_{11} = \sum \left(N_{u1}^2 \frac{l}{Ea} \right)_i$$

$$= \frac{1}{Ea}\left[3\left(-\frac{1}{\sqrt{2}} \right)^2 l + 2(1)^2\, l\sqrt{2} \right] = 4.328\frac{l}{Ea}$$

In Step 4 we solve the geometry (compatibility) equation (see Eq. 4.11)

$$[F_{1Case\ i} \quad F_{1Case\ ii}] = [f_{11}]^{-1}[-D_{1Case\ i} \quad -D_{1Case\ ii}]$$

$$[F_{1Case\ i} \quad F_{1Case\ ii}] = \left[4.328\frac{l}{Ea} \right]^{-1} \left[-2.707\frac{Pl}{Ea} \quad -0.7071\,\alpha\, T\, l \right]$$

$$= [-0.628P \quad -0.163Ea\,\alpha\, T]$$

Step 5 is done by inspection. Superposition of $\{N_s\}$ and $(-0.625P)\{N_{u1}\}$ (Figures 8.15c and d) gives the forces in the actual structure in case i (Figure 8.14e). For case ii, the forces in the actual structure are simply equal to $(-0.163\ E\ a\ \alpha\ T)\{N_{u1}\}$ (see Figure 8.15f).

Example 8.11: Arch with a tie: calculation of displacements needed in force method

Verify the values of D_1 and f_{11} used in Example 4.5 (Eqs. *b* and *d*).

The loads in Figure 4.5a, applied on the released structure in Figure 4.5b, produce zero axial force in the tie *AB* and induce bending moments that vary linearly over the arch segments; the bending moment ordinates in the left-hand half of the arch are:

$$\{M_{sA}, M_{sC}, M_{sD}, M_{sE}\} = \{0, 800, 1280, 1440\}\,\text{kN-m}$$

$$(N_s)_{AB} = 0$$

Equal and opposite forces $F_1 = 1$ on the released structure in Figure 4.5b give:

$$\{M_{u1A}, M_{u1C}, M_{u1D}, M_{u1E}\} = \{0, -2.222, -3.556, -4.000\}\,\text{N-m/N}$$

$$(N_{u1})_{AB} = 0$$

The lengths of the segments of the left-hand half of the arch are:

$$\{l_{AC}, l_{CD}, l_{DE}\} = \{4.575, 4.217, 4.025\}\,\text{m}$$

Considering only bending deformation of the arch and axial deformation of the tie,

$$D_{1Case\,1} = \int_{\text{Arch}} \frac{M_{u1} M_s}{EI}\,dl + \left(\frac{N_{u1} N_s l}{Ea}\right)_{\text{Tie}}$$

Because $N_s = 0$, the second term is nil. The integral in the first term is equal to two times the sum of its values for segments *AC*, *CD* and *DE*; e.g. for *CD*, Eq. 8.15 gives:

$$\int_C^D \frac{M_{u1} M_s}{EI}\,dl = \frac{10^3}{EI}\left[\frac{4.217}{6}(-2 \times 2.222 \times 800 - 2 \times 3.556 \times 1280 - 2.222 \times 1280 - 3.556 \times 800)\right]$$

$$= -0.15111\,\text{m}$$

$$D_{1\ Case\,1} = 2(-0.03177 - 0.15111 - 0.24267) = -0.85109\,\text{m}$$

The minus sign means widening the gap at the cut section in the tie. A rise in temperature of $T = 30°$ reduces the gap by $(\alpha T l)_{AB}$. Thus, the loads in Figure 4.5a combined with the rise in temperature of the tie give:

$$D_{1\ Case\,2} = -0.85109 + 10 \times 10^{-6}(30)24 = -0.84389\,\text{m}$$

Equal and opposite forces $F_1 = 1$ produce at coordinate 1 (Figure 4.5b) the displacement:

$$f_{11} = \int_{\text{Arch}} \frac{M_{u1}^2}{EI}\,dl + \left(\frac{N_{u1}^2 l}{Ea}\right)_{\text{Tie}}$$

$$= \frac{2}{85.32 \times 10^6}(7.529 + 35.822 + 57.516) + \frac{1 \times 24.0}{(2000 \times 10^{-6})(200 \times 10^9)}$$

$$= 2.4242 \times 10^{-6}\ \text{m/N}$$

Evaluation of $\int M_{u1}^2\,dl$ over the segments AC, CD and DE is determined by Eq. 8.15, giving 7.529, 35.822, and 57.516 m^3; the value of $(EI)_{\text{Arch}} = 85.32 \times 10^6\ \text{N-m}^2$.

8.9 General

The method of virtual work is general. It can be used for the calculation of the displacements in plane and space structures, statically determinate or indeterminate. However, in all cases the structure must first be analyzed and the stress resultants have to be determined. The basis of the method is the principle of virtual work relating a system of forces in equilibrium to a compatible system of displacements.

Calculation of displacement by virtual work involves the determination of the internal forces due to the actual loading and due to a unit load applied at each point where the displacement is required. In the general case of application of the method of virtual work, four types of stress resultants, axial force, bending moment, shear and torsion, contribute to the displacements. In pin-jointed trusses, the axial forces are the only contributors. The virtual work expressions involve integrals of a product of two functions; the integral can be conveniently evaluated by taking advantage of the fact that one of the two functions is generally linear.

To use the method of virtual work in frames, where loads are frequently applied at any point in the member, it is convenient to replace the actual loading by equivalent joint loading which induces the same displacements at the joints whose displacement is required as the real loading.

The procedure for the determination of deflection of beams and frames is straightforward. In frames, the displacements are mainly caused by the bending moments, and the other internal forces are often neglected. In some cases, for instance, in plate girders, it may, nevertheless, be prudent to verify that this is justified.

The examples in this chapter are limited to structures with straight members of constant cross section. The method of virtual work can, however, be applied also to structures with curved members and a variable cross section. One way of doing this is by approximating the actual structure to a structure composed of straight segments of constant cross section.

It is worth noting that the method of virtual work can take account of all four types of internal forces while the other methods discussed in Chapter 10 account for only one or the other type of stress resultant.

Problems

8.1 Using the method of virtual work, find D_1, the vertical deflection of joint H, and D_2, the relative translation in the direction of OB of joints O and B of the truss shown in the figure. The changes in length of the bars (in. or cm) are indicated in the figure.

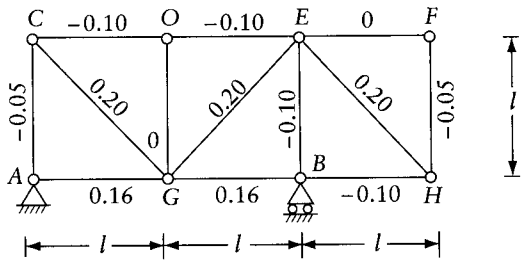

Prob. 8.1

8.2 Find the displacement at coordinate 1 which represents the relative translation of joints C and B of the truss in the figure. Assume $l/(Ea) = B$ to be constant for all members. If a member CB is added with the same $l/(Ea)$ value as the other members, what are the forces in the members caused by the same loading?

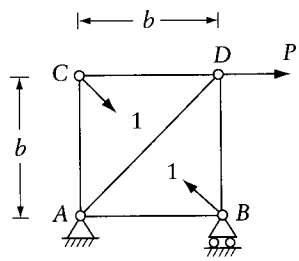

Prob. 8.2

8.3 Find the displacement along the line of action of the force P for the space truss shown in the figure. The value of Ea is the same for all members.

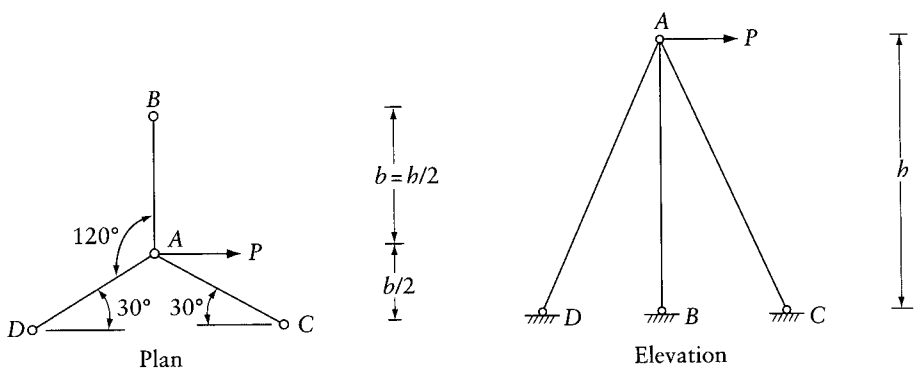

Prob. 8.3

8.4 For the plane truss shown in the figure, find: (a) the vertical deflection at E due to the given loads, (b) the camber at E in the unloaded truss if member EF is shortened by $b/2000$, and (c) the forces in all members if a member is added between C and F and the truss is subjected to the given loads. Consider Ea = constant for all members.

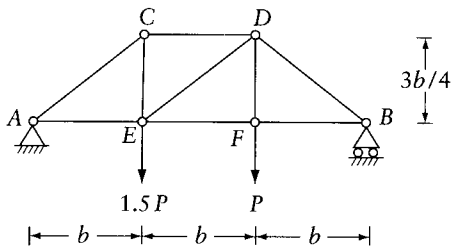

Prob. 8.4

8.5 Imperial units. For the plane truss shown in the figure, find: (a) the deflection at C due to the load P, (b) the vertical deflection at C in the unloaded truss if members DE and EC are each shortened by 1/8 in., and (c) the forces in all members if a member of cross-sectional area of 4 in.^{2} is added between B and D and the truss is subjected to the load P. Assume $E = 30,000$ ksi and the cross-sectional area of the members as indicated in the figure.

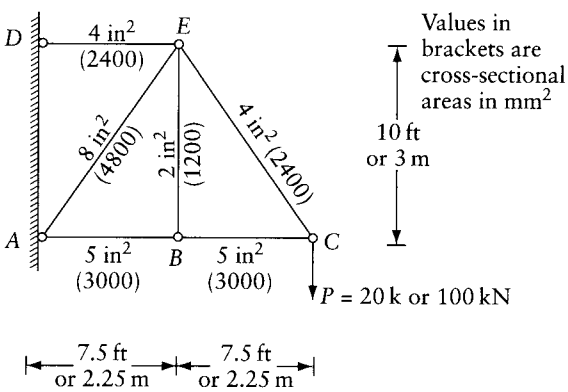

Prob. 8.5 (Imperial units) or *prob. 8.6* (SI units)

8.6 SI units. For the plane truss shown in the figure, find: (a) the deflection at C due to the load P, (b) the vertical deflection at C in the unloaded truss if members DE and EC are each shortened by 3 mm, and (c) the forces in all members if a member of cross-sectional area of 2400 mm^2 is added between B and D and the truss is subjected to the load P. Assume $E = 200$ GN/m^2 and the cross-sectional area of the members as indicated in the figure.

8.7 Find the forces in all members of the truss shown in the figure. Assume l/Ea to be the same for all members.

8.8 Determine the displacements D_1, D_2, and D_3 in directions x, y, and z respectively, at node A of the space truss in Prob. 2.2. Assume Ea = constant for all members.

8.9 The statically indeterminate space truss in Prob. 3.14 is released by cutting members AC, BD, AH, BE, CF, and DG. Find the displacements D_1 and D_2 in the x and y directions respectively, at node A. Also determine the flexibility coefficient f_{33} of the released structure, with coordinate 3 representing the axial force or the relative displacement at the cut section in member AC. Assume all members have the same value of Ea.

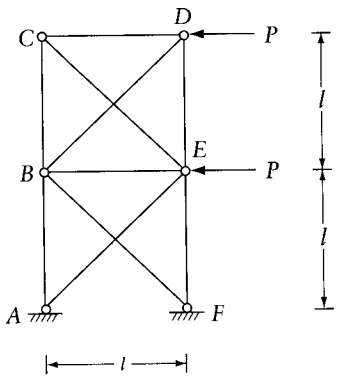

Prob. 8.7

8.10 Find the forces in the plane truss shown due to the combined effect of the force P and a drop of temperature T degrees of ABC only. Assume $Ea =$ constant for all members and $\alpha T = P/(aE)$, where $\alpha =$ coefficient of thermal expansion. Give the answers only for the six members numbered 1 to 6 in the figure.

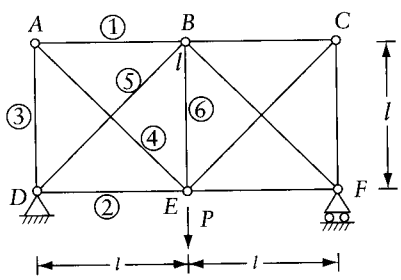

Prob. 8.10

8.11 For the space truss of Prob. 3.16, determine the forces in the members and the displacement at node A in the y direction due to a horizontal force P at the same location. Assume $a =$ constant for all members.

8.12 Find the fixed-end moments in the beam shown.

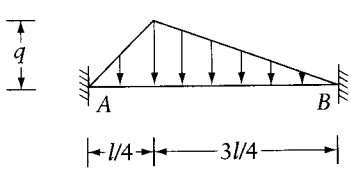

Prob. 8.12

8.13 Find the fixed-end moments in the beam shown.

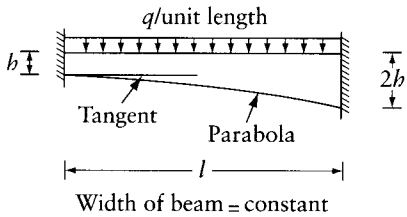

Prob. 8.13

8.14 Find the flexibility matrix corresponding to the coordinates 1 and 2 of the beam shown in the figure. Consider only bending deformation. Apply Eq. 8.32 evaluting the integral by Eq. 8.15 and verifying the answer by Eq. 8.18.

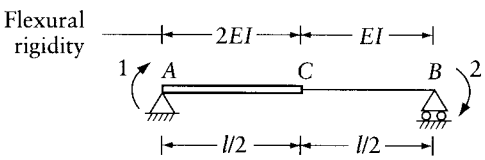

Prob. 8.14

8.15 Assuming that the displacement of the beam AB is prevented at any two of the coordinates shown, find the flexibility matrix corresponding to the other two. Consider both the bending and shear deformations. Use this matrix to derive the stiffness matrix corresponding to the four coordinates. Solution of this problem is included in Section 14.2.

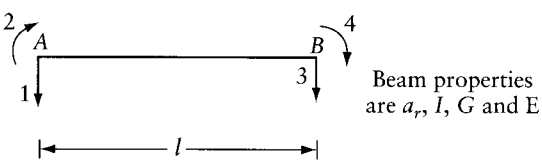

Prob. 8.15

8.16 Find the bending moment diagram for the tied arch shown, considering only the bending deformation in the arch and only the axial deformation in the tie. What is the force in the tie? Ea for tie $= (43/b^2)\,EI$ for arch.

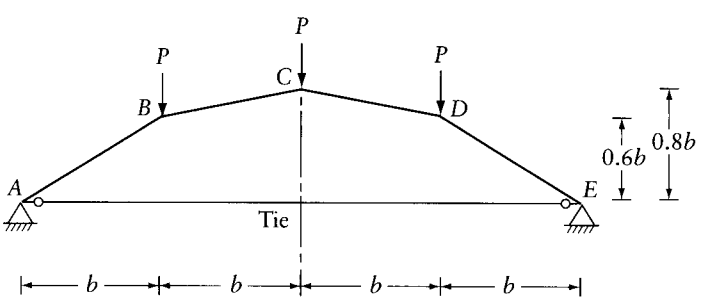

Prob. 8.16

8.17 Imperial units. Using the force method, find the tension in the tie and the horizontal reaction component at A for the frame of Prob. 4.22, with the hinge at C replaced by a rigid joint; draw the bending moment diagram. Consider only the bending deformation in the frame $ABCDE$ and only the axial deformation in the tie BD. $E = 30{,}000$ ksi, I for $ABCDE = 8000$ in.^{4}, area of tie $= 8$ in.^{2}, $l = 30$ ft, $q = 1$ kip/ft.

8.18 SI units. Using the force method, find the tension in the tie and the horizontal reaction component at A for the frame of Prob. 4.22 with the hinge at C replaced by a rigid joint; draw the bending moment diagram. Consider only the bending deformation in the frame $ABCDE$ and only the axial deformation in the tie BD. $E = 200\,\text{GN/m}^2$, I for $ABCDE = 3.1 \times 10^9\,\text{mm}^4$, area of tie $= 5000\,\text{mm}^2$, $l = 9$ m, $q = 1$ kN/m.

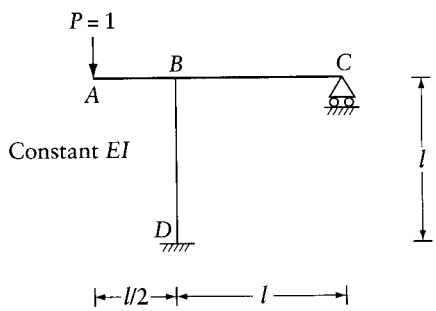

Prob. 8.19

8.19 Considering the deformations due to bending only, find the vertical deflection at A for the frame shown in the figure.

8.20 Solve Prob. 8.19 replacing the roller support at C by a hinge.

8.21 Find the vertical deflection at D and the angular rotation at A for the beam in the figure. Consider bending deformation only.

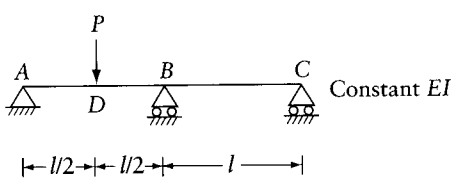

Prob. 8.21

8.22 What is the relative translation along EC of points E and C in the frame of Example 5.2?

8.23 Imperial units. Considering the tension F_1 and F_2 in the cables at C and D in Prob. 4.8 as redundants, find the flexibility matrix of the released structure. Consider only the bending deformation in AB and only the axial deformation in the cables.

8.24 SI units. Solve Prob. 8.23 by referring to Prob. 4.9 (instead of 4.8).

8.25 Considering only bending deformation, find the displacements at the three coordinates indicated in Figure 8.12b due to the loads shown in Figure 8.12a. Use the actual loading and verify that the same answers are obtained as with the equivalent joint loading in Example 8.8.

8.26 Show that the deflection at the center of a straight member with respect to its ends is given by

$$y_{\text{center}} = (\psi_1 + 10\psi_2 + \psi_3)l^2/96$$

where ψ_1 and ψ_3 are the curvatures at the two ends; l is the distance between the two ends; and ψ_2 is the curvature at the middle. The variation of ψ is assumed to be a second-degree parabola.

This is a geometric relation which can be derived by integration of the equation $\psi = -d^2y/dx^2$, where y is the deflection and x is the distance along the member, measured from the left end. The equation can be derived more easily by the method of elastic weights, using equivalent concentrated loading (Figure 10.11).

In practice, the expression derived can be used for continuous or simple beams having a constant or a variable cross section when the parabolic variation of ψ is acceptable.

8.27 The figure represents a pole serving as support of two cables subjected to a tensile force P. Determine the translations D_1, D_2, and D_3 at E in the positive directions of x, y, and z axes, assuming: (a) both cables are supported, and (b) only the cable at E is supported. Consider deformations due to bending moment and twisting moment and assume the cross section is constant hollow circular, with $EI = 1.3GJ$.

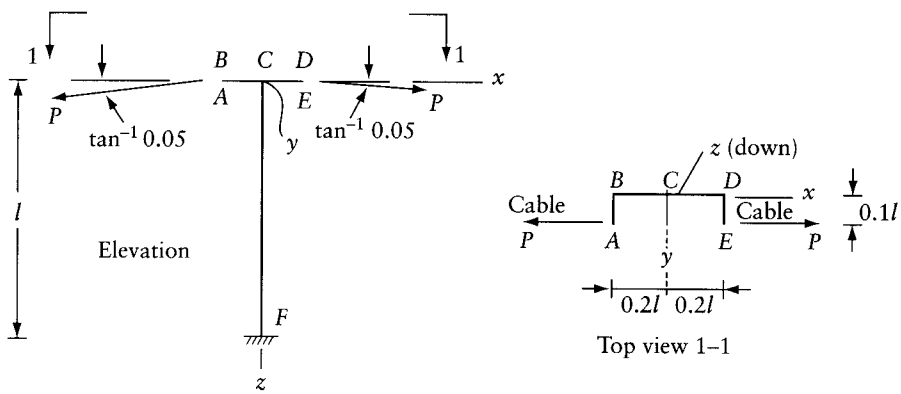

Prob. 8.27

8.28 Find the bending moment diagram for the beam shown due to a uniform load q/unit length over the whole length. The beam has a varying EI value as shown. What is the vertical reaction at A?

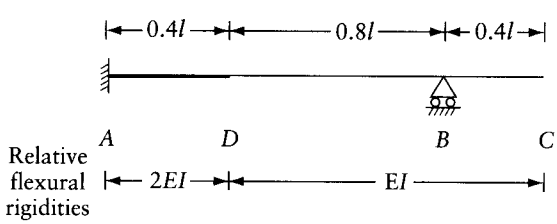

Prob. 8.28

8.29 Find the reaction components at B considering only bending deformation of AB and axial deformation of CD. Consider $(Ea)_{CD} = 20\,(EI)_{AB}/l^2$. What is the deflection at A?

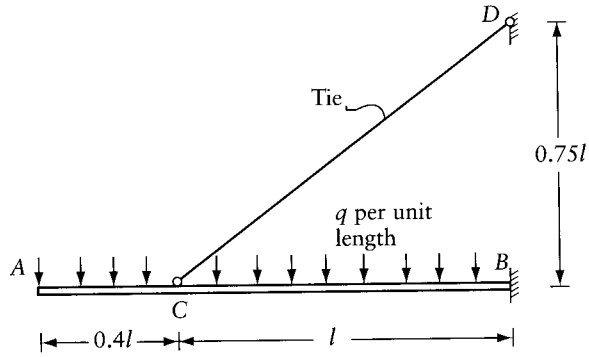

Prob. 8.29

8.30 The figure shows a top view of a curved member of a horizontal grid. Determine the fixed-end forces due to the self-weight of the member, q/unit length. Angle $\theta = 1$ radian. Assume constant cross section, with $GJ/EI = 0.8$. Give the answer as components in the directions of the coordinates shown. Consider only deformations due to bending and torsion. *Hint:* The only statically indeterminate force at the central section is a bending moment; the torsional moment and the shearing force are zero because of symmetry.

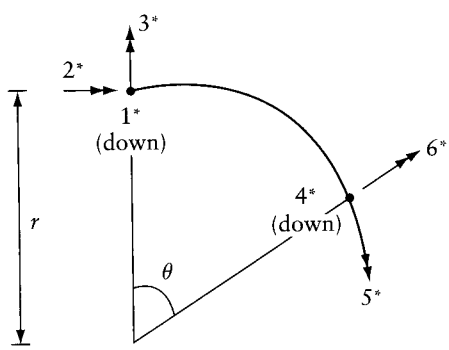

Prob. 8.30

8.31 Find the bending moment diagram for the frame in Figure 6.6d due to a uniform downward load on $ABCDE$ of intensity q/unit length of horizontal projection. Consider only bending deformation assuming $EI =$ constant and member lengths: $\{AB, BF, BC\} = l\{1.0, 1.0, \sqrt{2}\}$. The frame is symmetrical about a vertical line through C. The distance between F and $G = 2l$.

8.32 The figure represents half a symmetrical and symmetrically loaded three-span cable-stayed bridge. Find the changes in the cable forces and the bending moment diagram for AC and BD due to a uniform load q/unit length, covering the whole central span. Consider only axial deformation in the cables and bending deformation in AC and BD. Assume that the initial tension in the cable is sufficient to remain stretched under the effect of all subsequent loading. Ignore the effect of the initial tension on cable stiffness. Consider $EI =$ constant for AC and BD and $(Ea)_{\text{cable}} = 2000\,EI/l^2$.

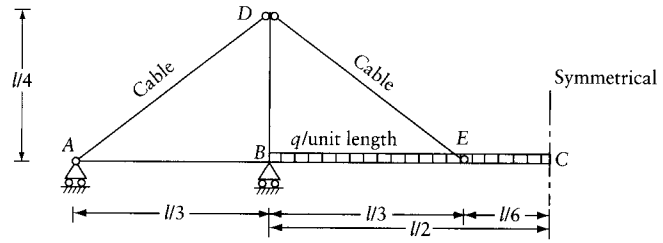

Prob. 8.32

8.33 The figure represents a chimney ABC stayed by four cables BD, BE, BF and BG. Find the reaction components at A due to a force P in the x direction at C. What is the displacement in the x direction at C? Assume that the cables have sufficient initial tension to remain stretched after deformation; ignore the effect of the initial tension on cable stiffness and the self-weight of the cables. Consider only bending deformation of the chimney and axial deformation of the cables; assume $(Ea)_{\text{cable}} = (20/l^2)\,(EI)_{\text{chimney}}$. The effect of the initial tension (ignored here) on the tension stiffness is discussed in Chapter 24.

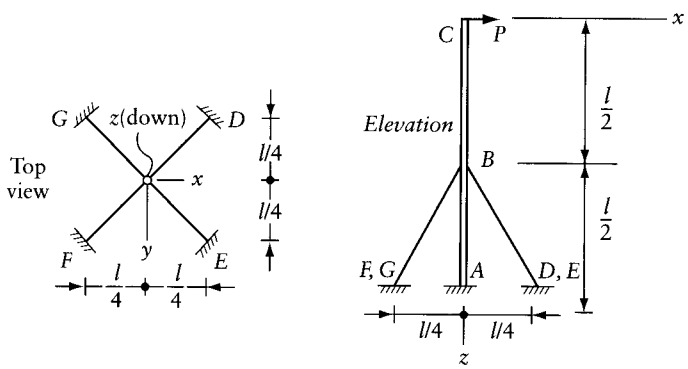

Prob. 8.33

8.34 For the frame in Figure 7.8, find the influence lines for the bending moment and the shearing force at a section just to the right of B.

8.35 Find the bending moment diagram of Prob. 4.22 due to uniform load q per unit length of horizontal projection on BC only.

8.36 Find the forces in the members of the plane truss shown. All members have the same axial rigidity Ea except member AB, whose axial rigidity is $Ea/2$.

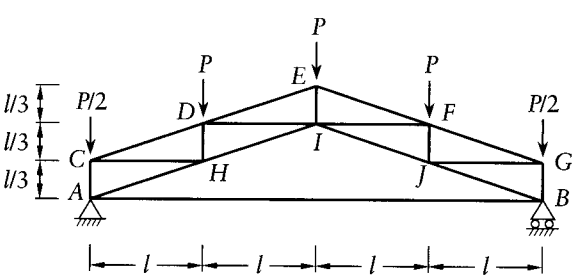

Prob. 8.36

8.37 Use virtual work to verify any number of the equations in Appendix B.

Chapter 9

Further energy theorems

9.1 Introduction

In Chapter 7 the concepts of strain energy and complementary energy were considered, mainly for the purpose of developing the principle of virtual work. There are several other energy theorems of interest in structural analysis, and these will now be discussed.

9.2 Betti's and Maxwell's theorems

Consider any structure, such as that shown in Figure 9.1a, with a series of coordinates 1, $2,\ldots,n,n+1,n+2,\ldots,m$ defined. The F system of forces $F_1,F_2,\ldots,F_n$ acts at coordinates 1 to n (Figure 9.1b), and the Q system of forces $Q_{n+1},Q_{n+2},\ldots,Q_m$ acts at the coordinates $n+1$ to m (Figure 9.1c). Let the displacements caused by the F system alone be $\{D_{1F},D_{2F},\ldots,D_{mF}\}$ and the displacements due to the Q system alone be $\{D_{1Q},D_{2Q}\ldots,D_{mQ}\}$.

Suppose that the F system alone is applied to the structure. The internal work and the external work are equal so that (see Eqs. 6.19 and 7.14)

$$\frac{1}{2}\sum_{i=1}^{n}F_iD_{iF}=\frac{1}{2}\int_v\{\sigma\}_F^T\{\epsilon\}_F dv \tag{9.1}$$

where $\{\sigma\}_F$ and $\{\epsilon\}_F$ are the stress and strain caused by the F system.

Imagine now that when the F system is being applied to the structure, the Q system is already acting, causing stresses σ_Q at any point. The external and internal work during the application of the F system are again equal, so that

$$\frac{1}{2}\sum_{i=1}^{n}F_iD_{iF}+\sum_{i=n+1}^{m}Q_iD_{iF}=\frac{1}{2}\int_v\{\sigma\}_F^T\{\epsilon\}_F dv+\int_v\{\sigma\}_Q^T\{\epsilon\}_F dv \tag{9.2}$$

The second term on each side of this equation is the work due to the Q system while moving along the displacement by the F system. From Eqs. 9.1 and 9.2,

$$\sum_{i=n+1}^{m}Q_iD_{iF}=\int_v\{\sigma\}_Q^T\{\epsilon\}_F dv \tag{9.3}$$

Equations 9.1 and 9.3 may be considered to be applications of the virtual work Eq. 7.46. Alternatively, the above may be considered as a proof of the same virtual work equation.

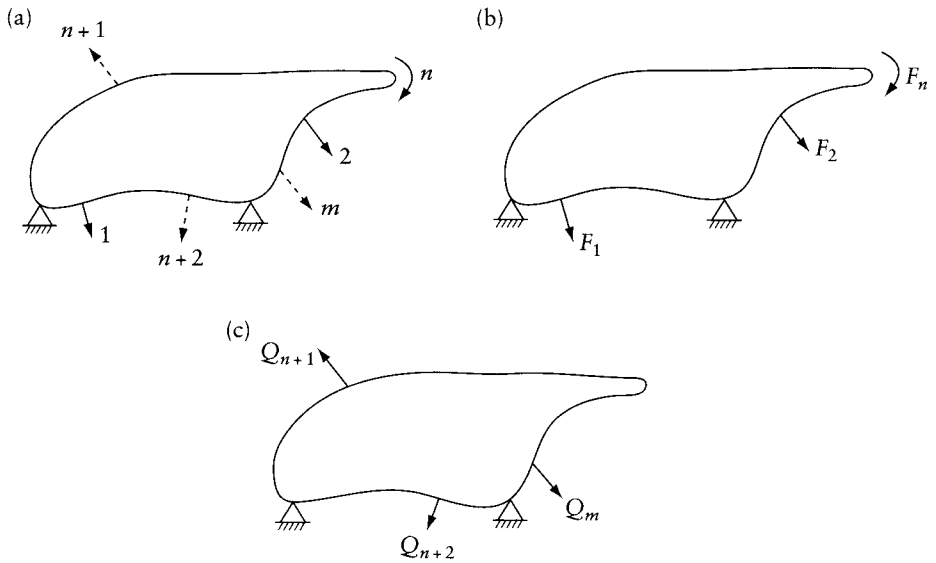

Figure 9.1 Betti's theorem. (a) Coordinate system: $1,2,\ldots,n,n+1,\ldots,m$. (b) F system of forces: $F_1,F_2,\ldots,F_n$; acting at coordinate: $1,2,\ldots,n$; causing displacements: $D_{1F},D_{2F},\ldots,D_{mF}$. (c) Q system of forces: $Q_{n+1},Q_{n+2},\ldots,Q_m$; acting at coordinates: $n+1,n+2,\ldots m$: causing displacements: $D_{1Q}, D_{2Q}, \ldots, D_{mQ}$.

Now, if we assume that the F system is applied first, causing stresses $\{\sigma\}_F$, and the Q system is added subsequently, causing additional stresses $\{\sigma\}_Q$ and strains $\{\epsilon\}_Q$, a similar equation is obtained:

$$\sum_{i=1}^{n} F_i D_{iQ} = \int_v \{\sigma\}_F^T \{\epsilon\}_Q dv \tag{9.4}$$

If the material of the structure obeys Hooke's law, $\{\epsilon\}_Q = [e]\,\{\sigma\}_Q$ and $\{\epsilon\}_F = [e]\,\{\sigma\}_F$; where $[e]$ is constant (see Eqs. 7.8 and 7.11). Therefore, substituting for $\{\epsilon\}$ in Eqs. 9.3 and 9.4, we find that the right-hand sides of the two equations are equal. Hence,

$$\sum_{i=1}^{n} F_i D_{iQ} = \sum_{i=n+1}^{m} Q_i D_{iF} \tag{9.5}$$

This equation is known as *Betti's theorem*, which can be expressed as follows. The sum of the products of the forces of the F system and the displacements at the corresponding coordinates caused by the Q system is equal to the sum of the products of the forces of the Q system and the displacements at the corresponding coordinates caused by the F system. We must remember that the theorem is valid only for linear elastic structures.

We shall now consider Maxwell's theorem, which is a special case of the more general Betti's theorem. Assume that there is only one force $F_i = 1$ in the F system acting at coordinate i, and one force $Q_j = 1$ in the Q system acting at j. Applying Eq. 9.5, we find

$$D_{iQ} = D_{jF} \tag{9.6}$$

Equation 9.6 can be written in the form

$$f_{ij} = f_{ji} \tag{9.7}$$

where f_{ij} is the displacement at i due to a unit force at j, and f_{ji} is the displacement at j due to a unit force at i. Equation 9.7 is called *Maxwell's reciprocal theorem*, which can be stated as follows. In a linear elastic structure, the displacement at coordinate i due to a unit force at coordinate j is equal to the displacement at j due to a unit force acting at i.

The displacements in Eq. 9.7 are the flexibility coefficients. For a structure in which m coordinates are indicated, the flexibility coefficients, when arranged in a matrix of the order $m \times m$, give the flexibility matrix of the structure. This matrix must be symmetrical, by virtue of Eq. 9.7; hence the word "reciprocal" in the theorem. The property of symmetry of the flexibility matrix was proved in another way in Section 6.6.

9.3 Application of Betti's theorem to transformation of forces and displacements

Betti's theorem can be used to transform the actual forces on a structure to equivalent forces at the coordinates.

Consider the structure of Figure 9.2a in which only the bending deformation need be taken into account. The degree of kinematic indeterminacy of the frame is three, as shown in Figure 9.2b (we recall that this represents the number of independent joint displacements). If the flexibility matrix for the frame is known, the independent displacements $\{D\}$ due to external applied forces $\{F\}$ can be determined by the equation $\{D\} = [f]\{F\}$ (Eq. 6.3), provided both the forces and the displacements are at the same three coordinates.

If the frame is subjected to an arbitrary system of forces (Figure 9.2c), they first have to be replaced by equivalent forces at the joints, as discussed in Section 8.7. The fixed-end forces are shown in Figure 9.2d; they are added at each joint and reversed to obtain the equivalent forces $\{F^*\}$ indicated in Figure 9.2e. The forces $\{F^*\}$ act at the coordinates $\{D^*\}$ which are not independent. The displacements $\{D^*\}$ are related to the displacement $\{D\}$ by the geometry of the deformed shape of the frame. These relations can be written as

$$\{D^*\} = [C]\{D\} \tag{9.8}$$

where $[C]$ is determined from the geometry of the frame.

For the frame shown in Figure 9.2a, we have

$$\{D^*\}_{6\times1} = \begin{bmatrix} 0 & 0 & 1 \\ 0 & 0 & 0.75 \\ 1 & 0 & 0 \\ 0 & 0 & 1 \\ 0 & 0 & 0 \\ 0 & 1 & 0 \end{bmatrix}_{6\times3} \{D\}_{3\times1} \tag{9.9}$$

The elements in each column of $[C]$ are the values of the displacements at the D^* coordinates corresponding to a unit displacement at one of the D coordinates. The first two columns are obvious; the elements in the third column can be obtained with the aid of the displacement diagram in Figure 9.2f. (The necessary principles of geometry are discussed in Sections 3.5 and 7.2.)

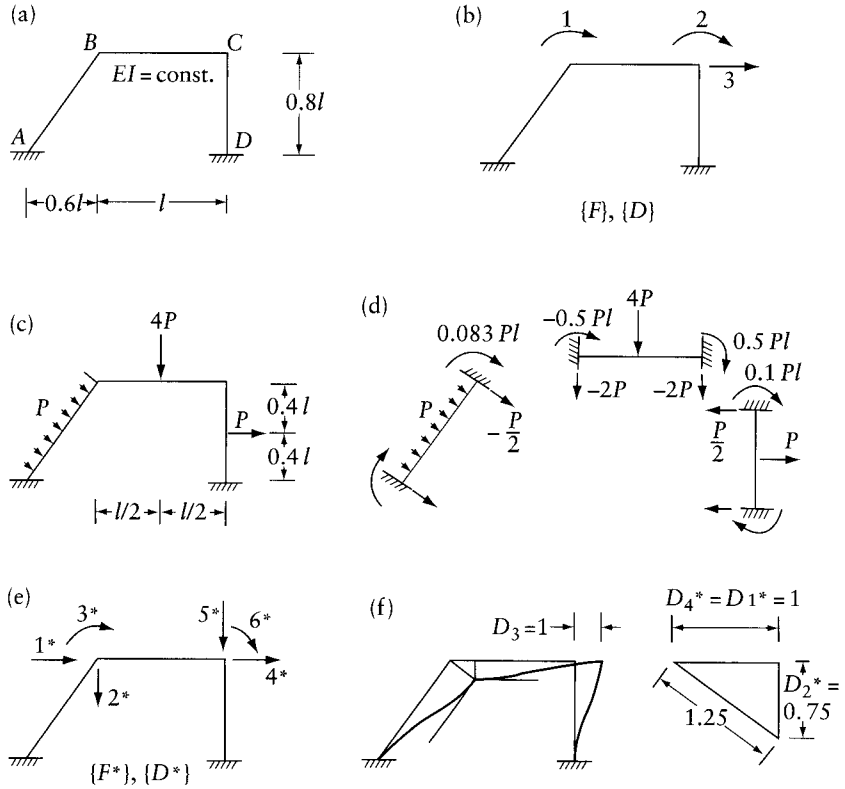

Figure 9.2 Transformation of forces and displacements.

Applying Betti's theorem (Eq. 9.5) to the two systems of forces in Figures 9.2b and e, we find

$$\sum_{i=1}^{3} F_i D_i = \sum_{j=1}^{6} F_j^* D_j^*$$

The second subscript of D and D^* (which indicates the cause of the displacements) is omitted since the F and F^* forces are known to cause the same joint displacements. The matrix form of this equation is

$$\{F\}^T \{D\} = \{F^*\}^T \{D^*\} \tag{9.10}$$

Substituting for $\{D^*\}$ from Eq. 9.8, and taking the transpose of both sides of Eq. 9.10, we obtain

$$\{D\}^T \{F\} = \{D\}^T [C]^T \{F^*\}$$

whence the equation for the transformation of forces is

$$\{F\} = [C]^T \{F^*\} \tag{9.11}$$

Equation 9.11 shows that if displacements $\{D\}$ are transformed to displacements $\{D^*\}$ using a transformation matrix $[C]$ (Eq. 9.8), then $[C]^T$ can be used to transform forces $\{F^*\}$ to forces $\{F\}$. The elements in the jth column of $[C]$ in Eq. 9.8 are the displacements at the D^* coordinates corresponding to a displacement $D_j = 1$ while the displacements are zero at the other D coordinates. It is therefore apparent that $[C]$ cannot be formed unless the displacements $\{D\}$ are independent of one another (see Section 3.5).

As an example of the use of Eqs. 9.8 and 9.11, consider the frame in Figure 9.3a. In a general case, when axial deformations are included, the frame has three degrees of freedom as shown in the figure by the coordinates referring to displacements $\{D\}$ or forces $\{F\}$. The displacements $\{D\}$ can be transformed to displacements $\{D^*\}$ along principal axes of the member cross sections by use of Eq. 9.8. The transformation matrix $[C]$ in this case is

$$[C] = \begin{bmatrix} [t]_1 \\ \hline [t]_2 \end{bmatrix}$$

where

$$[t]_i = \begin{bmatrix} \cos\alpha_i & \sin\alpha_i & 0 \\ -\sin\alpha_i & \cos\alpha_i & 0 \\ 0 & 0 & 1 \end{bmatrix}$$

and i refers to the number of the member. This type of transformation will be used in Chapter 21 for forces or displacements from coordinates along the principal axes of the member cross section to coordinates parallel to a common set of axes for the whole structure, referred to as global or general axes.

If we now apply Eq. 9.11, we transform forces at the ends of members $\{F^*\}$ to forces at the D coordinates, as follows:

$$\{F\} = \begin{bmatrix} \cos\alpha_1 & -\sin\alpha_1 & 0 & \cos\alpha_2 & -\sin\alpha_2 & 0 \\ \sin\alpha_1 & \cos\alpha_1 & 0 & \sin\alpha_2 & \cos\alpha_2 & 0 \\ 0 & 0 & 1 & 0 & 0 & 1 \end{bmatrix} \{F^*\}$$

The elements of the jth column of the rectangular matrix in this equation can be checked using the fact that they are the components of a force $F_j^* = 1$ at the coordinates in Figure 9.3a.

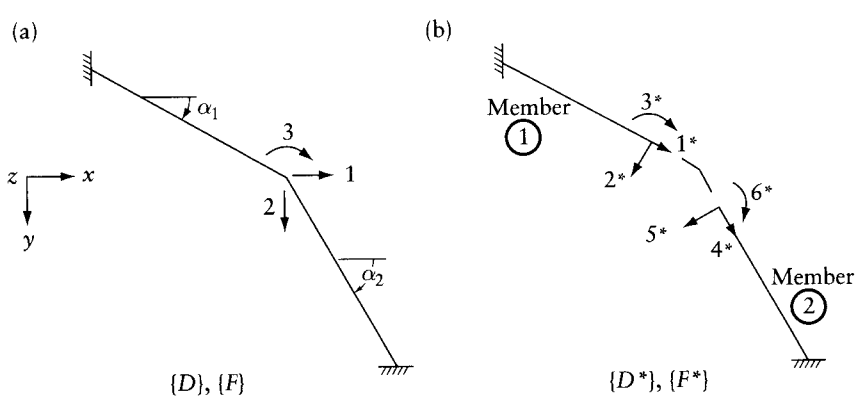

Figure 9.3 Transformation of forces and displacements from coordinates along principal axes of member cross sections to coordinates parallel to general axes.

In some cases, forces $\{F\}$ at global coordinates can be easily related to member end-forces $\{F^*\}$ at member coordinates by

$$\{F^*\} = [B]\,\{F\} \tag{9.12}$$

Using Betti's theorem, the corresponding displacements can be transformed by the equation

$$\{D\} = [B]^T\,\{D^*\} \tag{9.13}$$

For application of Eqs. 9.12 and 9.13, consider the global and member coordinates indicated on the statically determinate frame in Figures 9.4a and b. By simple statics, the transformation of forces in Eq. 9.12 can be made by

$$\{F^*\} = \left[\begin{array}{ccc} \cos\alpha_1 & \sin\alpha_1 & 0 \\ -\sin\alpha_1 & \cos\alpha_1 & 0 \\ -l_2\sin\alpha_2 & l_2\cos\alpha_2 & 1 \\ \hline -\cos\alpha_2 & -\sin\alpha_2 & 0 \\ \sin\alpha_2 & -\cos\alpha_2 & 0 \\ l_2\sin\alpha_2 & -l_2\cos\alpha_2 & -1 \end{array}\right] \{F\} \tag{9.14}$$

The 6×3 matrix in this equation stands for $[B]$ in Eq. 9.12. The elements in any column i of the matrix are equal to the member end-forces at 1^* to 6^* due to $F = 1$, with $i = 1, 2$ or 3 (Figure 9.4), and using Eq. 9.13, we write

$$\{D\} = \left[\begin{array}{ccc|ccc} \cos\alpha_1 & -\sin\alpha_1 & -l_2\sin\alpha_2 & -\cos\alpha_2 & \sin\alpha_2 & l_2\sin\alpha_2 \\ \sin\alpha_1 & \cos\alpha_1 & l_2\cos\alpha_2 & -\sin\alpha_2 & -\cos\alpha_2 & -l_2\cos\alpha_2 \\ 0 & 0 & 1 & 0 & 0 & -1 \end{array}\right] \{D^*\} \tag{9.15}$$

We can now check that the elements in the jth column of the rectangular matrix in this equation are the displacements $\{D\}$ corresponding to $D_j^* = 1$ with $D_i^* = 0$ when $i \neq j$.

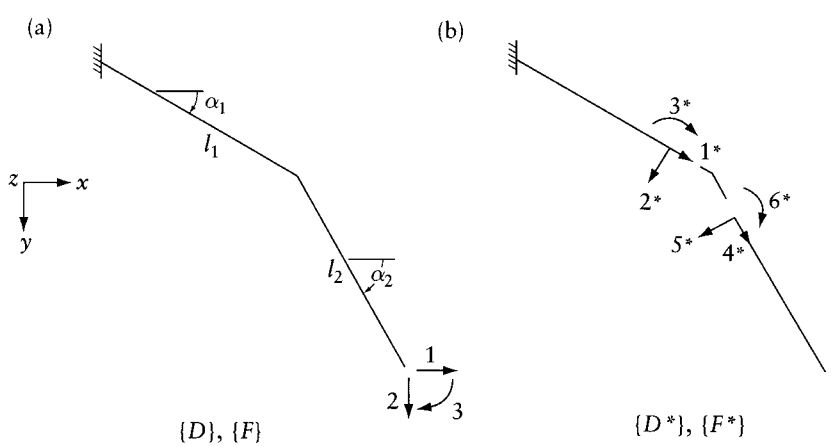

Figure 9.4 Transformation of forces and displacements using Eqs. 9.14 and 9.15.

We note that the elements in any column of matrix $[B]$ in Eq. 9.14 are member end-forces caused by a unit load at one of the D coordinates in Figure 9.4a (see Prob. 9.2).

Example 9.1: Plane frame in which axial deformation is ignored

Use Eq. 9.11 to determine the restraining forces at the three coordinates in Figure 9.2b corresponding to the external loading in Example 5.3 (see Figure 9.2c).

The components of the fixed-end forces (Figure 9.2d) along the coordinates $1,2,\ldots,6$ in Figure 9.2e are

$$\{F^*\} = \begin{Bmatrix} -0.4\,P \\ -2.3\,P \\ -0.417\,Pl \\ -0.5\,P \\ -2.0\,P \\ 0.6\,Pl \end{Bmatrix}$$

The first three elements of this vector are resultants of the internal forces at end B of members AB and BC. The remaining three elements of the vector can be calculated in a similar way.

Substituting for $[C]^T$ from Eq. 9.9 in Eq. 9.11, we obtain

$$\{F\} = \begin{bmatrix} 0 & 0 & 1 & 0 & 0 & 0 \\ 0 & 0 & 0 & 0 & 0 & 1 \\ 1 & 0.75 & 0 & 1 & 0 & 0 \end{bmatrix} P \begin{Bmatrix} -0.4 \\ -2.3 \\ -0.417l \\ -0.5 \\ -2.0 \\ 0.6 \end{Bmatrix} = P \begin{Bmatrix} -0.417l \\ 0.60l \\ -2.625 \end{Bmatrix}$$

which is identical with the forces calculated by resolving along the axes of the members in Example 5.3.

9.4 Transformation of stiffness and flexibility matrices

Consider a coordinate system on a linear structure defining the location and direction of forces $\{F\}$ and displacements $\{D\}$, and let the corresponding stiffness matrix be $[S]$ and the flexibility matrix $[f]$. Another system of coordinates is defined for the same structure referring to forces $\{F^*\}$ and displacements $\{D^*\}$, with the stiffness and flexibility matrices $[S^*]$ and $[f^*]$ respectively. If the displacements or forces at the two systems of coordinates are related by

$$\left.\begin{aligned} \{D\} &= [H]\,\{D^*\} \\ \text{or} \qquad & \\ \{F^*\} &= [H]^T\,\{F\} \end{aligned}\right\} \tag{9.16}$$

then the stiffness matrix $[S]$ can be transferred to $[S^*]$ by the equation

$$[S^*] = [H]^T\,[S]\,[H] \tag{9.17}$$

Also, when the forces at the two coordinate systems are related:

$$\left.\begin{aligned} &\{F\} = [L]\,\{F^*\} \\ \text{or} \qquad & \\ &\{D^*\} = [L]^T\,\{D\} \end{aligned}\right\} \tag{9.18}$$

the flexibility matrix $[f^*]$ can be derived from $[f]$ by

$$[f^*] = [L]^T[f]\,[L] \tag{9.19}$$

We should note that the transformation matrices $[H]$ or $[L]^T$ are formed by geometrical relations of the displacements $\{D\}$ and $\{D^*\}$, and it follows that these relations are valid regardless of the forces applied at the coordinates. The two systems of forces $\{F\}$ and $\{F^*\}$ are equivalent to each other, which means that the forces $\{F\}$ produce displacements $\{D\}$ and $\{D^*\}$ of the same magnitude as would be caused by the forces $\{F^*\}$. Also, the systems $\{F\}$ and $\{F^*\}$ do the same work to produce the displacement $\{D\}$ or $\{D^*\}$.

For the proof of Eq. 9.17, we assume that the structure is subjected to forces $\{F\}$ and we express the work done by these forces by Eq. 6.27, viz.

$$W = \frac{1}{2}[D]^T[S]\,\{D\} \tag{9.20}$$

Substituting for $\{D\}$ from Eq. 9.16, we obtain

$$W = \frac{1}{2}\{D^*\}^T[H]^T[S][H]\,\{D^*\}$$

Now, if we assume the structure to be subjected to forces $\{F^*\}$ and apply Eq. 6.27 again, we obtain

$$W = \frac{1}{2}\{D^*\}^T[S^*]\,\{D^*\}$$

A comparison of the two expressions for W gives the relation between the matrices $[S^*]$ and $[S]$, that is, Eq. 9.17.

If the work is expressed in terms of the forces and flexibility (Eq. 6.26), the proof of Eq. 9.19 is established.

For an application of Eqs. 9.17 and 9.19, consider the cantilever in Figure 9.5 with the part AB rigid and BC of flexural rigidity EI. Two coordinate systems are defined in Figures 9.5a and b. The stiffness matrix corresponding to the coordinates in Figure 9.5a is (see Appendix D)

$$[S] = \begin{bmatrix} \dfrac{12EI}{c^3} & \dfrac{6EI}{c^2} \\ \dfrac{6EI}{c^2} & \dfrac{4EI}{c} \end{bmatrix}$$

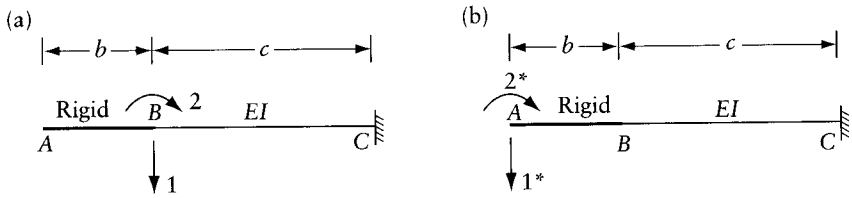

Figure 9.5 Cantilever used to illustrate the application of Eqs. 9.17 and 9.19. (a) Coordinate system referring to displacements $\{D\}$ and forces $\{F\}$. (b) Coordinate system referring to displacements $\{D^*\}$ and forces $\{F^*\}$.

From geometrical relations between the displacements at the two coordinates, the transformation matrix $[H]$ in Eq. 9.16 is

$$[H]=\begin{bmatrix} 1 & b \\ 0 & 1 \end{bmatrix}$$

and the application of Eq. 9.17 gives

$$[S^*]=EI\begin{bmatrix} \dfrac{12}{c^3} & \text{symmetrical} \\ \dfrac{12b}{c^3}+\dfrac{6}{c^2} & \dfrac{4}{c}+\dfrac{12b^2}{c^3}+\dfrac{12b}{c^2} \end{bmatrix}$$

For the application of Eq. 9.19, we first use geometrical relations to generate the transformation matrix $[L]^T$ defined in Eq. 9.18:

$$[L]^T=\begin{bmatrix} 1 & -b \\ 0 & 1 \end{bmatrix}$$

and

$$[f]=\begin{bmatrix} \dfrac{c^3}{3EI} & -\dfrac{c^2}{2EI} \\ -\dfrac{c^2}{2EI} & \dfrac{c}{EI} \end{bmatrix}$$

Substituting in Eq. 9.19 gives

$$[f^*]=\frac{1}{EI}\begin{bmatrix} \dfrac{c^3}{3}+bc^2+b^2c & \text{symmetrical} \\ -(c^2+bc) & c \end{bmatrix}$$

This matrix can be derived by calculation of the displacements $\{D^*\}$ due to unit values of the forces F_1^* and F_2^*, which should, of course, give the same result.

We recall that for the validity of Eqs. 9.17 and 9.19, the geometrical relations between $\{D\}$ and $\{D^*\}$ in Eqs. 9.16 and 9.18 must be true for all values of the forces $\{F\}$ and $\{F^*\}$, and it can

be easily seen that this is satisfied in the above example. If, however, the member AB is flexible, the geometrical relations do not hold when forces $\{F^*\}$ are applied and the transformation of stiffness and flexibility matrices cannot be made.

9.5 Stiffness matrix of assembled structure

The stiffness matrix $[S]$ of a structure formed by the assemblage of members can be obtained from the stiffness matrices of its members.

Consider the structure shown in Figure 9.6a and the coordinate system in Figure 9.6b. The external work, which is also equal to the strain energy of the structure, is $W = U = \frac{1}{2}\{D\}^T [S] \{D\}$, where $[S]$ is the stiffness matrix of the structure corresponding to the coordinates in Figure 9.6b.

The same strain energy is obtained from the sum of the values of strain energy of the individual members. This sum is equal to the work done by the member end-forces $\{F^*\}$ undergoing the displacements $\{D^*\}$ at the coordinates in Figure 9.6c. Thus,

$$U = \frac{1}{2}\{D^*\}^T [S_m] \{D^*\} \tag{9.21}$$

where $[S_m]$ is the stiffness matrix of the unassembled structure

$$[S_m] = \begin{bmatrix} [S_m]_1 & & \\ & [\ldots] & \\ & & [S_k] \end{bmatrix}$$

$[S_m]_i$ is the stiffness matrix of the ith member corresponding to the $\{D^*\}$ coordinates at its ends, and k is the number of members.

The displacements $\{D^*\}$ and $\{D\}$ are related by geometry so that $\{D^*\} = [C] \{D\}$; substituting this equation into Eq. 9.21, we obtain

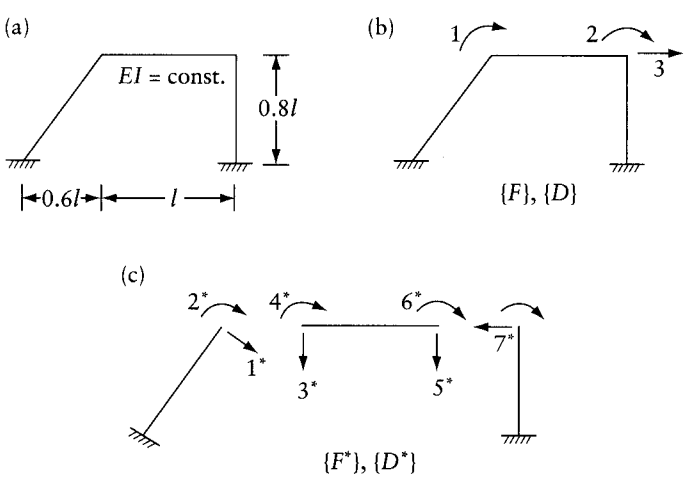

Figure 9.6 Frame considered in Example 9.2.

$$U = \frac{1}{2}\{D\}^T[C]^T[S_m]\,[C]\,\{D\} \tag{9.22}$$

From a comparison of Eqs. 9.20 and 9.22, it can be seen that

$$[S]_{n\times n} = [C]^T_{p\times n}\,[S_m]_{p\times p}\,[C]_{p\times n} \tag{9.23}$$

where n is the number of displacements $\{D\}$, and p is the number of displacements $\{D^*\}$.

Many of the elements of the matrices in this equation are zero. For this reason, it may be more convenient for computer programming to use Eq. 9.23 in the form

$$[S] = \sum_i^k [C]_i^T[S_m]_i\,[C]_i \tag{9.24}$$

where $[C]_i$ is the matrix relating the coordinates $\{D^*\}$ at the ends of the ith member to the structure coordinates $\{D\}$.

The member coordinates D^* are usually chosen along the principal axes of the member cross section at its two ends; thus, the member stiffness $[S_m]$ is normally readily available (see, for example, Eqs. 6.6, 6.7, and 6.8).

Example 9.2: Plane frame with inclined member

Find the stiffness matrix of the frame shown in Figure 9.6a using Eq. 9.24. (The stiffness matrix of the same frame was derived by a different procedure in Example 5.3.)

From geometry of the frame, [C] is determined as in Section 9.3:

$$[C] = \begin{bmatrix} [C]_1 \\ [C]_2 \\ [C]_3 \end{bmatrix} = \left[\begin{array}{ccc} 0 & 0 & 1.25 \\ 1 & 0 & 0 \\ - & - & - \\ 0 & 0 & 0.75 \\ 1 & 0 & 0 \\ 0 & 0 & 0 \\ 0 & 1 & 0 \\ - & - & - \\ 0 & 0 & -1 \\ 0 & 1 & 0 \end{array}\right]$$

Then,

$$[S_m] = \begin{bmatrix} [S_m]_1 & & \\ & [S_m]_2 & \\ & & [S_m]_3 \end{bmatrix}$$

where

$$[S_m]_1 = \begin{bmatrix} \dfrac{12EI}{l^3} & \text{symmetrical} \\ -\dfrac{6EI}{l^2} & \dfrac{4EI}{l} \end{bmatrix}$$

$$[S_m]_2 = \begin{bmatrix} \frac{12EI}{l^3} & & \text{symmetrical} & \\ \frac{6EI}{l^2} & \frac{4EI}{l} & & \\ -\frac{12EI}{l^3} & -\frac{6EI}{l^2} & \frac{12EI}{l^3} & \\ \frac{6EI}{l^2} & \frac{2EI}{l} & -\frac{6EI}{l^2} & \frac{4EI}{l} \end{bmatrix}$$

and

$$[S_m]_3 = \begin{bmatrix} \frac{12EI}{(0.8l)^3} & \text{symmetrical} \\ \frac{6EI}{(0.8l)^2} & \frac{4EI}{0.8l} \end{bmatrix}$$

Applying Eq. 9.24,

$$[S] = \sum_{i=1}^{3} [C]_i^T [S_m]_i [C]_i = EI \begin{bmatrix} \frac{8}{l} & & \text{symmetrical} \\ \frac{2}{l} & \frac{9}{l} & \\ \frac{-3}{l^2} & -\frac{4.875}{l^2} & \frac{48.938}{l^3} \end{bmatrix}$$

9.6 Potential energy

Consider an elastic structure subjected to force $\{F\}$ at n independent coordinates causing displacements $\{D\}$ at the same coordinates. If we assume the potential energy of the forces in the initial configuration to be zero, the *potential energy of the external forces* in the deformed configuration is defined as

$$V = -\sum_{i=1}^{n} F_i D_i \tag{9.25}$$

The sum of the potential energy of the external forces V and the strain energy U is called the *total potential energy:*

$$\Phi = V + U \tag{9.26}$$

Substituting Eqs. 9.25 and 7.7 in the above equation, we obtain

$$\Phi = -\sum_{i=1}^{n} F_i D_i + \sum_{m=1}^{6} \int_v \int_o^{\epsilon_{fm}} \sigma_m d\epsilon_m dv \tag{9.27}$$

where σ_m and ϵ_m are the values of the six stress and strain components as the forces increase from {0} to their final values {F}, and ϵ_{fm} is the final value of a strain component (see Section 7.3).

Now, let the structure acquire a configuration slightly different from the equilibrium position with the compatibility maintained at the supports, and let the corresponding change in {D} be the small virtual displacements $\{\overline{D}\}$ and the corresponding change in strain components at any point be the virtual strain vector $\{\overline{\epsilon}\}$. The change in the total potential energy is

$$\Delta\Phi = -\sum_{i=1}^{n} F_i\overline{D}_i + \int_v \{\sigma\}^T\{\overline{\epsilon}\}dv \tag{9.28}$$

where $\{\sigma\}$ are the final values of stress components.

By the principle of virtual work (Eq. 7.46), we have

$$\sum_{i=1}^{n} F_i\overline{D}_i = \int_v \{\sigma\}^T\{\overline{\epsilon}\}dv \tag{9.29}$$

and we conclude that the right-hand side of Eq. 9.28 is zero. Hence, there is no change in potential energy when the structure is given a compatible virtual small displacement from the equilibrium position.

This conclusion can serve a useful purpose when the actual deformed shape of the structure is not known. The actual displacement at any point (and hence the strain) is expressed by an assumed displacement function in terms of the unknown displacements {D}. The structure is then given a small virtual displacement ∂D_i at coordinate i, without change of the displacement at the other coordinates. Since the corresponding change in the total potential energy is zero, we can write

$$\frac{\partial\Phi}{\partial D_i} = 0 \tag{9.30}$$

By substituting $i = 1, 2, \ldots, n$ a system of simultaneous equations can be written from which the displacements {D} can be calculated. Equation 9.30 is, in fact, an equilibrium equation identical with Castigliano's Eq. 7.54. In other words, the use of potential energy concept leads to the same equations as Castigliano's theorem, Part I; the two approaches differ only in form.

Equation 9.30 is the *principle of stationary potential energy* and may be stated as follows. Of all deformed configurations compatible with support conditions, the one which satisfies equilibrium conditions corresponds to a stationary potential energy. It should be noted that this theorem is valid for linear and nonlinear structures.

It can be proved that the stationary value of the potential energy is minimum for stable structures and is maximum if the structure is unstable, and the principle can therefore be used for the derivation of critical loads.[1]

In the special case of a linear structure, the principle of stationary potential energy, Eq. 9.30, Castigliano's first theorem (Eq. 7.54) and the unit-displacement theorem (Eq. 7.50) all lead to the same equilibrium equation. We prove this by differentiating Eqs. 7.14 or 7.17 for the strain energy of a linear structure with respect to the final value D_j of the displacement at j; we obtain

$$\frac{\partial U}{\partial D_j} = \int_v \{\sigma\}^T \frac{\partial}{\partial D_j}\{\epsilon\}dv \tag{9.31}$$

1 Hoff, N. J., *The Analysis of Structures*, Wiley, New York, 1956. See also, Timoshenko, S. P. and Gere, J. M., *Theory of Elastic Stability* 2nd ed., McGraw-Hill, New York, 1961, Section 2.8.

where $\{\epsilon\}$ are the final strain components. From the condition of linearity, we have

$$\frac{\partial}{\partial D_j}\{\epsilon\} = \{\epsilon_{uj}\} \tag{9.32}$$

where $\{\epsilon_{uj}\}$ is the strain component at any point corresponding to a unit virtual displacement at j. Substitution of Eq. 9.32 in Eq. 9.31 and the result in Eq. 7.54 gives Eq. 7.50.

9.7 General

The energy principles are based on the law of conservation of energy which requires that the work done by external forces on an elastic structure be stored in the form of strain energy which is completely recovered when the load is removed. Betti's law derived from this law, applied to linear structures, serves a useful purpose in transformation of information given in one form into another. The equations derived in Sections 9.3, 9.4, and 9.5 are examples of transformation equations which are useful in structural analysis.

The energy theorems presented in the remaining sections lead, in the case of linear structures, to equations which were derived in a different manner in earlier chapters. For example, Castigliano's Eq. 7.54 and the principle of stationary potential energy, Eq. 9.30, are the same as the equilibrium equations used in the displacement method. It is therefore apparent that the energy principles are not merely methods of calculation of displacements but they can form the basis for derivation of equations satisfying the requirements of equilibrium and compatibility.

Some of the energy equations derived are valid both for linear and nonlinear structures, and this was pointed out in each case. The analysis of nonlinear structures leads to some mathematical difficulties owing to the form of the stress–strain relation.

Problems

9.1 From considerations of statical equilibrium derive the matrix $[B]$ in the equation $\{F^*\} = [B]\{F\}$ relating the forces in (a) of the figure to the corresponding member end-forces in (b). Then write: $\{D\} = [B]^T\{D^*\}$ and check by geometry columns 6, 9, 10, and 11 of $[B]^T$.

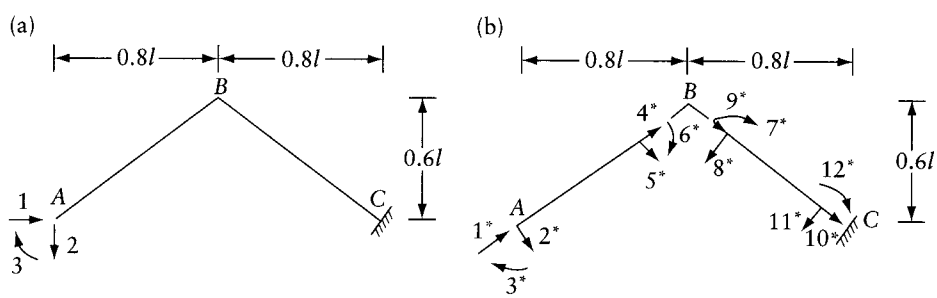

Prob. 9.1 (a) Forces $\{F\}$ and displacements $\{D\}$. (b) Member end-forces $\{F^*\}$ and displacements $\{D^*\}$.

9.2 Solve Prob. 9.1 considering the coordinates 3*, 6*, 9*, and 12* only. Then, neglecting shear and axial deformation, derive the flexibility matrix corresponding to the coordinates in Figure (a) using Eq. 8.32 and evaluating the integrals by Eq. 8.18.

9.3 Following the procedure used in Prob. 9.2, derive the flexibility matrix of the structure shown in the figure corresponding to the coordinates indicated. Ignore axial and shear deformations and assume EI constant.

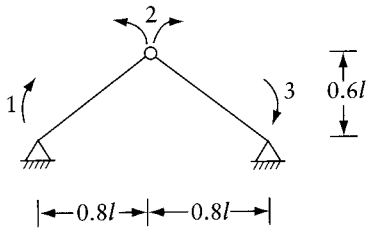

Prob. 9.3

9.4 Apply the requirements of Prob. 9.3 to the structure in the figure. Coordinates 1, 2, and 3 represent relative displacements of the two sides of a cut section at the top of the left column.

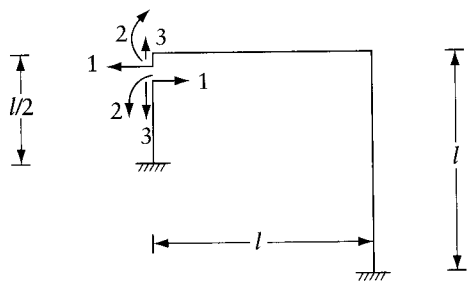

Prob. 9.4

9.5 Write the transformation matrix [C] in the equation $\{D^*\} = [C]\{D\}$, then use Eq. 9.24 to derive the stiffness matrix corresponding to the D coordinates indicated in the figure. Consider only the bending deformation and assume EI constant.

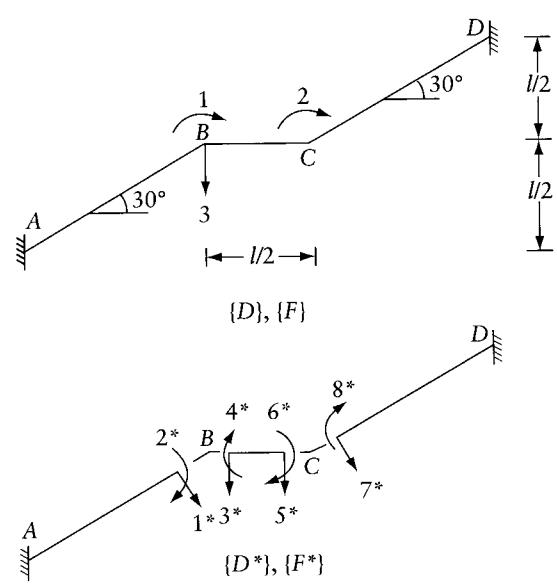

Prob. 9.5

9.6 If the structure in Prob. 9.5 is subjected to a uniform load q per unit length of horizontal projection, use Eq. 9.11 to derive the restraining forces $\{F\}$ necessary to prevent joint displacements.

9.7 Use Eq. 9.24 to solve Prob. 5.21.

9.8 The grid shown in the figure is composed of similar members of length l, flexural rigidity EI, and torsional rigidity GJ. Give the matrices required to derive the stiffness matrix of the grid using Eq. 9.24. Number the members in the order shown in the figure below and take the coordinates for member 3 to be the same as the structure coordinates indicated in the figure. Number the member coordinates for other members in the same order as for member 3.

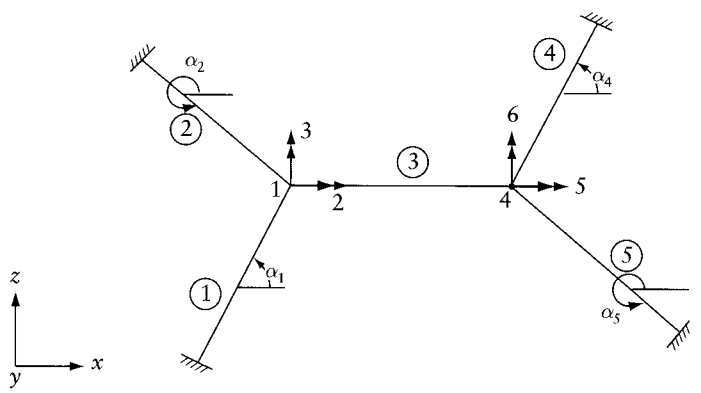

Prob. 9.8

9.9 Transform the stiffness matrix $[S]$ for a beam AB corresponding to the coordinates shown in (a) in the figure to a stiffness matrix $[S^*]$ corresponding to the coordinates shown in (b). The beam is prismatic of flexural rigidity EI and cross-sectional area a. Neglect shear deformations. In part (b) of the figure, AC and AD are rigid arms.

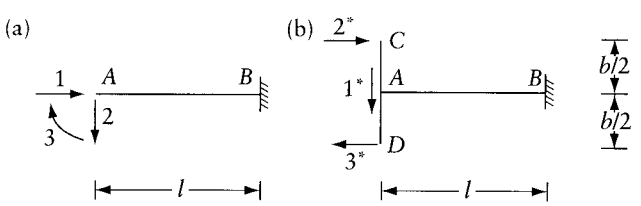

Prob. 9.9 (a) Coordinates representing $\{D\}$ and $\{F\}$. (b) Coordinates representing $\{D^*\}$ and $\{F^*\}$.

9.10 Use Eq. 9.19 to transform the flexibility matrix $[f]$ to $[f^*]$ in Prob. 9.9.

9.11 Write the stiffness matrix $[S]$ corresponding to the coordinate shown in (a), then use Eq. 9.17 to transform this matrix to a stiffness matrix $[S^*]$ corresponding to the coordinates in (b). Consider only bending deformation and take the beam flexural rigidity as EI.

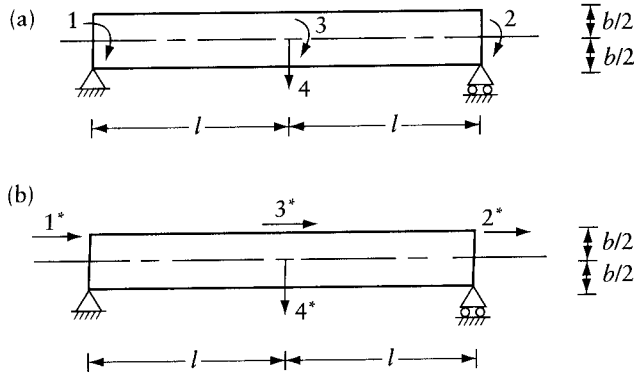

Prob. 9.11 (a) Coordinates for $\{D\}$ and $\{F\}$. (b) Coordinates for $\{D^*\}$ and $\{F^*\}$.

9.12 Use Castigliano's first theorem to find the force F_1 in terms of the displacement D_1 in the beam in the figure. Assume the following approximate equation for the deflection:

$$y = -\frac{D_1}{2} \sin \frac{\pi x}{l}$$

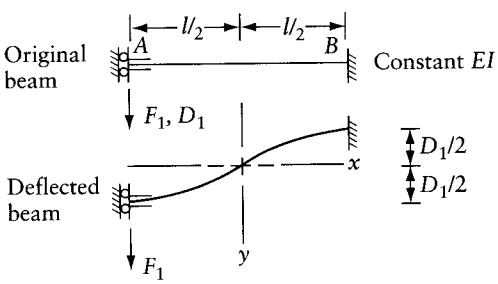

Prob. 9.12

9.13 Solve Prob. 9.12 using the principle of stationary potential energy and assuming that the beam is subjected at its two ends to two axial compressive forces $P = 4EI/l^2$ and that the horizontal movement of end A is allowed to take place freely. Assume the same approximate equation for the elastic line as in Prob. 9.12. *Hint:* The difference between the length of an element ds of the curved beam axis and its projection dx on the x axis is

$$ds - dx = dx\sqrt{1 + \left(\frac{dy}{dx}\right)^2} - dx \simeq \frac{1}{2}\left(\frac{dy}{dx}\right)^2 dx$$

and the horizontal displacement of A is

$$D_2 = \frac{1}{2}\int_{-l/2}^{l/2} \left[\frac{dy}{dx}\right]^2 dx$$

9.14 Solve Prob. 5.1 using Castigliano's theorem, Part I.

9.15 Solve Prob. 5.1 assuming that the stress and strain in an axial direction for any of the members are related by the equation $\sigma = C[\epsilon - (\epsilon^3/10)]$ where c is a constant. All members have the same length l and the same cross-sectional area a.

9.16 Figures a and b represent a typical member of a space truss. One end is supported, and a coordinate system 1* or 1,2, and 3 is defined at the other end. Write a geometry relation $\{D\} = [t]\{D^*\}$ between the displacements at the two coordinate systems; express $[t]$ in terms of $\lambda_{x^*x}, \lambda_{x^*y}$, and λ_{x^*z}, representing, respectively, the cosine of the angles between the local axis x^* and the global directions x, y, and z. Use $[t]$ to derive the member stiffness matrix $[S_m]$ corresponding to the coordinates in global directions (Figure b). Employ the derived stiffness matrix to determine the member forces in the space truss in Figure c by the displacement method. The structure is subjected to a force at A having the components: $\{F_x, F_y, F_z\} = P\{2.0, 2.0, 4.0\}$. Assume $Ea =$ constant.

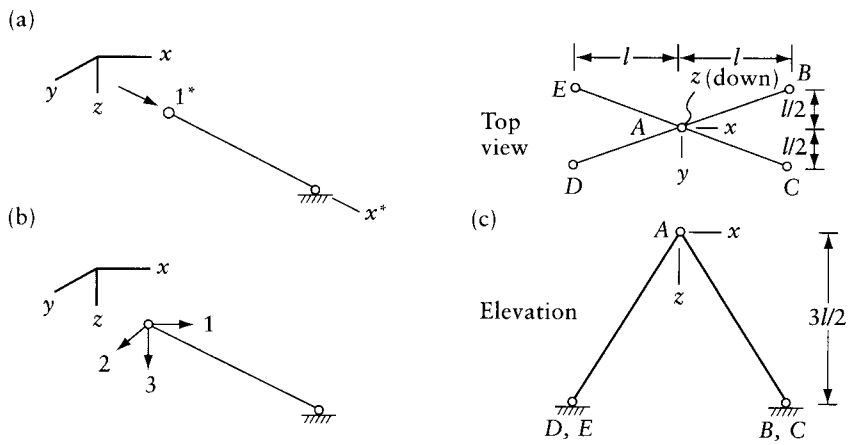

Prob. 9.16

Chapter 10

Displacement of elastic structures by special methods

10.1 Introduction

The calculation of displacements in elastic structures by the method of virtual work (considered in Chapter 8) represents probably the most general approach to the problem. However, in some cases, it may be convenient to apply other, more specialized, methods. Those among them which are most frequently used in practice will be developed in the present chapter.

10.2 Differential equation for deflection of a beam in bending

In Chapter 8 we saw that in the majority of cases the deflection of a beam is primarily due to bending. Thus, it is not unreasonable to ignore the contribution of shear to deflection and to obtain the elastic deflection of a beam by solving the differential equation of the deflected shape (also referred to as elastic line). In this section we shall derive the appropriate differential equations, and in subsequent sections deal with their solution.

Let us consider the beam of Figure 10.1a subjected to arbitrary lateral and axial loads.

Making the usual assumptions in the theory of bending, that plane transverse sections remain plane, and that the material obeys Hooke's law, we can show that (see Eq. 7.23)

$$M = -EI\frac{d^2y}{dx^2} \tag{10.1}$$

where y is the deflection and M is the bending moment at any section x (see Figure 10.1b); EI is the flexural rigidity, which may vary with x. The positive direction of y is indicated in Figure 10.1b and the bending moment is considered positive if it causes tensile stress at the bottom face of the beam.

An element of the beam of length dx is in equilibrium in a deflected position under the forces shown in Figure 10.1c. Summing the forces in the x and y directions, we obtain

$$\left.\begin{aligned} &\frac{dN}{dx} = -p \\ &\text{and} \\ &q = -\frac{dV}{dx} \end{aligned}\right\} \tag{10.2}$$

where N is the thrust, V is the shear, and p and q are the intensity, respectively, of the axial and lateral distributed load. The positive directions of q, p, y, M, V, and N are as indicated in Figure 10.1c.

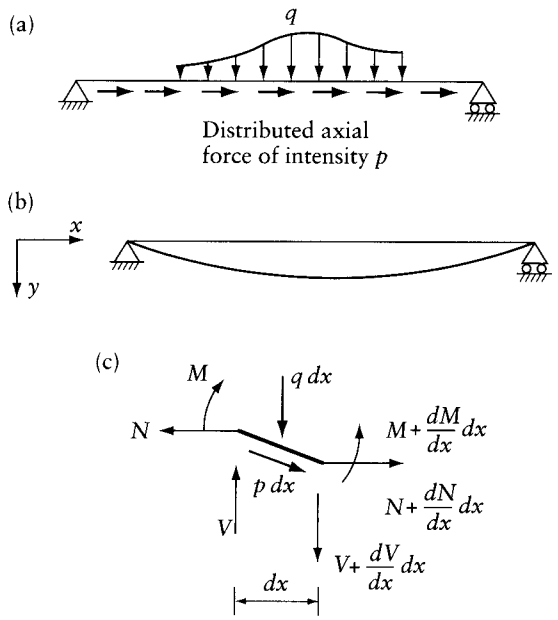

Figure 10.1 Deflection of a beam subjected to lateral and axial load. (a) Beam and loading. (b) Positive direction of deflection. (c) Positive directions of external and internal forces.

Taking moments about the right-hand edge of the element,

$$V dx - N\frac{dy}{dx}dx - \frac{dM}{dx}dx = 0 \tag{10.3}$$

whence

$$\frac{dV}{dx} - \frac{d}{dx}\left(N\frac{dy}{dx}\right) - \frac{d^2M}{dx^2} = 0 \tag{10.3a}$$

Substituting Eq. 10.2, we obtain the differential equation of the elastic line

$$\frac{d^2}{dx^2}\left(EI\frac{d^2y}{dx^2}\right) - \frac{d}{dx}\left(N\frac{dy}{dx}\right) = q \tag{10.4}$$

In the absence of axial forces (i.e. when $N = 0$), Eq. 10.4 becomes

$$\frac{d^2}{dx^2}\left(EI\frac{d^2y}{dx^2}\right) = q \tag{10.5}$$

If, in addition, the beam has a constant flexural rigidity EI, the differential equation of the elastic line is

$$\frac{d^4y}{dx^4} = \frac{q}{EI} \tag{10.6}$$

In a beam-column subjected to axial compressive forces P at the ends, $p = 0$ and $N = -P$, whence Eq. 10.4 becomes

$$\frac{d^2}{dx^2}\left(EI\frac{d^2y}{dx^2}\right) + P\frac{d^2y}{dx^2} = q \tag{10.7}$$

All the equations developed in this section can be applied with a slight modification to a beam on an elastic foundation, that is, to a beam which, in addition to the forces already mentioned, receives transverse reaction forces proportional at every point to the deflection of the beam. (As example, see Figures 10.17a and b.) Let the intensity of the distributed reaction be

$$\bar{q} = -ky$$

where k is the foundation modulus with dimensions of force per (length)^2. The modulus represents the intensity of the reaction produced by the foundation on a unit length of the beam due to unit deflection. The positive direction of reaction $\bar{q}$ is downward. We can therefore use Eqs. 10.1 to 10.7 for a beam on an elastic foundation if the term q is replaced by the resultant lateral load of intensity $q^* = (q + \bar{q}) = (q - ky)$. For example, Eq. 10.5 gives the differential equation of a beam with a variable EI on elastic foundation, subjected to lateral load q with no axial forces, as

$$\frac{d^2}{dx^2}\left[EI\frac{d^2y}{dx^2}\right] = q - ky \tag{10.5a}$$

The differential Eqs. 10.1, 10.4, 10.5, 10.6, and 10.7 have to be solved to yield the lateral deflection y. Direct integration is possible only in a limited number of cases, considered in standard books on strength of materials. In other cases, a solution of the differential equations by other means is necessary. In the following sections, we consider the method of elastic weights, the numerical method of finite differences, and solutions by series.

10.3 Moment–area theorems

The well-known Eq. 10.1 relates the deflection y to the bending moment M. Hence, we can relate the slope of the elastic line and its deflection to the area of the bending moment diagram and obtain two theorems.

(i) The difference in slope between any two points on the elastic curve is numerically equal to the area of the $M/(EI)$ diagram between these two points. This can be proved by integrating d^2y/dx^2 between any two points A and B in Figure 10.2a. From Eq. 10.1,

$$\frac{d^2y}{dx^2} = \frac{d\theta}{dx} = -\frac{M}{EI}$$

Integrating,

$$\int_A^B d\theta = -\int_A^B \frac{M}{EI}\,dx$$

whence

$$\theta_B - \theta_A = -\overline{w}_{AB} \tag{10.8}$$

where $\theta = dy/dx$ is the slope of the elastic line, and $\overline{w}_{AB}$ is the area of the M/(EI) diagram between A and B.

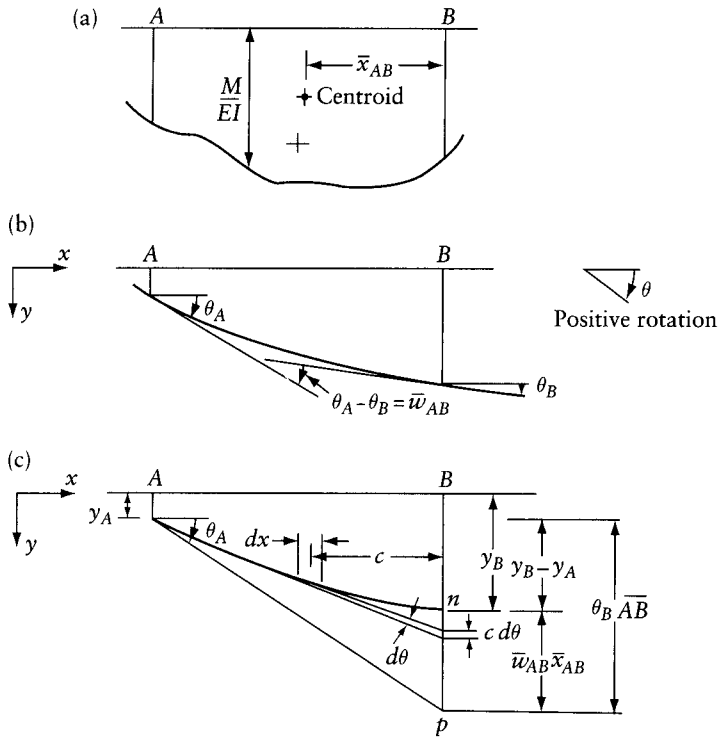

Figure 10.2 Slope, deflection, and moment–area relations. (a) $M/(EI)$ diagram. (b) Slope/moment–area relation. (c) Deflection/moment–area relation.

(ii) The deflection of B from the tangent to the elastic line at A (distance $\overline{np}$ in Figure 10.2c) is numerically equal to the moment of $\bar{w}_{AB}$ about B. From Figure 10.2c, we can see that

$$\overline{np} = \int_A^B c\,d\theta = \int_A^B c\left[\frac{M}{EI}\right] dx = \bar{w}_{AB}\bar{x}_{AB} \tag{10.9}$$

where c is the distance of an element dx from B, and $\bar{x}_{AB}$ is the distance of the centroid of $\bar{w}_{AB}$ from B. Note that the moment of $\bar{w}_{AB}$ is taken about the point where deflection is required.

The difference between the deflection at B and A is

$$y_B - y_A = \theta_A \overline{AB} - \bar{w}_{AB}\bar{x}_{AB} \tag{10.10}$$

According to the sign convention assumed in Eq. 10.2, the angle θ is positive if the deflection causes a rotation of the tangent to the beam in a clockwise direction. Thus, the rotations θ_A and θ_B as indicated in Figure 10.2b are positive. The area $\bar{w}_{AB}$ is positive for a positive bending moment.

Equations 10.8 and 10.10 can be used to calculate deflections in plane frames as shown by the following example.

Example 10.1: Plane frame: displacements at a joint

Determine the displacements D_1, D_2, and D_3 at the coordinates 1, 2, and 3 indicated on the frame in Figure 10.3a. The flexural rigidity of the frame, EI, is constant and only the deformations due to bending need be considered.

The bending moment diagram is drawn in Figure 10.3b. To conform to our sign convention when applying Eqs. 10.8 and 10.10, each member is looked at from inside of the frame as shown by the arrows in Figure 10.3b. The deflection y represents the translation perpendicular to the member considered.

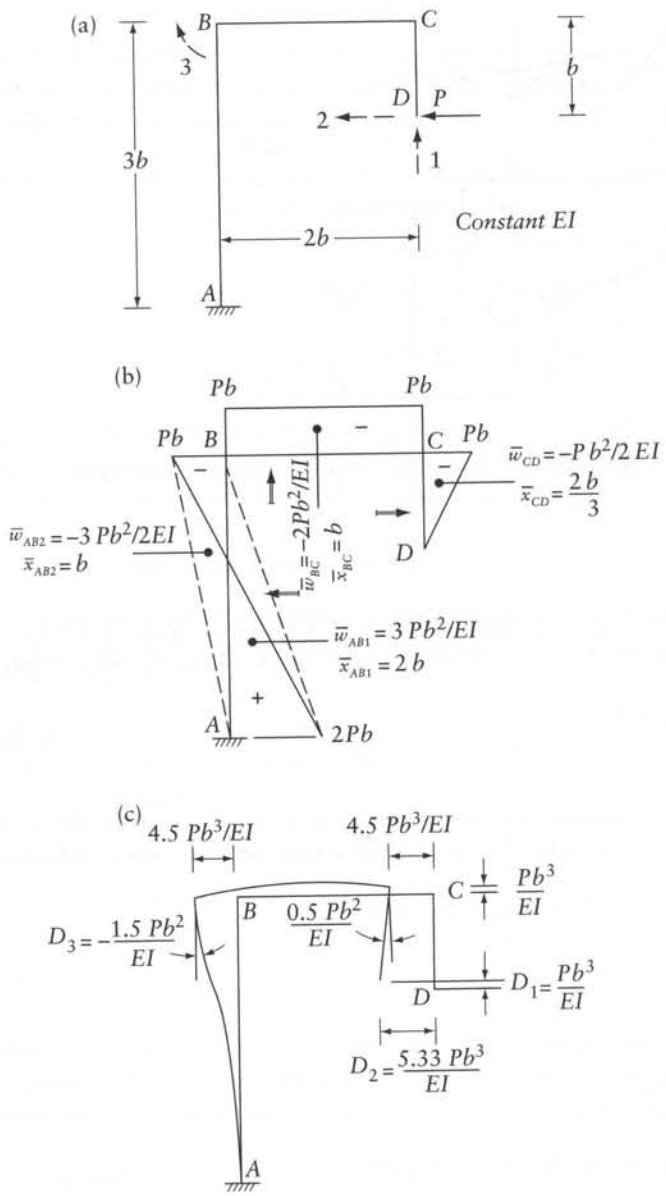

Figure 10.3 Deflection of the plane frame of Example 10.1 by moment–area method.

The deflection and rotation at the fixed end A are zero. Applying Eqs. 10.8 and 10.10 to AB, we obtain

$$\theta_B = -\overline{w}_{AB} = -\frac{1.5Pb^2}{EI}$$

and

$$y_B = -\overline{w}_{AB}\bar{x}_{AB} = -\frac{4.5Pb^3}{EI}$$

(The product $\overline{w}_{AB}\bar{x}_{AB}$ can be determined by adding algebraically the moments of the two triangles with areas $\overline{w}_{AB1}$ and $\overline{w}_{AB2}$.)

Similarly, applying the same equations to beam BC with θ_B as calculated above and the vertical deflection $y_B = 0$, we obtain

$$\theta_C = \theta_B - \overline{w}_{BC} = -\frac{1.5Pb^2}{EI} + \frac{2Pb^2}{EI} = \frac{0.5Pb^2}{EI}$$

and

$$y_C = \theta_B\overline{BC} - \overline{w}_{BC}\bar{x}_{BC} = -\frac{Pb^3}{EI}$$

Finally, we apply Eq. 10.10 to CD, with the horizontal deflection $yc = 4.5Pb^3/EI$, numerically equal to the horizontal translation of B, calculated earlier; hence,

$$y_D = y_C + \theta_C\overline{CD} - \overline{w}_{CD}\bar{x}_{CD} = \frac{Pb^3}{EI}\left[4.5 + 0.5 \times 1.0 + 0.5 \times \frac{2}{3}\right] = \frac{5.33Pb^3}{EI}$$

The deflected shape of the frame is sketched in Figure 10.3c, from which it can be seen that the required displacements are

$$D_1 = \frac{Pb^3}{EI}; \quad D_2 = \frac{5.33Pb^3}{EI}; \quad D_3 = -\frac{1.5Pb^2}{EI}$$

10.4 Method of elastic weights

The method of elastic weights is essentially equivalent to the moment–area method applied for a beam. The procedure is to calculate the rotation and the deflection respectively as the shearing force and the bending moment in a *conjugate beam* subjected to a load of intensity numerically equal to $M/(EI)$ for the actual beam. This load is referred to as elastic weight or, less aptly, as elastic load.

The conjugate beam is of the same length as the actual beam, but the conditions of support are changed, as discussed below. The $M/(EI)$ diagram of the actual beam is treated as the load on the conjugate beam, as shown in Figure 10.4. Positive moment is taken as a positive (downward) load. From the moment–area equations (Eqs. 10.8 and 10.9) it can be shown that at any point in the beam, the shear V and moment M in the conjugate beam are equal, respectively, to the rotation θ and deflection y at the corresponding point in the actual beam.

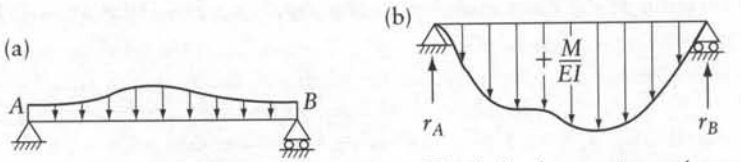

Figure 10.4 Load on actual and conjugate beams.

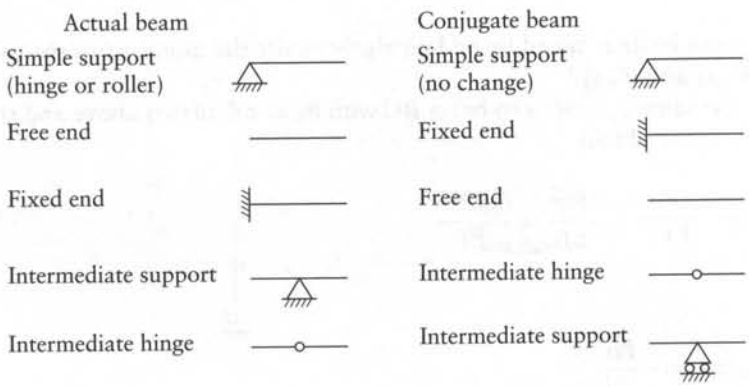

Figure 10.5 Type of support of actual and conjugate beams.

The changes in the type of support between the actual and the conjugate beam are shown in Figure 10.5. These changes are necessary to satisfy the known characteristics of the elastic line of the actual beam. For instance, at a fixed end of the actual beam, the slope and the deflection are zero: this corresponds to no shear and no bending moment in the conjugate beam. Therefore, the corresponding end of the conjugate beam must be free and unsupported.

With the changes in type of support of Figure 10.5, statically determinate beams have corresponding conjugate beams which are also statically determinate. Statically indeterminate beams appear to have unstable conjugate beams. However, such conjugate beams turn out to be in equilibrium with the particular elastic loading corresponding to the $M/(EI)$ diagram. This is illustrated in Example 10.4.

The method of elastic weights can be applied also to arches and portals. The procedure is to divide the axis of the structure into elements of length ds. The relative rotation of the sections at the two ends of the element is then $M\,ds/(EI)$. This quantity is considered as an elastic weight acting on a conjugate simply-supported horizontal beam of the same span as the arch (see, for instance, Prob. 10.6). The bending moment on the conjugate beam is then equal to the vertical deflection of the arch.

Example 10.2: Parity of use of moment–area theorems and method of elastic weights

Use the moment–area–deflection relations of Eqs. 10.8 and 10.10 to show that for a simple beam, such as the beam shown in Figure 10.6a, the slopes θ_A and θ_B at the ends and the deflection y_C at C are equal, respectively, to the shear and the bending of a conjugate simple

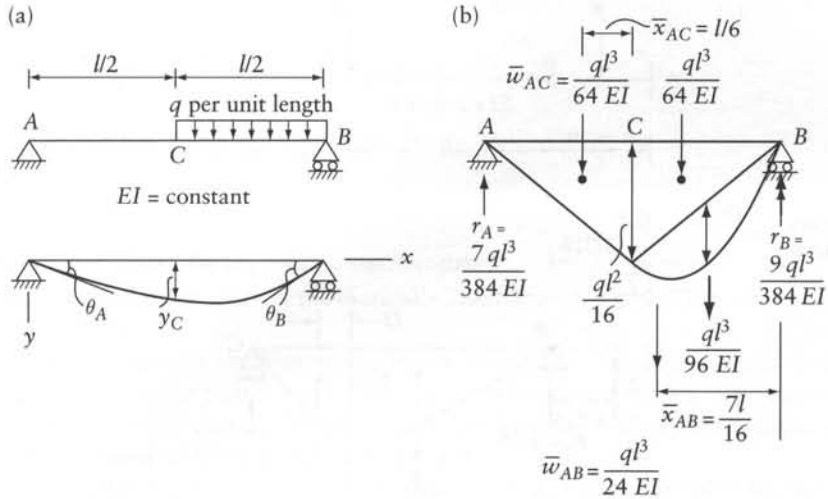

Figure 10.6 Calculations of end rotations and deflections in a simple beam. Example 10.2. (a) Beam dimensions and deflected shape. (b) Bending moment diagram, elastic weights and elastic reactions.

beam carrying the elastic weights shown in Figure 10.6b. Determine θ_A and θ_B and y_C for the beam shown in Figure 10.6a.

Application of Eqs. 10.8 and 10.10 to the bending moment diagrams between A and B and between A and C in Figure 10.6b gives:

$$\theta_B - \theta_A = -\overline{w}_{AB} \tag{a}$$

$$y_B - y_A = \theta_A \overline{AB} - \overline{w}_{AB}\bar{x}_{AB} \tag{b}$$

$$y_C - y_A = \theta_A \overline{AC} - \overline{w}_{AC}\bar{x}_{AB} \tag{c}$$

Substitute $y_A = y_B = 0$ in the above equations and compare the resulting equations with the shearing force and the bending moment due to the elastic weight:

$$\theta_A = \overline{w}_{AB}\bar{x}_{AB}/\overline{AB} = r_A = \text{shearing force at } A$$

$$\theta_B = -(\overline{w}_{AB} - \theta_A) = -r_B = \text{shearing force at } B$$

$$y_C = r_A \overline{AC} - \overline{w}_{AC}\bar{x}_{AC} = \text{bending moment at } C$$

For the beam considered, we can see that:

$$\theta_A = r_A = \frac{ql^3}{24\,EI}\frac{(7/16)l}{l} = \frac{7ql^3}{384\,EI};\quad \theta_B = -\left(\frac{ql^3}{24\,EI} - \frac{7ql^3}{384\,EI}\right) = -r_B = -\frac{9ql^3}{384\,EI}$$

$$y_C = \frac{7ql^3}{384\,EI}\left(\frac{l}{2}\right) - \frac{ql^3}{64\,EI}\left(\frac{l}{6}\right) = \frac{5}{768}\frac{ql^4}{EI}$$

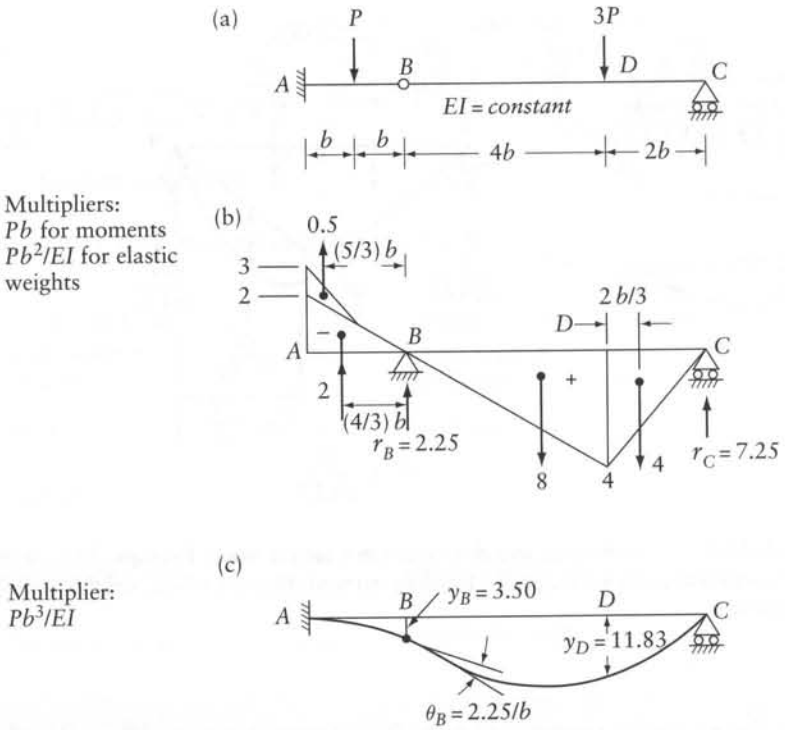

Figure 10.7 Deflection of the beam of Example 10.3 by method of elastic weights. (a) Actual beam. (b) Conjugate beam. (c) Elastic line.

Example 10.3: Beam with intermediate hinge

For the statically determinate beam of Figure 10.7a, find the deflections at B and D and the change in slope between the left- and right-hand sides of the hinge B. The beam has a constant value of EI.

The conjugate beam and the elastic weights on it are shown in Figure 10.7b. The elastic weights are obtained as areas of the different parts of the $M/(EI)$ diagram on the real beam, and they act at the respective centroids of each part. The *elastic reactions* for these elastic loads are calculated in the usual way:

$$r_B = \frac{2.25Pb^2}{EI} \uparrow \text{ and } r_C = \frac{7.25Pb^2}{EI} \uparrow$$

The sudden change θ_B in the slope of the elastic line at the hinge B in the actual beam is equal to the change in shear at the support B of the conjugate beam, which in turn is equal to the elastic reaction r_B. Therefore, the change in slope at B is $\theta_B = 2.25Pb^2/(EI)$ (radians) in the clockwise direction because r_B causes a sudden increase in shear.

The bending moments of the conjugate beam at B and D represent the deflections at these points:

$$y_B = \frac{Pb^2}{EI}\left(2 \times \frac{4}{3}b + 0.5 \times \frac{5}{3}b\right) = 3.5\frac{Pb^3}{EI}$$

and

$$y_D = \frac{Pb^2}{EI}\left(7.25 \times 2b - 4 \times \frac{2b}{3}\right) = 11.83\frac{Pb^3}{EI}$$

The elastic line is sketched in Figure 10.7c.

Example 10.4: Beam with ends encastré

Find the deflection at B in the statically indeterminate beam with constant EI, shown in Figure 10.8a.

The conjugate beam is shown in Figure 10.8b, in which the encastré ends of the actual beam are changed to free ends. The conjugate beam has therefore no supports, but it can be easily checked that the beam is in equilibrium under the elastic weights corresponding to the bending moment on the actual beam.

The elastic loading to the left of point B is equivalent to the components shown in Figure 10.8c. This can be verified by noting that, at any section, the sum of the ordinates of the two diagrams in part (c) of the figure is the same as the corresponding ordinate in part (b). The deflection y_B is equal to the moment of these components about B:

$$y_B = \frac{1}{EI}\left[\frac{Pc^2b^2}{2l^2}\frac{2c}{3} + \frac{Pc^2b}{2l^3}(c^2+b^2)\frac{c}{3} - \frac{Pc^2b}{2l}\frac{c}{3}\right]$$

With $(c+b)=l$, this equation reduces to $y_B = Pc^3b^3/(3EIl^3)$.

10.4.1 Equivalent concentrated loading

The calculation of reactions and bending moments in a beam due to an irregular loading can be simplified by the use of equivalent concentrated loads. This is particularly useful in the application of the method of elastic weights.

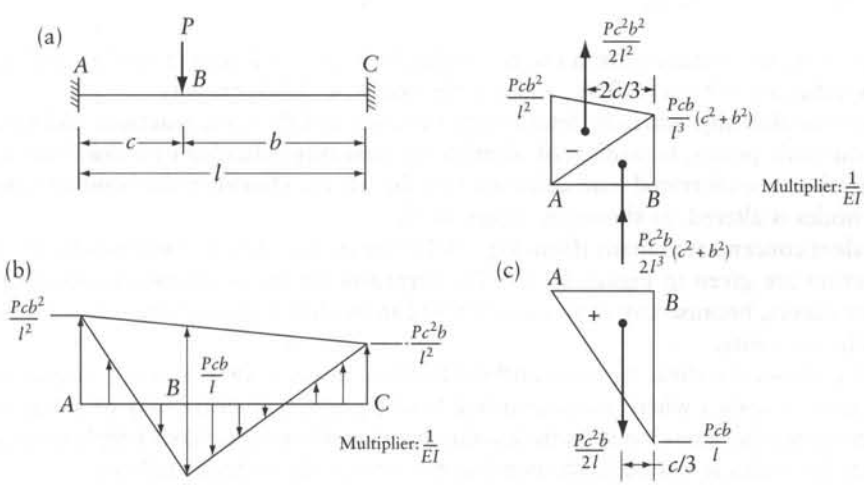

Figure 10.8 Deflection of the statically indeterminate beam of Example 10.4 by method of elastic weights. (a) Actual beam. (b) Conjugate beam. (c) Elastic weights.

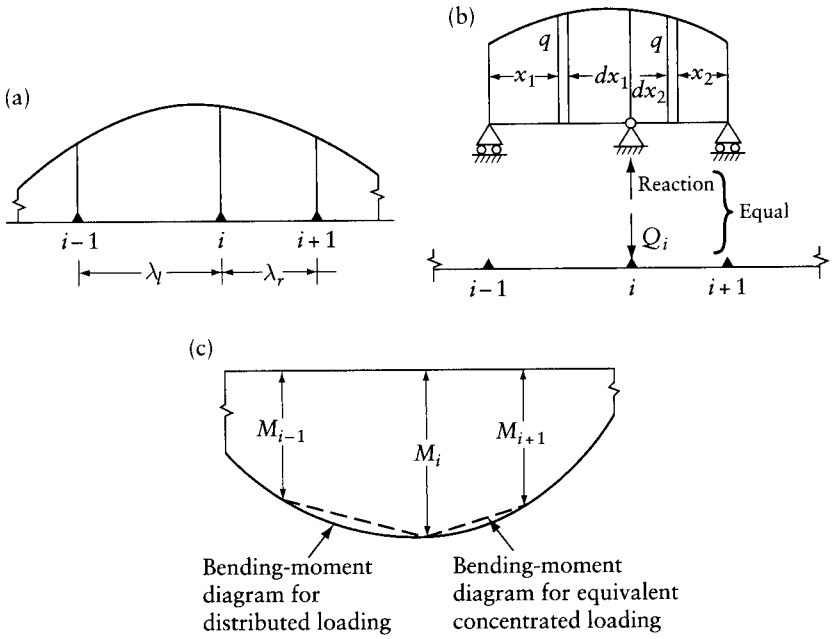

Figure 10.9 Bending moment using equivalent concentrated loading. (a) Distributed load. (b) Equivalent concentrated load at i. (c) Loadings (a) and (b) give the same bending moment at the nodes.

Figure 10.9a shows any three points $i-1$, i, and $i+1$ in a beam subjected to irregular loading. These points will be referred to as nodes. The concentrated load Q_i equivalent to this loading is equal and opposite to the sum of the reactions at i of two simply-supported beams between $i-1$, i, and $i+1$, carrying the same load as that on the actual beam between the nodes considered. Thus,

$$Q_i = \frac{1}{\lambda_l}\int_0^{\lambda_l} x_1 q\,dx_1 + \frac{1}{\lambda_r}\int_0^{\lambda_r} x_2 q\,dx_2 \tag{10.11}$$

where λ_l and λ_r are the distances from i to the nodes $i-1$ and $i+1$ respectively, x_1 and x_2 are the distances indicated in Figure 10.9b, and q is the (variable) load intensity.

It can be proved that any statically determinate structure has the same reactions and bending moments at the node points, regardless of whether the structure is loaded by a distributed load or by an equivalent concentrated load calculated by Eq. 10.11. However, the bending moment between the nodes is altered, as shown in Figure 10.9c.

The equivalent concentrated loads (from Eq. 10.11) for straight-line and second-degree parabolic distribution are given in Figure 10.10. The formulas for the parabolic variation can be used for other curves, because any continuous curve can be closely approximated by a series of small parabolic segments.

Figure 10.11 shows the shearing force and the bending moment diagrams for a beam in the vicinity of a general node i where a concentrated load Q_i acts. The beam may be subjected to loads at other nodes, but there must be no loading between the nodes. From simple statics, the shear between the nodes is related to the bending moment at the nodes as follows:

$$V_{i-\frac{1}{2}} = (M_i - M_{i-1})/\lambda_l$$

(a)

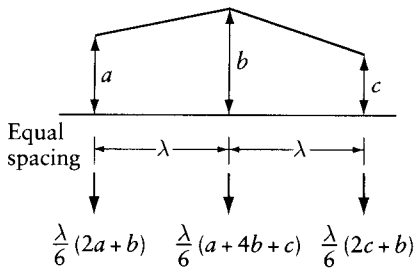

(b)

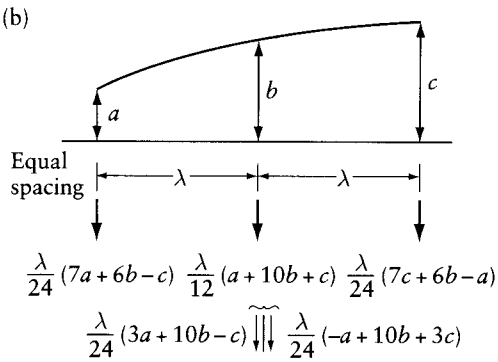

(c)

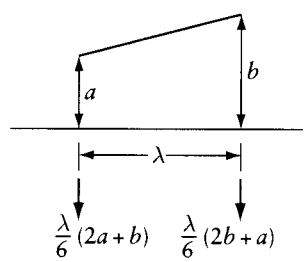

(d)

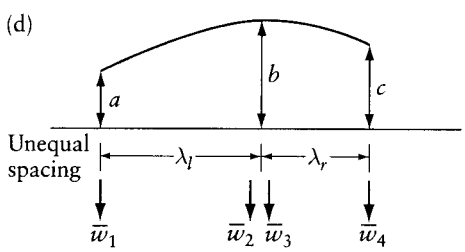

$$\bar{w}_1 = \frac{\lambda_l}{12}\left\{a\left[4-\frac{(\lambda_l/\lambda_r)}{1+(\lambda_l/\lambda_r)}\right]+b\left(2+\frac{\lambda_l}{\lambda_r}\right)-c\frac{(\lambda_l/\lambda_r)^2}{1+(\lambda_l/\lambda_r)}\right\}$$

$$\bar{w}_2 = \frac{\lambda_l}{12}\left\{a\left[2-\frac{(\lambda_l/\lambda_r)}{1+(\lambda_l/\lambda_r)}\right]+b\left(4+\frac{\lambda_l}{\lambda_r}\right)-c\frac{(\lambda_l/\lambda_r)^2}{1+(\lambda_l/\lambda_r)}\right\}$$

Figure 10.10 Equivalent concentrated loading for straight-line and second-degree parabolic distribution of load.

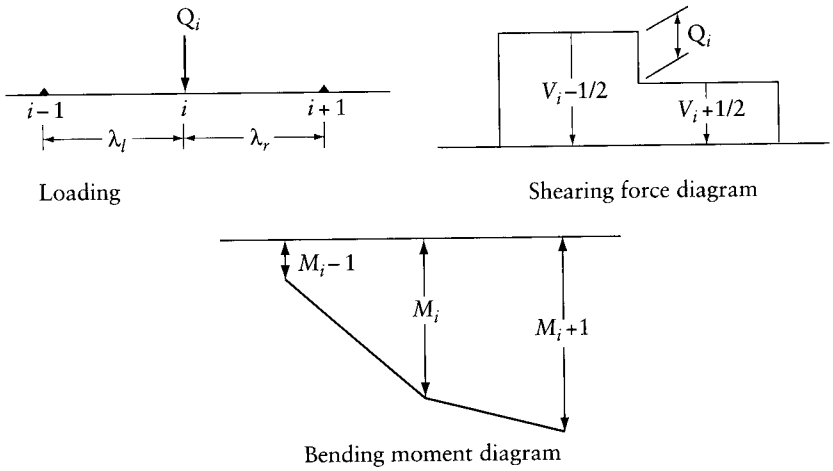

Figure 10.11 Bending moment diagram under the action of a concentrated load at nodes.

and

$$V_{i+\frac{1}{2}} = (M_{i+1} - M_i)/\lambda_r$$

where $V_{i-\frac{1}{2}}$ and $V_{i+\frac{1}{2}}$ are the shear in the intervals λ_l and λ_r respectively, and

$$Q_i = V_{i-\frac{1}{2}} - V_{i+\frac{1}{2}}$$

Substituting the first two of these equations into the last one, we find

$$-\frac{M_{i-1}}{\lambda_l} + M_i\left(\frac{1}{\lambda_l} + \frac{1}{\lambda_r}\right) - \frac{M_{i+1}}{\lambda_r} = Q_i \tag{10.12}$$

When $\lambda_l = \lambda_r = \lambda$, Eq. 10.12 becomes

$$\frac{1}{\lambda}(-M_{i-1} + 2M_i - M_{i+1}) = Q_i \tag{10.13}$$

If Eq. 10.12 or 10.13 is applied at several nodes in a beam, a system of simultaneous equations can be written, the solution of which gives the values of M.

When the deflection is calculated as the bending moment of elastic weights, we change Q_i to $\overline{w}_i$ and M to y in Eqs. 10.12 and 10.13, where $\overline{w}_i$ is the equivalent concentrated elastic weight and y is the deflection. Thus,

$$-\frac{y_{i-1}}{\lambda_l} + y_i\left(\frac{1}{\lambda_l} + \frac{1}{\lambda_r}\right) - \frac{y_{i+1}}{\lambda_r} = \overline{w}_i \tag{10.14}$$

and when $\lambda_l = \lambda_r = \lambda$,

$$\overline{w}_i = \frac{1}{\lambda}(-y_{i-1} + 2y_i - y_{i+1}) \tag{10.15}$$

The equivalent concentrated elastic loading is given by Eq. 10.11:

$$\overline{w}_i = \frac{1}{\lambda_l}\int_0^{\lambda_l} x_1 \frac{M}{EI}\,dx_1 + \frac{1}{\lambda_r}\int_0^{\lambda_r} x_2 \frac{M}{EI}\,dx_2 \tag{10.16}$$

Example 10.5: Simple beam with variable I

Find the deflection at C and the rotations at A and B for the beam of Figure 10.12. The variation in the second moment of area of the beam is as shown.

The elastic loading is shown in Figure 10.12b with the equivalent concentrated loads, calculated by the formulas in Figure 10.9. Applying Eq. 10.14 at C, with A, B, and C as nodes $i-1$, i, and $i+1$, and $y_A = y_B = 0$, we obtain

$$-0 + y_c\left[\frac{1}{(l/3)} + \frac{1}{(2l/3)}\right] - 0 = \frac{23M_0 l}{54EI_0}$$

whence

$$y_c = \frac{23M_0 l^2}{243EI_0}$$

The values of the slope at A and B are numerically equal to the elastic reactions r_A and r_B; thus,

$$\theta_A = r_A = \overline{w}_A + \frac{2}{3}\overline{w}_C = \frac{35M_0 l}{81EI_0}$$

$$\theta_B = -r_B = -\frac{\overline{w}_C}{3} - w_B = -\frac{47M_0 l}{162EI_0}$$

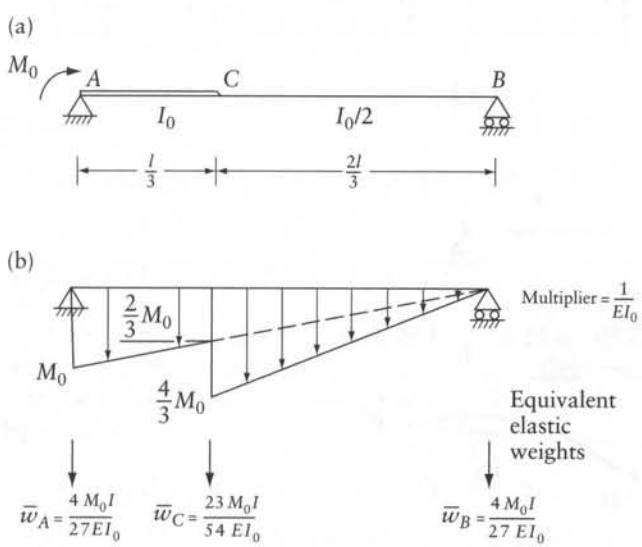

Figure 10.12 Deflection of the beam of Example 10.5 using equivalent concentrated elastic loading. (a) Actual loading. (b) Elastic loading.

Example 10.6: End rotations and transverse deflection of a member in terms of curvature at equally-spaced sections

Express the displacements D_1, D_2 and D_3 in the simple beam in Figure 10.13a in terms of the curvatures [ψ] at equally-spaced sections. (a) Use three sections (Figure 10.13b) and assume parabolic variation between the sections. (b) Use seven sections (Figure 10.13c) and assume linear variation between each adjacent two. Equations 10.21 to 10.23 and Eqs. 10.28 to 10.30 to be derived below are not limited to simple beams. They apply to any straight member of a plane frame. Figure 10.13d represents the deflected shape $A'B'$ of a typical straight member AB of a plane frame. Here, the displacements D_1, D_2 and D_3 represent rotations and transverse deflection measured from the chord joining A' and B'. The expressions relating the displacements to the curvatures are geometry relations that apply to prismatic or nonprismatic members. The equations are 'exact' when the variation of the curvature is as assumed in the derivation. When used in other cases, the error depends on how much the actual value of ψ differs from the assumed (see Example 10.7).

The curvature ψ can be treated as intensity of elastic weight (same as M/EI) and replace the distributed elastic weight by equivalent concentrated elastic weights (Figure 10.10). With ψ varying parabolically over Sections 1, 2 and 3 in Figure 10.13b,

$$\begin{Bmatrix} \overline{w}_1 \\ \overline{w}_2 \\ \overline{w}_3 \end{Bmatrix} = \frac{l}{48} \begin{bmatrix} 7 & 6 & -1 \\ 2 & 20 & 2 \\ -1 & 6 & 7 \end{bmatrix} \begin{Bmatrix} \psi_1 \\ \psi_2 \\ \psi_3 \end{Bmatrix} \tag{10.17}$$

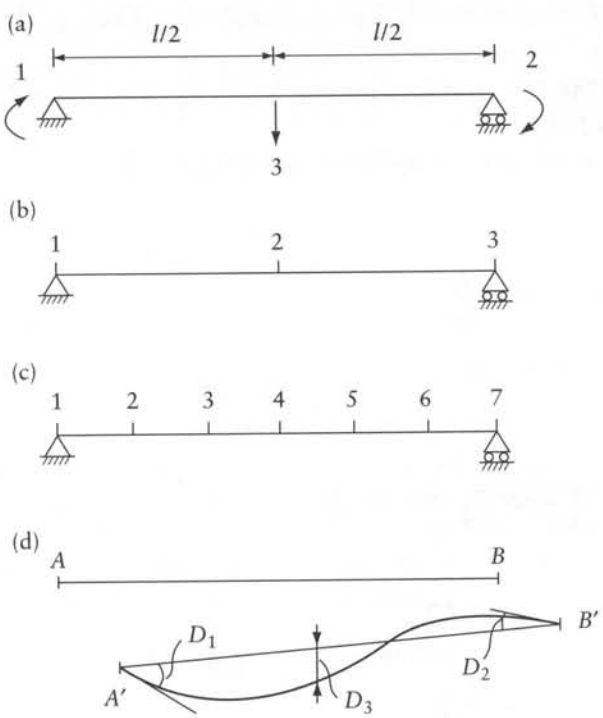

Figure 10.13 Derivation of expressions relating end rotations and deflection of a member of a plane frame in terms of the curvature at equally-spaced sections, Example 10.6. (a) Coordinate system. (b) Three sections. (c) Seven sections. (d) Deflected mirror.

The first column of the 3×3 matrix contains the equivalent concentrated loads when $\psi_1 = 1$ while ψ_2 and ψ_3 are equal to zero; the other two columns are derived in a similar way. The rotations D_1 and D_2 are equal to the shearing forces at the ends, and the deflection D_3 is the bending moment due to the equivalent concentrated elastic weights; thus,

$$D_1 = [1 \quad 1/2 \quad 0]\{\overline{w}\} \tag{10.18}$$

$$D_2 = -[0 \quad 1/2 \quad 1]\{\overline{w}\} \tag{10.19}$$

$$D_3 = l[0 \quad 1/4 \quad 0]\{\overline{w}\} \tag{10.20}$$

Substitution of Eq. 10.17 in Eqs. 10.18 to 10.20 gives expressions for the end rotations and the mid-length deflection for a straight member of a plane frame in terms of the curvatures at three equally-spaced sections, assuming parabolic variation (Figure 10.13b):

$$D_1 = \frac{l}{6}[1 \quad 2 \quad 0]\{\psi\} \tag{10.21}$$

$$D_2 = -\frac{l}{6}[0 \quad 2 \quad 1]\{\psi\} \tag{10.22}$$

$$D_3 = \frac{l^2}{96}[1 \quad 10 \quad 1]\{\psi \tag{10.23}$$

With ψ varying linearly between each two adjacent sections and a total of seven sections, the equivalent concentrated elastic weights (see Figure 10.10a) are:

$$\begin{Bmatrix} \overline{w}_1 \\ \overline{w}_2 \\ \overline{w}_3 \\ \overline{w}_4 \\ \overline{w}_5 \\ \overline{w}_6 \\ \overline{w}_7 \end{Bmatrix} = \frac{l}{36} \begin{bmatrix} 2 & 1 & 0 & 0 & 0 & 0 & 0 \\ 1 & 4 & 1 & 0 & 0 & 0 & 0 \\ 0 & 1 & 4 & 1 & 0 & 0 & 0 \\ 0 & 0 & 1 & 4 & 1 & 0 & 0 \\ 0 & 0 & 0 & 1 & 4 & 1 & 0 \\ 0 & 0 & 0 & 0 & 1 & 4 & 1 \\ 0 & 0 & 0 & 0 & 0 & 1 & 2 \end{bmatrix} \begin{Bmatrix} \psi_1 \\ \psi_2 \\ \psi_3 \\ \psi_4 \\ \psi_5 \\ \psi_6 \\ \psi_7 \end{Bmatrix} \tag{10.24}$$

The end rotations and the mid-length deflection are (same as shear forces and bending moment):

$$D_1 = (1/12)[12 \quad 10 \quad 8 \quad 6 \quad 4 \quad 2 \quad 0]\{\overline{w}\} \tag{10.25}$$

$$D_2 = (-1/12)[0 \quad 2 \quad 4 \quad 6 \quad 8 \quad 10 \quad 12]\{\overline{w}\} \tag{10.26}$$

$$D_3 = (l/12)[0 \quad 1 \quad 2 \quad 3 \quad 2 \quad 1 \quad 0]\{\overline{w}\} \tag{10.27}$$

Substitution of Eq. 10.24 in each of Eqs. 10.25 to 10.27 gives expressions for the end rotations and the deflection at mid-length of a straight member in terms of the curvatures at seven equally-spaced sections, assuming linear variation between each adjacent two (Figure 10.13c):

$$D_1 = (l/432)[34 \quad 60 \quad 48 \quad 36 \quad 24 \quad 12 \quad 2]\{\psi\} \tag{10.28}$$

$$D_2 = (-l/432)[2 \quad 12 \quad 24 \quad 36 \quad 48 \quad 60 \quad 34]\{\psi\} \tag{10.29}$$

$$D_3 = (l^2/432)[1 \quad 6 \quad 12 \quad 16 \quad 12 \quad 6 \quad 1]\{\psi\} \tag{10.30}$$

In a similar way we can derive the equations given below for use when the number of equally-spaced sections is five, instead of the seven sections shown in Figure 10.13:

With five sections:

$$D_1 = (l/192)[22 \quad 36 \quad 24 \quad 12 \quad 2]\{\psi\} \tag{10.28a}$$

$$D_2 = (-l/192)[2 \quad 12 \quad 24 \quad 36 \quad 22]\{\psi\} \tag{10.29a}$$

$$D_3 = (l^2/192)[1 \quad 6 \quad 10 \quad 6 \quad 1]\{\psi\} \tag{10.30a}$$

With nine sections:

$$D_1 = (l/768)[46 \quad 84 \quad 72 \quad 60 \quad 48 \quad 36 \quad 24 \quad 12 \quad 2]\{\psi\} \tag{10.28b}$$

$$D_2 = (-l/768)[2 \quad 12 \quad 24 \quad 36 \quad 48 \quad 60 \quad 72 \quad 84 \quad 46]\{\psi\} \tag{10.29b}$$

$$D_3 = (l^2/768)[1 \quad 6 \quad 12 \quad 18 \quad 22 \quad 18 \quad 12 \quad 6 \quad 1]\{\psi\} \tag{10.30b}$$

Example 10.7: Bridge girder with variable cross section

Figure 10.14 shows the elevation, the cross section and the bending moment diagram, due to a uniform load q/unit length, on an interior span of a continuous footbridge. Using the curvatures at seven equally-spaced sections (Figure 10.13c and Eqs. 10.28 to 10.30), find the end rotations D_1 and D_2 and the mid-span deflection D_3.

The values of the bending moment M, the second moment of area I and the curvature ψ ($= M/EI$, with E being modulus of elasticity) are:

Section	M	I	ψ
1 and 7	−100.0	266.7	−375.0
2 and 6	−30.5	94.8	−322.5
3 and 5	11.1	38.6	287.5
4	25.0	26.4	947.0
Multiplier	$ql^2/1000$	$10^{-9}\, l^4$	$10^3\, q/El^2$

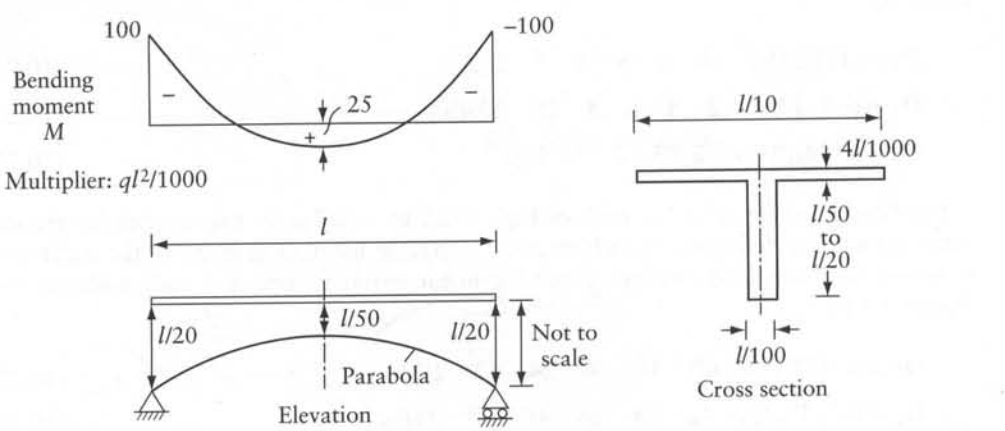

Figure 10.14 Interior span of a continuous footbridge subjected to uniform distributed load, Example 10.7.

The end rotations D_1 and D_2 and the mid-span deflection D_3 are (Eqs. 10.25 to 10.27):

$$D_1 = -D_2 = \frac{l}{432}[34 \quad 60 \quad 48 \quad 36 \quad 24 \quad 12 \quad 2] \begin{Bmatrix} -375.0 \\ -322.5 \\ 287.5 \\ 947.0 \\ 287.5 \\ -322.5 \\ -375.0 \end{Bmatrix} \frac{10^3 q}{EI^2} = 41.8 \times 10^3 \frac{q}{EI}$$

$$D_3 = \frac{l^2}{432}[2(-375.0) + 12(-322.5) + 24(287.5) + 16(947.0)] \frac{10^3 q}{EI^2} = 40.4 \times 10^3 \frac{q}{E}$$

Using 21 equally-spaced sections instead of seven gives the more accurate answers:

$$D_1 = -D_2 = 40.9 \times 10^3 q/(EI); \; D_3 = 42.9 \times 10^3 q/E$$

10.5 Method of finite differences

A numerical solution of the differential equation for deflection can be obtained by finite differences. If the bending moment is known, the second derivative in Eq. 10.1 can be put in finite-difference form in terms of the unknown deflections at three consecutive points (nodes), usually equally spaced along the beam. Hence, we obtain a finite-difference equation relating the deflection at node points to the bending moment. When the finite-difference equation is applied at all the nodes where the deflection is not known, a set of simultaneous equations is obtained, the solution of which gives the deflections.

A more useful application of the method of finite differences is in cases when the bending moment is not easy to determine; a solution is then first obtained for the differential equations relating the deflection to the external loading (Eqs. 10.4 to 10.7), and the stress resultants and reactions are found from the deflections by differentiation. Thus, a complete structural analysis can be carried out by finite differences. This method has a wide field of application, and for this reason it is treated in detail in Chapter 15.

In this section, the discussion is limited to the solution of Eq. 10.1 to obtain the deflection when the bending moment is known.

Consider a simple beam of variable flexural rigidity EI shown in Figure 10.15a. The differential equation governing the deflection is given by Eq. 10.1:

$$M = -EI \frac{d^2y}{dx^2} \tag{10.31}$$

Consider three equally-spaced points $i-1, i, i+1$ where the deflection is y_{i-1}, y_i, y_{i+1} respectively (Figure 10.12b). It can be easily shown[1] that the second derivative of the deflection at i can be approximated by

$$\frac{d^2y}{dx^2} \simeq \frac{1}{\lambda^2}(y_{i-1} - 2y_i + y_{i+1} \tag{10.32}$$

1 See Section 16.2.

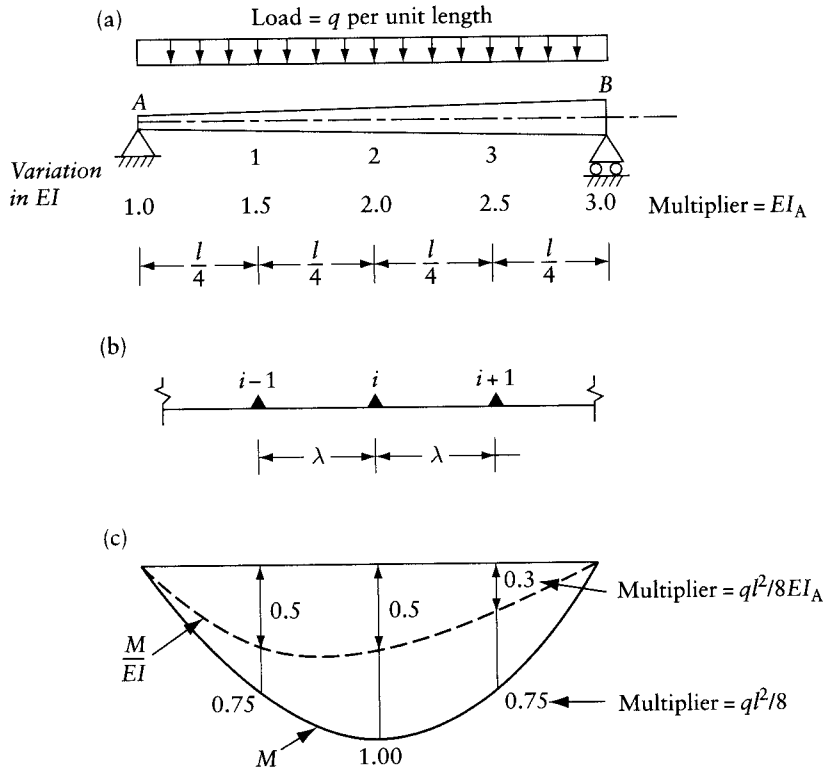

Figure 10.15 Calculation of deflections by finite differences.

The finite-difference form of Eq. 10.31 applied at node i is

$$\frac{1}{\lambda}(-y_{i-1} + 2y_i - y_{i+1} \simeq \left(\frac{M}{EI}\right)_i \lambda \tag{10.33}$$

where $(M/EI)_i$ is the value of the bending moment divided by the flexural rigidity at point i. This equation is approximate, and does not take into account the manner in which $M/(EI)$ varies between the nodes.

It may be useful to compare Eq. 10.33 with Eq. 10.15, in which the elastic concentrated weight $\overline{w}_i$ replaces the right-hand side of Eq. 10.33. The latter equation is approximate and its accuracy is increased if the number of nodes along the span is increased. However, for most practical cases, Eq. 10.33 gives sufficient accuracy even with a small number of divisions.

To compare the two expressions let us consider the beam of Figure 10.15a. The values of $M/(EI)$ at three nodes in the beam are indicated in Figure 10.15c. Applying Eq. 10.33 at nodes 1, 2, and 3, with the deflection at the supports $y_A = y_B = 0$, gives

$$\frac{1}{(l/4)}\begin{bmatrix} 2 & -1 & 0 \\ -1 & 2 & -1 \\ 0 & -1 & 2 \end{bmatrix}\begin{Bmatrix} y_1 \\ y_2 \\ y_3 \end{Bmatrix} \simeq \frac{ql^3}{32EI_A}\begin{Bmatrix} 0.5 \\ 0.5 \\ 0.3 \end{Bmatrix}$$

The solution of these equations is

$$y_1 = 2.10\left(\frac{ql^4}{384EI_A}\right) y_2 = 2.70\left(\frac{ql^4}{384EI_A}\right) \text{ and } y_3 = 1.8\left(\frac{ql^4}{384EI_A}\right)$$

Now, using Eq. 10.15 with the elastic weights $\overline{w}_i$ calculated by the expression

$$\overline{w}_i = \frac{\lambda}{12}\left[\left(\frac{M}{EI}\right)_{i-1} + 10\left(\frac{M}{EI}\right)_i + \left(\frac{M}{EI}\right)_{i+1}\right]$$

(see Figure 10.10), we obtain

$$\frac{1}{(l/4)}\begin{bmatrix} 2 & -1 & 0 \\ -1 & 2 & -1 \\ 0 & -1 & 2 \end{bmatrix}\begin{Bmatrix} y_1 \\ y_2 \\ y_3 \end{Bmatrix} = \frac{ql^3}{384EI_A}\begin{Bmatrix} 5.5 \\ 5.8 \\ 3.5 \end{Bmatrix}$$

whence

$$y_1 = 1.975\left(\frac{ql^4}{384EI_A}\right) y_2 = 2.575\left(\frac{ql^4}{384EI_A}\right) \text{ and } y_3 = 1.725\left(\frac{ql^4}{384EI_A}\right)$$

10.6 Representation of deflections by Fourier series

The equation of the deflected line of a simply-supported beam under any loading can be expressed in the form of a trigonometric series

$$y = \sum_{n=1}^{\infty} a_n \sin\frac{n\pi x}{l} \tag{10.34}$$

If the loading is represented as a Fourier series,

$$q = \sum_{n=1}^{\infty} b_n \sin\frac{n\pi x}{l} \tag{10.35}$$

where

$$b_n = \frac{2}{l}\int_0^1 q(x)\sin\frac{n\pi x}{l}\,dx \tag{10.36}$$

it can be seen that Eq. 10.34 is a solution of the differential equation $q = EI(d^4y/dx^4)$, provided that

$$a_n = \frac{l^4}{n^4\pi^4 EI} b_n \tag{10.37}$$

Equation 10.34 satisfies the end conditions of zero deflection ($y = 0$ at $x = 0, l$) and of zero moment ($-EI(d^2y/dx^2) = 0$ at $x = 0, l$).

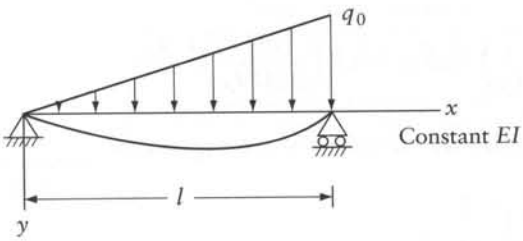

Figure 10.16 Representation of elastic line of the simple beam of Example 10.8 by a Fourier series.

Example 10.8: Triangular load on a simple beam

Find the deflection of the beam in Figure 10.16.

The intensity of load at any point distant x from the left-hand end is $q(x) = q_0 x/l$. From Eq. 10.36.

$$b_n = \frac{2q_0}{l^2}\int_0^l x \sin\frac{n\pi x}{l}\,dx = -\frac{2q_0}{n\pi}\cos n\pi$$

But $\cos n\pi = -1$ when $n = 1, 3, 5, \ldots$, and $\cos n\pi = 1$ for $n = 2, 4, 6, \ldots$ Therefore,

$$b_n = (-1)^{n+1}\frac{2q_0}{\pi n}$$

and from Eq. 10.37,

$$a_n = (-1)^{n+1}\frac{2q_0 l^4}{\pi^5 \pi^5 EI}$$

Substituting in Eq. 10.34, we obtain the deflection

$$y = \frac{2q_0 l^4}{\pi^5 EI}\sum_{n=1}^{\infty}\frac{(-1)^{n+1}}{n^5}\sin\frac{n\pi x}{l}$$

Using three terms of the series, we find for the mid-span $y_{(x=l/2)} = 0.00652 q_0 l^4/(EI)$, which agrees with the exact solution to two significant places. If only one term of the series is used, we have $y_{(x=l/2)} = 0.00654\, q_0 l^4/(EI)$. This does not differ greatly from the exact solution, and, indeed, in many cases sufficient accuracy is obtained by using only one term of the series.

10.7 Representation of deflections by series with indeterminate parameters

In the preceding section, we used a series to approximate loadings, and hence obtained the deflection function. Series may also be used to approximate the deflection function directly. Each term of the series includes a parameter which can be determined by one of several numerical

procedures.[2] In this section, the Rayleigh–Ritz method is used to find the deflection of beams. However, the principle of virtual work is employed instead of the minimization process of the total potential energy.

Consider the beam AB shown in Figure 10.17a, subjected to lateral and axial forces and resting on an elastic foundation. Let the deflection be expressed in the form

$$y = a_1 g_1 + a_2 g_2 + \ldots + a_n g_n \tag{10.38}$$

where g_i is any continuous function of x between A and B which satisfies the boundary conditions (for instance, at a fixed end, $y = 0$ and $dy/dx = 0$). The equilibrium conditions at the ends (for example, the condition that shear and bending moment at a free end are zero) are not necessarily satisfied by the functions g (as shear and bending moment are derivatives of y and therefore a function of a derivative of g).

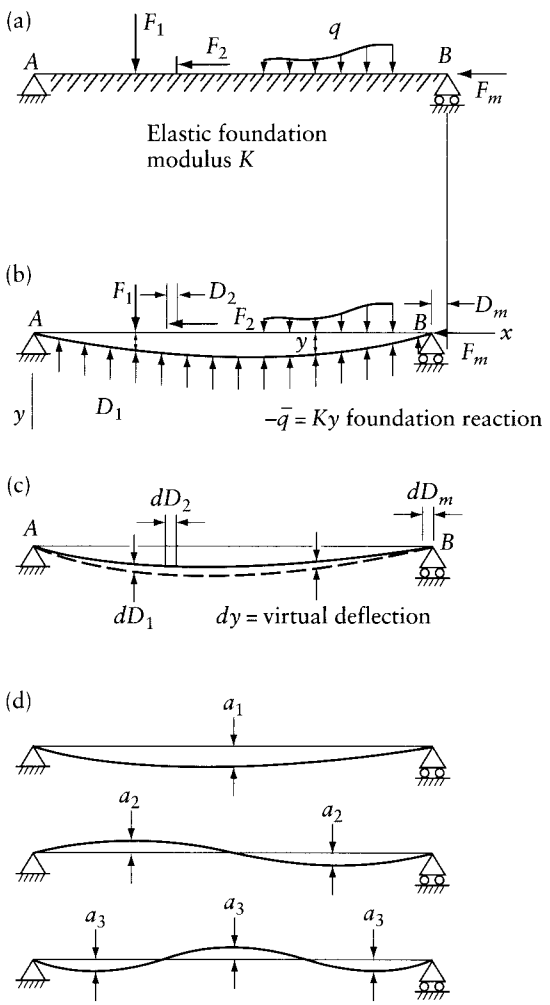

Figure 10.17 Representation of deflections by series with indeterminate parameters.

2 See, for example, Crandall, S. H., *Engineering Analysis*, McGraw-Hill, New York, 1956, pp. 230–232.

The values of the parameters $a_1, a_2, \ldots, a_n$ are determined by satisfying the energy criterion as follows.

Under the applied forces, the beam is in equilibrium in a deflected shape shown in Figure 10.17b. The displacements $D_1, D_2, \ldots, D_m$ are the movements along the line of action of the external forces $F_1, F_2, \ldots, F_m$. The resultant lateral load is $q^* = q - ky$, where ky is the intensity of the foundation reaction. Let the beam acquire a small virtual deflection from the equilibrium position. Assume that this virtual deflection varies in magnitude along the beam according to the equation

$$dy = da_i g_i \tag{10.39}$$

where da_i represents a small increase in the parameter a_i, while the other parameters remain unchanged. Thus, the virtual deflection dy varies along the beam in the same manner as the function g_i only. This is in contrast to the variation in y which depends on all the functions g_1, $g_2, \ldots, g_n$. The virtual deflection causes the forces $F_1, F_2, \ldots, F_m$ to move along their lines of action by amounts $dD_1, dD_2, \ldots, dD_m$, as shown in Figure 10.17c.

According to the principle of virtual work (see Section 7.5), if an elastic system in equilibrium undergoes a small virtual displacement, the work done by the external forces while moving along the virtual displacement is equal to the corresponding change in strain energy. The virtual work of the external forces is

$$dW = \sum_{j=1}^{m} F_j dD_j + \int_A^B q^*(dy)\, dx$$

This equation may also be written in the form

$$dW = da_i \left(\sum_{j=1}^{m} F_j \frac{\partial D_j}{\partial a_i} + \int_A^B q^* g_i \, dx \right)$$

where the partial derivative $\partial D_j / \partial a_i$ represents the change in the displacement D_j corresponding to a unit change in the parameter a_i, causing a virtual deflection which varies along the beam according to Eq. 10.39.

The two sections limiting an element of length dx of the beam will rotate relative to each other during the virtual deflection by an angle

$$d\theta = da_i \frac{d^2 g_i}{dx^2} dx$$

The change in strain energy of this element is $-M d\theta$ (see Section 7.3.2) and the total change in strain energy due to bending is

$$dU = -da_i \int_A^B M \frac{d^2 g_i}{dx^2} dx$$

The bending moment at any section is

$$M = -EI \frac{d^2 y}{dx^2} = -EI \left(a_1 \frac{d^2 g_1}{dx^2} + a_2 \frac{d^2 g_2}{dx^2} + \ldots + a_2 \frac{d^2 g_n}{dx^2} \right)$$

Substituting for moment in the strain-energy equation and equating the external and internal work, we obtain

$$\sum_{j=1}^{m} F_j \frac{\partial D_j}{\partial a_i} + \int_A^B q^* g_i dx = \int_A^B EI \left(a_1 \frac{d^2 g_1}{dx^2} + a_2 \frac{d^2 g_2}{dx^2} + \ldots + a_n \frac{d^2 g_n}{dx^2} \right) \frac{d^2 g_i}{dx^2} dx \tag{10.40}$$

Equation 10.40 represents a system of equations corresponding to $i = 1, 2, \ldots, n$, from which the parameters $a_1, a_2, \ldots, a_n$ can be determined; thus, by Eq. 10.38, an approximate equation to the elastic line is obtained.

The above procedure has been used extensively to treat buckling problems[3] and, to some extent, has also been applied to beams on elastic foundations.[4] For a simply-supported beam, the functions g are chosen as a sinusoidal curve along the beam length l

$$g_n = \sin \frac{n\pi x}{l} \qquad \frac{d^2 g_n}{dx^2} = -\frac{n^2 \pi^2}{l^2} \sin \frac{n\pi x}{l}$$

where $n = 1, 2, 3, \ldots$ These functions satisfy the boundary conditions of a simply-supported beam.[5] Thus, the deflection is represented by the series (see Eq. 10.34)

$$y = \sum_{n=1}^{\infty} a_n \sin \frac{n\pi x}{l} \tag{10.41}$$

This means that the deflection curve may be obtained by summing the ordinates of sine curves such as those shown in Figure 10.17d. The parameters $a_1, a_2, \ldots$ represent the maximum ordinates of these sine curves.

With this choice, and with the assumption that EI is constant, the integrals of the cross-products on the right-hand side of Eq. 10.40 vanish because

$$\int_0^l \sin \frac{n\pi x}{l} \sin \frac{r\pi x}{l} dx = \begin{cases} 0 \text{ if } n \neq r \\ \frac{1}{2} \text{ if } n = r \end{cases}$$

Therefore, in the case of a prismatic beam, Eq. 10.25 becomes

$$\sum_{j=1}^{m} F_j \frac{\partial D_j}{\partial a_n} + \int_0^l q^* g_n dx = a_n EI \int_0^l \left(\frac{d^2 g_n}{dx^2} \right)^2 dx$$

This equation has only one unknown parameter, and its solution gives the value of a_n:

$$a_n = \frac{2l^3}{n^4 \pi^4 EI} \left(\sum_{j=1}^{m} F_j \frac{\partial D_j}{\partial a_n} + \int_0^l q^* \sin \frac{n\pi x}{l} dx \right) \tag{10.42}$$

3 Timoshenko, S. and Gere, J. M., *Theory of Elastic Stability*, 2nd ed., McGraw-Hill, New York, 1961.

4 Hetényi, M., *Beams on Elastic Foundation*, The University of Michigan Press, Ann Arbor, 1947.

5 The functions which satisfy other end conditions are discussed in some detail in Chapter 18 in conjunction with the finite-strip method.

Equations 10.41 and 10.42 can be used to express the deflection in a prismatic beam with hinged ends, subjected to lateral and axial loads, such as the beam in Figure 10.17a. The same equations can be used in the analysis of beams with two hinged ends and with intermediate supports, the reactions at the intermediate supports being treated as any of the forces F. From the condition that $y = 0$ at the supports (or y has a known value), we obtain an equation from which the reaction can be determined. If the beam has intermediate spring supports (elastic supports) of stiffness k, the deflection condition at these supports is given by the equation for the reaction $F = ky$.

The above procedure is used in the following three examples for a beam loaded with a lateral load only, for a beam with lateral and axial loads, and for a beam resting on an elastic foundation.

Example 10.9: Simple beam with a concentrated transverse load

Find the deflection of a simply-supported beam carrying one vertical load P (Figure 10.18a). The beam is assumed to have a constant flexural rigidity EI.

Substituting in Eq. 10.42, $q^* = 0, F_1 = P$ and $\partial D_1/\partial a_n = \sin(n\pi c/l)$, we obtain

$$a_n = \frac{2Pl^3}{n^4\pi^4 EI} \sin\frac{n\pi c}{l}$$

Substituting for a_n in Eq. 10.41, we find

$$y = \frac{2Pl^3}{\pi^4 EI} \sum_{n=1}^{\infty} \frac{1}{n^4} \sin\frac{n\pi x}{l} \sin\frac{n\pi c}{l}$$

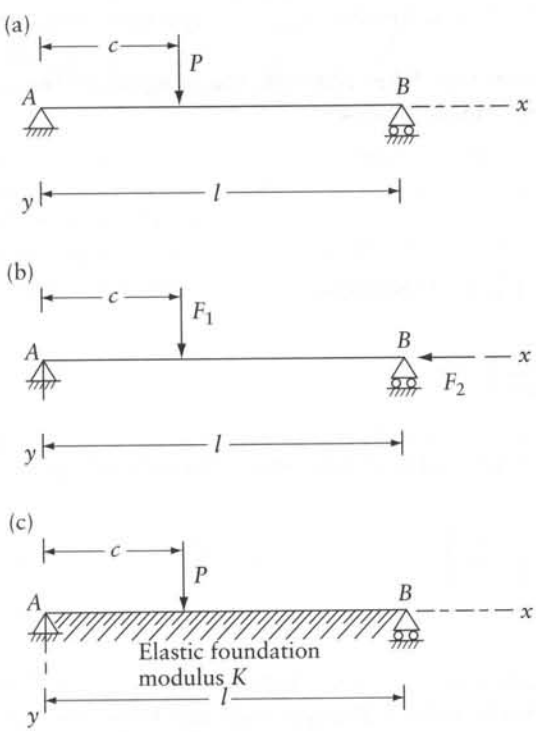

Figure 10.18 Beams considered in Examples 10.9, 10.10, and 10.11.

Example 10.10: Simple beam with an axial compressive force and a transverse concentrated load

Find the deflection of the beam in Figure 10.18b, carrying a vertical force F_1 and an axial compressive force F_2.

The deflection of the beam causes the roller at B to move toward the hinge A. The movement of B is equal to the difference between the length of the curve and the length of the chord AB. The length ds corresponding to a horizontal element dx is

$$ds = \sqrt{dx^2 + dy^2}$$

Dividing both sides of this equation by dx and expanding the square root by the binomial series, and retaining the first two terms only, we obtain

$$\frac{ds}{dx} = 1 + \frac{1}{2}\left(\frac{dy}{dx}\right)^2$$

Integrating both sides,

$$\int_0^l \frac{ds}{dx}\,dx = \int_0^l dx + \frac{1}{2}\int_0^l \left(\frac{dy}{dx}\right)^2 dx$$

whence the horizontal movement of B is

$$s - l = \frac{1}{2}\int_0^l \left(\frac{dy}{dx}\right)^2 dx$$

where s is the length of the curve AB.

For the beam considered, the deflection is expressed by Eq. 10.41 as

$$y = \sum_{n=1}^{\infty} a_n \sin\frac{n\pi x}{l}$$

and

$$D_2 = s - l = \frac{1}{2}\sum_{n=1}^{\infty}\int_0^l \left(a_n \frac{n\pi}{l}\cos\frac{n\pi x}{l}\right)^2 dx = \sum_{n=1}^{\infty}\frac{a_n^2 n^2\pi^2}{4l}$$

The partial derivative with respect to a_n is zero for all the terms in the above series except for the term containing a_n; therefore,

$$\frac{\partial D_2}{\partial a_n} = \frac{a_n n^2\pi^2}{2l}$$

Substituting in Eq. 10.42, $\partial D_1/\partial a_n = \sin(n\pi c/l)$, $\partial D_2/\partial a_n = a_n n^2\pi^2/(2l)$, and $q^* = 0$, and rearranging the terms, we obtain

$$a_n = \frac{2F_1 l^3 \sin(n\pi c/l)}{n^2\pi^4 EI[n^2 - F_2 l^2/(\pi^2 EI)]}$$

Therefore, from Eq. 10.41 the deflection equation is

$$y=\frac{2F_1l^3}{\pi^4EI}\sum_{n=1}^{\infty}\frac{\sin(n\pi c/l)\sin(n\pi x/l)}{n^2[n^2-F_2l^2/(\pi^2EI)]}$$

Example 10.11: Simple beam on elastic foundation with a transverse force

Find the deflection of a simple beam carrying a concentrated vertical load P and resting on an elastic foundation of modulus k (Figure 10.18c). The beam has a constant flexural rigidity EI.

The intensity of the resultant lateral load is

$$q^*=-ky=-k\sum_{n=1}^{\infty}a_n\sin\frac{n\pi x}{l}$$

Equation 10.42 gives

$$a_n=\frac{2l^3}{n^4\pi^4EI}\left[P\sin\frac{n\pi c}{l}-k\int_0^l\left(\sum_{r=1}^{\infty}a_r\sin\frac{r\pi x}{l}\sin\frac{n\pi x}{l}\right)dx\right]$$

The integral on the right-hand side of this equation is zero when $r\neq n$ and is equal to $a_nl/2$ when $r=n$. Therefore,

$$a_n=\frac{2Pl^8}{\pi^4EI}\left(\frac{\sin(n\pi c/l)}{n^4+kl^4/(\pi^4EI)}\right)$$

Substituting in Eq. 10.41,

$$y=\frac{2Pl^3}{\pi^4EI}\sum_{n=1}^{\infty}\frac{\sin(n\pi c/l)\sin(n\pi x/l)}{n^4+kl^4(\pi^4EI)}.$$

10.8 General

Several methods can be used to find the deflection due to bending of beams. The moment–area or the elastic-weight methods can be used when the variation of the bending moment along the beam is known. Both these methods are based upon relations between the area under the bending moment diagram and deflection. In the method of elastic weights, the calculation of angular rotation and deflection is similar to the routine calculation of shear and bending moment, except that the applied load and support conditions of the beam are generally altered.

The finite-difference method gives a numerical solution to the governing differential equations relating the deflection to bending moment or the deflection to loading. The use of finite differences is particularly advantageous when the bending moment is not known. From a numerical solution of the differential equation relating the loading to the deflection, the unknown stress resultants can be determined by differentiation. The details of this procedure can be found in Chapter 15.

If the loading is represented by a Fourier series, a solution to the differential equation giving the deflection can be obtained in the form of a trigonometric series. This can be applied to beams with hinged ends.

The deflection can also be represented as a series including an indeterminate parameter in each term. Several numerical methods can be used to determine the parameters which give a solution that approximately satisfies the differential equation. In the method discussed in this chapter, the parameters are chosen to satisfy the energy criterion. As in the case of the finite-difference method, the bending moment need not be known and the stress resultants can be determined from the deflection.

Problems

10.1 In Example 10.2 we use the moment–area–deflection relations of Eqs. 10.8 and 10.10 to prove that for a simple beam the slope and the deflection are equal, respectively, to the shear and the bending moment of the elastic weights. Verify that the displacements determined in the example for the beam in Figure 10.6 can also be calculated by the unit-load theorem to obtain the same answers.

10.2 Use the moment–area–deflection relations Eqs. 10.8 and 10.10 to verify that for the beam in Figures 10.7a and c the slope and the deflection at any section are equal, respectively, to the shear and the bending moment of the elastic weights on the conjugate beam in Figure 10.7b.

10.3 Imperial units. Determine the deflection and the angular rotation at C for the prismatic beam shown in the figure. Assume $I = 800\,\text{in.}^4$ and $E = 30 \times 10^6$ psi.

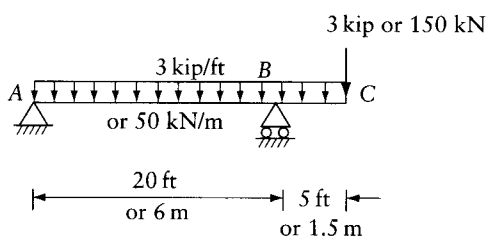

Prob. 10.3 or *10.4*

10.4 SI units. Determine the deflection and the angular rotation at C for the prismatic beam shown in the figure. Assume $I = 330 \times 10^6\,\text{mm}^4$ and $E = 200\,\text{GN/m}^2$.

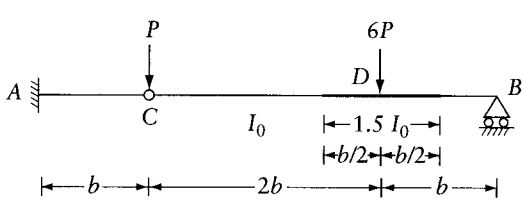

Prob. 10.5

10.5 Compute the deflection at D and C for the beam shown.

10.6 Show that the vertical deflection due to bending of the arch AB in the figure is numerically equal to the bending moment of the beam A′B′ loaded with the elastic loading $M\,ds/(EI)$,

where M is the bending moment in the arch, ds is the length of a typical element along the arch axis, and EI is the flexural rigidity.

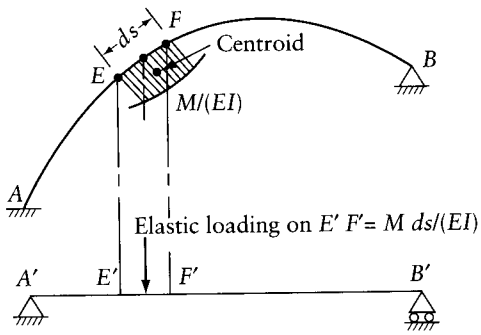

Prob. 10.6

10.7 Using the method of elastic weights, find the deflections at C, D, and E in the arch shown in the figure. Consider bending deformations only.

10.8 Obtain the stiffness matrix corresponding to the coordinates 1 and 2 of the beam shown. *Hint:* Find the angular rotations due to unit moment at each end, and form a flexibility matrix which, when inverted, gives the required stiffness matrix.

10.9 In Prob. 10.8 add coordinates 3 and 4 at B, representing downward translation and clockwise notation respectively. Write the stiffness matrix corresponding to the four coordinates. Use the condensation of stiffness matrix Eq. 5.17 to derive the 2×2 stiffness matrix required in Prob. 10.8.

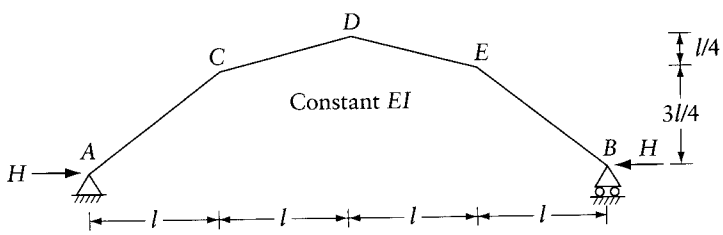

Prob. 10.7

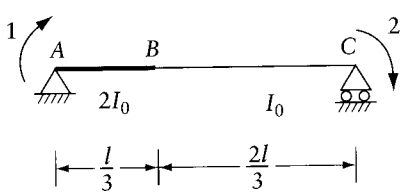

Prob. 10.8

10.10 Calculate the magnitude of two equal and opposite couples M necessary to produce an angular discontinuity of one radian at point D in the prismatic beam shown. Find the corresponding deflections at D and E. (These deflections are numerically equal to influence coefficients of the bending moment at D, in a continous beam ABC, having no hinge at D; see Section 12.3.)

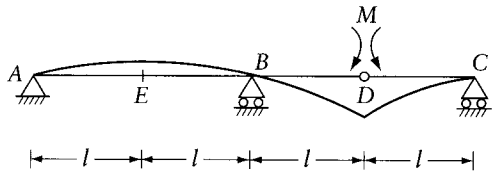

Prob. 10.10

10.11 (a) Find the deflection at D in the continuous beam on unyielding supports shown in the figure. The beam has a constant flexural rigidity EI.

(b) The bending moments at the supports in the above case are $M_A = -0.0711\,qb^2$ and $M_B = -0.1938\,qb^2$. A vertical settlement at B and a rotation at A change these moments to $M_A = 0$ and $M_B = -0.05\,qb^2$. Find the amount of the settlement and the rotation.

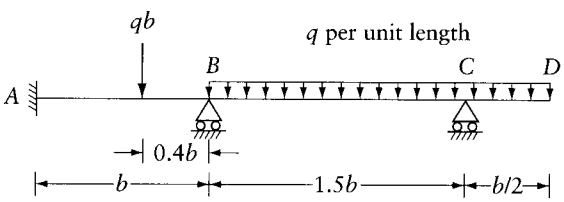

Prob. 10.11

10.12 Use the finite-difference method to calculate the deflection at nodes 1, 2, and 3 and the angular rotation at end A in the beam shown. Give the answers in terms of EI_0. To calculate the rotation at node A, use the approximate relation

$$\theta_i \simeq (y_{i+1} - y_i)/\lambda$$

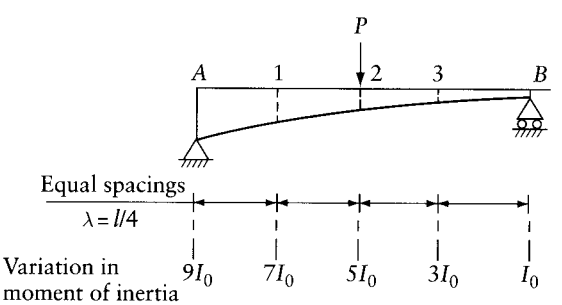

Prob. 10.12

10.13 Solve Prob. 10.12 representing the deflection by two terms of the series Eq. 10.34 and assuming the variation in the second moment of area: $I(x) = I_0(9 - 8\zeta)$; where $\zeta = x/l$, with x being the distance from A to any point and l being the span length. Apply Eq. 10.40 to obtain two simultaneous equations, whose solution gives the indeterminate parameters a_1 and a_2.

10.14 Use the Rayleigh–Ritz procedure to determine the deflection of a simple beam of constant EI, span l, loaded with a uniform transverse load of intensity q and an axial compressive force P at the ends. Represent the deflection by the series.

$$y = \sum_{n=1}^{\infty} a_n \sin \frac{n\pi x}{l}$$

10.15 Find the first three parameters in the series

$$y = \sum_{n=1}^{\infty} a_n \sin \frac{n\pi x}{l}$$

which represents the deflection of the prismatic beam shown in the figure.

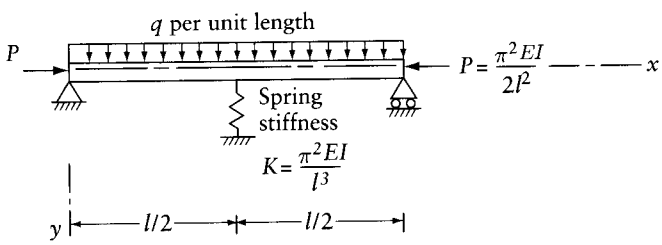

Prob. 10.15

10.16 Find the deflection of a prismatic beam on an elastic foundation symmetrically loaded by two concentrated loads as shown in the figure. Represent the deflection

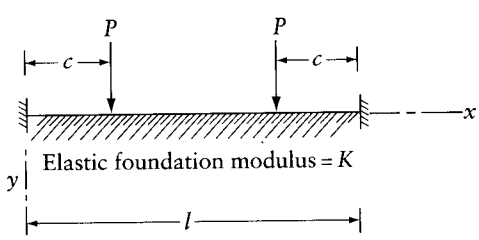

Prob. 10.16

by the series

$$y = \sum_{n=1}^{\infty} a_n \left(1 - \cos \frac{2n\pi x}{l}\right)$$

10.17 Express the end rotations D_1 and D_2 and the mid-length deflection D_3 of a straight member of length l (Figure 10.13) in terms of the curvatures ψ at five equally-spaced sections, assuming linear variation between each adjacent two (see Example 10.6). Use the derived expressions to find alternative answers to Prob. 10.12.

10.18 Use method of elastic weights to verify the set of equations relevant to any number of the beams shown in Appendix B.

Chapter 11

Applications of force and displacement methods: column analogy and moment distribution

11.1 Introduction

Applications of the force method and the displacement method have, in some cases, led to the classical procedures known as *column analogy* and *moment distribution*. Column analogy can be used in the analysis of a plane frame formed of one closed bent, and therefore statically indeterminate to a degree not higher than three. The analysis is by the force method, with the redundants chosen at a point called the elastic center, and involves calculations similar to those for stresses in a column cross section subjected to combined bending moment and a normal force. In this chapter the column analogy will be used only to determine the stiffness matrix of nonprismatic straight bars and their bending moment, considering only bending deformations. The use of column analogy to determine the bending moment in single-bay frames is omitted in the sixth edition to provide space for new material.

In the moment-distribution method, for analysis of plane frames considering only bending deformations, the joint displacements are first assumed restrained. The effect of joint displacements is then introduced by successive iterations, which can be continued to any desired precision. Thus, the moment distribution is also a displacement method of analysis. There is, however, a fundamental difference: in moment distribution generally no equations are solved to find the joint displacements; instead, these displacements are allowed to take place in succession, and their effect on the end-moments is introduced as a series of successive converging corrections. This absence of the need to solve simultaneous equations has made the moment-distribution method an extremely popular one, especially when the calculations are done by a simple calculator.

The moment-distribution procedure yields bending moments, and it is the value of the moments that are generally needed for design; thus, we avoid the procedure of first finding the joint displacements and then calculating the moments. A further advantage of the moment-distribution procedure is that it is easily remembered and easily applied.

Despite the use of computers, which can rapidly analyze frames with numerous joints and members, it is useful to analyze such frames (or their isolated parts) by hand, using moment distribution, in preliminary design or to check the computer results. Performing such a check is of great importance.

11.2 Analogous column: definition

Figure 11.1a shows a member of variable cross section idealized as a straight bar having a variable EI. Figure 11.1b, referred to as the cross section of the analogous column, has the shape of a strip of varying width $= 1/EI$ and length $= l$, the same as that of the member; where $EI \equiv EI(x)$ is the flexural rigidity at any point at a distance x from O, the centroid of the analogous column

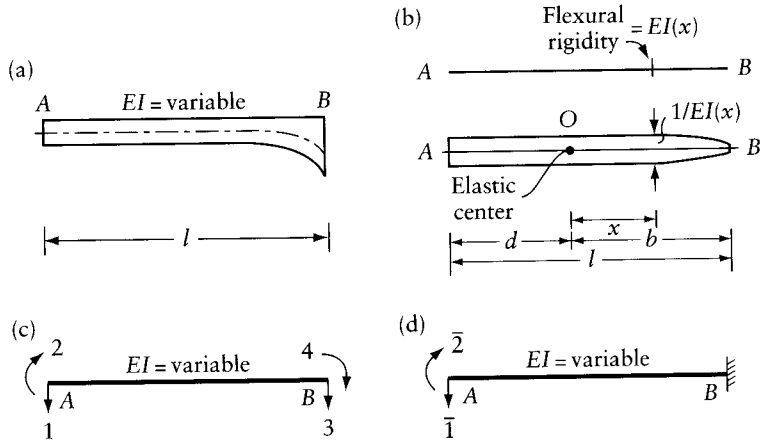

Figure 11.1 Derivation of the stiffness matrix of a nonprismatic member. (a) Nonprismatic member. (b) Idealization as a straight bar and its analogous column. (c) and (d) Coordinate systems.

(the elastic center). Thus, the area, the first moment of area, and the second moment of area about the centroidal y axis are, respectively,

$$a = \int \frac{dx}{EI}; \quad B_y = \int x \frac{dx}{EI} = 0; \quad I_y = \int x^2 \frac{dx}{EI} \tag{11.1}$$

11.3 Stiffness matrix of nonprismatic member

Figure 11.1c shows a system of four coordinates at ends A and B of the nonprismatic member in Figure 11.1a. We will derive the corresponding stiffness matrix $[S]$, using column analogy, thus considering only bending deformation. For this purpose, we use virtual work to derive the flexibility matrix $[\bar{f}]$ when end B is fixed (Figure 11.1d); see Eq. 8.5:

$$[\bar{f}] = \begin{bmatrix} \int \frac{M_{u1}^2 dx}{EI} & \text{symmetrical} \\ \int \frac{M_{u1} M_{u2} dx}{EI} & \int \frac{M_{u2}^2 dx}{EI} \end{bmatrix} \tag{11.2}$$

where

$$M_{u1} = -(x+d) \quad M_{u2} = 1 \tag{11.3}$$

with d being the distance between O and the left end A.

M_{u1} and M_{u2} are, respectively, equal to the bending moment at any section due to the separate effect of $F_1 = 1$ and $F_2 = 1$. Substitution of Eq. 11.3 into Eq. 11.2 gives

$$[\bar{f}] = \begin{bmatrix} \int \frac{(x+d)^2}{EI} dx & \text{symmetrical} \\ -\int \frac{(x+d)}{EI} dx & \int \frac{dx}{EI} \end{bmatrix} \tag{11.4}$$

Substitution of Eq. 11.1 into Eq. 11.4 gives

$$[\bar{f}] = \begin{bmatrix} I_y + ad^2 & -ad \\ -ad & a \end{bmatrix} \tag{11.5}$$

Inversion of Eq. 11.5 gives the stiffness matrix for the nonprismatic member when end B is fixed (Figure 11.1d):

$$[\bar{S}] = \begin{bmatrix} 1/I_y & d/I_y \\ d/I_y & (1/a) + (d^2/I_y) \end{bmatrix} \tag{11.6}$$

The forces in any column j of the stiffness matrix $[S]$ of the unsupported beam in Figure 11.1c represent a system in equilibrium; thus,

$$S_{3j} = -S_{1j} \quad \textit{and} \quad S_{4j} = S_{1j}(d+b) - S_{2j} \text{ (for } j = 1,\ 2,\ 3,\ 4) \tag{11.7}$$

Elements S_{11} and S_{21} are the forces at end A when end B is fixed (Figure 11.1d); thus, S_{11} and S_{21} are the same as $\bar{S}_{11}$ and $\bar{S}_{21}$. Similarly, S_{12} and S_{22} are the same as $\bar{S}_{12}$ and $\bar{S}_{22}$. Thus, using the equilibrium Eq. 11.7 and remembering that the stiffness matrix is symmetrical, we obtain the stiffness matrix of the nonprismatic member (Figure 11.1c):

$$[S] = \begin{bmatrix} 1/I_y & & \text{symmetrical} & \\ d/I_y & (1/a) + (d^2/I_y) & & \\ -1/I_y & -d/I_y & 1/I_y & \\ b/I_y & -(1/a) + (bd/I_y) & -b/I_y & (1/a) + (b^2/I_y) \end{bmatrix} \tag{11.8}$$

In the special case when $EI =$ constant, $a = l/EI$; $I_y = l^3/(12EI)$; $d = b = l/2$. Substitution of these values in Eq. 11.8 gives the same stiffness matrix as Eq. 6.8.

11.3.1 End rotational stiffness and carryover moment

The elements of columns 2 and 4 of the stiffness matrix of the nonprismatic beam in Figure 11.1c (Eq. 11.8) represent the end-forces when the beam is deflected as shown in Figures 11.2a and b respectively. Thus, the stiffness matrix of a nonprismatic member, Figure 11.1c, may be rewritten in the form

$$[S] = \begin{bmatrix} (S_{AB} + S_{BA} + 2t)/l^2 & (S_{AB} + t)/l & -(S_{AB} + S_{BA} + 2t)/l^2 & (S_{BA} + t)/l \\ (S_{AB} + t)/l & S_{AB} & -(S_{AB} + t)/l & t \\ -(S_{AB} + S_{BA} + 2t)/l^2 & -(S_{AB} + t)/l & (S_{AB} + S_{BA} + 2t)/l^2 & -(S_{BA} + t)/l \\ (S_{BA} + t)/l & t & -(S_{BA} + t)/l & S_{BA} \end{bmatrix} \tag{11.9}$$

This matrix can be generated by filling in the member end-forces in Figures 11.2a and b in columns 2 and 4, completing rows 2 and 4 by considering symmetry of the matrix, then completing the remaining four elements by considering that the four forces in any column are in equilibrium.

The member end-moment $S_{AB}(=S_{22})$, referred to as the *rotational stiffness* of end A of member AB (Figure 11.2a), is the moment required to produce unit rotation of end A while end B is fixed; the corresponding moment t at end B is referred to as the *carryover moment*. The ratio $C_{AB} = t/S_{AB}$ is referred to as the *carryover factor* from A to B.

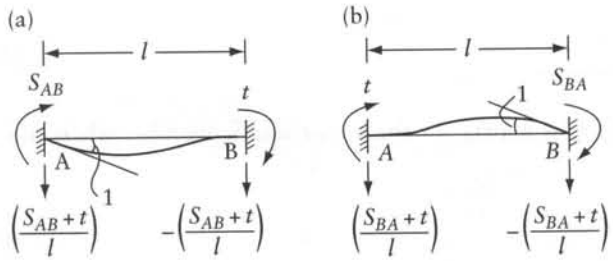

Figure 11.2 Member end-forces produced by unit rotations at the ends of a nonprismatic member. (a) and (b) Forces on columns 2 and 4, respectively, of the member in Figure 11.1c.

Similarly, with respect to Figure 11.2b, the rotational stiffness of end B of member AB, S_{BA}, is the moment at B required to produce unit rotation at B when end A is fixed; the corresponding carryover moment at A is also equal to t. This can be seen by applying Betti's theorem to the forces and displacements in Figures 11.2a and b. The carryover factor from B to A is $C_{BA} = t/S_{BA}$.

From Eq. 11.8 and the above definition, it is seen that the end rotational stiffness, the carryover moment, and the carryover factors for a nonprismatic beam are (Figure 11.1b)

$$S_{AB} = \frac{1}{a} + \frac{d^2}{I_y} \quad S_{BA} = \frac{1}{a} + \frac{b^2}{I_y} \quad t = -\frac{1}{a} + \frac{bd}{I_y} \tag{11.10}$$

$$C_{AB} = \frac{-(1/a) + (bd/I_y)}{(1/a) + (d^2/I_y)} \quad C_{BA} = \frac{(-1/a) + (bd/I_y)}{(1/a) + (b^2/I_y)} \tag{11.11}$$

In the special case of a prismatic member, the end rotational stiffness, the carryover moment, and the carryover factor are

$$S_{AB} = S_{BA} = \frac{4EI}{l} \quad t = \frac{2EI}{l} \quad C_{AB} = C_{BA} = \frac{1}{2} \tag{11.12}$$

The end rotational stiffnesses and the carryover factors will be used in the method of moment distribution (Section 11.4). Substitution of Eq. 11.12 in 11.9 gives the stiffness matrix for a prismatic member (Eq. 6.8). The introduction of simple supports at the ends of the nonprismatic member in Figure 11.1c prevents the displacements at coordinates 1 and 3; the stiffness matrix corresponding to the remaining coordinates (2 and 4, Figure 11.1c) will be given by Eq. 11.9 with the first and the third rows and columns removed; the resulting 2×2 matrix can be inverted to give the flexibility matrix for a nonprismatic simple beam, corresponding to clockwise arrows at its ends. (See Example 11.1)

Example 11.1: Nonprismatic member: end-rotational stiffness, carryover factors and fixed-end moments

Determine $S_{AB}, S_{BA}, t, C_{AB}$, and C_{BA} for a nonprismatic member AB, having a flexural rigidity $EI = EI_0(1 + \xi)$, where $\xi = \bar{x}/l$, with $\bar{x}$ being the distance from the left end; l is member length; $EI_0 =$ constant. Also, determine the fixed-end moments due to a uniform load q per unit length. Consider only bending deformation.

We may consider Figure 11.1a, with different variation of EI, as representing the member in this problem. The area of the analogous column is (Eq. 11.1)

$$a=\int \frac{d\bar{x}}{EI}=\frac{l}{EI_0}\int_0^1 \frac{d\xi}{1+\xi}=0.6931\frac{l}{EI_0}$$

To find the centroid, O of the analogous column, take the first moment of area about the end A. The distance between A and the centroid O is

$$d=\frac{1}{a}\int \frac{\bar{x}d\bar{x}}{EI}=\frac{l^2}{(0.6931l/EI_0)}\frac{1}{EI_0}\int_0^1 \frac{\xi d\xi}{1+\xi}$$

Hence

$$d=0.4427l \quad b=l-d=0.5573l$$

The distance between O and any point is: $x=\bar{x}-0.4427l$. The second moment of area of the analogous column, by Eq. 11.1, is

$$I_y=\int \frac{x^2dx}{EI}=\frac{l^3}{EI_0}\int_0^1 \frac{(\xi-0.4427)^2d\xi}{1+\xi}=0.0573\frac{l^3}{EI_0}$$

The end rotational stiffnesses, the carryover moments, and the carryover factors (Eqs. 11.10 and 11.11) are

$$S_{AB}=\frac{EI_0}{l}\left(\frac{1}{0.6931}+\frac{(0.4427)^2}{0.0573}\right)=4.863\frac{EI_0}{l}$$

$$S_{BA}=\frac{EI_0}{l}\left(\frac{1}{0.6931}+\frac{(0.5573)^2}{0.0573}\right)=6.863\frac{EI_0}{l}$$

$$t=\frac{EI_0}{l}\left(-\frac{1}{0.6931}+\frac{0.4427(0.5573)}{0.0573}\right)=2.863\frac{EI_0}{l}$$

$$C_{AB}=\frac{2.863}{4.863}=0.589 \quad C_{BA}=\frac{2.863}{6.863}=0.417$$

To determine the fixed-end moments $\{M_{AB}, M_{BA}\}$ due to uniform load, we use the force method selecting a simple beam as a released structure. Clockwise arrows 1 and 2 at the member ends represent the redundants:

$$\{F_1, F_2\}=\{M_{AB}, M_{BA}\}$$

The bending moment in the released structure due to load q/unit length, $F_1=1$ or $F_2=1$ is:

$$M_s=\frac{ql^2}{2}\xi(1-\xi) \quad M_{u1}=1-\xi \quad M_{u2}=-\xi$$

The displacements of the released structure (Eq. 8.4)

$$D_1 = \int_0^l \frac{M_s M_{u1}}{EI} d\bar{x} \quad D_2 = \int_0^l \frac{M_s M_{u2}}{EI} d\bar{x}$$

$$D_1 = \frac{ql^3}{2EI_0} \int_0^1 \frac{\xi(1-\xi)^2}{1+\xi} d\xi = 0.0304 \frac{ql^3}{EI_0}$$

$$D_2 = -\frac{ql^3}{2EI_0} \int_0^1 \frac{\xi^2(1-\xi)}{1+\xi} d\xi = -0.0265 \frac{ql^3}{EI_0}$$

The fixed-end moments (the redundants) are (Eqs. 4.9 and 6.1):

$$\begin{Bmatrix} F_1 \\ F_2 \end{Bmatrix} = -[f]^{-1}\{D\} = -[S]\{D\}$$

where $[f]$ and $[S]$ are the flexibility and stiffness matrices corresponding to the coordinates 1 and 2.

$$\begin{Bmatrix} M_{AB} \\ M_{BA} \end{Bmatrix} = -\begin{bmatrix} S_{AB} & t \\ t & S_{BA} \end{bmatrix}\{D\}$$

$$\begin{Bmatrix} M_{AB} \\ M_{BA} \end{Bmatrix} = \frac{EI_0}{l}\begin{bmatrix} 4.863 & 2.863 \\ 2.863 & 6.863 \end{bmatrix}\begin{Bmatrix} -0.0304 \\ 0.0265 \end{Bmatrix}\frac{ql^3}{EI_0} = \begin{Bmatrix} -0.0720 \\ 0.0940 \end{Bmatrix} ql^2$$

The integrals involved in this example are evaluated numerically, using a programmable calculator.

11.4 Process of moment distribution

The moment-distribution method of analysis of framed structures was introduced by Hardy Cross[1] in 1932, and was extended by others to the cases of structures subjected to high axial forces, and to axisymmetrical circular plates and shells of revolution.[2] In this section we deal mainly with plane frames supported in such a way that the only possible joint displacements are rotations without translation. Plane frames with joint translations are dealt with in Section 11.8.

Consider the beam ABC of Figure 11.3a, encastré at A and C, and continuous over support B. Let us assume first that the rotation of joint B is prevented by a restraining external couple acting at B. Due to the lateral loads on the members AB and BC, with the end rotations prevented at all ends, fixed-end moments (FEM) result at the ends A and B, and B and C.

Arbitrary values are assigned to these moments in Figure 11.3b, using the convention that a positive sign indicates a clockwise end-moment. The restraining moment required to prevent

1 Hardy Cross, "Analysis of Continuous Frames by Distributing Fixed-End Moments." *Trans. ASCE*. Paper 1793 (96) 1932.

2 See list of references: Gere, J. M., *Moment Distribution*, Van Nostrand, New York, 1963, pp. 247–268.

(a)

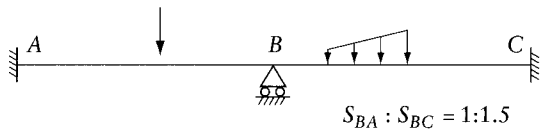

(b)

End	AB	BA	BC	CB
DF_s		0.4	0.6	
FEM's	−80	+100	−150	+180
One cycle; moment distribution and carryover	+10 ←	+20	+30 →	+15
Final moments	−70	120	−120	195

(c)

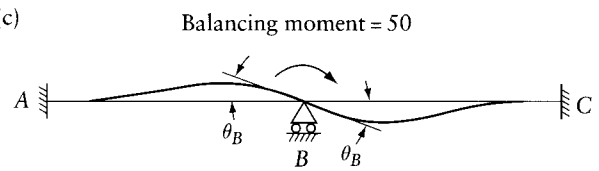

Figure 11.3 Analysis of a continuous beam by the moment-distribution method. (a) Beam. (b) Solution by moment distribution. (c) Beam deflection after release of joint B.

the rotation of joint B is equal to the algebraic sum of the fixed-end moments of the members meeting at B, that is -50.

So far, the procedure has been identical with the general displacement method considered in Chapter 5. However, we now recognize that the joint B is, in fact, not restrained, and we allow it to rotate by removing the restraining moment of -50. The same effect is achieved by applying to the joint B an external couple $M = +50$ (Figure 11.3c), that is, a moment equal and opposite to the algebraic sum of the fixed-end moments at the joint. This is known as the *balancing moment*. Its application causes the ends of the members BA and BC meeting at B to rotate through the same angle θ_B; hence, end-moments M_{BA} and M_{BC} develop. For equilibrium of the moments acting on joint B,

$$M = M_{BA} + M_{BC} \tag{11.13}$$

The end-moments M_{BA} and M_{BC} can be expressed in terms of the rotational stiffnesses of end B of members AB and BC, viz. S_{BA} and S_{BC}, thus,

$$M_{BA} = \theta_B S_{BA} \quad \text{and} \quad M_{BC} = \theta_B S_{BC} \tag{11.14}$$

From Eqs. 11.13 and 11.14, the end-moments can be expressed as a fraction of the balancing moment

$$\left.\begin{aligned} M_{BA} &= \left(\frac{S_{BA}}{S_{BA}+S_{BC}}\right)M \\ M_{BC} &= \left(\frac{S_{BC}}{S_{BA}+S_{BC}}\right)M \end{aligned}\right\} \tag{11.15}$$

This means that the balancing moment is distributed to the ends of the members meeting at the joint, the *distributed moment* in each member being proportional to its relative rotational stiffness. The ratio of the distributed moment in a member to the balancing moment is called *the distribution factor (DF)*. It follows that the distribution factor for an end is equal to the rotational stiffness of the end divided by the sum of the rotational stiffnesses of the ends meeting at the joint, that is,

$$(DF)_i = \frac{S_i}{\sum_{j=1}^{n} S_j} \tag{11.16}$$

where i refers to the near end of the member considered, and there are n members meeting at the joint.

It is clear that to determine the DFs we can use relative values of the rotational end stiffnesses rather than the actual values, so that Eq. 11.16 is valid also with S representing the *relative rotational end stiffness*. It is also evident that the sum of all the DFs of the ends meeting at a joint must be equal to unity.

Let the relative stiffnesses S_{BA} and S_{BC} for the beam in Figure 11.3a be 1 and 1.5. The DFs are therefore: $1/(1+1.5)=0.4$ for end BA, and $1.5/(1+1.5)=0.6$ for end BC. The balancing moment of $+50$ will be distributed as follows: $50\times 0.4=20$ to BA, and $50\times 0.6=30$ to BC. The distributed moments are recorded in a table in Figure 11.3b.

The rotation of joint B produced in the previous step induces end-moments at the far fixed ends A and C. These end-moments are referred to as *carryover moments*, their values being equal to the appropriate distributed moment multiplied by the carryover factor (COF): C_{BA} from B to A, and C_{BC} from B to C. The value of a carryover factor depends upon the variation in the cross section of the member; for a prismatic member, COF $=\frac{1}{2}$. A method of calculating the COFs is described in Section 11.3.1. When the far end of a member is pinned, the COF is, of course, zero.

The carryover moments in the beam considered are recorded in Figure 11.3b on the assumption that $C_{BA}=C_{BC}=\frac{1}{2}$, that is, the cross section is taken to be constant within each span. The two arrows in the table pointing away from joint B indicate that the rotation at B (or moment distribution at B) causes the carryover moment of the value indicated at the head of the arrow. The use of the arrows makes it easier to follow a proper sequence of operations and also facilitates checking.

The process of moment distribution followed by carrying over is referred to as one *cycle*. In the problem considered, no further cycles are required as there is no out-of-balance moment. The final end-moments are obtained by adding the end-moments in the restrained condition (FEMs) to the moments caused by the rotation of joint B in the cycle in Figure 11.3b. However, if rotation can occur at more than one joint, further cycles of distribution and carryover have to be performed, as shown in the following example.

Example 11.2: Plane frame: joint rotations without translations

Use the method of moment distribution to analyze the frame in Figure 11.4a. If the axial deformations are ignored, the only possible joint displacements are rotations at B and C.

(a)

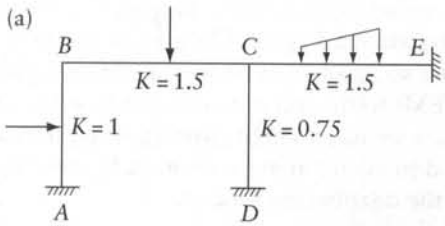

(b)

End	BA	BC	CB	CD	CE	EC	AB	DC
DF's	0.4	0.6	0.4	0.2	0.4			
FEM's	+150.0	-200.0	+285.0	0	-200.0	+200.0	-150.0	0
Cycle 1	+20.0	+30.0 →	+15.0				→ +10.0	
Cycle 2		-20.0 ←	-40.0	-20.0	-40.0 →	-20.0		-10.0←
Cycle 3	+8.0	+12.0 →	+6.0				→ 4.0	
Cycle 4		-1.2 ←	-2.4	-1.2	-2.4 →	-1.2		-0.6←
Cycle 5	+0.5	+0.7					→ 0.3	
Final moments	178.5	-178.5	263.6	-21.2	-242.4	178.8	-135.7	-10.6

Figure 11.4 Analysis of the plane frame in Example 11.2 by moment distribution without joint translation. (a) Plane frame without joint translation. (b) Moment distribution.

We assume the frame to have prismatic members so that the carryover factor in all cases is $\frac{1}{2}$. Then, the rotational end stiffness of any member is $S = 4EI/l$, where EI is the flexural rigidity of the cross section and l the length of the member. It follows that the relative rotational stiffnesses can be taken as $K = I/l$. The relative K values for all the members are shown in Figure 11.4a. The applied load is assumed to be of such a magnitude as to produce the FEMs given in Figure 11.4b.

The DFs are calculated by Eq. 11.16 and indicated in Figure 11.4b. The first cycle of moment distribution and carryover is done by allowing joint B to rotate; joint C continues to be restrained. This is done in the same way as in the previous example. In the second cycle, joint C is allowed to rotate, joint B now being restrained. The balancing moment for this cycle is equal to minus the algebraic sum of the FEMs at CB, CD, and CE plus the carryover moment caused by the rotation of joint B in the previous cycle – that is $-(285 + 0 - 200 + 15) = -100$. The second cycle is terminated by the carryover of moments to the far ends of the three members meeting at C, as shown by arrows. It is evident that cycle 2 has induced an imbalance at joint B, that is, if joint B is now released, a further rotation will occur. The effect of this release is followed through in the same way as in cycle 1, but with the balancing moment equal to minus the moment carried over to BC from the previous cycle.

The carryover in the third cycle results in an unbalanced moment at joint C. In order to remove the external constraint, joint C must be balanced again. The process is repeated until the unbalanced moments at all the joints are so small as to be considered negligible. The final moments are obtained by adding the FEMs to the end-moments produced by the joint displacement allowed in *all* the cycles. Because we reach a final position of equilibrium under the applied loading, the sum of the final end-moments at any joint must be zero. This fact can be used as a check on the arithmetic in the distribution process.

It may be interesting to note that moment distribution can be carried out experimentally on a model of a structure capable of being clamped at any joint.

In the preceding example, no distribution was carried out at the fixed ends A, D, and E because the ends of the members at these points can be imagined to be attached to a body of infinite rigidity. Thus, the DF for a built-in end of a frame is zero. We should also note that the moments introduced at the ends AB and DC in each cycle are equal to the COFs times the moment introduced respectively at ends BA and CD. It follows that the moments at ends AB and DC need not be recorded during the distribution process, and the final moments at these two ends can be calculated by

$$M_{AB} = (\text{FEM})_{AB} + C_{BA}[M_{BA} - (\text{FEM})_{BA}] \tag{11.17}$$

where M_{BA} is the final moment at end BA. A similar equation can be written for the end DC.

11.5 Moment-distribution procedure for plane frames without joint translation

We should recall that the process of moment distribution described in the previous section applies solely to structures in which the only possible displacement at the joints is rotation. It may be convenient to summarize the steps involved.

Step 1 Determine the internal joints which will rotate when the external load is applied to the frame. Calculate the relative rotational stiffnesses of the ends of the members meeting at these joints, as well as the carryover factors from the joints to the far ends of these members. Determine the distribution factors by Eq. 11.16. The rotational stiffness of either end of a prismatic member is $4EI/l$ and the COF from either end to the other is $\frac{1}{2}$. If one end of a prismatic member is hinged, the rotational end stiffness of the other end is $3EI/l$, and, of course, no moment is carried over to the hinged end. In a frame with all members prismatic, the relative rotational end stiffness can be taken as $K = I/l$, and when one end is hinged the rotational stiffness at the other end is $(\frac{3}{4})K = (\frac{3}{4})I/l$. The rotational end stiffnesses and the carryover factors for nonprismatic members can be determined by column analogy, as shown in Section 11.3.1.

Step 2 With all joint rotations restrained, determine the fixed-end moments due to the lateral loading on all the members.

Step 3 Select the joints to be released in the first cycle. It may be convenient to take these as alternate internal joints. (For example, in the frame of Figure 11.5, we can release in the first cycle either A, C, and E or D, B, and F.) Calculate the balancing moment at the selected joints; this is equal to minus the algebraic sum of the fixed-end moments. If an external clockwise couple acts at any joint, its value is simply added to the balancing moment.

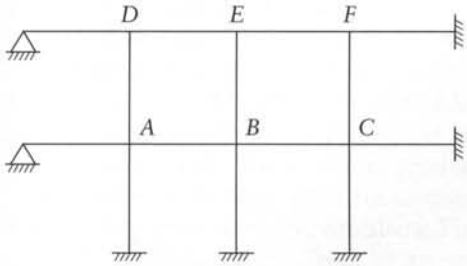

Figure 11.5 Plane frame without joint translation.

Step 4 Distribute the balancing moments to the ends of the members meeting at the released joints. The distributed moment is equal to the DF multiplied by the balancing moment. The distributed moments are then multiplied by the COFs to give the carryover moments at the far ends. Thus, the first cycle is terminated.

Step 5 Release the remaining internal joints, while further rotation is prevented at the joints released in the first cycle. The balancing moment at any joint is equal to minus the algebraic sum of the FEMs and of the end-moments carried over in the first cycle. The balancing moments are distributed and moments are carried over to the far ends in the same way as in Step 3. This completes the second cycle.

Step 6 The joints released in Step 3 are released again, while the rotation of the other joints is prevented. The balancing moment at a joint is equal to minus the algebraic sum of the end-moments carried over to the ends meeting at the joint in the previous cycle.

Step 7 Repeat Step 6 several times, for the two sets of joints in turn until the balancing moments become negligible.

Step 8 Sum the end-moments recorded in each of the steps 2 to 7 to obtain the final end-moments. The reactions or stress resultants if required may then be calculated by simple equations of statics.

If a frame has an overhanging part, its effect is replaced by a force and a couple acting at the joint of the overhang with the rest of the structure. This is illustrated in the following example.

Example 11.3: Continuous beam

Obtain the bending moment diagram for the continuous beam of Figure 11.6a.

The effect of the cantilever AB on the rest of the beam is the same as that of a downward force, qb and an anticlockwise couple of $0.6qb^2$ acting at B, as shown in Figure 11.6b. The end B is thus free, and the distribution has to be carried out at joints C, D, and E. During the distribution, joint B (Figure 11.6b) will be free to rotate so that B is considered to be a hinge. No moment is therefore carried over from C to B, and the relative end-rotational stiffness[3] of CB is $(\frac{3}{4})K = (\frac{3}{4})I/l$. Since I is constant throughout, it may be taken as unity.

3 See Eq. 11.21.

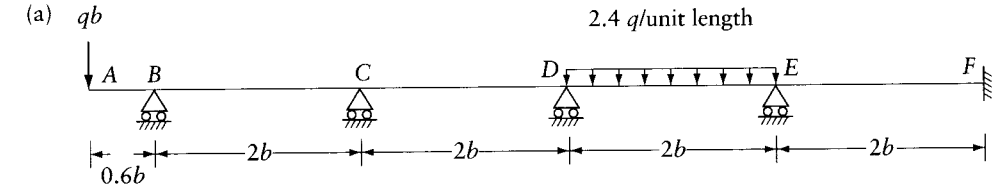

(c)

End	BC	CB	CD	DC	DE	ED	EF	FE	
Relative end rotational stiffness		(0.75/20)	(1/20)	(1/20)	(1/20)	(1/20)	(1/20)		
COFs		0	0.5	0.5	0.5	0.5	0.5		
DFs		0.43	0.57	0.5	0.5	0.5	0.5		Multiplier : $qb^2/100$
FEMs	−60	−30.0	0	0	−80.0	+80.0	0	0	
Five cycles of distribution and carryover			+20.0 ←	+40.0	+40.0 ←	+20.0			
			+5.7 →	+2.8	−25.0 ←	−50.0			
			+5.6 ←	+11.1	+11.1 →	+5.6			
			−3.2 ←	−1.6	−1.4 ←	−2.8			
			+0.8 ←	+1.5	+1.5 →	+0.8			
Distribution			−0.4			−0.4			
Final end-moments	−60	−28.5	28.5	53.8	−53.8	53.2	−53.2	−26.6	

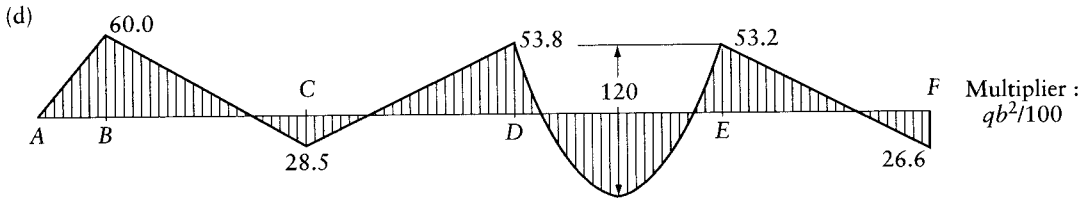

Figure 11.6 Analysis of the continuous beam in Example 11.3 by moment distribution. (a) Continuous beam. (b) Replacement of the actual load on overhang by equivalent loading at *B*. (c) Moment distribution. (d) Bending moment diagram.

The relative rotational stiffnesses of the ends at the three joints C, D, and E are recorded in Figure 11.6c, together with the COFs and the DFs.

The FEMs for ends BC and CB are those of a beam hinged at B, fixed at C, and subjected to a couple of $-0.6qb^2$ at B. The other FEMs are calculated in the usual way.

The moment distribution is performed at joint D in one cycle, and at joints C and E in the following cycle. The moments produced at ends CB, EF, and FE are not recorded; the final moments at these ends are calculated from the values of the final moments at the other end of the respective members. First, we write $M_{CB} = -M_{CD} = -0.285qb^2$, and $M_{EF} = -M_{ED} = -0.532qb^2$. Then, by an equation similar to Eq. 11.17,

$$M_{FE} = (\text{FEM})_{FE} + C_{EF}[M_{EF} - (\text{FEM})_{EF}]$$

The FEMs at the two ends of member EF are zero and $C_{EF} = \frac{1}{2}$; therefore, $M_{FE} = (\frac{1}{2})M_{EF} = -0.266qb^2$.

The final bending moment diagram of the beam is shown in Figure 11.6d.

11.6 Adjusted end-rotational stiffnesses

The process of moment distribution can be made shorter in certain cases if adjusted end-rotational stiffnesses are used instead of the usual stiffnesses. Expressions will be derived for these adjusted end-rotational stiffnesses of nonprismatic members but, because of their frequent use, values for prismatic members will also be given.

The end-rotational stiffness S_{AB} was defined in Section 11.3.1 as the value of the moment required at A to rotate the beam end A through a unit angle while the far end B is fixed. Similarly, S_{BA} is the end-moment to produce a unit rotation at B while end A is fixed. The deflected shapes of the beam corresponding to these two conditions are shown in Figure 11.7a. The moment t at the fixed end has the same value for the two deflected configurations. The rotated ends in Figure 11.7a are sketched with a roller support but they can also be represented as in Figures 11.2a and b. Both figures indicate the same conditions, that is, a unit rotation without transverse translation of the end. The axial and shear deformations are ignored for the present purposes. For a prismatic beam $S_{AB} = S_{BA} = 4EI/l$, and $t = 2EI/l$. For nonprismatic beams, values of S_{AB} and S_{BA} and the carryover factors may be calculated by Eqs. 11.10 and 11.11.

The special cases which we shall now consider are: (a) when rotation is applied at one end of a member whose far end is not fixed but hinged (Figure 11.7b); (b) when such a member is subjected to symmetrical or antisymmetrical end-forces and rotations (Figures 11.7c and d). The adjusted end-rotational stiffnesses in these cases will be denoted by S with a subscript indicating the beam end and a superscript indicating the conditions at the far end as defined in Figure 11.7.

Let us express the adjusted end-rotational stiffnesses $S^{①}_{AB}$, $S^{②}_{AB}$ and $S^{③}_{AB}$ in terms of the stiffnesses S_{AB}, S_{BA}, and t for the same beam.

The forces and displacements along the coordinates 1 and 2 in Figure 11.7a are related by

$$[S]\{D\} = \{F\} \tag{11.18}$$

where

$$[S] = \begin{bmatrix} S_{AB} & t \\ t & S_{BA} \end{bmatrix}$$

and where $\{D\}$ are the end-rotations and $\{F\}$ the end-moments.

(a)

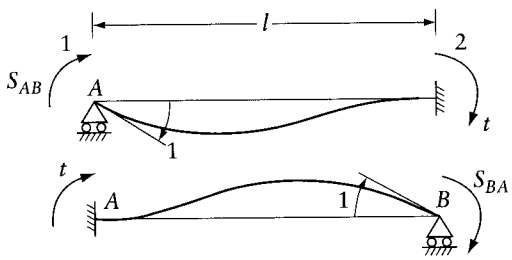

(b)

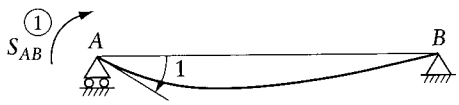

(c)

(d)

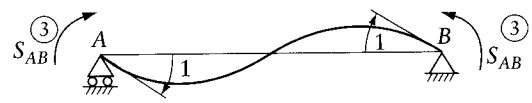

(e)

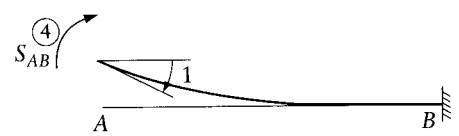

④
S_{AB} is given in Prob. 11.28.

(f)

Figure 11.7 End-rotational stiffnesses in special cases (Eqs. 11.18 to 11.25). (a) End-moments caused by a unit rotation at one end while the other end is fixed. (b) End-moment caused by a unit rotation at end A while end B is hinged. (c) End-moments caused by symmetrical unit rotations at ends A and B. (d) End-moments caused by antisymmetrical unit rotations at ends A and B. (e) End-moment at A caused by a unit rotation at A while B is fixed. The translation of A is not prevented. (f) Coordinates for calculation of $S_{AB}^{④}$.

Putting $D_1 = 1$ and $F_2 = 0$ in Eq. 11.18 represents the conditions in Figure 11.7b. The force F_1 in this case will be equal to the adjusted stiffness $S_{AB}^{①}$. Thus,

$$\begin{bmatrix} S_{AB} & t \\ t & S_{BA} \end{bmatrix} \begin{Bmatrix} 1 \\ D_2 \end{Bmatrix} = \begin{Bmatrix} S_{AB}^{①} \\ 0 \end{Bmatrix}$$

Solving,

$$S_{AB}^{①} = S_{AB} - \frac{t^2}{S_{BA}} \tag{11.19}$$

The same equation can be written in terms of the COFs, $C_{AB} = t/S_{AB}$ and $C_{BA} = t/S_{BA}$, thus,

$$S_{AB}^{①} = S_{AB}(1 - C_{AB}C_{BA}) \tag{11.20}$$

For a prismatic member, Eqs. 11.19 and 11.20 reduce to

$$S_{AB}^{①} = \frac{3EI}{l} \tag{11.21}$$

Referring again to Eq. 11.18, and putting $D_1 = -D_2 = 1$ represents the conditions in Figure 11.7c. The force $F_1 = -F_2$ is equal to the end-rotational stiffness $S_{AB}^{②}$. Thus,

$$\begin{bmatrix} S_{AB} & t \\ t & S_{BA} \end{bmatrix} \begin{Bmatrix} 1 \\ -1 \end{Bmatrix} = \begin{Bmatrix} S_{AB}^{②} \\ -S_{AB}^{②} \end{Bmatrix}$$

Solving either of the above equations, we obtain the end-rotational stiffness in case of symmetry:

$$S_{AB}^{②} = S_{AB} - t = S_{AB}(1 - C_{AB}) \tag{11.22}$$

For a prismatic member, this reduces to

$$S_{AB}^{②} = \frac{2EI}{l} \tag{11.23}$$

Similarly, if we put $D_1 = D_2 = 1$, Eq. 11.18 represents the conditions in Figure 11.7d. The end-forces are $F_1 = F_2 = S_{AB}^{③}$, and the end-rotational stiffness in the antisymmetrical case is

$$S_{AB}^{③} = S_{AB} + t = S_{AB}(1 + C_{AB}) \tag{11.24}$$

For a prismatic member, this reduces to

$$S_{AB}^{③} = \frac{6EI}{l} \tag{11.25}$$

11.7 Adjusted fixed-end moments

Figure 11.8a represents a beam with two fixed ends subjected to transverse loading. Let the end-moments for this beam be M_{AB} and M_{BA} and let the vertical reactions be F_A and F_B. The beam is assumed to be nonprismatic with end-rotational stiffnesses S_{AB} and S_{AB}, the carryover moment t, and the carryover factors C_{AB} and C_{BA}. Let us now find the end-moments for a similar beam subjected to the same transverse loading but with the support conditions of Figure 11.8b. In this figure, the end A is hinged; thus, rotation at A is free to take place and there is only one end-moment $M_{BA}^{①}$ to be determined.

To shorten the process of moment distribution, in some cases we can use the adjusted fixed-end moment $M_{BA}^{①}$ together with the adjusted end-rotational stiffnesses. Consider first the beam in Figure 11.8a with the end-displacements restrained; the end-moments are M_{AB} and M_{BA}. Now

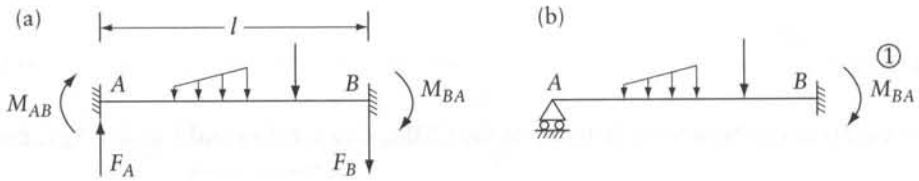

Figure 11.8 Adjusted fixed-end moments. (a) Two ends encastré. (b) Free rotation at *A*.

allow the end *A* to rotate by an amount such that a moment $-M_{AB}$ is developed at end *A*. The corresponding moment developed at *B* is $-C_{AB}M_{AB}$. Superposing the end-moments developed by the rotation will give a zero moment at *A*, and this represents the condition of the beam in Figure 11.8b. The adjusted FEM at *B* when end *A* is hinged is therefore

$$M_{BA}^{①} = M_{BA} - C_{AB}M_{AB} \tag{11.26}$$

where M_{AB} and M_{BA} are the FEMs of the same beam with the two ends encastré, and C_{AB} is the COF from *A* to *B*. For a prismatic beam, Eq. 11.26 becomes

$$M_{BA}^{①} = M_{BA} - \frac{M_{AB}}{2} \tag{11.27}$$

Example 11.4: Plane frame symmetry and antisymmetry

Find the bending moment in the symmetrical frame shown in Figure 11.9a by replacing the loading by equivalent symmetrical and antisymmetrical loadings.

Any load on a symmetrical structure can be replaced by the sum of a symmetrical and an antisymmetrical loading, as indicated in Figures 11.9b and c. The same concept can be used in computer analysis of large structures which exceeds the capacity of the available computer; by virtue of the structural symmetry, while the loading is not symmetrical, it is possible to find the solution by superposition of two or more analyses performed on a repetitive part of the structure (see Section 22.3).

We shall now introduce this concept for a relatively simple frame, using the adjusted stiffnesses and FEMs, although this does not achieve much saving in calculations.

With symmetry or antisymmetry of loading, the moment distribution need be done for one-half of the frame only. Figures 11.9d and e deal with the symmetrical and antisymmetrical cases respectively. The end-rotational stiffnesses for the members meeting at *B* are calculated using Eqs. 11.21, 11.23, and 11.25, and we find for the symmetrical case

$$S_{BA} : S_{BE} : S_{BC} = 3K_{BA} : 4K_{BE} : 2K_{BC}$$

and for the antisymmetrical case

$$S_{BA} : S_{BE} : S_{BC} = 3K_{BA} : 4K_{BE} : 6K_{BC}$$

where $K = I/l$. In this frame, *K* is the same for all members. The DFs are calculated in the usual way and are given in Figures 11.9d and e.

The FEM in end *BA* (for a beam with one end hinged) is obtained by the use of Appendix C and Eq. 11.26; thus, $(\text{FEM})_{BA} = 0.75\,Pb$ for both cases.

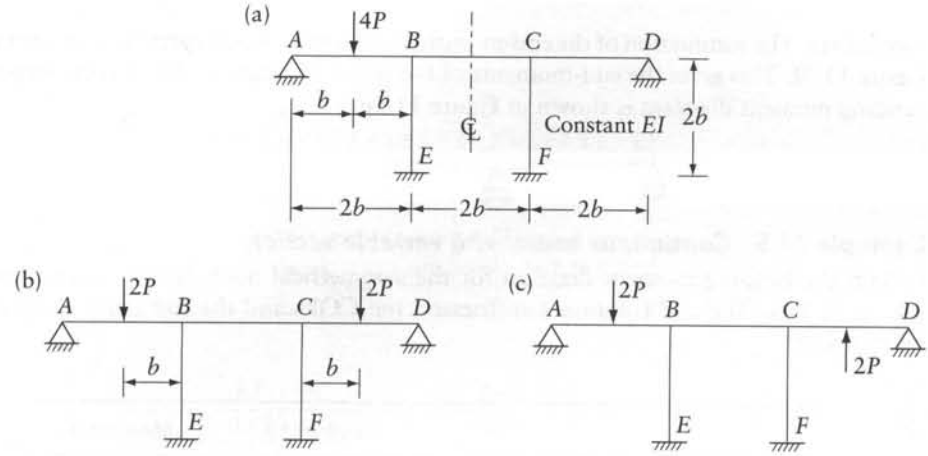

(d)

	BA	BE	BC
	0.33	0.45	0.22
Multiplier : *Pb*/100	← 0	↓ 0.5	0 →
	+75.0		
	−25.0	−33.4	−16.6
	+50.0	−33.4	−16.6

(e)

End	BA	BE	BC
DFs	0.23	0.31	0.46
COFs	← 0	↓ 0.5	0 →
FEMs	+75.0		
Distrib.	−17.2	−23.2	−34.6
Final end-moments	+57.8	−23.2	−34.6

(f)

End	*BA*	*BE*	*BC*	*EB*	*CD*	*CF*	*CB*	*FC*
Symmetrical loading	+50.0	−33.4	−16.6	−16.7	−50.0	+33.4	+16.6	+16.7
Antisymmetrical loading	+57.8	−23.2	−34.6	−11.6	+57.8	−23.2	−34.6	−11.6
Final end-moments for the frame in Fig.(a)	+107.8	−56.6	−51.2	−28.3	+7.8	+10.2	−18.0	+5.1

(g)

Multiplier : *Pb*/100

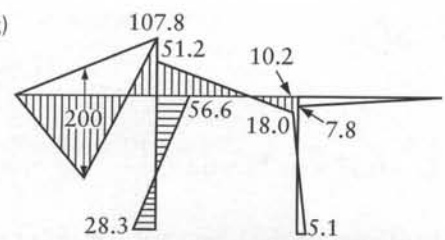

Figure 11.9 Analysis of frame in Example 11.4. (a) Frame properties and loading. (b) Symmetrical loading. (c) Antisymmetrical loading. (d) Moment distribution for the symmetrical case. (e) Moment distribution for the antisymmetrical case. (f) Summation of end-moments calculated in parts (d) and (e). (g) Bending moment diagram for the frame in part (a).

The COF $C_{BE} = 0.5$. No moments are carried over from *B* to *C* or from *B* to *A*. Thus, only one cycle of moment distribution is required at *B*, as shown in Figures 11.9d and e.

It is important to note that in the symmetrical case, the end-moments in the right-hand half of the frame are equal in magnitude and opposite in sign to the end-moments in the left-hand half, while in the antisymmetrical case they are equal and of the same sign in the

two halves. The summation of the end-moments in the two cases is carried out in the table in Figure 11.9f. This gives the end-moments of the frame in Figure 11.9a. The corresponding bending moment diagram is shown in Figure 11.9g.

Example 11.5: Continuous beam with variable section

Obtain the bending moment diagram for the symmetrical nonprismatic beam shown in Figure 11.10a. The end-rotational stiffnesses, the COFs and the fixed end-moments are given below.

	Member AB	*Member BC*
End-rotational stiffness	$S_{AB} = 4.2\dfrac{EI}{l_{AB}}$ $S_{BA} = 5.0\dfrac{EI}{l_{AB}}$	$S_{BC} = S_{CB} = 5.3\dfrac{EI}{l_{BC}}$
Carryover factor	$C_{AB} = 0.57$ $C_{BA} = 0.48$	$C_{BC} = C_{CB} = 0.56$
Fixed-end moment due to a uniform load of intensity q	$M_{AB} = -0.078ql_{AB}^2$ $M_{BA} = 0.095ql_{AB}^2$	$M_{BC} = -0.089ql_{BC}^2$ $M_{CB} = 0.089ql_{BC}^2$

The beam is symmetrical and symmetrically loaded. With adjusted stiffnesses and FEMs for ends BA and BC, the moment distribution needs to be carried out at joint B only.

The adjusted end-rotational stiffness for BA with end A hinged is given by Eq. 11.20; in our case,

$$S_{BA}^{①} = S_{BA}(1 - C_{AB}C_{BA})$$

or

$$S_{BA}^{①} = \frac{EI}{6b}(5.0)(1 - 0.57 \times 0.48) = 0.605\frac{EI}{b}$$

The adjusted end-stiffness for the symmetrical member BC is (from Eq. 11.22)

$$S_{BC}^{①} = S_{BC}(1 - C_{BC})$$

or

$$S_{BC}^{②} = \frac{EI}{8b}(5.3)(1 - 0.56) = 0.292\frac{EI}{b}$$

The distribution factors are

$$(DF)_{BA} = \frac{0.605}{0.605 + 0.292} = 0.67$$

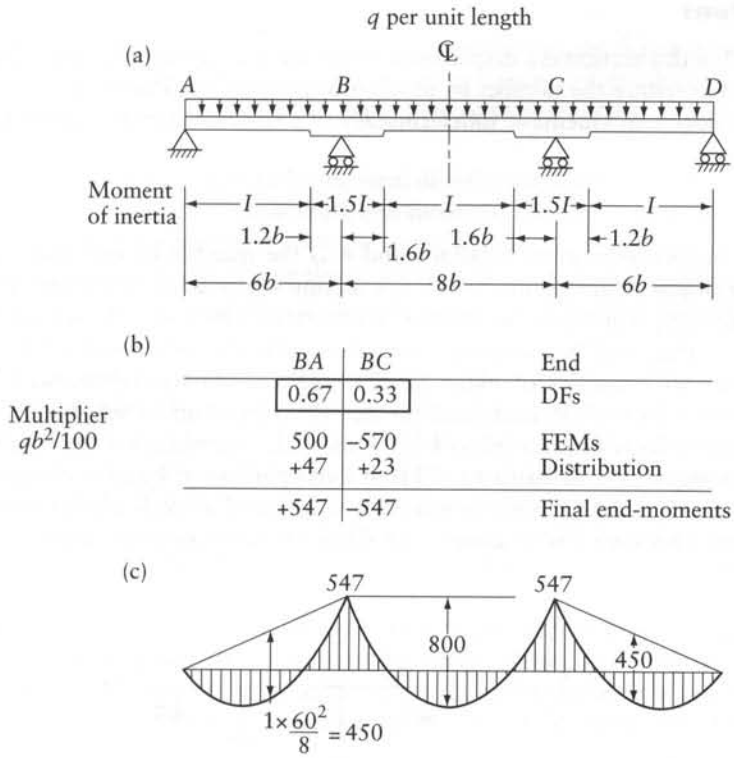

Figure 11.10 Analysis of beam in Example 11.5. (a) Beam properties and loading. (b) Moment distribution. (c) Bending moment diagram.

$$(DF)_{BC}=\frac{0.292}{0.605+0.292}=0.33$$

The adjusted FEM at B for member BA with end A hinged is (from Eq. 11.26)

$$M_{BA}^{①}=M_{BA}-C_{AB}M_{AB}$$

or

$$M_{BA}^{①}=ql_{AB}^2(0.095+0.57\times 0.078)=0.139ql_{AB}^2=5.00qb^2$$

The FEM at end ***BC*** is

$$M_{BC}=-0.089ql_{BC}^2=-5.70qb^2$$

One cycle of moment distribution is required with no carryover. This is shown in Figure 11.10b and the bending moment diagram is plotted in Figure 11.10c.

11.8 General moment distribution procedure: plane frames with joint translations

The procedure considered in this section is a displacement method of analysis of Chapter 5 with moment distribution used to reduce the number of simultaneous equations involved.

In the general case, the degree of kinematic indeterminacy of a structure can be expressed as

$$k = m + n$$

where m is the number of unknown joint rotations and n is the number of unknown joint translations. The number of joint translations, which is sometimes referred to as the number of *degrees of freedom in sidesway*, represents the number of equations which must be solved, and if n is much smaller than k, there will be a considerable reduction in computational effort.

Figure 11.11 shows several examples of plane frames with coordinates representing the unknown joint translations indicated. In each case the degree of freedom of sidesway n and the total number of unknown joint displacements k are indicated, assuming that the length of all members remains unchanged after deformations. From a comparison of k and n, we can see that the analysis by the method to be discussed involves the solution of a much smaller number of simultaneous equations. This saving is, of course, not significant in a computer analysis.

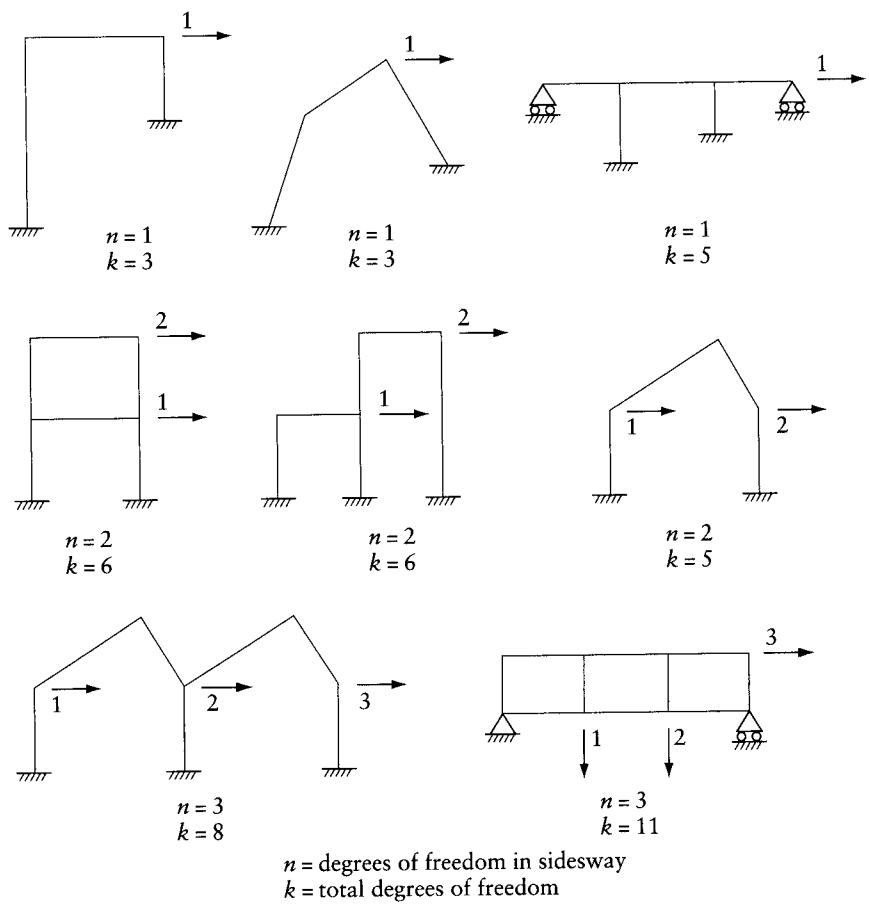

Figure 11.11 Joint displacements of plane frames.

The procedure is as follows.

Step 1 All the possible independent joint translations are first indicated by coordinates; their number is, of course, equal to the number of degrees of freedom in sidesway, n. Restraining forces $\{F\}_{n\times 1}$ are then introduced along these coordinates to prevent the translation of all joints.

Step 2 The frame is analyzed by moment distribution without joint translation (as in the preceding section), and the corresponding end-moments $\{A_r\}$ are determined. These are the moments on the ends of the members with the joints allowed to rotate but with translation restrained. The n restraining forces $\{F\}$ are then calculated by considering equilibrium of the members. This usually involves no more than the simple equations of static equilibrium.

Step 3 A unit displacement $D_1 = 1$ is introduced along the first of the n coordinates in the unloaded frame, while the translation along all the other coordinates is prevented. Assuming further that no joint rotations occur, the FEMs in the deformed members are calculated. With no further joint translation allowed, the moment distribution is now carried out. The end-moments obtained by the distribution correspond to a unit translational displacement along the coordinate 1, all the other joint translations being prevented, but joint rotations, of course, being allowed. From these moments, the forces required along the n coordinates in this deformed configuration are determined.

The process is repeated by allowing a unit value of translation to take place separately along each of the n coordinates. The resulting forces along the coordinates are then arranged in a matrix $[S]_{n\times n}$ representing the stiffness matrix of the frame. The end-moments are arranged in a matrix $[A_u]$ representing the end-moments caused by unit values of the translations.

Step 4 The loaded frame in the restrained state will have sidesway $(D_1, D_2, \ldots, D_n)$, which can be determined from the equation

$$[S]\{D\} = -\{F\} \tag{11.28}$$

Step 5 The end-moments in the actual structure are then calculated by a superposition equation

$$\{A\} = \{A_r\} + [A_u]\{D\} \tag{11.29}$$

It is obvious that in Step 3 we could have determined forces corresponding to an arbitrary value of the translation instead of unity. This, of course, would lead to a matrix $[S]$ which is not the real stiffness matrix and a vector $\{D\}$ which does not represent the real displacements, but Eq. 11.29 would still give the actual end-moments in the frame.

Example 11.6: Continuous beam on spring supports

Find the end-moments in each span of the prismatic continuous beam in Figure 11.12a. The beam is encastré at A and D and rests on elastic (spring) supports at B and C. The stiffness of the elastic supports, that is, the force required to compress any of the springs by a unit distance, is $2EI/l^3$.

The beam has two degrees of freedom of joint translation: vertical displacements at B and at C. Let the positive direction of these displacements be indicated by coordinates 1 and 2 in Figure 11.12b.

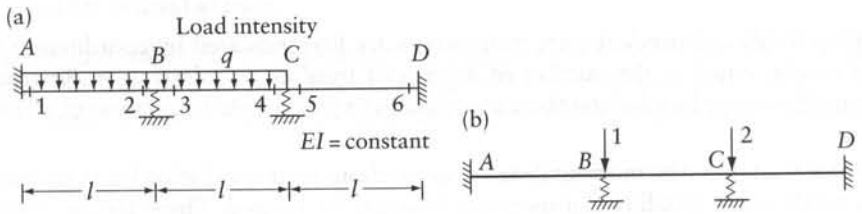

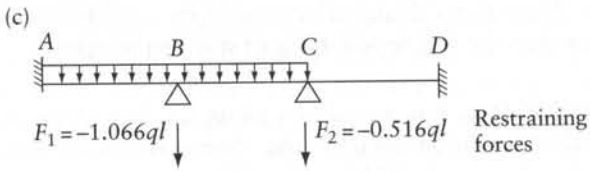

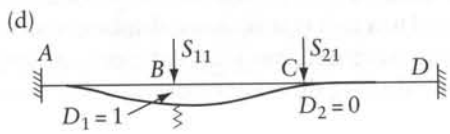

	AB	BA	BC	CB	CD	DC	End
		0.5	0.5	0.5	0.5		DFs
Multiplier $\frac{EI}{l^2}$	−6.00	−6.00	+6.00	+6.00			FEMs
			−1.50 ←	−3.00			Moment distribution and carry-over
			+0.75 →	+0.38			
			−0.09 ←	−0.19			
			+0.04 →	+0.02			
				−0.01			
	−5.60	−5.20	+5.20	+3.20	−3.20	−1.60	End-moments

Figure 11.12 Beam considered in Example 11.6. (a) Beam properties and loading. (b) Coordinate system. (c) Restraining forces ($D_1 = D_2 = 0$). (d) Calculation of the end-moments corresponding to $D_1 = 1$ and $D_2 = 0$.

First, the beam is analyzed with the translation of B and C prevented. The end-moments on ends 1, 2, . . ., 6 are

$$\{A_r\} = ql^2\{-0.078, 0.094, -0.094, 0.044, -0.044, -0.022\}$$

These moments can be obtained by moment distribution or by other methods. The restraining forces $\{F\}$ are equal to minus the reactions at B and C if these supports are rigid (Figure 11.12c), that is,

$$F = -ql\begin{Bmatrix} 1.066 \\ 0.516 \end{Bmatrix}$$

The FEMs due to $D_1 = 1$ and $D_2 = 0$, with no joint rotation allowed at B, are given in Figure 11.12d. The moment-distribution cycles are performed in the usual way and the end-moments are calculated. The forces S_{11} and S_{21} required to hold the beam in this deformed configuration are calculated from the end-moments, considering the equilibrium of each span as follows:

$$S_{11} = \left(\frac{2EI}{l^3}\right) - \frac{EI}{l^3}[(-5.2 - 5.60) - (5.20 + 3.2)] = 21.2\frac{EI}{l^3}$$

and

$$S_{21} = -\frac{EI}{l^3}[(3.2 + 5.2) - (-3.2 - 1.6)] = -13.2\frac{EI}{l^3}$$

The term $2EI/l^3$ included in S_{11} is the force required at 1 to compress the spring at A by a unit amount.

Because the structure is symmetrical, we can see that the forces S_{12} and S_{22} (at 1 and 2 respectively) corresponding to the displacements $D_1 = 0$ and $D_2 = 1$ are

$$S_{12} = -13.2\frac{EI}{l^3}$$

and

$$S_{22} = 21.2\frac{EI}{l^3}$$

The moments on the ends, 1, 2,..., 6 (see Figure 11.12a) due to the two deformed configurations considered above can be arranged in a matrix:

$$[A_u] = \frac{EI}{l^2}\begin{bmatrix} -5.6 & 1.6 \\ -5.2 & 3.2 \\ 5.2 & -3.2 \\ 3.2 & -5.2 \\ -3.2 & 5.2 \\ -1.6 & 5.6 \end{bmatrix}$$

Applying Eq. 11.28,

$$\frac{EI}{l^3}\begin{bmatrix} 21.2 & -13.2 \\ -13.2 & 21.2 \end{bmatrix}\begin{Bmatrix} D_1 \\ D_2 \end{Bmatrix} = ql\begin{Bmatrix} 1.066 \\ 0.516 \end{Bmatrix}$$

Hence,

$$\{D\} = \begin{Bmatrix} D_1 \\ D_2 \end{Bmatrix} = \frac{ql^4}{EI}\begin{Bmatrix} 0.107 \\ 0.091 \end{Bmatrix}$$

The final end-moments for the beam of Figure 11.12a are obtained from Eq. 11.29 by substituting the values calculated. Hence, the final end-moments are

$$\{A\} = ql^2 \begin{Bmatrix} -0.533 \\ -0.172 \\ 0.172 \\ -0.086 \\ 0.086 \\ 0.360 \end{Bmatrix}$$

In the present example, the end-moments due to a unit displacement at 1 or at 2 and the forces corresponding to these displacements could have been taken directly from the tables in Appendix E without the need for moment distribution. However, these tables apply only to continuous beams with equal spans.

11.9 General

The end-rotational stiffnesses, the carryover moment, and the stiffness matrix can be conveniently determined by the use of column analogy. It is to be noted that the method of column analogy considers bending deformations only.

The moment distribution is used in this chapter for the analysis of plane frames considering bending deformations only. Solution of simultaneous equations is avoided in structures not involving translation of the joints. The amount of computation can be further reduced for symmetrical frames subjected to symmetrical or antisymmetrical loading (and any loading can be resolved into such components) by using adjusted end-rotational stiffnesses and FEMs.

For plane frames with joint translations, moment distribution is used to limit the number of equations required in the displacement method to the number of unknown joint translations.

Problems

11.1 to 11.5

Considering bending deformations only, find the bending moment diagram and the reactions (if any) for the plane frame shown. *Hint:* Where possible, take advantage

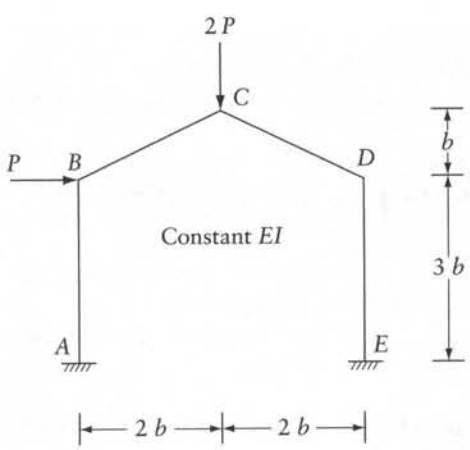

Prob. 11.1

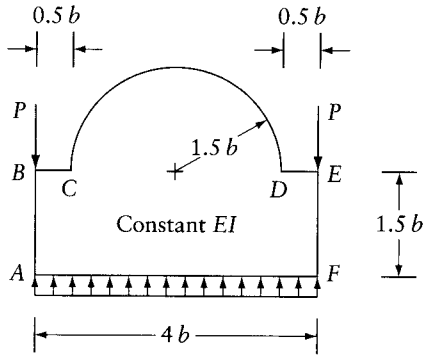

Prob. 11.2

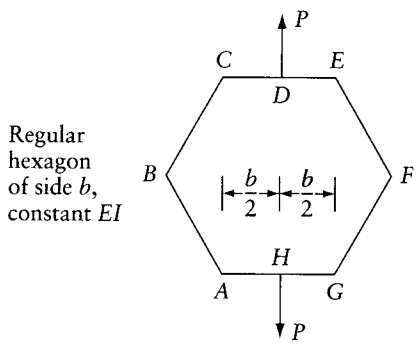

Prob. 11.3

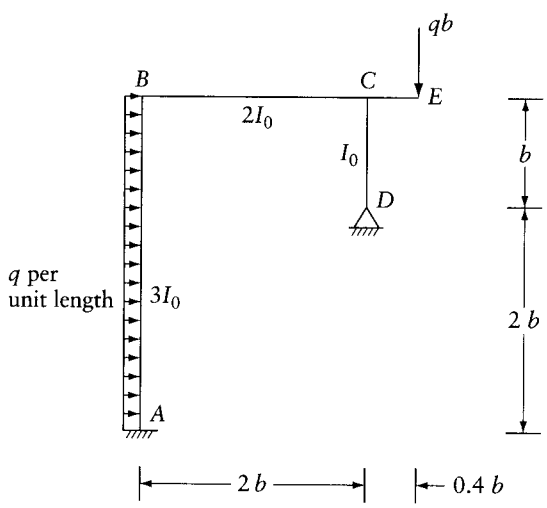

Prob. 11.4

HINT: The statically determinate parts AC and GH must not be included in the analogous column.

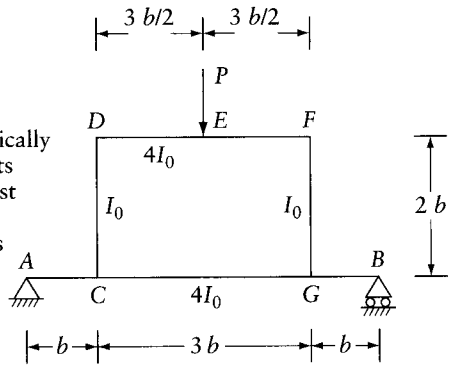

Prob. 11.5

of the symmetry of the structure or of both the structure and the loading. In the latter case, cutting a section at an axis of symmetry gives a released structure with two unknown internal forces, instead of three (the third one is known to be nil).

11.6 Find the forces at the ends A and B of the gable frame shown, subjected to a uniform vertical load of intensity q per unit length of horizontal projection. The frame is assumed to be encastré at A and B. Consider bending deformations only.

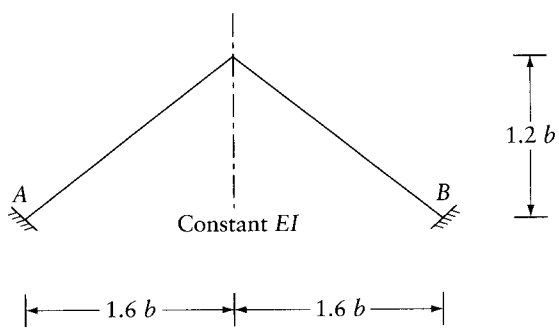

Prob. 11.6

11.7 and 11.8

Find the end-rotational stiffness S_{AB}, S_{BA}, and the carryover factors C_{AB} and C_{BA} for the beam in the figure.

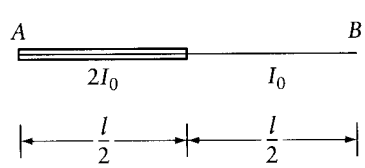

Prob. 11.7

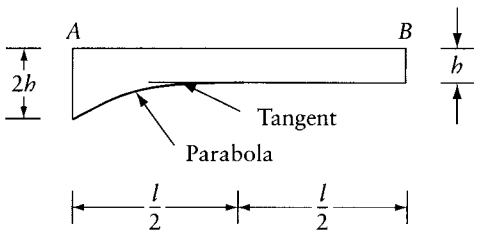

EI varies as the cube of the depth

Prob. 11.8

11.9 Find the fixed-end moments in the beam of Prob. 11.7 subjected to a uniform transverse load q per unit length.

11.10 Find the fixed-end moments in the beam of Prob. 11.8 loaded by a concentrated transverse force P at the center.

11.11 Find the bending moment diagram for the frame shown in the figure. Find the three reaction components at A.

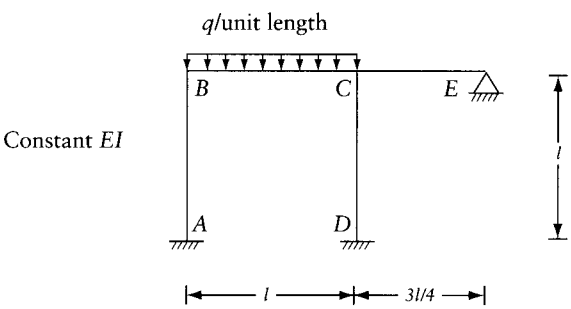

Prob. 11.11

11.12 Solve Prob. 11.11 with the end E supported on a roller which allows horizontal translation instead of the hinged support shown in the figure.

11.13 Draw the bending moment diagram for the bridge frame in the figure due to a uniform load of q per unit length on AD. The end-rotational stiffnesses, the carryover moment, and the FEMs for the members of variable I are given below the figure.

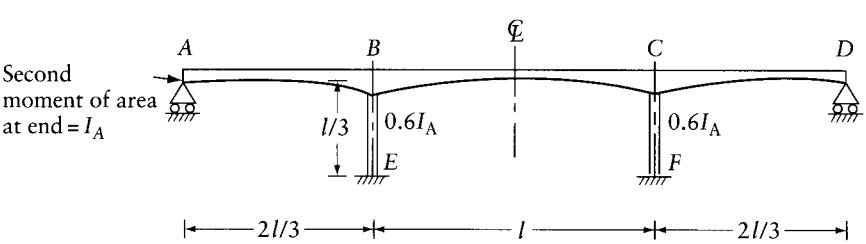

Prob. 11.13

The end-rotational stiffnesses and carryover moments are as follows:

Member $AB: S_{AB} = 5.4\dfrac{EI_A}{l_{AB}}, S_{BA} = 14.6\dfrac{EI_A}{l_{AB}}$, and $t_{AB} = 4.9\dfrac{EI_A}{l_{AB}}$

Member $BC: S_{BC} = S_{CB} = 12.0\dfrac{EI_A}{l_{BC}}$, and $t_{BC} = 8.3\dfrac{EI_A}{l_{BC}}$

The FEMs due to a uniform load of intensity w are:

$$M_{AB} = -0.057wl_{AB}^2, M_{BA} = 0.103\ wl_{AB}^2$$

$$M_{CB} = -M_{BC} = 0.103\ wl_{BC}^2$$

11.14 For the bridge frame of Prob. 11.13, find the bending moment diagram due to a horizontal force H to the left, along the axis of AD.

11.15 For the bridge frame of Prob. 11.13, find the bending moment diagram due to a unit settlement at F. Give the ordinates of the bending moment diagram in terms of EI_A.

11.16 The beam in the figure is subjected to a dead load and a live load of intensities q and $2q$ per unit length respectively. Draw the curve of maximum moment.
Hint: Solve for the following four cases of loading:

(i) D.L. on AD with L.L. on AB
(ii) D.L. on AD with L.L. on AC
(iii) D.L. on AD with L.L. on BC
(iv) D.L. on AD with L.L. on CD.

Draw the four bending moment diagrams in one figure to the same scale. The curve which has the maximum ordinates at any portion of the beam is the required curve.

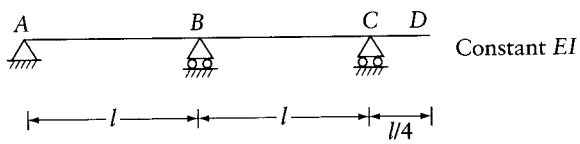

Prob. 11.16

11.17 Find the bending moment diagram for the frame shown in the figure.

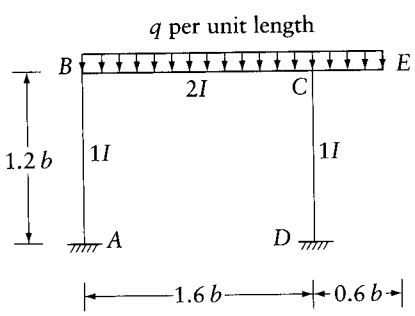

Prob. 11.17

11.18 Imperial units. For the frame shown in the figure, considering bending deformations only,

(a) draw the bending moment diagram due to a distributed vertical load 1 k/ft of horizontal projection.
(b) find the reactions due to a rise of temperature of 40° F with no loading on the frame.

$EI = 2 \times 10^6$ ft^{2}k

Coefficient of thermal expansion $\alpha = 0.6 \times 10^{-5}$ per °F.

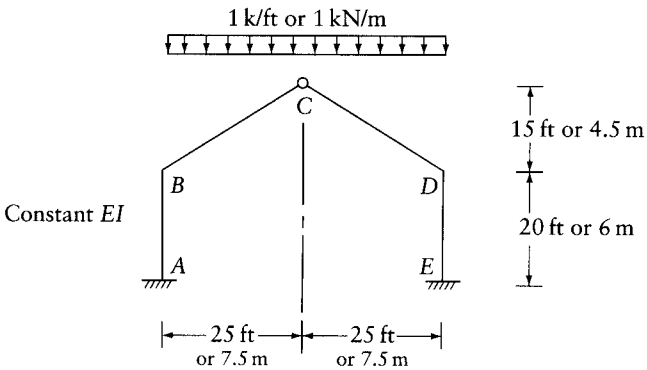

Prob. 11.18 Imperial units or Prob. 11.19 SI units.

11.19 SI units. For the frame shown in the figure, considering bending deformations only,

(a) draw the bending moment diagram due to a distributed vertical load 1 kN/m of horizontal projection.
(b) find the reactions due to a rise of temperature of 25° C with no loading on the frame.

$EI = 800$ MN m^2

Coefficient of thermal expansion $\alpha = 1 \times 10^{-5}$ per degree Celsius.

11.20 Imperial units. Find the bending moment at points A, B, C, and D of the frame shown in the figure due to:

(a) a uniform shrinkage strain=0.0002
(b) vertical settlement of $\frac{1}{2}$ in. at support A
(c) rotation of B in the clockwise direction by 0.20°

Assume $I = 4$ ft^4 and $E = 2 \times 10^6$ psi.
Consider bending deformations only.

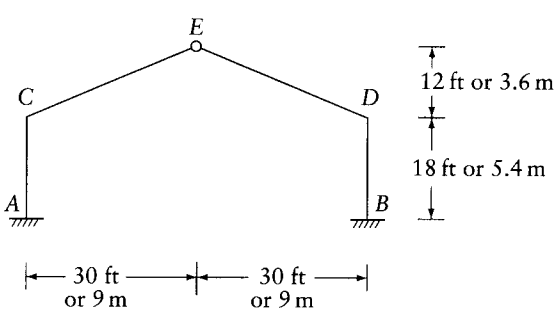

Prob. 11.20 Imperial units or Prob. 11.21 SI units.

11.21 SI units. Find the bending moment at points A, B, C, and D of the frame shown in the figure due to:

(a) a uniform shrinkage strain = 0.0002
(b) vertical settlement of 10 mm at support A
(c) rotation of B in the clockwise direction by 0.20°

Assume $I = 30 \times 10^9$ mm^4 and $E = 15$ GN/m^2.
Consider bending deformations only.

11.22 Part (a) of the figure shows a bridge frame subjected to a horizontal force P at the deck level. Assuming that the deck has an infinite rigidity,

(a) find the bending moment diagram in the piers.
(b) if hinges are introduced below the deck at the top of the piers BF and DH, as shown in part (b), find the shearing force at the bottom of the three piers.

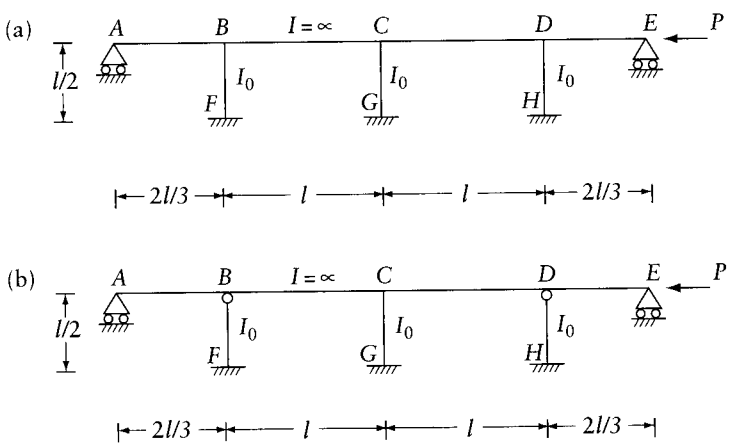

Prob. 11.22

11.23 Find the bending moment diagram for the left-hand half of the frame shown, considering bending deformations only. *Hint:* Because of symmetry, the rotation and the horizontal displacement at D are zero. Also, because the change in length of member is ignored, no

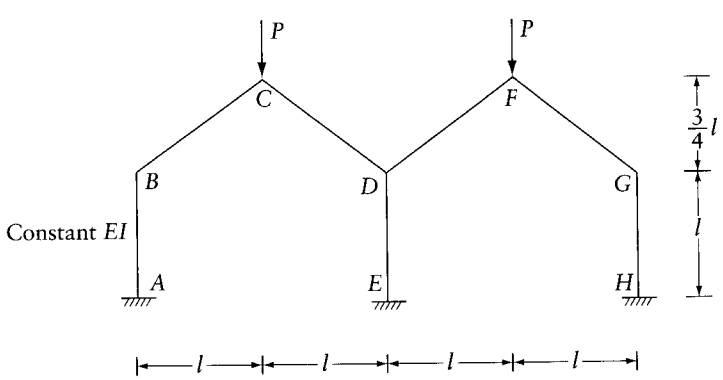

Prob. 11.23

vertical displacement occurs at *D*. Thus, we can analyze the part *ABCD* only, assuming *A* and *D* to be totally fixed joints.

11.24 Apply the requirements of Prob. 11.23, considering that the frame has only one bay *ABCDE*.

11.25 The figure shows one of the concrete frames supporting an elevated water tank. The wind pressure causes the loads shown to act on the frame. Assuming that the tank elements are of infinite rigidity compared to the rigidity of the horizontal bracing beams, find the bending moment in the frame. Consider bending deformations only. *Hint*: Because of symmetry of the structure, the bending moment and the vertical displacements are zero at the middle of CF and BG. Analyze the left-hand half of the frame carrying *P*, *P*/4, *P*/4 at D, C and B respectively. The degrees of freedom can be a horizontal translation at each of D, C and B and a rotation at each of C and B.

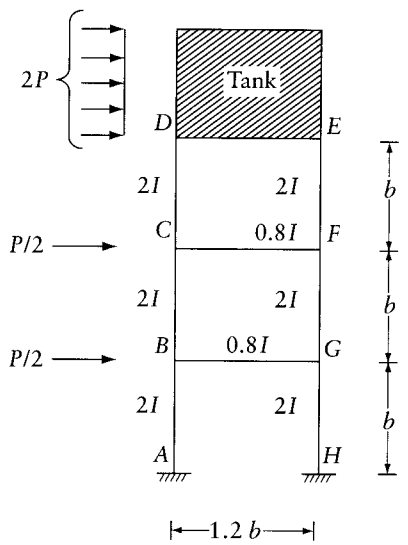

Prob. 11.25

11.26 Find the bending moment diagram for the Vierendeel girder shown in the figure. Consider bending deformations only. Use a computer program (e.g. PLANEF, Appendix L); verify the results. Cut ends G and B of members FG and AB and verify that the internal forces at the cut sections are statistical equivalents to the shearing force and the bending moment in a simple beam AE carrying the same loads. Check the angular rotation at A and the vertical deflection at C by virtual work, accepting the bending moments given by the computer.

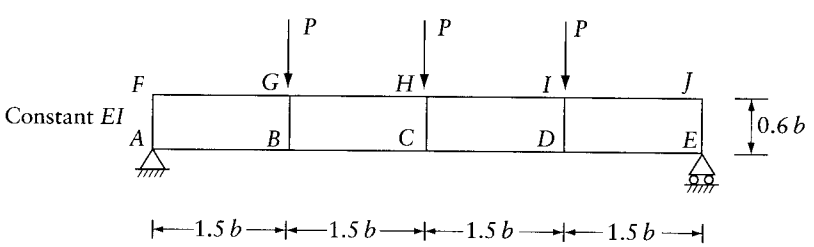

Prob. 11.26

11.27 Find the bending moment diagram in the frame shown. Consider only bending deformation. This becomes a problem of a symmetrical frame with antisymmetrical loading by the replacement of the force P at C by a force $= P/2$ at each of C and D; similarly, replace the force $2P$ at B by a force $= P$ at each of B and E. The mid-points of CD and BE are inflection points of zero vertical displacement. Introduce a roller support at each of the two points and analyze only the left-hand half of the structure by the force method, considering the vertical forces at the roller supports as the statically indeterminate redundants.

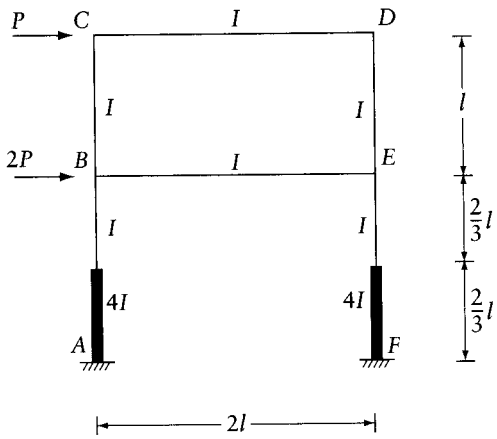

Prob. 11.27

11.28 Figure 11.7e and 11.7f represent a straight non-prismatic cantilever subjected at coordinates 1* and 2* to $F_{1*} = S^{④}_{AB}$ and $F_{2*} = 0$. Verify that for $D^*_1 = 1$, the adjusted end-rotational stiffness, $S^{④}_{AB}$ is:

$$S^{④}_{AB} = \frac{S_{AB}S_{BA} - t^2}{S_{AB} + S_{BA} + 2t}$$

where S_{AB}, S_{BA} and t are the end-rotational stiffnesses and the carry-over moment for the same member (Fig. 11.7a). Verify that for a prismatic member, $S^{④}_{AB} = EI/l$.

Chapter 12

Influence lines

12.1 Introduction

The effect of live loads which can have different positions on a structure can be conveniently analyzed and succinctly described in graphical form by the use of influence lines. An influence line shows the value of any action due to a unit point load moving across the structure. For example, the influence line for the bending moment at a section of a continuous beam shows the variation in the bending moment at this section as a unit transverse load traverses the beam.

In this chapter we deal with the methods of obtaining influence lines for statically indeterminate structures but, by way of introduction and review, influence lines for statically determinate structures, introduced in Section 2.6, will be further discussed.

12.2 Concept and application of influence lines

A transverse concentrated load at a general position on a member of a structure causes various actions. These actions, which may be a bending moment, shearing force, normal force, or displacement at a section, or a reaction at a support, vary as the load moves across the structure.

If the values of any action A are plotted as ordinates at all the points of application of a unit transverse load, we obtain the influence line of the action A. In this chapter, we use η to represent the influence ordinate – which may also be referred to as *influence coefficient* – of any action due to a unit moving concentrated load acting at right angles to the member over which the load is moving. Our sign convention is to plot positive influence ordinates in the same direction as the applied concentrated load. Thus, influence lines for gravity loads on horizontal members are drawn positive downwards.

Let us now illustrate the use of influence lines in analysis. The value of any action A due to a system of concentrated loads $P_1, P_2, \ldots, P_n$ (Figure 12.1a) can be obtained from the influence ordinates by

$$A = \eta_1 P_1 + \eta_2 P_2 + \cdots + \eta_n P_n \tag{12.1}$$

or

$$A = \sum_{i=1}^{n} \eta_i P_i \tag{12.1a}$$

The value of the actions due to a distributed transverse load of intensity p over a length $\overline{BC}$ (Figure 12.1b) is

$$A = \int_B^C \eta p \, dx$$

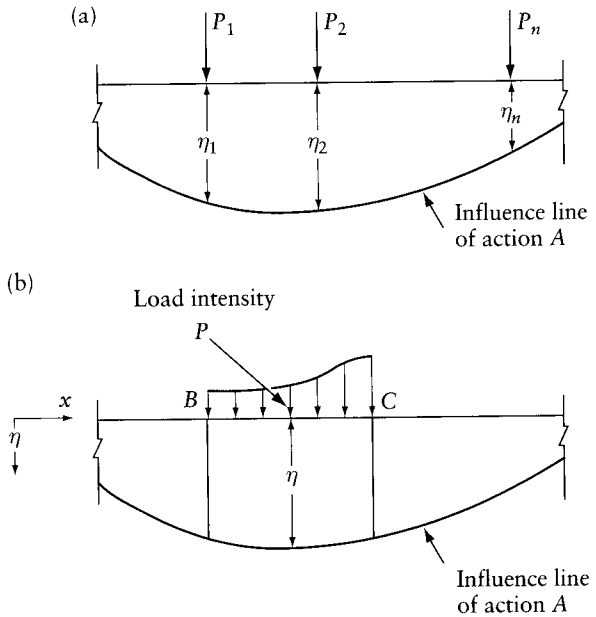

Figure 12.1 Determination of the value of an action due to loading using the influence line.

For a uniform load of intensity q,

$$A = q \int_B^C \eta \, dx \tag{12.2}$$

The value of the integral in this equation is the area under the influence line between B and C.

The knowledge of the shape of an influence line indicates which part or parts of a structure should be loaded to obtain maximum effects. In Figure 12.4, influence lines are sketched for a plane frame, and in Figure 12.5 for a grid. The ordinates plotted on the column EB in Figure 12.4 represent the value of the action considered due to a horizontal load on the column. As always, the value is positive if the load is applied in the direction of the positive ordinate. The ordinates of the influence lines for the grid are vertical to represent the effect of a unit vertical load, as shown in the pictorial view in Figure 12.5.

We can see that, for instance, in the case of shear at section n in the frame of Figure 12.4, a maximum negative value occurs when a distributed load covers Bn as well as the span CD, without a load on the remainder of the frame. Likewise, the bending moment at n_3 in Figure 12.5 is maximum positive when loads cover the members CD and the central part of GI, without a load on AB or EF.

12.3 Müller-Breslau's principle

One of the most effective methods of obtaining influence lines is by the use of Müller-Breslau's principle, which states that the ordinates of the influence line for any action in a structure are equal to those of the deflection curve obtained by releasing the restraint corresponding to this action and introducing a corresponding unit displacement in the remaining structure.

The principle is applicable to any structure, statically determinate or indeterminate, and can be easily proved, using Betti's theorem.

Consider a loaded beam in equilibrium, as in Figure 12.2a. Remove the support B and replace its effect by the corresponding reaction R_B, as shown in Figure 12.2b. If the structure is now subjected to a downward load F at B such that the deflection at B equals unity, the beam will

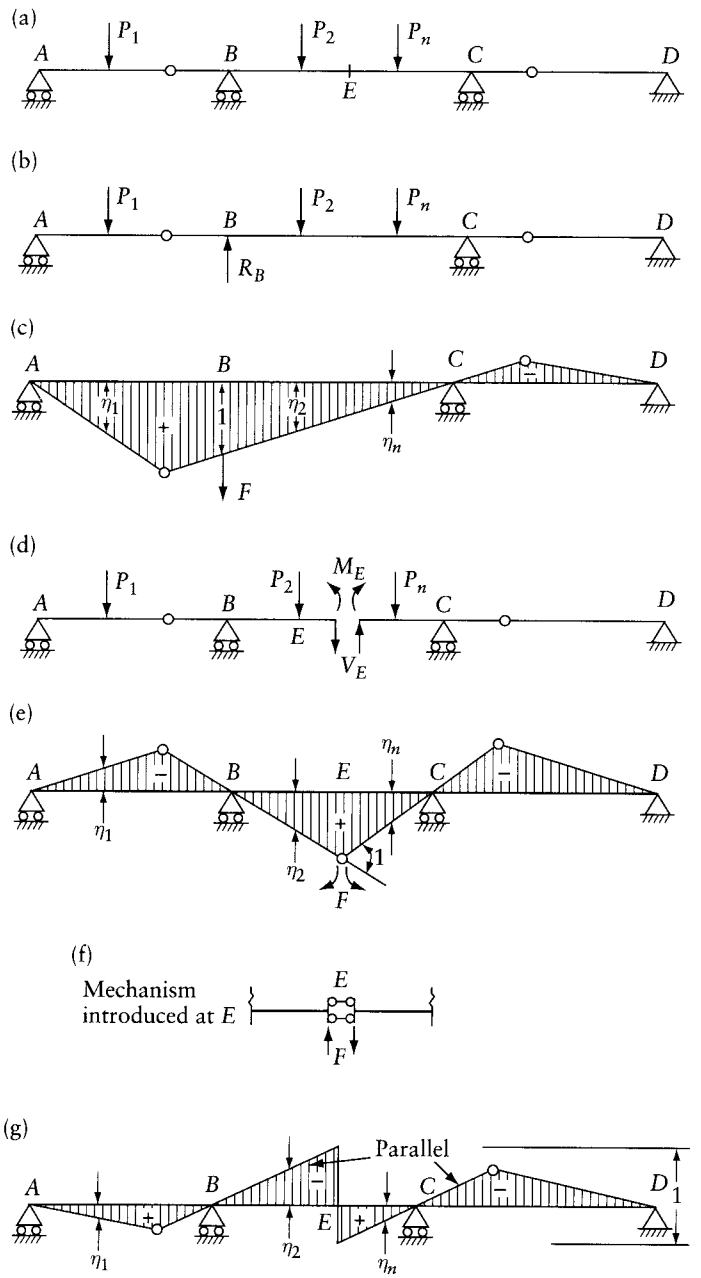

Figure 12.2 Influence line for a statically determinate beam. (a) Loaded beam in equilibrium. (b) Support B replaced by R_B. (c) Influence line for R_B. (d) Equilibrium maintained by forces M_E and V_E. (e) Influence line for M_E. (f) and (g) Influence line for V_E and mechanism inserted at E.

assume the deflected form in Figure 12.2c. Because the original structure is statically determinate, the release of one restraining force turns the structure into a mechanism, and, therefore, the force F required to produce the displacements in Figure 12.2c is zero. However, the release of one restraining force in a statically indeterminate structure leaves a stable structure so that the value of the force F is generally not equal to zero.

Applying Betti's theorem (Eq. 9.5) to the two systems of forces in Figures 12.2b and c, we write

$$\eta_1 P_1 + \eta_2 P_2 + \cdots + \eta_n P_n - 1 \times R_B = F \times 0$$

This equation expresses the fact that the external virtual work done by the system of forces in Figure 12.2b during the displacement by the system in Figure 12.2c is the same as the external virtual work done by the system in Figure 12.2c during the displacement by the system in Figure 12.2b. This latter quantity must be zero because no deflection occurs at B in Figure 12.2b.

The preceding equation can be written

$$R_B = \sum_{i=1}^{n} \eta_i P_i$$

Comparing this equation with Eq. 12.1a, we see that the deflection line in Figure 12.2c is the influence line of the reaction R_B. This shows that the influence line of the reaction R_B can be obtained by releasing its effect, that is, removing the support B, and introducing a unit displacement at B in the downward direction, that is, opposite to the positive direction of the reaction.

Using simple statics, we can readily check that the deflection ordinate at any point in Figure 12.2c is, in fact, equal to the reaction R_B if a unit load is applied at this point in the beam of Figure 12.2a.

Let us now use Müller-Breslau's principle in the case of the influence line of the bending moment at any section E. We introduce a hinge at E, thus releasing the bending moment at this section. We then apply two equal and opposite couples F to produce a unit relative rotation of the beam ends at E (Figure 12.2e). In order to prove that the deflection line in this case is the influence line of the bending moment at E, cut the beam in Figure 12.2a at section E and introduce two pairs of equal and opposite forces M_E and V_E to maintain the equilibrium (Figure 12.2d). Applying Betti's theorem to the systems in Figures 12.2d and e, we can write

$$\eta_1 P_1 + \eta_2 P_2 + \cdots + \eta_n P_n - 1 \times M_E = F \times 0$$

or

$$M_E = \sum_{i=1}^{n} \eta_i P_i$$

This demonstrates that the deflection line in Figure 12.2e is the influence line for the bending moment at E.

The influence line for shear at section E can be obtained by introducing a unit relative translation without relative rotation of the two beam ends at E (Figure 12.2g). This is achieved by introducing at E a fictitious mechanism such as that shown in Figure 12.2f and then applying two equal and opposite vertical forces F. With this mechanism the two ends at E remain parallel

as shown in Figure 12.2g. Applying Betti's theorem to the systems in Figures 12.2d and g, we can write

$$\eta_1 P_1 + \eta_2 P_2 + \cdots + \eta_n P_n - 1 \times V_E = F \times 0$$

or

$$V_E = \sum_{i=1}^{n} \eta_i P_i$$

which shows that the deflection line in Figure 12.2g is the influence line for the shear at E.

All the influence lines considered so far are composed of straight-line segments. This is the case for any influence line in any statically determinate structure. Thus, one computed ordinate and the known shape of the influence line are sufficient to draw it. This ordinate may be calculated from considerations of statics, or from the geometry of the influence line.

All influence lines for statically indeterminate structures are composed of curves, and, therefore, several ordinates must be computed. In Figure 12.3, Müller-Breslau's principle is used to obtain the general shape of the influence lines for a reaction, bending moment, and shear at a

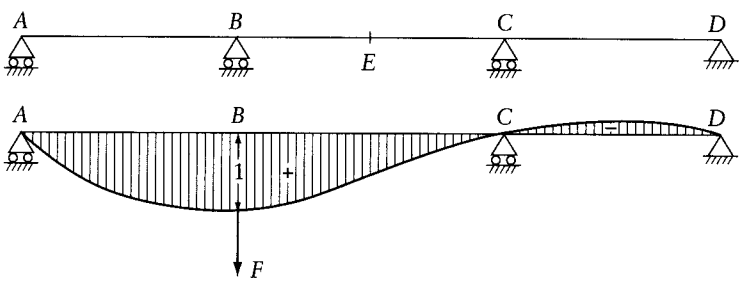

Influence line for R_B

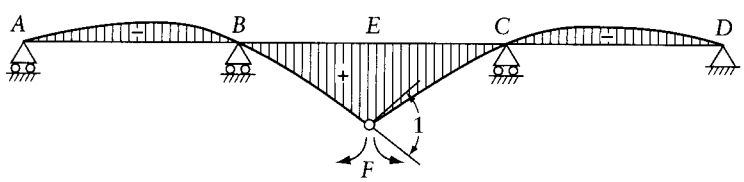

Influence line for M_E

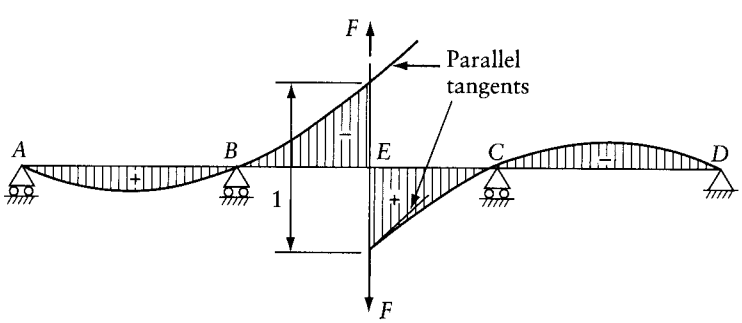

Influence line for V_E

Figure 12.3 Influence lines for a continuous beam.

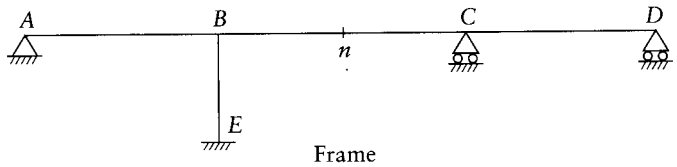

Frame

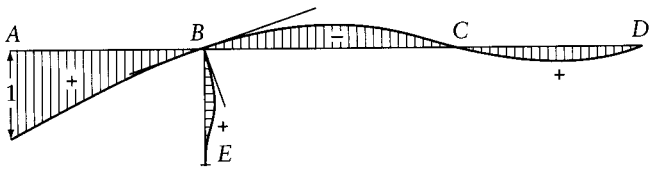

Influence line for vertical reaction at A

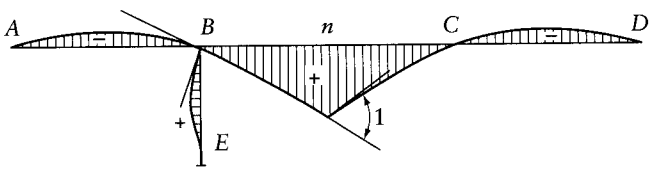

Influence line for bending moment at n

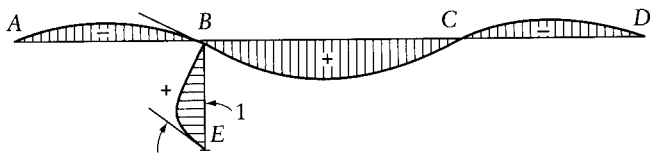

Influence line for end moment M_{EB} (postive clockwise)

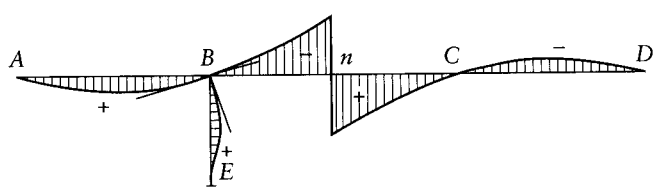

Influence line for shear at n

Figure 12.4 Shape of influence lines for a plane frame using Müller-Breslau's principle.

section in a continuous beam. Sketches of influence lines for several actions in a plane frame and in a grid are deduced by Müller-Breslau's principle in Figures 12.4 and 12.5.

12.3.1 Procedure for obtaining influence lines

The steps followed in Section 12.3 to obtain the influence line for any action can be summarized as follows.

1. The structure is released by removal of the restraint corresponding to the action considered. The degree of indeterminacy of the released structure compared with the original structure is reduced by one. It follows that, if the original structure is statically determinate, the released structure is a mechanism.

2. Introduce a unit displacement in the released structure in a direction opposite to the positive direction of the action. This is achieved by applying a force (or a pair of equal and opposite forces) corresponding to the action.
3. The ordinates of the deflection line thus obtained are the influence ordinates of the action. The ordinates of the influence line are positive if they are in the same direction as the external applied load.

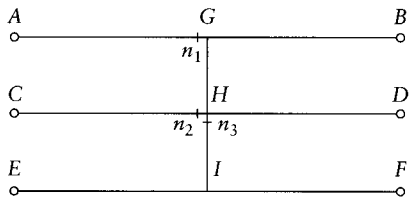

Ends A, C, E, B, D and F are simply supported

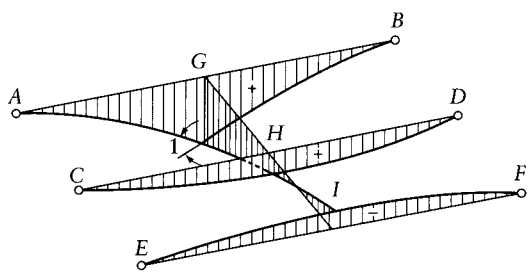

Influence line for bending moment at n_1

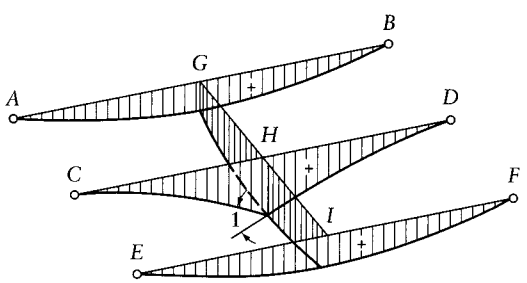

Influence line for bending moment at n_2

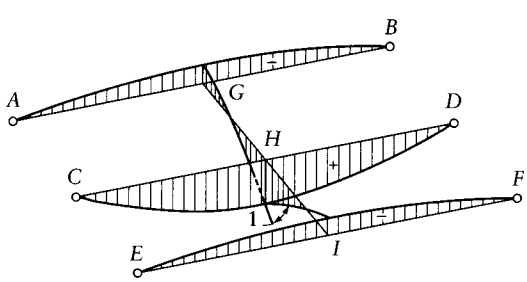

Influence line for bending moment at n_3

Figure 12.5 Shape of influence lines for a grid using Müller-Breslau's principle.

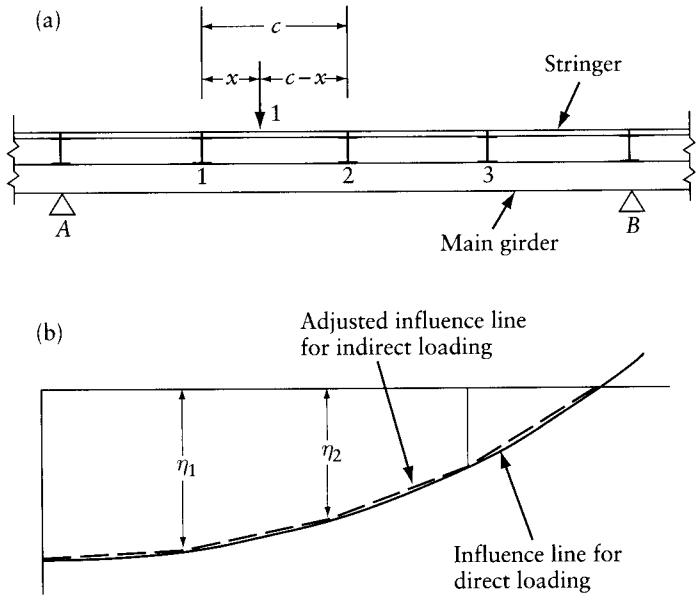

Figure 12.6 Correction of influence lines for indirect loading. (a) Indirect loading on main girder. (b) Influence line for any action A in main girder.

12.4 Correction for indirect loading

In some cases, loads are not applied directly to the structure for which the influence lines are desired, but through smaller beams assumed to be simply supported on the main structure. For instance, the main girder in Figure 12.6a supports cross-girders at nodes A, 1, 2, 3, and B, and these in turn carry stringers to which the live load is applied. Let the solid curve in Figure 12.6b represent the influence line of any action A, drawn on the assumption that the unit load is applied directly to the beam. But the unit load can be transmitted to the main girder at the cross-girders only, and we have to correct the influence line accordingly.

A unit load applied at an arbitrary point between nodes 1 and 2 is transmitted to the main girder as two concentrated loads equal to $(c-x)/c$ and x/c at 1 and 2 respectively. The value of the action A due to these two loads is

$$A = \frac{x}{c}\eta_2 + \frac{c-x}{c}\eta_1 \tag{12.3}$$

where c is the panel length and x is the distance indicated in Figure 12.6a. This is the equation of the straight line between points 1 and 2 shown dashed in Figure 12.6b. Thus, the corrected influence line is composed of straight segments between the node points.

In pin-connected trusses, all the loads are assumed to act at the joints; thus, influence lines for trusses are composed of straight segments between the joints.

12.5 Influence lines for a beam with fixed ends

Let us now use Müller-Breslau's principle to find the influence lines for the end-moments of a beam with fixed ends. From these, by equations of statics, influence lines for reaction, shear, and bending moments at any section can be determined. We use – as in previous chapters – the convention that a clockwise end-moment is positive.

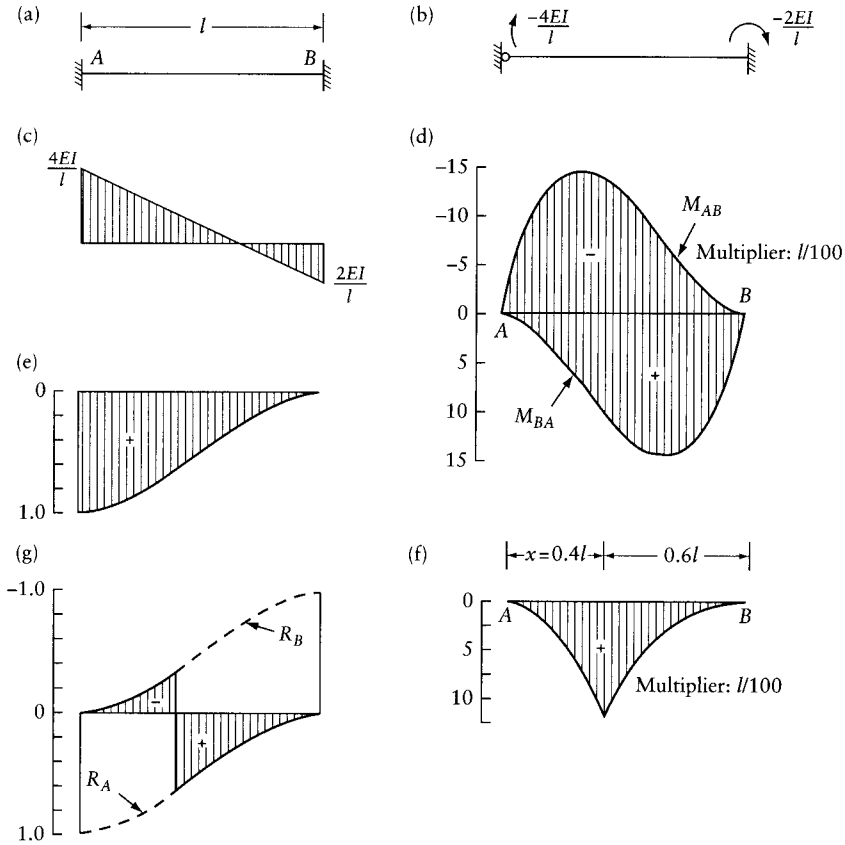

Figure 12.7 Influence lines for a prismatic beam with fixed ends. (a) Beam. (b) End-moments corresponding to a unit angular rotation at end A. (c) Bending moment diagram for the beam in part (b). (d) Influence lines for end-moments. (e) Influence line for R_A. (f) Influence line for $M_{(x=0.4l)}$. (g) Influence line for $V_{(x=0.4l)}$.

To find the influence line for the end-moment M_{AB} in the beam in Figure 12.7a, we introduce a hinge at A and apply there an anticlockwise moment to produce a unit angular rotation of the end A (Figure 12.7b). This moment must be equal in magnitude to the end-rotational stiffness S_{AB}. The corresponding end-moment at B is $t = C_{AB}S_{AB}$, where S_{AB}, C_{AB} and t are the end-rotational stiffness, the carryover factor, and the carryover moment respectively. The deflection line corresponding to the bending moment diagram in Figure 12.7c is the required influence line.

When the beam has a constant flexural rigidity EI and length l, the end-moments at A and B are respectively $-4EI/l$ and $-2EI/l$. These values can be substituted in the expression for the deflection[1] y in a prismatic member AB due to clockwise end-moments M_{AB} and M_{BA}

$$y = \frac{l^2}{6EI}[M_{AB}(2\zeta - 3\zeta^2 + \zeta^3) - M_{BA}(\zeta - \zeta^3)] \tag{12.4}$$

1 When the beam ends A and B deflect, Eq. 12.5 gives the deflection measured from the straight line joining the displaced position of A and B.

where $\zeta = x/l$, x is the distance from the left-hand end A, and l is the length of the member. Equation 12.4 can be proved by the method of elastic weights (see Section 10.4). The values of y due to unit end-moments are given in Appendix I.

Substituting $M_{AB} = -4EI/l$ and $M_{BA} = -2EI/l$ in Eq. 12.4, we obtain the equation of the influence line for the end-moment M_{AB}:

$$\eta_{MAB} = -l\zeta(1-\zeta)^2 \tag{12.5}$$

Similarly, substituting $M_{AB} = -2EI/l$ and $M_{BA} = -4EI/l$, we obtain the equation of the influence line for the end-moment M_{BA}:

$$\eta_{MBA} = l\zeta^2(1-\zeta) \tag{12.6}$$

The influence lines of the two end-moments are plotted in Figure 12.7d.

The reaction R_A may be expressed as

$$R_A = R_{As} - \frac{M_{AB} + M_{BA}}{l} \tag{12.7}$$

where R_{As} is the statically determinate reaction of the beam AB if simply supported. Equation 12.7 is valid for any position of a unit moving load. We can therefore write:

$$\eta_{RA} = \eta_{RAs} - \frac{1}{l}(\eta_{MAB} + \eta_{MBA}) \tag{12.8}$$

where η is the influence ordinate of the action indicated by the subscript. The influence line of R_{As} is a straight line (Figure 2.15):

$$\eta_{RAs} = 1 - \zeta \tag{12.9}$$

Substitution of Eqs. 12.5, 12.6, and 12.9 in Eq. 12.8 gives the influence line for the reaction R_A (Figure 12.7e):

$$\eta_{RA} = 1 - 3\zeta^2 + 2\zeta^3 \tag{12.10}$$

Similarly, the influence ordinate for the bending moment at any section distance x from the left-hand end is given by

$$\eta_M = \eta_{Ms} + \frac{(l-x)}{l}\eta_{MAB} - \frac{x}{l}\eta_{MBA} \tag{12.11}$$

where η_M and η_{Ms} are the influence ordinates for the bending moment at the section for a beam with fixed ends and simply supported respectively (Figure 2.15a). The ordinates η_M for a section at $x = 0.4l$ are calculated in Table 12.1, and Figure 12.7f plots the relevant influence line.

The influence ordinates h of the shear at any section can be calculated by the equation

$$\eta_V = \eta_{Vs} - \frac{1}{l}(\eta_{MAB} + \eta_{MBA}) \tag{12.12}$$

where η_{Vs} is the influence ordinate for the shear at the same section in a simply-supported beam. The influence line for shear at a section at $x = 0.4l$ is shown in Figure 12.7g. It can be seen that this influence line can be formed by parts of the influence lines for R_A and R_B.

Table 12.1 Ordinates of the Influence Line for $M_{(x=0.4l)}$

Distance from left-hand end	*0.1l*	*0.2l*	*0.3l*	*0.4l*	*0.5l*	*0.6l*	*0.7l*	*0.8l*	*0.9l*	*Multiplier*
η_{Ms}	0.060	0.120	0.180	0.240	0.200	0.160	0.120	0.080	0.040	1
$0.6\ \eta_{MAB}$	−0.049	−0.077	−0.088	−0.086	−0.075	−0.058	−0.038	−0.019	−0.005	1
$-0.4\ \eta_{MBA}$	−0.004	−0.013	−0.025	−0.038	−0.050	−0.058	−0.059	−0.051	−0.032	1
Influence ordinates for $M_{(x=0.4l)}$	0.007	0.030	0.067	0.116	0.075	0.044	0.023	0.010	0.003	1

The influence lines for continuous prismatic beams with equal spans or with unequal spans in certain ratios are given in various references, and in most cases they need not be calculated. On the other hand, influence lines are often calculated in the design of bridges of variable l or with irregularly varying spans forming continuous beams, and also of frames and grids.

12.6 Influence lines for plane frames

In the preceding section we have seen that the influence lines for shear or bending moment at any section of a member can be determined from the influence lines for the end-moments by simple equations of statics. We shall now show how to use moment distribution to find the influence lines for the end-moments of continuous plane frames.

Let us assume that we want to find the influence line for the end-moment M_{BC} in the frame of Figure 12.8a. According to the Müller-Breslau principle, the influence ordinates are the ordinates of the deflected shape of the frame corresponding to a unit angular discontinuity at end BC. Assume that such a unit angular rotation is introduced at end BC without other displacements at the joints, as shown in Figure 12.8b. The end-moments corresponding to this configuration are $-S_{BC}$ and $-t_{BC} = -C_{BC}S_{BC}$, where S_{BC} is the end-rotational stiffness, t_{BC} the carryover moment, and C_{BC} the carryover factor from B to C.

We now allow joint rotations (and joint translations, if any) to take place and find the corresponding moments at the ends of the members by moment distribution in the usual way. The corresponding bending moment diagram will be a straight line for each member (Figure 12.8c). The deflections, which are the influence line ordinates, are calculated by superposition of the deflections due to the end-moments as in the previous section.

For prismatic members, the values given in Appendix I may be used. For members of variable I, we can use the influence line ordinates of the moment at a fixed end of a member with the other end hinged.[2] To obtain the deflection due to a unit couple applied at one end, these ordinates should be divided by the adjusted end-rotational stiffness at the fixed end while the other end is hinged (see Figure 12.9 and Eq. 11.20).

The shape of the influence line for the end moment M_{BC} for the frame considered is shown in Figure 12.8d. The ordinates plotted on the columns BE and CF can be used to find the value of M_{BC} if a unit horizontal load is applied to either of the columns. The value will be positive if the load points toward the left. If, however, a horizontal load on a column cannot occur, the influence ordinates on BE and CF need not be plotted.

2 Influence-line ordinates of FEMs in beams with a variable I can be found in *Handbook of Frame Constants*, Portland Cement Association, Chicago, III. and Guldan, R., *Rahmentragwerke und Durchlauftrager*, Springer, Vienna, 1959.

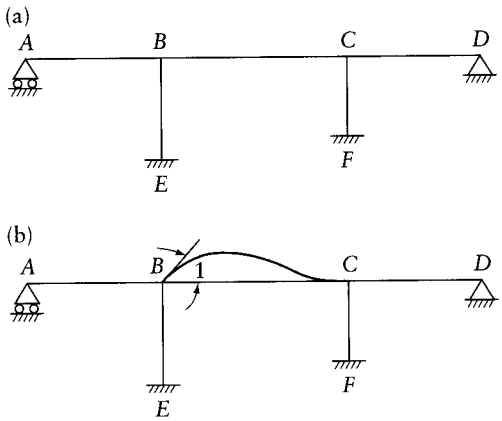

End-moments are:
$M_{BC} = -S_{BC}$, $M_{CB} = -C_{BC}\, S_{BC}$
and equal to zero at all other ends

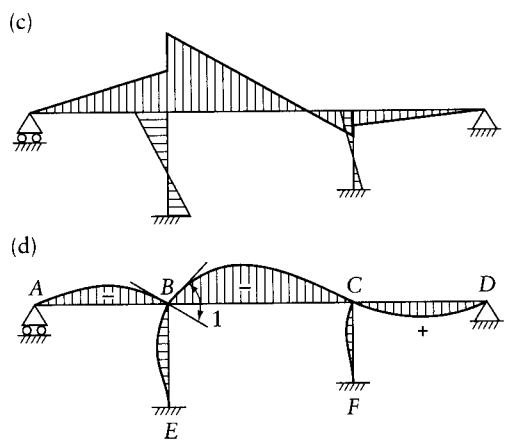

Figure 12.8 Determination of influence line for end-moment in a plane frame. (a) Plane frame. (b) Unit angular rotation of end BC without other joint displacements. (c) Bending moment diagram corresponding to the elastic line in part (d). (d) Influence line for the end-moment M_{BC}.

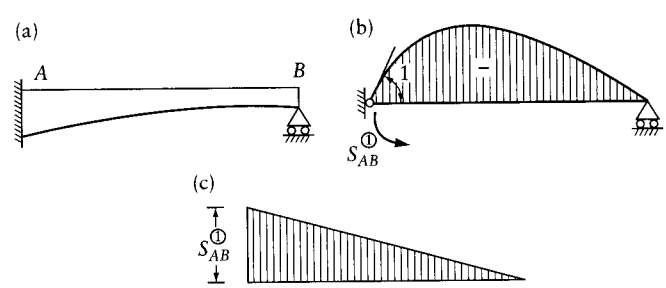

Figure 12.9 Deflection of a nonprismatic beam due to a couple applied at one end with the other end hinged. (a) Beam. (b) Influence line for end-moment M_{AB}. (c) Bending moment diagram corresponding to the deflection line in part (b).

Example 12.1: Bridge frame: influence line for member end moment

Obtain the influence line for the end-moment M_{BA} in the bridge frame in Figure 12.10a. Use this influence line to find the influence ordinate of the bending moment M_G at the center of AB and of the shear V_n at a section n just to the left of B. The relative values of I are shown in the figure.

A unit rotation in an anticlockwise direction is introduced at end B of BA, as shown in Figure 12.10b. The corresponding end-moments are $M_{BA} = -3(EI/l)_{BA} = -1.85EI/b$ and zero for all the other ends. These values are the initial FEMs for which a moment distribution is carried out in Figure 12.10c. The deflections of members AB, BC, and CD due to the final end-moments are calculated in Table 12.2 at $0.3l$, $0.5l$, and $0.7l$ of each span by the use of the tabulated values in Appendix I. These deflections, which are the influence ordinates of the end-moment M_{BA}, are plotted in Figure 12.10d. As always, a positive sign indicates a clockwise end-moment.

The ordinates of the influence lines for M_G and V_n are determined by superposition Eqs. 12.11 and 12.12 respectively. The calculations are performed in Tables 12.3 and 12.4, and the influence lines are plotted in Figures 12.11a and b.

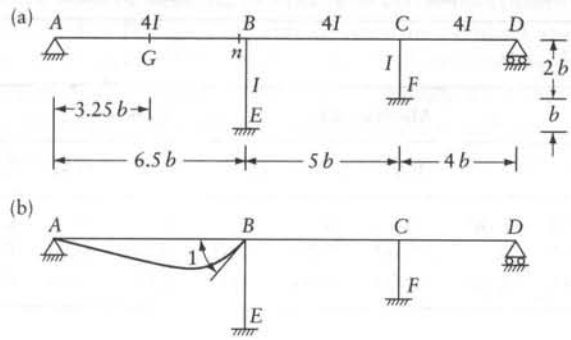

(c)

End	*BA*	*BE*	*BC*	*CB*	*CF*	*CD*
	0.29	0.21	0.5	0.39	0.24	0.37
FEMs	−185	0	0	0	0	0
Multiplier: *EI*/(IOOb)	+53	+39	+93 →	+47		
			−9 ←	−18	−12	−17
	+2	+2	+5 →	+3		
				−1	−1	−1
Final end-moments	−130	+41	+89	+31	−13	−18

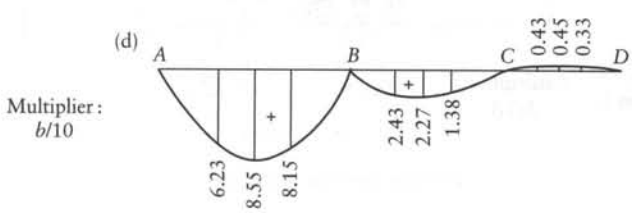

Figure 12.10 Influence line for an end-moment in Example 12.1. (a) Frame properties. (b) Unit angular rotation introduced at end BA. (c) Moment distribution. (d) Influence line of end-moment M_{BA}.

Table 12.2 Ordinates of Influence Line for End-Moment $M_{BA}(b/10)$

Deflection due to end-moment at	*Member AB*			*Member BC*			*Member CD*		
	0.3l	*0.5l*	*0.7l*	*0.3l*	*0.5l*	*0.7l*	*0.3l*	*0.5l*	*0.7l*
Left-hand end	0	0	0	3.31	3.48	2.53	−0.43	−0.45	−0.33
Right-hand end	6.23	8.55	8.15	−0.88	−1.21	−1.15	0	0	0
Influence ordinate	6.23	8.55	8.15	2.43	2.27	1.38	−0.43	−0.45	−0.33

Table 12.3 Ordinates of Influence Line for the Bending Moment M_G at G $(b/10)$

Influence coefficient	*Member AB*			*Member BC*			*Member CD*		
	0.3l	*0.5l*	*0.7l*	*0.3l*	*0.5l*	*0.3l*	*0.7l*	*0.5l*	*0.7l*
η_{Ms}	9.75	16.25	9.75	0	0	0	0	0	0
$-\frac{1}{2}\,\eta_{MBA}$	−3.12	−4.28	−4.08	−1.22	−1.14	−0.69	0.22	0.23	0.17
Influence ordinate	6.63	11.97	5.67	−1.22	−1.14	−0.69	0.22	0.23	0.17

Table 12.4 Ordinates of Influence Line for Shear V_n

Influence coefficient	*Member AB*				*Member BC*			*Member CD*		
	0.3l	*0.5l*	*0.7l*	*l*	*0.3l*	*0.5l*	*0.7l*	*0.3l*	*0.5l*	*0.7l*
η_{Vs}	−0.30	−0.50	−0.70	−1.00	0	0	0	0	0	0
$-(6.5b)^{-1}\,\eta_{MBA}$	−0.10	−0.13	−0.13	0	−0.04	−0.04	−0.02	0.01	0.01	0.005
Influence ordinate	−0.40	−0.63	−0.83	−1.00	−0.04	−0.04	−0.02	0.01	0.01	0.005

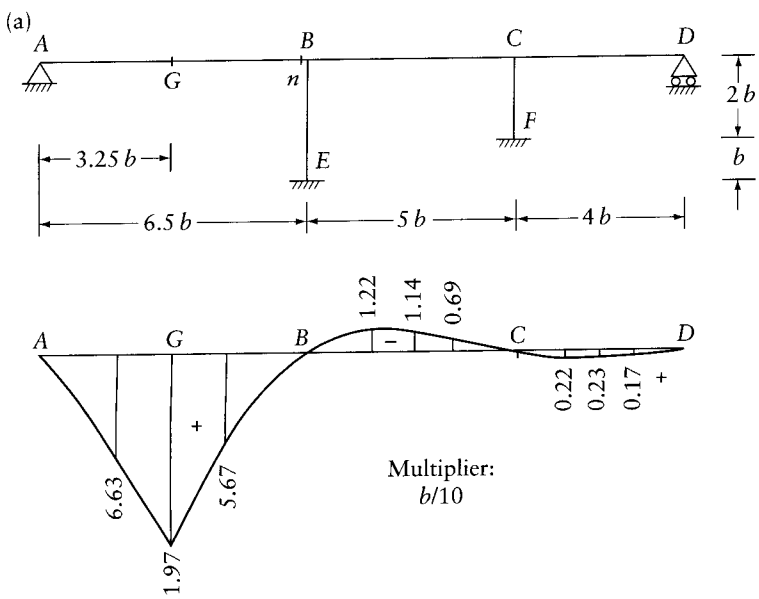

Figure 12.11 Influence line for bending moment and shear at a section of the frame in Example 12.1. (a) Influence line for M_G. (b) Influence line for V_n.

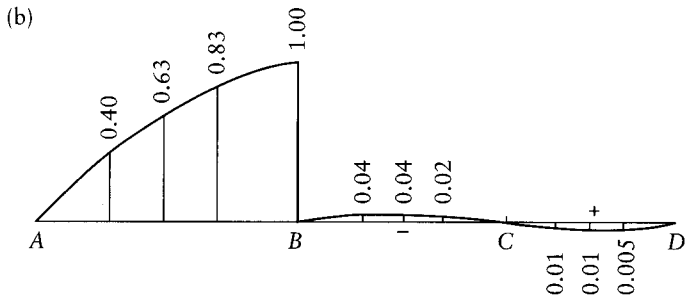

Figure 12.11 (Continued).

12.7 Influence lines for grids

The grid in Figure 12.12a represents the main and cross-girders of a bridge deck for which influence lines of bending moments at certain sections of the members are required. All joints are assumed to be rigid, capable of resisting bending and torsion.

For the analysis of this grid by the displacement method each of the internal joints has three unknown displacements: v, θ_x, and θ_z (Figure 12.12a). At each support two rotations, θ_x and θ_z are possible. One method of obtaining the influence lines is to carry out the analysis of the structure for a number of loading cases (see Section 5.4) with a unit vertical load at various

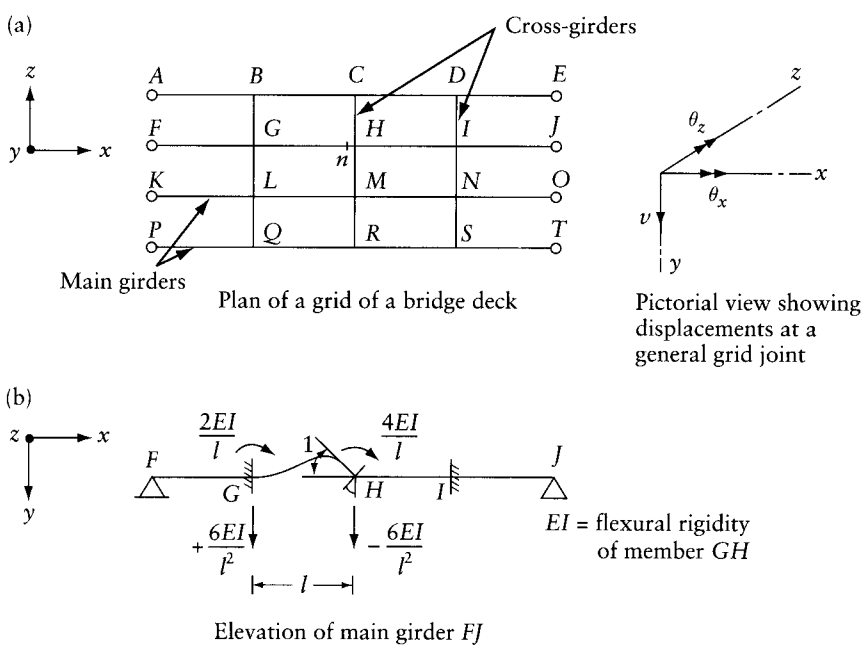

Figure 12.12 Determination of the influence line for the bending moment at section n of a grid. (a) Grid plan. (b) Restraining forces corresponding to a unit angular discontinuity at n without joint displacements.

positions. Each loading case gives one ordinate for each influence line required. This method is satisfactory when a computer is used as little additional effort in programming is required compared with that necessary for the dead-load analysis.

Another method of obtaining the influence lines, and one which requires less computing, is by the use of Müller-Breslau's principle, as discussed below.

Assume that we require the influence line for the bending moment M_n at section n, just to the left of H. We induce a rotation at the end H of member HG in the vertical plane, as shown in the elevation of girder FJ in Figure 12.12b. The forces required to hold the structure in this configuration are two couples and two vertical forces shown in the figure, with no forces at all the other joints. If these forces are now released, the grid will deform maintaining a unit angular discontinuity at H between the members HG and HI. The vertical deflections of the grid are therefore the ordinates of the required influence line. The displacements can be determined by solution of the equation

$$[S]\{D\} = -\{F\} \tag{12.13}$$

where $[S]$ is the stiffness matrix, $\{D\}$ is the vector of the nodal displacements, and $\{F\}$ is the vector of nodal forces preventing the displacements, while member GH is deformed as shown in Figure 12.12b. The restraining forces are zero at all nodes except G and H; thus,

$$\{F\} = \left\{\ldots, \frac{6EI}{l^2}, 0, \frac{2EI}{l}, -\frac{6EI}{l^2}, 0, \frac{4EI}{l}, \ldots\right\} \tag{12.14}$$

where the elements not shown are zero; the first three forces given are at G and the remaining forces are at H.

The vertical deflections v, included in $\{D\}$, are equal to the coordinates η_{Mn} of the bending moment at section n (Figure 12.12a).

The variation of the deflection v over the length of any member can be expressed in terms of the two v-values at the ends and the two end-rotations θ_z or θ_x:

$$v = [L_1\ L_2\ L_3\ L_4] \begin{Bmatrix} v_l \\ \theta_l \\ v_r \\ \theta_r \end{Bmatrix} \tag{12.15}$$

where the subscripts l and r refer to the left- and right-hand ends of the member; θ refers to θ_z for the members running in the x direction and to θ_x for members running in the z direction; for these, the left-hand end means the end closer to the top of the page (Figure 12.12a). The functions L_1 to L_4 describe the deflected shapes of the member when one of the four end displacements is equal to unity while the others are zero:

$$L_1 = 1 - 3\xi^2 + 2\xi^3 \quad L_2 = l\xi(\xi - 1)^2 \quad L_3 = \xi^2(3 - 2\xi) \quad L_4 = l\xi^2(\xi - 1) \tag{12.16}$$

where ξl is the distance from the left-hand end of the member to any section. The bending moment corresponding to any of the four deflected shapes can be expressed by a straight-line equation: $M = C_1 + C_2\xi$, where C_1 and C_2 are constants. Substitution of this equation

in Eq. 10.1 and integration give L_1, L_2, L_3, and L_4, satisfying the appropriate boundary conditions.

The vector $\{D\}$ includes the displacements required to apply Eq. 12.15 to any member; an exception is θ_r, of member GH whose value is given by $\theta_r = \theta_{z\ at\ H} + 1$. The added unity represents the rotation introduced while $\{D\} = \{0\}$, Figure 12.12b.

Example 12.2: Grid: influence line for bending moment in a section

Find the influence line for the bending moment at section n, just to the left of joint C, in the grid of Figure 12.13a. The main girders are encastré. The relative value of I is 4 for all main girders and 1 for the cross-girders. The ratio of the torsional rigidity GJ to the flexural rigidity EI is 1:4 for all members.

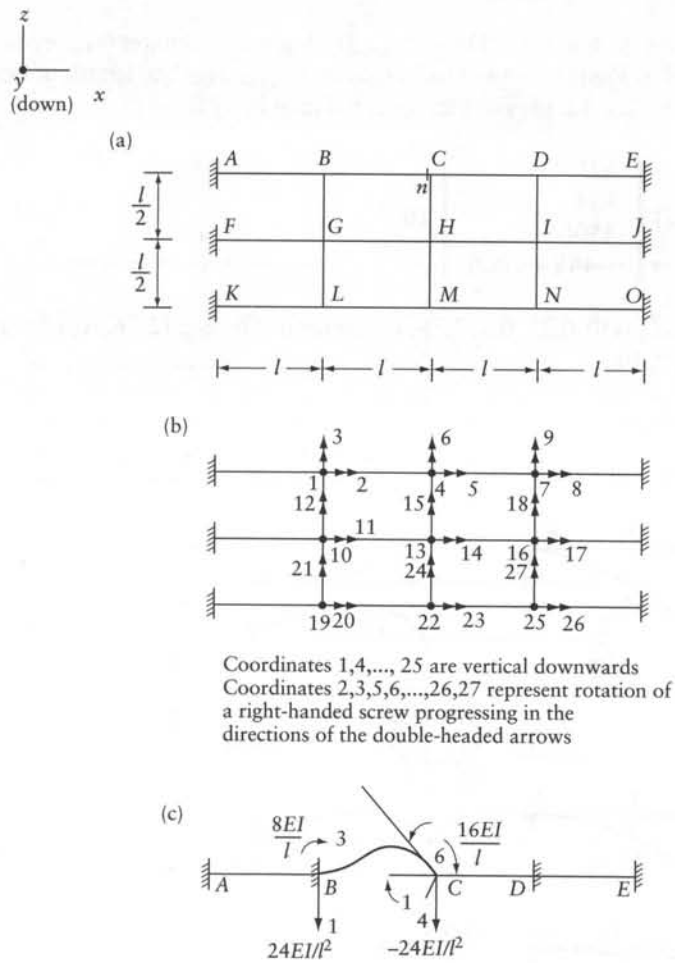

Figure 12.13 Analysis of the grid of Example 12.2. (a) Grid plan. (b) Coordinate system. (c) Restraining forces corresponding to a unit angular discontinuity at n without joint displacements.

Figure 12.13b shows a coordinate system, with three coordinates at each node. The restraining forces corresponding to a unit angular discontinuity at n without joint displacements are (Figure 12.13c)

$$\{F\}_{27\times1} = \left\{\frac{24EI}{l^2}, 0, \frac{8EI}{l}, -\frac{24EI}{l^2}, 0, \frac{16EI}{l}, \ldots\right\}$$

where the elements not shown are zero.

Application of the restraining forces in reversed directions on the grid gives the following displacements (determined by computer program PLANEG, Appendix L):

$$\{D\} = 10^{-3}\{\{62l, 35, 134\}, \{350l, 381, -488\}, \{66l, 49, -140\},$$
$$\{54l, 58, 106\}, \{140l, 331, -10\}, \{51l, 64, -101\},$$
$$\{10l, 102, 10\}, \{10l, 198, -2\}, \{8l, 99, -91\}\}$$

The displacements v in the y direction $(D_1, D_4, \ldots, D_{25})$ are coordinates η_{Mn} of the influence line of M_n, plotted in Figure 12.14. The variation of η_{Mn} over the length of any member can be determined by Eq. 12.15. For example, for member BC

$$(\eta_{Mn})_{BC} = [L_1\ L_2\ L_3\ L_4]\begin{Bmatrix} 62l \\ 134 \\ 350l \\ -488 + 1000 \end{Bmatrix} 10^{-3}$$

Substituting the L-values at $\xi = \{0, 0.25, 0.5, 0.75, 1\}$ determined by Eq. 12.16, we obtain: $\{\eta_{Mn}\} = l\{62, 102, 159, 239, 350\}$.

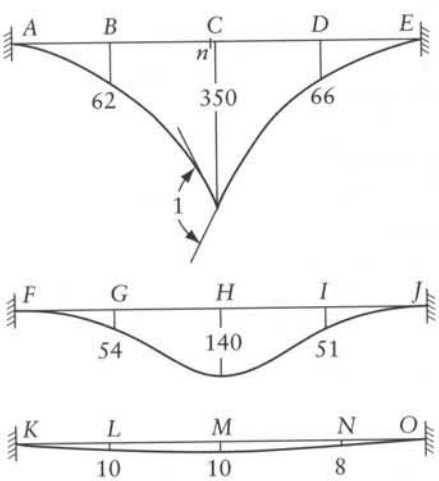

Figure 12.14 Influence line for the bending moment M_n at section n of the grid in Example 12.2.

Example 12.3: Torsionless grid

Neglecting the torsional rigidity of the girders, find for the interconnected bridge system of Figure 12.15a the influence lines for the following actions:

(a) bending moment at the center of girder AB
(b) bending moment at the center of girder CD
(c) bending moment in the cross-girder at J
(d) reaction R_c at support C

The main girders are simply supported and have a second moment of area of $4I$, where I is the second moment of area of the cross-girders.

The stiffness matrix of the grid corresponding to vertical downward coordinates at N, J, K, and L (Figure 12.15b) can be calculated from the values tabulated in Appendix E. We obtain

$$[S] = \frac{EI}{l^3}\begin{bmatrix} 537.6 & & \text{symmetrical} & \\ -777.6 & 2265.6 & & \\ 518.4 & -1814.4 & 2265.6 & \\ -86.4 & 518.4 & -777.6 & 537.6 \end{bmatrix} \qquad \text{(a)}$$

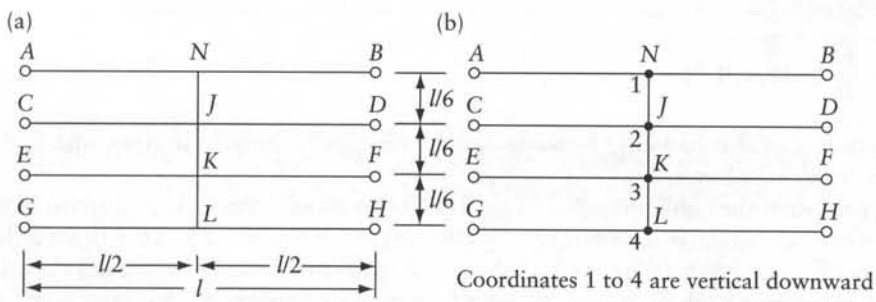

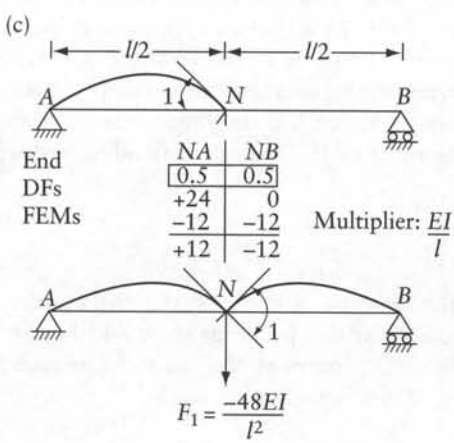

Figure 12.15 Analysis of the torsionless grid in Example 12.3. (a) Grid plan. (b) Coordinate system. (c) Calculation of the restraining force F_1 corresponding to a unit angular discontinuity in main girder at N, with no displacements along the coordinate.

As an example, we calculate element S_{11} as follows:

$$S_{11} = 6.0(EI/l^3)_{AN} + 1.6(EI/l^3)_{NJ} = 537.6EI/l^3$$

The two terms in this equation are read from Table E.1 as the reactions at N, treating ANB and $NJKL$ as continuous beams of two and three spans respectively.

To find the influence line of the bending moment at the center of girder AB, we introduce a unit angular discontinuity just to the left (or right) of joint N (Figure 12.15c) with the vertical joint displacements prevented. The end-moment M_{NA} corresponding to this configuration is

$$\frac{3E(4I)}{l/2} = 24\frac{EI}{l}$$

Moment distribution for the beam ANB is carried out in Figure 12.15c, and the restraining force F_1 required to prevent the deflection at N is

$$F_1 = -48\frac{EI}{l^2}$$

It is obvious that no forces are required at the other three coordinates. Thus, the matrix $\{F\}$ is

$$\{F\} = \frac{EI}{l^2}\{-48, 0, 0, 0\}$$

The force F_1 can also be found by the use of the reactions tabulated in Appendix E, the procedure being as follows.

In order to reach the configuration of Figure 12.16a we can proceed in two steps. First, we introduce a unit angular discontinuity by allowing the left-hand end of the beam to lift by a distance $l/2$, as shown in Figure 12.16b; no forces are involved. In the second step, the support A is brought back to its original level by a vertical downward force at A without a change in the angle between the ends of the members meeting at N. From Appendix E, the value of the reaction at N due to a unit downward displacement of support A is $3E(4I)/(l/2)^3$ upward. Therefore, the value of the restraining force is $F_1 = -48(EI/l^2)$, which is the reaction at N corresponding to a downward displacement of $l/2$ at A.

Similarly, to find the influence line for the bending moment at the center of CD, we introduce a unit rotation at the end J of JC. The corresponding restraining forces are

$$\{F\} = \frac{EI}{l^2}\{0, -48, 0, 0\}$$

For the influence line for the bending moment in the cross-girder at section J, a unit angular discontinuity is introduced at this point, as shown in Figure 12.16c, causing the lifting of end N by a distance $l/6$. The forces at N, J, K, and L required to bring joint N to its original position, determined from Appendix E, are

$$\{F\} = \frac{EI}{l^2}\{57.6, -129.6, 86.4, -14.4\}$$

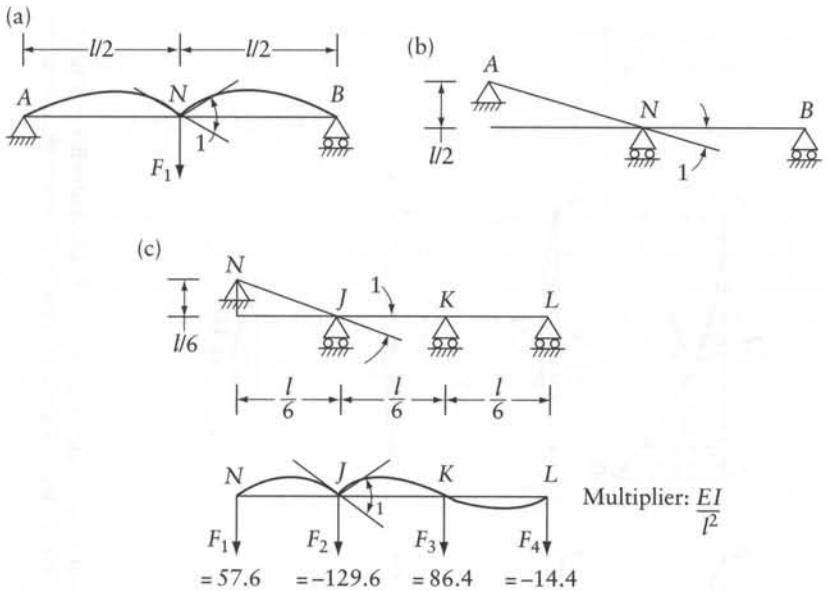

Figure 12.16 Analysis of members of the torsionless grid in Example 12.3. (a) Unit angular discontinuity at N with the vertical deflection restrained by the force F_1. (b) Unit angular discontinuity introduced at N without restraining forces. (c) Determination of the restraining forces corresponding to a unit angular discontinuity in the cross-girder at J by use of tabulated values in Appendix E.

For the influence line of the reaction R_c, a unit downward displacement is introduced at C. The restraining force at J is taken from Appendix E, and the other restraining forces are zero. Therefore,

$$\{F\} = \frac{EI}{l^3}\{0, -96, 0, 0\}$$

The influence ordinates for each of the four effects are summarized in the equation

$$[S][D] = -\frac{EI}{l^2}\begin{bmatrix} -48 & 0 & 57.6 & 0 \\ 0 & -48 & -129.6 & -\frac{96}{l} \\ 0 & 0 & 86.4 & 0 \\ 0 & 0 & -14.4 & 0 \end{bmatrix} \qquad \text{(b)}$$

where $[S]$ is the stiffness matrix in Eq. (a). The solution of Eq. (b) gives

$$[D] = \begin{bmatrix} 0.194l & 0.082l & -0.038l & 0.164 \\ 0.082l & 0.097l & 0.055l & 0.194 \\ 0.010l & 0.062l & 0.006l & 0.124 \\ -0.034l & 0.010l & -0.024l & 0.020 \end{bmatrix}$$

The influence lines for the four actions are plotted in Figure 12.17. They include ordinates between joints, and as an example of calculation of such ordinates, the computation for

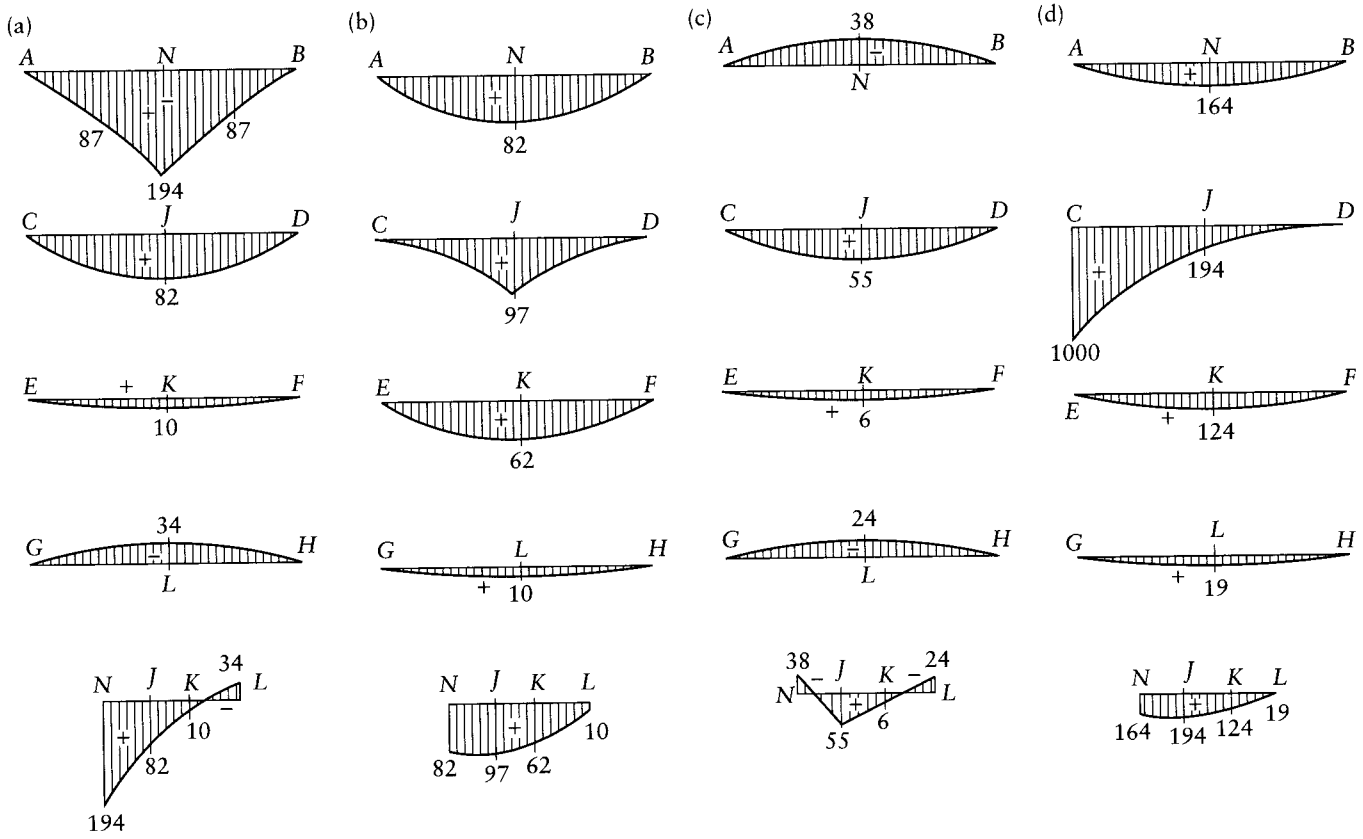

Figure 12.17 Influence lines for the grid in Example 12.3. (a) Influence line for bending moment in main girder at center of AB, multiplier $= l/1000$. (b) Influence line for bending moment in main girder at center of CD, multiplier $= l/1000$. (c) Influence line for bending moment in cross-girder at joint J, multiplier $= l/1000$. (d) Influence line for reaction at C, multiplier $= 1/1000$.

AN is given below for the influence line for the bending moment in Figure 12.17a. The end-moment at N of member AN corresponding to the deflected shape in Figure 12.17a is

$$M_{NA} = 12\frac{EI}{l} - \left[\frac{3E(4I)}{(l/2)^2}\right]0.194l = 2.688\frac{EI}{l}$$

The first term in this equation is the end-moment when the vertical joint displacements are restrained, and the second term is the end-moment caused by the vertical displacement. The bending moments caused by unit values of the vertical displacement are tabulated in Appendix E. The deflection measured from the straight line between A and N can be calculated by Eq. 12.4 or by the use of Appendix I (noting that AN has a second moment of area $=4I$ and length $=l/2$). Therefore, the equation of the influence line between A and N is

$$\eta = l[0.194\xi - 0.028(\xi - \xi^3)]$$

where $\xi = (2x/l)$, and x is the distance from A to the desired point on AN.

12.8 General superposition equation

The concept of adding influence coefficients for statically determinate and statically indeterminate cases in Eq. 12.11 in order to obtain the influence coefficient for bending moment at a section of a straight member will be extended now for any action in a statically indeterminate structure.

The influence coefficients for any action in a linearly elastic statically indeterminate structure can be obtained by adding the influence coefficients for the same action in a released structure and the influence coefficients for the redundants multiplied by the values of the action due to unit values of the redundants. Let p be the number of influence coefficients to be calculated for any action of a structure statically indeterminate to the nth degree. If a unit point load is applied at j, one of the p locations where the influence coefficients are required, the influence coefficient $\eta_j = A_j$ is the value of the action in the statically indeterminate structure determined by the superposition equation

$$A_j = A_{sj} + [F_{1j}F_{2j}\ldots F_{nj}]\{A_u\} \tag{12.17}$$

where $A_{sj} = \eta_{sj}$ is the value of the action due to a unit load at j in a released structure, $F_{ij} = \eta_{Fij}$ is the value of the ith redundant due to a unit load at j, and the elements of $\{A_u\}$ are the values of the action considered due to unit values of the redundants on the released structure.

If the statically indeterminate structure is subjected to a unit load acting separately at each of the p locations and Eq. 12.17 is applied, we obtain the following equation of superposition of influence coefficients:

$$\{\eta\}_{p\times 1} = \{\eta_s\}_{p\times 1} + [\{\eta_{F1}\} \vdots \{\eta_{F2}\} \vdots \ldots \vdots \{\eta_{Fn}\}]_{p\times n}\{A_u\}_{n\times 1} \tag{12.18}$$

in which the elements of the submatrices $\{\eta_{Fi}\}$ are the p influence coefficients of the redundants F_i.

To use Eq. 12.18 the influence lines for the redundants must first be determined. These can be obtained by an analysis for p locations of the unit load. For each position, the n redundants are determined, thus giving one of the p ordinates of the influence line for each redundant.

Influence lines for the redundants can also be determined by direct application of Müller-Breslau's principle.

The use of Eq. 12.18 for arches and trusses will be considered in the following two sections.

12.9 Influence lines for arches

Influence lines are very useful in the analysis of arch bridges. Here, the load is applied through vertical members supporting the deck (Figure 12.18a). Let us consider the influence lines due to a unit vertical load in any position E on CD. This load is assumed to be transmitted to the arch at F vertically below E.

The fixed arch in Figure 12.18a is statically indeterminate to the third degree. The simply-supported arch in Figure 12.18b is chosen as the released structure with the clockwise end-moments M_{AB} and M_{BA}, and the inward horizontal force H as the redundants. The influence lines for the three redundants can be obtained by application of Müller-Breslau's principle. For the influence line for M_{AB}, an anticlockwise unit rotation is introduced at end A: the resulting vertical displacements of the arch axis are the influence ordinates. Similarly, for the influence line for M_{BA}, we introduce an anticlockwise unit rotation at B, and for the influence line for H a unit horizontal displacement is introduced outwards at either A or B.

The bending moment M corresponding to these end displacements can be obtained by the general force method.

The corresponding vertical deflection may be determined by the method of elastic weights (see Section 10.4 and Prob. 10.6). This procedure ignores the effect of axial deformation of the arch. In extremely flat arches, however, the axial deformations may have a non-negligible effect. While a computer is commonly used for analysis of arch bridges, it is useful to discuss below the shapes of influence lines to be expected; these make possible a broad check of the calculations.

Simple expressions can be derived for the redundants H, M_{AB}, and M_{BA} in a parabolic arch in which the flexural rigidity EI varies as the secant of the inclination of the arch axis; thus, $EI = EI_0 \sec\alpha$, where EI_0 is the flexural rigidity at the crown (Figure 12.19a). The equations of the influence lines are

$$\eta_H = \frac{15l}{64h}(1-\xi^2)^2 \tag{12.19}$$

$$\eta_{MAB} = \frac{l}{32}(1-\xi)^2(5\xi^2+6\xi+1) \tag{12.20}$$

$$\eta_{MBA} = -\frac{l}{32}(1+\xi)^2(5\xi^2-6\xi+1) \tag{12.21}$$

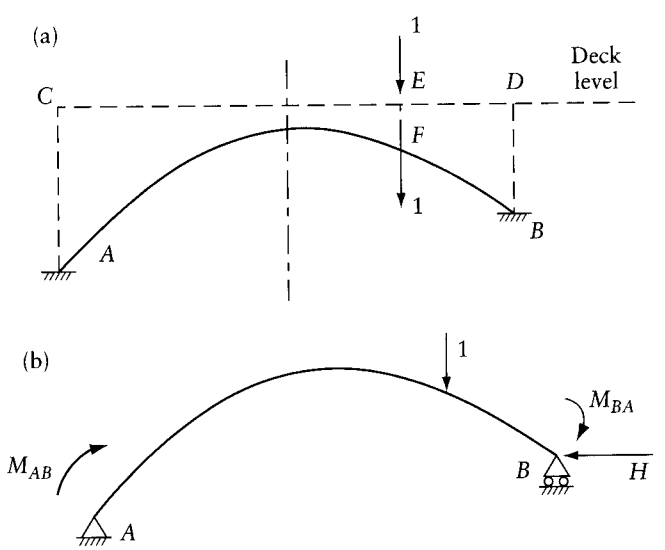

Figure 12.18 Fixed arch and a released structure. (a) Arch supporting a bridge deck. (b) Statically determinate released structure.

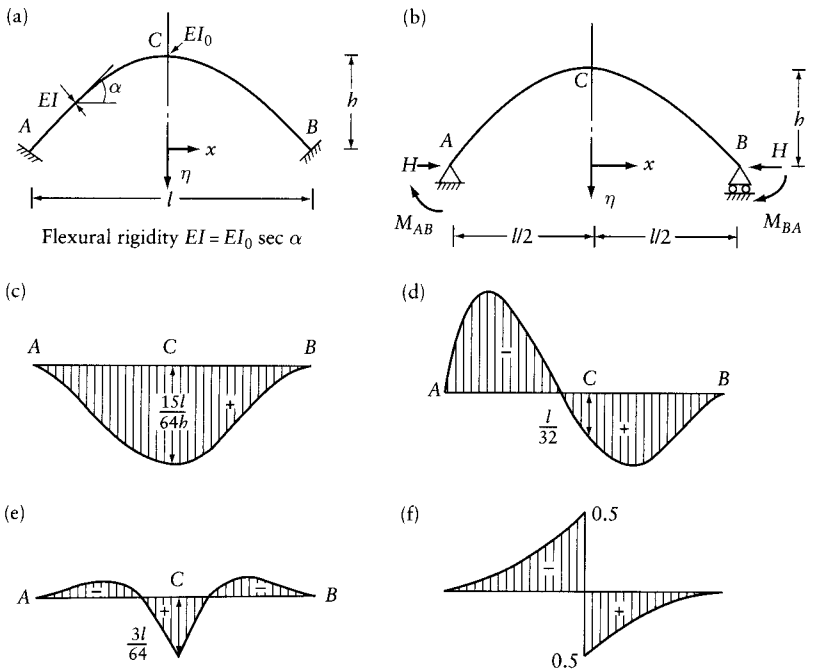

Figure 12.19 Influence lines for a parabolic arch with secant variation of flexural rigidity. (a) Parabolic arch with secant variation in EI. (b) Positive direction of the redundants. (c) Influence line for H. (d) Influence line for M_{AB}. (e) Influence line for M_C. (f) Influence line for V_c.

where $\xi = x/(0.5l)$; l is the span, and h is the rise. Equations 12.20 and 12.21 are plotted in Figures 12.19c and d.

The influence line for the stress resultant at any section of the arch in Figure 12.19a can be determined by Eq. 12.18. For example, to obtain the influence line of the bending moment M_c at the crown, we first find the values of this action due to unit values of the redundants on the released structure of Figure 12.19b; $\{A_u\} = \{-h, \frac{1}{2}, -\frac{1}{2}\}$, in which the order of the redundants is H, M_{AB}, and M_{BA}. The influence line η_s for the moment M_c in the released structure is formed by two straight segments (as for a simple beam):

$$\left.\begin{aligned} \eta_s &= \frac{l}{4}(1-\xi) \quad \text{for } 0 < \xi < 1 \\ \eta_s &= \frac{l}{4}(1+\xi) \quad \text{for } 0 > \xi > -1 \end{aligned}\right\} \tag{12.22}$$

The influence ordinates η_{MC} are given by Eq. 12.18:

$$\eta_{MC} = \eta_s + \left(-h\eta_H + \frac{1}{2}\,\eta_{MAB} - \frac{1}{2}\,\eta_{MBA}\right)$$

The influence ordinates between the brackets in this equation are given by Eqs. 12.19 to 12.21. The shape of the influence line for M_c is shown in Figure 12.19e.

The influence line for shear V_c at the crown can be obtained in a similar manner; its shape is shown in Figure 12.19f.

It can be shown that the horizontal thrust H due to a uniform load q per unit length of the horizontal projection of a parabolic arch, with any variation in EI and with hinged or fixed supports, is

$$H = \frac{ql^2}{8h} \tag{12.23}$$

and that the bending moment and the shear are zero at all sections. Since the area under an influence line is equal to the value of the action considered due to a uniform load $q = 1$ (see Eq. 12.19), it follows that the area under η_H (Figure 12.20c) is $l^2/8h$ and the area is zero under the other three influence lines in Figure 12.19.

12.10 Influence lines for trusses

Influence lines for the reactions or forces in the members of pin-connected trusses can be obtained by solving for several cases with the unit load at different joints. The influence lines can also be obtained from Eq. 12.18, which applies to any linearly elastic structure. To use this equation, we need the influence line for a statically determinate released truss, the influence lines for the redundants, and the values of the action due to unit values of the redundants. The procedure is illustrated by the following example.

Example 12.4: Continuous truss

Find the influence line for the reaction at B and the forces in the members labeled Z_1 and Z_2 in the truss of Figure 12.20a. The unit load can act at the nodes of the lower chord only. All the members are assumed to have the same value of l/aE, l being the length defined in Figure 12.20a, and a the cross-sectional area of the members.

A released structure is shown in Figure 12.20b, in which the redundants F_1 and F_2 are taken as the forces in members Z_3 and Z_4 respectively. The influence ordinates η_s for the values of the required actions in the released structure are plotted in Figures 12.20c, d, and e. These can be checked by simple statics.

According to Müller-Breslau's principle, the influence line for F_1 can be obtained by cutting the member Z_3 and applying equal and opposite forces (causing compression in Z_3) to the remaining truss, so as to produce a relative unit displacement at the cut section.

Then, the deflected shape of the bottom chord of the truss gives the influence line for F_1. This is the same as finding the deformations in the actual structure due to a unit extension of member Z_3, such as that caused by a rise in temperature or a lack of fit in this member.

The flexibility matrix of the released structure is

$$[f] = \frac{l}{8Ea}\begin{bmatrix} 57 & 3 \\ 3 & 57 \end{bmatrix}$$

The elements of this matrix can be checked by virtual work (see Section 8.6). For convenience, the forces in the members due to $F_1 = 1$ are shown in Figure 12.20f. Making use of symmetry of the structure, the forces in members due to $F_2 = 1$ can also be deduced from this figure.

Forcing member Z_3, with unit elongation, to fit has the same effect as introducing the imposed displacements $\{\Delta\} = \{-1, 0\}$ at the coordinates in Figure 12.20b; the values of the redundants necessary to produce $\{\Delta\}$ are (Eq. 4.11)

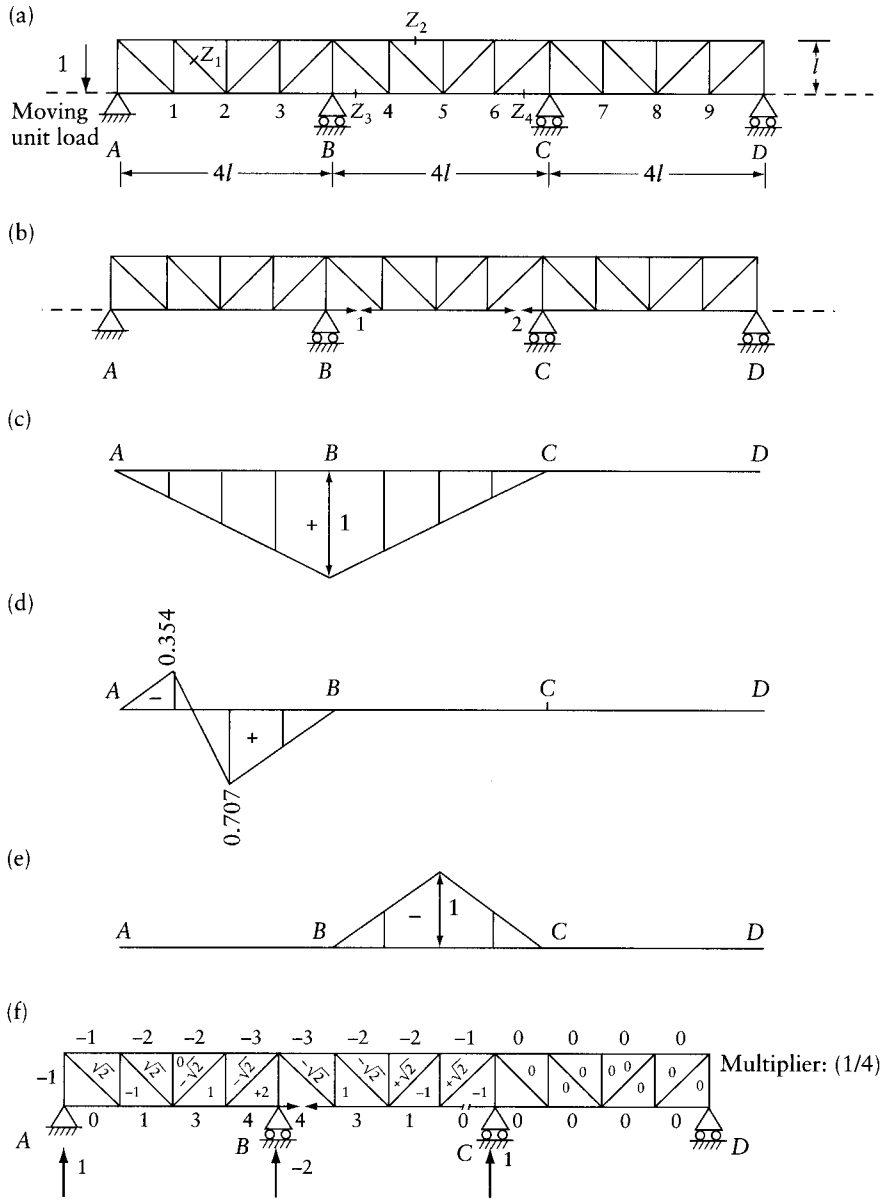

Figure 12.20 Analysis of the continuous truss of Example 12.4. (a) Continuous truss. (b) Released structure and coordinate system. (c) Influence line for R_B in the released structure. (d) Influence line for the force in Z_1 in the released structure. (e) Influence line for the force in Z_2 in the released structure. (f) Reactions and forces in members due to $F_1 = 1$.

$$[f]\begin{Bmatrix} F_1 \\ F_2 \end{Bmatrix} = -\begin{Bmatrix} 1 \\ 0 \end{Bmatrix}$$

Solution of this equation gives $\{F\} = (Ea/405l)\{-57, 3\}$. By superposition (Eq. 4.12), using the values given in Figure 12.20f, we can determine the forces in the actual truss due to a unit extension of member Z_3. The corresponding deflections can be determined by virtual work (Eq. 8.20), giving the influence line ordinates at the joints 1, 2, ..., 9 of the redundant F_1 (Figure 12.21a).

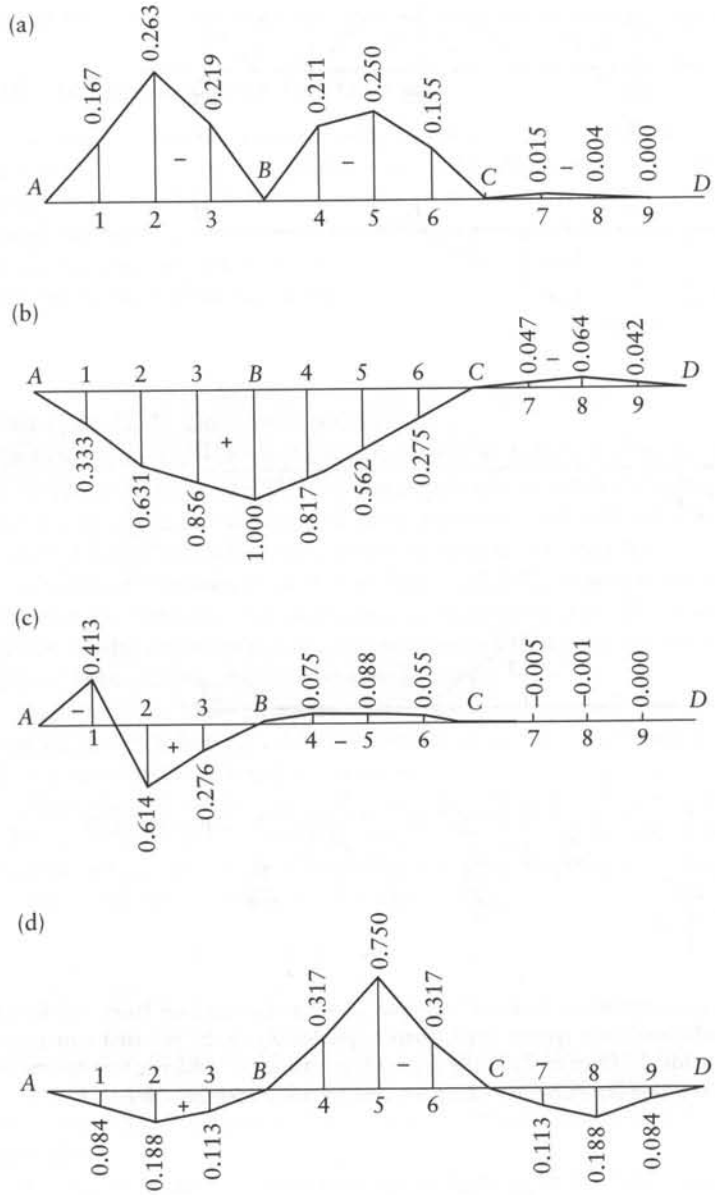

Figure 12.21 Influence lines for the continuous truss of Figure 12.20 (Example 12.4). (a) Influence line for redundant F_1 (force in member Z_3). (b) Influence line for vertical reaction at B. (c) Influence line for force in member Z_1. (d) Influence line for force in member Z_2.

The values in this figure can, of course, be verified by a computer program for analysis of plane trusses (such as PLANET, Appendix L). The analysis needs to be done for one load case, namely, that of a unit elongation of member Z_3. Because the structure is symmetrical, the same ordinates in reversed order are the ordinates at the nine joints of the influence line for F_2.

For the influence line of the reaction at B, we use Eq. 12.18 to determine the coordinates at the joints 1, 2, ..., 9:

$$\{\eta\}_{9\times1} = \{\eta_s\}_{9\times1} + [\{\eta_{F1}\} \vdots \{\eta_{F2}\}]_{9\times2} \{A_u\}_{2\times1} \tag{12.24}$$

The elements of $\{A_u\}$ are the reactions at B due to $F_1 = 1$ and $F_2 = 1$ (see Figure 12.20f)

$$\{A_u\} = \begin{Bmatrix} -0.5 \\ 0.25 \end{Bmatrix}$$

An upward reaction is considered positive. Substituting in Eq. 12.18, we obtain the influence ordinates for R_B:

$$\{\eta\} = \begin{Bmatrix} 0.250 \\ 0.500 \\ 0.750 \\ 0.750 \\ 0.500 \\ 0.250 \\ 0 \\ 0 \\ 0 \end{Bmatrix} + 10^{-3} \begin{bmatrix} -167 & 0 \\ -263 & -4 \\ -219 & -15 \\ -211 & -155 \\ -250 & -250 \\ -155 & -211 \\ -15 & -219 \\ -4 & -263 \\ 0 & -167 \end{bmatrix} \begin{Bmatrix} -0.5 \\ 0.25 \end{Bmatrix} = 10^{-3} \begin{Bmatrix} 333 \\ 631 \\ 856 \\ 817 \\ 562 \\ 275 \\ -47 \\ -64 \\ -42 \end{Bmatrix}$$

The influence line for R_B is plotted in Figure 12.21b. The influence lines for the forces in members Z_1 and Z_2 are determined by Eq. 12.18 in the same way, and the results are plotted in Figures 12.21c and d.

12.11 General

The influence line for any action in a structure can be obtained by repeating the analysis for several cases of loading with a unit load at different positions: each loading case gives one ordinate of the required influence line. This method is convenient only with a computer.

Using Müller-Breslau's principle, influence lines can be represented as deflection lines. The use of this principle makes it possible to determine without any special calculations the shape of the influence line, and this indicates the parts of the structure to be loaded in order to obtain the maximum effects. The principle is also used to calculate the ordinates of the influence line, and can be applied to continuous frames, grids, and trusses.

When a computer is used to determine influence lines, Müller-Breslau's principle can give a single loading case for which the deflections are the influence line ordinates. The study of influence lines in this chapter should help to predict the shape of influence lines to be expected and to verify computer analysis.

The general superposition Eq. 12.18 is shown to facilitate the derivation of influence lines for arches and trusses.

Problems

12.1 Obtain the influence lines for the reaction at B, and bending moment and shear at E in the statically determinate beam shown in the figure. From the influence ordinates, determine the maximum positive values of these actions resulting from a uniform traveling live load q/unit length. The live load is to be applied on parts of the beam such that it produces maximum effect.

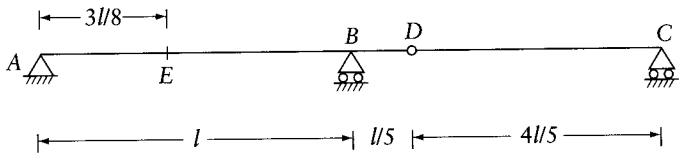

Prob. 12.1

12.2 Obtain the influence lines for the forces in the members marked Z_1 and Z_2 of the truss shown.

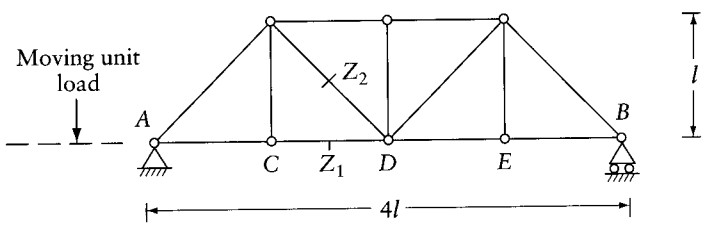

Prob. 12.2

12.3 Obtain the influence lines of the horizontal component of the reaction at A and the bending moment at D for the three-hinged parabolic arch shown in the figure. What are the maximum positive and negative values of the bending moment at D due to a uniform live load of q/unit length of horizontal projection?

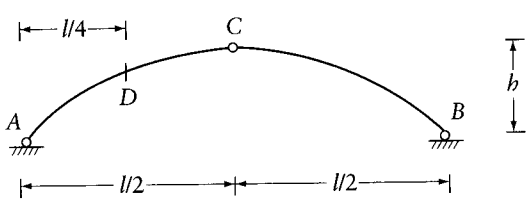

Prob. 12.3

12.4 For the bridge frame shown, calculate the influence ordinate at $0.3l$, $0.5l$, and $0.7l$ of each span and draw the influence lines for the following actions:

(a) Bending moment at n
(b) Bending moment at center of span AB
(c) Shearing force at n

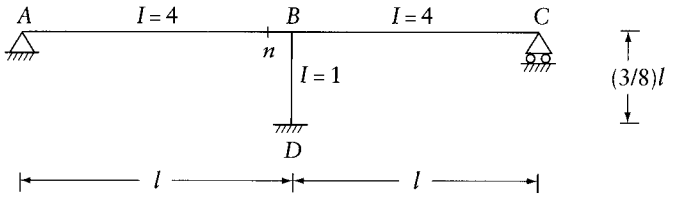

Prob. 12.4

12.5 The continuous prismatic beam shown in the figure is totally fixed at A and supported at B and C on elastic supports of stiffness EI/l^3, where EI is the flexural rigidity of the beam. Obtain the influence lines for R_A, R_B and the end-moment at A. Give the ordinates at the supports and the middle of each span.

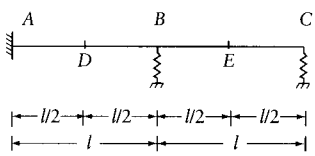

Prob. 12.5

12.6 Replace the hinged support at A of the frame of Prob. 12.4 by a roller support, then obtain the influence line of the end-moment DB. Give the ordinates at $0.3l$, $0.5l$, and $0.7l$ for each of the spans AB and BC.

12.7 Find the influence line of the bending moment at section n of the grid shown in the figure. The relative EI values are given alongside the girders. The ratio $GJ/(EI) = \frac{1}{4}$ for all members. Give ordinates at G, H, and I only. The end supports prevent the rotations about the x axis as well as the vertical displacements in the y direction.

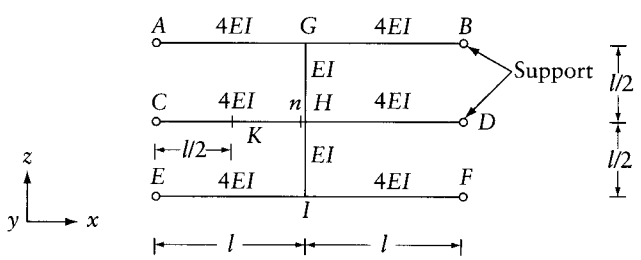

Prob. 12.7

12.8 Solve Prob. 12.7 with $GJ = 0$. Give the influence ordinates at G, H, I, and the center of CH.

12.9 Prove Eq. 12.16.

12.10 Prove Eq. 12.19.

12.11 Obtain the influence line for the reaction components X_A, Y_A, and M_{AB} in the arch shown due to a unit vertical load. This load can be applied at the panel points A, B, C, D, and E. Consider bending deformations only.

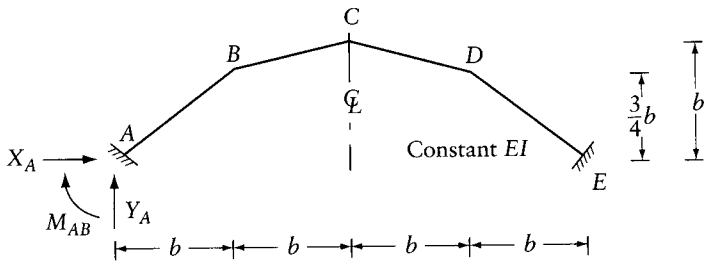

Prob. 12.11

12.12 Obtain the influence line for the component X_A of the reaction at A in the two-hinged truss in the figure. Use this influence line to obtain the influence line for the force in member DE. Assume that all the members are of the same cross section.

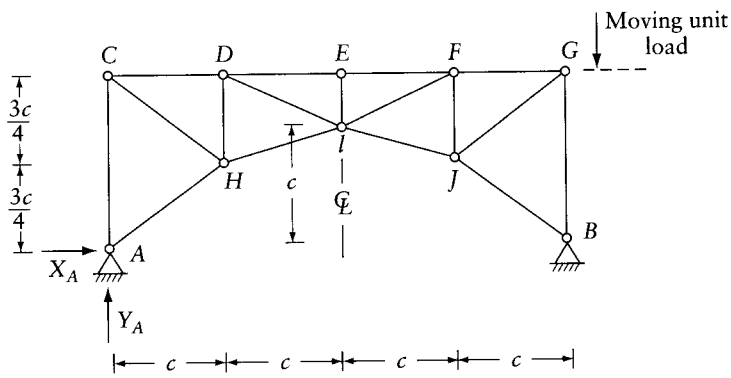

Prob. 12.12

12.13 Find the influence lines for the forces in members Z_1 and Z_2 of the truss in the figure. Assume that all the members have the same $b/(aE)$ value, b and a being the length defined in the figure and the cross-sectional area of the member.

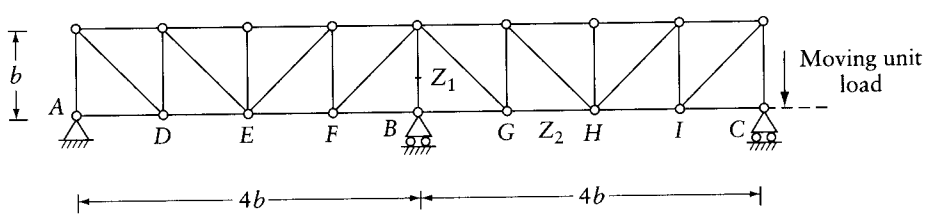

Prob. 12.13

Chapter 13

Effects of axial forces on flexural stiffness

13.1 Introduction

The forces required to cause a unit rotation or translation in the transverse direction at one end of a member decrease when the member is subjected to axial compressive force, and conversely increase if the axial force is tensile. When the axial forces in members of frames are relatively high, the change in stiffness arising from bending by the axial force can be of importance. This effect of the axial force is important in slender members only, and is referred to as the *beam–column effect* (or, casually, *P-delta effect).*

In the following sections, the beam–column effect is discussed for analysis of plane frames. Calculation of the critical buckling loads for members and frames is also presented.

13.2 Stiffness of a prismatic member subjected to an axial force

We recall that the force and displacement methods of analysis considered in the previous chapters are for linear structures for which the principle of superposition holds. In such structures, the deformations are proportional to the applied loads, and the displacements or the internal forces caused by a set of effects can be obtained by superposition.

In Section 3.6, we saw that the superposition of deflections cannot be applied in the case of a strut subjected to axial compression together with a transverse load because of the additional moment caused by the change in geometry of the member by the loading. If, however, the strut is subjected to a system of loads or end displacements all acting in the presence of an unaltered axial force, the effects of these loads and the displacements can be superimposed. Thus, the axial force can be looked upon as a parameter which affects the stiffness or the flexibility of the member and, once these have been determined, the methods of analysis of linear structures can be applied.

In the analysis of rigid frames with very slender members, the axial forces are generally not known at the outset of the analysis. A set of axial forces is estimated, the stiffness (or flexibility) of the members is determined accordingly, and the frame is analyzed as a linear structure. If the results show that the axial forces obtained by this analysis differ greatly from the assumed values, the calculated values are used to find new stiffness (or flexibility) values and the analysis is repeated.

Let us now consider in detail the effects of an axial compressive and axial tensile force on the stiffness of a prismatic member.

13.3 Effect of axial compression

The differential equation governing the deflection y of a prismatic member AB subjected to a compressive force P and any end restraint (Figure 13.1a and Eq. 10.7) is

$$\frac{d^4y}{dx^4} + \frac{P}{EI}\frac{d^2y}{dx^2} = \frac{q}{EI} \tag{13.1}$$

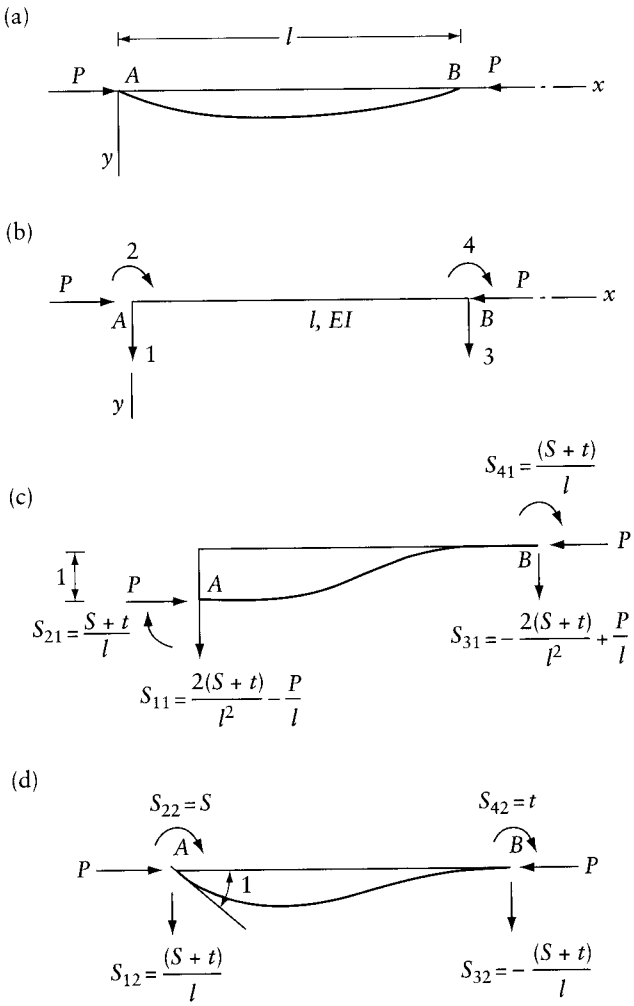

Figure 13.1 Stiffness of a strut. (a) Deflection of a strut assumed to be subjected to end-forces and end-displacements at the coordinates indicated in part (b). (b) Coordinate system corresponding to the stiffness matrix of a strut in Eq. 13.14. (c) End-forces corresponding to $D_1 = 1$ while $D_2 = D_3 = D_4 = 0$. (d) End-forces corresponding to $D_2 = 1$ while $D_1 = D_3 = D_4 = 0$.

where q is the intensity of transverse loading. When $q = 0$, the general solution of Eq. 13.1 is

$$y = A_1 \sin u\frac{x}{l} + A_2 \cos u\frac{x}{l} + A_3 x + A_4 \tag{13.2}$$

where

$$u = l\sqrt{\frac{P}{EI}} \tag{13.3}$$

and A_1, A_2, A_3, and A_4 are the integration constants to be determined from the boundary conditions.

Equation 13.2 will now be used to derive the stiffness matrix of an axially compressed member corresponding to the coordinates 1, 2, 3, and 4 in Figure 13.1b. The displacements $\{D\}$ at the four coordinates

$$D_1 = (y)_{x=0} \quad D_2 = \left(\frac{dy}{dx}\right)_{x=0} \quad D_3 = (y)_{x=l} \quad D_4 = \left(\frac{dy}{dx}\right)_{x=l}$$

are related to the constants $\{A\}$ by the equation

$$\begin{Bmatrix} D_1 \\ D_2 \\ D_3 \\ D_4 \end{Bmatrix} = \begin{bmatrix} 0 & 1 & 0 & 1 \\ \frac{u}{l} & 0 & 1 & 0 \\ s & c & l & 1 \\ \frac{u}{l}c & -\frac{u}{l}s & 1 & 0 \end{bmatrix} \begin{Bmatrix} A_1 \\ A_2 \\ A_3 \\ A_4 \end{Bmatrix} \tag{13.4}$$

where $s = \sin u$, and $c = \cos u$.

Equation 13.4 can be written

$$\{D\} = [B]\{A\} \tag{13.5}$$

where $[B]$ is the 4×4 matrix in Eq. 13.4.

The forces $\{F\}$ at the four coordinates are the shear and bending moment at $x = 0$ and $x = l$; thus,

$$\begin{Bmatrix} F_1 \\ F_2 \\ F_3 \\ F_4 \end{Bmatrix} = \begin{Bmatrix} (-V)_{x=0} \\ (M)_{x=0} \\ (V)_{x=l} \\ (-M)_{x=l} \end{Bmatrix} = EI \begin{Bmatrix} \left(\frac{d^3y}{dx^3} + \frac{u^2}{l^2}\frac{dy}{dx}\right)_{x=0} \\ \left(-\frac{d^2y}{dx^2}\right)_{x=0} \\ \left(-\frac{d^3y}{dx^3} - \frac{u^2}{l^2}\frac{dy}{dx}\right)_{x=l} \\ \left(\frac{d^2y}{dx^2}\right)_{x=l} \end{Bmatrix} \tag{13.6}$$

Equation 10.1 expresses the bending moment M in terms of the deflections. Using this equation with Eqs. 10.3 and 13.3, the shear can be expressed as

$$V = \frac{dM}{dx} - P\frac{dy}{dx} = EI\left(-\frac{d^3y}{dx^3} - \frac{u^2}{l^2}\frac{dy}{dx}\right) \tag{13.7}$$

Differentiating Eq. 13.2 and substituting in Eq. 13.6 give

$$\begin{Bmatrix} F_1 \\ F_2 \\ F_3 \\ F_4 \end{Bmatrix} = EI \begin{bmatrix} 0 & 0 & \frac{u^2}{l^2} & 0 \\ 0 & \frac{u^2}{l^2} & 0 & 0 \\ 0 & 0 & -\frac{u^2}{l^2} & 0 \\ -\frac{su^2}{l^2} & -\frac{cu^2}{l^2} & 0 & 0 \end{bmatrix} \begin{Bmatrix} A_1 \\ A_2 \\ A_3 \\ A_4 \end{Bmatrix} \tag{13.8}$$

or

$$\{F\} = [C]\{A\} \tag{13.9}$$

where $[C] = EI$ times the 4×4 matrix in Eq. 13.8.

Solving for $\{A\}$ from Eq. 13.5 and substituting into Eq. 13.9,

$$\{F\} = [C][B]^{-1}\{D\} \tag{13.10}$$

Putting

$$[S] = [C][B]^{-1} \tag{13.11}$$

Eq. 13.10 takes the form

$$\{F\} = [S]\{D\}, \tag{13.12}$$

where $[S]$ is the required stiffness matrix. The inverse of $[B]$ is

$$[B]^{-1} = \frac{1}{2-2c-us}\left[\begin{array}{c|c|c|c} -s & \frac{l}{u}(1-c-us) & s & -\frac{l}{u}(1-c) \\ (l-c) & \frac{l}{u}(s-uc) & -(1-c) & \frac{l}{u}(u-s) \\ \frac{u}{l}s & (l-c) & -\frac{u}{l}s & (1-c) \\ (l-c-us) & -\frac{l}{u}(s-uc) & (l-c) & -\frac{l}{u}(u-s) \end{array}\right] \tag{13.13}$$

Substituting Eq. 13.13 into Eq. 13.11, we obtain the stiffness of a strut corresponding to the coordinates in Figure 13.1b:

$$[S] = EI\begin{bmatrix} \frac{u^3 s}{l^3(2-2c-us)} & & \text{symmetrical} & \\ \frac{u^2(1-c)}{l^2(2-2c-us)} & \frac{u(s-uc)}{l(2-2c-us)} & & \\ -\frac{u^3 s}{l^3(2-2c-us)} & -\frac{u^2(1-c)}{l^2(2-2c-us)} & \frac{u^3 s}{l^3(2-2c-us)} & \\ \frac{u^2(1-c)}{l^2(2-2c-us)} & \frac{u(u-s)}{l(2-2c-us)} & -\frac{u^2(1-c)}{l^2(2-2c-us)} & \frac{u(s-uc)}{l(2-2c-us)} \end{bmatrix} \tag{13.14}$$

When the axial force P vanishes, $u \to 0$, and the above stiffness matrix becomes identical with the stiffness matrix in Eq. 6.8. Thus,

$$\lim_{u\to 0}[S]\begin{bmatrix} \frac{12EI}{l^3} & \text{symmetrical} & & \\ \frac{6EI}{l^2} & \frac{4EI}{l} & & \\ -\frac{12EI}{l^3} & -\frac{6EI}{l^2} & \frac{12EI}{l^3} & \\ \frac{6EI}{l^2} & \frac{2EI}{l} & \frac{6EI}{l^2} & \frac{4EI}{l} \end{bmatrix} \tag{13.15}$$

The elements in the first and second column of [S] in Eq. 13.14 are the forces necessary to hold the member in the deflected configuration shown in Figures 13.1c and d. The two end-moments in Figure 13.1d are the end-rotational stiffness $S(=S_{AB}=S_{BA})$ and the carry-over moment t, which are needed for moment distribution. Thus, the end-rotational stiffness and the carryover moment for a prismatic member subjected to an axial compressive force P (Figure 13.1d) are

$$S=\frac{u(s-uc)}{(2-2c-us)}\frac{EI}{l} \tag{13.16}$$

and

$$t=\frac{u(u-s)}{(2-2c-us)}\frac{EI}{l} \tag{13.17}$$

where $s=\sin u$, $c=\cos u$, and $u=l\sqrt{P/(EI)}$. The carryover factor $C(=C_{AB}=C_{BA})$ is

$$C=\frac{t}{S}=\frac{u-s}{s-uc} \tag{13.18}$$

When u tends to zero, S, t, and C tend to $4EI/l$, $2EI/l$, and 1/2 respectively. It can be seen thus that the axial compressive force reduces the value of S and increases C. When the force P reaches the critical buckling value, S becomes zero, which means that the displacement D_2 can be caused by an infinitely small value of the force F_2, and the value of C approaches infinity. From Eq. 13.16, S is zero when $s=uc$ or $\tan u=u$. The smallest value of u to satisfy this equation is $u=l\sqrt{P_{cr}/(EI)}=4.49$. Thus, the buckling load of the strut with the end conditions of Figure 13.1d is $P_{cr}=20.19(EI/l^2)$.

The critical buckling load corresponding to any end conditions can be derived from the stiffness matrix in Eq. 13.14.

The deflected shape in Figure 13.1c can be achieved in two stages. First, a unit downward translation is introduced at A while the end-rotations are allowed to occur freely; this condition can be represented by a straight line (a chord) joining A and B. Second, clockwise end-rotations, through angles equal to $1/l$, at A and B produce the deflected shape in Figure 13.1c, and require the end-moments $M_{AB}=S_{21}=(S+t)/l$ and $M_{BA}=S_{41}=(S+t)/l$. The vertical forces S_{11} and S_{31} can now be determined by considering the equilibrium of the system of forces in Figure 13.1c. Thus, the elements in the first column of the stiffness matrix corresponding to the coordinates in Figure 13.1b can be expressed in terms of S and t. The end-moments S and t in Figure 13.1d are, respectively, equal to S_{22} and S_{42}; again, considering equilibrium of the forces in this figure, $S_{12}=(S+t)/l=-S_{32}$. This gives the elements in the second column of [S] in terms of S and t.

In a similar way, the elements in the remaining two columns of [S] can be derived. Thus, the stiffness matrix for a prismatic member subjected to a compressive axial force (Figure 13.1b) can be expressed as

$$[S]=\begin{bmatrix} \dfrac{2(S+t)}{l^2}-\dfrac{P}{l} & & \text{symmetrical} & \\ \dfrac{S+t}{l} & S & & \\ -\dfrac{2(S+t)}{l^2}+\dfrac{P}{l} & -\dfrac{(S+t)}{l} & \dfrac{2(S+t)}{l^2}-\dfrac{P}{l} & \\ \dfrac{S+t}{l} & t & -\dfrac{(S+t)}{l} & S \end{bmatrix} \tag{13.19}$$

If we substitute $P=u^2EI/l^2$ in the above equation, it becomes apparent that all the elements of the stiffness matrix are a function of the dimensionless parameter u, the member length l, and the flexural rigidity EI. Figure 13.2 shows the values of the end-rotational stiffness S and the carryover moment t in terms of the dimensionless parameter $u=\sqrt{P/(EI)}$; Table 13.1 lists

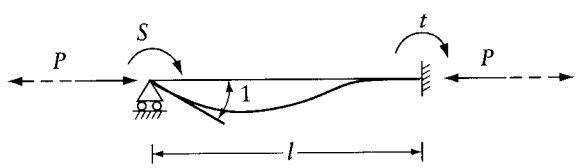

P = absolute value of the axial force (tension or compression)

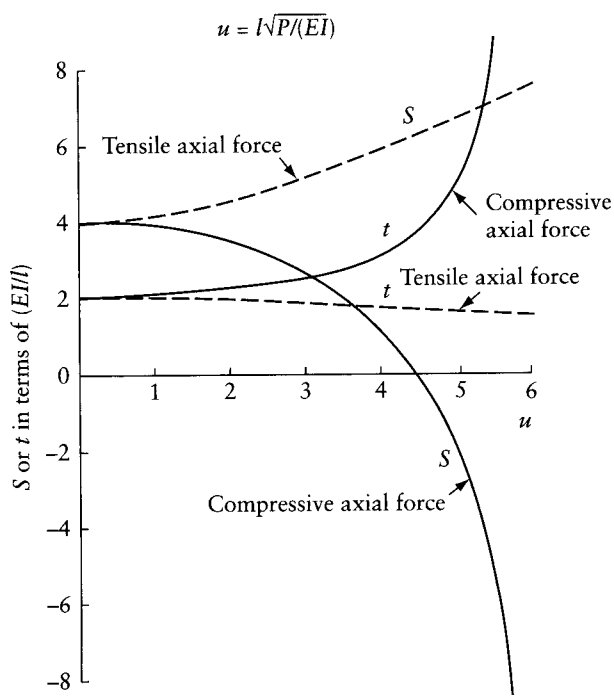

Figure 13.2 End-rotational stiffness and carryover moment for a prismatic member subjected to an axial force.

Table 13.1 Values of End-rotational Stiffness S and Carryover Moment *t* in Terms of *EI/l* for Prismatic Members Subjected to Axial Forces (Eqs. 13.16, 13.17, 13.20, and 13.21; see Figure 13.2)

Axial compressive force P						*Axial tensile force P*					
u^*	S	t	u	S	t	u	S	t	u	S	t
0.0	4.000	2.000	3.0	2.624	2.411	0.0	4.000	2.000	3.0	5.081	1.766
0.1	3.998	2.000	3.1	2.515	2.450	0.1	4.001	1.999	3.1	5.147	1.754
0.2	3.995	2.001	3.2	2.399	2.492	0.2	4.005	1.999	3.2	5.214	1.742
0.3	3.988	2.003	3.3	2.276	2.538	0.3	4.012	1.997	3.3	5.283	1.730
0.4	3.977	2.005	3.4	2.146	2.588	0.4	4.021	1.995	3.4	5.353	1.718
0.5	3.967	2.008	3.5	2.008	2.642	0.5	4.033	1.992	3.5	5.424	1.706
0.6	3.952	2.012	3.6	1.862	2.702	0.6	4.048	1.988	3.6	5.497	1.694
0.7	3.934	2.016	3.7	1.706	2.767	0.7	4.065	1.984	3.7	5.570	1.683
0.8	3.914	2.022	3.8	1.540	2.838	0.8	4.085	1.979	3.8	5.645	1.671
0.9	3.891	2.028	3.9	1.363	2.917	0.9	4.107	1.974	3.9	5.720	1.659
1.0	3.865	2.034	4.0	1.173	3.004	1.0	4.132	1.968	4.0	5.797	1.648
1.1	3.836	2.042	4.1	0.970	3.100	1.1	4.159	1.961	4.1	5.874	1.636
1.2	3.804	2.050	4.2	0.751	3.207	1.2	4.188	1.954	4.2	5.953	1.625
1.3	3.769	2.059	4.3	0.515	3.327	1.3	4.220	1.946	4.3	6.032	1.614
1.4	3.732	2.070	4.4	0.259	3.462	1.4	4.255	1.938	4.4	6.112	1.603
1.5	3.691	2.081	4.5	−0.019	3.614	1.5	4.292	1.930	4.5	6.193	1.592
1.6	3.647	2.093	4.6	−0.323	3.787	1.6	4.330	1.921	4.6	6.275	1.581
1.7	3.599	2.106	4.7	−0.658	3.984	1.7	4.372	1.912	4.7	6.357	1.571
1.8	3.548	2.120	4.8	−1.029	4.211	1.8	4.415	1.902	4.8	6.440	1.561
1.9	3.494	2.135	4.9	−1.443	4.475	1.9	4.460	1.892	4.9	6.524	1.551
2.0	3.436	2.152	5.0	−1.909	4.785	2.0	4.508	1.881	5.0	6.608	1.541
2.1	3.374	2.170	5.1	−2.439	5.151	2.1	4.557	1.871	5.1	6.693	1.531
2.2	3.309	2.189	5.2	−3.052	5.592	2.2	4.608	1.860	5.2	6.779	1.521
2.3	3.240	2.210	5.3	−3.769	6.130	2.3	4.661	1.849	5.3	6.865	1.512
2.4	3.166	2.233	5.4	−4.625	6.798	2.4	4.716	1.837	5.4	6.952	1.503
2.5	3.088	2.257	5.5	5.673	7.647	2.5	4.773	1.826	5.5	7.039	1.494
2.6	3.005	2.283	5.6	−6.992	8.759	2.6	4.831	1.814	5.6	7.127	1.485
2.7	2.918	2.312	5.7	−8.721	10.269	2.7	4.891	1.802	5.7	7.215	1.476
2.8	2.825	2.342	5.8	−11.111	12.428	2.8	4.953	1.791	5.8	7.303	1.468
2.9	2.728	2.376	5.9	−14.671	15.745	2.9	5.016	1.779	5.9	7.392	1.460

*$u = l\sqrt{P/EI}$. Enter the table with the dimensionless parameter u and read the corresponding values of $S/(EI/l)$ and $t/(EI/l)$.

the numerical data. All these values apply to prismatic members only. The negative values of S correspond to P values higher than the critical buckling load, so that the negative sign indicates that a restraining moment is needed to hold the end rotation at a value not exceeding unity.

13.4 Effect of axial tension

The stiffness of a prismatic member in tension can be derived from the expressions for a member in compression by replacing P by $(-P)$. Accordingly, the notation $u = l\sqrt{P/(EI)}$ is to be replaced by $l\sqrt{-P/(EI)} = iu$, where $i = \sqrt{-1}$. Applying this to Eqs. 13.16 to 13.18 and making use of the fact that

$$\sinh u = -i \sin iu$$

and

$$\cosh u = \cos iu$$

we obtain the end-rotational stiffness, carryover moment, and carryover factor for a prismatic member subjected to an axial tensile force P:

$$S = \frac{u(u\cosh u - \sinh u)}{(2 - 2\cosh u + u\sinh u)}\frac{EI}{l} \tag{13.20}$$

$$t = \frac{u(\sinh u - u)}{(2 - 2\cosh u + u\sinh u)}\frac{EI}{l} \tag{13.21}$$

and

$$C = \frac{t}{S} = \frac{\sinh u - u}{u\cosh u - \sinh u} \tag{13.22}$$

where $u = l\sqrt{P/(EI)}$, P being the absolute value of the axial tensile force. The values of S and t calculated by the above equations are included in Table 13.1 and are plotted against u in Figure 13.2.

Considering equilibrium, we can readily see that the stiffness matrix corresponding to the coordinates in Figure 13.1b for a member in tension is

$$[S] = \left[\begin{array}{c|c|c} \frac{2(S+t)}{l^2} + \frac{P}{l} & & \\ \frac{S+t}{l} & S & \text{symmetrical} \\ -\frac{2(S+t)}{l^2} - \frac{P}{l} & -\frac{(S+t)}{l} & \frac{2(S+t)}{l^2} + \frac{P}{l} \\ \frac{S+t}{l} & t & -\frac{(S+t)}{l} \end{array}\right| \left.\begin{array}{c} \\ \\ \\ \\ S \end{array}\right] \tag{13.23}$$

13.5 General treatment of axial force

Summarizing the above discussion, we can see that the axial force is considered as a parameter affecting the stiffness of the member, and the forces corresponding to unit end-displacements are expressed in terms of S and t, which are functions of the dimensionless parameter $u = l\sqrt{P/(EI)}$. Once the stiffness of the member is known, any one of the displacement methods of analysis considered in the previous chapters can be used.

The end-forces corresponding to unit end-displacement of a prismatic member subjected to an axial force are listed in Table 13.2. All forces are given in terms of S and t, which may be defined as the end-moments F_1 and F_2 corresponding to the end conditions in case (b) of the table. The values of S and t can be taken from Table 13.1 or calculated by Eqs. 13.16 and 13.17 or Eqs. 13.20 and 13.21. When the axial force is zero, S and t become $4EI/l$ and $2EI/l$ respectively, and the forces listed in Table 13.2 become the same as the forces listed in Appendix D. Table 13.2 is to be used for the same purpose and in the same way as Appendix D, but with Table 13.2 the axial force P must be known (or assumed) and the corresponding values of S and t calculated in advance.

In some cases, it may be more convenient to substitute for $P = u^2(EI/l^2)$ in the equations in Table 13.2. With S and t expressed in terms of EI/l, all the forces in the table can be expressed in terms of EI and l.

Table 13.2 End-forces Caused by End-displacements of a Prismatic Member Subjected to Axial Compressive or Tensile Force

Bar	*End-Forces*	
	Axial compressive force P	*Axial tensile force P*
(a) 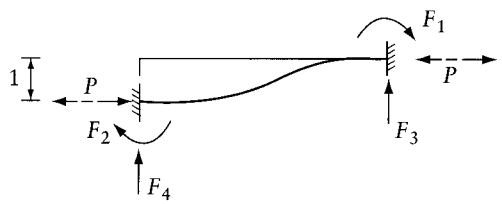	$F_1 = F_2 = \frac{S+t}{l}$ $F_3 = -F_4$ $F_4 = \frac{2(S+t)}{l^2} - \frac{P}{l}$	$F_1 = F_2 = \frac{S+t}{l}$ $F_3 = -F_4 =$ $\frac{2(S+t)}{l^2} + \frac{P}{l}$
(b) 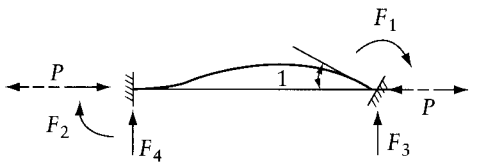	$F_1 = S$ $F_2 = t$ $F_3 = -F_4 = \frac{S+t}{l}$	$F_1 = S$ $F_2 = t$ $F_3 = -F_4 = \frac{S+t}{l}$
(c) 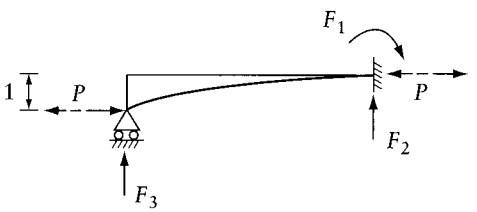	$F_1 = \frac{S-(t^2/S)}{l}$ $F_2 = -F_3 =$ $\frac{S-(t^2/S)-Pl}{l^2}$	$F_1 = \frac{S-(t^2/S)}{l}$ $F_2 = -F_3 =$ $\frac{S-(t^2/S)-Pl}{l^2}$
(d) 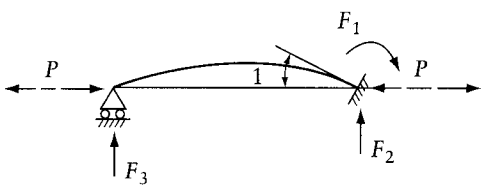	$F_1 = S-(t^2/S)$ $F_2 = -F_3 =$ $\frac{S-(t^2/S)}{l}$	$F_1 = S-(t^2/S)$ $F_2 = -F_3 =$ $\frac{S-(t^2/S)}{l}$

Note: S and t are given in terms of $u = l\sqrt{P/(EI)}$ in Table 13.1. EI is flexural rigidity and l is the length of the member. P may be expressed as $P = u^2 EI/l^2$.

13.6 Adjusted end-rotational stiffness for a prismatic member subjected to an axial force

We recall that the end-rotational stiffness S of a beam is the moment required to rotate one end of the beam through unity while the far end is encastré (Figure 13.1d). Following the same procedure as in Section 11.6, the adjusted end-rotational stiffness of a beam subjected to an axial force can be derived for various end conditions. In the following, the adjusted end-rotational stiffnesses which are needed for analysis by moment distribution are given for beams subjected to the conditions shown in Figure 11.7 as well as to an axial compressive or tensile force of value P (not shown in the figure).

For the end conditions in Figure 11.7b:

$$S_{AB}^{①} = S(1 - C^2) = S - (t^2/S) \tag{13.24}$$

For the symmetrical conditions in Figure 11.7c:

$$S_{AB}^{②} = S(1 - C) = S - t \tag{13.25}$$

For the antisymmetrical case in Figure 11.7d:

$$S_{AB}^{③} = S(1 + C) = S + t \tag{13.26}$$

For the cantilever in Figure 11.7e:

$$S_{AB}^{④} = S - \frac{(S + t)}{2 \pm Pl/(S + t)} \tag{13.27}$$

The carryover factor in the last case is

$$C_{AB}^{④} = \frac{t^2 - S^2 \pm tPl}{S^2 - t^2 \pm SPl} \tag{13.28}$$

The sign of the terms containing $Pl(=u^2(EI/l))$ in Eqs. 13.27 and 13.28 is plus when the axial force is tensile and minus when compressive. The values of S, t, and C to be used in Eqs. 13.24 to 13.28 should be calculated by Eqs. 13.16 to 13.18 for compression members and by Eqs. 13.20 to 13.22 for tension members, or by Table 13.1 for both cases. Equation 13.27 can be derived by the condensation of $[S^*]$ corresponding to coordinates 1^* and 2^* in Figure 11.7f, considering $D_1^* = 1$ while $F_2^* = 0$ (Section 6.5).

13.7 Fixed-end moments for a prismatic member subjected to an axial force

Consider a straight member subjected to transverse loading and an axial force shown in Figure 13.3. The end-displacement along the beam axis can take place freely but the end-rotation is prevented, so that fixed-end moments are induced. The presence of an axial compressive force causes an increase in the fixed-end moments whereas a tensile force results in a decrease. Two cases of loading will be considered: a uniform load and a concentrated load.

13.7.1 Uniform load

The deflection of the prismatic strut AB in Figure 13.3a carrying a transverse load of constant intensity q is governed by the differential Eq. 13.1, for which the solution is

$$y = G_1 \sin u\frac{x}{l} + G_2 \cos u\frac{x}{l} + G_3 x + G_4 + \frac{qx^2}{2P} \tag{13.29}$$

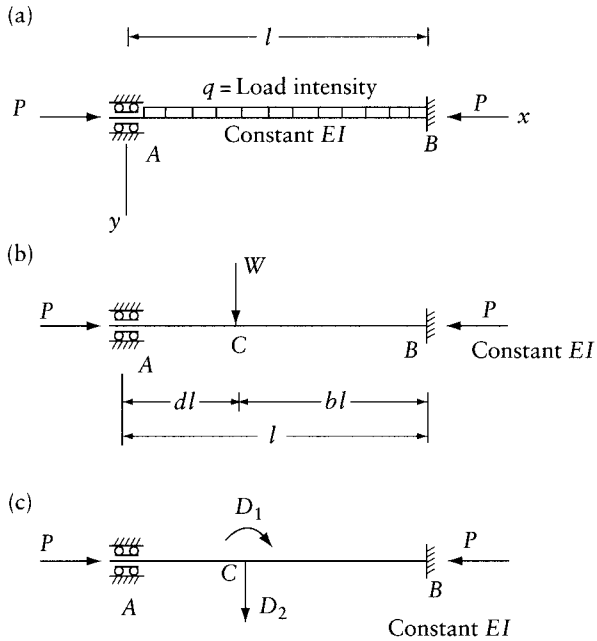

Figure 13.3 Straight prismatic member subjected to an axial force and transverse loading. (a) Loading corresponding to the FEM Eqs. 13.31 or 13.33. (b) Loading corresponding to the FEM Eq. 13.34 and Table 13.3. (c) Degrees of freedom (D_1 and D_2) considered for the analysis of the strut in part (b).

The integration constants $\{G\}$ are determined from the boundary conditions $y = 0$ and $(dy/dx) = 0$ at $x = 0$ and $x = l$. It can be checked that these four conditions can be put in the form

$$[B] = \begin{Bmatrix} G_1 \\ G_2 \\ G_3 \\ G_4 \end{Bmatrix} + \frac{q}{P} \begin{Bmatrix} 0 \\ 0 \\ l^2/2 \\ l \end{Bmatrix} = \{0\}$$

where $[B]$ has the same meaning as in Eq. 13.5. Solving for the integration constants, we obtain

$$\begin{Bmatrix} G_1 \\ G_2 \\ G_3 \\ G_4 \end{Bmatrix} = -\frac{ql^2}{u^2 EI} [B]^{-1} \begin{Bmatrix} 0 \\ 0 \\ l^2/2 \\ l \end{Bmatrix} \tag{13.30}$$

where $[B]^{-1}$ is that given by Eq. 13.13.

Considering the end-moments to be positive if clockwise and making use of symmetry of the member, the two fixed-end moments are related to the deflection by

$$M_{AB} = -M_{BA} = -EI \left(\frac{d^2 y}{dx^2} \right)_{x=0}$$

Differentiating twice Eq. 13.29 and substituting in the above equation, we obtain

$$M_{AB} = -M_{BA} = EI\left(\frac{u^2}{l^2}G_2 - \frac{q}{P}\right)$$

With G_2 from Eq. 13.30 substituted in the above equation, the fixed-end moments due to a uniform load on a member subjected to an axial compression are

$$M_{AB} = -M_{BA} = -ql^2\frac{1}{u^2}\left(1 - \frac{u}{2}\cot\frac{u}{2}\right) \tag{13.31}$$

If the axial force is tensile, the expression for fixed-end moments becomes

$$M_{AB} = -M_{BA} = -ql^2\frac{1}{u^2}\left(\frac{u}{2}\coth\frac{u}{2} - 1\right) \tag{13.32}$$

The fixed-end moments due to a uniform transverse load given by Eqs. 13.31 and 13.32 can be expressed in the form

$$M_{AB} = -M_{BA} = -\frac{EI}{2l(S+t)}ql^2 \tag{13.33}$$

where the values of S and t are determined as a function of $u = l\sqrt{P/(EI)}$ (P being the absolute value of the axial compressive or tensile force) by Eqs. 13.16 and 13.17, or by Eqs. 13.20 and 13.21, or by Table 13.1. When the axial force P vanishes, $u \to 0$, and Eqs. 13.31, 13.32, or 13.33 give $M_{AB} = -M_{BA} = -ql^2/12$.

13.7.2 Concentrated load

Consider the prismatic strut AB in Figure 13.3b carrying a transverse load W at a distance dl and bl from the left- and right-hand ends respectively. The strut can be treated as an assemblage of two members AC and CB with the two degrees of freedom indicated in Figure 13.3c, for which the stiffness matrix can be derived from the stiffness of the individual members (Eq. 13.19). Thus,

$$[S] = \begin{bmatrix} (S_d + S_b) & \text{symmetrical} \\ \left[\frac{(S_b + t_b)}{bl} - \frac{(S_d + t_d)}{dl}\right] & \left[\frac{(2S_d + t_d)}{d^2l^2} + \frac{(2S_b + t_b)}{b^2l^2} - \frac{P}{dbl}\right] \end{bmatrix}$$

where the subscripts d and b refer to members AC and BC respectively. The values of S and t for the two members are given by Eqs. 13.16 and 13.17, with du or bu in place of u.

The displacements at the two coordinates are given by

$$\begin{Bmatrix} D_1 \\ D_2 \end{Bmatrix} = [S]^{-1}\begin{Bmatrix} 0 \\ W \end{Bmatrix}$$

and the fixed-end moment at A (considered positive if clockwise) is given by

$$M_{AB} = t_d D_1 - (S_d + t_d)\frac{D_2}{dl}$$

Table 13.3 Influence Coefficient of the Fixed-end Moment M_{AB}* Due to a Unit Transverse Load on a Prismatic Beam Subjected to an Axial Force $M_{AB} = -$Coefficient $\times\, l$ (Refer to Figure 13.3b, Calculations by Eqs. 13.34 and 13.35)

Force P $u = l\sqrt{\frac{P}{EI}}$	Value of d										
	0	0.1	0.2	0.3	0.4	0.5	0.6	0.7	0.8	0.9	1.0
0	0	0.0810	0.1280	0.1470	0.1440	0.1250	0.0960	0.0630	0.0320	0.0090	0
Compressive											
1.0	0	0.0815	0.1294	0.1493	0.1467	0.1276	0.0981	0.0644	0.0327	0.0091	0
2.0	0	0.0831	0.1342	0.1569	0.1558	0.1365	0.1054	0.0692	0.0350	0.0097	0
3.0	0	0.0863	0.1438	0.1725	0.1747	0.1552	0.1208	0.0796	0.0402	0.0111	0
4.0	0	0.0922	0.1624	0.2037	0.2136	0.1946	0.1540	0.1022	0.0515	0.0141	0
5.0	0	0.1057	0.2070	0.2820	0.3150	0.3009	0.2459	0.1662	0.0843	0.0229	0
6.0	0	0.1943	0.5218	0.8689	1.1150	1.1750	1.0288	0.7282	0.3789	0.1039	0
Tensile											
1.0	0	0.0805	0.1265	0.1447	0.1413	0.1224	0.0939	0.0616	0.0313	0.0088	0
2.0	0	0.0791	0.1226	0.1386	0.1341	0.1155	0.0883	0.0579	0.0295	0.0083	0
3.0	0	0.0770	0.1168	0.1297	0.1239	0.1058	0.0806	0.0529	0.0271	0.0077	0
4.0	0	0.0745	0.1100	0.1196	0.1125	0.0951	0.0722	0.0474	0.0244	0.0070	0
5.0	0	0.0718	0.1029	0.1093	0.1012	0.0848	0.0641	0.0423	0.0220	0.0064	0
6.0	0	0.0690	0.0959	0.0996	0.0908	0.0754	0.0569	0.0377	0.0198	0.0059	0

*A fixed-end moment is positive when clockwise. To find the fixed-end moment at the right-hand end enter the value of b in lieu of d and change the sign of the moment. P is the absolute value of the axial compressive or tensile force.

The above procedure can also be followed for members subjected to axial tension. Thus, the fixed-end moment in member AB subjected to an axial compression (Figure 13.3b) is

$$M_{AB} = -Wl\frac{(bu\cos u - \sin u + \sin du + \sin bu - u\cos bu + du)}{u(2 - 2\cos u - u\sin u)} \tag{13.34}$$

and when the axial force P is tension,

$$M_{AB} = -Wl\frac{(bu\cosh u - \sinh u + \sinh du + \sinh bu - u\cosh bu + du)}{u(2 - 2\cosh u - u\sinh u)} \tag{13.35}$$

Equations 13.34 and 13.35 are used to calculate influence coefficients of the fixed-end moment M_{AB} in Table 13.3, by fixing a value for u and varying d (and $b = 1 - d$). The same table can be used for the fixed-end moments at the right-hand end M_{BA} by considering d in the table to represent b and changing the sign of the moment given.

13.8 Adjusted fixed-end moments for a prismatic member subjected to an axial force

With the end-moments M_{AB} and M_{BA} for a beam with two fixed ends subjected to an axial force (Figure 13.4a), we can derive the adjusted end-moments due to the same loading but with different end conditions. The parameters involved, in addition to M_{AB} and M_{BA}, are the end-rotational stiffness S and the carryover moment t. Following the same procedure as in Section 11.7, we obtain for the beam in Figure 13.4b, with a hinged end A, the end-moment at B.

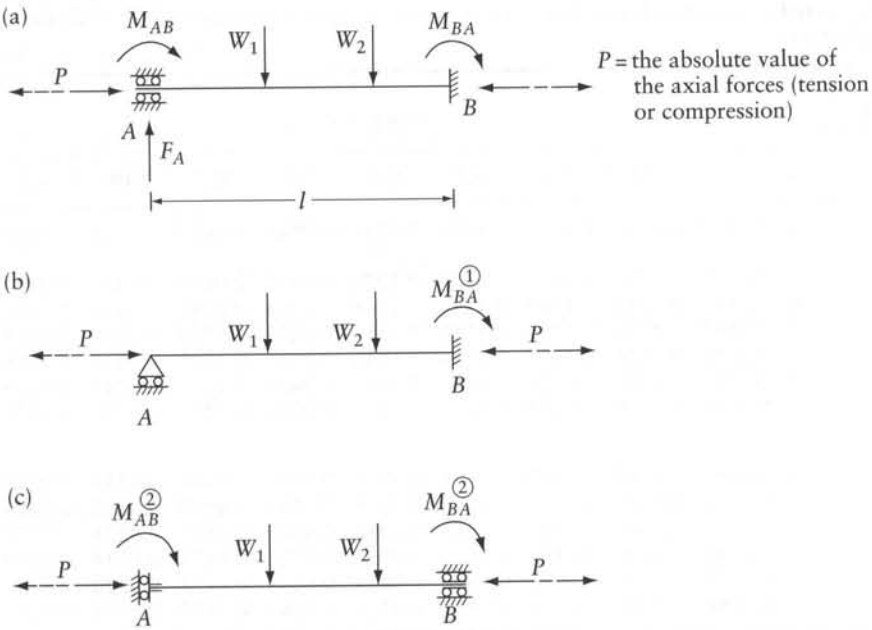

Figure 13.4 Adjusted fixed-end moments. (a) Rotation and translation in the transverse direction prevented at both ends. (b) Free rotation at A. (c) Vertical translation at A is allowed with no rotation.

$$M_{BA}^{①} = M_{BA} - CM_{AB} \tag{13.36}$$

where $C = t/S$. This equation is valid regardless of whether the axial force is compressive or tensile.

For the beam in Figure 13.4c, with translation of end A in the transverse direction allowed but rotation prevented, the end-moments are

$$M_{AB}^{②} = M_{AB} + F_A l \frac{(S+t)}{2(S+t) \pm Pl} \tag{13.37}$$

$$M_{BA}^{②} = M_{BA} + F_A l \frac{(S+t)}{2(S+t) \pm Pl} \tag{13.38}$$

where M_{AB}, M_{BA}, and F_A are the end-moments and reaction for the same beam but with the end condition of Figure 13.4a; the positive directions of these forces are indicated in the figure. The sign of the term Pl[that is, equal to $u^2(EI/l)$] in the denominator in the last two equations is plus when the axial force is tensile and minus when compressive.

Example 13.1: Plane frame without joint translations

Find the end-moments for the members in the frame of Figure 13.5a, taking into account the beam–column effect.

We assume approximate values of the axial forces in the members: $P_{AB} = P_{BC} = 5qb$ tensile, and $P_{BD} = 12.5qb$ compressive. The corresponding values of $u = l\sqrt{P/(EI)}$ are: $u_{AB} = u_{BC} = 1.41$, and $u_{BD} = 2.53$.

(a)

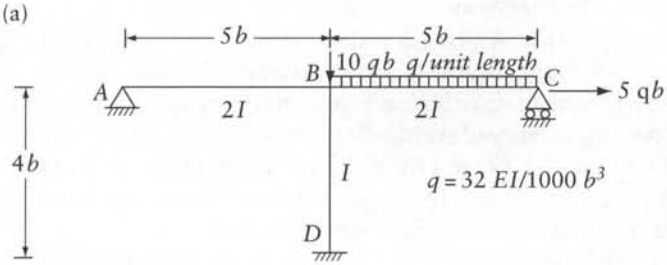

(b)

End	BA	BD	BC
DFs	0.39	0.22	0.39
FEMs			−295
Distribution	115	65	115
Final moments	115	65	−180

Multiplier : $qb^2/100$

COF $C_{BD} = 0.74$ $M_{DB} = 0.74 \times 65 = 48$

Figure 13.5 Analysis of the frame of Example 13.1 by moment distribution taking into account the beam– column effect. (a) Frame properties and loading. (b) Moment distribution.

From Eqs. 13.20 and 13.21, or from Table 13.1, we find for members AB and BC: $S = 4.26(EI/l)$; $t = 1.94(EI/l)$; and $C = t/S = 0.46$.

Similarly, from Eqs. 13.16 and 13.17, or from Table 13.1, the values of S and t for member BD are: $S = 3.06(EI/l)$, $t = 2.26(EI/l)$, and $C = t/S = 0.74$.

The adjusted rotational stiffness of end B of members BA and BC, to account for the hinged ends at A and C, is (from Eq. 13.24) $S_{BA} = S_{BC} = S(1 - C^2) = 3.36EI/l$.

We now substitute the relative values of EI/l for the individual members in the above expressions, then calculate the distribution factors in the usual way (Figure 13.5b).

From Eq. 13.36, the fixed-end moment is $M_{BC}^{①} = M_{BC} - CM_{CB}$, where M_{BC} and M_{CB} are the end-moments when both B and C are encastré. Using Eq. 13.33,

$$M_{BC} = -M_{CB} = -\frac{EI}{2l(S+t)}ql^2 = -\frac{ql^2}{2(4.26+1.94)}$$

$$= -0.081ql^2 = -2.02qb^2$$

Thus, the adjusted fixed-end moment is

$$M_{BC}^{①} = -(2.02 + 0.46 \times 2.02)qb^2 = -2.95qb^2$$

The moment distribution is carried out in the usual way in Figure 13.5b, and the end-moments thus obtained are (in terms of $qb^2/100$): $M_{BA} = 115$, $M_{BC} = -180$, $M_{BD} = 65$, and $M_{DB} = 48$.

More accurate values of the axial forces can now be determined and the above calculations may be repeated. It is clear, however, that in this example no appreciable change in values will result.

Example 13.2: Plane frame with sidesway

Solve Example 13.1 with the support at A being a roller instead of a hinge, but for the loading being that in Figure 13.6a. Note also the change in relative I values.

A solution can be obtained by moment distribution similar to the procedure followed in Example 13.1, but the adjusted end-rotational stiffness and the carryover factor have to be calculated for BD by Eqs. 13.27 and 13.28, and the fixed-end moments for ends BD and DB have to be determined by Eqs. 13.37 and 13.38. This solution is not given here, but instead we analyze the structure by the general displacement method.

The approximate values of the axial forces are: $P_{AB} = 0$, $P_{BC} = 0.05qb$ tensile, and $P_{BD} = 7qb$ compressive; the corresponding u values are: $u_{AB} = 0$, $u_{BC} \simeq 0$, and $u_{BD} = 1.34$. For member BD, $S = 3.75EI/l$ and $t = 2.06EI/l$. With these values, the end-forces corresponding to unit end displacements can be calculated using Table 13.2.

The stiffness matrix of the structure corresponding to the coordinates 1 and 2 in Figure 13.6b is

$$[S] = \begin{bmatrix} 3\left(\frac{EI}{l}\right)_{BA} + 3\left(\frac{EI}{l}\right)_{BC} + 3.75\left(\frac{EI}{l}\right)_{BD} & \text{symmetrical} \\ -(3.75+2.06)\left(\frac{EI}{l^2}\right)_{BD} & 2(3.75+2.06)\left(\frac{EI}{l^3}\right)_{BD} - \left(\frac{P}{l}\right)_{BD} \end{bmatrix}$$

The fixed-end moments at end B of members BA, BC, BD, and DB are $2.5qb^2$, $-3.125qb^2$, 0 and 0 respectively. The restraining forces at coordinates 1 and 2 to prevent displacements at B are

$$\{F\} = \begin{Bmatrix} -0.625qb^2 \\ -0.05qb \end{Bmatrix}$$

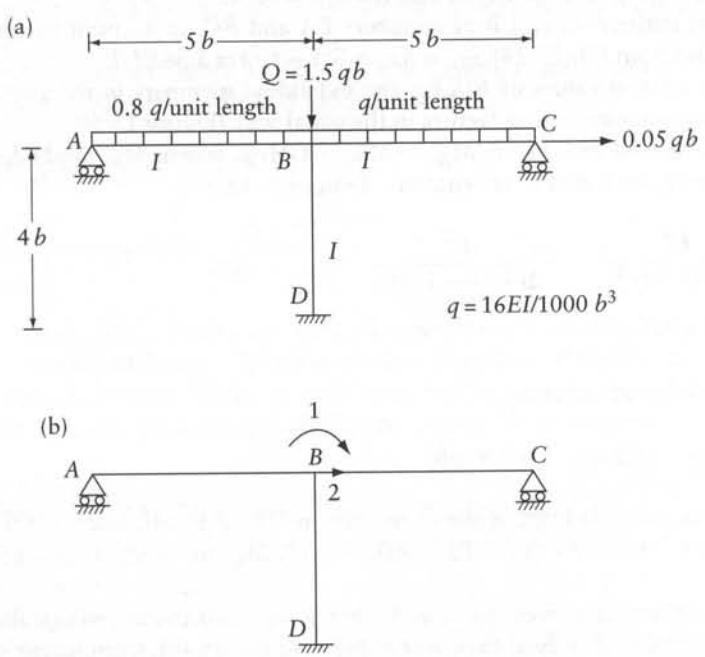

Figure 13.6 Analysis of the frame of Example 13.2 by the general displacement method taking into account the beam–column effect. (a) Frame properties and loading. (b) Coordinate system.

The displacements at the coordinates are given by Eq. 5.3.

$$\{D\} = [S]^{-1}\{-F\}$$

Substituting the values of I, l, and $P(= u^2[EI/l^2])$ into $[S]$ and inverting it, then substituting in Eq. 5.3, we obtain

$$\{D\} = \frac{qb^2}{EI}\begin{Bmatrix} 0.58 \\ 1.71b \end{Bmatrix}$$

The end-moments M_{BA}, M_{BC}, M_{BD}, and M_{DB} are then determined by Eq. 5.5:

$$\{A\} = \{A_r\} + [A_u]\{D\}$$

$$\begin{Bmatrix} M_{BA} \\ M_{BC} \\ M_{BD} \\ M_{DB} \end{Bmatrix} = qb^2 \begin{Bmatrix} 2.50 \\ -3.125 \\ 0 \\ 0 \end{Bmatrix} + \left[\begin{array}{c|c} 3.00\left(\frac{EI}{l}\right)_{BA} & 0 \\ 3.00\left(\frac{EI}{l}\right)_{BC} & 0 \\ 3.75\left(\frac{EI}{l}\right)_{BD} & -(3.75+2.06)\left(\frac{EI}{l^2}\right)_{BD} \\ 2.06\left(\frac{EI}{l}\right)_{DB} & -(3.75+2.06)\left(\frac{EI}{l^2}\right)_{DB} \end{array}\right] \{D\}$$

Substituting for $\{D\}$, the final end-moments are obtained

$$\begin{Bmatrix} M_{BA} \\ M_{BC} \\ M_{BD} \\ M_{DB} \end{Bmatrix} = \frac{qb^2}{100}\begin{Bmatrix} 285 \\ -277 \\ -8 \\ -32 \end{Bmatrix}$$

13.9 Elastic stability of frames

In design based on a definite load factor, failure loads must be known. Broadly speaking, failure can occur by yielding of the material at a sufficient number of locations to form a mechanism (see Chapters 18 and 19) or by buckling due to axial compression without the stresses exceeding the elastic limit.

Buckling of individual members was considered in Section 13.3. In the present section, we shall deal with buckling of rigidly jointed plane frames in which the members are subjected to axial forces only.

Consider a plane frame subjected to a system of forces $\{Q\}$ (Figure 13.7a) causing axial compression in some of the members. The buckling, or critical, loading $\alpha\{Q\}$ is defined by the value of the scalar α at which the structure can be given small displacements without application of disturbing forces. In other words, when the buckling loading $\alpha\{Q\}$ acts, it is possible to maintain the structure in a displaced configuration without additional loading, as shown in Figure 13.7b.

If, for the frame considered, an estimate is made of the value of α and the corresponding values of the axial forces $\{P(\alpha)\}$ are computed, it becomes possible to find the stiffness matrix $[S(\alpha)]$ of the structure corresponding to any chosen coordinate system. The elements of this matrix are

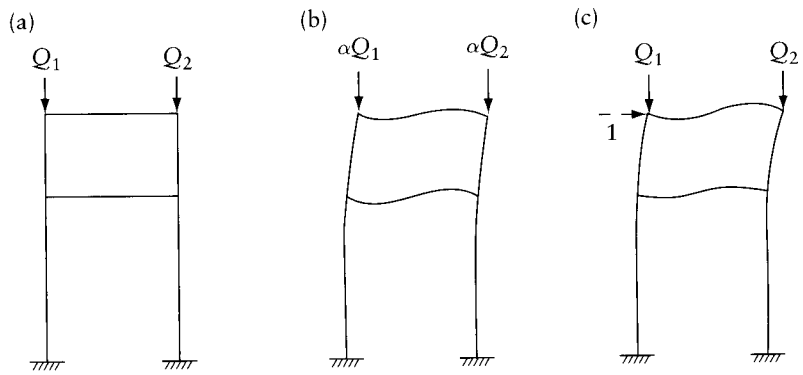

Figure 13.7 Buckling of a plane frame.

functions of the value α. Any system of forces $\{F\}$ and displacements $\{D\}$ at the coordinates are related by the equation

$$[S(\alpha)]\{D\} = \{F\}$$

If α corresponds to the critical buckling value, then it is possible to let the structure acquire some small displacements $\{\delta D\}$ without application of forces, and the last equation thus becomes

$$[S(\alpha)]\{\delta D\} = \{0\}$$

For a nontrivial solution to exist, the stiffness matrix $[S(\alpha)]$ must be singular – that is, the determinant

$$|S(\alpha)| = 0 \tag{13.39}$$

The collapse loading is that which has the smallest value of α which satisfies Eq. 13.39. In general, there is more than one value of α which satisfies this equation, and each value has associated with it values of $\{\delta D\}$ of arbitrary magnitude but in definite proportions defining an associated critical mode.

To solve Eq. 13.39 for α, the value of the determinant is calculated for a set of values of α, and the value corresponding to a zero value of the determinant is obtained by interpolation. Once α has been calculated, the associated displacement vector, if required, can be obtained in a way similar to that used in the calculation of eigenvectors in Section A.3 of Appendix A.

The above procedure may involve a large amount of numerical work so that access to a computer is necessary. However, in most structures, it is possible to guess the form of the critical mode associated with the lowest critical load. For example, it can be assumed that when the buckling load is reached in the frame of Figure 13.7a, a small disturbing force at coordinate 1 will cause buckling in sidesway (Figure 13.7c). At this stage, the force at 1 required to produce a displacement at this coordinate is zero, that is $S_{11} = 0$. This condition can be used to determine the critical load. A value of α lower than the critical value is estimated and the stiffness coefficient $S_{11}(\alpha)$ corresponding to coordinate 1 is determined. As α is increased the value of S_{11} decreases and it vanishes when the critical value of α is attained. If a set of values of α is assumed and plotted against S_{11}, the value of α corresponding to $S_{11} = 0$ can be readily determined.

The critical buckling loads for a straight prismatic member with various end conditions are given in Figure 13.8. These may be used to establish lower and upper bounds to the buckling load of a frame and hence are of help in estimating the approximate values of α.

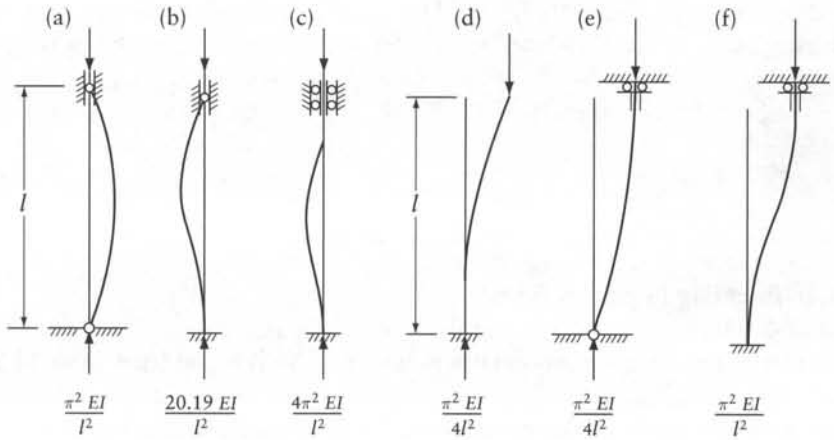

Figure 13.8 Critical buckling load for a prismatic member.

Example 13.3: Column buckling in plane frame

Find the value of the force Q at B which causes buckling of the frame of Example 13.2 (Figure 13.6a). The frame is not subjected to loads other than the force Q.

Let $Q=\alpha$. The axial forces in the members are $P_{BA}=P_{BC}=0$ and $P_{BD}=\alpha$, compressive. The stiffness matrix of the frame corresponding to the coordinates in Figure 13.6b, expressed as function of α, is

$$[S(\alpha)]=\begin{bmatrix} 3\left(\frac{EI}{l}\right)_{BA}+3\left(\frac{EI}{l}\right)_{BC}+S_{BD} & \text{symmetrical} \\ -(S_{BD}+t_{BD})/l_{BD} & \frac{2(S_{BD}+t_{BD})}{l_{BD}^2}-\frac{\alpha}{l_{BD}} \end{bmatrix} \tag{a}$$

where S_{BD} and t_{BD} are functions of α to be calculated by Eqs. 13.16 and 13.17 or from Table 13.1.

When α corresponds to the buckling load, the determinant $|S(\alpha)|=0$, so that

$$\text{determinant}=S_{11}S_{22}-S_{21}^2 \tag{b}$$

where S_{ij} are elements of the stiffness matrix in Eq. (a).

Upper and lower bounds of the critical load are established if we consider that the rotation at end B of BD is partially restrained. Thus, the buckling load for BD is some value between $\pi^2EI/(4l^2)=0.154EI/b^2$ and $\pi^2EI/l^2=0.617EI/b^2$, corresponding to the conditions in Figures 13.8d and f respectively. As a first trial, let us take the average value between these two bounds, that is $\alpha=0.386EI/b^2$. The corresponding value of the determinant in Eq. (b) is 0.0279 $(EI)^2/b^4$. In the second trial, we take $\alpha=0.5EI/b^2$, giving a value of $-0.0354(EI)^2/b^4$ for the determinant. By linear interpolation, we choose for the third trial

$$\alpha=\left[0.386+\frac{(0.5-0.386)\ 0.0279}{0.0279+0.0354}\right]\frac{EI}{b^2}=0.436\frac{EI}{b^2}$$

for which the determinant is $-0.0004(EI)^2/b^4$. This value is negligible compared with the preceding values; thus, $\alpha = 0.436EI/b^2$ can be considered as the buckling value. Therefore, the critical load is

$$Q_{cr} = 0.436\frac{EI}{b^2}$$

Example 13.4: Buckling in portal frame

Find the value of Q which causes buckling of the frame in Figure 13.9a.

The stiffness matrix for the three coordinates in Figure 13.9b is found from Table 13.2:

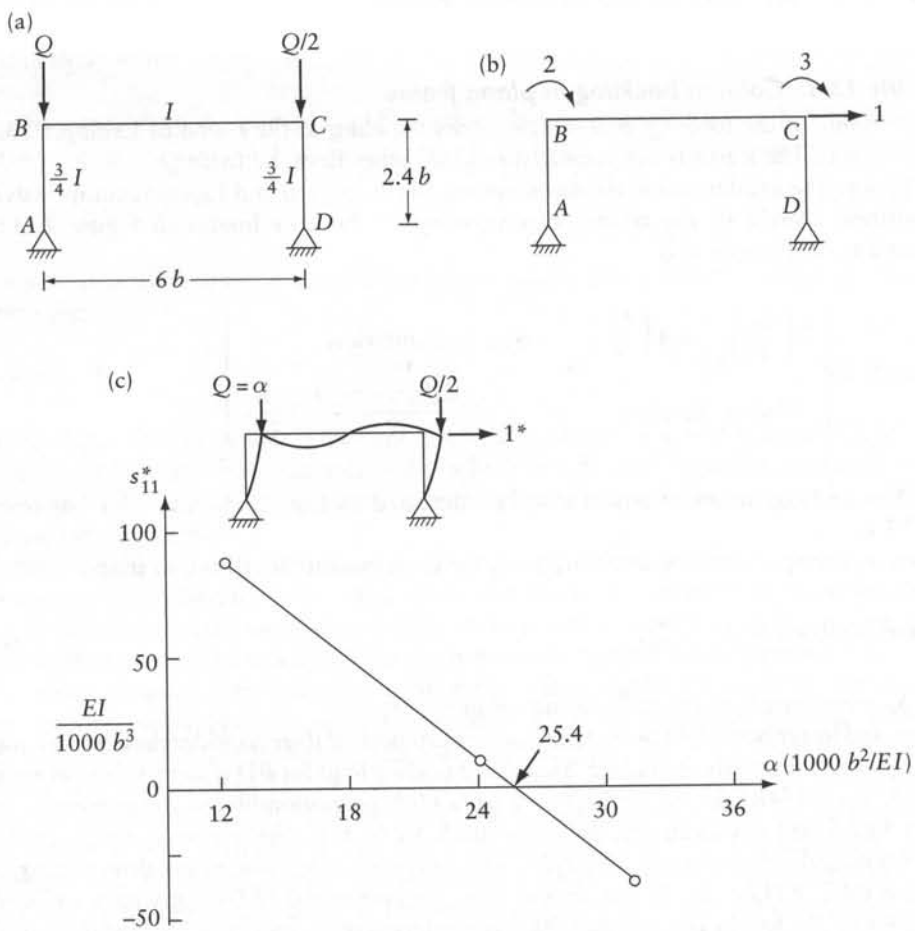

Figure 13.9 Determination of the critical load on the frame of Example 13.4 by consideration of stiffness reduction. (a) Frame dimensions and loading. (b) Coordinate system; the corresponding stiffness matrix in presence of the Q and $Q/2$ forces is given in Eq. (a). (c) Variation of stiffness S^*_{11} with α.

$$[S]=\left[\begin{array}{c|c|c} \left(\frac{S-t^2/S-u^2EI/l}{l^2}\right)_{BA}+\left(\frac{S-t^2/S-u^2EI/l}{l^2}\right)_{CD} & \text{symmetrical} & \\ \hline -\left(\frac{S-t^2/S}{l}\right)_{BA} & (S-t^2/S)_{BA}+4\left(\frac{EI}{l}\right)_{BC} & \\ \hline -\left(\frac{S-t^2/S}{l}\right)_{CD} & 2\left(\frac{EI}{l}\right)_{BC} & (S-t^2/S)_{CD}+4\left(\frac{EI}{l}\right)_{BC} \end{array}\right] \quad \text{(a)}$$

The lowest buckling load for this frame corresponds to a sidesway by a small disturbing force at coordinate 1. It can be shown that the stiffness S_{11}^* corresponding to coordinate 1* (Figure 13.9c) is given by (see Section 6.5, Eq. 6.18):

$$S_{11}^* = S_{11} - \frac{S_{21}^2 S_{33} - 2S_{21}S_{31}S_{32} + S_{31}^2 S_{22}}{(S_{22}S_{33} - S_{32}^2)} \tag{13.40}$$

where S_{ij} are elements of the matrix in Eq. (a). Equation 13.40 can, in fact, be used for condensation of any 3 × 3 stiffness matrix when the forces at coordinates 2 and 3 are zero.

Let the buckling load occur when $Q = \alpha$. Considering that the rotation of end C of member CD is partially restrained, it can be concluded that the buckling load is lower than the value $(\pi^2 EI/4l^2)_{BA}$ which corresponds to the conditions in Figure 13.8e. Thus, an upper bound for α is

$$\alpha < \left(\frac{\pi^2 EI}{4l^2}\right)_{BA} = 0.32\frac{EI}{b^2}; \quad Q < 0.32\frac{EI}{b^2}$$

The values of α are assumed, the corresponding u values for BA and CD are determined, and the corresponding S and t values are taken from Table 13.1:

$\alpha(b^2/EI)$	u_{BA}	$\frac{S_{BA}}{(EI/l)_{BA}}$	$\frac{t_{BA}}{(EI/l)_{BA}}$	u_{CD}	$\frac{S_{CD}}{(EI/l)_{CD}}$	$\frac{t_{CD}}{(EI/l)_{CD}}$
0.12	0.960	3.876	2.031	0.679	3.938	2.015
0.24	1.357	3.747	2.066	0.960	3.876	2.031
0.31	1.543	3.672	2.086	1.091	3.839	2.041

Substituting into Eqs. (a) and 13.40, we obtain the following value of S_{11}^*:

$\alpha(b^2/EI)$	$S_{11}^*(b^3/EI)$
0.12	0.0888
0.24	0.0092
0.31	−0.0376

The above values are plotted in Figure 13.9c from which it is seen that $S_{11}^* = 0$ when $\alpha = 0.254EI/b^2$. Thus, the buckling load $Q_{cr} = 0.254EI/b^2$.

13.10 Calculation of buckling load for frames by moment distribution

We shall first consider frames without sidesway, and then adapt the method to the case when sidesway is possible. The critical buckling load of frames with no joint translation may be determined by examining the convergence of moment distribution. Consider the frame in Figure 13.10a, for which the critical value of the force Q is required. We assume a value for Q, and determine the end-rotational stiffness of the members and the carryover factors. We now assume an arbitrary disturbing moment at one (or more) joint and carry out the moment distribution. The significance of the operation lies in the fact that the behavior under moment distribution depends on the magnitude of the load relative to its critical value. Specifically, as the load is increased to approach the critical value, the final moments approach positive or negative infinity, whereas if the load is less than the critical load the results converge, that is, the moments become smaller after each cycle of moment distribution and finite values of the end-moments can be reached.

(a)

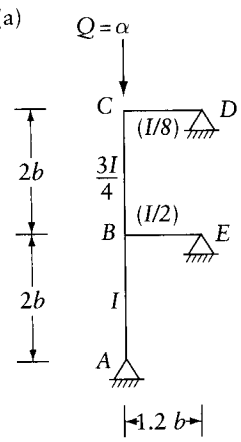

(b)

α	Joint	B				C		Remarks
	End	BA	BE	BC		CB	CD	
$\frac{2.7EI}{b^2}$	DFs	−0.16	0.79	0.37	1.83	0.65	0.35	$\frac{80.6}{100} < 1.00$
	COFs				⟷			
	Apply a clockwise moment = 100 at B							
	Distribution	−16.0	79.0	37.0	⟶	67.7		$\therefore \alpha_{cr} > \frac{2.7EI}{b^2}$
	CO			−80.6	⟵	−44.0		
$\frac{2.9EI}{b^2}$	DFs	−0.41	1.01	0.40	2.27	0.61	0.39	$\frac{125.6}{100} > 1.00$
	COFs				⟷			
	Apply a clockwise moment = 100 at B							
		−41.0	101.0	40.0	⟶	90.8		$\therefore \alpha_{cr} < \frac{2.9EI}{b^2}$
				−125.6	⟵	−55.3		
$\frac{2.8EI}{b^2}$	DFs	−0.27	0.89	0.38	2.02	0.63	0.37	$\frac{97.7}{100} \approx 1.00$
	COFs				⟷			
	Apply a clockwise moment = 100 k ft at B							
		27.0	89.0	38.0	⟶	76.8		$\therefore \alpha_{cr} = \frac{2.8EI}{b^2}$
				−97.7	⟵	−48.4		

Figure 13.10 Calculation of the critical buckling load for Example 13.5. (a) Frame dimensions and loading. (b) Moment distribution.

When the assumed load is only slightly below the critical load, the results converge slowly, and, as already stated, above the critical load the results diverge. Therefore, to find the critical load, it is not necessary to continue the moment distribution for a great many cycles: if, after one cycle, it is seen that the moments converge, then the load chosen is smaller than the critical load.

Example 13.5: Buckling in a frame without joint translations

Using moment distribution, find the value of Q which will cause buckling of the frame in Figure 13.10a.

First, the upper and lower bounds of the critical load $Q_{cr} = \alpha$ have to be established. Member AB can rotate freely at its bottom end while the rotation at the top end is partially restrained. Therefore, the buckling load for this member has a value lying between the critical loads for the conditions shown in Figures 13.8a and b. Thus,

$$\left(\frac{\pi^2 EI}{l^2}\right)_{AB} < Q_{cr} < 20.19\left(\frac{EI}{l^2}\right)_{AB}$$

or

$$2.47\frac{EI}{b^2} < Q_{cr} < 5.05\frac{EI}{b^2}$$

Consider now the member BC. The rotation at both ends is restrained so that the buckling load for BC lies between the critical loads for the conditions in Figures 13.8a and c. Therefore,

$$\left(\frac{\pi^2 EI}{l^2}\right)_{BC} < Q_{cr} < \left(\frac{4\pi^2 EI}{l^2}\right)_{BC}$$

$$1.85\frac{EI}{b^2} < Q_{cr} < 7.40\frac{EI}{b^2}$$

Hence, α lies between $1.85EI/b^2$ and $5.05EI/b^2$. For the first trial, take $\alpha = 3.6EI/b^2$; the values of u, S, and t are, respectively, $3.79, 1.56(EI/l)_{AB}$, and $2.83(EI/l)_{AB}$, for AB, and $4.38, 0.32(EI/l)_{BC}$, and $3.43(EI/l)_{BC}$, for BC. The rotational stiffnesses of the member ends meeting at joint B are (Eq. 13.24)

$$S_{BA} = \frac{EI}{2b}\left(1.56 - \frac{2.83^2}{1.56}\right) = -1.79EI/b$$

$$S_{BC} = \frac{E(0.75)I}{2b} \times 0.32 \quad = 0.12EI/b$$

$$S_{BE} = \frac{3.0E(0.5)I}{1.2b} \quad = 1.25EI/b$$

$$\text{Sum} = -0.42EI/b$$

The sum of the rotational stiffnesses of the ends meeting at B is negative, indicating that even with the top end of member BC totally fixed, the assumed value of α is greater than the critical value.

For a second trial, take $\alpha = 2.7EI/b^2$; the corresponding end-rotational stiffness and carryover moments are calculated as before. The corresponding distributing and carryover

factors are given in Figure 13.10b. A disturbing clockwise moment of 100 is applied at joint B, an appropriate moment is carried over to joint C, joint C is balanced, and a moment of −80.6 is carried back to joint B, thus ending the first cycle. If a second cycle of distribution were to be performed, it would begin by the distribution of a balancing moment of +80.6, which is less than the starting moment of 100. It is clear, therefore, that the calculation converges, indicating that the critical load has not been reached.

Two additional trials are shown in Figure 13.10b from which we conclude that the critical load is $Q_{cr} = 2.8EI/b^2$.

Let us now consider frames with sidesway. The value of Q which causes buckling of the frame in Figure 13.9a can be obtained by moment distribution. The approach is similar to that followed in Example 13.4 in that we seek the value of Q such that sidesway can be produced without a horizontal force at the level of BC ($F_1^* = 0$ in Figure 13.9c).

The procedure is to assume a value *of* Q, then introduce a unit sidesway at the level of BC; the member end-moments are determined by moment distribution and the force F_1^* is found by static equilibrium. If F_1^* is positive, the frame is stable and the value of Q is less than the critical load. The calculation is repeated with new values of Q until F_1^* reaches a zero value.

13.11 General

By inspection of the numerical values of S and t in Table 13.1, we can see that the stiffness of a member is appreciably affected by an axial force P only when $u = l\sqrt{P/(EI)}$ is relatively large, say 1.5. However, a lower value of u appreciably changes the shear required to produce a unit translation. For example, if the axial force is compressive, the element S_{11} of the stiffness matrix in Eq. 13.19 (see also Table 13.2, case (a))

$$S_{11} = \frac{2(S+t)}{l^2} - \frac{P}{l} = \frac{2(S+t)}{l^2} - \frac{u^2 EI}{l^3}$$

is equal to $10.8\,EI/l^3$ when $u = 1$. The value of S_{11} is $12EI/l^3$ when the axial force vanishes.

In the plane structures considered in this chapter, the deflections and bending moments are assumed to be in the plane of the structure, while displacements normal to this plane are assumed to be prevented. For space structures, similar methods of analysis can be developed but they become complicated by the possibility of torsional-flexural buckling.

When the axial force is compressive and the value of P is the critical buckling load, the force required to produce a unit displacement at a coordinate becomes zero. Thus, when $S_{11} = 0$ in the stiffness matrix of Eq. 13.14, the value of the axial load is the critical buckling value for a strut with the displacement at coordinate 1 (Figure 13.1b) allowed to take place freely, while the displacements at the coordinates 2, 3, and 4 are restrained. Similarly, $S_{22} = 0$ corresponds to a critical buckling load of a strut when D_2 is free to occur while $D_1 = D_4 = D_4 = 0$. At higher values of the axial loads, the elements on the diagonal of $[S]$ become negative which means that a restraining force is necessary to limit the displacement to unity at one of the coordinates.

The force or displacement methods of analysis for linear structures can be used for structures in which the axial forces in the members affect their stiffness, provided that a set of axial forces is assumed to be present in the members in all the steps of the calculations. These forces are regarded as known parameters of the members, just like E, I, and l. Tables 13.1 and 13.2 based on a dimensionless parameter can be used for the calculation of the stiffness of prismatic members subjected to axial forces.

If, after carrying out the analysis, the axial forces determined by considering the static equilibrium of the members differ from the assumed values, revised values of the member stiffnesses or flexibilities based on the new axial forces have to be used, and the analysis is repeated. However, the repetition is usually unnecessary, as in most practical problems a reasonably accurate estimate of the axial forces in the members can be made. If a computer is used, the calculation may be repeated until the assumed and calculated axial forces agree to any desired degree.

Buckling of frames subjected to forces acting at joints only, causing axial compressive forces in the members, can be treated by a trial-and-error approach seeking the lowest load that leads to divergent moment distribution or to a singular stiffness matrix. A transverse load within the length of a member can be replaced by statically equivalent concentrated loads at the joints. The critical load thus obtained is slightly higher than that obtained from a more accurate analysis in which account is taken of the bending moment produced by the load acting at intermediate points.

Transverse deflection of a straight member subjected to a large axial force produces bending moment, which is considered in the analysis presented in this chapter. The transverse deflection also produces a change in member length, which is ignored here as is generally done in linear analysis. Considering this effect requires nonlinear analysis, discussed in Chapter 23. Nevertheless, the quasi-linear analysis discussed in the present chapter is sufficiently accurate for many practical applications.

Problems

13.1 or 13.2

Determine the end-moments in the frame shown in the figure, taking into account the change in length of members and the beam–column effect.

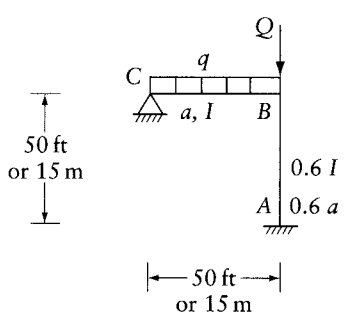

Imperial units, Prob. 13.1:
$Q = 200$ k; $q = 2$ k/ft;
$a = 25$ in^2; $I = 1000$ in^4,
$E = 30{,}000$ k/in^2

SI units, Prob. 13.2:
$Q = 900$ kN; $q = 30$ kN/m;
$a = 16 \times 10^3$ mm^2; $I = 400 \times 10^6$ mm^4;
$E = 200$ GPa

Prob. 13.1 or *13.2*

13.3 or 13.4

Apply the requirements of Prob. 13.1 to the frame shown.

13.5 Apply the requirements of Prob. 13.1 to the frame shown. Assume $Q = 5EI/l^2$; $al^2/I = 40{,}000$.

13.6 Prove Eqs. 13.27 and 13.28.

13.7 Verify the critical buckling loads given in Figure 13.8 for a prismatic member with different end conditions. *Hint:* Determine S_{11} corresponding to a rotational or a translational coordinate 1, and verify that $S_{11} = 0$, assuming that the member is subjected to an axial compressive force equal to the critical value given in the figure.

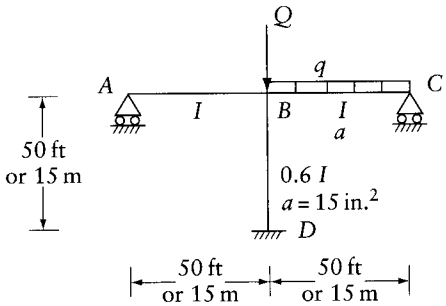

Imperial units, Prob. 13.3:
$Q = 150$ k; $q = 0.2$ k/ft;
$a = 15$ in^2; $I = 1000$ in^4;
$E = 30{,}000$ k/in^2

SI units, Prob. 13.4:
$Q = 675$ kN; $q = 3.0$ kN/m;
$a = 10 \times 10^3$ mm^2; $I = 400 \times 10^6$ mm^4;
$E = 200$ GPa

Prob. 13.3 or *13.4*

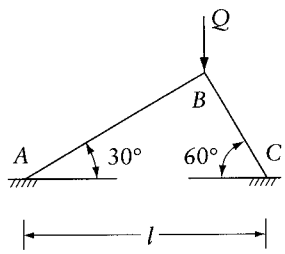

Constant section
of area a and
flexural rigidity EI

Prob. 13.5

13.8 Obtain the bending moment diagram for beam ABC shown in the figure. The beam is fixed at A, on a roller at C and on a spring support of stiffness $= 3EI/l^3$ at B.

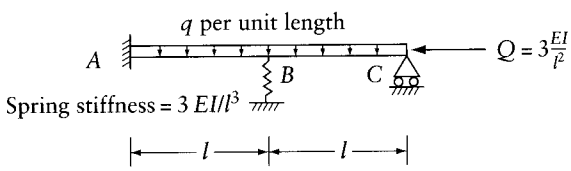

Prob. 13.8

13.9 Solve Example 13.3, with the roller support at C changed to a hinged support.

13.10 Find the value of the force Q which causes buckling of the frame of Prob. 13.5. Assume $I_{AB} = 1.73 I_{BC}$. Ignore axial deformations.

13.11 Find the value of Q which causes buckling of the beam in Prob. 13.8. The beam is not subjected to distributed loads in this case.

13.12 Show that the critical load Q associated with sidesway mode for the frame in the figure is given by the equation

$$(S+t)^2 = \left(S + 6\frac{EI_1}{l}\right)(2S + 2t - Qh)$$

where S and t are respectively the end-rotational stiffness and carryover moment for BA (S and t are defined in Figure 13.2).

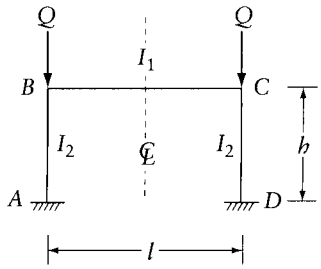

Prob. 13.12

13.13 Solve Example 13.4 by moment distribution.

13.14 Determine the value of Q which causes instability of the structure shown in the figure. Assume E = constant.

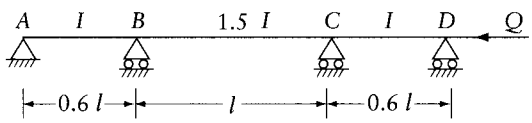

Prob. 13.14

13.15 Apply the requirements of Prob. 13.14 to the structure shown.

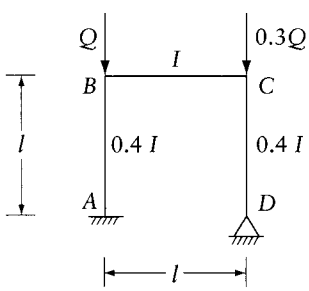

Prob. 13.15

13.16 Derive the stiffness matrix for the member in Figure 13.1b when $P=0$ (Eq. 5.7), following the procedure employed to derive Eq. 13.14. The solution of the differential Eq. 13.1 governing the deflection when P and q are zero is: $y = A_1 + A_2x + A_3x^2 + A_4x^3$.

Chapter 14

Analysis of shear-wall structures

14.1 Introduction

In high-rise buildings, it is important to ensure adequate stiffness to resist lateral forces induced by wind, or seismic or blast effects. These forces can develop high stresses, and produce sway movement or vibration, thereby causing discomfort to the occupants. Concrete walls, which have high in-plane stiffness, placed at convenient locations, are often economically used to provide the necessary resistance to horizontal forces. This type of wall is called a shear wall. The walls may be placed in the form of assemblies surrounding lift shafts or stair wells; this box-type structure is efficient in resisting horizontal forces. Columns, of course, also resist horizontal forces, their contribution depending on their stiffness relative to the shear walls. The object of the analysis for horizontal forces is to determine in what proportion are the external loads at each floor level distributed among shear walls and the columns.

The horizontal forces are usually assumed to act at floor levels. The stiffness of the floors in the horizontal direction is very large compared with the stiffness of shear walls or columns. For this reason, it is common to assume that each floor diaphragm is displaced in its horizontal plane as a rigid body. This rigid-body movement can be defined by translations along horizontal perpendicular axes and a rotation about a vertical axis at an arbitrary point in the floor (Figure 14.1c).

The assumption of rigid-body in-plane behavior is important in that it reduces considerably the degree of kinematic indeterminacy. However, even so, the analysis of the general case as a three-dimensional structure represents a complex problem, and further assumptions are usually made in order to produce an analysis at a reasonable cost and in moderate time. These assumptions differ with the chosen method of analysis or the type of structure, but the assumption that the floor diaphragms are rigid in their own plane is generally accepted.[1]

A major simplification of the problem is achieved if the analysis can be limited to a plane structure composed of shear walls and frames subjected to horizontal forces in their plane. This is possible when the building is laid out in a symmetrical rectangular grid pattern, so that the structure can be assumed to be made up of two sets of parallel frames acting in perpendicular directions (Figure 14.1b). Very often, even in an irregular building, an idealized plane structure is used to obtain an approximate solution. The majority of published papers on the analysis of shear-wall structures deal with this type of two-dimensional problems.

The unsymmetrical arrangement of shear walls in the building in Figure 14.1c causes the diaphragms to rotate and translate under the action of symmetrical horizontal forces. The shear

1 For further reading on analysis of shear-wall structures and an extensive list of references, see Smith, B. S. and Coull, A., *Tall Building Structures: Analysis and Design*, J. Wiley & Sons, New York, 1991, 537 pp.

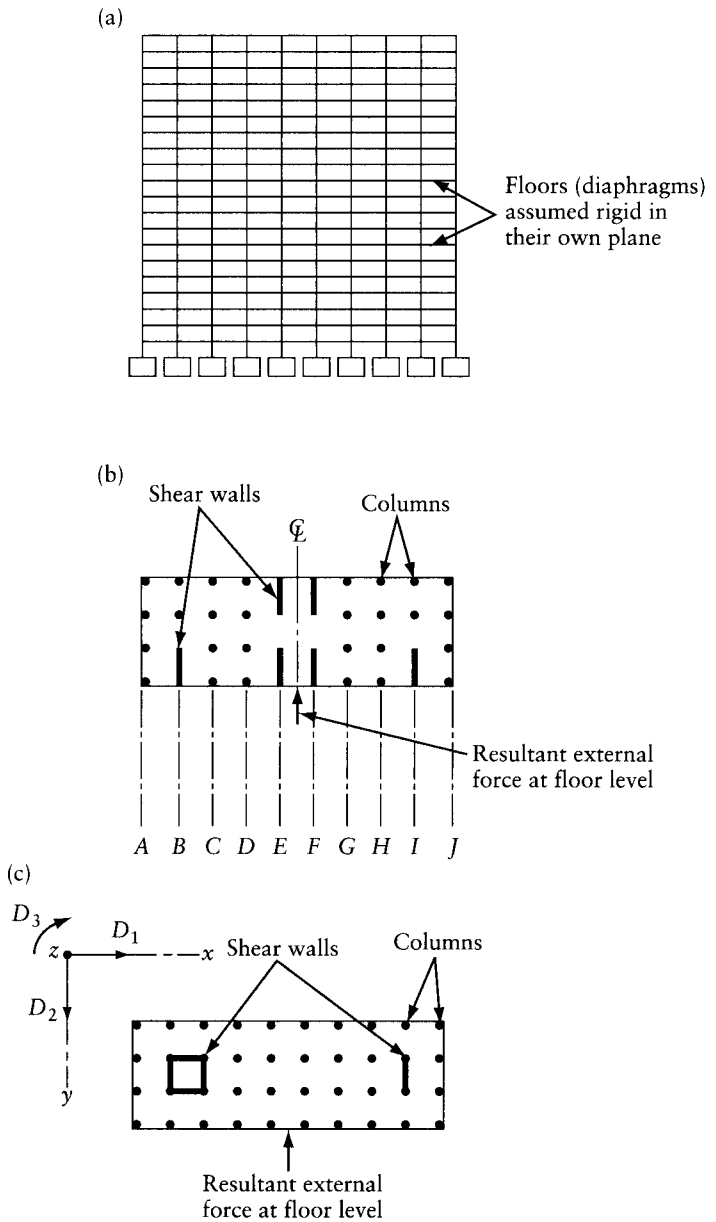

Figure 14.1 Illustration of shear walls and some assumptions involved in their analysis. (a) Elevation of a multistorey structure. (b) Plan for a regular symmetric building. (c) Plan of unsymmetrical building (rigid-body translation of the floor is defined by displacements at the coordinates D_1, D_2, and D_3).

walls in this case are subjected to twisting moments which cannot be calculated if the analysis is limited to an idealized plane structure.

In the following sections, the analysis of an idealized plane shear-wall structure is treated on the basis of certain simplifying assumptions. The three-dimensional problem is also considered, including further simplifying assumptions.

14.2 Stiffness of a shear-wall element

In the analysis to follow, we shall treat shear walls as vertical deep beams transmitting loads to the foundations. The effect of shear deformations in these walls is of greater importance than in conventional beams, where the span–depth ratio is much larger. The stiffness matrix of an element of a shear wall between two adjacent floors (Figure 14.2a) will now be derived, shear deformation being taken into consideration.

Consider the cantilever AB in Figure 14.2b. The flexibility matrix corresponding to the two coordinates indicated at A is

$$[f] = \begin{bmatrix} \dfrac{h}{EI} & \text{symmetrical} \\ \dfrac{h^2}{2EI} & \left(\dfrac{h^3}{3EI} + \dfrac{h}{Ga_r}\right) \end{bmatrix} \tag{14.1}$$

The term h/Ga_r is the shear deflection at A due to a unit transverse load at A, with the notation: G is the shear modulus of elasticity, a_r is the effective shear area (see Section 7.3.3), and h is the floor height.

The stiffness matrix corresponding to the coordinates in Figure 14.2b is obtained by inverting $[f]$. Thus,

$$[f]^{-1} = \frac{1}{(1+\alpha)} \begin{bmatrix} (4+\alpha)\dfrac{EI}{h} & \text{symmetrical} \\ -\dfrac{6EI}{h^2} & \dfrac{12EI}{h^3} \end{bmatrix} \tag{14.2}$$

where

$$\alpha = \frac{12EI}{h^2 Ga_r} \tag{14.3}$$

From the elements of the stiffness matrix of Eq. 14.2 and by considering equilibrium, the stiffness matrix corresponding to the coordinates in Figure 14.2c can be derived. Thus, the stiffness matrix for a prismatic bar (Figure 14.2c), or the shear-wall element in Figure 14.2a, with the shear deformation considered, is

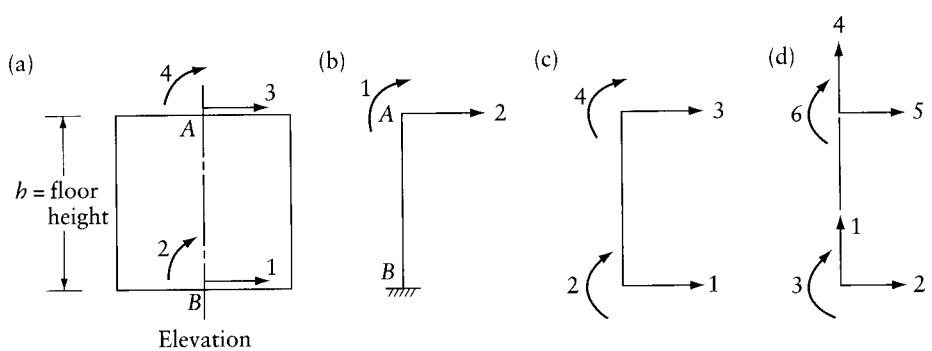

Figure 14.2 Flexibility and stiffness of a member considering shear, bending, and axial deformations. (a) Shear-wall element. (b), (c), and (d) Coordinates corresponding to the flexibility or stiffness matrices in: (b) Eqs. 14.1 and 14.2, (c) Eq. 14.4, and (d) Eq. 14.5.

$$[S]=\frac{1}{1+\alpha}\begin{bmatrix} \frac{12EI}{h^3} & & \text{symmetrical} & \\ \frac{6EI}{h^2} & (4+\alpha)\frac{EI}{h} & & \\ -\frac{12EI}{h^3} & -\frac{6EI}{h^2} & \frac{12EI}{h^3} & \\ \frac{6EI}{h^2} & (2-\alpha)\frac{EI}{h} & -\frac{6EI}{h^2} & (4+\alpha)\frac{EI}{h} \end{bmatrix} \tag{14.4}$$

Putting $\alpha = 0$, the stiffness matrix becomes identical with the matrix in Eq. 6.8 in which the shear deformations are ignored.

In some cases, it is necessary to consider the axial deformation so that the stiffness matrix has to be written for six coordinates as shown in Figure 14.2d. The stiffness matrix corresponding to these coordinates taking into account bending, shear, and axial deformation is

$$[S]=\begin{matrix} 1 \\ 2 \\ 3 \\ 4 \\ 5 \\ 6 \end{matrix}\begin{bmatrix} \frac{Ea}{h} & & & & \text{symmetrical} & \\ & \frac{12EI}{(1+\alpha)h^3} & & & \text{elements not} & \\ & \frac{6EI}{(1+\alpha)h^2} & \frac{(4+\alpha)EI}{(1+\alpha)h} & & \text{shown are zero} & \\ -\frac{Ea}{h} & & & \frac{Ea}{h} & & \\ & -\frac{12EI}{(1+\alpha)h^3} & -\frac{6EI}{(1+\alpha)h^2} & & \frac{12EI}{(1+\alpha)h^3} & \\ & \frac{6EI}{(1+\alpha)h^2} & \frac{(2-\alpha)EI}{(1+\alpha)h} & & -\frac{6EI}{(1+\alpha)h^2} & \frac{(4+\alpha)EI}{(1+\alpha)h} \end{bmatrix} \tag{14.5}$$

where a is the area of a cross section perpendicular to the axis, and α is as before (Eq. 14.3). If we put $a = 0$, Eq. 14.5 becomes the same as Eq. 6.7 with the shear deformations ignored.

14.3 Stiffness matrix of a beam with rigid end parts

Shear walls are usually connected by beams, and for purposes of analysis we have to find the stiffness of such a beam corresponding to coordinates at the wall axis. Consider the beam AB of Figure 14.3a. We assume that the beam has two rigid parts AA' and $B'B$ (Figure 14.3b). The displacements $\{D^*\}$ at A and B are related to the displacements $\{D\}$ at A' and B' by geometry as follows:

$$\{D\}=[H]\{D^*\} \tag{14.6}$$

where

$$[H]=\begin{bmatrix} 1 & \delta l & 0 & 0 \\ 0 & 1 & 0 & 0 \\ 0 & 0 & 1 & -\beta l \\ 0 & 0 & 0 & 1 \end{bmatrix} \tag{14.7}$$

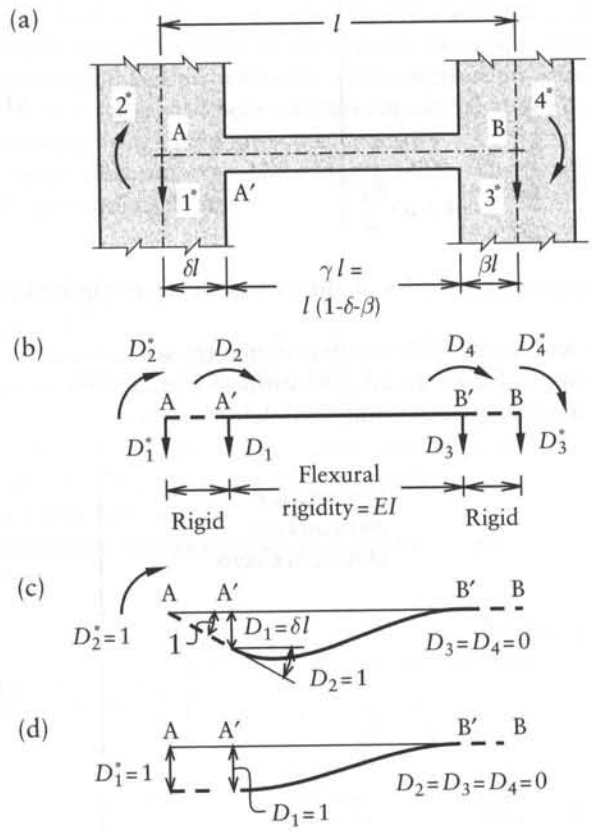

Figure 14.3 Coordinate system corresponding to the stiffness matrices in Eqs. 14.8 and 14.10 of a beam between shear walls. (a) Elevation of a beam between shear walls. (b) Coordinate systems. (c) and (d) Deflected configurations corresponding to $D_2^* = 1$ and $D_1^* = 1$ respectively.

The elements in the first and second column of $[H]$, which are the $\{D\}$ displacements due to $D_1^* = 1$ and $D_2^* = 1$ respectively, can be checked by examining Figure 14.3c.

If shear deformations are to be considered, the stiffness matrix $[S]$ of the beam corresponding to the $\{D\}$ coordinates is the same as in Eq. 14.4 with γl substituted for h. Thus,

$$[S] = \frac{1}{1+\alpha}\begin{bmatrix} \frac{12EI}{(\gamma l)^3} & & & \text{symmetrical} \\ \frac{6EI}{(\gamma l)^2} & (4+\alpha)\frac{EI}{\gamma l} & & \\ -\frac{12EI}{(\gamma l)^3} & -\frac{6EI}{(\gamma l)^2} & \frac{12EI}{(\gamma l)^3} & \\ \frac{6EI}{(\gamma l)^2} & (2-\alpha)\frac{EI}{\gamma l} & -\frac{6EI}{(\gamma l)^2} & (4+\alpha)\frac{EI}{\gamma l} \end{bmatrix} \tag{14.8}$$

where $\gamma = 1 - \delta - \beta$, and δ and β are the ratios of the lengths of the rigid parts of the beam to the total length l.

From Eq. 9.17, the stiffness matrix corresponding to the $\{D^*\}$ coordinates is given by

$$[S^*] = [H]^T [S] [H] \tag{14.9}$$

Substituting Eqs. 14.7 and 14.8 into Eq. 14.9 gives

$$[S^*] = \frac{EI}{1+\alpha} \begin{bmatrix} \frac{12}{(\gamma l)^3} & & & \text{symmetrical} \\ \frac{6}{(\gamma l)^2} + \frac{12\delta}{\gamma^3 l^2} & \frac{4+\alpha}{\gamma l} + \frac{12\delta}{\gamma^2 l} + \frac{12\delta^2}{\gamma^3 l} & & \\ -\frac{12}{(\gamma l)^3} & -\frac{6}{(\gamma l)^2} - \frac{12\delta}{\gamma^3 l^2} & \frac{12}{(\gamma l)^3} & \\ \frac{6}{(\gamma l)^2} + \frac{12\beta}{\gamma^3 l^2} & \frac{2-\alpha}{\gamma l} + \frac{6\delta+6\beta}{\gamma^2 l} + \frac{12\delta\beta}{\gamma^3 l} & -\frac{6}{(\gamma l)^2} - \frac{12\beta}{\gamma^3 l^2} & \frac{4+\alpha}{\gamma l} + \frac{12\beta}{\gamma^2 l} + \frac{12\beta^2}{\gamma^3 l} \end{bmatrix} \tag{14.10}$$

Equation 14.10 thus gives the stiffness matrix corresponding to $\{D^*\}$ coordinates (Figure 14.3a) for a prismatic bar of length l with parts δl and βl at the ends of infinite flexural rigidity (Figure 14.3b). The term $\alpha = (12EI)/(\gamma^2 l^2 G a_r)$ accounts for the shear deformations; if these are to be ignored, α is set equal to zero. The end-rotational stiffness of member AB in Figure 14.3c, $S_{AB} = S^*_{22}$; the carryover factors $C_{AB} = S^*_{42}/S^*_{22}$ and $C_{BA} = S^*_{42}/S^*_{44}$; where S_{ij} is any element of $[S^*]$. The adjusted end-rotational stiffness, $S^1_{AB} = S_{AB}(1 - C_{AB}C_{BA})$ (see Section 11.6, Eq. 11.20 and Figures 11.7a and b). When $\beta = 0$ and shear deformation is ignored, this equations becomes:

$$S^{①}_{AB} = \frac{3EI}{l}(1-\delta)^3 \tag{14.11}$$

This is the end moment at A to deform AB as shown in Figure 11.7b, assuming that the member has a rigid part of length δl adjacent to A.

14.4 Analysis of a plane frame with shear walls

Consider the structure shown in Figure 14.1b, composed of frames parallel to the axis of symmetry. Some of these frames include shear walls. Because of symmetry in structure and in loading, the diaphragms translate without rotation. With the diaphragms assumed rigid in their own planes, all the frames sway by the same amount D^* at a given floor level, as shown in Figure 14.4a.

The stiffness matrix $[S^*]_i$ (of the order $n \times n$, where n is the number of floors), corresponding to the $\{D^*\}$ coordinates is calculated for each plane frame. The matrices are then added to obtain the stiffness $[S^*]$ of the entire structure

$$[S^*] = \sum_{i=1}^{m} [S^*]_i \tag{14.12}$$

where m is the number of the frames.

The sway at the floor levels is calculated by

$$[S^*]_{n\times n} \{D^*\}_{n\times 1} = \{F^*\}_{n\times 1}$$

where $\{F^*\}$ are the resultant horizontal forces at floor levels, and n is the number of floors.

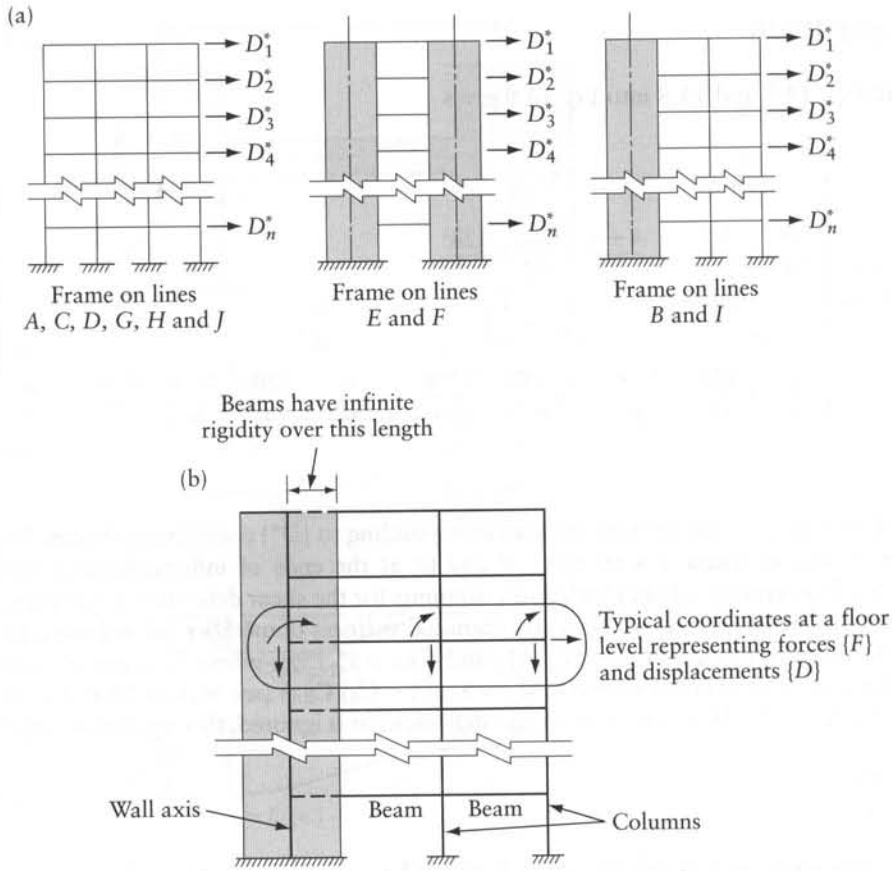

Figure 14.4 Plane frames considered in the analysis of the symmetrical three-dimensional structure of Figure 14.1b. (a) Frames parallel to the line of symmetry in the building of Figure 14.1b. (b) Coordinate system corresponding to the stiffness matrix $[S]_i$ for the frame on lines *B* and *I*.

In order to determine $[S^*]_i$ for any frame, say, the frame on line *B* or *I* (Figure 14.4a), coordinates are taken at the frame joints as shown in Figure 14.4b. These represent rotation and vertical displacement at each joint and sway of the floor as a whole. The corresponding stiffness matrix $[S]_i$ (of the order $7n \times 7n$, in this case) is first derived using the stiffness of the shear wall and beam attached to it (as obtained in Sections 14.2 and 14.3). The stiffness matrix $[S]_i$ is then condensed into matrix $[S^*]_i$ corresponding to coordinates for the sidesway at floor level (see Section 6.5). The elements of $[S^*]_i$ are forces at floor levels corresponding to unit horizontal displacements at alternate floors with the rotations and vertical joint displacements allowed to take place.

After solving Eq. 14.12 for $\{D^*\}$, the horizontal forces at floor levels for each plane frame are determined by

$$[S^*]_i \{D^*\} = \{F^*\}_i \tag{14.13}$$

When the horizontal forces $\{F^*\}_i$ are applied at the floors of the *i*th frame, without forces at the other coordinates in Figure 14.4b, the displacements at all the other coordinates in this figure can be calculated. From these, the stress resultants in any element can be determined.

Clough et al.[2] give details of an analysis involving the same assumptions as in the above approach and describe an appropriate computer program. It may be interesting to give here the results of their analysis of a 20-storey structure with the plan arrangement shown in Figure 14.5a, subjected to wind loading in the direction of the x axis. Storey heights are 10 ft (3.05 m), except for the ground floor which is 15 ft (4.58 m) high. All columns and shear walls are fixed at the base. The properties of the structural members are listed in Table 14.1.

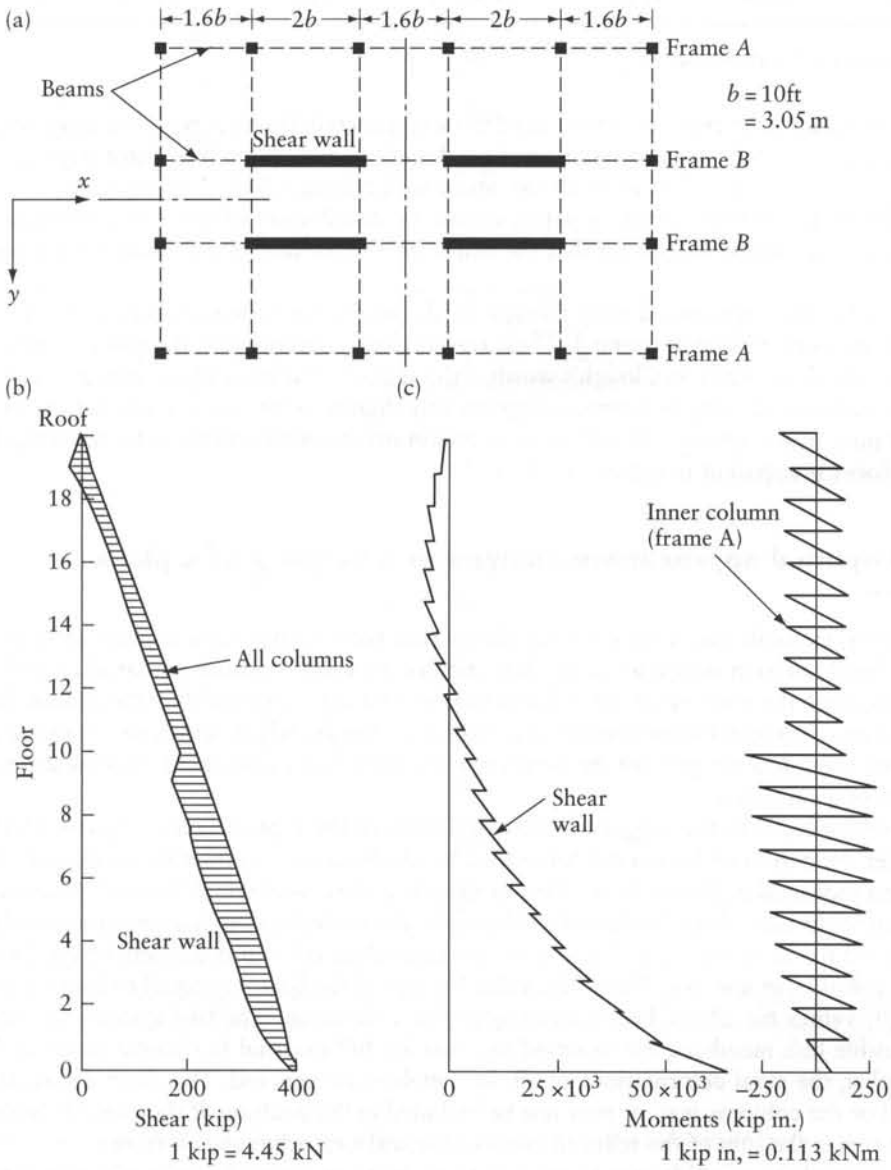

Figure 14.5 Example of a building analyzed by Clough, King, and Wilson. (a) Plan. (b) Shearing force distribution. (c) Moments in vertical members.

2 Clough, R. W., King, I. P. and Wilson, E. L., "Structural Analysis of Multistorey Buildings," *Proc. ASCE*, (90), No. ST3, Part 1 (1964), pp. 19–34.

Table 14.1 Member Properties for the Example of Figure 14.5

	Columns		*Shear Walls*		*Girders*	
	I, in.^{4}	*Area, in.*^{2}	*I, in.*^{4}	*Area, in.*^{2}	*I, in.*^{4}	*Area, in.*^{2}
Stories 11–20	3437	221.5	1793×10^4	3155	6875	—
Stories 1–10	9604	313.5	2150×10^4	3396	11295	—

1 in.^{2} = 645 mm^2; 1 in.^{4} = 416 000 mm^4.

For this structure, two types of frames need to be considered: frame *A* with five bays, with all columns considered to be of zero width in the *x* direction; and frame *B* of three bays: 26, 36, and 26 ft (7.93, 10.98, and 7.93 m) with two shear-wall columns 20 ft (6.10 m) wide.

Figure 14.5b, taken from Clough's paper, shows the distribution of shear force between the columns and shear walls; we can see that the major part of the lateral resistance is provided by the shear walls.

Figure 14.5c, also reproduced from Clough et al., shows the bending moment in the shear wall and in an inner column of frame *A*. These results clearly demonstrate the different behavior of columns and shear walls: in Clough's words, "the shear wall is basically a cantilever column, with frame action modifying its moment diagram only slightly, whereas the single column shows essentially pure frame action." The effect of discontinuity in column stiffness between the 10th and 11th floors is apparent in Figures 14.5b and c.

14.5 Simplified approximate analysis of a building as a plane structure

The preceding example (see Figure 14.5c) shows that the columns have a point of inflection within the height of each storey, while the deflection of the walls is similar to that of a cantilever. This is so because the rotation of the column ends is elastically restrained by the beams. When the walls have a very high *I* value compared to that of the beams, which is the case in practice, the beams cannot significantly prevent the rotation at the floor levels associated with the deflection in the form of a cantilever.

This behavior leads to the suggestion that structures of the type shown in Figures 14.1b or 14.5a under the action of horizontal forces can be idealized into a structure composed of the two systems indicated in Figure 14.6a. One of these is a shear wall which has an *I* value in any storey equal to the sum of the *I* values of all the walls; the second system is an equivalent column rigidly jointed to the beams. The I_c value for the equivalent column is the sum of the *I* values for all the columns in a storey. The $(I/l)_b$ value for any of the beams is equal to four times the sum of (I/l) values for all the beams running in the *x* direction. The two systems, connected by inextensible link members, are assumed to resist the full external horizontal forces at floor levels. Further, the axial deformations of all the members are ignored. The shear deformations of the wall or the columns may or may not be included in the analysis. If they are, the reduced (effective) area is the sum of the reduced areas of the walls or columns in a storey.

Replacement of the actual frames by the substitute frame in Figure 14.6a implies the assumption that, under the effect of horizontal forces at floor levels, the beams deflect with a point of inflection (zero bending moment) at their middle; e.g. see the frame of Problem 11.27. For this frame, we can verify that the displacements at C or B are the same as those of a substitute frame subjected to the same forces as the actual structure. The substitute frame represents the left-hand half of the actual frame, with roller supports preventing the vertical displacements at the middle of CD and BE; I_{AB} or I_{BC} in the substitute frame = the sum of the *I*-values of the columns on the

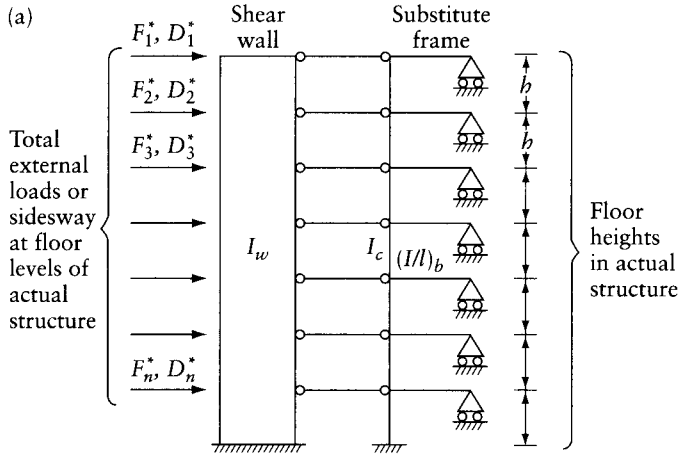

For the shear wall: $I_w = \Sigma I_{wi}$

For the substitute frame: $I_c = \Sigma I_{ci}$ *and* $(I/l)_b = 4\Sigma (I/l)_{bi}$

i is for all walls, columns or beams in a floor. Subscripts w, c, and b refer to wall, column, and beam respectively.

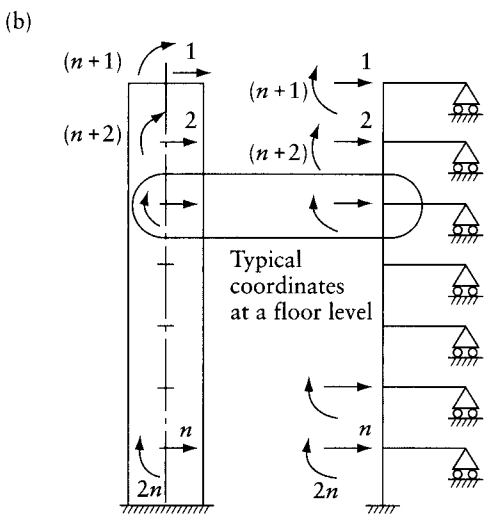

Figure 14.6 Simplified analysis of a building frame of the type shown in Figures 14.1b or 14.5a. (a) Idealized structure. (b) Coordinates corresponding to stiffness matrices $[S_w]$ and $[S_r]$.

opposite sides of the actual frame; for the beam at C or D in the substitute frame, $(I/l)_{\text{beam}} =$ four times $(I/l)_{\text{CD or BE}}$.

The idealized structure in Figure 14.6a is assumed to have n degrees of freedom representing the sidesway of the floors. The stiffness matrix $[S^*]_{n\times n}$ of this structure is obtained by summation of the stiffness matrices of the two systems. Thus,

$$[S^*] = [S^*]_w + [S^*]_r \tag{14.14}$$

where $[S^*]_w$ and $[S^*]_r$ are the stiffness matrices, respectively, of the shear wall and the substitute frame, corresponding to n horizontal coordinates at the floor levels. For the determination of $[S^*]_w$ or $[S^*]_r$ two degrees of freedom (a rotation and sidesway) are considered at each floor level for the wall and at each beam–column connection in the substitute frame. A stiffness matrix $[S]_w$ or $[S]_r$ of order $2n \times 2n$ corresponding to the coordinates in Figure 14.6b is written, then these matrices are condensed to $[S^*]_w$ and $[S^*]_r$ which relate horizontal forces to sidesway with the rotations unrestrained (see Section 6.5).

The sidesway at floor levels of the actual structure is then calculated by solving

$$[S^*]_{n\times n}\{D^*\}_{n\times 1} = \{F^*\}_{n\times 1} \tag{14.15}$$

The displacements $\{D^*\}$ represent the horizontal translation at floor levels of all columns or shear walls in the building. The external forces $\{F^*\} = \{F^*\}_w + \{F^*\}_r$, where $\{F^*\}_w$ and $\{F^*\}_r$ are, respectively, the forces resisted by walls and by the substitute frame, can be calculated from

$$[F^*]_w = \{S^*\}_w\{D^*\} \tag{14.16}$$

and

$$[F^*]_r = \{S^*\}_r\{D^*\} \tag{14.17}$$

These forces are then applied to the shear wall and to the substitute frame, and the member end-moments are determined in each system. If these end-moments are apportioned to the walls, columns, and beams of the actual structure according to their (EI/h) or (EI/l) values, approximate values of the actual member end-moments can be obtained. The apportionment in this manner may result in unbalanced moments at some of the joints. Improved values can be rapidly reached by performing one or two cycles of moment distribution.

It is important to note that if the shear walls differ considerably from one wall to another or if there are variations in cross section at different levels, the above method of calculation can lead to erroneous results. In such a case, it may be necessary to consider an idealized structure composed of more than one wall attached by links to the substitute frame and to derive the stiffness of each separately; the stiffness of the idealized structure is then obtained by summation.

14.5.1 Special case of similar columns and beams

When the column cross section and height are the same in all stories and $(I/l)_b$ is the same at all floors, the stiffness matrix of the substitute frame in the right-hand side of Figure 14.6b is

$$[S]_{r_{2n\times 2n}} = \begin{bmatrix} [S_{11}]_r & [S_{12}]_r \\ [S_{21}]_r & [S_{22}]_r \end{bmatrix} \tag{14.18}$$

The submatrices are

$$[S_{11}]_r = \frac{2(S+t)}{h^2}\begin{bmatrix} 1 & -1 & & & & & \\ -1 & 2 & -1 & & & & \\ & -1 & 2 & -1 & & & \\ & & \cdots & \cdots & \cdots & & \\ \text{Elements} & \text{not} & & \cdots & \cdots & \cdots & \\ \text{shown} & \text{are} & \text{zero} & & -1 & 2 & -1 \\ & & & & & -1 & 2 \end{bmatrix}_{n\times n} \tag{14.19}$$

$$[S_{21}]_r = [S_{12}]_r^T = \frac{(S+t)}{h}\begin{bmatrix} & -1 & 1 & & & & \\ & -1 & 0 & 1 & & & \\ & & -1 & 0 & 1 & & \\ & & & \cdots & \cdots & \cdots & \\ \text{Elements} & \text{not} & & \cdots & \cdots & \cdots & \\ \text{shown} & \text{are} & \text{zero} & & -1 & 0 & 1 \\ & & & & & -1 & 0 \end{bmatrix}_{n\times n} \tag{14.20}$$

and

$$[S_{22}]_r = S\begin{bmatrix} (1+\beta) & C & & & & & \\ C & (2+\beta) & C & & & & \\ & C & (2+\beta) & C & & & \\ & & \cdots & \cdots & \cdots & & \\ \text{Elements} & \text{not} & & \cdots & \cdots & \cdots & \\ \text{shown} & \text{are} & \text{zero} & & C & (2+\beta) & C \\ & & & & & C & (2+\beta) \end{bmatrix}_{n\times n} \tag{14.21}$$

where

$$\beta = \frac{3E}{S}(I/l)_b \tag{14.22}$$

$$S = \frac{(4+\alpha)}{(1+\alpha)}\frac{EI_c}{h} \tag{14.23}$$

$$t = \frac{(2-\alpha)}{(1+\alpha)}\frac{EI_c}{h} \tag{14.24}$$

and

$$C = (t/S) \tag{14.25}$$

The term S is the column rotational stiffness at one end with the far end fixed; t is the carryover moment (refer to Eq. 14.4); and C the carryover factor. The shear deformation of the vertical members is accounted for by the term

$$\alpha = \frac{12EI_c}{h^2 G a_{rc}} \tag{14.26}$$

while the shear deformation of the beams is ignored. The values I_c and $(I/l)_b$ are the properties respectively of the column and of the beam in the substitute frame (see Figure 14.6a). The cross-sectional area $a_{rc} = \Sigma a_{rci}$ is the sum of the reduced (effective) cross-sectional areas of all the columns in the frame.

The general case in which the column cross section and height vary from storey to storey and the beams do not have the same values of $(I/l)_b$ at all floor levels is considered in Prob. 14.2.

The above equations can be used to obtain the stiffness matrix $[S]_w$ of the wall corresponding to the coordinates in Figure 14.6b. For this purpose, we put $\beta = 0$ and substitute the subscript w for c.

Example 14.1: Structures with four and with twenty stories

Find the approximate values of the end-moments in a column and a shear wall in a structure which has the same plan as in Figure 14.5a, and has four stories of equal height $h = b$. The frame is subjected to a horizontal force in the x direction of magnitude $P/2$ at top floor and P at each of the other floor levels. The properties of members are as follows: for any column $I = 17 \times 10^{-6} b^4$, for any beam $I = 34 \times 10^{-6} b^4$, and for any wall $I = 87 \times 10^{-3} b^4$. Take $E = 2.3G$. The area of wall cross section is $222 \times 10^{-3} b^2$. Consider shear deformation in the walls only.

The wall and the substitute frame of the idealized structure are shown in Figure 14.7a. In the actual structure there are 16 columns, 4 walls, 12 beams of length $1.6b$, and 4 beams of length $2b$. The properties of members of the idealized structure are

$$I_c = \Sigma I_{ci} = 16 \times 17 \times 10^{-6} b^4 = 272 \times 10^{-6} b^4$$

$$(I/l)_b = 4\Sigma(I/l)_{bi} = 4 \times 34 \times 10^{-6} b^4 \left(\frac{12}{1.6b} + \frac{4}{2.0b} \right) = 1292 \times 10^{-6} b^3$$

$$I_w = \Sigma I_{wi} = 4 \times 87 \times 10^{-3} b^4 = 348 \times 10^{-3} b^4$$

$$a_{rw} = \Sigma a_{rwi} = 4 \times \frac{5}{6} \times 222 \times 10^{-3} b^2 = 740 \times 10^{-3} b^2$$

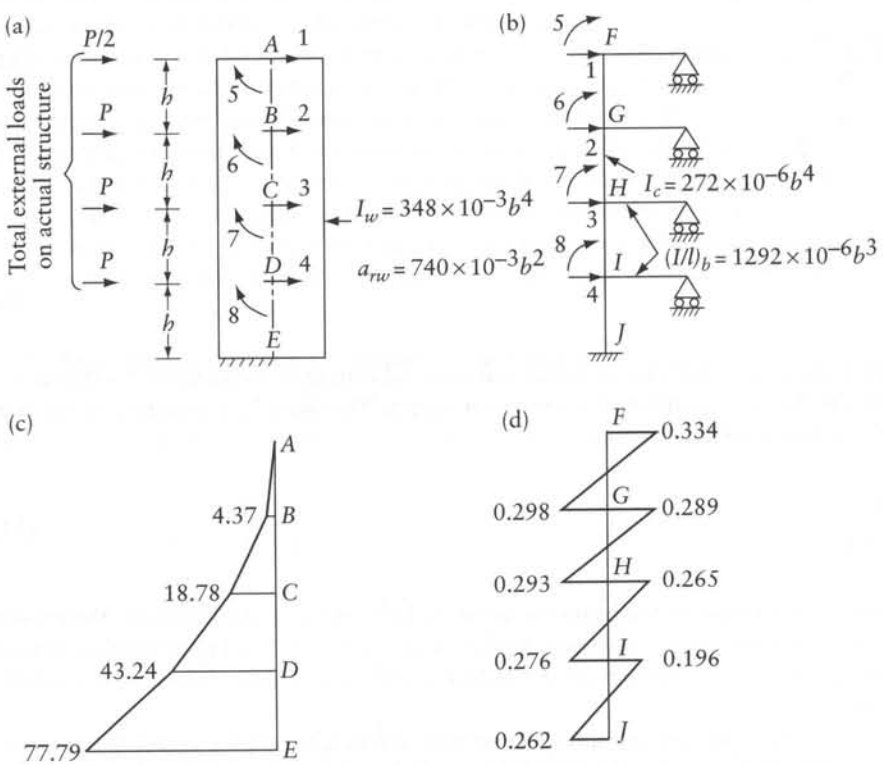

Figure 14.7 Analysis of the four-storey building in Example 14.1. (a) Shear wall. (b) Substitute frame. (c) Sum of moments in walls in terms of $Ph/10$. (d) Sum of moments in columns in terms of $Ph/10$.

For the derivation of the stiffness matrix of the wall and the substitute frame, the following quantities are calculated by Eqs. 14.22 to 14.26.

	Wall	Substitute frame
α:	12.9	0
S:	$0.423Eh^3$	$1.09 \times 10^{-3}\, Eh^3$
t:	$-0.273Eh^3$	$0.54 \times 10^{-3}\, Eh^3$
C:	-0.65	0.5
β:	—	3.56

To obtain the stiffness matrix of the substitute frame, we substitute in Eqs. 14.19 to 14.21 to calculate the submatrices of $[S_r]$:

$$[S_{11}]_r = 3.26 \times 10^{-3} Eh \begin{bmatrix} 1 & -1 & & \\ -1 & 2 & -1 & \\ & -1 & 2 & -1 \\ & & -1 & 2 \end{bmatrix}$$

$$[S_{21}]_r = [S_{12}]_r^T = 1.63 \times 10^{-3} Eh^2 \begin{bmatrix} -1 & 1 & & \\ -1 & 0 & 1 & \\ & -1 & 0 & 1 \\ & & -1 & 0 \end{bmatrix}$$

$$[S_{22}]_r = 1.09 \times 10^{-3} Eh^3 \begin{bmatrix} 4.56 & 0.5 & & \\ 0.5 & 5.56 & 0.5 & \\ & 0.5 & 5.56 & 0.5 \\ & & 0.5 & 5.56 \end{bmatrix}$$

The condensed stiffness matrix corresponding to the four sidesway coordinates is (by Eq. 5.17)

$$[S^*]_r = [S_{11}]_r - [S_{12}]_r [S_{22}]_r^{-1} [S_{21}]_r \tag{14.27}$$

Substituting, we obtain

$$[S^*]_r = 10^{-4} Eh \begin{bmatrix} 23.55 & & \text{symmetrical} & \\ -27.16 & 55.08 & & \\ 3.93 & -31.93 & 56.03 & \\ -0.36 & 4.40 & -32.40 & 60.37 \end{bmatrix}$$

In a similar way, the stiffness matrix of the wall corresponding to horizontal coordinates at the floor level is

$$[S^*]_w = 10^{-2} Eh \begin{bmatrix} 13.98 & & \text{symmetrical} & \\ -22.76 & 51.22 & & \\ 5.70 & -31.84 & 53.77 & \\ 2.33 & 2.55 & -30.19 & 56.33 \end{bmatrix}$$

The stiffness matrix of the idealized structure (wall and substitute frame connected) is obtained by Eq. 14.14:

$$[S^*] = [S^*]_w + [S^*]_r$$

$$= 10^{-4}Eh \begin{bmatrix} 1421.40 & \text{symmetrical} & & \\ -2303.05 & 5177.15 & & \\ 574.22 & -3215.76 & 5433.34 & \\ 232.28 & 259.64 & -3051.41 & 5692.92 \end{bmatrix}$$

Substituting $[S^*]$ from the above equation and $\{F^*\} = P\{0.5, 1.0, 1.0, 1.0\}$ in Eq. 14.15 and solving for $\{D^*\}$, we find the sidesway of the actual structure at floor levels

$$\{D^*\} = \frac{10P}{Eh} \begin{Bmatrix} 11.47 \\ 8.32 \\ 5.03 \\ 2.03 \end{Bmatrix}$$

Multiplying $[S^*]_w$ or $[S^*]_r$ by $\{D^*\}$, we obtain the forces resisted by the wall and by the substitute frame (Eqs. 14.16 and 14.17):

$$\{F^*\}_w = P \begin{Bmatrix} 0.4368 \\ 1.0050 \\ 1.0041 \\ 1.0083 \end{Bmatrix}; \quad \{F^*\}_r = P \begin{Bmatrix} 0.0632 \\ -0.0050 \\ -0.0041 \\ -0.0083 \end{Bmatrix}$$

The joint rotations of the substitute frame $\{D_2\}_r$, can be determined by

$$\{D_2\}_r = -[S_{22}]_r^{-1}[S_{21}]_r\{D_1\}_r \tag{14.28}$$

where $\{D_1\}_r = \{D^*\}$ are the displacements at the first n coordinates in Figure 14.7b. A part of the calculations required for the equation has already been done in the operations for Eq. 14.27. From the rotation and translation of the joints in the column, the end-moments can be easily calculated. The bending moment diagram of the substitute frame is shown in Figure 14.7d. The moment in the shear walls is calculated by applying the forces $\{F^*\}_w$ on a cantilever and is plotted in Figure 14.7c.

Because all the walls are of the same cross section, and likewise the columns, the moment in each wall is $\frac{1}{4}$ of the value in Figure 14.7c, and in each column 1/16 of the value in Figure 14.7d.

The solution of the same problem with the number of stories $n = 20$, instead of 4, gives the results shown in Figure 14.8. The external applied forces are $P/2$ on the top diaphragm and P on each of the others. All stories have the same height h.

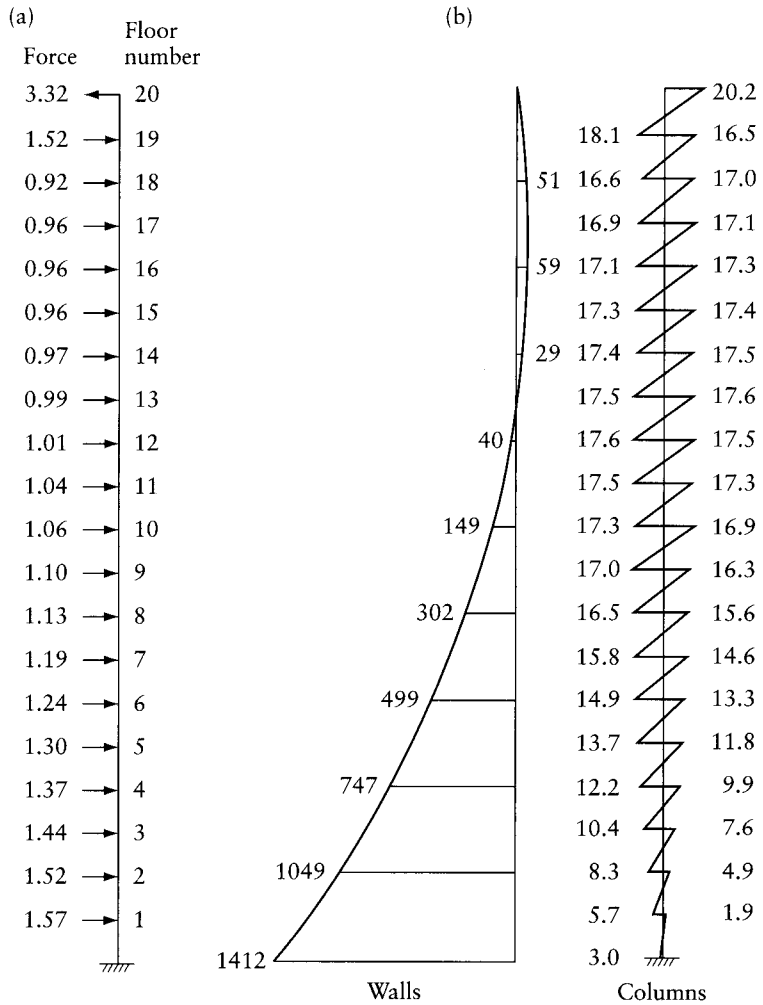

Figure 14.8 Forces and moments in a 20-storey building shown in plan in Figure 14.5a, using analysis in Example 14.1. (a) Forces resisted by shear walls in terms of P. (b) Moments in vertical members in terms of $Ph/10$.

14.6 Shear walls with openings

Figures 14.9a and b show the types of walls which are often used in dwelling blocks. The two types shown differ in the size of openings and in their location. An exact treatment of this problem would require the solution of the governing plane-stress elasticity equations, but this is difficult and cannot be used in practice. A reasonable solution can be obtained by the finite-element method (see Chapter 16) or by idealizing the wall into different types of latticed frames composed of small elements; however, the calculation generally requires the solution of a large number of equations. These methods are used in the analysis of walls with openings arranged in any pattern, and they give a better picture of the stress distribution than the much more simplified analysis described below.

In the simplified analysis, walls with a row of openings of the type shown in Figures 14.9a and b are idealized to a frame composed of two wide columns connected by beams with end

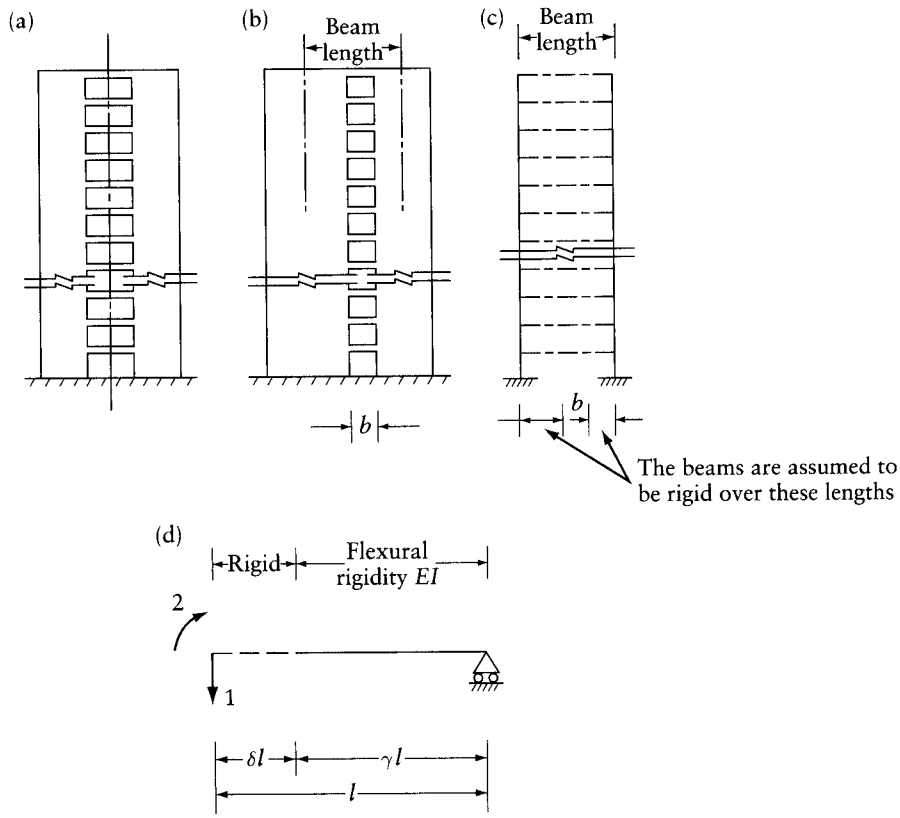

Figure 14.9 Idealized structure for the analysis of a wall with row of openings. (a) Symmetrical wall. (b) Wall with a row of openings. (c) Idealized structure for the analysis of the wall in part (b). (d) Coordinates corresponding to the stiffness matrix $\bar{S}$ given by Eq. 14.29.

parts infinitely rigid. The stiffness of the elements forming such a structure and the method of analysis are given in Sections 14.2 and 14.3. MacLeod[3] showed by model testing that the idealization of a wall of this type by a frame gives a good estimate of stiffness (corresponding to sidesway) for most practical cases. It seems, therefore, that the finite-element idealization offers little advantage in this respect.

The symmetrical wall in Figure 14.9a can be analyzed using a suitable frame composed of one column rigidly connected to beams (see Figure 14.7b). Each beam has a rigid part near its connection with the column. The stiffness matrix of such a beam with one end hinged, corresponding to the coordinates in Figure 14.9d can be easily derived from Eq. 14.10 and is

$$\left[\bar{S}\right] = \begin{bmatrix} S^*_{11} - \dfrac{S^{*2}_{14}}{S^*_{44}} & \text{symmetrical} \\ S^*_{21} - \dfrac{S^*_{24}S_{41}}{S^*_{44}} & S^*_{22} - \dfrac{S^{*2}_{24}}{S^*_{44}} \end{bmatrix} \tag{14.29}$$

3 MacLeod, I. A., "Lateral Stiffness of Shear Walls with Openings in Tall Buildings," *Proceedings of a Symposium on Tall Buildings, Southampton,* Pergamon Press, New York, 1967, pp. 223–244.

where S^*_{ij} are elements of the stiffness matrix in Eq. 14.10 with $b = 0$. If the axial deformation is ignored in the special case of a symmetrical wall having the same height and cross section in all stories and the beams between the windows are the same in all floors, Eqs. 14.18 to 14.26 can be used to derive the stiffness matrix of the substitute frame, but β of Eq. 14.22 must be replaced by

$$\beta' = \frac{\bar{S}_{22}}{S} \tag{14.30}$$

where $\bar{S}_{22}$ is an element of the stiffness matrix in Eq. 14.29 and S is defined by Eq. 14.23. The reason for this is that in Eq. 14.22, the quantity $3E(I/l)_b$ is the adjusted end-rotational stiffness of a prismatic horizontal beam in the substitute frame. The corresponding quantity for the beam in Figure 14.9d is $\bar{S}_{22}$.

14.7 Three-dimensional analysis

A joint in a three-dimensional framed structure has in general six degrees of freedom: three rotations and three translations in the x, y, and z directions (Figure 14.10a). The assumption that the diaphragms in a multistorey building are rigid constrains three of the displacements (D_1, D_2 and D_3) to be the same at all joints in one floor. Even with this important simplification, the analysis is complicated in the case of three-dimensional structures incorporating members having an arbitrary orientation in space.

This section deals with the case of a structure formed of shear walls in a random arrangement. Any two or more walls which are monolithic will be referred to as a *wall assembly*. A typical wall assembly is shown in plan in Figure 14.10b. The structure is analyzed to determine the forces resisted by different shear walls when horizontal forces in any direction are applied at floor levels. In addition to the rigid-diaphragm assumption used in the previous sections, we assume here that the floors do not restrain the joint rotations about the x and y axes (D_4 and D_5 in Figure 14.10a). This assumption is equivalent to considering that the diaphragm has a small flexural rigidity compared with the walls and can therefore be ignored. With this additional assumption, horizontal forces result in no axial forces in the walls; thus, the vertical displacements (D_6 in Figure 14.10a) are zero.

Given all these assumptions, the analysis by the stiffness method will now be performed for a single-storey structure and then extended to a multistorey building.

14.7.1 One-storey structure

Imagine that the building shown in plan in Figure 14.10b has one storey of height h and the walls are totally fixed at the base. The displacement of the walls at the floor level is completely defined if the displacements $\{D\}$ at the coordinates 1, 2, and 3 are known at any arbitrary point O in the floor level. A horizontal force anywhere in the plane of the floor can be analyzed into three components $\{F\}$ along the three coordinates.

The forces and displacements at the shear center at the top of any wall assembly are related by

$$\left[\bar{S}\right]_i \{q\}_i = \{Q\}_i \tag{14.31}$$

where $[\bar{S}]_i$ is the stiffness matrix of the ith wall assembly, and $\{q\}_i$ and $\{Q\}_i$ are respectively displacements and forces at three local coordinates in that assembly; they represent translations (or forces) at the shear center of this wall at the floor level parallel to the x and y axes and a rotation (or a couple) about the z axis (Figure 14.10b).

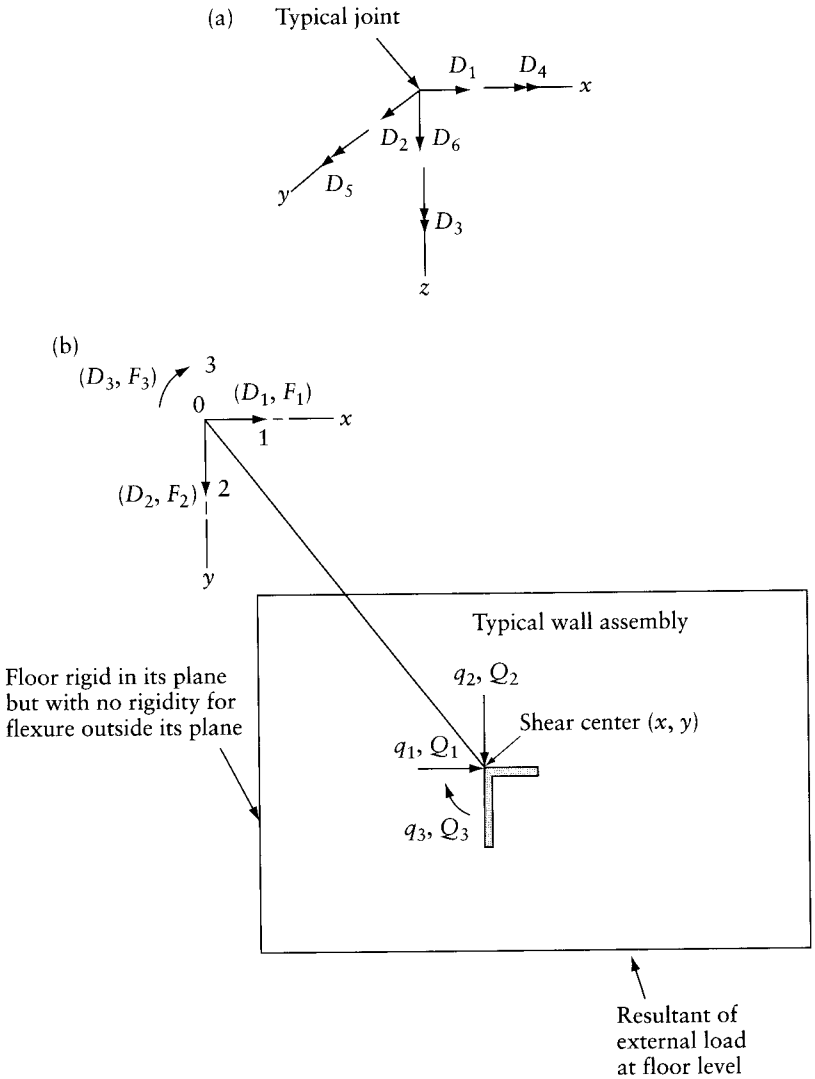

Figure 14.10 Coordinate system for the analysis of a single-storey shear-wall structure. (a) Degrees of freedom of a typical joint in a building frame. (b) Coordinate system.

To derive the stiffness matrix $[\bar{S}]_i$ consider any wall AB in Figure 14.11a fixed at the base and free at the top. The flexibility matrix corresponding to the coordinates in Figure 14.11b, of which 1* and 2* are parallel to the principal axes of inertia of the cross section, is

$$[f^*]_i = \begin{bmatrix} \left(\frac{h^3}{3EI_v} + \frac{h}{Ga_{rv}}\right) & & \\ & \left(\frac{h^3}{3EI_u} + \frac{h}{Ga_{ru}}\right) & \\ \text{Elements not shown are zero} & & \frac{h - (\tanh \Gamma h)/\Gamma}{GJ} \end{bmatrix}_i \tag{14.32}$$

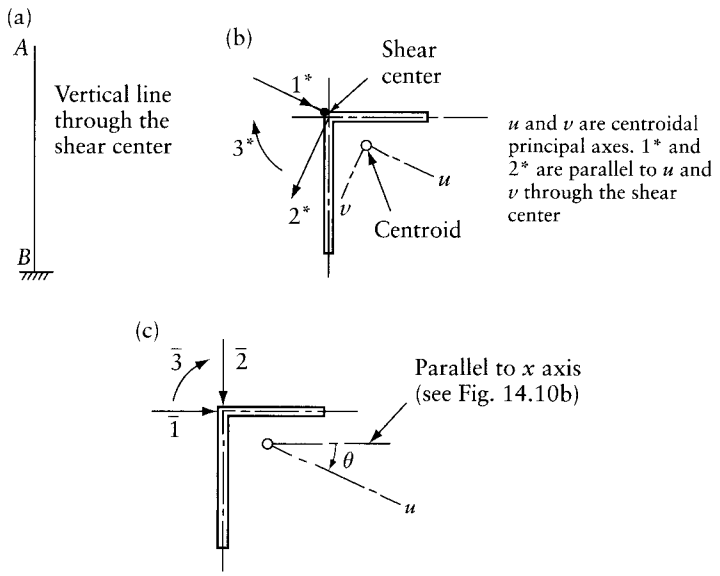

Figure 14.11 Coordinate systems corresponding to the flexibility and stiffness matrices of a wall assembly in Eqs. 14.32, 14.34, and 14.37. (a) Elevation. (b) Plan showing coordinates corresponding to the flexibility matrix in Eq. 14.32. (c) Coordinates corresponding to matrix in Eq. 14.34 or 14.37.

where I_v and I_u are the second moments of the cross-sectional area about the principal axes v and u respectively; and a_{rv} and a_{ru} are reduced (effective) areas of the cross section corresponding to loading in the vertical plane through axes u and v respectively. The second term in the expressions for f_{11}^* and f_{22}^* in the above matrix accounts for shear deformation, while the second term in f_{33}^* is included because the warping of the cross section at the bottom of the wall is prevented.[4] The parameter Γ is given by

$$\Gamma = \sqrt{\frac{GJ}{EK}} \tag{14.33}$$

where J is the torsion constant (length^4) and K is the warping constant (length^6) of the cross section. If shear deformation is ignored and the warping at the two ends is not prevented, or the warping effect is ignored, the three diagonal terms in Eq. 14.32 become: $h^3/(3EI_v)$, $h^3/(3EI_u)$, and $h/(GJ)$ (which are the displacements given in Appendix B).

The nondiagonal elements in $[f^*]_i$ are all zero because the three coordinates are chosen through the shear center, and 1* and 2* are parallel to the principal axes of the section: a force applied through the shear center produces no twisting of the cross section; further, if this force is parallel to one of the principal axes, then the deflection takes place in a plane parallel to this axis.

The stiffness matrix $[\bar{S}]_i$ corresponding to the coordinates in Figure 14.11c can be derived by inversion of $[f^*]_i$ and transformation (see Eq. 9.17).

$$\left[\bar{S}\right]_i = \begin{bmatrix} \bar{S}_{11} & \bar{S}_{12} & 0 \\ \bar{S}_{21} & \bar{S}_{22} & 0 \\ 0 & 0 & \bar{S}_{33} \end{bmatrix}_i \tag{14.34}$$

4 See Timoshenko, S. P., *Strength of Materials,* Part II, 3rd ed., Van Nostrand, New York, 1956, 260 pp.

where

$$\left.\begin{aligned}
\bar{S}_{11} &= \frac{E}{h^3}\left[\frac{12\cos^2\theta}{(4+\alpha_v)}I_v + \frac{12\sin^2\theta}{(4+\alpha_u)}I_u\right] \\
\bar{S}_{22} &= \frac{E}{h^3}\left[\frac{12\sin^2\theta}{(4+\alpha_v)}I_v + \frac{12\cos^2\theta}{(4+\alpha_u)}I_u\right] \\
\bar{S}_{12} &= \bar{S}_{21} = \frac{E}{h^3}\left[\sin\theta\cos\theta\left(\frac{12I_v}{(4+\alpha_v)} - \frac{12I_u}{(4+\alpha_u)}\right)\right] \\
\bar{S}_{33} &= \frac{GJ}{h-(\tanh\Gamma h)/\Gamma}
\end{aligned}\right\} \tag{14.35}$$

$$\left.\begin{aligned}
\alpha_u &= \frac{12EI_u}{h^2 G a_{ru}} \\
\alpha_v &= \frac{12EI_v}{h^2 G a_{rv}}
\end{aligned}\right\} \tag{14.36}$$

and θ = the angle between the x and u axes.

If the shear deformation and the warping effect are ignored, the stiffness matrix in Eq. 14.34 corresponding to the three coordinates in Figure 14.11c becomes

$$\left[\bar{S}\right]_i = \begin{bmatrix} \frac{3EI_y}{h^3} & \text{symmetrical} & \\ \frac{3EI_{xy}}{h^3} & \frac{3EI_x}{h^3} & \\ 0 & 0 & \frac{GJ}{h} \end{bmatrix}_i \tag{14.37}$$

where I_y and I_x are the moments of inertia about axes parallel to the y and x axes through the centroid, and I_{xy} is the product of inertia about the same axes.

The displacements $\{q\}_i$ of the ith wall are related to the floor displacement $\{D\}$ by geometry as follows:

$$\{q\}_i = [C]_i\{D\} \tag{14.38}$$

where

$$[C]_i = \begin{bmatrix} 0 & 0 & -y \\ 0 & 1 & x \\ 0 & 0 & 1 \end{bmatrix}_i \tag{14.39}$$

Here, $[C]_i$ is a transformation matrix for the ith wall, and x and y are the Cartesian coordinates of the shear center of this wall (Figure 14.10b). The transpose of this matrix relates the forces $\{Q\}_i$ to equivalent forces $\{F\}_i$ at the $\{D\}$ coordinates (see Section 9.3):

$$\{F\}_i = [C]_i^T\{Q\}_i$$

Applying Eq. 9.17, the stiffness matrix of the ith wall corresponding to the $\{D\}$ coordinates is

$$[S]_i = [C]_i^T\left[\bar{S}\right]_i[C]_i \tag{14.40}$$

This equation transforms the stiffness matrix $[\bar{S}]_i$ corresponding to the $\{q\}$ coordinates to a stiffness matrix $[S]_i$ corresponding to the $\{D\}$ coordinates. Performing the multiplication in Eq. 14.40 gives

$$[S]_i = \begin{bmatrix} \bar{S}_{11} & & \\ \bar{S}_{21} & \bar{S}_{22} & \text{symmetrical} \\ \left(-\bar{S}_{11}y+\bar{S}_{21}x\right) & \left(-\bar{S}_{12}y+\bar{S}_{22}x\right) & \left(\bar{S}_{11}y^2-2\bar{S}_{21}xy+\bar{S}_{22}x^2+\bar{S}_{33}\right) \end{bmatrix} \tag{14.40a}$$

The stiffness matrix of the structure can now be obtained by summation, thus,

$$[S]=\sum_{i-1}^{m}[S]_i \tag{14.41}$$

where m is the number of wall assemblies.

The floor displacement can be determined by the equation

$$\{F\}_{3\times1}=[S]_{3\times3}\{D\}_{3\times1} \tag{14.42}$$

and the forces $\{Q\}_i$ on each wall assembly are calculated by Eqs. 14.38 and 14.31.

The above analysis for a single-storey structure is given separately not only because of its intrinsic importance but also because it serves as an introduction to the multistorey case. Some designers use the single-storey solution to each storey of a multistorey structure in turn in order to obtain an approximate solution. However, for an accurate solution, all the floors must be treated simultaneously.

The above solution can also be used to calculate the displacement of bridge decks due to horizontal forces at the deck level. This is particularly useful for skew or curved bridges. The stiffness $[S]_i$ of the elements in this case would be that of a supporting pier or elastomeric bearing pad or a combination of these (see Prob. 14.8).

Example 14.2: Structure with three shear walls

Find the horizontal force resisted by each of the shear walls 1, 2, and 3 in a single-storey building whose plan is shown in Figure 14.12a. All the walls are fixed to the base. Take shear deformation into consideration but ignore warping. Assume $E=2.3\,G$.

The axes x and y are chosen to pass through the center of the shaft as shown in Figure 14.12b, in which the coordinate system is indicated. In the present case, the shear center of each wall coincides with its centroid, for which the x and y coordinates are given in brackets. (The principal axes for each wall are parallel to the x and y axes.) The values of I_u, I_v, J, a_{ru}, and a_{rv}, for each wall are given below:

	I_u	I_v	J	a_{ru}	a_{rv}
Wall 1:	$0.03413b^4$	$0.03413b^4$	$0.0512b^4$	$0.16b^2$	$0.16b^2$
Wall 2 or 3:	$0.0342b^4$	$0.00013b^4$	$0.00053b^4$	$0.133b^2$	$0.133b^2$

Substituting in Eq. 14.34 with $\theta=0$ and neglecting the warping term, we obtain

$$\left[\bar{S}\right]_1=10^{-4}Eb\begin{bmatrix} 414.2 & 0 & 0 \\ 0 & 414.2 & 0 \\ 0 & 0 & 223.0b^2 \end{bmatrix}$$

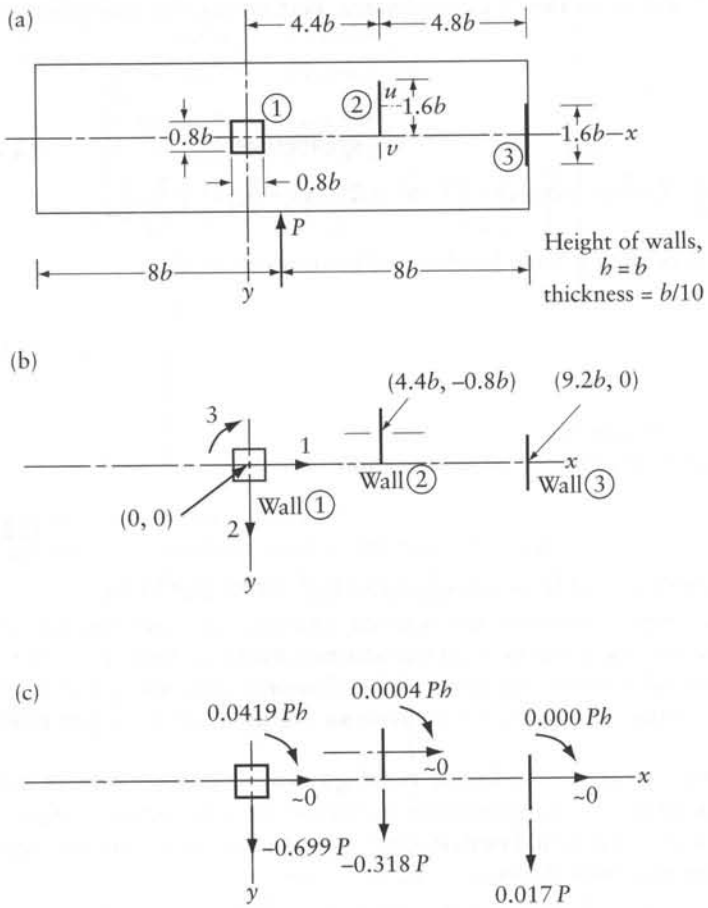

Figure 14.12 A one-storey structure considered in Example 14.2. (a) Plan of shear walls. (b) Coordinate system. (c) Forces resisted by the various walls.

No transformation is needed for this matrix, because of the choice of the origin at the shear center of the shaft. Thus,

$$[S]_1 = \left[\bar{S}\right]_1$$

Similarly, Eq. 14.34 applied to wall 2 or 3 gives

$$\left[\bar{S}\right]_{2 \text{ or } 3} = 10^{-4} Eh \begin{bmatrix} 3.87 & 0 & 0 \\ 0 & 370 & 0 \\ 0 & 0 & 2.3h^2 \end{bmatrix}$$

Substituting in Eq. 14.40a, we obtain

$$[S]_2 = Eh \begin{bmatrix} 0.387 \times 10^{-3} & & \text{symmetrical} \\ 0 & 37 \times 10^{-3} & \\ 0.3099 \times 10^{-3} h & 0.1627h & 716.46 \times 10^{-3} h^2 \end{bmatrix}$$

and

$$[S]_3 = Eh \begin{bmatrix} 0.387 \times 10^{-3} & & \text{symmetrical} \\ 0 & 37 \times 10^{-3} & \\ 0 & 0.3402h & 3130.4 \times 10^{-3}h^2 \end{bmatrix}$$

The stiffness matrix of the structure is given by Eq. 14.41 with $m = 3$:

$$[S] = Eh \begin{bmatrix} 42.2 \times 10^{-3} & & \text{symmetrical} \\ 0 & 115.4 \times 10^{-3} & \\ 0.31 \times 10^{-3}h & 0.503h & 3869.1 \times 10^{-3}h^2 \end{bmatrix}$$

The forces at the coordinates equivalent to the external applied load are

$$\{F\} = P \begin{Bmatrix} 0 \\ -1 \\ -1.2h \end{Bmatrix}$$

Substituting in Eq. 14.42 and solving for $\{D\}$, we obtain

$$\{D\} = \frac{P}{Eh} \begin{Bmatrix} -0.0138 \\ -16.8782 \\ 1.884/h \end{Bmatrix}$$

Combining Eqs. 14.38 and 14.31, we find the forces resisted by any one of the wall assemblies

$$\{Q\}_i = \left[\bar{S}\right]_i [C]_i \{D\}$$

For example, the forces on wall 2 are

$$\{Q\}_2 = \left[\bar{S}\right]_2 \begin{bmatrix} 1 & 0 & 0.8h \\ 0 & 1 & 4.4h \\ 0 & 0 & 1 \end{bmatrix} \{D\} = P \begin{bmatrix} 0.0000 \\ -0.3176 \\ 0.00044h \end{bmatrix}$$

The forces on all three walls are shown in Figure 14.12c.

14.7.2 *Multistorey structure*

A typical wall assembly in a building with n floors is shown in Figure 14.13a. Figure 14.13b is an isometric view of a vertical axis through the shear center of a shear wall assembly i. The local coordinates 1^* to n^* and $(n+1)^*$ to $(2n)^*$ lie in vertical planes parallel to the principal axes of inertia of the cross sections u and v respectively (Figure 14.13b). The directions of u and v are assumed to be the same at all floors for a given wall. The third set of coordinates,

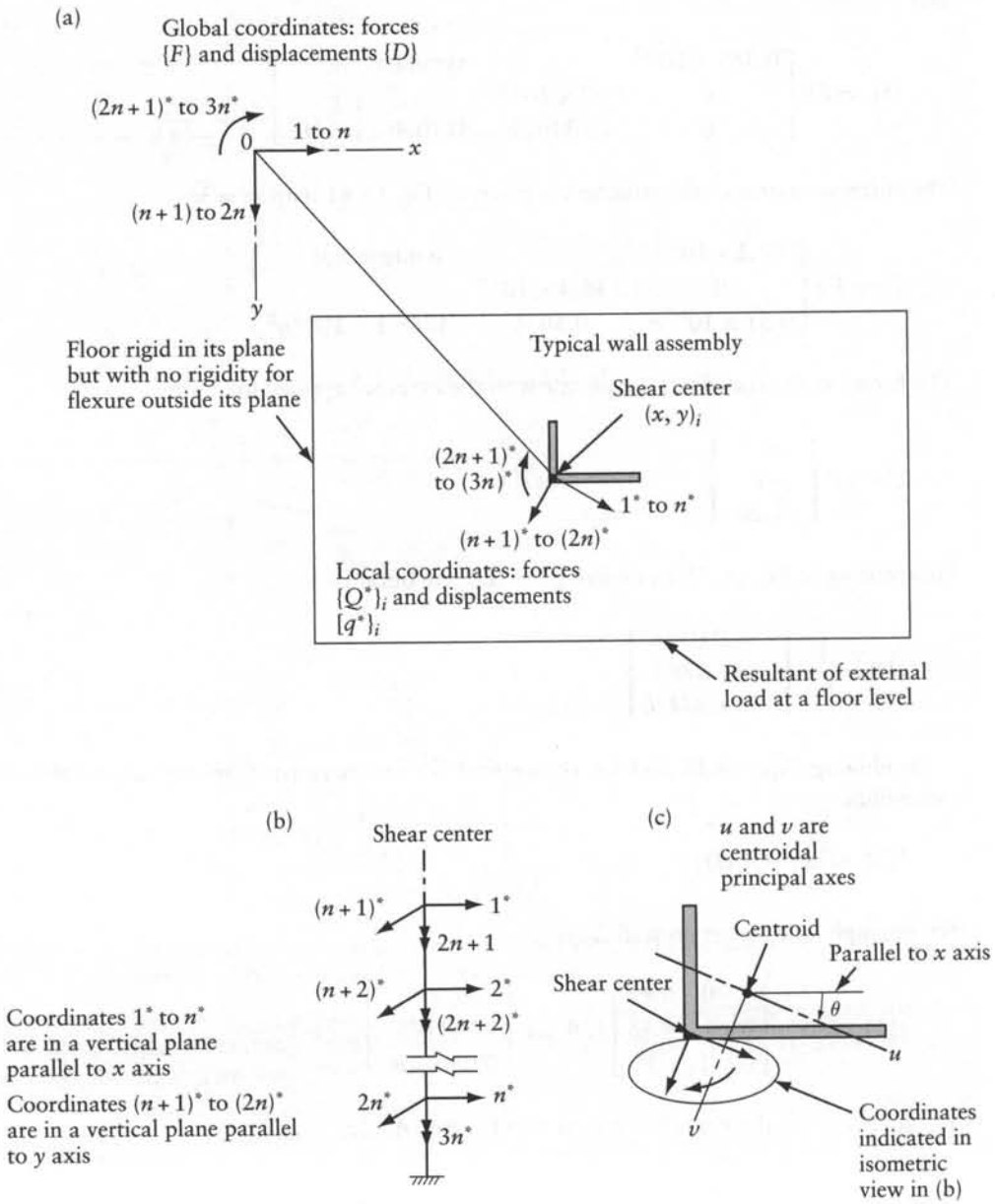

Figure 14.13 Coordinates for the analysis of a multistorey shear wall structure. (a) Coordinate system. (b) Local coordinates for a typical wall. (c) Plan of a typical wall assembly.

$(2n+1)^*$ to $(3n)^*$, represent angles of twist or twisting couples. The stiffness matrix for the ith wall corresponding to these coordinates is of the form

$$[S^*]_i = \begin{bmatrix} [S_u^*] & & \\ & [S_v^*] & \\ \text{Submatrices not} & & [S_\theta^*] \\ \text{show are zero} & & \end{bmatrix} \tag{14.43}$$

Each of the submatrices $[S_u^*]_i$ and $[S_v^*]_i$ can be determined separately in a way similar to that used for a plane structure in Sections 14.4 and 14.5 (using Eq. 5.17). If warping is ignored and the wall is encastré at the base, the submatrix $[S_\theta^*]_i$ will be

$$[S_\theta^*]_i = \left[\begin{array}{c|cc|cc|c} \left(\frac{GJ}{h}\right)_1 & & & & & \\ -\left(\frac{GJ}{h}\right)_1 & \left(\frac{GJ}{h}\right)_1+\left(\frac{GJ}{h}\right)_2 & & \text{symmetrical} & & \\ & -\left(\frac{GJ}{h}\right)_2 & & \left(\frac{GJ}{h}\right)_2+\left(\frac{GJ}{h}\right)_3 & & \\ & & & \cdots & & \\ & & & & \cdots & \\ & & & & -\left(\frac{GJ}{h}\right)_{n-1} & \left(\frac{GJ}{h}\right)_{n-1}+\left(\frac{GJ}{h}\right)_n \end{array}\right]_i \tag{14.43a}$$

where the subscripts refer to the storey number reckoned from the top of the structure.

In order to consider the effect of warping in a rational way, the angles of twist can be calculated at floor levels due to a unit twisting couple acting separately at each floor,[5] thus forming a flexibility matrix which, when inverted, gives $[S_\theta^*]$. At a fixed base, the warping is restrained whereas it is free to occur in the upper stories in a high building. Thus, neglecting warping underestimates the torsional stiffness at the floors near the base.

The displacements $\{q^*\}_i$ and the forces $\{Q^*\}_i$ at the coordinates in Figure 14.13b are related by

$$\{Q^*\}_i = [S^*]_i \{q^*\}_i \tag{14.44}$$

A global coordinate system is defined in Figure 14.13a, in which the coordinates 1 to n, and $(n+1)$ to $2n$ represent translations or horizontal forces at the floor levels at an arbitrary point O, and $(2n+1)$ to $3n$ are floor rotations or twisting couples. The displacements $\{q^*\}_i$ and $\{D\}$ are related by geometry so that

$$\{q^*\}_{i3n\times 1} = [B]_{i3n\times 3n} \{D\}_{3n\times 1} \tag{14.45}$$

where

$$[B]_i = \left[\begin{array}{ccc} \lceil\cos\theta,\ldots\rfloor & \lceil\sin\theta,\ldots\rfloor & \lceil(x\sin\theta - y\cos\theta),\ldots\rfloor \\ \hline \lceil-\sin\theta,\ldots\rfloor & \lceil\cos\theta,\ldots\rfloor & \lceil(x\cos\theta + y\sin\theta),\ldots\rfloor \\ \hline [0] & [0] & [I] \end{array}\right] \tag{14.46}$$

5 See reference in footnote 4 of this chapter: use Eq. (p), p. 260 of that reference.

The special brackets used indicate diagonal submatrices, each of order $n \times n$. The diagonal term for each of these submatrices is given above. The principal axes of any wall are assumed to have the same directions in all floors. If, in addition, the x and y coordinates of the shear center are the same in all floors, the submatrices have a diagonal element repeated in each row. For example,

$$[B_{11}]_i = \lceil \cos\theta, \cos\theta, \ldots, \cos\theta \rfloor_i = \cos\theta_i \, [I]$$

If the coordinates x and y change from floor to floor, the submatrix $[B_{13}]_i$ is

$$[B_{13}]_i = \lceil (x_1 \sin\theta - y_1 \cos\theta), \ldots, (x_j \sin\theta - y_j \cos\theta), \ldots \rfloor$$

where the subscripts of x and y indicate the floor (1 means the top floor and n the lowest floor). A similar equation can be written for $[B_{23}]_i$.

Applying Eq. 9.17, the stiffness matrix of the ith wall corresponding to the global coordinates can be obtained from

$$[S]_i = [B]_i^T \, [S^*]_i \, [B]_i \tag{14.47}$$

If $[B]_i$ is divided into submatrices $[B_1]_i$, $[B_2]_i$, and $[B_3]_i$ (each of order $n \times 3n$) along the horizontal dashed lines in Eq. 14.46, then Eq. 14.47 can be written in a more convenient form

$$[S]_i = \sum_{r=1}^{3} [B_r]_i^T \, [S_r^*]_i \, [B_r]_i \tag{14.47a}$$

where $[S_r^*]_i$ with $r = 1,2,3$ are the three submatrices $[S_u^*]$, $[S_v^*]$ and $[S_\theta^*]$ of $[S^*]_i$ defined in Eq. 14.43.

When x_i and y_i coordinates are the same at all floors, Eq. 14.47a yields

$$[S]_i = \left[\begin{array}{c|c|c} c^2 [S_u^*] + S^2 [S_v^*] & & \text{symmetrical} \\ \hline cs([S_u^*] - [S_v^*]) & s^2 [S_u^*] + c^2 [S_v^*] & \\ \hline c(xs - yc)[S_u^*] & s(xs - yc - [S_u^*]) & (xs - yc)^2 [S_u^*] + \\ s(xc + ys)[S_v^*] & c(xc + ys)[S_v^*] & (xc + ys)^2 [S_v^*] + [S_\theta^*] \end{array}\right]_i \tag{14.47b}$$

where $c = \cos\theta$ and $s = \sin\theta$.

The stiffness matrix of the structure corresponding to the global coordinates is obtained by summation

$$[S] = \sum_{i=1}^{m} [S]_i \tag{14.48}$$

where m is the number of wall assemblies.

The displacements at the global coordinates can now be determined by solving the equation

$$\{F\}_{3n\times 1} = [S]_{3n\times 3n} \{D\}_{3n\times 1} \tag{14.49}$$

where $\{F\}$ are forces at the global coordinates equivalent to the external loading. The forces on each wall assembly can be calculated by Eqs. 14.44 and 14.45.

Example 14.3: Three-storey structure

Analyze the structure of Example 14.2 but with three stories instead of one.

Let the center of the global coordinates be chosen at the center of the shaft (wall 1 in Figure 14.12b) with the coordinates 1, 2, and 3 representing translation in the x direction, 4, 5, and 6 translation in the y direction, and 7, 8, and 9 rotation in the clockwise direction. The stiffness matrix $[S]_2$ of wall 2 with respect to the global coordinates is derived below in some detail. For simplicity, deformation due to shear forces is ignored.

First, a stiffness matrix of order 6×6 is generated corresponding to a translation in the u direction and a rotation about the v axis at each floor level.[6] This matrix is then condensed by Eq. 5.17 to obtain

$$[S_u^*]_2 = 10^{-3}Eh \begin{bmatrix} 0.2100 & \text{symmetrical} & \\ -0.4800 & 1.320 & \\ 0.3600 & -1.380 & 2.400 \end{bmatrix}$$

By a similar procedure, we obtain

$$[S_v^*]_2 = \frac{Eh}{10} \begin{bmatrix} 0.5525 & \text{symmetrical} & \\ -1.263 & 3.473 & \\ 0.9471 & -0.3631 & 0.6314 \end{bmatrix}$$

Because the cross section and the height of wall 2 are the same in all floors and warping is ignored, Eq. 14.43a gives

$$[S_\theta^*]_2 = 0.2304 \times 10^{-3}Eh^3 \begin{bmatrix} 1 & \text{symmetrical} & \\ -1 & 2 & \\ 0 & -1 & 2 \end{bmatrix}$$

For the transformation of the stiffness matrix $[S^*]_2$ corresponding to local coordinates into the matrix $[S]_2$ referring to the global coordinates (using Eq. 14.47) we need the transformation matrix $[B]_2$ given by Eq. 14.46. Substituting in this equation $i=2$, $\theta=0$, $x=4.4b$, and $y=-0.8b$, we obtain

$$[B]_2 = \begin{bmatrix} [I] & [0] & h\lceil 0.8, 0.8, 0.8 \rfloor \\ [0] & [I] & h\lceil 4.4, 4.4, 4.4 \rfloor \\ [0] & [0] & [I] \end{bmatrix}$$

Equation 14.47 or 14.47b gives

$$[S]_2 = E \begin{bmatrix} h \begin{bmatrix} 2100e-7 & & \\ -4800e-7 & 1320e-6 & \\ 3600e-7 & -1380e-6 & 2400e-6 \end{bmatrix} & \text{symmetrical} & \\ h \begin{bmatrix} 0 & 0 & 0 \\ 0 & 0 & 0 \\ 0 & 0 & 0 \end{bmatrix} & h \begin{bmatrix} 5525e-5 & & \\ -1263e-4 & 3473e-4 & \\ 9471e-5 & -3631e-4 & 6314e-4 \end{bmatrix} & \\ h^2 \begin{bmatrix} 1680e-7 & -3840e-7 & 2880e-7 \\ -3840e-7 & 1056e-6 & -1104e-6 \\ 2880e-7 & -1104e-6 & 1920e-6 \end{bmatrix} & h^2 \begin{bmatrix} 2431e-4 & -5556e-4 & 4167e-4 \\ 5556e-4 & 1528e-3 & -1597e-3 \\ 4167e-4 & -1597e-3 & 2778e-3 \end{bmatrix} & h^3 \begin{bmatrix} 1070e-3 & & \\ -2445e-3 & 6724e-3 & \\ 1834e-3 & -7030e-3 & 1223e-2 \end{bmatrix} \end{bmatrix}$$

6 See answer to Prob. 14.2 for a general form of the matrix required.

By a similar procedure, $[S]_1$ and $[S]_3$ for walls 1 and 3 are derived and added to $[S]_2$ to obtain the stiffness matrix of the structure (Eq. 14.48).

The forces at the global coordinates equivalent to the external applied loads are

$$\{F\} = P\{0, 0, 0, -1, -1, -1, -1.2h, -1.2h, -1.2h\}$$

Solving for $\{D\}$ in Eq. 14.49, we obtain

$$\{D\} = \frac{P}{Eh}\{-0.9923e - 1, -0.5423e - 1, -0.1669e - 1, -0.2948e + 3, -0.1608e + 3,$$
$$-0.4935e + 2, 0.3280e + 2/h,\ 0.1793e + 2/h, 0.5516e + 1/h\}$$

Substitution in Eqs. 14.44 and 14.45 gives the forces in the walls at each of the three stories; these are given in Figure 14.14.

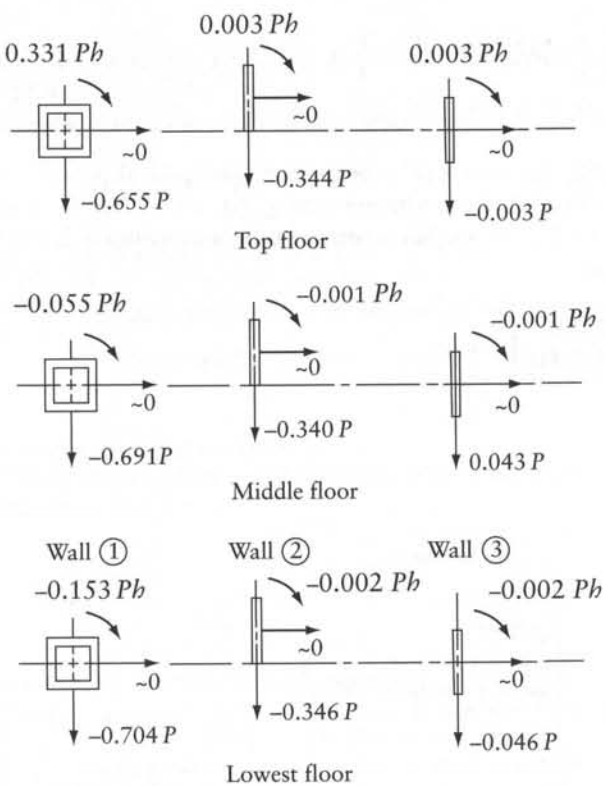

Figure 14.14 Forces resisted by various walls in Example 14.3.

14.8 Outrigger-braced high-rise buildings

The drift of a tall building caused by horizontal forces due to wind or earthquake can be reduced by the provision of outriggers. Figure 14.15a represents plan of a typical floor of a tall building, in which the core is composed of two halves; each consists of concrete walls housing the elevator shafts. The core is the main lateral force-resistant component. The maximum horizontal displacement (the drift) is limited by codes for the stability of the building and for the comfort of its occupants. Also, the codes limit the interstorey drift ratio, defined as the difference of drift in two consecutive floors divided by the vertical distance between them. The sum of the moments at the ends of a column at a floor level is a couple transferred, in the opposite direction, to the floor; the floor must be designed for the flexural and shear stress caused by the transfer. The moments transferred between the columns and the floors are mainly dependent on the interstorey drift ratio.

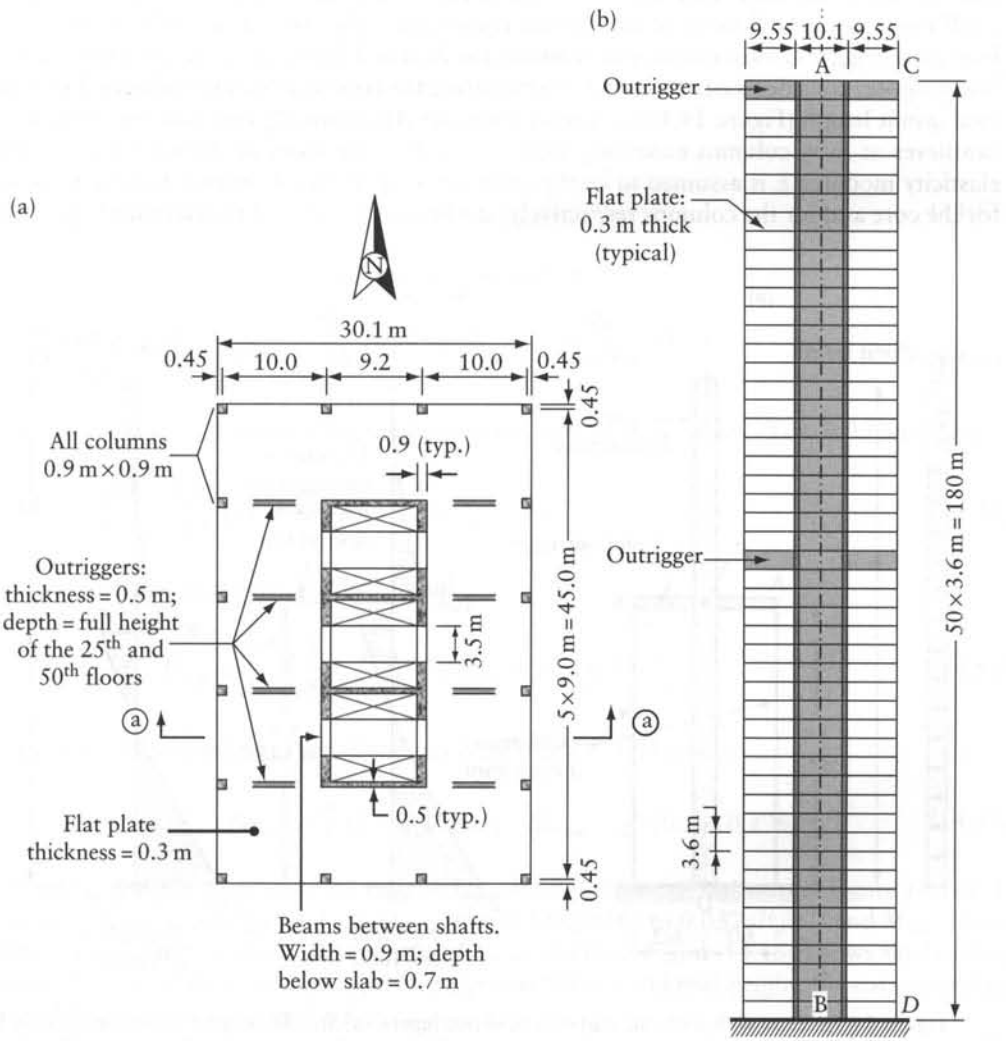

Figure 14.15 Tall building with outriggers (Example 14.4). (a) Plan of a typical floor. (b) Sectional elevation a-a.

The outriggers are relatively stiff horizontal members, of depth commonly equal to one-storey height, connecting the core to the exterior columns, inducing in them tensile and compressive forces, forming stabilizing couples that reduce the maximum drift and the interstorey drift ratio. The outriggers can be at one level or at two levels (Figure 14.15b), or at up to four levels in very tall buildings. For lateral loads in the west–east direction on the building in Figure 14.15, the columns at the east and the west extremities of the outriggers are subjected to tensile and compressive forces respectively; the corresponding internal forces act downward and upward at the east and the west extremities, respectively, of the outriggers. A stiff spandrel girder or truss on the periphery can also be provided to connect the outer ends of the outriggers and also to mobilize the columns on the north and west ends of the building to stiffen the core.

14.8.1 Location of the outriggers

The outriggers are walls that impair the use of the floor area; thus, they are usually located in a tall building in the floor(s) of mechanical equipments. However, it is useful to study at what level an outrigger is most effective in reducing the drift and the bending moment in the core. For this purpose, consider a cantilever CD representing the core of a building subjected to uniform load q/unit length (Figure 14.16a). A rigid outrigger AB elastically restrains the rotation of the cantilever at E by columns extending from A and B to the base, at the same level as D. The elasticity modulus E is assumed to be the same for all members. Constant I and a are assumed for the core and for the columns respectively; the flexural rigidity of the columns is ignored and

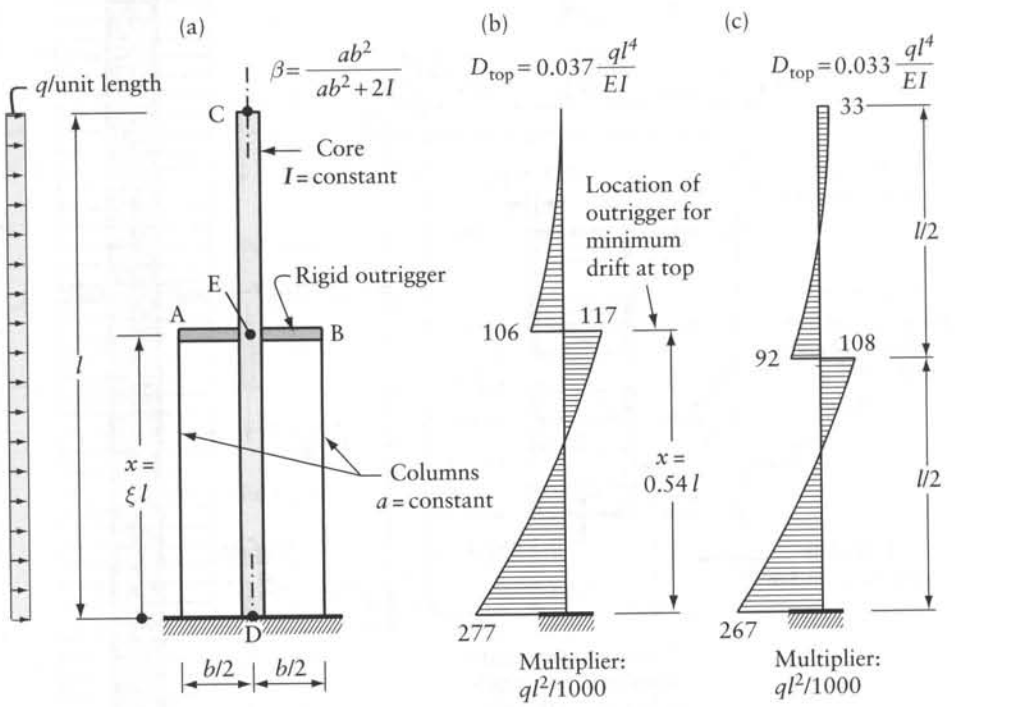

Figure 14.16 Core wall with one and two rigid outriggers. (a) Simplified model considering only bending deformation of the core and axial deformation of the columns. (b) Bending moment in core with one outrigger at $x = 0.54l$, with $\beta = 0.8$. (c) Bending moment in core with outriggers at top and at mid-height, with $\beta = 0.8$.

only their axial deformation and the bending deformation of the core are considered. The floors connecting the core to the exterior columns also restrain the free rotation and translation of the core; the existence of these floors is ignored here, but it is assumed that their presence excludes buckling of the exterior columns. We analyze the structure by the force method, releasing a single redundant F_1 representing the moment connecting AB to the cantilever at E; the redundant F_1 is a clockwise couple on AB and anticlockwise on the core. The incompatible rotation of the released core at E is (Eq. B.28):

$$D_1 = -\frac{ql^3}{6EI}\left(3\xi - 3\xi^2 + \xi^3\right) \tag{14.50}$$

where $\xi = x/l$. The relative rotation of the released core relative to AB at E due to $F_1 = 1$ is (Eq. B.31):

$$f_{11} = \frac{\xi l}{EI} + \frac{2\xi l}{Eab^2} \tag{14.51}$$

$$f_{11} = \frac{\xi l}{\beta EI} \tag{14.52}$$

where

$$\beta = ab^2/(ab^2 + 2I) \tag{14.53}$$

Thus, the redundant $F_1 (= -D_1/f_{11})$ can be expressed as:

$$F_1 = \frac{ql^2}{6}\beta(3 - 3\xi + \xi^2) \tag{14.54}$$

The drift at the top and the bending moment at the base of the core are (Eqs. B.29 and B.32):

$$D_{\text{top}} = \frac{ql^4}{8EI} - \frac{F_1 l^2}{EI}\xi(1 - 0.5\xi);\ M_{\text{base}} = \frac{ql^2}{2} - F_1 \tag{14.55}$$

When the outrigger is at the top, $\xi = 1.0$ and

$$F_1 = \frac{ql^2\beta}{6};\quad D_{top} = \frac{ql^4}{EI}\left(\frac{1}{8} - \frac{\beta}{12}\right);\quad M_{\text{base}} = ql^2\left(0.5 - \frac{\beta}{6}\right) \tag{14.56}$$

The location of the outrigger that minimizes D_{top} is at $\xi = 0.54$ giving:

$$F_1 = 0.279\beta ql^2;\quad D_{\text{top}} = \tfrac{ql^4}{EI}\left(\tfrac{1}{8} - 0.110\beta\right);\quad M_{\text{base}} = ql^2(0.5 - 0.279\beta) \tag{14.57}$$

The bending moment diagram of the core with $\xi = 0.54$ and $\beta = 0.8$ is shown in Figure 14.16b. It can be seen that the outrigger reduces D_{top} (from $0.125ql^2/EI$ to $0.037ql^2/EI$) and M_{base} (from $0.500ql^2$ to $0.278ql^2$) without affecting the shear at the base. Figure 14.16c shows the bending moment diagram of the core with rigid outriggers at the top and mid-height; the corresponding drift at the top is also given in the figure.

Considering the flexibility of the outrigger in the above equations will only increase f_{11} (Eq. 14.51) to become $\bar{f}_{11} = f_{11} + b(1 - \delta)^3/(12EI_o)$, where EI_o is the flexural rigidity of the outrigger, δ is a ratio (=the length of the rigid part of AB divided by $\overline{AB}$ (see Eq. 14.11)). For

practical values of I_o/I, considering the flexibility of the outriggers will have a small effect on the values given in Figures 14.16b and c; see the answers to Probs. 14.9 and 14.10.

Example 14.4: Concrete building with two outriggers subjected to wind load

The 50-storey reinforced concrete building shown in Figure 14.15 is analyzed for the effect of wind load in the east–west direction. For simplicity, uniform load q per unit height of the building is considered. The building is idealized as a plane frame subjected to a uniform load of intensity q (Figure 14.17a). Line AB represents the centroidal axis of the core; at each floor level, AB is connected to rigid elements representing the parts within the shaft width. Members on line CD represent the six columns on the east façade. The two columns, away from the corners, on the north and the south façades can contribute to resisting the wind load by framing with the corner columns; this relatively small contribution is here ignored for simplicity of presentation.

In calculating the cross-sectional properties of the members given in Figure 14.17a, the gross concrete sections are considered for the core (AB) and for the edge columns on CD; to account for cracking, half the gross concrete sections are considered for the floor slabs. Within the width of the core, the horizontal members are considered rigid. A single value of the elasticity modulus is assumed for all members.

The reactions at B and D and the bending moments in AB and CD are given in Figures 14.17a, b and c respectively. The applied moment of the wind load about the base is $500 \times 10^{-3} ql^2$. This is partly resisted by the anticlockwise moment reactions at B, D, and F; the total moment value $= (0.322 + 0.308 + 280)10^{-3} ql^2 = 281 \times 10^{-3} ql^2$, representing 56 percent of the applied moment. The remainder of the applied moment is resisted by the couple induced by the upward and downward vertical reactions at B and D respectively (Figure 14.17a); the resisting moment of the vertical reaction components $= 1.35ql \times 0.1622l = 219 \times 10^{-3} ql^2$.

If the wind load were resisted totally by the core, the horizontal displacement at the top would be $125 \times 10^{-3} ql^4/(EI)$, with $I = 744.9\,\text{m}^4 =$ the second moment of area of the core about its centroidal axis. Because of the interaction of the core with other members, the drift at the top is reduced to $D_{top} = 44 \times 10^{-3} ql^4/(EI)$. Repetition of the analysis with the cross-sectional area properties of the outriggers reduced by a factor of 0.5 (e.g. to account for cracking) gives results that are not significantly different.

In the above elastic analysis, a reduction factor of 0.5 is applied to the gross concrete cross-sectional area properties to obtain effective values that account for cracking of the slabs. Codes differ in their requirements for the reduction factors that account for the variation in concrete cracking of the structural components; different reduction factors are required for the slabs, the core, and the columns. The results in Figure 14.17 are obtained (using PLANEF, Appendix L) assuming that the length of the flexible parts of the outriggers is equal to their clear length (outside the faces of the core walls). To account for the high-strain penetration in the wall, an effective length – longer than the clear length (e.g. by 20%) – may be used. When reduction factors of 0.5 and 0.25 are applied to the gross concrete cross-sectional properties of all horizontal members, the outriggers and the slabs respectively, the following results are obtained: $D_{top} = 47 \times 10^{-3} ql^4/(EI)$; the anticlockwise moment reactions at F, B and $D = 0.328 \times 10^{-3} ql^2$, $296 \times 10^{-3} ql^2$, and $0.303 \times 10^{-3} ql^2$ respectively; the downward and upward reactions at F and $D = 1.253ql$. As expected, D_{top} and the bending moments in the shaft are increased.

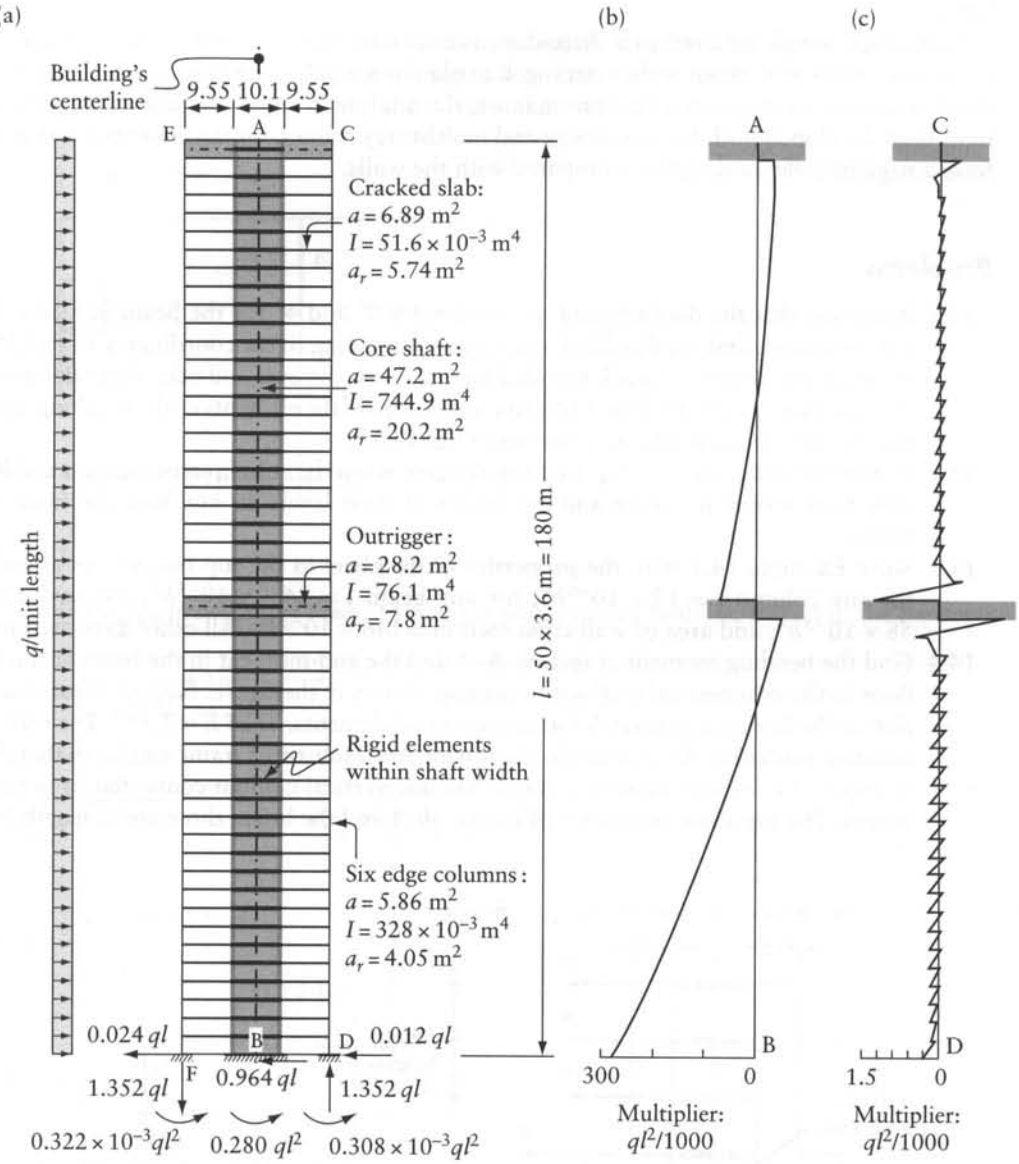

Figure 14.17 The tall building of Figure 14.15 analyzed for the effect of uniform wind load (Example 14.4). (a) Plane frame idealization of the right-hand half of the building. (b) Bending moment in the core. (c) Total bending moment in the six columns on the east edge.

14.9 General

The analysis of the effect of horizontal forces on building frames with shear walls is simplified by the assumption that each floor is infinitely rigid in its own plane, so that the degree of kinematic indeterminacy of the frame is considerably reduced.

Some regular building frames can be analyzed as plane structures, two procedures being available (Sections 14.4 and 14.5). In the simplified approximate method of Section 14.5 the

problem is reduced to the analysis of one wall and one substitute frame connected by inextensible links.

A relatively simple analysis of a three-dimensional structure is possible when it is composed of frames – with or without walls – arranged in plan in a regular rectangular pattern. When the shear walls are arranged in a random manner, the analysis is rather complex, but procedures have been developed both for one-storey and multistorey frames, on the assumption that floors have a negligible flexural rigidity compared with the walls.

Problems

14.1 Assuming that the displacement at coordinates 3* and 4* for the beam in Figure 14.3a are restrained, find the flexibility matrix corresponding to the coordinates 1* and 2*. Use the principle of virtual work to calculate the displacements and take shear deformation into account. Invert the derived matrix and compare the elements of the resulting stiffness matrix with the appropriate elements in Eq. 14.10.

14.2 Derive the submatrices in Eq. 14.18 in the case when the column cross section and height vary from storey to storey and the beams at floor levels do not have the same $(I/l)_b$ values.

14.3 Solve Example 14.1 with the properties of members in the top two stories as follows: for any column $I = 17 \times 10^{-6} b^4$; for any beam $I = 24.3 \times 10^{-6} b^4$; for any wall $I = 58 \times 10^{-3} b^4$; and area of wall cross section $= 146 \times 10^{-3} b^2$. All other data unchanged.

14.4 Find the bending moment at section A–A and the end-moment in the beam at the lower floor in the symmetrical wall with openings shown in the figure. Neglect shear deformation in the beams and axial deformations in all elements. Take $E = 2.3\,G$. The wall has a constant thickness. To idealize the shear wall, use a substitute frame similar to that shown in Figure 14.7b. The substitute frame has one vertical column connected to horizontal beams. The top three beams are of length $3b/4$ and the lower three are of length b.

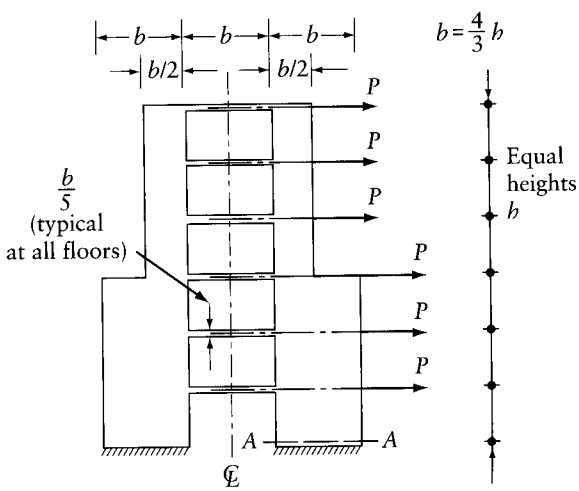

Prob. 14.4

14.5 Solve Prob. 14.4 by moment distribution. Use a substitute frame similar to the one in Figure 14.7b. and for any of the beams given in Eq. 14.29 (element $\bar{S}_{22}$ of the matrix in this equation). Because of the small stiffness of the beams in the substitute frame compared to

the stiffness of the column, the moment distribution in the above solution will converge slowly.

14.6 Find the forces on each of the shear walls in a single-storey building shown in the figure. All walls have thickness $= b/12$ and height $= b$ and are totally fixed to a rigid foundation. Neglect the warping effect of the shear walls. Take $E = 2.3\,G$.

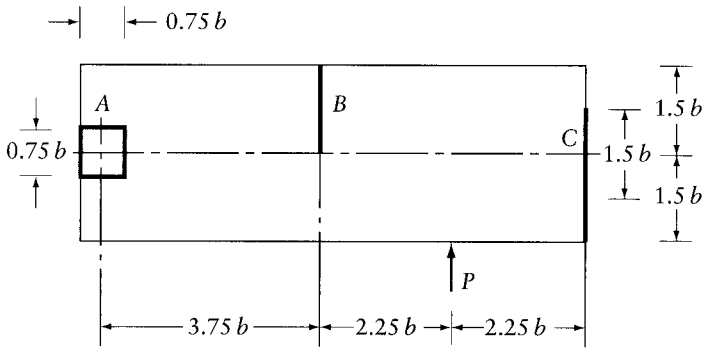

Prob. 14.6

14.7 Apply the requirements of Prob. 14.6 to the single-storey building shown in the figure.

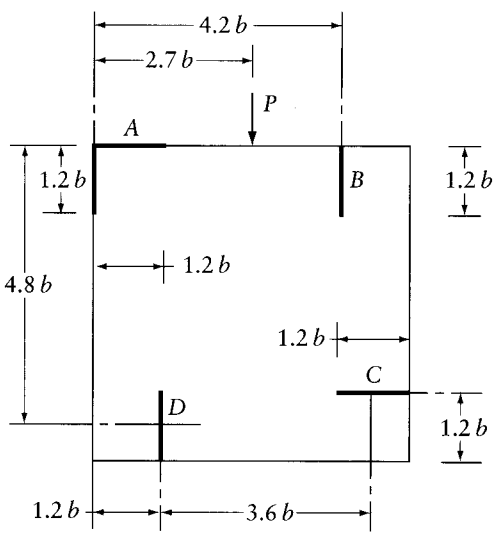

Prob. 14.7

14.8 Imperial units or 14.9 SI units. The figure shows a plan view of a curved slab bridge deck, supported on piers at B and C and on bearing pads above rigid abutments at A and D. The piers are assumed to be pin-connected to an infinitely rigid bridge deck. Each pier has a cross section 2 ft × 8 ft (or 0.6 m × 2.4 m) and is 40 ft (or 12 m) high and encastré at the base. The bearing pads at A and D have an area of 4 ft^2 (or 0.36 m^2), thickness 1.25 in. (or 32 mm) and shear modulus of elasticity $= 300$ lb/in^2 or (2.1 N/mm^2). Find the three displacement components of the deck and the forces on each of the supporting elements A, B, C, and D due to a force P at the deck level, as shown. Assume for the pier material: $E = 2.3G = 4000$ kip/in^2 (or 28 GN/m^2), and that the bearing pads at A and

D are strips of total length 8 ft, width 6 in. and height 1.25 in. (or length 2.4 m, width 0.15 m and height 32 mm).

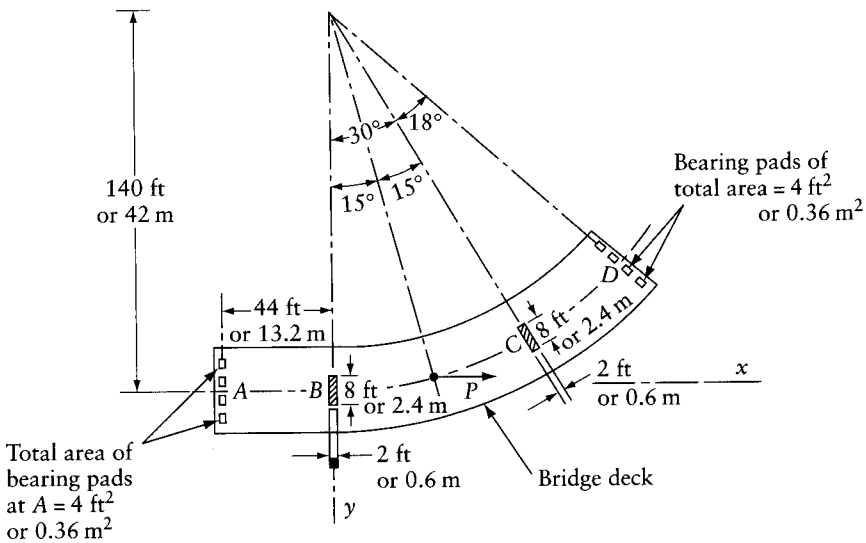

Prob. 14.8 or 14.9

14.10 Find the drift at the top and the bending moment diagram in the core wall in Figure 14.16 with rigid outriggers at the top and at mid-height. The outer columns have constant cross section, the area of which is $a = 8I/b^2$, where I is the second moment of the cross-sectional area of the core. Consider only bending deformation of the core and axial deformation of the columns; E = constant for all members. The answers are given in Figure 14.16c.

14.11 Solve Prob. 14.10 considering flexible outriggers with $I_o/I = 0.2$ or 2.0; where I_o is the second moment of the cross-sectional area of the outriggers about their centroidal axis. Assume: $b = l/5$; $\delta = 1/15$ =ratio of the length of rigid part of each outrigger (=the width of the core) to its total length b (Figure 14.16a). The answers to this problem and Prob. 14.10 show the effect of varying I_o/I as follows: $I_o/I = 0.2$, 2.0, and ∞.

Chapter 15

Method of finite differences

15.1 Introduction

We should bear in mind that all methods of structural analysis are essentially concerned with solving the basic differential equations of equilibrium and compatibility, although in some of the methods this fact may be obscured. Analytical solutions are limited to the cases when the load distribution, section properties, and boundary conditions can be described by mathematical expressions, but for complex structures numerical methods are in general a more practical means of analysis.

One of these is the finite-difference method, in which a numerical solution of the differential equation for displacement or stress resultant is obtained for chosen points on the structure, referred to as *nodes* or *pivotal points,* or simply as points of division. The numerical solution is thus obtained from differential equations which are applicable to the actual continuous structure. This is different from the *finite-element* method (dealt with in Chapters 16 and 17), in which the actual continuous structure is idealized into an assembly of discrete elements, for which force-displacement relations and stress distributions are determined (or assumed), and the complete solution is obtained by combining the individual elements into an idealized structure for which the conditions of equilibrium and compatability are satisfied at the junctions of these elements.

The numerical solution by finite differences generally requires replacing the derivatives of a function by difference expressions of the function at the nodes. The differential equation governing the displacement (or stress) is applied in a difference form at each node, relating the displacement at the given node and at nodes in its vicinity to the external applied load. This usually provides a sufficient number of simultaneous equations for the displacements (or stresses) to be determined. The finite-difference coefficients of the equations applied at nodes on, or close to, the boundary have to be modified, compared with the coefficients used at interior points, in order to satisfy the boundary conditions of the problem. Therein lies one of the difficulties of the method of finite differences and a disadvantage in its use compared with the finite-element method. Nevertheless, the finite-difference method can be conveniently used for a variety of problems, and, when it is used, the number of simultaneous equations required (for a comparable degree of accuracy) is generally only about a half or a third of the number of the equations needed in the finite-element method.

15.2 Representation of derivatives by finite differences

Figure 15.1 represents a function $y = f(x)$, which for our purposes can, for example, be the deflection of a beam. Consider equally-spaced abscissae x_{i-1}, x_i and x_{i+1} and the corresponding ordinates y_{i-1}, y_i, and y_{i+1}. The derivative (or the slope) of the curve at point $x_{i-\frac{1}{2}}$ midway between i and $i-1$ can be approximated by

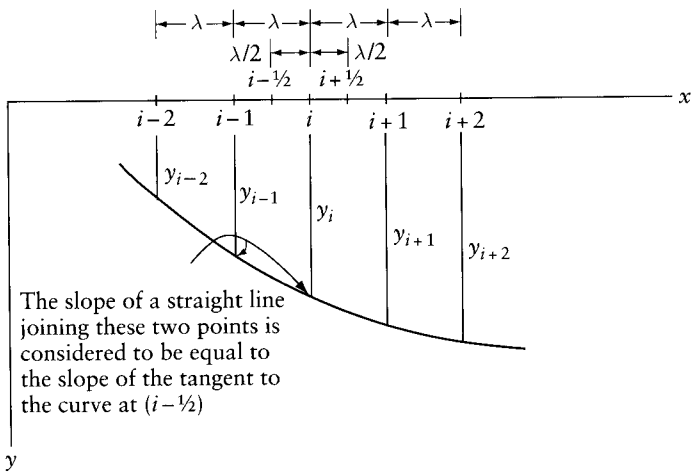

Figure 15.1 Graph of function $y = f(x)$.

$$\left(\frac{dy}{dx}\right)_{i-\frac{1}{2}} \cong \frac{1}{\lambda}(y_i - y_{i-1}) \tag{15.1}$$

where λ is the spacing of the abscissae. Similarly, the slope of the curve midway between i and $i+1$ is

$$\left(\frac{dy}{dx}\right)_{i+\frac{1}{2}} \cong \frac{1}{\lambda}(y_{i+1} - y_i) \tag{15.2}$$

The second derivative at i (which is the rate of change of slope) is approximately equal to the difference between the slope at $i+\frac{1}{2}$ and at $i-\frac{1}{2}$ divided by λ thus,

$$\left(\frac{d^2y}{dx^2}\right)_i \cong \frac{1}{\lambda}\left[\left(\frac{dy}{dx}\right)_{i+\frac{1}{2}} - \left(\frac{dy}{dx}\right)_{i-\frac{1}{2}}\right]$$

Substituting from Eqs. 15.1 and 15.2,

$$\left(\frac{d^2y}{dx^2}\right)_i \cong \frac{1}{\lambda^2}(y_{i+1} - 2y_i + y_{i-1}) \tag{15.3}$$

In the above expressions we have used *central differences* because the derivative of the function in each case was expressed in terms of the values of the function at points located symmetrically with respect to the point considered. The process can be repeated to calculate higher derivatives, in which case the values of y at a greater number of equally-spaced points are required. This is done in the finite-difference pattern of coefficients as shown in Figure 15.2.

The first derivative at i can also be expressed in terms of y_{i-1} and y_{i+1} with interval 2λ. Similarly, the third derivative at i can be expressed from the difference of the second derivatives at $i+1$ and $i-1$ with interval 2λ. The resulting coefficients are given in the last two rows of Figure 15.2.

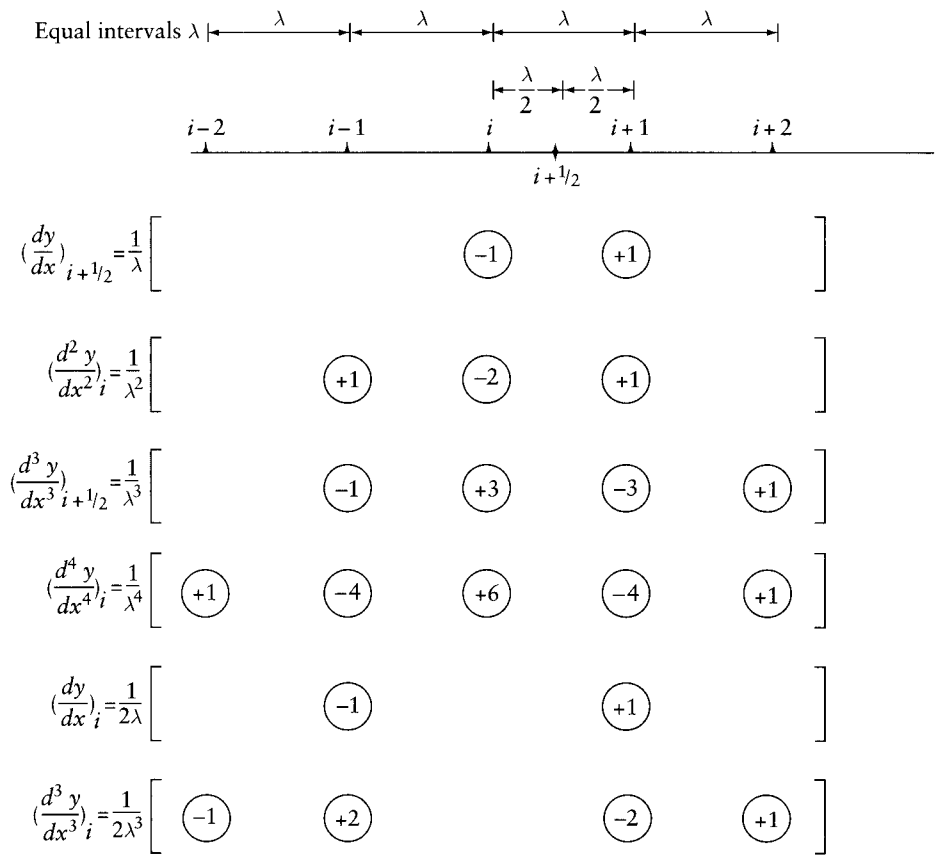

Figure 15.2 Finite-difference pattern of coefficients, using central differences.

Other finite-difference expressions can be obtained by considering *forward or backward differences*, in which the derivative at any point is expressed in terms of the value of the function at points in ascending or descending order with respect to the point under consideration. The central differences are more accurate than either forward or backward differences and they will be used in this chapter.

15.3 Bending moments and deflections in a statically determinate beam

Consider a simple beam AB subjected to vertical loading of varying intensity, as shown in Figure 15.3. The bending moment M and the load intensity q are related by the differential equation (see Eqs 10.1 and 10.5)

$$\frac{d^2M}{dx^2} = -q \tag{15.4}$$

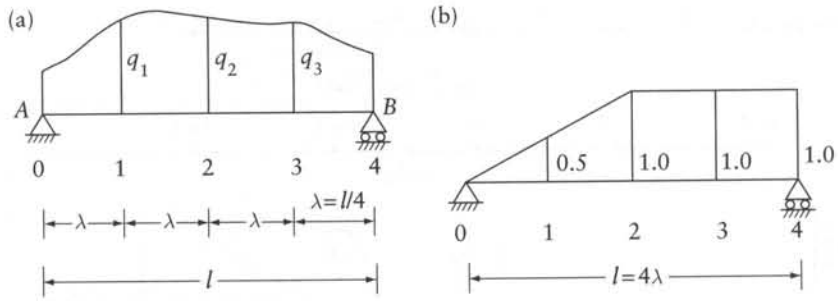

Figure 15.3 Simple beam subjected to nonuniform loading. (a) Beam divisions used in the finite-difference Eq. 16.14. (b) Beam considered in Example 15.1.

which, when applied at a general point i, can be put in the finite-difference form (see Figure 15.2)

$$[1 \quad -2 \quad 1] \begin{Bmatrix} M_{i-1} \\ M_i \\ M_{i+1} \end{Bmatrix} \cong -q_i \lambda^2 \tag{15.5}$$

The load q is positive when downward and M is positive when the bottom fiber is in tension; x is measured from the left-hand end of the beam.

The bending moment at the ends of the beam of Figure 15.3a is $M_0 = M_4 = 0$. Writing Eq. 15.13 at each of the three interior points, we obtain

$$\begin{bmatrix} 2 & -1 & 0 \\ -1 & 2 & -1 \\ 0 & -1 & 2 \end{bmatrix} \begin{Bmatrix} M_1 \\ M_2 \\ M_3 \end{Bmatrix} \cong \lambda^2 \begin{Bmatrix} q_1 \\ q_2 \\ q_3 \end{Bmatrix} \tag{15.6}$$

With the load q known, the solution of these three simultaneous equations gives the moments M_1, M_2, and M_3.

In the beam considered, we have found it possible to carry out the analysis by using only the finite-difference equations relating the bending moment to the external loading. This is so because the bending moment at the ends of the beam is known to be zero, so that the finite-difference equations at the internal points are sufficient in number to determine the unknown moments. If, however, the beam is statically indeterminate, e.g. when the ends A and B are encastré, the end-moments are unknown. However, the deflection and slope at the ends are known to be zero, and we therefore use finite-difference equations relating the deflection to the applied loading, discussed in Section 15.4.

Example 15.1: Simple beam

Determine the bending moments in a simple beam with the loading shown in Figure 15.3b:

Applying Eq. 16.14 for the loading: $q_1 = 0.50$, $q_2 = 1.00$, and $q_3 = 1.00$, and solving, we obtain $\{M\} = l^2\{0.0703, 0.1094, 0.0859\}$. The exact answer is $\{M\} = l^2\{0.0677, 0.1042, 0.0833\}$.

15.3.1 Use of equivalent concentrated loading

We should note that the solution of Eq. 15.14 depends upon the intensity of loading at the nodes but does not take into account the manner in which the loading varies between these points. More accurate values would be obtained if the beam were divided into smaller intervals, thereby requiring a larger number of equations.

Exact values can be obtained if the actual loading is replaced by equivalent concentrated loads; the finite-difference Eq. 15.13 at a general point is then replaced by the exact equation

$$\begin{bmatrix} 1 & -2 & 1 \end{bmatrix} \begin{Bmatrix} M_{i-1} \\ M_i \\ M_{i+1} \end{Bmatrix} = -Q_i \lambda \tag{15.7}$$

where Q_i is an equivalent concentrated load replacing $(q_i \lambda)$ in Eq. 15.5. We should note that we no longer use $\cong$ but $=$, as Eq. 15.7 is exact. The method of calculating the equivalent concentrated load Q_i and the proof of Eq. 15.7 are given in Section 10.4.1 (refer to Eq. 10.13).

The bending moment M and the deflection y are related by the differential equation (see Section 10.2).

$$EI \frac{d^2y}{dx^2} = -M \tag{15.8}$$

where EI is the flexural rigidity of the beam, and x is the distance from its left-hand end. Comparing this equation with Eq. 15.4, we can write the approximate finite-difference form of Eq. 15.8 by replacing M and q in Eq. 15.5 by y and $M/(EI)$ respectively. Similarly, an exact form can be obtained by replacing M and Q in Eq. 15.7 by y and $\overline{w}_i$ where $\overline{w}_i$ is an equivalent elastic loading (refer to Eqs. 10.15 and 10.16). An example of the use of the approximate and exact equations in the calculation of deflection is given in Section 10.5.

15.4 Finite-difference relation between beam deflection and applied loading

The equations relating deflection to the bending moment can be used to calculate the deflections when the moments are known, as is the case in statically determinate beams. In statically indeterminate structures, it is more convenient to relate the deflections to the applied loads, and solve for deflections which can then be used to determine the unknown stress resultants.

From Eqs. 15.12 and 15.16, the deflection y and the intensity of loading q can be related by the differential equation

$$\frac{d^2}{dx^2}\left(EI \frac{d^2y}{dx^2}\right) = q \tag{15.9}$$

This equation can be put in finite-difference form in two steps as follows. First, the term in brackets (which is equal to minus the bending moment) is replaced by finite differences, using Eq. 15.3:

$$M_i \cong -\frac{EI_i}{\lambda^2}(y_{i-1} - 2y_i + y_{i+1}) \tag{15.10}$$

Then the second derivative of the moment is put in finite-difference form, again using Eq. 15.2:

$$\frac{d^2}{dx^2}\left(EI\frac{d^2y}{dx^2}\right) = -\left(\frac{d^2M}{dx^2}\right) \cong -\frac{1}{\lambda^2}(M_{i-1} - 2M_i + M_{i+1}) \tag{15.11}$$

The values of M_{i-1} and M_{i+1} can be expressed in terms of deflections by using Eq. 15.10 with $i-1$ and $i+1$ in place of i. Substituting these values in Eq. 15.11 and combining it with Eq. 15.9, we obtain the finite-difference equation applied at a general point i:

$$\frac{E}{\lambda^4}\left[I_{i-1}\middle|-2(I_{i-1}+I_i)\middle|(I_{i-1}+4I_i+I_{i+1})\middle|-2(I_i+I_{i+1})\middle|I_{i+1}\right] \times \begin{Bmatrix} y_{i-2} \\ y_{i-1} \\ y_i \\ y_{i+1} \\ y_{i+2} \end{Bmatrix} \cong q_i \tag{15.12}$$

The accuracy of this equation is improved if the equivalent concentrated load Q_i is used instead of $q_i\lambda$. Then Eq. 15.12 becomes

$$\frac{E}{\lambda^3}\left[I_{i-1}\middle|-2(I_{i-1}+I_i)\middle|(I_{i-1}+4I_i+I_{i+1})\middle|-2(I_i+I_{i+1})\middle|I_{i+1}\right] \times \begin{Bmatrix} y_{i-2} \\ y_{i-1} \\ y_i \\ y_{i+1} \\ y_{i+2} \end{Bmatrix} \cong Q_i \tag{15.13}$$

This equation is, in fact, a combination of the exact Eq. 15.7 and the approximate Eq. 15.10, and is therefore an approximate relation for beams of variable I. The pattern of coefficients of Eq. 15.13 is shown in Figure 15.4a.

When the beam is prismatic, i.e. I is constant, Eq. 15.13 simplifies to Eq. 15.21a, given in Figure 15.5a.

15.4.1 Beam with a sudden change in section

Consider the beam shown in Figure 15.6, which has a sudden change in the flexural rigidity at a node i. We propose to show that, if the flexural rigidities are EI_{il} and EI_{ir} at sections just to the left and just to the right of i respectively, Eqs. 15.12 and 15.13 are applicable with an effective flexural rigidity EI_i at i, where

$$\left.\begin{aligned} EI_i &= \left(\frac{2}{1+\alpha}\right) EI_{ir} \\ \text{and} \qquad \alpha &= \frac{EI_{ir}}{EI_{il}} \end{aligned}\right\} \tag{15.14}$$

Let the deflection at three equally-spaced points on the beam be y_{i-1}, y_i, and y_{i+1}. Extend the two parts AB and CB of the deflection line, respectively, to fictitious points C' and A' (Figure 15.6b) whose ordinates are y^f_{i+1} and y^f_{i-1}. For compatibility, the slope of the two curves are the same. Thus,

	Position of node i	Coefficient of the deflection in terms of E/λ^3					Right-hand side	Equation number
		Y_{i-2}	Y_{i-1}	Y_i^*	Y_{i+1}	Y_{i+2}		
(a)	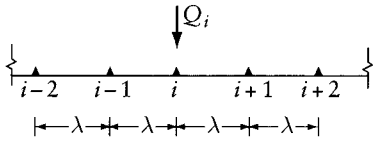	I_{i-1}	$-2(I_{i-1}+I_i)$	$(I_{i-1}+4I_i+I_{i+1})$	$-2(I_i+I_{i+1})$	I_{i+1}	$=Q_i$	15.13
(b)	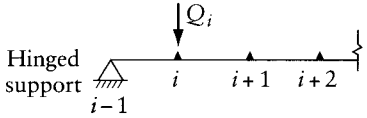	–	–	$(4I_i+I_{i+1})$	$-2(I_i+I_{i+1})$	I_{i+1}	$=Q_i$	15.19
(c)	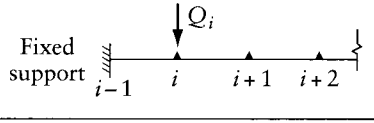	–	–	$(2I_{i-1})+4I_i+I_{i+1}$	$-2(I_i+I_{i+1})$	I_{i+1}	$=Q_i$	15.20
(d)	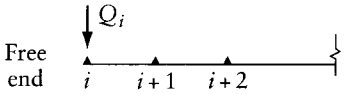	–	–	I_{i+1}	$-2I_{i+1}$	I_{i+1}	$=Q_i$	15.21
(e)	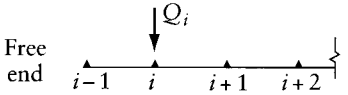	–	$-2I_i$	$(4I_i+I_{i+1})$	$-2(I_i+I_{i+1})$	I_{i+1}	$=Q_i$	15.22

* For a beam on elastic foundation of modulus K_i (force/length^2), add $K_i\lambda/2$ to the coefficient of Y_i in Eq. 15.21 and $K_i\lambda$ in other equation. If the beam is on elastic spring at i of stiffness K_i (force/length), add K_i to the coefficient of Y_i in all equations.

Figure 15.4 Finite-difference equations relating beam deflection to applied load.

	Position of node i	Coefficient of the deflection in terms of E/λ^3					Right-hand side	Equation number
		Y_{i-2}	Y_{i-1}	Y_i^*	Y_{i+1}	Y_{i+2}		
(a)	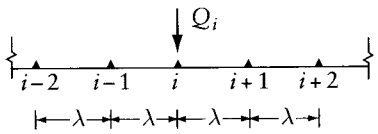	1	–4	6	–4	1	$=Q_i$	15.13a
(b)	Hinged support 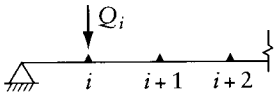	–	–	5	–4	1	$=Q_i$	15.19a
(c)	Fixed support 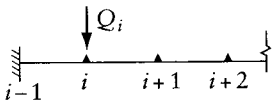	–	–	7	–4	1	$=Q_i$	15.20a
(d)	Free end 	–	–	1	–2	1	$=Q_i$	15.21a
(e)	Free end 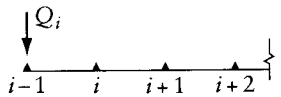	–	–2	5	–4	1	$=Q_i$	15.22a

* For a beam on elastic foundation of modulus K_i (force/length^2), add $K_i\lambda/2$ to the coefficient of Y_i in Eq. 16.29 and $K_i\lambda$ in other equation. If the beam is on elastic spring at i of stiffness K_i (force/length), add K_i to the coefficient of Y_i in all equations.

Figure 15.5 Finite-difference equations relating beam deflection to applied load, when I is constant.

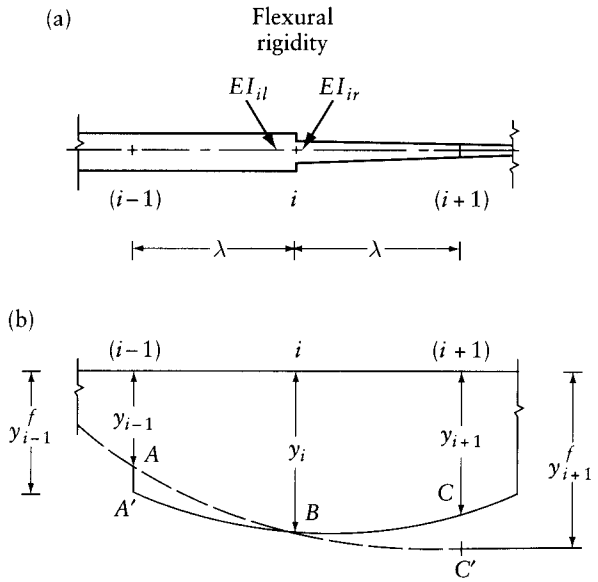

Figure 15.6 Deflection of a beam with a sudden change in section. (a) Beam properties. (b) Deflection line.

$$\frac{1}{2\lambda}(-y^f_{i-1}+y_{i+1})=\frac{1}{2\lambda}(y^f_{i+1}-y_{i-1}) \tag{15.15}$$

Also, for equilibrium, the bending moment just to the right and just to the left of node i must be the same, that is,

$$M_{il}=M_{ir}=M_i$$

Applying Eq. 15.10,

$$M_i=M_{il}=-\left(EI\frac{d^2y}{dx^2}\right)_{il}\cong-\frac{EI_{il}}{\lambda^2}(y_{i-1}-2y_i+y^f_{i+1}) \tag{15.16}$$

and

$$M_i=M_{ir}=-\left(EI\frac{d^2y}{dx^2}\right)_{ir}\cong-\frac{EI_{ir}}{\lambda^2}(y^f_{i-1}-2y_i+y_{i+1}) \tag{15.17}$$

From Eqs. 15.15 to 15.17, by eliminating the fictitious deflections, we obtain

$$M_i\cong-\left(\frac{2}{1+\alpha}\right)\frac{EI_{ir}}{\lambda^2}\begin{bmatrix}1 & -2 & 1\end{bmatrix}\begin{Bmatrix}y_{i-1}\\ y_i\\ y_{i+1}\end{Bmatrix} \tag{15.18}$$

If the quantity $2EI_{ir}/(1+\alpha)$ in this equation is substituted by an effective flexural rigidity EI_i (as defined in Eq. 15.14), Eq. 15.18 becomes identical with Eq. 15.10.

	Type of support		Coefficient of the deflection in terms of E/λ^3 when I is variable, or in terms of EI/λ^3 when I is constant					Right-hand side	Equation number
			Y_{i-2}	Y_{i-1}	Y_i^*	Y_{i+1}	Y_{i+2}		
(a)	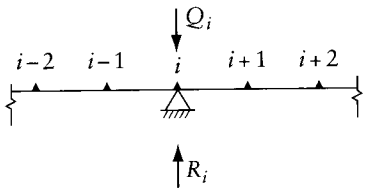 Intermediate support	Variable I	$-I_{i-1}$	$2(I_{i-1}+I_i)$	$-(I_{i-1}+4I_i+I_{i+1})$	$2(I_i+I_{i+1})$	$-I_{i+1}$	$=(R_i-Q_i)$	15.25
		Constant I	−1	4	−6	4	−1	$=(R_i-Q_i)$	15.25a
(b)	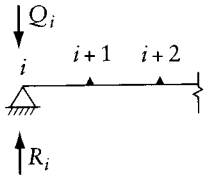 Hinged end	Variable I	–	–	$-I_{i+1}$	$2I_{i+1}$	$-I_{i+1}$	$=(R_i-Q_i)$	15.26
		Constant I	–	–	−1	2	−1	$=(R_i-Q_i)$	15.26a
(c)	Fixed-end moment M_i (given by) Eq. 16-36) 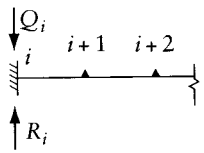 Rotation at i is prevented	Variable I	–	–	$-2(I_i+I_{i+1})$	$2(I_i+I_{i+1})$	$-I_{i+1}$	$=(R_i-Q_i)$	15.29
		Constant I	–	–	−3	4	−1	$=(R_i-Q_i)$	15.29a

* For a beam on elastic foundation of modulus k_i (force/length^2), add to the coefficient of y_i the value $(-k_i\lambda)$ in the first two equations and $(-k_i\lambda/2)$ in the other equations of this table.

Figure 15.7 Finite-difference equations relating beam deflection to reaction.

If the derivation of Eqs. 15.12 and 15.13 is reviewed, it can be seen that the sudden variation in the flexural rigidity can be accounted for simply by using an effective flexural rigidity (calculated by Eq. 15.14) at the node where the sudden change occurs. The same applies to all the other finite-difference equations in Figures 15.4, 15.5, and 15.7.

15.4.2 Boundary conditions

When the finite-difference Eq. 15.13 relating the deflection to external loading is applied at or near a discontinuous end, the deflections at fictitious nodes outside the beam are included. These deflections are then expressed in terms of the deflections at other nodes on the beam, the procedure for different end conditions being as follows.

(a) *SIMPLE SUPPORT.* The deflection and the bending moment are zero. Referring to Figure 15.4b, $y_{i-1} = 0$, and $M_{i-1} = 0$.

These two conditions are satisfied if the beam is considered to be continuous with another similar beam with similar loading acting in the opposite direction. Therefore, at a fictitious point $i-2$ (not shown in the figure), the deflection $y_{i-2} = -y_i$, and the finite-difference Eq. 15.13, when applied at a point i adjacent to a simple support, takes the form of Eq. 15.9 in Figure 15.4b.

(b) *FIXED END.* The deflection and the slope are zero. Referring to Figure 15.4c,

$$y_{i-1} = 0 \quad \text{and} \quad \left(\frac{dy}{dx}\right)_{i-1} = 0$$

These two conditions are satisfied if the beam is considered continuous with a similar beam loaded in the same manner as the actual beam. Therefore, $y_{i-2} = y_i$, and the finite-difference Eq. 15.13, when applied at a point i adjacent to a fixed support, takes the form of Eq. 15.20 in Figure 15.4c.

(c) *FREE END.* The bending moment is zero. Referring to Figure 15.4d, and considering simple statics, we can write

$$M_{i+1} = -Q_i\lambda$$

Substituting for M_{i+1} in terms of the deflections from Eq. 15.10, we obtain the finite-difference Eq. 15.21 applied at point i at the free end, given in Figure 15.4d.

Referring to Figure 15.4e, and applying Eq. 15.7, with $M_{i-1} = 0$, we obtain

$$-\frac{1}{\lambda}(-2M_i + M_{i+1}) = Q_i$$

Substituting for M_i. and M_{i+1} in terms of deflection from Eq. 15.10, we obtain the finite-difference Eq. 15.22 applied at point i adjacent to a free end, given in Figure 15.4e.

When the beam has a constant second moment of area, the equations listed in Figure 15.4 simplify to the form given in Figure 15.5.

15.5 Finite-difference relation between beam deflection and stress resultant or reaction

The finite-difference method can be used in the analysis of structures also for the purpose of determining the internal forces. First, the deflection is related to the loading by a finite-difference equation applied at each node where the deflection is unknown. The appropriate equation to be

used at each node is selected from Figures 15.4 or 15.5. Thus, we obtain a system of simultaneous linear equations which can be put in the form

$$[K]\{y\} = \{Q\} \tag{15.23}$$

Examination of the finite-difference coefficients of y in the equations listed in Figures 15.4 or 15.5 will show that the matrix $[K]$ is symmetrical. For example, the coefficient of y_{i+1} when the finite-difference equation is applied at node i in Figure 15.4d is the same as the coefficient of y_i when the equation is applied at node $i+1$ (see Figure 15.4e). In Section 15.15 we shall use the matrix $[K]$ as an equivalent stiffness matrix.

A solution of the equation $[K]\{y\} = \{Q\}$ makes it possible to find the nodal deflections $\{y\}$. With the deflections known, the bending moment, shear, and reactions can be calculated by the finite-difference equations derived below.

The shear midway between nodes i and $i+1$ is

$$V_{i+\frac{1}{2}} \cong \frac{1}{\lambda}(M_{i+1} - M_i)$$

Substituting for M_i from Eq. 15.10,

$$V_{i+\frac{1}{2}} \cong \frac{E}{\lambda^3}[I_i y_{i-1} - (2I_i + I_{i+1})y_i + (I_i + 2I_{i+1})y_{i+1} - I_{i+1}y_{i+2}] \tag{15.24}$$

The same value represents also the shear at any point between the nodes i and $i+1$ when no load acts between those nodes.

The reaction at an intermediate support i in a continuous beam is given in Figure 15.7a as

$$R_i = Q_i - \frac{E}{\lambda^3}[I_{i-1}y_{i-2} - 2(I_{i-1} + I_i)y_{i-1} + (I_{i-1} + 4I_i + I_{i+1})y_i - 2(I_i + I_{i+1})y_{i+1} + I_{i+1}y_{i+2}] \tag{15.25}$$

where Q_i is the equivalent concentrated load acting directly above the support.

The reaction at a hinged end i (Figure 15.7b) is

$$R_i = Q_i + \frac{M_{i+1}}{\lambda}$$

Substituting for M_{i+1} from Eq. 15.10,

$$R_i \cong Q_i - \frac{EI_{i+1}}{\lambda^3}(y_i - 2y_{i+1} + y_{i+2}) \tag{15.26}$$

The reaction at a totally fixed end is

$$R_i = Q_i + \frac{1}{\lambda}(M_{i+1} - M_i) \tag{15.27}$$

The moment M_i at a fixed end i where rotation is prevented but transverse displacement y_i can occur (Figure 15.7c) is

$$M_i \cong \frac{EI}{\lambda^2}(2y_i - 2y_{i+1}) \tag{15.28}$$

The bending moment M_i is, of course, numerically equal to the fixed-end moment. A positive M_i indicates a clockwise moment for a left-hand end of the beam.

Substituting for M_{i+1} and M_i in Eq. 15.28 in terms of deflection, we obtain the reaction at a totally fixed end i:

$$R_i = Q_i + \frac{E}{\lambda^3}[-(2I_i + I_{i+1})y_i + 2(I_i + I_{i+1})y_{i+1} - I_{i+1}y_{i+2}] \tag{15.29}$$

The various equations are collected in Figure 15.7, together with the corresponding equations for the case when I is constant. When there is no settlement at the support, $y_i = 0$ in the appropriate equation.

15.6 Beam on an elastic foundation

The basic differential equation for a beam resting on an elastic foundation is (see Eq. 10.5a)

$$\frac{d^2}{dx^2}\left(EI\frac{d^2y}{dx^2}\right) = q - ky \tag{15.30}$$

where k is the foundation modulus, that is, the foundation reaction per unit length of the beam per unit deflection (force/length^2), and the remaining notation is the same as used in Eq. 15.9.

The finite-difference form of Eq. 16.38 when applied at a general point i is

$$\frac{E}{\lambda^4}[I_{i-1}| - 2(I_{i-1} + I_i)|(I_{i-1} + 4I_i + I_{i+1})| - 2(I_i + I_{i+1})|I_{i+1}] \times \begin{Bmatrix} y_{i-2} \\ y_{i-1} \\ y_i \\ y_{i+1} \\ y_{i+2} \end{Bmatrix} \cong qi - k_i y_i \tag{15.31}$$

Equation 15.31 can be derived in the same way as Eq. 15.12. Using the equivalent concentrated load Q_i to replace $q_i\lambda$ and rearranging terms, Eq. 15.31 becomes

$$\frac{E}{\lambda^3}\left[I_{i-1}| - 2(I_{i-1} + I_i)|\left(I_{i-1} + 4I_i + I_{i+1} + \frac{k_i\lambda^4}{E}\right)| - 2(I_i + I_{i+1})|I_{i+1}\right] \times \begin{Bmatrix} y_{i-2} \\ y_{i-1} \\ y_i \\ y_{i+1} \\ y_{i+2} \end{Bmatrix} \cong Qi \tag{15.32}$$

This equation can be applied to a beam of variable section resting on a foundation of variable modulus. Comparing Eqs. 15.13 and 15.32, we see that the presence of the elastic foundation can be accounted for simply by adding the term $k_i\lambda$ to the coefficient of y_i. If, instead of an elastic foundation, a spring of stiffness K_i (force/length) is placed at point i, the term to be added to the coefficient of y_i is equal to K_i.

With a similar modification, all the other equations in Figures 15.4 and 15.5 can be used for a beam on an elastic foundation. The modification is indicated at the bottom of these two figures.

Example 15.2: Beam on elastic foundation

Determine the deflection, bending moment, and end support reactions for the beam of Figure 15.8a, which has a constant EI. The beam is resting on an elastic foundation between the supports with a modulus $k = 0.1024EI/\lambda^4$, where $\lambda = l/4$.

The dimensionless term is

$$\frac{k\lambda^4}{EI} = 0.1024$$

Applying the appropriate finite-difference equations from Figure 15.5 at each point of division, we can write

$$\frac{EI}{\lambda^3}\begin{bmatrix}(5+0.1024) & -4 & 1\\ -4 & (6+0.1024) & -4\\ 1 & -4 & (5+0.1024)\end{bmatrix}\begin{Bmatrix}y_1\\ y_2\\ y_3\end{Bmatrix} = q\lambda\begin{Bmatrix}1\\ 1\\ 1\end{Bmatrix}$$

for which the solution is

$$y_1 = y_3 = 1.928q\frac{\lambda^4}{EI} \quad \text{and} \quad y_2 = 2.692q\frac{\lambda^4}{EI}$$

or

$$y_1 = y_3 = 0.00753ql^4/EI \quad \text{and} \quad y_2 = 0.0105ql^4/EI$$

We may note in passing that we could have made use of symmetry of the structure by putting $y_1 = y_3$; hence, only two simultaneous equations would have required solving.

Applying Eq. 15.10 at points 1 and 2, we obtain

$$M_1 = -\frac{EI}{\lambda^2} \times q\frac{\lambda^4}{I}(0 - 2 \times 1.928 + 2.692) = 1.164q\lambda^2 = 0.0728ql^2$$

and

$$M_2 = -\frac{EI}{\lambda^2} \times q\frac{\lambda^4}{I}(1.928 - 2 \times 2.692 + 1.928) = 1.528q\lambda^2 = 0.0955ql^2$$

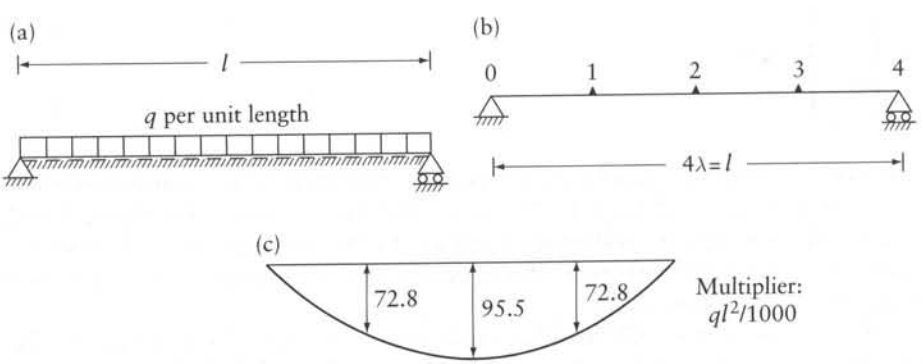

Figure 15.8 Beam on an elastic foundation considered in Example 15.2. (a) Beam on an elastic foundation. (b) Nodes. (c) Bending moment diagram.

The bending moment diagram for the beam is plotted in Figure 15.8c. The reaction at 0 is given by Eq. 15.34a (Figure 15.7b) as

$$\frac{EI}{\lambda^3}(2y_1 - y_2) = (R_0 - Q_0)$$

Substituting for y the values calculated previously and $Q_0 = q\lambda/2 = ql/8$, we find

$$R_0 = R_4 = 0.416ql$$

The exact values using an analytical solution[1] are: $y_1 = y_3 = 0.00732ql^4/EI$, $y_2 = 0.0102ql^4/EI$, $M_1 = M_3 = 0.0745ql^2$, $M_2 = 0.0978ql^2$, and $R_0 = R_4 = 0.414ql$.

15.7 Axisymmetrical circular cylindrical shell

Consider a thin-walled elastic cylinder subjected to any axisymmetrical radial loading. Because of symmetry, any section of the shell perpendicular to the cylinder axis will remain circular, while the radius r will undergo a change $\Delta r = y$. We need therefore to consider the deformation of only one strip parallel to the generatrix of the cylinder (Figure 15.9a). Let the width of the strip be unity.

The radial displacement y must be accompanied by a circumferential (or hoop) force (Figure 15.9b) whose magnitude per unit length of the generatrix is

$$N = \frac{Eh}{r}y \tag{15.33}$$

where h is the thickness of the cylinder and E is the modulus of elasticity. The hoop forces are considered positive when tensile. The radial deflection and loading are positive when outward.

The resultant of the hoop forces N on the two edges of the strip acts in the radial direction opposing the deflection, and its value per unit length of the strip is

$$-\frac{N}{r} = -\frac{Eh}{r^2}y \tag{15.34}$$

Hence, the strip may be regarded as a beam on an elastic foundation whose modulus is

$$k = \frac{Eh}{r^2} \tag{15.35}$$

Because of the axial symmetry of the deformation of the wall, the edges of any strip must remain in radial planes, and lateral extension or contraction (caused by bending of the strip in a radial plane) is prevented. This restraining influence is equivalent to a bending moment in a circumferential direction.

$$M_\phi = \nu M \tag{15.36}$$

1 See Hetényi, M., *Beams on Elastic Foundation*, University of Michigan Press, Ann Arbor, 1952, p. 60.

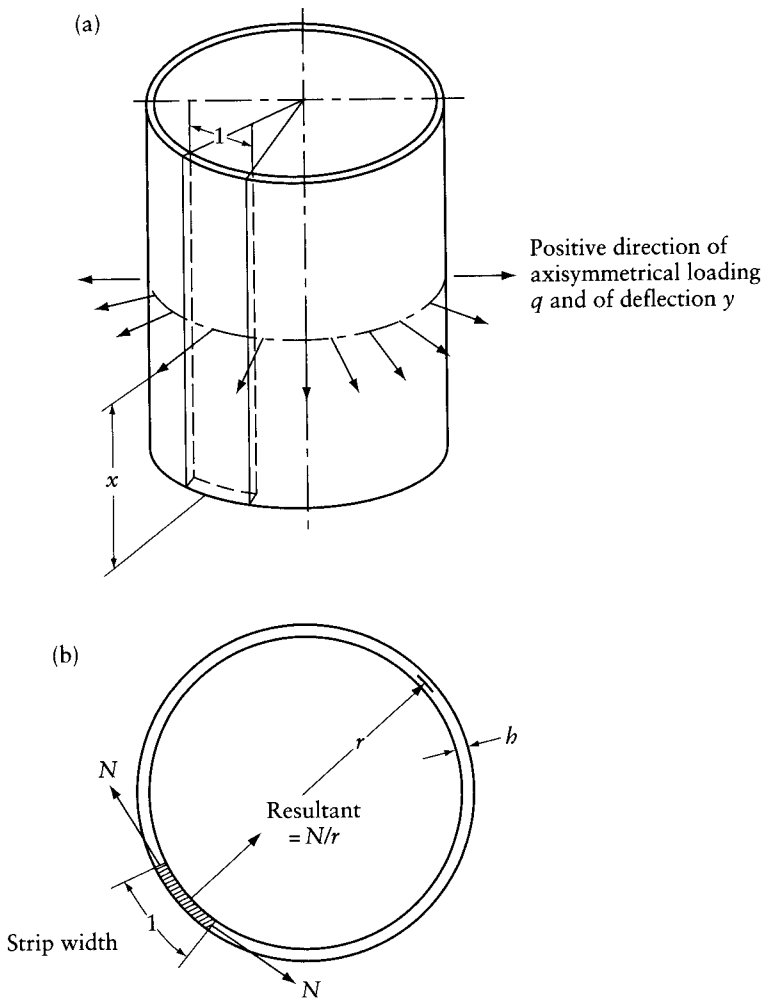

Figure 15.9 A strip parallel to the generatrix of an axisymmetrical cylindrical wall considered analogous to a beam on an elastic foundation. (a) Pictorial view. (b) Cross section.

where M is the bending moment parallel to a generatrix and ν is Poisson's ratio of the material. It can be shown that the stiffening effect of M_ϕ on the bending deformation of the beam strip can be taken into account by increasing the second moment of area of the strip in the ratio $1/(1-\nu^2)$; hence, the flexural rigidity of the strip of unit width is

$$EI = \frac{Eh^3}{12(1-\nu^2)} \tag{15.37}$$

The differential equation for the deflection of a beam resting on an elastic foundation (Eq. 15.30) can thus be used for the cylinder with y indicating the deflection in the radial direction, and x the distance from the lower edge of the wall (Figure 15.9a); EI and k are as defined earlier, and q is the intensity of radial pressure on the wall.

When the thickness of the wall is variable both EI and k vary. However, this does not cause an appreciable difficulty in the finite-differences solution.

The finite-difference equations derived for beams and listed in Figures 15.4, 15.5, and 15.7 can be used for circular cylindrical shells subjected to axisymmetrical loading, the equivalent concentrated load Q_i being taken for a strip of unit width.

Example 15.3: Circular cylindrical tank wall

Determine the lateral radial deflection caused by hydrostatic pressure on the wall of a cylindrical water tank shown in Figure 15.10a. Calculate also the hoop force, the bending moment along the wall, and the reaction at its top and bottom. The wall is assumed pinned at both edges. Neglect the effect of Poisson's ratio.

The nodes are chosen as shown in Figure 15.10b, with $\lambda = H/5$. The terms $k_i\lambda^4/E$ and Q_i required in the calculation of the coefficients of the finite-difference equations are given in Figure 15.10b. Substituting for k_i from Eq. 15.35,

$$\frac{k_i\lambda^4}{E} = \frac{Eh_i}{r^2}\frac{\lambda^4}{E} = \frac{h_i\lambda^4}{r^2}$$

The value of Q_i is calculated using the expression for the equivalent concentrated loading from Figure 10.9.

(a)

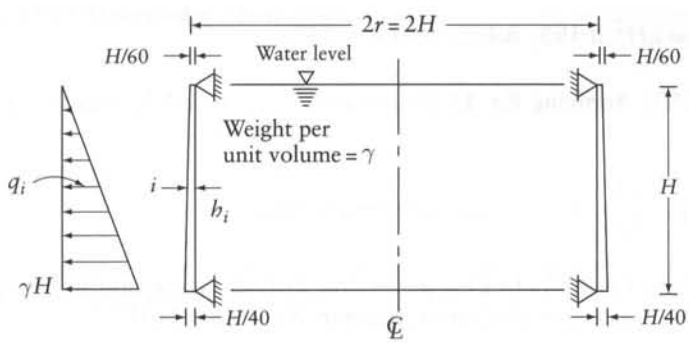

Hydrostatic pressure

(b)

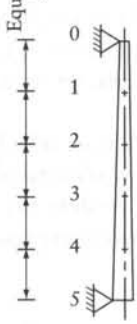

i	h_i $(H/40)$	$I_i = \frac{h_i^3}{12}$ $(H/40)^3$	$\frac{k_i\lambda^4}{E} = \frac{h_i\lambda^4}{r^2}$ $(H/40)^3$	Q_i (γH^2)
0	0.667	0.025		0.0067
1	0.733	0.033	1.876	0.0400
2	0.800	0.043	2.048	0.0800
3	0.867	0.054	2.220	0.1200
4	0.933	0.068	2.388	0.1600
5	1.00	0.083		0.0933

Figure 15.10 Wall of the water tank considered in Example 15.3. (a) Wall. (b) Calculation of $k_i\lambda^4/E$ and Q_i.

(a) *DEFLECTIONS.* Applying the appropriate finite-difference equation from Figure 15.4 at each of the nodes 1, 2, 3, and 4, we write

$$\left(\frac{E}{\lambda^3}\right)\left(\frac{H}{40}\right)^3 \times$$

$$\begin{bmatrix} (4\times 0.033+0.043+1.876) & -2(0.033+0.043) & 0.043 & 0 \\ -2(0.033+0.043) & (0.033+4\times 0.043+0.054+2.048) & -2(0.043+0.054) & 0.054 \\ 0.043 & -2(0.043+0.054) & (0.043+4\times 0.054+0.068+2.220) & -2(0.054+0.068) \\ 0 & 0.054 & -2(0.054+0.068) & (0.054+4\times 0.068+2.388) \end{bmatrix}$$

$$\begin{Bmatrix} y_1 \\ y_2 \\ y_3 \\ y_4 \end{Bmatrix} = \lambda H^2 \begin{Bmatrix} 0.040 \\ 0.080 \\ 0.120 \\ 0.160 \end{Bmatrix}$$

The solution of these equations is

$$\{y_1, y_2, y_3, y_4\} = \frac{\lambda H^2}{E}\{10.88,\ 20.12,\ 28.57,\ 32.35\}$$

(b) *HOOP FORCES.* Substituting in Eq. 15.33 for y_i, we find

$$\{N_1,\ N_2,\ N_3,\ N_4\} = \lambda H^2\{0.199,\ 0.402,\ 0.619,\ 0.755\}$$

(c) *BENDING MOMENT.* Applying Eq. 15.18 at points 1, 2, 3, and 4, with $y_0 = y_5 = 0$, we obtain

$$\{M_1,\ M_2,\ M_3,\ M_4\} = \frac{\gamma H^3}{1000}\{0.021,\ 0.013,\ 0.099,\ 0.960\}$$

(d) *REACTIONS.* Applying Eq. 15.26 (see Figure 15.7b), we find the reaction at the top support $R_0 = 0.0068\gamma H^2$, and the reaction at the bottom support $R_5 = 0.0981\gamma H^2$.

15.8 Representation of partial derivatives by finite differences

Thin plates subjected to transverse (normal) loading are subjected to bending and are therefore referred to as *plates in bending*. They undergo transverse deflections which are small compared with the dimensions of the plate. As a result, the stretching of the middle plane of the plate is negligible, and the in-plane displacement of points on the middle plane is assumed to be zero. Thus, the displacement at any point on the middle plane (or surface) of the plate, say, the $x-y$ plane, can be defined by a translation in the z direction and two rotations about the x and y axes. The plate-bending problem involves the solution of a partial differential equation, for which the finite-difference method will be used.

Figure 15.11 shows a mesh drawn on a surface representing a function $w = f(x, y)$, which can, for example, be the deflected surface of a plate in bending. The derivative of w with respect to x or y can be expressed as a difference of the values of w at the nodes of the mesh in the same manner as the ordinary finite differences considered in Section 15.4. In the following expressions, central differences are used to express values at point O.

The slope of the surface in the x direction is

$$\left(\frac{\partial w}{\partial x}\right)_0 \cong \frac{1}{2\lambda_x}[-1 \quad 1]\begin{Bmatrix} w_1 \\ w_2 \end{Bmatrix} \tag{15.38}$$

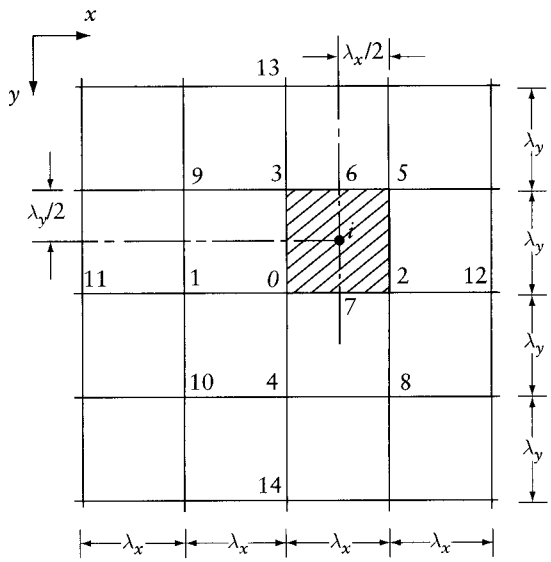

Figure 15.11 Mesh used in a finite-difference representation of the derivatives of a function $w = f(x, y)$.

and the curvature in the x direction is

$$\left(\frac{\partial^2 w}{\partial x^2}\right)_0 \cong \frac{1}{\lambda_x^2}[1 \quad -2 \quad 1]\begin{Bmatrix} w_1 \\ w_0 \\ w_2 \end{Bmatrix} \tag{15.39}$$

Similar expressions can be written for derivatives with respect to y.

The Laplacian operator in the x and y variables

$$\nabla^2 = \frac{\partial^2}{\partial x^2} + \frac{\partial^2}{\partial y^2} \tag{15.40}$$

applied at a general point O can be put in the finite-difference form

$$(\nabla^2 w)_0 \cong \frac{1}{\lambda_x^2}[1 \quad -2 \quad 1]\begin{Bmatrix} w_1 \\ w_0 \\ w_2 \end{Bmatrix} + \frac{1}{\lambda_y^2}[1 \quad -2 \quad 1]\begin{Bmatrix} w_3 \\ w_0 \\ w_4 \end{Bmatrix} \tag{15.41}$$

The mixed derivative at point i, the center of the hatched rectangle in Figure 15.11, is

$$\left(\frac{\partial^2 w}{\partial x \partial y}\right)_i \cong \frac{1}{\lambda_y}\left[\left(\frac{\partial w}{\partial x}\right)_7 - \left(\frac{\partial w}{\partial x}\right)_6\right]$$

whence

$$\left(\frac{\partial^2 w}{\partial x \partial y}\right)_i \cong \frac{1}{\lambda_y \lambda_x}[1 \quad -1 \quad 1 \quad -1]\begin{Bmatrix} w_2 \\ w_0 \\ w_3 \\ w_5 \end{Bmatrix} \tag{15.42}$$

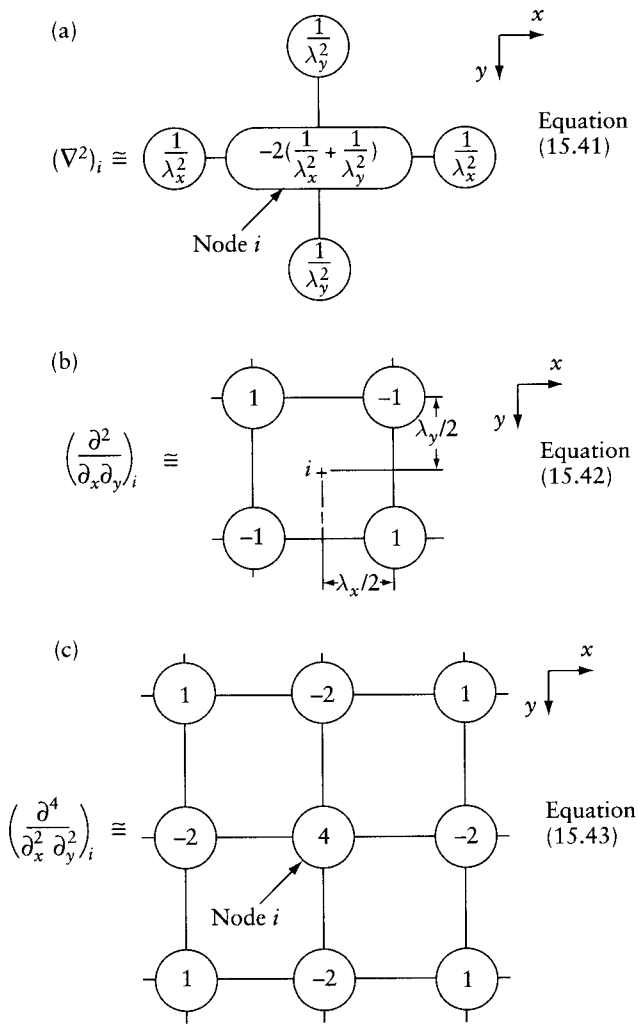

Figure 15.12 Coefficients for central-difference approximations of partial derivatives (λ_x and λ_y are mesh widths in x and y directions). (a) Equation 15.41. Laplacian operator in two variables. (b) Equation 15.42. Multiplier for all coefficients: $1/(\lambda_x^2\lambda_y^2)$. (c) Equation 15.43. Multiplier for all coefficients: $1/(\lambda_x^2\lambda_y^2)$.

The mixed derivative at node O can be expressed in a way similar to Eq. 15.42 in terms of w at the four corners of the rectangle of size $2\lambda_x \times 2\lambda_y$ whose center is the node O.

The coefficients of w at the nodes in Eqs. 15.41 and 15.42 applied at a general node i are given in Figures 15.12a and b. The coefficients of ω for the derivative $\partial^4 w/(\partial x^2 \partial y^2)_i$ are given in Eq. 15.43 in Figure 15.12c.

15.9 Governing differential equations for plates subjected to in-plane forces

The method of finite differences can be used in the analysis of thin plates. Two different problems arise depending on the type of loading. In this section, we consider the case when all the forces

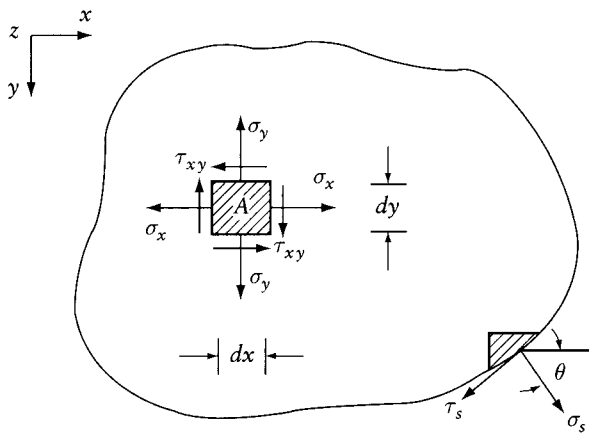

Figure 15.13 Positive direction of stresses.

are applied in the plane of the plate, say, the $x-y$ plane: the stresses produced are σ_x, σ_y, and $\tau_{xy}(=\tau_{yx})$, while σ_z, τ_{zx}, τ_{xz}, τ_{zy}, and τ_{yz} are zero (see Figures 6.4 and 15.13).

This is referred to as *plane-stress* distribution and the forces involved are called *in-plane forces*. The displacement at any point in the plane of the plate can be completely defined by two components in the x and y directions.

However, the finite-differences solution of the plane-stress problem is omitted in the present edition of this book because it has no advantage over the finite-element method (Chapters 16 and 17).

Nevertheless, we give below the equations of equilibrium and compatibility and boundary conditions for plates subjected to in-plane forces because they serve as an introduction to the plate-bending problem (Section 15.10) and will also be used in Chapter 16.

(a) *EQUILIBRIUM.* Considering the forces in the x and y directions acting on a small rectangular block A with sides dx, dy, and h, where h is the plate thickness (Figure 15.13), we can write the following differential equations of equilibrium:

$$\frac{\partial \sigma_x}{\partial x}+\frac{\partial \tau_{xy}}{\partial y}+X=0 \tag{15.44}$$

and

$$\frac{\partial \sigma_y}{\partial y}+\frac{\partial \tau_{xy}}{\partial x}+Y=0 \tag{15.45}$$

where X and Y are components of body force per unit volume in the x and y directions. The positive direction of stresses is shown in Figure 15.13.

(b) *COMPATIBILITY.* If u and v are the in-plane displacements of a general point in the x and y directions, the strain components ϵ_x, ϵ_y and γ_{xy} can be expressed as

$$\epsilon_x=\frac{\partial u}{\partial x};\quad \epsilon_y=\frac{\partial v}{\partial y};\quad \gamma_{xy}=\frac{\partial u}{\partial y}+\frac{\partial v}{\partial x} \tag{15.46}$$

The three strain components ϵ_x, ϵ_y, and γ_{xy} are not independent, but must satisfy the compatibility equation

$$\frac{\partial^2 \epsilon_x}{\partial y^2} + \frac{\partial^2 \epsilon_y}{\partial x^2} = \frac{\partial^2 \gamma_{xy}}{\partial x \partial y^2} \tag{15.47}$$

which can be derived from Eq. 15.46.

The stress–strain relations (Hooke's law, Eq. 6.6) for an isotropic thin plate with a plane-stress distribution can be written in the form

$$\begin{Bmatrix} \epsilon_x \\ \epsilon_y \\ \lambda_{xy} \end{Bmatrix} = \frac{1}{E} \begin{bmatrix} 1 & -\nu & 0 \\ -\nu & 1 & 0 \\ 0 & 0 & 2(1+\nu) \end{bmatrix} \begin{Bmatrix} \sigma_x \\ \sigma_y \\ \tau_{xy} \end{Bmatrix} \tag{15.48}$$

where E is the modulus of elasticity, and n is Poisson's ratio. Combining Eqs. 15.44 to 15.48, the compatibility condition in terms of stress components becomes

$$\nabla^2(\sigma_x + \sigma_y) = -(1+\nu)\left(\frac{\partial X}{\partial x} + \frac{\partial Y}{\partial y}\right) \tag{15.49}$$

(c) *BOUNDARY CONDITIONS.* Considering the equilibrium of forces acting on a triangular block B at the plate boundary (Figure 15.13), the external applied stresses normal (σ_a) and tangential (τ_a) to the boundary can be related to the stress components σ_x, σ_y, and τ_{xy} near the boundary by

$$\begin{Bmatrix} \sigma_a \\ \tau_a \end{Bmatrix} = \begin{bmatrix} \cos^2 & \sin^2\theta & \sin 2\theta \\ -\dfrac{\sin 2\theta}{2} & \dfrac{\sin 2\theta}{2} & \cos 2\theta \end{bmatrix} \begin{Bmatrix} \sigma_x \\ \sigma_y \\ \tau_{xy} \end{Bmatrix} \tag{15.50}$$

where θ is the angle between the normal to the boundary and the x axis (see Figure 15.13).

15.10 Governing differential equations for plates in bending

In this section we deal with thin plates subjected to transverse loading causing deflections which are small compared with the plate thickness (Figure 15.14a). If the orthogonal axes x and y are chosen in the middle surface of the plate, we can neglect, at all points on this surface, the displacements u and v parallel to the x and y axes, the stresses σ_x and σ_y and the deformations caused by the stress σ_z. Further, we assume that a normal to the middle surface remains straight across the plate thickness and is normal to the deflected middle surface. This is analogous to the assumption in the bending theory that plane cross sections remain plane after bending, which is normally made for beams long in comparison with their cross-sectional dimensions.

Figure 15.14b shows the forces acting on a small rectangular block A of sides dx, dy, and h. If dx and dy are taken equal to unity, the internal forces M_x, M_y, M_{xy}, V_x, and V_y on the block edges are equal to the resultants of the appropriate stresses on the element sides. The positive directions of these stress resultants are indicated in Figure 15.14b, and the positive directions of stresses are shown in Figure 7.4. The stress resultants are related to the stresses σ_x, σ_y, and τ_{xy} as follows:

$$M_x = \int_{-h/2}^{h/2} \sigma_x z dz; \quad M_y = \int_{-h/2}^{h/2} \sigma_x z\, dz \tag{15.51}$$

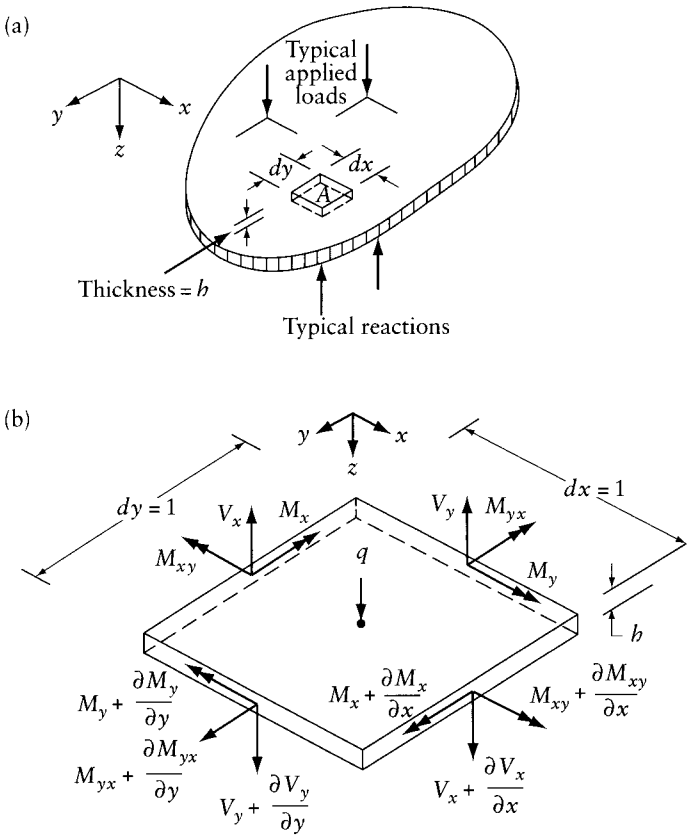

Figure 15.14 (a) Plate in bending. (b) Forces acting on the block A in part (a). This figure also indicates the positive directions of the stress resultants.

$$M_{yx} = -M_{xy} = \int_{-h/2}^{h/2} \tau_{xy} z \, dz \tag{15.52}$$

and

$$V_x = \int_{-h/2}^{h/2} \tau_{xz} dz \quad \text{and} \quad V_y = \int_{-h/2}^{h/2} \tau_{yz} \, dz \tag{15.53}$$

To solve for the stress resultants we consider the equilibrium and the deformation of the block.

(a) *EQUILIBRIUM.* The sum of the vertical forces is zero and the sum of the moments about edges dx and dy equals zero. Thus,

$$\left.\begin{aligned} &\frac{\partial V_x}{\partial x} + \frac{\partial V_y}{\partial y} + q = 0 \\ &\frac{\partial M_x}{\partial x} + \frac{\partial M_{yx}}{\partial y} - V_x = 0 \\ \text{and} \quad &-\frac{\partial M_y}{\partial y} + \frac{\partial M_{xy}}{\partial x} + V_y = 0 \end{aligned}\right\} \tag{15.54}$$

where q is the intensity of the applied load per unit area. These three equations can be combined in one equation:

$$\frac{\partial^2 M_x}{\partial x^2} - 2\frac{\partial^2 M_{xy}}{\partial x \partial y} + \frac{\partial^2 M_y}{\partial y^2} = -q \tag{15.55}$$

(b) *DEFORMATION.* The displacements u and v (in the direction of the x and y axes) at any point at a distance z from the middle surface can be expressed in terms of the slope of the deflected surface by

$$u = -z\frac{\partial w}{\partial x} \quad \text{and} \quad v = -z\frac{\partial w}{\partial y} \tag{15.56}$$

where w is the deflection in the direction of the z axis. The partial derivatives represent the slope of the deflected surface which is also equal to the rotation of the normal to the middle surface.

The strain at the same point is expressed in terms of the displacements by Eq. 15.46, from which we obtain

$$\epsilon_x = -z\frac{\partial^2 w}{\partial x^2} \quad \epsilon_y = -z\frac{\partial^2 w}{\partial y^2} \quad \text{and} \quad \gamma_{xy} = -2z\frac{\partial^2 w}{\partial x \partial y} \tag{15.57}$$

The stress is related to strain by Hooke's law, which for a homogeneous, isotropic plate is expressed by Eq. 15.48. Using this equation and Eq. 15.57, the stress can be expressed in terms of the deflection of the middle surface:

$$\begin{Bmatrix} \sigma_x \\ \sigma_y \\ \tau_{xy} \end{Bmatrix} = -\frac{Ez}{(1-\nu^2)} \begin{bmatrix} 1 & \nu & 0 \\ \nu & 1 & 0 \\ 0 & 0 & (1-\nu) \end{bmatrix} \begin{Bmatrix} \dfrac{\partial^2 w}{\partial x^2} \\ \dfrac{\partial^2 w}{\partial y^2} \\ \dfrac{\partial^2 w}{\partial x \partial y} \end{Bmatrix} \tag{15.58}$$

Substituting for the stress from Eq. 15.48 into Eqs. 15.51 and 15.52, we obtain

$$\begin{Bmatrix} M_x \\ M_y \\ M_{xy} \end{Bmatrix} = -N \begin{bmatrix} 1 & \nu & 0 \\ \nu & 1 & 0 \\ 0 & 0 & -(1-\nu) \end{bmatrix} \begin{Bmatrix} \dfrac{\partial^2 w}{\partial x^2} \\ \dfrac{\partial^2 w}{\partial y^2} \\ \dfrac{\partial^2 w}{\partial x \partial y} \end{Bmatrix} \tag{15.59}$$

where

$$N = \frac{Eh^3}{12(1-\nu^2)} \tag{15.60}$$

represents the flexural rigidity of a strip of the plate having a unit width.

From last two of Eq. 15.54 and Eq. 15.59, the shear can also be expressed in terms of the deflection:

$$V_x = -N\frac{\partial}{\partial x}(\nabla^2 w) \quad \text{and} \quad V_y = -N\frac{\partial}{\partial y}(\nabla^2 w) \tag{15.61}$$

where ∇^2 is the Laplacian operator.

(c) *DERIVATION.* Substitution of Eq. 15.59 into Eq. 15.55 gives

$$\frac{\partial^4 w}{\partial x^4} + 2\frac{\partial^4 w}{\partial x^2 \partial y^2} + \frac{\partial^4 w}{\partial y^4} = \frac{q}{N} \tag{15.62}$$

which can be written in the form

$$\nabla^2(\nabla^2 w) = q/N \tag{15.63}$$

In the analysis of plates in bending, deflection is obtained by solving Eq. 15.62 satisfying the conditions at the plate boundaries; the stress resultants are then determined by Eqs. 15.59 and 15.61. In the following, the solution for the deflection will be obtained by the method of finite differences.

15.11 Finite-difference equations at an interior node of a plate in bending

Equation 15.41 gives the finite-difference form of the Laplacian operator ∇^2 for a function of x and y, and the finite-difference coefficients are schematically represented in Figure 15.12a. Applying Laplace's operator ∇^2 to the function $\nabla^2 w$ and using the pattern of coefficients of Figure 15.12a, we obtain the finite-difference form of the derivative $\nabla^2(\nabla^2 w)$. The pattern of coefficients for the operator $\nabla^2(\nabla^2)$ applied at a node i for a function which varies with x and y is shown in Figure 15.15a. When the mesh widths are such that $\lambda_x = \lambda_y = \lambda$, the pattern of

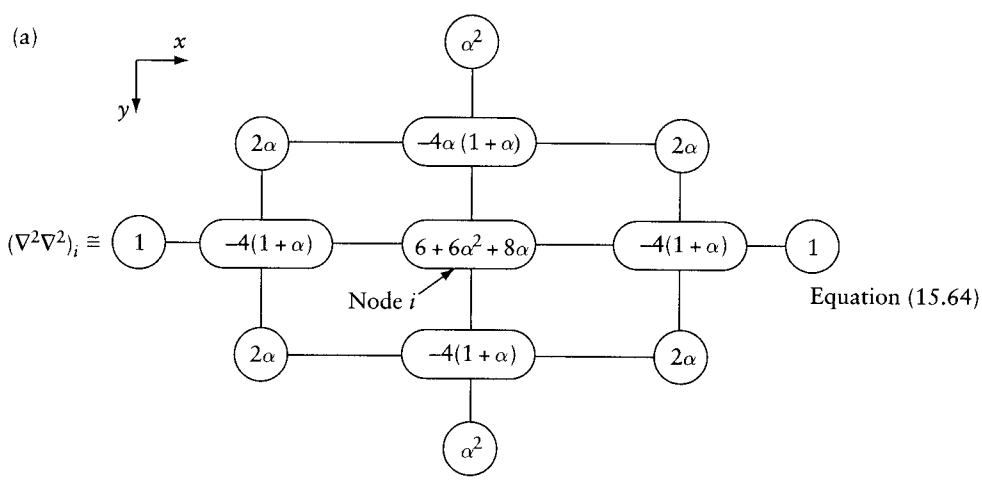

Figure 15.15 Central-difference approximation of the partial derivative $(\nabla^2\nabla^2)_i$. The above coefficients are to be used in the finite-difference form of Eq. 15.62 or 15.63 as follows: [coefficients] $\{w\} \cong q_i/N$. (a) Rectangular mesh; $\alpha = (\lambda_x/\lambda_y)^2$; λ_x and λ_y are mesh widths in the x and y directions. (b) Square mesh; the mesh width is λ in the x and y directions.

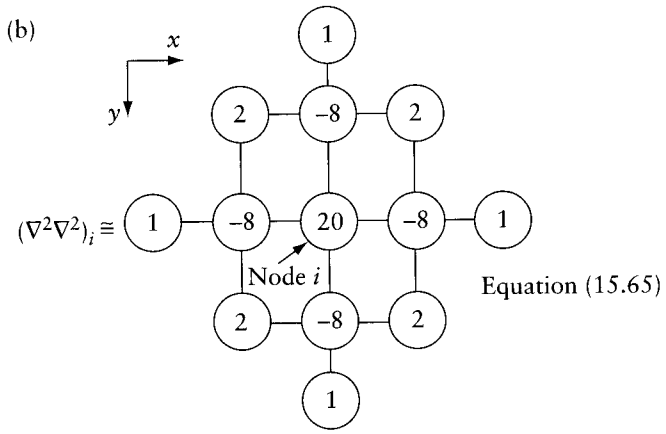

Figure 15.15 (Continued).

coefficients is as shown in Figure 15.15b. Hence, the finite-difference form of Eq. 15.62, applied at a general interior node i, is

$$[\text{coefficients}]\{w\} \cong q_i/N \tag{15.66}$$

where the coefficients are as indicated in Figure 15.15. This equation relates the deflection w_i at i and at 12 other nodes in its vicinity to the load intensity q_i.

The stress resultants at an interior node can be expressed in terms of the node deflections w by the finite-difference form of Eqs. 15.59 and 15.61. The pattern of coefficients for these approximations is given in Figure 15.16.

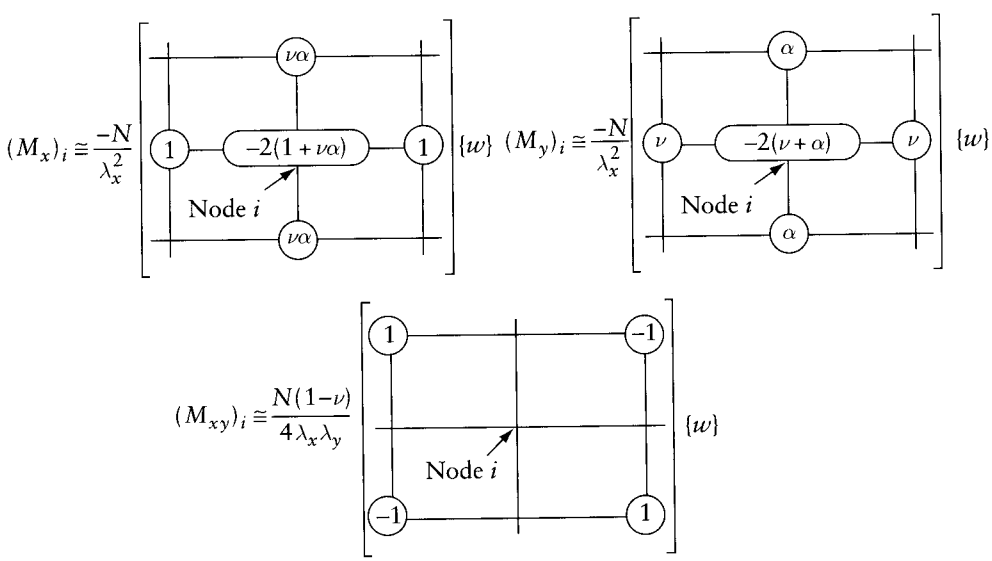

Figure 15.16 Finite-difference forms of Eqs. 15.59 and 15.61 using a rectangular mesh.

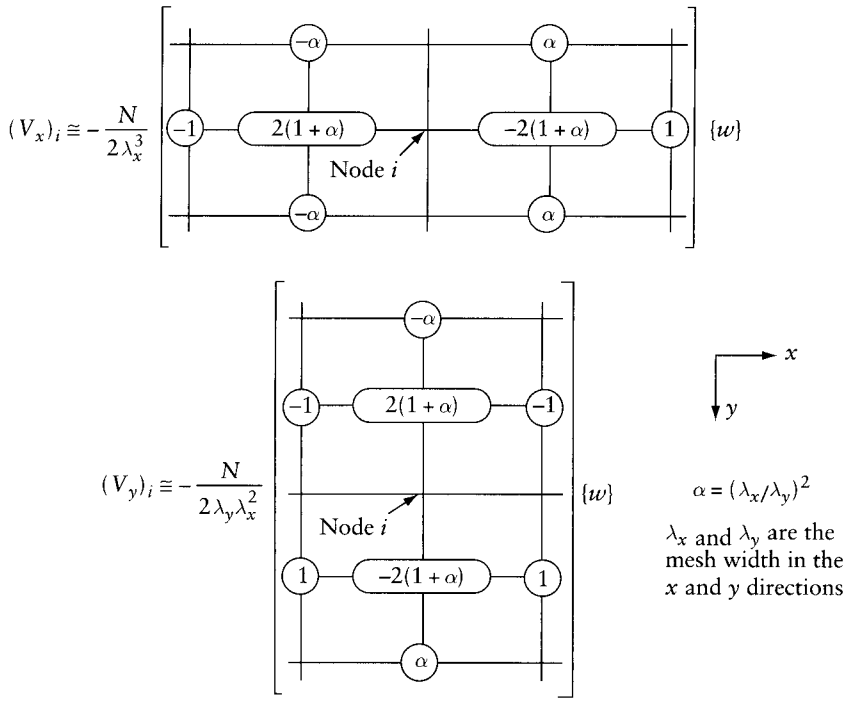

Figure 15.16 (Continued)

15.12 Boundary conditions of a plate in bending

In Figure 15.17 the orthogonal coordinates n and t are taken normal and tangential to plate boundary. Considering equilibrium of the small block B (see Figure 15.17b), the bending and twisting moment at the boundary can be related to M_x, M_y, and M_{xy} by

$$\begin{Bmatrix} M_n \\ M_{nt} \end{Bmatrix} = \begin{bmatrix} \cos^2\theta & \sin^2\theta & -\sin 2\theta \\ \frac{\sin 2\theta}{2} & -\frac{\sin 2\theta}{2} & \cos 2\theta \end{bmatrix} \begin{Bmatrix} M_x \\ M_y \\ M_{xy} \end{Bmatrix} \tag{15.67}$$

The boundary shear V_n is related to V_x and V_y by

$$V_n = V_x \cos\theta + V_y \sin\theta \tag{15.68}$$

At a plate edge, one or more of the stress resultants or the deflection or slope of the deflected surface can be known. This information is taken into account when writing the finite-difference equations relating the deflection to the applied loads. The different edge conditions are considered below.

(a) *BUILT-IN EDGE.* The deflection at all points on a built-in edge and the slope of the deflected surface normal to the edge are zero, so that

$$w = 0 \quad \text{and} \quad \frac{\partial w}{\partial n} = 0 \tag{15.69}$$

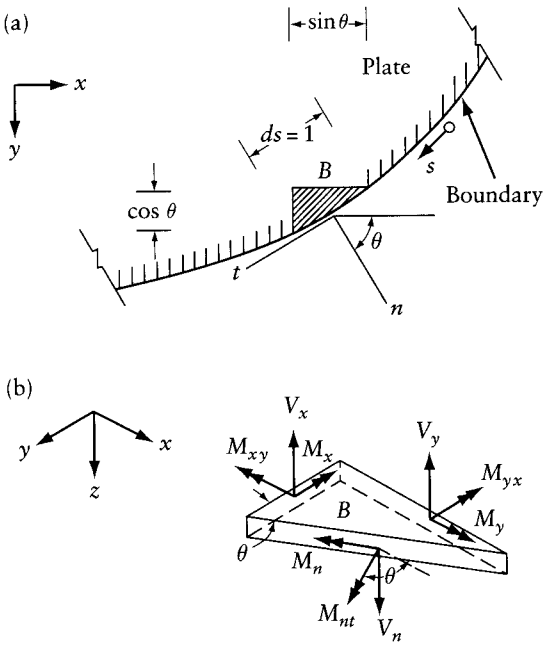

Figure 15.17 A block near the boundary of a plate in bending considered in the derivation of Eqs. 15.67 and 15.68. (a) Top view of a plate. (b) Forces acting on block B in part (a). This figure also indicates the positive directions of V_n, M_n, and M_{nt}.

Consider the case when the plate edge is straight. The conditions of Eq. 15.69 will be satisfied if the plate is considered continuous with a symmetrical fictitious plate subjected to symmetrical loading so that its deflected middle surface is a mirror image of the actual deflected middle surface.

If the built-in edge is parallel to the x axis, as in Figure 15.18a, the conditions of Eq. 15.69 give $w_D = w_B = w_E = 0$ and $w_C = w_A$. When the finite-difference Eq. 15.66 is applied at node A, the deflection at the fictitious node C is put equal to W_A and the deflection of the edge nodes is taken as zero. Hence, we obtain an equation relating the deflection at the interior nodes to the intensity of the applied load at A. The finite-difference Eq. 15.66 applied at each interior node gives a sufficient number of simultaneous equations for the nodal deflections to be calculated.

(b) *SIMPLY-SUPPORTED EDGE.* The deflection w and the moment M_n vanish at all points of a simply-supported edge, that is,

$$w = 0 \quad \text{and} \quad M_n = 0 \tag{15.70}$$

Combining Eqs. 15.67 and 15.59, the second boundary condition can be represented in terms of the deflection by

$$(1-\nu)\left(\frac{\partial^2 w}{\partial x^2}\cos^2\theta + 2\frac{\partial^2 w}{\partial x \partial y}\sin\theta\cos\theta + \frac{\partial^2 w}{\partial y^2}\sin^2\theta\right) + \nu\nabla^2 w = 0 \tag{15.71}$$

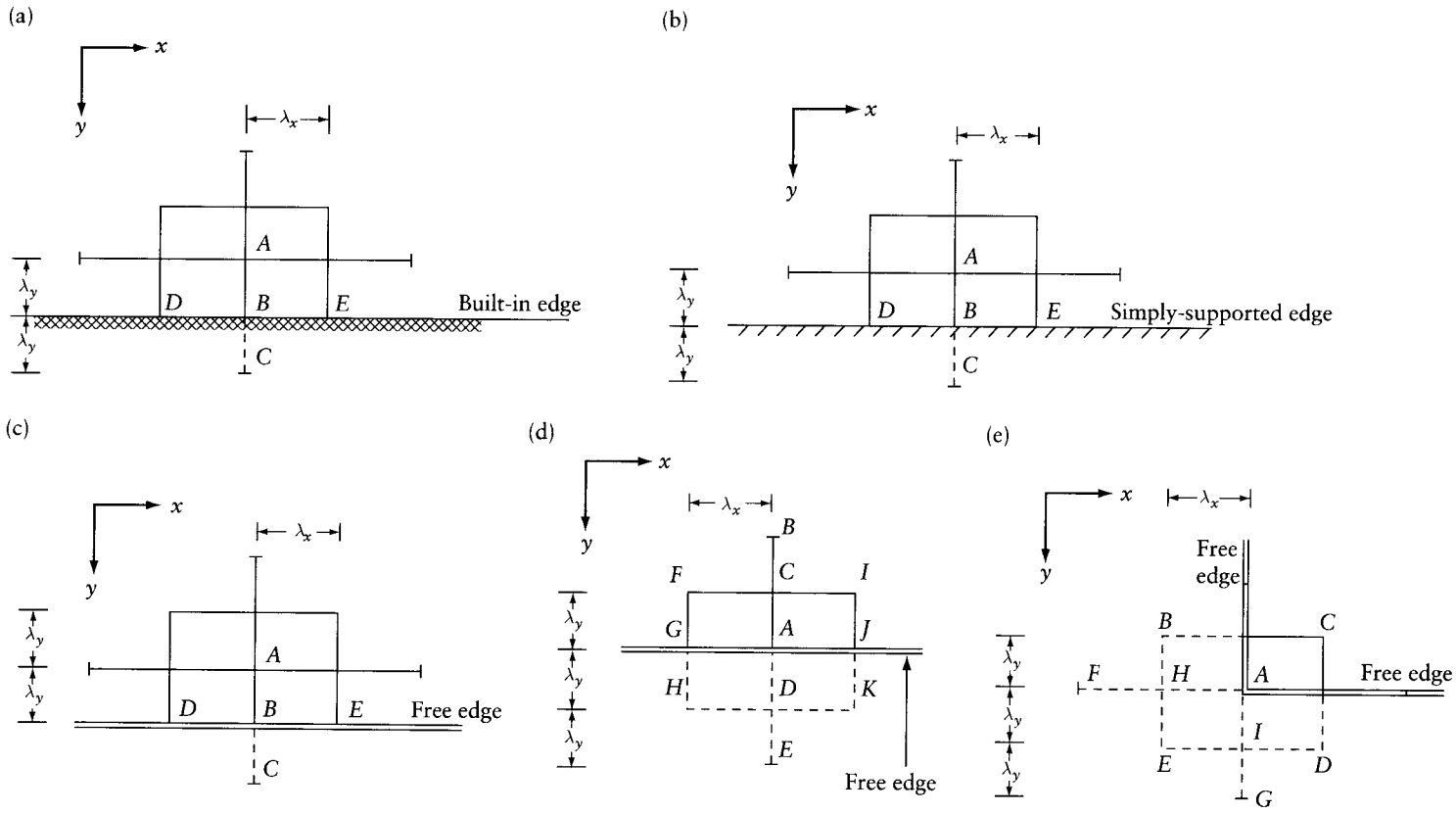

Figure 15.18 Use of boundary conditions for the elimination of the deflection at fictitious nodes when the finite-difference Eq. 15.66 is applied at a node A on or near a plate edge. (a) Node A near a fixed edge. (b) Node A near a simply-supported edge. (c) Node A near a free edge. (d) Node A on a free edge. (e) Node A at a corner.

When the plate edge is straight, the two conditions of Eq. 15.70 will be satisfied if the plate is considered continuous with a fictitious symmetrical plate subjected to antisymmetrical loading so that the deflections of the middle surface are equal and opposite at symmetrical points.

If the simply-supported edge is parallel to the x axis, as in Figure 15.18b, the conditions of Eq. 15.70 give $w_D = w_B = w_E = 0$ and $w_C = -w_A$. These equations are substituted in the finite-difference Eq. 15.66 applied at node A in a manner similar to that used for the built-in edge.

(c) *FREE EDGE.* The bending moment at any point on a free edge is zero, that is, $M_n = 0$. This means that Eq. 15.71 must be satisfied. Further, at a free edge there should be no transverse forces. Now, the shear V_n and the twisting moment M_{nt} (Figure 15.17) can be reduced to transverse forces only[2] and, since these vanish at a free edge, we can write

$$V_n - \frac{\partial M_{nt}}{\partial s} = 0 \tag{15.72}$$

Using Eqs. 15.59, 15.61, 15.67, and 15.68, this condition can be represented in terms of the deflection in the form

$$\begin{aligned}(1-\nu)\frac{\partial}{\partial s}\left[\left(\frac{\partial^2 w}{\partial x^2} - \frac{\partial^2 w}{\partial y^2}\right)\sin\theta\cos\theta - \frac{\partial^2 w}{\partial x \partial y}(\cos^2\theta - \sin^2\theta)\right] \\ -\left(\frac{\partial^3 w}{\partial x^3} + \frac{\partial^3 w}{\partial x \partial y^2}\right)\cos\theta - \left(\frac{\partial^3 w}{\partial y^3} + \frac{\partial^3 w}{\partial y \partial x^2}\right)\sin\theta = 0\end{aligned} \tag{15.73}$$

When the free edge is parallel to the x axis ($\theta = 90°$ and $\partial s = -\partial x$), the conditions at the free edge become

$$\frac{\partial^2 w}{\partial y^2} + \nu\frac{\partial^2 w}{\partial x^2} = 0 \tag{15.74}$$

and

$$\frac{\partial^3 w}{\partial y^3} + (2-\nu)\frac{\partial^3 w}{\partial y \partial x^2} = 0 \tag{15.75}$$

When the finite-difference Eq. 15.66 is applied at node A on the first mesh line inside the boundary (Figure 15.18c), the deflection at a fictitious node C can be eliminated using the following finite-difference form of Eq. 15.74 applied at node B:

$$\frac{1}{\lambda_y^2}(w_C - 2w_B + w_A) + \frac{\nu}{\lambda_x^2}(w_E - 2w_B + w_D) \cong 0 \tag{15.76}$$

Application of Eq. 15.66 at node A on a free edge (Figure 15.18d) includes the deflection at the fictitious nodes H, D, K, and E. The deflection w_E can be expressed in terms of the deflection at the other nodes, using the following finite-difference form of Eq. 15.75 applied at A:

$$\frac{1}{2\lambda_y^3}(w_E - 2w_D + 2w_C - w_B) + \frac{(2-\nu)}{2\lambda_y}\left(\frac{w_K - 2w_D + w_H}{\lambda_x^2} - \frac{w_I - 2w_C + w_F}{\lambda_x^2}\right) \cong 0 \tag{15.77}$$

2 See Timoshenko, S. and Wojnowsky-Krieger, S., *Theory of Plates and Shells,* 2nd ed., McGraw-Hill, New York, 1959.

Three equations similar to Eq. 15.76 can be applied at nodes G, A, and J (Figure 15.18d) and used to eliminate the fictitious deflections w_H, w_D, and w_K.

(d) *CORNER.* At a corner where two free edges parallel to the x and y axes meet (Figure 15.18e), the boundary conditions of Eqs. 15.74 and 15.75 apply (as to all the nodes on the edge parallel to the x axis). Two similar equations apply to the nodes on the edge parallel to the y axis. In addition, at a corner,[3] the twisting moment $M_{xy} = 0$; this can be written in finite-difference form (see Figure 15.16) as

$$\frac{N(1-\nu)}{4\lambda_x\lambda_y}(w_B - w_C + w_D - w_E) \cong 0 \tag{15.78}$$

Application of Eq. 15.66 at a corner node A (Figure 15.18e) includes deflections at the fictitious nodes B, D, G, F, H, I, and E. The deflection at E can be eliminated by the use of Eq. 15.78, and the other fictitious deflections are eliminated using the remainder of the boundary conditions in the same manner as for the free edge.

15.13 Analysis of plates in bending

The procedure outlined in the preceding sections leads to linear equations relating the deflections at nodes within the boundary to the external applied load. These equations will have one of the forms given in Figure 15.19 when applied at a node i, which may be a general interior node or a node on or near the boundary. Any one of these forms can be expressed as

$$(N\lambda_y/\lambda_x^3)\,[\text{coefficients}]\,\{w\} \cong Q_i \tag{15.79}$$

where the coefficients are as given in Figure 15.19, and Q_i is an equivalent concentrated load at i. When the load is uniform and of intensity q, and i is an interior node, $Q_i = q\lambda_x\lambda_y$. The values of Q where i is on an edge or at a corner are, respectively, $q\lambda_x\lambda_y/2$ and $q\lambda_x\lambda_y/4$.

In the case of nonuniform loading, the equivalent concentrated load can be calculated from the equations given in Section 10.4.1. For example, if we use the expression for parabolic variation (see Figure 10.9) to find the equivalent concentrated load Q_0 at node O of the mesh in Figure 15.11, we write

$$\left.\begin{aligned} p_3 &= \frac{\lambda_x}{12}(q_9 + 10q_3 + q_5) \\ p_0 &= \frac{\lambda_x}{12}(q_1 + 10q_0 + q_2) \\ p_4 &= \frac{\lambda_x}{12}(q_{10} + 10q_4 + q_8) \end{aligned}\right\} \tag{15.80}$$

where the q terms are the load intensities at the nodes (force/area) and the p values are line load intensities (force/length) on a line parallel to the y axis through 0. Applying the same expression for the load p, we obtain

$$Q_0 = \frac{\lambda_y}{12}(p_3 + 10p_0 + p_4) \tag{15.81}$$

3 For a discussion of this condition, see reference in footnote 4 in this chapter.

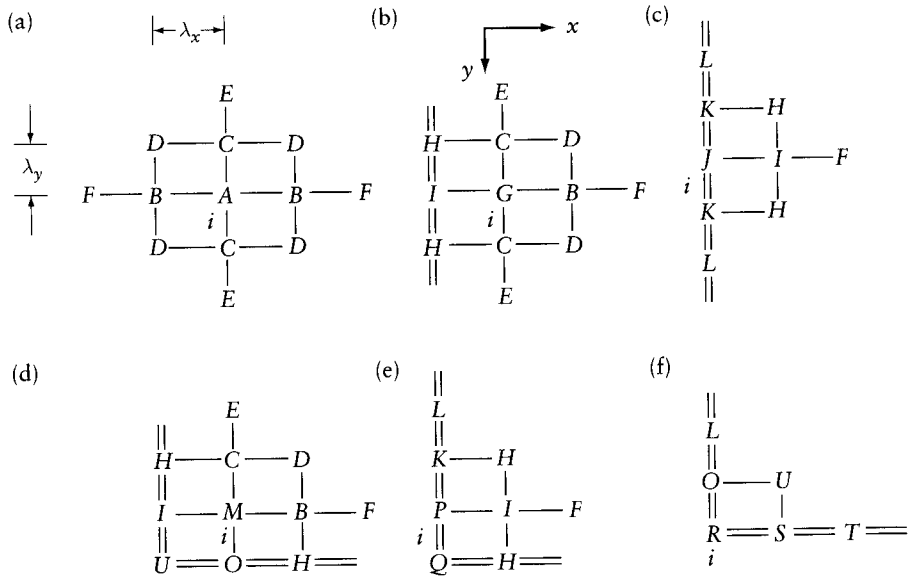

Figure 15.19 Finite-difference coefficients in Eq. 15.79 applied at node i on or near the edge of a plate in bending (from reference in footnote 6 in this chapter).

Combining Eqs. 15.80 and 15.81, we find

$$Q_0 = \frac{\lambda_x \lambda_y}{144}[100q_0 + 10(q_1 + q_2 + q_3 + q_4) + (q_9 + q_5 + q_{10} + q_8)] \tag{15.82}$$

For other forms of load variation, or for edge or corner nodes, the other equations for the line loads given in Figure 10.10 can be used to derive corresponding expressions for the equivalent concentrated load.

Applying the finite-difference equations at all mesh points where the deflection is not known leads to a system of simultaneous equations which may be written in matrix form

$$[K]\{w\} \cong \{Q\} \tag{15.83}$$

where $[K]$ is a square matrix formed by the finite-difference coefficients. Examination of the coefficients in Figure 15.19 shows that the matrix $[K]$ is symmetrical. For example, the finite-difference equation applied at a corner node (Figure 15.19f) has a coefficient $U = 2\alpha(1-\nu)$ for

the deflection at a diagonally opposite node, and, when the equation is applied at this latter node (see Figure 15.19d) the coefficient at the corner is also equal to U. We may consider the matrix $[K]$ as an equivalent stiffness matrix, and we shall so use it in the following chapter.

The procedure of the analysis of plates in bending by finite differences can be summarized as follows. A system of linear simultaneous equations is written in the form of Eq. 15.83, in which $\{Q\}$ are the known forces and $\{w\}$ are the unknown deflections. The elements of the matrix $[K]$ are determined using Figure 15.19, which covers the majority of practical cases. The solution of Eq. 15.83 gives the deflections, and these are then substituted in the finite-difference equations in Figure 15.16 to determine the stress resultants.

The finite-difference equations in Figure 15.19 can be used for a plate with a simply-supported edge by substituting zero for the deflection at nodes on this edge. A figure similar to Figure 15.19 can be prepared for the finite-difference equations applied at nodes on the first mesh line inside the boundary parallel to a built-in edge. This figure is not given here as it is easy to derive from Figure 15.19a if we observe that the deflections at fictitious nodes outside the boundary are a mirror image of the deflections at corresponding nodes within the boundary. When the free edge is inclined to the x and y directions, the finite-difference equations can also be derived by a similar procedure.[4]

When a plate has a curved boundary, the nodes of a rectangular mesh may not fall on the plate edge. In this case, the finite-difference expressions have to be used for unevenly-spaced nodes.[5]

In the analysis of a parallelogram-shaped plate, it may be more suitable to use skew coordinate axes and a skew mesh in the finite-difference equations.[6] In some other cases, a mesh formed by arcs of circles and radial lines may be used. The coefficients of the finite-difference equations for these types of meshes are not given here, but the basic ideas in the analysis are the same in all cases.

15.13.1 Stiffened plates

If a plate is stiffened by beams located on mesh lines and assumed to be connected to the plate in the idealized fashion indicated in Figures 15.20a or b, the effect of the stiffening can be easily included by substituting $[K]=[K]_p+[K]_b$ in Eq. 15.83, where $[K]_p$ is the plate equivalent stiffness matrix for the plate alone, obtained as described before from the finite-difference coefficients, and $[K]_b$ is the equivalent stiffness matrix for the beams, defined by

$$[K]_b\,\{w\}=\{Q\}_b \tag{15.84}$$

Here, $\{w\}$ are the nodal deflections of the composite system beam-plate, $\{Q\}_b$ is a vector of the part of $\{Q\}$ carried by the beams alone, and $[K]_b$ is an equivalent stiffness matrix for the beams. The elements of $[K]_b$ can be derived from the finite-difference coefficients given in Figures 15.4 and 15.5.

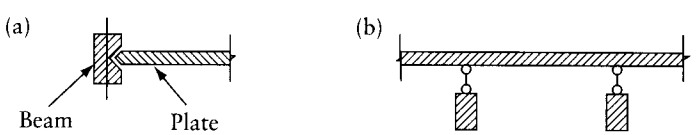

Figure 15.20 Idealized plate-beam connections.

4 See Ghali, A. and Bathe, K.-J., "Analysis of Plates in Bending Using Large Finite Elements," *International Association for Bridges and Structural Engineering*, 30/II, Zurich, 1970.

5 For further discussion, see Crandall, S. H., *Engineering Analysis*, McGraw-Hill, New York, 1956.

6 Jensen, V. P., *Analysis of Skew Slabs*, University of Illinois Engineering Experiment Station, Bulletin No. 332.

Example 15.4: Square plate simply supported on three sides

Find the deflection and moment M_y at node 2 and the moments M_x and M_y at node 6 in the plate shown in Figure 15.21, subjected to a uniform load q per unit area. The plate is of constant thickness h, and has three edges simply supported and one edge free. Assume Poisson's ratio $\nu = 0.3$.

Applying Eq. 15.79 at each of the eight nodes (see Figure 15.21) and using the finite-difference patterns of coefficients in Figure 15.19, the following simultaneous equations can be written:

$$\frac{N}{\lambda^2}\begin{bmatrix} J & K & I & H & F & & & \\ 2K & J & 2H & I & & F & & \\ I & H & G & C & B & D & F & \\ 2H & I & 2C & G & 2D & B & & F \\ F & & B & D & A & C & B & D \\ & F & 2D & B & 2C & A & 2D & B \\ & & F & & B & D & G & C \\ & & & F & 2D & B & 2C & G \end{bmatrix} \begin{Bmatrix} w_1 \\ w_2 \\ w_3 \\ w_4 \\ w_5 \\ w_6 \\ w_7 \\ w_8 \end{Bmatrix} \cong q\lambda^2 \begin{Bmatrix} 0.5 \\ 0.5 \\ 1.0 \\ 1.0 \\ 1.0 \\ 1.0 \\ 1.0 \\ 1.0 \end{Bmatrix}$$

where the coefficients A, B, ... are defined in Figure 15.19. The square matrix on the left-hand side can be made symmetrical by multiplying by 2 each of the first, third, fifth, and seventh equations. The figure 2 represents the number of nodes of the mesh which have the same deflection as each of w_1, w_3, w_5, and w_7. The property of symmetry is useful to detect any mistakes which may have been made in forming the equations.

Substituting the values of the coefficients A, B, ... and solving, we obtain

$$\{w\} \cong \frac{q\lambda^4}{N}\{2.3984,\ 3.3516,\ 1.9361,\ 2.7033,\ 1.4899,\ 2.0749,\ 0.8641,\ 1.1979\}$$

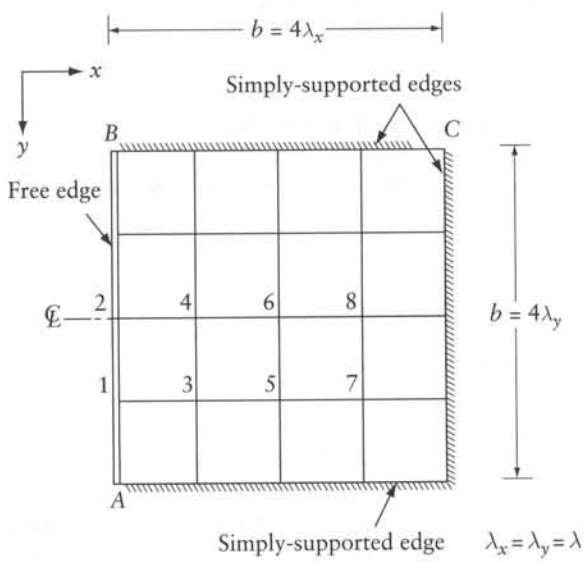

Figure 15.21 Square plate subjected to a uniform transverse load analyzed by finite difference in Example 15.4.

The required deflection at node 2 is $w_2 \cong 0.1429qb^4/Eh^3$. At node 2 the moment M_y on the free edge is (from Eq. 15.59)

$$(M_y)_2 = -N\left(\frac{\partial^2 w}{\partial y^2} + \nu\frac{\partial^2 w}{\partial x^2}\right)_2$$

and the moment M_x is

$$(M_x)_2 = -N\left(\frac{\partial^2 w}{\partial x^2} + \nu\frac{\partial^2 w}{\partial y^2}\right)_2 = 0$$

Hence,

$$(M_y)_2 = -N(1-\nu^2)\frac{\partial^2 w}{\partial y^2}$$

Using finite-difference approximation for the derivatives, we obtain

$$(M_y)_2 \cong -N\frac{(1-\nu^2)}{\lambda_y^2}(2w_1 - 2w_2) = 0.1084qb^2$$

Substituting for w in the M_x and M_y equations in Figure 15.16, we obtain

$$(M_x)_6 \cong 0.0374qb^2 \quad \text{and} \quad (M_y)_6 \cong 0.0777qb^2$$

Exact answers[7] to this problem are: $w_2 = 0.1404qb^4/Eh^3$, $(M_y)_2 = 0.112qb^2$, $(M_x)_6 = 0.039qb^2$, and $(M_y)_6 = 0.080qb^2$.

15.14 Stiffness matrix equivalent

In this chapter we have shown that the use of finite differences for solving differential equations relating the transverse load to the deflection in beams and slabs results in a system of simultaneous linear equations of the form

$$[K]\{D\} \cong \{F\} \tag{15.85}$$

where $[K]$ is a matrix formed by the finite-difference coefficients of the transverse deflections at the nodes $\{D\}$, and $\{F\}$ are nodal transverse loads (compare with Eqs. 15.23 and 15.83).

Comparing Eq. 15.85 with the fundamental equation

$$[S]\{D\} = \{F\} \tag{15.86}$$

we see that replacing the stiffness matrix $[S]$ by $[K]$ results in the approximate Eq. 15.85. The matrix $[K]$ can, therefore, be treated as equivalent to the stiffness matrix. The inverse of the equivalent stiffness matrix gives the approximate influence coefficients of transverse deflections. From these, influence coefficients of the stress resultants and reactions can be calculated.

7 Taken from reference in footnote 4 in this chapter.

The equivalent stiffness matrix [K] is easily generated by the use of the finite-difference patterns of coefficients given in this chapter. The matrix [K] which corresponds to coordinates representing transverse deflections can be transformed to stiffness matrices corresponding to other sets of coordinates.

The principles discussed are general and can be applied to a variety of structures, such as continuous beams, frames, grids, slabs, and shells.

15.15 Comparison between equivalent stiffness matrix and stiffness matrix

Consider a beam on an elastic foundation (Figure 15.22a) which for simplicity is assumed to have a constant flexural rigidity EI, and a constant foundation modulus k per unit length per unit deflection.

Let the beam be divided into five equal intervals λ. Using the finite-difference pattern of coefficients of Figure 15.5, we can generate the following equivalent stiffness matrix relating the nodal transverse deflections to nodal transverse forces:

$$[K]=\frac{EI}{\lambda^3}\begin{bmatrix} \left(1+\frac{k\lambda^4}{2EI}\right) & & & & & \text{symmetrical} \\ -2 & \left(5+\frac{k\lambda^4}{EI}\right) & & & & \\ 1 & -4 & \left(6+\frac{k\lambda^4}{EI}\right) & & & \\ & 1 & -4 & \left(6+\frac{k\lambda^4}{EI}\right) & & \\ \text{Elements are} & \text{not shown} & 1 & -4 & \left(5+\frac{k\lambda^4}{EI}\right) & \\ \text{zero} & & & 1 & -2 & \left(1+\frac{k\lambda^4}{EI}\right) \end{bmatrix} \tag{15.87}$$

Replace the elastic foundation by elastic supports (springs) of stiffness equal to $k\lambda$ at nodes 2, 3, 4, and 5, and equal to $k\lambda/2$ at the end nodes 1 and 6. The elements of the stiffness matrix of this beam are the support reactions of the continuous beam in Figure 15.22b when one support undergoes a unit downward displacement. These can be obtained from Appendix E. Thus,

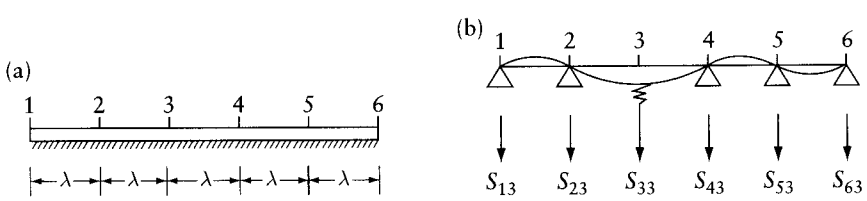

Figure 15.22 Beam on an elastic foundation considered in Section 15.15. (a) Points of division in a beam on an elastic foundation. (b) Forces in the third column of the stiffness matrix [S], Eq. 15.88.

$$[S]=\frac{EI}{\lambda^3}\begin{bmatrix}\left(1.6077+\frac{k\lambda^4}{2EI}\right) & & & & & \\ -3.6459 & \left(9.8756+\frac{k\lambda^4}{EI}\right) & & \text{symmetrical} & & \\ 2.5837 & -9.5024 & \left(14.0096+\frac{k\lambda^4}{EI}\right) & & & \\ -0.6890 & 4.1340 & -10.5359 & \left(14.0096+\frac{k\lambda^4}{EI}\right) & & \\ 0.1723 & -1.0335 & 4.1340 & -9.5024 & \left(9.8756+\frac{k\lambda^4}{EI}\right) & \\ -0.0287 & 0.1723 & -0.6890 & 2.5837 & -3.6459 & \left(1.6077+\frac{k\lambda^4}{2EI}\right)\end{bmatrix} \tag{15.88}$$

We can now verify that the equivalent stiffness matrix $[K]$ in Eq. (15.87) has all the general properties of stiffness matrices discussed in Section 6.6. The sum of the elements of any column (or row) of $[K]$ or $[S]$ is equal to the value $k\lambda$ (or $k\lambda/2$). This value is the additional force required at the displaced support to overcome the stiffness of the spring below this support, so that either matrix satisfies the equilibrium condition that the sum of the reactions produced by the displacement of one support of a continuous beam is zero. If k is zero, that is, if the elastic foundation is removed, the beam becomes unstable. This is reflected in both the stiffness matrix and the equivalent stiffness matrix: their determinants vanish and both $[S]$ and $[K]$ become singular.

The two matrices $[K]$ and $[S]$, when inverted, give the flexibility matrices $[\bar{f}]$ and $[f]$, in which any element $\bar{f}_{ij} \cong f_{ij}$, the degree of approximation depending on the chosen node spacing. If, for example, we take $k\lambda^4/(EI)=0.1$ in Eqs. (15.87) and (15.88) and invert, we obtain the following flexibility matrices, which can be compared:

$$[\bar{f}]=[K]^{-1}=\frac{\lambda^3}{EI}\begin{bmatrix}8.569 & & & \text{symmetrical} & & \\ 5.285 & 4.095 & & & & \\ 2.572 & 2.642 & 2.583 & & & \\ 0.474 & 1.250 & 2.003 & 2.583 & & \\ -1.224 & -0.017 & 1.250 & 2.642 & 4.095 & \\ -2.782 & -1.224 & 0.474 & 2.572 & 5.284 & 8.569\end{bmatrix} \tag{15.89}$$

and

$$[f]=[S]^{-1}=\frac{\lambda^3}{EI}\begin{bmatrix}8.489 & & & \text{symmetrical} & & \\ 5.304 & 4.062 & & & & \\ 2.605 & 2.654 & 2.529 & & & \\ 0.483 & 1.265 & 2.001 & 2.529 & & \\ -1.242 & -0.020 & 1.265 & 2.654 & 4.062 & \\ -2.807 & -1.242 & 0.483 & 2.605 & 5.304 & 8.489\end{bmatrix} \tag{15.90}$$

The methods of condensation of the stiffness matrix discussed in Section 6.5 can also be used with the equivalent stiffness matrix. For example, if in the beam of Figure 15.22a the displacement at node 6 is prevented by the introduction of a support, the deflection $D_6=0$, and the stiffness matrix of the resulting structure is obtained by deletion of the 6th row and

column from [K]. The last row of [K] can then be used to find the force F_6 at the support introduced:

$$F_6 = [K_{61} K_{62} \ldots K_{65}] \begin{Bmatrix} D_1 \\ D_2 \\ \ldots \\ D_5 \end{Bmatrix} \tag{15.91}$$

15.16 General

The problems treated in this chapter, ranging from beams to plates in bending, involve the solution of differential equations using the method of finite differences. Thus, derivatives of the deflection are represented by finite differences and the problem reduces to the solution of simultaneous algebraic equations. The number of equations depends upon the number of nodes chosen to approximate the deflection. The accuracy of the solution is improved with a decrease in the node spacing and an increase in the number of equations. However, in many problems adequate accuracy can be achieved with a small number of equations.

When the pattern of the finite-difference coefficients is known, the formation of the simultaneous equations is an easy process and the finite-difference solution can be used to advantage. All the steps of the analysis can be easily programmed for the use of computers. However, in some cases, such as with irregular boundaries, it is rather difficult to derive the finite-difference equations which suit the boundary conditions.

The finite-difference method can also be used to solve structural problems not included in this chapter, for example, a stretched membrane, or torsion, shell vibration problems. In all these cases we find solution of a partial differential equation using finite differences in a manner similar to that used in plate problems.

Problems

15.1 Find the deflections at points 1, 2, and 3 in the beam in Figure 10.15a using the approximate equations listed in Figure 15.4. Compare the answers with the values obtained in Section 10.5.

15.2 Determine the deflection, the bending moment at the nodes, and the support reactions for the beam in the figure, with a constant EI. The beam is on an elastic foundation between the supports A, B, and C with a modulus $k = 1184EI/l^4$.

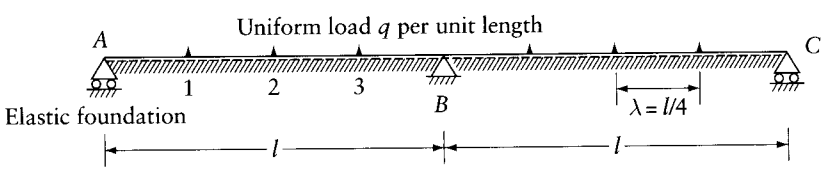

Prob. 15.2

15.3 Using finite differences, find the rotation at end A due to a unit couple applied at A for the beam in the figure and compare the result with the exact answer ($l/4EI$). *Hint:* Replace the couple by two equal and opposite forces at A and at node 1, and find the deflections using the equations listed in Figure 15.5. The slope is then calculated from the deflection using the expression given in Figure 15.2.

15.4 Using finite differences, find the flexibility matrix [f] corresponding to coordinates 1 and 2 of the cantilever in the figure. Compare the answer with accurate values from

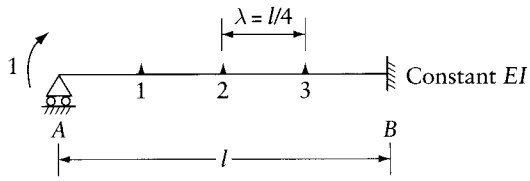

Prob. 15.3

Appendix B. *Hint:* A couple at coordinate 2 can be replaced by two equal and opposite forces at nodes 1 and 2. To calculate f_{21}, that is, the rotation at coordinate 2 due to a unit force at 1, we use the fact that the slope of the elastic line at 1 is approximately equal to the slope of the line joining the deflected position of nodes 1 and 2. This is acceptable because, for this loading, the bending moment, and hence the rate of change of slope at node 1, are zero. To calculate f_{22}, use the expression given in Figure 15.2.

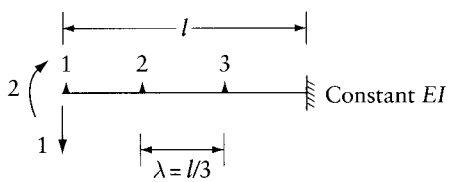

Prob. 15.4

15.5 Using finite differences, find the end-rotational stiffness at A and the carryover moment at B for the beam of Prob. 15.3. The beam is subjected to an axial compressive force $P = 9EI/l^2$ (not shown in the figure). Compare your results with the exact answers from Table 13.1. See the hint given for Prob. 15.3.

15.6 Using finite differences, find the end-moment at B in the beam-column shown in the figure.

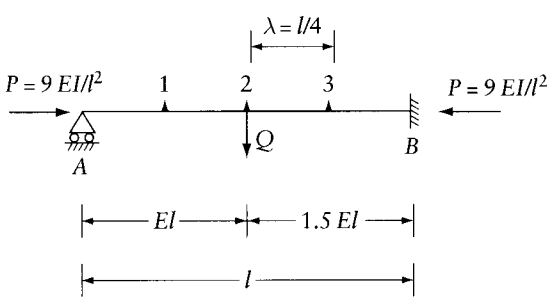

Prob. 15.6

15.7 Using finite differences, find the deflection at the nodes 1, 2, and 3 on the base of the long rectangular water tank shown in the figure. Consider a strip of unit width of the wall and base as a frame $ABCD$ of constant flexural rigidity EI. Neglect the self-weight of the frame. *Hint:* Walls AB and DC are subjected to a linearly varying outward horizontal load of $yl/2$ at the bottom and zero at the top, and the base BC is subjected to a uniform

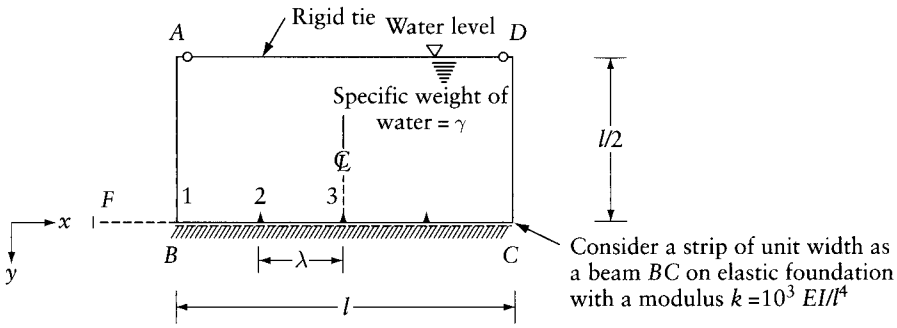

Prob. 15.7

vertical load $\lambda l/2$. Analyze the symmetrical beam BC by finite differences. One of the end conditions at B is: $M_B = -\lambda l^3/120 - 6Ely'_B/l = -Ely''_B$; where $|\lambda l^3/120|$ is absolute value of moment at end B when its rotation is prevented; $|6EI/l|$ is absolute value of the end moment due to unit rotation; $y'_B = (y_2 - y_F)/(2\lambda)$; $y''_B = (y_F - 2y_1 + y_2)/\lambda^2$; y_F is the deflection at a fictitious point F.

15.8 Find the radial deflection caused by hydrostatic pressure on the wall of a circular cylindrical water tank shown in the figure. Calculate also the hoop force, the bending moment in the vertical direction along the wall height, and the reaction at the bottom. Assume Poisson's ratio $\nu = 1/6$. The answers to this problem are given at the end of the book, using two solutions: one with $\lambda = H/5$ as shown in the figure, and the other with $\lambda = H/20$. A comparison of the two results gives an indication of the accuracy gained by reducing λ. With $\lambda = H/5$, five simultaneous equations have to be solved. Readers may either solve the equations or use the given answers to verify their equations.

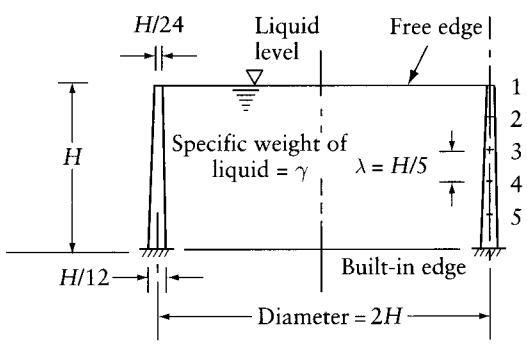

Prob. 15.8

15.9 Using finite differences with the mesh shown in the figure, find the deflection at the nodes and the bending moment M_y at nodes 1 and 2 of the plate shown. The plate is subjected to a uniform transverse load q, has a constant thickness h, and Poisson's ratio $\nu = 0$.

15.10 Solve Prob. 15.9 with the width of the plate in the x direction of 2b, and use the same mesh with $\lambda_x = 2\lambda_y$.

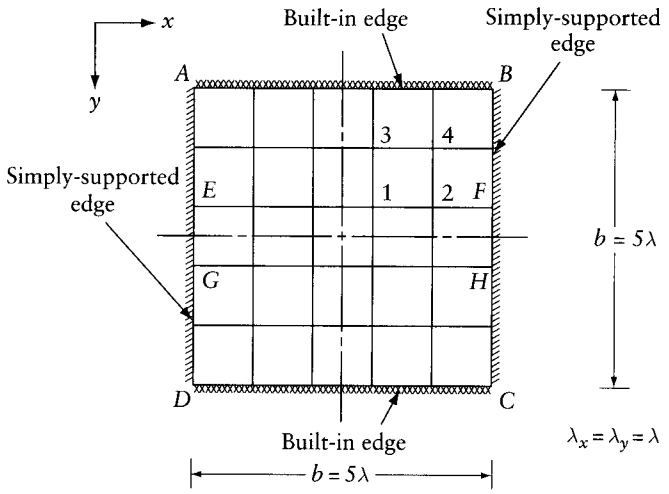

Prob. 15.9

15.11 Solve Prob. 15.9 with the plate subjected (in lieu of q) to a uniform positive bending moment M on the two edges AD and BC. *Hint:* Replace the edge moments by two equal and opposite transverse loads on the edge nodes and at nodes on a mesh line at distance λ_x from the edge.

15.12 Solve Prob. 15.9 with the plate reinforced by beams of flexural rigidity $EI = 2N\lambda$ along mesh lines EF and GH. The beams are assumed to be attached to the plate in the idealized fashion indicated in Figure 15.20b and have the ends simply supported. What is the bending moment in beam EF at node 1?

15.13 Using finite differences with the mesh shown in the figure, find the deflections at the nodes and M_y at points A, B, and C of the plate in the figure. The plate has a constant thickness h, Poisson's ratio $\nu = 0$, and is loaded by one concentrated load P on the free edge DE, as shown.

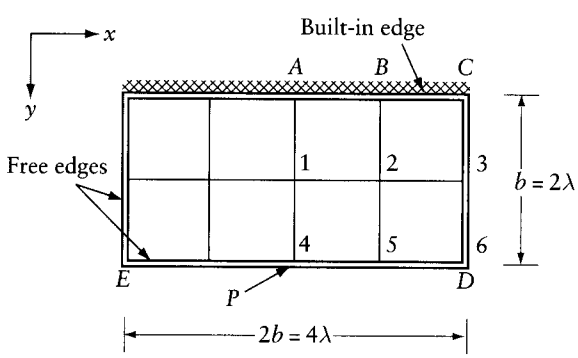

Prob. 15.13

15.14 Solve Prob. 15.13 with the plate reinforced by a beam along DE with free ends and a flexural rigidity $EI = 2N\lambda$. The beam is assumed to be attached to the plate in the idealized fashion indicated in Figure 15.20a.

15.15 Using finite differences with the mesh shown in the figure, find the deflections at the nodes and the reaction at the support A of the plate in the figure. The plate has a constant thickness h, Poisson's ratio $\nu = 0$, is built-in along two edges, free at the other two and has a support at A which can provide a transverse reaction only. The load intensity on the plate varies as shown. *Hint:* Apply the finite-difference equations in Figure 15.19 at nodes 1, 2, and 3, solve for the deflections, and then use the equation in Figure 15.19f to calculate the reaction at A.

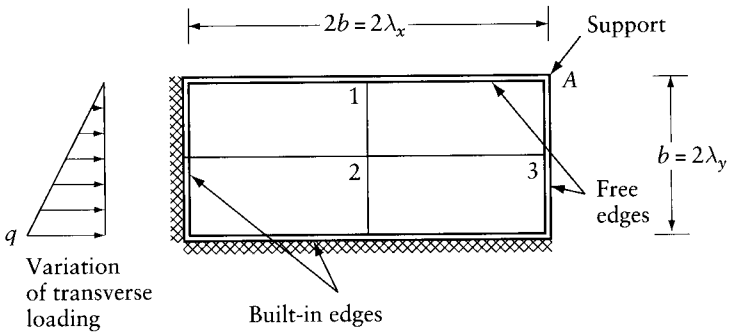

Prob. 15.15

Chapter 16

Finite-element method

16.1 Introduction

The finite-element method is widely used in structural analysis. The method is also used in a wide range of physical problems[1] including heat transfer, seepage, flow of fluids, and electrical and magnetic potential. In the finite-element method, a continuum is idealized as an assemblage of finite elements with specified nodes. The infinite number of degrees of freedom of the continuum is replaced by specified unknowns at the nodes.

In essence, the analysis of a structure by the finite-element method is an application of the displacement method. In frames, trusses, and grids, the elements are bars connected at the nodes; these elements are considered to be one-dimensional. Two-dimensional or three-dimensional finite elements are used in the analysis of walls, slabs, shells, and mass structures. The finite elements can have many shapes with nodes at the corners or on the sides (Figure 16.1). The unknown displacements are nodal translations or rotations or derivatives of these.

The use of a computer is essential in the finite-element method because of the large number of degrees of freedom commonly involved. Chapters 21 to 23 discuss the computer analysis of structures; the approach there applies to structures which are composed of finite elements of any type. However, the matrices for individual elements, given explicitly in earlier chapters (e.g. Eqs. 6.6 to 6.7) and in Chapters 21 to 23, are for one-dimensional bar elements. The present chapter is mainly concerned with the generation of matrices for finite elements other than bars. The element matrices required are: the stiffness matrix, relating nodal forces to nodal displacements; the stress matrix, relating the stress or internal forces at any point within an element to its nodal displacements; and vectors of restraining nodal forces for use when the external forces are applied away from the nodes or when the element is subjected to temperature variation.

For finite elements other than bars, "exact" element matrices cannot be generated. The displacements (e.g. u and v) within an element are expressed in terms of the nodal displacement. *Assumed* displacement fields (e.g. a polynomial in x and y) are used. The corresponding strains are determined by differentiation and the stress by using Hooke's law. Use of the principle of virtual work or minimization of the total potential energy (Sections 7.5, 7.6 and 9.6) with respect to the element nodal displacements gives the desired element matrices.

Use of displacement fields as described above is similar to the Rayleigh-Ritz method presented in Section 10.7, where the deflection of a beam is represented by a series of assumed functions with indeterminate parameters. The unknown parameters are derived by the principle of virtual work. They can also be derived by minimization of total potential energy. In the finite-element

1 See Zienkiewicz, O.C. and Taylor, R.L., *The Finite Element Method*, 6th ed., McGraw-Hill, London, 2005.

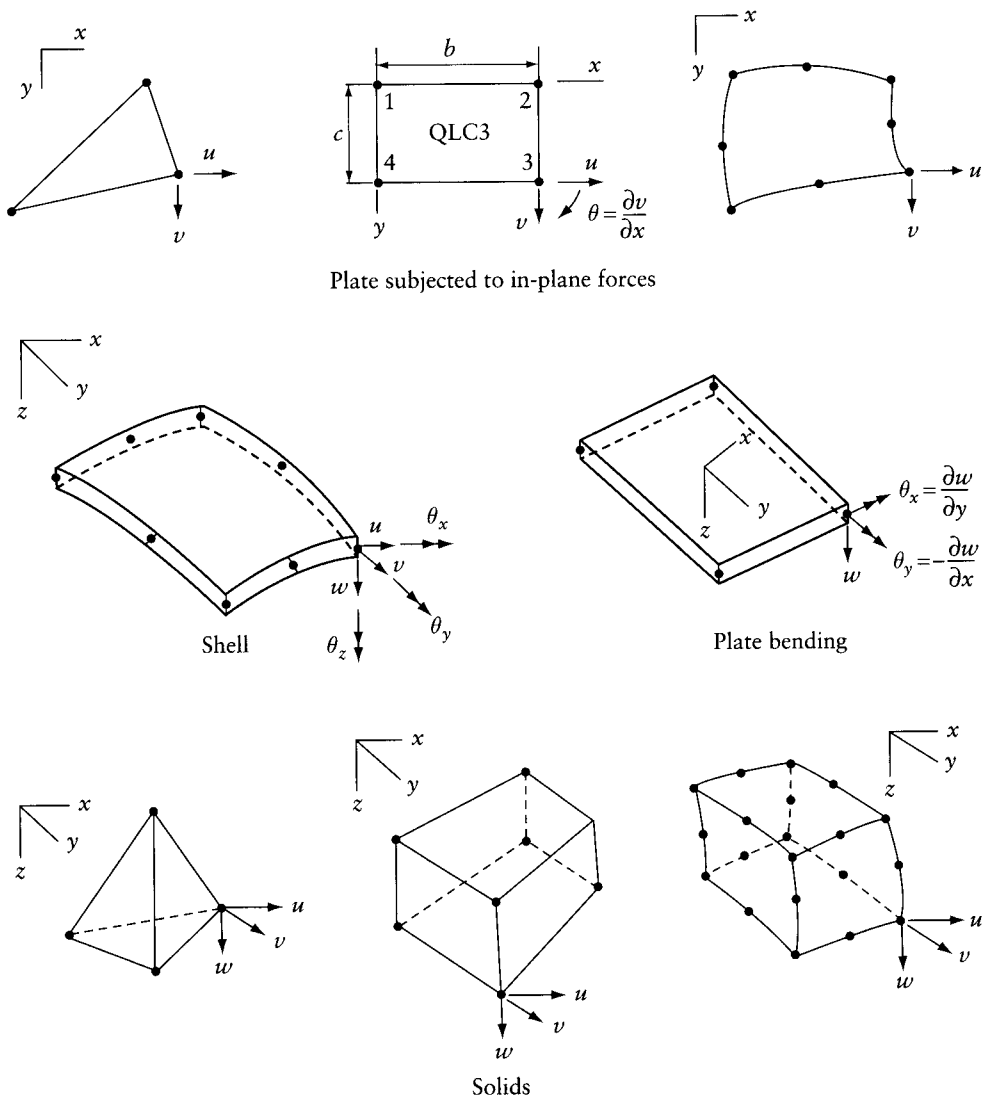

Figure 16.1 Examples of finite elements with nodal degrees of freedom shown at a typical node only.

formulation, using assumed displacement fields, the indeterminate parameters are the nodal displacements. As in the Rayleigh-Ritz method, the solution obtained by the finite-element method is approximate; however, convergence to the exact solution is achieved as the number of unknown parameters is increased. In other words, when a finer finite-element mesh is used, more unknown displacements are involved and a greater accuracy is achieved.

The use of smaller elements for convergence is not required when the true displacement shapes can be derived and used to generate the element matrices. This is the case with prismatic bar elements.

This chapter gives the general procedures to derive matrices for finite elements of any type. This is explained by reference to bar elements and to plate elements subjected to in-plane forces or to bending. Other element types are discussed in Chapter 17.

It is most common to derive the matrices for finite elements using assumed displacement fields, and this method will be mainly used in this chapter. It is also possible to generate the element matrices using assumed fields for displacements and for stresses (or strains): this results in what are known as *hybrid elements*. The unknowns will then be the stress (or strain) parameters, in addition to the nodal displacements. However, all the unknown parameters other than the nodal displacements are eliminated at the element level; the global system of equations for the structure involves nodal displacements only. When the same number of equations is solved, a more accurate analysis is obtained with hybrid elements compared with the analysis using displacement-based finite elements. Thus, the use of hybrid elements represents a convenient practical approach. Section 17.13 discusses the generation of stiffness and stress matrices for hybrid elements.

16.2 Application of the five steps of displacement method

In essence, the analysis of a structure by the finite-element method is an application of the five steps of the displacement method summarized in Section 5.6. This analysis is explained below by reference to a plate subjected to in-plane forces (Figure 16.2) which is idealized as an assemblage of rectangular finite elements. Each element has four nodes with two degrees of freedom per node, that is, translations u and v in the x and y directions respectively. The purpose of the analysis is to determine the stress components $\{\sigma\} = \{\sigma_x, \sigma_y, \tau_{xy}\}$ at O, the center of each element. The external loads are nodal forces $\{F_x, F_y\}_i$ at any node i, and body forces with intensities per unit volume of $\{p_x, p_y\}_m$ distributed over any element m. Other loadings can also be considered, such as the effects of temperature variation or of shrinkage (or swelling).

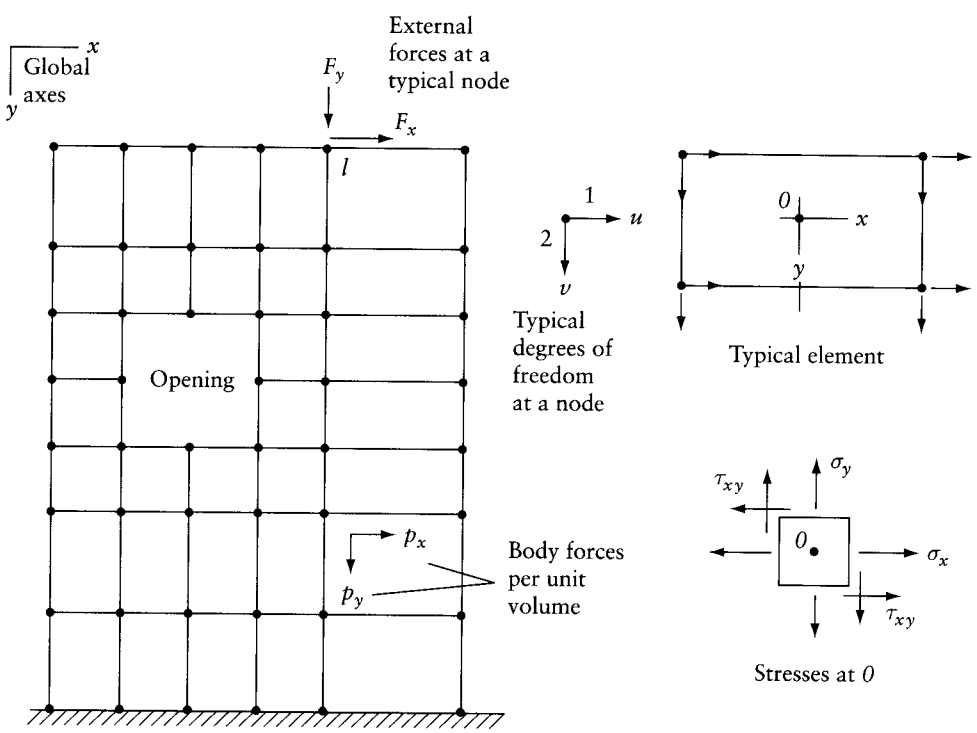

Figure 16.2 Example of a finite-element model for the analysis of stresses in a wall subjected to in-plane forces.

The five steps in the analysis are as follows:

Step 1 Define the unknown degrees of freedom by two coordinates u and v at each node. The actions to be determined for any element m are $\{A\}_m \equiv \{\sigma\}_m = \{\sigma_x, \sigma_y, \tau_{xy}\}_m$.

Step 2 With the loading applied, determine the restraining forces $\{F\}$ to prevent the displacements at all coordinates. Also, for any element, determine $\{A_r\}_m \equiv \{\sigma_r\}_m$, which represents the values of the actions (the stresses) with the nodal displacements prevented.

The stresses $\{\sigma_r\}$ are produced only when effects of temperature are considered; $\{\sigma_r\}$ due to body forces is commonly ignored.

The vector $\{F\}$ is considered equal to the sum of two vectors:

$$\{F\} = \{F_a\} + \{F_b\} \tag{16.1}$$

The vector $\{F_a\}$ is composed of the external nodal forces reversed in sign; $\{F_b\}$ is generated by assemblage of $\{F_b^*\}_m$ for individual elements. The vector $\{F_b^*\}_m$ is composed of forces at the nodes of element m in equilibrium with the external forces on the element body away from the nodes; in the case of temperature variation, $\{F_b^*\}_m$ represents a system of nodal forces in equilibrium producing stresses $\{\sigma_r\}$. (Eq. 6.43 gives the nodal forces due to temperature variation for a member of a plane frame; for other finite elements, see Section 16.6.1.)

Step 3 Generate the structure stiffness matrix $[S]$ by assemblage of the stiffness matrices $[S]_m$ of individual elements. Also, generate $[A_u]_m \equiv [\sigma_u]_m$, which represents the stress components at O in any element due to unit displacement introduced separately at the element nodal coordinates. For the example considered in Figure 16.2, $[\sigma_u]_m$ will be a 3×8 matrix.

Step 4 Solve the equilibrium equations

$$[S]\{D\} = -\{F\} \tag{16.2}$$

This gives the structure nodal displacements $\{D\}$. In the example considered, the number of elements in $\{D\}$ is twice the number of nodes.

Step 5 Calculate the required stress components for each element:

$$\{A\}_m = \{A_r\}_m [A_u]_m \{D\}_m \tag{16.3}$$

or

$$\{\sigma\}_m = \{\sigma_r\}_m + [\sigma_u]_m \{D\}_m \tag{16.4}$$

The values $\{D\}_m$ are the nodal displacements for the element m; in the example considered (Figure 16.2), $\{D\}_m$ has eight values (subset of the structure displacement vector $\{D\}$).

Ignoring $\{\sigma_r\}$ caused by body forces (steps 2 and 5) produces an error which diminishes as the size of the finite elements is reduced. However, when the elements are bars (in framed structures), $\{\sigma_r\} \equiv \{A_r\}$, and the other matrices for individual members can be determined exactly; for this reason, $\{\sigma_r\}$ is commonly not ignored and the exact answers can be obtained without the need to reduce the size of the elements for convergence.

Assemblage of the structure load vector and of the stiffness matrix may be done by Eqs. 21.34 and 21.31. The nonzero elements of $[S]$ are generally limited to a band adjacent to the diagonal.

This property, combined with the symmetry of $[S]$, is used to conserve computer storage and to reduce the number of computations. These topics and the methods of solution of Eq. 16.2 to satisfy displacement constraints are discussed in Chapters 21 and 22. Examples of displacement constraints are a zero or a prescribed value for the displacement at a support.

16.3 Basic equations of elasticity

The stresses and strains in an elastic body are related by Hooke's law, which can be written in the generalized form

$$\{\sigma\} = [d]\{\epsilon\} \tag{16.5}$$

where $\{\sigma\}$ and $\{\epsilon\}$ are generalized stress and strain vectors respectively, and $[d]$ is a square symmetrical matrix referred to as the *elasticity matrix*.

The strain components are defined as derivatives of the displacement component by the generalized equation

$$\{\epsilon\} = [\partial]\{f\} \tag{16.6}$$

where $[\partial]$ is a matrix of the differential operator, and $\{f\}$ is a vector of functions describing the displacement field.

The symbols $\{\sigma\}$ and $\{\epsilon\}$ will be used to represent stress or strain components in one-, two-, or three-dimensional bodies. The displacement field $\{f\}$ will have one, two, and three components: u, v, and w in the direction of orthogonal axes x, y, and z. The differential operator matrix $[\partial]$ will represent derivatives with respect to one, two, or three of the variables x, y, and z.

In a bar subjected to an axial force (Figure 7.5a), each of $\{\sigma\}$ and $\{\epsilon\}$ has one component and $[d]$ has one element equal to E, the modulus of elasticity. The strain ϵ is equal to du/dx, where u is displacement along the beam axis and x is distance measured in the same direction. Thus, we can use Eqs. 16.5 and 16.6 for the uniaxial stress state, with the symbols having the following meanings:

$$\{\sigma\} \equiv \sigma \quad \{\epsilon\} \equiv \epsilon \quad [d] \equiv E \quad \{f\} \equiv u \quad [\partial] = d/dx \tag{16.7}$$

We shall also use the symbol $\{\sigma\}$ to represent a vector of stress resultants. For the bar considered above, we can take $\{\sigma\} \equiv N$, the axial force on the bar cross section, and $[d] \equiv Ea$, where a is the cross-sectional area. Again, Eqs. 16.5 and 16.6 apply, with the symbols having the following meanings:

$$\{\sigma\} \equiv N \quad \{\epsilon\} \equiv \epsilon \quad [d] \equiv Ea \quad \{f\} \equiv u \quad [\partial] = d/dx \tag{16.8}$$

The generalized Eqs. 16.5 and 16.6 apply to a bar in bending (Figure 6.5b), with the symbols having the following meanings:

$$\{\sigma\} \equiv M \quad \{\epsilon\} \equiv \psi \quad [d] \equiv EI \quad \{f\} \equiv v \quad [\partial] = d^2/dx^2 \tag{16.9}$$

where M is the bending moment, ψ is the curvature, I is the second moment of area about the centroidal axis, and v is the displacement in the y direction.

The product $\{\sigma\}^T\{\epsilon\}$ integrated over the volume of an element appears in the strain energy Eq. 7.14 and in the virtual work Eq. 7.46, both of which will be frequently used. When $\{\sigma\}$ represents stress resultants over a cross section of a bar, the integral over the volume has to be replaced by an integral over the length (see Eq. 7.32). For plates in bending, we shall use $\{\sigma\}$ to represent bending and twisting moments $\{M_x, M_y, M_{xy}\}$ and the integral will be over the area.

In the following subsections we shall apply the generalized Eqs. 16.5 and 16.6 in three stress states.

16.3.1 Plane stress and plane strain

Consider a plate subjected to in-plane forces (Figure 16.13). At any point, the stress , strain, and displacement components are

$$\{\sigma\} = \{\sigma_x, \sigma_y, \tau_{xy}\} \quad \{\epsilon\} = \{\epsilon_x, \epsilon_y, \gamma_{xy}\} \quad \{f\} = \{u, v\} \tag{16.10}$$

The strains are defined as derivatives of $\{f\}$ by the generalized Eq. 16.6, with the differential operator matrix

$$[\partial] = \begin{bmatrix} \partial/\partial x & 0 \\ 0 & \partial/\partial y \\ \partial/\partial y & \partial/\partial x \end{bmatrix} \tag{16.11}$$

The stress and strain vectors are related by generalized Hooke's law (Eq. 16.5) with the elasticity matrix $[d]$ given by one of the Eqs. 16.12 or 16.13.

When strain in the z direction is free to occur, $\sigma_z = 0$ and we have the state of plane stress. Deep beams and shear walls are examples of structures in a state of plane stress. When strain in the z direction cannot occur, $\epsilon_z = 0$ and we have the state of plane strain. The state of plane strain occurs in structures which have a constant cross section perpendicular to the z direction and also have the dimension in the z direction much larger than those in the x and y directions. Concrete gravity dams and earth embankments are examples of structures in this category. The analysis of these structures may be performed for a slice of unit thickness in a state of plane strain.

For an isotropic material, the elasticity matrix in a plane-stress state is

$$[d] = \frac{E}{1-\nu^2} \begin{bmatrix} 1 & \nu & 0 \\ \nu & 1 & 0 \\ 0 & 0 & (1-\nu)/2 \end{bmatrix} \tag{16.12}$$

where E is the modulus of elasticity in tension or in compression, and ν is Poisson's ratio.

The elasticity matrix for a plane-strain state is

$$[d] = \frac{E(1-\nu)}{(1+\nu)(1-2\nu)} \begin{bmatrix} 1 & \nu/(1-\nu) & 0 \\ \nu/(1-\nu) & 1 & 0 \\ 0 & 0 & (1-2\nu)/2(1-\nu) \end{bmatrix} \tag{16.13}$$

Equation 16.12 can be derived from Eq. 6.6 or by inversion of the square matrix in Eq. 15.53. Equation 16.13 can also be derived from Eq. 7.8 by setting $\epsilon_z = 0$ (in addition to $\tau_{xz} = \tau_{yz} = 0$). The same equations give the normal stress in the z direction in the plane-strain state

$$\sigma_z = \nu(\sigma_x + \sigma_y) \tag{16.14}$$

16.3.2 Bending of plates

For a plate in bending (Figure 15.14), the generalized stress and strain vectors are defined as

$$\{\sigma\} = \{M_x, M_y, M_{xy}\} \tag{16.15}$$

and

$$\{\epsilon\} = \left\{-\partial^2 w/\partial x^2, -\partial^2 w/\partial y^2, 2\partial^2 w\,(\partial x \partial y)\right\} \tag{16.16}$$

One component of body force and one component of displacement exist:

$$\{p\} \equiv \{q\} \tag{16.17}$$

$$\{f\} \equiv \{w\} \tag{16.18}$$

where q is force in the z direction per unit area and w is deflection in the same direction. The generalized Eqs. 16.5 and 16.6 apply to a plate in bending, with

$$[\partial] \begin{Bmatrix} -\partial^2/\partial x^2 \\ -\partial^2/\partial y^2 \\ 2\partial^2/(\partial x \partial y) \end{Bmatrix} \tag{16.19}$$

For an orthotropic plate in bending, the elasticity matrix is

$$[d] = \frac{h^3}{12} \begin{bmatrix} E_x/(1-\nu_x\nu_y) & \nu_x E_y/(1-\nu_x\nu_y) & 0 \\ \nu_x E_y/(1-\nu_x\nu_y) & E_y/(1-\nu_x\nu_y) & 0 \\ 0 & 0 & G \end{bmatrix} \tag{16.20}$$

where E_x, E_y are moduli of elasticity in tension or in compression in the x and y directions; ν_x and ν_y are Poisson's ratios; G is shear modulus of elasticity; and h is the plate thickness. The shear modulus of elasticity

$$G = \sqrt{E_x E_y}/[2(1+\sqrt{\nu_x \nu_y})]$$

When the plate is isotropic, we set $E = E_x = E_y$ and $\nu = \nu_x = \nu_y$ in Eq. 16.20:

$$[d] = \frac{Eh^3}{12(1-\nu^2)} \begin{bmatrix} 1 & \nu & 0 \\ \nu & 1 & 0 \\ 0 & 0 & (1-\nu)/2 \end{bmatrix} \tag{16.21}$$

It can be noted that, for a plate in bending, the generalized Eq. 16.5 is simply a condensed form of Eq. 15.64.

16.3.3 Three-dimensional solid

For a three-dimensional body, the generalized Eqs. 16.5 and 16.6 apply again, with the vectors $\{p\}$ and $\{f\}$ having the following meaning:

$$\{p\} = \{p_x, p_y, p_z\} \tag{16.22}$$

$$\{f\} = \{u, v, w\} \tag{16.23}$$

where $\{p_x, p_y, p_z\}$ are body forces per unit volume, and $\{u, v, w\}$ are translations in the x, y, and z directions (Figure 7.4). The stress and strain vectors $\{\sigma\}$ and $\{\epsilon\}$ are defined by Eqs. 7.9 and 7.10, and the $[d]$ matrix is given by Eq. 7.13. The differential operator is

$$[\partial]^T = \begin{bmatrix} \partial/\partial x & 0 & 0 & \partial/\partial y & \partial/\partial z & 0 \\ 0 & \partial/\partial y & 0 & \partial/\partial x & 0 & \partial/\partial z \\ 0 & 0 & \partial/\partial z & 0 & \partial/\partial x & \partial/\partial y \end{bmatrix} \tag{16.24}$$

16.4 Displacement interpolation

In the derivation of element matrices, interpolation functions are required to define the deformed shape of the element. For a finite element of any type, the displacement at any point within the element can be related to the nodal displacement by the equation

$$\{f\} = [L]\{D^*\} \tag{16.25}$$

where $\{f\}$ is a vector of displacement components at any point; $\{D^*\}$ is a vector of nodal displacements; and $[L]$ is a matrix of functions of coordinates defining the position of the point considered within the element (e.g. x and y or ξ and η in two-dimensional finite elements).

The interpolation functions $[L]$ are also called *shape functions;* they describe the deformed shape of the element due to unit displacements introduced separately at each coordinate. Any interpolation function L_i represents the deformed shape when $D_i^* = 1$ while the other nodal displacements are zero.

The accuracy of a finite element depends upon the choice of the shape functions. These should satisfy conditions which will ensure convergence to correct answers when a finer finite-element mesh is used. The derivation of the shape functions and the conditions which should be satisfied are discussed in Sections 16.8 and 16.9. Examples of shape functions with various types of elements are given below.

16.4.1 Straight bar element

For the axial deformation of a bar (Figure 16.3), $\{f\} \equiv \{u\}$ is the translation in the x direction at any section, and $\{D^*\} = \{u_1, u_2\}$ is the translation at the two ends. The matrix $[L]$ may be composed of two linear interpolation functions:

$$[L] = [1 - \xi, \xi] \tag{16.26}$$

where $\xi = x/l$, and l is the bar length.

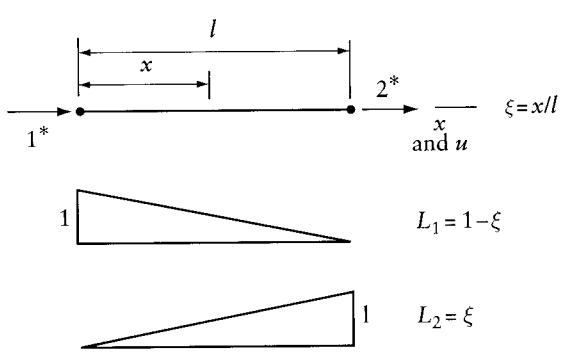

Figure 16.3 Linear interpolation functions. Shape functions for a bar subjected to an axial force.

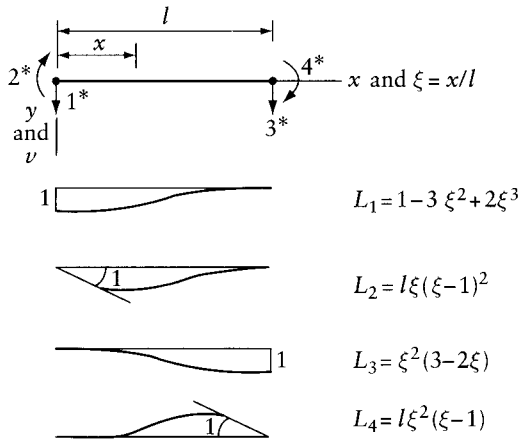

Figure 16.4 Shape functions for deflection of a bar in bending.

The shape functions which can be used for a bar in bending are given in Figure 16.4. For this element, $\{f\} \equiv \{v\}$ is the transverse deflection in the y direction at any section; the nodal displacements are defined as

$$\{D^*\} = \left\{v_{x=0}, \left(\frac{dv}{dx}\right)_{x=0}, v_{x=1}, \left(\frac{dv}{dx}\right)_{x=1}\right\} \tag{16.27}$$

The shape functions $[L]$ can be the four cubic polynomials

$$[L] = \left[1 - 3\xi^2 + 2\xi^3 \,|\, l\xi\,(\xi - 1)^2 \,|\, \xi^2\,(3 - 2\xi) \,|\, l\xi^2\,(\xi - 1)\right] \tag{16.28}$$

Each shape function L_i in Eqs. 16.26 and 16.28 satisfies the requirement that $D_i^* = 1$ with other displacements zero. This requirement is sufficient to derive the functions (see Section 16.8).

The shape functions in Eqs. 16.26 and 16.28 correspond to the true deformed shapes of a prismatic bar (with shear deformation ignored). The same shape functions may be used to derive matrices for nonprismatic bars (see Examples 16.4 and 16.5).

We can recognize that the shape functions in Figures 16.3 and 16.4 are the same as the influence lines for the nodal forces, reversed in sign. (Compare, for example, L_2 and L_4 in Figure 16.4 with the influence lines of the member end-moments in Figure 12.7d.)

The shape functions L_1 in Figure 16.4 can be considered to be equal to the sum of the straight lines $1 - \xi$ and $(L_2 + L_4)/l$; the latter term represents the deflected shape corresponding to clockwise rotations, each equal to $1/l$ at the two ends. By similar reasoning, we can verify that $L_3 = \xi - (L_2 + L_4)/l$.

16.4.2 Quadrilateral element subjected to in-plane forces

Figure 16.5 shows a quadrilateral element with corner nodes and two degrees of freedom per node. The element may be used in plane-stress and plane-strain analyses. In this case, the symbols in the generalized Eq. 16.25 have the following meaning:

$$[f] = \{u, v\} \tag{16.29}$$

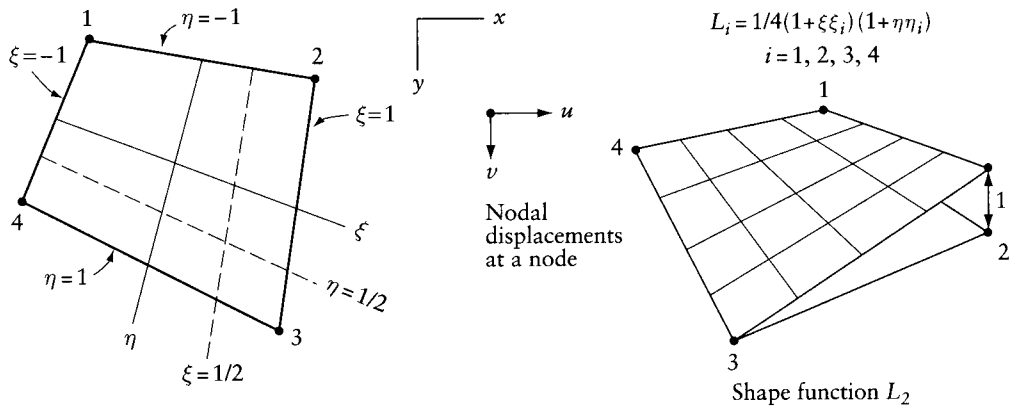

Figure 16.5 Plane-stress or plane-strain quadrilateral element. Natural coordinates ξ and η define the location of any point. Pictorial view of a shape function (hyperbolic paraboloid).

where u and v are translations in the x and y directions, and

$$\{D^*\}=\{u_1,v_1,u_2,v_2,u_3,v_3,u_4,v_4\} \tag{16.30}$$

where u_i and v_i are translations at node i in the x and y directions. The $[L]$ matrix for the element in Figure 16.5 is

$$[L]=\begin{bmatrix} L_1 & 0 & L_2 & 0 & L_3 & 0 & L_4 & 0 \\ 0 & L_1 & 0 & L_2 & 0 & L_3 & 0 & L_4 \end{bmatrix} \tag{16.31}$$

The function L_i is a sum of bilinear functions in the natural coordinates ξ and η, defined in Figure 16.5. The value of L_i is unity at node i and zero at the other three nodes; any of the four shape functions may be expressed as

$$L_i=\frac{1}{4}(1+\xi\xi_i)(1+\eta\eta_i) \quad \text{with } i=1,2,3,4 \tag{16.32}$$

If the value of L_i is plotted perpendicular to the surface of the element, a hypersurface is obtained. Along the lines $\xi=$ constant or $\eta=$ constant, the surface follows straight lines. The shape function L_2 is plotted in pictorial view in Figure 16.5; at node 2, $\xi_i=1$ and $\eta_i=-1$, and the function L_2 defining the hypersurface is obtained by substitution of the two values in Eq. 16.32.

Equation 16.32 represents one of a family of functions used for interpolation in the *isoparametric elements*, discussed in Section 17.2. We should note that the sum of the values of the four L_i functions at any point is unity.

16.4.3 Rectangular plate-bending element

The rectangular element in Figure 16.6, used in the analysis of plates in bending, has twelve degrees of freedom (three at each corner), defined as

$$\{D^*\}=\left\{(w,\theta_x,\theta_y)_1 \;\vdots\; (w,\theta_x,\theta_y)_2 \;\vdots\; (w,\theta_x,\theta_y)_3 \;\vdots\; (w,\theta_x,\theta_y)_4\right\} \tag{16.33}$$

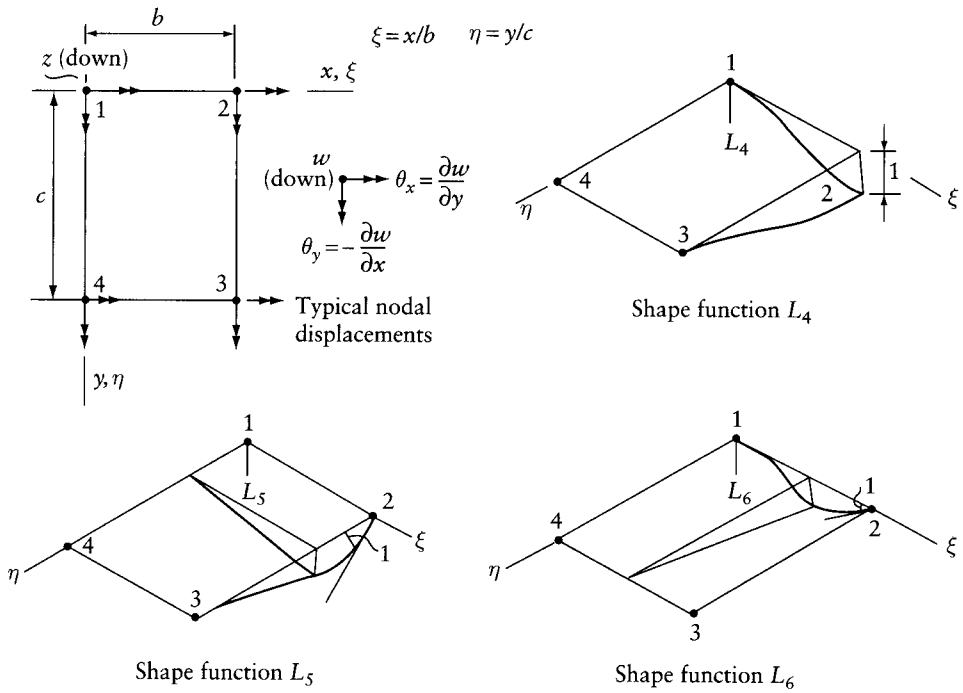

Figure 16.6 Plate-bending element.

Here, the displacement $f \equiv w$ is the deflection at any point. The rotations θ are treated as derivatives of w:

$$\theta_x = \partial w/\partial y \quad \theta_y = -\partial w/\partial x \tag{16.34}$$

The shape functions for the rectangular bending element (Figure 16.6) are

$$[L] = \Big[\begin{array}{ll} (1-\xi)(1-\eta) - \frac{1}{b}(L_3 + L_6) + \frac{1}{c}(L_2 + L_{11}) & 1 \\ c\eta(\eta-1)^2(1-\xi) & 2 \\ -b\xi(\xi-1)^2(1-\eta) & 3 \\ \xi(1-\eta) + \frac{1}{b}(L_3 + L_6) + \frac{1}{c}(L_5 + L_8) & 4 \\ c\eta(\eta-1)^2\xi & 5 \\ -b\xi^2(\xi-1)(1-\eta) & 6 \\ \xi\eta + \frac{1}{b}(L_9 + L_{12}) - \frac{1}{c}(L_5 + L_8) & 7 \\ c\eta^2(\eta-1)\xi & 8 \\ -b\xi^2(\xi-1)\eta & 9 \\ (1-\xi)\eta - \frac{1}{b}(L_9 + L_{12}) - \frac{1}{c}(L_2 + L_{11}) & 10 \\ c\eta^2(\eta-1)(1-\xi) & 11 \\ -b\xi(\xi-1)^2\eta \Big] & 12 \end{array} \tag{16.35}$$

where b and c are lengths of element sides; $\xi = x/b$ and $\eta = y/c$. The functions L_2, L_3, L_5, L_6, L_8, L_9, L_{11}, L_{12} are shape functions given explicitly in Eq. 16.35 on lines 2, 3, 5, 6, 8, 9, 11, and 12 respectively; they correspond to unit rotations. Pictorial views of three deflected shapes, L_4, L_5, and L_6, corresponding to unit displacements at node 2, are included in Figure 16.6. It can be seen that L_6 is zero along three edges, while along the fourth edge (1-2) the function is the same as the shape function for a beam (compare with L_4 in Figure 16.4, reversed in sign). Along any line $\xi =$ constant, L_6 varies linearly, as shown in Figure 16.6. Similarly, L_5 has the same shape as a deflected bar along the edge 3-2 and varies linearly along any line $\eta =$ constant.

The shape functions L_1, L_4, L_7, L_{10}, corresponding to $w = 1$ at the corners, are expressed as the sum of bilinear shape functions (similar to the one shown in Figure 16.5) and the shape functions corresponding to rotations at the nodes equal to $\pm(1/b)$ or $\pm(1/c)$. Each of the four functions has values along two edges which are the same as the shape functions of a bar (L_1 or L_3 in Figure 16.4). At any point, the sum $L_1 + L_4 + L_7 + L_{10}$ is equal to unity.

We should note that the deflected surface defined by any of the twelve shape functions does not generally have a zero slope normal to the element edges. This can produce incompatibility of slopes in adjacent elements; the effects of these incompatibilities will be discussed in Section 16.9.

16.5 Stiffness and stress matrices for displacement-based elements

Equation 16.25 defines the element displacement field in terms of the nodal displacement. By appropriate differentiation, we can derive the strain (Eq. 16.6):

$$\{f\} = [L]\{D^*\} \tag{16.36}$$

$$\{\epsilon\} = [\partial][L]\{D^*\} \tag{16.37}$$

Thus, the strain at any point in a displacement-based element is

$$\{\epsilon\} = [B]\{D^*\} \tag{16.38}$$

where

$$[B] = [\partial][L] \tag{16.39}$$

The matrix $[B]$ may be referred to as the nodal displacement-strain transformation matrix. Any column j of $[B]$ represents the strain components $\{\epsilon_{uj}\}$ due to $D_j^* = 1$. Use of Hooke's law (Eq. 16.5) gives the stress at any point in a displacement-based element:

$$\{\sigma\} = [d][B]\{D^*\} \tag{16.40}$$

or

$$\{\sigma\} = [\sigma]_u \{D^*\} \tag{16.41}$$

where $[\sigma_u]$ is the *stress matrix* for the element:

$$[\sigma_u] = [d][B] \tag{16.42}$$

The elements of any column j of $[\sigma_u]$ are the stress components at any point due to $D_j^* = 1$.

An element S^*_{ij} of the stiffness matrix is the force at coordinate i corresponding to unit displacement at j; S^*_{ij} can be determined by the unit-displacement theorem (Eq. 7.47):

$$S^*_{ij} = \int_v \{\sigma_{uj}\}^T \{\epsilon_{ui}\}\, dv \tag{16.43}$$

where $\{\sigma_{uj}\}$ represents the "actual" stresses at any point due to unit displacement at j; $\{\epsilon_{ui}\}$ represents the strains at the same point corresponding to unit virtual displacement at i; and dv is an elemental volume.[2] The integral over the volume is replaced by an integral over the length in the case of a bar and over the area in the case of a plate. For this purpose, the symbols $\{\sigma\}$ and $\{\epsilon\}$ in Eq. 16.43 represent generalized stress and strain respectively. For example, in a bar, $\{\sigma\}$ represents internal forces at a section; in a plate in bending, $\{\epsilon\}$ represents curvatures (Eq. 16.16).

Using the shape functions $[L]$ to determine the actual stresses and the virtual strains via Eqs. 16.39 and 16.42, substitution in Eq. 16.43 gives any element of the stiffness matrix:

$$S^*_{ij} = \int_v \{B\}_j^T [d] \{B\}_i\, v \tag{16.44}$$

where $\{B\}_i$ and $\{B\}_j$ are the ith and jth columns of $[B]$. The stiffness matrix of a finite element is given by

$$[S^*] \int_v [B]^T [d] [B] dv \tag{16.45}$$

In Eqs. 16.43 and 16.44 we are accepting an assumed displacement field, namely L_j, as actual. However, in general, the assumed shape is different from the actual. What we are doing then is tantamount to imposing the assumed configuration by the application of small distributed forces on the element body in addition to the nodal forces. The distributed forces have the effect of changing the actual configuration to the assumed shape; these forces, not accounted for, cause the stiffness calculated by Eq. 16.45 to be an overestimate. In other words, a finite-element analysis in which the element stiffness matrices are derived by the above procedure is expected to give smaller displacements than the actual ones.

16.6 Element load vectors

The vector of restraining forces, to be used in the equilibrium Eq. 16.2, includes a component $\{F_b\}$ representing the forces in equilibrium with the external loads applied on the body of the elements away from the nodes (Eq. 16.1). Considering a single element, the equilibrant at node j to the body forces can be determined by

$$F_{bj} = -\int_v \{L_j\}^T \{p\}\, dv \tag{16.46}$$

where $\{p\}$ represents the magnitudes per unit volume of forces applied in the same directions as the displacements $\{f\}$.

Equation 16.46 can be explained by the principle of virtual work (Eq. 7.46) and also, succinctly, by Betti's theorem (Section 9.2). Here, the body forces and the nodal equilibrants form

2 The symbol dv representing elemental volume should not be confused with v, which represents a translational displacement.

one system; the element subjected only to those nodal forces which produce the displacement configuration L_j represents the second system. According to Betti's theorem, the work of the forces of the first system during displacements by the second system is equal to the work of the second system during displacements by the first system. Now, the second quantity is zero because the second system has forces at the nodes only, and the nodal displacements in the first system are all zero.

By the use of Eq. 16.46, we are treating the shape function L_j as the influence line (or influence surface) of the nodal force at j, reversed in sign (see Section 12.3). We should remember that an approximation is involved in Eq. 16.46 by the acceptance of an assumed deflected shape as the actual displacement field.

The vector of nodal forces in equilibrium with the forces applied on the element away from the nodes is

$$\{F_b^*\} = -\int_v [L]^T \{p\} dv \tag{16.47}$$

This vector is referred to as the element *consistent load vector* because the same shape functions $[L]$ are used to generate $[S^*]$ and $\{F_b^*\}$. The superscript * is used here to refer to local coordinates of an individual element.

When the external forces are applied to the surface of the element, the integral in Eq. 16.47 should be taken over the area of the element. When concentrated forces act, the integral is replaced by a summation of the forces multiplied by the values of $[L]^T$ at the load positions.

16.6.1 Analysis of effects of temperature variation

When an element is subjected to temperature variation (or to shrinkage), with the displacements restrained, the stresses at any point are given by (Eq. 16.5)

$$\{\sigma_r\} = -[d]\{\epsilon_0\} \tag{16.48}$$

where $\{\epsilon_0\}$ represents the strains which would exist if the change in volume were free to occur. In a two-dimensional plane-stress or plane-strain state, a rise of temperature of T degrees produces the free strain

$$\{\epsilon_0\} = \alpha T \begin{Bmatrix} 1 \\ 1 \\ 0 \end{Bmatrix} \tag{16.49}$$

where α is the coefficient of thermal expansion.

For an element subjected to volume change, the consistent vector of restraining forces is given by

$$\{F_b^*\} = -\int_v [B]^T [d] \{\epsilon_0\} dv \tag{16.50}$$

Again, the unit-displacement theory may be used to derive Eq. 16.50. With the actual stress being $\{\sigma_r\} = -[d]\{\epsilon_0\}$ and the virtual strain being $\{\epsilon_{uj}\} = \{B\}_j$, Eq. 7.50 gives the jth element of the consistent load vector.

In most cases, the integrals involved in generating the stiffness matrix and the load vectors for individual elements are evaluated numerically using Gaussian quadrature (see Section 17.9).

16.7 Derivation of element matrices by minimization of total potential energy

The element stiffness matrix $[S^*]$ and the consistent load vector $\{F_b^*\}$ (Eqs. 16.45 and 16.47) can be derived by the principle of total potential energy (Section 9.6). Consider a finite element subjected to body forces $\{p\}$ and nodal forces $\{Q^*\}$. The total potential energy is defined as the sum of potential energy and strain energy (Eq. 9.27):

$$\Phi = -\{D^*\}^T[Q^*] - \int_v \{f\}^T\{p\}\,dv + \frac{1}{2}\int_v \{\sigma\}^T\{\epsilon\}\,dv \tag{16.51}$$

where $\{f\}$ are displacement components at any point; $\{p\}$ are body forces per unit volume applied in the same directions as $\{f\}$; $\{\sigma\}$ are stresses; $\{\epsilon\}$ are strains; and $\{D^*\}$ are nodal displacements. Substitution of Eqs. 16.36, 16.38, and 16.40 in the above equation gives

$$\Phi = -\{D^*\}^T\{Q^*\} - \int_v \{D^*\}^T[L]^T\{p\}\,dv + \frac{1}{2}\int_v \{D^*\}^T[B]^T[d][B]\{D^*\}\,dv \tag{16.52}$$

The principle of minimum total potential energy can be expressed as (Eq. 9.30)

$$\frac{\partial \Phi}{\partial D_i^*} = 0 \tag{16.53}$$

where the subscript i refers to any of the nodal displacements. Partial differentiation[3] with respect to each nodal displacement gives

$$\frac{\partial \Phi}{\partial \{D^*\}} = -\{Q^*\} - \int_v [L]^T\{p\}\,dv + \int_v [B]^T[d][B]\{D^*\}\,dv = 0 \tag{16.54}$$

Equation 16.54 can be rewritten in the form

$$[S^*]\{D^*\} = -\{F^*\} \tag{16.55}$$

where $\{F^*\}$ are nodal forces which would prevent the nodal displacements. The restraining forces are the sum of the nodal forces $\{Q^*\}$ in a reversed direction and of the nodal equilibrants of the body forces. Thus,

$$\{F^*\} = \{F_a^*\} + \{F_b\} \tag{16.56}$$

where $\{F_a^*\} = -\{Q^*\}$, and $\{F_b^*\}$ is the element consistent load vector. The matrix $[S^*]$ is the element stiffness matrix. Combining Eqs. 16.55 and 16.56 and comparing with Eq. 16.54, we obtain, by analogy, Eqs. 16.47 and 16.45.

3 It can be shown that if a scalar quantity y is expressed as a sum of products of matrices $y = (1/2)\{x\}^T[a]\{x\} + \{x\}^T\{b\}$, where $[a]$ and $\{b\}$ are constants and $[a]$ is symmetrical, differentiation of y with respect to x_i for $i = 1, 2, \ldots$ gives $\partial y/\partial\{x\} = \{\partial y/\partial x_1, \partial y/\partial x_2, \ldots\} = [a]\{x\} + \{b\}$.

16.8 Derivation of shape functions

The displacement field $\{f\}$ may be expressed as polynomials of the coordinates x and y (or ξ and η) defining the position of any point. For example, the deflection w in a plate-bending element or the translations u and v in a plane-stress or a plane-strain element may be expressed as

$$f(x,y) = \left[1, x, y, x^2, \ldots\right]\{A\} = [P]\{A\} \tag{16.57}$$

where $\{A\}$ is a vector of constants, yet to be determined; and $[P]$ is a matrix of polynomial terms, the number of which equals the number of nodal degrees of freedom. Pascal's triangle (Figure 16.7) can be used to select the polynomial terms to be included in $[P]$. In general, the lower-degree terms are used. Examples of the polynomial terms used in several elements are given later in this section.

The nodal displacements $\{D^*\}$ can be related to the constants $\{A\}$ by substituting x and y (or ξ and η) values at the nodes in Eq. 16.57 (or its derivatives). This gives

$$\{D^*\} = [C]\{A\} \tag{16.58}$$

The elements of $[C]$ are known values depending upon (x_i, y_i), with $i = 1, 2, \ldots$ referring to the node numbers. The undetermined constants $\{A\}$ can now be expressed in terms of $\{D^*\}$ by inversion:

$$\{A\} = [C]^{-1}\{D^*\} \tag{16.59}$$

Substituting Eq. 16.59 into Eq. 16.57, and by analogy of the resulting equation with Eq. 16.36, we obtain the shape functions

$$[L] = [P][C]^{-1} \tag{16.60}$$

As an example of polynomial selection, let us consider the bar element shown in Figure 16.3, which is subjected to an axial force. With two degrees of freedom, $[P]$ has only two terms:

$$[P] = \begin{bmatrix} 1 & \xi \end{bmatrix} \tag{16.61}$$

For a bar in bending (Figure 16.4),

$$[P] = \begin{bmatrix} 1 & \xi & \xi^2 & \xi^3 \end{bmatrix} \tag{16.62}$$

$$\begin{array}{ccccc} & & 1 & & \\ & x & & y & \\ x^2 & & xy & & y^2 \\ x^3 & & x^2y & & xy^2 \qquad y^3 \\ x^4 & & x^3y & & x^2y^2 \qquad xy^3 \qquad y^4 \end{array}$$

Figure 16.7 Pascal's triangle.

For a plate element subjected to in-plane forces (Figure 16.5), each of the displacements u and v is associated with four nodal displacements. A polynomial with four terms is used for each of u and v:

$$[P] = [1 \quad \xi \quad \eta \quad \xi\eta] \tag{16.63}$$

For the plate-bending element in Figure 16.6, with twelve degrees of freedom, we express the deflection as $w = [P]\{A\}$, with

$$[P] = [1 \quad \xi \quad \eta \quad \xi^2 \quad \xi\eta \quad \eta^2 \quad \xi^3 \quad \xi^2\eta \quad \xi\eta^2 \quad \eta^3 \quad \xi^3\eta \quad \xi\eta^3] \tag{16.64}$$

For elements with two or more variables, such as x and y (or x, y, and z), the terms included in $[P]$ should be invariant if the reference axes x and y (or x, y, and z) are interchanged. Thus, in Eq. 16.63 we should not replace the terms $\xi\eta$ by ξ^2 or by η^2. Similarly, in Eq. 16.64 we should not replace $\xi^3\eta$ or $\xi\eta^3$ by $\xi^2\eta^2$. In other words, $[P]$ includes symmetrical terms from Pascal's triangle (Figure 16.7). When this requirement is satisfied, the element does not have a "preferred" direction. In consequence, the use of such an element in the analysis of the structure shown in Figure 16.2 will give the same answers regardless of whether the global axes x and y are as shown or are rotated through 90° so that x becomes vertical.

The invariance requirement is relaxed for the rectangular plate element subjected to in-plane forces included in Figure 16.1. The element has four nodes with three nodal displacements per node: u, v, $\partial v/\partial x$. The inclusion of $\partial v/\partial x$ (but not of other derivatives of u and v) makes the element behave differently in the x and y directions. The polynomials used for u and for v are different:

$$u(x,y) = [1 \quad x \quad y \quad xy]\{A\}_u \tag{16.65}$$

$$v(x,y) = [1 \quad x \quad y \quad x^2 \quad xy \quad x^3 \quad x^2y \quad x^3y]\{A\}_v \tag{16.66}$$

The variation of v in the x direction is cubic, while a linear variation is used for v in the y direction and for u in both the x and y directions. The shape functions for the element are given in Eq. 16.67 (see Example 16.3).

This element[4] gives excellent accuracy when used for structures which have beam-like behavior, e.g. folded plates and box girders. For this use, the element local x axis must be in the direction of the "beam". For comparison of accuracy of results of this element with other elements, see Prob. 17.18.

Example 16.1: Beam in flexure

Derive the shape functions for the bar element in Figure 16.4. The deflection v is expressed as a cubic polynomial of ξ, where $\xi = x/l$ (Eqs. 16.57 and 16.62).

$$v = [\,1 \quad \xi \quad \xi^2 \quad \xi^3\,]\{A\} = [P]\{A\}$$

4 The rectangular element considered here is a special case of the quadrilateral element referred to as QLC3. See Sisodiya, R., Cheung, Y. K. and Ghali, A., "New Finite Element with Application to Box Girder Bridges," *Proceedings, The Institution of Civil Engineers,* London, Supplement 1972, Paper 7495, pp. 207–225. The combination of QLC3 with the rectangular bending element shown in Figure 16.6 gives a good shell element with three translations and three rotations per node for the analysis of spatial structures (See 17.10.1).

The nodal displacements defined by Eq. 16.27 are substituted in the above equations to give

$$\{D^*\} = \begin{bmatrix} 1 & 0 & 0 & 0 \\ 0 & 1/l & 0 & 0 \\ 1 & 1 & 1 & 1 \\ 0 & 1/l & 2/l & 3/l \end{bmatrix} \{A\}$$

Inversion of the square matrix in the above equation gives

$$[C]^{-1} = \begin{bmatrix} 1 & 0 & 0 & 0 \\ 0 & l & 0 & 0 \\ -3 & -2l & 3 & -l \\ 2 & l & -2 & l \end{bmatrix}$$

The product $[P]\,[C]^{-1}$ gives the shape functions $[L]$ (Eq. 16.28).

Example 16.2: Quadrilateral plate subjected to in-plane forces

Derive the shape functions for the plane-stress or plane-strain quadrilateral element shown in Figure 16.5.

We have u or $v = [P]\{A\}$, with $[P]$ given in Eq. 16.63. Substituting for ξ and η by their values at the four corners, we write for u:

$$\begin{Bmatrix} u_1 \\ u_2 \\ u_3 \\ u_4 \end{Bmatrix} = \begin{bmatrix} 1 & -1 & -1 & 1 \\ 1 & 1 & -1 & -1 \\ 1 & 1 & 1 & 1 \\ 1 & -1 & 1 & -1 \end{bmatrix} \{A\}$$

Inversion of $[C]$, which is the square matrix in this equation, gives

$$[C]^{-1} = (1/4) \begin{bmatrix} 1 & 1 & 1 & 1 \\ -1 & 1 & 1 & -1 \\ -1 & -1 & 1 & 1 \\ 1 & -1 & 1 & -1 \end{bmatrix}$$

Substitution in Eq. 16.60 gives

$$[L_1, L_2, L_3, L_4] = \tfrac{1}{4}[1-\xi-\eta+\xi\eta, \quad 1+\xi-\eta-\xi\eta, \quad 1+\xi+\eta+\xi\eta, \quad 1-\xi+\eta-\xi\eta]$$

which is the same as Eq. 16.32. The same shape functions apply to v.

Example 16.3: Rectangular element QLC3

Using the polynomials in Eq. 16.66, derive the shape functions for the displacement v in a rectangular plate element QLC3 subjected to in-plane forces (Figure 16.1).

The nodal displacements are defined as

$$\{D^*\} = \left\{ \left(u, v, \frac{\partial v}{\partial x}\right)_1, \left(u, v, \frac{\partial v}{\partial x}\right)_2, \left(u, v, \frac{\partial v}{\partial x}\right)_3, \left(u, v, \frac{\partial v}{\partial x}\right)_4 \right\}$$

Using the symbols $\xi = x/b$ and $\eta = y/c$, Eq. 16.66 can be written as $v = [P]\{\bar{A}\}$, with

$$[P] = [1 \quad \xi \quad \eta \quad \xi^2 \quad \xi\eta \quad \xi^3 \quad \xi^2\eta \quad \xi^3\eta]$$

The nodal displacements associated with v are

$$\{D_v^*\} = \{D_2^*, D_3^*, D_5^*, D_6^*, D_8^*, D_9^*, D_{11}^*, D_{12}^*\}$$

Substituting for ξ and η by their values at the nodes, we can write $\{D_v^*\} = [C]\{\bar{A}\}$, with

$$[C] = \begin{array}{c} \\ 2 \\ 3 \\ 5 \\ 6 \\ 8 \\ 9 \\ 11 \\ 12 \end{array} \begin{bmatrix} 1 & 0 & 0 & 0 & 0 & 0 & 0 & 0 \\ 0 & 1/b & 0 & 0 & 0 & 0 & 0 & 0 \\ 1 & 1 & 0 & 1 & 0 & 1 & 0 & 0 \\ 0 & 1/b & 0 & 2/b & 0 & 3/b & 0 & 0 \\ 1 & 1 & 1 & 1 & 1 & 1 & 1 & 1 \\ 0 & 1/b & 0 & 2/b & 1/b & 3/b & 2/b & 3/b \\ 1 & 0 & 1 & 0 & 0 & 0 & 0 & 0 \\ 0 & 1/b & 0 & 0 & 1/b & 0 & 0 & 0 \end{bmatrix}$$

Inversion of $[C]$ and substitution in Eq. 16.60 gives the eight shape functions associated with v: $L_2, L_3, L_5, L_6, L_8, L_9, L_{11}, L_{12}$. For reference, we give the complete shape functions for the element as follows:

$$\begin{array}{lll} L_1 = (1-\xi)(1-\eta) & L_2 = (1-3\xi^2+2\xi^3)(1-\eta) & L_3 = b\xi(\xi-1)^2(1-\eta) \\ L_4 = \xi(1-\eta) & L_5 = \xi^2(3-2\xi)(1-\eta) & L_6 = b\xi^2(\xi-1)(1-\eta) \\ L_7 = \xi\eta & L_8 = \xi(3-2\xi)\eta & L_9 = b\xi^2(\xi-1)\eta \\ L_{10} = (1-\xi)\eta & L_{11} = (1-3\xi^2+2\xi^3)\eta & L_{12} = b\xi(\xi-1)^2\eta \end{array} \tag{16.67}$$

These functions can be used to express u and v by the equation $\{u, v\} = [L]\{D^*\}$ (see Eq. 16.25), with

$$[L] = \begin{bmatrix} L_1 & 0 & 0 & L_4 & 0 & 0 & L_7 & 0 & 0 & L_{10} & 0 & 0 \\ 0 & L_2 & L_3 & 0 & L_5 & L_6 & 0 & L_8 & L_9 & 0 & L_{11} & L_{12} \end{bmatrix} \tag{16.68}$$

16.9 Convergence conditions

In principle, it is possible to use any continuous shape function for the displacement field of a finite element; however, polynomials are commonly used. For monotonic convergence to the correct answer as smaller elements are used, the shape functions should satisfy the following three requirements:

1. The displacements of adjacent elements along a common boundary must be identical.

It can be seen that this condition is satisfied in the plane-stress or plane-strain element in Figure 16.5 and in the plate-bending element in Figure 16.6. Along any side 1-2, the translations u and v in Figure 16.5 or the deflection w in Figure 16.6 are functions of the nodal displacements at 1 and 2 only. It thus follows that two adjacent elements sharing nodes 1 and 2 will have the same nodal displacements at the two nodes and the same u and v or w along the line 1-2.

In some cases, the first partial derivatives of the element should also be compatible. This condition needs to be satisfied in plate-bending elements but not in plane-stress or plane-strain elements.

Two adjacent elements of the type shown in Figure 16.6 have the same deflection and hence the same slope along the common edge. However, normal to the common edge, the tangents of the deflected surfaces of the two elements have the same slope only at the nodes. Away from the nodes, the tangents normal to a common edge can have slopes differing by an angle a. The quantity $(1/2)\int M_n\alpha\, ds$ represents, for the assembled structure, strain energy not accounted for in the process of minimizing the total potential energy (see Eq. 16.52); here, M_n is the resultant of stresses normal to the common edge and ds is an elemental length of the edge.

The rule to ensure convergence is that the compatibility be satisfied for $[L]$ and its derivatives of order one less than the derivatives included in $[B]$. For a plate-bending element, $[B]$ includes second derivatives (Eqs. 16.39 and 16.19): $-\partial^2 w/\partial x^2, -\partial^2 w/\partial y^2, 2\partial^2 w/\partial x\partial y$. Thus, compatibility is required for $\partial w/\partial x$ and $\partial w/\partial y$ in addition to w.

Several elements, said to be incompatible or nonconforming, such as the element in Figure 16.6, do not satisfy the requirement of compatibility of displacement derivatives, and yet some of these elements give excellent results. An explanation of this behavior is that the excess stiffness, which is a characteristic of displacement-based finite elements, is compensated by the increase in flexibility resulting from a lack of compatibility of slopes.

Nonconforming elements converge towards the correct answer when the incompatibilities disappear as the mesh becomes finer and the strains within the element tend to be constants.

2. When the nodal displacements $\{D^*\}$ correspond to rigid-body motion, the strains $[B]\{D^*\}$ must be equal to zero.

This condition is easily satisfied when the polynomial matrix $[P]$ in Eq. 16.57 includes the lower-order terms of Pascal's triangle. For example, for the plate-bending element (Figure 16.6), inclusion of the terms $1, x, y$ would allow w to be represented by the equation of an inclined plane.

We can verify that the shape functions in Eq. 16.35 for the element shown in Figure 16.6 allow translation as a rigid body by setting $w = 1$ at the four corners and $\theta_x = \theta_y = 0$ at all nodes; Eq. 16.25 will then give $w = 1$, representing unit downward translation. (This is because $L_1 + L_4 + L_7 + L_{10} = 1$, as noted earlier.) To check that the shape functions allow rigid-body rotation, let $w = 1$ at nodes 1 and 2, and $\theta_x = -1/c$ at the four nodes of the element, while all other nodal displacements are zero. It can be seen that substitution of these nodal displacements and of Eq. 16.35 in Eq. 16.25 gives $w = 1 - \eta$, which is the equation of the plane obtained by rotation of the element through an angle $\theta_x = -1/c$ about the edge 4-3. In a similar way, we can verify that the shape functions allow a rigid-body rotation $\theta_y =$ constant.

3. The shape functions must allow the element to be in a state of constant strain.

This is required because, as the elements become smaller, the strains within individual elements tend to constants. Thus, a smooth curve (or surface) representing the strain variation can be approximated by step variation.

This requirement will be satisfied when the polynomial $[P]$ in Eq. 16.57 includes the lower terms which contribute to the strain. For example, for the rectangular bending element shown in Figure 16.6, the strains are $\{\epsilon\} = \{-\partial^2 w/\partial x^2, -\partial^2 w/\partial y^2, 2\partial^2 w/(\partial x \partial y)\}$; the terms x^2, xy, and y^2 of Pascal's triangle must be included in $[P]$.

We can verify that the shape functions in Eq. 16.35 allow a constant curvature, i.e. $-\partial^2 w/\partial x^2 = \text{constant}$, by setting $\theta_y = 1$ at nodes 1 and 4, and $\theta_y = -1$ at nodes 2 and 3, while the remaining nodal displacements are equal to zero. Substitution in Eq. 16.36 gives $w = b\xi(1-\xi)$, which represents the surface of a cylinder with a constant curvature of $2/b$.

For the same element, $2\partial^2 w(\partial x \partial y)$ will be constant $(= -4/bc)$ when the element is twisted so that $w = 1$ at nodes 2 and 4, with the edges remaining straight. Thus, the nodal displacements will be: $w = 0$ at 1 and 3; $w = 1$ at 2 and 4; $\theta_x = 1/c$ at 1 and 4; $\theta_x = -1/c$ at 2 and 3; $\theta_y = -1/b$ at 1 and 2; and $\theta_y = 1/b$ at 3 and 4.

Requirement 2 can be considered to be a special case of requirement 3 when the constant strain is zero. The "patch test" (Section 16.10) is a numerical method for nonconforming elements to verify that an assemblage of elements can assume a constant-strain state.

16.10 The patch test for convergence

It is advisable to perform a patch test before a new computer program or a new element is adopted.[5] The test is conducted on a patch of several elements (Figure 16.8). Prescribed displacements are introduced at boundary nodes which correspond to constant-strain conditions. If the strains determined by the analysis are constant, the patch test is passed. If the test is not passed, convergence with an arbitrary fine mesh is not ensured. Passing the patch test for conforming or nonconforming elements means that convergence requirements 2 and 3 in the preceding section are satisfied.

In the patch of plane-stress or plane-strain elements shown in Figure 16.8, a constant-strain state should exist for all elements of the patch when the displacement at the boundary nodes are prescribed by

$$u = a_1 x + a_2 y + a_3 \qquad v = a_4 x + a_5 y + a_6$$

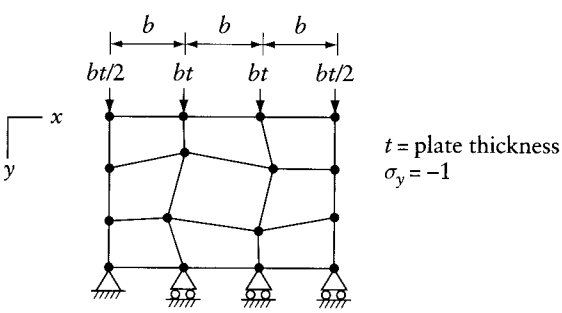

Figure 16.8 Model for the patch test for the plane-stress or plane-strain element of Figure 16.5. Consistent nodal forces correspond to a uniform stress $\sigma_y = -1$ on the top edge of the patch.

5 The importance of the patch test, what it achieves and the philosophy behind it are the subject of a chapter in Irons, B. M. and Ahmad, S., *Techniques of Finite Elements*, Ellis Horwood, Chichester, England, and Halsted Press (Wiley), New York, 1980 (see pp. 149–162).

where a_1 to a_6 are arbitrary constants. The inner nodes should be left free. The expected strains are (Eq. 16.6): $\{\epsilon_x, \epsilon_y, \gamma_{xy}\} = \{a_1, a_5, (a_2 + a_4)\}$. When the patch test is passed, the computed strains agree with the exact values to the limit of computer accuracy.

Alternatively, appropriate supports and consistent nodal forces (calculated by Eq. 16.47) may be introduced to represent the state of constant stress. An example of this is shown in Figure 16.8, in which is represented a constant stress $\sigma_y = -1$. Other constant-stress (or constant-strain) states and more than one geometry should be tested to guarantee convergence.

Example 16.4: Axial forces and displacements of a bar of variable cross section

Generate the stiffness matrix and the vector of restraining forces due to a uniform rise in temperature of T degrees for the bar shown in Figure 16.3. Assume that the cross section varies as $a = a_0(2 - \xi)$, where a_0 is constant. The coefficient of thermal expansion is α and the modulus of elasticity is E.

Using the shape functions of Eq. 16.26, the $[B]$ matrix is (Eq. 16.39)

$$[B] = \frac{d}{dx}\,[1 \quad -\xi \quad \xi] = \frac{d}{l\,d\xi}\,[1 \quad -\xi \quad \xi] = \frac{1}{l}\,[-1 \quad 1]$$

The elasticity matrix in this case has one element $[d] \equiv [E]$. Substitution in Eq. 16.45 gives the stiffness matrix:

$$[S^*] = l \int_0^1 \frac{1}{l} \begin{Bmatrix} -1 \\ 1 \end{Bmatrix} [E] \frac{1}{l} [-1, \textit{phantom}{-}1]\, a_0 (2 - \xi)\, d\xi$$

or

$$[S^*] = \frac{Ea_0}{l} \begin{bmatrix} 1 & -1 \\ -1 & 1 \end{bmatrix} \left[2\xi - \frac{\xi^2}{2}\right]_0^1 = \frac{1.5Ea_0}{l} \begin{bmatrix} 1 & -1 \\ -1 & 1 \end{bmatrix}$$

If the effect of the temperature change is not restrained, the strain is $\epsilon_0 = \alpha T$. The nodal forces to restrain nodal displacements (Eq. 16.50) are then

$$\{F_b\}_m = -l \int_0^1 \frac{1}{l} \begin{Bmatrix} -1 \\ 1 \end{Bmatrix} E\alpha T a_0 (2 - \xi)\, d\xi = 1.5E\alpha T a_0 \begin{Bmatrix} 1 \\ -1 \end{Bmatrix}$$

The same results would be obtained if the member were treated as a prismatic bar with a constant cross-sectional area equal to the average of the values at the two ends. The exact answer for the stiffness matrix is the same as above with the constant 1.5 replaced by $(1/\ln 2) = 1.443$ (obtained by considering the true deformed shape). As expected, the use of assumed shape functions resulted in an overestimate of stiffness.

Example 16.5: Stiffness matrix of a beam in flexure with variable cross section

Determine element S^*_{12} of the stiffness matrix for the bar shown in Figure 16.4, assuming the second moment of the cross section to vary as $I = I_0(1 + \xi)$, where I_0 is constant. Consider bending deformations only; E = constant. Also, generate the vector of nodal equilibrants of a uniform load q per unit length covering the entire length.

For a beam in bending, $[d] \equiv [EI]$, $\{\sigma\} \equiv \{M\}$, and $\{\epsilon\} \equiv -d^2v/dx^2$. Using the shape functions in Figure 16.4, the $[B]$ matrix is (Eq. 16.39)

$$[B] = -\frac{d^2}{dx^2}\left[1-3\xi^2+2\xi^3 \quad l\xi(\xi-1)^2 \quad \xi^2(3-2\xi) \quad l\xi^2(\xi-1)\right]$$

$$[B] = -\frac{1}{l^2}\left[-6+12\xi \quad l(6\xi-4) \quad 6-12\xi \quad l(16\xi-2)\right]$$

The required element of the stiffness matrix (Eq. 16.44) is

$$S_{12}^* = \int_0^1 \left(\frac{6-12\xi}{l^2}\right) EI_0(1+\xi)\left(\frac{-6\xi+4}{l}\right) l\,d\xi = 8\frac{EI_0}{l^2}$$

The exact answer can be calculated by Eq. 11.15, giving $S_{12}^* = 7.72\ EI_0/l^2$. As expected, the stiffness is overestimated by the use of the assumed shape function L_2 instead of the true deflected shape due to $D_2^* = 1$.

The entire stiffness $[S^*]$ derived by Eq. 16.45 may be compared with the exact stiffness matrix (by Eq. 11.15) in the answers to Prob. 16.1

The nodal forces in equilibrium with the uniform load q, with nodal displacements prevented, are (Eq. 16.47)

$$\{F_b\}_m = -\int_0^1 \begin{Bmatrix} 1-3\xi^2+2\xi^3 \\ 1\xi(\xi-1)^2 \\ \xi^2(3-2\xi) \\ 1\xi^2(\xi-1) \end{Bmatrix} ql\,d\xi = \begin{Bmatrix} -ql/2 \\ -ql/12 \\ -ql/2 \\ -ql^2/12 \end{Bmatrix}$$

These are the same forces as for a prismatic beam; again, an approximation is involved in accepting the deflected shapes of a prismatic bar for a bar with a variable I.

Example 16.6: Stiffness matrix of a rectangular plate subjected to in-plane forces

Determine element S_{22}^* of the stiffness matrix for a rectangular plane-stress element of constant thickness h (Figure 16.1). The shape functions for this element are derived in Example 16.3. Determine also the stresses at any point due to $D_2^* = 1$.

Due to $D_2^* = 1$, the displacements at any point are given by (Eqs. 16.67 and 16.68) as

$$\begin{Bmatrix} u \\ v \end{Bmatrix} = \begin{Bmatrix} 0 \\ L_2 \end{Bmatrix} = \begin{Bmatrix} 0 \\ (1-3\xi^2+2\xi^3)(1-\eta) \end{Bmatrix}$$

The strain at any point (Eqs. 16.39 and 16.11) is

$$\{B\}_2 = \begin{Bmatrix} 0 \\ (1/c)(-1+3\xi^2-2\xi^3) \\ (1/b)(-6\xi+6\xi^2)(1-\eta) \end{Bmatrix}$$

The required element of the stiffness matrix is given by Eq. 16.44 as

$$S_{22}^* = bch\int_0^1\int_0^1 \{B\}_2^T[d]\{B\}_2\,d\xi\,d\eta$$

Substituting for $[d]$ from Eq. 16.12 and performing the integral gives

$$S_{22}^{*}=1\frac{Eh}{1-\nu^2}\left[\frac{13}{35}\left(\frac{b}{c}\right)+\frac{1}{5}\left(\frac{c}{b}\right)(1-\nu)\right]$$

The stress at any point due to $D_2^{*}=1$ is (Eq. 16.42)

$$\{\sigma_u\}_2=[d]\{B\}_2$$
$$=\frac{E}{1-\nu^2}\left\{\frac{\nu}{c}\left(-1+3\xi^2-2\xi^3\right),\right.$$
$$\left.\frac{1}{c}\left(-1+3\xi^2-2\xi^3\right),\frac{3(1-\nu)}{b}(1-\eta)\left(-\xi+\xi^2\right)\right\}$$

16.11 Constant-strain triangle

The triangular element shown in Figure 16.9 may be used in a plane-stress or plane-strain analysis. The element has three nodes at the corners, with two nodal displacements u and v. The

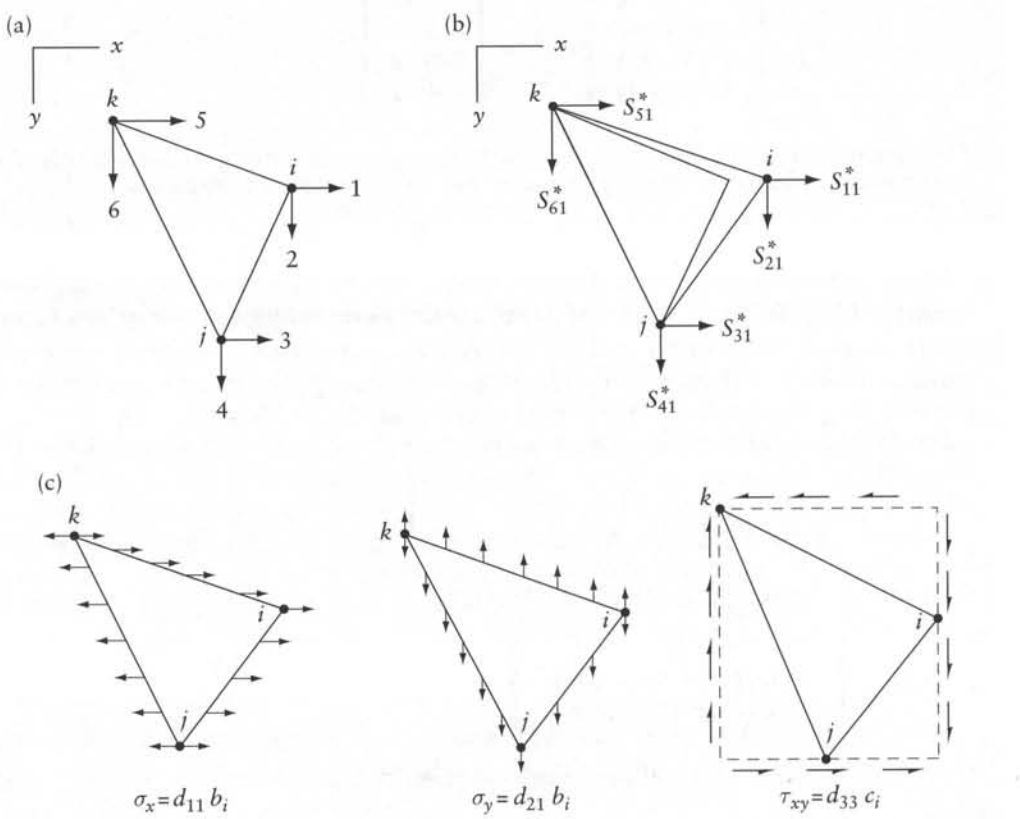

Figure 16.9 Triangular plane-stress or plane-strain element. (a) Nodal coordinates. (b) and (c) Stresses on element edges lumped in equivalent forces at the nodes.

element is called a constant-strain triangle because the strain, and hence the stress, within the element is constant.

Each of u and v is associated with three of the six nodal displacements. The same polynomial may therefore be used for the two variables:

$$[P] = [1,\ x,\ y] \tag{16.69}$$

We shall now derive the shape functions associated with u, which are the same as the shape functions associated with v. At the three nodes we have

$$\begin{Bmatrix} u_i \\ u_j \\ u_k \end{Bmatrix} = \begin{bmatrix} 1 & x_i & y_i \\ 1 & x_j & y_j \\ 1 & x_k & y_k \end{bmatrix} \{A\} \tag{16.70}$$

or

$$\{u\} = [\mathrm{C}]\ \{A\} \tag{16.71}$$

Inversion of [C], using Cramer's rule (Appendix A, Section A.9) or other methods, gives

$$[\mathrm{C}]^{-1} = \frac{1}{2\Delta} \begin{bmatrix} a_i & a_j & a_k \\ b_i & b_j & b_k \\ c_i & c_j & c_k \end{bmatrix} \tag{16.72}$$

where 2Δ is the determinant of $[\mathrm{C}] = 2\times$ area of triangle. Here,

$$a_i = x_j y_k - y_j x_k \quad b_i = y_i - y_k \quad c_i = x_k = x_j \tag{16.73}$$

By cyclic permutation of the subscripts i, j, and k, similar equations can be written for $\{a_j, b_j, c_j\}$ and for $\{a_k, b_k, c_k\}$.

Substitution in Eq. 16.60 gives the shape functions:

$$[L] = \frac{1}{2\Delta} \left[(a_i + b_i x + c_i y) \quad (a_j + b_j x + c_j y) \quad (a_k + b_k x + c_k y)\right] \tag{16.74}$$

The displacements $\{u,\ v\}$ at any point may be expressed in terms of the nodal displacements (Eq. 16.25):

$$\begin{Bmatrix} u \\ v \end{Bmatrix} = \begin{bmatrix} L_1 & 0 & L_2 & 0 & L_3 & 0 \\ 0 & L_1 & 0 & L_2 & 0 & L_3 \end{bmatrix} \{D^*\} \tag{16.75}$$

where

$$\{D^*\} = \{u_i, v_i, u_j, v_j, u_k, v_k\}$$

The matrix $[B]$, relating strains $\{\epsilon\}$ to $\{D^*\}$ is (Eqs. 16.39 and 16.11)

$$[B] = \frac{1}{2\Delta} \begin{bmatrix} b_i & 0 & b_j & 0 & b_k & 0 \\ 0 & c_i & 0 & c_j & 0 & c_k \\ c_i & b_i & c_j & b_j & c_k & b_k \end{bmatrix} \tag{16.76}$$

The product $[d]\,[B]$ gives the stresses due to unit nodal displacements (Eq. 16.42):

$$[\sigma_u] = \frac{1}{2\Delta}\begin{bmatrix} d_{11}b_i & d_{21}c_i & d_{11}b_j & d_{21}c_j & d_{11}b_k & d_{21}c_k \\ d_{21}b_i & d_{22}c_i & d_{21}b_j & d_{22}c_j & d_{21}b_k & d_{22}c_k \\ d_{33}c_i & d_{33}b_i & d_{33}c_j & d_{33}b_j & d_{33}c_k & d_{33}b_k \end{bmatrix} \tag{16.77}$$

where d_{ij} are elements of the elasticity matrix $[d]$, given by Eqs. 16.12 and 16.13 for the states of plane stress and plane strain respectively. It can be seen that all the elements of $[B]$ and $[\sigma_u]$ are constants, indicating constant strain and stress. If the thickness h is constant, the stiffness matrix of the element is (Eq. 16.45)

$$[S^*] = h\Delta\,[B]^T\,[d]\,[B] = h\Delta\,[B]^T\,[\sigma_u] \tag{16.78}$$

that is,

$$[S^*] = \frac{h}{4\Delta}\begin{bmatrix} d_{11}b_i^2 + d_{33}c_i^2 & & & & \text{symmetrical} & \\ d_{21}b_ic_i + d_{33}b_ic_i & d_{22}c_i^2 + d_{33}b_i^2 & & & & \\ d_{11}b_ib_j + d_{33}c_ic_j & d_{21}c_ib_j + d_{33}c_jb_i & d_{11}b_j^2 + d_{33}c_j^2 & & & \\ d_{21}b_ic_j + d_{33}b_jc_i & d_{22}c_ic_j + d_{33}b_ib_j & d_{21}b_jc_j + d_{33}c_jb_j & & & \\ d_{11}b_ib_k + d_{33}c_ic_k & d_{21}c_ib_k + d_{33}b_ic_k & d_{11}b_jb_k + d_{33}c_jc_k & & & \\ d_{21}b_ic_k + d_{33}b_kc_i & d_{22}c_ic_k + d_{33}b_ib_k & d_{21}b_jc_k + d_{33}c_jb_k & & & \end{bmatrix}$$

$$\begin{bmatrix} d_{22}c_j^2 + d_{33}b_j^2 & & \\ d_{21}c_jb_k + d_{33}b_jc_k & d_{11}b_k^2 + d_{33}c_k^2 & \\ d_{22}c_jc_k + d_{33}b_jb_k & d_{21}b_kc_k + d_{33}c_kc_k & d_{22}c_k^2 + d_{33}b_k^2 \end{bmatrix} \tag{16.79}$$

If the element is subjected to uniform body forces with intensities per unit volume of $\{p\} = \{q_x, q_y\}$ the equilibrants at the nodes, when the nodal displacements are prevented, are (Eq. 16.47)

$$\{F_b^*\} = -h\int\int \begin{bmatrix} L_1 & 0 & L_2 & 0 & L_3 & 0 \\ 0 & L_1 & 0 & L_2 & 0 & L_3 \end{bmatrix}^T \begin{Bmatrix} q_x \\ q_y \end{Bmatrix} dx\,dy \tag{16.80}$$

Evaluation of the integrals is simplified by noting that $\int\int dx\,dy = \Delta$; $\int\int x dx\,dy$ is the first moment of area about the y axis, so that $\int\int y dx\,dy = (\Delta/3)(y_i + y_j + y_k)$. The consistent vector of forces in equilibrium with the body forces thus becomes

$$\{F_b^*\} = \frac{\Delta h}{3}\{q_x, q_y, q_x, q_y, q_x, q_y\} \tag{16.81}$$

This means that one-third of the load on the triangle is assigned to each node. The same distribution could have been suggested intuitively. (However, it is not always possible to determine $\{F_b^*\}$ intuitively; see Figure 17.7.)

The consistent vector of restraining forces when the element is subjected to a rise in temperature of T degrees is obtained by substitution of Eqs. 16.49 and 16.76 into Eq. 16.50:

$$\{F_b\}_m = -\frac{\alpha T h}{2}(d_{11} + d_{21})\{b_i, c_i, b_j, c_j, b_k, c_k\} \tag{16.82}$$

Here, we have assumed that the material is isotropic ($d_{22} = d_{11}$).

16.12 Interpretation of nodal forces

In the derivation of the stiffness matrix of individual elements, the forces distributed along the edges of the elements are replaced by equivalent forces lumped at the nodes. The equivalent forces are determined by the use of the principle of virtual work.

This approach can be seen in the example of the constant-strain triangular element shown in Figure 16.9. For a unit nodal displacement, say, $D_1^* = 1$, while other nodal displacements are zero, the stresses are (Eq. 16.77, first column of $[\sigma_u]$)

$$\{\sigma\} = \frac{1}{2\Delta}\{d_{11}b_i, d_{21}b_i, d_{33}c_i\} \tag{16.83}$$

where d_{ij} are elements of the elasticity matrix $[d]$ given in Eqs. 16.12 and 16.13 for plane-stress or plane-strain states respectively; $b_i = y_j - y_k$; $c_i = x_k - x_j$; and Δ = area of the triangle.

The stresses are represented by uniform forces on the edges of the element in Figure 16.9c.

The distributed forces in Figure 16.9c are lumped at the nodes in Figure 16.9b. The force in the x or y direction at a node is equal to the sum of one-half of the distributed load on each of the two sides connected to the node. For example, the horizontal force at node k is one-half of the load on edges ki and kj; thus,

$$S_{51}^* = h\left\{\frac{\sigma_x}{2}[(y_i - y_k) - (y_j - y_k)] + \frac{\tau_{xy}}{2}[(x_j - x_k) - (x_i - x_k)]\right\} \tag{16.84}$$

We can now verify that this is the same as element S_{51}^* of the stiffness matrix in Eq. 16.79. Any other element of the stiffness matrix can be verified in a similar way.

Equation 16.84 means that the virtual work of force S_{51}^* during nodal displacement $D_1^* = 1$ is the same as the work done by the forces distributed over edges ki and kj during their corresponding virtual displacements (which, in this example, vary linearly).

The consistent load vector also represents the distributed forces lumped at the nodes. If the element shown in Figure 16.9b is subjected to a rise in temperature of T degrees and the element expansion is restrained, the stresses in an isotropic material will be (Eqs. 16.48 and 16.49)

$$\{\sigma_r\} = -[d]\{\epsilon_0\} = -\alpha T(d_{11} + d_{21})\begin{Bmatrix} 1 \\ 1 \\ 0 \end{Bmatrix} \tag{16.85}$$

where a is the coefficient of thermal expansion.

Under the conditions of restraint, uniform forces act on the edges so as to produce $\sigma_x = \sigma_y = -\alpha T(d_{11} + d_{21})$. Lumping one-half of the distributed load on any edge at the two end nodes gives the nodal forces of Eq. 16.82.

16.13 General

The displacement method of analysis is applicable to structures composed of finite elements which may be one-, two-, or three-dimensional. The analysis requires the generation of stiffness and stress matrices and of load vectors for individual elements. Exact element matrices can be generated only for bars. Procedures to generate approximate matrices for elements of any type have been presented in this chapter. Convergence to the exact solution can be ensured as a finer finite-element mesh is used. The general procedures have been applied to bar elements and to plate elements subjected to in-plane forces and to bending. Other finite elements are discussed in Chapter 17.

Assemblage of stiffness matrices and load vectors of individual elements, generation of structure equilibrium equations and their solutions, and the use of computers are discussed in Chapters 21 and 22. This is done mainly for structures composed of bar elements (framed structures). However, the same techniques apply when any type of finite element is used.

Problems

16.1 Determine any element S^*_{ij} for the bar of Example 16.5, using the shape functions in Figure 16.4. Compare the answer with an exact value as given by Eq. 11.15.

16.2 Consider the member of Prob. 1 as a cantilever fixed at the end $x = l$ and subjected to a transverse concentrated *load* P at the free end. Find the deflection at the tip of the cantilever, using the two matrices given in the answers to Prob. 1.

16.3 For the prismatic bar shown, generate the stiffness matrix corresponding to the three coordinates indicated. Use the following shape functions: $L_1 = -(1/2)\xi(1-\xi); L_2 = (1/2)\xi(1+\xi); L_3 = 1-\xi^2$ (Lagrange polynomials, Figure 17.3). Condense the stiffness matrix by elimination of node 3.

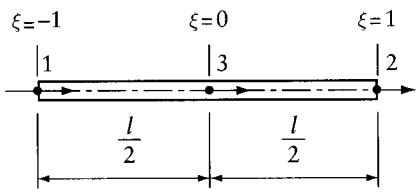

Prob. 16.3

16.4 Assume that the displacement at coordinate 1 of the bar element of Prob. 16.3 is prevented. A spring support is provided at coordinate 2 so that $F_2 = -Ku_2$, where F_2 and u_2 are, respectively, the force and the displacement at coordinate 2, and K is the spring constant equal to $Ea/(3l)$. What will be the displacements at coordinates 2 and 3 and the stress in the bar when it is subjected to a rise in temperature of $T = (1/2)T_0(1+\xi)$ where T_0 is a constant? Use the shape functions given in Prob. 16.3. Do you expect exact answers?

16.5 Determine $S^*_{11}, S^*_{21}, S^*_{31}, S^*_{41}$, and S^*_{51} of the stiffness matrix of the plane-stress finite element in Figure 16.5. Assume that the element is rectangular with sides b and c parallel to the x and y axes respectively, and is made of an isotropic material with $\nu = 0.2$. Element thickness is constant and equal to h. The nodal displacement vector and shape functions are defined by Eqs. 16.30 to 16.32.

16.6 Determine the consistent vector of restraining forces $\{F^*_b\}$ for a rectangular plane-stress element (Example 16.2) subjected to a uniform temperature rise of T degrees. Assume an isotropic material with $\nu = 0.2$. Only the first two elements of the vector need to be determined by Eq. 16.50; the remaining elements can be generated by consideration of equilibrium and symmetry.

16.7 Considering symmetry and equilibrium, use the results of Prob. 16.5 to generate $[S^*]$ for the element when $b = c$. For a comparison of the accuracy of this element with other elements, see Prob. 17.18.

16.8 Use the results of Prob. 16.5 to calculate the deflection at the middle of a beam idealized by two elements as shown. Take the beam width as h and Poisson's ratio as 0.2. Compare the result with that obtained by beam theory, considering bending and shear deformations. Note that the deflection calculated by the finite-element method is smaller than the more accurate value obtained by beam theory and that the percentage error increases with an increase in the ratio b/c.

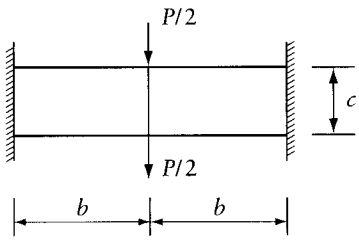

Prob. 16.8

16.9 Use the displacement determined in Prob. 16.8 to calculate the stresses in the top fiber at the fixed end.

16.10 Determine the consistent vector of restraining forces $\{F_b^*\}$ for the rectangular plane-stress element considered in Example 16.3 when it is subjected to a uniform temperature rise of T degrees. Assume an isotropic material. Only the first three elements of the vector need to be determined by Eq. 16.50; the remaining elements can be obtained by considering equilibrium and symmetry.

16.11 Determine S_{11}^* for the rectangular plate-bending element shown in Figure 16.6. The nodal displacement vector and the shape functions are defined in Eqs. 16.33 to 16.35. Use the result to calculate the central deflection of a rectangular plate $2b \times 2c$ with built-in edges and subjected to a concentrated load P at mid-point. Consider an isotropic material with $\nu = 0.3$. Idealize the plate by four elements and perform the analysis for one element only, taking advantage of symmetry. Use Figure 16.6 to represent the element analyzed with node 1 at the center of the plate. Determine also M_x at node 2.

16.12 The answers to this problem are given in terms of the ratio b/c. For comparison, we give here the exact[6] answers for a square plate ($b/c = 1$): deflection $= 0.244\,Pb^2/Eh^3$; M_x at node $2 = -0.126\,P$. The deflection is smaller than the finite-element solution: why?

16.13 The figure shows identical plane-stress elements with three coordinate systems. For the system in (a), calculate S_{11}^*, S_{21}^*, S_{31}^*, S_{33}^*, S_{34}^*, and S_{44}^*, and, by considering equilibrium and symmetry, generate the remaining elements of $[S^*]$. What are the transformation matrix $[T]$ and the equation to be used to transform $[S^*]$ into $[S]$ for the coordinate

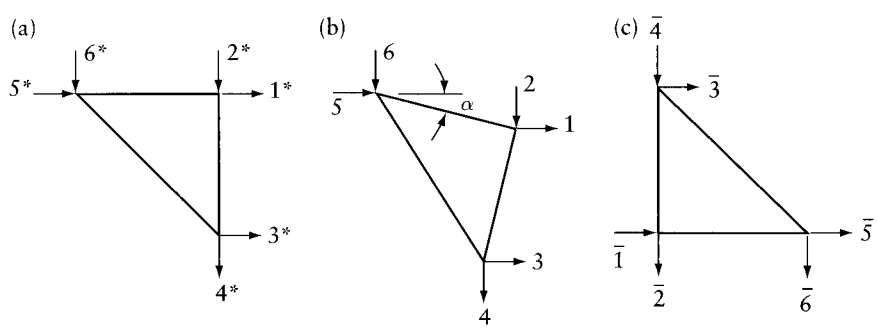

Prob. 16.13

6 From Timoshenko, S. and Goodier, J. N., *Theory of Elasticity*, 2nd ed., McGraw-Hill, New York, 1951.

system in (b)? What is the value of the angle a to be substituted in the equations to give $[S]$ corresponding to the coordinates in (c)? Consider an isotropic material with Poisson's ratio $\nu = 0$. Element thickness is h; element sides are b, b, $b\sqrt{2}$.

16.14 Using the answers of Prob. 16.2 and taking advantage of symmetry, determine, for the beam shown, the nodal displacements and the stress in element 2-6-3. The beam is of isotropic material; $\nu = 0$; beam width is h. The structure idealization is composed of isosceles right-angle triangles of the same size. The equilibrium equations can be checked by substitution of $\{D\}$ given in the answers.

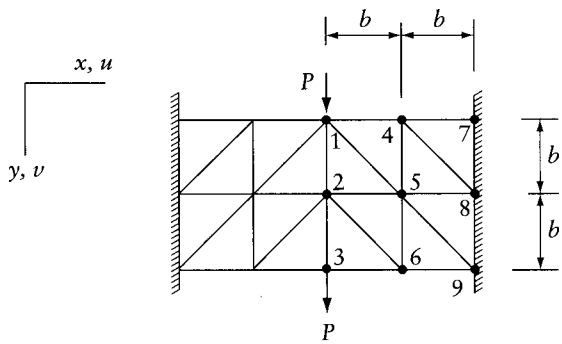

Prob. 16.14

16.15 Generate columns 1, 2 and 3 of the $[B]$ matrix for element QLC3 (Figure 16.1).

16.16 Calculate any stiffness coefficient S^*_{ij} for a rectangular plane-stress element QLC3 (Figure 16.1 and Example 16.3). Consider an isotropic square element of side b, constant thickness h and Poisson's ratio $\nu = 0.2$. The stiffness matrix is given in the answers and is used in Prob. 17.18 to compare the accuracy of results when using this approach and two other types of element (the element in Figure 16.5 and the hybrid element of Example 17.6).

Chapter 17

Further development of finite-element method

17.1 Introduction

This chapter is a continuation of Chapter 16, introducing various types of finite elements which are frequently used in practice.

The isoparametric formulation[1] is widely used because of its effectiveness and because it allows the elements to have curved shapes. In this chapter it is used for one-, two-, and three-dimensional elements. For this purpose, functions in natural coordinates ξ, (ξ, η) or (ξ, η, ζ) are used to describe the geometry of the element, and the same functions are used as shape functions describing the variation of the displacement components over the elements.

The integration involved in the generation of the finite-element matrices is, in the majority of cases, evaluated numerically. The Gauss quadrature method, which is frequently used, is discussed in Section 17.9.

Sections 17.10 and 17.11 present elements suitable for the analysis of shell structures and solids of revolution.

Instead of the division of a structure into elements by a mesh in two or three directions, it is possible to perform the analysis on an assemblage of finite strips or finite prisms. For this purpose the structure is divided in one dimension or in two dimensions only, instead of two or three dimensions respectively. The division results in finite strips or finite prisms running the full length of the structure. The analysis using this structural idealization is discussed in Section 17.12.

Section 17.13 is an introduction to the hybrid elements which were briefly discussed in Section 16.1.

17.2 Isoparametric elements

Isoparametric elements can be in the form of a curved bar, a triangular or quadrilateral plate with curved edges, or a three-dimensional brick with curved edges. The quadrilateral plane-stress or plane-strain element in Figure 16.5 is an example of an isoparametric element. The nodal displacements for the element are

$$\{D^*\} = \{u_1, v_1, u_2, v_2, u_3, v_3, u_4, v_4\} \tag{17.1}$$

The displacements u and v at any point are determined from the nodal displacements, using shape functions:

$$u = \Sigma L_i u_i \quad v = \Sigma L_i v_i \tag{17.2}$$

1 The technique was developed by B. M. Irons: see the following two papers by this author: "Numerical Integration Applied to Finite Element Methods". *Conf. Use of Digital Computers in Struct. Eng.*, Univ. of Newcastle, 1966, and, "Engineering Application of Numerical Integration in Stiffness Method", *JAIAA* (14), 1966, pp. 2035–2037.

where L_i with $i = 1, 2, 3, 4$ represents shape functions of the natural coordinates ξ and η. The shape functions for this element are given by Eq. 16.32, which is repeated here:

$$L_i = \frac{1}{4}(1 + \xi\xi_i)(1 + \eta\eta_i) \tag{17.3}$$

The natural coordinates varying between -1 and 1 (Figure 16.5) define the relative position of any point with respect to the corner nodes. The same shape functions can be used to determine the (x, y) coordinates of any point in terms of ξ and η:

$$x = \Sigma L_i x_i \quad y = \Sigma L_i y_i \tag{17.4}$$

where (x_i, y_i) with $i = 1, 2, 3, 4$ represent cartesian coordinates at the nodes. The element is called isoparametric because the same interpolation functions are used to express the location of a point and the displacement components in terms of ξ and η.

The strain components at any point involve derivatives $\partial/\partial x$ and $\partial/\partial y$ with respect to the cartesian coordinates. Derivatives of any variable g with respect to the natural coordinates are obtained by the chain rule:

$$\frac{\partial g}{\partial \xi} = \frac{\partial g}{\partial x}\frac{\partial x}{\partial \xi} + \frac{\partial g}{\partial y}\frac{\partial y}{\partial \xi} \quad \frac{\partial g}{\partial \eta} = \frac{\partial g}{\partial x}\frac{\partial x}{\partial \eta} + \frac{\partial g}{\partial y}\frac{\partial y}{\partial \eta} \tag{17.5}$$

We can rewrite Eq. 17.5 in matrix form:

$$\begin{Bmatrix} \partial g/\partial \xi \\ \partial g/\partial \eta \end{Bmatrix} = [J] \begin{Bmatrix} \partial g/\partial x \\ \partial g/\partial y \end{Bmatrix}; \quad \begin{Bmatrix} \partial g/\partial x \\ \partial g/\partial y \end{Bmatrix} = [J]^{-1} \begin{Bmatrix} \partial g/\partial \xi \\ \partial g/\partial \eta \end{Bmatrix} \tag{17.6}$$

Here, $[J]$ is the *Jacobian matrix;* it serves to transform the derivatives of any variable with respect to ξ and η into derivatives with respect to x and y, and vice versa. The elements of $[J]$ are given by

$$[J] = \begin{bmatrix} \partial x/\partial \xi & \partial y/\partial \xi \\ \partial x/\partial \eta & \partial y/\partial \eta \end{bmatrix} \tag{17.7}$$

When Eq. 17.4 applies, the Jacobian can be expressed as

$$[J] = \Sigma \begin{bmatrix} x_i(\partial L_i/\partial \xi) & y_i(\partial L_i/\partial \xi) \\ x_i(\partial L_i/\partial \eta) & y_i(\partial L_i/\partial \eta) \end{bmatrix} \tag{17.8}$$

The element geometry is defined by the cartesian coordinates (x, y) at the four nodes. For a given quadrilateral, the Jacobian varies, with ξ and η defining the position of any point.

The strains at any point are given by $\{\epsilon\} = [\partial]\{u, v\}$; the derivative operator $[\partial]$ is defined by Eq. 16.11. Substitution of Eq. 17.2 gives

$$\{\epsilon\} = \sum_{i=1}^{n} \left\{ [B]_i \begin{Bmatrix} u_i \\ v_i \end{Bmatrix} \right\} \tag{17.9}$$

where n is the number of nodes; for the quadrilateral element in Figure 16.5, $n = 4$. Here,

$$[B]_i = \begin{bmatrix} \dfrac{\partial L_i}{\partial x} & 0 \\ 0 & \dfrac{\partial L_i}{\partial y} \\ \dfrac{\partial L_i}{\partial y} & \dfrac{\partial L_i}{\partial x} \end{bmatrix}; \quad [B] = [[B]_1\,[B]_2 \ldots [B]_n] \tag{17.10}$$

When $[J]$ and its inverse are determined at a particular point, numerical values of the derivatives $(\partial L_i/\partial x)$ and $(\partial L_i/\partial y)$ required for generating $[B]_i$ are calculated from $\partial L_i/\partial \xi$ and $\partial L_i/\partial \eta$ via Eq. 17.6. The integrals involved in the generation of the element stiffness matrix and of the consistent load vector are obtained numerically.

The element stress matrix relating the stresses at any point to nodal displacements (Eq. 16.42) is

$$[\sigma_u] = [d][B] \tag{17.11}$$

The element stiffness matrix is given by (Eq. 16.45)

$$[S^*] = h\int_{-1}^{1}\int_{-1}^{1} [B]^T [d][B]\,|J|\,d\xi\,d\eta \tag{17.12}$$

where h is the element thickness, which is assumed constant, and

$$|J|\,d\xi\,d\eta = da \tag{17.13}$$

Here, da is the elemental area (parallelogram) shown in Figure 17.1. The determinant of the Jacobian serves as a scaling factor (length^2) to transform the dimensionless product $d\xi\,d\eta$ into an elemental area. The validity of Eq. 17.13 can be verified by considering the following areas:

$$\text{parallelogram } ABCD = \text{rectangle } EFGH - 2(\text{triangle } EAD + \text{triangle } AFB)$$

If the element is subjected to a rise in temperature of T degrees and the expansion is restrained, the stress $\{\sigma_r\}$ will be the same as given by Eq. 16.48, and the consistent vector of restraining forces will be given by (Eq. 16.50)

$$\{F_b^*\} = -h\int_{-1}^{1}\int_{-1}^{1} [B]^T [d]\{\epsilon_0\}\,|J|\,d\xi\,d\eta \tag{17.14}$$

where $\{\epsilon_0\}$ represents the change in strains if the expansion is free to occur (Eq. 16.49).

For a quadrilateral element, the determinant $|J|$ at the center of the element is equal to one-quarter of its area. For a rectangle, $[J]$ is constant. In general, the determinant $|J|$ is positive,

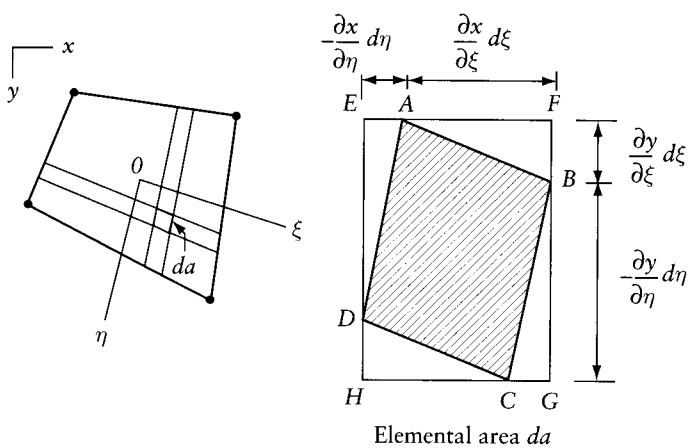

Figure 17.1 Verification of Eq. 17.12.

the matrix $[J]$ is nonsingular, and the matrix inversion in Eq. 17.6 is possible. If two corners of the quadrilateral coincide, the element becomes triangular. At the point where they coincide, $[J]$ is singular, indicating that the strains cannot be determined at this point. When the internal angle at each of the four corners of a quadrilateral is smaller than 180°, $[J]$ is nonsingular at all points and its determinant is positive.

Equations 17.2 and 17.4 to 17.14 are general for any isoparametric plane-stress or plane-strain element, with two degrees of freedom per node. The shape functions $[L]$ differ depending on the number of nodes and the arrangement of the nodes in each element. Methods of derivation of shape functions for various isoparametric elements are given in Sections 17.4 and 17.5.

Example 17.1: Quadrilateral element: Jacobian matrix at center

Determine the Jacobian matrix at the center of the quadrilateral element shown in Figure 16.5, using the following (x, y) coordinates: node 1(0, 0); node 2(7, 1); node 3(6, 9); node 4(−2, 5). Use the determinant of the Jacobian to calculate the area of the quadrilateral.

The derivatives of the shape function in Eq. 17.3 at $\xi = \eta = 0$ are

$$\frac{\partial L_i}{\partial \xi} = \frac{\xi_i}{4}; \quad \frac{\partial L_i}{\partial \eta} = \frac{\eta_i}{4}$$

The Jacobian is (Eq. 17.8)

$$[J] = \begin{bmatrix} 0\left(\frac{-1}{4}\right) & 0\left(\frac{-1}{4}\right) \\ 0\left(\frac{-1}{4}\right) & 0\left(\frac{-1}{4}\right) \end{bmatrix} + \begin{bmatrix} 7\left(\frac{1}{4}\right) & 1\left(\frac{1}{4}\right) \\ 7\left(\frac{-1}{4}\right) & 1\left(\frac{-1}{4}\right) \end{bmatrix}$$
$$+ \begin{bmatrix} 6\left(\frac{1}{4}\right) & 9\left(\frac{1}{4}\right) \\ 6\left(\frac{1}{4}\right) & 9\left(\frac{1}{4}\right) \end{bmatrix} + \begin{bmatrix} -2\left(\frac{-1}{4}\right) & 5\left(\frac{-1}{4}\right) \\ -2\left(\frac{1}{4}\right) & 5\left(\frac{1}{4}\right) \end{bmatrix}$$
$$= \begin{bmatrix} \frac{15}{4} & \frac{5}{4} \\ -\frac{3}{4} & \frac{13}{4} \end{bmatrix}$$

$$\text{Area} = 4|J| = 4(13.125) = 52.5$$

17.3 Convergence of isoparametric elements

One of the requirements for the shape functions for a finite element is that they allow a constant-strain state (see Section 16.9). To verify that the shape functions of isoparametric elements satisfy this requirement, let the element acquire nodal displacements given by

$$u_i = a_1 x_i + a_2 y_i + a_3 \quad v_i = a_4 x_i + a_5 y_i + a_6 \tag{17.15}$$

where a_1 to a_6 are arbitrary constants, and i is the node number. The displacement at any point (ξ, η) is given by substitution of Eq. 17.15 in Eq. 17.2:

$$u = a_1 \sum L_i x_i + a_2 \sum L_i y_i + a_3 \sum L_i \qquad (17.16)$$
$$v = a_4 \sum L_i x_i + a_5 \sum L_i y_i + a_6 \sum L_i$$

We note that $\Sigma L_i x_i = x$ and $\Sigma L_i y_i = y$ (Eq. 17.4). If $\Sigma L_i = 1$, Eq. 17.16 can be rewritten as

$$u = a_1 x + a_2 y + a_3 \quad v = a_4 x + a_5 y + a_6 \qquad (17.17)$$

Equation 17.17 indicates that the strains are constant when the sum $\Sigma L_i = 1$. This condition is satisfied for the shape functions in Eq. 17.3. It is also satisfied for the shape functions of other isoparametric elements discussed below.

Another requirement for convergence is that the shape functions allow rigid-body motion with zero strains. This represents a special case of the state of constant strain. This then verifies the fact that the shape functions allow the element to move as a rigid body.

17.4 Lagrange interpolation

Consider a function $g(\xi)$ for which the n values $g_1, g_2, \ldots, g_n$ are known at $\xi_1, \xi_2, \ldots, \xi_n$ (Figure 17.2). The Lagrange equation gives a polynomial $g(\xi)$ which passes through the n points. The equation takes the form of a summation of n polynomials:

$$g(\xi) = \sum_{i=1}^{n} g_i L_i \qquad (17.18)$$

where L_i is a polynomial in ξ of degree $n-1$. Equation 17.18 can be used to interpolate between $g_1, g_2, \ldots, g_n$ to give the g value at any intermediate ξ. Figure 17.3 shows *Lagrange interpolation functions* for $n = 2$, 3, and 4. It can be seen that any function L_i has a unit value at ξ_i and a zero value at ξ_j, where $j \neq i$.

Lagrange interpolation functions are expressed as a product of $n-1$ terms:

$$L_i = \frac{\xi - \xi_1}{\xi_i - \xi_1} \frac{\xi - \xi_2}{\xi_i - \xi_2} \cdots \frac{\xi - \xi_{i-1}}{\xi_i - \xi_{i-1}} \frac{\xi - \xi_{i+1}}{\xi_i - \xi_{i+1}} \cdots \frac{\xi - \xi_n}{\xi_i - \xi_n} \qquad (17.19)$$

which gives polynomials of order $n-1$.

Equation 17.19 can be used to derive any of the functions L_i in Figure 17.3, which are linear, quadratic, and cubic corresponding to $n = 2$, 3, and 4 respectively. It can be verified that, for any n, the sum $(L_1 + L_2 + \cdots + L_n)$ is equal to 1 for any value of ξ.

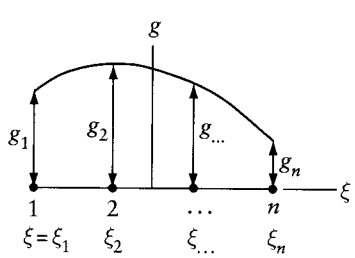

Figure 17.2 Function $g(\xi)$ with n known values $g_1, g_2, \ldots, g_n$ at $\xi = \xi_1, \xi_2, \ldots, \xi_n$.

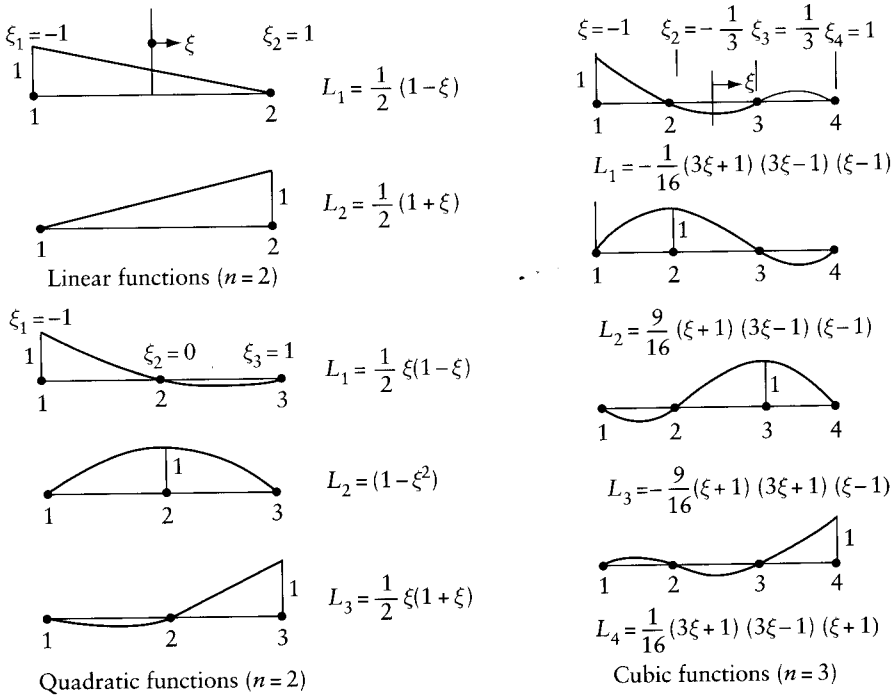

Figure 17.3 Linear, quadratic, and cubic Lagrange polynomials used to give the value of a function at any point in terms of n known values, with $n = 2$, 3, and 4 respectively (Eq. 17.18).

17.5 Shape functions for two- and three-dimensional isoparametric elements

Figure 17.4 shows a quadrilateral element with corner nodes and also intermediate nodes on the edges. This element can be used for plane-stress or plane-strain analysis; the degrees of freedom at each node are u and v, representing translations in x and y directions. The nodes are equally spaced on each edge. The number of intermediate nodes on any edge can be 0, 1, 2, ..., but the most commonly used elements have one or two intermediate nodes on each edge.

The shape functions are represented by Lagrange polynomials at one edge (or at two adjacent edges) with linear interpolation between each pair of opposite edges. As an example, the shape functions L_5 and L_6 for the element in Figure 17.4 are

$$L_5 = \tfrac{1}{2}\left(1-\xi^2\right)(1-\eta) \tag{17.20}$$

$$L_6 = \tfrac{1}{2}\left(1-\eta^2\right)(1+\xi) \tag{17.21}$$

The shape functions L are used for interpolation of u or v and also for the coordinates x and y between nodal values of the same parameters. Figure 17.4 includes pictorial views of L_5 and L_6 plotted perpendicular to the surface of the element.

For corner node 2, the shape function is

$$L_2 = \tfrac{1}{4}(1+\xi)(1-\eta) - \frac{L_5}{2} - \frac{L_6}{2} \tag{17.22}$$

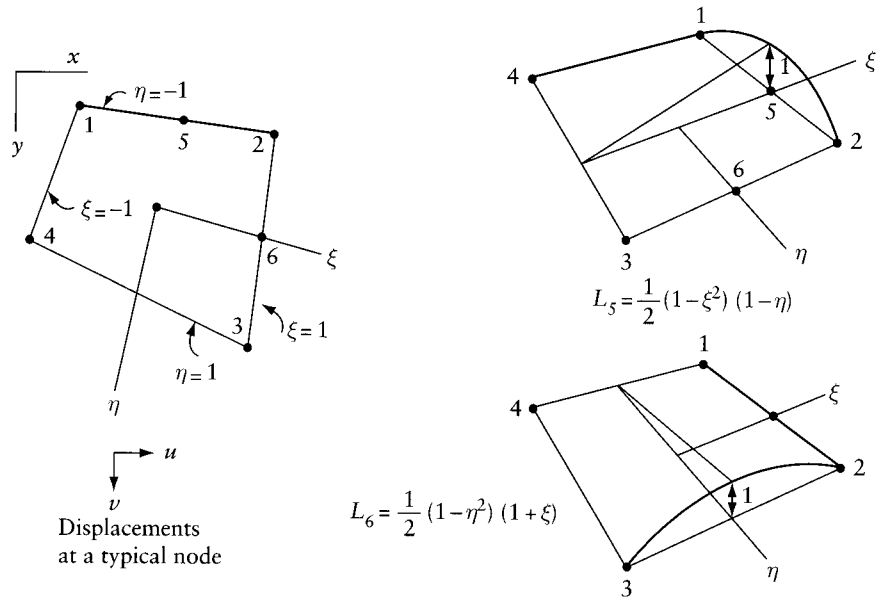

Figure 17.4 Generation of shape functions by superposition of shapes. The function L_2 is the shape function shown in Figure 16.5 minus one-half of $(L_5 + L_6)$ of this figure.

The first term in this equation is the shape function for the same corner node in an element without mid-side nodes (Figure 16.5). The terms $L_5/2$ and $L_6/2$ are subtracted to make L_2 equal to zero at the two added mid-side nodes 5 and 6.

The use of Lagrange polynomials at the edges and linear interpolation between opposite sides, in the manner described above, enables us to write directly (by intuition) the shape functions for any corner or intermediate node on the element edges. Figure 17.5 gives the shape functions for an eight-node element; such an element is widely used in plane-stress or plane-strain analysis because it gives accurate results. In general form, the edges are curved (second-degree parabola) and the coordinates ξ and η are curvilinear. The shape functions given in this figure can be used with Eq. 17.2 and Eqs. 17.4 to 17.14 to generate a stiffness matrix and a load vector without any complication caused by the curvilinear coordinates.

The above approach can be extended directly to three-dimensional solid elements with three degrees of freedom per node, u, v, and w, in the global x, y, and z directions. The shape functions

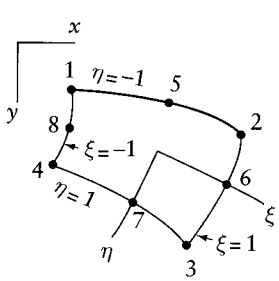

$$L_i = \frac{1}{4}(1+\xi\xi_i)(1+\eta\eta_i)(\xi\xi_i+\eta\eta_i-1) \quad \text{with } i = 1, 2, 3, 4$$

$$L_i = \frac{1}{2}(1-\xi^2)(1+\eta\eta_i) \quad \text{with } i = 5, 7$$

$$L_i = \frac{1}{2}(1-\eta^2)(1+\xi\xi_i) \quad \text{with } i = 6, 8$$

Figure 17.5 Shape functions for a two-dimensional element with corner and mid-side nodes.

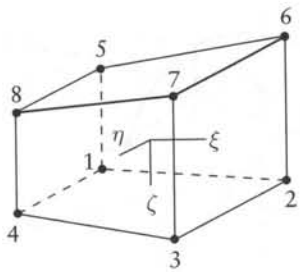

8-node solid

$$L_i = \frac{1}{8}(1+\xi\xi_i)(1+\eta\eta_i)(1+\zeta\zeta_i) \text{ with } i = 1 \text{ to } 8$$

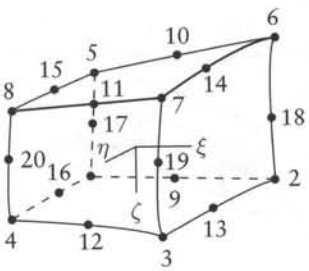

20-node solid

$$L_i = \frac{1}{8}(1+\xi\xi_i)(1+\eta\eta_i)(1+\zeta\zeta_i)(\xi\xi_i+\eta\eta_i+\xi\xi_i-2) \text{ with } i = 1 \text{ to } 8$$

$$L_i = \frac{1}{4}(1-\xi^2)(1+\eta\eta_i)(1+\zeta\zeta_i) \text{ with } i = 9 \text{ to } 12$$

$$L_i = \frac{1}{4}(1-\eta^2)(1+\xi\xi_i)(1+\zeta\zeta_i) \text{ with } i = 13 \text{ to } 16$$

$$L_i = \frac{1}{4}(1-\zeta^2)(1+\xi\xi_i)(1+\eta\eta_i) \text{ with } i = 17 \text{ to } 20$$

Figure 17.6 Shape functions for isoparametric solid elements with eight and twenty nodes.

are given in Figure 17.6 for an element with corner nodes and for an element with corner as well as mid-edge nodes. With the addition of mid-edge nodes, the accuracy is increased and the element can have curved edges.

For the three-dimensional isoparametric elements shown in Figure 17.6, the shape functions $L(\xi, \eta, \zeta)$ are used for interpolation of displacements u, v, w and coordinates x, y, z as follows:

$$u = \sum L_i u_i \quad v = \sum L_i v_i \quad w = \sum L_i w_i \tag{17.23}$$

$$x = \sum L_i x_i \quad y = \sum L_i y_i \quad z_i = \sum L_i z_i \tag{17.24}$$

with $i = 1$ to 8 or 1 to 20.

It is of interest to note that, by use of Lagrange polynomials, the sum of the interpolation functions at any point equals unity. This can be verified for the two- and three-dimensional elements discussed above.

Example 17.2: Element with four corner nodes and one mid-edge node

Construct shape functions for the isoparametric element shown in Figure 17.5 with four corner nodes and only one mid-edge node 5 (nodes 6, 7, and 8 are deleted).

The shape functions can be generated by intuition as explained in Section 17.5. The shape function L_5 is

$$L_5 = \tfrac{1}{2}\left(1-\xi^2\right)(1-\eta)$$

For L_1 and L_2, combine the shape functions in Figure 16.5 with L_5:

$$L_1 = \tfrac{1}{4}(1-\xi)(1-\eta) - \frac{L_5}{2} \quad L_2 = \tfrac{1}{4}(1+\xi)(1-\eta) - \frac{L_5}{2}$$

The shape functions L_3 and L_4 are the same as in Figure 16.5:

$$L_3 = \tfrac{1}{4}(1+\xi)(1+\eta) \quad L_4 = \tfrac{1}{4}(1-\xi)(1+\eta)$$

17.6 Consistent load vectors for rectangular plane element

Equations 16.47 and 16.50 can be used to determine the consistent load vectors due to body forces or due to temperature variation for the plane-stress or plane-strain element shown in Figure 17.5. Consider a special case when the element is a rectangle subjected to a uniform load of q_x per unit volume (Figure 17.7). The consistent vector of restraining forces is (Eq. 16.47)

$$\{F_b^*\} = -\frac{hbc}{4}\int_{-1}^{1}\int_{-1}^{1}\begin{bmatrix} L_1 & 0 & L_2 & 0 & \dots & L_8 & 0 \\ 0 & L_1 & 0 & L_2 & \dots & 0 & L_8 \end{bmatrix}^T \begin{Bmatrix} q_x \\ 0 \end{Bmatrix} d\xi\, d\eta \tag{17.25}$$

where b and c are the element sides and h is its thickness; L_1 to L_8 are given in Figure 17.5. The integrals in Eq. 17.25 give the consistent nodal forces shown in Figure 17.7.

Note the unexpected result: the forces at corner nodes are in the opposite direction to the forces at mid-side nodes. But, as expected, the sum of the forces at the eight nodes is equal to $q_x hbc$. Apportionment of the load on the nodal forces intuitively may be sufficient when the finite-element mesh is fine, but greater accuracy is obtained using the consistent load vector, particularly when the mesh is coarse.

Let the element in Figure 17.7 be subjected to a temperature rise of T degrees; if the expansion is restrained, the stresses are

$$\{\sigma\}_r = -[E\alpha T/(1-\nu)]\{1,1,0\} \tag{17.26}$$

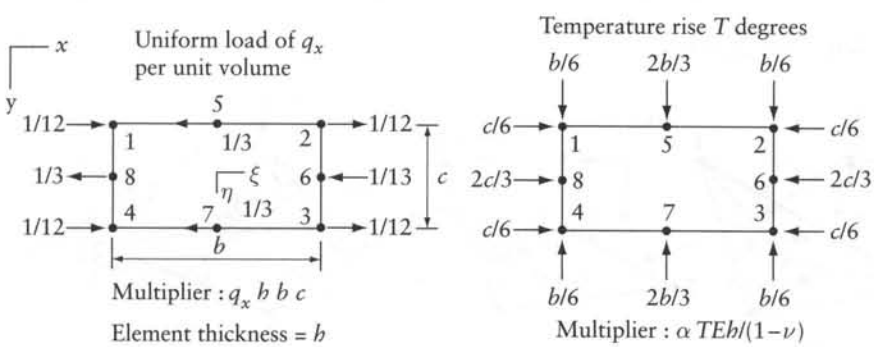

Figure 17.7 Rectangular plane-stress element. Consistent nodal forces due to a uniform load q_x and due to a rise in temperature of T degrees, with the nodal displacements prevented.

where E, ν, and α are modulus of elasticity, Poisson's ratio, and coefficient of thermal expansion of the material (assumed isotropic). The corresponding consistent nodal forces can be determined by substitution of Eqs. 17.10, 17.26, and 16.48 into 16.50, using the shape functions in Figure 17.5. The resulting nodal forces are included in Figure 17.7.

The same results can be obtained by integration, over the length of the edges, of the product of σ_{rx} or σ_{ry} and the shape functions, with the result multiplied by the thickness h. For example, the force at node 8 is

$$F_8 = \sigma_{rx} h \int_{-\frac{c}{2}}^{\frac{c}{2}} (L_8)_{\xi=-1}\, dy = \sigma_{rx} \frac{hc}{2} \int_{-1}^{1} (1-\eta^2) d\eta = \tfrac{2}{3}\sigma_{rx} hc \tag{17.27}$$

Here again, the consistent load vector cannot be generated by intuition.

17.7 Triangular plane-stress and plane-strain elements

Consider the triangular element 1.2.3 shown in Figure 17.8a, which has an area Δ. Joining any point (x,y) inside the triangle to its three corners divides Δ into three areas, A_1, A_2, and A_3. The position of the point can be defined by the dimensionless parameters α_1, α_2, and α_3, where

$$\alpha_1 = A_1/\Delta \quad \alpha_2 = A_2/\Delta \quad \alpha_3 = A_3/\Delta \tag{17.28}$$

and

$$\alpha_1 + \alpha_2 + \alpha_3 = 1 \tag{17.29}$$

The parameters α_1, α_2, and α_3 are called *area coordinates* or *areal coordinates*. Any two of them are sufficient to define the position of a point within the element. Lines parallel to the sides of the triangle are lines of equal α_i (Figure 17.8b).

Figure 17.8c is a pictorial view of the shape function L_1 for the constant-strain triangle discussed in Section 16.11. The element has three corner nodes with degrees of freedom u and n per node, representing translations in the x and y directions. The ordinates L_1, which are plotted perpendicular to the surface of the triangle, represent the variation in u or v when the nodal displacement u_1 or v_1 equals unity. If we plot lines of equal L_1, they will be identical to the lines of equal α_1, indicating that α_1 is equal to L_1. Thus, the shape functions α_1, α_2, and α_3 can serve as shape functions L_1, L_2, and L_3 for the constant-strain triangle.

Therefore, we can express the displacement at any point by

$$u = \sum L_i u_i \quad v = \sum L_i v_i \tag{17.30}$$

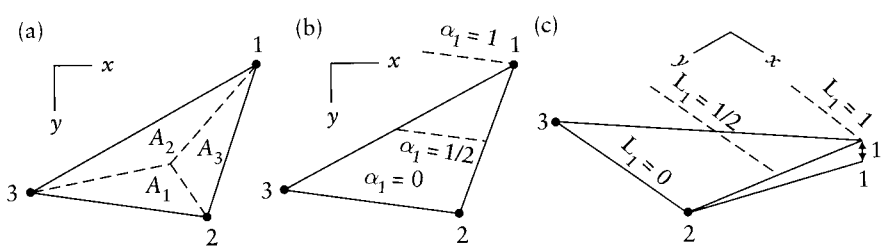

Figure 17.8 Constant-strain triangle. (a) Area coordinates $\{\alpha_1,\alpha_2,\alpha_3\} = (1/\Delta)\{A_1,A_2,A_3\}$. (b) Lines of equal α_1. (c) Pictorial view of shape function $L_1 = \alpha_1$.

It can be shown (by linear interpolation) that

$$x = \sum L_i x_i \quad y = \sum L_i y_i \tag{17.31}$$

Equations 17.30 and 17.31 are the same as Eqs. 17.2 and 17.4, indicating that the constant-strain triangle is an isoparametric element in which the area coordinates serve as shape functions:

$$L_1 = \alpha_1 \quad L_2 = \alpha_2 \quad L_3 = \alpha_3 \tag{17.32}$$

For a triangle with *straight* edges (Figure 17.8a), the area coordinates can be expressed in terms of x and y by combining Eqs. 17.29, 17.31 and 17.32, giving

$$\{\alpha_1, \alpha_2, \alpha_3\} = \frac{1}{2\Delta}\{a_1 + b_1 x + c_1 y, \quad a_2 + b_2 x + c_2 y, \quad a_3 + b_3 x + c_3 y\} \tag{17.33}$$

where

$$a_1 = x_2 y_3 - y_2 x_3 \quad b_1 = y_2 - y_3 \quad c_1 = x_3 - x_2 \tag{17.34}$$

By cyclic permutation of the subscripts 1, 2, and 3, similar equations can be written for a_2, b_2, c_2 and a_3, b_3, c_3.

17.7.1 Linear-strain triangle

An isoparametric triangular element with corner and mid-side nodes is shown in Figure 17.9a. This element is widely used in practice for plane-stress or plane-strain analysis because it gives accurate results. The nodal displacements are u_i and v_i with $i = 1, 2, \ldots, 6$. Equations 17.30 and 17.31 apply to this element, with the shape functions L_1 to L_6 derived by superposition for various shapes, in a way similar to that used for the quadrilateral element in Figure 17.4.

The shape functions for the mid-side nodes in Figure 17.9a are

$$L_4 = 4\alpha_1\alpha_2 \quad L_5 = 4\alpha_2\alpha_3 \quad L_6 = 4\alpha_3\alpha_1 \tag{17.35}$$

A pictorial view of L_4, plotted perpendicular to the plane of the element, is shown in Figure 17.9b. The function is quadratic along edge 1–2, but linear along lines α_1 or α_2 = constant.

The shape functions for corner nodes are obtained by an appropriate combination of L_4, L_5, and L_6 with the shape functions for the three-node element. For example, combining the shape

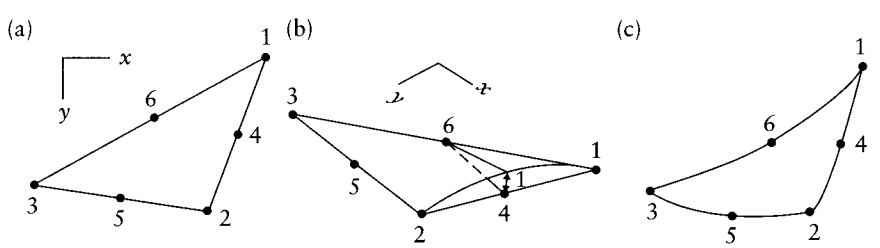

Figure 17.9 Triangular isoparametric element for plane-stress or plane-strain analysis. Two degrees of freedom per node: u and v in x and y directions. (a) Node numbering. (b) Pictorial view of shape function L_4. (c) General quadratic triangle.

function of Figure 17.8 with $-L_4/2$ and $-L_6/2$ gives shape function L_1 for the six-node element. The function obtained in this way has a unit value at 1, and a zero value at all other nodes, as it should. The shape functions for the three corner nodes for the element in Figure 17.9a are

$$L_1 = \alpha_1(2\alpha_1 - 1) \quad L_2 = \alpha_2(2\alpha_2 - 1) \quad L_3 = \alpha_3(2\alpha_3 - 1) \tag{17.36}$$

It can be seen from Eqs. 17.35 and 17.36 that the shape functions are quadratic, but the first derivatives, which give the strains, are linear. The six-node triangular element is sometimes referred to as a *linear-strain* triangle.

The six-node element can have curved sides. The x, y coordinates of any point are given by Eq. 17.31, using the shape functions in Eqs. 17.35 and 17.36. The lines of equal α will not be straight in this case, and Eq. 17.33 does not apply.

The stiffness matrix and the consistent load vectors for the six-node isoparametric triangular element can be generated using the equations given in Section 17.2 for a quadrilateral element, replacing ξ and η by α_1 and α_2 respectively. The third parameter α_3 is eliminated from the shape functions by substituting $\alpha_3 = 1 - \alpha_1 - \alpha_2$.

The integrals involved in the derivation of the matrices of triangular elements can be put in the form

$$\int_a f(\alpha_1, \alpha_2)\, da = \int_0^1 \int_0^{1-\alpha_1} f(\alpha_1, \alpha_2)\, |J|\, d\alpha_2 d\alpha_1 \tag{17.37}$$

where $f(\alpha_1, \alpha_2)$ is a function of α_1 and α_2, and $|J|$ is the determinant of the Jacobian. The inner integral on the right-hand side represents the value of the integral over a line of constant α_1; over such a line, the parameter α_2 varies between 0 and $1 - \alpha_1$.

The Jacobian can be determined by Eq. 17.8, replacing ξ and η as mentioned above. We can verify that, when the sides of the triangle are straight, $[J]$ is constant and its determinant is equal to twice the area.

The integral on the right-hand side of Eq. 17.37 is commonly evaluated numerically, using Eq. 17.48. However, in the case of a triangle with *straight* edges, the determinant $|J|$ can be taken out of the integral and the following closed-form equation can be used to evaluate the functions in the form

$$\int_a \alpha_1^{n_1} \alpha_2^{n_2} \alpha_3^{n_3}\, da = 2\Delta \frac{n_1! n_2! n_3!}{(n_1 + n_2 + n_3 + 2)!} \tag{17.38}$$

where n_1, n_2, and n_3 are any integers; the symbol ! indicates a factorial.

17.8 Triangular plate-bending elements

A desirable triangular element which can be used for the analysis of plates in bending and for shell structures (when combined with plane-stress elements) should have three degrees of freedom per node, namely w, θ_x, and θ_y, representing deflection in a global z direction and two rotations θ_x and θ_y (Figure 17.10a). With nine degrees of freedom, the deflection w should be expressed by a polynomial with nine terms. Pascal's triangle (Figure 16.7) indicates that a complete quadratic polynomial has six terms and a cubic polynomial has ten. Leaving out one of the terms x^2y or xy^2 gives an element for which the outcome is dependent upon the choice of x and y axes.

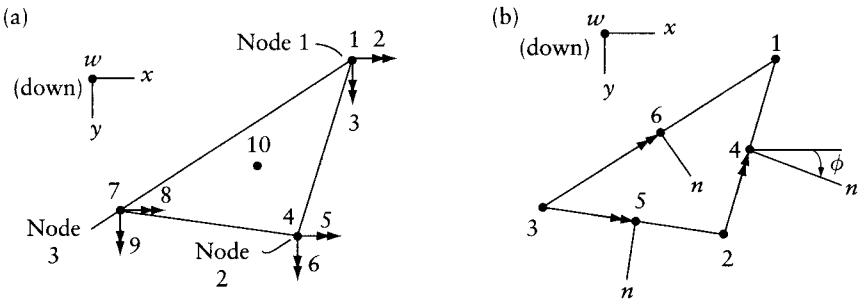

Figure 17.10 Triangular bending elements. (a) Number of degrees of freedom 10: w, θ_x, θ_y at each corner and w at centroid. (b) Number of degrees of freedom 6: w at corners and $\partial w/\partial n$ at mid-side nodes.

It is possible to express w using area coordinates and a polynomial of nine terms (which are not a simple selection). This gives a nonconforming element[2] which is widely used in practice because its results are accurate (although it does not pass the patch test, Section 16.10).

The two triangular elements shown in Figure 17.10b. and 17.10a have six and ten degrees of freedom respectively. The deflection w for the two elements can be represented by complete quadratic and cubic polynomials respectively, containing the top six or ten terms of Pascal's triangle (Figure 16.7).

The six degrees of freedom for the element in Figure 17.10b. are

$$\{D^*\} = \left\{ w_1, w_2, w_3, \left(\frac{\partial w}{\partial n}\right)_4, \left(\frac{\partial w}{\partial n}\right)_5, \left(\frac{\partial w}{\partial n}\right)_6 \right\} \tag{17.39}$$

where $\partial w/\partial n$ is the slope of a tangent normal to the sides half-way between the nodes. The positive direction of the normal vector is pointing either inwards or outwards, so that the angle ϕ, measured in the clockwise direction from the global x axis to the normal, is smaller than π. Thus, for the triangle in Figure 17.10b, the normal at node 6 points inwards. However, for an adjacent triangle (not shown) sharing side 1–3, the normal points outwards; the two triangles share the same degree of freedom $\partial w/\partial n$, which is indicated in a positive direction (Figure 17.10b). The derivative $\partial w/\partial n$ can be expressed as

$$\frac{\partial w}{\partial n} = \frac{\partial w}{\partial x}\cos\phi + \frac{\partial w}{\partial y}\sin\phi \tag{17.40}$$

The deflection is expressed by the upper six terms of Pascal's triangle (Figure 16.7):

$$w = \left[1\, x\, y\, x^2\, xy\, y^2\right]\{A\} = [P]\{A\} \tag{17.41}$$

Substituting for x and y by their values at the nodes, the nodal displacements can be expressed by $[D^*] = [C]\{A\}$, with

2 See Bazeley, G. P., Cheung, Y. K., Irons, B. M. and Zienkiewicz, O. C., "Triangular Elements in Plate Bending: Conforming and Non-Conforming Solutions," *Proceedings of the Conference on Matrix Methods in Structural Mechanics*, Air Force Institute of Technology, Wright Patterson Base, Ohio, 1965.

$$[C]=\begin{bmatrix} 1 & x_1 & y_1 & x_1^2 & x_1y_1 & y_1^2 \\ 1 & x_2 & y_2 & x_2^2 & x_2y_2 & y_2^2 \\ 1 & x_3 & y_3 & x_3^2 & x_3y_3 & y_2^2 \\ 0 & c_4 & s_4 & 2x_4c_4 & y_4c_4+x_4s_4 & 2y_4s_4 \\ 0 & c_5 & s_5 & 2x_5c_5 & y_5c_5+x_5s_5 & 2y_5s_5 \\ 0 & c_6 & s_6 & 2x_6c_6 & y_6c_6+x_6s_6 & 2y_6s_6 \end{bmatrix} \tag{17.42}$$

where $s_i=\sin\phi_i$, $c_i=\cos\phi_i$.

The shape functions can be derived by Eq. 16.60, the $[B]$ matrix by Eqs. 16.39 and 16.19, and the stiffness matrix and consistent load vectors by Eqs. 16.45, 16.47, and 16.50. The strains for this element are constant and the element matrices are relatively simple to derive (see Prob. 17.8).

Despite its simplicity, the element with six degrees of freedom (Figure 17.10b) gives fairly accurate results. It can be shown that the element is nonconforming because the inter-element deflections and their derivatives are not compatible. However, the element passes the patch test and the results converge quickly to the exact solution as the finite-element mesh is refined.[3]

The element in Figure 17.10a has ten degrees of freedom $\{D^*\}$, as shown. The tenth displacement is a downward deflection at the centroid. The deflection can be expressed as $w=[L]\{D^*\}$, where $[L]$ is composed of ten shape functions given in terms of area coordinates α_1, α_2, and α_3 (Eq. 17.28) as follows:

$$\begin{aligned} L_1&=\alpha_1^2(\alpha_1+3\alpha_2+3\alpha_3)-7\alpha_1\alpha_2\alpha_3 \\ L_2&=\alpha_1^2(b_2\alpha_3-b_3\alpha_2)+(b_3-b_2)\alpha_1\alpha_2\alpha_3 \\ L_3&=\alpha_1^2(c_2\alpha_3-c_3\alpha_2)=(c_3-c_2)\alpha_1\alpha_2\alpha_3 \\ L_{10}&=27\alpha_1\alpha_2\alpha_3 \end{aligned} \tag{17.43}$$

where b_i and c_i are defined by Eq. 17.34. The equation for L_1 can be used for L_4 and L_7 by cyclic permutation of the subscripts 1, 2, and 3. Similarly, the equation for L_2 can be used for L_5 and L_8, and the equation for L_3 can be used for L_6 and L_9. We can verify that the ten shape functions and their derivatives take unit or zero values at the nodes, as they should. This involves the derivatives $\partial\alpha_i/\partial x$ and $\partial\alpha_i/\partial y$ which are, respectively, equal to $b_i/2\Delta$ and $c_i/2\Delta$, where Δ is the area of the triangle (see Eq. 17.33).

The inter-element displacement compatibility for $\partial w/\partial n$ is violated with the shape functions in Eq. 17.43, but the values of w of two adjacent elements are identical along a common side. This element does not give good accuracy.

However, the accuracy of the element shown in Figure 17.10a can be improved by imposing constraints in the solution of the equilibrium equations of the assembled structure (Section 22.4). The constraints specify continuity of normal slopes $\partial w/\partial n$ at mid-points of element sides. With such treatment, the accuracy of this element will be better than that of the element shown in Figure 17.10b.

3 Numerical comparison of results obtained by various types of triangular bending elements and convergence as the mesh is refined can be seen in Gallagher, R. H., *Finite Element Analysis Fundamentals*, Prentice-Hall, Englewood Cliffs, NJ, 1975, p. 350. The same book includes other triangular elements and a list of references on this topic.

17.9 Numerical integration

The Gauss method of integration is used extensively in generating the matrices of finite elements. The method is given below without derivation[4] for one-, two-, and three-dimensional integration.

A definite integral of a one-dimensional function $g(\xi)$ (Figure 17.11) can be calculated by

$$\int_{-1}^{1} g(\xi)d\xi \simeq \sum_{i=1}^{n} W_i g_i \tag{17.44}$$

where g_i represents the values of the function at n sampling points $\xi_1, \xi_2, \ldots, \xi_n$ and W_i represents the weight factors. The sampling points are sometimes referred to as *Gauss points*. The values ξ_i and W_i are given to 15 decimal places in Table 17.1 for n between 1 and 6.[5] The values of ξ_i and W_i used in computer programs should include as many digits as possible.

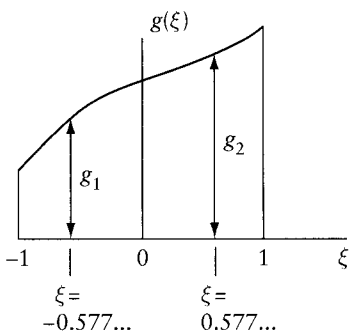

Figure 17.11 Gauss numerical integration of function $g(\xi)$ by Eq. 17.44. Example for a number of sampling points $n = 2$.

Table 17.1 Location of Sampling Points and Weight Factors for Gauss Numerical Integration by Eqs. 17.44 to 17.46

n	ξ_i, η_i or ζ_i	W_i
1	0.000 000 000 000 000	2.000 000 000 000 000
2	±0.577 350 269 189 626	1.000 000 000 000 000
3	0.000 000 000 000 000	0.888 888 888 888 888
	±0.774 596 669 241 483	0.555 555 555 555 556
4	±0.339 981 043 584 856	0.652 145 154 862 546
	±0.861 136 311 594 053	0.347 858 485 137 454
	0.000 000 000 000 000	0.568 888 888 888 889
5	±0.538 469 310 105 683	0.478 628 670 499 366
	±0.906 179 845 938 664	0.236 926 885 056 189
	±0.238 619 186 083 197	0.467 913 934 572 691
6	±0.661 209 386 466 265	0.360 761 573 048 139
	±0.932 469 514 203 152	0.171 324 492 379 170

4 Derivation can be found in Irons, B. M. and Shrive, N. G., *Numerical Methods in Engineering and Applied Science,* Ellis Horwood, Chichester, England and Halsted Press (Wiley), New York, 1987.

5 Values of ξ_i and W_i for n between 1 and 10 can be found on p. 79 of the reference in footnote 4 in this chapter. See also Kopal, Z., *Numerical Analysis,* 2nd ed., Chapman & Hall, 1961.

The location of the sampling points, specified by the values of ξ_i in the table, is chosen to achieve the maximum accuracy for any given n. The sampling points are located symmetrically with respect to the origin.

If the function is a polynomial, $g = a_0 + a_1\xi + \cdots + a_m\xi^m$, Eq. 17.44 is exact when the number of sampling points is $n \geqslant (m+1)/2$. In other words, n Gauss points are sufficient to integrate exactly a polynomial of order $2n-1$. For example, we can verify that using $n=2$ (Figure 17.11) gives exact integrals for each of the functions $g = a_0 + a_1\xi$, $g = a_0 + a_1\xi + a_2\xi^2$ and $g = a_0 + a_1\xi + a_2\xi^2 + a_3\xi^3$. The two sampling points are at $\xi = \pm 0.577\ldots$ and the weight factors are equal to unity.

We should note that the sum of the weight factors in Eq. 17.44 is 2.0.

A definite integral for a two-dimensional function $g(\xi, \eta)$ can be calculated by

$$\int_{-1}^{1}\int_{-1}^{1} g(\xi,\eta)d\xi\,d\eta \simeq \sum_{j}^{n_n}\sum_{i}^{n_\xi} W_j W_i g(\xi_i, \eta_j) \tag{17.45}$$

where n_ξ and n_η are the number of sampling points on ξ and η axes respectively. Figure 17.12 shows two examples of sampling points. In most cases, n_ξ and n_η are the same (equal to n); then $n \times n$ Gauss points integrate exactly a polynomial $g(\xi, \eta)$ of order $2n-1$.

Equation 17.45 can be derived from Eq. 17.44 by integrating first with respect to ξ and then with respect to η. For 3×2 Gauss points ($n_\xi = 3, n_\eta = 2$), Eq. 17.45 can be rewritten (Figure 17.12) as

$$\begin{aligned}\int_{-1}^{1}\int_{-1}^{1} g(\xi,\eta)d\xi\,d\eta &\simeq (1.0)(0.555\cdots)g_1 + (1.0)(0.888\cdots)g_2 + (1.0)(0.555\cdots)g_3 \\ &\quad + (1.0)(0.555\cdots)g_4 + (1.0)(0.888\cdots)g_5 + (1.0)(0.555\cdots)g_6\end{aligned} \tag{17.46}$$

We can note that the sum of the multipliers of g_1 to g_6 is 4.0.

For a function in three dimensions, $g(\xi, \eta, \zeta)$, the integral is

$$\int_{-1}^{1}\int_{-1}^{1}\int_{-1}^{1} g(\xi,\eta,\zeta)d\xi\,d\eta\,d\zeta \simeq \sum_{k}^{n_\zeta}\sum_{j}^{n_n}\sum_{i}^{n_\xi} W_k W_j W_i g(\xi_i, \eta_j, \zeta_k) \tag{17.47}$$

Equations 17.44, 17.45, and 17.47 can be used for one-, two-, and three-dimensional elements with curvilinear axes.

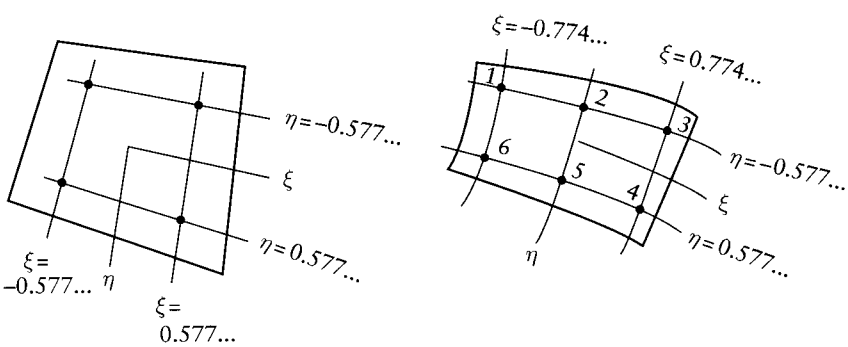

Figure 17.12 Examples of sampling points for two-dimensional Gauss numerical integration.

When the element is triangular and the area coordinates α_1, α_2, and α_3 are used (Figure 17.8a), any variable over the area of the element can be expressed as a function $f(\alpha_1, \alpha_2)$, in which α_3 is eliminated by substituting $\alpha_3 = 1 - \alpha_1 - \alpha_2$. The integral $\int f\, da$ over the area of the triangle is expressed by Eq. 17.37, and can be evaluated numerically using

$$\int_0^1 \int_0^{1-\alpha_1} g(\alpha_1, \alpha_2) d\alpha_2 d\alpha_1 \simeq \sum_{i=1}^{n} W_i g_i \tag{17.48}$$

In this equation, the symbol $g(\alpha_1, \alpha_2)$ stands for the product $f(\alpha_1, \alpha_2)|J|$ in Eq. 17.37, where $|J|$ is the determinant of the Jacobian.

The location of the sampling points and the corresponding weight factors for use in Eq. 17.48 are given in Figure 17.13.[6] These values give the exact integrals when g is linear, quadratic, cubic, and quintic, as indicated.

We should note that the sum of the weight factors for all the sampling points of any triangle is equal to one-half. For a triangle with straight edges, $|J| = 2\Delta$, where Δ is the area. If we set

	Point	α_1 or α_2	Point	Weight factor
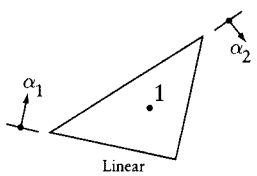	1	0.333 333 333 3	1	$W_1 = 0.5000000000$
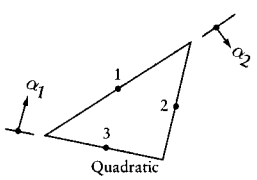	3 1,2	0.000 000 000 0 0.500 000 000 0	1 2,3	$W_{1,2,3} = 0.1666666667$
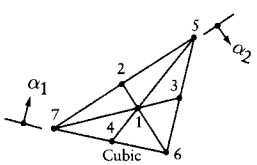	4,6,7 1 2,3 5	0.000 000 000 0 0.333 333 333 3 0.500 000 000 0 1.000 000 000 0	2,5,7 1 3,4 6	$W_1 = 0.2250000000$ $W_{2,3,4} = 0.0666666667$ $W_{5,6,7} = 0.0250000000$
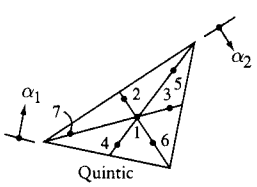	4 6,7 1 2,3 5	0.059 715 871 8 0.101 286 507 3 0.333 333 333 3 0.470 142 064 1 0.797 426 985 4	2 5,7 1 3,4 6	$W_1 = 0.1125000000$ $W_{2,3,4} = 0.0661970764$ $W_{5,6,7} = 0.0629695903$

Figure 17.13 Numerical integration of function $g(a_1, a_2, a_3)$ over the area of a triangle. Values of a_1, a_2, and a_3 defining sampling points and weight factors W_i for use in Eq. 17.48 ($a_3 = 1 - a_1 - a_2$).

6 See Cowper, G. R., "Gaussian quadrature formulas for triangles", *Int. J. Num. Math. Eng.* (7), (1973), pp. 405–408; and Zienkiewicz, O. C, *The Finite Element Method in Engineering Science*, 4th ed., McGraw-Hill, London, 1989.

$f(\alpha_1,\alpha_2)=1$, the function $g(\alpha_1,\alpha_2)=2\Delta$, and the value of the integral given by Eq. 17.48 is equal to $(2\Delta)\Sigma W_i=\Delta$, as it should.

The number of sampling points in the numerical integration to generate the stiffness matrices of finite elements influences the accuracy and the convergence. The appropriate choice of sampling points is discussed in more detail in references devoted specifically to the finite-element method.[7]

A small number of points is generally used in order to reduce computation. Furthermore, the use of a small number of points tends to reduce the stiffness, thus compensating for the excess in stiffness associated with displacement-based finite elements (see Section 16.5). However, the number of sampling points cannot be reduced without limit. Some elements have a *spurious mechanism* when a specified pattern of sampling points is used in the integration for the derivation of the stiffness matrix. This mechanism occurs when the element can deform in such a way that the strains at the sampling points are zero.

Two-by-two sampling points are frequently used in quadrilateral plane linear elements with corner nodes only or in quadratic elements with corner and mid-side nodes. Three or four sampling points in each direction are used when the elements are elongated or in cubic[8] elements.

Example 17.3: Stiffness matrix of quadrilateral element in plane-stress state

Determine coefficient S^*_{11} of the stiffness matrix of the quadrilateral element of Example 17.1 and Figure 16.5. The element is of isotropic material; Poisson's ratio $\nu=0.2$. Also find the consistent restraining force at coordinate 1 when the element is subjected to a constant rise of temperature of T degrees. Use only one Gauss integration point.

The displacement field corresponding to $D^*_1=1$ is $\{u,v\}=\{L_1,0\}$, where

$$L_1=\tfrac{1}{4}(1-\xi)(1-\eta)$$

Derivatives of L_1 with respect to x and y at the center ($\xi=\eta=0$) are (using Eq. 17.6, with $[J]$ from Example 17.1)

$$\begin{Bmatrix}\partial L_1/\partial x\\ \partial L_1/\partial y\end{Bmatrix}=\begin{bmatrix}15/4 & 5/4\\ -3/4 & 13/4\end{bmatrix}^{-1}\begin{Bmatrix}-(1-\eta)/4\\ -(1-\xi)/4\end{Bmatrix}=\frac{1}{210}\begin{Bmatrix}-8\\ -18\end{Bmatrix}$$

When $D^*=1$, the strains at the same point are (Eq. 17.10)

$$\{B\}_1=\frac{1}{210}\{-8,0,-18\}$$

The value of the product in the stiffness matrix of Eq. 17.12 at the center of the element (Eq. 16.12) is

$$\begin{aligned}g_1&=h\{B\}_1^T[d]\{B\}_1|J|\\&=\frac{1}{(210)^2}[-8,0,-18]-\frac{Eh}{1-(0.2)^2}\begin{bmatrix}1 & 0.2 & 0\\ 0.2 & 1 & 0\\ 0 & 0 & (1-0.2)/2\end{bmatrix}\begin{Bmatrix}-8\\ 0\\ -18\end{Bmatrix}|J|\\&=4.57\times10^{-3}Eh\,|J|\end{aligned}$$

7 See, for example, the reference in footnote 5 in Chapter 16. Other selected books are included in the References to this book.

8 For example, element QLC3; see footnote 4 in Chapter 16, and Example 16.3.

The determinant of the Jacobian is 13.125 (see Example 17.1). Substitution in Eq. 17.45 with $W_1 = 2$ (from Table 17.1) gives

$$S_{11}^* = 2 \times 2(4.57 \times 10^{-3})Eh(13.125) = 0.240Eh$$

The free strains due to the temperature rise are $\alpha T\{1,1,0\}$. Substitution in Eq. 17.14 gives

$$F_{b1}^* = 2 \times 2(13.125)(-h)\left(\frac{1}{210}\right)[-8,0,-18] \times \frac{E}{1-(0.2)^2}\begin{bmatrix} 1 & 0.2 & 0 \\ 0.2 & 1 & 0 \\ 0 & 0 & (1-0.2)2 \end{bmatrix}\begin{Bmatrix} 1 \\ 1 \\ 0 \end{Bmatrix}\alpha T = 2.5E\alpha Th$$

Example 17.4: Triangular element with parabolic edges: Jacobian matrix

Determine the Jacobian at $(\alpha_1, \alpha_2) = (1/3, 1/3)$ in a triangular isoparametric element with corner and mid-side nodes, where α_1 and α_2 are area coordinates. The (x, y) coordinates of the nodes are: $(x_1, y_1) = (0,0)$; $(x_2, y_2) = (1,1)$; $(x_3, y_3) = (0,1)$; $(x_4, y_4) = ((\sqrt{2})/2, 1-(\sqrt{2})/2)$; $(x_5, y_5) = (0.5, 1)$; $(x_6, y_6) = (0, 0.5)$. These correspond to a quarter of a circle with its center at node 3 and a radius of unity. By numerical integration of Eq. 17.48, determine the area of the element, using only one sampling point.

The shape functions L_1 to L_6 are given by Eqs. 17.35 and 17.36. We eliminate α_3 by substituting $\alpha_3 = 1 - \alpha_1 - \alpha_2$, and then determine the derivatives $\partial L_i/\partial\alpha_1$ and $\partial L_i/\partial\alpha_2$ at $(\alpha_1, \alpha_2) = (1/3, 1/3)$. The Jacobian at this point (from Eq. 17.8, replacing ξ and η by α_1 and α_2) is

$$[J] = \begin{bmatrix} 0\left(\frac{1}{3}\right) & 0\left(\frac{1}{3}\right) \\ 0(0) & 0(0) \end{bmatrix} + \begin{bmatrix} 1(0) & 1(0) \\ 1\left(\frac{1}{3}\right) & 1\left(\frac{1}{3}\right) \end{bmatrix} + \begin{bmatrix} 0\left(-\frac{1}{3}\right) & 1\left(-\frac{1}{3}\right) \\ 0\left(-\frac{1}{3}\right) & 1\left(-\frac{1}{3}\right) \end{bmatrix}$$
$$+ \begin{bmatrix} \frac{\sqrt{2}}{2}\left(\frac{4}{3}\right) & \left(1-\frac{\sqrt{2}}{2}\right)\left(\frac{4}{3}\right) \\ \frac{\sqrt{2}}{2}\left(\frac{4}{3}\right) & \left(1-\frac{\sqrt{2}}{2}\right)\left(\frac{4}{3}\right) \end{bmatrix} + \begin{bmatrix} 0.5\left(-\frac{4}{3}\right) & 1\left(-\frac{4}{3}\right) \\ 0.5(0) & 1(0) \end{bmatrix}$$
$$+ \begin{bmatrix} 0(0) & 0.5(0) \\ 0\left(-\frac{4}{3}\right) & 0.5\left(-\frac{4}{3}\right) \end{bmatrix} = \begin{bmatrix} 0.2761 & -1.2761 \\ 1.2761 & -0.2761 \end{bmatrix}$$

The area of the element (from Eq. 17.48 with W_1 from Figure 17.13) is

$$\text{area} = \int_0^1 \int_0^{1-\alpha_1} |J|\, d\alpha_2 d\alpha_1 = 0.5\,|J| = 0.7761$$

17.10 Shells as assemblage of flat elements

Finite elements in the form of flat quadrilateral or triangular plates can be used to idealize a shell (Figure 17.14). In general, the elements will be subjected to in-plane forces and to bending. The element matrices derived separately in earlier sections for elements in a state of plane stress and for bending elements can be combined for a shell element as discussed below.

Idealization of a shell, using curved elements, may be necessary if large elements are employed, particularly in double-curved shells. However, in practice, many shells, particularly those of cylindrical shape, have been analyzed successfully using triangular, quadrilateral, or rectangular elements.

Flat shell elements can be easily combined with beam elements to idealize edge beams or ribs, which are common in practice.

17.10.1 Rectangular shell element

Figure 17.15 represents a rectangular shell element with six nodal displacements at each corner, three translations $\{u,v,w\}$ and three rotations $\{\theta_x,\theta_y,\theta_z\}$. The derivation of the matrices for a plane-stress rectangular element with nodal displacements u, v, and θ_z at each corner was discussed in Section 16.8 (see Example 16.3). A rectangular bending element with nodal displacements w, θ_x, and θ_y at each corner was discussed in Section 16.43.

The stiffness matrix for the shell element in Figure 17.15 can be written in the form

$$[S^*]=\begin{bmatrix} [S_m^*] & [0] \\ [0] & [S_b^*] \end{bmatrix} \tag{17.49}$$

where $[S_m^*]$ is a 12×12 membrane stiffness matrix relating forces to the displacements u, v, and θ_z, and $[S_b^*]$ is a 12×12 bending stiffness matrix relating forces to the displacements w, θ_x, and θ_y. The off-diagonal submatrices in Eq. 17.49 are null because the first set of displacements produces no forces in the directions of the second set, and vice versa. The two sets of displacements are said to be *uncoupled*.

For convenience in coding, the degrees of freedom at each node are commonly arranged in the order $\{u,v,w,\theta_x,\theta_y,\theta_z\}$. The columns and rows in the 24×24 stiffness matrix in Eq. 17.49 are

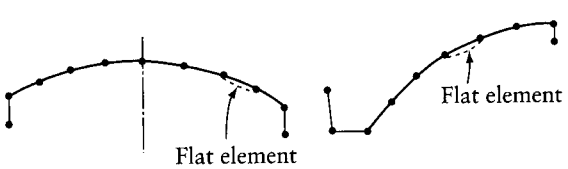

Figure 17.14 Cylindrical shells idealized as an assemblage of flat elements.

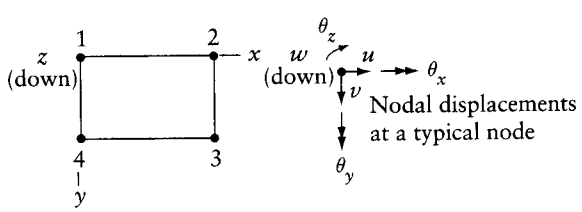

Figure 17.15 Rectangular flat shell element.

rearranged so that the nodal coordinates are numbered in the following sequence: six coordinates at node 1, followed by six coordinates at node 2, and so on.

17.10.2 Fictitious stiffness coefficients

The majority of plane-stress elements have two degrees of freedom per node, u and v. Combining such an element with a bending element (with nodal displacements w, θ_x, and θ_y) so as to form a shell element will leave the θ_z coordinate unused. The five degrees of freedom, u, v, w, θ_x, and θ_y, are not sufficient to analyze a spatial structure. This can be seen by considering elements in two intersecting planes; no matter how the global axes are chosen, the structure will, in general, have three rotation components in the three global directions at the nodes on the line of intersection.

We may think of generating a stiffness matrix for the shell element with six degrees of freedom per node, with zero columns and rows corresponding to the θ_z coordinates. However, when elements situated in one plane meet at a node, a zero will occur at the diagonal of the stiffness matrix of the assembled structure; this will result in an error message with common computer equation solvers (Sections 21.11 and A.9) when attempting to divide a number by the stiffness coefficient on the diagonal. To avoid this difficulty Zienkiewicz[9] assigns fictitious stiffness coefficients, instead of zeros, in the columns and rows corresponding to θ_z. For a triangular element with three nodes, the fictitious coefficients are

$$[S]_{\text{fict}} = \beta E \begin{bmatrix} 1 & -0.5 & -0.5 \\ -0.5 & 1 & -0.5 \\ -0.5 & -0.5 & 1 \end{bmatrix} (\text{volume}) \tag{17.50}$$

where E is the modulus of elasticity, the multiplier at the end is the volume of the element, and β is an arbitrarily chosen coefficient. Zienkiewicz suggested a value $\beta = 0.03$ or less. We can note that the sum of the fictitious coefficients in any column is zero, which is necessary for equilibrium.

17.11 Solids of revolution

Figure 17.16 represents a solid of revolution which is subjected to axisymmetrical loads (not shown). For the analysis of stresses in this body, it is divided into finite elements in the form of rings, the cross sections of which are triangles or quadrilaterals. The element has nodal circular

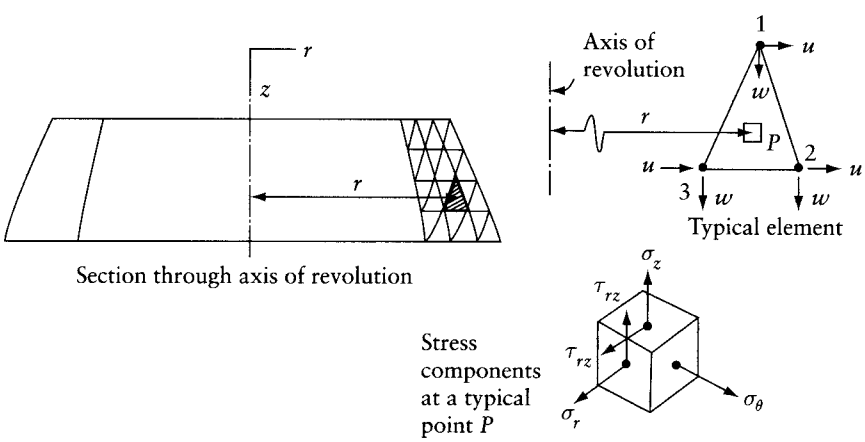

Figure 17.16 Finite-element idealization of a solid of revolution.

9 See reference mentioned in footnote 1 of Chapter 16.

lines, rather than point nodes. The displacements at the nodes are u and w in the radial direction r and in the z direction respectively.

The arrangement of the nodes and the shape functions used for plane-stress and plane-strain elements (Sections 16.42, 16.11, 17.2, 17.5, and 17.7) can be used for axisymmetric solid elements. The parameters x, y, u, and v used for plane elements have to be replaced by r, z, u, and w respectively.

One additional strain component needs to be considered in solids of revolution, namely, the hoop strain ϵ_θ, which represents elongation in the tangential direction, normal to the plane of the element. Thus, the strain vector has four components:

$$\{\epsilon\} = \begin{Bmatrix} \epsilon_r \\ \epsilon_z \\ \epsilon_\theta \\ \gamma_{rz} \end{Bmatrix} = \begin{bmatrix} \dfrac{\partial}{\partial r} & 0 \\ 0 & \dfrac{\partial}{\partial w} \\ \dfrac{1}{r} & 0 \\ \dfrac{\partial}{\partial w} & \dfrac{\partial}{\partial r} \end{bmatrix} \begin{Bmatrix} u \\ w \end{Bmatrix} \tag{17.51}$$

The stress vector has also one additional component, the hoop stress σ_θ (Figure 17.16). The stress–strain relation for solids of revolution of isotropic material is

$$\{\sigma\} = [d]\,\{\epsilon\} \tag{17.52}$$

where

$$\{\sigma\} = \{\sigma_r, \sigma_z, \sigma_\theta, \gamma_{rz}\} \tag{17.53}$$

and

$$\{d\} = \frac{E}{(1+\nu)(1-2\nu)} \begin{bmatrix} 1-\nu & \nu & \nu & 0 \\ \nu & 1-\nu & \nu & 0 \\ \nu & \nu & 1-\nu & 0 \\ 0 & 0 & 0 & \dfrac{1-2\nu}{2} \end{bmatrix} \tag{17.54}$$

The element stiffness matrix for an axisymmetric solid element is given by (see Eq. 16.45)

$$[S^*] = 2\pi \int\int [B]^T [d][B] r\, dr\, dz \tag{17.55}$$

When the natural coordinates ξ and ν are used, the elemental area $dr\,dz$ is replaced by $|J|d\xi d\eta$, where $|J|$ is the determinant of the Jacobian (Eq. 17.7 or 17.8). The limits for each of the two integrals become -1 to 1.

Any element S^*_{ij} of the stiffness matrix represents $2\pi r_i$ multiplied by the intensity of a uniform load distributed on a nodal line at node i when the displacement at j is 1. Thus, S^*_{ij} has the units of force per length.

If the element is subjected to a rise in temperature of T degrees and the expansion is restrained, the stress at any point is

$$\{\sigma_0\} = -E\alpha T[d]\,\{1,1,1,0\} \tag{17.56}$$

and the consistent vector of restraining forces is

$$\{F_b\} = 2\pi \int\int [B]^T \{\sigma_0\} r \, dr \, dz \tag{17.57}$$

17.12 Finite strip and finite prism

Figure 17.17 shows a top view of a simply-supported bridge with three types of cross section. Analysis of stress and strain can be performed by treating the structure as an assemblage of finite strips or finite prisms as shown.[10] Similar to the elements used in the analysis of solids of revolution (Section 17.11), the finite strips and finite prisms have nodal lines rather than node points.

Over a nodal line, any displacement component is expressed as a sum of a series $\Sigma_{k=1}^{n} a_k Y_k$, where the values a are unknown amplitudes. The terms Y are functions of y which satisfy *a priori* the displacement conditions at the extremities of the strip.

An example of Y functions suitable for the determination of the deflection of a simply-supported strip is

$$Y_k = \sin \frac{\mu_k y}{l} \quad \text{with } \mu_k = k\pi \tag{17.58}$$

Over the width of the strip, or over the cross-sectional area of the prism, the displacement components are assumed to vary as polynomials of x or of x and z. The same polynomials as

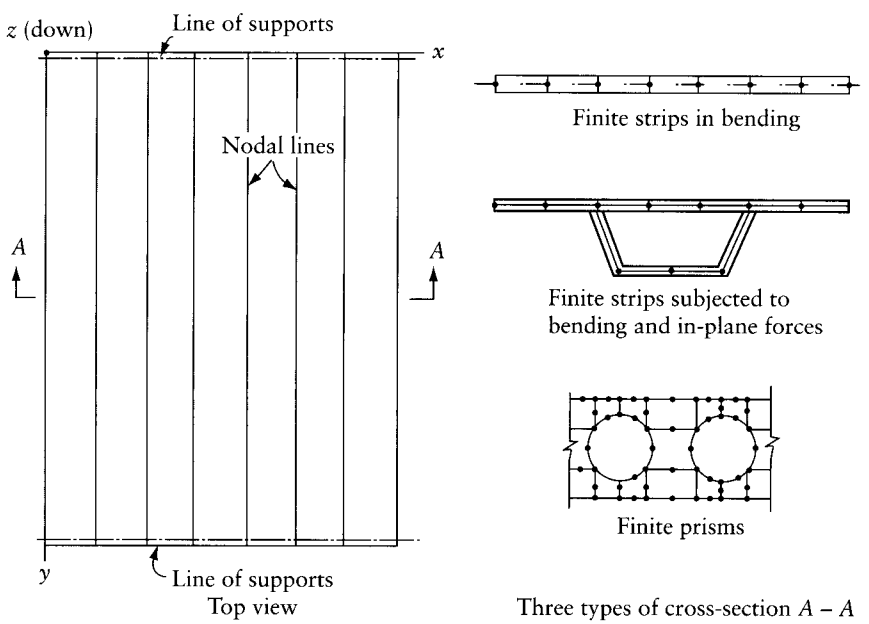

Figure 17.17 Example of the use of finite strips and finite prisms for the analysis of a simply-supported bridge with three types of cross section: slab, box, and voided slab.

10 The theory and applications of finite strips and finite prisms are discussed in more detail in Cheung, Y. K., *Finite Strip Method in Structural Analysis,* Pergamon Press, Oxford, New York, Toronto, 1976.

used for one-dimensional or two-dimensional elements are generally used for the strip and the prism respectively.

In general, the displacement components in a finite strip or a finite prism are expressed as

$$\{f\} = \sum_{k=1}^{n} [L]_k \{D^*\}_k \tag{17.59}$$

where $\{D^*\}_k$ is a vector of nodal parameters (displacement amplitudes, i.e. the a values), and $[L]_k$ is a matrix of shape functions pertaining to the kth term of the series. The nodal displacement parameters for a strip or a prism are

$$\{D^*\} = \{\{D^*\}_1, \{D^*\}_2, \ldots, \{D^*\}_n\} \tag{17.60}$$

For the finite strip in Figure 17.18a, usable for the analysis of plates in bending, the displacement field $\{f\} \equiv \{w\}$ represents deflection, and the nodal parameters are defined as

$$\{D^*\}_k = \{w_1, \theta_1, w_2, \theta_2\}_k \tag{17.61}$$

where the subscripts 1 and 2 refer to nodal lines along the sides of the strip; $\theta = \theta_y = -\partial w/\partial x$. The strip has $4n$ degrees of freedom.

The shape functions for a finite strip in bending are (Figure 17.18a)

$$[L]_k = [1 - 3\xi^2 + 2\xi^3, -b\xi(\xi - 1)^2, \xi^2(3 - 2\xi), -b\xi^2(\xi - 1)]Y_k \tag{17.62}$$

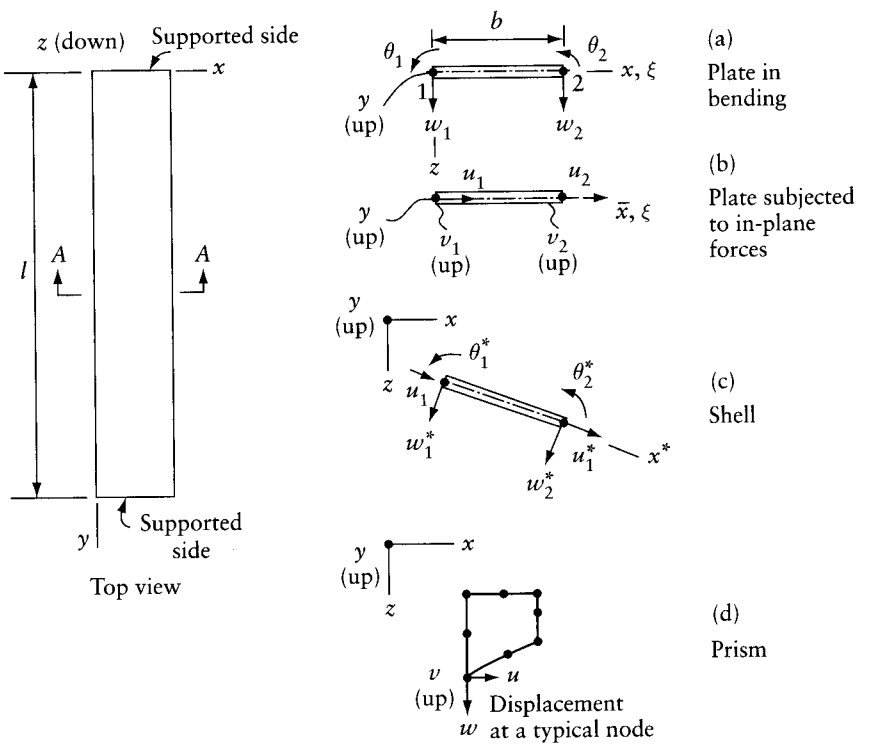

Figure 17.18 Top view and cross section *A–A* showing nodal displacement parameters for (a) finite strip in bending. (b) finite strip subjected to in-plane forces. (c) finite strip subjected to bending combined with in-plane forces (a shell). (d) finite prism.

We recognize that the functions in the 1×4 matrix are the same as the shape functions for a bar in bending (Figure 16.4); here, b is the width of the strip and $\xi = x/b$.

A finite strip suitable for the analysis of plates subjected to in-plane forces is shown in Figure 17.18b. The displacement components at any point are $\{f\} \equiv \{u, v\}$ and the nodal displacement parameters are

$$\{D^*\}_k = \{u_1, v_1, u_2, v_2\} \tag{17.63}$$

The same Y functions which are used for plates in bending are suitable to describe the variation of u in the y direction. However, for the variation of v it is suitable to use the derivative $Y' = dY/dy$. This choice can represent the behavior of a beam in bending with the same cross section as the strip and subjected to forces in the x direction.

The u displacement represents the deflection in the direction of the applied load. If the beam is simply supported, the sinusoidal Y function (Eq. 17.58) can be used to represent the variation of u in the y direction. However, the displacement in the v direction (caused by the shortening or elongation of the fibers due to bending) is equal to Y' multiplied by the distance from the neutral axis of the beam.

In general, to describe the variation of the displacement components in the y direction, we use the Y_k functions for u and w, and $Y_k' l/\mu_k$ for v. Thus, when Y is a sine series (Eq. 17.58), the variation of v is described by a cosine series.

The shape functions for a finite strip subjected to in-plane forces (Figure 17.18b) are

$$[L]_k = \begin{bmatrix} (1-\xi)Y_k & 0 & \xi & 0 \\ 0 & (1-\xi)\dfrac{1}{\mu_k}Y_k' & 0 & \xi\dfrac{1}{\mu_k}Y_k' \end{bmatrix} \tag{17.64}$$

For the variation of each of u and w over the width of the strip, we use linear functions (Figure 17.3).

When a strip is subjected to bending combined with in-plane forces, the nodal displacement parameters will be those defined by Eqs. 17.61 and 17.63 combined. We should note that the two sets of displacements are uncoupled. Thus, the stiffness matrix of a finite strip, suitable for the analysis of shells, folded plates, or box girders, is obtained by combining the stiffness matrices of a bending strip and a plane-stress strip as shown in Eq. 17.49.

The finite strip for shell analysis is shown in Figure 17.18c in a general inclined position. The nodal displacement parameters are indicated in local directions. The stiffness matrix has to be derived with respect to these local directions and then transformed to correspond to the global directions before the assemblage of strip matrices can be performed (see Sections 21.8 and 21.9).

The nodal displacement parameters for the finite prism in Figure 17.18d are

$$\{D^*\}_k = \{u_1, v_1, w_1, u_2, v_2, w_2, \ldots, u_8, v_8, w_8\}_k \tag{17.65}$$

The shape functions for the finite prism can be expressed by the shape functions for the plane-stress element shown in Figure 17.5 multiplied by Y_k or by $(l/\mu_k)Y_{ik}'$.

17.12.1 Stiffness matrix

The strains at any point in a finite strip or a finite prism are given by Eq. 16.6:

$$\{\epsilon\} = [\partial]\{f\} \tag{17.66}$$

The differential operator $[\partial]$ is given by Eqs. 16.19, 16.11, and 16.24 for the elements in Figures 17.18a, b, and d respectively.

Substitution of Eq. 17.59 into Eq. 17.66 gives

$$\{\epsilon\} = [B]\{D^*\} = \sum_{k=1}^{n} [B]_k \{D^*\}_k \tag{17.67}$$

The $[B]$ matrix is thus partitioned into n submatrices, given by

$$\{B\}_k = [\partial][L]_k \tag{17.68}$$

The stiffness matrix of a finite strip or a finite prism can be generated by Eq. 16.45, which is repeated here:

$$[S^*] = \int_v [B]^T [d][B]\, dv \tag{17.69}$$

The number of rows or columns in $[S^*]$ is $n_1 n_2 n$, where n_1 is the number of nodal lines in the finite strip or prism, n_2 is the number of degrees of freedom per node, and n is the number of terms in the Y series.

The matrix $[S^*]$ can be partitioned into $n \times n$ submatrices, of which a typical submatrix is

$$[S^*]_{kr} = \int_v [B]_k^T [d][B]_r\, dv \tag{17.70}$$

Generation of the stiffness submatrix $[S^*]_{kr}$ by Eq. 17.70 involves integration over the length of nodal lines of the products $Y_k Y_r$, $Y''_k Y''_r Y'_k Y'_r$ and $Y_k Y''_r$. For $k \neq r$, the integrals for the first two products are zero when Y is given by any of Eqs. 17.58 or 17.79 to 17.81. However, the integrals of the remaining two products are also zero only when Y is a sine series (Eq. 17.58). Because of these properties, with $k \neq r$, Eq. 17.70 gives submatrices $[S^*]_{kr}$ equal to zero only when Y is a sine series. In this case, the stiffness matrix of the finite strip or finite prism takes the form

$$[S^*] = \begin{bmatrix} [S^*]_{11} & & \text{submatrices} & \text{not} \\ & [S^*]_{22} & \text{shown are} & \text{null} \\ & & \cdots & \\ & & & [S^*]_{nn} \end{bmatrix} \tag{17.71}$$

The stiffness matrices of individual strips or prisms have to be assembled to obtain the stiffness matrix of the structure (see Section 21.9).

The stiffness matrix of the assembled structure will also have the form of Eq. 17.71 when Y is a sine series. Thus, the equilibrium equations $[S]\{D\} = -\{F\}$ will uncouple, which means that, instead of a large set of simultaneous equations having to be solved, n subsets (of much smaller band width) are solved separately. Each subset is of the form $[S]_k\{D\}_k = -\{F\}_k$ and its solution gives the nodal displacement parameters for the kth term of the Y series. This results in a substantial reduction in computing.

The variation of a displacement component over a nodal line is given by

$$D_i = \sum_{k=1}^{n} D_{ik} Y_k \tag{17.72}$$

where $D_{i1}, D_{i2}, \ldots, D_{in}$ are the nodal parameters for D_i obtained by the solution of the equilibrium equations.

17.12.2 Consistent load vector

When a strip or a prism is subjected to body forces $\{p\}$ per unit volume, the consistent vector of restraining forces is given by Eq. 16.47, which is repeated here:

$$\{F_b^*\} = -\int_v [L]^T \{p\}\, dv \tag{17.73}$$

The vector $\{F_b^*\}$ can be partitioned into n subvectors, given by

$$\{F_b^*\}_k = -\int_v [L]_K^T \{p\}\, dv \tag{17.74}$$

Similarly, the consistent vector of forces to restrain a temperature expansion is given by Eq. 16.50. The vector can be partitioned into subvectors, given by

$$\{F_b^*\}_k = -\int_v [B]_K^T [d]\{\epsilon_0\}\, dv \tag{17.75}$$

where $\{\epsilon_0\}$ represents the strains if the expansion were free to occur.

Element matrices for a finite strip for the analysis of plates in bending (Figure 17.18a) are given explicitly in Section 17.12.4.

We shall now consider the case when an external load of intensity q per unit length is applied on a nodal line in the direction of one of the nodal coordinates. The displacement due to this loading can be restrained by a consistent force equal to the sum of n terms of the form

$$F_{ak}^* = -\int_0^1 qY_k dy \tag{17.76}$$

When a concentrated force P is applied on the nodal line, the integral in Eq. 17.74 is replaced by the product $PY_k(y_p)$, where $Y_k(y_p)$ is the value of Y_k at y_p defining the location of P:

$$F_{ak}^* = -PY_k(y_p) \tag{17.77}$$

The vector of restraining forces to prevent the nodal displacements is (Eq. 21.32)

$$\{F\} = \{F_a\} + \{F_b\} \tag{17.78}$$

where $\{F_a\}$ accounts for external forces applied on the nodal lines, calculated by Eqs. 17.76 and 17.77 and transformed to global directions. The vector $\{F_b\}$ accounts for body forces. Consistent force vectors for individual strips or prisms are calculated by Eqs. 17.73 to 17.75, transformed to global directions and assembled into one vector by Eq. 21.34.

17.12.3 Displacement variation over a nodal line

The variation of all displacement components in the y direction is described by the y functions which satisfy the boundary conditions at $y=0$ and $y=l$. Functions of the shape of free vibration modes of prismatic beams are suitable.[11]

11 Derivations of the Y functions used here are given in Vlasov, V. Z., *General Theory of Shells and its Applications in Engineering;* Translated from Russian by NASA; distributed by Office of Technical Services, Department of Commerce, Washington, DC, 1949, pp. 699–707. This reference gives Y functions suitable for other boundary conditions not included above.

For simply-supported finite strips of prisms, Y and Y'' are zero at $y=0$ and $y=l$; these conditions are satisfied when Y is a sine series (Eq. 17.58). When one end is simply supported and the other end is built in, Y and Y'' are zero at $y=0$ while Y and Y'' are zero at $y=l$. These conditions are satisfied by

$$Y_k = \sin\frac{\mu_k y}{l} - \alpha_k \sinh\frac{\mu_k y}{l} \tag{17.79}$$

where

$$\mu_k = 3.927, 7.068, \ldots, \frac{4k+1}{4}\pi \qquad \alpha_k = \frac{\sin\mu_k}{\sinh\mu_k}$$

When both ends of a finite strip or prism are built in, Y and Y' are zero there, so that

$$Y_k = \sin\frac{\mu_k y}{l} - \sinh\frac{\mu_k y}{l} + \alpha_k\left(\cosh\frac{\mu_k y}{l} - \cos\frac{\mu_k y}{l}\right) \tag{17.80}$$

where

$$\mu_k = 4.730, 7.853, \ldots, \frac{2k+1}{2}\pi \qquad \alpha_k = \frac{\sinh\mu_k - \sin\mu_k}{\cosh\mu_k - \cos\mu_k}$$

When the end $y=0$ is built in and the other end is free, Y and Y' are zero at $y=0$ while Y'' and Y''' are zero at $y=l$. These conditions are satisfied by

$$Y_k = \sin\frac{\mu_k y}{l} + \sinh\frac{\mu_k y}{l} + \alpha_k\left(\cosh\frac{\mu_k y}{l} - \cos\frac{\mu_k y}{l}\right) \tag{17.81}$$

where

$$\mu_k = 1.875, 4.694, \ldots, \frac{2k-1}{2}\pi \qquad \alpha_k = \frac{\sinh\mu_k + \sin\mu_k}{\cosh\mu_k + \cos\mu_k}$$

17.12.4 Plate-bending finite strip

The strains at any point in the finite strip shown in Figure 17.18a are given by Eq. 17.67, in which the matrix $[B]_k$ is (Eqs. 17.68, 16.19, and 17.62)

$$[B]_k = \begin{bmatrix} \frac{1}{b^2}(6-12\xi)Y_k & \frac{1}{b}(-4+6\xi)Y_k & \frac{1}{b^2}(12\xi-6)Y_k & \frac{1}{b}(-2+6\xi)Y_k \\ -(1-3\xi^2+2\xi^3)Y_k'' & b\xi(\xi-1)^2Y_k'' & -\xi^2(3-2\xi)Y_k'' & 6\xi^2(\xi-1)Y_k'' \\ \frac{2}{b}(-6\xi+6\xi^2)Y_k' & 2(-3\xi^2+4\xi-1)Y_k' & \frac{1}{b}(6\xi-6\xi^2)Y_k' & 2(-3\xi^2+2\xi)Y_k' \end{bmatrix} \tag{17.82}$$

For a simply-supported strip, $Y_k = \sin(k\pi y/l)$, and the stiffness matrix submatrices $[S^*]_{kr}$ are nonzero only when $k=r$.

Equation 17.70 can be rewritten in the form

$$[S^*]_{kk} = b\int_0^1\int_0^1 [B]_k^T[d][B]_k\,d\xi\,dy \tag{17.83}$$

The elasticity matrix $[d]$ for a plate in bending is given by Eq. 16.20 or Eq. 16.21. For a strip of constant thickness, the integrals involved in Eq. 17.83 can be expressed explicitly, noting that

$$\int_0^1 Y_k^2 dy = \frac{1}{2}; \int_0^1 Y_k Y_k'' dy = \frac{k^2\pi^2}{2l}$$
$$\int_0^1 (Y_k'')^2 dy = \frac{k^4\pi^4}{2l^3}; \int_0^1 (Y_k')^2 dy = \frac{k^2\pi^2}{2l} \tag{17.84}$$

Thus, the submatrix $[S^*]_{kk}$ of a simply-supported finite strip is (Figure 17.18a)

$$[S^*]_{kk} = b \begin{bmatrix} \frac{6l}{b^4}d_{11} + \frac{13k^4\pi^4}{70l^3}d_{22} + \frac{6k^2\pi^2}{5b^2l}d_{21} + \frac{12k^2\pi^2}{5b^2l}d_{33} & & & \\ -\frac{3l}{b^3}d_{11} - \frac{11bk^4\pi^4}{420l^3}d_{22} - \frac{3k^2\pi^2}{5bl}d_{21} - \frac{k^2\pi^2}{5bl}d_{33} & \frac{2l}{b^2}d_{11} + \frac{b^2k^4\pi^4}{210l^3}d_{22} + \frac{2k^2\pi^2}{15l}d_{21} + \frac{4k^2\pi^2}{15l}d_{33} & \text{symmetrical} & \\ -\frac{6l}{b^4}d_{11} + \frac{9k^4\pi^4}{140l^3}d_{22} - \frac{6k^2\pi^2}{5b^2l}d_{21} - \frac{12k^2\pi^2}{5b^2l}d_{33} & \frac{3l}{b^3}d_{11} - \frac{13bk^4\pi^4}{840l^3}d_{22} + \frac{k^2\pi^2}{10bl}d_{21} + \frac{k^2\pi^2}{5bl}d_{33} & \frac{6l}{b^4}d_{11} + \frac{13k^4\pi^4}{70l^3}d_{22} + \frac{6k^2\pi^2}{5b^2l}d_{21} + \frac{12k^2\pi^2}{5b^2l}d_{33} & \\ -\frac{3l}{b^3}d_{11} + \frac{13bk^4\pi^4}{840l^3}d_{22} - \frac{k^2\pi^2}{10bl}d_{21} - \frac{k^2\pi^2}{5bl}d_{33} & \frac{1}{b^2}d_{11} - \frac{b^2k^4\pi^4}{280l^3}d_{22} - \frac{k^2\pi^2}{30l}d_{21} - \frac{k^2\pi^2}{15l}d_{33} & \frac{3l}{b^3}d_{11} + \frac{11bk^4\pi^4}{420l^3}d_{22} + \frac{3k^2\pi^2}{5bl}d_{21} + \frac{k^2\pi^2}{5bl}d_{33} & \frac{2l}{b^2}d_{11} + \frac{b^2k^4\pi^4}{210l^3}d_{22} + \frac{2k^2\pi^2}{15l}d_{21} + \frac{4k^2\pi^2}{15l}d_{33} \end{bmatrix} \tag{17.85}$$

where d_{ij} represents elements of the elasticity matrix (Eq. 16.20 or Eq. 16.21).

When a strip is subjected to a load in the z direction, distributed over a rectangle (Figure 17.19), the consistent subvector of restraining forces is (see Eq. 17.74)

$$\{F_b^*\}_k = -b \int_{y_1}^{y_2} \int_{\xi_1}^{\xi_2} q_z [L]_k^T d\xi dy \tag{17.86}$$

where q_z is the load intensity.

When a concentrated load P is applied at (x_p, y_p) (Figure 17.19), Eq. 17.86 becomes

$$\{F_b^*\}_k = -p[L(\xi_p, y_p)]_k^T \quad \text{with } \xi_p = x_p/b \tag{17.87}$$

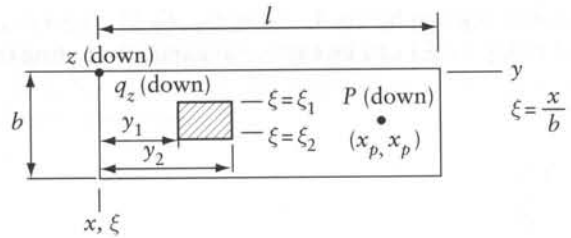

Figure 17.19 Finite strip loads considered in Eqs. 17.86 and 17.87.

When the load q_z is constant over the whole area of the strip, Eq. 17.86 becomes

$$\{F_b^*\}_k = -q_z \left\{ \frac{b}{2}, \quad -\frac{b^2}{12}, \quad \frac{b}{2}, \quad \frac{b^2}{12} \right\} \int_0^1 Y_k dy \tag{17.88}$$

When a sine series is used for Y_k (Eq. 17.58), the integral in Eq. 17.88 is replaced by $2l/k\pi$ or by zero when k is odd or even respectively.

When a plate in bending is stiffened by a beam running along a nodal line, compatibility of displacement will be ensured by assuming that the deflection w and the angle of twist θ vary over the beam length according to the same Y function as used for the finite strips. To account for the contribution of the beam to the stiffness of the system, we can derive flexural and torsional stiffness for the beam (see answers to Prob. 17.5) and add them to the diagonal coefficients, corresponding to w and θ, in the stiffness matrix of the finite strips assemblage.

Example 17.5: Simply-supported rectangular plate

For a horizontal rectangular plate with sides of length l and c, determine the deflection at the center due to: (a) a downward line load of p per unit length along the axis of symmetry parallel to the dimension l, and (b) a uniform downward load of q per unit area. The plate is simply supported at its four sides, has a constant thickness h, and is of isotropic material with a modulus of elasticity E and Poisson's ratio $\nu = 0.3$. The aspect ratio is $l/c = 2$.

Divide the slab into two strips parallel to the l dimension. Because of symmetry, only one strip needs to be considered; this strip can be represented by Figure 17.18a, with nodal lines 1 and 2 running along the supported edge and the slab center line respectively. The width of the strip is $b = c/2 = l/4$. The displacement parameters w_1 and θ_2 are zero. This leaves only two unknowns:

$$\{D\} = \{\theta_1, w_2\}$$

In case (a), only one-half of the line load intensity $(p/2)$ is applied to the half-slab considered.

For an isotropic slab with thickness h, the elements of the elasticity matrix are (Eq. 16.21).

$$d_{11} = d_{22} = \frac{Eh^3}{12(1-\nu^2)} = 91.58 \times 10^{-3} Eh^3$$
$$d_{21} = \nu d_{11} = 27.47 \times 10^{-3} Eh^3$$
$$d_{33} = \frac{Eh^3}{24(1+\nu)} = 32.05 \times 10^{-3} Eh^3$$

The submatrix $[S]_{kk}$ for the half-slab is given by Eq. 17.85 after deletion of the first and the fourth rows and columns:

$$[S]_{kk}=10^{-3}Eh^3\begin{bmatrix} 732.6+0.6637k^4+30.13k^2 & \text{symmetrical} \\ \frac{1}{c}(2198-4.314k^4+45.19k^2) & \frac{1}{c^2}(8791+103.5k^4+1085k^2) \end{bmatrix}$$

The consistent subvectors of restraining forces for the two loading cases are null for values of k which are even numbers. For $k=1,3,\ldots$, the subvectors are (Eqs. 17.76 and 17.88)

$$[F]_k=-\begin{bmatrix} 0 & -\frac{b^2}{12}\left(\frac{2l}{k\pi}\right) \\ \frac{p}{2}\frac{2l}{k\pi} & q\frac{b}{2}\left(\frac{2l}{k\pi}\right) \end{bmatrix}=\begin{bmatrix} 0 & q\frac{c^3}{12k\pi} \\ -\frac{2pc}{k\pi} & -\frac{qc^2}{k\pi} \end{bmatrix}$$

The equilibrium equations are

$$[S]_k\{D\}_k=-\{F\}_k$$

Substitution and solution with $k=1$ and $k=3$ gives the nodal displacement parameters in the two cases of loading:

$$[D]_1=\frac{c^2}{Eh^2}\begin{bmatrix} -0.5470p & -0.3751qc \\ 0.1865pc & 0.1161qc^2 \end{bmatrix}$$

$$[D]_3=\frac{c^2}{Eh^3}\begin{bmatrix} -0.0205p & -0.0205qc \\ 0.0096pc & 0.0057qc^2 \end{bmatrix}$$

It can be seen that the contribution of the third term ($k=3$) is much smaller than the contribution of the first term. Using $k=1$ and $k=3$, the deflection at the center of the slab ($\xi=1$; $y=l/2$) is as follows (Eq. 17.59):

Case (a):

$$w_{\text{center}}=\frac{pc^3}{Eh^3}\left(0.1865\sin\frac{\pi}{2}+0.0096\sin\frac{3\pi}{2}\right)=0.1769\frac{pc^3}{Eh^3}$$

Case (b):

$$w_{\text{center}}=\frac{qc^4}{Eh^3}\left(0.1161\sin\frac{\pi}{2}+0.0057\sin\frac{3\pi}{2}\right)=0.1104\frac{qc^4}{Eh^3}$$

The "exact" answers[12] to the same problem are $0.1779pc^3/Eh^3$ and $0.1106qc^4/Eh^3$ respectively.

While high accuracy in the calculation of deflection is achieved with only two strips and two nonzero terms, for the same accuracy in the calculation of moments a larger number of strips and of terms may be necessary, particularly with concentrated loads.

Finally, the displacement parameters can be used to calculate the strains (curvatures) and the stresses (moments) at any point by Eqs. 17.82, 16.15, and 16.40.

12 See Timoshenko, S. and Wojnowsky-Krieger, S., *Theory of Plates and Shells*, 2nd ed., McGraw-Hill, New York, 1959.

17.13 Hybrid finite elements

In displacement-based finite elements, the displacement components are assumed to vary as (Eq. 16.25)

$$\{f\} = [L]\{D^*\} \tag{17.89}$$

where $\{D^*\}$ are nodal displacements and $[L]$ are displacement shape functions. The strain and the stress components are determined from the displacements by Eqs. 16.37 to 16.40.

Two techniques of formulating hybrid finite elements will be discussed: *hybrid stress* and *hybrid strain* formulations.[13] In the first of these, the displacements are assumed to vary according to Eq. 17.89 and the stresses according to an assumed polynomial

$$\{\sigma\} = [P]\{\beta\} \tag{17.90}$$

In the second technique, in addition to the displacement field (Eq. 17.89), a strain field is assumed:

$$\{\epsilon\} = [P]\{\alpha\} \tag{17.91}$$

In the last two equations, $[P]$ represents assumed polynomials; $\{\beta\}$ and $\{\alpha\}$ are unknown multipliers referred to as the stress parameter and the strain parameter respectively.

In the hybrid stress or hybrid strain formulation, a finite element has two sets of unknown parameters, $\{D^*\}$ with $\{\beta\}$ or $\{D^*\}$ with $\{\alpha\}$. However, the parameters $\{\beta\}$ or $\{\alpha\}$ are eliminated, by condensation, before assemblage of the element matrices in order to obtain the stiffness matrix of the structure. The equilibrium equations $[S]\{D\} = -\{F\}$ are generated and solved by the general techniques discussed in Sections 21.9 to 21.11.

In the formulation of displacement-based elements and hybrid elements, the forces applied on the body of the element are represented by a vector of consistent restraining nodal forces (Eq. 16.47):

$$\{F_b^*\} = -\int_v [L]^T\{p\}\, dv \tag{17.92}$$

where $\{p\}$ are body forces per unit volume.

17.13.1 Stress and strain fields

We give here, as an example, the polynomials $[P]$ selected successfully[14] to describe the stress field by Eq. 17.90 in a plane-stress or plane-strain hybrid stress element, with corner nodes and two degrees of freedom per node (Figure 17.20):

$$[P] = \begin{bmatrix} 1 & y & 0 & 0 & 0 \\ 0 & 0 & 1 & x & 0 \\ 0 & 0 & 0 & 0 & 1 \end{bmatrix} \tag{17.93}$$

The stress vector in this example is $\{\sigma\} = \{\sigma_x, \sigma_y, \tau_{xy}\}$.

13 The material in this section is based on Ghali, A. and Chieslar, J., "Hybrid Finite Elements," *Journal of Structural Engineering*, 112 (11) (November 1986), American Society of Civil Engineers, pp. 2478–2493.

14 Pian, T. H. H. and Sumihara, K. "Rational Approach for Assumed Stress Finite Elements," *International Journal for Numerical Methods in Engineering*, 20 (1984), pp. 1685–1695.

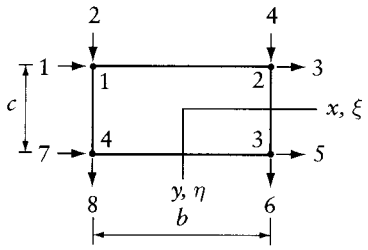

Figure 17.20 Hybrid finite element for plane-stress and plane-strain analysis.

For a general quadrilateral, x and y can be replaced by the natural coordinates ξ and η, and the use of the Jacobian matrix will be necessary in the derivation of element matrices (Section 17.2). The same matrix $[P]$ can be used for a hybrid strain element.

The number of stress or strain parameters, $\{\beta\}$ or $\{\alpha\}$, must be at least equal to the difference between the number of degrees of freedom of the element and the minimum number of degrees of freedom at which displacements have to be restrained in order to prevent rigid-body motion. The element shown in Figure 17.20 has eight degrees of freedom, and rigid-body motion will not occur if the displacements are prevented at three coordinates (e.g. two in the x direction and one in the y direction). Thus, for this element, the minimum number of parameters in $\{\beta\}$ or $\{\alpha\}$ is five.

17.13.2 Hybrid stress formulation

For this formulation we shall use the principle of virtual work (Eq. 6.36), which is rewritten here as

$$\{F^*\}^T\{D^*\} = \int \{\sigma\}^T\{\epsilon\}\, dv \tag{17.94}$$

We recall that two interpretations are possible for the symbols in this equation. In one, $\{F^*\}$ and $\{\sigma\}$ represent actual nodal forces and corresponding stresses, while $\{D^*\}$ and $\{\epsilon\}$ represent virtual nodal displacements and the corresponding strains. In the second interpretation, $\{D^*\}$ and $\{\epsilon\}$ are real while $\{F^*\}$ and $\{\sigma\}$ are virtual.

The two interpretations will be used in the formulation of hybrid elements. Equations 17.90 and 17.91 will be considered to represent real stresses and strains, but the virtual strains are chosen as the derivatives of the displacement shape functions (Eq. 16.39):

$$[B] = [\partial][L] = [\{B\}_1\{B\}_2 \ldots \{B\}_n] \tag{17.95}$$

where $[\partial]$ is a matrix of differential operators (see, for example, the 3×2 matrix in Eq. 16.11), and n is the number of nodal displacements. Each column of $[B]$ may be used to represent a virtual strain field.

We apply the principle of virtual work (Eq. 17.94) to a finite element subjected to nodal forces $\{F^*\}$ producing stresses $\{\sigma\} = [P]\{\beta\}$. The virtual displacement field is assumed to correspond to $D_1^* = 1$, while the other nodal displacements are zero. The corresponding virtual strains are

$$\{\epsilon\}_1 = \{B\}_1 = [\partial]\{L\}_1 \tag{17.96}$$

For this application, Eq. 17.94 gives

$$\{F^*\}^T \begin{Bmatrix} 1 \\ 0 \\ \ldots \end{Bmatrix} = \int_v \{\sigma\}^T\{\epsilon\}_1\, dv \tag{17.97}$$

Substitution of Eq. 17.90 produces

$$\{F^*\}^T \begin{Bmatrix} 1 \\ 0 \\ \dots \end{Bmatrix} = \int_v ([P]\{\beta\})^T \{B\}_1 \, dv \tag{17.98}$$

By repeated application of Eq. 17.94, using pairs of virtual vectors $\{0, 1, 0, \dots\}$ and $\{B\}_2$, and so on, and combining the resulting equations, we obtain

$$\{F^*\}^T [I] = \{\beta\}^T \int_v [P]^T [B] \, dv \tag{17.99}$$

We can rewrite Eq. 17.99 as

$$\{F^*\} = [G]^T \{\beta\} \tag{17.100}$$

where

$$[G] = \int_v [P]^T [B] \, dv \tag{17.101}$$

The elements in any row i of $[G]$ are forces at the nodes when the stresses are represented by the ith column of $[P]$. The elements in any row of $[G]$ form a set of self-equilibrating forces (see Example 17.6).

The procedure to generate $[G]$, used above, is tantamount to a repeated application of the unit-displacement theorem (Eq. 6.40) in order to determine nodal forces corresponding to given stress fields $\{\sigma\} = [P]\{\beta\}$.

The strains in the element considered above can be determined from the stresses by

$$\{\epsilon\} = [e]\{\sigma\} = [e][P]\{\beta\} \tag{17.102}$$

where

$$[e] = [d]^{-1}$$

Here, $[d]$ is the material elasticity matrix (Eqs. 6.11, 16.12, 16.13, 16.20, and 16.21); $[e]$ is given in Eq. 6.9 for an isotropic three-dimensional solid.

Let us now apply again the principle of virtual work (Eq. 17.94) but this time with $\{D^*\}$ and $\{[e][P]\{\beta\}\}$ representing real displacements and strains, and $[G]^T$ and $[P]$ representing virtual forces and stresses:

$$[G][D^*] = \int_v [P]^T [e][P]\{\beta\} \, dv \tag{17.103}$$

or

$$[G]\{D^*\} = [H]\{\beta\} \tag{17.104}$$

where

$$[H] = \int [P]^T [e][P] \, dv \tag{17.105}$$

The matrix $[H]$ is a symmetrical matrix which we refer to as the *quasi-flexibility* matrix. The explanation of this term is as follows. For a regular flexibility matrix, we should integrate the product of stress and strain produced by unit forces at the nodes. For the quasi-flexibility matrix, we also integrate the product of stress and strain, but these correspond to nodal forces $[G]$. We can obtain the stiffness matrix of the hybrid stress element by inverting $[H]$ and pre- and post-multiplying by $[G]^T$ and $[G]$ respectively:

$$[S^*]_{\text{hybrid stress}} = [G]^T[H]^{-1}[G] \tag{17.106}$$

This equation can be derived from Eq. 17.100 by elimination of $\{\beta\}$ using Eq. 17.104:

$$[G]^T[H]^{-1}[G]\{D^*\} = \{F^*\} \tag{17.107}$$

or

$$[S^*]\{D^*\} = \{F^*\} \tag{17.108}$$

A comparison of the last two equations gives Eq. 17.106.

When the nodal displacements have been determined (by the solution of the equilibrium equations for the structure) the stress parameters for individual hybrid stress elements can be determined by Eq. 17.104:

$$\{\beta\} = [H]^{-1}[G]\{D^*\} \tag{17.109}$$

The stresses due to unit nodal displacements in the hybrid stress element are

$$[\sigma_u]_{\text{hybird stress}} = [\text{P}][\text{H}]^{-1}[\text{G}] \tag{17.110}$$

Here, $[\sigma_u]$ is referred to as the *stress matrix*. The product $[P][H]^{-1}[G]$ is the equivalent of the product $[d][B]$ in displacement-based finite elements (Eqs. 16.41 and 16.42).

Example 17.6: Rectangular element in plane-stress state

Generate the matrices $[G]$ and $[H]$ for a hybrid stress rectangular element for plane-stress analysis (Figure 17.20). The element has a constant thickness h, modulus of elasticity E, and Poisson's ratio ν. Use the polynomial matrix of Eq. 17.93 and the shape functions given by Eqs. 16.31 and 16.32.

$$[B] = \begin{bmatrix} \partial/\partial x & 0 \\ 0 & \partial/\partial y \\ \partial/\partial y & \partial/\partial x \end{bmatrix} [L]$$

$$= \frac{1}{4}\begin{bmatrix} -\frac{2}{b}(1-\eta) & 0 & \frac{2}{b}(1-\eta) & 0 & \frac{2}{b}(1+\eta) & 0 & \frac{2}{b}(1+\eta) & 0 \\ 0 & -\frac{2}{c}(1-\xi) & 0 & -\frac{2}{c}(1+\xi) & 0 & \frac{2}{c}(1+\xi) & 0 & \frac{2}{c}(1-\xi) \\ -\frac{2}{c}(1-\xi) & -\frac{2}{b}(1-\eta) & -\frac{2}{c}(1+\xi) & \frac{2}{b}(1-\eta) & \frac{2}{c}(1+\xi) & \frac{2}{b}(1+\eta) & \frac{2}{c}(1-\xi) & -\frac{2}{b}(1+\eta) \end{bmatrix}$$

Substitution in Eq. 17.101 gives

$$[G]=\int_v [P]^T[B]\,dv = h\frac{bc}{4}\int_{-1}^{1}[P]^T[B]d\xi\,d\eta$$

$$=hbc\begin{bmatrix} -1/(2b) & 0 & 1/(2b) & 0 & 1/(2b) & 0 & -1/(2b) & 0 \\ c/(12b) & 0 & -c/(12b) & 0 & c/(12b) & 0 & -c/(12b) & 0 \\ 0 & -1/(2c) & 0 & -1/(2c) & 0 & 1/(2c) & 0 & 1/(2c) \\ 0 & b/(12c) & 0 & -b/(12c) & 0 & b/(12c) & 0 & -b/(12c) \\ -1/(2c) & -1/(2b) & -1/(2c) & -1/(2b) & 1/(2c) & 1/(2b) & 1/(2c) & -1/(2b) \end{bmatrix}$$

The inverse of the elasticity matrix for the plane-stress state is (Eq. 16.12)

$$[e]=[d]^{-1}=\frac{1}{E}\begin{bmatrix} 1 & -\nu & 0 \\ -\nu & 0 & 0 \\ 0 & 0 & 2(1+\nu) \end{bmatrix}$$

Substitution of this matrix and of Eq. 17.93 in Eq. 17.105 gives

$$[H]=\frac{hbc}{E}\begin{bmatrix} 1 & & & & \text{symmetrical} \\ 0 & c^2/12 & & & \\ -\nu & 0 & 1 & & \\ 0 & 0 & 0 & b^2/12 & \\ 0 & 0 & 0 & 0 & 2(1+\nu) \end{bmatrix}$$

The accuracy of the results obtained by this element is compared with two displacement-based elements in Prob. 17.14.

17.13.3 Hybrid strain formulation

We shall now consider an element in which the strain field is assumed to be $\{\epsilon\}=[P]\{\alpha\}$ (Eq. 17.91) while the corresponding stress field is determined from

$$\{\sigma\}=[d]\{\epsilon\}=[d][P]\{\alpha\} \tag{17.111}$$

Application of the principle of virtual work (Eq. 17.94) in two different ways, as was done in Section 17.13.2, gives

$$\{F^*\}=[\overline{G}]\{\alpha\} \tag{17.112}$$

and

$$[\overline{G}]\{D^*\}=[\overline{H}]\{\alpha\} \tag{17.113}$$

where

$$[\overline{G}]=\int_v [P]^T[d][B]\,dv \tag{17.114}$$

and

$$[\overline{H}]=\int_v [P]^T[d][P]\,v \tag{17.115}$$

The elements in any row i of $[\overline{G}]$ are the nodal forces which produce the strain vector represented by the ith column of $[P]$. The symmetrical matrix $[\overline{H}]$ is referred to as the *quasi-stiffness* matrix.

The stiffness matrix of a hybrid strain element is

$$[S^*]_{\text{hybrid strain}} = [\overline{G}]^T[\overline{H}]^{-1}[\overline{G}] \tag{17.116}$$

The strain parameters are given by (Eq. 17.113)

$$\{\alpha\} = [\overline{H}]^{-1}[\overline{G}]\{D^*\} \tag{17.117}$$

The stress matrix for a hybrid strain element is

$$[\sigma_u]_{\text{hybrid strain}} = [d][P][\overline{H}]^{-1}[\overline{G}] \tag{17.118}$$

The product of the four matrices in this equation can be used to replace the product $[d][B]$ in displacement-based finite elements.

The assumption that the strain field is continuous over the element (rather than the stresses being continuous) is more representative of actual conditions in some applications. These include composite materials and materials with a nonlinear stress–strain relationship.

17.14 General

In this chapter and in Chapter 16 we have discussed the main concepts and techniques widely used in the analysis of structures by the finite-element method. This was possible because the finite-element method is an application of the displacement method, which is extensively discussed in earlier chapters and also in Chapters 21 and 22.

Selected books on the finite-element method are included in the References to this book. Some of these books contain extensive lists of references on the subject.

Problems

17.1 Generate $[S]$ for the isoparametric bar element of Prob. 17.3, assuming that the cross-sectional area equals $2a_0, a_0$, and $1.25a_0$ at nodes 1, 2, and 3 respectively. For interpolation between these values, use the displacement shape functions. Evaluate the integrals numerically with two sampling points. Would you expect a change in the answer if three or four sampling points were used?

17.2 The figure shows two load distributions on an element boundary. Determine the consistent vectors of restraining forces, assuming that the variation of displacement is: (a) linear between each two adjacent nodes, and (b) quadratic polynomial. Use Lagrange interpolation (Figure 17.3). The answers to (a) are included in Figure 10.9. Compare the answers to (b) when $q_1 = q_2 = q_3 = q$ with the consistent nodal forces due to a rise in temperature as given in Figure 17.7.

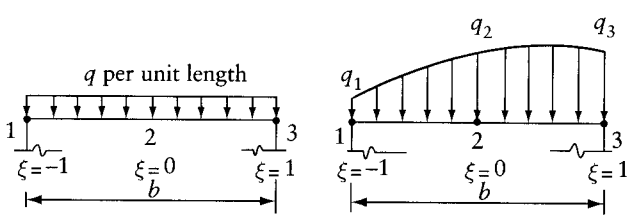

Prob. 17.2

17.3 Use the shape functions in Figure 17.5 to verify the consistent vectors of restraining nodal forces given in Figure 17.7.

17.4 Using Lagrange polynomials (Figure 17.3), construct shape functions L_1, L_2, L_{10}, and L_{11} for the element shown. Using these shape functions and considering symmetry and equilibrium, determine the consistent vector of nodal forces in the y direction when the element is subjected to a uniform load of q_y per unit volume.

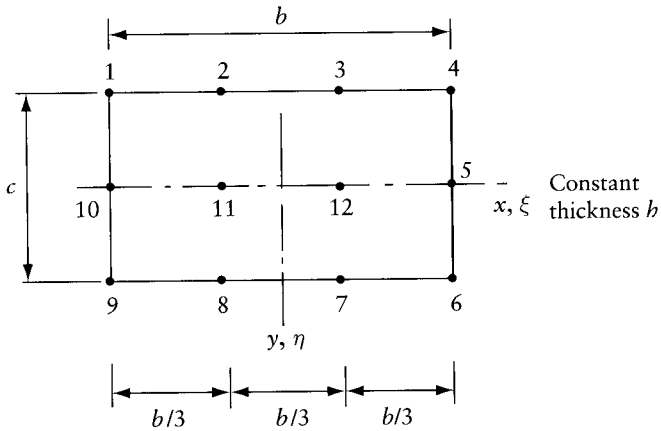

Prob. 17.4

17.5 Determine the strains at nodes 1, 2, and 3 in the linear-strain triangle (Figure 17.9) due to $D_1^* \equiv u_1 = 1$ and to $D_2^* \equiv v_1 = 1$.

17.6 Show that the shape functions of Eqs. 17.35 and 17.36 give linear strains in the element shown in Figure 17.9. The answers to Prob. 17.5 give the strains at the three corners of the triangle. By linear interpolation, using area coordinates, determine the strains at any point in the element. These give the first two columns of the $[B]$ matrix.

17.7 Use the answers to Prob. 17.6 to determine S_{11}^* and S_{12}^* of the linear-strain triangle (Figure 17.9).

17.8 Derive $[B]$ and $[S^*]$ for the triangular bending element with equal sides l shown. Assume a constant thickness h and an isotropic material with $\nu = 0.3$.

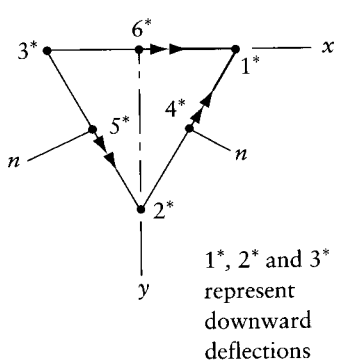

Prob. 17.8

17.9 The hexagonal horizontal plate shown is simply supported at the corners and carries a downward concentrated load P at the center. Calculate the deflection at this point and the moments at A by idealizing the plate as an assemblage of six triangular elements identical to the element of Prob. 17.8. Check the value of M_x by taking the moment of the forces situated to the left or to the right of the y axis.

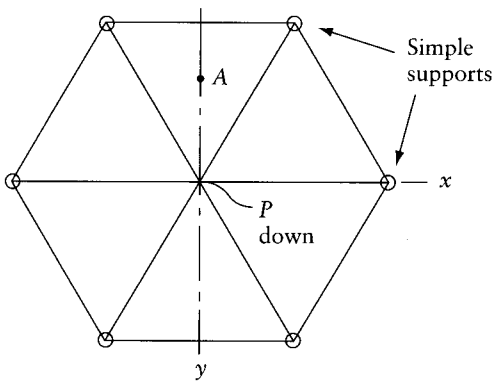

Prob. 17.9

17.10 If the plate in Prob. 17.9 is built-in along the edges, find the deflection at the center and the moments M_x, M_y, and M_{xy} at A caused by a change in temperature of $T/2$ and $-T/2$ degrees at the bottom and top surfaces respectively, with a linear variation over the thickness. Take the coefficient of thermal expansion as α.

17.11 Using one strip and one term of the series, calculate the deflection at A and also M_x at B in the plate shown. The plate is subjected to a uniform load of q per unit area. Assume a constant thickness h and Poisson's ratio $\nu = 0.2$.

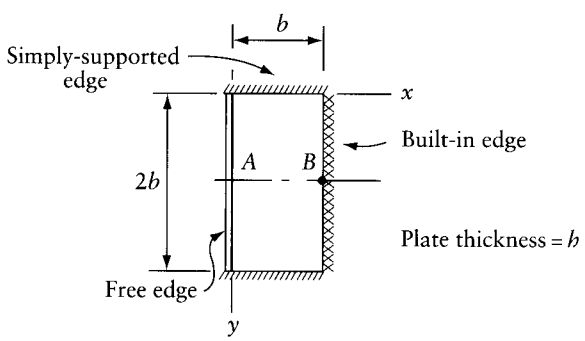

Prob. 17.11

17.12 Solve Prob. 17.11 for a uniform line load of p per unit length applied along the plate center line parallel to the x axis.

17.13 Find the deflection at the center of a square, simply-supported plate due to a uniform load of q per unit area. Assume a constant thickness h, a length of side l, and an isotropic material with $\nu = 0.3$. Divide the slab into two finite strips and use one term of the series.

17.14 Find the variation in the deflection of the plate in Example 17.5 along the center line parallel to the l dimension, due to a hydrostatic pressure $q_z = q_0 y/l$. Divide the plate into two strips of length l and width $c/2$, and use three terms of the series.

17.15 The figure shows a top view of a rectangular plate simply supported at two edges, with each of the other two edges stiffened by a beam. The centroid of the beam cross section is in the plane of middle surface of the plate; the cross-sectional area properties of the beam are $I = 3lh^3/100$ and $J = 4lh^3/100$. Poisson's ratio $\nu = 0$. The plate is subjected to a concentrated load P at the center.

(a) Derive the flexural and torsional stiffnesses for the beam which can be combined with the finite-strip stiffness. Use a sine series (Eq. 17.58) to describe the variation in the deflection of the beam, w, and in the angle of twist, θ.

(b) Find the deflection at the center of the slab and the bending moment in the edge beams at mid-span. Divide the plate into two strips and use one term of the series.

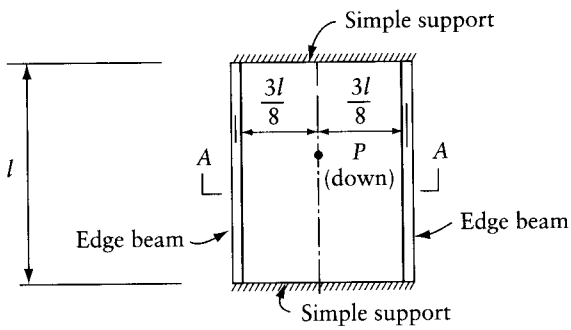

Prob. 17.15

17.16 Derive S^*_{11}, S^*_{21}, S^*_{31}, S^*_{41}, and S^*_{51} for the hybrid plane-stress element in Figure 17.20. Assume a constant thickness h and an isotropic material with $\nu = 0.2$.

17.17 Use the results of Prob. 17.16 and consider symmetry and equilibrium to generate $[S^*]$ for the hybrid rectangular element when $b = c$.

17.18 Use the stiffness matrices generated in Probs. 16.7, 16.15 and 17.17 to calculate the deflection at A, the stress σ_x at B, and τ_{xy} at C for one or more of the cantilevers shown. The answers to this problem are given in the figure, which indicates the degree of accuracy when we use two displacement-based elements and a hybrid element. The stresses are determined at two points on a vertical section at the middle of an element rather than at the corners because, at the chosen locations, the stresses are more accurate.

Width of cantilevers = h: $\gamma = 0.2$

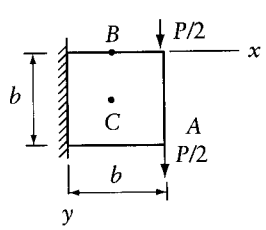

Element type	Deflection at A	Normal stress σ_x at B	Shear stress τ_{xy} at C
1	4.46	2.14	1.00
2	5.01	3.00	1.17
3	5.40	3.00	1.00
Exact	6.88	3.00	1.50

Prob. 17.18

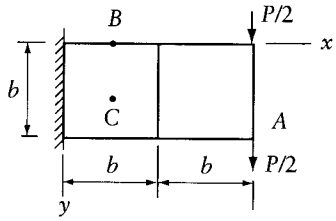

Element type	Deflection at A	Normal stress σ_x at B	Shear stress τ_{xy} at C
1	25.4	6.43	1.00
2	33.3	9.00	1.15
3	34.8	9.00	1.00
Exact	37.8	9.00	1.50

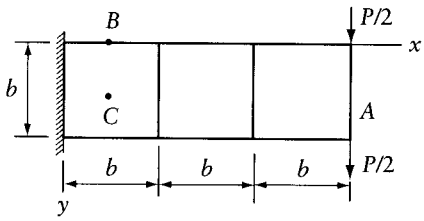

1	79.2	10.7	1.00
2	107.7	15.0	1.15
3	112.2	15.0	1.00
Exact	116.6	15.0	1.50

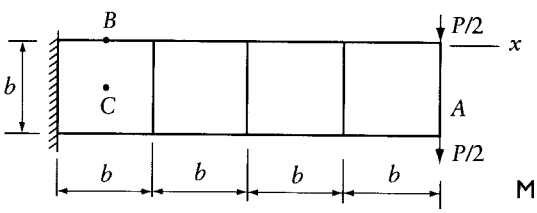

1	182.4	15.0	1.00
2	251.2	21.0	1.15
3	261.6	21.0	1.00
Exact	267.5	21.0	1.50
Multipliers	P/Eh	P/hb	

Element types:
1 Displacement-based, 8 degrees of freedom (Example 16.2)
2 Displacement-based, 12 degrees of freedom (element QLC3, Example 16.2)
3 Hybrid-stress, 8 degrees of freedom (Example 17.6)

Prob. 17.18 (Continued)

Chapter 18

Plastic analysis of continuous beams and frames

18.1 Introduction

An elastic analysis of a structure is important to study its performance, especially with regard to serviceability, under the service loading for which the structure is designed. However, if the load is increased until yielding occurs at some locations, the structure undergoes elastic-plastic deformations and, on further increase, a fully plastic condition is reached, at which a sufficient number of *plastic hinges* are formed to transform the structure into a mechanism. This mechanism would collapse under any additional loading. A study of the mechanism of failure and the knowledge of the magnitude of the collapse load are necessary to determine the load factor in analysis. Alternatively, if the load factor is specified, the structure can be designed so that its collapse load is equal to, or higher than, the product of the load factor and the service loading.

Design of structures based on the plastic approach (referred to as *limit design*) is accepted by various codes of practice, particularly for steel construction. The material is assumed to deform in the idealized manner shown in Figure 18.1. The strain and stress are proportional to one another up to the yield stress, at which the strain increases indefinitely without any further increase in stress. This type of stress–strain relation is not very different from that existing in mild steel. However, there exists a reserve of strength due to strain hardening but this will not be allowed for in the analysis in this chapter.

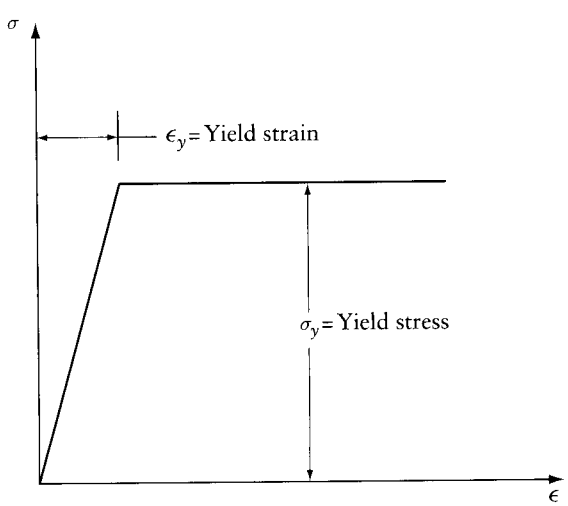

Figure 18.1 Idealized stress–strain relation.

We shall now consider the principles of plastic analysis of plane frames in which buckling instability is prevented and fatigue or brittle failure is not considered possible. In most cases, the calculation of the collapse load involves trial and error, which may become tedious in large structures. A general procedure of limit analysis by the displacement method suitable for use with computers will be discussed in Chapter 22.

18.2 Ultimate moment

Consider a beam whose cross section has an axis of symmetry as shown in Figure 18.2a. Let the beam be subjected to bending in the plane of symmetry. If the bending moment is small, the stress and the strain vary linearly across the section, as shown in Figure 18.2b. When the moment is increased, yield stress is attained in the top fiber (Figure 18.2c), and with a further increase the yield stress is reached in the bottom fiber as well, as shown in Figure 18.2d. If the bending moment continues to increase, yield will spread from the outer fibers inward until the two zones of yield meet (Figure 18.2e); the cross section in this state is said to *be fully plastic.*

The value of the ultimate moment in the fully plastic condition can be calculated in terms of the yield stress σ_y. Since the axial force is zero in the case considered, the neutral axis in the fully plastic condition divides the section into two equal areas, and the resultant tension and compression are each equal to $(a\sigma_y/2)$, forming a couple equal to the ultimate moment:

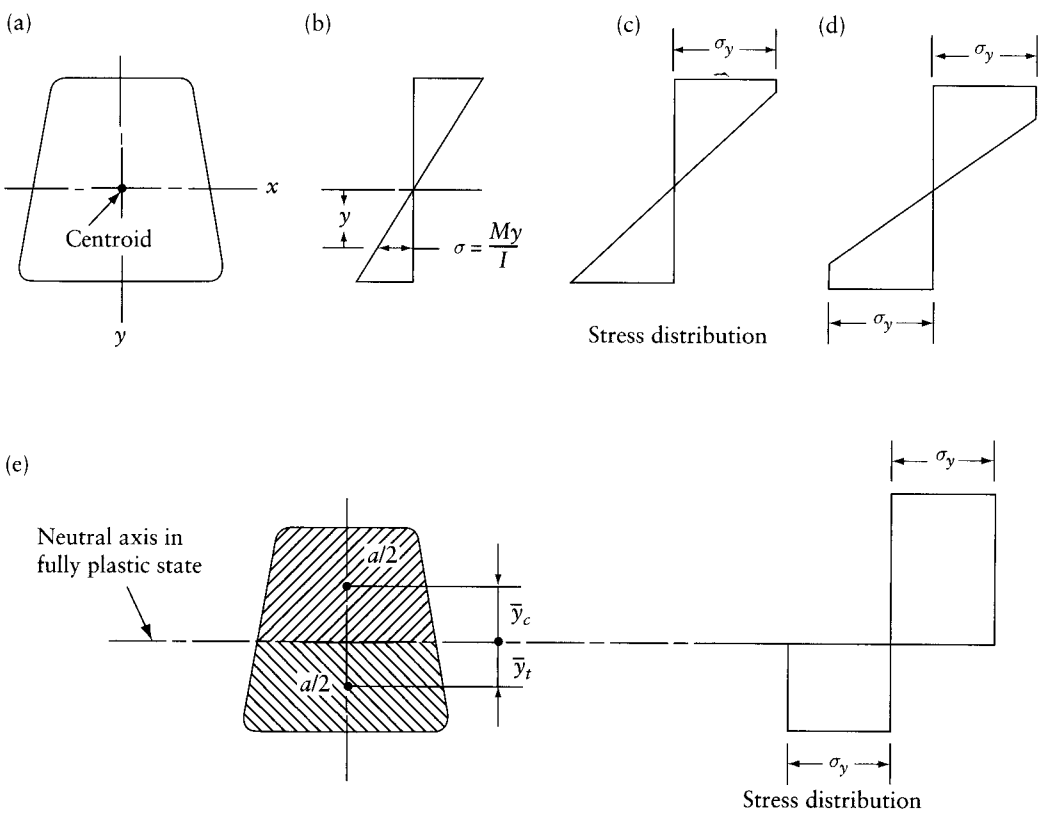

Figure 18.2 Stress distribution in a symmetrical cross section subjected to a bending moment of increasing magnitude. (a) Beam cross section. (b) Elastic. (c) Plastic at top fiber. (d) Plastic at top and bottom fibers. (e) Fully plastic state.

$$M_p = \frac{1}{2} a\, \sigma_y (\bar{y}_c + \bar{y}_t) \tag{18.1}$$

where $\bar{y}_c$ and $\bar{y}_t$ are, respectively, the distance of the centroid of the compression and tension area from the neutral axis in the fully plastic condition.

The maximum moment which a section can carry without exceeding the yield stress is $M_y = \sigma_y Z$, where Z is the section modulus. The ratio $\alpha = M_p/M_y$ depends on the shape of the cross section and is referred to as the *shape factor*; it is always greater than unity.

For a rectangular section of breadth b and depth d, $Z = bd^2/6$, $M_p = \sigma_y bd^2/4$; hence $\alpha = 1.5$. For a solid circular cross section $\alpha = 1.7$, while for I-beams and channels α varies within the small range of 1.15 to 1.17.

18.3 Plastic behavior of a simple beam

To consider displacements let us assume an idealized relation between the bending moment and curvature at a section, as shown in Figure 18.3.

If a load P at the mid-span of a simple beam (Figure 18.4a) is increased until the bending at the mid-span cross section reaches the fully plastic moment M_p, a plastic hinge is formed at this section and collapse will occur under any further load increase. According to the assumed idealized relation, the curvature, and hence the rotation, at the plastic hinge increase at a constant load; so does deflection. The collapse load P_c can be easily calculated from statics:

$$P_c = 4M_p/l \tag{18.2}$$

The bending moment at sections other than mid-span is less than M_p, and by virtue of the assumed idealized relations the beam remains elastic away from this section. The deflected configurations of the beam in the elastic and plastic stages are shown in Figure 18.4b. The increase in deflection during collapse is caused by the rotation at the central hinge without a concurrent change in curvature of the two halves of the beam. Figure 18.4c represents the change in deflection during collapse; this is a straight line for each half of the beam. The same figure shows also the collapse mechanism of the beam.

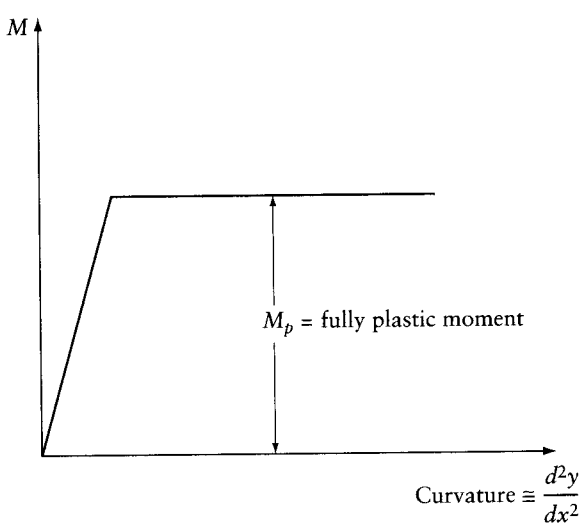

Figure 18.3 Idealized moment–curvature relation.

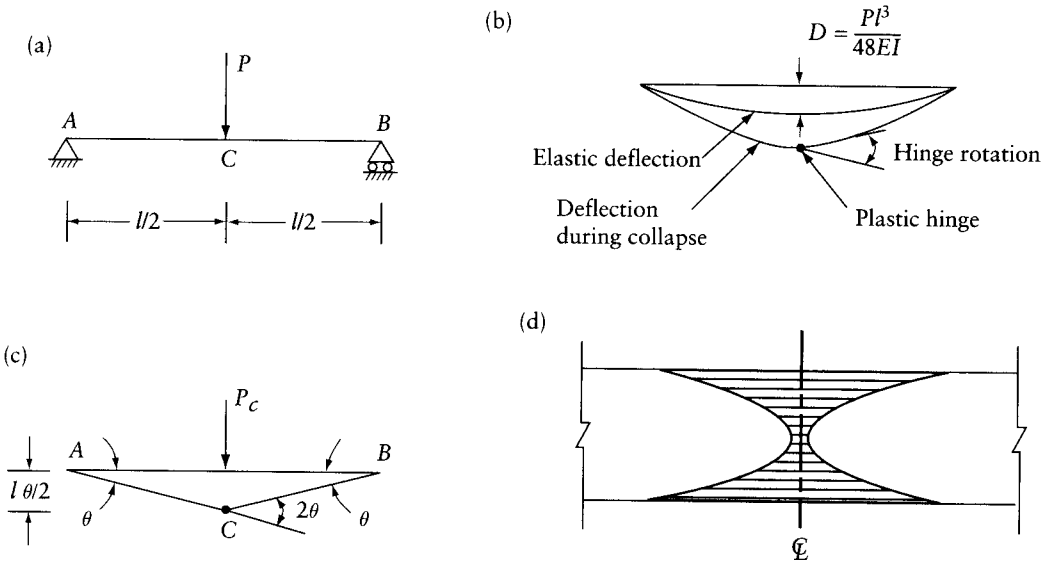

Figure 18.4 Plastic behavior of a simple beam. (a) Beam. (b) Deflection lines. (c) Change in deflection during collapse. (d) Elevation of beam showing yielding near the mid-span section.

The collapse load of the beam (and this applies also to statically indeterminate structures) can be calculated by equating the external and internal work during a virtual movement of the collapse mechanism. Let each half of the beam in Figure 18.4c acquire a virtual rotation θ, so that the corresponding rotation at the hinge is 2θ, and the downward displacement of the load P_c is $l\theta/2$. Equating the work done by P_c to the work of the moment M_p at the plastic hinge, we obtain

$$P_c = \frac{l\theta}{2} = M_p 2\theta \tag{18.3}$$

which gives the same result as Eq. 18.2.

The idealized relation between load and central deflection for this beam is represented by the line *OFM* in Figure 18.5. When the collapse load corresponding to point *F* in Figure 18.5 is reached, the elastic deflection at mid-span is

$$D_F = P_c \frac{l^3}{48EI} \tag{18.4}$$

However, the actual load–deflection relation follows the dashed curve *GKE*. When the yield moment $M_y (= \sigma_y Z)$ is reached at the mid-span section, the upper or the lower fiber, or both, yield and the elastic behavior comes to an end. If the load is increased further, the yield spreads inward at this section and also laterally to other nearby sections. Figure 18.4d illustrates this spread of yield. After M_y has been reached, the deflection increases at a greater rate per unit increase of load until M_p is reached, as indicated by the curve *GK* in Figure 18.5. In practice, rolled steel sections continue to show a small rise in the load–deflection curve during collapse (line *KE*); this is due to strain hardening which is generally not considered in ordinary plastic analysis.

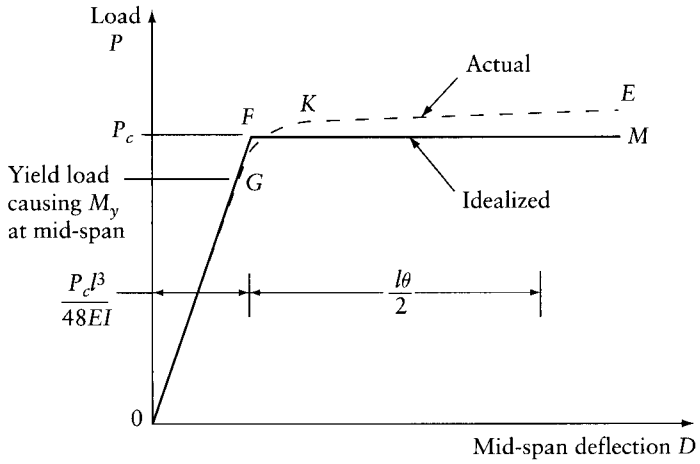

Figure 18.5 Load–deflection relation for the beam in Figure 18.4.

18.4 Ultimate strength of fixed-ended and continuous beams

Consider a prismatic fixed-ended beam subjected to a uniform load of intensity q (Figure 18.6a). The resulting bending moments are $M_A = M_C = -ql^2/12$ and $M_B = ql^2/24$. When the load intensity is increased to q_1 such that the moments at the supports reach the fully plastic moment $M_p = q_1 l^2/12$, hinges are formed at A and C. If q is further increased, the moment at the supports will remain constant at M_p; free rotation will take place there so that the deflection due to the load in excess of q_1 will be the same as in a simply-supported beam. The collapse will occur at a load intensity q_c which produces the moment at mid-span of magnitude M_p, so that a third hinge is formed at B. The bending moment diagrams due to load intensity q for the cases $q = q_1$, $q_1 < q < q_c$, and $q = q_c$ are shown in Figure 18.6b and the collapse mechanism in Figure 18.6c. The collapse load q_c is calculated by the virtual-work equation

$$M_p(\theta + 2\theta + \theta) = 2\left(\frac{q_c l}{2}\right)\frac{\theta l}{4} \tag{18.5}$$

where θ, 2θ, and θ are the virtual rotations at the plastic hinges A, B, and C respectively, and $\theta l/4$ is the corresponding downward displacement of the resultant load on one-half of the beam. Equation 18.5 gives the intensity of the collapse load:

$$q_c = \frac{16M_p}{l^2} \tag{18.6}$$

If the beam is of solid rectangular section, $M_p = 1.5\,M_y$ and the maximum load intensity computed by elastic theory with the maximum fiber stress σ_y is $q_E = 12\,M_y/l^2$. Thus, the ratio $q_c/q_E = 2$, which clearly indicates that the design of the beam considered by elastic theory is conservative.

In plastic design of continuous beams, we draw the bending moment diagram for each span as a simple beam loaded with the design load multiplied by the load factor. Arbitrary values may be chosen for the bending moment at the supports and a closing line such as $AB'C'D$ in Figure 18.7d is drawn. The value of the bending moment at any section will then be the ordinate between the closing line and the simple-beam moment diagram. The beam will have the required

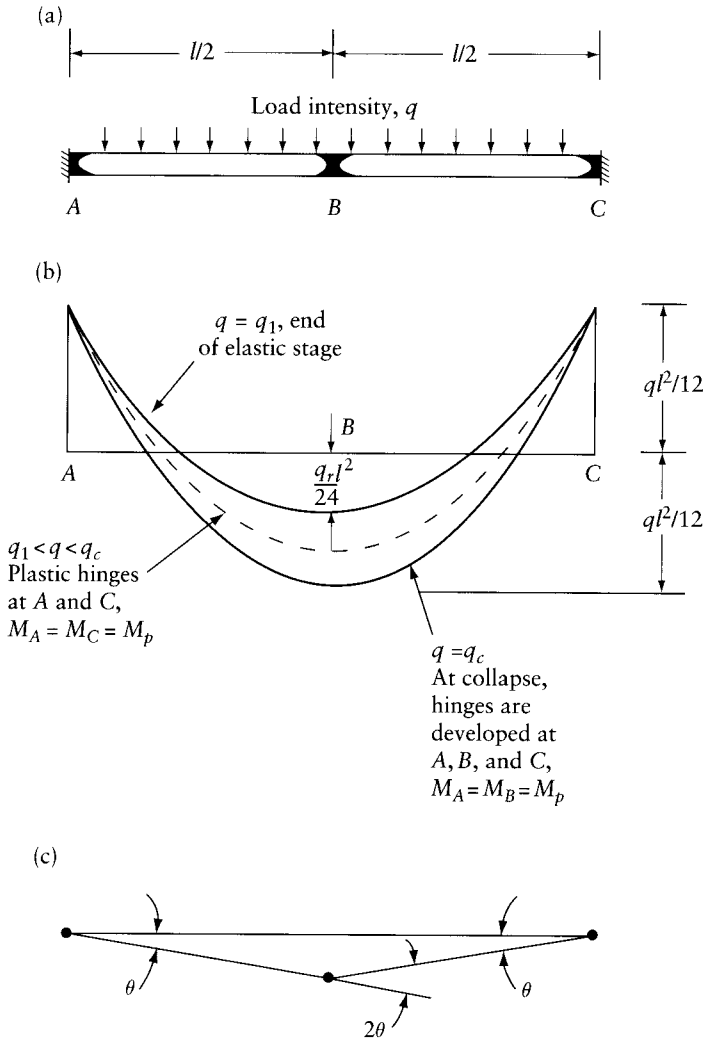

Figure 18.6 Collapse of a beam with fixed ends under a uniformly distributed load. (a) Beam. (b) Bending moment diagrams for three load intensities. (c) Collapse mechanism.

ultimate capacity if the sections are then selected so that the plastic moment of resistance is everywhere equal to or in excess of the bending moment. However, the most economical design is generally attained when a regular section is used of size such that a collapse mechanism develops.

If the beam sections are given or assumed, the values of the collapse load corresponding to all possible mechanisms are determined; the actual collapse load is the smallest one of these. Consider, for example, the continuous beam in Figure 18.7a which has constant section with a plastic moment of resistance M_p. We want to find the value of the two equal loads P which causes collapse; denote this value by P_c. Failure can occur only by one of the two mechanisms shown in Figures 18.7b and c. By a virtual-work equation for each of the two mechanisms, we obtain

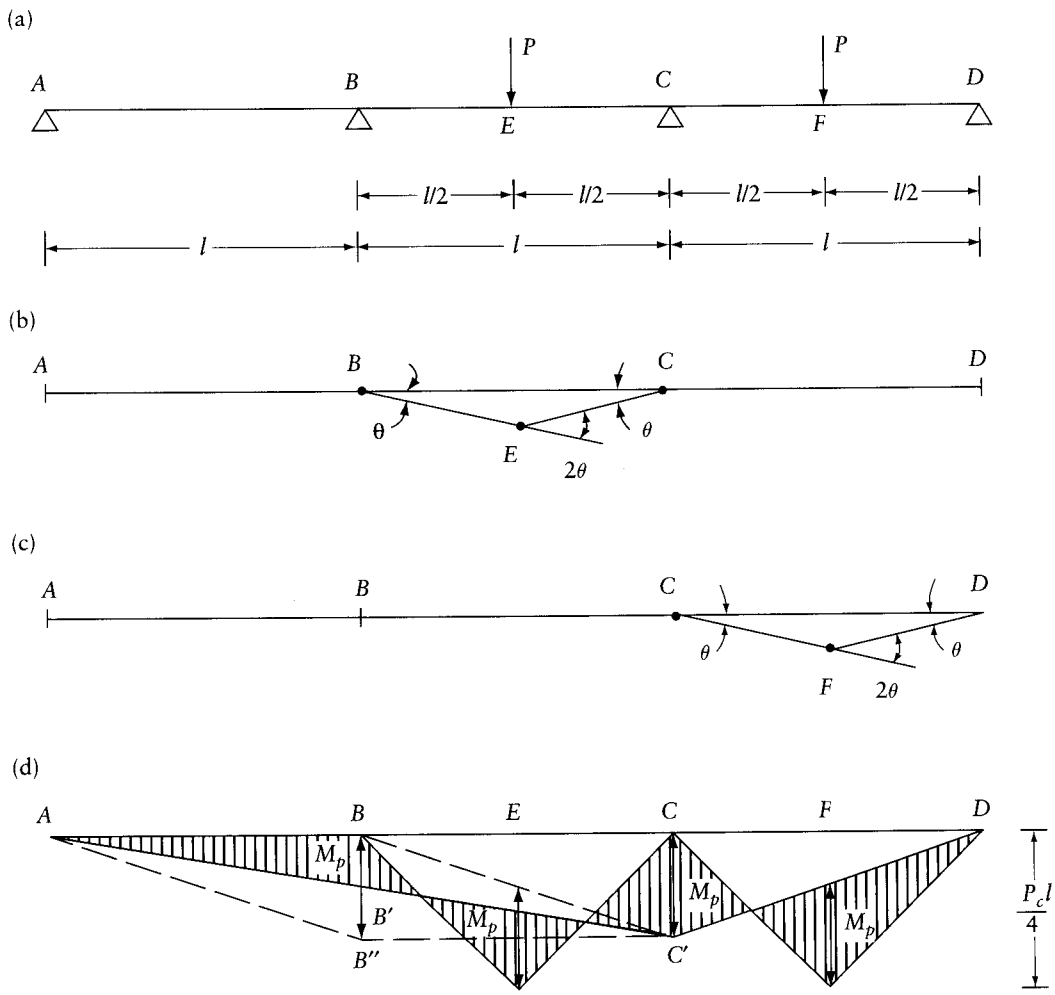

Figure 18.7 Plastic analysis of a continuous beam. (a) Continuous beam of constant section and of plastic moment of resistance M_p. (b) Collapse mechanism 1. (c) Collapse mechanism 2. (d) Bending moment diagram.

$$P_{c1}\left(\frac{l\theta}{2}\right) = M_p(\theta + 2\theta + \theta) \quad \text{(see Figure 18.7b)}$$

whence

$$P_{c1} = 8M_p/l \tag{18.7}$$

and

$$P_{c2}\left(\frac{l\theta}{2}\right) = M_p(\theta + 2\theta) \quad \text{(see Figure 18.7c)}$$

whence

$$P_{c2} = 6M_p/l \tag{18.8}$$

The smaller of these two values is the true collapse load, $P_c = 6\,M_p/l$. The corresponding bending moment diagram is shown in Figure 18.7d, in which the values of the bending moment at C and F are equal to M_p. When the collapse occurs, the part of the beam between A and C is still in the elastic stage, and the value of the bending moment at B can be calculated by analyzing a continuous beam ABC, hinged at A and C, and subjected to a clockwise couple of magnitude M_p at C and a vertical load $P_c = 6\,M_p/l$ at E. However, this calculation has no practical value in limit design. It is clear that the closing line $AB'C'$ of the bending moment diagram can take any position between the limiting lines $AB''C'$ and ABC' with the bending moment at no section exceeding M_p.

18.5 Rectangular portal frame

Let us determine the collapse load for the frame shown in Figure 18.8a, assuming the plastic moment of resistance $2\,M_p$ for the beam BC and M_p for the columns. There are only three possible collapse mechanisms, which are shown in Figures 18.8b, c, and d.

A virtual-work equation for each of these mechanisms gives

$$M_p(\theta + \theta) + 2M_p(2\theta) = 2P_{c1}\left(\frac{l\theta}{2}\right) \quad \text{(see Figure 18.8b)}$$

or

$$P_{c1} = \frac{6M_p}{l} \tag{18.9}$$

$$M_p(\theta + \theta + \theta + \theta) = P_{c2}(0.6l\theta) \quad \text{(see Figure 18.8c)}$$

or

$$P_{c2} = 6.67\frac{M_p}{l} \tag{18.10}$$

and

$$M_p(\theta + \theta + 2\theta) + 2M_p(2\theta) = P_{c3}(0.6l\theta) + 2P_{c3}\left(\frac{l\theta}{2}\right) \quad \text{(see Figure 18.8d)}$$

or

$$P_{c3} = 5\frac{M_p}{l} \tag{18.11}$$

The collapse load is the smallest of P_{c1}, P_{c2}, and P_{c3}; thus, $P_c = 5\,M_p/l$, and failure of the frame will occur with the mechanism of Figure 18.8d. The corresponding bending moment diagram in Figure 18.8e has an ordinate M_p at the plastic hinges A, C, and D and $2M_p$ at E, with the plastic moment of resistance exceeded nowhere. A check on the calculations can be made by verifying that the bending moment diagram in Figure 18.8e satisfies static equilibrium.

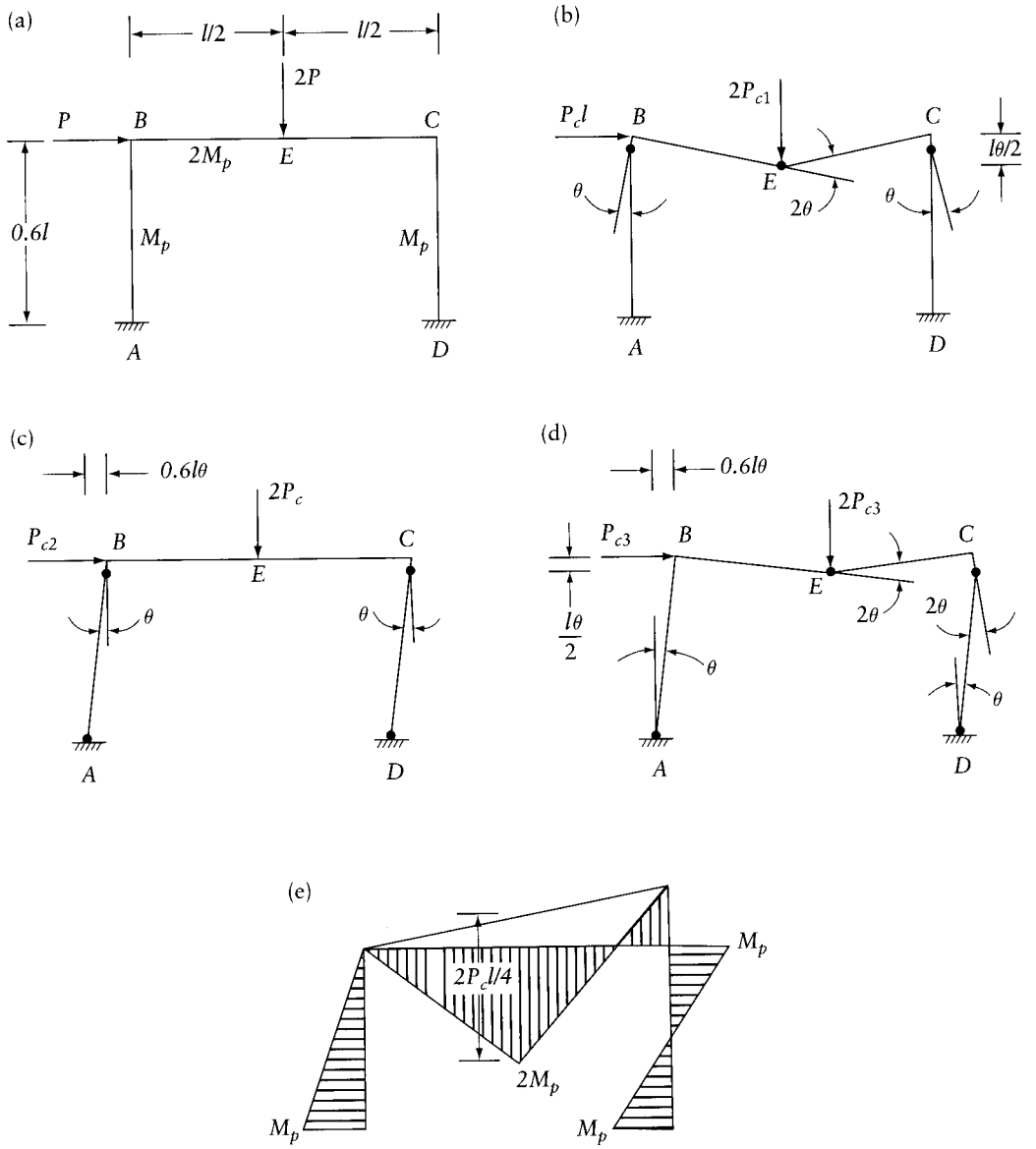

Figure 18.8 Plastic analysis of a rectangular portal frame. (a) Frame loading and properties. (b) Mechanism corresponding to collapse load P_{c1}. (c) Mechanism corresponding to collapse load P_{c2}. (d) Mechanism corresponding to collapse load P_{c3}. (e) Bending moment diagram at collapse.

18.5.1 Location of plastic hinges under distributed loads

Consider the frame analyzed in the previous section, but with a vertical load 4 P distributed over the beam BC, as shown in Figure 18.9a; the horizontal load P is unchanged. In this case, the position of the maximum positive bending moment in BC is not known, so that the location of the plastic hinge has to be determined.

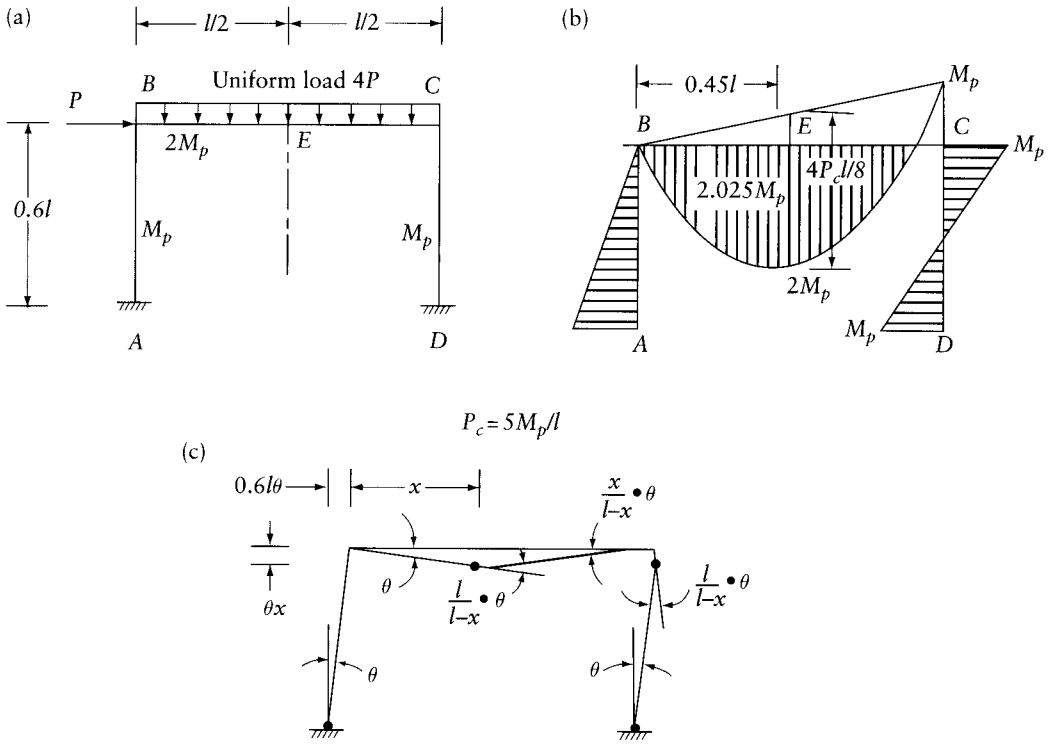

Figure 18.9 Frame subjected to distributed load analyzed in Section 18.5.1. (a) Frame loading and properties. (b) Bending moment diagram due to loading in part (a) on the mechanism in Figure 18.8d. (c) Mechanism corresponding to collapse load P_c in Eq. 18.14.

Let us apply the virtual-work equation to the mechanism in Figure 18.8d, loaded as in Figure 18.9a, with the hinge in the beam assumed at mid-span. Each half of the beam is subjected to a vertical load whose resultant $2P_{c3}$ moves through a vertical distance $l\theta/4$.

The internal virtual work and the external virtual work of the horizontal force are the same as before (Eq. 18.11); thus,

$$M_p(\theta + \theta + 2\theta) + 2M_p(2\theta) = P_{c3}(0.6l\theta) + 2 \times 2P_{c3}\left(\frac{l\theta}{4}\right) \tag{18.12}$$

This equation gives the same value of the collapse load as Eq. 18.11.

The bending moment diagram for the mechanism in Figure 18.8d with the loads in Figure 18.9a is shown in Figure 18.9b, from which it can be seen that the fully plastic moment $2M_p$ is slightly exceeded in the left-hand half of the beam.

This maximum moment occurs at a distance $x = 0.45l$ from B, and its value is $2.025M_p$. It follows that the assumed collapse mechanism is not correct, the reason for this being that the plastic hinge in the beam should not be located at mid-span. The calculated value of $P_c = 5M_p/l$ is an upper bound on the value of the collapse load. If the load P_c is given, the structure must be designed for a plastic moment M_p slightly greater than $P_c l/5$, and this value is to be considered a lower bound on the required plastic moment. It is clear that the structure will be safe if designed for

$$M_p = \frac{2.025}{2}\left(\frac{P_c l}{5}\right) = 1.0125\frac{P_c l}{5}$$

Therefore, the required value of M_p is

$$\frac{P_c l}{5} < M_p < 1.0125\frac{P_c l}{5} \tag{18.13}$$

These limits define the value of M_p to within 1.25 percent and are accurate enough for practical purposes. However, the precise value of M_p can be calculated considering the mechanism in Figure 18.9c, with a plastic hinge F at a distance x from B. By a virtual-work equation M_p can be derived in terms of x. The value of x is then chosen so that M_p is a maximum, that is, $dM_p/dx = 0$.

The rotation at the hinges and the translation of the loads are shown in Figure 18.9c, and the virtual-work equation is

$$M_p\left(\theta + \theta + \frac{l}{l-x}\theta\right) + 2M_p\left(\frac{l}{l-x}\theta\right) = P_c(0.6l\theta) + \frac{4P_c}{l}x\left(\frac{x\theta}{2}\right) + \frac{4P_c}{l}(l-x)\left(\frac{x\theta}{2}\right)$$

or

$$M_p = P_c\frac{(0.6l^2 + 1.4lx - 2x^2)}{(5l - 2x)} \tag{18.14}$$

Putting $dM_p/dx = 0$, we obtain

$$4x^2 - 20lx + 8.2l^2 = 0 \tag{18.15}$$

whence $x = 0.4505l$. Substituting in Eq. 18.14, we obtain the maximum value of M_p:

$$M_p = 1.0061\frac{P_c l}{5} \tag{18.16}$$

The values of x and M_p differ slightly from the approximate value $x = 0.45l$ and from the conservative value of $M_p = 1.0125\ (P_c l/5)$ obtained from the bending moment diagram in Figure 18.9b.

18.6 Combination of elementary mechanisms

We can now consider the plastic analysis of plane frames in general. A sufficient number of plastic hinges are introduced at assumed locations to form a mechanism and the corresponding collapse load is calculated by virtual work. The value determined in this way is an upper bound on the correct load capacity, that is, the load indicated is greater than the correct load. In other words, if the plastic moment M_p required for any specified collapse is calculated according to any mechanism, then the resulting value of M_p is a lower bound on the necessary plastic resisting moment. In practical calculation, the correct mechanism may be reached by considering elementary mechanisms and combining them to obtain the lowest, that is, the correct, load capacity.

Consider the frame of Figure 18.10a with prismatic members; the relative values of the fully plastic moment are indicated. Three elementary mechanisms are shown in Figures 18.10b, c, and d and the work equation for each is given alongside.

Mechanism 2 gives the lowest P_c, and we combine it with the other mechanisms to reach a smaller value of P_c. Two combinations are shown in Figures 18.10e and f. Mechanism 4 is a

(a)

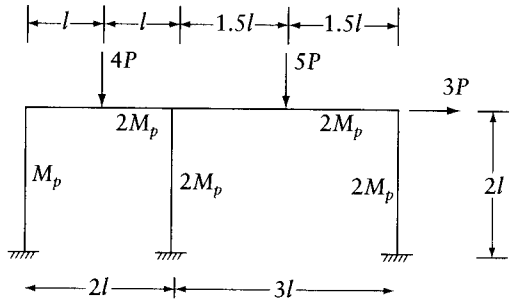

(b)

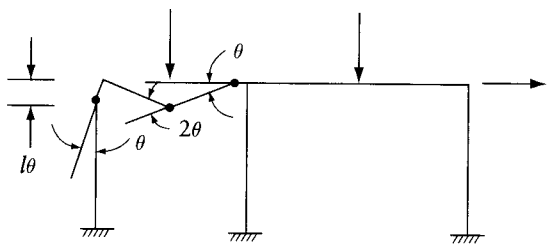

$$M_p\theta + 2M_p(2\theta + \theta) = 4P_{c1}(l\theta)$$
$$P_{cl} = 1.75M_p/l$$

(c)

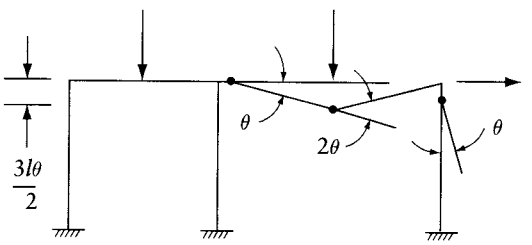

$$3M_P(\theta + 2\theta) + 2M_p\theta = 5P_{c2}(\tfrac{3}{2}l\theta)$$
$$P_{c2} = 1.47M_p/l$$

(d)

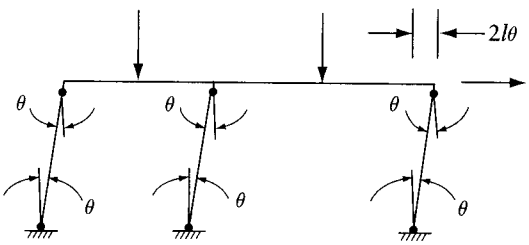

$$M_p(\theta + \theta) + 2M_p(\theta + \theta + \theta + \theta) = 3P_{c3}(2l\theta)$$
$$P_{c3} = 1.67M_p/l$$

(e)

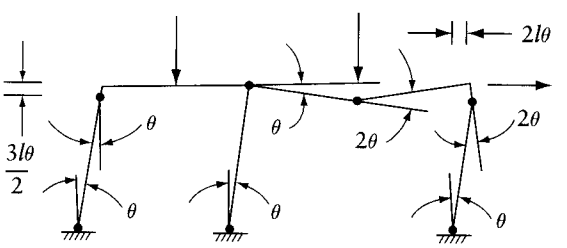

$$M_p(2\theta) + 2M_p(5\theta) + 3M_p(2\theta) = 5P_{c4}(\tfrac{3l\theta}{2}) + 3P_{c4}(2l\theta)$$
$$P_{c4} = 1.33M_p/l$$

(f)

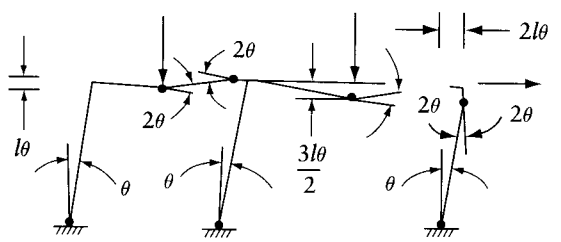

$$M_p(\theta) + 2M_p(8\theta) + 3M_p(2\theta) = 4P_{c5}(l\theta) + 5P_{c5}(\tfrac{3l\theta}{2}) + 3P(2l\theta)$$
$$P_{c5} = 1.31M_{p/l}$$

Figure 18.10 Plastic analysis of a multibay frame. (a) Frame properties and loading. (b) Mechanism 1. (c) Mechanism 2. (d) Mechanism 3. (e) Mechanism 4. (f) Mechanism 5.

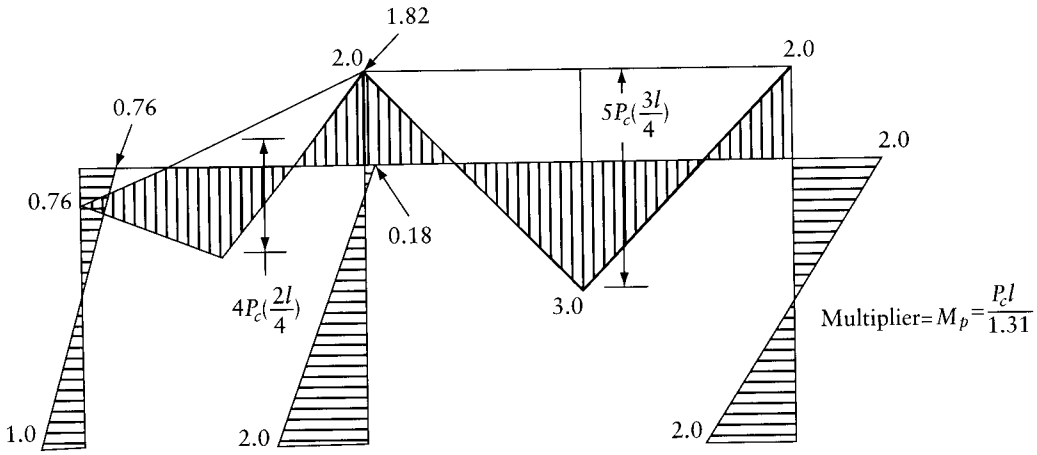

Figure 18.11 Bending moment diagram for mechanism 5 in Figure 18.10f.

combination of mechanisms 2 and 3 with a modification of the location of the hinge above the central column. The resulting collapse load is P_{c4} 1.33 Mp/l. Mechanism 5 is a combination of mechanisms 1, 2, and 3, again with the same modification, giving a value $P_{c5} = 1.31\, M_p/l$, which is lower than all the previous values.

To find whether or not P_{c5} is the lower bound on P_c, the corresponding bending moment diagram is drawn. If the moment at no section is greater than its plastic moment, P_{c5} is the lower bound and the solution is correct. The bending moment diagram of Figure 18.11 shows that mechanism 5 is the correct mechanism. In the construction of this diagram, the known values of moments at the plastic hinges were first plotted, and the other ordinates were then derived by simple statics.

It is possible that, on plotting the bending moment diagram, we find that the moment at some section exceeds the plastic moment of resistance. If the excess is small, say 5 percent, then it is safe to consider that the frame can carry the loads previously calculated, each reduced by 1/1.05. Some publications[1] suggest that, if, for a specified collapse load calculated for a wrong mechanism, the plastic moment of resistance is nowhere exceeded by more than 30 percent, a fairly close estimate of the required bending strength can be obtained by increasing the computed value of M_p by one-half of the largest excess moment.

18.7 Frames with inclined members

In computing the angle between the ends of members at a plastic hinge in a nonrectangular frame, it may be convenient to locate the instantaneous center about which a part of the frame rotates during collapse.

Consider the gable frame in Figure 18.12a, for which a trial mechanism 1 is given in Figure 18.12b. Joining the plastic hinges at A and C and extending the line AC to meet GF, locates O, the center of rotation of the part CDF. Parts ABC and GF rotate about A and G respectively. During collapse points C and F move along the normals to the lines AO and GO respectively, that is, along the common tangent to circles having their centers located at the

1 See *Plastic Design of Steel*, The American Institute of Steel Construction, New York, 1959, p. 7.

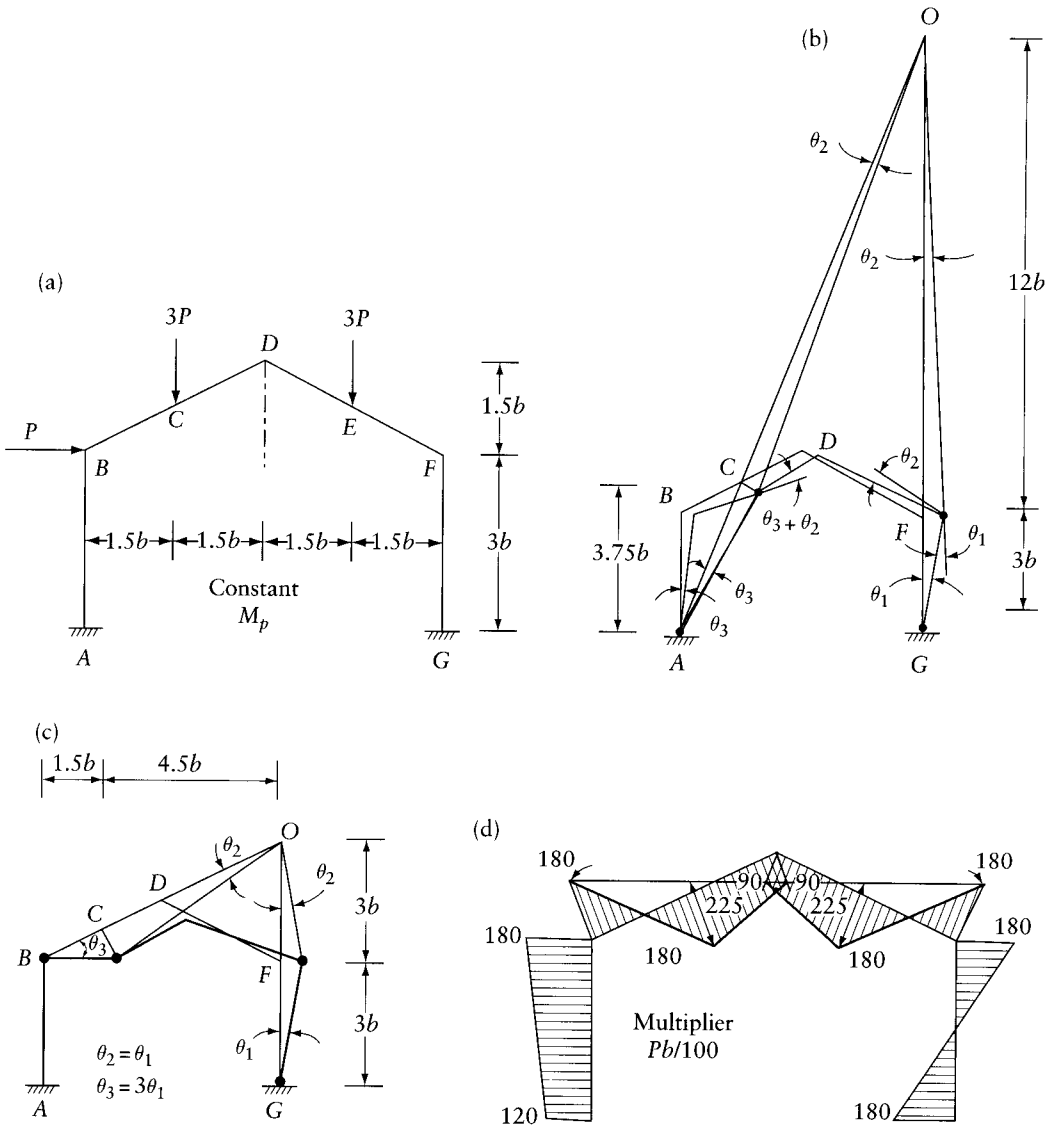

Figure 18.12 Plastic analysis of a gable frame. (a) Frame properties and loading. (b) Mechanism 1. (c) Mechanism 2. (d) Bending moment diagram for mechanism 2.

centers of rotation A, O, and G. Assuming the angle of rotation of GF to be θ_1, the angles of rotation of the frame parts about their instantaneous centers can be determined easily by geometry: $\theta_2 = \theta_1/4$ and $\theta_3 = 3\theta_2 = 3\theta_1/4$. The relative rotations of frame parts at the plastic hinges are indicated in Figure 18.12b, and the corresponding internal virtual work W is the sum of the work done at the four hinges A, C, F, and G; thus,

$$W = M_p[\theta_3 + (\theta_3 + \theta_2) + (\theta_2 + \theta_1) + \theta_1]$$
$$= 4M_p\theta_1$$

The translation of the external loads corresponding to the above rotations is calculated from the geometry of the mechanism, and the external virtual work is obtained as follows.

Load point	*Displacement*	*Load*	*External work*
B	$0.75\theta_1 \times 3b = 2.25\theta_1 b$	P	$2.25Pb\theta_1$
C	$0.75\theta_1 \times 1.5b = 1.125\theta_1 b$	$3P$	$3.375Pb\theta_1$
E	$0.25\theta_1 \times 1.5b = 0.375\theta_1 b$	$3P$	$1.125Pb\theta_1$
			Total $= 6.75Pb\theta_1$

Equating the external and internal work, we obtain

$$M_p = 1.6875Pb$$

If the bending moment corresponding to this mechanism is sketched, it will be clear that the value $M_p = 1.6875Pb$ is exceeded at several points, which means that mechanism 1 is not the correct collapse mechanism. A second mechanism is shown in Figure 18.12c, for which the instantaneous centers are B, O, and G for frame parts BC, CF, and FG respectively. An arbitrary small virtual rotation θ_1 is assumed for FG, and the corresponding rotations for the other parts are determined in terms of θ_1 by considering the geometry of the mechanism. The work equation for this mechanism gives $M_p = 1.8Pb$. The corresponding bending moment diagram is shown in Figure 18.12d: the value of M_p is not exceeded, indicating that collapse takes place according to mechanism 2.

18.8 Effect of axial forces on plastic moment capacity

In previous sections we assumed that the fully plastic state at a hinge is induced solely by the bending moment M_p. However, in the presence of a high axial compressive or tensile force, a plastic hinge can be formed at a moment M_{pc} lower than the value M_p. We shall now derive an expression for M_{pc} for a rectangular cross section subjected to a tensile or compressive axial force; any buckling effect will be ignored.

Figures 18.13a to e show the changes in stress distribution in a rectangular cross section $b \times d$ subjected to an axial compressive force P together with a bending moment M in the vertical plane, as the magnitude of M and P is increased at a constant value of M/P until the fully plastic stage is reached. The values of the axial force and the moment at this stage are

$$P = 2\sigma_y b y_0 \tag{18.17}$$

and

$$M_{pc} = \frac{\sigma_y b}{4}(d^2 - 4y_0^2) \tag{18.18}$$

where σ_y is the yield stress and y_0 is the distance from the centroid of the section to the neutral axis.

In the absence of the axial force, $y_0 = 0$, and the fully plastic moment is then

$$M_p = \sigma_y \frac{bd^2}{4} \tag{18.19}$$

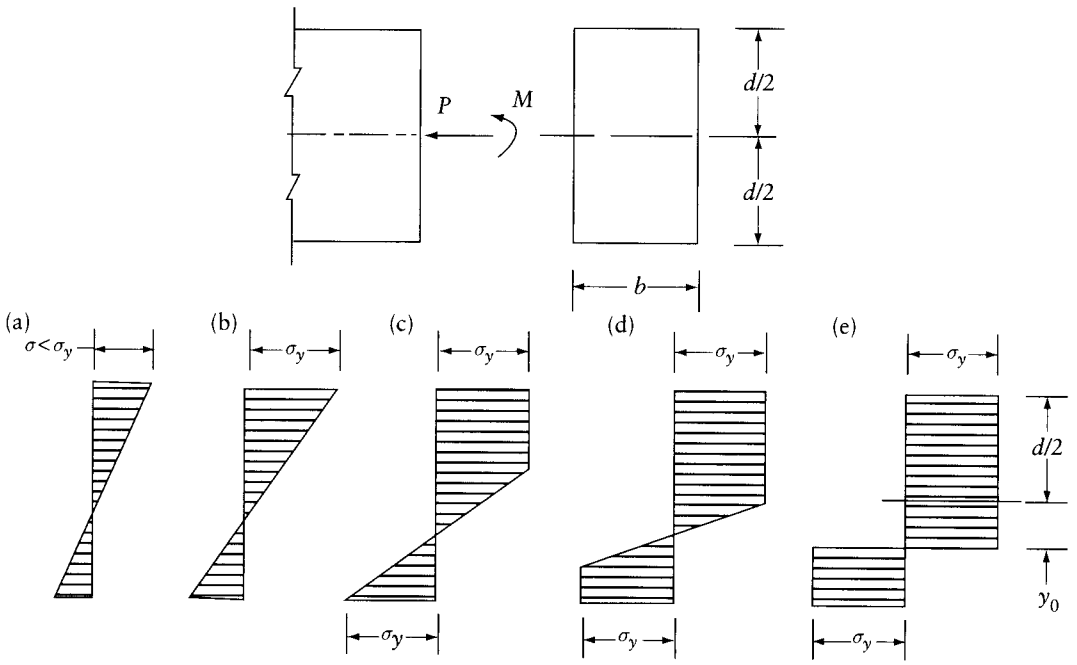

Figure 18.13 Stress distribution in a rectangular section subjected to an increasing bending moment M and axial force P at a constant value of M/P.

On the other hand, if the axial force alone causes a fully plastic state, its magnitude is

$$P_y = \sigma_y bd \tag{18.20}$$

From Eqs. 18.17 to 18.20 we can obtain the interaction equation

$$\frac{M_{pc}}{M_p} = 1 - \left(\frac{P}{P_y}\right)^2 \tag{18.21}$$

The interaction curve of M_{pc}/M_p plotted against P/P_y in Figure 18.14 can be used to determine the strength of a section under combined loading of an axial force and a bending moment from the strengths in two simple types of loading: axial force only and bending moment only.

The shape of the interaction curve depends on the geometry of the cross section. For all wide-flange I-sections used in steel construction, the interaction curves fall within a narrow band and may be approximated by two straight lines[2] shown in Figure 18.14. From this figure it is apparent that when $P/P_y \leq 0.15$, the effect of the axial load is neglected, and when $P/P_0 \geq 0.15$,

2 Joint Committee of the Welding Research Council and the American Society of Civil Engineers, Commentary on Plastic Design in Steel, *ASCE Manual of Engineering Practice*, No. 41, New York, 1961.

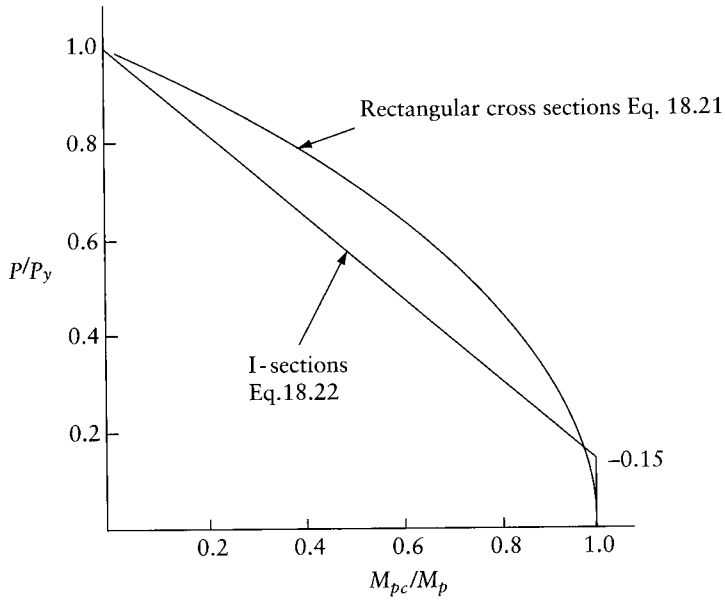

Figure 18.14 Axial-force/bending moment interaction curves for rectangular cross sections and for wide-flange I-sections.

we use the equation

$$\frac{M_{pc}}{M_p} = 1.18\left(1 - \frac{P}{P_y}\right) \tag{18.22}$$

18.9 Effect of shear on plastic moment capacity

The presence of shear at a section at which the bending moment is high may limit the ultimate load capacity of a structure to a value below that which produces the fully plastic moment M_p at the location of the plastic hinges. Although in the majority of practical cases the influence of shear is small, there are circumstances when shear may produce a plastic hinge at a bending moment M_{ps} appreciably smaller than M_p.

The main assumptions made in deriving an interaction equation for M_{ps}/M_p for rectangular and wide-flange I-sections are:

1. The outer portions of the beam (the flanges and a part of the web) are in a yield state and resist bending only, while the middle portion is in an elastic state and resists shear.
2. The shearing stress in the (rectangular) center portion is calculated by ordinary elastic equations.

The resistance of the section is assumed to be exhausted when the shearing stress in the center portion reaches yield under pure shear, which, according to von Mises-Hencky yield criterion, equals $\sigma_y/\sqrt{3}$. With these assumptions, the following equation can be derived:[3]

$$\frac{M_{ps}}{M_p} = \frac{8bc^2}{9\alpha Z}\left(\sqrt{1+\frac{9}{4}\frac{\alpha Z}{bc^2}}-1\right) \tag{18.23}$$

where b is the width of the rectangular section or of the web of an I-section, Z is the section modulus, α is as defined at the end of Section 18.2, and c is the shear span (= bending moment/shearing force).

18.10 General

This chapter is no more than an introduction to the structural analysis required in the plastic design of steel structures. For safe and efficient use of plastic design of continuous framed structures, it is important to understand the restrictions and limitations of this design method, such as the effect of repeated loading, instability, and also to be able to estimate deflections at working and ultimate loads.[4]

Problems

18.1 Find the required plastic moment resistance of the cross section(s) for the beam in the figure, which is to be designed to carry the given loads with a load factor of 1.7. Assume that the beam has: (a) a constant cross section, (b) two different cross sections one from A to C, and the other from C to D.

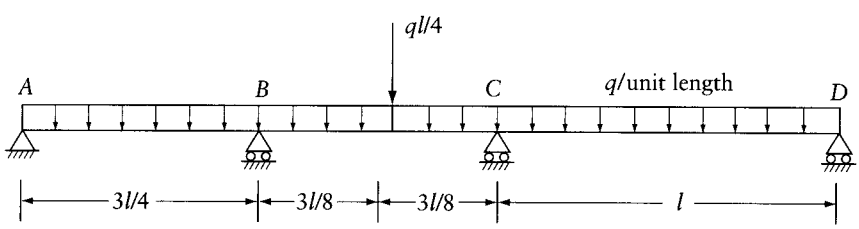

Prob. 18.1

3 See pp. 35–40 of the reference in footnote 2 in this chapter for proof and limitations of this equation, and also for the combined effect of shear and axial force.

4 See, for instance, Neal, B.G., *The Plastic Methods of Structural Analysis*, 2nd ed., Chapman and Hall, London, 1963. A list of other references can be found at the end of the manual referred to in footnote 2 in this chapter.

18.2 Determine the fully plastic moment for the frames shown, with the collapse loads indicated. Ignore the effects of shear and axial forces.

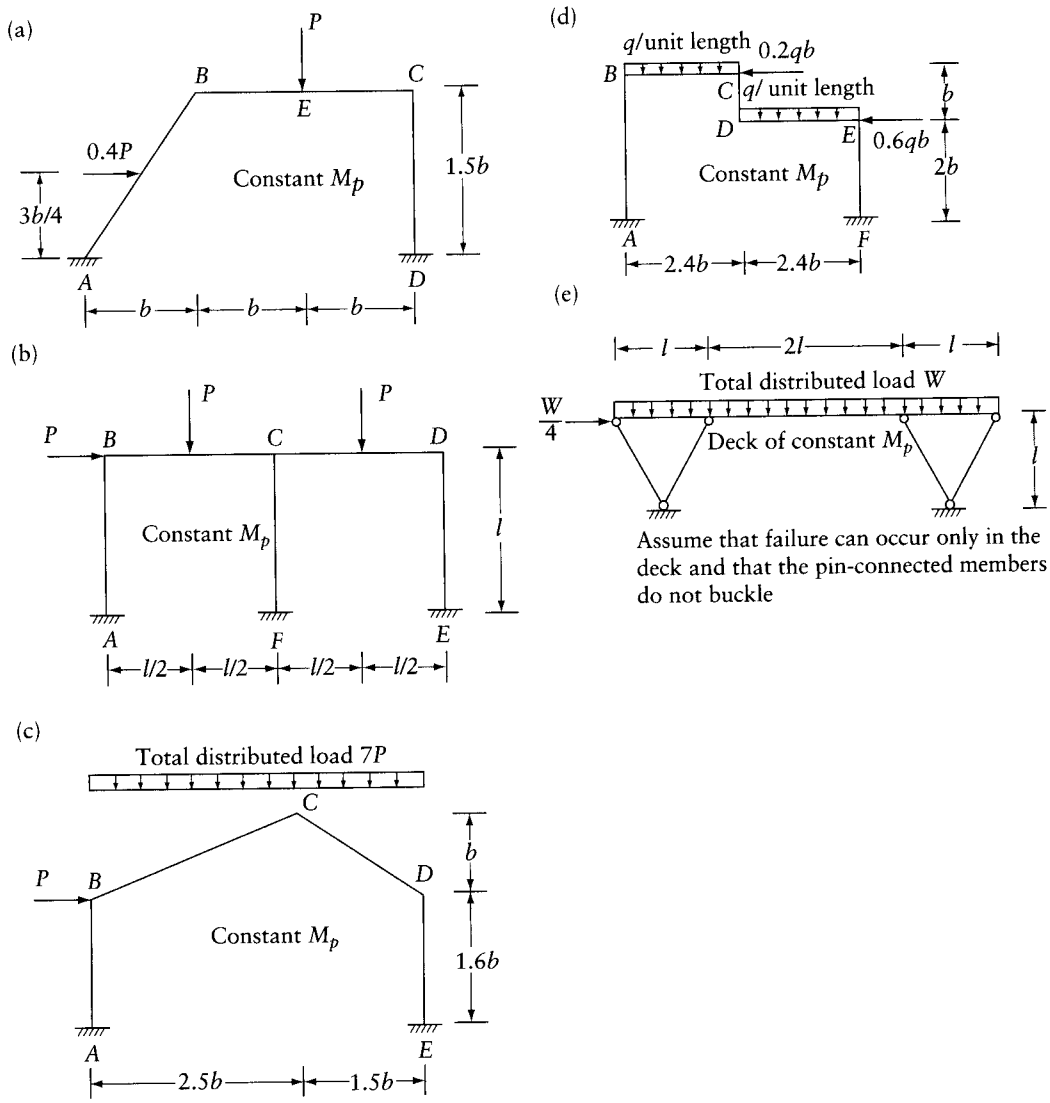

Assume that failure can occur only in the deck and that the pin-connected members do not buckle

Prob. 18.2

18.3 What is the value of M_p for the frame in Prob. 18.2b, if the axial force effect (excluding buckling) is taken into account? Assume that the frame has a constant rectangular section $b \times d$, with $d = l/15$.

18.4 What is the value of M_p for the beam in Prob. 18.1, if the shear effect is taken into account? Assume that the beam has a constant rectangular section $b \times d$, with $d = l/30$.

Chapter 19

Yield-line and strip methods for slabs

19.1 Introduction[1]

This chapter deals in a general way with plates but many of the applications are virtually limited to reinforced concrete slabs. For this reason, the term slab will be generally used.

An elastic analysis of a reinforced concrete slab gives no indication of its ultimate load-carrying capacity and further analyses have to be made for this condition. An exact solution for the ultimate flexural strength of a slab can be found only rarely, but it is possible to determine upper and lower bounds to the true collapse load.

The yield-line method of analysis gives an upper bound to the ultimate load capacity of a reinforced concrete slab by a study of assumed mechanisms of collapse. This method, developed by Johansen,[2] is a powerful tool for estimating the required bending resistance and hence the necessary reinforcement, especially for slabs of nonregular geometry or loading. Two approaches are possible in yield-line theory. The first one is an energy method in which the external work done by the loads during a small virtual movement of the collapse mechanism is equated to the internal work. The alternative approach is by the study of the equilibrium of the various parts of the slab into which the slab is divided by the yield lines. We may note that it is the equilibrium of slab parts that is considered and not the equilibrium of forces at all points of the yield line.

In contrast to the above, lower-bound solutions to the collapse load are obtained by satisfying equilibrium at *all* points in the slab, and necessitate the determination of a complete bending moment field in equilibrium with the applied loading. We shall restrict our discussion of these lower-bound solutions to the special case where twisting moments are absent – the so-called strip method. This strip method is more of a direct design procedure than the yield-line method as the designer chooses the layout of reinforcement as the calculation progresses.

Ultimate load designs according to the yield-line or strip methods do not guarantee safety against cracking or excessive deformations. Therefore, an understanding of elastic behavior is necessary for the effective distribution of reinforcement when an ultimate load design is made.

19.2 Fundamentals of yield-line theory

The slab is assumed to collapse at a certain ultimate load through a system of yield lines or fracture lines, called the pattern of fracture. The working load is obtained by dividing this ultimate load by the required load factor. For design, the working load is multiplied by the load factor, and the required ultimate moment of resistance is determined.

1 Sections 19.1, 19.5, 19.6, 19.8, 19.9, and 19.10 were written in collaboration with Dr. J. Harrop, University of Leeds.

2 Johansen, K. W., *Yield-Line Theory*, Cement and Concrete Association, London, 1962, p. 181.

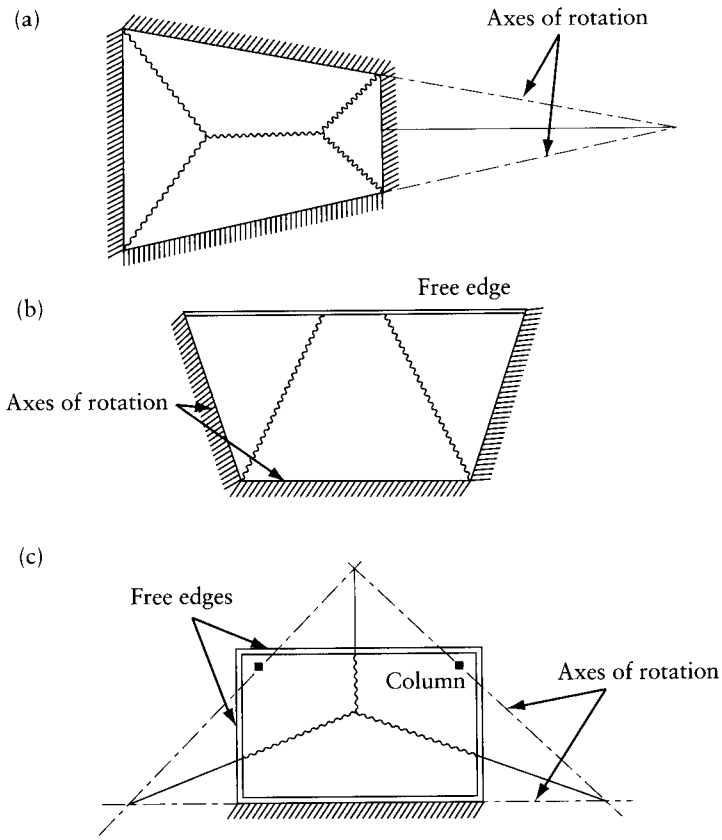

Figure 19.1 Typical fracture patterns in slabs. (a) Slab simply supported on four sides. (b) Slab simply supported on three sides and free along the fourth side. (c) Slab simply supported on two columns and on one side.

The basic fundamentals and main assumptions of the yield-line theory are as follows:

1. At fracture, the bending moment per unit length along all the fracture lines is constant and equal to the yield value corresponding to the steel reinforcement. The fracture is assumed to occur due to the yield of the steel.
2. The slab parts rotate about axes along the supported edges. In a slab supported directly on columns, the axes of rotation pass through the columns. Figure 19.1 shows some typical fracture patterns.
3. At fracture, elastic deformations are small compared with the plastic deformations and are therefore ignored. From this assumption and the previous one, it follows that fractured slab parts are plane and therefore they intersect in straight lines. In other words, the yield lines are straight.
4. The lines of fracture on the sides of two adjacent slab parts pass through the point of intersection of their axes of rotation.

Figure 19.2 shows the fracture pattern of a uniformly loaded slab simply supported on three sides. It is readily seen that the pattern satisfies the requirements given above. Each of the three

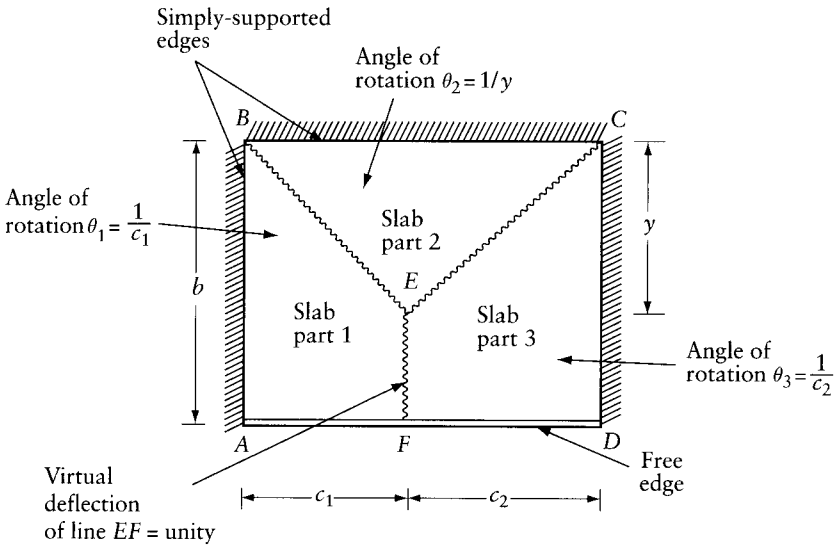

Figure 19.2 Angular rotation of slab parts.

slab parts rotates about its axis of rotation by an angle θ_i which is related to the rotation of the other parts. Let points E and F have a virtual downward displacement $w = 1$. The rotations of the slab parts are then

$$\theta_1 = \frac{1}{c_1} \quad \theta_2 = \frac{1}{y} \text{ and } \quad \theta_3 = \frac{1}{c_2}$$

19.2.1 Convention of representation

The different conditions of supports will be indicated thus:

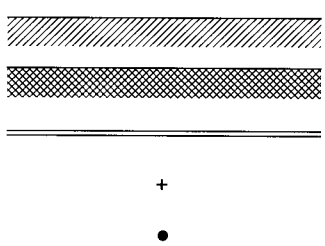

A positive ultimate moment m per unit length causes yield of the bottom reinforcement. A yield line formed by a positive moment is referred to as a positive yield line. Negative ultimate moment m' per unit length causes yield of the top reinforcement along a negative yield line.[3]

3 There are several methods of calculation of the value of the ultimate moment in terms of the depth, area of reinforcement and the strengths of concrete and of steel. Refer, for example, to the American Concrete Institute Standard 318–08 Building Code Requirements for Reinforced Concrete.

19.2.2 Ultimate moment of a slab equally reinforced in two perpendicular directions

Consider a slab reinforced in two perpendicular directions, x and y, with different reinforcement corresponding to ultimate positive moments m_1 and m_2 (Figure 19.3a). For equilibrium of the element shown in Figure 19.3b, the bending (m_α) and twisting (m_t) moments at a fracture line making an angle α with the x axis are

$$\left.\begin{aligned} m_\alpha &= m_1 \cos^2\alpha + m_2 \sin^2\alpha \\ m_t &= (m_1 - m_2) \sin\alpha \cos\alpha \end{aligned}\right\} \tag{19.1}$$

The moments are represented in Figure 19.3b (as usual) by double-headed arrows in the direction of the progress of a right-hand screw rotating in the same direction as the moment.

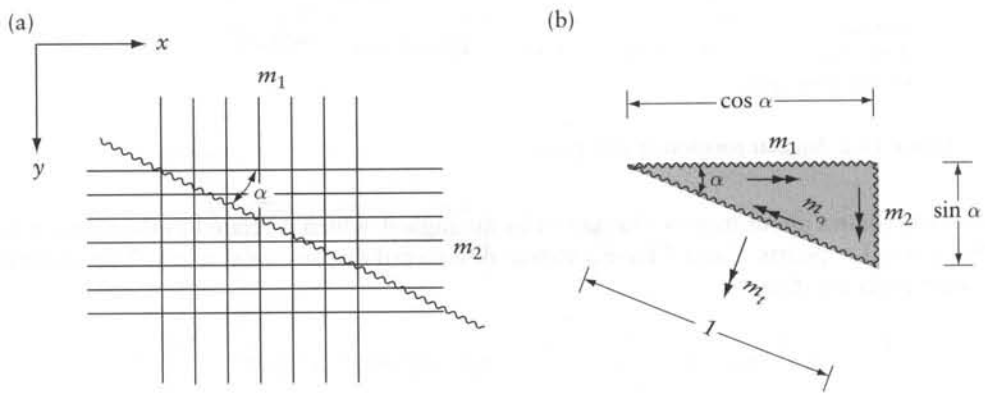

Figure 19.3 Moments at a fracture line inclined to the direction of reinforcement.

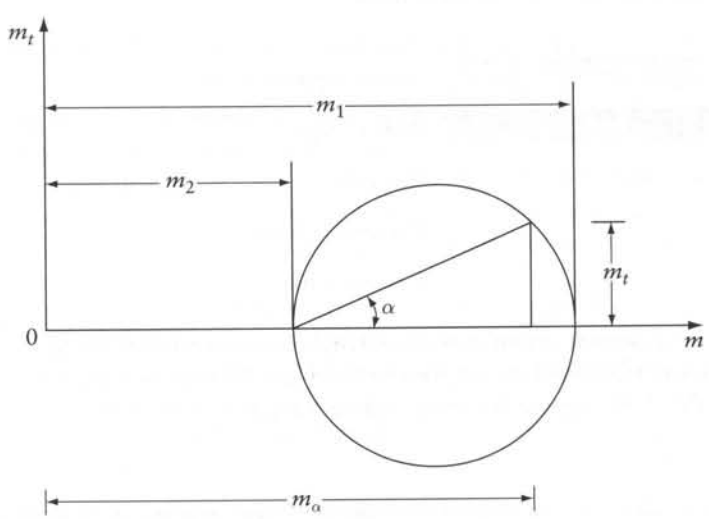

Figure 19.4 Moments on an inclined fracture line by Mohr's circle.

In an isotropic slab (that is, one equally reinforced in two perpendicular directions) $m_1 = m_2 = m$, and the moment on any inclined fracture line is

$$\left.\begin{aligned} & m_\alpha = m(\cos^2\alpha + \sin^2\alpha) = m \\ \text{and} \quad & \\ & m_t = 0 \end{aligned}\right\} \tag{19.2}$$

The values of m_α and m_t can also be determined by Mohr's circle as shown in Figure 19.4.

19.3 Energy method

In this method, the pattern of fracture is assumed and the slab is allowed to deflect in the fractured state as a mechanism. Each slab part will rotate a small virtual angle θ about its axis of rotation. The relation between the rotation of the slab parts is defined by the choice of the fracture pattern. The internal energy dissipated on the yield lines during the virtual rotation is equated to the external virtual work done in deflecting the slab. From this equation, the value of the ultimate moment is obtained. We should note, when calculating the internal energy, that only the ultimate moments in the yield lines do work during rotation.

The virtual-work equation (similar to the equation used for plastic analysis of frames, Chapter 18) gives either the correct ultimate moment or a value smaller than the correct value. In other words, if the virtual-work equation is used to find the ultimate load for a slab with an assumed bending resistance, then the value obtained will be an upper bound on the carrying capacity of the slab. This means that the solution obtained is either correct or unsafe. In practical calculations, one or two fracture patterns are assumed, and the value obtained is usually within 10 percent of the correct value. It seems to be a reasonable design procedure to increase the moment obtained by the work equation by a small percentage, depending on the number of trials and on the uncertainty of the chosen fracture pattern. The theoretical exact pattern is that for which the ultimate moment is a maximum. This can be reached, if we define the fracture pattern by certain parameters $x_1, x_2, \ldots$; the work equation will then give the value of m as a function of these parameters, i.e. $m = f(x_1, x_2, \ldots)$. The value of the parameters corresponding to the maximum moment is determined by partial differentiation: $(\partial f/\partial x_1) = 0$, $(\partial f/\partial x_2) = 0$, etc. This process can become laborious except for simple slabs in which the designer can define a reasonable pattern and proceed as suggested above.

The internal work done during a virtual rotation θ of a slab part is equal to the scalar product of a vector $\vec{M} = \vec{ml}$ and a vector $\vec{\theta}$ along the axis of rotation (Figure 19.5). The internal work for this slab part is then $\vec{M}.\vec{\theta} = ml\,(\cos\alpha)\theta$, where α is the angle between the two vectors. This means that, for any part of the slab, the internal work is equal to the rotation of that part multiplied by the projection of the ultimate moment upon the axis of rotation. It is sometimes convenient to consider the components of the moments in two perpendicular directions x and y in the plane of the slab. The total internal virtual work for all the slab parts is then

$$U = \sum \vec{M}.\vec{\theta} = \Sigma M_x.\theta_x + \Sigma M_y.\theta_y \tag{19.3}$$

where θ_x and θ_y are the x and y components of the rotation vector, and M_x and M_y are the x and y components of the vector $\vec{ml}$. The symbol U represents the work done by the plastic moment to produce rotation of the plastic hinge. The arrow shown on the yield line in Figure 19.5 represents the effect of the plastic hinge on the slab part; the moment exerted by the slab part on the plastic hinge is in the opposite direction.

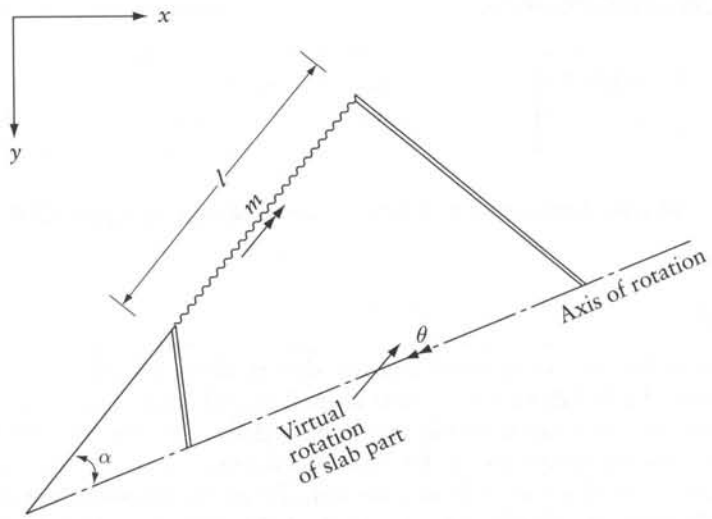

Figure 19.5 Data for calculation of internal virtual work.

If x and y are the coordinates of any point on the slab and w is the vertical displacement corresponding to the virtual rotation of the slab parts, then the total external virtual work is

$$W = \iint qw \, dx \, dy \tag{19.4}$$

where q is the load intensity. The virtual-work equation is

$$W = U \tag{19.5}$$

whence

$$\sum (M_x.\theta_x + M_y.\theta_y) = \iint qw \, dx \, dy \tag{19.6}$$

Example 19.1: Isotropic slab simply supported on three sides

Determine the ultimate moment of a square isotropic slab simply supported on three sides and subjected to a uniform load q per unit area.

Because of symmetry, the fracture pattern is fully determined by one parameter x, as shown in Figure 19.6. Let the junction of the three fracture lines have a virtual displacement $w = 1$. The rotations of the slab parts are

$$\theta_1 = \frac{1}{x} \quad \theta_2 = \theta_3 = \frac{2}{l}$$

The internal virtual work is

$$U = ml\frac{1}{x} + 2ml\frac{2}{l}$$

where the first term applies to Part 1 and the second to Parts 2 and 3.

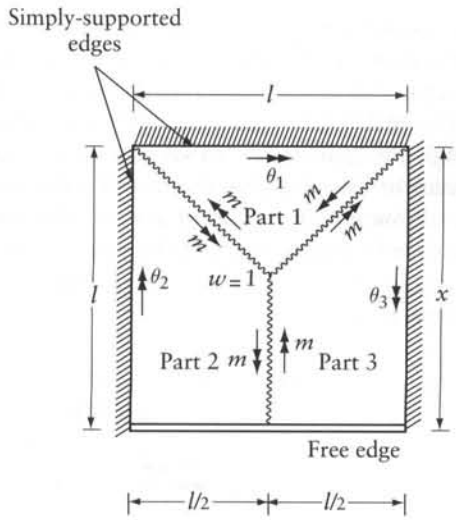

Figure 19.6 Slab considered in Example 19.1.

The work done by the distributed load is equal to the resultant on each part multiplied by the vertical displacement of its point of application. Thus,

$$W = q\left\{l\frac{x}{2}\frac{1}{3} + 2\left[(l-x)\frac{l}{2}\frac{1}{2} + \frac{xl}{4}\frac{1}{3}\right]\right\}$$

Here again, the first term is for Part 1 and the second term Parts 2 and 3. Equating the internal and external work,

$$m\left(\frac{l}{x} + 4\right) = ql^2\left(\frac{1}{2} - \frac{x}{6l}\right)$$

whence

$$m = ql^2\left[\frac{3 - \frac{x}{l}}{6\left(\frac{l}{x} + 4\right)}\right]$$

The maximum value of m is obtained when $dm/dx = 0$, which gives $x/l = 0.65$. The corresponding ultimate moment is

$$m = ql^2/14.1$$

19.4 Orthotropic slabs

The analysis of certain types of orthotropic slabs is simplified by Johansen to that of an isotropic affine slab for which the length of the sides and the loading are altered in certain ratios depending on the ratio of the ultimate resistance of the orthotropic slab in the two perpendicular directions.

Consider a part of a slab *ABCDEF* shown in Figure 19.7, limited by positive and negative yield lines and a free edge, assumed to rotate through a virtual angle θ about an axis of rotation $R - R$. Assume that the bottom and top reinforcement are placed in the x and y directions. Let the reinforcement in the y direction[4] provide ultimate moments of m and m', and let the corresponding values in the x direction be ϕm and $\phi m'$; this means that the ratio of the top to the bottom reinforcement is the same in both directions. The vectors $\vec{c}$ and $\vec{b}$ represent the resultants of the positive and negative moments respectively.

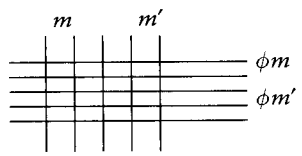

Moments of resistance provided by reinforcement in x and y directions

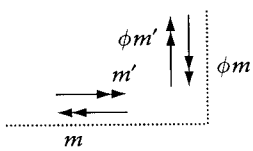

Ultimate moments: m and ϕm positive; m' and $\phi m'$ negative

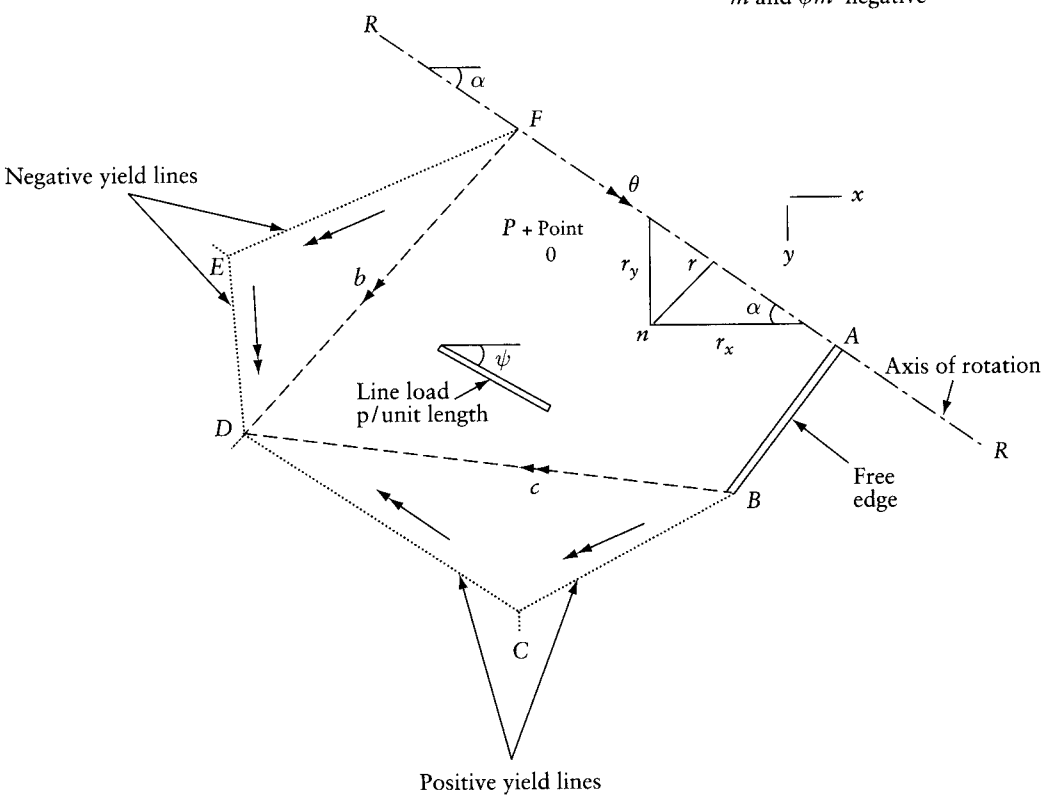

Figure 19.7 Conversion of an orthotropic slab to an isotropic affine slab.

4 The ultimate moments in the x and y directions are indicated by vectors in the right-hand top corner of Figure 19.7.

The internal virtual work for this slab part is

$$U = (mc_x + m'b_x)\,\theta_x + \phi(mc_y + m'b_y)\theta_y \tag{19.7}$$

where c_x, c_y and b_x, b_y are the projections in the x and y directions of the lengths c and b, and θ_x and θ_y are the x and y components of the rotation vector $\vec{\theta}$.

Assuming that the virtual deflection at a point n, distance r from the axis $R-R$, is unity, the rotation θ and its components can be written as

$$\theta = \frac{1}{r} \quad \theta_x = \theta\,\cos\alpha = \frac{1}{r_y} \quad \theta_y = \theta\,\sin\alpha = \frac{1}{r_x} \tag{19.8}$$

where α is the angle between the x axis and the axis of rotation. Substituting Eq. 19.8 into Eq. 19.7, we obtain

$$U = \theta[(mc_x + m'b_x)\,\cos\,\alpha + \phi(mc_y + m'b_y)\,\sin\,\alpha] \tag{19.9}$$

Let us assume now that the loading on the slab part consists of a uniformly distributed load q per unit area, a line load p per unit length on a length l in a direction making an angle ψ with the x axis and a concentrated load P at point O. The external virtual work of the loads on this slab part is

$$W = \iint qw\,dx\,dy + \int pw_l\,dl + Pw_p \tag{19.10}$$

where w is the deflection at any point (x, y), w_l deflection of any point below the line load, and w_P the deflection below the concentrated load. The integration is carried out for the whole area and for the loaded length. The virtual-work equation is

$$\sum\left[(mc_x + m'b_x)\frac{1}{r_y} + \phi(mc_y + m'b_y)\frac{1}{r_x}\right] = \sum\left(\int\int qw\,dx\,dy + \int pw_l dl + Pw_p\right) \tag{19.11}$$

where the summation is for all slab parts.

Consider an affine slab equally reinforced in the x and y directions so that the ultimate positive and negative moments are m and m' respectively. Suppose that this affine slab has all its dimensions in the x direction equal to those of the actual slab multiplied by a factor λ. The pattern of fracture remains similar and the corresponding points can still have the same vertical displacements. The internal virtual work for the part of the affine slab is

$$U' = (m\lambda c_x + m'\lambda b_x)\frac{1}{r_y} + (mc_y + m'b_y)\frac{1}{\lambda r_x} \tag{19.12}$$

Let the loading on the affine slab be a distributed load of q' per unit area, a line load p' per unit length, and a concentrated load P'. The external work for this part of the affine slab is

$$W' = \iint q'w\lambda\,dx\,dy + \int p'w_l\sqrt{(dy)^2 + \lambda^2(dx)^2} + P'w_p \tag{19.13}$$

Dividing both the internal and external work by λ will not change the work equation, which then becomes

$$\sum(mc_x + m'b_x)\frac{1}{r_y} + \frac{1}{\lambda^2}\sum(mc_y + m'b_y)\frac{1}{r_x}$$
$$= \sum\left(\int\int q'w\,dx\,dy + \int p'w_l\sqrt{\frac{(dy)^2}{\lambda^2} + (dx)^2} + \frac{P'}{\lambda}w_p\right) \tag{19.14}$$

All terms of the virtual-work Eqs. 19.11 and 19.14 are identical provided that

$$\phi = \frac{1}{\lambda^2} \text{ or } \lambda = \sqrt{\frac{1}{\phi}} \tag{19.15}$$

$$q' = q \tag{19.16}$$

$$p'\sqrt{\frac{(dy)^2}{\lambda^2} + (dx)^2} = p\,dl$$

or

$$p' = \frac{p}{\sqrt{\phi\sin^2\psi + \cos^2\psi}} \tag{19.17}$$

and

$$P' = P\sqrt{\frac{1}{\phi}} \tag{19.18}$$

It follows that an orthotropic slab with positive and negative ultimate moments m and m' in the x direction and ϕm and $\Phi m'$ in the y direction, can be analyzed as an isotropic slab with moments m and m' but with the linear dimensions in the x direction multiplied by $\sqrt{1/\phi}$. The intensity of a uniformly distributed load remains the same. A linear load has to be multiplied by $(\phi\sin^2\psi + \cos^2\psi)^{1/2}$, with ψ being the angle between the load line and the x axis. A concentrated load has to be multiplied by $\sqrt{1/\phi}$.

Example 19.2: Rectangular slab

A rectangular orthotropically reinforced slab is shown in Figure 19.8a. Find the dimensions of an isotropic affine slab.

We have $\phi = \frac{1}{2}$, so that side AB is to be changed to $l\sqrt{1/\phi} = 1.414l$ for an isotropic affine slab with ultimate moments of $2m$ and $2m'$. The same orthotropic slab can also be analyzed as an isotropic slab for which side AB remains unchanged and side AD is changed to $(3l/4)/\sqrt{2} = 0.530l$, the ultimate moments being m and m' (Figure 19.8c).

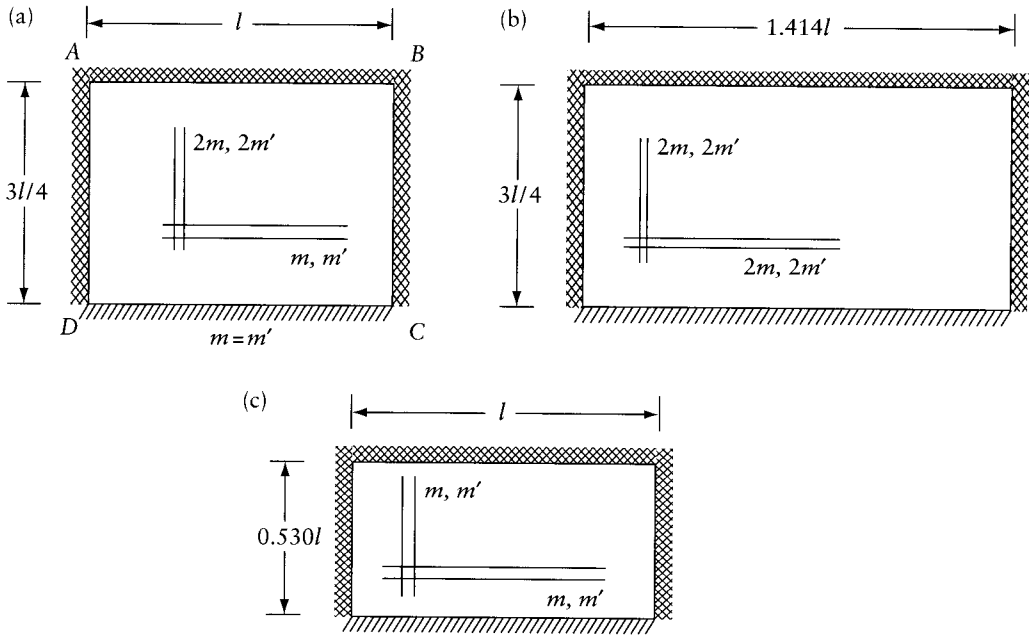

Figure 19.8 Orthotropic slab and affine slabs considered in Example 19.2. (a) Orthotropic slab. (b) Affine slab. (c) Alternative affine slab.

19.5 Equilibrium of slab parts

The energy method of the last two sections gives, it will be remembered, an upper-bound value to the collapse load and can always be used for any assumed mechanism of collapse. Where the mechanism is complex and its layout is defined by several initially unknown dimensions, the algebraic manipulation necessary to obtain a solution can be long and tedious. There can, however, be a saving of work in many cases by considering the equilibrium of the slab parts.

In this approach, we abandon the virtual-work equations of the energy method and consider instead the equilibrium of each slab part when acted upon by the external applied load, and by the forces acting at a fracture line. In general, these are: bending moment, shearing force acting perpendicular to the slab plane, and twisting moment.

To establish the equilibrium conditions it is not necessary to know the precise distribution of the shear and of the twisting moment: they can be replaced by two forces perpendicular to the plane of the slab, one at each end of the fracture line. These two forces are referred to as nodal forces and are denoted by V; they are considered positive when acting upwards.

19.5.1 Nodal forces

The formulas given here follow the original theory of Johansen. There are some restrictions on their use, although in the majority of cases they give a satisfactory solution. These restrictions have been studied by Wood and Jones.[5]

5 "Recent Developments in Yield Line Theory." *Magazine of Concrete Research*, May 1965. See also Jones, L. L. and Wood, R. H., "Yield Line Analysis of Slabs," Thames and Hudson, Chatto and Windus, London, 1967, p. 405.

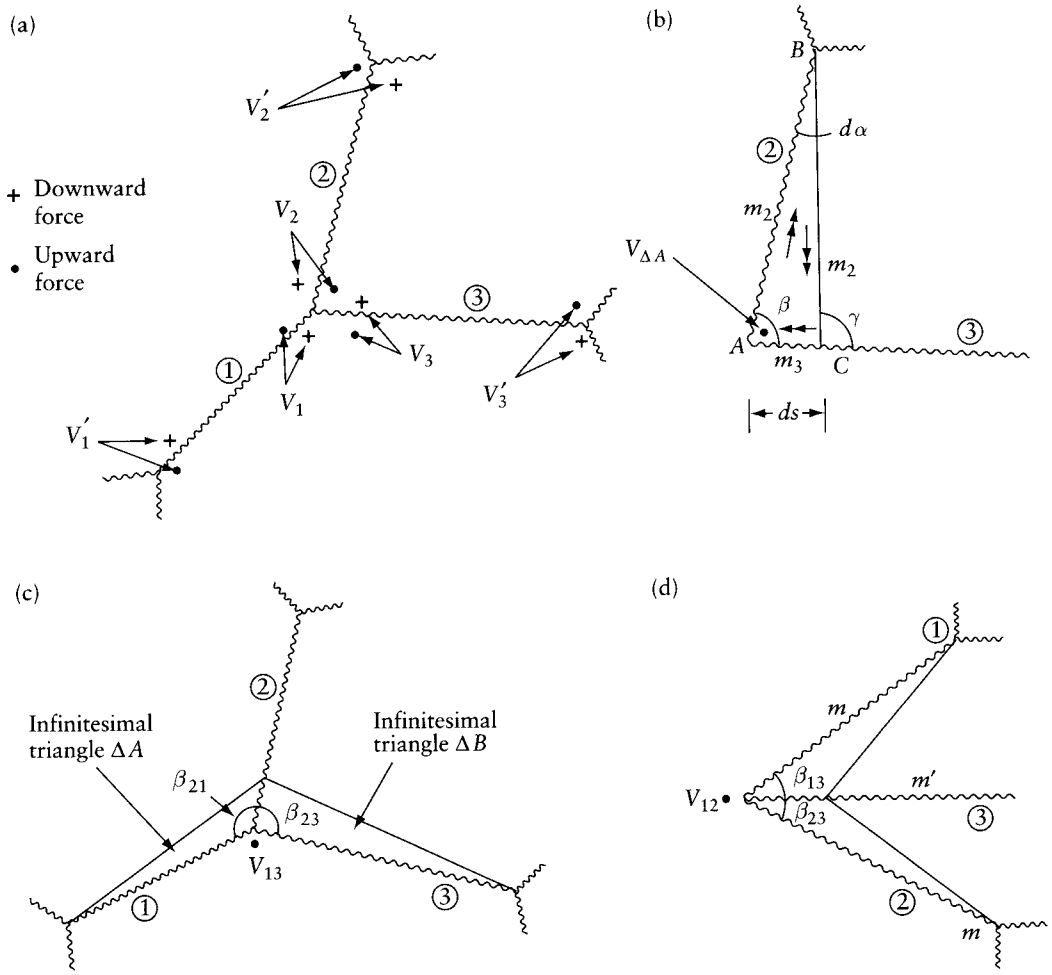

Figure 19.9 Nodal forces at a junction of fracture lines.

In Figure 19.9a the shears and twists on fracture lines (1), (2), and (3) are represented by the equivalent nodal forces V_1 and V_1', etc., on ends of lines (1), (2), and (3). The nodal forces are equal and opposite on the two sides of each fracture line. It follows that a summation of all the nodal forces at any junction of the fracture lines is zero.

Consider an elemental triangle ABC of area ΔA limited by positive fracture lines (2) and (3) (Figure 19.9b) and any adjacent line at a small angle $d\alpha$ to fracture line (2). This adjacent line is assumed to have the same bending moment m_2 as line (2) to a first-order approximation. The resultant moment on the triangle $\Delta\alpha$ is $(m_3 - m_2)\,ds$ directed from C to A. For equilibrium of the triangle ABC, the moments about BC vanish:

$$V_{\Delta A}\,ds\,\sin\gamma + (m_3 - m_2)ds\cos(180° - \gamma) - dP\frac{ds\,\sin\,\gamma}{3} = 0$$

where $V_{\Delta A}$ is the nodal force at A replacing the twisting moment and shearing force on the fracture line (2) and the length ds of the fracture line (3), and dP is the external load on the

triangle ABC, assumed to be uniformly distributed. As the triangle ΔA tends to zero, $\gamma \to \beta$ and $dP \to 0$, so that

$$V_{\Delta A} = (m_3 - m_2)\cot\beta \tag{19.19}$$

The general form of this equation is

$$V_{\Delta A} = (m_{ds} - m_{\text{long side}})\cot\beta(\text{acting upward}) \tag{19.20}$$

where the subscripts of m indicate the bending moment per unit length on the sides ds and on the long side of the infinitesimal triangle.

Equation 19.20 can be used to find the value of the nodal force V between any two lines at the junction of fracture lines. The nodal force between lines (1) and (3) in Figure 19.9c is equal and opposite to the sum of the two nodal forces $V_{\Delta A}$ and $V_{\Delta B}$ of the infinitesimal triangles ΔA and ΔB, that is,

$$V_{13} = -V_{\Delta A} - V_{\Delta B}$$

or

$$V_{13} = -(m_2 - m_1)\cot\beta_{21} - (m_2 - m_3)\cot\beta_{23} \tag{19.21}$$

It follows from the above that, when the reinforcement is equal in two orthogonal directions, the moments are $m_1 = m_2 = m_3 = m$, and all the nodal forces are zero at the junction of fracture lines of the same sign.

At a junction where two positive fracture lines (1) and (2) meet one negative fracture line (3) in an isotropic slab (Figure 19.9d) the nodal forces are

$$V_{12} = -(-m' - m)\cot\beta_{13} - (-m' - m)\cot\beta_{23}$$

or

$$V_{12} - (m' + m)(\cot\beta_{13} + \cot\beta_{23}) \tag{19.22}$$

where m' is the absolute value of the bending moment on the negative fracture line. Similar equations can be written for the forces between other lines. When a fracture line meets a free or simply-supported edge (Figure 19.10a), we have $V_{12} = m\cot\beta$. When the fracture line is positive, the nodal force V is downward in the acute angle.

If the edge rotation is restrained or otherwise subjected to a negative moment m' (Figure 19.10b), the nodal force is $V_{12} = (m + m')\cot\beta$, acting downward in the acute angle.

19.6 Equilibrium method

As mentioned earlier, the slab parts are in equilibrium under the effect of the external loading, the moments on the yield lines, the nodal forces, and the support reactions. For each slab part, three equations of equilibrium can be written, viz. two moment equations about two axes in the plane of the slab and an equation for the forces perpendicular to the plane of the slab, each of which adds up to zero.

The fracture pattern for a slab is completely defined if the axes of rotation are known, together with the ratios of the rotations $\theta_1, \theta_2, \ldots, \theta_n$ of slab parts when the mechanism acquires a small virtual deflection. For n parts, we require $(n-1)$ ratios. The fracture pattern in Figure 19.11a is

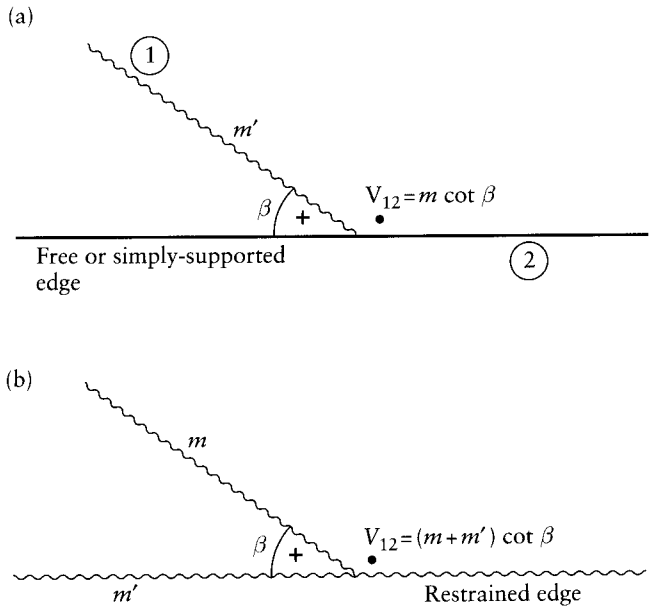

Figure 19.10 Nodal force at a free or simply-supported edge and at a restrained edge.

determined by drawing contour lines of the deflected mechanism. The contour line of deflection w is composed of n straight segments parallel to the axes of rotation and distant from them by w/θ_1, $w/\theta_2, \ldots, w/\theta_n$ (see Figure 19.11b). The intersections of the segments define points on the fracture lines.

For a part supported on one side, the position and magnitude of the reaction are unknown, thus representing two unknowns. For a part supported on a column, the axis of rotation passes through the column, but its direction is unknown and so is, of course, the magnitude of the reaction; hence, again, there are two unknowns for the part of the slab. For a nonsupported part, the direction and position of the axis of rotation are unknown, so that, once again, we have two unknowns.

For n parts of a slab the unknowns are: the value of the ultimate moment m, $(n-1)$ relations between the rotations of the parts, and two unknowns for each part. Hence, the total number of unknowns is $3n$, that is, the same as the number of equations of equilibrium (three for each part).

The formulation of the equilibrium equations becomes complicated except in simple cases such as the slabs considered below.

(a) Isotropic square slab, simply supported on four edges and carrying distributed load q per unit area. The fracture pattern is shown in Figure 19.12.
Taking the moment about a supported edge for one of the parts, we obtain

$$lm = \frac{ql^2 l}{4 \times 6}$$

whence

$$m = \frac{ql^2}{24} \tag{19.23}$$

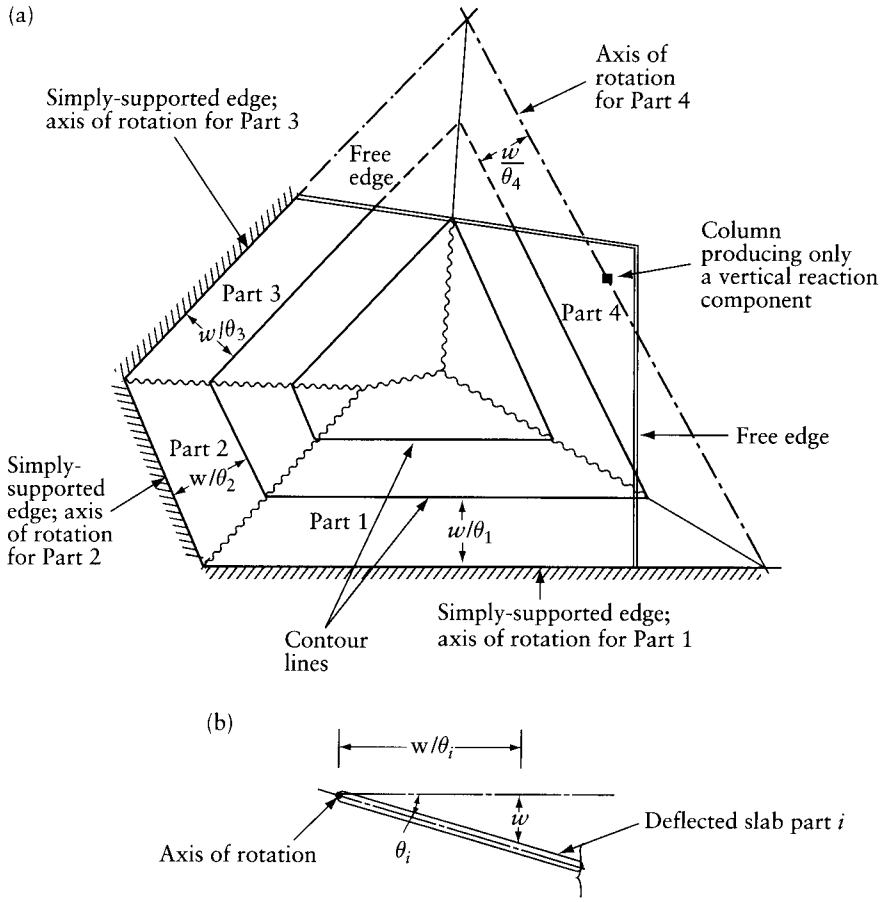

Figure 19.11 Determination of the fracture pattern from axes of rotation and the ratios between the virtual rotations of slab parts. (a) Fracture pattern. (b) Cross section through the *i*th slab part in a direction perpendicular to its axis of rotation.

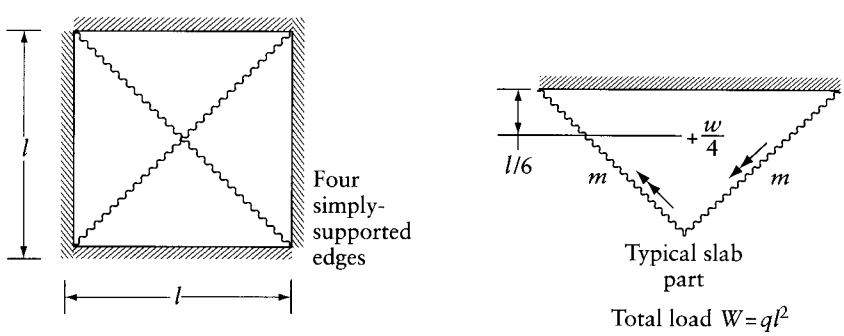

Figure 19.12 Equilibrium condition for an isotropic square slab under a uniformly distributed load of total magnitude W.

or

$$m = \frac{W}{24} \tag{19.23a}$$

where W is the total load.

(b) Isotropic polygonal slab simply supported on n equal sides, carrying a uniform load whose total magnitude is W. The fracture pattern is shown in Figure 19.13. Taking moments about the edge for any slab part, it can be shown that

$$m = \frac{W}{6n\tan(\pi/n)} \tag{19.24}$$

The values of the ultimate moment for simply-supported slabs in the form of different regular polygons are given in Figure 19.14. They are calculated by Eq. 19.24 with n tending to infinity for the circular slab.

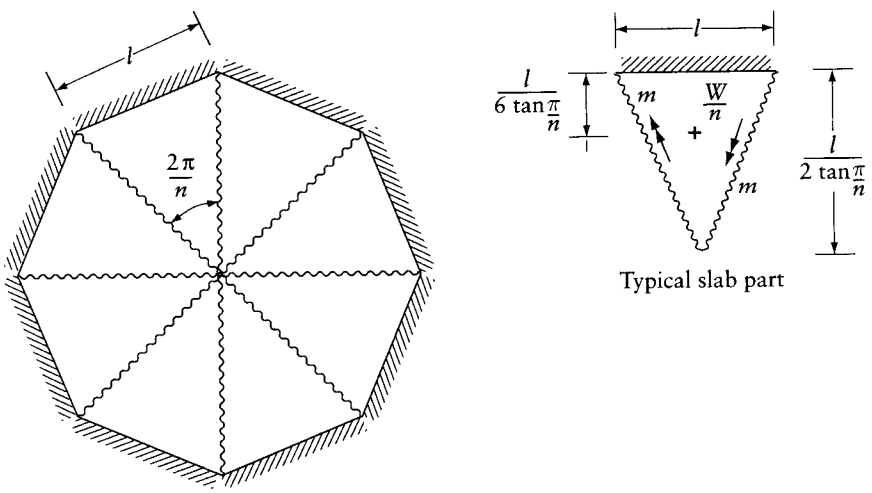

Figure 19.13 Equilibrium condition for an isotropic polygonal slab under uniformly distributed load of total magnitude W.

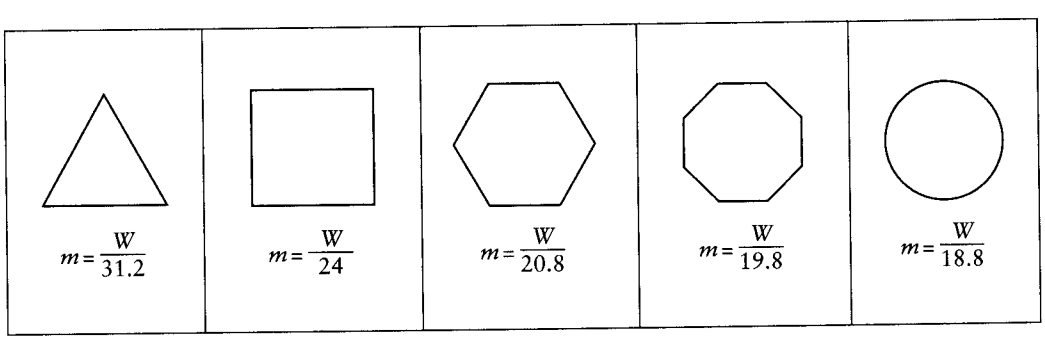

Figure 19.14 Ultimate moment for simply-supported polygonal slabs under a uniform load of total magnitude W.

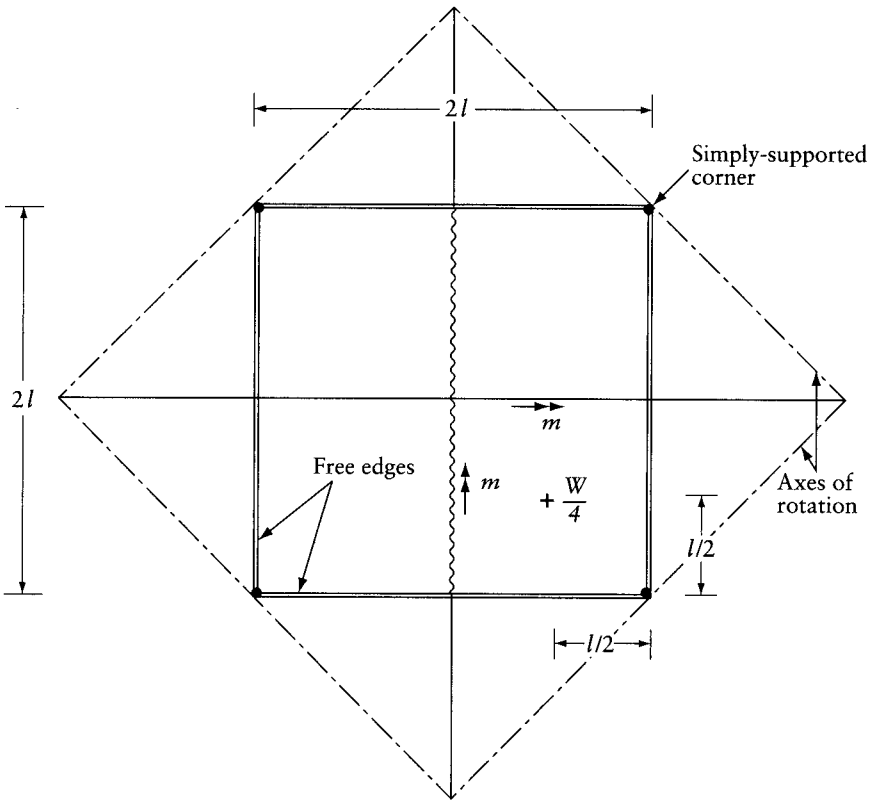

Figure 19.15 Equilibrium condition for an isotropic square slab supported at corners and carrying a uniformly distributed load of total magnitude W.

(c) Isotropic square slab simply supported at corners, carrying a uniform load whose total magnitude is W. Taking moment for one slab part (Figure 19.15) about the axis of rotation passing through the corner support and inclined at 45° to the edges, we find

$$m = \frac{W}{8}$$

19.7 Nonregular slabs

In the case of slabs of nonregular shape or loading, the calculation of the ultimate moment is as follows.

(a) A fracture pattern is assumed, and the corresponding ultimate moment is computed by considering the equilibrium of each slab part. A moment equation about the axis of rotation of each part will give different values of the ultimate moment. For the correct yield pattern, all yield moment values must be equal.

(b) In general, the ultimate moments computed for the first assumed fracture pattern are not equal and the values will indicate how the pattern should be corrected. The procedure is then repeated with a "more correct" pattern until the exact pattern is obtained. This then is an iteration method.

(c) If, for an assumed pattern, the values of the ultimate moment obtained by equilibrium considerations do not differ much from one another, the application of the work equation for this fracture mechanism will give a value of the ultimate moment very close to the correct answer.

Example 19.3: Rectangular slab with opening

Find the ultimate moment for the isotropic slab shown in Figure 19.16a. The ultimate positive and negative moments are equal.

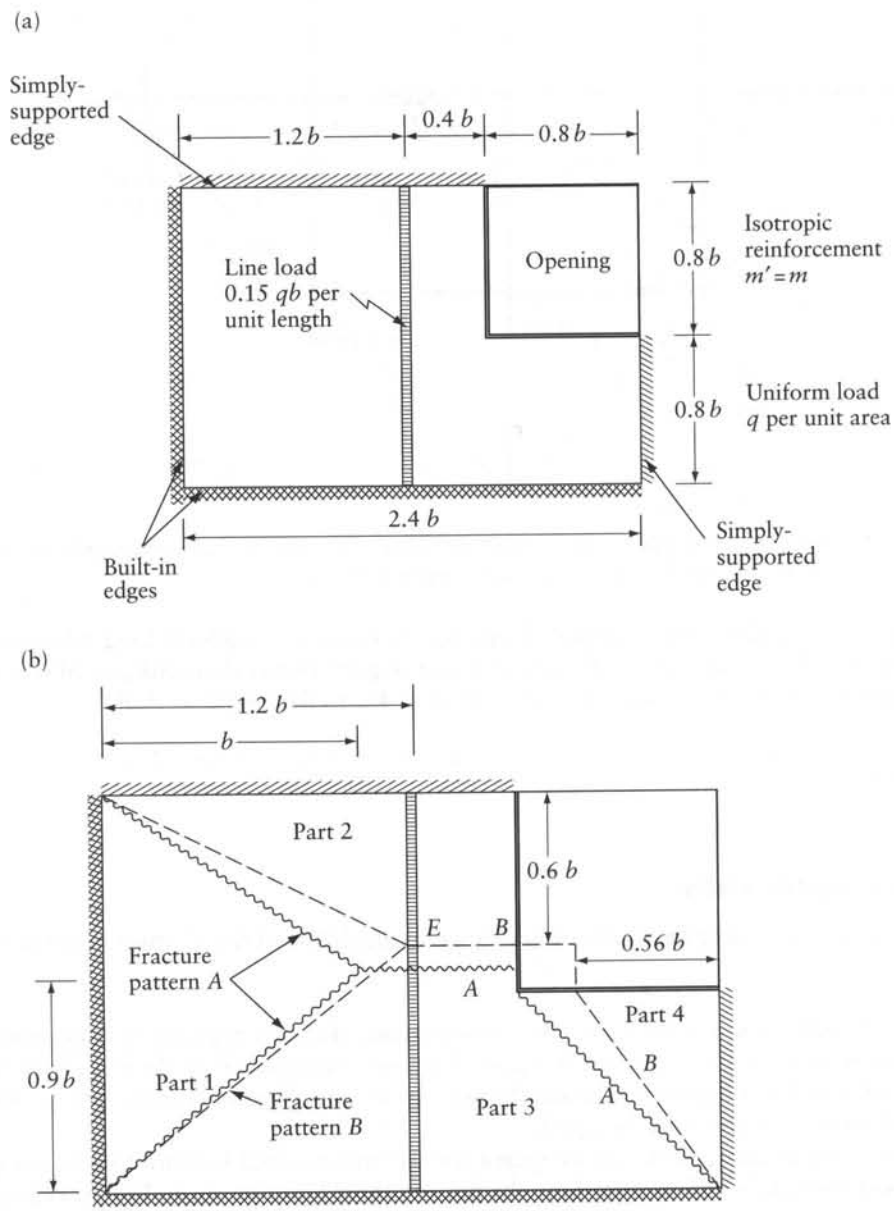

Figure 19.16 Slab analyzed in Example 19.3. (a) Slab dimensions and loading. (b) Fracture patterns.

For the first trial, we assume the fracture pattern *A* of Figure 19.16b. The only nodal forces that need to be considered are those at the intersection of the inclined fracture line from the slab corner with the free edge. A moment equation about the axis of rotation of each slab part gives

Part 1:

$$2m(1.6b) = \frac{q(1.6b)b^2}{6} \quad \therefore\ m = 0.0833qb^2$$

Part 2:

$$m(1.6b) = q\left[\frac{b(0.7b)^2}{6} + \frac{0.6b(0.7b)^2}{2} + 0.15qb\frac{(0.7b)^2}{2}\right] \quad \therefore\ m = 0.1659qb^2$$

Part 3:

$$2m(2.4b) = q\left[\frac{b(0.9b)^2}{6} + \frac{0.6b(0.9b)^2}{2} + \frac{0.8b(0.8b)^2}{6}\right]$$
$$+ 0.15qb\frac{(0.9b)^2}{2} - m\frac{0.8b}{0.8b}(0.8b) \quad \therefore\ m = 0.0936qb^2$$

Part 4:

$$m(0.8b) = q\frac{(0.8b)(0.8b)^2}{6} + m\frac{0.8b}{0.8b}(0.8b) \quad \therefore\ m = \infty$$

It is clear that the chosen pattern is not the correct one. However, the moment values for the various slab parts indicate the way in which we should move the yield lines to achieve a better result. Specifically, we can see that Parts 1 and 3 should be increased in size and Parts 2 and 4 decreased. The amended pattern *B* is therefore chosen for the second trial. The moment equation gives

Part 1:

$$2m(1.6b) = q\frac{(1.6b)(1.2b)^2}{6} \quad \therefore\ m = 0.1200qb^2$$

Part 2:

$$m(1.6b) = q\left[\frac{1.2b(0.6b)^2}{6} + \frac{0.4b(0.6b)^2}{2}\right] + 0.15qb\frac{(0.6b)^2}{2} \quad \therefore\ m = 0.1069qb^2$$

Part 3:

$$m(2.4b + 2.16b) = q\left[\frac{1.2bb^2}{6} + \frac{0.4bb^2}{2} + \frac{0.24b(0.8b)^2}{2} + \frac{0.56b(0.8b)^2}{6}\right]$$
$$+ 0.15qb\frac{b^2}{2} - m\frac{0.56b}{0.8b}(0.8b) \quad \therefore\ m = 0.1194qb^2$$

Part 4:

$$m(0.8b) = q\frac{(0.8b)(0.56b)^2}{6} + m\frac{0.56b}{0.8b}(0.56b) \quad \therefore\ m = 0.1025qb^2$$

Assuming that the mechanism corresponding to pattern B acquires a unit virtual deflection at point E, the corresponding rotation of slab parts will be $1/(1.2b)$, $1/(0.6b)$, $1/b$, and $1/(1.7b)$ for slab Parts 1, 2, 3, and 4 respectively. Equating the internal and external virtual work gives

$$2m(1.6b)\frac{1}{1.2b} + m(1.6b)\frac{1}{0.6b} + (2.4b + 2.6b)m\frac{1}{b} + m(0.8b)\frac{1}{0.7b} = q\left[1.2b(1.6b)\frac{1}{3} + 0.4b(1.6b)\frac{1}{2} + 0.24b(0.8b)\left(\frac{0.8b}{b}\right)\frac{1}{2} + 0.56b(0.8b)\left(\frac{0.8b}{b}\right)\frac{1}{3}\right] + 0.15qb(1.6b)\frac{1}{2}$$

whence $m = 0.1156qb^2$.

19.8 Strip method

We remember that the yield-line method of analysis for slabs always gives an upper bound to the true collapse load, though for certain simple cases the exact collapse load can be intuitively achieved by guessing the correct mechanism of failure. It is clear that for design purposes we might justifiably consider a lower bound to the true collapse load to be preferable.

Any lower-bound solution for a slab with given loading must have a moment field which satisfies the governing equilibrium equation at all points, and must not violate the particular yield criterion anywhere. The equilibrium equation in rectangular coordinates is (see Eq. 15.55)

$$\frac{\partial^2 M_x}{\partial x^2} + \frac{\partial^2 M_y}{\partial y^2} - 2\frac{\partial^2 M_{xy}}{\partial x \partial y} = -q \tag{19.25}$$

This equation must hold for both lower-bound and exact solutions regardless of the material properties of the slab, and it is evident that there is an infinite number of moment fields which satisfy Eq. 19.25. If we derive a complete moment field in equilibrium with the desired ultimate load and then provide reinforcement such that the ultimate moments of resistance at all points exceed or are equal to the equilibrium moments, then a lower-bound solution will be achieved. A yield-line analysis of the completed design will, of course, give an upper bound to the collapse load.

Because of the infinite number of possible equilibrium moment fields for a given slab and loading, and the difficulties of proportioning reinforcement in the cases where twisting moments are present, Hillerborg[6] suggested that the twisting moments M_{xy} be made zero at the outset of the analysis. In this case, the equilibrium Eq. 19.25 reduces to

$$\frac{\partial^2 M_x}{\partial x^2} + \frac{\partial^2 M_x}{\partial y^2} = -q \tag{19.26}$$

6 Hillerborg, A., "A Plastic Theory for the Design of Reinforced Concrete Slabs," *Proc. 6th Congr. Int Ass. Bridg. Struct. Eng.*, Stockholm, 1960; Hillerborg, A., "Jamviktsteori för Armerade Betongplattor," *Betong* 41(4) (1956), pp. 171–182.

and the load q is carried by strips running in the x and y directions. This strip method has been critically examined by Wood,[7] who found that if the reinforcement in the slab is curtailed so that precise correspondence between the ultimate moment field and the equilibrium moment field is obtained, then the strip method gives an exact correspondence between the design load and the collapse load.

To determine how the load is shared between the strips in the x and y directions, we partition Eq. 19.26 as follows:

$$\left.\begin{aligned} \frac{\partial^2 M_x}{\partial x^2} &= -\alpha q \\ \frac{\partial^2 M_y}{\partial y^2} &= -(1-\alpha) q \end{aligned}\right\} \tag{19.27}$$

where the parameter α governs the way in which load is dispersed at all points in the slab. This load-dispersion parameter may have any value between 0 and 1, and can vary from point to point in the slab. In practice, for simplicity of design, α will normally have a constant value in specified zones within the slab. Because we are now dealing with beam equations of the type of Eq. 19.27, the moment profiles are easily obtained.

Consider the design of a simply-supported slab shown in Figure 19.17a, which carries a uniformly distributed load q per unit area. We can assume the load-dispersion discontinuity

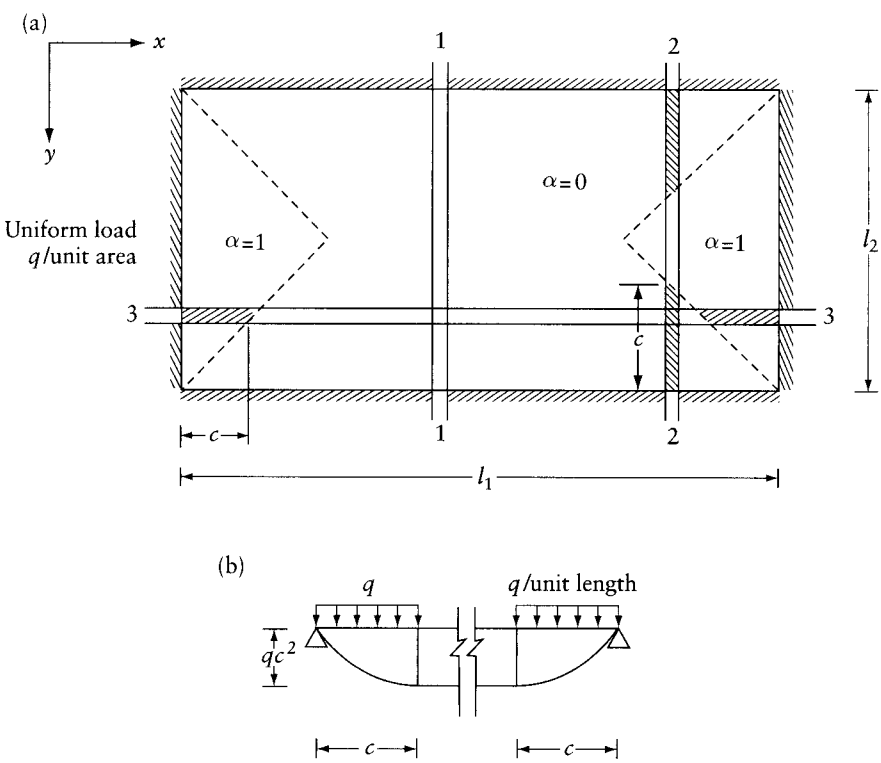

Figure 19.17 Loading in the strip method. (a) Assumed α values. (b) Loading and bending moment diagrams for strips of unit width, 2.2 and 3.3.

7 Wood, R. H. and Armer, G. S. T., "The Theory of the Strip Method for Design of Slabs," *Proc. I.C.E.* 41 (1968), pp. 285–311.

lines as shown in the figure: they are consistent with the major part of the slab spanning one-way in the short-span direction. The slab strip 1.1 carries then the full load q over its full length and the maximum moment will be $ql^2/8$. Slab strips 2.2 and 3.3 are loaded over the end regions only as shown in Figure 19.17b. In these cases, the maximum moment is $qc^2/2$, the moment being constant in the unloaded region.

Since the full bending moment pattern for the slab is known, the reinforcement can be provided at all points to ensure that the ultimate moment of resistance is greater than the calculated value. For efficiency in design, variable reinforcement in the end-loaded strips (Figure 19.17b) will be necessary. This is difficult to handle in practical cases and it is preferable to use reinforcement in distinct uniform bands.

19.9 Use of banded reinforcement

Wherever the load-dispersion discontinuity lines are not parallel to the support lines of the particular strip, the maximum moment varies from strip to strip. We can, however, ensure that the moment profiles for strips within a given bandwidth are the same by making the load-dispersion discontinuity lines parallel to the support lines of the band.

Consider again the simply-supported slab in Figure 19.17a. We know that the elastic curvature of the slab parallel to and near the edges is small and only small amounts of reinforcement need to be placed there. We choose then the load-dispersion zones of Figure 19.18a. The size of the various zones is quite arbitrary, as are the load-dispersion proportions in the corner regions.

The maximum moments in the four different bands are then

Strip 1.1 $M_{max} = ql^2/8$

Strip 2.2 $M_{max} = qc^2/4$

Strip 3.3 $M_{max} = qb^2/2$

Strip 4.4 $M_{max} = qb^2/4$

The reinforcement is provided accordingly, but it can be curtailed, if desired for economy reasons, in accordance with the moment profiles of Figure 19.18b.

One advantage of the strip method is that the reactions to strips are known and hence the loading on any supporting beam is immediately established. Continuity at the supports poses no difficulty; all that is necessary is to provide an arbitrary value of moment at these points, with consequent reduction in the interior slab moments. In the case of slabs having a free edge, all load dispersion adjacent to the free edge must take place parallel to the edge. This will necessitate in general a strong band of reinforcement parallel to the edge. Strips normal to the edge are supported on this strong band and on the remote support. Figure 19.19 shows an example of a slab with one free edge, the opposite edge continuous, and the remaining edges simply supported, and gives the moment profiles in the various bands of the slab. The uniformly distributed reaction, R, to strip 1.1 can be calculated once the continuity moment value has been fixed. The loading on strip 3.3 includes the reaction R in addition to the uniformly distributed external loading q.

Because of the large measure of freedom in using the strip method, the designer will find an appreciation of the elastic moment fields particularly useful. Provided the equilibrium moment field derived is not too far removed from that expected in elastic design, the working load behavior in terms of cracking and deflections will generally be satisfactory.

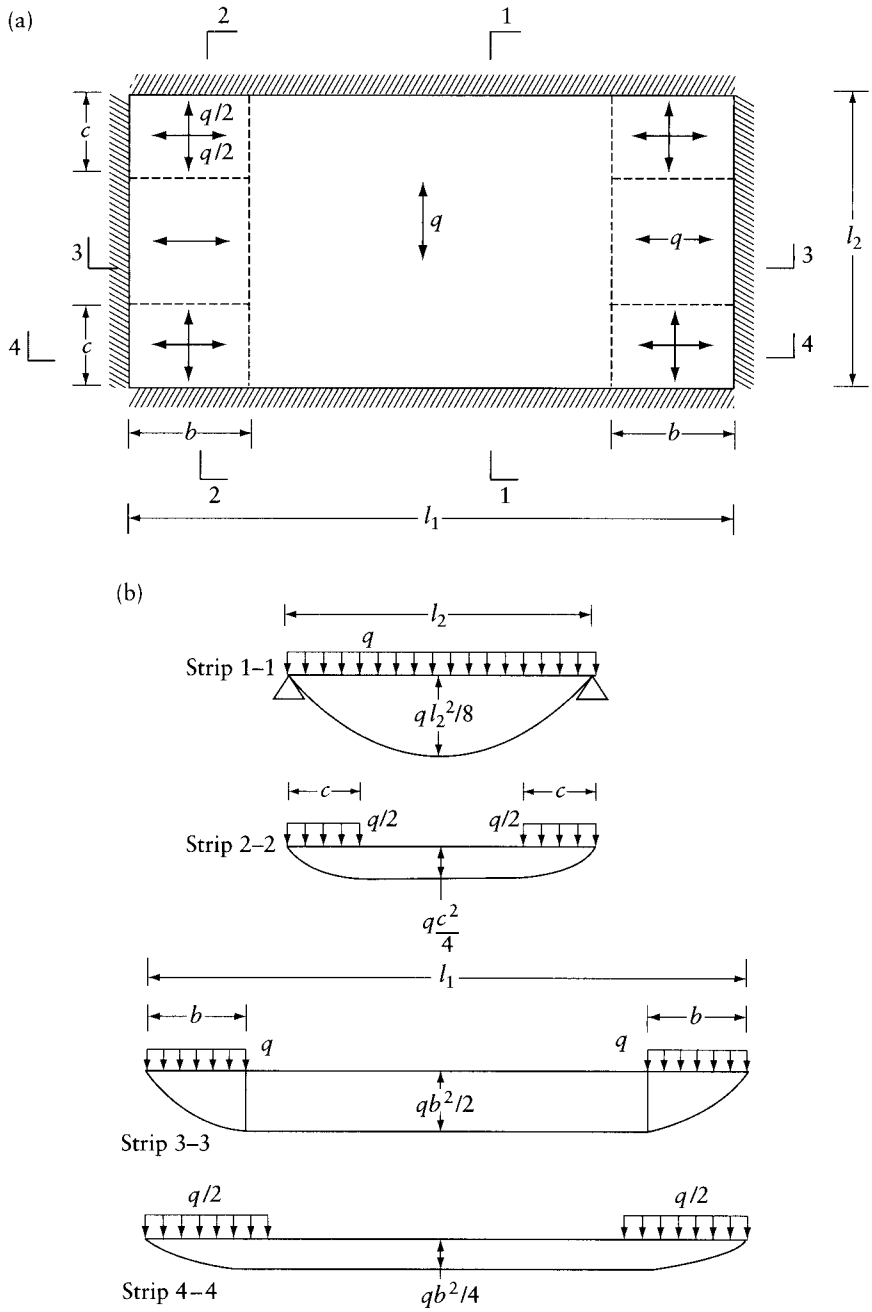

Figure 19.18 Load-dispersion zones and moment profiles for the slab in 19.17a. (a) Load-dispersion zones. (b) Loading and bending moment diagrams for strips of unit width.

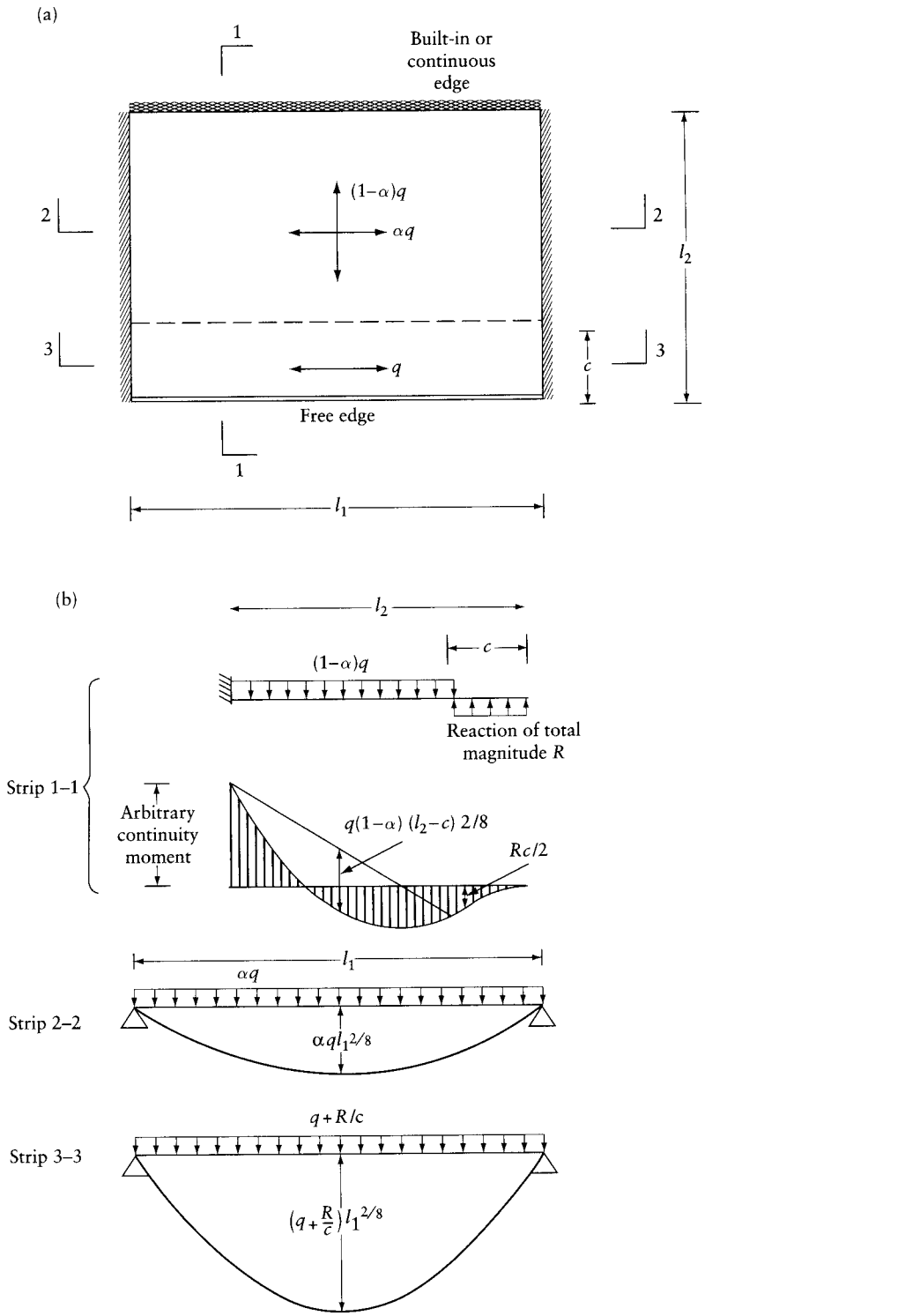

Figure 19.19 Strip method for a slab with a free edge. (a) Slab details and load dispersion. (b) Loading and bending moment diagrams for strips of unit width.

19.10 General

The methods considered in this chapter are of two basic types: the energy and equilibrium methods of yield-line theory are, strictly speaking, methods of analysis, while the strip method is a direct design procedure. For simple cases of slab geometry and loading, the yield-line method can be safely used as a design method since the fracture pattern to give an upper bound close to the correct collapse load can be readily obtained. For complex cases of geometry and loading, care must be exercised in the choice of fracture patterns, particularly where concentrated loads occur, since local modes of collapse, called fan modes, can occur. A fracture pattern involving fan modes will generally give lower collapse load than that obtained from the corresponding straight line pattern.

Although the collapse loads given by the yield-line method are theoretically upper-bound values, in practice the actual collapse load of a reinforced concrete slab may be above the calculated value because of the presence of various secondary effects.

It has been assumed in the analysis that Eq. 19.1 can be used for calculating the moment of resistance in a yield line at any angle to a set of orthogonal reinforcement. This method tends to underestimate the true moment of resistance which can be increased by up to 14 percent for the case of a yield line at 45° to an isotropic orthogonal set of reinforcement. The reason for this is that the analysis takes no account of kinking of reinforcement, which places the reinforcement almost at right angles to the fracture line and therefore increases the moment of resistance.

Where the boundaries of any slab are restrained from horizontal movement (as might occur in the interior panels of a continuous slab) the formation of the collapse mechanism develops high compressive forces in the plane of the slab with a consequent increase in carrying capacity. At very large deflections of the slab, it is possible finally to develop tensile membrane action where cracks go right through the slab so that the load is supported on the net of reinforcement.

These secondary effects will also occur in the actual behavior of slabs designed by the strip method. The strip method will always give a lower-bound or correct value for the collapse load depending on the degree of curtailment of reinforcement that the designer imposes. An advantage of the strip method is that the reactions on the supports to the slab are precisely determined.

Whenever variable reinforcement is required in a slab as a move toward efficiency, then the strip method is preferable, since economy can be readily achieved by suitable choice of the load-dispersion parameter. The use of the yield-line method with variable reinforcement involves the consideration of a large number of differing yield-line patterns.

Neither the yield-line method nor the strip method of ultimate load design guarantees satisfactory deflection and cracking behavior at working loads, though tests carried out on slabs designed by both methods generally exhibit satisfactory behavior. Distribution of reinforcement within the slab which is not too far removed from that expected with an elastic distribution of bending moments will generally ensure satisfactory working-load behavior. In the context of elastic analyses we should also remember that the bending moment distribution can change markedly for changes in the relative stiffnesses of the slab and its supporting beams and that many of the design tables based on elastic analyses are consistent only with nondeflecting supporting beams.

Problems

The representation of the different edge conditions of the slabs in the following problems is made according to the convention indicated in Section 19.21.

19.1 Using the yield-line theory, find the ultimate moment for the isotropic slabs shown in the figures under the action of uniformly distributed load. Show in a pictorial view the forces on the fractured slab parts in Prob. 19.1a. The columns in Prob. 19.1d and e are assumed to produce only a normal concentrated reaction component.

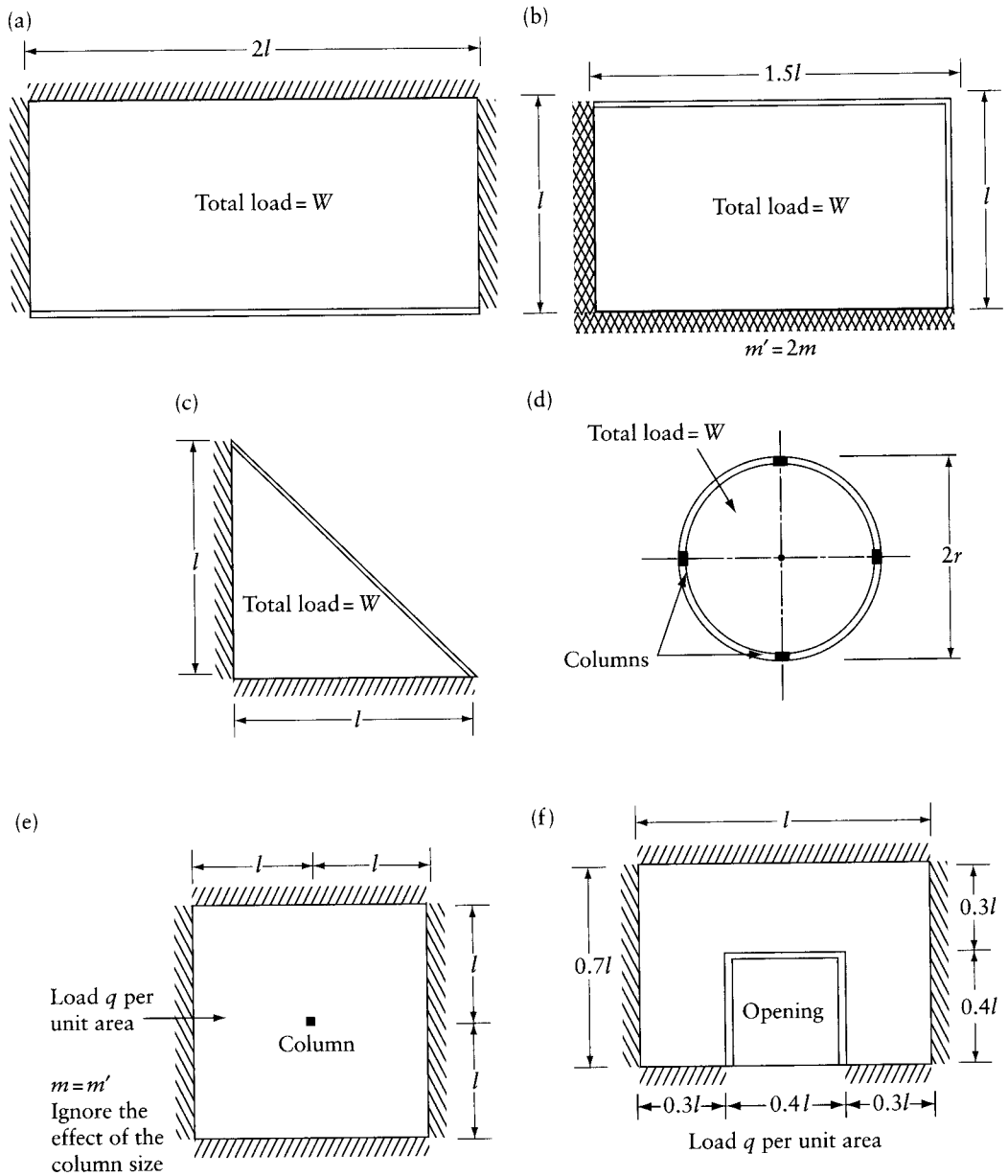

Prob. 19.1

19.2 Using the yield-line theory, find the ultimate moment for the slabs shown assuming the given ratio of reinforcement in each case. Assume that the columns in Prob. 19.2b produce only a normal concentrated reaction component.

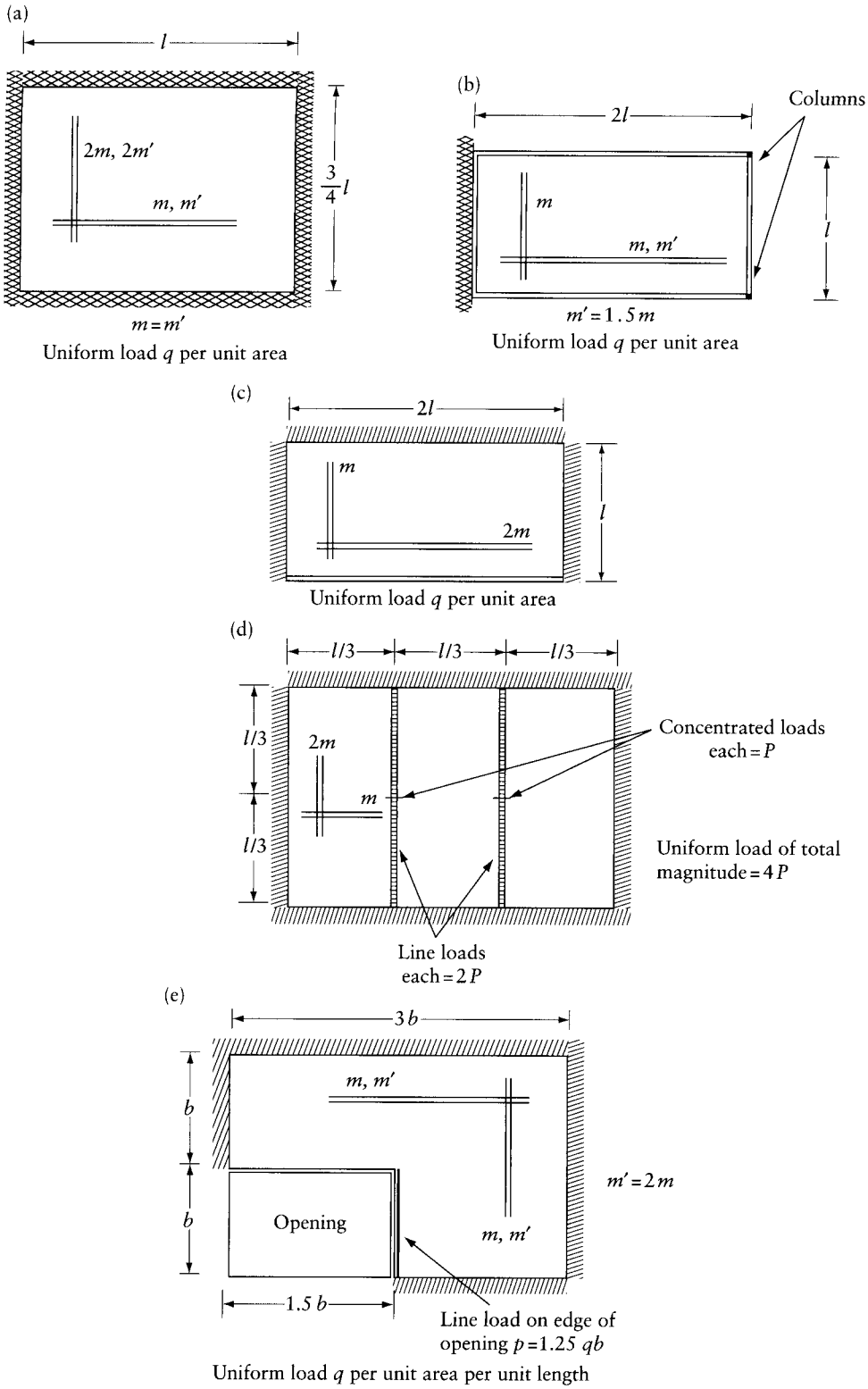

Prob. 19.2

Chapter 20

Structural dynamics

20.1 Introduction

The previous chapters dealt with structures subjected to static forces producing displacements that do not vary with time. We now consider dynamic problems, in which the forces are time dependent and cause vibration of the structure; hence, it is necessary to take into account the forces produced by the inertia of the accelerating masses. For this purpose we use Newton's second law of motion, which states that the product of the mass and its acceleration is equal to the force. In practice, dynamic loading is produced by seismic forces, nonsteady wind, blast, reciprocating machinery, or impact of moving loads.

An elastic structure disturbed from its equilibrium condition by the application and removal of forces will oscillate about its position of static equilibrium. Thus, the displacement at any point on the structure will vary periodically between specific limits in either direction. The distance of either of these limits from the position of equilibrium is called the "amplitude of the vibration." In the absence of external forces, the motion is called *free vibration*, and may continue with the same amplitude for an indefinitely long time. In practice, energy is lost through effects such as friction, air resistance, or imperfect elasticity, and these cause the amplitude to diminish gradually until motion ceases. These effects are termed *damping*, and this type of motion is then called *damped vibration*.

If external forces are applied, we have *forced motion*. This may be *damped* or *undamped*, depending on the presence or absence of these energy losses. In structural analysis, damping effects are modeled as *damping forces*, which are often assumed to be viscous (i.e. they are assumed to be proportional to the velocity). This is called "viscous damping" because the resistance of a liquid or a gas to a moving mass (at a low velocity) is proportional to the velocity.

20.2 Lumped mass idealization

In any structure, the mass is distributed throughout the structure and its elements, and thus the *inertial forces* are also distributed. This can cause difficulties, as seen in Figure 20.1a, where an infinite number of coordinates are required to define the displacement configuration. However, if we imagine that the beam mass is lumped into two bodies, with the force-displacement properties of the beam unchanged (Figure 20.1b), and assume that the external forces causing the motion are applied at these two masses, the deflected shape of the beam at any time can be completely defined by 12 coordinates, 6 at each mass (Figure 20.1c). The idealized model in Figure 20.1b, which has 12 degrees of freedom may, therefore, conveniently be considered in dynamic problems in place of the actual structure. A more accurate representation can be obtained by using a larger number of masses at closer intervals, but this requires a greater number of coordinates.

To demonstrate further the use of the lumped mass idealization, consider the motion of the multistorey frame in its own plane (Figure 20.2a). For the idealized model, we ignore axial

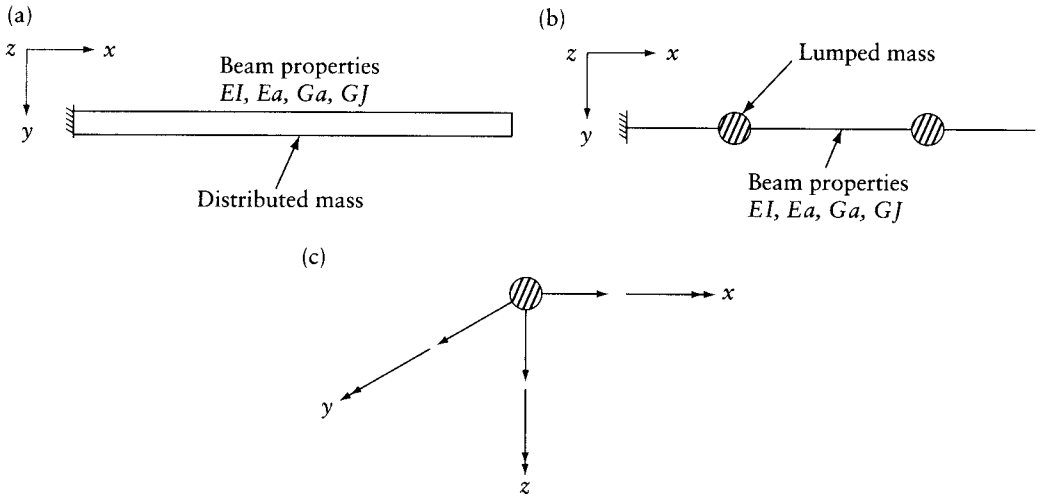

Figure 20.1 Idealization of a distributed mass by a lumped-mass system. (a) A vibrating beam has infinite degrees of freedom. (b) Idealization of the beam in part (a) into a lumped-mass system. (c) Typical degrees of freedom at a lumped mass.

deformations of the members, and distribute the mass of the columns to the adjacent floors, and assume that the total mass is mounted on a simple beam (Figure 20.2b), so that the mass can sidesway only. Typically, this mass will be the mass of the floor plus one-half of the mass of the columns and walls above and below the floor.

Let the horizontal displacements at floor levels at any time be $D_1, D_2, \ldots, D_i, \ldots, D_n$ and let the corresponding masses be $m_1, m_2, \ldots, m_i, \ldots, m_n$. As each degree of freedom of the frame is displaced, restraining forces will be developed as a function of the stiffness of the connecting elements (in this case, the columns), see Figure 20.2d. There may also be external forces, P_i, acting at the coordinates, which generally are functions of time. Thus, the total force acting on the ith mass is:

$$P_i - S_i D_i \tag{20.1}$$

Applying Newton's second law to the ith mass, we get:

$$m_i \ddot{D}_i = P_i - S_i D_i \tag{20.2}$$

where $\ddot{D}_i$, the acceleration of the ith mass, is equal to the second derivative of the displacement D_i with respect to time t, $(d^2 D_i/dt^2)$. Rearranging this equation for the ith mass gives the corresponding *equation of motion*:

$$m_i \ddot{D}_i + S_i D_i = P_i \tag{20.3}$$

For n masses, we can write this equation in matrix form:

$$[m]\{\ddot{D}\} + [S]\{D\} = \{P(t)\} \tag{20.4}$$

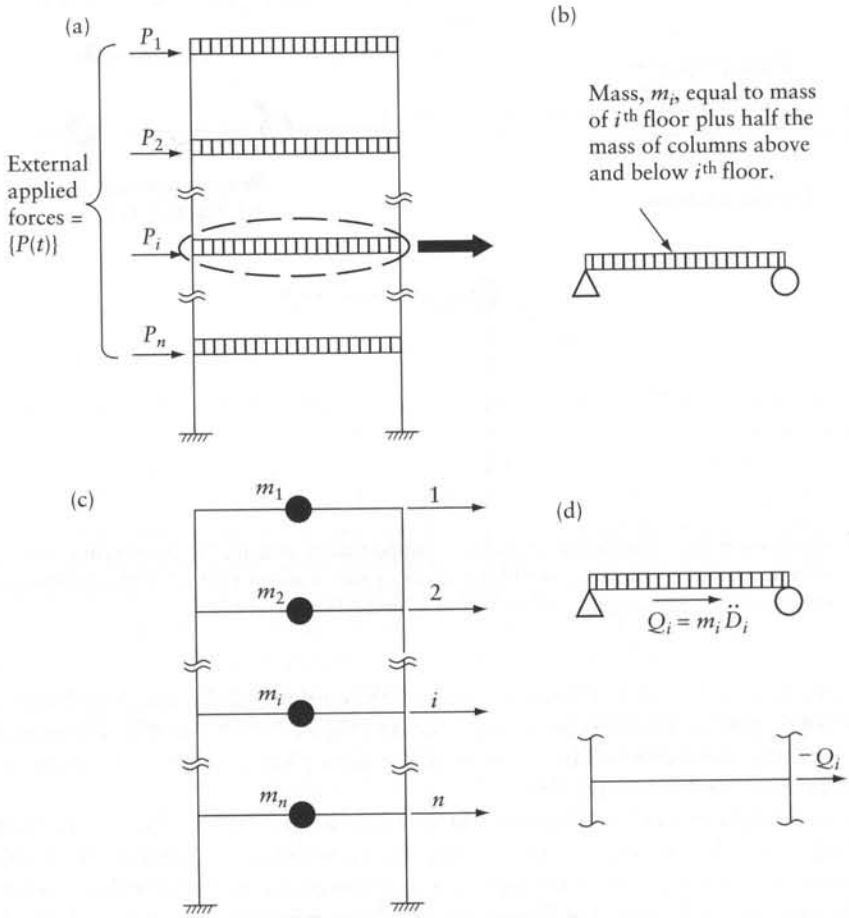

Figure 20.2 A multi-degree-of-freedom system. (a) Plane frame. (b) Idealization of the mass at a typical floor. (c) Coordinate system representing positive directions of forces and displacements. (d) Application of Newton's second law to the mass of the i^{th} floor.

where $[m]$ is a diagonal matrix:

$$[m] = \begin{bmatrix} m_1 & & & \\ & m_2 & & \\ & & \cdots & \\ & & & m_n \end{bmatrix} \tag{20.5}$$

When the system is vibrating freely, $\{P(t)\} = \{0\}$ and the equation of motion becomes (undamped free vibration):

$$[m]\{\ddot{D}\} + [S]\{D\} = \{0\} \tag{20.6}$$

Equations 20.4 and 20.6 are termed the *undamped multi-degree-of-freedom* equations of motion for forced and free vibration respectively. Corresponding equations for a single degree of freedom can be obtained by writing the equations in scalar form.

20.3 Consistent mass matrix

In the preceding section we saw that, when a structure is vibrating, the mass of the various structural elements is arbitrarily lumped at nodes, resulting in a diagonal mass matrix. The motion of these lumped masses must be related to the translations and rotations of the structural degrees of freedom. An alternative representation of the distributed mass can be achieved using the *consistent* mass matrix. The terms, m_{ij}, of the mass matrix represent the inertial force in the ith coordinate due to unit acceleration in the jth coordinate. Using displacement interpolation functions L_i (see Section 16.4) and the principle of virtual work, the term m_{ij} is given by:

$$m_{ij} = \int_{\text{vol}} \gamma L_i L_j \, dv \tag{20.7}$$

where $\gamma(x, y, z)$ is the mass per unit volume and dv is the elemental volume. It is apparent from the form of Eq. 20.7, that $m_{ij} = m_{ji}$, and the consistent mass matrix is symmetric.

As an example of the development of the consistent mass, consider a prismatic beam of cross-sectional area a and the four coordinates in Fig 20.3a, and use the displacement functions of Eq. 16.28, which can be written as:

$$[L] = \left[\left(1 - \frac{3x^2}{l^2} + \frac{2x^3}{l^3}\right) \quad \left(x - \frac{2x^2}{l} + \frac{x^3}{l^2}\right) \quad \left(\frac{3x^2}{l^2} - \frac{2x^3}{l^3}\right) \quad \left(-\frac{2x^2}{l} + \frac{x^3}{l^2}\right)\right] \tag{20.8}$$

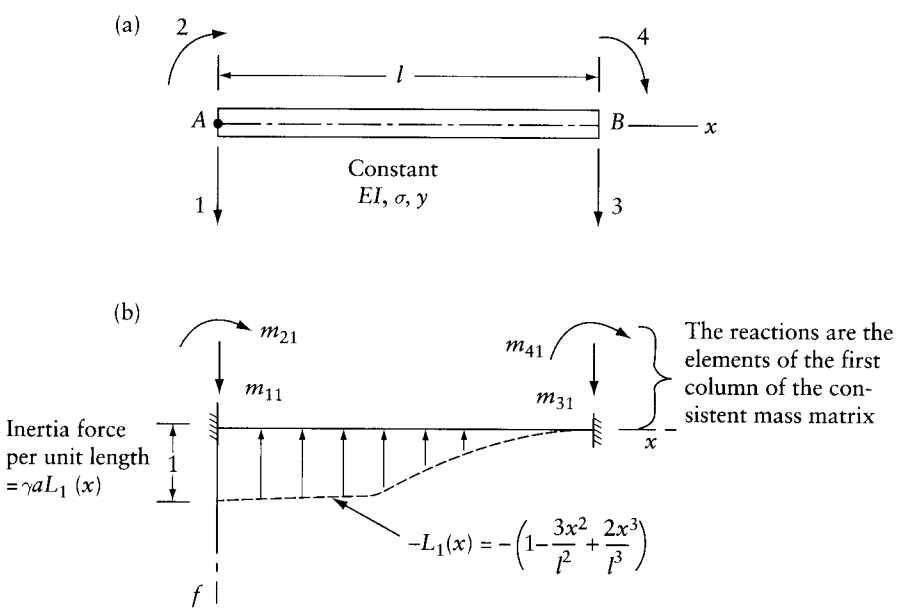

Figure 20.3 Derivation of the consistent mass matrix for a prismatic beam. (a) Prismatic beam of total mass γal. (b) Distributed inertia forces associated with acceleration $\ddot{D}_1 = 1$.

where l is the length of the beam. Equation 20.7 can be written as:

$$m_{ij} = \gamma a \int_0^l L_i L_j \, dx \tag{20.9}$$

Substituting for L_i and L_j from Eq. 20.8 into Eq. 20.9, the following consistent mass matrix is obtained:

$$[m] = \frac{\gamma a l}{420} \begin{bmatrix} 156 & & \text{symm.} & \\ 22l & 4l^2 & & \\ 54 & 13l & 156 & \\ -13l & -3l^2 & -22l & 4l^2 \end{bmatrix} \tag{20.10}$$

Figure 20.3b shows the inertia forces associated with $\ddot{D}_1 = 1$, with the motion prevented at the other coordinates defined in Figure 20.3a.

20.4 Undamped vibration: single-degree-of-freedom system

For a single-degree-of-freedom system, the undamped equation of motion, using the scalar version of Eq. 20.4, is:

$$m\ddot{D} + SD = P(t) \tag{20.11}$$

Examples of such a system are the frame in Figure 1.13c with the mass concentrated at the top, and the beam in Figure 20.1 with one lumped mass. The homogeneous case of this equation, with $P(t) = 0$, defines free vibration of a single-degree-of-freedom system:

$$m\ddot{D} + SD = 0 \tag{20.12}$$

This equation can be rewritten as:

$$\ddot{D} + \omega^2 D = 0 \tag{20.13}$$

where ω is the *natural frequency* of the single-degree-of-freedom system, with units of radian/sec:

$$\omega = \sqrt{S/m} \tag{20.14}$$

The solution to the differential equation (Eq. 20.13) is:

$$D = C_1 \sin \omega t + C_2 \cos \omega t \tag{20.15}$$

This equation represents periodic motion, where the *natural period of vibration*, T, is given by:

$$T = 2\pi/\omega \tag{20.16}$$

The reciprocal of the period T, $f = \omega/(2\pi)$, is called the *cyclic natural frequency*, and has units of cycle/s = Hertz.

The integration constants C_1 and C_2 in Eq. 20.15 can be determined from the initial conditions at time $t = 0$, of displacement D_0, and velocity $\dot{D}_0$. Substituting these values into Eq. 20.15 and its first derivative with respect to time, we obtain:

$$C_1 = \dot{D}_0/\omega \; ; \; C_2 = D_0 \tag{20.17}$$

The complete solution for the free vibration of a single-degree-of-freedom system is then:

$$D = \frac{\dot{D}_0}{\omega} \sin \omega t + D_0 \cos \omega t \tag{20.18}$$

The amplitude of vibration (Figure 20.4) is the maximum value of the displacement which, using Eq. 20.18, is:

$$D_{\max} = \overline{D} = \sqrt{D_0^2 + \left(\frac{\dot{D}_0}{\omega}\right)^2} \tag{20.19}$$

Equation 20.19 can be written in terms of the amplitude:

$$D = \overline{D} \sin (\omega t + \alpha) \tag{20.20}$$

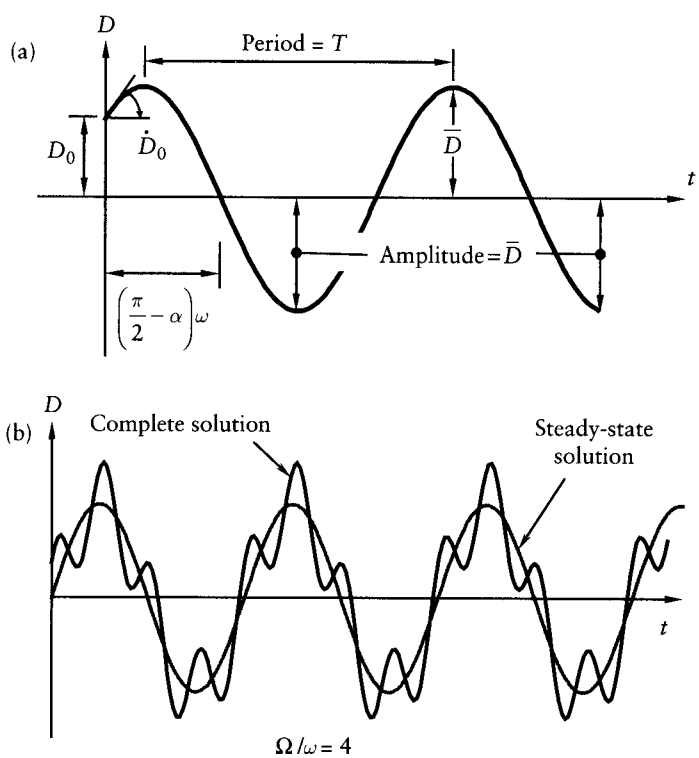

Figure 20.4 Displacement versus time of an undamped single-degree-of-freedom system. (a) Free vibration. (b) Motion forced by a force varying harmonically.

where α is called the *phase angle*, given as:

$$\alpha = \tan^{-1}\left(D_0\,\omega/\dot{D}_0\right) \tag{20.21}$$

A graph of D against t from Eq. 20.18 or Eq. 20.20 is shown in Figure 20.4a.

Example 20.1: Light cantilever with heavy weight at top

A water tower is idealized as a light prismatic cantilever fixed at the base having a lumped mass, $m = W/g$ at the top; where $W = 400\,\text{kN}$ and g = gravity acceleration $= 9.81\,\text{m/s}^2$. The length of the cantilever is $l = 50\,\text{m}$ and its flexural rigidity is $EI = 30 \times 10^9\,\text{N-m}^2$. Find the natural angular frequency ω and the natural period of vibration T. If motion is initiated by displacing the mass horizontally a distance D_0, then the system is left to vibrate, what is the displacement at $t = T/8$? What are the values of T with l reduced to 25 m or increased to 75 m?

The static force that produces unit drift at the tip of the cantilever (Appendix E):

$$S = 3EI/l^3 = 3\left(30 \times 10^9\right)/(50)^3 = 720 \times 10^3\,\text{N/m}$$

Equations 20.14, 20.16 and 20.18 give:

$$\omega = \sqrt{S/m} = \left[720 \times 10^3/\left(400 \times 10^3/9.81\right)\right]^{1/2} = 4.202\,\text{rad/s}$$

$$T = 2\pi/\omega = 2\pi/4.202 = 1.495\,\text{s};\quad D_{t=T/8} = D_0 \cos(\pi/4) = 0.707\,D_0$$

With $l = 25$, 50, and 75 m, $T = 0.529$, 1.495, and 2.747 s respectively; we can see that T is proportional to $l^{1.5}$.

20.4.1 Forced motion of an undamped single-degree-of-freedom system: harmonic force

When an external harmonic force is applied to a single-degree-of-freedom system, the equation of motion becomes:

$$m\ddot{D} + S\,D = P_0 \sin \Omega t \tag{20.22}$$

where P_0 is the force amplitude and Ω is the *impressed* or *forcing frequency*. This type of loading can be caused by centrifugal forces resulting from imbalance in rotating machines, but many periodic loads can be represented by a summation of harmonic loads, using Fourier analysis. Using the definition of ω from Eq. 20.14, Eq. 20.22 can be written as:

$$\ddot{D} + \omega^2 D = \frac{P_0}{m} \sin \Omega t \tag{20.23}$$

The solution of this equation consists of two components: the complementary solution (Eq. 20.15), and a particular solution, which is of the form:

$$D = C_3 \sin \Omega t \tag{20.24}$$

Substituting this solution into Eq. 20.24 and solving for C_3, and adding this solution to the homogeneous solution, the complete solution becomes:

$$D = C_1 \sin \omega t + C_2 \cos \omega t + \frac{P_0}{S}\left[\frac{1}{1-(\Omega/\omega)^2}\right] \sin \Omega t \tag{20.25}$$

The constants C_1 and C_2 are again determined from the initial conditions. The first and second terms of Eq. 20.25 are called the *transient response*, while the third term is called the *steady-state response*. The transient response is so-called because, under damped conditions, these terms rapidly decay to zero. However, for the undamped condition, for a single-degree-of-freedom system, which starts from rest at its equilibrium position, the constants are:

$$C_1 = -\frac{\Omega P_0}{\omega S}\left[\frac{1}{1-(\Omega/\omega)^2}\right] \; ; \; C_2 = 0 \tag{20.26}$$

The complete solution is then

$$D = \frac{P_0}{S}\left[\frac{1}{1-(\Omega/\omega)^2}\right]\left(\sin \Omega t - \frac{\Omega}{\omega} \sin \omega t\right) \tag{20.27}$$

This solution is plotted in Figure 20.4b, from which it may be seen that the transient solution is oscillating about the steady-state response (the last term in Eq. 20.25). The quantity P_0/S is the displacement of the system under a static load, P_0. The first bracket, $1/\{1-(\Omega/\omega)^2\}$, is termed the *amplification factor*. This factor is ~1.0 when the *frequency ratio* Ω/ω is close to zero, but is infinity when this ratio is 1.0. This condition is termed *resonance*, in which the amplitude of vibration increases indefinitely. In practice, damping will limit the maximum amplitude to finite values but these may still be large enough to cause damage to the system. As the frequency ratio becomes large, $\Omega/\omega >> 1$, the magnitude of the amplification factor decreases, eventually to zero.

20.4.2 Forced motion of an undamped single-degree-of-freedom system: general dynamic forces

Analysis for a general dynamic loading resulting from blasts, wind gusts, or seismic effects is accomplished by considering the loading as a sequence of *impulse* loads, and integrating for the effect of these impulses to obtain the system response. This integration can either be carried out in closed form, if the load function is fairly simple, or numerically, if the function is complex.

Consider the time-dependent loading shown in Figure 20.5, which begins to act at $t = 0$, when the mass is at rest; thus, $D_0 = 0$ and $\dot{D}_0 = 0$. At time $t = \tau$, we show an impulse: $I = P(\tau)\mathrm{d}\tau$. Such an impulse causes a change in momentum of the system. As the mass is constant, the change is in the velocity of the system:

$$\mathrm{d}\dot{D} = \frac{P(\tau)\,\mathrm{d}\tau}{m} \tag{20.28}$$

This change in velocity may be considered as an initial condition at time $t = \tau$, for which the subsequent displacement is given by Eq. 20.18 (initial velocity only):

$$\mathrm{d}D = \frac{\mathrm{d}\dot{D}}{\omega} \sin \omega (t - \tau) \tag{20.29}$$

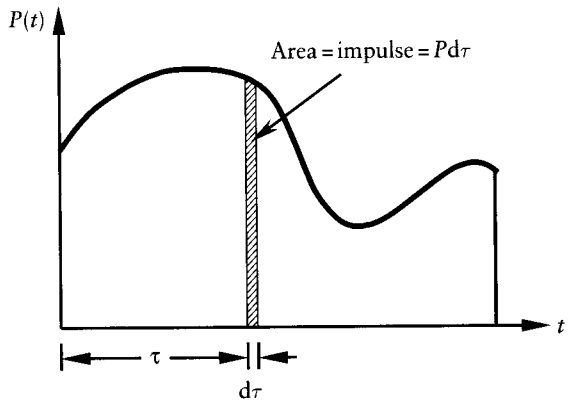

Figure 20.5 General force–time relation.

Substituting Eq. 20.29, and integrating from time $t = 0$, we obtain the displacement at time t for any arbitrary time-dependent load:

$$D = \frac{1}{m\omega} \int_0^t P(\tau) \sin \omega (t - \tau) \, d\tau \tag{20.30}$$

This is called the *Duhamel integral.* Using the trigonometric identity:

$$\sin \omega (t - \tau) = \sin \omega t \cdot \cos \omega \tau - \cos \omega t \cdot \sin \omega \tau$$

we can rewrite Eq. 20.30 in the form:

$$D = \frac{1}{m\omega} [\psi_1 (t) \sin \omega t - \psi_2 (t) \cos \omega t] \tag{20.31}$$

where $\psi_1 (t) = \int_0^t P(\tau) \cos (\omega\tau) \, d\tau$; $\psi_2 (t) = \int_0^t P(\tau) \sin (\omega\tau) \, d\tau$.

Depending on the nature of the function $P(\tau)$, these integrals may be evaluated in closed form, or numerically, using any numerical integration system (e.g. Simpson's rule).

20.5 Viscously damped vibration: single-degree-of-freedom system

Generally, the most widely used form of damping is *viscous damping*, where the actual damping effects are replaced by forces proportional to the velocity. Thus, the damping force is:

$$F_c = c\dot{D} \tag{20.32}$$

where c is the *damping coefficient*. The equation of motion for a viscously damped single degree of freedom then becomes (from Eq. 20.11):

$$m\ddot{D} + c\dot{D} + SD = P(t); \ \ddot{D} + 2\zeta\omega\dot{D} + \omega^2 D = P(t)/m \tag{20.33}$$

$$\zeta = c/(2m\omega) \tag{20.34}$$

where ω is the natural frequency (Eq. 20.14), and ζ is the damping ratio = ratio between the actual damping coefficient and the critical damping coefficient ($= 2m\omega$, discussed below).

20.5.1 Viscously damped free vibration

Setting $P(t)$ equal to zero in Eq. 20.33, we obtain the free vibration equation of motion for a damped system:

$$\ddot{D} + 2\zeta\omega\dot{D} + \omega^2 D = 0 \tag{20.35}$$

Substituting $D = e^{\lambda t}$, we obtain the characteristic equation:

$$\lambda^2 + 2\zeta\omega\lambda + \omega^2 = 0 \tag{20.36}$$

which has the roots:

$$\lambda_{1,2} = \omega\left(-\zeta \pm i\sqrt{1-\zeta^2}\right) \tag{20.37}$$

where $i = \sqrt{-1}$ and the solution to Eq. 20.35 becomes:

$$D = e^{-\zeta\omega t}\left(C_1 e^{i\omega_d t} + C_2 e^{-i\omega_d t}\right) \tag{20.38}$$

$$\omega_d = \omega\sqrt{1-\zeta^2} \tag{20.39}$$

where ω_d is the *damped natural frequency*; C_1 and C_2 are constants. Equation 20.38 can be rewritten using the relationships between trigonometric functions and exponential functions as:

$$D = e^{-\zeta\omega t}\left(\overline{C}_1 \sin\omega_d t + \overline{C}_2 \cos\omega_d t\right) \tag{20.40}$$

Using the initial conditions, D_0 and $\dot{D}_0$, Eq. 20.40 is written as:

$$D = e^{-\zeta\omega t}\left[\left(\frac{\dot{D}_0 + \zeta\omega D_0}{\omega_d}\right)\sin\omega_d t + D_0\cos\omega_d t\right] \tag{20.41}$$

When $\zeta = 1$, the system is said to be critically damping, with critical damping coefficient $= 2m\omega$. At critical damping, the initial displacement D_0 of a system, starting from rest, dies out gradually without oscillation. ζ is the ratio between the actual damping coefficient and the critical damping coefficient. For buildings and bridges, ζ varies between 0.01 and 0.2. Figure 20.6 illustrates this equation for a system that starts at rest with displacement D_0. The *natural period of damped vibration* is:

$$T_d = 2\pi/\omega_d = T/\sqrt{1-\zeta^2} \tag{20.42}$$

The ratio of the displacement at time t to that at time $t + T_d$ is constant and the natural logarithm of this ratio is called the *logarithmic decrement*, δ:

$$\delta = \ln\left(\frac{D_t}{D_{t+T_d}}\right) = \ln\left(e^{\zeta\omega T_d}\right) = \frac{2\pi\zeta}{\sqrt{1-\zeta^2}} \cong 2\pi\zeta \tag{20.43}$$

This property of the free vibration response of a damped system is often used as a means of estimating the damping ratio of real structures from measurements of the displacements.

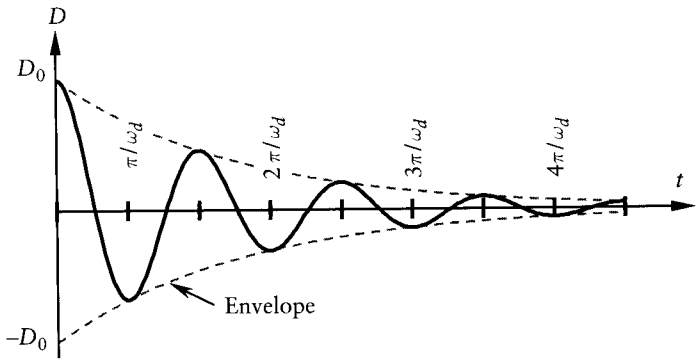

Figure 20.6 Damped free vibration, with $\dot{D} = 0$ at $t = 0$.

20.5.2 *Viscously damped forced vibration – harmonic loading: single-degree-of-freedom system*

When a damped single-degree-of-freedom system is subject to a harmonically applied load, the equation of motion becomes:

$$\ddot{D} + 2\zeta\omega\dot{D} + \omega^2 D = \frac{P_0}{m}\sin\Omega t \tag{20.44}$$

The complete solution of Eq. 20.44 consists of two parts, the complementary solution (as given by Eq. 20.40), and the particular solution representing the response to the harmonic force, given by:

$$D_{\text{Steady state}} = \frac{P_0}{S}\left\{\frac{[1-(\Omega/\omega)^2]\sin\Omega t - (2\zeta\Omega/\omega)\cos\Omega t}{[1-(\Omega/\omega)^2]^2 + (2\zeta\,\Omega/\omega)^2}\right\} \tag{20.45}$$

The complementary solution (Eq. 20.40) is also called the *transient solution*, and is damped out after a few cycles. The particular solution of Eq. 20.45 is called the *steady-state displacement* and it is this solution that defines the response of the system to the external load $P(t)$. Equation 20.45 can be written in terms of its displacement amplitude, $\overline{D}$, and phase angle, α:

$$D_{\text{Steady state}} = \overline{D}\sin(\Omega t + \alpha) \tag{20.46}$$

$$\overline{D} = \chi\frac{P_0}{S} \tag{20.47}$$

$$\alpha = \tan^{-1}\left[\frac{-2\zeta\Omega/\omega}{1-(\Omega/\omega)^2}\right] \tag{20.48}$$

$$\chi = \left[\left\{1-(\Omega/\omega)^2\right\}^2 + (2\zeta\Omega/\omega)^2\right]^{-1/2} \tag{20.49}$$

The complete solution of Eq. 20.44 is then given by the sum of Eqs. 20.40 and 20.46:

$$D = e^{-\zeta\omega t}(\overline{C}_1\sin\omega_d t + \overline{C}_2\cos\omega_d t) + \overline{D}\sin(\Omega t + \alpha) \tag{20.50}$$

The amplitude $\overline{D}$ of the steady-state displacement is equal to the static displacement (P_o/S) multiplied by the amplification factor, χ (Eq. 20.49). Figure 20.7 represents χ versus Ω/ω for

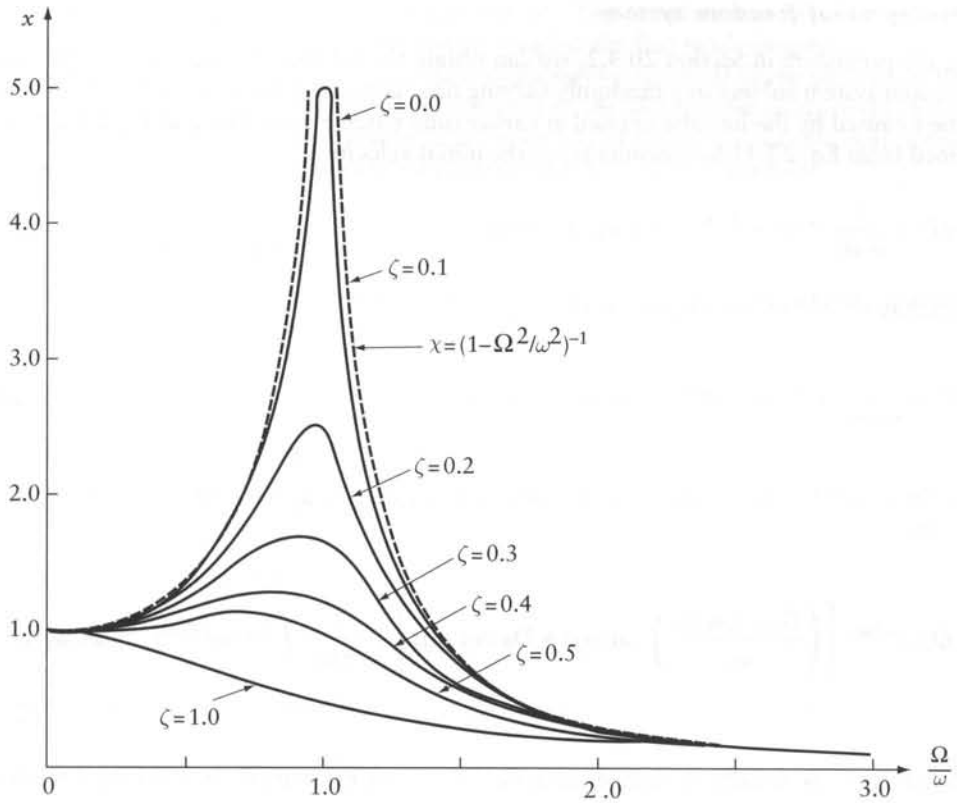

Figure 20.7 Magnification factor defined by Eq. 20.57 for a damped system subjected to harmonic disturbing forces.

various values of the damping ratio, ζ. At resonance, $\Omega = \omega$, the amplification factor $= 1/(2\zeta)$. The dashed curve in Figure 20.7 is for the theoretical case of undamped motion (Eq. 20.27). The other curves indicate that, even with a small amount of damping, finite displacements occur at resonance. Nevertheless, this condition is generally avoided.

Example 20.2: Damped free vibration of a light cantilever with a heavy weight at top

For the system in Example 20.1, find the damped natural frequency, ω_d, the natural period of damped vibration, T_d, and the displacement at $t = 3T_d$. Assume a damping ratio $\zeta = 0.05$.

Using the results of Example 20.1 and applying Eqs. 20.39, 20.42 and 20.41 gives:

$$\omega_d = \omega\sqrt{1-\zeta^2} = 4.202\left[1-(0.05)^2\right]^{1/2} = 4.197\,\text{rad/s}$$

$$T_d = 2\pi/\omega_d = 1.497\,\text{s}$$

$$D_{t=3T_d} = D_0\,e^{-\zeta\omega(3T_d)} = D_0\,e^{-0.05(4.202)(3\times1.497)} = 0.389\,D_0$$

We can see that with $\zeta = 0.05$ the amplitude drops to $0.39D_0$ in three cycles; in six cycles ($t = 6T_d$), it drops to $0.15D_0$.

20.5.3 Viscously damped forced vibration – general dynamic loading: single-degree-of-freedom system

Using the procedure in Section 20.4.2, we can obtain the solution for a damped single-degree-of-freedom system subject to a randomly varying time-dependent force, $P(\tau)$. The displacement at time t caused by the impulse applied at earlier time τ (see Figure 20.5 and Eq. 20.29) can be obtained from Eq. 20.41 by considering as the initial velocity :

$$\mathrm{d}D = \frac{1}{m\omega_d} P(\tau)\, \mathrm{e}^{-\zeta\omega(t-\tau)} \sin\omega_d (t-\tau)\, \mathrm{d}\tau \tag{20.51}$$

Integrating, we obtain the displacement:

$$D = \frac{1}{m\omega_d} \int_o^t P(\tau)\, \mathrm{e}^{-\zeta\omega(t-\tau)} \sin\omega_d (t-\tau)\, \mathrm{d}\tau \tag{20.52}$$

Using Eq. 20.41 for the solution for the initial conditions, D_0 and $\dot{D}_0$, the complete solution is given by:

$$D = \mathrm{e}^{-\zeta\omega t}\left[\left(\frac{\dot{D}_0 + \zeta\omega D_0}{\omega_d}\right)\sin\omega_d t + D_0 \cos\omega_d t\right] + \frac{1}{m\omega_d}\int_o^t P(\tau)\,\mathrm{e}^{-\zeta\omega(t-\tau)}\sin\omega_d(t-\tau)\,\mathrm{d}\tau \tag{20.53}$$

Equation 20.53 is usually evaluated numerically, except in unusual cases where $P(\tau)$ can be described by a simple function.

20.6 Undamped free vibration of multi-degree-of-freedom systems

In Section 20.2 we developed the equation of motion for the free vibration of a system with n degrees of freedom (Eq. 20.6). This is a system of second-order differential equations for which the solution is a set of equations of the form:

$$\{D\} = \{\overline{D}\}\sin(\omega t + \alpha) \tag{20.54}$$

The elements of $\{\overline{D}\}$ are the amplitudes of vibration corresponding to n degrees of freedom. Differentiation of Eq. 20.54 with respect to time gives the acceleration vector:

$$\{\ddot{D}\} = -\omega^2 \{D\} \tag{20.55}$$

Substituting Eq. 20.55 into Eq. 20.6, we obtain:

$$[S]\{D\} = \omega^2 [m]\{D\} \tag{20.56}$$

Pre-multiplying both sides by $[m]^{-1}$ gives:

$$[B]\{D\} = \omega^2 \{D\} \tag{20.57}$$

$$[B] = [m]^{-1}[S] \tag{20.58}$$

Equation 20.57 is called an *eigenvalue equation* (see Section A.3), and its solution provides n characteristic values (*eigenvalues*) of the quantity ω^2. The ω values are called the *natural* or *modal frequencies* of the system, and the lowest is called the *first mode* frequency.

For each characteristic value, a corresponding *eigenvector* or *mode shape* $\{\phi\}$ can be found. A value is selected (e.g. unity) for one of the elements of $\{\phi\}$ and the remaining $(n-1)$ values are found in terms of this value. This results in a vector $\{\phi\}$ of modal amplitudes that define the relationship between the magnitudes of vibration of the n degrees of freedom.

20.6.1 Mode orthogonality

The mode shapes of a multi-degree-of-freedom system have one important property that greatly facilitates analysis of such systems. Apply Eq. 20.56 to the rth mode:

$$\omega_r^2 [m] \{\phi_r\} = [S] \{\phi_r\} \tag{20.59}$$

Pre-multiplying by $\{\phi_s\}^T$, we obtain:

$$\omega_r^2 \{\phi_s\}^T [m] \{\phi_r\} = \{\phi_s\}^T [S] \{\phi_r\} \tag{20.60}$$

Now, consider sth mode, $\{\phi_s\}$:

$$\omega_s^2 [m] \{\phi_s\} = [S] \{\phi_s\} \tag{20.61}$$

Pre-multiplying by $\{\phi_r\}^T$, we obtain:

$$\omega_s^2 \{\phi_r\}^T [m] \{\phi_s\}^T = \{\phi_r\}^T [S] \{\phi_s\} \tag{20.62}$$

Transpose this equation, and recall that $[m]$ and $[S]$ are symmetrical matrices:

$$\omega_s^2 \{\phi_s\}^T [m] \{\phi_r\} = \{\phi_s\}^T [S] \{\phi_r\} \tag{20.63}$$

Subtraction of Eq. 20.63 from Eq. 20.60 gives:

$$\left(\omega_r^2 - \omega_s^2\right) \{\phi_s\}^T [m] \{\phi_r\} = 0 \tag{20.64}$$

When $\omega_r \neq \omega_s$, then:

$$\{\phi_s\}^T [m] \{\phi_r\} = 0; \ \{\phi_s\}^T [S] \{\phi_r\} = 0 \tag{20.65}$$

Equation 20.65 means that the natural modes are orthogonal with respect to $[m]$ or $[S]$.

$$[\phi]^T [m] [\phi] = [M]; \ [\phi]^T [S] [\phi] = [K] \tag{20.66}$$

where $[M]$ and $[K]$ are diagonal matrices; the rth elements on the diagonals are:

$$M_r = \{\phi_r\}^T [m] \{\phi_r\}; \ K_r = \{\phi_r\}^T [S] \{\phi_r\} \tag{20.67}$$

$$K_r = \omega_r^2 M_r \tag{20.68}$$

M_r and K_r are, respectively, called *generalized mass* and *generalized stiffness* for the rth mode. We recall that $\{\phi_r\}$ is generated by setting one of its elements $= 1$, and the remaining elements are

ratios between the elements defining the shape of the rth mode (see Section 20.6). It is convenient to use a *normalized mode matrix* $[\Phi]$ in lieu of $[\phi]$, obtained by the division of the rth column of $[\phi]$ by $\sqrt{M_r} = \left(\{\phi_r\}^T [m] \{\phi_r\}\right)^{1/2}$, with $r = 1, 2, \ldots, n$.

The use of $[\Phi]$ is convenient because of the relationships:

$$[\Phi]^T [m][\Phi] = [I]; \; [\Phi]^T [S][\Phi] = [\omega^2] \tag{20.69}$$

where $[I]$ and $[\omega^2]$ are diagonal matrices. Each element on the diagonal of $[I]$ is equal to 1.0. The elements on the diagonal of $[\omega^2]$ are: $\omega_1^2, \omega_2^2, \ldots, \omega_n^2$.

20.7 Modal analysis of damped or undamped multi-degree-of-freedom systems

The equation of motion of an undamped n-degree-of-freedom system is (Eq. 20.4 and Figure 20.2):

$$[m]\{\ddot{D}\} + [S]\{D\} = \{P(t)\} \tag{20.70}$$

Use the normalized modal matrix to express $\{D\}$ as sum of its modal contributions:

$$\{D\} = [\Phi]\{\eta\} \tag{20.71}$$

This equation transforms the displacements $\{D\}$ into modal coordinates $\{\eta\}$. Substitution of Eq. 20.71 into Eq. 20.70 and pre-multiplication by $[\Phi]^T$ gives:

$$[\Phi]^T [m][\Phi]\{\ddot{\eta}\} + [\Phi]^T [S][\Phi]\{\eta\} = [\Phi]^T \{P(t)\} \tag{20.72}$$

Substitution of Eq. 20.69 in this equation gives the uncoupled set of equations of motion in modal coordinates.

$$\{\ddot{\eta}\} + [\omega^2]\{\eta\} = \{P^*(t)\} \tag{20.73}$$

$\{p^*(t)\}$ = vector of generalized forces, given by:

$$\{P^*(t)\} = [\Phi]^T \{P(t)\} \tag{20.74}$$

The typical r^{th} equation of the set in Eq. 20.73 is the equation of motion of the r^{th} mode for the undamped system:

$$\ddot{\eta}_r + \omega_r^2 \eta_r = P_r^*(t) \tag{20.75}$$

The equation of motion of a damped n-degree-of-freedom system is:

$$[m]\{\ddot{D}\} + [C]\{\dot{D}\} + [S]\{D\} = \{P(t)\} \tag{20.76}$$

where $[C]$ is the damping matrix. We limit our discussion to classical damping, which is reasonable for many structures, with $[C] = a_0[m] + a_1[S]$, where a_0, a_1 are constants. Pre-multiplication by $[\Phi]^T$, post-multiplication by $[\Phi]$, and substituting Eq. 20.69 gives:

$$[\Phi]^T [C][\Phi] = a_0[I] + a_1[\omega^2] \tag{20.77}$$

Substituting Eqs. 20.69, 20.71, 20.74 and 20.77 in Eq. 20.76, we can derive:

$$\{\ddot{\eta}\} + 2[\zeta\omega]\{\dot{\eta}\} + \lfloor\omega^2\rfloor\{\eta\} = \{P^*(t)\}$$

where $[\zeta\omega]$ is a diagonal matrix of the products of the modal damping ratio times the modal frequency.

This is a set of uncoupled equations; a typical uncoupled equation of motion of the rth mode of the damped system is:

$$\ddot{\eta}_r + 2\zeta_r\omega_r\dot{\eta}_r + \omega_r^2\eta_r = P_r^*(t) \tag{20.78}$$

The uncoupled equations of motion (Eq. 20.75 and 20.78) make it possible to determine the response of each mode as that of a single-degree-of-freedom system. The contribution of the n-modes is then summed up by Eq. 20.71 to give $\{D\}$ at any time. Comparison of Eq. 20.75 or 20.77 with Eq. 20.11 or 20.33, respectively, indicates that we can solve for η_r by using the equations of single-degree-of-freedom system by replacing D, S, m, and $P(t)$ by η_r, ω_r^2, 1.0, and $P^*(t)$ respectively.

Example 20.3: Cantilever with three lumped masses

Find the natural frequencies $\{\omega\}$ and the normalized mode shapes $[\Phi]$ for the cantilever in Figure 20.8a. Verify the orthogonality of Eq. 20.69.

The system has three degrees of freedom indicated by the three coordinates in Figure 20.8b. The corresponding stiffness matrix is (using Table E.3, Appendix E):

$$[S] = \frac{EI}{l^3}\begin{bmatrix} 1.6154 & & \text{symmetrical} \\ -3.6923 & 10.1538 & \\ 2.7692 & -10.6154 & 18.4615 \end{bmatrix} \tag{a}$$

The mass matrix is:

$$[m] = \frac{W}{g}\begin{bmatrix} 4 & 0 & 0 \\ 0 & 1 & 0 \\ 0 & 0 & 1 \end{bmatrix} \tag{b}$$

where g is the acceleration due to gravity. Substituting in Eq. 20.58, we obtain

$$[B] = \frac{gEI}{Wl^3}\begin{bmatrix} 0.4039 & -0.9231 & 0.6923 \\ -3.6923 & 10.1538 & -10.6154 \\ 2.7692 & -10.6154 & 18.4615 \end{bmatrix} \tag{c}$$

Substituting this equation in Eq. 20.57 and solving for the eigenvalues, ω^2 (or solving the eigenvalue problem in the form of Eq. 20.56), we obtain

$$\omega_1^2 = 0.02588\frac{gEI}{Wl^3};\ \omega_2^2 = 3.09908\frac{gEI}{Wl^3};\ \omega_3^2 = 25.89415\frac{gEI}{Wl^3} \tag{d}$$

or

$$\omega_1 = 0.1609\sqrt{\frac{gEI}{Wl^3}};\ \omega_2 = 1.7604\sqrt{\frac{gEI}{Wl^3}};\ \omega_3 = 5.0886\sqrt{\frac{gEI}{Wl^3}} \tag{e}$$

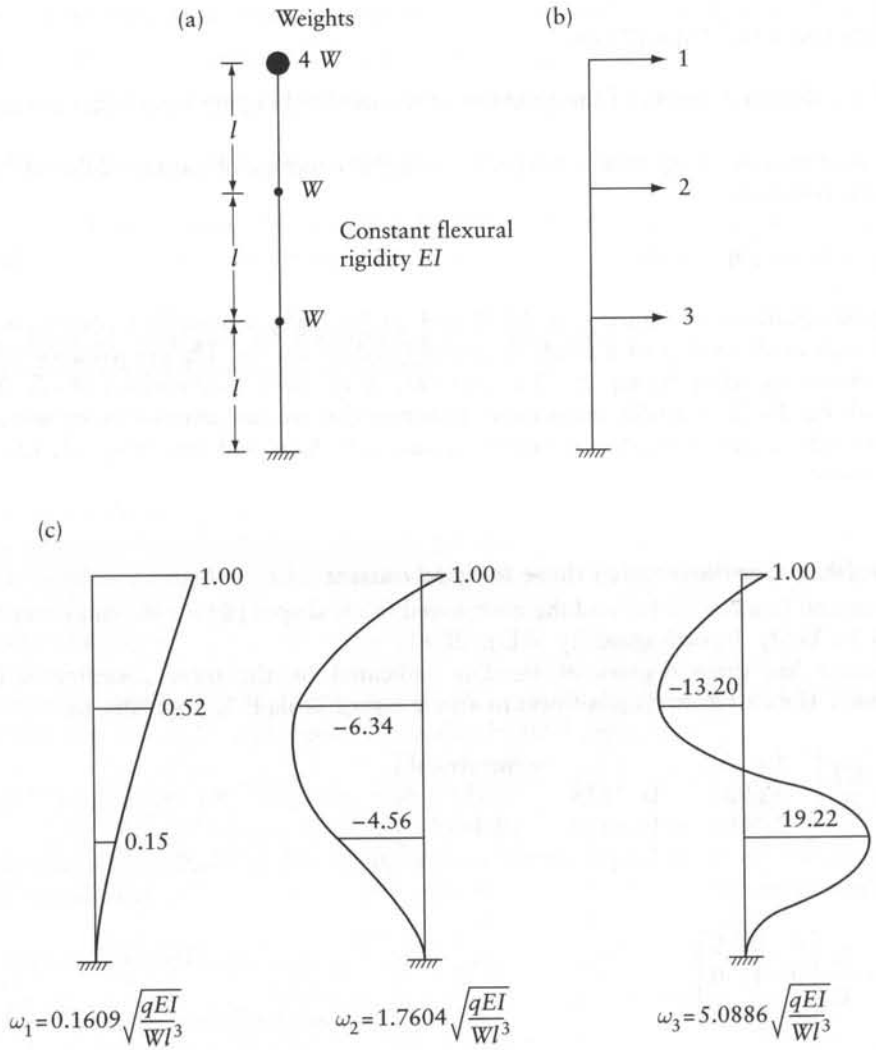

Figure 20.8 Free vibration of the beam of Example 21.2. (a) System properties. (b) Coordinate system. (c) Mode characteristic shapes.

If we choose $D_1 = 1$, the modal vectors corresponding to the above angular frequencies are

$$[\phi] = \begin{bmatrix} 1.0 & 1.0 & 1.0 \\ 0.5224 & -6.3414 & -13.1981 \\ 0.1506 & -4.5622 & 19.2222 \end{bmatrix} \tag{f}$$

The values of $\sqrt{M_r} = \sqrt{\{\phi_r\}^T [m] \{\phi_r\}}$, with $r = 1$, 2, and 3 are, respectively, $= 2.073\sqrt{W/g}$, $8.064\sqrt{W/g}$, and $23.400\sqrt{W/g}$; multiply columns 1, 2, and 3 of $[\phi]$, respectively, by $(2.073)^{-1}$, $(8.064)^{-1}$, and $(23.400)^{-1}$ to obtain:

$$[\Phi]=\begin{bmatrix}0.4825 & 0.1240 & 0.0427\\ 0.2521 & -0.7864 & -0.5640\\ 0.0727 & -0.5658 & 0.8214\end{bmatrix}\left(\frac{g}{W}\right)^{1/2} \tag{g}$$

We can verify $[\Phi]$ by Eq. 20.69:

$$[\Phi]^T\begin{bmatrix}4 & 0 & 0\\ 0 & 1 & 0\\ 0 & 0 & 1\end{bmatrix}[\Phi]\frac{W}{g}=\begin{bmatrix}1 & 0 & 0\\ 0 & 1 & 0\\ 0 & 0 & 1\end{bmatrix}$$

$$\frac{EI}{l^3}[\Phi]^T\begin{bmatrix}1.6154 & & \text{symmetrical}\\ -3.6923 & 10.1538 & \\ 2.7692 & -10.6154 & 18.4615\end{bmatrix}[\Phi]$$

$$=\begin{bmatrix}0.02588 & 0 & 0\\ 0 & 3.09908 & 0\\ 0 & 0 & 25.8445\end{bmatrix}\frac{gEI}{Wl^3}$$

Example 20.4: Harmonic forces on a cantilever with three lumped masses

Find the steady-state displacements of the system shown in Figure 20.8a subjected to harmonic forces $\{P(t)\}=P_0\sin\Omega t\,\{2,1,1\}$, with $\Omega=\omega_1/2$; where ω_1 = frequency of the first natural mode. Use the results of Example 20.3.

The steady-state displacement of undamped single-degree-of-freedom system is (the last term of Eq. 20.25):

$$D=\frac{P_0\sin\Omega t}{S}\left(1-\frac{\Omega^2}{\omega^2}\right)^{-1} \tag{20.79}$$

Replace D by η_r, $P_0\sin\Omega t$ by $P_r^*(t)$, and S by ω_r^2 to obtain the rth mode of displacement in modal coordinate:

$$\eta_r=\frac{P_r^*(t)}{\omega_r^2}\left(1-\frac{\Omega^2}{\omega_r^2}\right)^{-1} \tag{20.80}$$

In this problem, $\Omega^2=(\omega_1)^2/4=6.47\times10^{-3}[gEI/(Wl^3)]$. The generalized forces can be expressed as (Eq. 20.74):

$$P_r^*(t)=[\Phi]^T\{P(t)\}$$

$$=\left(\frac{g}{W}\right)^{\frac{1}{2}}\begin{bmatrix}0.4825 & 0.2521 & 0.0727\\ 0.1240 & -0.7864 & -0.5640\\ 0.0427 & -0.5640 & 0.8214\end{bmatrix}\begin{Bmatrix}2\\1\\1\end{Bmatrix}P_0\sin\Omega t$$

$$=\left(\frac{g}{W}\right)^{\frac{1}{2}}\begin{Bmatrix}1.2898\\ -1.1042\\ 0.3428\end{Bmatrix}P_0\sin\Omega t$$

The steady-state displacements in natural coordinates are:

$$\eta_1 = \left(\frac{W}{g}\right)^{\frac{1}{2}} \frac{P_0 \sin \Omega t (1.2898)}{(EI/l^3)(0.02588)} \left[1 - \frac{6.47 \times 10^{-3}}{0.02588}\right]^{-1} = 66.45 \left(\frac{W}{g}\right)^{\frac{1}{2}} \frac{P_0 l^3}{EI} \sin \Omega t$$

$$\eta_2 = \left(\frac{W}{g}\right)^{\frac{1}{2}} \frac{P_0 \sin \Omega t (-1.1042)}{(EI/l^3)(3.0991)} \left[1 - \frac{6.47 \times 10^{-3}}{3.0991}\right]^{-1} = -0.3570 \left(\frac{W}{g}\right)^{\frac{1}{2}} \frac{P_0 l^3}{EI} \sin \Omega t$$

$$\eta_3 = \left(\frac{W}{g}\right)^{\frac{1}{2}} \frac{P_0 \sin \Omega t (0.3428)}{(EI/l^3)(25.8914)} \left[1 - \frac{6.47 \times 10^{-3}}{25.8914}\right]^{-1} = 0.0136 \left(\frac{W}{g}\right)^{\frac{1}{2}} \frac{P_0 l^3}{EI} \sin \Omega t$$

The displacements are (Eq. 20.71):

$$\{D\} = \left(\tfrac{W}{g}\right)^{\frac{1}{2}} [\Phi] \begin{Bmatrix} 66.45 \\ -0.3570 \\ 0.0136 \end{Bmatrix} \frac{P_0 l^3}{EL} \sin \Omega t = \begin{Bmatrix} 32.02 \\ 17.03 \\ 5.044 \end{Bmatrix} \frac{P_0 l^3}{EI} \sin \Omega t$$

20.8 Single- or multi-degree-of-freedom systems subjected to ground motion

Consider the response of the single-degree-of-freedom damped system in Figure 20.9 subjected to support motion described in terms of its acceleration $\ddot{u}_g(t)$. At any instant, the displacement of the mass m relative to the ground is:

$$D = u - u_g \tag{20.81}$$

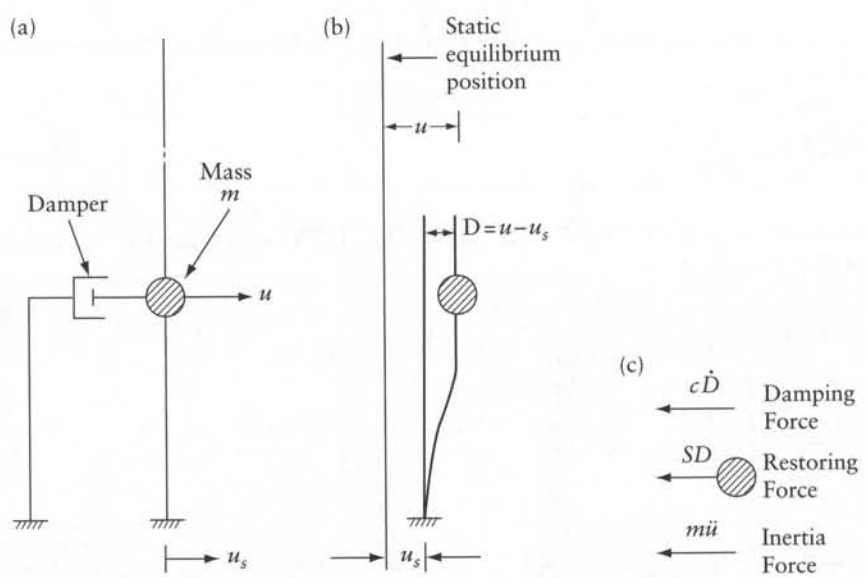

Figure 20.9 A single-degree-of-freedom system subjected to support movements. (a) Positive directions of u and u_s. (b) Deformed shape at any time t. (c) Forces acting on mass at any time t.

The forces acting on the mass are: an inertial force $m\ddot{u}$, a damping force $c\dot{D}$, and a restoring force SD; where S is the stiffness of the structure with respect to the coordinate shown. The equation of motion is:

$$m\ddot{u} + c\dot{D} + SD = 0 \tag{20.82}$$

where c = damping coefficient, $\zeta = c/(2m\omega)$ = damping ratio (Eq. 20.34), and $\omega = \sqrt{S/m}$ = natural frequency (Eq. 20.14). Substituting for c and S and Eq. 20.81 in Eq. 20.82, the equation of motion of a single-degree-of-freedom damped system subjected to ground motion becomes:

$$\ddot{D} + 2\zeta\omega\dot{D} + \omega^2 D = -\ddot{u}_g \tag{20.83}$$

Comparison of Eq. 20.83 with Eq. 20.33 shows that the effect of ground motion is the same as that of the force:

$$P(t) = -\ddot{u}_g m \tag{20.84}$$

The modal analysis (Section 20.7) can determine the response of a damped multi-degree-of-freedom system (Figure 20.2) subjected to ground motion, described by its acceleration, $\ddot{u}_g$. For this purpose, apply Eq. 20.78.

$$\ddot{\eta}_r + 2\zeta\omega,\dot{\eta}_r + \omega_r^2\eta_r = P_r^*(t)$$

Here, D is replaced by η and $(-\ddot{u}_g)$ by the generalized force $P_r^*(t)$; where

$$\{P_r^*(t)\} = -\ddot{u}_g [\Phi]^T \begin{Bmatrix} m_1 \\ m_2 \\ \cdots \\ m_n \end{Bmatrix} \tag{20.85}$$

Equation 20.78, combined with the rth element of $\{P_r^*(t)\}$, gives the uncoupled equation of the rth mode.

The effect of a particular earthquake can be analyzed by the substitution of its record of $\ddot{u}_g$ in Eq. 20.83 or 20.85. Solution of these differential equations is commonly done by numerical "time-stepping" methods.

Example 20.5: Cantilever subjected to harmonic support motion

Find the steady-state displacements of the system shown in Figure 20.8a subjected to harmonic support acceleration $\ddot{u}_g = (g/5)\sin\Omega t$, where $\Omega = \omega_1/2$ and ω_1 is the frequency of the first natural mode. Use the results of Example 20.3.

The vector of generalized forces is (Eq. 20.85)

$$\{P^*(t)\} = -\frac{g}{5}\sin\Omega t \begin{bmatrix} 0.4825 & 0.2521 & 0.0727 \\ 0.1240 & -0.7865 & -0.5640 \\ 0.0427 & -0.5640 & 0.8214 \end{bmatrix} \begin{Bmatrix} 4 \\ 1 \\ 1 \end{Bmatrix} \left(\frac{W}{g}\right)^{\frac{1}{2}}$$

$$= -\frac{g}{5}\sin\Omega t \begin{Bmatrix} 2.2548 \\ -0.8545 \\ 0.4282 \end{Bmatrix} \left(\frac{W}{g}\right)^{\frac{1}{2}} = g\sin\Omega t \begin{Bmatrix} -0.45096 \\ 0.17090 \\ -0.08564 \end{Bmatrix} \left(\frac{W}{g}\right)^{\frac{1}{2}}$$

Given: $\Omega = \omega_1/2$; $\Omega^2 = \frac{\omega_1^2}{4} = \frac{0.02588}{4}\frac{gEI}{Wl^3}$. Equation 20.80 gives the displacements of the three modes in natural coordinates:

$$\eta_1 = \left(\frac{W}{g}\right)^{\frac{1}{2}} \frac{-0.45096}{0.02588}\left[1 - \frac{0.02588}{4(0.02588)}\right]^{-1} \frac{Wl^3}{EI} \sin \Omega t = -23.23\left(\frac{W}{g}\right)^{\frac{1}{2}} \frac{Wl^3}{EI} \sin \Omega t$$

$$\eta_2 = \left(\frac{W}{g}\right)^{\frac{1}{2}} \frac{0.17090}{3.09908}\left[1 - \frac{0.02588}{4(3.09908)}\right]^{-1} \frac{Wl^3}{EI} \sin \Omega t = 0.0553\left(\frac{W}{g}\right)^{\frac{1}{2}} \frac{Wl^3}{EI} \sin \Omega t$$

$$\eta_3 = \left(\frac{W}{g}\right)^{\frac{1}{2}} \frac{-0.08564}{25.89415}\left[1 - \frac{0.02588}{4(25.89415)}\right]^{-1} \frac{Wl^3}{EI} \sin \Omega t = -0.0033\left(\frac{W}{g}\right)^{\frac{1}{2}} \frac{Wl^3}{EI} \sin \Omega t$$

The displacements are (Eq. 20.71):

$$\{D\} = [\Phi]\{\eta\} = \begin{Bmatrix} -11.200 \\ -5.893 \\ -1.723 \end{Bmatrix} \frac{Wl^3}{EI} \sin \Omega t$$

20.9 Earthquake response spectra

The equation of motion of a single-degree-of-freedom system (Eq. 20.83) indicates that for a given ground acceleration $\ddot{u}_g(t)$ the response is dependent only upon the natural frequency ω and the damping ratio ζ. Thus, systems having the same ω (or $T = 2\pi/\omega$) and same ζ have the same displacement response, although they may differ in mass and stiffness. For typical ground motions, a structure will respond primarily in its fundamental mode, with a period close to its fundamental T. Structures with higher fundamental period T will experience greater peak displacement. Damping decreases the peak displacement; higher ζ corresponds to smaller peak displacement.

The variations of ground acceleration $\ddot{u}_g(t)$ recorded during strong earthquakes have been used to derive *pseudo-acceleration response spectra*. The jagged line in Figure 20.10a is a sketch of the spectrum derived from the record of the earthquake at El Centro, California, 1940. (More accurate graphs can be found in more specialized references.[1]) The spectrum shown in Figure 20.10 is for $\zeta = 0.02$. For any T value, a numerical solution (in time steps) of the equation of motion (Eq. 20.83) gives the variation of the acceleration for the whole duration of the earthquake record; the absolute peak value of the acceleration gives the ordinate S_a of the pseudo-acceleration spectrum. Repetition of the solution varying T (keeping $\zeta = 0.02$) gives the spectrum shown in Figure 20.10a. Commonly, curves for three to five ζ values are plotted on the same graph (e.g. $\zeta = 0$, 0.02, 0.05, 0.10, and 0.20). Note that S_a is the peak acceleration of a vibrating mass relative to the support (Figure 20.9); thus, S_a is different from the peak acceleration of the ground and also different from the peak acceleration of the mass; the prefix *pseudo* is used to differentiate between the accelerations.

From the same ground acceleration record, it is also possible to prepare *pseudo-velocity response* and *pseudo-displacement response* spectra. For specific values of ζ and T, the velocity and displacement spectra, S_v and S_d are approximately related to S_a:

$$S_v = S_a(T/2\pi);\ S_d = S_a(T/2\pi)^2 \tag{20.86}$$

1 See references at the end of this chapter.

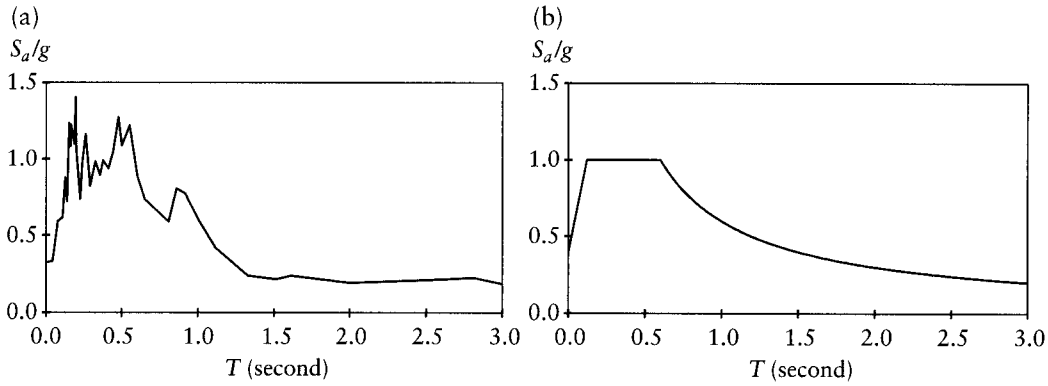

Figure 20.10 Pseudo-acceleration response spectrum. (a) Sketch of the response spectrum for El Centro (1940) ground motion with $\zeta = 0.02$. (b) Simplified spectrum.

Figure 20.10b is a simplified version of the spectrum in Figure 20.10a. Modern codes use the spectra of available earthquake records to develop simplified design spectra giving $S_a(\zeta, T)$ that vary with the geographic location of the structure; the codes also provide soil multipliers to S_a to account for the conditions of the soil (higher multipliers for softer soil). Figure 20.11a is an example[2] of acceleration design spectrum for $\zeta = 0.05$. The use of acceleration design spectra is demonstrated in Examples 20.6, 20.7 and 20.8.

20.10 Peak response to earthquake: single-degree-of-freedom system

Figure 20.11b shows a single-degree-of-freedom system with mass m and stiffness S. We can calculate $T = 2\pi/\sqrt{S/m}$ and use the design spectral acceleration S_a for the site (such as the

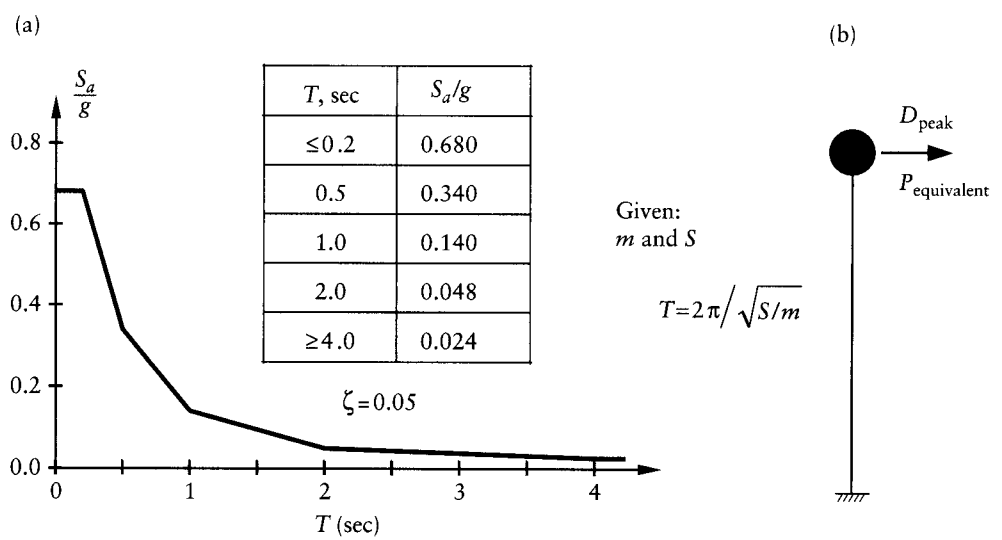

T, sec	S_a/g
≤0.2	0.680
0.5	0.340
1.0	0.140
2.0	0.048
≥4.0	0.024

Figure 20.11 Typical design data. (a) Spectral acceleration[2]. (b) Single degree of freedom.

2 National Building Code of Canada (NBCC 2005). The values shown are for Montreal, Quebec.

one shown in Figure 20.11a) to determine peak displacement D_{peak} and equivalent static force $P_{equivalent}$:

$$D_{peak} = S_a (T/2\pi)^2 \tag{20.87}$$

$$P_{equivalent} = m S_a \tag{20.88}$$

Example 20.6: A tower idealized as a single-degree-of-freedom system subjected to earthquake

A tower is idealized as a weightless vertical cantilever of length $l = 40$ m, carrying a weight $W = 160$ kN at its tip. Find the equivalent static force at the tip, the peak drift at the tip, the shearing force and the bending moment at the base. Given $E = 200$ GPa, $I = 30 \times 10^{-3}$ m^4, and the damping ratio $\zeta = 0.05$, the spectral acceleration for the site is shown in Figure 20.11a. Gravitational acceleration, $g = 9.81$ m/s^2.

The stiffness is (see Appendix B, inverse of Eq. B.19):

$$S = 3EI/l^3 = 3\left(200 \times 10^9\right)\left(30 \times 10^{-3}\right)/(40)^3 = 281 \times 10^3 \text{ N/m}$$

$$\omega^2 = S/m = S/(W/g) = 281 \times 10^3 / \left[\left(160 \times 10^3\right)/9.81\right] = 17.22 \text{ s}^{-2}$$

$$T = 2\pi/\omega = 2\pi/\sqrt{17.22} = 1.51 \text{ s}$$

Figure 20.11a gives: $S_a = 0.093\,g = 0.093(9.81) = 0.913$ m/s^2.

Peak displacement: $D_{peak} = S_a (T/2\pi)^2 = 0.913\ (1.51/2\pi)^2 = 0.053$ m

Equivalent static force: $P_{equivalent} = mS_a = \dfrac{W}{g} S_a = \dfrac{160 \times 10^3}{9.81}\ (0.913) = 14.9 \times 10^3$ N

Shearing force at the base $= 14.9 \times 10^3$ N

Bending moment at the base $= 14.9 \times 10^3 (40) = 596 \times 10^3$ N-m

20.11 Generalized single-degree-of-freedom system

The response of a multi-degree-of-freedom system to earthquake can be analyzed (approximately) using a generalized single-degree-of-freedom system. Consider the plane frame in Figure 20.2c, idealized as a system having n degrees of freedom and n lumped masses. It is required to determine the peak displacements, the equivalent static forces, the base shear, and the base overturning moment due to earthquake movement described by a spectral acceleration, S_a, as function of ζ and T.

We assume that the structure can deflect in a single assumed shape, Ψ, which is an approximation of the fundamental mode shape. For a multistorey building, the fundamental mode has the same sign at all coordinates. Generally, one of a variety of shape functions can be selected. For a multistorey building, examples of shape functions are:

$$\Psi = \xi;\ \Psi = \left(3\xi^2 - \xi^3\right)/2;\ \Psi = \left(6\xi^2 - 4\xi^3 + \xi^4\right)/3 \tag{20.89}$$

where $\xi = x/l$, with x and l being the distance between the base and any coordinate and between the base and the top coordinate respectively. Each function gives $\Psi = 0$ and 1 at the base and the top. The first function is simply linear; the second and the third represent the deflected shape of a prismatic cantilever subjected to a lateral force at its tip and to a uniform load respectively (see Eqs. B.22 and B.29, Appendix B). The shape function must satisfy the boundary conditions that coincide with any of the n degrees of freedom. Sometimes the shape function Ψ is taken

as the deflected shape of the frame due to static forces mg at the coordinates, where g is the gravitational acceleration. The natural frequency of the generalized system is given by:

$$\omega_n^2 = \frac{S_n}{m_n};\ S_n = \{\Psi\}^T[S]\{\Psi\};\ m_n = \{\Psi\}^T[m]\{\Psi\} \tag{20.90}$$

This is known as Rayleigh's equation; S_n and m_n are called *generalized stiffness* and *generalized mass* respectively; the equation is exact when Ψ is the true fundamental mode shape. This can be verified by dividing the second of Eqs. 20.69 by the first. When Ψ is assumed, Eq. 20.90 gives an approximate value for ω_n, always greater than the exact value. Rayleigh's equation can also be verified by virtual work. The natural period of vibration of the generalized system is:

$$T_n = 2\pi/\omega_n \tag{20.91}$$

Calculate the mass participation parameter L_n, defined as:

$$L_n = \sum_{i=1}^{n} \Psi_i m_i \tag{20.92}$$

The peak displacement of the generalized system is:

$$D_{n\ \text{peak}} = L_n S_a / \left(m_n \omega_n^2\right) \tag{20.93}$$

This is the peak displacement at the point whose $\xi = 1$. The equivalent static force at any coordinate i is:

$$p_{ni} = L_n m_i \Psi_i S_a / m_n \tag{20.94}$$

The equivalent static shearing force and overturning moment at the base and the effective height are:

$$V_{\text{base}} = \sum_{i=1}^{n} p_{ni};\ M_{\text{base}} = \sum_{i=1}^{n} p_{ni}\, h_i;\ h_{\text{effective}} = M_{\text{base}}/V_{\text{base}} \tag{20.95}$$

where h_i is the distance from the base to coordinate i.

Example 20.7: A cantilever with three lumped masses subjected to earthquake: use of a generalized single-degree-of-freedom system

The structure in Figure 20.8a is subjected to earthquake characterized by the design spectrum in Figure 20.11a ($\zeta = 0.05$). Find the shearing force and the bending moment at the base and the peak displacement at the top. Use a generalized single-degree-of-freedom system. Assume $Wl^3/(gEI) = 950 \times 10^{-6}\ \text{s}^2$; $g = 9.81\ \text{m/s}^2$.

The stiffness matrix of the three-degrees-of-freedom system in Figure 20.8b is (Table E.3, Appendix E):

$$[S] = \frac{EI}{l^3}\begin{bmatrix} 1.6154 & & \text{symmetrical} \\ -3.6923 & 10.1538 & \\ 2.7692 & -10.6154 & 18.4615 \end{bmatrix}$$

The mass matrix is:

$$[m] = \frac{W}{g}\begin{bmatrix} 4 & 0 & 0 \\ 0 & 1 & 0 \\ 0 & 0 & 1 \end{bmatrix}$$

We select the shape function:

$$\psi = \left(3\xi^2 - \xi^3\right)/2 \text{ with } \xi = x/(3l)$$

$$\psi_1 = 1;\ \psi_2 = 0.5185;\ \psi_3 = 0.1481$$

The generalized stiffness and the generalized mass are (Eq. 20.90):

$$S_n = \{\psi\}^T\ [S]\ \{\psi\} = 0.1112\, EI/l^3;\ m_n = \{\psi\}^T\ [m]\ \{\psi\} = 4.291\ W/g$$

$\omega_n^2 = \dfrac{S_n}{m_n} = \dfrac{0.1112}{4.291}\dfrac{gEI}{Wl^3} = 25.92 \times 10^{-3}\dfrac{gEI}{Wl^3}$ (slightly greater than ω_1^2, for the fundamental mode determined in Example 20.3)

$$T_n = 2\pi/\omega_n = \left[2\pi/\sqrt{25.92 \times 10^{-3}}\right]\left(\frac{gEI}{Wl^3}\right)^{-1/2}$$

$$= 39.03\left(\frac{gEI}{Wl^3}\right)^{-1/2} = 39.03\left(950 \times 10^{-6}\right)^{1/2} = 1.2 \text{ second}$$

From Figure 20.11a, $S_a = 0.122g = 0.122(9.81) = 1.197$ m/s^2

The mass participation parameter (Eq. 20.92):

$$L_n = \sum_{i=1}^{n} \psi_i m_i = \frac{W}{g}\left[1.0\ (4.0) + 0.5185\ (1.0) + 0.1481\ (1.0)\right] = 4.667\,\frac{W}{g}$$

The peak displacement of the generalized system is:

$$D_{n\ \text{peak}} = L_n S_a/\left(m_n \omega_n^2\right) = \frac{4.667\ (1.197)}{4.291\left[25.92 \times 10^{-3}/\left(950 \times 10^{-6}\right)\right]} = 0.0477\,\text{m}$$

The equivalent static forces at the coordinates are (Eq. 20.94):

$$\{p_n\} = \{p_n\} = \frac{L_n S_a}{m_n}\{m_i \psi_i\} = \frac{4.667\ (0.122)}{4.291}\begin{Bmatrix} 4.0\ (1.0) \\ 1.0\ (0.5185) \\ 1.0\ (0.1481) \end{Bmatrix} W = \begin{Bmatrix} 0.5309 \\ 0.0688 \\ 0.0197 \end{Bmatrix} W$$

The equivalent static shearing force and overturning moment at the base and the effective height $h_{\text{effective}}$ are (Eq. 20.95):

$$V_{\text{base}} = W\,(0.5309 + 0.0688 + 0.0197) = 0.6195\ W$$
$$M_{\text{base}} = W\,l\,(0.5309 \times 3 + 0.0688 \times 2 + 0.0197) = 1.789\ W\,l$$
$$h_{\text{effecive}} = M_{\text{base}}/V_{\text{base}} = (1.789/0.6195)\ l = 2.888l$$

20.12 Modal spectral analysis

The spectral acceleration graphs of $S_a(\zeta, T)$ (e.g. Fig. 20.11a) can be used to obtain the peak response (forces or displacements) of a multi-degree-of-freedom system to earthquakes. Consider the plane frame in Fig. 20.2 having n degrees of freedom and n lumped masses. The steps of analysis are:

1. Generate the stiffness and mass matrices, $[S]$ and $[m]$, the product $[m]^{-1}[S]$, the corresponding eigenvalues $\{\omega^2\}$, and modal shapes $[\phi]$. Divide a typical rth column of $[\phi]$ by $\left(\{\phi_r\}^T\ [m]\ \{\phi_r\}\right)^{1/2}$ to obtain the modal shapes $[\Phi]$ normalized with respect to the masses. Calculate the natural vibration periods, $\{T\} = \left\{2\pi \Big/ \sqrt{\omega^2}\right\}$. The calculation involved in this step is demonstrated in Example 20.3.
2. Calculate the *mass participation parameters* $\{\alpha\}$ and the *mass participation factors* $\{MPF\}$ defined as:

$$\{\alpha\} = [\Phi]^T\ [m] \begin{Bmatrix} 1 \\ 1 \\ \cdots \\ 1 \end{Bmatrix} \tag{20.96}$$

$$\{MPF\} = \left(\sum_{i=1}^{n} m_i\right)^{-1} \left\{\alpha^2\right\} \tag{20.97}$$

Note that $\sum_{i=1}^{n} MPF_i = 1.0$.

3. Read the spectral accelerations $\{S_a(\zeta, T)\}$ from spectral graphs similar to Figure 20.11a.
4. The contribution of the modes to the equivalent static base shear is given by:

$$\{V\}_{\text{base}} = \left\{\alpha^2\, S_a\right\} = \left(\sum_{i=1}^{n} m_i\right) \{MPF \cdot S_a\} \tag{20.98}$$

A typical rth element V_{rbase} of this vector is equal to the sum of the equivalent static forces at the coordinates for the rth mode; to find the force at individual coordinates, partition V_{rbase} proportional to $m_i \Phi_{ir}$, with $i=1, 2, \ldots, n$. The contribution of the rth mode to the equivalent static forces at the coordinates is:

$$\{p\}_r = \frac{V_{r\,\text{base}}}{\sum_{i=1}^{n} m_i\, \Phi_{ir}} \begin{Bmatrix} m_1\, \Phi_{1r} \\ m_2\, \Phi_{2r} \\ \cdots \\ m_n\, \Phi_{nr} \end{Bmatrix} = \frac{V_{r\,\text{base}}}{\alpha_r} \begin{Bmatrix} m_1\, \Phi_{1r} \\ m_2\, \Phi_{2r} \\ \cdots \\ m_n\, \Phi_{nr} \end{Bmatrix} \tag{20.99}$$

The *equivalent static overturning moment* and the *model height* for the rth mode are:

$$M_{r\,\text{base}} = \sum_{i=1}^{n} p_{ir}\, h_i;\ h_r = M_{r\,\text{base}} / V_{r\,\text{base}} \tag{20.100}$$

5. Apply the equivalent static forces $\{p\}_r$ on the structure to calculate displacements, internal forces, or reactions (as required) for the rth mode.

6. Find the contribution of each mode *separately* to any required action (e.g. displacement or internal force) before combining the modal contributions, by one of the methods in Section 20.12.1, to obtain the peak value of the action.

20.12.1 Modal combinations

The peak values for different modes do not occur at the same instant. The sum of the absolute peak values is an upper bound of the total response:

$$r_{\text{upper bound}} = \sum_{i=1}^{n} |r_i|\, h_i \tag{20.101}$$

where r refers to generalized response (displacement or force) and i refers to the mode number. The use of the upper bound in design is conservative. The *square root of the sum of the squares* (SRSS) gives a more realistic estimate of the peak response:

$$r_{SRSS} = \left(\sum_{i=1}^{n} r_i^2 \right)^{1/2} \tag{20.102}$$

This equation is appropriate except when the natural frequencies are close to each other. In this case, the *complete quadratic combination* (CQC) method is considered more appropriate.

The contribution of the fundamental mode to the response is commonly much higher than the remaining modes. When the number of degrees of freedom n is high, it is commonly sufficient to use the contribution of m modes, with $m < n$, such that $\sum_{i=1}^{m} MPF_i > 0.9$. The SRSS (Eq. 20.102) applies to combine the displacements or the forces obtained for separate modes. However, the displacements calculated by the SRSS equation do not give accurate results if used to calculate forces; similarly, the forces obtained by the SRSS equation should not be used to calculate displacements.

Example 20.8: Response of a multistorey plane frame to earthquake: modal spectral analysis

A three-storey building is idealized as a plane frame with masses lumped at three coordinates (Fig. 20.12). Calculate the equivalent static shearing force and overturning moment at the base for the effect of an earthquake whose design acceleration response spectrum, $S_a(\zeta, T)$, is given in Figure 20.11a (with $\zeta = 0.05$). Assume rigid floors and consider only bending deformation for the columns. Gravitational acceleration, $g = 9.81 \text{m/s}^2$.

The stiffness and the mass matrices are:

$$[S] = \frac{12EI}{l^3} \begin{bmatrix} 2 & -2 & 0 \\ -2 & 4 & -2 \\ 0 & -2 & 4 \end{bmatrix}; [m] = \frac{10^3}{g} \begin{bmatrix} 200 & 0 & 0 \\ 0 & 280 & 0 \\ 0 & 0 & 280 \end{bmatrix}$$

$$[m]^{-1}\,[S] = 10^3 \begin{bmatrix} 0.8591 & -0.8591 & 0 \\ -0.6136 & 1.227 & -0.6136 \\ 0 & -0.6136 & 1.227 \end{bmatrix} \text{s}^{-2}$$

The eigenvalues are: $\{\omega_1^2, \omega_2^2, \omega_3^2\} = \{143.3, 1079, 2091\}\ \text{s}^{-2}$

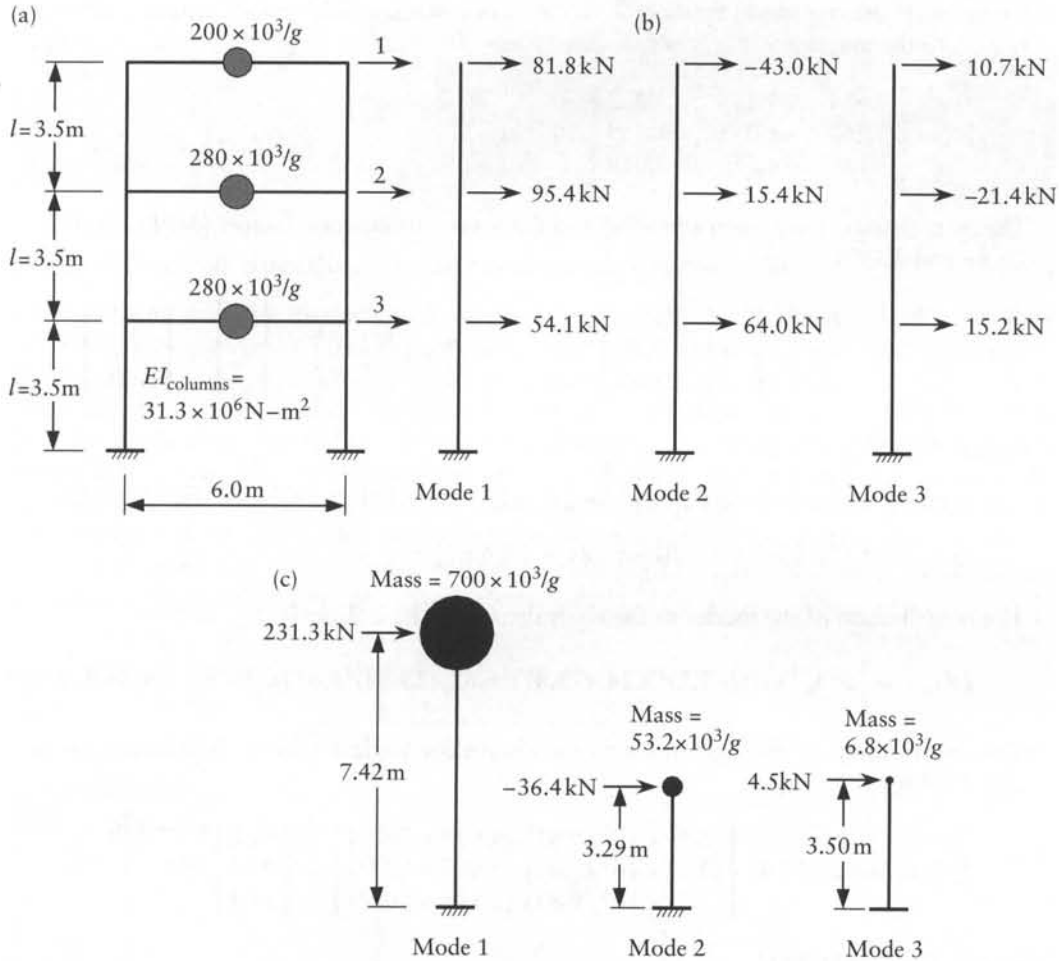

Figure 20.12 The plane frame of Example 20.8 subjected to earthquake. (a) Idealization, coordinates and lumped masses. (b) Mode contributions to the equivalent static forces. (c) Effective modal masses, heights and static forces.

The natural periods of vibration are ($T = 2\pi/\omega$):

$\{T\} = \{0.525, 0.191, 0.137\}$s

The modal shapes are:

$$[\phi] = \begin{bmatrix} 1 & 1 & 1 \\ 0.833 & -0.256 & -1.434 \\ 0.472 & -1.062 & 1.019 \end{bmatrix}$$

$$\left\{\sqrt{M_r}\right\} = \left\{\left(\{\phi_r\}^T\,[m]\,\{\phi_r\}\right)^{1/2}\right\} = \{216, 233, 330\}\ \text{kg}^{1/2}$$

Divide each column of $[\phi]$ by its $\sqrt{M_r}$ value to obtain the modal shapes normalized with respect to the masses:

$$[\Phi] = \begin{bmatrix} 4.634 & 4.285 & 3.032 \\ 3.861 & -1.098 & -4.349 \\ 2.186 & -4.550 & 3.089 \end{bmatrix} 10^{-3}\,\text{kg}^{-1/2}$$

The mass participation parameters $\{\alpha\}$ and the mass participation factors $\{MPF\}$ are (Eqs. 20.96 and 20.97):

$$\{\alpha\} = [\Phi]^T [m] \begin{Bmatrix} 1 \\ 1 \\ 1 \end{Bmatrix} = \begin{Bmatrix} 267.2 \\ -73.87 \\ 25.88 \end{Bmatrix} \text{kg}^{1/2}; \{MPF\} = \left(\sum_{i=1}^{n} m_i\right)^{-1} \begin{Bmatrix} \alpha_1^2 \\ \alpha_2^2 \\ \alpha_3^2 \end{Bmatrix} = \begin{Bmatrix} 0.921 \\ 0.070 \\ 0.009 \end{Bmatrix}$$

Check: $\sum_{i=1}^{3} MPF_i = 1.000$.

The spectral accelerations $S_a(\zeta, T)$ for $\{T\} = \{0.525, 0.191, 0.137\}$s are (Fig. 20.11a):

$$\{S_a\} = g\{0.330, 0.680, 0.680\} = \{3.24, 6.67, 6.67\}\, m/s^2$$

The contribution of the modes to the equivalent static base shear is (Eq. 20.98):

$$\{V\}_{\text{base}} = \left\{\alpha^2 S_a\right\} = \{(267.2)^2 3.24, (73.87)^2 6.69, (25.88)^2 6.67\} = 10^3\{231.3, 36.4, 4.5\}N$$

The contribution of the first mode to the equivalent static forces at the coordinates is (Eq. 20.99):

$$\{p\}_1 = 267.2\ (3.24) \begin{Bmatrix} (200 \times 10^3/9.81)\ (4.634 \times 10^{-3}) \\ (280 \times 10^3/9.81)\ (3.861 \times 10^{-3}) \\ (280 \times 10^3/9.81)\ (2.186 \times 10^{-3}) \end{Bmatrix} = \begin{Bmatrix} 81.8 \\ 95.4 \\ 54.1 \end{Bmatrix} \text{kN}$$

Check: Sum = 231.3 kN

Similar calculations for the second and third modes give:

$$\{p\}_2 = \begin{Bmatrix} -43.0 \\ 15.4 \\ 64.0 \end{Bmatrix} \text{kN}; \qquad \{p\}_3 = \begin{Bmatrix} 10.7 \\ -21.4 \\ 15.2 \end{Bmatrix} \text{kN}$$

Check: Sum = 36.4 kN Sum = 4.5 kN

The effective height and the overturning moment for each mode are (Eq. 20.100):

$$h_1 = [81.8(3 \times 3.5) + 95.4(2 \times 3.5) + 54.1(3.5)]/231.3 = 7.42 \text{ m}; \; M_{1\text{base}} = 1716 \text{ kN-m}$$

$$h_2 = [-43.0(3 \times 3.5) + 15.4(2 \times 3.5) + 64.0(3.5)]/36.4 = -3.29 \text{ m}; \; M_{2\text{base}} = -120 \text{ kN-m}$$

$$h_3 = [10.7(3 \times 3.5) - 21.4(2 \times 3.5) + 15.2(3.5)]/4.5 = 3.50 \text{ m}; \; M_{3\text{base}} = 16 \text{ kN-m}$$

Figure 20.12b shows the mode contributions to the equivalent static forces at the nodes. Figure 20.12c is a physical interpretation of the results. The effective mass for typical mode r is equal to $\left(\sum_{i=1}^{n} m_i\right) MPF_r$; this mass multiplied by S_{ar} gives the equivalent static force

(sum of p_{1r}, p_{2r}, and p_{3r}). We use the SRSS (Eq. 20.102) to calculate the required answers; the equivalent static shearing force and overturning moment at the base are:

$$V_{base} = [(231.3)^2 + (36.4)^2 + (4.5)^2]^{1/2} = 234.2 \text{ kN}$$

$$M_{base} = [(1716)^2 + (120)^2 + (16)^2]^{1/2} = 1720 \text{ kN-m}$$

20.13 Effect of ductility on forces due to earthquakes

The maximum drift due to earthquake excitation is roughly the same for elastic or plastic structures. But, when yielding occurs, the maximum forces are limited by the yield strengths. The dashed and solid lines in Figure 20.13 compare the load-deflection graphs of an elastic and a perfectly elastoplastic pendulum subjected to the same maximum displacement $D > D_y$, where D_y is the displacement at yielding. For the elastic member, the loading and unloading paths are the same (A to B, and B to A), without loss of energy. When the yield strength F_y is reached, the paths are ACD and DE for loading and unloading respectively. The area enclosed within $ACDE$ is the energy lost. In seismic design of structures, codes specify forces smaller than the elastic forces and require that the structures possess the ductility to ensure that plastic deformations can occur without failure (see specialized references[3]).

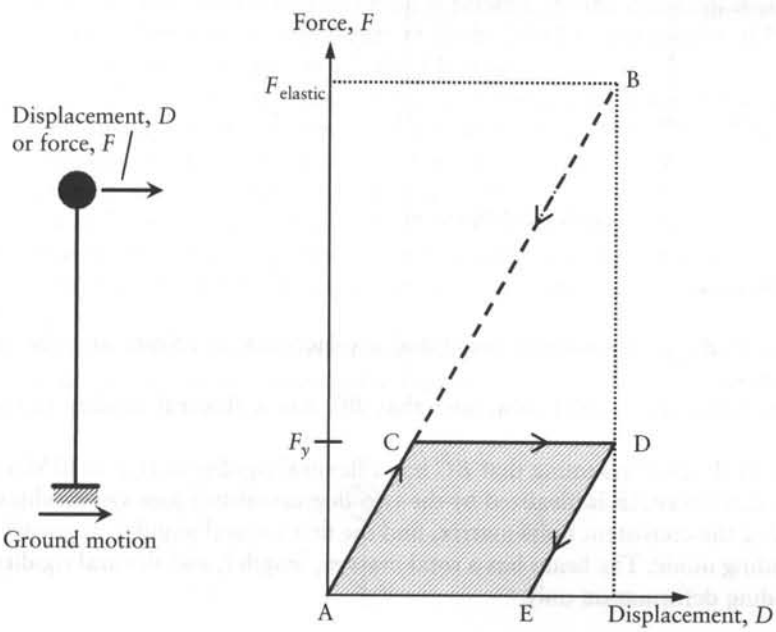

Figure 20.13 Force–displacement relationship in an elastic structure compared with elastoplastic structure.

3 Chopra, A. K., *Dynamics of Structures*, Pearson Prentice-Hall, Upper Saddle River, New Jersey, 2007, 876 pp.; Penelis, G. G. and Kappos, A. J., *Earthquake-Resistant Concrete Structures*, E&FN Spon, London, 1997, 572 pp.; Priestly, M. J., Seible, F. and Calvi, G. M., *Seismic Design and Retrofit of Bridges*, J. Wiley & Sons, London, 1996, 686 pp.; Paz, M., *Structural Dynamics, Theory and Computation*, 3rd ed., Van Nostrand Reinhold, New York, 1991, 626 pp.; Clough, R. W. and Penzien, J., *Dynamics of Structures*, 2nd ed., McGraw-Hill, New York, 1993, 738 pp.; Humar, J., *Dynamics of Structures*, Prentice-Hall, Engelwood Cliffs, New Jersey, 1990, 780 pp.

20.14 General

This chapter should be considered only as an introduction to the subject of structural dynamics. For more complete treatment, reference can be made to specialized publications.

Problems

Take the acceleration of gravity $g = 32.2\,\text{ft/sec}^2$ $(386\,\text{in./sec}^2)$ or $9.81\,\text{m/sec}^2$ whenever it is needed in the solution of the following problems.

20.1 Imperial units. Compute the natural angular frequency of vibration in sidesway for the frame in the figure, and calculate the natural period of vibration. Idealize the frame as a one-degree-of-freedom system. Neglect the axial and shear deformations, and the weight of the columns. If initially the displacement is 1 in. and the velocity is 10in./sec, what is the amplitude and what is the displacement at $t = 1$ sec?

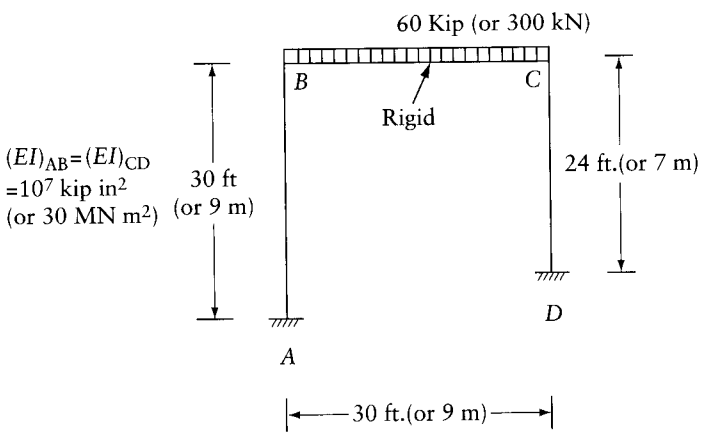

Prob. 20.1 or Prob. 20.2

20.2 SI units. Solve Prob. 20.1 assuming the initial displacement is 25 mm and the initial velocity 0.25 m/sec.

20.3 Imperial units. Solve Prob. 20.1 assuming that BC has a flexural rigidity $(EI)_{BC} = 10^7\,\text{kip in.}^2$.

20.4 SI units. Solve Prob. 20.2 assuming that BC has a flexural rigidity $(EI)_{BC} = 30\,\text{MN m}^2$.

20.5 The prismatic cantilever AB is idealized by the two-degrees-of-freedom system shown in the figure. Using the consistent mass matrix, find the first natural angular frequency and the corresponding mode. The beam has a total mass m, length l, and flexural rigidity EI. Consider bending deformation only.

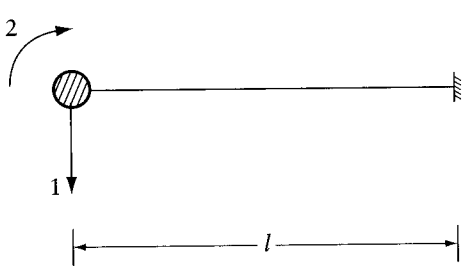

Prob. 20.5

20.6 Find the consistent mass matrix for the beam element of Prob. 20.5 assuming that the area of the cross section varies linearly between a_1 and a_2 at ends A and B respectively. Use the displacement functions of Eq. 20.11.

20.7 Imperial units. The frame in Prob. 20.1 is disturbed from rest by a horizontal force of 8 kip at C, suddenly applied at time $\tau = 0$ and removed at time $\tau = T/2$, where T is the natural period of vibration. What is the displacement and velocity at the removal of the force? What is the displacement at time $\tau = 11T/8$?

20.8 SI units. Solve Prob. 20.7 taking the force value to be 40 kN.

20.9 Imperial units. Solve Prob. 20.7 assuming that the disturbing force increases linearly from zero at $\tau = 0$ to 8 kip at $\tau = T/4$, then decreases linearly to zero at $\tau = T/2$, at which time the force is removed.

20.10 SI units. Solve Prob. 20.9 replacing the value 8 kip by 40 kN.

20.11 Imperial units. If the system of Prob. 20.1 has a damping coefficient $\xi = 0.1$, what are the damped natural circular frequency ω_d and the natural period of damped vibration T_d? What is the displacement at $t = 1$ sec, if $\dot{D}_0 = 1$ in. and $\dot{D}_0 = 10$ in./*sec*?

20.12 SI units. Answer the questions of Prob. 20.11 for the system of Prob. 20.2, with $\dot{D}_0 =$ 25 mm and $\dot{D}_0 = 0.25$ m/section.

20.13 If the amplitude of free vibration of a system with one degree of freedom decreases by 50 percent in 3 cycles, what is the damping coefficient?

20.14 Imperial units. Determine the maximum steady-state sidesway in the frame of Prob. 20.1 when it is subjected to a harmonic horizontal force at the level of BC of magnitude 4 sin $14t$ (kip), and (a) no damping is present, (b) the damping coefficient = 0.10.

20.15 SI units. Apply the requirements of Prob. 20.14 to the system of Prob. 20.2, replacing the value 4 sin $14t$ (kip) by 20 sin $14t$ (kN).

20.16 Imperial units. Assume that the frame in Prob. 20.1 has a damping coefficient = 0.05 and it is disturbed from rest by a horizontal force of 8 kip at C. The force is suddenly applied at time $\tau = 0$ and removed at time $\tau = T_d/2$, where T_d is the natural period of damped vibration. What are the displacements at the removal of the force and at time $\tau = 11T_d/8$? (Compare the answers with the undamped case, Prob. 20.7.)

20.17 SI units. Apply the requirements of Prob. 20.16 to the frame of Prob. 20.2, replacing the value 8 kip by 40 kN. (Compare the answers with the undamped case, Prob. 20.8.)

20.18 and 20.19

Determine the natural circular frequencies and characteristic shapes for the two-degrees-of-freedom systems shown in the figure.

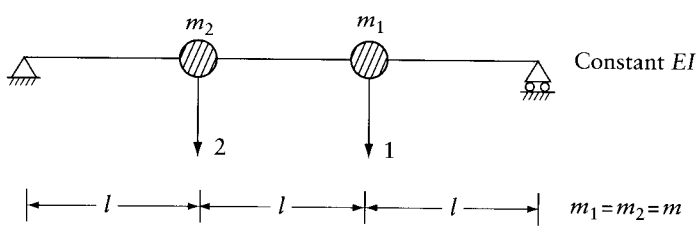

Prob. 20.18

20.20 Write the uncoupled equations of motion for the undamped system in Prob. 20.19, assuming that a force P_1 is suddenly applied at time $t = 0$ and continues to act after this. Find the time–displacement relations for D_1 and for D_2.

20.21 If in Prob. 20.20 the force $P_1 = P_0$ sin Ωt, what is the amplitude of the steady-state vibration of m_1?

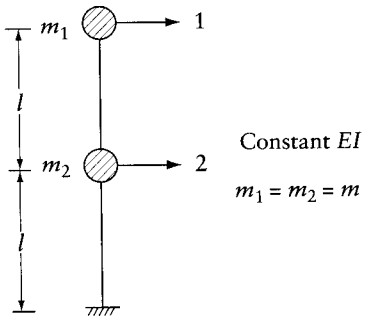

Prob. 20.19

20.22 Imperial units. The supports of the frame in Prob. 20.1 move horizontally with an acceleration indicated in the figure. What is the maximum displacement of BC relative to the support? Neglect damping.

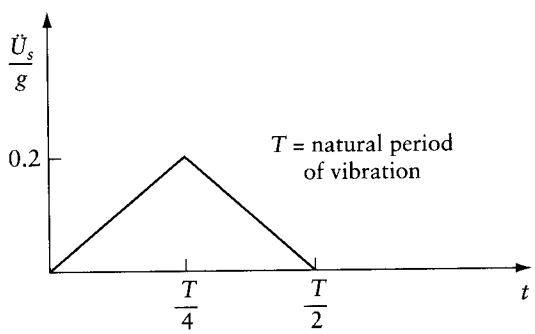

Prob. 20.22

20.23 SI units. Apply the requirement of Prob. 20.22 to the frame of Prob. 20.2.

20.24 If the support in Prob. 20.19 has a horizontal acceleration $\ddot{u}_s = (g/4) \sin \Omega t$, determine the maximum displacement of the mass m_1 relative to the support.

20.25 Solve Example 20.8 using a generalized single-degree-of-freedom system with the shape function ψ taken as the deflected shape of the frame due to static forces $\{m\}g$ at the coordinates.

20.26 Consider the plane frame in Figure 20.12 modified by the removal of the columns and the beam of the top storey. Number the coordinates 1 and 2, with one being the coordinate at the top of the modified frame. Calculate the equivalent static shearing force and overturning moment at the base for the effect of an earthquake whose design acceleration response spectrum $S_a(\zeta, T)$ is given in Figure 20.11a (with $\zeta = 0.05$). Consider only bending deformation of all members, and assume that EI for each member is 31.3×10^6 N-m^2.

Chapter 21

Computer analysis of framed structures

21.1 Introduction

This chapter discusses the use of computers in the analysis of large structures by the displacement (stiffness) method. Although the concepts discussed apply to all types of structure, the matrices involved in the analysis are given explicitly only for framed structures composed of prismatic straight members. Five types of framed structure are considered: plane and space trusses with pin joints, plane and space frames with rigid joints, and grids with rigid joints.[1]

The nodes (joints) and the members are numbered sequentially 1 to n_j and 1 to n_m respectively. The coordinates representing the degrees of freedom are also numbered sequentially, following at each node the order indicated in Figure 21.1. For example, at the ith node of a plane truss, the translations in the global x and y directions are represented by coordinate numbers $(2i-1)$ and $2i$ respectively. The origin and the directions of the orthogonal x, y (and z) axes are chosen arbitrarily.

The analysis of framed structures is commonly performed to determine the nodal displacements and the member end-forces. While the nodal displacements are determined in the global directions, the member end-forces are calculated in local directions of the individual members. These are defined in the following section.

Before proceeding with this chapter, some readers may find it beneficial to go over the summary given in Section 21.13.

21.2 Member local coordinates

The stiffness matrix $[S^*]$ of a member of a framed structure is first generated with respect to local coordinates in the directions of the centroidal axis and the principal axes of the member cross section; $[S^*]$ is then transformed to coordinates parallel to the global directions. This is necessary before the stiffness matrix of individual members can be assembled to obtain the structure stiffness matrix $[S]$. Also, the member end-actions are generally determined in local coordinates.

Typical nodal coordinates in global directions are shown in Figure 21.1, while the local coordinates for typical members of framed structures are shown in their positive directions in Figure 21.2.

The local coordinates are parallel to local axes x^*, y^*, and z^*. The local x^* axis is directed along the centroidal axis from the first node to the second node of the member. The first node

1 A summary of the steps involved in the analysis by the displacement method is given in Section 5.6. Appendix L describes a series of microcomputer programs available on disk for analysis of each of the five types of framed structure. The disk include executable files and FORTRAN-language files of the codes. Appendix L also gives address of a web site from which the files for linear analysis can be downloaded. An order form at the end of the book can be used to obtain nonlinear analysis programs.

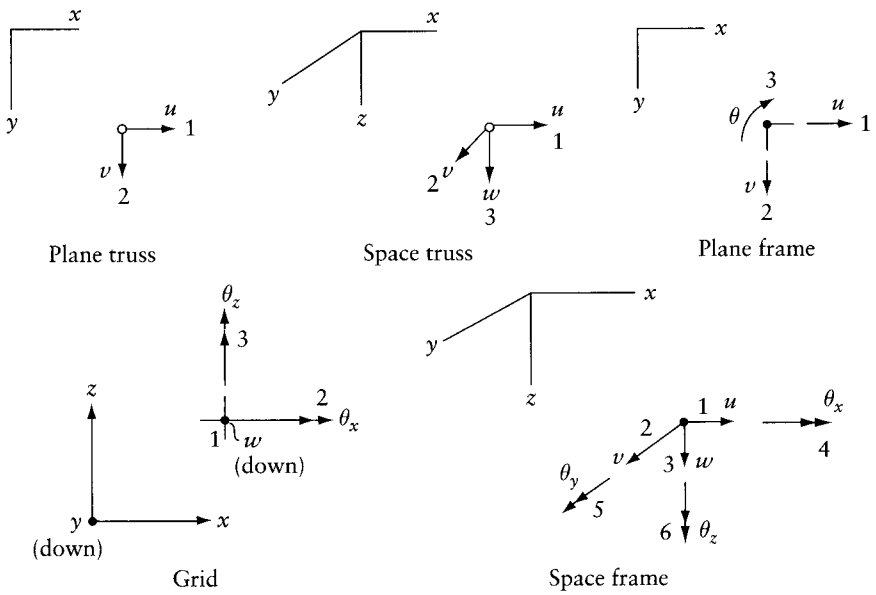

Figure 21.1 Global axes, degrees of freedom, and order of numbering of the coordinates at typical nodes of framed structures.

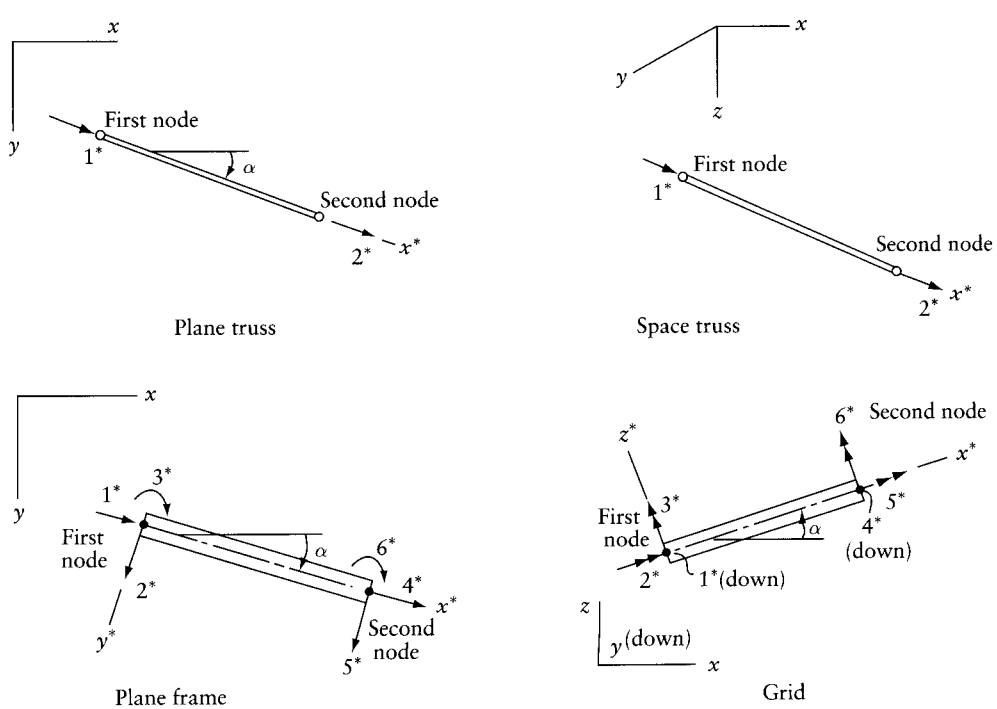

Figure 21.2 Local coordinates for typical members of framed structures.

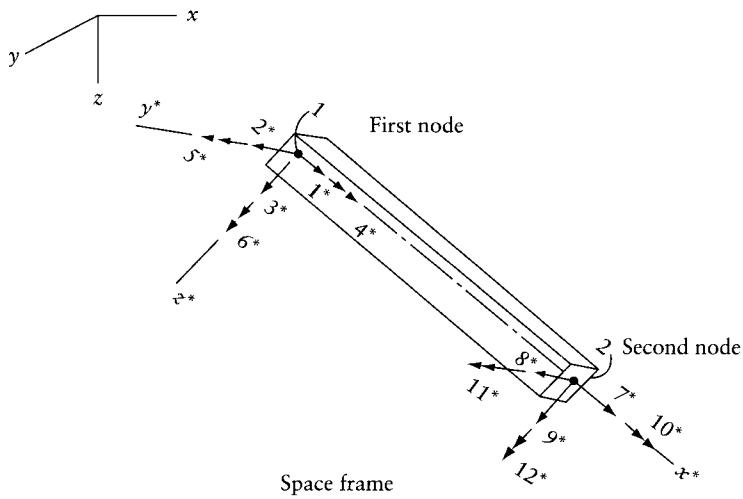

Figure 21.2 (Continued).

of a member is specified arbitrarily by the analyst by the order in which the two nodes at the ends of a member are listed in the member information in the input data (see Section 21.4).

Each of the sets of global and local axes is an orthogonal right-hand triad.

With the above system of numbering of coordinates and the choice of member local coordinates, the first step of the displacement method is completed when the numbering of nodes and elements is terminated. We recall that the first step involves the definition of the degrees of freedom and of the required actions and their positive directions.

21.3 Band width

As mentioned in Section 5.3, any element S_{ij} of the stiffness matrix $[S]$ of a structure is nonzero only when the coordinates i and j are adjacent to each other. In a framed structure, $S_{ij} \neq 0$ only when i and j are at one node or when i and j are at the two ends of one member. Generally, the nonzero elements of $[S]$ are limited to a band adjacent to the diagonal (Figure 21.3). This property of $[S]$, combined with the fact that the matrix is symmetrical, is used to conserve computer storage space and to reduce the number of computations. Only the diagonal elements of $[S]$ and the part of the band above the diagonal are generated and stored in a rectangular matrix of n rows and n_b columns (Figure 21.3). Here n is the number of degrees of freedom; n_b is referred to as the *half-band width* or simply the *band width* and is given by

$$n_b = s(|k-j|_{\text{largest}} + 1) \tag{21.1}$$

where s is the number of degrees of freedom per node, namely 2, 3, 3, 3, and 6 respectively, for plane truss, plane frame, grid, space truss, and space frame. The term $|k-j|$ is the absolute value of the difference between the node numbers at the ends of a member. The band width is determined by the member for which $|k-j|$ is a maximum.

A large portion of the computer time in the analysis of a structure is spent in the solution of the equilibrium equations

$$[S][D] = -[F]$$

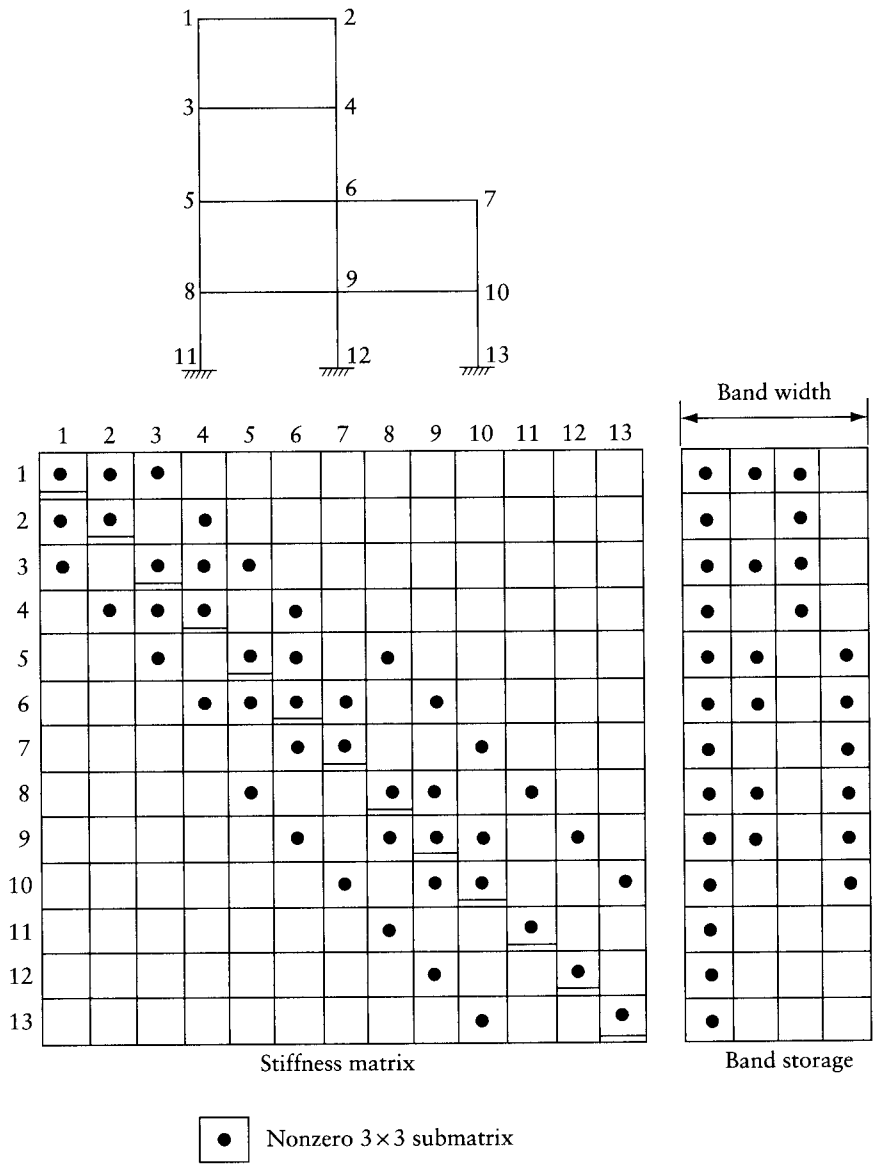

Figure 21.3 Node numbering and band width for a plane frame.

where [D] and [F] are, respectively, the unknown displacements and the forces at the coordinates to prevent the displacements due to loading. The respective columns of [D] and [F] correspond to the same loading case. The number of arithmetic operations in the solution of the equilibrium equations increases linearly with n and with n_b^2. Thus, we have an interest in reducing n_b.

For a given structure, a narrower band width is generally achieved by numbering the nodes sequentially across the side which has a smaller number of nodes. An example of a plane frame with suggested node numbering, the corresponding [S], and the band to be generated and stored in computing is shown in Figure 21.3. For the same structure, $n_b = 18$ (instead of 12) when the nodes are numbered sequentially down the columns. Note that [S] generally has zeros within the band (as in Figure 21.3).

There exist several techniques[2] aimed at efficiency and accuracy in equation solvers by automatic renumbering of the nodes to minimize n_b, by generating and operating only on the nonzero entries of [S] and by estimating and controlling round-off errors.

The stiffness matrix discussed above (Figure 21.3) is for a free (unsupported) structure. Elimination of rows and columns corresponding to the coordinates where the displacements are zero results in a condensed stiffness matrix of the supported structure (see Section 5.5). The condensed matrix is the one to be used in the equilibrium equations to be solved.

It is, of course, possible[3] to avoid generating the nonrequired rows and columns of [S]. However, for simplicity in computer programming, at the expense of more computing, it is possible to work with the stiffness matrix of the free structure by adjusting [S]. The adjustment, discussed in Section 21.10, causes the displacement to be equal to zero or equal to a prescribed value at any specified coordinates. This can be used when the analysis is for the effect of support movements.

21.4 Input data

The input data for computer analysis must be sufficient to define the material and geometric properties of the structure as well as the loading. Two basic units are used: unit of length and unit of force. These units must be employed consistently in the data.

The data for the geometric properties of a plane truss or a space truss are defined by the following: the modulus of elasticity E; the (x, y) or (x, y, z) coordinates of the nodes; the cross-sectional area of each member; two integers identifying the nodes at its ends; and the support conditions. The support conditions are defined by giving the number of the node and a restraint indicator for each of its two coordinates (u, v). The convention used here is to put 1 to indicate a free (unrestrained) displacement and 0 to indicate that the displacement at this coordinate is prescribed. When the restraint indicator is zero, the magnitude of the prescribed displacement must be given (zero for a support with no settlement). In Example 21.1, the input data for the plane truss in Figure 21.4 are given in Table 21.1.

When preparing the data for support conditions, it is important to ensure that the structure cannot translate or rotate freely as a rigid body. This requirement for stability should be verified before the computer analysis of any structure (particularly, spatial structures).

Ideally, a truss should be loaded only at the nodes so that there are only axial forces in the members. The input data for the load at a node are the node number and the components (F_x, F_y) or (F_x, F_y, F_z).

When a truss member is subjected to a temperature rise, the data are the member number and the two end-forces $\{A_r\}$ (along the local coordinates) which occur when the nodal displacements are prevented. This produces an axial compressive force of magnitude αTEa, where α is the coefficient of thermal expansion, T is the temperature rise, E is the modulus of elasticity, and a is the cross-sectional area.

As mentioned in Section 21.3, the effect of a prescribed displacement at a support can be accounted for by adjusting the stiffness matrix, but this can be done only when the analysis is for a single loading case. To avoid this restriction, we calculate the member end-forces when the prescribed displacements occur while the other displacements are zero (see Section 4.2). These member end-forces are then included in the data in the same way as the data for temperature. It is obvious that this needs to be done only for the members connected to nodes with prescribed displacements.

2 See Bathe, K. J. and Wilson, E. L., *Numerical Methods in Finite Element Analysis*, Prentice-Hall, Englewood Cliffs, NJ, 1976. See also Holzer, S. M., *Computer Analysis of Structures*, Elsevier, New York, 1985 (a list of references on this topic is given on pp. 325–327 of Holzer).

3 A computer coding for this purpose is discussed in Section 2.9 of Cook, R. D., *Concepts and Application of the Finite Elements*, 2nd ed., Wiley, New York, 1981.

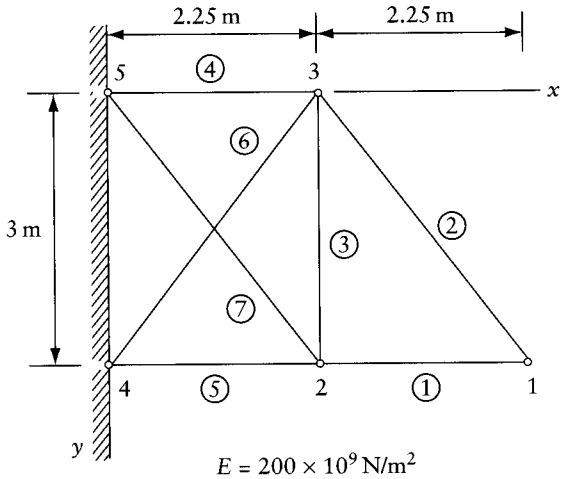

Basic units:
m for length
N for force

$E = 200 \times 10^9$ N/m^2

Cross-sectional area of members (m^2):

1, 5	0.0030
2, 4	0.0024
3	0.0012
6, 7	0.0048

Figure 21.4 Plane truss of Example 21.1.

Table 21.1 Input Data for a Plane Truss (Figure 21.4)

$E = 200 \times 10^9$

Nodal coordinates

Node	x	Y
1	4.5	3.0
2	2.25	3.0
3	2.25	0.0
4	0.0	3.0
5	0.0	0.0

Element information

Element	First node	Second node	a
1	2	1	0.0030
2	3	1	0.0024
3	2	3	0.0012
4	5	3	0.0024
5	4	2	0.0030
6	4	3	0.0048
7	5	2	0.0048

Support conditions

Node	Restraint indicator		Prescribed displacement	
	u	v	u	v
4	0	0	0.0	0.0
5	0	0	0.0	0.0

Loading case 1
Forces applied at nodes

Node	F_x	F_y
1	0.0	100×10^3

Loading case 2
Member end-forces with displacements restrained

Member	A_{r1}	A_{r2}
4	96×10^3	-96×10^3

Loading case 3
Member end-forces with displacements restrained

Member	A_{r1}	A_{r2}
6	-410×10^3	410×10^3

Example 21.1: Plane truss

Prepare the input data for the analysis of the plane truss in Figure 21.4 with the following loading cases: (1) A single downward force of 100×10^3 N at node 1; (2) a temperature rise of 20 degrees of member 4, the coefficient of thermal expansion being 10^{-5} per degree; and (3) a downward movement of 0.002 m of node 4.

Table 21.1 gives the required input data. The member end-forces in the data for loading case (3) are calculated in a similar way to the procedure included in Example 5.1.

For a plane frame, the input data differ from a plane truss in that the second moment of area of the cross section must also be given; at a supported node, three displacements u, v, and θ must be described; the forces at each member end have three components along the local coordinates (Figure 21.2); and when a member is subjected to forces away from the nodes, the data should include the member end-forces $\{A_r\}$ with the nodal displacements restrained. Example 21.2 gives the data for a plane frame.

The input data for a grid are similar to those for a plane frame except that the cross-sectional torsion constant J (Appendix G) is required for the members, instead of their area; the modulus of elasticity in shear G is also required. The displacement components at a typical node and the local coordinates of a typical member of a grid are shown in Figures 21.1 and 21.2.

The data defining the geometric properties of a space frame are the (x, y, z) coordinates of the nodes and, for each member, two integers identifying the nodes at its ends, the area a of the cross section, its torsion constant J, and its second moments of area I_y^* and I_z^* about the centroidal principal axes parallel to the local y^* and z^* axes (Figure 21.2). While the direction of the local x^* axis is defined by the (x, y, z) coordinates of the nodes, the y^* direction needs further definition. For this reason, we include in the data for each member the direction cosines of y^*: $\lambda_{y^*x}, \lambda_{y^*y}, \lambda_{y^*z}$. Here, the λ values are the cosines of the angles between the local y^* axis and the global directions. The third direction z^* is orthogonal to the other two local axes and thus does not require additional data.

In most practical cases, the global axes are selected in horizontal and vertical directions and the member cross sections have one of their principal axes horizontal or vertical. The y^* axis can be considered in such a direction and its direction cosines will be easy to find (see Prob. 22.1 and Eq. 21.9a).

The data for loading of a space frame are similar to those for a plane frame, noting that the forces at the nodes have six components in the global directions and each member end has six forces defined in Figures 21.1 and 21.2.

Example 21.2: Plane frame

Prepare the input data for the analysis of the plane frame in Figure 21.5 for the following loadings: (1) the loads shown; (2) displacements $u = 0.2b$ and $v = 0.5b$ of the support at node 1.

Table 21.2 gives the required input data. The member end-forces included in the data may be calculated using Appendices C and D. See also answer to Problem 22.2.

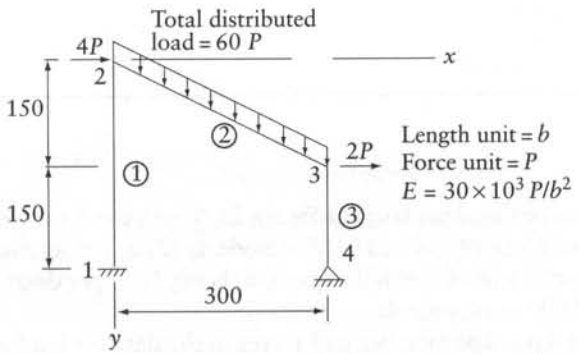

Properties of cross section of members

Member	a (b^2)	I (b^4)
1	30	3000
2	40	5000
3	30	3000

Figure 21.5 Plane frame of Example 21.2.

Table 21.2 Input Data for a Plane Frame (Figure 21.5)

$E = 30{,}000.0$

Nodal coordinates

Node	x	y
1	0.0	300.0
2	0.0	0.0
3	300.0	150.0
4	300.0	300.0

Element information

Element	First node	Second node	a	I
1	1	2	30.0	3000.0
2	2	3	40.0	5000.0
3	3	4	30.0	3000.0

Support conditions

Node	Restraint indicator			Prescribed displacement		
	u	v	θ	u	v	θ
1	0	0	0	0.0	0.0	0.0
4	0	0	1	0.0	0.0	–

Table 21.2 (Continued)

Loading case 1
Forces applied at nodes

Node	F_x	F_y
2	4.0	0.0
3	2.0	0.0

Member end-forces with displacements restrained

Member	A_{r1}	A_{r2}	A_{r3}	A_{r4}	A_{r5}	A_{r6}
2	−13.42	−26.83	−1500.0	−13.42	−26.83	1500.0

Loading case 2
Member end-forces with displacements restrained

Member	A_{r1}	A_{r2}	A_{r3}	A_{r4}	A_{r5}	A_{r6}
1	−1500.0	8.0	1200.0	1500.0	−8.0	1200.0

21.5 Direction cosines of element local axes

The direction cosines λ of the member local x^*, y^*, z^* axes will be used in the transformation matrices. The coordinates (x,y) defining the position of the nodes give the λ values for the local x^* axis. For a member of a plane truss or a plane frame,

$$\lambda_{x^*x} = \frac{x_2 - x_1}{l_{12}};\ \lambda_{x^*y} = \frac{y_2 - y_1}{l_{12}} \tag{21.2}$$

where

$$l_{12} = [(x_2 - x_1)^2 + (y_2 - y_1)^2]^{\frac{1}{2}} \tag{21.3}$$

The subscripts 1 and 2 refer to the first and second nodes of the member.

In a plane frame, the y^* axis for any member is perpendicular to x^* (Figure 21.2), so that the λ values for the y^* axis are

$$\lambda_{y^*x} = -\lambda_{x^*y} \quad \lambda_{y^*y} = \lambda_{x^*x} \tag{21.4}$$

For a member of a grid in the $x-z$ plane, the direction cosines required for the local x^* and z^* axes are λ_{x^*x}, λ_{x^*z}, λ_{z^*x}, and λ_{z^*z}. These are given by Eqs. 21.2 to 21.4, replacing y by z and y^* by z^*.

The direction cosines of the local x^* axis of a member of a space truss or a space frame are

$$\lambda_{x^*x} = \frac{x_2 - x_1}{l_{12}};\quad \lambda_{x^*y} = \frac{y_2 - y_1}{l_{12}};\quad \lambda_{x^*z} = \frac{z_2 - z_1}{l_{12}} \tag{21.5}$$

where

$$l_{12} = [(x_2 - x_1)^2 + (y_2 - y_1)^2 + (z_2 - z_1)^2]^{1/2} \tag{21.6}$$

As mentioned in the preceding section, the λ values for the local y^* axis of each member are included in the input data. The direction cosines of the local z^* axis are obtained from the cross product of two unit vectors in the x^* and y^* directions:

$$\lambda_{z^*x} = \lambda_{x^*y}\lambda_{y^*z} - \lambda_{x^*z}\lambda_{y^*y} \tag{21.7}$$

$$\lambda_{z^*y} = \lambda_{x^*z}\lambda_{y^*x} - \lambda_{x^*x}\lambda_{y^*z} \tag{21.8}$$

$$\lambda_{z^*z} = \lambda_{x^*x}\lambda_{y^*y} - \lambda_{x^*y}\lambda_{y^*x} \tag{21.9}$$

As mentioned in Section 21.5, in practice the global x and y axes for space frames are selected in horizontal directions and the local axis y^* for most members can be considered horizontal. To simplify the input data, the computer program SPACEF (available from a web site whose address is given in Appendix L) requires that the direction cosines for axis y^* be given only for a special member when the assumption that its y^* axis is parallel to the global $x-y$ plane is not acceptable. When the direction cosines of the local y^* axis are not given for any member, the program assumes that the axis is parallel to the global $x-y$ plane and calculates its direction cosines by Eq. 21.9a:

$$\lambda_{y^*x} = \frac{y_1 - y_2}{[(x_2-x_1)^2 + (y_2-y_1)^2]^{\frac{1}{2}}}; \lambda_{y^*y} = \frac{x_2 - x_1}{[(x_2-x_1)^2 + (y_2-y_1)^2]^{\frac{1}{2}}}; \lambda_{y^*z} = 0 \tag{21.9a}$$

21.6 Element stiffness matrices

The stiffness matrices of individual members of a framed structure with respect to local coordinates (Figure 21.2) can be generated from Appendix D.

For a member of a *plane truss* or a *space truss* (Figure 21.2), the stiffness matrix is

$$[S^*] = \frac{Ea}{l}\begin{bmatrix} 1 & -1 \\ -1 & 1 \end{bmatrix} \tag{21.10}$$

The stiffness matrix for a member of a *plane frame* (Figure 21.2), given in Eq. 5.6 is

$$[S^*] = \begin{bmatrix} Ea/l & & & & \text{symmetrical. Elements} & & \\ & 12EI/l^3 & & & \text{not shown are zero} & & \\ & 6EI/l^2 & 4EI/l & & & & \\ -Ea/l & & & Ea/l & & & \\ & -12EI/l^3 & -6EI/l^2 & & 12EI/l^3 & & \\ & 6EI/l^2 & 2EI/l & & -6EI/l^2 & 4EI/l & \end{bmatrix} \tag{21.11}$$

In the above equation, each member has its centroidal axis in the $x-y$ plane, and $I \equiv I_{z^*}$ with z^* perpendicular to the same plane.

The stiffness matrix for a member of a *grid* is (Figure 21.2)

$$[S^*] = \begin{bmatrix} 12EI/l^3 & & \text{symmetrical} & & & \\ 0 & GJ/l & & & & \\ 6EI/l^2 & 0 & 4EI/l & & & \\ -12EI/l^3 & 0 & -6EI/l^2 & 12EI/l^3 & & \\ 0 & -GJ/l & 0 & 0 & GJ/l & \\ 6EI/l^2 & 0 & 2EI/l & -6EI/l^2 & 0 & 4EI/l \end{bmatrix} \tag{21.12}$$

Here, the centroidal axes of the members are in the $x-z$ plane, and $I \equiv I_{z^*}$, with z^* situated in the same plane.

The stiffness matrix for a member of a *space frame* (Figure 21.2) is given by Eq. 6.5.

In the above matrices, the shear deformations are ignored. To take shear deformations into account, the elements of $[S^*]$ associated with coordinates representing shear or bending have to be adjusted as discussed in Section 14.2. The stiffness matrix of a typical member of a plane frame accounting for deformations due to axial force, bending and shear is given by Eq. 14.5.

21.7 Transformation matrices

The displacements $\{D^*\}$ in local directions at the end of a member of a framed structure of any type (Figure 21.2) are related to the displacements at the same node in global directions (Figure 21.1) by the geometrical relation

$$\{D^*\} = [t]\{D\} \tag{21.13}$$

where $[t]$ is a transformation matrix which is generated in terms of the direction cosines of the local axes x^*, y^*, z^* with respect to the global directions. The $[t]$ matrix for the different types of framed structures is given below.

Plane truss
$$[t] = [\lambda_{x^*x} \quad \lambda_{x^*y}] \tag{21.14}$$

Space truss
$$[t] = [\lambda_{x^*x} \quad \lambda_{x^*y} \quad \lambda_{x^*z}] \tag{21.15}$$

Plane frame
$$[t] = \begin{bmatrix} \lambda_{x^*x} & \lambda_{x^*y} & 0 \\ \lambda_{y^*x} & \lambda_{y^*y} & 0 \\ 0 & 0 & 1 \end{bmatrix} \tag{21.16}$$

Grid
$$[t] = \begin{bmatrix} 1 & 0 & 0 \\ 0 & \lambda_{x^*x} & \lambda_{x^*z} \\ 0 & \lambda_{z^*x} & \lambda_{z^*z} \end{bmatrix} \tag{21.17}$$

Space frame
$$[t] = \begin{bmatrix} \lambda_{x^*x} & \lambda_{x^*y} & \lambda_{x^*z} \\ \lambda_{y^*x} & \lambda_{y^*y} & \lambda_{y^*z} \\ \lambda_{z^*x} & \lambda_{z^*y} & \lambda_{z^*z} \end{bmatrix} \tag{21.18}$$

The transformation matrix given in the last equation is used to relate the three translations $\{u^*, v^*, w^*\}$ to $\{u, v, w\}$. The same matrix can be used to relate $\{\theta_x^*, \theta_y^*, \theta_z^*\}$ to $\{\theta_x, \theta_y, \theta_z\}$.

A member stiffness matrix $[S^*]$, with respect to local coordinates, can be transformed into a stiffness matrix $[S_m]$ corresponding to coordinates in the global directions (see Eq. 9.17) by

$$[S_m] = [T]^T[S^*][T] \tag{21.19}$$

where

$$[T] = \begin{bmatrix} [t] & [0] \\ [0] & [t] \end{bmatrix} \tag{21.20}$$

The above equation may be used for members of a plane truss, a space truss, a plane frame, or a grid, substituting for $[t]$ from one of the Eqs. 21.14 to 21.17. However, for a member of a space frame,

$$[T] = \begin{bmatrix} [t] & & & \\ & [t] & & \\ & & [t] & \\ & & & [t] \end{bmatrix} \begin{matrix} \text{submatrices not} \\ \text{shown are null} \end{matrix} \tag{21.21}$$

where $[t]$ is given by Eq. 21.18.

The $[T]$ matrices may be used to transform the actions in local directions at the ends of a member into equivalent forces along nodal coordinates in the global directions (see Eq. 9.16):

$$\{F\}_m = [T]_m^T \{A_r\}_m \tag{21.22}$$

where the subscript m refers to element number.

The elements of the matrices $[S_m]$ and $\{F\}_m$ are forces in the global directions; they represent contributions of one member. Summing the matrices for all members gives the stiffness matrix and load vector of the assembled structure, as shown in Section 21.9.

21.8 Member stiffness matrices with respect to global coordinates

Equation 21.19 expresses the stiffness matrix $[S_m]$ for a member of a framed structure with respect to coordinates at its two ends in the direction of the global axes. Instead of the matrix product in Eq. 21.19, the stiffness matrix $[S_m]$ is given below in explicit form for a member of framed structures of various types.

Plane truss

$$[S_m] = \frac{Ea}{l} \begin{bmatrix} c^2 & cs & -c^2 & -cs \\ cs & s^2 & -cs & -s^2 \\ -c^2 & -cs & c^2 & cs \\ -cs & -s^2 & cs & s^2 \end{bmatrix} \tag{21.23}$$

where $c = \cos\alpha = \lambda_{x^*x}$; $s = \sin\alpha = \lambda_{x^*y}$; and α is the angle defined in Figure 22.2 with its positive sign convention.

Space truss

$$[S_m] = \begin{bmatrix} [S_{11}] & [S_{12}] \\ [S_{21}] & [S_{22}] \end{bmatrix}_m \tag{21.24}$$

where

$$[S_{11}]_m = \frac{Ea}{l}\begin{bmatrix} \lambda_{x^*x}^2 & & \text{symmetrical} \\ \lambda_{x^*y}\lambda_{x^*x} & \lambda_{x^*y}^2 & \\ \lambda_{x^*z}\lambda_{x^*x} & \lambda_{x^*z}\lambda_{x^*y} & \lambda_{x^*z}^2 \end{bmatrix} \tag{21.25}$$

$$[S_{22}]_m = [S_{11}]_m; \quad [S_{21}]_m = -[S_{11}]_m; \quad [S_{12}]_m = [S_{21}]_m^T \tag{21.26}$$

Plane frame

$$[S_m] = \left[\begin{array}{ccc:ccc} \frac{Eac^2}{l} + \frac{12EIs^2}{l^3} & & & & \text{symmetrical} & \\ \left(\frac{Ea}{l} - \frac{12EI}{l^3}\right)cs & \frac{Eas^2}{l} + \frac{12EIc^2}{l^3} & & & & \\ -\frac{6EI}{l^2}s & \frac{6EI}{l^2}c & \frac{4EI}{l} & & & \\ \hdashline -\frac{Eac^2}{l} - \frac{12EIs^2}{l^3} & -\left(\frac{Ea}{l} - \frac{12EI}{l^3}\right)cs & \frac{6EI}{l^2}s & \frac{Eac^2}{l} + \frac{12EIs^2}{l^3} & & \\ -\left(\frac{Ea}{l} - \frac{12EI}{l^3}\right)cs & -\frac{Eas^2}{l} - \frac{12EIc^2}{l^3} & -\frac{6EI}{l^2}c & \left(\frac{Ea}{l} - \frac{12EI}{l^3}\right)cs & \frac{Eas^2}{l} + \frac{12EIc^2}{l^3} & \\ -\frac{6EI}{l^2}s & \frac{6EI}{l^2}c & \frac{2EI}{l} & \frac{6EI}{l^2}s & -\frac{6EI}{l^2}c & \frac{4EI}{l} \end{array}\right] \tag{21.27}$$

where $c = \cos\alpha = \lambda_{x^*x} = \lambda_{y^*y}$; $s = \sin\alpha = \lambda_{x^*y} = -\lambda_{y^*x}$; and α is the angle defined in Figure 21.2 with its positive sign convention.

Grid

$$[S_m] = \begin{bmatrix} \frac{12EI}{l^3} & & & & \text{symmetrical} & \\ -\frac{6EI}{l^2}s & \frac{GJc^2}{l} + \frac{4EIs^2}{l} & & & & \\ \frac{6EI}{l^2}c & \left(\frac{GJ}{l} - \frac{4EI}{l}\right)cs & \frac{GJs^2}{l} + \frac{4EIc^2}{l} & & & \\ -\frac{12EI}{l^3} & \frac{6EI}{l^2}s & -\frac{6EI}{l^2}c & \frac{12EI}{l^3} & & \\ -\frac{6EI}{l^2}s & -\frac{GJc^2}{l} + \frac{2EIs^2}{l} & \left(-\frac{GJ}{l} - \frac{2EI}{l}\right)cs & \frac{6EIs}{l^2} & \frac{GJc^2}{l} + \frac{4EIs^2}{l} & \\ \frac{6EI}{l^2}c & \left(-\frac{GJ}{l} - \frac{2EI}{l}\right)cs & -\frac{GJs^2}{l} + \frac{2EIc^2}{l} & -\frac{6EI}{l^2}c & \left(\frac{GJ}{l} - \frac{4EI}{l}\right)cs & \frac{GJs^2}{l} + \frac{4EIc^2}{l} \end{bmatrix} \tag{21.28}$$

where $c = \cos\alpha = \lambda_{x^*x} = \lambda_{z^*z}$; $s = \sin\alpha = \lambda_{x^*z} = -\lambda_{z^*x}$; and a is the angle defined in Figure 21.2 with its positive sign convention.

To save computing, Eqs. 21.23 to 21.28 may be used in lieu of the matrix product in Eq. 21.19.

The stiffness matrix $[S_m]$ for a member of a *space frame* with respect to global coordinates is too long to be included here.

21.9 Assemblage of stiffness matrices and load vectors

Consider a typical member of a framed structure whose first and second nodes are numbered j and k respectively. Let $[S_m]$ be the stiffness matrix of the member with respect to coordinates in the global directions at the two nodes. $[S_m]$ may be partitioned as follows:

$$[S_m] = \begin{bmatrix} [S_{11}] & [S_{12}] \\ [S_{21}] & [S_{22}] \end{bmatrix}_m \tag{21.29}$$

The same partitioning is made by dashed lines in Eqs. 21.23, 21.24, 21.27, and 21.28. The elements above the horizontal dashed line represent the forces at the first node (the jth node), and the elements below the same line represent forces at the second node (the kth node). The elements to the left of the vertical dashed line are produced by unit displacements at node j, and the elements to the right of the same line correspond to unit displacements at node k. Each of the submatrices in Eq. 21.29 is of size $s \times s$, where s is the number of degrees of freedom per node.

Let the structure stiffness matrix $[S]$ be also partitioned into $n_j \times n_j$ submatrices, each of size $s \times s$, where n_j is the number of nodes. The submatrices of the element stiffness matrix in Eq. 21.29 may be arranged in a matrix of the same size and partitioned in the same way as $[S]$:

$$[\bar{S}_m] = \begin{array}{c} \\ j \\ \\ k \\ \\ \end{array} \begin{bmatrix} & j & & k & \\ & \cdots & & & \\ \cdots & [S_{11}] & \cdots & [S_{12}] & \cdots \\ & \cdots & & & \\ & [S_{21}] & \cdots & [S_{22}] & \cdots \\ & \cdots & & \cdots & \end{bmatrix}_m \tag{21.30}$$

In this equation only the submatrices associated with nodes j and k are shown while all other submatrices are null. The above matrix represents the contribution of the mth member to the structure stiffness. The structure stiffness matrix can now be obtained by a summation:

$$[S] = \sum_{m=1}^{n_m} [\bar{S}_m] \tag{21.31}$$

where n_m is the number of members.

We should note that each column of the stiffness matrix $[\bar{S}_m]$ for an element represents a set of forces in equilibrium, and an assemblage of such matrices gives a structure stiffness matrix $[S]$ which has the same property.

The matrix $[S]$ generated as described above represents the stiffness of a free unsupported structure. It is a singular matrix which cannot be used to solve for the unknown displacements before it has been adjusted to account for the support conditions (see Section 21.10).

If the structure is to be analyzed for one case of loading, we need to solve the equilibrium equations $[S]\{D\} = -\{F\}$. The vector $\{F\}$ of the forces necessary to prevent the nodal displacements may be considered as the sum of two vectors:

$$\{F\} = \{F_a\} + \{F_b\} \tag{21.32}$$

Here, $\{F_a\}$ accounts for the external forces at the nodes, and $\{F_b\}$ for other forces (between the nodes), for temperature variation, and for support movements. $\{F_a\}$ is generated simply by listing the nodal forces given in the input data with a reversed sign. The vector $\{F_b\}$ is generated from the restraining forces $\{A_r\}_m$ given in the input data for individual members.

First, Eq. 21.22 is used to transform $\{A_r\}_m$ into equivalent nodal forces $\{F\}_m$ in global directions at member ends. The vector $\{F\}_m$, which has $2s$ elements (s being the number of degrees of freedom per node), may be partitioned in two submatrices, $\{\{F_1\}\ \{F_2\}\}_m$, each having s elements representing forces at one end. The two submatrices may be rearranged into a vector of the same size as $\{F_b\}$ (or $\{F\}$):

$$\{\bar{F}\}_m = \begin{matrix} \\ j \\ \\ k \\ \end{matrix} \begin{Bmatrix} \cdots \\ \{F_1\} \\ \cdots \\ \{F_2\} \\ \cdots \end{Bmatrix}_m \tag{21.33}$$

This vector has n_j submatrices, all of which are null with the exception of the jth and the kth, where j and k are the node numbers at the two ends of the mth member. The vector $\{\bar{F}\}_m$ represents the contribution of the mth member to the load vector $\{F_b\}$: thus, summing for all members,

$$\{F_b\} = \sum_{m=1}^{n_m} \{\bar{F}\}_m \tag{21.34}$$

where n_m is the number of members.

Enlarging the element stiffness and the force matrices to the size of the structure stiffness matrix and of its load vector (Eqs. 21.30 and 21.33) requires formidable computer storage space. The actual computations are carried out using one matrix for stiffness and another for the load vector(s) of the assembled structure. The matrices are null at the start, and then, for each member, the elements of $[S_m]$ and $\{\bar{F}\}_m$ are generated and added in the appropriate location by an algorithm. Furthermore, advantage is taken of the symmetry of the structure stiffness matrix and of its banded nature; thus, for $[S]$, only the elements within the band on and above the diagonal are generated, as discussed in Section 21.3.

Example 21.3: Stiffness matrix and load vectors for a plane truss

Generate the stiffness matrix and the load vectors for the three loading cases in Example 21.1 (Figure 21.4). The input data are given in Table 21.1.

To save space, we give below the member stiffness matrices $[S_m]$ and $[\bar{S}_m]$ for two members only. The submatrices not shown are null.

We start with the structure stiffness matrix $[S] = [0]$.

For member 1, having its first node $j = 2$ and second node $k = 1$ (see Table 21.1), Eqs. 21.23 and 21.30 give

$$[S_1] = \frac{200 \times 10^9 (0.0030)}{2.25} \begin{bmatrix} 1 & 0 & -1 & 0 \\ 0 & 0 & 0 & 0 \\ -1 & 0 & 1 & 0 \\ 0 & 0 & 0 & 0 \end{bmatrix}$$

and

$$[\bar{S}_1] = \begin{array}{c} \\ 1 \\ \\ 2 \\ \\ 3 \\ \\ 4 \\ \\ 5 \end{array} \begin{array}{c} \begin{array}{cccccc} 1 & & 2 & & 3 & & 4 & & 5 \end{array} \\ \begin{bmatrix} 267 & 0 & -267 & 0 & & & & & \\ 0 & 0 & 0 & 0 & & & & & \\ -267 & 0 & 267 & 0 & & & & & \\ 0 & 0 & 0 & 0 & & & & & \\ & & & & & & & & \\ & & & & & & & & \\ & & & & & & & & \\ & & & & & & & & \\ & & & & & & & & \end{bmatrix} \end{array} 10^6$$

Adding $[\bar{S}_1]$ to the existing structure stiffness matrix $[S]$ gives the new matrix $[S]$, which, in this case, is the same as $[\bar{S}_1]$ and therefore not repeated here.

A repetition of the above calculations for member 2, which has $j = 3$ and $k = 1$, gives

$$[S_2] = \frac{200 \times 10^9 (0.0024)}{3.75} \begin{bmatrix} 0.36 & 0.48 & -0.36 & -0.48 \\ 0.48 & 0.64 & -0.48 & -0.64 \\ -0.36 & -0.48 & 0.36 & 0.48 \\ -0.48 & -0.64 & 0.48 & 0.64 \end{bmatrix}$$

and

$$[\bar{S}_2] = \begin{array}{c} \\ 1 \\ \\ 2 \\ \\ 3 \\ \\ 4 \\ \\ 5 \end{array} \begin{array}{c} \begin{array}{ccccccccc} 1 & & 2 & & 3 & & 4 & & 5 \end{array} \\ \begin{bmatrix} 46 & 61 & & & -46 & -61 & & & \\ 61 & 82 & & & -61 & -82 & & & \\ & & & & & & & & \\ & & & & & & & & \\ -46 & -61 & & & 46 & 61 & & & \\ -61 & -82 & & & 61 & 82 & & & \\ & & & & & & & & \\ & & & & & & & & \\ & & & & & & & & \end{bmatrix} \end{array} 10^6$$

Adding this matrix to the existing matrix $[S]$, we obtain the new matrix $[S]$:

$$[S] = \begin{array}{c} \\ 1 \\ \\ 2 \\ \\ 3 \\ \\ 4 \\ \\ 5 \\ \\ \end{array} \begin{array}{c} \begin{array}{cccccccccc} 1 & & 2 & & 3 & & 4 & & 5 & \end{array} \\ \left[\begin{array}{cccccccccc} 313 & 61 & -267 & 0 & -46 & -61 & & & & \\ 61 & 82 & 0 & 0 & -61 & -82 & & & & \\ -267 & 0 & 267 & 0 & & & & & & \\ 0 & 0 & 0 & 0 & & & & & & \\ -46 & -61 & & & 46 & 61 & & & & \\ -61 & -82 & & & -61 & 82 & & & & \\ & & & & & & & & & \\ & & & & & & & & & \\ & & & & & & & & & \\ & & & & & & & & & \end{array}\right] \end{array} 10^6$$

Repetition of the above computations for members 3 to 7 leads to the structure stiffness matrix:

$$[S] = \begin{array}{c} \\ 1 \\ \\ 2 \\ \\ 3 \\ \\ 4 \\ \\ 5 \\ \\ \end{array} \begin{array}{c} \begin{array}{cccccccccc} 1 & & 2 & & 3 & & 4 & & 5 & \end{array} \\ \left[\begin{array}{cccccccccc} 313 & 61 & -267 & 0 & -46 & -61 & & & & \\ 61 & 82 & 0 & 0 & -61 & -82 & & & & \\ -267 & 0 & 625 & 123 & 0 & 0 & -267 & 0 & -92 & -123 \\ 0 & 0 & 123 & 244 & 0 & -80 & 0 & 0 & -123 & -164 \\ -46 & -61 & 0 & 0 & 352 & -62 & -92 & 123 & -213 & 0 \\ -61 & -82 & 0 & -80 & -62 & 326 & 123 & -164 & 0 & 0 \\ & & -267 & 0 & -92 & 123 & 359 & -123 & & \\ & & 0 & 0 & 123 & -164 & -123 & 164 & & \\ & & -92 & -123 & -231 & 0 & & & 305 & 123 \\ & & -123 & -164 & 0 & 0 & & & 123 & 164 \end{array}\right] \end{array} 10^6$$

The load vector for case 1 is

$$\{F\} = \{0, -100 \times 10^3, 0, 0, 0, 0, 0, 0, 0, 0\}$$

For cases 2 and 3, we need a transformation matrix for member 4, which has its first node 5 and the second node 3. Equations 21.2, 21.14 and 21.20 give

$$[t] = [1 \quad 0] \quad \text{and} \quad [T] = \begin{bmatrix} 1 & 0 & 0 & 0 \\ 0 & 0 & 1 & 0 \end{bmatrix}$$

For the same member, Eqs. 21.22 and 21.33 give for loading case 2

$$\{F\}_4 = \begin{bmatrix} 1 & 0 \\ 0 & 0 \\ 0 & 1 \\ 0 & 0 \end{bmatrix} \begin{Bmatrix} 96 \times 10^3 \\ -96 \times 10^3 \end{Bmatrix} = \begin{Bmatrix} 96 \\ 0 \\ -96 \\ 0 \end{Bmatrix} \times 10^3$$

and

$$\{\bar{F}\}_4 = \{0, 0, 0, 0, -96 \times 10^3, 0, 0, 0, 96 \times 10^3, 0\}$$

Because member 4 is the only member which has restraining forces listed in the input data (Table 21.1), this vector is the global vector $\{F\}$ for load case 2. Similar calculations are made for case 3, and the load vectors for the three cases are combined into one matrix:

$$[F] = \begin{array}{c} \\ 1 \\ \\ 2 \\ \\ 3 \\ \\ 4 \\ \\ 5 \\ \\ \end{array} \begin{bmatrix} 0 & \\ -100 & \\ & \\ & \\ & -96 & 246 \\ & 0 & -328 \\ & & -246 \\ & & 328 \\ & 96 & \\ & 0 & \end{bmatrix} 10^3$$

21.10 Displacement support conditions and support reactions

To find the unknown displacements we need to solve the equilibrium equation

$$[S]\{D\} = -\{F\} \tag{21.35}$$

where $[S]$ is the structure stiffness matrix, $\{D\}$ is a vector of nodal displacements, and $\{F\}$ is a vector of artificial restraining forces which prevent the nodal displacements.

In general, some elements of $\{D\}$ are known to be zero or have prescribed values at the supports, while the corresponding elements of $\{F\}$ are unknown. The total number of unknowns is n, which is equal to the number of equations.

The stiffness matrix $[S]$, generated as described in the preceding section, is the stiffness of a free (unsupported) structure. It is theoretically possible to rearrange the rows and columns in the matrices in Eq. 21.35 so that the known elements of $\{D\}$ are listed first. The equation can then be separated into two sets (see Section 5.5). One set, containing only the unknown displacements, can be solved and the result is then substituted in the second set to give the reactions. However, rearranging the equations increases the band width.

Without disturbing the arrangement, it is possible to adjust Eq. 21.35 so that its solution ensures that, at any coordinate k, the displacement $D_k = c_k$, where c_k can be zero in the case of a support without movement or can be a known value of support movement. In one method, the kth row and column of the matrices in Eq. 21.35 are modified as follows:

$$\begin{array}{c} \\ 1 \\ k \\ n \end{array}\begin{array}{c} \begin{array}{ccccc} 1 & & k & & n \end{array} \\ \begin{bmatrix} & & 0 & & \\ & & \cdots & & \\ 0 & \cdots & 1 & \cdots & 0 \\ & & \cdots & & \\ & & 0 & & \end{bmatrix} \end{array} \begin{Bmatrix} D_1 \\ \cdots \\ D_k \\ \cdots \\ D_n \end{Bmatrix} = \begin{bmatrix} -F_1 - S_{1k}c_k \\ \cdots \\ c_k \\ \cdots \\ -F_n - S_{nk}c_k \end{bmatrix} \tag{21.36}$$

The kth equations are now replaced by $D_k = c_k$; the terms $S_{1k}\ c_k$, $S_{2k}\ c_k, \ldots$ represent the forces at nodes $1, 2, \ldots$ when $D_k = c_k$ and the other displacements are prevented. The modifications shown in Eq. 21.36 have to be repeated for all the prescribed displacements. The solution of the modified equations gives the unknown displacements, but not the unknown reactions. To determine the force F_k we substitute in the kth row of Eq. 21.35 the D values, which are now all known:

$$F_k = \sum_{j=1}^{n} S_{kj} D_j \tag{21.37}$$

The reaction at a supported node in the direction of the kth coordinate is given by

$$R_k = F_k + F'_k \tag{21.38}$$

where F'_k is the kth element of the original load vector, i.e. before Eq. 21.35 was modified. This element represents a reaction at coordinate k with $\{D\} = \{0\}$. The value F'_k will be nonzero only when an external force is applied at the supported node or over the members meeting at the node, or when the members meeting at the node are subjected to temperature change.

As mentioned in Section 21.3, computer storage space is commonly saved by storing $[S]$ in a compact form which takes advantage of its symmetry and its banded nature. The same space is used to store the reduced matrix needed for the solution; thus, the original $[S]$ is lost when $\{D\}$ is determined. To be able to use Eq. 21.37 at this stage, the necessary rows of $[S]$ must be stored. Also, the element F'_k of the original load vector must be retained for use in Eq. 21.38.

Another method of prescribing a displacement $D_k = c_k$ which requires fewer operations is to modify the kth row of the original equations as follows:

$$\begin{bmatrix} \cdots & & & & \\ S_{k1} & \cdots & S_{kk} \times 10^6 & \cdots & S_{kn} \\ \cdots & & & & \end{bmatrix} \begin{Bmatrix} D_1 \\ \cdots \\ D_k \\ \cdots \\ D_n \end{Bmatrix} = \begin{Bmatrix} -F_1 \\ \cdots \\ S_{kk} \times 10^6 c_k \\ \cdots \\ -F_n \end{Bmatrix} \tag{21.39}$$

where the 10^6 is an arbitrarily chosen large number. The change in Eq. 21.39 is equivalent to providing a fixed support connected to the structure by a very strong spring of stiffness $(10^6 - 1)S_{kk}$ at the kth coordinate and applying a large force of $S_{kk} \times 10^6 c_k$. For all practical purposes, Eq. 21.39 satisfies with sufficient accuracy the condition that D_k equals c_k. This is so because the division of both sides of the kth row in Eq. 21.39 by $10^6 S_{kk}$ reduces the term $S_{kk} \times 10^6$ to 1; the other S terms become negligible, and the kth row reduces to $D_k \simeq c_k$.

After modification of the original equations for each prescribed displacement, a solution will give a vector $\{D\}$ of the displacements at all nodes. The force F_k can now be determined by Eq. 21.37, which requires storage of the kth row of the original $[S]$ matrix. Alternatively, F_k can be obtained by combining Eq. 21.37 and the kth row of Eq. 21.39:

$$F_k = S_{kk} \times 10^6 (c_k - D_k) + D_{kk} D_k \tag{21.40}$$

The difference $c_k - D_k$ needs to be determined with sufficient number of significant figures (three or more). After calculating F_k by the above equation, substitution in Eq. 21.38 gives the support reaction.

The condition that D_k equals c_k can also be satisfied by replacing S_{kk} on both sides of Eq. 21.39 by $(S_{kk} + 1)$. In this case, F_k can be calculated using Eq. 21.40 and replacing S_{kk} in the first term on the right-hand side by $(S_{kk} + 1)$. This option should be used when S_{kk} can be zero (e.g. in trusses).

When a structure is analyzed for a number of load cases, the vectors $\{D\}$ and $\{F\}$ in Eq. 21.35 are replaced by rectangular matrices $[D]$ and $[F]$, with the respective columns of the two matrices representing one load case; however, the same stiffness matrix $[S]$ is used for all cases. Modification of $[S]$, as suggested by Eq. 21.36 or Eq. 21.39, indicates that a loading case representing the effect of support movements cannot be solved simultaneously with other loading cases unless the prescribed displacements are valid for all cases. This will be the condition when all the prescribed displacements are zero, thus representing supports without movement.

In order to analyze for a nonzero prescribed displacement $D_k = c_k$ at the same time as for other loading cases, we may prepare the support conditions in the input data as if c_k were zero. However, the effect of $D_k = c_k$ must then be presented in the forces $\{A_r\}$ included in the data; $\{A_r\}$ represents the end-forces for the members connected to the coordinate k when $D_k = c_k$ when the displacements at the other coordinates are restrained (see Example 21.1).

The techniques presented in this section require the solution of a larger number of equations than the number of unknown displacements. The extra computing is justified by simpler coding and by the fact that the solution gives the unknown displacements as well as the unknown forces.

As mentioned in Section 21.3, it is possible to generate only the equilibrium equations corresponding to the unknown displacements. After the solution of these equations, the displacements, which become known at all coordinates, are used to determine the forces $\{A\}$ at member ends in the directions of local axes (see Section 21.12). The reactions at a supported node (with or without support movement) can then be obtained by summing the forces at the ends of the members meeting at the node:

$$\{R\} = \sum ([t]^T \{A\})_i - \{F_s\} \tag{21.41}$$

Here, $\{R\}$ represents s reaction components in global directions, s being the number of degrees of freedom per node; the $[t]$ matrix is included to transform the member end-forces from local to global directions (Eq. 21.22); the subscript i refers to a member number, and the summation is performed for the members meeting at the supported node; and $\{F_s\}$ represents forces applied direct at the supported node, producing no displacements and no member end-forces.

21.11 Solution of banded equations

The solution of the equilibrium Eq. 21.35 was expressed in earlier chapters in the succinct form $\{D\} = -[S]^{-1}\{F\}$. However, a solution by matrix inversion involves more operations than the Gauss elimination or the Cholesky method, discussed later in this section.

Consider a system of n linear equations.

$$[a]\{x\} = \{c\} \tag{21.42}$$

The elements of $[a]$ and $\{c\}$ are known, and it is required to determine the vector of unknowns $\{x\}$.

The standard Gauss elimination (see Eq. A.44, Appendix A) reduces the original equations to

$$[u]\{x\} = \{d\} \tag{21.43}$$

where $[u]$ is a unit upper triangular matrix in which all the diagonal elements are equal to 1, and the elements below the diagonal are zero. Back substitution, starting from the last row, gives successively the unknowns x_n, $x_{n-1}, \ldots, x_1$.

The Gauss elimination can be achieved by a computer, using compact storage space. In Crout's procedure, presented in Section A.9, the Gauss elimination is achieved by generating auxiliary matrices $[b]$ and $\{d\}$ of the same size as $[a]$ and $\{c\}$. The elements above the diagonal in $[b]$ are the same as the corresponding elements of $[u]$; thus,

$$u_{ij} \equiv b_{ij} \quad \text{with } i < j \tag{21.44}$$

For structural analysis, we are interested in the case when $[a]$ is symmetrical and banded. In such a case, $[b]$ is also banded and has the same band width. Also, any element b_{ij} above the diagonal is equal to b_{ji}/b_{ii}. Thus, when only the half-band of $[a]$ is stored in a rectangular matrix (Figure 21.3), $[b]$ can be stored in a matrix of the same size with no need to store the elements below the diagonal.

Examination of the equations which give the elements of $[b]$ (see Eqs. A.42 and A.43 and the numerical example in Section A.9) will indicate that, starting from the top row, the elements of $[b]$ can be calculated one by one. Each element b_{ij} can be stored in the same space occupied by a_{ij} because the latter term is no longer needed. In other words, the $[b]$ matrix can be generated in a band form and can replace $[a]$ using the same storage space. The vector $\{d\}$ is generated in a similar way and is stored in the same space originally occupied by $\{c\}$.

The Cholesky method offers some advantages when $[a]$ is symmetrical and banded.[4] In this method, the symmetrical matrix $[a]$ is decomposed into the product of three matrices:

$$[a] = [u]^T[e][u] \tag{21.45}$$

Here again, $[u]$ is a unit upper triangular matrix and therefore its transpose $[u]^T$ is a unit lower triangular matrix; $[e]$ is a diagonal matrix.

Let

$$[e][u] = [b] \tag{21.46}$$

where $[b]$ is an upper triangular matrix. Also, let

$$[b]\{x\} = \{g\} \tag{21.47}$$

Substitution of Eqs. 21.45 to 21.47 into Eq. 21.42 gives

$$[u]^T\{g\} = \{c\} \tag{21.48}$$

Forward substitution in this equation gives $\{g\}$, and using the result with backward substitution in Eq. 21.47 gives the required vector $\{x\}$.

The operations involved in the matrix product in Eq. 21.45 and in the forward and backward substitutions are relatively small, compared with the operations involved in the decomposition to generate $[u]$ and $[e]$.

4 See the references in footnote 2 in this chapter.

Performing the matrix product in Eq. 21.45 gives

$$a_{ij} = e_{ii}u_{ij} + \sum_{k=1}^{i-1} e_{kk}u_{kj}u_{ki} \quad \text{with } i < j \tag{21.49}$$

and

$$a_{jj} = e_{jj} + \sum_{k=1}^{j-1} e_{kk}u_{kj}^2 \tag{21.50}$$

To avoid the triple products in the above summations and thereby reduce the number of operations, let us introduce the symbol

$$\overline{u}_{ij} = e_{ii}u_{ij} \tag{21.51}$$

Substitution of Eq. 21.51 into Eqs. 21.49 and 21.50 and rearrangement of term give

$$\overline{u}_{ij} = a_{ij} - \sum_{k=1}^{i-1} \overline{u}_{kj}u_{ki} \quad \text{with } i < j \tag{21.52}$$

and

$$e_{jj} = a_{jj} - \sum_{k=1}^{i-1} \overline{u}_{kj}u_{kj} \tag{21.53}$$

Here again, when $[a]$ is symmetrically banded, only the elements within the band, on and above the diagonal, are stored in the computer. The same storage space is reused; the elements e_{jj} replace a_{jj}, and u_{ij} replace a_{ij} (with $i < j$).

Working down the jth column, the nonzero elements $\overline{u}_{ij}$ are calculated by Eq. 21.52 and temporarily stored in place of a_{ij}. Then, the first nonzero u_{ij} in the column is calculated from $\overline{u}_{ij}$ by Eq. 21.51; the product $\overline{u}_{ij}\ u_{ij}$ is deducted from a_{jj}, and u_{ij} replaces $\overline{u}_{ij}$. Repetition of this step for the remaining $\overline{u}_{ij}$ in the jth column results in the replacement of a_{ii} by e_{ii} (see Eq. 21.53).

Unlike the Gauss eliminations, with Cholesky's method only the matrix $[a]$ is reduced, while $\{c\}$ is used in the forward substitution without change (Eq. 21.46).

In the following example, the same equations which are solved in Section A.9 are solved here by Cholesky's method.

Example 21.4: Four equations solved by Cholesky's method

Use Cholesky's method to solve the equations $[a]\{x\} = \{c\}$. The vector $\{c\}$ is $\{1, -4, 11, -5\}$. The matrix $[a]$ is

$$\begin{bmatrix} 5 & -4 & 1 & 0 \\ & 6 & -4 & 1 \\ & & 6 & -4 \\ \text{symmetrical} & & & 7 \end{bmatrix}$$

Equations 21.49 to 21.53 are used to generate

$$\begin{bmatrix} e_{11} & u_{12} & u_{13} & 0 \\ - & e_{22} & u_{23} & u_{24} \\ - & - & e_{33} & u_{34} \\ - & - & - & e_{44} \end{bmatrix} = \begin{bmatrix} 5 & -4/5 & 1/5 & 0 \\ - & 14/5 & -8/7 & 5/14 \\ - & - & 15/7 & -4/3 \\ - & - & - & 17/6 \end{bmatrix}$$

Equation 21.48 and forward substitution give

$$\begin{bmatrix} 1 & 0 & 0 & 0 \\ -4/5 & 1 & 0 & 0 \\ 1/5 & -8/7 & 1 & 0 \\ 0 & 5/14 & -4/3 & 1 \end{bmatrix} \begin{Bmatrix} g_1 \\ g_2 \\ g_3 \\ g_4 \end{Bmatrix} = \begin{Bmatrix} 1 \\ -4 \\ 11 \\ -5 \end{Bmatrix}$$

whence

$$\{g\} = \{1, -16/5, 50/7, 17/3\}$$

Equation 21.46 and 21.47 and backward substitution give

$$\begin{bmatrix} 5 & -4 & 1 & 0 \\ & 14/5 & -16/5 & 1 \\ & & 15/7 & -20/7 \\ & & & 17/6 \end{bmatrix} = \begin{Bmatrix} x_1 \\ x_2 \\ x_3 \\ x_4 \end{Bmatrix} = \begin{Bmatrix} 1 \\ -16/5 \\ 50/7 \\ 17/3 \end{Bmatrix}$$

whence

$$\{x\} = \{3,\ 5,\ 6,\ 2\}$$

21.12 Member end-forces

The last step in the displacement method (see Section 4.6) is the superposition to determine the required actions

$$\{A\} = \{A_r\} + [A_u]\{D\} \tag{21.54}$$

where $\{A_r\}$ are the values of the actions with $\{D\} = \{0\}$, and $[A_u]$ are the values of the actions due to unit displacements introduced separately at each coordinate.

In a framed structure, the required actions are commonly the forces at the member ends in the local directions for individual members. The superposition is done separately for individual members.

After solution of the equilibrium equations, we have a vector $\{D\}$ of the nodal displacements in the global directions at all the nodes. Let $\{D\}$ be partitioned into submatrices, each having s values of the displacements at a node, where s is the number of degrees of freedom per node. For the mth member, having its first and second node j and k respectively, the displacements at the two ends in local coordinates are given by (Eq. 21.13)

$$\{D^*\}_m = \begin{Bmatrix} \{D^*\}_1 \\ \{D^*\}_2 \end{Bmatrix}_m = \begin{bmatrix} [t] & [0] \\ [0] & [t] \end{bmatrix}_m \begin{Bmatrix} \{D\}_j \\ \{D\}_k \end{Bmatrix} \tag{21.55}$$

where $\{D\}_j$ and $\{D\}_k$ are submatrices of $\{D\}$, corresponding to nodes j and k, and $[t]_m$ is a transformation matrix for the mth member given by one of Eqs. 21.14 to 21.18.

To apply the superposition Eq. 21.54 in order to find member end-forces, we have $\{A_r\}$ given in the input data. The values of the member end-forces due to unit displacements introduced separately at each local coordinate (Figure 21.2) are the elements of the member stiffness matrix $[S^*]$, given by one of Eqs. 21.10 to 21.12 or by Eq. 5.5. Thus, in this application, the product $[S^*]\{D^*\}$ stands for $[A_u]\{D\}$. The member end-forces for any member are therefore given by

$$\{A\} = \{A_r\} + [S^*]\{D^*\} \tag{21.56}$$

The stiffness matrices of individual members need to be calculated again in this step, unless they have been stored.

Example 21.5: Reactions and member end-forces in a plane truss

Find the reactions and the end-forces in member 6 in the truss of Figure 21.4 for each of the three cases in Example 21.1.

The stiffness matrix and the load vectors for the three cases have been determined in Example 21.3. Zero displacement is prescribed in the x and y directions at nodes 4 and 5; therefore, multiply the diagonal coefficient in each of rows 7, 8, 9, and 10 by 10^6 and set zeros in the same rows of the load vectors (see Eq. 21.39). Because we accounted for the support movement in the member end-forces by $\{A_r\}$ used in the input data, we put here $c_k = 0$. The adjusted equilibrium equations are

$$10^6 \times \begin{bmatrix} 313 & 61 & -267 & 0 & -46 & -61 & & & & \\ & 82 & 0 & 0 & -61 & -82 & & & & \\ & & 625 & 123 & 0 & 0 & -267 & 0 & -92 & -123 \\ & & & 244 & 0 & -80 & 0 & 0 & -123 & -164 \\ & & & & 352 & -62 & -92 & 123 & -213 & 0 \\ & & & & & 326 & 123 & -164 & 0 & 0 \\ & \text{symmetrical. Submatrices} & & & & & 359 \times 10^6 & -123 & & \\ & \text{not shown are null} & & & & & & 164 \times 10^6 & & \\ & & & & & & & & 305 \times 10^6 & 123 \\ & & & & & & & & & 164 \times 10^6 \end{bmatrix}$$

$$[D]=\begin{bmatrix} 0 & 0 & 0 \\ 100 & 0 & 0 \\ 0 & 0 & 0 \\ 0 & 0 & 0 \\ 0 & +96 & -246 \\ 0 & 0 & +328 \\ 0 & 0 & 0 \\ 0 & 0 & 0 \\ 0 & 0 & 0 \\ 0 & 0 & 0 \end{bmatrix} \times 10^3$$

The solution is

$$[D]=\begin{bmatrix} -0.6510\times10^{-3} & -0.3223\times10^{-5} & -0.1912\times10^{-3} \\ 0.3016\times10^{-2} & 0.5688\times10^{-3} & 0.1372\times10^{-2} \\ -0.3698\times10^{-3} & -0.3223\times10^{-5} & -0.1912\times10^{-3} \\ 0.4694\times10^{-3} & 0.9411\times10^{-4} & 0.5582\times10^{-3} \\ 0.5925\times10^{-3} & 0.4097\times10^{-3} & -0.2390\times10^{-3} \\ 0.8627\times10^{-3} & 0.2374\times10^{-3} & 0.1408\times10^{-2} \\ -0.4180\times10^{-9} & -0.1013\times10^{-15} & -0.6856\times10^{-9} \\ 0.4183\times10^{-9} & -0.6994\times10^{-10} & 0.1587\times10^{-8} \\ 0.4910\times10^{-9} & 0.3142\times10^{-9} & 0.3782\times10^{-15} \\ 0.1921\times10^{-9} & 0.6994\times10^{-10} & 0.4149\times10^{-9} \end{bmatrix} \begin{matrix} 1 \\ \\ 2 \\ \\ 3 \\ \\ 4 \\ \\ 5 \\ \end{matrix}$$

The forces at the supported nodes 4 and 5 (Eq. 21.40) are

$$\begin{Bmatrix} F_7 \\ F_8 \\ F_9 \\ F_{10} \end{Bmatrix} = 10^3 \times \begin{bmatrix} 150 & 0 & 246 \\ -69 & 11 & -260 \\ -150 & -96 & 0 \\ -31 & -11 & -68 \end{bmatrix}$$

These forces are calculated by the multiplication of the nodal displacement with reversed sign by the diagonal elements of the adjusted stiffness matrix. (The last term in Eq. 21.40 is negligible and $c_k = 0$.) Addition of the above forces to the corresponding rows of the original load vector (generated in Example 21.3) gives the reactions (Eq. 21.38):

$$\begin{Bmatrix} R_7 \\ R_8 \\ R_9 \\ R_{10} \end{Bmatrix} = 10^3 \times \begin{bmatrix} 150 & 0 & 0 \\ -69 & 11 & 68 \\ -150 & 0 & 0 \\ -31 & -11 & -68 \end{bmatrix}$$

The first and second nodes of member 6 are $j=4$ and $k=3$ (see input data, Table 21.1). The transformation matrix is (Eq. 21.14)

$$[t]=[0.6 \quad -0.8]$$

Let us transform the nodal displacements for the three cases of nodes 4 and 3 from global to local directions (Eq. 21.55):

$$[D^*]=\begin{bmatrix}0.6 & -0.8 & 0 & 0\\ 0 & 0 & 0.6 & -0.8\end{bmatrix} \times \begin{bmatrix}-0.4180\times10^{-9} & -0.1013\times10^{-15} & -0.6856\times10^{-9}\\ 0.4183\times10^{-9} & -0.6994\times10^{-10} & 0.1587\times10^{-8}\\ 0.5925\times10^{-3} & 0.4097\times10^{-2.5} & -0.2390\times10^{-3}\\ 0.8687\times10^{-3} & 0.2374\times10^{-3} & 0.1408\times10^{-2}\end{bmatrix}$$

whence

$$[D^*]=\begin{bmatrix}-0.5854\times10^{-9} & 0.5595\times10^{-10} & -0.1681\times10^{-8}\\ -0.3347\times10^{-3} & 0.5590\times10^{-4} & -0.1270\times10^{-2}\end{bmatrix}$$

The end-forces for member 6 in the three cases are (Eq. 21.54)

$$[A]=10^3\times\begin{bmatrix}0 & 0 & -410\\ 0 & 0 & 410\end{bmatrix}+256\times10^6\begin{bmatrix}1 & -1\\ -1 & 1\end{bmatrix}[D^*]$$

whence

$$[A]=10^3\times\begin{bmatrix}86 & -14 & -85\\ -86 & +14 & 85\end{bmatrix}$$

21.13 General

The analysis of framed structures by computer to give the nodal displacements and the member end-forces is summarized below. The nodal displacements are in the directions of arbitrarily chosen global axes x, y, (and z) (Figure 21.1), while the member end-forces are in local coordinates pertaining to individual members (Figure 21.2).

The input data are composed of: the material properties E (and G); the x, y (and z) coordinates of the nodes; the number of the two nodes at the ends of each member; the cross-sectional properties a, L, J etc. of each member; the support conditions; the external forces applied at the nodes; and the end-forces $\{A_r\}$ for the members subjected to loads away from the nodes. The elements of $\{A_r\}$ are forces in local coordinates at the member ends when the nodal displacements are restrained.

The five steps of the displacement method summarized in Section 4.6 are executed as follows:

Step 1 The nodes and the members are numbered sequentially by the analyst, from 1 to n_j and from 1 to n_m respectively. This will automatically define the degrees of freedom and the required end-actions according to the systems specified in Figures 21.1 and 21.2.

Step 2 The forces $\{A_r\}$ included in the input data are transformed into global directions and assembled to give a vector $\{F_b\}$ of restraining nodal forces (Eqs. 21.22 and 21.34). A vector $\{F_a\}$ is also generated, simply by listing from the input data, the nodal forces with a reversed sign. The sum $\{F_a\}$ plus $\{F_b\}$ gives a vector of the restraining forces $\{F\}$ which are necessary to prevent the nodal displacements (Eq. 21.32).

Step 3 To generate the stiffness matrix of the structure, start with $[S] = [0]$ and partition this matrix into $n_j \times n_j$ submatrices each of size $s \times s$, where s is the number of degrees of freedom per node. The stiffness matrix of the first member is generated by one of Eqs. 21.23, 21.24, 21.27, 21.28, or 5.5 and partitioned into 2×2 submatrices, each of size $s \times s$. The four submatrices are added to the appropriate submatrices of $[S]$ according to Eqs. 21.30 and 21.31. By repeating this procedure for all the members, the stiffness matrix of a free unsupported structure is generated.

When one of Eqs. 21.23, 21.24, 21.27, or 21.28 is used, the stiffness matrix of a member is obtained with respect to coordinates in global directions. However, Eq. 5.5 gives the stiffness matrix of a member of a space frame with respect to local coordinates. Transformation is necessary according to Eq. 21.19 before the assemblage of the stiffness matrices can be performed by Eq. 21.31.

The structure stiffness matrix $[S]$ is symmetrical and generally has the nonzero elements limited to a band adjacent to the diagonal. To save computer space, only the diagonal element of $[S]$ and the elements above the diagonal within the band are stored in a rectangular matrix as shown in Figure 21.3. The node numbering selected by the analyst in step 1 affects the band width and hence the width of the rectangular matrix used to store $[S]$. A narrower band width is generally obtained by numbering the nodes sequentially across that side of the frame which has a smaller number of nodes (as an example, see Figure 21.3).

Step 4 Before the equilibrium equations $[S]\{D\} = -\{F\}$ can be solved, $[S]$ and $\{F\}$ must be adjusted according to the displacements prescribed in the input data (Eqs. 21.36 or 21.39).

Two methods of solution of the equilibrium equations are discussed in Section 21.11. The solution gives the unknown displacements $\{D\}$ and these are used to calculate the reactions by Eq. 21.38 and one of Eqs. 21.37 or 21.40.

Step 5 The end-forces for each member are obtained by the superposition Eq. 21.56, which sums $\{A_r\}$ given in the input data and the product $([S^*]\{D^*\})$, with $[S^*]$ and $\{D^*\}$ being, respectively, the member stiffness matrix and the displacements at the member ends in local coordinates. For this reason, the displacements obtained in step 4 have to be transformed from global directions to local directions by Eq. 21.55 before the superposition can proceed.

The general approach in this chapter is followed in Chapter 22 by a discussion of special topics related to use of computers in structural analysis.

Problems for Chapter 21 are included at the end of Chapter 22.

Chapter 22

Implementation of computer analysis

22.1 Introduction

Analysis of structures by the displacement method requires the solution of the equilibrium equations $[S]\ \{D\} = \{-F\}$. The solution must satisfy the displacement boundary conditions. In Chapter 21 we assumed that the displacements $\{D\}$ and the forces $\{F\}$ are in directions of global axes. In Section 21.10, we discussed a method in which the stiffness matrix $[S]$ generated for a free, unsupported structure is adjusted, together with the vector $\{F\}$ to satisfy the condition that the displacement at a coordinate equals zero or a prescribed value. In Section 22.2, we shall consider the case when the prescribed displacement is in a direction inclined to global axes; this may be so at a roller support.

In the analysis of a large structure, it is often possible to consider only a part of the structure rather than the whole. This approach is useful to reduce the cost of preparing the data, of computing and of interpretation of the results. When an isolated part of a structure is analyzed, it is crucial that the displacement boundary conditions accurately represent the conditions in the actual structure. If this is not so, the results can be grossly erroneous.

Structures which are composed of symmetrical sectors can be analyzed by considering one sector with appropriate displacement constraints imposed at the boundaries with adjacent sectors. The displacement boundary conditions for different types of symmetry are discussed in Sections 22.3 and 22.5.

A displacement component may be constrained so as to be equal to a prescribed value or to zero. For instance, the constraint may be specified by imposing the value of the displacement at one coordinate to be equal to the displacement at another coordinate; more generally, the displacement at one coordinate may be required to be a linear combination of the displacement at two other coordinates. Section 22.4 shows how the equilibrium equations can be adjusted to satisfy the displacement constraints, and gives examples of structures in which such constraints are required.

The analysis of a large structure can be reduced to a series of analyses of substructures which are easier to handle one at a time. This is discussed in Section 22.6.

Section 22.7 is concerned with the use of computers for the plastic analysis of plane frames on the basis of the assumptions adopted in Chapter 18.

Section 22.8 gives a method for generating the stiffness matrix of a member with a variable section or with a curved axis. The stiffness matrix is derived from the flexibility matrix of the member treated as a cantilever.

22.2 Displacement boundary conditions in inclined coordinates

In the analysis of structures by computer, using the displacement method, the coordinates at the nodes typically represent displacement components in the directions of one set of global axes. It is, however, sometimes necessary to express the boundary conditions at a node as prescribed

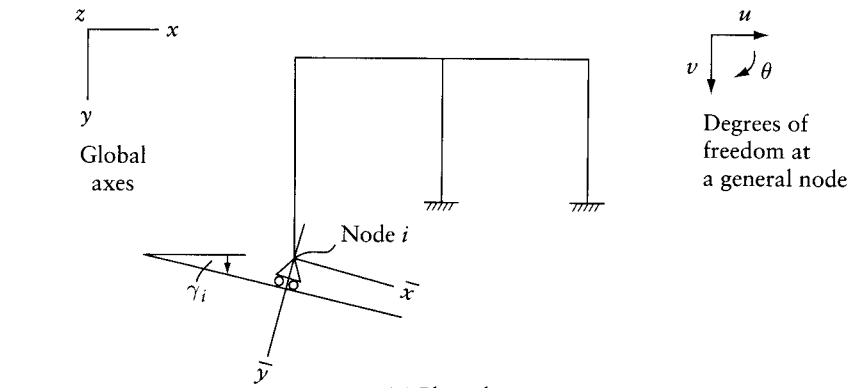

(a) Plane frame

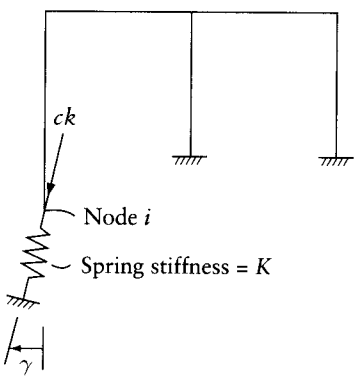

(b) Addition of a fictitious spring

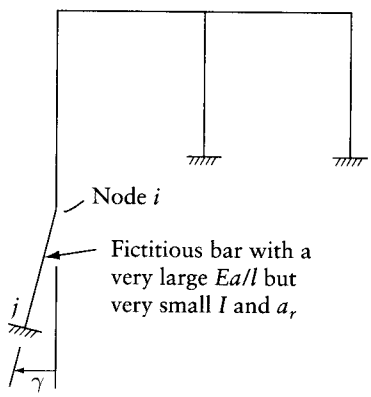

(c) Addition of a fictitious bar

Figure 22.1 Introduction of displacement boundary conditions in directions inclined to the global axes.

displacements in directions inclined to the global axes. An example of this situation is at the roller support at node i of the plane frame in Figure 22.1a. The support allows a free translation $\bar{u}$ in the $\bar{x}$ direction, parallel to a plane inclined at an angle γ_i to the global x axis, but prevents translation $\bar{v}$ in the $\bar{y}$ direction. Alternatively, $\bar{v}$ may take a prescribed value c.

For the analysis of the structure in Figure 22.1a, we need a stiffness matrix $[S]$ corresponding to degrees of freedom u, v, θ in the global x, y, z directions at each node except node i, where the degrees of freedom are $\bar{u}$, $\bar{v}$ and $\bar{\theta}$ in the $\bar{x}$, $\bar{y}$, $\bar{z}$ directions. One way to achieve this is first to generate the stiffness matrix $[S]$, in the usual way, corresponding to degrees of freedom in the global x, y, z directions, and subsequently to adjust $[S]$ to $[\bar{S}]$ as discussed below.

In general, a geometrical relation can be written:

$$\{D\}_i = [H]_i \{\bar{D}\}_i \tag{22.1}$$

where $\{D\}_i$ and $\{\bar{D}\}_i$ are nodal displacements at i in the global x, y, z directions and in the $\bar{x}$, $\bar{y}$, $\bar{z}$ directions respectively. The matrix $[H]_i$ is a transformation matrix for node i. However, Eq. 6.6 gives the stiffness matrix the forces at node i in the two coordinate systems can also be related by using the same transformation matrix (see Eq. 9.16):

$$\{\bar{F}\}_i = [H]_i^T \{F\}_i \tag{22.2}$$

In the example considered in Figure 22.1a, the transformation matrix is

$$[H]_i = \begin{bmatrix} \cos\gamma & -\sin\gamma & 0 \\ \sin\gamma & \cos\gamma & 0 \\ 0 & 0 & 1 \end{bmatrix}_i \tag{22.3}$$

Using the stiffness matrix $[S]$, we can write the equilibrium equations

$$[S]\,\{D\} = -\{F\} \tag{22.4}$$

Let us now partition $[S]$ into $n_j \times n_j$ submatrices each of size $s \times s$, where n_j is the number of nodes and s is the number of degrees of freedom per node. The partitioned equilibrium equation will appear as follows:

$$\begin{bmatrix} & & S_{1i} & \\ & & S_{2i} & \\ & & \cdots & \\ S_{i1} & S_{i2} & \cdots\ S_{ii} & \cdots \\ & & \cdots & \end{bmatrix} \begin{Bmatrix} D_1 \\ D_2 \\ \cdots \\ D_i \\ \cdots \end{Bmatrix} = - \begin{Bmatrix} F_1 \\ F_2 \\ \cdots \\ F_i \\ \cdots \end{Bmatrix} \tag{22.5}$$

In this equation and in the following two, only the elements in the ith row and ith column of the square matrix on the left-hand side are written.

The term $\{D\}_i$ in Eq. 22.5 may be eliminated by the use of Eq. 22.1, giving

$$\begin{bmatrix} & & S_{1i}H_i & \\ & & S_{2i}H_i & \\ & & \cdots & \\ S_{i1} & S_{i2} & \cdots\ S_{ii}H_i & \cdots \\ & & \cdots & \end{bmatrix} \begin{Bmatrix} D_1 \\ D_2 \\ \cdots \\ \overline{D}_i \\ \cdots \end{Bmatrix} = - \begin{Bmatrix} F_1 \\ F_2 \\ \cdots \\ F_i \\ \cdots \end{Bmatrix} \tag{22.6}$$

The submatrix $\{F\}_i$ in this equation may also be eliminated by multiplication of the ith row by $[H]_i^T$ and substitution of Eq. 22.2:

$$\begin{bmatrix} & & S_{1i}H_i & \\ & & S_{2i}H_i & \\ & & \cdots & \\ H_i^T S_{i1} & H_i^T S_{i2} & \cdots\ H_i^T S_{ii}H_i & \cdots \\ & & \cdots & \end{bmatrix} \begin{Bmatrix} D_1 \\ D_2 \\ \cdots \\ \overline{D}_i \\ \cdots \end{Bmatrix} = - \begin{Bmatrix} F_1 \\ F_2 \\ \cdots \\ \overline{F}_i \\ \cdots \end{Bmatrix} \tag{22.7}$$

The square symmetrical matrix on the left-hand side of Eq. 22.7 is the stiffness matrix $[\overline{S}]$ in which the boundary conditions can be introduced as discussed in Section 21.10. In practice, the adjustment to obtain $[\overline{S}]$ can be conveniently made to the stiffness matrices of the elements connected to node i (see Example 22.1).

An alternative to the above procedure is to add a spring of stiffness K at node i in the $\overline{y}$ direction (Figure 22.1b). The stiffness K is much larger than the diagonal elements of $[S]$, e.g. 10^5 times larger than their values. When a displacement c is prescribed in the $\overline{y}$ direction, a force cK has to be applied in the $\overline{y}$ direction at node i. Because the stiffness of the structure is negligible compared with that of the spring, the force cK produces the prescribed displacement c at i.

The stiffness matrix of the added spring with respect to the coordinates $\bar{u}$, $\bar{v}$, and $\bar{\theta}$ in Figure 22.1b is

$$[\bar{S}]_k = \begin{bmatrix} 0 & 0 & 0 \\ 0 & K & 0 \\ 0 & 0 & 0 \end{bmatrix} \tag{22.8}$$

Before assemblage of $[S]$ (see Section 21.9), the above stiffness matrix for the spring must be transformed to correspond to the global directions:

$$[S]_K = [H]_i [\bar{S}]_k [H]_i^T \tag{22.9}$$

where $[H]_i$ is the transformation matrix in Eq. 22.3. Equation 22.9 is derived from Eq. 9.17, noting that the inverse of $[H]_i$ is equal to its transpose.

The concept discussed above is general and it can be used for any structure in which a displacement is prescribed in an inclined direction.

For the frame in Figure 22.1a, the conditions that, at node i, $\bar{v} = c$ while $\bar{u}$ is free, can be achieved by connecting to i a fictitious bar with end j fixed (Figure 22.1c). The length l and cross-sectional area a of the fictitious bar must be chosen so that $Ea/l = K$, K being the same as for the spring considered earlier. Very small values should be assigned to the second moment of area I (and to the reduced area a_r when shear deformations are considered). Prescribed displacements in the global directions $u_j = -c \sin \gamma$ and $v_j = c \cos \gamma$, introduced at node j instead of node i, will produce the desired effect. This method has the advantage that the required boundary conditions are achieved by entering appropriate input data without changing the computer program which performs the analysis. It should be mentioned, however, that a numerical difficulty in solving the equilibrium equations may be encountered if the stiffness of the added member is excessive.

Example 22.1: Stiffness of member of plane frame with respect to inclined coordinates

Generate the stiffness matrix of a prismatic member of a plane frame with respect to the coordinates shown in Figure 22.2a.

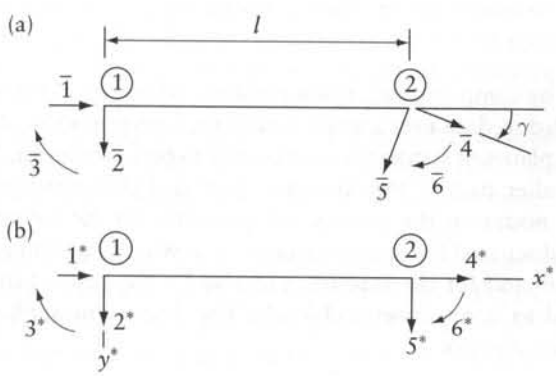

Figure 22.2 Member of a plane frame. (a) Inclined coordinates. (b) Coordinates parallel to member local axes.

The transformation matrix relating $\{\overline{D}\}$ to $\{D^*\}$ at node 2 is (see Eqs. 22.1 and 22.2)

$$[H]_2 = \begin{bmatrix} c & -s & 0 \\ s & c & 0 \\ 0 & 0 & 0 \end{bmatrix}_2$$

where $c = \cos\gamma$ and $s = \sin\gamma$.

The stiffness matrix $[S^*]$ with respect to the coordinates parallel to the member local axes (Figure 22.2b) is given by Eq. 21.11. Application of Eq. 22.7 gives

$$\begin{bmatrix} S_{11} & S_{12}H_2 \\ H_2^T S_{21} & H_2^T S_{22} H_2 \end{bmatrix} \begin{Bmatrix} \overline{D}_1 \\ \overline{D}_2 \end{Bmatrix} = \begin{Bmatrix} \overline{F}_1 \\ \overline{F}_2 \end{Bmatrix}$$

where S_{ij} represents the 3×3 submatrix given in Eq. 21.11; $\overline{D}_1 \equiv D_1^*$ and $\overline{F}_1 \equiv F_1^*$ are subvectors representing, respectively, the three displacements and forces at member end 1.

Substitution for S_{ij} and H_2 gives the stiffness matrix with respect to the coordinates in Figure 22.2a:

$$[\overline{S}] = \left[\begin{array}{ccc:ccc} \frac{Ea}{l} & & & & & \\ 0 & \frac{12EI}{l^3} & & & & \\ 0 & \frac{6EI}{l^2} & \frac{4EI}{l} & & & \\ \hdashline -\frac{cEa}{l} & -\frac{12sEI}{l^3} & -\frac{6sEI}{l^2} & \frac{c^2Ea}{l} + \frac{12s^2EI}{l^3} & & \\ +\frac{sEa}{l} & -\frac{12cEI}{l^3} & -\frac{6cEI}{l^2} & -\frac{scEa}{l} + \frac{12scEI}{l^3} & \frac{s^2Ea}{l} + \frac{12c^2EI}{l^3} & \\ 0 & \frac{6EI}{l^2} & \frac{2EI}{l} & -\frac{6sEI}{l^2} & -\frac{6cEI}{l^2} & \frac{4EI}{l} \end{array}\right] \tag{22.10}$$

22.3 Structural symmetry

Large structures are commonly analyzed by computer and, when possible, advantage is taken of symmetry so as to reduce the effort needed in data preparation and in the interpretation of the results. When a structure has one or more planes of symmetry it is possible to perform the analysis on one-half, one-quarter or an even smaller part of the structure, provided that appropriate boundary conditions are applied at the nodes on the plane(s) of symmetry. In the following sections, these boundary conditions are discussed for spatial structures in which the symmetry exists both for the structure configuration and for the loading, and also for the case when the structure is symmetrical but is subjected to nonsymmetrical loads. The discussion applies to structures composed of bars or other finite elements.

22.3.1 *Symmetrical structures subjected to symmetrical loading*

Figure 22.3a is a top view of a spatial structure with two vertical planes of symmetry: xz and yz. It follows that, for all the elements and applied forces (not shown in the figure) on one side of a

(a)

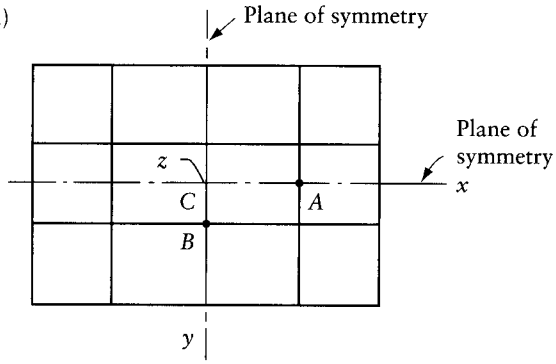

(b)

Boundary conditions for typical nodes

Node	u	v	w	θ_x	θ_y	θ_z
A	1	0	1	0	1	0
B	0	1	1	1	0	0
C	0	0	1	0	0	0

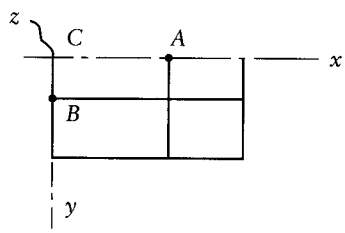

0 ≡ Displacement prevented

1 ≡ Displacement free

Figure 22.3 Spatial structure with two planes of symmetry subjected to symmetrical loading. (a) Top view. (b) Quarter structure to be analyzed.

plane of symmetry, there exists a set of mirror-image elements and forces on the opposite side. The analysis of a structure of this type needs to be performed on one-quarter of the structure only (Figure 22.3b).

Let us assume the degrees of freedom at a typical node to be three translations u, v, w in the global x, y, z directions and three rotations θ_x, θ_y, θ_z in the same directions. The global directions x, y, z are chosen parallel to the planes of symmetry. In the part of the structure to be analyzed, the elements situated on a plane of symmetry must have adjusted properties. For example, when the elements on a plane of symmetry are bars, their cross-sectional properties (a, I, J, and a_r) to be used in the analysis must be assumed to be equal to one-half of the values in the actual structure. It is also possible, instead of changing the cross-sectional properties, to reduce correspondingly (i.e. by one-half) the material properties E and G. Also, the forces applied at the nodes on a plane of symmetry must be assumed to be one-half of the actual values.

Because of symmetry, some of the displacement components at the nodes on the planes of symmetry are known to be zero. The table in Figure 22.3b indicates 0 or 1 for each of the six degrees of freedom at typical nodes A, B, and C on the planes of symmetry. The value 0 indicates zero displacement, and 1 indicates that the displacement is free to occur.

As mentioned in Section 21.4, the displacement boundary conditions must be sufficient to ensure that the structure analyzed cannot translate or rotate as a free rigid body. Now, the boundary conditions prescribed in Figure 22.3b are not sufficient to prevent translation in the z direction; to prevent this translation, at least one node must have $w = 0$.

22.3.2 *Symmetrical structures subjected to nonsymmetrical loading*

Let us assume that the spatial structure shown in Figure 22.3a is subjected to forces P_1 and P_2 (where $P_1 \neq P_2$) at the symmetrical nodes D, E, F, and G, as shown in Figure 22.4a. The system of forces in Figure 22.4a may be considered to be equivalent to the sum of a symmetrical and an antisymmetrical system, shown in Figure 22.4b. The magnitude of the symmetrical component P_s and that of the antisymmetrical component P_a must satisfy the equations

$$P_s + P_a = P_1 \quad -P_s + P_a = P_2 \tag{22.11}$$

whence

$$P_s = \frac{P_1 - P_2}{2} \quad P_a = \frac{P_1 + P_2}{2} \tag{22.12}$$

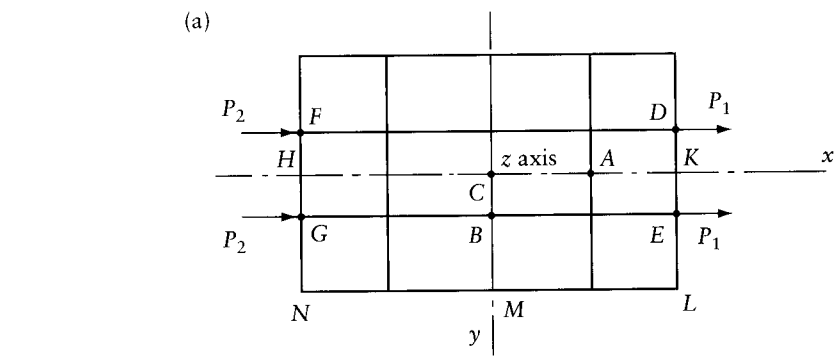

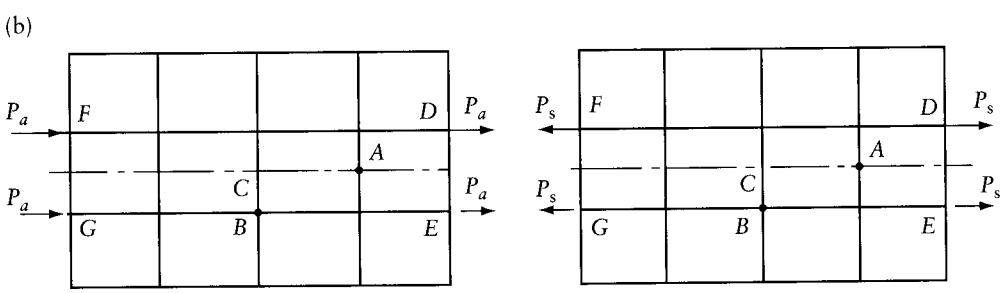

(c)

Boundary conditions for antisymmetrical case

Node	u	v	w	θ_x	θ_y	θ_z
A	1	0	1	0	1	0
B	1	0	0	0	1	1
C	1	0	0	0	1	0

0 ≡ displacement prevented

1 ≡ displacement free

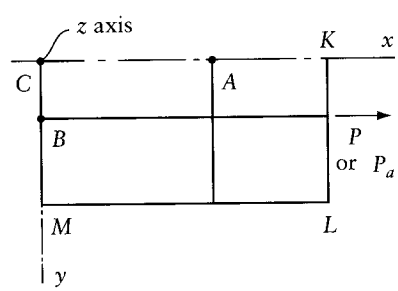

Figure 22.4 Spatial structure with two planes of symmetry subjected to nonsymmetrical loading. (a) Top view. (b) Symmetrical and antisymmetrical load components. (c) Quarter structure to be analyzed.

The analyses for the symmetrical and for the antisymmetrical loading can be performed separately for the quarter structure *CKLM*. For the symmetrical loading, the boundary conditions are as indicated in Figure 22.3b. The boundary conditions for the antisymmetrical loading case are shown in Figure 22.4c.

The results of the two analyses, when added, give the displacements and the internal forces for the quarter structure *CKLM* due to the actual nonsymmetrical loading (Figure 22.4a). By subtracting the results for the antisymmetrical loading from the results for the symmetrical loading, we obtain a mirror image of the displacements and the internal forces in the quarter structure *CHNM* due to the actual nonsymmetrical loading. In other words, the results for the antisymmetrical loading subtracted from the results for the symmetrical loading give the displacements and the internal forces in the quarter structure *CKLM* when the two forces at *F* and *G* (Figure 22.4a) are interchanged with the two forces at *D* and *E*, and the four forces are reversed in direction.

It should be noted that the procedure described above involves two separate analyses of quarter structures, each requiring the solution of a set of equations which differ both in the right-hand side and in the left-hand side. However, each set involves a smaller number of unknown displacements than if a half structure were analyzed. The results of the two analyses of the quarter structure must be stored and the two solutions are combined. The procedure is advantageous only in very large structures to save computing time for the solution of the equations or when the capacity of the computer would otherwise be exceeded.

22.4 Displacement constraints

In Section 21.10 we discussed the methods to be used in order to satisfy the condition that the displacement at a coordinate is zero or has a prescribed value. In this section, we consider a method to impose relations between nodal displacements.

As an example we can consider the plane frame shown in Figure 22.5a, which is composed of an infinite number of bays identical in geometry and in loading. The analysis needs to be performed for a single isolated bay $ABCB'$ with the following relation between the displacements at nodes B and B':

$$\{u, v, \theta\}_{B'} = \{u, v, \theta\}_B \tag{22.13}$$

Another example is shown in Figure 22.5b, which represents a square plate in bending, with symmetry in geometry and in loading about the vertical planes through the x and y axes and about the two diagonals. A finite-element analysis of this structure can be performed using the square elements for the shaded part of the plate. The degrees of freedom at a typical node can be taken as $\{w, \theta_x, \theta_y\}$, as shown in the figure. For symmetry of displacements, the following constraints apply:

$$(\theta_x)_C = -(\theta_y)_C \quad (\theta_x)_D = -(\theta_y)_D \quad (\theta_x)_E = -(\theta_y)_E \tag{22.14}$$

$$\{w, \theta_x, \theta_y\}_{A'} = \{w, -\theta_y, -\theta_x\}A$$

$$\{w, \theta_x, \theta_y\}_{B'} = \{w, -\theta_y, -\theta_x\}_B \tag{22.15}$$

Another example where displacement constraints can be used in finite-element analysis is shown in Figure 22.5c. A plane-stress quadrilateral element with nodes at its corners is connected to a beam element. The constraint equations in this case can be taken as

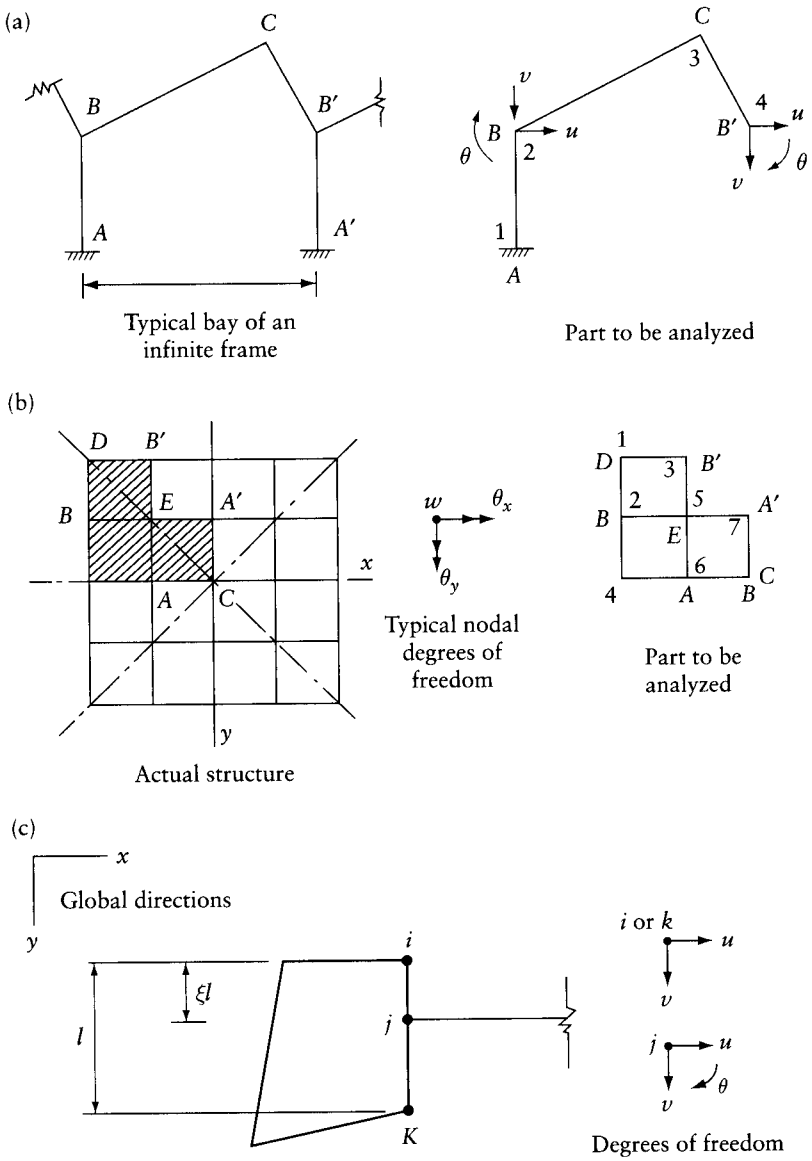

Figure 22.5 Examples for use of displacement constraints. (a) Plane frame of many bays. (b) Plate in bending. (c) Beam-to-wall connection.

$$
\begin{aligned}
u_j &= (1-\xi)u_i + \xi u_k \\
v_j &= (1-\xi)v_i + \xi v_k \\
\theta_j &= \left(\frac{1}{l}\right)u_i - \left(\frac{1}{l}\right)u_k
\end{aligned}
\tag{22.16}
$$

Displacement constraints can also be used in structures with cyclic symmetry (see Section 22.5).

A typical constraint equation may be written in the form

$$D_j = \beta_i D_i \tag{22.17}$$

where β_i is a constant. (A second term $\beta_k D_k$ is added to the right-hand side for the constraints of Eq. 22.16.)

Each constraint equation reduces the number of unknown displacements by one. Thus, in the equilibrium equations $[S]\{D\} = -\{F\}$, the constraint Eq. 22.17 may be used to eliminate D_j so that we can solve the equations for the remaining unknowns, but this requires renumbering of the unknowns. A method[1] of adjusting the equilibrium equations $[S]\{D\} = -\{F\}$ to satisfy any number of constraints of this type is discussed below. The adjustment does not require changes in the number of equations to be solved or in the arrangement of the unknowns.

For each constraint Eq. 22.17, the adjustments are limited to the ith and jth columns of $[S]$ and the ith and jth rows of $[S]$ and of $\{F\}$. The adjustments are performed in steps. First, the elements in the jth column of $[S]$ are multiplied by β_i and added to the ith column. Then, the elements in the jth row of $[S]$ and of $\{F\}$ are multiplied by β_i and added to the ith row. Element S_{jj} is replaced by 1 and the off-diagonal elements in the jth row and column of $[S]$ are replaced by zero. The adjusted columns and rows now become

$$\begin{array}{c} \\ 1 \\ 2 \\ \\ i \\ \\ j \\ \\ \end{array}\!\!\begin{array}{c} \begin{array}{ccccccc} 1 & & i & & & & j \end{array} \\ \begin{bmatrix} & & (s_{1i}+\beta_i S_{1j}) & & 0 & & \\ & & (s_{2i}+\beta_i S_{2j}) & & 0 & & \\ \cdots & & \cdots & & \cdots & & \\ (s_{i1}+\beta_i S_{j1}) & \cdots & (s_{ii}+2\beta_i S_{ij}+\beta_i^2 S_{jj}) & \cdots & 0 & \cdots & \\ \cdots & & \cdots & & \cdots & & \\ 0 & \cdots & 0 & \cdots & 1 & & \\ \cdots & & & & \cdots & & \end{bmatrix} \end{array} \{D\}$$

$$= -\begin{Bmatrix} F_1 \\ F_2 \\ \cdots \\ F_i + \beta_i F_j \\ \cdots \\ 0 \\ \cdots \end{Bmatrix} \tag{22.18}$$

The above adjustments consist of the elimination of D_j in all equations and multiplication of both sides of the ith equation by β_i to maintain symmetry; the jth equation is replaced by the dummy equation $D_j = 0$. Solution of the adjusted equations gives the unknown displacements, including a zero for D_j. This answer must be replaced by $D_j = \beta_i D_i$.

The adjustment of the equilibrium equations as described above can be repeated for each constraint equation.

As mentioned earlier, for the example in Figure 22.5c, each constraint equation can be written in the form: $D_j = \beta_i D_i + \beta_k D_k$. The adjustment of the equilibrium equation to satisfy this equation has to be done as described above for the ith column of $[S]$ and the ith row of $[S]$

1 Other methods are discussed in the reference in footnote 3 in Chapter 21.

and $\{F\}$. Similar adjustments have to be made for the kth column and row of the same matrices before replacing S_{jj} by 1 and the off-diagonal elements in the jth column and row by zero. This procedure causes external forces at node j to be replaced by static equivalents added to the external forces at nodes i and k.

The adjusted stiffness matrix will continue to be symmetrical, but the band width can increase. Equation 21.1 can be used to calculate the new band width, noting that any element connected to node i is also "connected" to node j by the constraint Eq. 23.17. For the plane frame $ABCB'$ in Figure 22.5a, with the number of degrees of freedom per node $s=3$ and a constraint equation relating displacements at B' and B, the band width is governed by member AB. Thus, element AB is considered to be connected to nodes 1, 2, and 4 and the band width is (Eq. 21.1)

$$n_b = 3[(4-1)+1] = 12$$

We should note that, in the adjusted equations, F_i is added to $\beta_i F_j$. For this reason, external forces at B in the actual frame in Figure 22.5a, which are the same as at B', must be applied in the analysis at either node 2 or node 4, but not at both nodes. Similarly, in the structure in Figure 22.5b, the forces at A, which are the same as at A', should be applied at either node 6 or at node 7; and so on.

22.5 Cyclic symmetry

Each of the structures shown in top view in Figure 22.6 is composed of r sectors which are identical in terms of geometry, material properties, and loading.[2] The global structure can be generated by successive rotations of the hatched sector through an angle $2\pi/r$ about a vertical axis through O, where r is an integer. The structures can be two-dimensional or three-dimensional and they may be idealized by bar elements or other finite elements. The analysis can be performed for the hatched sectors isolated as shown by imposing the following displacement constraints:

$$\{D_n, D_t, D_z\}_j = \{D_n, D_t, D_z\}_i \tag{22.19}$$

$$(D_n)_0 = (D_t)_0 = 0 \tag{22.20}$$

where i and j are nodes at equal distances from O on the common sector boundaries OA and OA' (indicated by heavy lines); D_n and D_t are displacement components (translations or rotations) in the directions of the normal n and the tangent t to the common boundaries; and D_z is a displacement component in a vertical downward direction. Equation 22.20 means that, at nodes on a vertical axis through O, the displacements can be nonzero only in the z direction.

The equilibrium equations $[S]\{D\} = \{-F\}$ have to be generated for all the degrees of freedom in the sector; the equations are then adjusted as discussed in Section 22.4.

The use of Eq. 22.19 requires that the degrees of freedom at the boundaries be in the n, t, and z directions. The necessary transformation is discussed in Section 22.2.

Members or elements located on the common boundaries may be situated either on plane OA or on plane OA', but not on both. Similarly, forces at the nodes on the common boundaries must be applied on the nodes situated on one of the two vertical planes. At a node on the vertical through O the forces on the actual structure (in the z direction) must be divided by r when applied on the sector analyzed.

2 Further discussion of symmetry can be found in Glockner, P. G., "Symmetry in Structural Mechanics," *Proceedings American Society of Civil Engineers*, 99 (ST1), 1973, pp. 71–89.

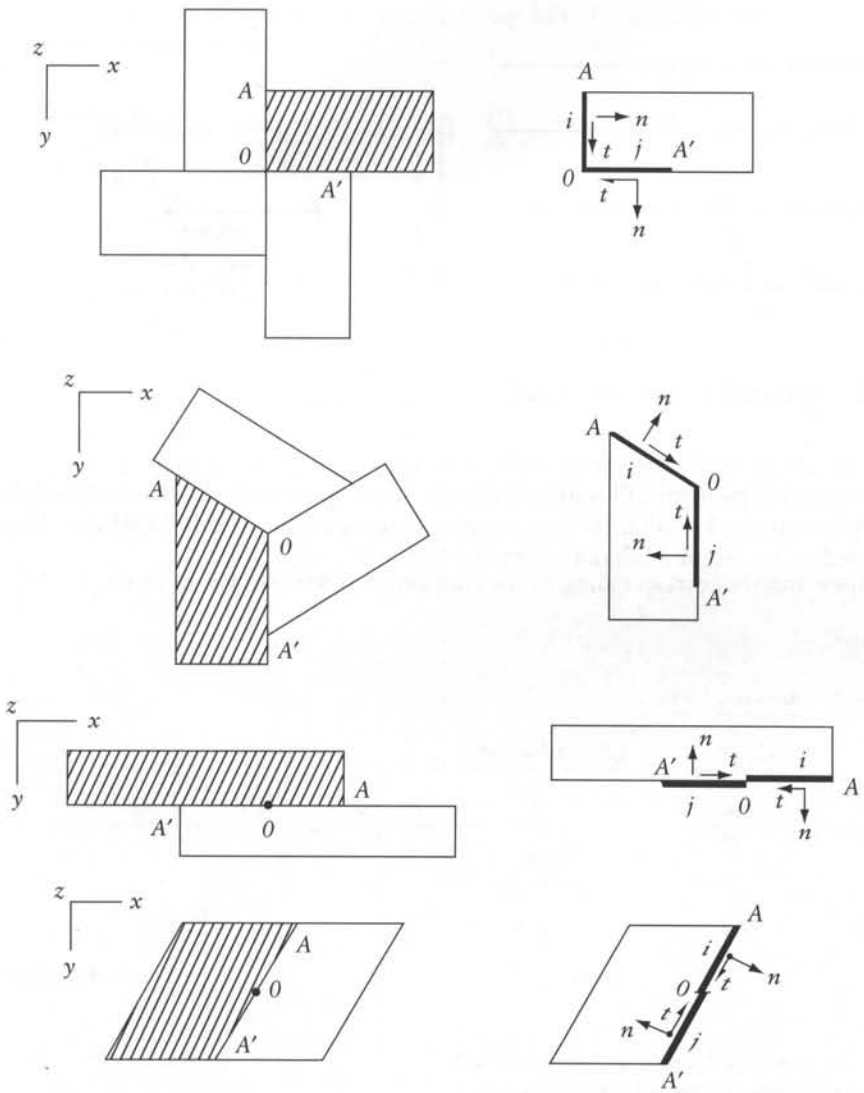

Figure 22.6 Structures with cyclic symmetry.

Example 22.2: Grid: skew bridge idealization

Find the nodal displacements for the horizontal grid shown in top view in Figure 22.7. The grid is subjected to a uniform downward load of q per unit length on DOF only. Assume that all members have the same cross section with $GJ/EI = 0.6$.

The structure is composed of two identical sectors, one of which is shown in the figure. This sector will be analyzed using seven degrees of freedom: downward deflection and two rotations at each of the nodes B and H, and downward deflection only at O. The restraining forces are

$$\{F\} = \{0, 0, 0, -0.5ql, 0, 0, 0\}$$

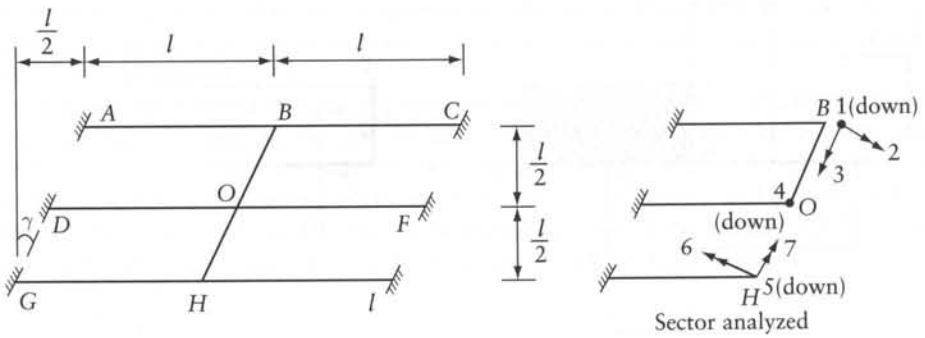

Figure 22.7 Horizontal grid of Example 22.2.

We should note that member OB is included in the sector analyzed but OH is omitted. For the cyclic symmetry to be valid, the two members must be identical, and OH could have been included in the sector analyzed instead of OB.

The stiffness matrix corresponding to the coordinate system shown in Figure 22.7 is

$$[S]=\begin{bmatrix}
\frac{12+96c^3}{l^3} & & & & & & \\
\frac{6s+24c^2}{l_2} & \frac{4s^2+0.6c^2+8c}{l} & & & & & \\
\frac{6c}{l^2} & \frac{4sc-0.6sc}{l} & \frac{1.2c+4c^2+0.60s^2}{l} & & & & \\
-\frac{96c^3}{l^3} & -\frac{24c^2}{l^2} & 0 & \frac{12+96c^3}{l^3} & & & \\
0 & 0 & 0 & 0 & \frac{12}{l^3} & & \\
0 & 0 & 0 & 0 & -\frac{6s}{l^2} & \frac{0.6c^2+4s^2}{l} & \\
0 & 0 & 0 & 0 & \frac{6c}{l^2} & \frac{4cs-0.6cs}{l} & \frac{4c^2+0.6s^2}{l}
\end{bmatrix} EI$$

where $s=\sin\gamma=1/\sqrt{5}$ and $c=\cos\gamma=2/\sqrt{5}$.

The displacement constraint equations are

$$D_1=D_5 \quad D_2=D_6 \quad D_3=D_7$$

Substitution for s and c by their values and adjustment of the equilibrium equations gives (Eq. 22.18)

$$EI\begin{bmatrix}
\frac{92.692}{l^3} & & & \\
\frac{19.2}{l^2} & \frac{9.715}{l} & & \\
0 & \frac{2.720}{l} & \frac{7.713}{l} & \\
\frac{68.692}{l^3} & \frac{19.20}{l^2} & 0 & \frac{80.692}{l^3}
\end{bmatrix}\begin{Bmatrix} D_1 \\ D_2 \\ D_3 \\ D_4 \end{Bmatrix}=ql\begin{Bmatrix} 0 \\ 0 \\ 0 \\ +0.5 \end{Bmatrix}$$

The last three equations, which become dummy, have been omitted here. The solution of the above equations yields

$$\{D\} = \{10.68l,\ 21.13,\ -7.45,\ 20.31l\}\frac{9l^3}{1000EI}$$

22.6 Substructuring

A large structure may be divided into substructures to make its analysis possible by a small computer. Such substructuring breaks a large problem into smaller parts, thus replacing a long computer analysis by several shorter analyses. We shall explain the relevant procedure using the structure shown in top view in Figure 22.8; this structure is partitioned into seven substructures, with six connection boundaries. The steps in the analysis are as follows:

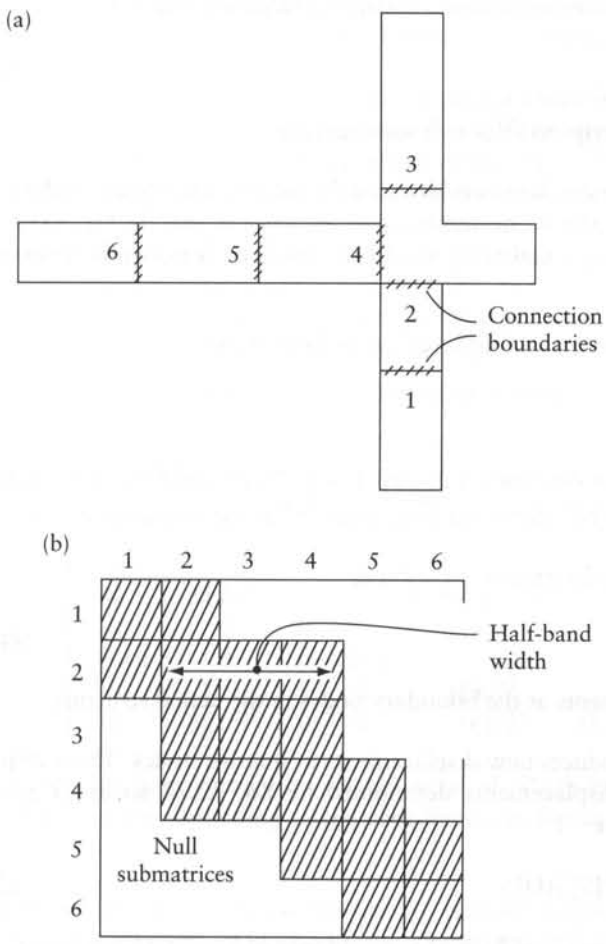

Figure 22.8 Substructuring. (a) Top view of actual structure. (b) Band width of assembled stiffness matrix $[S_b]$.

Step 1 The equilibrium equations for a substructure are written in the form

$$\begin{bmatrix} S^*_{bb} & S^*_{bi} \\ S^*_{ib} & S^*_{ii} \end{bmatrix} \begin{Bmatrix} D^*_b \\ D^*_i \end{Bmatrix} = - \begin{Bmatrix} F^*_b \\ F^*_i \end{Bmatrix} \tag{22.21}$$

In this equation, the displacement and force vectors are partitioned into connection-boundary coordinates and interior coordinates, referred to by subscripts b and i respectively. Coordinates at real supports are treated as interior coordinates.

The displacements of the substructure are now prevented at the supported nodes and also at the connection-boundary nodes. With the connection-boundary nodes artificially restrained, $\{D^*_b\} = \{0\}$, the displacements at interior coordinates are given by

$$\{D^*_i\}_{\text{boundaries fixed}} = -[S^*_{ii}]^{-1}\{F^*_i\} \tag{22.22}$$

The restraining forces are

$$\{F^*_b\} = [S^*_{bi}][S^*_{ii}]^{-1}\{F^*_i\} \tag{22.23}$$

Step 2 For each substructure, a condensed stiffness matrix is calculated (Eq. 5.17):

$$[\overline{S^*_b}] = [S^*_{bb}] - [S^*_{bi}][S^*_{ii}]^{-1}[S^*_{ib}] \tag{22.24}$$

An asterisk is used here as a superscript to refer to a substructure.

Step 3 The condensed stiffness matrices are assembled into the stiffness matrix $[S_b]$ of the global structure. The connection boundary should be numbered in sequence so that the $[S_b]$ have small band width. An example of boundary numbering and of the resulting band width is shown in Figures 22.8a and b.

Step 4 A vector is generated for the restraining forces at the boundaries:

$$F_{bj} = \sum F^*_{bj} - P_{bj} \tag{22.25}$$

where j refers to a coordinate, F^*_{bj} is determined in step 1 (Eq. 22.23), and P_{bj} is the external force at j. The summation is for the two substructures connected at the boundary considered.

Step 5 The displacements $\{D_b\}$ are determined by solving

$$[S_b]\{D_b\} = -\{F_b\} \tag{22.26}$$

Here, $\{D_b\}$ represents the displacements at the boundary nodes in the actual structure.

Step 6 Elimination of restraint produces new displacements at interior nodes. These displacements have to be added to the displacements determined by Eq. 22.22 so as to give the displacements in the actual structure:

$$\{D^*_i\} = \{D^*_i\}_{\text{boundaries fixed}} - [S^*_{ii}]^{-1}[S^*_{ib}]\{D^*_b\} \tag{22.27}$$

The last term in this equation is determined from the second row of Eq. 22.21 by setting

$$\{F^*_i\} = \{0\}.$$

Step 7 By steps 5 and 6, the displacements at all nodes in the actual structure have been determined; these are used in the usual way to determine the internal forces or stresses in individual elements.

Substructuring requires more complicated coding and may not always be advantageous, particularly when the substructures involve no repetition.

22.7 Plastic analysis of plane frames

This section discusses the use of a computer for the plastic analysis of plane frames[3] on the basis of the assumptions made in Chapter 18, in particular, the bilinear moment–curvature relationship of Figure 18.3. The frames are assumed to have prismatic members with known cross-sectional properties a, I, and M_p, where a and I are the area and the second moment of area respectively, and M_p is the fully plastic moment (see Section 18.2). A set of forces is applied and their magnitudes are increased in stages, without changing their relative values, until a collapse mechanism is formed. A plastic hinge is assumed to occur when M_p is reached, ignoring the effects of axial and shear forces on the plastic moment capacity (see Sections 18.8 and 18.9).

An elastic analysis is performed for each load increment and the member end-moments are recorded. When M_p is reached at a section, a hinge is inserted there and the structure stiffness matrix [S] is changed accordingly. Collapse is reached when: (a) [S] becomes singular (determinant close to zero); or (b) a diagonal element S_{ii} becomes zero; or (c) very large deflections are obtained.

For each load stage, the analysis is carried out for a unit increment in one of the loads ($P_i = 1$), with proportionate increments in the other loads. The corresponding member end-moments are used to determine a load multiplier which causes M_p to be reached at any one section, thus developing a new plastic hinge. The sum of the multipliers in all stages is the value of P_j at collapse.

For each loading stage, we generate a stiffness matrix for a structure with hinges located at the ends of members, as determined in earlier stages. The stiffness matrix for an individual member with a hinge at one or both ends is discussed below.

22.7.1 *Stiffness matrix of a member with a hinged end*

The stiffness matrix of a prismatic member of a plane frame (Figure 21.2) is given by Eq. 21.11, which ignores the effect of shear deformation and the beam-column effect (Chapter 13). After the development of a hinge at end 1 (left-hand end), the stiffness matrix of the member becomes

$$[S^*_{H1}] = \begin{bmatrix} Ea/l & & & & & \\ 0 & 3EI/l^3 & & & \text{symmetrical} & \\ 0 & 0 & 0 & & & \\ -Ea/l & 0 & 0 & Ea/l & & \\ 0 & -3EI/l^3 & 0 & 0 & 3EI/l^3 & \\ 0 & 3EI/l^2 & 0 & 0 & -3EI/l^2 & 3EI/l \end{bmatrix} \tag{22.28}$$

This matrix can be generated by condensation of [S^*] in Eq. 21.11 (using Eq. 5.17) to obtain a 5×5 matrix corresponding to the coordinates in Figure 21.2, with coordinate 3* omitted.

3 The method presented in this section and the example included are taken from Wang, C. K., "General Computer Program for Limit Analysis," *Proceedings American Society of Civil Engineers*, 89 (ST6) (December 1963), pp. 101–117. Appendix L includes a description of a microcomputer program, available on diskette, which performs the plastic analysis presented in this section. The diskette includes an executable file and a FORTRAN-language file of the code.

The original size of the matrix and the coordinate numbering are maintained by the insertion of a column and a row of zeros, as shown in Eq. 22.28.

In a similar way, when a hinge develops at end 2 instead of end 1, the member stiffness will be

$$[S^*_{H2}] = \begin{bmatrix} Ea/l & & & & & \\ 0 & 3EI/l^3 & & & \text{symmetrical} & \\ 0 & 3EI/l^2 & 3EI/l & & & \\ -Ea/l & 0 & 0 & Ea/l & & \\ 0 & -3EI/l^3 & -3EI/l^2 & 0 & 3EI/l^3 & \\ 0 & 0 & 0 & 0 & 0 & 0 \end{bmatrix} \tag{22.29}$$

When hinges are developed at both ends, the member stiffness matrix will be the same as Eq. 22.28 or Eq. 22.29, with zero substituted for all the matrix elements which include I.

It should be pointed out that, in this section, we limit the discussion to frames subjected to concentrated loads applied at nodes only. Thus, plastic hinges can develop only at member ends.

Example 22.3: Single-bay gable frame

Determine the value of P_c to produce collapse for the load system shown in Figure 22.9. For the seven members in the figure, the values of M_p, in terms of P_b, are {765, 765, 1275, 1275, 1015, 1015, 616}; the values of a and I are given in the same figure.

Load stage 1 With the value $P_c = 1$, the load system produces the end-moments $\{M_u^{(I)}\}$ listed in Table 22.1. From these values, it can be seen that a multiplier $P_c = 34.458$ will cause M_p to be reached so that the first plastic hinge is developed at node 7 in member 7. The corresponding

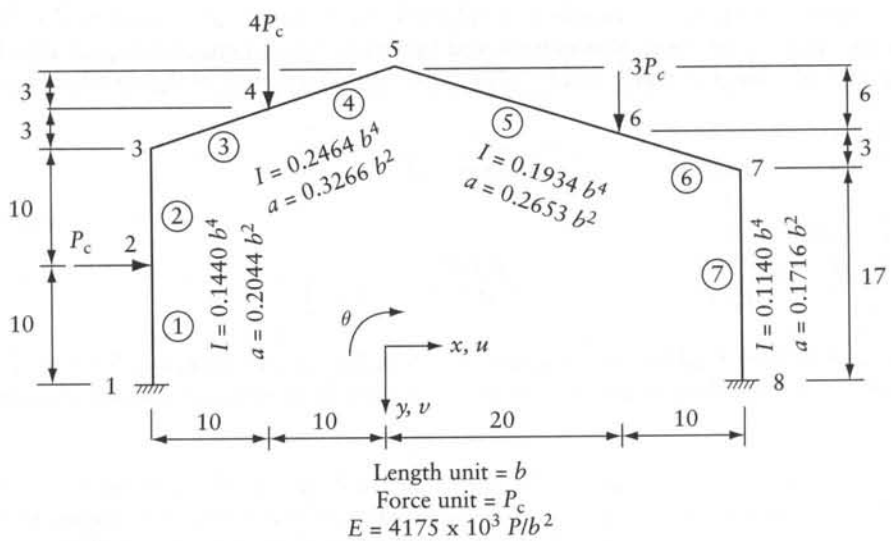

Figure 22.9 Plane frame of Example 22.3.

Table 22.1 Member End-Moments at the Termination of Stage 1 (in terms of Pb)

Member	*Node at member end*	*Plastic moment capacity* M_p	*Moment due to* $P_c = 1$ $M_u^{(1)}$	*Load multiplier*	*Number of the stage in which a hinge is formed*	*Moment at the end of stage 1* $M^{(1)}$
1	1	765.0	7.56			260.61
	2	765.0	0.56			19.36
2	2	765.0	–0.56			–19.36
	3	765.0	18.69			643.92
3	3	1275.0	–18.69			–643.92
	4	1275.0	–12.95			–446.23
4	4	1275.0	12.95			446.23
	5	1275.0	–4.59			–158.06
5	5	1015.0	4.59			158.06
	6	1015.0	–9.61			–331.18
6	6	1015.0	9.61			331.18
	7	1015.0	17.88			616.00
7	7	616.0	–17.88	34.458		–616.00
	8	616.0	–12.94			–445.75

nodal displacements, listed for nodes 1 to 8 in the order u, v, θ and given in terms of length unit b or radian, are

$$\{D^{(1)}\} = 34.458 \times 10^{-6}$$
$$\times \{0, 0, 0, -403.5, 43.44, -58.19, -436.50, 86.92, 101.8$$
$$-27.80, 1524, -130.9,\ 198.2,\ 2321,\ 41.94$$
$$399.4, 1531, -141.6,\ 808.8, 78.11, -88.20,\ 0, 0, 0\}$$

Load stage 2 A new stiffness matrix is generated for the structure with a hinge introduced in member 7 at node 7. The member end-moments $\{M_u^{(2)}\}$, for $P_c = 1$, given in Table 22.2, show that a multiplier $P_c = 5.871$ will cause a second hinge to develop at node 3 in member 2. The member end-moments after application of this load increment are

$$\{M^{(2)}\} = \{M^{(1)}\} + 5.871\{M_u^{(2)}\}$$

The corresponding displacements are calculated in a way similar to that used for stage 1, giving

$$\{D^{(2)}\} = 5.871 \times 10^{-6}$$
$$\times \{0, 0, 0,\ 245.2, 48.33, 61.79,\ 1768, 96.67, 282.2$$
$$2726, 3358, 305.4,\ 3400, 5643, 156.5$$
$$3744, 4406, -328.1,\ 5024, 68.21, -485.6,\ 0, 0, 0\}$$

We should note that, with a hinge existing at the connection of member 7 to node 7, the rotation at node 7, included in the above equation, represents the rotation at the node, and not at the top end of member 7.

Load stage 3 A second hinge is introduced and the process described in stage 2 is repeated, giving (Table 22.3)

$$\{M^{(3)}\} = \{M^{(2)}\} + 1.522\{M_u^{(3)}\}$$

Table 22.2 Member End-Moments at Termination of Stage 2 (in Terms of Pb)

Member	*Node at member end*	$M_p - \lvert M^{(1)}\rvert$	*Moment due to* $P_c = 1$ $M_u^{(2)}$	*Load multiplier*	*Number of the stage in which a hinge is formed*	$5.871\ M_u^{(2)}$	*Moment at the end of stage 2* $M^{(2)}$
1	1	504.39	−1.42			−8.31	252.30
	2	745.64	6.02			35.34	54.71
2	2	745.64	−6.02			−35.34	−54.71
	3	121.08	20.62	5.871	2	121.08	765.00
3	3	631.08	−20.62			−121.08	−765.00
	4	828.77	−16.24			−95.38	−541.61
4	4	828.77	16.24			95.38	541.61
	5	1116.94	−13.11			−76.98	−235.04
5	5	856.94	13.11			76.98	235.04
	6	683.82	−24.37			−143.08	−474.26
6	6	683.82	24.37			143.08	474.26
	7	399.00	0.00			0.00	616.00
7	7	0	0		1	0	−616.00
	8	170.25	−24.83			−145.79	−591.54

Table 22.3 Member End-Moments at Termination of Stage 3 (in Terms of Pb)

Member	*Node at member end*	$M_p - \lvert M^{(2)}\rvert$	*Moment due to* $P_c = 1$ $M_u^{(3)}$	*Load multiplier*	*Number of the stage in which a hinge is formed*	$1.522\ M_u^{(3)}$	*Moment at the end of stage 3* $M^{(3)}$
1	1	512.70	8.91			13.56	265.86
	2	710.29	−9.45			−14.39	40.32
2	2	710.29	9.45			14.39	−40.32
	3	0	0		2	0	765.00
3	3	515.00	−0.00			−0.00	−765.00
	4	733.39	−34.60			−52.66	−594.27
4	4	733.39	34.60			52.66	594.27
	5	1039.96	−29.19			−44.44	−279.48
5	5	779.96	29.19			44.44	279.48
	6	540.74	−29.73			−45.25	−519.52
6	6	540.74	29.73			45.25	519.52
	7	399.00	0.00			−0.00	616.00
7	7	0	0		1	0	−616.00
	8	24.46	−16.07	1.522	3	−24.46	−616.00

The corresponding displacement after the third load stage is

$$\{D^{(3)}\} = 1.522 \times 10^{-6}$$
$$\times \{0,0,0,\ -755.4, 43.86, -152.6,\ -2805, 87.75, 709.3,$$
$$-867.5, 6600, 533.8,\ 288.9, 10275, 210.2,$$
$$1228, 6880, -551.6,\ 3251, 77.26, -743.9,\ 0,0,0\}$$

Table 22.4 Member End-Moments at Termination of Stage 4 (in Terms of Pb)

Member	*Node at member end*	$M_p - \lvert M^{(3)}\rvert$	*Moment due to* $P_c = 1$ $M_u^{(4)}$	*Load multiplier*	*Number of the stage in which a hinge is formed*	$15.489\, M_u^{(2)}$	*Moment at the end of stage 4* $M^{(4)}$
1	1	499.14	−10.00			−154.84	111.01
	2	714.68	0.00			0	40.32
2	2	714.68	−0.00			−0.00	−40.32
	3	0	0		2	0	765.00
3	3	515.00	−0.00			−0.00	−765.00
	4	680.73	−38.00			−588.402	−1182.67
4	4	680.73	38.00			588.40	1182.67
	5	995.52	−36.00			−557.44	−836.92
5	5	735.52	36.00			557.44	836.92
	6	495.48	−32.00			−495.48	−1015.00
6	6	495.48	32.00	15.484	4	495.48	1015.00
	7	399.00	0.00			−0.00	616.00
7	7	0	0		1	0	−616.00
	8	0	0		3	0	−616.00

Load stage 4 Introducing a third hinge at node 8 in member 7 and repeating the above procedure gives (Table 22.4):

$$\{M^{(4)}\} = \{M^{(3)}\} + 15.484\ \{M_u^{(4)}\}$$

$$\{D^{(4)}\} = 15.484 \times 10^{-6} \times \{0,0,0,\ 554.1,44.53,83.11,\ 1385,89.08,812.6,\ 3623,7575,\ 619.8,\ 4914,11883,245.0\ 6136,7805,-634.7,\ 8442,75.92,-841.6,\ 0,0,0\}$$

The fourth hinge changes the structure into a mechanism so that an additional loading stage would give extremely large displacements. The collapse load is therefore the sum of the load increments in the four stages, namely,

$$P_c = (34.458 + 5.871 + 1.522 + 15.484)P = 57.335\ P$$

22.8 Stiffness matrix of member with variable cross section or with curved axis

A procedure for generating the stiffness matrix of a member of a framed structure of any type is presented below. The procedure can be used when the member has a variable cross section or a curved axis, and also in nonlinear analysis of reinforced concrete structures where cracking reduces the effective area[4] of the cross section.

4 See the first reference mentioned in footnote 1 in Chapter 1.

Any of the stiffness matrices given in Chapter 21 for individual members of framed structures (Figure 21.2) may be partitioned as follows:

$$[S^*] = \begin{bmatrix} [S^*_{11}] & [S^*_{12}] \\ [S^*_{21}] & [S^*_{22}] \end{bmatrix} \tag{22.30}$$

The submatrices in the first row contain forces at the first node of the member. Equilibrants of these forces at the second node form the elements in the submatrices in the second row. Because of this equilibrium relationship and the symmetry of $[S^*]$, Eq. 22.30 may be rewritten as

$$[S^*] = \begin{bmatrix} [S^*_{11}] & [S^*_{11}][R]^T \\ [R][S^*_{11}] & [R][S^*_{11}][R]^T \end{bmatrix} \tag{22.31}$$

where $[R]$ is a matrix generated by static equilibrium. As an example, considering a member of a plane frame (Figure 21.2), we have

$$[R] = \begin{bmatrix} -1 & 0 & 0 \\ 0 & -1 & 0 \\ 0 & l & -1 \end{bmatrix} \tag{22.32}$$

Here, the elements in the first column of $[R]$ are values of forces at coordinates 4*, 5*, and 6* in equilibrium with $F^*_1 = 1$. Similarly, the second and third columns correspond to $F^*_2 = 1$ and $F^*_3 = 1$ respectively.

The submatrix $[S^*_{11}]$ can be determined by

$$[S^*_{11}] = [f]^{-1} \tag{22.33}$$

where $[f]$ is the flexibility matrix of the member when it is treated as a cantilever fixed at the second node. Any element f_{ij} of the flexibility matrix can be calculated by the unit-load theorem (Section 7.6):

$$f_{ij} = \int N_{ui} N_{uj} \frac{dl}{Ea} + \int M_{ui} M_{uj} \frac{dl}{EI} + \int V_{ui} V_{uj} \frac{dl}{Ga_r} + \int T_{ui} T_{uj} \frac{dl}{GJ} \tag{22.34}$$

where N, M, V, and T are axial force, bending moment, shearing force, and twisting moment respectively; subscripts ui and uj refer to the effect of unit force $F_i = 1$ and $F_j = 1$ respectively, applied separately at coordinate i and j; E is the modulus of elasticity in tension or compression, and G is the modulus of elasticity in shear; a, I, and J are, respectively, the cross-sectional area, second moment of area, and torsion constant; and a_r is the reduced area of the cross section (see Section 7.3.3).

When the cross-sectional properties vary arbitrarily, the integrals in this equation are evaluated numerically. Substitution in Eqs. 22.33 and 22.31 generates the stiffness matrix of the member.

Example 22.4: Horizontal curved grid member

Generate the stiffness matrix for a horizontal grid member curved in the form of circular arc of radius r (Figure 22.10a). Consider deformations due to bending and torsion only. The member has a constant cross section with $GJ/EI = 0.8$; $\theta = 1$ radian.

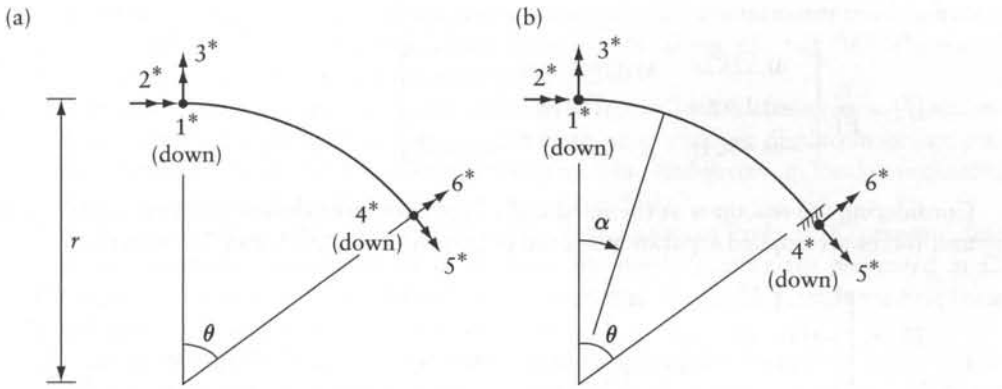

Figure 22.10 Top view of a curved grid member. (a) Coordinate system. (b) Member fixed at one end to generate the flexibility matrix.

A unit load applied at coordinate 1, 2, or 3 on the cantilever in Figure 22.10b produces the following internal forces:

$$M_{u1} = -rs \quad M_{u2} = s \quad M_{u3} = c \tag{22.35}$$

$$T_{u1} = r(1-c) \quad T_{u2} = c \quad T_{u3} = -s \tag{22.36}$$

where $s = \sin\alpha$ and $c = \cos\alpha$, with α defined in Figure 22.10b. The elements of the flexibility matrix of the cantilever shown in Figure 22.10b are given by (Eq. 22.34)

$$f_{ij} = \frac{r}{EI}\int_0^\theta M_{ui}M_{uj}d\alpha + \frac{r}{GJ}\int_0^\theta T_{ui}T_{uj}d\alpha \tag{22.37}$$

The flexibility matrix can thus be considered as

$$[f] = [f_M] + [f_T] \tag{22.38}$$

where $[f_M]$ and $[f_T]$ represent bending and torsion contributions to be calculated by the first and second term of Eq. 22.37 respectively.

Substitution of Eqs. 22.35 and 22.36 into Eq.22.37 and evaluation of the integrals gives

$$[f_M] = \frac{r}{EI}\begin{bmatrix} 0.2727r^2 & \text{symmetrical} & \\ -0.2727r & 0.2727 & \\ -0.3540r & 0.3540 & 0.7273 \end{bmatrix}$$

$$[f_T] = \frac{r}{GJ}\begin{bmatrix} 0.0444r^2 & \text{symmetrical} & \\ 0.1141r & 0.7273 & \\ -0.1057r & -0.3540 & 0.2727 \end{bmatrix}$$

and

$$[f] = \frac{r}{EI}\begin{bmatrix} 0.3282r^2 & \text{symmetrical} & \\ -0.1300r & 1.1818 & \\ -0.4861r & -0.0885 & 1.0682 \end{bmatrix}$$

Considering the reactions at the fixed end of the cantilever shown in Figure 22.10a when unit forces are applied separately at each of coordinates 1*, 2*, and 3*, we write

$$[R] = \begin{bmatrix} -1 & 0 & 0 \\ -r(1-c) & -c & s \\ rs & -s & -c \end{bmatrix}$$

where c and s are $\cos\theta$ and $\sin\theta$ respectively.

Inversion of $[f]$ and substitution in Eq. 22.31 gives

$$[S^*] = \frac{EI}{r}\left[\begin{array}{ccc:ccc} 12.158/r^2 & & & & \text{symmetrical} & \\ 1.763/r & 1.107 & & & & \\ 5.679/r & 0.894 & 3.595 & & & \\ \hdashline -12.158/r^2 & -1.763/r & -5.679/r & 12.158/r^2 & & \\ -1.763/r & -0.656 & -0.069 & 1.763/r & 1.107 & \\ 5.679/r & 0.069 & 2.084 & -5.679/r & -0.894 & 3.595 \end{array}\right]$$

22.9 General

The techniques presented in Chapters 21 and 22 can be used to analyze fairly large structures idealized as bars or other finite elements. There exist more sophisticated techniques to make optimum use of computer storage and to minimize computing time.

The problems given below are related to Chapters 21 and 22.

Problems

22.1 Change the space truss of Prob. 3.14 into a space frame with rigid joints. Assume that each member has a hollow rectangular cross section, arranged so that at least two opposite

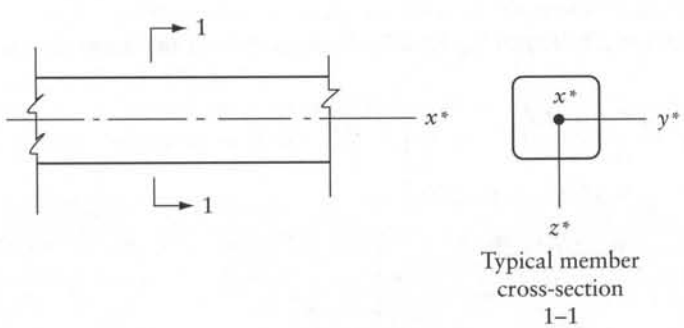

Prob. 22.1

sides are in vertical planes. With this arrangement, local axis y^* (see figure here) for each member will be parallel to one of the global axes. Generate the transformation matrices $[t]$ for members AC and DG, which have local x^* axes along AC and DG. The global x, y, z axes are indicated in the figure for Prob. 3.14.

22.2 The right-hand end of the plane frame member in Figure 21.2 is subjected to prescribed displacements $\{D\} = \{u, v, \theta\}$ in global x, y, z directions, while the displacements are prevented at the left-hand end. The corresponding member end-forces, in local coordinates, can be expressed as $\{A_r\} = [G]\{D\}$. Generate matrix $[G]$.

22.3 Find the forces at the ends of member CD of the plane frame of Prob. 5.16 corresponding to a unit downward displacement of D while the displacements are prevented at C. Consider the end-forces in local directions as shown in Figure 21.2, with the first three coordinates at C. Ignore deformations due to shear.

22.4 Use the answer of Prob. 22.2 to calculate the member end-forces $\{A_r\}$ of member 1 of the frame in Figure 21.5 due to $u = 0.2b$ and $v = 0.5b$ at the bottom end while the displacements are prevented at the top end. The answers to this problem are given in the last row of Table 21.2 (see Example 21.2).

22.5 Use Eq. 21.41 to verify the reactions determined at node 4 in Example 21.5 for loading case 3, Figure 21.4.

22.6 Use the nodal displacements determined in Example 21.5 to calculate the end-forces for member 4 in the truss of Figure 21.4 due to a rise in temperature of the same member (loading case 2).

22.7 Analysis of the frame in Figure 21.5 for the loads shown gives the following displacements: $\{D\} = 10^{-3}\{-68.14 \times 10^{-6}, 8.119 \times 10^{-6}, -0.1601 \times 10^{-6}, 39.83, 8.119, 0.7198, 38.25, 5.941, -0.4722, 27.28 \times 10^{-6}, 5.941 \times 10^{-6}, 0.6186\}$. The displacements are listed in the order u, v, θ for nodes 1, 2, 3, and 4. In obtaining the solution, the displacements at the supports were prescribed as indicated by Eq. 21.39. Find:
(a) The reactions at node 1 using Eq. 21.40 and check the results by Eq. 21.41.
(b) The forces at the ends of member 2.

22.8 Generate the stiffness matrix for a member of a plane frame corresponding to the coordinates in Figure 21.2, assuming that the member has a rectangular cross section of width b and a depth which varies as shown in Prob. 11.8.

22.9 The stiffness matrix of a grid member shown in Figure 21.2 is given by Eq. 21.12. Adjust the stiffness matrix so that it will correspond to coordinates 5* and 6* rotated through an angle γ in the clockwise direction, without a change in the remaining coordinates.

22.10 Derive the stiffness matrix for a member of a plane truss with the coordinates as shown. Verify that when $\alpha_1 = \alpha_2 = \alpha$, $[S]$ will be given by Eq. 21.23.

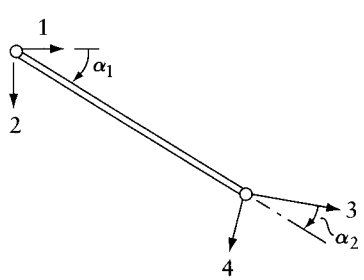

Prob. 22.10

22.11 The figure represents the top view of a typical panel of a horizontal pipeline composed of an infinite number of identical panels. Assuming that, in each panel, the pipe has supports

at A, B, C, and D, which can provide vertical reaction components only, find θ_x and θ_z at B. Obtain the bending moment and twisting moment diagrams for EBH due to uniform downward load of q per unit length, representing the self-weight of the pipe and its contents. Take $GJ/EI = 0.8$. (By symmetry, the unknown displacement components can be reduced to two.)

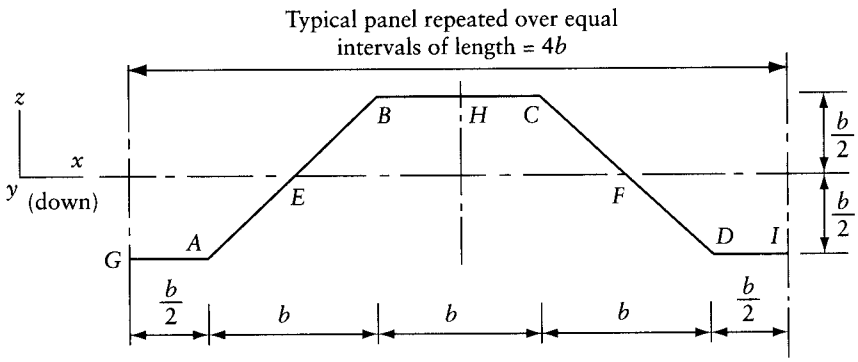

Prob. 22.11

22.12 Solve Prob. 22.11 for a uniform rise in temperature of T degrees. The coefficient of thermal expansion is α; the cross-sectional area of the pipe is $a = 100I/b^2$. Do not consider the self-weight of the pipe in this problem.

22.13 The figure is a top view of a horizontal beam EF subjected to a gravity load of q per unit length. AB and CD are rigid bars connecting E and F to supports at A, B, C, and D which can provide vertical components only. Obtain the bending moment and twisting moment diagrams for EF, assuming $GJ/EI = 0.6$. Take advantage of symmetry to reduce the unknown displacement components to one. (This structure may be considered as a simplified idealization of a bridge girder over skew supports.)

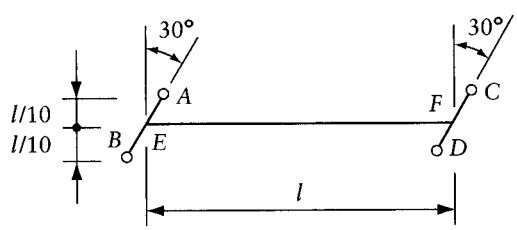

Prob. 22.13

22.14 The figure is a top view of a horizontal beam EF subjected to a gravity load of q per unit length. AB, CD, and GH are rigid bars connecting E, O, and F to supports at A, B, C, D, G, and H which can provide vertical components only. Obtain the bending moment and twisting moment diagrams for EF, assuming $GJ/EI = 0.6$. Also find the reactions at supports G and H. Take advantage of cyclic symmetry to reduce the unknown displacement components to one.

22.15 The figure is the top view of a horizontal grid. Find the displacements at node B due to the self-weight of the members of q per unit length. All members have the same cross section, with $GJ = 0.6EI$. Take advantage of symmetry to reduce the unknown displacement components to three.

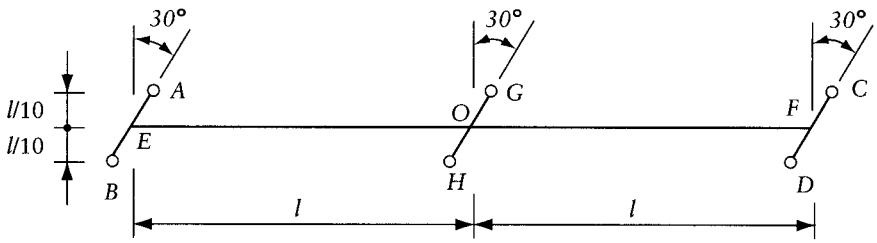

Prob. 22.14

For all members, $GJ/EI = 0.6$ and EI = constant

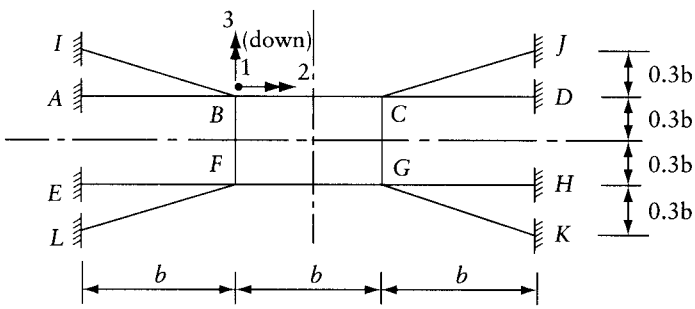

Prob. 22.15

22.16 The grid of Prob. 22.15 is subjected to a downward force P at each of B and C. Replace the actual load by symmetrical and antisymmetrical components and perform analyses for a quarter structure to determine the three displacement components at B and F.

22.17 The figure is the top view of a horizontal grid with all members subjected to a uniform downward load of q per unit length. Find the displacement components at node E by analyzing part AEF, considering cyclic symmetry. Also, take advantage of symmetry about an appropriate plane to reduce the unknown displacement components to two. All members have same length l and the same cross section, with $GJ/EI = 0.5$.

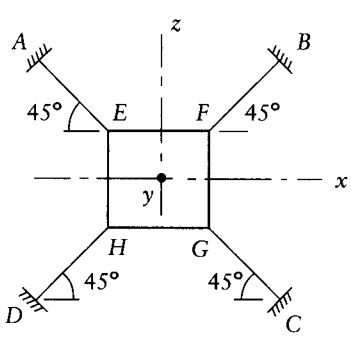

Prob. 22.17

22.18 The figure is the top view of a horizontal grid which has supports at A, B, C, D, E, and F providing vertical reaction components only. Find the deflection at O and bending moments at member ends marked 1, 2, and 3 due to uniform load of q per unit length on all members. All members have the same length l and the same cross section. Considering cyclic symmetry, perform the analysis for FAO. In addition, take advantage of symmetry about an appropriate plane to reduce the number of unknown displacements to two.

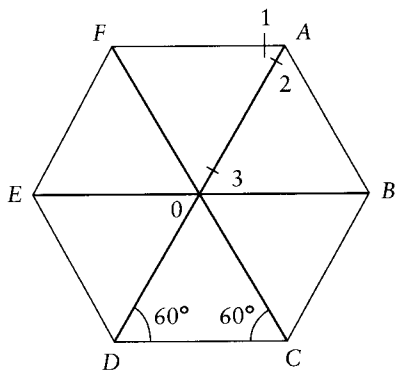

Prob. 22.18

Chapter 23

Nonlinear analysis

23.1 Introduction

In linear analysis of structures, the equations of equilibrium are based on the undeformed geometry existing before load application. This is sufficiently accurate for many practical cases. However, some structures, such as cable nets and fabrics, trusses, and frames with slender members may have large deformations, so that it is necessary to consider equilibrium in the real deformed configurations. This requires nonlinear analysis involving iteration, which can be done using Newton-Raphson's technique. The equilibrium equations are based on trial displacement values, whose accuracy is improved by iterations, so as to satisfy the equilibrium of the nodes or the members in their displaced positions or their deformed shapes. Nonlinearity caused by large deformations is referred to as *geometric nonlinearity*. We are dealing here with large deformation, but small strain with linear stress–strain relationship.

Nonlinearity can also arise when the stress–strain relationship of the material is nonlinear in the elastic or in the plastic range; this is called *material nonlinearity*.

A member subjected to a large axial force combined with transverse loads or to transverse end translation or rotation represents a geometric nonlinear problem, often referred to as a beam-column problem, or casually, a *P*-delta problem. The equilibrium of the member is considered in its deformed shape, as was done in Chapter 13, where a quasi-linear analysis is employed for the analysis of plane frames, including calculation of the critical buckling loads. This is achieved by considering trial values of the axial forces in the members as constants unchanged by the nodal displacements. In this way a linear analysis is possible because of the fact that, in the presence of a constant axial force P, the magnitude of the transverse deflection y due to any pattern of transverse loads $\alpha\{q\}$ varies linearly with the value of α (see the governing differential Eq. 13.1).

It should be noted that the *P*-delta analysis of Chapter 13 ignores the change in length of members associated with the transverse deflection. For example, the left-hand end of the member in Figure 13.2a is assumed to acquire a unit transverse translation without change in the magnitude of the axial force, in spite of the fact that the length of the curved deflected line is longer than the initial length. Such an assumption may cause inaccuracy when the deformations are very large. This source of error is avoided in the geometric nonlinear analysis presented in this chapter for plane and space trusses, cable nets, and plane frames. The length of a deflected member of a frame is assumed to be equal to the length of the straight line joining its ends (the chord). In all these cases, the geometric nonlinearity caused by axial forces, particularly prestressing of cables, can be of prime importance.

Material nonlinearity is considered in the computer plastic analysis of plane frames presented in Section 22.7. By assuming a bilinear moment–curvature relationship (Figure 18.3), the structure behaves linearly until the first hinge has developed. Under increasing load the structure continues to behave linearly, generally with a reduced stiffness, until a second hinge is formed.

The same behavior continues under increasing load until sufficient hinges have developed to form the failure mechanism.

In the present chapter there are presented[1] several techniques that can be used in analysis of structures in general, considering material nonlinearity. Simple examples of trusses and plane frames will be analyzed.

23.2 Geometric stiffness matrix

When the load on a geometrically nonlinear structure is applied in small increments, the force and displacement may be related by

$$[S]\{\Delta D\} = \{\Delta F\} \tag{23.1}$$

where $\{\Delta F\}$ and $\{\Delta D\}$ are increments of forces and displacements at a coordinate system. The stiffness matrix $[S]$ changes with the change in geometry; moreover, in framed structures $[S]$ depends also upon the axial forces in the members. As $\{\Delta F\}$ tends to $\{0\}$, $[S]$ tends to $[S_t]$ referred to as the *tangent stiffness matrix* and is expressed as the sum of two matrices:

$$[S_t] = [S_e] + [S_g] \tag{23.2}$$

where $[S_e]$ is the conventional *elastic stiffness matrix*, based on the initial geometry of the structure at the start of loading increment and $[S_g]$ is the *geometric stiffness matrix*, to be generated in this chapter for prismatic members of plane and space trusses and of plane frames with rigid joints and for triangular membrane elements. $[S_g]$ depends upon the deformed geometry of the structure and the axial forces in the members. The displacements change node positions; thus, $[S_e]$ also varies during the analysis.

When the members are subjected to initial forces (e.g. initial prestress in cables), the initial geometric stiffness matrix is not null.

23.3 Simple example of geometric nonlinearity

As a simple example, consider a wire stretched between two points with initial tension $N^{(0)}$ (Figure 23.1a). Define one coordinate at the middle as shown. Application of a force Q at the coordinate produces a displacement D and the tension in the cable becomes N. Assuming elastic material, the tension in the cable can be expressed as

$$N = N^{(0)} + (2Ea/b)\{[b/2)^2 + D^2]^{1/2} - b/2\} \tag{23.3}$$

where b is the initial length of cable, a is the cross-sectional area, and E is the modulus of elasticity.

Considering equilibrium of node B in the deflected position, we write

$$Q = 2ND[(b/2)^2 + D^2]^{-1/2} \tag{23.4}$$

For this simple structure, with a single degree of freedom, a value of D can be assumed and successive use of Eqs. 23.3 and 23.4 can give a plot of D versus Q, as done below in Example 24.1.

1 For additional reading on nonlinear analysis, see: Levy, R. and Spillers, W.R., *Analysis of Geometrically Nonlinear Structures*, Chapman and Hall, New York, 1995, 199 pp. See also, Crisfield, M.A., *Non-linear Finite Element Analysis of Solids and Structures*, Wiley, Chichester, England, 1991, Vol. 1, 345 pp.

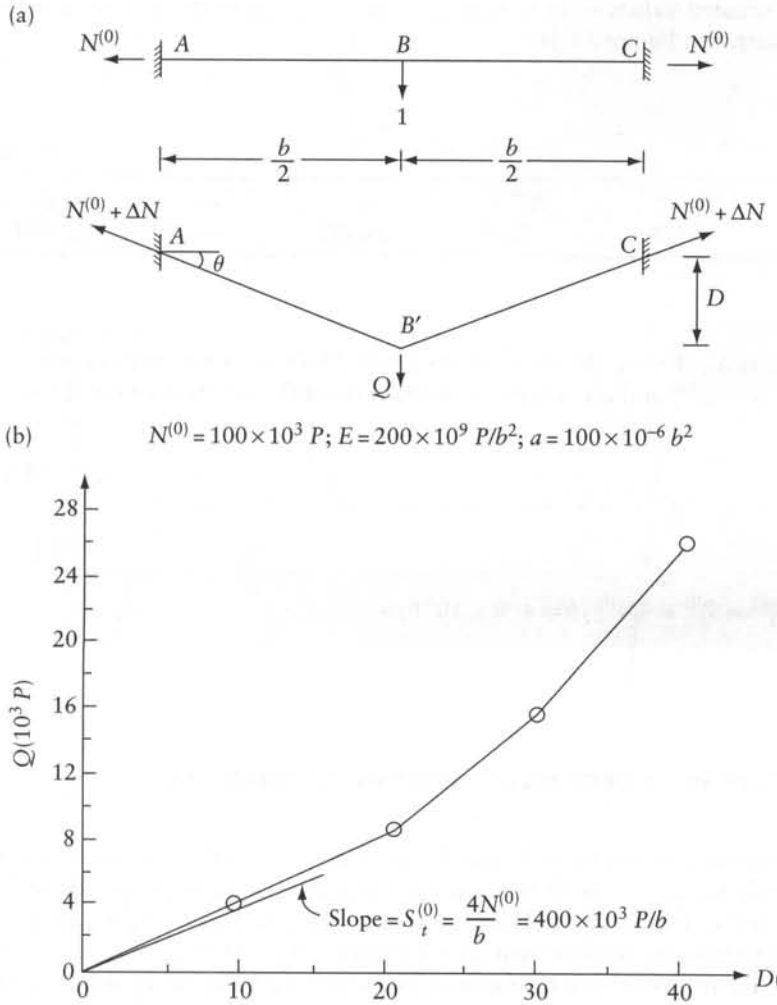

Figure 23.1 A wire stretched between two fixed points. (a) Geometry and forces before and after application of force Q. (b) Plot of force Q versus displacement D.

With multiple degrees of freedom (e.g. when the cable is carrying several concentrated forces), the equilibrium can be checked by equations similar to Eq. 23.4 using trial values of $\{D\}$. The solution is reached only when the force in each member (in various parts of the cable example) satisfies an elastic relation similar to Eq. 23.3. This is achieved by iterative calculations discussed in several sections of the present chapter.

Example 23.1: Prestressed cable carrying central concentrated load

Plot a graph of D versus Q for the structure in Figure 23.1, assuming $.N^{(0)} = 100 \times 10^3 P$, $a = 100 \times 10^{-6} b^2$, and $E = 200 \times 10^9 P/b^2$, where P and b are, respectively, force and length units. What are the initial values $S_g^{(0)}$ and $S_t^{(0)}$?

Substitution of selected values of D in Eqs. 23.3 and 23.4 gives the following values of Q, which are plotted in Figure 23.1b:

						Multiplier:
D	0	10	20	30	40	$10^{-3}b$
Q	0	4.159	9.272	16.287	26.140	$10^{3}P$

The tangent stiffness S_t, that is, the slope of the graph Q–D, increases with an increase in D. When D=0, $N = N^{(0)}$ and the tangent stiffness is (by differentiation of Eq. 23.4)

$$S_t^{(0)} = \frac{4N^{(0)}}{b} \tag{23.5}$$

In this case,

$$S_e^{(0)} = 0 \text{ and } S_t^{(0)} = S_g^{(0)} = 4N^{(0)}/b = 400 \times 10^3 P/b$$

23.4 Newton-Raphson's technique: solution of nonlinear equations

Newton-Raphson's rapidly converging technique is presented here for the solution of nonlinear equations with a single variable or with n unknown variables. For this purpose, consider the symmetrical plane truss in Figure 23.2a. Define a system composed of a single coordinate as shown. It is required to find the displacement D, for a given value of the force F.

The D–F diagram (Figure 23.2b) can be obtained by assuming a value for D and determining the value of F, following the equilibrium equation of the displaced node B' (Figure 23.2a):

$$F = -2N \sin\theta \tag{23.6}$$

where

$$\sin\theta = (h - D)/l \tag{23.7}$$

$$l = [b^2 + (h - D)^2]^{1/2} \tag{23.8}$$

$$N = Ea(l - l_{in})/l_{in} \tag{23.9}$$

Here, N is the axial force in the members; θ is the angle between the horizontal and the displaced position of member ($B'C$), l_{in} and l are the initial length (BC) and the length after deformation ($B'C$) of each member, E is the modulus of elasticity, and a is the cross-sectional area. Linear stress–strain relation for the material is assumed.

In a multi-degree-of-freedom system with n unknown displacements, it is not simple to assume a set of displacements $\{D\}$ to satisfy equilibrium and geometry equations similar to Eqs. 23.6

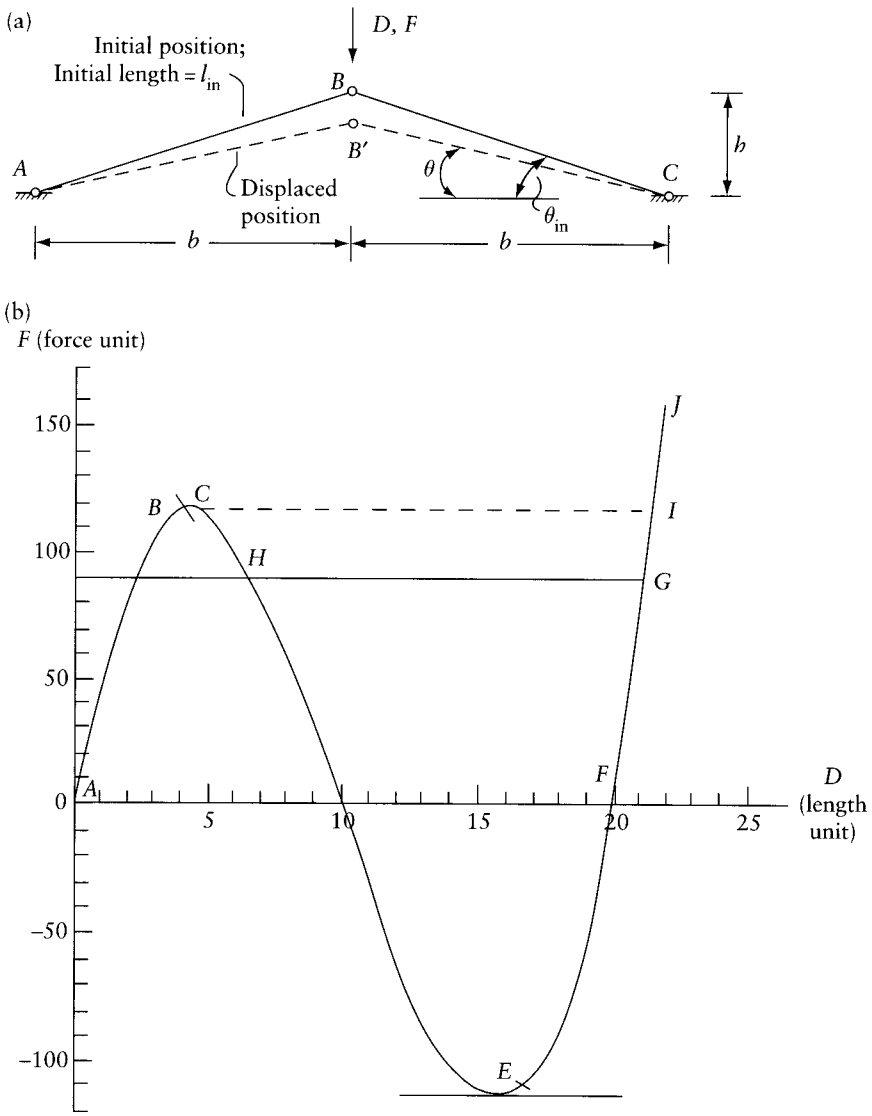

Figure 23.2 Geometric nonlinearity of a plane truss with a single degree of freedom. (a) Plane truss. Example values: b = 300 and h = 10 (length unit); $Ea = 8 \times 10^6$ (force unit). (b) Force versus displacement at coordinate 1.

and 23.9 at all nodes and for all members. The problem can be solved by iteration, which is explained first with reference to the single-degree-of-freedom system in Figure 23.2a.

In the present section, we limit our discussion to the case when h is small compared to l_{in} (Figure 23.2a); the angle θ_{in} between the horizontal and the initial position of BC is small and the geometric nonlinearity is too important to be ignored. Crisfield[2] gives the following approximate relation between F and D:

$$F \simeq (Ea/l_{in}^3)(2h^2D - 3hD^2 + D^3) \tag{23.10}$$

2 See Crisfield, M.A., mentioned in footnote 1 of this chapter.

We can verify that Eq. 23.10 satisfies approximately Eq. 23.6 for values of D in the range considered ($0 \leq D \leq 2.5h$), assuming as an example $b = 300$ and $h = 10$ (length unit) respectively, and $Ea = 8 \times 10^6$ (force unit). The second moment of area of the cross section is considered to be sufficiently large to preclude buckling of individual members.

To determine D corresponding to a specified value of F by Newton-Raphson's technique, Eq. 23.10 is rewritten:

$$g(D) = (Ea/l_{in}^3)(2h^2D - 3hD^2 + D^3) - F = 0 \tag{23.11}$$

For the correct value of D, the function $g(D)$ should be zero. We start by an estimated answer $D^{(0)}$, for which $g(D)$ is a nonzero value representing an out-of-balance force. A more accurate value of D is given by the recursion equations

$$D^{(1)} = D^{(0)} + \Delta D \tag{23.12}$$

Here,

$$\Delta D = -[S_t(D^{(0)})]^{-1} g(D) \tag{23.13}$$

and $S_t(D^{(0)})$ is the value of the tangent stiffness when the value of the unknown is $D^{(0)}$. The tangent stiffness can be determined by differentiation:

$$S_t = dF/dD \tag{23.14}$$

Calculating g with a trial value of D and determining an improved estimate of D by Eq. 23.12 represent one iteration cycle. The cycle is repeated until the out-of-balance force is sufficiently small. The procedure converges rapidly as demonstrated below.

As an example, consider the structure in Figure 23.2; it is required to find the value of D when $F = 90$. The tangent stiffness is (by differentiation of Eq. 23.10)

$$S_t = dF/dD = (Ea/l_{in}^3)(2h^2 - 6hD + 3D^2) \tag{23.15}$$

This equation applies only for the simple truss in Figure 23.2, with $\theta_{in} \ll 1.0$. General equations which can be used for plane or space trusses are derived in Section 23.6.

At D = 0, $S_t = 59.16$. We use this value to obtain the approximate answer, corresponding to linear analysis: $D^{(0)} = (59.16)^{-1}(90) = 1.52$. With D = 1.52, the out-of-balance force and the tangent stiffness are (Eqs. 23.11 and 23.15)

$$g(D^{(0)}) = -19.54(\text{force unit}) \quad S_t(D^{(0)}) = 34.23(\text{force/length})$$

The improved estimate of D at the end of the first cycle is (Eqs. 23.12 and 23.13)

$$D^{(1)} = 1.52 - (34.23)^{-1}(-19.54) = 2.09(\text{length unit})$$

The second and third iteration cycles give, respectively, $D = 2.18$ and $D = 2.19$. The latter value is accurate to two decimal places.

The above procedure, represented in Figure 23.3, can be used to find points on the curve AB before reaching the buckling load, corresponding to point C in Figure 23.2b. At this point the iteration fails because $S_t = 0$ and its inverse cannot be used in Eq. 23.13. If a model of the structure is tested experimentally, it would be possible to follow the path AB by increasing the value of F up to a value just below the buckling load; the structure will then suddenly snap through to

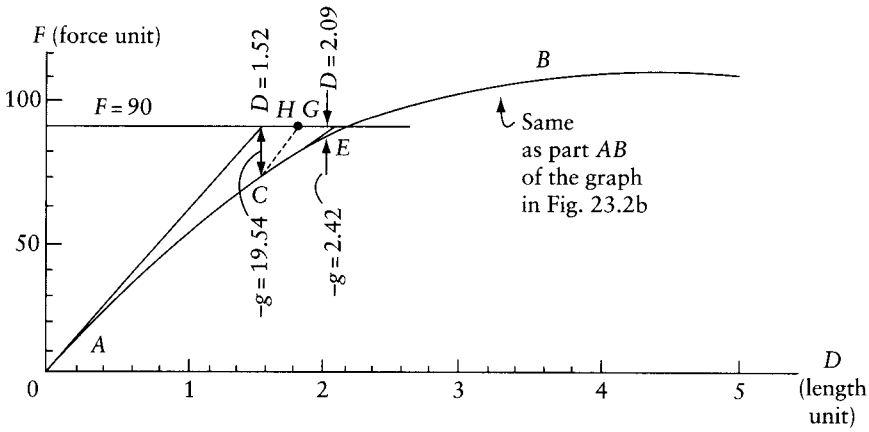

Figure 23.3 The Newton-Raphson iterative procedure applied to the structure in Figure 23.2a. Two iteration cycles are shown; the third iteration converges to the solution $D = 2.19$ (point E).

reach the equilibrium position represented by point I. The path $CHEFI$ can be obtained only by a displacement-controlled experiment.

The same path can be followed analytically by appropriate selection of the trial values of D. We can verify that the values $D = 6.55$ and $D = 21.27$ (length unit) are valid answers corresponding to $F = 90$ (force unit) (points H and G in Figure 23.2b).

When Newton-Raphson's technique is employed to solve a system of n equations, each of Eqs. 23.12 to 23.14 becomes a system of n equations:

$$\{D\}^{(1)} = \{D\}^{(0)} + \{\Delta D\} \tag{23.16}$$

$$\{\Delta D\} = -[S_t(\{D\}^{(0)})]^{-1}\{g\} \tag{23.17}$$

$$[S_t] = \begin{bmatrix} \partial F_1/\partial D_1 & \partial F_1/\partial D_2 & \dots & \partial F_1/\partial D_n \\ \partial F_2/\partial D_1 & \partial F_2/\partial D_2 & \dots & \partial F_2/\partial D_n \\ \dots & & & \\ \partial F_n/\partial D_1 & \partial F_n/\partial D_2 & \dots & \partial F_n/\partial D_n \end{bmatrix} \tag{23.18}$$

23.4.1 Modified Newton-Raphson's technique

In practical nonlinear analysis, the external forces are introduced in stages; Newton-Raphson's technique is employed to reduce the out-of-balance forces $\{g\}$ to tolerably small values before introducing a new stage. The tangent stiffness matrix $[S_t]$ is determined by considering the geometry and forces in the members at the start of a loading stage; the same matrix $[S_t]$ can be used in the iteration cycles, in order to save computing a new stiffness matrix in each cycle.

For application of Eq. 23.17, $[S_t]$ must be nonsingular. The matrix $[S_t]$ can become singular when instability is reached, for example, because of buckling of the system.

Figure 23.3 can also be used to explain the difference between Newton-Raphson's technique and the modified Newton-Raphson's technique. Point E on the curve represents the value $D = 2.19$ (length unit) corresponding to $F = 90$ (force unit) on the structure in Figure 23.2a. The values of D obtained in three iteration cycles by Newton-Raphson's technique in Section 23.4 are: 1.52, 2.09, 2.18, and 2.19. The line AB (Figure 23.3) with slope $S_t^{(0)} = 59.16$ intersects the line $F = 90$ at $D = 1.52$; the line CG with slope $(S_t)_{\text{at } D=1.52} = 34.23$ intersects the line $F = 90$ at

$D = 2.09$; the second and third iterations cannot be represented in Figure 23.3 because $D = 2.09$ is very close to the exact answer.

If the modified Newton-Raphson's technique is used, line CG in the first cycle will be replaced by CH, whose slope is 59.16, and the improved value of D at the end of the first cycle will be $[1.52 - (59.16)^{-1}(-19.54)] = 1.85$. More cycles will be required to reach the correct answer. We can verify the following answers for D, determined in seven cycles: 1.52, 1.85, 2.00, 2.08, 2.13, 2.15, 2.17, 2.18.

23.5 Newton-Raphson's technique applied to trusses

The analysis discussed below applies to plane and space trusses and cable nets. Cable nets can be treated as trusses, provided that the cables are pretensioned so that the members remain in tension after the nodal displacements. As usual, the external forces must be applied only at the nodes. Thus, the self-weight of a truss member or of a cable must be represented in the analysis by concentrated forces at the nodes. With this assumption, a cable is idealized as composed of straight segments between the nodes. The tangent stiffness of a cable segment is the same as that of a truss member with the same tensile force, cross-sectional area, and length, but because a cable segment cannot carry a compressive force, its tangent stiffness is null whenever, in the analysis, the force in the segment becomes compressive.

Consider a plane or a space truss with m members and n degrees of freedom, representing nodal displacements in directions of global axes (x, y) or (x, y, z); n is two or three times the number of nodes in a plane truss or a space truss respectively. It is required to find the nodal displacements $\{D\}$ and the change in member forces $\{\Delta N\}$ due to external applied loads and temperature variations. The geometric nonlinearity is not to be ignored.

Assume that in the initial state the nodal displacements $\{D\}_{n\times 1} = \{0\}$, the member lengths $= \{l_{in}\}_{m\times 1}$ and the forces in the members $= \{N_{in}\}_{m\times 1}$; the initial member forces may be caused, for example, by prestressing or by initial nodal forces $\{F_{in}\}$. The analysis discussed below is not concerned with the displacements occurring during the initial prestressing or nodal forces to produce the forces $\{N_{in}\}$. Unlike linear analysis, the initial member forces are required in the input data because the tangent stiffness of individual members depends upon the geometry and material properties as well as on the magnitude of the axial forces (see Section 23.6).

As in linear analysis (Section 4.6), the forces $\{F\}$ necessary to prevent the nodal displacements are determined. For the consideration of geometric nonlinearity, the forces at the nodes must be in equilibrium in their displaced position. This condition is expressed by

$$-[G]^T\{N\} = -\{F\} + \{F_{in}\} \tag{23.19}$$

$[G]_{m\times n}$ is a geometry matrix composed of one row for each member. The kth row contains the components, in the directions of the global axes of the two equal and opposite forces exerted by the member, on the two nodes i and j at its ends, when $\Delta N_k = 1$. Thus, the kth row of $[G]$ is

$$\begin{matrix} & i & & j & \\ [\cdots & [t]_k & \cdots & [-t]_k & \cdots] \end{matrix} \tag{23.20}$$

This row is composed of submatrices whose number equals the number of nodes; all submatrices except the ith and the jth are null. The submatrix $[t_k]$ is the transformation matrix given by Eqs. 21.14 and 21.15 and repeated here:

$$[t]_k = [\lambda_{x^*x}\ \lambda_{x^*y}]_k \text{(plane truss member } k) \tag{23.21}$$

and

$$[t]_k = [\lambda_{x^*x}, \lambda_{x^*y}\, \lambda_{x^*z}]_k \text{ (space truss member } k) \tag{23.22}$$

where λ_{x^*x}, λ_{x^*y}, and λ_{x^*z} are cosines of the angles between the global axes x, y, and z and the vector x^* joining node i to node j in their displaced positions (Figure 21.2). Thus, $[G]$ depends upon the unknown displacements $\{D\}$.

Assuming that the material is linearly elastic, the force in any member can be expressed as (positive when tensile)

$$N = N_{\text{in}} + \Delta N \quad \Delta N = N_r + \frac{Ea}{l_{\text{in}}}(l - l_{\text{in}}) \tag{23.23}$$

where E is the modulus of elasticity, a is the cross-sectional area, l_{in} and l are the member lengths before and after the displacements of the nodes, and N_r is the force in the member due to temperature variation with the nodal displacements r artificially restrained.

No approximation needs to be involved in calculating the change in length of members; Eqs. 21.3 or 21.6 can be applied to give l_{in} and l, using the x, y, and z coordinates of the nodes in their initial and displaced positions respectively. Thus, $\{N\}$ generated by Eq. 23.23 is dependent upon the unknown displacements $\{D\}$.

The iterative Newton-Raphson's technique can be used to determine $\{D\}$ to satisfy Eq. 23.19. Each iteration cycle involves the calculations specified below.

23.5.1 Calculations in one iteration cycle

The cycle starts with trial displacements $\{D^{(0)}\}$ and the corresponding out-of-balance forces $\{g^{(0)}\}$. The cycle terminates with more accurate displacements $\{D^{(1)}\}$ and smaller out-of-balance forces $\{g^{(1)}\}$. A cycle is completed in four steps:

Step 1 Generate the structure stiffness matrix $[S_t^{(0)}]$, expressed as the sum of the elastic stiffness matrix $[S_e^{(0)}]$ and the geometric stiffness matrix $[S_g^{(0)}]$. Both matrices are dependent upon the displacements $\{D^{(0)}\}$; the latter matrix also depends on member forces $\{N^{(0)}\}$. The superscript (0) refers to values known at the start of the current cycle. The geometric stiffness matrices of individual members of plane and space trusses are derived in Section 23.6. Assemblage of the stiffness matrices of members to obtain the stiffness matrix of the structure is discussed in Section 21.9.

Step 2 Determine the displacement increments $\{\Delta D\}$ by solving

$$[S_t^{(0)}]\{\Delta D\} = \{g^{(0)}\} \tag{23.24}$$

Step 3 Calculate the new, more accurate displacements:

$$\{D^{(1)}\} = \{D^{(0)}\} + \{\Delta D\} \tag{23.25}$$

Using the new displacements $\{D^{(1)}\}$ and Eq. 23.23, generate new member forces $\{N^{(1)}\}$. For this purpose, the (x, y) or (x, y, z) coordinates of the nodes in their new displaced positions must be calculated.

Step 4 Compute the new out-of-balance forces:

$$\{g^{(1)}\} = -\{F\} + [G^{(1)}]^T\{N^{(1)}\} + \{F_{\text{in}}\} \tag{23.26}$$

Here, $[G^{(1)}]$ and $\{N^{(1)}\}$ are to be generated by Eqs. 23.20 and 23.23 respectively, based on the new position of the nodes (with displacements $D^{(1)}$). This terminates the iteration cycle.

If the out-of-balance forces calculated at the end of the cycle are sufficiently small, the analysis is complete. If not, a new cycle is started with $\{D^{(1)}\}$ and $\{g^{(1)}\}$ equal to the improved values determined at the end of the preceding cycle.

23.5.2 *Convergence criteria*

The iteration cycles discussed above may be terminated when the following criterion is satisfied:

$$(\{g\}^T\{g\})^{1/2} \leq \beta(\{F\}^T\{F\})^{1/2} \tag{23.27}$$

where β is tolerance value, say, 0.01 to 0.001. This criterion ensures that the out-of-balance forces are small compared to the forces $\{F\}$.

When the analysis is for the effect of prescribed displacements, Eq. 23.27 cannot be used because $\{F\}$ can be equal to $\{0\}$, while the nonzero forces are only at the coordinates where the displacements are prescribed (including the supports). In such a case, the iteration cycles may be terminated when

$$(\{g\}^T\{g\})^{1/2} \leq \beta(\{R\}^T\{R\})^{1/2} \tag{23.28}$$

where $\{R\}$ is vector of the forces at the coordinates for which the displacements are prescribed, including the support reactions.

As mentioned in Section 23.4.1, in practical use of nonlinear analysis, the load is introduced in stages, with iterations and convergence achieved in each stage. Slow convergence or its lack indicates instability, which can be monitored by looking for a negative or zero value on the diagonal element of the tangent stiffness matrix $[S_t]$ during the Gauss elimination process to solve Eq. 23.24. Thus, by introducing the load in stages, the analysis can give a range of the load level in which buckling occurs.

The Newton-Raphson rapid convergence occurs when the trial values are near the correct answer. This is why convergence occurs more quickly when the load is applied in increments; in some problems, convergence may fail when the full load is applied in one stage.

As mentioned above, each iteration cycle is started with trial displacements $\{D^{(0)}\}$, which are taken as displacements determined in the preceding iteration cycle. In the first cycle of the first load stage, the starting displacements may simply be $\{D^{(0)}\} = \{0\}$.

23.6 Tangent stiffness matrix of a member of plane or space truss

The tangent stiffness matrix required in the Newton-Raphson iteration is an assemblage of the tangent stiffness matrices of individual members. We derive below the tangent stiffness matrix $[S_t]_m$ of a member of a space truss; deletion of appropriate rows and columns from this matrix results in the tangent stiffness matrix for a plane truss member.

Figure 23.4a represents a member of a space truss and a system of coordinates in directions of global axes x, y, and z. It is required to determine the tangent stiffness matrix relating small increment of forces $\{\Delta F\}$ to the corresponding displacements $\{\Delta D\}$:

$$[S_t]_m\{\Delta D\} = \{\Delta F\} \tag{23.29}$$

Before application of $\{\Delta F\}$, the member is assumed to have an axial force N, positive when tensile. We derive first the tangent stiffness matrix $[S_t]$ for the member AB with end B supported as shown in Figure 23.4b.

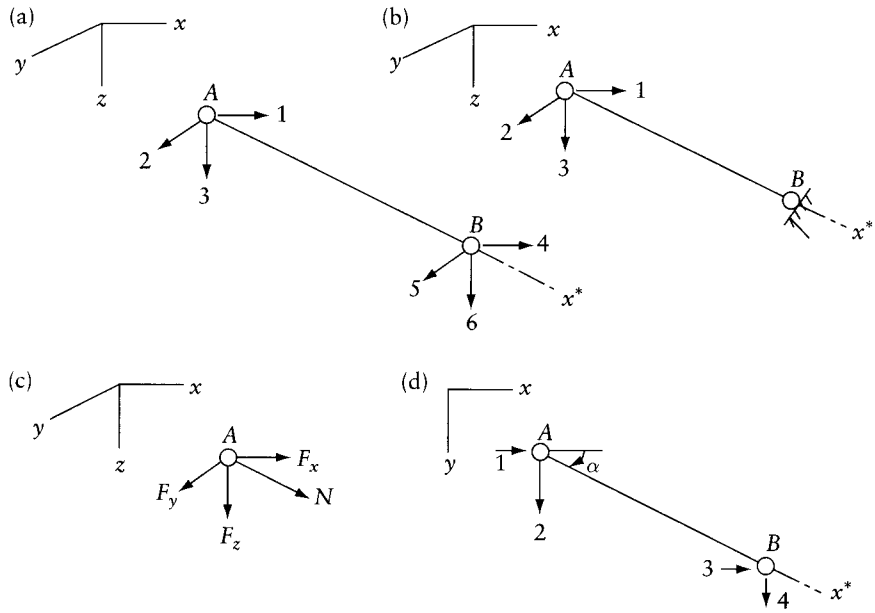

Figure 23.4 Derivation of the geometric stiffness matrices for a member of a plane or space truss with an axial force N. (a) Coordinate system for a space truss member. (b) Same as (a) but with end B supported. (c) Free-body diagram of node A. (d) Coordinate system for a plane truss member.

The following equilibrium equation applies to node A treated as a free body (Figure 23.4c):

$$[t]^T N = -\{F\} \tag{23.30}$$

where $[t]$ is the transformation matrix (Eq. 21.15):

$$[t] = [\lambda_{x^*x}\ \lambda_{x^*y}\ \lambda_{x^*z}] \tag{23.31}$$

The terms λ are cosines of the angles between the member local axis x^* in its position before application of $\{\Delta F^*\}$ and the global axes x, y, and z.

By definition, the tangent stiffness matrix can be expressed as

$$[\bar{S}_t] = \left[\frac{\partial}{\partial\{D\}}\{F\}^T\right]^T \tag{23.32}$$

This equation may be rewritten in the form

$$[\bar{S}_t] = \begin{bmatrix} \partial F_1/\partial D_1 & \partial F_1/\partial D_2 & \partial F_1/\partial D_3 \\ \partial F_2/\partial D_1 & \partial F_2/\partial D_2 & \partial F_2/\partial D_3 \\ \partial F_3/\partial D_1 & \partial F_3/\partial D_2 & \partial F_3/\partial D_3 \end{bmatrix} \tag{23.33}$$

Substitution of Eq. 23.30 into Eq. 23.32 and performing the differentiation gives $[\bar{S}_t] = [\bar{S}_e]$ when $[t]$ is considered constant. However, when $[t]$ is considered variable, the result will be: $[\bar{S}_t] = [\bar{S}_e] + [\bar{S}_g]$. In linear analysis we assume $[t]$ = constant and employ the elastic stiffness

$$[\overline{S_e}] = \left[-\frac{\partial N}{\partial \{D\}} [t] \right]^T \tag{23.34}$$

where $\partial N/\partial\{D\} = \{\partial N/\partial D_1, \partial N/\partial D_2, \partial N/\partial D_3\}$. For elastic material, we have for a truss member

$$\frac{\partial N}{\partial \{D\}} = -\frac{Ea}{l}[t]^T \tag{23.35}$$

Substitution of Eq. 23.35 into Eq. 23.34 gives the elastic stiffness matrix, used in conventional linear analysis (see Eq. 21.25):

$$[\overline{S_e}] = \frac{Ea}{l}[t]^T[t] \tag{23.36}$$

Considering both N and $[t]$ as variables and substituting Eq. 23.30 in Eq. 23.32 gives the tangent stiffness matrix

$$[\overline{S_t}] = \left[-\frac{\partial N}{\partial \{D\}} [t] - N \frac{\partial [t]}{\partial \{D\}} \right]^T \tag{23.37}$$

The first term on the right-hand side of this equation is $[\overline{S_e}]$. Recognizing that $[\overline{S_t}] = [\overline{S_e}] + [\overline{S_g}]$(see Eq. 23.2), we conclude that the geometric stiffness matrix is

$$[\overline{S_g}] = \left[-N \frac{\partial [t]}{\partial \{D\}} \right]^T \tag{23.38}$$

Substitution of Eq. 23.31 in this equation gives

$$[\overline{S_g}] = -N \begin{bmatrix} \partial \lambda_{x^*x}/\partial D_1 & \partial \lambda_{x^*x}/\partial D_2 & \partial \lambda_{x^*x}/\partial D_3 \\ \partial \lambda_{x^*y}/\partial D_1 & \partial \lambda_{x^*y}/\partial D_2 & \partial \lambda_{x^*y}/\partial D_3 \\ \partial \lambda_{x^*z}/\partial D_1 & \partial \lambda_{x^*z}/\partial D_2 & \partial \lambda_{x^*z}/\partial D_3 \end{bmatrix} \tag{23.39}$$

The following geometry relations apply:

$$\lambda_{x^*x} = \frac{l_x}{l} \quad \lambda_{x^*y} = \frac{l_y}{l} \quad \lambda_{x^*z} = \frac{l_z}{l} \quad l = (l_x^2 + l_y^2 + l_z^2)^{1/2} \tag{23.40}$$

$$\frac{\partial}{\partial D_1} = -\frac{\partial}{\partial l_x} \quad \frac{\partial}{\partial D_2} = -\frac{\partial}{\partial l_y} \quad \frac{\partial}{\partial D_3} = -\frac{\partial}{\partial l_z} \tag{23.41}$$

where l_x, l_y, and l_z are the x, y, and z components of a vector of magnitude l directed from node A to node B (Figure 23.4b).

Substitution of Eqs. 23.40 and 23.41 into Eq. 23.39 gives the geometric stiffness matrix for the space truss member in Figure 23.4b:

$$[\overline{S_g}] = \frac{N}{l} \begin{bmatrix} 1 - \lambda_{x^*x}^2 & & \text{symmetrical} \\ -\lambda_{x^*x}\lambda_{z^*y} & 1 - \lambda_{x^*y}^2 & \\ -\lambda_{x^*x}\lambda_{x^*y} & -\lambda_{x^*y}\lambda_{x^*z} & 1 - \lambda_{x^*z}^2 \end{bmatrix} \tag{23.42}$$

Considering the fact that, for equilibrium, the forces at ends A and B are equal and opposite, the matrices $[\bar{S}_e]$ and $[\bar{S}_g]$ for the supported member in Figure 23.4b can be used to generate the stiffness matrices for the space and plane truss members in Figures 23.4a and d. Simple deletion of the rows and columns associated with the coordinates in the z direction reduces the stiffness matrices for a space member to those of a member of a plane truss situated in the x–y plane. For easy reference, the member stiffness matrices required for the nonlinear analysis of space and plane trusses are listed below.

For a member of a space or a plane truss, the tangent stiffness matrix is (Figure 23.4a or d)

$$[S_t]_m = [S_e]_m + [S_g]_m \tag{23.43}$$

$$[S_e]_m = \begin{bmatrix} [\bar{S}_e] & -[\bar{S}_e] \\ -[\bar{S}_e] & [\bar{S}_e] \end{bmatrix}; \quad [\bar{S}_g]_m = \begin{bmatrix} [\bar{S}_g] & -[\bar{S}_g] \\ -[\bar{S}_g] & [\bar{S}_g] \end{bmatrix} \tag{23.44}$$

For a space truss member, the elastic and geometric stiffness submatrices are

$$[\bar{S}_e] = \frac{Ea}{l_{\text{in}}} \begin{bmatrix} \lambda_{x^*x}^2 & \text{symmetrical} & \\ \lambda_{x^*x}\lambda_{x^*y} & \lambda_{x^*y}^2 & \\ \lambda_{x^*x}\lambda_{x^*z} & \lambda_{x^*y}\lambda_{x^*z} & \lambda_{x^*z}^2 \end{bmatrix} \quad \text{for } [\bar{S}_g] \text{ see Eq. 23.42} \tag{23.45}$$

where l_{in} is the initial length.

For a plane truss member, the elastic and geometric stiffness matrices are

$$[\bar{S}_e] = \frac{Ea}{l_{\text{in}}} \begin{bmatrix} c^2 & cs \\ cs & s^2 \end{bmatrix}; \quad [\bar{S}_g] = \frac{N}{l} \begin{bmatrix} s^2 & -cs \\ -cs & c^2 \end{bmatrix} \tag{23.46}$$

where $c = \cos\alpha$ and $s = \sin\alpha$; angle α and its positive sign convention are defined in Figure 23.4d.

Example 23.2: Prestressed cable carrying central concentrated load: iterative analysis

Perform two Newton-Raphson iteration cycles to determine, for the prestressed cable in Figure 23.1a, the deflection D at mid-point and the tension N in the cable when the transverse force $Q = 16P$. Use the elastic and the geometric stiffness matrices in Eq. 23.46. Take $E = 200 \times 10^6 P/b^2$; $a = 100 \times 10^{-6} b^2$; initial tension=$100P$; where P and b are, respectively, force and length units.

Because of symmetry, the system has one degree of freedom shown in Figure 23.1a; use of Eq. 23.46 gives the following stiffness for the structure:

$$S_e = \frac{4Ea}{b} \sin^2\theta \quad S_g = 2\left(\frac{N}{l}\right)_{AB'} \cos^2\theta$$

For this structure, the out-of-balance force is (Eq. 23.26)

$$g = Q - 2N_{AB'} \sin\theta$$

The angle θ is defined in Figure 23.1a.

We start the cycles with $D = 0$ and $g = Q$. The four calculation steps specified in Section 23.5.1 are performed:

Iteration cycle 1

1. $D^{(0)} = 0$; $g^{(0)} = 16P$; $N_{AB'}^{(0)} = 100P$; $\theta^{(0)} = 0$; $\sin\theta^{(0)} = 0$; $\cos\theta^{(0)} = 1$; $l_{AB'} = 0.5b$; $S_e = 0$; $S_g = 400P/b$; $S_t = 0 + (400P/b) = 400P/b$.
2. $\Delta D = (400/b)^{-1}(16) = 0.04b$.
3. $D^{(1)} = 0 + 0.04b = 0.04b$.
4. Equation 23.23 gives $N_{AB'} = 163.9P$; $\sin\theta^{(1)} = 0.04[(0.04)^2 + (0.5)^2]^{-1/2} = 79.7 \times 10^{-3}$; $g^{(1)} = -10.140P$.

Iteration cycle 2

1. $D^{(0)} = 0.04b$; $g^{(0)} = -10.140P$; $N_{AB'}^{(0)} = 163.9P$; $\sin\theta^{(0)} = 79.7 \times 10^{-3}$; $\cos\theta^{(0)} = 0.9968$; $l_{AB'} = 0.5016b$; $S_e = 508.7P/b$; $S_g = 649.4P/b$; $S_t = 1158.1P/b$.
2. $\Delta D = (1158.1/b)^{-1}(-10.140) = -8.76 \times 10^{-3}b$.
3. $D^{(1)} = (0.04 - 8.76 \times 10^{-3})b = 31.24 \times 10^{-3}b$.
4. Equation 23.23 gives $N_{AB'} = 139.0P$; $\sin\theta^{(0)} = 62.3 \times 10^{-3}$; $g^{(1)} = -1.330P$.

A third iteration gives: $D = 29.7 \times 10^{-3}b$; $N_{AB'} = 135.3P$. The exact answers satisfying Eqs. 23.3 and 23.4 are: $D = 29.6 \times 10^{-3}b$; $N = 135.2P$.

23.7 Nonlinear buckling

Consider the plane truss in Figure 23.2a and assume that its individual members have sufficient flexural rigidities such that buckling of individual members is precluded. In the analysis in Section 23.4, we saw that the system becomes unstable and the structure snaps through when point C on the $F - D$ graph in Figure 23.2b is reached. This corresponds to $D = 4.23$ (length unit) and $F = 114$ (force unit). Thus, it can be concluded that the critical buckling value of F for this system is $F_{cr} = 114$ (force unit).

The tangent stiffness corresponding to the single coordinate shown at B in Figure 23.2a is (Eqs. 23.6 and 23.46)

$$S_t = S_e + S_g \tag{a}$$

or

$$S_t = \frac{2Ea}{l}s^2 + \left[-\frac{F}{sl}\right]c^2 \tag{b}$$

where $s = \sin\theta$ and $c = \cos\theta$, with θ being the angle between $B'C$ (position of BC in the displaced position) and the horizontal. The buckling load F_{cr} is the value of F that makes S_t = zero; thus, we can write

$$F = 2Ea\frac{s^3}{c^2} \tag{c}$$

We can verify that this equation gives $F_{cr} = 114$ (force unit) for $\theta = \tan^{-1}[(h - D)/b]$, with $h = 10, b = 300$, and $D = 4.23$ (length unit).

The value of F_{cr} based on the displaced positions of the nodes is referred to as the *nonlinear buckling load*. For shallow plane or space trusses the risk of buckling can be examined by nonlinear analysis which considers equilibrium of the nodes in their displaced positions.

If we use Eq. (c) to calculate F_{cr} based on the initial geometry (with $\theta_{in} = \tan^{-1}(h/b)$), we would obtain the erroneous result $F_{cr} = 593$ (force unit), which is 5.2 times larger than the correct answer. Calculation of the critical buckling load based on the initial geometry gives what is

referred to as the *linear buckling load*. For the single-degree-of-freedom system considered, the buckling is calculated by setting S_t equal to zero and solving for the value of F. For a multi-degree-of-freedom system, the determinant $|S_t|$ is set equal to zero and the solution gives several values of F of which the lowest is the critical value.

It can be shown[3] that the nonlinear buckling load for the plane truss in Figure 23.2a is

$$F_{cr} = 2Ea(1 - c_{in}^{2/3})^{3/2} \qquad (d)$$

where $c_{in} = \cos\theta_{in}$, with θ_{in} being the angle between BC (the initial position of the member) and the horizontal.

23.8 Tangent stiffness matrix of a member of plane frame

In this section, we derive the tangent stiffness matrix $[S_t]_m$ for a plane frame member AB (Figure 23.5a) with respect to coordinates at the two ends in the directions of global axes.

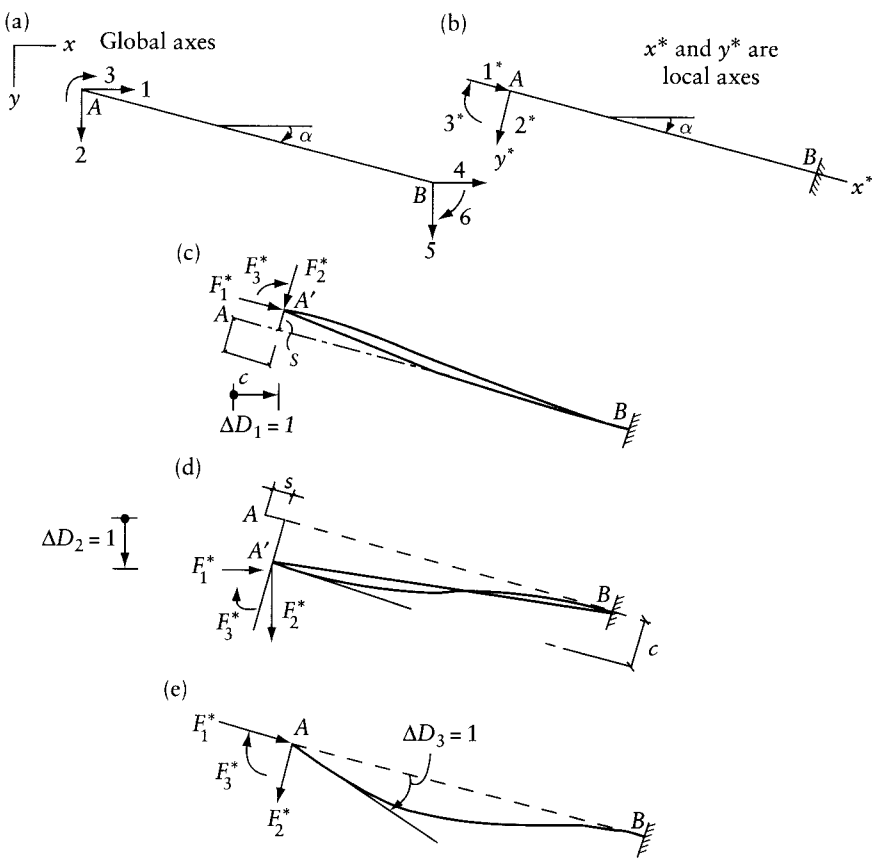

Figure 23.5 Derivation of tangent stiffness matrix for a plane frame member. (a) Coordinate system. (b) Local coordinates at end A with end B fixed. (c), (d), and (e) Introduction of unit displacements in direction of global axes at end A.

3 See the first reference in footnote 1 of this chapter.

The tangent stiffness matrix relates small increments of forces $\{\Delta F\}$ to the corresponding displacements $\{\Delta D\}$:

$$[S_t]_m\{\Delta D\} = \{\Delta F\} \tag{23.47}$$

The member end-forces at A existing before applications of $\{\Delta F\}$ are $\{F^*\}$ in the direction of local axes (Figure 23.5b). We derive first the tangent stiffness matrix $[\bar{S}_t]$ for the member with end B encastré, as shown in Figure 23.5b. The forces and displacements at coordinates 1, 2, 3 (Figure 23.5a) are related to the forces and displacements at coordinates 1*, 2*, 3* (Figure 23.5b) by equations

$$\{D^*\} = [t]\{D\} \qquad \{F\} = [t]^T\{F^*\} \tag{23.48}$$

where $[t]$ is transformation matrix (Eq. 21.16):

$$[t] = \begin{bmatrix} c & s & 0 \\ -s & c & 0 \\ 0 & 0 & 1 \end{bmatrix} \tag{23.49}$$

with $c = \cos\ \alpha$ and $s = \sin\ \alpha$; where α is the angle between local axis x^*, before application of $\{\Delta F\}$, and the global x axis.

The tangent stiffness matrix can be derived by differentiation, as was done for truss members in Section 23.6. However, an alternative approach is used here to derive the tangent stiffness matrix $[\bar{S}_t]$ for the member in Figure 23.5b (with end B encastré) with respect to three coordinates in the global directions (not shown in Figure 23.5b for clarity, but shown at end A in Figure 23.5a). Figures 23.5c, d, and e show the deformed shapes of the member with small displacements $\Delta D_1 = 1, \Delta D_2 = 1$, and $\Delta D_3 = 1$ respectively. The end-forces $\{F^*\}$ existing before the introduction of the displacements, are shown in the figures, but the forces $\{\Delta F\}$ – in the global directions – necessary for equilibrium in the three deformed configurations are not shown. By definition, the tangent stiffness matrix Eq. 23.33 may be written in the form

$$[\bar{S}_t] = \mathrm{Lim}_{(\Delta D)\to\{0\}}\left[(\Delta D_1)^{-1}\{\Delta F\}_1 \quad (\Delta D_2)^{-1}\{\Delta F\}_2 \quad (\Delta D_3)^{-1}\{\Delta F\}_3\right] \tag{23.50}$$

where $\{\Delta F\}_i$ represents force increments corresponding to displacement change ΔD_i at coordinate i while the displacement increments are zero at other coordinates.

To maintain equilibrium at end A, when $\Delta D_1 = 1$, the forces $\{\Delta F^*\}$ – in the x^* and y^* directions – must be added to the forces existing before displacement (Figure 23.5c). The force increments $\{\Delta F^*\}$ are

$$\{\Delta F^*\}_{\Delta D_1=1} = \begin{Bmatrix} c(Ea/l_{\text{in}}) \\ -2s(S+t)/l^2 \\ -s(S+t)/l \end{Bmatrix} + \frac{F_1^*}{l}\begin{Bmatrix} 0 \\ s \\ 0 \end{Bmatrix} + \frac{F_2^*}{l}\begin{Bmatrix} -s \\ c \\ 0 \end{Bmatrix} \tag{23.51}$$

where E = modulus of elasticity, a = cross-sectional area, l_{in} is the initial member length before any deformation; S and t are the end-moments at A and B respectively, when a unit rotation is introduced at A while B is encastré (Figure 23.5e). S and t are given by Eqs. 13.16 and 13.17 when the axial force is compressive, and by Eqs. 13.20 and 13.21 when the axial force is tensile, l is member length before introducing ΔD_1. In verifying Eqs. 23.51, note that as ΔD_1 tends to zero, the cosine of the angle between the chord $A'B$ and the original member direction tends to 1.0. Also, note that F_1^* is in the direction of the chord before and after displacement. Similarly,

F_2^* is perpendicular to the chord before and after displacement. Similarly, equilibrium equations can be written for end A of the deformed beams in Figures 23.5d and e and the results combined:

$$[\Delta F^*] = \left[\{\Delta F^*\}_{\Delta D_1=1} \quad \{\Delta F^*\}_{\Delta D_2=1} \quad \{\Delta F^*\}_{\Delta D_3=1}\right] \tag{23.52}$$

$$[\Delta F^*] = \begin{bmatrix} c(Ea/l_{\text{in}}) & s(Ea/l_{\text{in}}) & 0 \\ -2s(S+t)/l^2 & 2c(S+t)/l^2 & (S+t)/l \\ -s(S+t)/l & c(S+t)/l & S \end{bmatrix} + \frac{F_1^*}{l}\begin{bmatrix} 0 & 0 & 0 \\ s & -c & 0 \\ 0 & 0 & 0 \end{bmatrix} + \frac{F_2^*}{l}\begin{bmatrix} -s & c & 0 \\ c & s & 0 \\ 0 & 0 & 0 \end{bmatrix} \tag{23.53}$$

The forces $[\Delta F^*]$ in local directions can be transformed to the global directions by Eq. 23.48 to give the tangent stiffness matrix for the beam in Figure 24.5b, corresponding to coordinates at A, in global directions, shown in Figure 24.5a.

$$[\bar{S}_t] = [t]^T [\Delta F^*] \tag{23.54}$$

Combining Eqs. 23.50 to 23.54 gives

$$[\bar{S}_t] = [\bar{S}_e] + [\bar{S}_g] \tag{23.55}$$

where $[\bar{S}_e]$ is the elastic stiffness matrix

$$[\bar{S}_e] = \begin{bmatrix} c^2Ea/l_{\text{in}} + 2s^2(S+t)/l^2 & \text{symmetrical} & \\ sc[Ea/l_{\text{in}} - 2(S+t)/l^2] & s^2Ea/l_{\text{in}} + 2c^2(S+t)/l^2 & \\ -s(S+t)/l & c(S+t)/l & S \end{bmatrix} \tag{23.56}$$

where l_{in} is the initial length of the member and $[\bar{S}_g]$ is the geometric stiffness matrix

$$[\bar{S}_g] = \frac{F_1^*}{l}\begin{bmatrix} -s^2 & sc & 0 \\ sc & -c^2 & 0 \\ 0 & 0 & 0 \end{bmatrix} + \frac{F_2^*}{l}\begin{bmatrix} -2sc & c^2-s^2 & 0 \\ c^2-s^2 & 2sc & 0 \\ 0 & 0 & 0 \end{bmatrix} \tag{23.57}$$

Considering the fact that the forces in each column of the stiffness matrices are in equilibrium, the tangent stiffness for a plane frame member (Figure 23.5a) is generated:

$$[S_t]_m = [S_e]_m + [S_g]_m \tag{23.58}$$

where $[S_e]_m$ is the elastic stiffness matrix

$$[S_e]_m = \begin{bmatrix} \frac{c^2Ea}{l_{\text{in}}} + \frac{2s^2}{l^2}(S+t) & & \text{symmetrical} & & & \\ cs\left[\frac{Ea}{l_{\text{in}}} - \frac{2}{l^2}(S+t)\right] & \frac{s^2Ea}{l_{\text{in}}} + \frac{2c^2}{l^2}(S+t) & & & & \\ -\frac{s}{l}(S+t) & \frac{c}{l}(S+t) & S & & & \\ -S_{11} & -S_{12} & -S_{13} & S_{11} & & \\ -S_{21} & -S_{22} & -S_{23} & -S_{24} & S_{22} & \\ -\frac{s}{l}(S+t) & \frac{c}{l}(S+t) & t & \frac{s}{l}(S+t) & -\frac{c}{l}(S+t) & S \end{bmatrix} \tag{23.59}$$

The parameters S and t are dependent upon the value of the axial force F_1^*. When $F_1^* = 0$, $S = 4EI/l$ and $t = 2EI/l$, Eq. 23.59 becomes the same as Eq. 21.27; here, I is the second moment of cross-sectional area.

The geometric stiffness matrix corresponding to the coordinates in Figure 23.5a is

$$[S_g]_m = \begin{bmatrix} [\bar{S}_g] & -[\bar{S}_g] \\ -[\bar{S}_g] & [\bar{S}_g] \end{bmatrix} \tag{23.60}$$

where $[\bar{S}_g]$ is given by Eq. 23.57.

The tangent stiffness derived above differs from the stiffness matrices generated in Chapter 13 only by the presence of the last term containing F_2^* in Eq. 23.57. Thus, if the angle $\alpha = 0$ ($s = 0$; $c = 1$) and the last term in Eq. 23.57 is ignored, $[S_t]$ generated by the equations derived in this section will be the same as that given by Eq. 13.19 when the axial force is compressive, or by Eq. 13.23 when the axial force is tensile. Alternatively, if the stiffness matrix in Eq. 13.19 or 13.23 is transformed to correspond to global coordinates (by Eq. 21.19), the resulting matrix will be the same as the matrix obtained by the equations derived in this section if the transverse force F_2^* is assumed equal to zero.

In derivation of $[S_t]_m$ (Eq. 23.58), the member local axis x^* is assumed to be the chord joining the member ends. However, in general, the member axis is curved due to earlier loading. The difference between the chord and the curved member axis can be reduced by a division of the member into segments. Unlike linear analysis, in nonlinear analysis of a frame, if, for example, a member is represented by two elements, by adding a node at its mid-length, different results (generally more accurate) will be obtained.

23.9 Application of Newton-Raphson's technique to plane frames

Consider a plane frame with m members and n degrees of freedom (n being three times the number of nodes) subjected to forces applied only at the nodes. The members may also be subjected to temperature changes. We discuss below the geometrically nonlinear analysis to determine the displacements $\{D\}_{n\times 1}$ and the corresponding changes in the member end-forces caused by the applied forces combined with the thermal effects. First, the displacements are artificially restrained by restraining nodal forces $\{F\}_{n\times 1}$; in this state, the temperaturee change produces member end-forces $\{F^*\}_r$. The asterisk refers to the directions of the local axes x^* and y^*.

At all stages of the analysis, the three forces at the second node of a member can be determined from the three forces at the first node by the equilibrium equation (Figure 23.6a):

$$\begin{Bmatrix} F_4^* \\ F_5^* \\ F_6^* \end{Bmatrix}_{\text{mem}} = [R]_{\text{mem}} \begin{Bmatrix} F_1^* \\ F_2^* \\ F_3^* \end{Bmatrix}_{\text{mem}} ; \quad [R]_{\text{mem}} = \begin{bmatrix} -1 & 0 & 0 \\ 0 & -1 & 0 \\ 0 & l & -1 \end{bmatrix}_{\text{mem}} \tag{23.61}$$

where l is the member length at the stage considered; the subscript "mem" refers to an individual member.

Define vector $\{F^*\}_{3m\times 1}$ containing the required member restraining forces at end 1 of all members. In addition to initial geometry of the structure, the elasticity modulus E, the cross-sectional area a, the second moment of area I, and $\{F_{\text{in}}^*\}_{3m\times 1}$ are included in the input data. $\{F_{\text{in}}^*\}$ contains initial member end-forces at the first node of all members. Assume that in the initial state the displacements $\{D\}_{n\times 1} = \{0\}$, the member lengths$= \{l_{\text{in}}\}_{m\times 1}$. The initial member forces may be caused, for example, by prestressing or by initial nodal forces$= \{F_{\text{in}}\}_{n\times 1}$. The analysis discussed below is to determine the displacement changes $\{D\}_{n\times 1}$. It is also required to determine the final member end-forces.

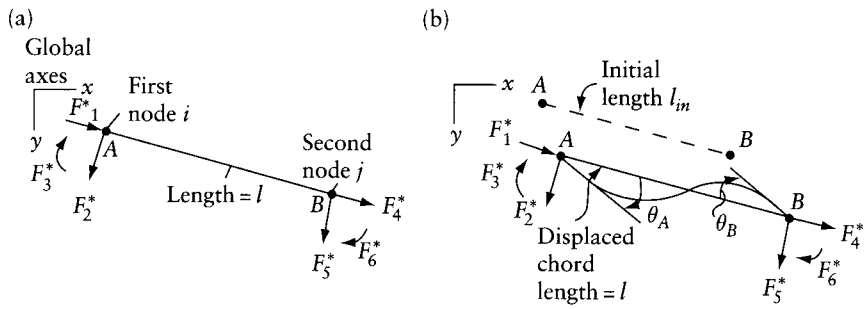

Figure 23.6 Member end-forces. (a) Definition of symbols and positive directions of $\{F^*\}$. (b) A typical member in initial and displaced positions.

The same procedure of analysis for trusses as discussed in Sections 23.5 and 23.5.1 can be used, with the following differences. Equation 23.19 for equilibrium of the nodes is to be replaced by

$$[G]^T\{F^*_{\text{final}}\}_{3m\times 1} = -\{F\}_{n\times 1} + \{F_{\text{in}}\}_{n\times 1} \tag{23.62}$$

where $\{F^*\}$ represents the changes in end-forces at the first node of all members from the initial stage to the final values, $\{F^*_{\text{final}}\}$. Note that $\{F^*\} \neq \{F^*_{\text{final}}\} - \{F^*_{\text{in}}\}$ because not all the initial and the final member end-forces are in the same directions.

The geometry matrix $[G]_{3m\times n}$ can be divided into m submatrices, one for each member. The submatrix for the kth member is

$$\begin{bmatrix} & i & & j & \\ \dots & [\bar{t}]_k & \dots & [\bar{t}]_k & \dots \end{bmatrix} \tag{23.63}$$

In this equation the $3 \times n$ submatrix is partitioned into submatrices, each 3×3, all of which are null with the exception of the ith and the jth, where i and j are, respectively, the first and second node of the kth member. The submatrix $[t]_k$ is the same as the transformation matrix given by Eq. 23.49. The submatrix $[\bar{t}]_k$ is given by

$$[\bar{t}]_k = [t]_k[R]^T = \begin{bmatrix} -c & -s & sl \\ s & -c & cl \\ 0 & 0 & -1 \end{bmatrix} \tag{23.64}$$

where $c = \cos\alpha$ and $s = \sin\alpha$, α being the angle between the global x axis and the local member axis x^* after deformation.

After r iteration cycles the axial forces at member ends become

$$F^{*(1)}_{1r} = F^{*(1)}_{1\text{in}} - (Ea/l_{\text{in}})(l^{(1)}_r - l_{\text{in}}); \quad F^{*(1)}_{4r} = -F^{*(1)}_{1r} \tag{23.65}$$

As before, the superscript (1) refers to the state at cycle end. The first subscript (e.g. 1 or 4) refers to the local coordinates (Figure 23.6a), the second subscript r refers to the cycle number. Approximate values of the end moments F^*_3 and F^*_6 can be determined by summation of the

increments occurring in the iteration cycles. Then, the values of F_3^* and F_6^* can be employed to determine the corresponding equilibrating forces F_2^* and F_5^*:

$$\left.\begin{aligned} F_{3r}^{*(1)} &= F_{3\text{in}}^* + \sum_{i=1}^{r}[S^{(0)}(\theta_A^{(1)} - \theta_A^{(0)}) + t^{(0)}(\theta_B^{(1)} - \theta_B^{(0)})]_i \\ F_{6r}^{*(1)} &= F_{6\text{in}}^* + \sum_{i=1}^{r}[S^{(0)}(\theta_B^{(1)} - \theta_B^{(0)}) + t^{(0)}(\theta_A^{(1)} - \theta_A^{(0)})]_i \\ F_{2r}^{*(1)} &= (F_{3r}^{*(1)} + F_{6r}^{*(1)})/l_r^{(1)} \\ F_{5r}^{*(1)} &= -F_{2r}^{*(1)} \end{aligned}\right\} \tag{23.66}$$

where θ_A and θ_B are the angles between the chord connecting ends A and B and the tangents of the deflected member at the same sections (Figure 23.6b). The subscript i refers to the iteration cycle. The magnitudes of the end-rotational stiffness $S_i^{(0)}$ and the carryover moment $t_i^{(0)}$ are dependent upon the value of the axial force at the start of the ith cycle ($= F_{4i}^{(0)}$).

The out-of-balance forces at the end of each cycle are determined by Eq. 23.67 (corresponding to Eq. 23.26 used for trusses):

$$\{g^{(1)}\} = -\{F\} - [G^{(1)}]^T\{F_{\text{final}}^{*(1)}\} + \{F_{\text{in}}\} \tag{23.67}$$

The end-forces $\{F_3^*$ and $F_6^*\}_r^{(1)}$ and the equilibrating forces $\{F_2^*$ and $F_5^*\}_r^{(1)}$ may be determined more accurately by using the value of the axial force ($F_{4r}^{*(1)}$) to calculate values of $S_r^{(1)}$ and $t_r^{(1)}$ employing these combined with the final end rotations to determine the member end moments:

$$\left.\begin{aligned} F_{3r}^{*(1)} &= F_{3\text{in}}^* + S_r^{(1)}(\theta_{Ar}^{(1)} - \theta_{A\text{in}}) + t_r^{(1)}(\theta_{Br}^{(1)} - \theta_{B\text{in}}) \\ F_{6r}^{*(1)} &= F_{6\text{in}}^* + S_r^{(1)}(\theta_{Br}^{(1)} - \theta_{B\text{in}}) + t_r^{(1)}(\theta_{Ar}^{(1)} - \theta_{A\text{in}}) \\ F_{2r}^{*(1)} &= (F_{3r}^{*(1)} + F_{6r}^{*(1)})/l_r^{(1)} \\ F_{5r}^{*(1)} &= -F_{2r}^{*(1)} \end{aligned}\right\} \tag{23.68}$$

However, employing Eqs. 23.68, successively, to replace Eqs. 23.66 may hamper convergence. This is so because the values of $S^{(0)}$ and $t^{(0)}$ employed in the generation of the stiffness matrix are not the same as $S^{(1)}$ and $t^{(1)}$ used in the calculation of the member end-forces and the corresponding out-of-balance forces.

In a computer program named NLPF (Nonlinear Analysis of Plane Frames), described briefly in Appendix L, Eqs. 23.66 are used during the iteration with $S = 4EI/l_{\text{in}}$ and $t = S/2$, where E is the modulus of elasticity and I is the second moment of cross-sectional area. This implies that the influence of axial force on member end-rotational stiffness and carryover moment is ignored. After convergence, the analysis gives approximate values of the axial forces, which are subsequently employed to determine more accurate values of S and t (Eqs. 13.16, 13.17, 13.20, and 13.21) and new member end-forces are calculated by Eqs. 23.65 and 23.68. Application of Eq. 23.67 commonly gives new out-of-balance forces, which are eliminated by a few refinement iteration cycles in which S and t values are unchanged. Usually the refinement cycles produce small changes in the values of axial forces which are too small to justify further analysis. However, if this is not the case, the refinement cycles are repeated using an updated set of axial forces.

Example 23.3: Frame with one degree of freedom

Perform two iteration cycles to determine the vertical downward displacement D at joint B of the toggle shown in Figure 23.7a due to a load $Q = 120$. What are the corresponding forces at the ends of member BC? Take $Ea = 8.40 \times 10^6$; $EI = 26.6 \times 10^6$. The data (with units newton and mm) represent a model in an experiment reported by Williams.[4]

We give below the equations which will be used in the iteration cycles. Because of symmetry, there is a single degree of freedom, representing the deflection D at B. The elastic and the geometric stiffnesses are (derived by Eqs. 23.59 and 23.60)

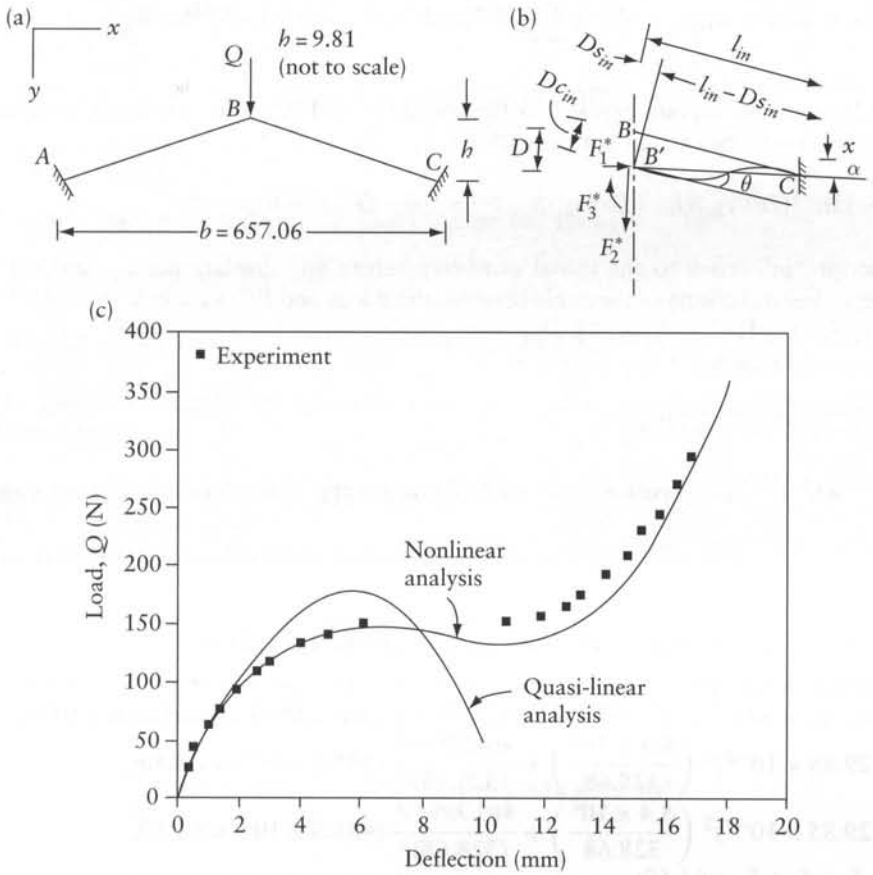

Figure 23.7 Plane frame of Example 23.3. (a) Initial shape. (b) Deformed shape of the right-hand half. (c) Comparison of analytical and experimental results.

4 Williams, F.W., "An Approach to the Nonlinear Behaviour of the Members of a Rigid-Jointed Plane Framework with Finite Deflections," *Quarterly Journal of Mechanics and Applied Mathematics*, XVII, Pt. 4, 1964, pp. 451-469. Alternative methods which account for the geometric nonlinearity are applied to analyze the same model in Salami, A.T. and Morley, C.T., "Finite Element Analysis of Geometric Nonlinearity in Plane Frameworks," *The Structural Engineer*, 70, (15), (1992), pp. 268–271.

$$S_e = 2(s^{(0)})^2(Ea/l_{in}) + [4(c^{(0)})^2/l^2](S^{(0)} + t^{(0)}) \quad (a)$$

$$S_g = -2(c^{(0)})^2(F_1^{*(0)}/l^{(0)}) + 4s^{(0)}c^{(0)}(F_2^{*(0)}/l^{(0)}) \quad (b)$$

where the superscript (0) refers to the geometry and member end-forces known at the start of the cycle; $s = \sin\alpha$, $c = \cos\alpha$, α is the angle between the x direction and the chord $B'C$, $\{F^*\}$ are forces at end B' (Figure 23.7b), S and t are the end-rotational stiffness and the carryover moment (the values of S and t are dependent upon the axial force (Eqs. 13.16 and 13.17)), l_{in} is the initial length of BC, and $l^{(0)}$ is the length of the chord $B'C$.

Each cycle starts with trial displacement $D^{(0)}$ and ends with a more accurate value $D^{(1)}$. In a typical rth iteration, the forces at end B of member BC are (Eqs. 23.65 and 23.66)

$$F_1^{*(1)} = -\frac{Ea}{l_{in}}(l^{(1)} - l_{in}); \quad F_3^{*(1)} = \sum_{i=1}^{r}[(S^{(0)} + t^{(0)})(\theta^{(1)} - \theta^{(0)})]_i; \quad F_2^{*(1)} = \frac{2F_3^{*(1)}}{l^{(1)}} \quad (c)$$

The term between the square brackets is the change in end-moment in a single iteration. The summation is to be carried out for cycles $1, 2, \ldots, r$.

$$\theta^{(1)} = \tan^{-1}[D^{(1)}c_{in}/(l_{in} - D^{(1)}s_{in})]; \quad l^{(1)} = [(h - D^{(1)})^2 + b^2/4]^{1/2} \quad (d)$$

The subscript "in" refers to the initial geometry before any displacement; s and c are, respectively, sine and cosine of the angle between the x axis and BC. $s_{in} = h(h^2 + b^2/4)^{-1/2}$; $c_{in} = 0.5b(h^2 + b^2/4)^{-1/2}$; $l_{in} = 328.68$

The out-of-balance force (Eq. 23.67) is

$$g = Q - 2(s^{(1)}F_1^{*(1)} + c^{(1)}F_2^{*(1)}) \quad (e)$$

where $s^{(1)}$ and $c^{(1)}$ are based on the updated geometry with the displacement equal to $D^{(1)}$.

Iteration cycle 1 $s^{(0)} = s_{in} = 29.85 \times 10^{-3}$; $c^{(0)} = c_{in} = 0.9996$; $l_{in} = 328.68$.

1. $D^{(0)} = 0$; $g^{(0)} = 120$; $\{F^{*(0)}\} = \{0\}$.
2. $s^{(0)} = 4EI/l_{in} = 323.7 \times 10^3$; $t^{(0)} = 2EI/l_{in} = 161.9 \times 10^3$; $S^{(0)} + t^{(0)} = 485.6 \times 10^3$;

$$S_e = 2(29.85 \times 10^{-3})^2\left(\frac{8.4 \times 10^6}{328.68}\right) + \frac{4(0.9996)^2}{(328.68)^2}(485.6 \times 10^3) = 63.50;$$

$$S_e = 2(29.85 \times 10^{-3})^2\left(\frac{8.4 \times 10^6}{328.68}\right) + \frac{4(0.9996)^2}{(328.68)^2}(485.6 \times 10^3) = 63.50;$$

$S_g = 0$; $S_t = S_e + S_g = 63.50$;
$\Delta D = (63.50)^{-1}(120) = 1.890$

3. $D^{(1)} = D^{(0)} + \Delta D = 1.890$; $s^{(1)} = 24.10 \times 10^{-3}$; $c^{(1)} = 0.9997$; $l^{(1)} = 328.63$.
4. The difference between the length of the chord $l^{(1)}$ and the initial member length l_{in} is -50.98×10^{-3}. From Eq. (d), $\theta^{(1)} = 5.749 \times 10^{-3}$. The member end-forces (Eq. (c)) are

$$\{F^*\}^{(1)} = \left\{-\frac{8.4 \times 10^6}{328.68}(-50.98 \times 10^{-3}), \frac{2(5.749 \times 10^{-3})(485.6 \times 10^3)}{328.63}, \right.$$

$$\left. 5.749 \times 10^{-3}(485.6 \times 10^3)\right\}$$

whence

$\{F^*\}^{(1)} = \{1303, 16.99, 2792\}$

The out-of-balance force (Eq. (e)) is

$g = 120 - 2[24.10 \times 10^{-3}(1303) + 0.9997(16.99)] = 23.20$

Iteration cycle 2 $s^{(0)} = 24.1 \times 10^{-3}$; $c^{(0)} = 0.9997$

1. $D^{(0)} = 1.890$; $g^{(0)} = 23.2$; $\{F^{*(0)}\} = \{1303, 16.99, 2791\}$.
2. With an axial compressive force of 1303, Eqs. 13.16 and 13.17 give
   $S^{(0)} = 3.2395EI/l_{in} = 262.2 \times 10^3$; $t^{(0)} = 2.2102EI/l_{in} = 178.9 \times 10^3$
   $S^{(0)} + t^{(0)} = 441.1 \times 10^3$
   $S_e = 46.03 \quad S_e = -7.92 \quad S_t = 38.11$
   $\Delta D = (38.11)^{-1}(23.2) = 0.609$
3. $D^{(1)} = D^{(0)} + \Delta D = 2.499$; $s^{(1)} = 22.25 \times 10^{-3}$; $c^{(1)} = 0.9998$; $l^{(1)} = 328.61$.
4. $l^{(1)} - l_{in} = -65.09 \times 10^{-3}$; $\theta^{(1)} - \theta^{(0)} = 1.853 \times 10^{-3}$. The updated member end-forces are (Eq. (c))

$$F_1^{*(1)} = 1664; \; F_3^{*(1)} = 2792 + 441.1 \times 10^3 \, (1.853 \times 10^{-3}) = 3609$$

$$F_2^{*(1)} = \frac{2(3609)}{328.61} = 21.96$$

$\Delta\{F^*\} = \{361, 4.97, 817\} \qquad \{F^*\} = \{1664, 21.96, 3609\}$

The out-of-balance force (Eq. (e)) is

$$g = 120 - 2[22.25 \times 10^{-3}(1664) + 0.9998(21.96)] = 2.05$$

After the third iteration, the updated downward displacement at B and the end-forces at end B of member BC are

$D = 2.566 \qquad \{F^*\} = \{1701, 22.49, 3695\}$

The corresponding out-of-balance force is calculated by Eq. (e):

$s = 22.04 \times 10^{-3} \qquad c = 0.9998 \qquad g = 0.02$

With member BC subjected to an axial force of -1701 (compressive), end-rotational stiffness and carryover moment are (Eqs. 13.16 and 13.17)

$$S = 2.9807\frac{EI}{l_{in}} \quad t = 2.2913\frac{EI}{l_{in}} \quad \text{and} \quad (S + t) = 426.67 \times 10^3$$

Application of Eqs. 23.65, 23.68, and Eq. (e) shows that with the displacement configuration obtained, the more accurate values of the forces at end B of member BC and the corresponding out-of-balance force are

$\theta_A = \theta_B = 7.8053 \times 10^{-3} \quad \{F^*\} = \{1701, 20.27, 3330\} \quad g = 4.46$

The computer program NLPF, discussed in the preceding section, performs refinement cycles to eliminate the new out-of-balance force and gives more accurate answers:

$D = 2.729 \quad \{F^*\} = \{1792, 21.39, 3514\}$

We may now verify the accuracy of the answers. The change in member length $= -70.11 \times 10^{-3}$, corresponding to an axial force$= -1792$ (compressive); $(S+t) = 5.2310EI/l_{in}$ (Eqs. 13.16 and 13.17), $\theta = 8.297 \times 10^{-3}$; and member end-moments at each of B and $C = (S+t)\theta = 3514$. Length of BC after deformations is $l^{(1)} = 328.61$ and the absolute value of the shearing force in the member is$= 2\theta(S+t)/l^{(1)} = 21.39$. The resultant of the forces at end B of members AB and BC is the same as the external force applied at B, indicating zero out-of-balance force.

As mentioned earlier, the accuracy of the solution can be improved by introducing the load in stages and partitioning members AB and BC. The results of analyses, with each of these two members subdivided into four segments of equal length, are compared with the experimental results in Figure 23.7c. In the analyses, prescribed D values are used to determine the corresponding Q values. When $D > h$, B is situated below A and C, and the compressive axial force in AB and BC decreases, this being accompanied by an increase in stiffness, represented by increase in the slope of the Q–D graph.

Figure 23.7c includes the results of quasi-linear analyses (P-delta, Chapter 13). These analyses, which do not rigorously consider the geometry of the structure after deformation, cannot give accurate results when the displacements are large; in this example, when D is greater than, say, 4. Instead of using Eqs. (d) and (e), the quasi-linear analyses consider $l^{(1)} = l_{in} - D \sin \alpha_{in}$ and $Q = 2(F_1^* \sin \alpha_{in} + F_2^* \cos \alpha_{in})$, where α_{in} is the angle between the global x axis and the initial direction of member BC (Figure 23.7a).

Example 23.4: Large deflection of a column

Determine the horizontal and vertical displacements at the top of the column shown in Figure 23.8a. What are the reaction components at the bottom? Take $l_{in} = 75$(length unit); $Q = P = 150$ (force unit); $Ea = 10 \times 10^6$ (force unit); $EI = 1.0 \times 10^6$ (force $\times$ length^2). Assume elastic material. The forces P and Q are assumed to maintain their original directions after deformation.

We give below the equations to be used in the iteration cycles, the superscripts (0) and (1) referring to the values available at the start of a cycle and the values determined at its end respectively. In a typical cycle, the updated member end-forces at A are (Figure 23.8c and Eqs. 23.65 and 23.66)

$$F_1^* = -\frac{Ea}{l_{in}}(l^{(1)} - l_{in}); \quad F_3^{*(1)} = S\theta_A^{(1)} + t\theta_B^{(1)}; \quad F_2^{*(1)} = \frac{(S+t)}{l^{(1)}}(\theta_A^{(1)} + \theta_B^{(1)}) \tag{a}$$

where $S = 4EI/l_{in}$ and $t = 2EI/l_{in}$ (effects of axial force on S and t ignored)

$$\left.\begin{aligned} \theta_A^{(1)} &= D_3^{(1)} + \tan^{-1}[D_2^{(1)}/(l_{in} - D_1^{(1)})] \\ \theta_B^{(1)} &= \tan^{-1}[D_2^{(1)}/(l_{in} - D_1^{(1)})] \end{aligned}\right\} \tag{b}$$

The out-of-balance forces are

$$\{g^{(1)}\} = \begin{Bmatrix} P \\ Q \\ 0 \end{Bmatrix} - \begin{bmatrix} c^{(1)} & -s^{(1)} & 0 \\ s^{(1)} & c^{(1)} & 0 \\ 0 & 0 & 1 \end{bmatrix} \{F^{*(1)}\} \tag{c}$$

$$s^{(1)} = \frac{D_2^{(1)}}{l^{(1)}}; \; c^{(1)} = \frac{l_{in} - D_1}{(1)}; \; l^{(1)} = [(l_{in} - D_1^{(1)})^2 + (D_2^{(1)})^2]^{1/2} \tag{d}$$

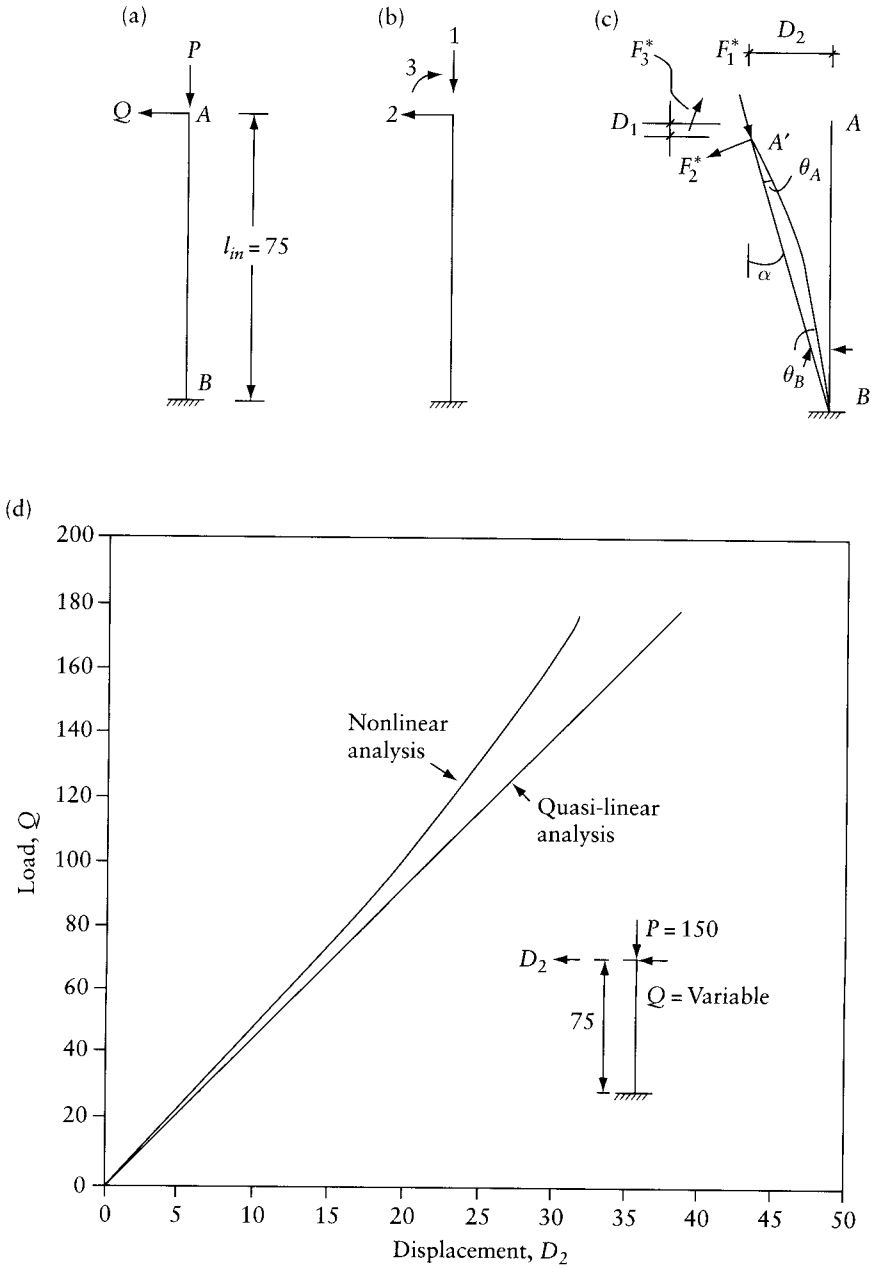

Figure 23.8 Column analyzed in Example 23.4. (a) Initial geometry and applied loads. (b) Coordinate system. (c) Deflected shape and forces at top end. (d) $Q - D_2$ graph with P constant.

Iteration cycle 1 $\{D^{(0)}\}=\{0\}$; $\{F^{*(0)}\}=\{0\}$; $s^{(0)}=0$; $c^{(0)}=1$.

1. $\{g^{(0)}\}=\{150,150,0\}$; $S=4EI/l_{\text{in}}$; $t=2EI/l_{\text{in}}$; $[S_t]=[S_e]+[S_g]$; $[S_g]=[0]$. Equation23.56 gives

$$[S_t]=[S_e]=\begin{bmatrix} 0.13333\times10^6 & \text{symmetrical} & \\ 0 & 0.28444\times10^2 & \\ 0 & 0.10667\times10^4 & 0.53333\times10^5 \end{bmatrix}$$

2. $\{\Delta D\}=[S_t]^{-1}\{g^{(0)}\}=\{0.11250\times10^{-2},0.21094\times10^2,-0.42188\}$
3. $\{D^(1)\}=\{D^{(0)}\}+\{\Delta D\}=\{0.11250\times10^{-2},0.21094\times10^2,-0.42188\}$
4. Equations (a) to (d) give

$$l^{(1)}=0.77909\times10^2 \qquad s^{(1)}=-0,27075 \qquad c^{(1)}=0.96265$$

$$l^{(1)}-l^{(0)}=0.29088\times10 \qquad \theta_A^{(1)}=-0.14770 \qquad \theta_B^{(1)}=0.27417$$

$$\{F^{*(1)}\}=\{-0.38784\times10^6,0.12987\times10^3,-0.56629\times10^3\}$$

$$\{g^{(1)}\}=\{0.37347\times10^6,-0.10498\times10^6,0.56629\times l0^3\}$$

Iteration cycle 2 $\{D^{(0)}\}=\{0.11250\times10^{-2},\ 0.21094\times10^2,\ -0.42188\}$; $\{g^{(0)}\}=\{0.37347\times10^6,\ -0.10498,\ 0.56629\times10^3\}$

1. Substitution of $s=-0.27075$, $c=0.96265$, $l=77.909$, and $(Ea/l)\equiv(Ea/l_{\text{in}})=10^6/75$ in Eq. 23.56 gives the elastic stiffness matrix

$$[S_e]=\begin{bmatrix} 0.12356\times10^6 & & \text{symmetrical} \\ -0.34745\times10^5 & 0.97985\times10^4 & \\ 0.27802\times10^3 & 0.98849\times10^3 & 0.53333\times10^5 \end{bmatrix}$$

Substitution of $F_1^*=-0.38784\times10^6$, $F_2^*=0.12987\times10^3$, and $l=77.909$ in Eq. 23.57 gives the geometric stiffness matrix

$$[S_g]=\begin{bmatrix} 0.36579\times10^3 & \text{symmetrical} & \\ 0.12989\times10^4 & 0.46123\times10^4 & \\ 0 & 0 & 0 \end{bmatrix}$$

$$[S_t]=[S_e]+[S_g]$$

2. $\{\Delta D\}=[S_t]^{-1}\{g^{(0)}\}=0.28030\times10,-0.78016,0.10466\times10^{-1}\}$
3. $\{D^{(1)}\}=\{D^{(0)}\}+\{\Delta D\}=\{0.28042\times10,0.20314\times10^2,-0.41141\}$
4. Equations (a) to (c) give

$$l^{(1)}=0.74999\times10^2 \qquad s^{(1)}=-0.27085 \qquad c^{(1)}=0.96262$$

$$l^{(1)}-l_{\text{in}}=0.77790\times10^{-3} \qquad \theta_A^{(1)}-0.13713 \qquad \theta_B^{(1)}=0.27428$$

The updated member forces at end A in this cycle are

$$\{F^{*(1)}\}=\{0.10372\times10^3,0.14629\times10^3,0.31483\}$$

The out-of-balance forces (Eq. (c)) are

$$\{g^{(1)}\} = \{0.10538 \times 10^2, 0.37271 \times 10^2, -0.31483\}.$$

After six iteration cycles, and refinement cycles in which S and t are considered functions of the axial force, the solution is

$$\{D\} = \{0.52711 \times 10, 0.27619 \times 10^2, -0.57027\}$$

The member end-forces are

$$\{F^*\} = \{0.84221 \times 10^2, 0.19470 \times 10^3, 0, -0.84221 \times 10^2,$$
$$-0.19470 \times 10^3, 0.14602 \times 10^5\}$$

Quasi-linear analysis For comparison, we give below the results of a quasi-linear analysis, in which the stiffness matrix is determined by Eq. 13.14, for a member subjected to an axial compressive force of 150. Furthermore, this analysis ignores the downward movement of the tip A associated with the lateral deflection. The displacements at A and the six member end-forces obtained by the quasi-linear analysis are

$$\{D\} = \{1.125 \times 10^{-3}, 31.908, -0.64754\}$$
$$\{F^*\} = \{150, 150, 0, -150, -150, 16036\}$$

The graph in Figure 23.8d shows the results of nonlinear and quasi-linear analyses for the structure in Figure 23.8a, maintaining P = constant = 150 and varying Q. As expected, the quasi-linear analysis is represented by a straight line. The nonlinear analysis gives smaller values of the lateral deflection because, in the displaced position, the force Q is closer to the fixed end than in its initial position.

23.10 Tangent stiffness matrix of triangular membrane element

The stiffness of membrane elements is discussed here because it is required in the analysis of shell structures and fabric structures composed of cable nets and fabric material. We generate below the tangent stiffness matrix for a triangular plane element whose corner nodes i, j, and k are defined by their (x, y, z) coordinates with respect to global orthogonal axes (Figure 23.9a). The element local orthogonal axes (x^*, y^*, z^*) have the same origin O as the global axes, and the $x^* - y^*$ plane is parallel to the plane of the element (Figure 23.9b). Furthermore, the local axis x^* is parallel to the vector connecting node i to node j; the local axis y^* is the perpendicular to x^*, pointing toward node k in direction away from line ij.

We will derive the tangent stiffness matrix with respect to coordinates $1^*, 2^*, \ldots, 9^*$ in the directions of the local axes[5] (Figure 23.9b). The tangent stiffness matrix is the sum of the elastic stiffness matrix $[S_e^*]$ and the geometric stiffness matrix $[S_g^*]$. The stiffness matrices corresponding to the nine coordinates in the global directions can be determined by the transformation equation

$$[S]_{e\,org} = [T]^T [S^*]_{e\,org} [T] \tag{23.69}$$

5 See Levy and Spillers, footnote 1 of this chapter.

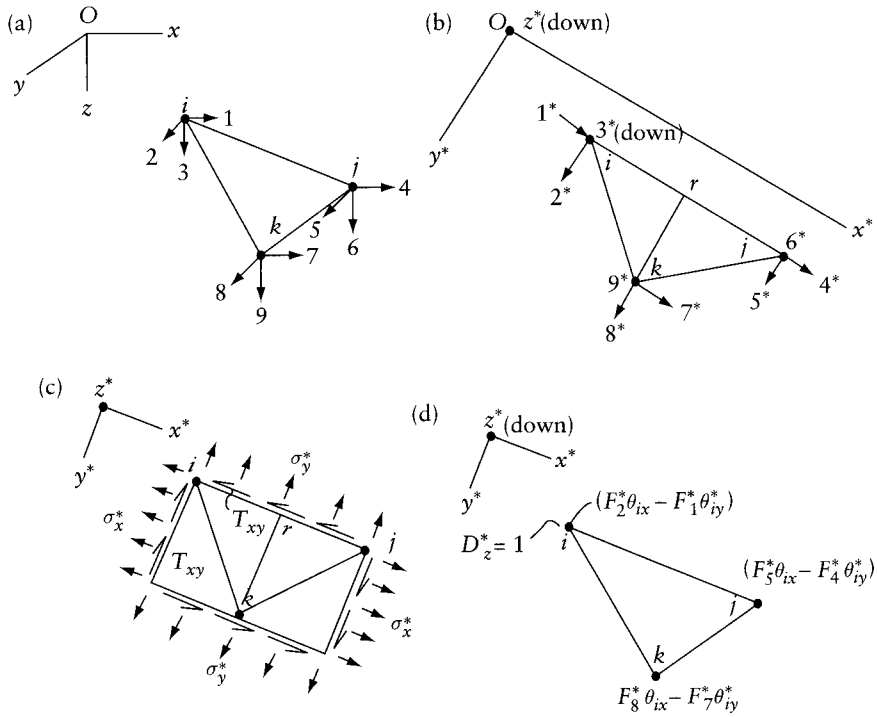

Figure 23.9 Derivation of geometric stiffness matrix of triangular membrane element. (a) Coordinate system in global directions. (b) View of the plane of the element and local coordinate system. (c) Stresses on element edges. (d) Forces necessary to maintain equilibrium when $D_z^* = 1$.

where

$$[T] = \begin{bmatrix} [t] & & \\ & [t] & \\ & & [t] \end{bmatrix}; \text{ submatrices not shown are null}$$

with $[t]$ being a 3×3 matrix consisting of cosines of the angles between the local and global axes (Eq. 21.18). At any corner of the triangle, the nodal coordinates, the nodal displacements, and the nodal forces in the local and global directions are related as follows:

$$\begin{Bmatrix} x^* \\ y^* \\ z^* \end{Bmatrix} = [t] \begin{Bmatrix} x \\ y \\ z \end{Bmatrix} \tag{23.70}$$

$$\begin{Bmatrix} D_x^* \\ D_y^* \\ D_z^* \end{Bmatrix} = [t] \begin{Bmatrix} D_x \\ D_y \\ D_z \end{Bmatrix} \quad \begin{Bmatrix} F_x \\ F_y \\ F_z \end{Bmatrix} = [t]^T \begin{Bmatrix} F_x^* \\ F_y^* \\ F_z^* \end{Bmatrix} \tag{23.71}$$

The stresses on the edges of the element are constant and are represented in their positive directions in Figure 23.9c (see Section 16.12 and Figure 16.9c). The nodal forces in the x^* and y^* directions at a node are equal to the sum of one-half of the distributed load on each of the two sides connected to the node (see Eq. 16.84). Thus,

$$\begin{Bmatrix} F_1^* \\ F_2^* \\ F_3^* \\ F_4^* \\ F_5^* \\ F_6^* \\ F_7^* \\ F_8^* \\ F_9^* \end{Bmatrix} = \frac{h}{2} \begin{bmatrix} -(y_k^* - y_j^*) & 0 & -(x_j^* - x_k^*) \\ 0 & (x_k^* - x_j^*) & -(y_k^* - y_j^*) \\ 0 & 0 & 0 \\ \hline -(y_i^* - y_k^*) & 0 & -(x_k^* - x_i^*) \\ 0 & (x_i^* - x_i^*) & -(y_i^* - y_k^*) \\ 0 & 0 & 0 \\ \hline 0 & 0 & -(x_i^* - x_j^*) \\ 0 & (x_j^* - x_i^*) & 0 \\ 0 & 0 & 0 \end{bmatrix} \begin{Bmatrix} \sigma_x^* \\ \sigma_y^* \\ \tau_{xy}^* \end{Bmatrix} \tag{23.72}$$

where h is the thickness of the element, or

$$\{F^*\} = [G]\{\sigma^*\} \tag{23.73}$$

where $[G]$ is the 9×3 matrix in Eq. 23.72, multiplied by $h/2$.

The elastic stiffness matrix for the constant-strain triangle was derived in Section 16.11 (Eq. 16.79). The same equation can be used here, by insertion of three rows and three columns composed of zeros, corresponding to coordinates 3*, 6*, and 9*. This is so because the membrane element has no out-of-plane stiffness.

The geometric stiffness matrix will be derived by differentiation of Eq. 23.73, holding $\{\sigma^*\}$ constant. A general element of the geometric stiffness matrix (see Eq. 23.33) is

$$S_{gnm}^* = \frac{\partial F_n^*}{\partial D_m^*} \quad (\text{with} \{\sigma^*\} = \text{constant}) \tag{23.74}$$

Noting that differentiation with respect to D^* is the same as differentiation with respect to x^* or y^* at the appropriate node, substitution of the nth row of Eq. 23.72 into Eq. 23.74 gives

$$S_{gnm}^* = \frac{\partial}{\partial D_m^*} [G_{n1}\ G_{n2}\ G_{n3}]\{\sigma^*\} \tag{23.75}$$

For example, for $n = 4$ and $m = 2$, we obtain

$$S_{g42}^* = \frac{h}{2} \frac{\partial}{\partial y_i^*} [-(y_i^* - y_k^*) \quad 0 \quad -(x_k^* - x_i^*)]\{\sigma^*\} \tag{23.76}$$

or

$$S_{g42}^* = -\frac{h}{2}\sigma_x^* \tag{23.77}$$

Columns 1, 2, 4, 5, 7, and 8 of $[S_g^*]$ can be generated by Eq. 23.75. The remaining columns of $[S_g^*]$ represent changes in the nodal forces resulting from separate out-of-plane displacement $D_z^* = 1$ at each of the three nodes. For example, to derive the third column of $[S_g]$, we introduce $D_3^* = D_{zi}^* = 1$, resulting in rotations of the plane of the element through angles θ_{ix}^* and θ_{iy}^* about the x^* and y^* axes. To maintain equilibrium, the following nonzero changes in the nodal forces must occur (Figure 23.9d):

$$S_{g33}^* = F_2^*\theta_{ix}^* - F_1^*\theta_{ij}; \quad S_{g63}^* = F_5^*\theta_{ix}^* - F_4^*\theta_{iy}^*; \quad S_{g93}^* = F_8^*\theta_{ix}^* - F_7^*\theta_{iy}^* \tag{23.78}$$

To verify the first of these three equations, consider the equilibrium of the membrane element in the rotated position. Forces F_1^* and F_2^* at node i are in a plane parallel to the initial plane of the element. Addition at node i of upward and downward forces of magnitudes $F_1^*\theta_{iy}$ and $F_2^*\theta_{ix}$, respectively, causes the resultant nodal forces to be situated in the rotated plane of the element. For the same purpose, forces are required at nodes j and k expressed by the second and the third of Eqs. 23.78.

The complete geometric stiffness matrix of the membrane triangular element with respect to the local coordinates in Figure 23.9b is

$$[S_g]=\begin{array}{c}\\1\\2\\3\\4\\5\\6\\7\\8\\9\end{array}\begin{bmatrix}
0 & 0 & 0 & -h\tau_{xy}^*/2 & h\sigma_x/2 & 0 & h\tau_{xy}^*/2 & -h\sigma_x/2 & 0\\
0 & 0 & 0 & -h\sigma_y^*/2 & h\tau_{xy}^*/2 & 0 & h\sigma_y^*/2 & -h\tau_{xy}^*/2 & 0\\
0 & 0 & F_2^*\theta_{ix}^*-F_1^*\theta_{iy}^* & 0 & 0 & F_2^*\theta_{jx}^*-F_1^*\theta_{jy}^* & 0 & 0 & F_2^*\theta_{kx}^*\\
\hdashline
h\tau_{xy}^*/2 & -h\sigma_x^*/2 & 0 & 0 & 0 & 0 & -h\tau_{xy}^*/2 & h\sigma_x^*/2 & 0\\
h\sigma_y^*/2 & -h\tau_{xy}^*/2 & 0 & 0 & 0 & 0 & -h\sigma_y^*/2 & h\tau_{xy}^*/2 & 0\\
0 & 0 & F_5^*\theta_{ix}^*-F_4^*\theta_{iy}^* & 0 & 0 & F_5^*\theta_{jx}^*-F_4^*\theta_{jy}^* & 0 & 0 & F_5^*\theta_{kx}^*\\
\hdashline
-h\tau_{xy}^*/2 & h\sigma_x^*/2 & 0 & h\tau_{xy}^*/2 & -h\sigma_x^*/2 & 0 & 0 & 0 & 0\\
-h\sigma_y^*/2 & h\tau_{xy}^*/2 & 0 & h\sigma_y^*/2 & -h\tau_{xy}^*/2 & 0 & 0 & 0 & 0\\
0 & 0 & F_8^*\theta_{ix}^*-F_7^*\theta_{iy}^* & 0 & 0 & F_8^*\theta_{jx}^*-F_7^*\theta_{jy}^* & 0 & 0 & F_8^*\theta_{kx}^*
\end{bmatrix} \tag{23.79}$$

where θ_{ix}^* and θ_{iy}^* are rotations of the element, with respect to axes x^* and y^*, when $D_{zi}^*=1$; in a similar way, θ_{jx}^*, θ_{jy}^*, θ_{kx}^* and θ_{ky}^* are defined. We can verify the following geometric relations:

$$\theta_{ix}^*=-\left(\frac{x_j^*-x_k^*}{x_j^*-x_i^*}\right)\left(\frac{1}{y_k^*-y_j^*}\right)\qquad \theta_{iy}^*=\frac{1}{x_j^*-x_i^*} \tag{23.80}$$

$$\theta_{jx}^*=-\left(\frac{x_k^*-x_i^*}{x_j^*-x_i^*}\right)\left(\frac{1}{y_k^*-y_j^*}\right)\qquad \theta_{jy}^*=\frac{1}{x_j^*-x_i^*} \tag{23.81}$$

$$\theta_{kx}^*=1/(y_k^*-y_j^*)\quad \theta_{ky}^*=0 \tag{23.82}$$

It is to be noted that in this case $[S_g^*]$ is a nonsymmetric matrix.

The iterative Newton-Raphson technique (Section 23.5.1) can be employed to determine the nodal displacements which define the geometry of triangular element after deformation. Let the line rk in Figure 23.9b be parallel to the y^* axis passing through node k in its initial position and in its displaced position. The element strains may be calculated from the length changes (Figure 23.9b).

$$\delta_{ij}=l_{ij}-(l_{ij})_{\text{in}}\quad \delta_{rk}=l_{rk}-(l_{rk})_{\text{in}}\quad \delta_{ir}=l_{ir}-(l_{ir})_{\text{in}}$$

where the subscript "in" refers to initial lengths. With respect to the local axes x^*, y^*, and z^* (Figures 23.9b and c), the changes in strain from the initial state are given by

$$\epsilon_x^*=\frac{\delta_{ij}}{(l_{ij})_{\text{in}}}\qquad \epsilon_y^*=\frac{\delta_{rk}}{(l_{rk})_{\text{in}}}\qquad \gamma_{xy}^*=\frac{1}{(l_{rk})_{\text{in}}}[\delta_{ir}-\epsilon_x^*(l_{ir})_{\text{in}}] \tag{23.83}$$

In verifying the equation for γ_{xy}^*, note that δ_{ir} represents the combined effects of ϵ_x^* and τ_{xy}^* on the translation in the x^* direction of k with respect to i; $\epsilon_x^*(l_{ir})_{\text{in}}$ represents the part of this translation attributed to ϵ_x^*.

The stresses after deformation are given by (Figure 23.9c)

$$\begin{bmatrix} \sigma_x^* \\ \sigma_y^* \\ \tau_{xy}^* \end{bmatrix} = [d] \begin{bmatrix} \epsilon_x^* \\ \epsilon_y^* \\ \gamma_{xy}^* \end{bmatrix} + \begin{bmatrix} \sigma_{xin}^* & (l_{rk})_{in}/l_{rk} \\ \sigma_{yin}^* & (l_{ij})_{in}/l_{ij} \\ (\tau_{xy}^*)_{in} & \Delta_{in}/\Delta \end{bmatrix} \tag{23.84}$$

where $[d]$ is the material elasticity matrix (Eq. 16.12), $\{\sigma_x^*, \sigma_y^*, \tau_{xy}^*\}_{in}$ are stresses existing in the initial state, and Δ_{in} and Δ are areas of the element in initial and deformed states respectively.

The last term in Eq. 23.84 represents adjusted stresses equivalent to the initial stresses $\{\sigma_x^*, \sigma_y^*, \tau_{xy}^*\}_{in}$. Considering the rectangular element in Figure 23.9c, we see that the resultants of the initial and the adjusted stress normal to any of the sides are the same. Also, the initial and the adjusted shear stress on each pair of opposite sides have equal resultant couples ($\tau_{xy}\, l_{ij}\, l_{rk}$).

23.11 Analysis of structures made of nonlinear material

Figure 23.10 shows examples of the shape of the stress–strain relation for nonlinear materials in practice. In this section, we discuss the simplest analysis technique known as the *incremental method*.

The applied forces $\{F\}$ are divided into increments $\beta_i\{F\}$. The load increments are applied one at a time and an elastic analysis is used. For the ith load increment, the following equilibrium equation is solved:

$$[S]_i\{\Delta D\}_i = \{\Delta F\}_i \tag{23.85}$$

The stiffness matrix $[S]_i$ depends upon the stress level reached in the preceding increment; thus, for the ith increment, the modulus of elasticity is the slope of the stress–strain diagram at the stress level reached in the increment $(i-1)$. The displacements obtained by the solution of Eq. 23.85 for each load increment are summed to give the final displacements:

$$\{D\} = \Sigma\{\Delta D\}_i \tag{23.86}$$

Similarly, the final stresses or stress resultants are determined by the sum of the increments calculated in all the linear analyses.

A typical plot of the displacement at any coordinate and the corresponding nodal force is composed of straight segments (Figure 23.11). It can be seen that the error in the results of the incremental method increases as the load level is increased. However, the accuracy can be improved by using smaller load increments.

The advantage of the incremental method is its simplicity. It can also be used for geometrically nonlinear analysis. For this purpose, the stiffness matrix $[S]_i$ for increment i is based on the geometry of the structure and the member end-forces determined in the preceding increment, $(i-1)$.

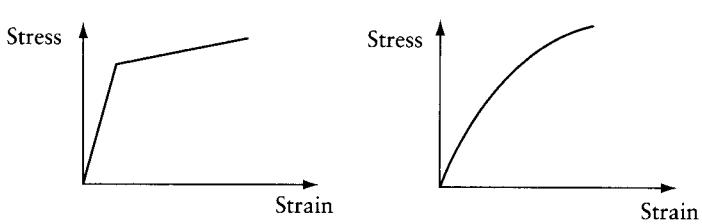

Figure 23.10 Examples of stress–strain relations.

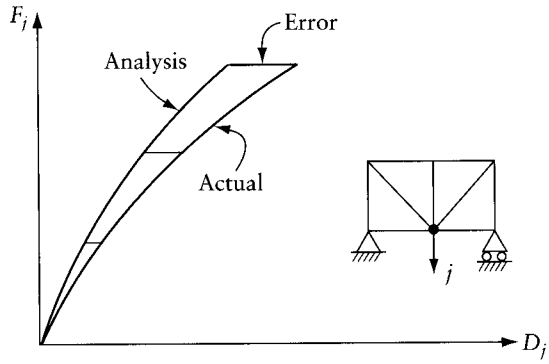

Figure 23.11 Typical result of incremental method of analysis.

23.12 Iterative methods for analysis of material nonlinearity

Newton-Raphson's and the modified Newton-Raphson's techniques discussed in Sections 23.4, 23.4.1, 23.5, and 23.9 can also be used to analyze structures with material nonlinearity. Figure 23.12 represents two analysis schemes. In Figure 23.12a the full load is introduced, and an approximate solution is obtained and corrected by a series of iterations. A linear analysis is performed in each iteration, using approximate stiffness, and giving approximate displacements and hence the strain in each member (or in each finite element). Using the stress–strain relation, the corresponding stress is determined. From the stress, the forces at member ends (or at the local coordinates of finite elements) are determined by Eq. 23.88 (discussed below). These forces are assembled to determine a vector of nodal forces $\{\bar{F}\}$ which maintain the equilibrium of the structure in the approximate deformed configuration determined in this iteration cycle. The difference between $\{\bar{F}\}$ and the known nodal forces represents out-of-balance forces to be eliminated by iteration:

$$\{g\} = -\{F\} - \{\bar{F}\} \tag{23.87}$$

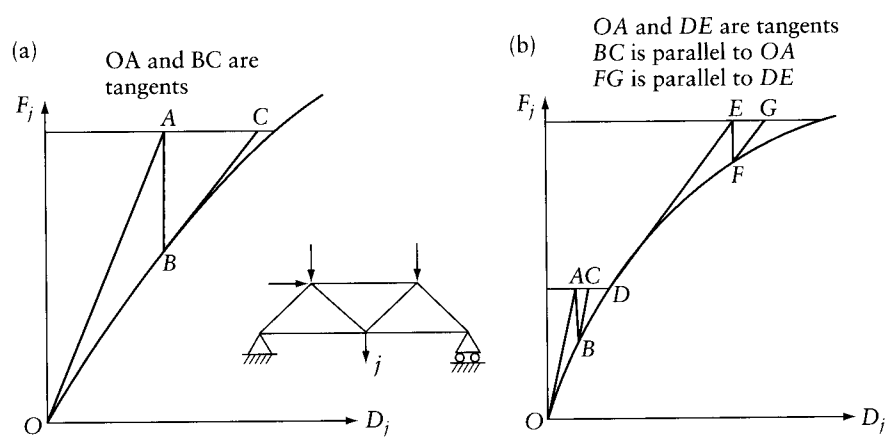

Figure 23.12 Load-displacement analysis in two consecutive iterative cycles. (a) Use of new tangent stiffness matrix in each iteration. (b) Application of the load in increments and use of new tangent stiffness matrix only in the first cycle after introduction of each new load increment.

where $\{F\}$ represents the forces which artificially prevent the nodal displacements; $\{\bar{F}\}$ represents the forces balanced by the internal forces in the members in the trial deformed configuration.

In each iteration cycle, a new stiffness matrix is used, based on the stress level in each member (or finite element) at the end of the preceding cycle. This is represented in Figure 23.12a, which is a graph of the force versus displacement at a typical coordinate. The slopes of OA and BC are different, indicating different stiffnesses in consecutive iterations.

The scheme presented in Figure 23.12b employs the modified Newton-Raphson's technique. The load is introduced in stages, and in each stage iteration cycles are employed to determine the nodal displacements. To avoid generating a new stiffness matrix in each iteration cycle, the stiffness matrix determined in the first cycle in each load stage is employed in all subsequent cycles until convergence has been achieved, before proceeding to the next load stage. This is schematically represented in Figure 23.12b in which the slopes of OA and BC are the same, indicating the same stiffness in two cycles.

In both schemes described above, we need to determine the nodal forces for a member (or finite element) for which the stress $\{\sigma\}$ is known. The unit-displacement theorem can be used for this purpose (Eq. 6.40). For a finite element, the nodal forces are given by

$$\{\bar{F}\}_{\text{element}} = \int_v [B]^T \{\sigma\} dv \tag{23.88}$$

where $[B]$ is the matrix expressing the strain at any point within the element in terms of the displacements at the nodes of the element (Eq. 16.38); $\{\sigma\}$ = the last determined stress at any point.

Analysis for material nonlinearity is illustrated in the following examples.

Example 23.5: Axially loaded bar

The bar shown in Figure 23.13a is made of two material types, whose stress–strain relations are shown in Figure 23.13b. Find the axial force in segments AB, BC, and CD due to $F_1 = 160$. The bar cross-sectional area = 4. Assume that the given stress–strain graphs apply both in tension and in compression.

A system of two coordinates is defined in Figure 23.13a. The forces necessary to restrain the displacements are $\{F\} = \{-160,\ 0\}$.

Iteraction cycle I We start with $\{D^{(0)}\} = \{0\}$ and the stress is zero in the three elements. The slope of the $\sigma - \epsilon$ graph at this stress level is 30 000, and the stiffness matrix corresponding to the coordinates in Figure 23.12a is

$$[S^{(1)}] = \frac{30\,000(4.0)}{10} \begin{bmatrix} 2 & -1 \\ 1 & 2 \end{bmatrix}$$

The out-of-balance forces at the start of this cycle are: $\{g^{(0)}\} = -\{F\} = \{160, 0\}$. We have

$$\{\Delta D\} = [S^{(1)}]^{-1}\{g^{(0)}\} = 4444 \times 10^{-6}\{2, 1\}$$

The improved displacement values are

$$\{D^{(1)}\} = \{D^{(0)}\} + \{\Delta D\} = \{8889, 4444\}10^{-6}$$

The strains in the three elements are: $\{\epsilon\} = m10^{-6}\{-889, 444, 444\}$. Entering the stress–strain graphs with these strain values gives the stress in the elements:

$$\{\sigma\} = \{-26.7, 4.0, 13.3\}$$

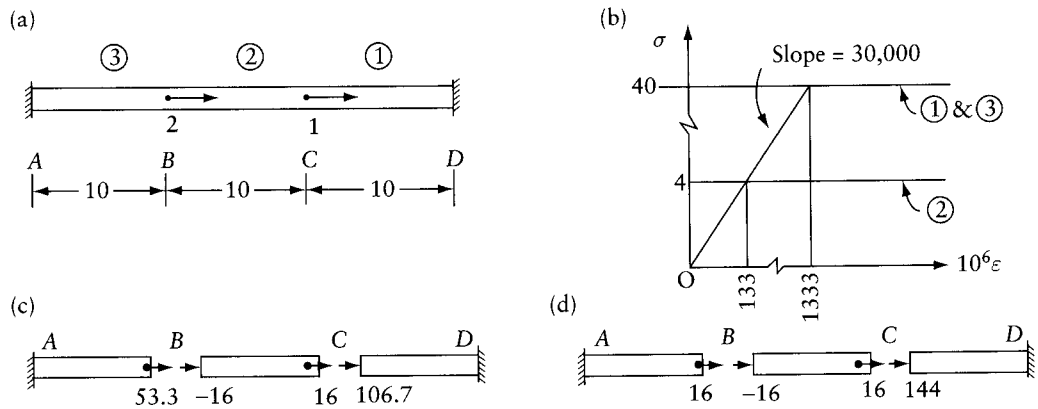

Figure 23.13 Bar analyzed in Example 23.5. (a) Bar dimensions. (b) $\sigma - \epsilon$ graphs for three elements. (c) and (d) Element nodal forces determined in iteraction cycles 1 and 2.

The corresponding member end-forces are shown in Figure 23.13c. The nodal forces to maintain equilibrium are

$$(\bar{F}) = \{122.7, 37.3\}$$

The out-of-balance forces are

$$\{g^{(1)}\} = \{-F\} - \{\bar{F}\} = \{37.3, -37.3\}$$

Iteration cycle 2 We now start with $\{D^{(0)}\} = \{8889, 4444\}10^{-6}; \{g^{(0)}\} = \{37.3, -37.3\}$. Entering the $\sigma - \epsilon$ graphs with the strain values determined in cycle 1 gives the values of slope E of 30 000, 0, 30 000 for elements 1, 2, and 3 respectively. The corresponding stiffness matrix for the structure is

$$[S^{(1)}] = \frac{30\,000(4)}{10}\begin{bmatrix} 1 & 0 \\ 0 & 1 \end{bmatrix}$$

Note in verifying this matrix that element 2 has zero stiffness. We have

$$\{\Delta D\} = [S^{(1)}]^{-1}\{g^{(0)}\} = \{3111, -3111\}10^{-6}$$

The improved displacements are

$$\{D^{(1)}\} = \{D^{(0)}\} + \{\Delta D\} = \{12\,000, 1333\}10^{-6}$$

The strains in the three elements are $\{\epsilon\} = 10^{-6}\{-1200, 1067, 133\}$. The corresponding stresses are $\{\sigma\} = \{-36, 4, 4\}$. The member end-forces are shown in Figure 23.13d and the corresponding nodal forces are

$$\{\bar{F}\} = \{160, 0\}$$

The out-of-balance forces are

$$\{g^{(1)}\} = \{-F\} - \{\bar{F}\} = \{0\}$$

Thus, the exact answers are: $\{D\} = 10^{-6}\{12\,000, 1333\}$ and the member end-forces are as shown in Figure 23.13d.

Example 23.6: Plane truss

Find the displacements at A and the forces in members AB, AC, and AD of the truss shown in Figure 23.14a, assuming the stress–strain diagram in Figure 23.14b. All members have the same cross-sectional area, a. The applied force $P = 1.75\sigma_y a$.

The restraining forces at the coordinates in Figure 23.14c are

$$\{F\} = \{0, -P\} = -1.75\sigma_y a\{0, 1\}$$

In accordance with the $\sigma - \epsilon$ graph in Figure 23.14b, the axial force in any member is

$$N = aE_1\epsilon \text{ (with } \epsilon \leq \epsilon_y) \quad N = a[\sigma_y + E_2(\epsilon - \epsilon_y)] \text{ (with } \epsilon > \epsilon_y)$$

From the geometry of the structure (Figure 23.14a), the strain in the members is expressed in terms of the nodal displacements:

$$\{\epsilon\} = \begin{Bmatrix} \epsilon_{AB} \\ \epsilon_{AC} \\ \epsilon_{AD} \end{Bmatrix} = \frac{1}{l}\begin{bmatrix} -1 & 0 \\ 0 & 1 \\ 0.707 & 0.707 \end{bmatrix}\{D\}$$

The stiffness matrix for m members connected at one node (Figure 23.14b) is

$$[S_t] = \sum_{i=1}^{m}\left[\frac{E\alpha}{l}\begin{bmatrix} c^2 & sc \\ sc & s^2 \end{bmatrix}\right]_i \tag{23.89}$$

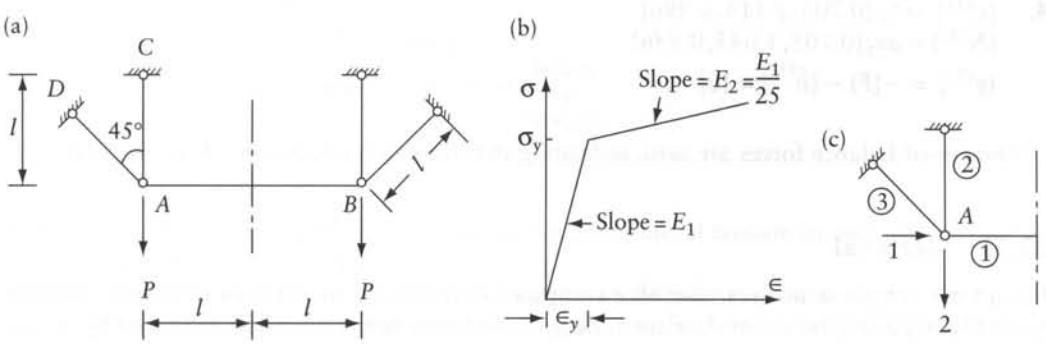

Figure 23.14 Plane truss of Example 23.6. (a) Truss geometry. (b) Stress–strain relation. (c) Coordinate system.

where $s_i = \sin\theta_i$, $c_i = \cos\theta_i$ and θ_i is the angle, measured in the clockwise direction, between the x axis and the member. For the same type of structure, the forces at the nodes balanced by the axial forces $\{N\}$ in the m members are

$$\{\bar{F}\} = -\sum_{i=1}^{m} \left\{ N \begin{Bmatrix} c \\ s \end{Bmatrix} \right\}_i \tag{23.90}$$

The four calculation steps outlined in Section 23.5.1 follow below.

Iteration cycle 1

1. $\{D^{(0)}\} = \{0\}$; $\{g^{(0)}\} = 1.75\,\sigma_y\,a\,\{0, 1\}$
2. $\{\epsilon^{(0)}\} = \{0\}$ and E for all members equals E_1. Equation 23.89 gives

$$[S_t] = E_1 \frac{a}{l} \begin{bmatrix} 1.5 & 0.5 \\ 0.5 & 1.5 \end{bmatrix}$$

$$\{\Delta D\} = [S_t]^{-1}\{g^{(0)}\} = \sigma_y l/E_1)\{-0.438, 1.313\}$$

3. $\{D^{(1)}\} = \{D^{(0)}\} + \{\Delta D\} = (\sigma_y l/E_1)\{-0.438, 1.313\}$
4. $\{\epsilon^{(1)}\} = \epsilon_y\,\{0.438,\ 1.313,\ 0.619\}$
   $\{N^{(1)}\} = a\sigma_y\{0.438, 1.013, 0.619\}$
   Application of Eq. 23.90 gives
   $\{g^{(1)}\} = -\{F\} - \{\bar{F}^{(1)}\} = a\sigma_y\{0, 0.299\}$

Iteration cycle 2

1. $\{D^{(0)}\} = (\sigma_y l/E_1)\{-0.438, 1.313\}$; $\{g^{(0)}\} = a\sigma_y\{0, 0.299\}$; $\{\epsilon^{(0)}\} = \epsilon_y\,\{0.438, 1.313, 0.619\}$. At this strain level, E is equal to E_1 for members 1 and 3, and to E_2 for member 2. Use of Eq. 23.89 gives

$$[S_t] = \frac{a}{l} E_1 \begin{bmatrix} 1.5 & 0.5 \\ 0.5 & 0.54 \end{bmatrix}$$

2. $\{\Delta D\} = [S_t]^{-1}\ \{g^{(0)}\} = (\sigma_y l/E_1)\ \{-0.267,\ 0.801\}$
3. $\{D^{(1)}\} = \{D^{(0)}\} + \{\Delta D\} = (\sigma_y l/E_1)\ \{-0.705.\ 2.114\}$
4. $\{\epsilon^{(1)}\} = \epsilon_y\,\{0.705, 2.114, 0.996\}$
   $\{N^{(1)}\} = a\sigma_y\{0.705, 1.045, 0.996\}$
   $\{g^{(1)}\} = -\{F\} - \{\bar{F}^{(1)}\} = \{0\}$

The out-of-balance forces are zero, indicating that the exact solution has been reached.

23.13 General

Except for simple structures, use of a computer is necessary to perform nonlinear analysis, generally requiring iterations. Understanding of nonlinear behavior can be enhanced by the use of computer programs which permit the introduction of loads in multi-stages, allow changing the number of iteration cycles, and give the out-of-balance forces at the end of each iteration cycle. Available computer programs, described in Appendix L, may be used for this purpose.

Problems

23.1 Perform two iteration cycles to determine, for $F = 90$, the corresponding value of D and the forces in the members of the truss in Figure 23.2, using the tangent stiffness matrix derived in Section 23.6. Approximate answers are given in Figure 23.3.

23.2 SI units. Calculate the displacements at B and C and the tension in segments AB, BC, and CD of the prestressed cable shown. Initial prestress = 100 kN, $E = 200$ GPa; cross-sectional area = 100 mm^2; $b = 1$ m.

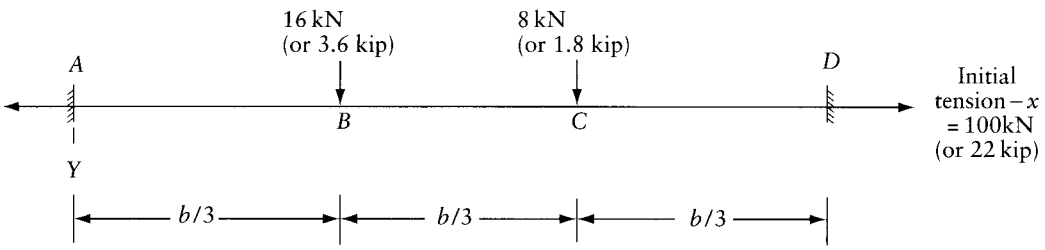

Prob. 23.2 or 23.3

23.3 Imperial units. Solve Prob. 23.2 with the following data: initial prestress = 22 kip; $E = 29\,000$ ksi; cross-sectional area = 0.15 in^2; $b = 40$ in.

23.4 By trial, using Eqs. 23.6 to 23.9, determine the maximum value of the force F that can be applied to the structure in Figure 23.2a (corresponding to point C on the graph in Figure 23.2b). Take $Ea = 8 \times 10^6$ and the ratio $h/b = 1/15$. Note that the answer depends only on the ratio h/b, not on the two separate values of h and b.

23.5 SI units. Determine the downward deflection D at B and the tension in AB and BC in the initially horizontal cable net shown, due to four downward forces $P = 12$ kN at each of B, C, F, and G. Take initial tension in each cable to be 180 kN and $Ea = 60$ MN.

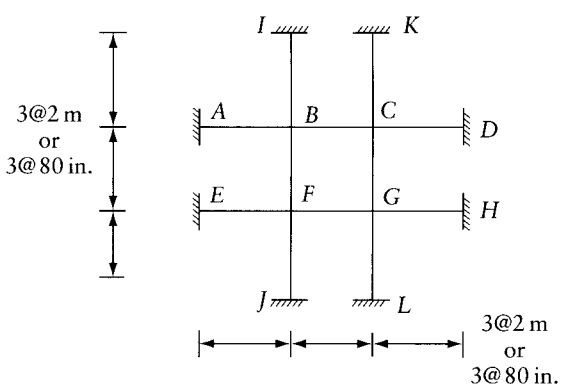

Prob. 23.5 or 23.6

23.6 Imperial units. Solve Prob. 23.5 taking $P = 3$ kip, initial tension in each cable equal to 40 kip and $Ea = 13\,500$ kip.

23.7 The figure shows the top view and elevation of a shallow space truss. Determine the vertical deflection of node A and the forces in the members due to a downward force $P = 100$ at the same node. Take $Ea = 40\,000$ for all members.

23.8 Determine the value of P which produces buckling of the space truss of Prob. 23.7, with the direction of the force P reversed.

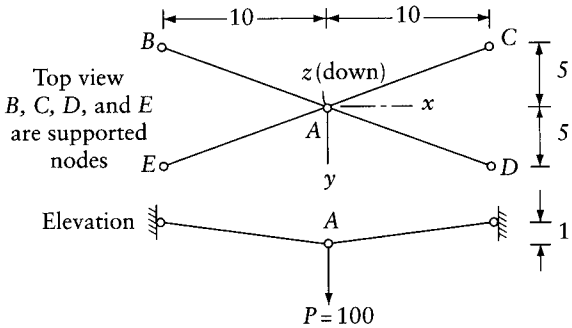

Prob. 23.7

23.9 The figure shows the top view of a cable network. The z coordinates of the nodes in their initial positions are given by $z = xy/(8l)$. The nodes on the external perimeter $ABCD$ are supported, while each of the internal nodes is subjected to a downward force $F_z = Q$. Determine the displacements at nodes 5, 6, 7, and 11 and the forces after loading the cable segments 5-6, 6-7, 1-5, 2-6, 6-11, and 3-7. Take $Ea = 10 \times 10^3 Q$, and $P = 30Q$, where P is the initial tension in the cable. (The given equation for z describes a hyperbolic parabolic surface, with concave and convex curvatures along AC and BD respectively. The surface is casually referred to as a saddle dome.) Solution of this problem is too long to be done by hand; however, the equilibrium equations of the nodes can be generated and verified using the displacement values given in the answers.

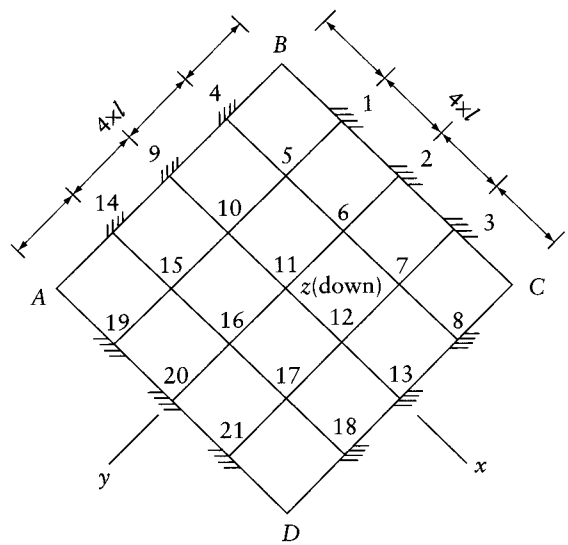

Prob. 23.9

23.10 Determine the displacements at B and the member end-forces for AB and BC of the structure shown. Take $b = 100$; $h = 2$; $Q = 0.8$; $Ea = 1.0 \times 10^6$; $EI = 0.1 \times 10^6$, where a and I are the cross-sectional area and the second moment of area of all members.

23.11 The plane frame of Prob. 13.12 is subjected, in addition to the downward forces Q at B and C, to two horizontal forces at the same nodes, each equal to $Q/10$ pointing to the right-hand side. Find the nodal displacements and the member end-forces. Take $l = 6c$;

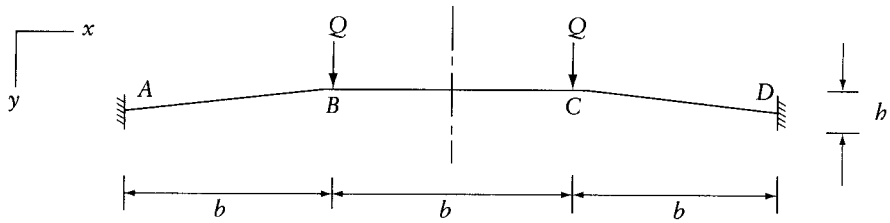

Prob. 23.10

$h = 2.4c$; for all members, $a = 25 \times 10^{-3}c^2$, $I = 60 \times 10^{-6}c^4$, and $E = 40 \times 10^9$ (F/c^2); $Q = 1.5 \times 10^6$ F, where c and F are force and length units respectively.

23.12 Find the displacement D due to an axial force F applied at the end of a straight prismatic bar of length l, assuming the stress–strain relation $\sigma = C(\epsilon - \epsilon^2/4)$, where $C =$ constant. Take $F = 0.7Ca$, with a being the cross-sectional area. Apply Newton-Raphson's technique and give the answers for two iterations.

23.13 Determine the displacement D at node B of the structure shown due to a force $F = 1000a$, where a is the cross-sectional area of each of the two parts AB and BC. The stress–strain graph for the two parts is shown in the figure, with

$$\{\sigma_y, E, \bar{E}\}_{AB} = \{500, 200 \times 10^3, 20 \times 10^3\}$$

and

$$\{\sigma_y, E, \bar{E}\}_{BC} = \{400, 200 \times 10^3, 0\}$$

What are the axial forces in AB and BC? Assume that the stress–strain relations given apply when the stress is tensile or compressive.

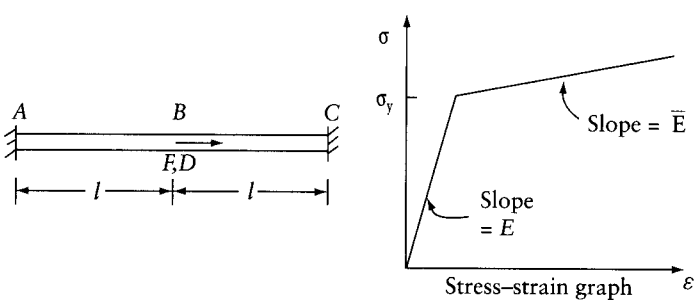

Prob. 23.13

23.14 Determine the forces in the members of the truss of Prob. 4.1. Assume that all members have the same cross-sectional area a and length l, and that the stress–strain relationship for part AB of the structure in Prob. 23.13 applies to all members of the truss. Take $P = 3.3 \times 10^{-3}$, $Ea = 660a$. Ignore geometric nonlinearity. Assume that the same stress–strain relationship applies when the stress is tensile or compressive.

Chapter 24

Reliability analysis of structures[1]

24.1 Introduction

The building process includes planning, design, construction, operation/use, and demolition. All components of the process involve uncertainties. These uncertainties can be put into two major categories with regard to causes: human and natural. Human causes include intended and unintended departures from optimum realization. In the design, this can be due to approximation, calculation error, communication problem, omission, lack of knowledge, and so on. Similarly, in the construction, uncertainties are due to use of inadequate materials, inappropriate methods of construction, bad connections, or changes without analysis. During operation/use, the structure can be subjected to overloading, inadequate maintenance, misuse, or even an act of sabotage. Natural causes of uncertainty result from unpredictability of loads such as wind, earthquake, snow, ice, water pressure, or live load, and also material properties, which vary from sample to sample and within the sample. This chapter presents reliability analysis that quantifies the uncertainties by means of a reliability index. The basic reliability theory, employed in the analysis, is presented in Appendix M.

24.2 Limit states

Structural performance can be acceptable or unacceptable. A structure fails if it cannot perform its function any longer. However, this is a rather vague definition, as it requires the definition of a function that can be the capacity to carry the loads, the stiffness to avoid excessive deflection, cracking, and so on. An example of a failure definition: a compact steel section fails if the bending moment, $M > M_p$, where M_p is the ultimate moment in the fully plastic condition (Eq. 18.1). The limit state is the limit at which the performance transits from acceptable to unacceptable. There are different types of limit states: strength or ultimate limit states, serviceability limit states, fatigue limit states, and extreme events limit states. Each limit state can be described by a limit state function. A simple example of a limit state function is:

$$g = R - Q \tag{24.1}$$

where R is the resistance (load-carrying capacity), Q is the load, and $g \geq 0$ for acceptable performance and $g < 0$ for unacceptable performance (failure). In the case of an ultimate limit state of flexural carrying capacity, R represents the bending moment carrying capacity and Q is the bending moment caused by the load. In the case of the serviceability limit state of deflection, R can represent the maximum acceptable deflection for the considered structure and Q can

1 This chapter was written in collaboration with the authors by Professor Andrzej S. Nowak, University of Nebraska, Lincoln, USA.

Table 24.1 Probability of Failure, P_f, for Selected Values of Reliability Index β

β	1.0	1.5	2.0	2.5	3.0	3.5	4.0	4.5	5.0	5.5
P_f	1.59E-1	6.68E-2	2.28E-2	6.21E-3	1.35E-3	2.33E-4	3.17E-5	3.40E-6	2.87E-7	1.90E-8

represent the deflection caused by the load. However, the limit state function can be more complex (e.g. non-linear) and the parameters can vary with time.

24.3 Reliability index definition

The reliability, that is, the probability of reaching the failure limit state of Eq. 24.1, is:

$$P_f = P((R - Q) < 0) = P(g < 0) \tag{24.2}$$

The probability P_f is equal to the *cumulative distribution function* (CDF) for the random variable g, defined by Eq. 24.1. The *reliability index* is defined as a function of P_f:

$$\beta = -\Phi^{-1}(P_f) \text{ or } P_f = \Phi(-\beta) \tag{24.3}$$

where Φ and Φ^{-1} are the *standard normal cumulative distribution function* (Table M.1) and its inverse (Eq. M.34). Table 24.1 lists values of P_f for selected β values.

24.3.1 Linear limit state function

When R and Q are independent (uncorrelated) normally distributed random variables, the reliability index is given by:

$$\beta = \frac{\overline{R} - \overline{Q}}{\sqrt{\sigma_R^2 + \sigma_Q^2}} \tag{24.4}$$

where $\overline{R}$ and $\overline{Q}$ are mean values of R and Q respectively; σ_R^2 and σ_Q^2 are their variance values. Equation 24.4 can be derived from Eqs. M.44, M.51, and M.53. If the independent random variables R and Q have log-normal distribution, the reliability index is given by:

$$\beta = \frac{\overline{y_R} - \overline{y_Q}}{\sqrt{\sigma_{y_R}^2 + \sigma_{y_Q}^2}} \tag{24.5}$$

where $\overline{y_R}$, $\overline{y_Q}$, $\sigma_{y_R}^2$, or $\sigma_{y_Q}^2$ is the mean or the variance of:

$$y_R = \ln R; \qquad y_Q = \ln Q \tag{24.6}$$

The variance and the mean of the Y random variables are given in terms of the variance and the mean of R or Q by Eqs. M.51 and M.53. Application of Eq. 24.4 or 24.5 requires the knowledge of the mean and the standard deviation, or the mean and the coefficient of variation, of R and Q.

The general limit state equation is:

$$g = R - Q = 0 \tag{24.7}$$

We can think of R and Q as the "capacity" and the "demand" respectively. When $R = Q$, the limit between safety and failure is reached. Equation 24.4 takes the form of Eq. 24.9 or 24.11 when g is expressed as a linear combination of random variables.

$$g\,(\{X\}) = a_0 + \sum_{i=1}^{n} (a_i X_i) = a_0 + \{a\}^T \{X\} \tag{24.8}$$

The reliability index is:

$$\beta = \overline{g} \Big/ \left[\sum_{i=1}^{n} (a_i \sigma_{X_i})^2 \right]^{1/2} \tag{24.9}$$

where $\overline{g}$ is the mean value of g:

$$\overline{g} = a_0 + \sum_{i=1}^{n} (a_i \overline{x}_i) = a_0 + \{a\}^T \{\overline{x}\} \tag{24.10}$$

The term in the square brackets in Eq. 24.9 is the variance of g. When $\{x\}$ contains correlated variables, Eq. 24.9 takes the form:

$$\beta = \overline{g} / \left(\{a\}^T [C] \{a\} \right)^{1/2} \tag{24.11}$$

where [C] is the covariance matrix (see Section M.13). The reliability index given by Eq. 24.4, 24.9, or 24.11 is sometimes called the *second mean value reliability index*, because it is expressed in terms of the mean and the variance.

Example 24.1: Probability of flexural failure of a simple beam

Calculate the reliability index β and the probability of failure P_f for a simple beam of span $l = 6$ m, subjected to uniform load q/unit length, combined with a concentrated load W at midspan. Assume that q, W, and the moment capacity at midspan M_r are uncorrelated normal random variables given the distribution parameters: $\overline{q} = 16$ kN/m; $V_q = 10\%$; $\overline{W} = 55$ kN; $V_W = 15\%$; $\overline{M_r} = 270$ kN-m; $V_{M_r} = 12\%$.

The standard deviation is equal to the product of the mean and the coefficient of variation, and thus the variance σ^2 of q, W, and M_r are:

$$\sigma_q^2 = [0.1(16)]^2 = 2.56; \quad \sigma_W^2 = [0.15\ (55)]^2 = 68.1; \quad \sigma_{M_r}^2 = [0.12\ (270)]^2 = 1050$$

Apply the limit state Eq. 24.1 with:

$$R = M_r; \quad Q = \left(\frac{l^2}{8}\right) q + \left(\frac{l}{4}\right) W; \quad g = R - Q$$

The mean and the variance of R are:

$$\overline{R} = \overline{M_r} = 270; \quad \sigma_R^2 = \sigma_{M_r}^2 = 1050$$

The mean and the variance of Q are (Eqs. M.51 and M.53):

$$\overline{Q} = \left(\frac{l^2}{8}\right)\overline{q} + \left(\frac{l}{4}\right)\overline{W} = \left(\frac{6^2}{8}\right)16 + \left(\frac{6}{4}\right)55 = 154.5$$

$$\sigma_Q^2 = \left(\frac{l^2}{8}\right)^2 \sigma_q^2 + \left(\frac{l}{4}\right)^2 \sigma_W^2 = \left(\frac{6^2}{8}\right)^2 (2.56) + \left(\frac{6}{4}\right)^2 (68.1) = 205.1$$

The reliability index (Eq. 24.4):

$$\beta = \frac{\overline{R} - \overline{Q}}{\sqrt{\sigma_R^2 + \sigma_Q^2}} = \frac{270 - 154.5}{\sqrt{1050 + 205.1}} = 3.26$$

The probability of failure (Eq. 24.3 and Table M.1);

$$P_f = \Phi(-\beta) = \Phi(-3.26) = 0.557 \times 10^{-3}$$

Example 24.2: Plastic moment resistance of a steel section

The plastic moment capacity of a steel section is expressed as (Eq. 18.1): $M_p = f_y Z$, where f_y is the yield stress and Z is the plastic section modulus. Let Q be the bending moment that the section has to resist (the demand). Find the reliability index and the probability of failure. Assuming that f_y, Z, and Q are independent log-normal random variables whose mean values and coefficient of variations are: $\overline{f_y} = 300$ MPa (300×10^3 kN/m^2); $V_{f_y} = 10\%$; $\overline{Z} = 0.9 \times 10^{-3}$ m^3; $V_Z = 5\%$; $\overline{Q} = 160$ kN-m; $V_Q = 12\%$.

The probability of failure,

$$P_f = P\left(\frac{M_p}{Q} < 1\right) = P\left[\left(\frac{f_y Z}{Q}\right) < 1\right]$$

The variance of f_y, Z, and Q are:

$$\sigma_{f_y}^2 = \left[0.10\left(300 \times 10^3\right)\right]^2 = 900 \times 10^6; \quad \sigma_Z^2 = \left[0.05\left(0.9 \times 10^{-3}\right)\right]^2 = 2.025 \times 10^{-9};$$

$$\sigma_Q^2 = [0.12\ (160)]^2 = 9.437 \times 10^6$$

Let $Y_1 = \ln f_y$; $Y_2 = \ln Q$; $Y_3 = \ln Z$

The variance and the mean of Y_1, Y_2, and Y_3 are (Eqs. M.38 and M.39):

$$\sigma_{Y_1}^2 = \ln\left(V_{Y_1}^2 + 1\right) = \ln\left[(0.1)^2 + 1\right] = 9.95 \times 10^{-3};$$

$$\overline{y_1} = \ln \overline{f_y} - \frac{1}{2}\sigma_{Y_1}^2 = \ln\left(300 \times 10^3\right) - \frac{1}{2}\left(9.95 \times 10^{-3}\right) = 12.6$$

$$\sigma_{Y_2}^2 = \ln\left(V_{Y_2}^2 + 1\right) = \ln\left[(0.12)^2 + 1\right] = 14.3 \times 10^{-3};$$

$$\overline{y_2} = \ln \overline{Q} - \frac{1}{2}\sigma_{Y_2}^2 = \ln(160) - \frac{1}{2}\left(14.3 \times 10^{-3}\right) = 5.0609$$

$$\sigma^2_{Y_3} = \ln\left(V^2_{Y_3} + 1\right) = \ln\left[(0.05)^2 + 1\right] = 2.50 \times 10^{-3};$$

$$\overline{y_3} = \ln \overline{Z} - \frac{1}{2}\sigma^2_{Y_3} = \ln\left(0.9 \times 10^{-3}\right) - \frac{1}{2}\left(2.50 \times 10^{-3}\right) = -7.0144$$

Let $X_0 = \ln\left(\frac{f_y Z}{Q}\right)$; let $Y = \ln X_0 = \ln f_y + \ln Z - \ln Q = Y_1 + Y_3 - Y_2$

The mean and variance of Y are (Eqs. M.58 and M.59):

$$\overline{y} = \overline{y_1} + \overline{y_3} - \overline{y_2} = 12.60 + (-7.014) - 5.0609 = 0.5247$$

$$\sigma^2_Y = \sigma^2_{Y_1} + \sigma^2_{Y_2} + \sigma^2_{Y_3} = 10^{-3}\,(9.95 + 14.3 + 2.50) = 26.75 \times 10^{-3}$$

The probability of failure (Table M.1):

$$P_f = P\left[\left(\frac{f_y Z}{Q}\right) < 1\right] = \Phi\left[\frac{\ln(1) - \overline{y}}{\sigma_Y}\right] = \Phi\left[\frac{0 - 0.5247}{\sqrt{26.75 \times 10^{-3}}}\right]$$

$$= \Phi\,[-3.21] = 0.664 \times 10^{-3}$$

The reliability index, $\beta = 3.21$.

Example 24.3: Probability of shear failure

Calculate the probability of shear failure at the section just to the left of D for the structure in Prob. 12.1, subjected to uniform dead load q/unit length and moving concentrated loads P_1 and P_2, spaced at a distance $= l/15$. Assume that $l = 25$ m and q, P_1, P_2, and the shear strength V_D are random normally distributed variables, whose mean and standard deviation values are:

$$\overline{q} = 360\,\text{kN/m}; \quad \overline{P_1} = 400\,\text{kN}; \quad \overline{P_2} = 300\,\text{kN}; \quad \overline{V_D} = 6000\,\text{kN}$$

$$\sigma_q = 36\,\text{kN/m}; \quad \sigma_{P_1} = 60\,\text{kN}; \quad \sigma_{P_2} = 45\,\text{kN}; \quad \sigma_{V_D} = 1000\,\text{kN}$$

Consider that only P_1 and P_2 are correlated with $COV = 2500\,(\text{kN})^2$. What is the mean value $\overline{V_D}$ that brings β up to 3.0 and reduces the probability of failure to 1.35×10^{-3}?

Use the limit state equation: $g = R - Q = 0$, with $R \equiv V_D$ and $Q \equiv$ the maximum shear force at the section.

$$g = V_D - (0.4l)\,q - P_1 - (2/3)\,P_2 = 0$$

$$g = \{a\}^T\,\{x\}; \quad \{a\} = \{1, -0.4\,(25), -1, -(2/3)\}; \quad \{x\} = \{V_D, q, P_1, P_2\}$$

$$COV\left[\{x\}^T\,\{x\}\right] = \begin{bmatrix} (1000)^2 & & & \text{symmetrical} \\ 0 & (36)^2 & & \\ 0 & 0 & (60)^2 & \\ 0 & 0 & 2500 & (45)^2 \end{bmatrix} \text{ kN and m units}$$

$$\sigma^2_g = \{a\}^T\,[C]\,\{a\} = 1.137 \times 10^6; \quad \sigma_g = 1066.5\,\text{kN}$$

The reliability index and the probability of failure are (Eqs. M.44, M.51, and 24.3):

$$\beta = \overline{g}/\sigma_g = [6000 - 0.4 \times 25 \times 360 - 400 - 300\,(2/3)]/(1066.5) = 1.69$$

Table M.1 gives: $P_f = \Phi(-1.69) = 45.5 \times 10^{-3}$. To reduce this relatively high probability, increase the reliability index to $\beta = 3.0$ by the increase of shear strength to $V_D = 7400$ kN.

24.3.2 Linearized limit state function

Consider a nonlinear limit state function of uncorrelated random variables, $\{X\}_{n\times 1}$. The first two terms of Taylor's expansion transform the function to a linear equation:

$$g(X_1, X_2, \ldots, X_n) \approx \overline{g} + \sum_{i=1}^{n} \left[(X_i - \overline{x_i}) \frac{\partial g}{\partial X_i} \right] \tag{24.12}$$

where $\overline{g}$ is a value of g calculated with chosen values of the variables. One choice is: the mean values of the random variables, giving an approximate mean value of g:

$$\overline{g} = g(\overline{x_1}, \overline{x_2}, \ldots, \overline{x_n}) = g(\{\overline{x}\}) \tag{24.13}$$

The first term in Eq. 24.12 is a constant, the remaining terms are linear combinations of the variables $(X_i - \overline{x_i})$, with $\overline{x_i}$ = constant; thus, Eq. 24.9 can be used to give an approximate reliability index:

$$\beta \approx \overline{g} \Big/ \left[\sum_{i=1}^{n} (a_i X_i)^2 \right]^{1/2} \quad \text{with } a_i = \left. \frac{\partial g}{\partial X_i} \right|_{\text{at } \{\overline{x}\}} \tag{24.14}$$

Because we use the first term of Taylor's expansion, the reliability index given by Eq. 24.14 is sometimes called *first-order second-moment mean-value reliability index*.

Example 24.4: Probability of flexural failure of a rectangular reinforced concrete section

A rectangular reinforced concrete section is subjected to a bending moment = Q. Find the probability of flexural failure and the reliability index using:

$$R = A_s f_y \left(d - 0.59 \frac{A_s f_y}{b f_c'} \right)$$

where R is the capacity of the cross section (the bending moment that it can carry); A_s and f_y are the cross-sectional area and the specified yield strength of the steel reinforcement respectively; f_c' is the specified compressive strength of concrete; b is the width of the section; and d is the distance between the steel reinforcement and the extreme compression fiber. Consider $b = 0.3$ m; $d = 0.45$ m; $\{A_s, f_y, f_c', Q\}$ = random variables normally distributed having mean and standard deviation values:

$$\overline{A_s} = 2.6 \times 10^{-3}\,\text{m}^2; \quad \sigma_{A_s} = 0.05 \times 10^{-3}\,\text{m}^2; \quad \overline{f_y} = 400\,\text{MPa}; \quad \sigma_{f_y} = 45\,\text{MPa};$$

$$\overline{f_c'} = 30\,\text{MPa}; \quad \sigma_{f_c'} = 4\,\text{MPa}; \quad \overline{Q} = 290 \times 10^3\,\text{N-m}; \quad \sigma_Q = 24 \times 10^3\,\text{N-m}.$$

Let: $\{X_1, X_2, X_3, X_4\} = \{A_s, f_y, f'_c, Q\}$; $g = R - Q$.

The mean values of the limit state function (Eq. 24.13):

$$\bar{g} \approx g(\{\bar{x}\}) = 0.0026\left(400 \times 10^6\right)\left[0.45 - \frac{0.59\,(0.0026)\,(400 \times 10^6)}{0.3\,(30 \times 10^6)}\right] - 290 \times 10^3$$

$$= 107.1 \times 10^3 \text{ N-m}$$

At the mean values $\{\bar{x}\}$, the partial derivatives are:

$$a_1 = \partial g/\partial X_1 = 125.2 \times 10^6 \text{ N/m}; \quad a_2 = \partial g/\partial X_2 = 813.7 \times 10^{-6} \text{ m}^3;$$

$$a_3 = \partial g/\partial X_3 = 2340 \times 10^{-6} \text{ m}^3; \quad a_4 = \partial g/\partial X_4 = -1.$$

The reliability index and the probability of failure are (Eq. 24.14 and Table M.1):

$$\beta = 107.1 \times 10^3 \left\{\left[125.2\,(0.05)\,10^3\right]^2 + [813.7\,(45)]^2 + [2340\,(4)]^2 + \left[(-1)\,24 \times 10^3\right]^2\right\}^{-1/2}$$

$$\beta = 2.37; P_f = \Phi(-2.37) = 8.89 \times 10^{-3}.$$

24.3.3 Comments on the first-order second-moment mean-value reliability index

The use of Eq. 24.14 to find an approximate value of the reliability index is easy; but the equation does not consider different distributions of random variables. The result can be inaccurate when the tails of the distributions are far from the normal distribution. Furthermore, the value of β calculated using Eq. 24.14 for a specific nonlinear limit state function can depend on the form in which the function is written (see Example 24.5). The methods discussed in Section 24.4 do not exhibit this problem.

Example 24.5: Drift at top of a concrete tower

A concrete tower is idealized as a vertical prismatic cantilever fixed at the base and subjected to uniform load q/unit length. It is required that the elastic drift (horizontal displacement) at the top, $D = ql^4/(8EI)$ does not exceed $l/500$; where l is the length of the cantilever; E is the modulus of elasticity; I is the second moment of cross-sectional area. The limit state equation can be written as: $g = R - Q = (EI/l^3) - (500/8)\,q = 0$. The same limit state function can be expressed in terms of the permissible drift or in terms of the bending moment at the base as:

$$g_1 = \frac{l}{500} - \frac{ql^4}{8EI}; \quad g_2 = \frac{EI}{125l} - \frac{ql^2}{2}$$

Use Eq. 24.14 to determine β_1 using g_1 and β_2 using g_2. Given data:

$l = 50$ m; q, E, and I are random variables with: $\bar{q} = 10$ kN/m; $\sigma_q = 1.5$ kN/m; $\bar{E} = 30$ GPa; $\sigma_E = 3$ GPa; $\bar{I} = 4.0\,\text{m}^4$; $\sigma_I = 0.8\,\text{m}^4$.

Use g_1 as limit state equation:

$$\overline{g_1} = \frac{50}{500} - \frac{10 \times 10^3 \,(50)^4}{8\,(30 \times 10^9)\,(4.0)} = 0.0349\,\text{m}$$

$$a_1 = -6.51 \times 10^{-6}\,\text{m}^2/\text{N}; \quad a_2 = 2.17 \times 10^{-12}\,\text{m}^3/\text{N}; \quad a_3 = 16.3 \times 10^{-3}\,\text{m}^{-3}$$

$$\beta_1 \approx 0.0349 \left\{ \left[6.51 \times 10^{-6} \left(1.5 \times 10^3\right)\right]^2 + \left[2.17 \times 10^{-12} \left(3 \times 10^9\right)\right]^2 + \left[16.3 \times 10^{-3}\,(0.8)\right]^2 \right\}^{-1/2} = 1.99$$

Use g_2 as limit state equation:

$$\overline{g_2} = \frac{30 \times 10^9\,(4.0)}{125\,(50)} - \frac{10 \times 10^3\,(50)^2}{2} = 6.70 \times 10^6\,\text{N-m}$$

$$a_1 = -1250\,\text{m}^2; \quad a_2 = 0.640 \times 10^{-3}\,\text{m}^3; \quad a_3 = 4.80 \times 10^6\,\text{N-m}^3$$

$$\beta_2 \approx 6.7 \times 10^6 \left\{ \left[-1250 \left(1.5 \times 10^3\right)\right]^2 + \left[0.640 \times 10^{-3} \left(3 \times 10^9\right)\right]^2 + \left[4.8 \times 10^6\,(0.8)\right]^2 \right\}^{-1/2} = 1.43$$

24.4 General methods of calculation of the reliability index

The methods presented in this section and Sections 24.4.1 and 24.4.2 give, for any specified limit state equation, the same answer for the reliability index β, regardless of the form in which the equation is set. Consider the limit state equation:

$$g\,(\{X\}) = g\,(X_1, X_2, \ldots, X_n) = 0 \tag{24.15}$$

where $\{X\}_{n\times 1}$ is a random variable whose mean $\{\overline{x}\}$ and standard deviation $\{\sigma_X\}$ values are given. It is required to find the reliability index β.

Transform $\{X\}$ to $\{Z\}$ = standard normal random variables, using Eq. M.28:

$$Z_i = (X_i - \overline{x_i})/\sigma_{X_i}; \quad X_i = \overline{x_i} + Z_i \sigma_{X_i} \tag{24.16}$$

Substitution of Eq. 24.16 gives the limit state equation as a function of $\{Z\}$:

$$g\,(\{Z\}) = g\,(Z_1, Z_2, \ldots, Z_n) = 0 \tag{24.17}$$

Imagine n-dimensional space with origin O at $\{Z\} = \{0\}$. Figure 24.1 is a three-dimensional representation of $g(Z_1, Z_2)$, a function of two random variables. The horizontal axes Z_1 and Z_2 represent $\{Z\}$. The curve SB is the intersection of the surface $g(\{Z\})$ with $Z_1 - Z_2$ plane; any point on SB satisfies the limit state Eq. 24.17. The curve SB represents a boundary between the safe and the failure zones.

Now, let the vertical upward axis in Figure 24.1 represent also the probability density function, $\phi(z)$, Eq. M.26. Imagine rotating the curve of $\phi(z)$ in Figure M.1a about the vertical axis to obtain a surface of rotation, whose contour lines are the circles shown in Figure 24.1. The shortest distance $\overline{OL}$ between O and the boundary SB is equal to reliability index β. Point L on

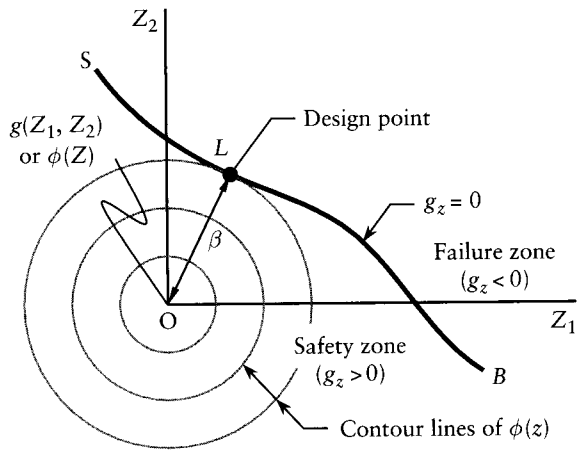

Figure 24.1 Three-dimensional representation of standard normal space, with limit state function of two random variables. Top view.

SB is called the *point of maximum likelihood* or the *design point*. A vertical plane through *OL* intersects the surface of revolution in a curve whose vertical coordinates are $\phi(z)$; the area below the curve between *L* and infinity is equal to P_f, the probability of failure. Its value is maximum when $\overline{OL}$ is minimum. The reliability index in the case of two random variables only is:

$$\beta = \left(Z_1^{*2} + Z_2^{*2}\right)^{1/2} \tag{24.18}$$

where $\{Z^*\}$ are coordinates of the design point.

When there are n random variables, the problem of finding $\{Z^*\}_{n\times 1}$ that gives minimum β and satisfies Eq. 24.17 amounts to the solution of:

$$\beta = \min\left(\{Z\}^T\{Z\}\right)^{1/2} \text{ with } g(\{Z\}) = 0 \tag{24.19}$$

This is called a *constrained maximization problem*, for which commercial computer programs exist (e.g. Excel of Microsoft). An iterative solution is given in Section 24.4.2.

24.4.1 Linear limit state function

When $g(\{Z\})$ in Eq. 24.17 is a linear combination of two random variables only, the safety boundary *SB* in Figure 24.1 will be a straight line and *OL* is perpendicular to it. However, when the limit state Eq. 24.15 is a linear combination of $\{X\}_{n\times 1}$ (Eq. 24.15), the reliability index can be determined by Eq. 24.9 or 24.11, without the need of using standardized variables (Eq. 24.16).

24.4.2 Arbitrary limit state function: iterative procedure

An iterative procedure is presented here to solve the problem discussed in Section 24.4. The solution starts with guess values for β and the coordinates $\{Z^*\}$ of the design point, with:

$$Z_i^* = \alpha_i \beta \tag{24.20}$$

In the case of two random variables represented in Figure 24.1, α_1 or α_2 is equal to cosine the angle between OL and the Z_1 or Z_2 axis. The iteration is performed to satisfy Eq. 24.21:

$$\alpha_i = -\frac{\partial g(\{Z\})}{\partial Z_i}\left[\sum_{k=1}^{n}\left(\frac{\partial g(\{Z\})}{\partial Z_k}\right)^2\right]^{-1/2} \tag{24.21}$$

Equation 24.20 gives:

$$\frac{\partial g(\{Z\})}{\partial Z_i} = \beta^{-1}\left(\frac{\partial g(\{Z\})}{\partial \alpha_i}\right) \tag{24.22}$$

Thus, the partial derivatives in Eq. 24.21 can be replaced by partial derivatives with respect to $\alpha_1, \alpha_2, \ldots, \alpha_n$. The values $\{\alpha\}$ calculated using Eq. 24.21 satisfy the equation:

$$\alpha_1^2 + \alpha_2^2 + \cdots + \alpha_n^2 = 1 \tag{24.23}$$

The iteration may start with $\alpha_i^2 = 1/n$ and $\alpha_i = \pm\sqrt{1/n}$, for all i values. The plus or minus sign should be selected to match the expected sign of α_i in Eq. 24.21. In general, the positive sign is used for the variable that represents the load effect, and the negative sign is used for the resistance. Express the limit state Eq. 24.17 in terms of β and $\{\alpha\}$, and then perform the following iterative steps:

1. Use the limit state equation to solve for improved β; the solution will, in general, include terms with β and $\{\alpha\}$; for these substitute the latest values.
2. Calculate improved $\{\alpha\}$ using Eq. 24.21; here again, substitute the latest values of β and $\{\alpha\}$ in the right-hand side of the equation.

Repeat the iterative steps until the value of β does not change substantially in consecutive iterations.

Example 24.6: Iterative calculation of the reliability index

Find the reliability index β for the concrete tower of Example 24.5, using the limit state equation for the lateral drift at the top:

$$g = \left(\frac{l}{500}\right) EI - \left(\frac{l^4}{8}\right) q$$

Consider that E, I, and q are uncorrelated normal random variables whose mean and standard deviation values are as given in Example 24.5. Assume $l = 50$ m.

Let $\{X_1, X_2, X_3\} = \{E, I, q\}$.

The standardized normal random variables are (Eq. 24.16):

$$\{X_1, X_2, X_3\} = \{10^9\,(30 + 3Z_1), (4 + 0.8Z_2), 10^3\,(10 + 1.5Z_3)\}$$

Substitution in the limit state equation gives:

$$g(\{Z\}) = \frac{50 \times 10^9}{500}\,(30 + 3Z_1)\,(4 + 0.8Z_2) - \frac{(50)^4 \times 10^3}{8}\,(10 + 1.5Z_3)$$

With $Z_i = \beta\,\alpha_i$, the limit state equation is rewritten:

$$g\,(\{Z\}) = 10^6\left(1200\,\beta\,\alpha_1 + 2400\,\beta\,\alpha_2 + 240\,\beta^2\,\alpha_1\,\alpha_2 - 1171.9\,\beta\,\alpha_3 + 4187.5\right) = 0$$

Solve for β:

$$\beta = -4187.5\,(1200\,\alpha_1 + 2400\,\alpha_2 + 240\,\beta\,\alpha_1\,\alpha_2 - 1171.9\,\alpha_3)^{-1} \qquad \text{(a)}$$

Equation 24.21 gives:

$$\alpha_1 = -\frac{(1200 + 240\,\alpha_2)}{(\text{Sum})^{1/2}};\quad \alpha_2 = -\frac{(2400 + 240\,\beta\,\alpha_1)}{(\text{Sum})^{1/2}};\quad \alpha_3 = \frac{1171.9}{(\text{Sum})^{1/2}} \qquad \text{(b)}$$

where Sum is the quantity in the square brackets in Eq. 24.21. Start the iteration by: $\beta = 2.5$; $\alpha_1 = \alpha_2 = -\sqrt{1/3}$; $\alpha_3 = \sqrt{1/3}$.

Substitution of these values in the recurrent Eqs. (a) and (b) gives the improved values in column 3 of Table 24.2; repetition gives the values in columns 4 to 6. The last two columns are almost the same. Thus, $\beta = 1.49$.

24.5 Monte Carlo simulation of random variables

This section is a brief introduction to the Monte Carlo method for calculating the probability of failure. The procedure uses uniformly distributed random numbers between 0 and 1, $\{u_1, u_2, \ldots, u_n\}$ to generate standard normal numbers $\{z_1, z_2, \ldots, z_n\}$. Any number u_i is related to z_i by:

$$z_i = \Phi^{-1}\,(u_i) \qquad (24.24)$$

The numbers $\{z\}$ can be used to generate values of the standard normal random variable X using Eq. M.28:

$$X_i = \bar{x}_i + Z_i\,\sigma_{X_i} \qquad (24.25)$$

where $\bar{x}_i$ and σ_{X_i} are mean and standard deviation values of X_i.

Uniformly distributed random numbers $\{u\}$ of between 0 and 1 can be used to generate standard normal numbers $\{z\}$ using Eq. 24.24; then, the z values can be used to generate values of a log-normal random variable X, whose mean and coefficient of variation, $\bar{x}$ and V_X, are known.

$$X_i = \exp\,(\bar{y} + Z_i\,\sigma_Y) \qquad (24.26)$$

Table 24.2 Results of Iterative Calculation in Example 24.6

(1)	*Guess values*	*Improved values*			
	(2)	(3)	(4)	(5)	(6)
β	2.500	1.639	1.493	1.486	1.486
α_1	$-\sqrt{1/3}$	−0.340	−0.326	−0.331	−0.331
α_2	$-\sqrt{1/3}$	−0.817	−0.840	−0.840	−0.839
α_3	$\sqrt{1/3}$	0.466	0.434	0.431	0.431

where

$$\bar{y} = \ln \bar{x} - \frac{1}{2}\sigma_Y^2 \approx \ln \bar{x} \tag{24.27}$$

$$\sigma_Y^2 = \ln\left(1 + V_X^2\right) \approx V_X^2 \tag{24.28}$$

The approximate formulas can be applied if the coefficient of variation does not exceed 0.2. Using the approximate formulas, the following expression is obtained,

$$X_i = \bar{x}_i \exp\left(Z_i V_{X_i}\right) \tag{24.29}$$

A general procedure can be formulated for any type of distribution function. Consider a random variable X with a CDF of $F_X(x)$. To generate values of X_i, the following steps can be taken

1. Generate u_i, uniformly distributed, such that $0 \leq u_i \leq 1$.
2. Calculate X_i from the following formula

$$X_i = F_X^{-1}(u_i) \tag{24.30}$$

where F_X^{-1} is the inverse of F_X.

Example 24.7: Generation of uniformly distributed random variables

Generate 10 uniformly distributed random variables for the dead load D on a structure given that: $\overline{D} = 200\,\text{kN/m}$; $\sigma_D = 20\,\text{kN/m}$. Use the $\{u\}$ values of uniformly distributed variables given in Table 24.3.

In Table 24.3, the values of z are calculated using Eq. 24.24 (or Eq. M.34) and the D values are calculated using Eq. 24.25.

24.5.1 Reliability analysis using the Monte Carlo method

For a given limit state function, $g = g(X_1, \ldots, X_n)$, where $X_1, \ldots, X_n$ are random variables with CDFs of $F_1, \ldots, F_n$ respectively, the probability of failure and the reliability index can be determined by generating a sufficiently large number of values for the random variables $X_1, \ldots, X_n$. For each set of values of $X_1, \ldots, X_n$ generated, the value of g is calculated and saved. The process is repeated M times. The probability of failure, P_f, can be determined in one of the following ways:

1. $P_f = m/M$, where m is the number of negative values of g. However, use of this formula requires at least 10 negative values of g ($m > 10$). If there are no negative values of g ($m = 0$), or if m is less than 10, more values of g have to be generated. The reliability index can be calculated using the previously shown relationship between β and P_f.
2. Plot the CDF of the generated values of g on normal probability paper. The obtained CDF intersects with the vertical axis at the probability of failure (or negative value of the reliability index). If the CDF does not intersect the vertical axis, then either generate more values of g, or extrapolate the lower tail of the CDF.

Table 24.3 Generation of Uniformly Distributed Random Variables from Uniformly Distributed Variables: Example 24.7

u_i	0.25089	0.74099	0.97455	0.74801	0.74908	0.05048	0.92514	0.38575	0.98618	0.03064
z_i	−0.6714	0.6461	1.9527	0.6679	0.6713	−1.6407	1.4408	−0.2900	2.2027	−1.8719
$D_i\left(\frac{\text{kN}}{\text{m}}\right)$	186.6	212.9	239.1	213.4	213.4	167.2	228.8	194.2	244.1	162.6

The Monte Carlo technique is now considered to be the most accurate and most efficient method of the reliability analysis. It is applicable to linear and nonlinear limit state functions. The correlated random variables require special treatment.

24.6 System reliability

In earlier examples in this chapter, the reliability analysis was applied to the calculation of the reliability index of individual components or members of structures. However, most structures consist of systems of interconnected components and members. When considering the system reliability, it is important to recognize that the failure of a single component may or may not cause failure of the structure. Therefore, there is a need to present some techniques to determine (or at least estimate or bound) the probability of failure for a whole structure (system).

There are two extreme types of structural elements (components) that are commonly considered in system reliability analyses. These extreme types are brittle members and ductile members. A member is classified as brittle if the member becomes completely ineffective after it fails. Examples of members that can be classified as brittle include non-reinforced concrete members in tension or a timber beam. Conversely, a ductile element is able to maintain its

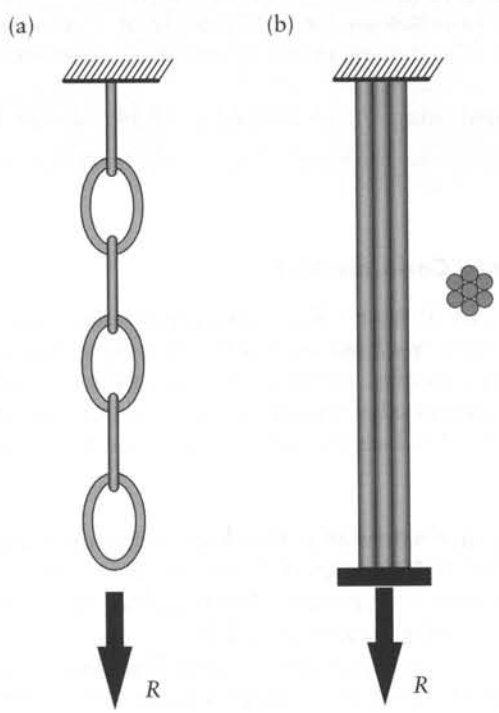

Figure 24.2 Examples of structural systems. (a) Series system. (b) Parallel system.

load-carrying capacity after it fails. An example of a member with ductile behavior would be a member made of low-carbon steel.

There are two idealized types of structural systems. In a series system, the failure of one member leads to immediate failure of the entire system. In contrast, in a parallel system all the members must fail before the system fails. Figures 24.2a and b show examples of the two systems.

24.6.1 Series systems

A series system is sometimes referred to as a *weakest-link system*, because failure of the system corresponds to failure of the weakest element in the system (Figure 24.2a). A statically determinate truss having n members is a series system, because if any member i fails the truss will be unable to carry its load without collapsing. The upper bound of the probability of failure of the series system is:

$$P_f = 1 - \prod_{i=1}^{n} (1 - P_{fi}) \tag{24.31}$$

The lower bound of the probability of failure is $\max(P_{fi})$.

Example 24.8: Probability of failure of a statically determinate truss

A statically determinate truss has 20 members; the reliability index of each is $\beta = 2.0$. What is the probability of failure of the truss?

$$p_{Fi} = \Phi(-\beta) = -\Phi(-2.0) = 22.8 \times 10^{-3}$$

The probability of failure for the truss (Eq. 24.31) is:

$$P_f = 1 - (1 - 22.8 \times 10^{-3})^{20} = 370 \times 10^{-3}$$

In practice, the axial forces in the members are generally different from each other and the reliability index β will not be the same for all members. However, this example shows that P_f of a series system is greater than P_{fi} of its individual elements.

Example 24.9: Probability of failure of a two-hinged frame

Find the probability of failure of the frame shown in Figure 24.3, subjected to independent normally distributed variable loads F_1 and F_2. Define the failure of the system as the event when $g = R - Q < 0$ at sections A or B; where R and Q are the flexural strength and the bending moment due to the applied loads, respectively (assuming that moment redistribution cannot occur). Given: $l_1 = 20$ m; $l_2 = 8$ m; $\overline{F_1} = 100$ kN; $\sigma_{F_1} = 10$ kN; $\overline{F_2} = 10$ kN; $\sigma_{F_2} = 1.5$ kN; EI = constant; $\overline{R_A} = 180$ kN-m; $\overline{R_B} = 260$ kN-m; $\sigma_{R_A} = 18$ kN-m; $\sigma_{R_B} = 26$ kN-m.

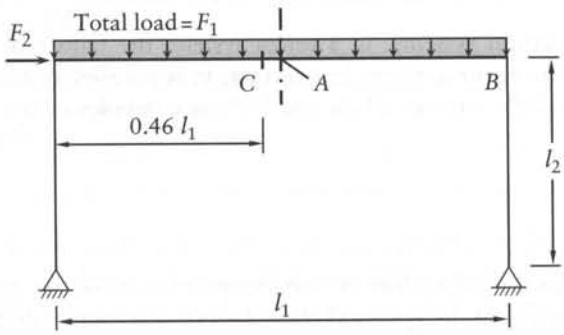

Figure 24.3 The frame of Example 24.9.

The absolute values of the bending moment at A and B are:

$$Q_A = 1.184F_1; \quad Q_B = 1.316F_1 + 4.0F_2$$

$$\overline{g_A} = \overline{R_A} - \overline{Q_A} = 180 - 118.4 = 61.6\,\text{kN-m}$$

$$\overline{g_B} = \overline{R_B} - \overline{Q_B} = 260 - 171.6 = 88.4\,\text{kN-m}$$

Equations M.53 and 24.4 give:

$$\sigma_{g_A} = \sqrt{\sigma_{R_A}^2 + \sigma_{Q_A}^2} = \sqrt{(18)^2 + (1.184 \times 10)^2} = 21.5\,\text{kN-m}$$

$$\sigma_{g_B} = \sqrt{\sigma_{R_B}^2 + \sigma_{Q_B}^2} = \sqrt{(26)^2 + (1.316 \times 10)^2 + (4.0 \times 1.5)^2} = 29.7\,\text{kN-m}$$

The reliability indices and probabilities of failure are:

$$\beta_A = \overline{g_A}/\sigma_{g_A} = 61.6/21.5 = 2.87; \quad P_{f_A} = \Phi(-\beta_A) = \Phi(-2.87) = 2.05 \times 10^{-3}$$

$$\beta_B = \overline{g_B}/\sigma_{g_B} = 88.4/29.7 = 2.98; \quad P_{f_B} = \Phi(-\beta_B) = \Phi(-2.98) = 1.44 \times 10^{-3}$$

The probability of failure of the system (using Eq. 24.31) is in the range between 1.44×10^{-3} and $\left[1 - (1 - 2.05 \times 10^{-3})\,(1 - 1.44 \times 10^{-3})\right] = 3.49 \times 10^{-3}$. The structure is treated as a series system because the failure is defined as the event when the moment at *one* of the sections at A or B reaches a specified limit; this would not be the case when the frame is ductile (see Prob. 24.7 or 24.8).

24.6.2 Parallel systems

A parallel system (Figure 24.2b) can consist of ductile or brittle elements. A parallel system with n *perfectly ductile* elements (e.g. see Figure 18.1) is in a state of failure when all of its elements fail (i.e. yield). Let R_i represent the strength of the ith element in such a system. The system strength will be the sum of all the strengths of the elements, or

$$R = \sum_{i=1}^{n} R_i \tag{24.32}$$

If the strengths of the individual elements are all *uncorrelated normal* variables, then the system strength is also normal with mean and variance values, $\overline{R}$ and σ_R^2 given by:

$$\overline{R} = \sum_{i=1}^{n} \overline{R_i}; \quad \sigma_R^2 = \sum_{i=1}^{n} \sigma_{R_i}^2 \tag{24.33}$$

In practice, it is reasonable to assume R to be normally distributed, even in cases where the R_i variables are non-normal, provided that n is not too small.

Now, let us consider a special case of the parallel system with uncorrelated, perfectly ductile elements. If the R_i variables are identically distributed (i.e. they have the same probability density function and the same cumulative distribution function), then the mean and variance given in Eq. 24.33 become:

$$\overline{R} = n\overline{R_i}; \quad \sigma_R^2 = n\sigma_{R_i}^2 \tag{24.34}$$

The corresponding coefficient of variation would be

$$V_R = \frac{\sigma_R}{\overline{R}} = \frac{\sqrt{n\sigma_{R_i}^2}}{n\overline{R_i}} = \frac{\sigma_{R_i}}{\sqrt{n}\overline{R_i}} = \frac{V_{R_i}}{\sqrt{n}} \tag{24.35}$$

Thus, the coefficient of variation for a system of n parallel, identically distributed elements is smaller than the coefficient of variation of each element. The probability of failure due to a deterministic load on a system of n parallel elements is:

$$P_f = \prod_{i=1}^{n} P_{fi} \tag{24.36}$$

The probability of failure, P_f, of a parallel system is generally much less than that of any of its elements, P_{fi}; e.g. with $n = 2$, probability index $\beta_1 = \beta_2 = 1$, $P_{f1} = P_{f2} = 1.59 \times 10^{-3}$ and $P_f = (1.59 \times 10^{-3})^2 = 2.53 \times 10^{-6}$.

Now consider a parallel system consisting of n *perfectly brittle* elements. For this type of system, if one of the brittle elements fails, it loses its capacity to carry load. The load must be redistributed to the remaining $(n-1)$ elements. If, after the load has been redistributed, the system does not fail, the load can be increased until the next element fails. Then, the load is redistributed among the remaining $(n-2)$ elements. This process of failure and load redistribution continues until overall failure of the system.

Let $R_1, R_2, \ldots, R_n$ represent the strengths of n perfectly brittle elements arranged such that $R_1 < R_2 < \ldots < R_n$. The strength of the system, R, is

$$R = \max[nR_1, (n-1)R_2, (n-2)R_3, \ldots, 2R_{n-1}, R_n] \tag{24.37}$$

When the maximum of Eq. 24.37 is defined by the ith element, the variance of the system is $(n-i+1)\,\sigma_{R_i}^2$. Substitution of this value and R in Eq. 24.4 gives the reliability index β of the system; then Eq. 24.3 can give the probability of the system, p_F.

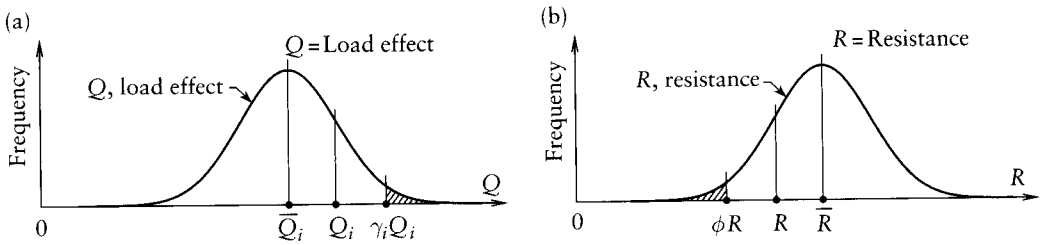

Figure 24.4 Mean, design and factored values of load effect, Q and resistance, R. (a) Load effect. (b) Resistance.

24.7 Load and resistance factors in codes

The basic design formula in load and resistance factor design codes is of the form:

$$\gamma_D D + \gamma_L L + \ldots \leq \phi R \tag{24.38}$$

where D is the dead load, γ_D is the dead load factor, L is the live load, γ_L is the live load factor, R is the resistance, and ϕ is the resistance factor.

To provide an adequate safety level, the design values for load and resistance have to be conservative: design loads are overestimated and load-carrying capacity (resistance) is underestimated (Figures 24.4a and b).

24.8 General

An introduction to the relatively new topic of reliability analysis of structures is presented in this chapter. For more complete study of the subject, refer to specialized publications.[2]

Problems

24.1 SI units. A reinforced concrete cantilever of length $l = 4.0$ m carries at its free end a load W combined with a uniform load w/unit length. Both W and w are normal random variables whose mean and standard deviation values are: $\overline{W} = 860$ kN; $\sigma_W = 160$ kN; $\overline{w} = 40$ kN/m; $\sigma_w = 3$ kN/m. What is the probability that the bending moment exceeds 4300 kN-m? What is the probability that the shearing force exceeds 1200 kN?

24.2 Imperial units. What is the probability that the bending moment in the cantilever in Prob. 24.1 exceeds 3170 kip-ft? What is the probability that the shearing force exceeds 270 kips? Data: $l = 13.1$ ft; $\overline{W} = 193$ kips; $\sigma_W = 36$ kips; $\overline{w} = 2.75$ kip/ft; $\sigma_w = 2.1$ kip/ft.

2 Nowak, A.S. and Collins, K.R., *Reliability of Structures*, McGraw-Hill, New York, 2000, 338 pp.; Melchers, R.E., *Structural Reliability Analysis and Prediction*, Ellis Horwood Limited, Chichester, John Wiley and Sons, 2nd ed. 1999, 437 pp.; Thoft-Christensen, P. and Murotzu, M., *Application of Structural Systems Reliability Theory*, Springer Verlag, Berlin, 1986; Stewart, M. and Melchers, R.E., *Probabilistic Risk Assessment of Engineering Systems*, Chapman & Hall, 1997; Madsen, H.O., Krenk, S. and Lind, N.C., *Methods of Structural Safety*, Prentice Hall Inc., Englewood Cliffs, New Jersey, 1986; Walpole, R.E., Myers, R.H., Myers, S.L. and Ye, K., *Probability & Statistics For Engineers and Scientists*, Prentice Hall, Upper Saddle River, NJ, 07458, 8th Edition, 2007, 816 pp.

24.3 SI units. Calculate the probability of failure P_{fM} of the cantilever in Prob. 24.1. Also, calculate the probability of shear failure P_{fV}. Assume that the flexural and the shear strengths, R_M and R_V, are normal random variables, whose values of the mean and the standard deviation are: $\overline{R_M} = 4300$ kN-m; $\sigma_{R_M} = 430$ kN-m; $\overline{R_V} = 1200$ kN; $\sigma_{R_V} = 420$ kN.

24.4 Imperial units. Calculate the probability of flexural failure P_{fM} of the cantilever in Prob. 24.2. Also, calculate the probability of shear failure P_{fV}. Assume that the flexural and the shear strengths, R_M and R_V, are normal random variables, whose values of the mean and the standard deviation are: $\overline{R_M} = 3170$ kip-ft; $\sigma_{R_M} = 317$ kip-ft; $\overline{R_V} = 270$ kips; $\sigma_{R_V} = 90$ kips.

24.5 SI units. A horizontal steel beam ABC has length $l = 20$ m, a totally fixed support at A, and a roller support at C. The beam is subjected to a downward concentrated load W at section B, middle of the span. Calculate the probability of flexural failure as a mechanism with plastic hinges at A and B. Consider that failure occurs when: $g = 1.5\,M_p - (W\,l/4) > 0$ (see Chapter 18), where M_p is the the absolute value of the fully plastic moment strength at A or B. Assume that W and M_p are normal random variables, whose mean and standard deviation values are: $\overline{W} = 200$ kN; $\sigma_W = 40$ kN; $\overline{M_p} = 1150$ kN-m; $\sigma_{M_p} = 120$ kN-m.

24.6 Imperial units. Solve Prob. 24.5 with $l = 60$ ft, $\overline{W} = 45$ kips, $\sigma_W = 9$ kips, $\overline{M_p} = 900$ kip-ft, $\sigma_{M_p} = 100$ kip-ft.

24.7 SI units. Calculate the probability of flexural failure of the frame shown in Figure 24.3 (with $l_1 = 20$ m; $l_2 = 8$ m) as a mechanism with plastic hinges at C and B. Consider that failure occurs when $g = 1.24\,F_1 + 2.16\,F_2 - M_p > 0$ (see Chapter 18), where M_p is the absolute value of the fully plastic hinges at C and B. Assume that F_1, F_2, and M_p are normal random values, whose mean and standard deviation values are: $\overline{F_1} = 100$ kN; $\sigma_{F_1} = 10$ kN; $\overline{F_2} = 10$ kN; $\sigma_{F_2} = 1.5$ kN; $\overline{M_p} = 210$ kN-m; $\sigma_{M_p} = 21$ kN-m.

24.8 Imperial units. Solve Prob. 24.7 with the data: $\overline{F_1} = 22.5$ kips; $\sigma_{F_1} = 2.25$ kips; $\overline{F_2} = 2.25$ kips; $\sigma_{F_2} = 0.34$ kips; $\overline{M_p} = 155$ kip-ft; $\sigma_{M_p} = 15.5$ kip-ft; $l_1 = 65.6$ ft; $l_2 = 26.2$ ft; $g = 4.07\,F_1 + 7.09\,F_2 - M_p > 0$.

24.9 Imperial (or SI) units. Using the Monte Carlo method, calculate the probability of failure of a steel beam. The limit state function is $g = f_y Z - (D + L)$. Assume that the yield stress, f_y, and the bending moments due to dead load, D, and live load, L, are random variables with the statistical parameters given below, and the plastic section modulus is $Z = 80$ in.^{3} (1.31×10^{-3} m^3) (deterministic value).

Parameter	*Mean*	*V*	*Type of distribution*
f_y	60 ksi (414 MPa)	0.09	Log-normal
D	80 k-ft (108 kN-m)	0.10	Normal
L	120 k-ft (163 kN-m)	0.18	Extreme type I

Appendix A

Matrix algebra

A.1 Determinants

The determinant of a square matrix is denoted by $|S|$. This indicates specified arithmetical operations with the elements of the square matrix $[S]$, which result in a single number. A determinant $|S|$ is said to be of order n if $[S]$ is a square matrix of order $n \times n$.

A second-order determinant is defined as

$$|S| = \begin{vmatrix} S_{11} & S_{12} \\ S_{21} & S_{22} \end{vmatrix} = S_{11}\, S_{22} - S_{12}\, S_{21} \tag{A.1}$$

The operations for a determinant of higher order will be defined later in this section.

The *minor* M_{ij} of element S_{ij} in determinant $|S|$ is defined as the determinant obtained by omission of the ith row and jth column of $|S|$. For example, in the third-order determinant

$$|S| = \begin{vmatrix} S_{11} & S_{12} & S_{13} \\ S_{21} & S_{22} & S_{23} \\ S_{31} & S_{32} & S_{33} \end{vmatrix}$$

the minor M_{32} is given by

$$M_{32} = \begin{vmatrix} S_{11} & S_{13} \\ S_{21} & S_{23} \end{vmatrix}$$

It is apparent that if $|S|$ is of order n, any minor is a determinant of order $n-1$.

The *cofactor* Co_{ij} of element S_{ij} is obtained from the minor M_{ij} as follows:

$$Co_{ij} = (-1)^{i+j} M_{ij} \tag{A.2}$$

Thus, in the above example,

$$Co_{32} = (-1)^{3+2}\, M_{32} = -M_{32}$$

A determinant of order n can be evaluated from the cofactors of any row i, thus:

$$|S| = \sum_{j=i}^{n} S_{ij}\, Co_{ij} \tag{A.3}$$

Alternatively, the determinant can be evaluated from the cofactors of any column j, thus:

$$|S| = \sum_{i=1}^{n} S_{ij}\, Co_{ij} \tag{A.4}$$

Equations A.3 and A.4 are called *Laplace expansion equations*.

Properties of determinants. Some useful properties of determinants are listed below.

1. If all elements in one row or one column are zero, the determinant is zero.
2. When any two rows or two columns are interchanged, the sign of the determinant is changed.
3. The determinant of a matrix is the same as the determinant of its transpose.
4. If the elements in a row (or column) are multiplied by a constant and the result added to the corresponding elements in another row (or column), the determinant is not changed.
5. If one row (or column) can be generated by linear combination of other row(s) (or columns), the determinant is zero. From this it follows that if two rows or columns are identical, the determinant is zero.
6. The sum of the product of the elements in one row i by the corresponding cofactors of another row m is zero. Thus, for a matrix $[S]_{n\times n}$,

$$\sum_{j=1}^{n} S_{ij}\, Co_{mj} = 0 \text{ (when } i \neq m) \tag{A.5}$$

This is the general form of Laplace expansion; it can be compared with Eq. A.3, which gives the value of the determinant $|S|$ when $m = i$. Similarly, when the product is for the elements in a column j with the cofactors of another column m, we can write

$$\sum_{i=1}^{n} S_{ij}\, Co_{im} = 0 \text{ (when } j \neq m) \tag{A.6}$$

The summation is equal to $|S|$ when $m = j$ (see Eq. A.4).

This last property will be used to derive the inverse of a matrix.

Matrix inversion using cofactors: Consider a matrix $[S]_{n\times n}$ for which the inverse $[S]^{-1}$ is to be derived. We form a new matrix $[Co]$ consisting of cofactors Co_{ij} of the elements of $[S]$, and then form the product

$$[S]_{n\times n}\, [Co]^{T}_{n\times n} = [B]_{n\times n} \tag{A.7}$$

From the definition of matrix multiplication, any element of $[B]$ is

$$B_{ij} = \sum_{r=1}^{n} S_{ir}\, Co_{jr}$$

From Eqs. A.3 and A.5 we can see that the summation in the above equation is zero when $i \neq j$, and equals $|S|$ when $i = j$. Therefore, $[B]$ is a diagonal matrix with all the diagonal elements equal to $|S|$. Thus, we can write $[B] = |S|\,[I]$. Hence, by substituting in Eq. A.35 and dividing by $|S|$, we obtain

$$\frac{1}{|S|}\,[S]\,[Co]^{T} = [S]\,[S]^{-1} = [I]$$

whence

$$[S]^{-1} = \frac{[Co]^T}{|S|} \tag{A.8}$$

From Eq. A.36 it is apparent that the division by $|S|$ is possible only when $|S| \neq 0$. It follows that only matrices which have a nonzero determinant have an inverse. When its determinant is zero, a matrix is said to be *singular* (and its inverse does not exist).

A.2 Solution of simultaneous linear equations

Consider a system of n linear equations with n unknowns

$$[a]_{n\times n}\,\{x\}_{n\times 1} = \{c\}_{n\times 1} \tag{A.9}$$

If all the elements in $\{c\}$ are zero, the system is called *homogeneous*. This system occurs in *eigenvalue* or *characteristic-value* problems, such as stability and vibration problems in structural analysis. In this section, we shall deal only with *nonhomogeneous* equations for which not all the elements of $\{c\}$ are zero.

A unique solution of a system of nonhomogeneous equations exists when the determinant $|a|$ is nonzero. If $|a| = 0$, that is, if matrix $[a]$ is singular, Eq. A.9 may have no solution or may have an infinite number of solutions. If the determinant $|a|$ is small compared with the cofactors of $[a]$, the system of equations is said to be *ill-conditioned*, in contrast to *well-conditioned* equations. The determinant $|a|$ of ill-conditioned equations is said to be *almost singular*.

For the purposes of this book, it is useful to mention two methods of solving a system of simultaneous equations. According to one of these, known as *Cramer's rule*, the solution of Eq. A.9 is:

$$\left.\begin{aligned}
x_1 &= \frac{1}{|a|}\begin{vmatrix} c_1 & a_{12} & \dots & a_{1n} \\ c_2 & a_{12} & \dots & a_{2n} \\ \dots & \dots & \dots & \dots \\ c_n & a_{n2} & \dots & a_{nn} \end{vmatrix} \\
x_2 &= \frac{1}{|a|}\begin{vmatrix} a_{11} & c_1 & \dots & a_{1n} \\ a_{21} & c_2 & \dots & a_{2n} \\ \dots & \dots & \dots & \dots \\ a_{n1} & c_n & \dots & a_{nn} \end{vmatrix} \\
x_n &= \frac{1}{|a|}\begin{vmatrix} a_{11} & a_{12} & \dots & c_1 \\ a_{21} & a_{22} & \dots & c_2 \\ \dots & \dots & \dots & \dots \\ a_{n1} & a_{n2} & \dots & c_n \end{vmatrix}
\end{aligned}\right\} \tag{A.10}$$

Each of the unknowns x_i is found by multiplying the reciprocal of the determinant $|a|$ by the determinant of a matrix which has the same elements as $|a|$ except that the ith column is replaced by the column vector $\{c\}$. The evaluation of the determinants involves a large number of operations, and Cramer's rule is perhaps the most suitable method when the number of equations is 2 or 3. When the number of equations is greater, other methods require fewer operations. However, Cramer's rule serves to explain some of the preceding statements related to the case when the determinant $|a|$ is small or zero.

As an example of the use of Cramer's rule, let us consider the equations

$$\begin{bmatrix} S_{11} & S_{12} \\ S_{21} & S_{22} \end{bmatrix} \begin{Bmatrix} D_1 \\ D_2 \end{Bmatrix} = \begin{Bmatrix} F_1 \\ F_2 \end{Bmatrix} \tag{A.11}$$

Applying Eq. A.38,

$$\left.\begin{aligned} D_1 &= \frac{\begin{vmatrix} F_1 & S_{12} \\ F_2 & S_{22} \end{vmatrix}}{\begin{vmatrix} S_{11} & S_{12} \\ S_{21} & S_{22} \end{vmatrix}} = \frac{F_1 S_{22} - F_2 S_{12}}{S_{11} S_{22} - S_{12} S_{21}} \\ \text{and} \\ D_2 &= \frac{\begin{vmatrix} S_{11} & F_1 \\ S_{21} & F_2 \end{vmatrix}}{\begin{vmatrix} S_{11} & S_{12} \\ S_{21} & S_{22} \end{vmatrix}} = \frac{F_2 S_{11} - F_1 S_{21}}{S_{11} S_{22} - S_{12} S_{21}} \end{aligned}\right\} \tag{A.12}$$

The inverse of $[S]$ may be found, as explained in Section A.7, by solving Eq. A.12 twice: once with $\{F_1, F_2\} = \{1, 0\}$ and the second time with $\{F_1, F_2\} = \{0, 1\}$. Thus,

$$\begin{bmatrix} S_{11} & S_{12} \\ S_{21} & S_{22} \end{bmatrix}^{-1} = \frac{1}{(S_{11} S_{22} - S_{12} S_{21})} \begin{bmatrix} S_{22} & -S_{12} \\ -S_{21} & S_{11} \end{bmatrix} \tag{A.13}$$

We can see then that the inverse of a matrix of order 2×2 is the product of the reciprocal of the determinant and of a matrix in which the two elements on the main diagonal of the original matrix are interchanged, and the other two elements change sign.

The method which is most commonly used to solve linear equations (and to invert matrices) is the method of elimination, introduced in elementary algebra. Several procedures of the elimination process have been developed,[1] and standard programs are now available for computers. A discussion of these procedures and of their advantages is beyond the scope of this book, and we shall limit ourselves here to one procedure suitable for the use of a small calculator.

In the procedure suggested by P.D. Crout,[2] the calculation is arranged in two tables. Let us consider it with reference to a system of four equations $[a]_{4\times4}\ \{x\}_{4\times1} = \{C\}_{4\times1}$. The tables are:
Given equations

a_{11}	a_{12}	a_{13}	a_{14}	c_1
a_{21}	a_{22}	a_{23}	a_{24}	c_2
a_{31}	a_{32}	a_{33}	a_{34}	c_3
a_{41}	a_{42}	a_{43}	a_{44}	c_4

1 See references on numerical procedures, for example, Crandall, S.H., *Engineering Analysis,* McGraw-Hill, New York, 1956.

2 Crout, P. D., "A Short Method for Evaluating Determinants and Solving Systems of Linear Equations with Real or Complex Coefficients," *Trans. AIEE,* 60 (1941), pp. 1235–1240.

Auxiliary quantities

b_{11}	b_{12}	b_{13}	b_{14}	d_1
b_{21}	b_{22}	b_{23}	b_{24}	d_2
b_{31}	b_{32}	b_{33}	b_{34}	d_3
b_{41}	b_{42}	b_{43}	b_{44}	d_4

Solution

x_1	x_2	x_3	x_4

The first table requires no computation, and is simply formed by the elements of $[a]$ and $\{c\}$.

The second table contains auxiliary quantities which are determined following a set pattern of computation. The elements in the first column of this table $\{b_{11}, b_{21}, b_{31}, b_{41}\}$ are the same as the column $\{a_{11}, a_{21}, a_{31}, a_{41}\}$, and are simply copied from the first table. The quantities in the first row are determined as follows:

$$[b_{12}\ b_{13}\ b_{14}\ d_1] = \frac{1}{b_{11}}[a_{12}\ a_{13}\ a_{14}\ c_1]$$

Then the second column (b_{22} to b_{42}) is completed from the following:

$$\begin{Bmatrix} b_{22} \\ b_{32} \\ b_{42} \end{Bmatrix} = \begin{Bmatrix} (a_{22} - b_{21}\ \ b_{12}) \\ (a_{32} - b_{31}\ \ b_{12}) \\ (a_{42} - b_{41}\ \ b_{12}) \end{Bmatrix}$$

Next, the second row (b_{23} to d_2) is completed from

$$[b_{23}\ b_{24}\ d_2] = \frac{1}{b_{22}}[(a_{23} - b_{21}\ b_{13}), (a_{24} - b_{21}\ b_{14}), (c_2 - b_{21}\ d_1)]$$

Proceeding diagonally downward, a column is completed starting from the diagonal element b_{ii}, followed by a row to the right of the diagonal. The elements required to complete the third column and the third row in the above example are calculated as follows:

$$\begin{Bmatrix} b_{33} \\ b_{43} \end{Bmatrix} = \begin{Bmatrix} (a_{33} - b_{31}\ \ b_{13} - b_{32}\ \ b_{23}) \\ (a_{43} - b_{41}\ \ b_{13} - b_{42}\ \ b_{23}) \end{Bmatrix}$$

$$[b_{34}\ d_3] = \frac{1}{b_{33}}[(a_{34} - b_{31}\ b_{14} - b_{32}\ b_{24}), (c_3 - b_{31}\ d_1 - b_{32}\ d_2)]$$

Finally, to complete the last row, the elements b_{44} and d_4 are determined:

$$b_{44} = a_{44} - b_{41}\ b_{14} - b_{42}\ b_{24} - b_{43}\ b_{34}$$

$$d_4 = \frac{1}{b_{44}}(c_4 - b_{41}\ d_1 - b_{42}\ d_2 - b_{43}\ d_3)$$

From the above we can see that the diagonal elements b_{11}, b_{22}, b_{33}, and b_{44} and the elements below the diagonal in Crout's second table are determined by one pattern of operations. The

same pattern is followed for the remainder of the table, except that division by the diagonal element b_{ii} has also to be carried out.

All these operations can be summarized as follows. Any element b_{ij}, such that $j \leq i$, is calculated by

$$b_{ij} = a_{ij} - \sum_{r=1}^{j-1} b_{ir}\, b_{rj} \tag{A.14}$$

An element b_{ij}, such that $i < j$, is determined by

$$b_{ij} = \frac{1}{b_{ii}} \left[a_{ij} - \sum_{r=1}^{i-1} b_{ir}\, b_{rj} \right] \tag{A.15}$$

The elements $d_1, \ldots, d_4$ are determined by Eq. A.15, treating the columns $\{c\}$ and $\{d\}$ as if they were the last columns of matrices $[a]$ and $[b]$ respectively.

The above procedure is, in fact, a process of elimination in which the original equations are reduced to

$$\begin{bmatrix} 1 & b_{12} & b_{13} & b_{14} \\ 0 & 1 & b_{23} & b_{24} \\ 0 & 0 & 1 & b_{34} \\ 0 & 0 & 0 & 1 \end{bmatrix} \begin{Bmatrix} x_1 \\ x_2 \\ x_3 \\ x_4 \end{Bmatrix} = \begin{Bmatrix} d_1 \\ d_2 \\ d_3 \\ d_4 \end{Bmatrix} \tag{A.16}$$

The values of x_i can now be determined by a process of back substitution starting from the last equation, thus,

$$\left.\begin{aligned} x_4 &= d_4 \\ x_3 &= d_3 - b_{34}\, x_4 \\ x_2 &= d_2 - b_{23}\, x_3 - b_{24}\, x_4 \\ x_1 &= d_1 - b_{12}\, x_2 - b_{13}\, x_3 - b_{14}\, x_4 \end{aligned}\right\} \tag{A.17}$$

In practice, Eqs. A.16 and A.17 need not be written down, and the answers are put directly in a row below the tables. From Eq. A.17 we can see that, in a general case, each of the unknowns x_j is determined by

$$x_j = d_j - \sum_{r=j+1}^{n} b_{jr}\, x_r \tag{A.18}$$

where n is the number of the unknowns (or of equations).

If we want to invert $[a]$, the columns $\{c\}$ are replaced by n columns forming a unit matrix. These columns are treated in the same way as $\{c\}$ in the preceding discussion, and the column $\{d\}$ is replaced by a matrix $[d]_{n \times n}$. Back substitution in Eq. A.18 with the elements of d in each column of this matrix gives a column of the inverse matrix.

If matrix $[a]$ is symmetrical, which is usually the case in equations needed in structural analysis, the arithmetical operations are reduced considerably as each of the auxiliary quantities b_{ij} to the right of the diagonal is related to an element b_{ji} below the diagonal by

$$b_{ij} = \frac{b_{ji}}{b_{ii}} \quad i < j \tag{A.19}$$

The following tables are an example of the application of Crout's procedure to the solution of four symmetrical equations.

Given equations

5	−4	1	0	1
−4	6	−4	1	−4
1	−4	6	−4	11
0	1	−4	7	−5

Auxiliary quantities

5	$-\frac{4}{5}$	$\frac{1}{5}$	0	$\frac{1}{5}$
−4	$\frac{14}{5}$	$-\frac{8}{7}$	$\frac{5}{14}$	$-\frac{8}{7}$
1	$-\frac{16}{5}$	$\frac{15}{7}$	$-\frac{4}{3}$	$\frac{10}{3}$
0	1	$-\frac{20}{7}$	$\frac{17}{6}$	2

Solution

3	5	6	2

A.3 Eigenvalues

In the preceding section we mentioned the solution of the equation $[a]_{n\times n}\{x\}_{n\times 1}=\{0\}$. This is of interest when $[a]=[b]_{n\times n}-\lambda[I]_{n\times n}$ and λ is unknown. In other words, we require the solution of

$$([b]_{n\times n}-\lambda[I]_{n\times n})\{x\}_{n\times 1}=\{0\} \tag{A.20}$$

Equation A.20 can also be written as

$$[b]_{n\times n}\{x\}_{n\times 1}=\lambda\{x\}_{n\times 1} \tag{A.21}$$

which means that pre-multiplying a column vector by a matrix results in a multiple of the column vector. Such a column vector is known as an *eigenvector* of the matrix, and the multiplier is called an *eigenvalue* or characteristic value.

Equation A.20 represents a system of n homogenous linear equations, and its solution arising from $\{x\}=\{0\}$, is given by the determinant

$$|[b]-\lambda[I]|=0 \tag{A.22}$$

For example, if we want to find the eigenvalues of the matrix

$$[b] = \begin{bmatrix} 3 & 7 & 9 \\ 7 & 11 & 7 \\ 9 & 7 & 9 \end{bmatrix}$$

we can write from Eq. A.50

$$\begin{vmatrix} 3-\lambda & 7 & 9 \\ 7 & 11-\lambda & 7 \\ 9 & 7 & 9-\lambda \end{vmatrix} = 0$$

Expanding this determinant with the aid of Eq. A.4,

$$|a| = \sum_{j=1}^{3} a_{ij}\, Co_{ij}$$

and choosing $i = 1$, we obtain

$$|a| = (3-\lambda)[(11-\lambda)(9-\lambda) - 7 \times 7] - 7[7(9-\lambda) - 7 \times 9] + 9[7 \times 7 - (11-\lambda) \times 9] = 0$$

from which

$$\lambda^3 - 23\lambda^2 - 20\lambda + 300 = 0$$

Hence, the three values of λ are 23.31, 3.44, and -3.75. As expected, the number of eigenvalues is equal to the order of the matrix. In many practical problems, it is only the largest eigenvalue that is of interest.

In general, when $[b]$ is of order n, expansion of the determinant in Eq. A.22 gives a polynomial in λ of the form

$$\lambda^n + c_1\lambda^{n-1} + c_2\lambda^{n-2} + \cdots + c_n = 0 \tag{A.23}$$

This equation is called the *characteristic equation* of the matrix $[b]$, and its solution gives the eigenvalues $\lambda_1, \lambda_2, \ldots, \lambda_n$ which satisfy the conditions

$$\sum_{i=1}^{n} \lambda_i = \sum_{i=1}^{n} b_{ii} \tag{A.24}$$

and

$$\lambda_1 \times \lambda_2 \times \cdots \times \lambda_n = |b| \tag{A.25}$$

The eigenvalues obtained in the preceding examples can be checked by these two equations.

The eigenvector corresponding to the λ values can be found by substituting for λ in Eq. A.20 and solving. Since Eq. A.20 is homogeneous, only relative values of x can be determined for each eigenvalue. We can assume $x_1 = 1$, solve for the other values using $(n-1)$ equations and the last equation can be used to check the calculations.

Instead of evaluating the determinant, we may use an iteration method which leads to the eigenvalue with the *largest absolute value*. In this we assume the value of the eigenvector $\{x\}$ and

substitute it in the left-hand side of Eq. A.21. Hence, we find a value of λ and a new value of $\{x\}$. If this new value of $\{x\}$ is equal to the assumed value, then we have solved the problem: λ is the required eigenvalue, and $\{x\}$ the eigenvector. If, however, there is a discrepancy between the two values of $\{x\}$, we use the new value as an assumed value in the second cycle of evaluating $[b]\{x\}$. We repeat this procedure until Eq. A.21 is satisfied.

In many practical problems, a good estimate of $\{x\}$ corresponding to the largest λ can be made from the physical data available, and rapid convergence is obtained.

As an example, let us consider the matrix $[b]$ given earlier, and assume the vector $\{x^{(1)}\}$ as below. Then

$$\begin{matrix} & & & & \{x^{(1)}\} & & & & \{x^{(2)}\} \\ & & & & \downarrow & & & & \downarrow \\ \begin{bmatrix} 3 & 7 & 9 \\ 7 & 11 & 7 \\ 9 & 7 & 9 \end{bmatrix} & \begin{Bmatrix} 1.0 \\ 1.2 \\ 1.1 \end{Bmatrix} & = & \begin{Bmatrix} 22.2 \\ 28.6 \\ 27.3 \end{Bmatrix} & = 22.2 & \begin{Bmatrix} 1.00 \\ 1.29 \\ 1.23 \end{Bmatrix} \end{matrix}$$

Since $\{x^{(2)}\} \neq \{x^{(1)}\}$, we repeat the multiplication with $\{x^{(2)}\}$:

$$\begin{matrix} & & & & \{x^{(2)}\} & & & & \{x^{(3)}\} \\ & & & & \downarrow & & & & \downarrow \\ \begin{bmatrix} 3 & 7 & 9 \\ 7 & 11 & 7 \\ 9 & 7 & 9 \end{bmatrix} & \begin{Bmatrix} 1.00 \\ 1.29 \\ 1.23 \end{Bmatrix} & = & \begin{Bmatrix} 23.10 \\ 29.80 \\ 29.10 \end{Bmatrix} & = 23.10 & \begin{Bmatrix} 1.00 \\ 1.29 \\ 1.26 \end{Bmatrix} \end{matrix}$$

Since $\{x^{(2)}\} \cong \{x^{(3)}\}$, we have found the eigenvector, and $\lambda \cong 23.1$ is the largest eigenvalue. A third repetition of the multiplication using $\{x^{(3)}\}$ gives $\lambda = 23$, which is very close to the exact solution.

Problems

A.1 Given the matrices

$$[A] = \begin{bmatrix} 1 & 0 & 2 \\ 3 & 1 & 1 \end{bmatrix}; \quad [B] = \begin{bmatrix} 4 & 2 \\ 2 & 3 \end{bmatrix}$$

execute the following matrix operations, if possible:

(a) $[A]\,[B]$ (b) $[A]^T\,[B]$
(c) $[A]^T[B]\,[A]$ (d) $[A]\,[B]^T\,[A]^T$
(e) Prove that, if $[B]$ is symmetrical, the product $[A]^T[B]\,[A]$ must also be symmetrical.

A.2 Given $[A]$ and $[B]$ as in Prob. A.1 and

$$[C] = \begin{bmatrix} 3 & 2 & 0 \\ 1 & 0 & 2 \end{bmatrix}$$

execute the following operations:

(a) $[B]\,[A+C]$ (b) $[B]\,[A]+[B]\,[C]$

Note that the distributive law $[B]\,[A+C]=[B]\,[A]+[B]\,[C]$ applies to matrices.

A.3 Prove that the transpose of the product of two or more matrices is the product of the transposes of the matrices in a reversed order.

A.4 Find the inverse of the following matrices:

$$(a)\begin{bmatrix} 5 & -2 \\ -2 & 3 \end{bmatrix} \quad (b)\begin{bmatrix} 2 & -1 & 0 \\ -1 & 2 & -1 \\ 0 & -1 & 2 \end{bmatrix}$$

$$(c)\begin{bmatrix} 5 & -4 & 1 \\ -4 & 6 & -4 \\ 1 & -4 & 7 \end{bmatrix}$$

A.5 The coordinates 1 and 2 in part (a) of the figure represent the positive directions of forces F_1 and F_2 and displacements D_1 and D_2 at the end A of cantilever AB. The displacements (deflection or rotation) due to unit values of the forces (vertical load or couple) are given in parts (b) and (c); these displacements are arranged in the flexibility matrix

$$[f]=\begin{bmatrix} f_{11} & f_{12} \\ f_{21} & f_{22} \end{bmatrix}=\begin{bmatrix} l/(EI) & -l^2/(2EI) \\ -l^2/(2EI) & l^3/(3EI) \end{bmatrix}$$

Assuming that the displacements $\{D_1, D_2\}$ due to forces $\{F_1, F_2\}$ can be obtained by the superposition equation

$$\begin{bmatrix} f_{11} & f_{12} \\ f_{21} & f_{22} \end{bmatrix}\begin{Bmatrix} F_1 \\ F_2 \end{Bmatrix}=\begin{Bmatrix} D_1 \\ D_2 \end{Bmatrix}$$

(a) Find the displacements due to $F_1=\frac{Pl}{2}$ and $F_2=P$ acting simultaneousy.
(b) Find the forces S_{11} and S_{21} corresponding to the displacements $D_1=1$ and $D_2=0$. Sketch the deflected shape of the beam.
(c) Find the forces S_{12} and S_{22} corresponding to the displacement $D_1=0$ and $D_2=1$. Sketch the deflected shape of the beam.
(d) Show that the stiffness matrix formed by the forces obtained in (b) and (c)

$$[S]=\begin{bmatrix} S_{11} & S_{12} \\ S_{21} & S_{22} \end{bmatrix}$$

is the inverse of the flexibility matrix $[f]$.

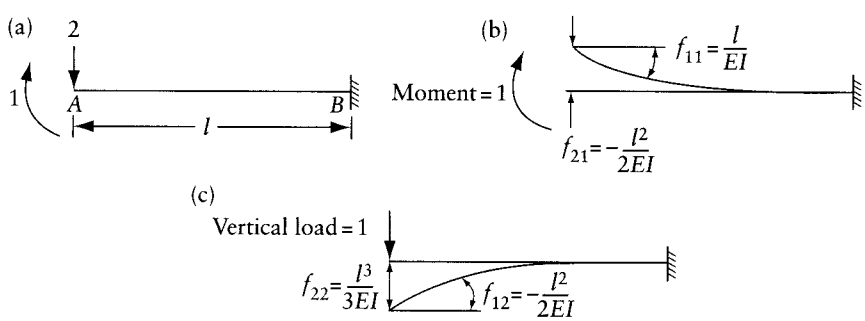

Prob. A.5

A.6 The stiffness matrix for the beam in the figure is

$$[S]=\frac{EI}{l^3}\begin{bmatrix} 9.6 & -8.4 \\ -8.4 & 9.6 \end{bmatrix}$$

The forces $\{F\}=\{F_1, F_2\}$ and the corresponding displacements $\{D\}=\{D_1, D_2\}$ along the coordinates 1 and 2 are related as follows: $[S]\{D\}=\{F\}$.

(a) Sketch the deflected shape of the beam when the forces applied are $F_1 = S_{11}$ and $F_2 = S_{21}$.
(b) Find the inverse of the stiffness matrix $[S]$. What does the resulting matrix signify?

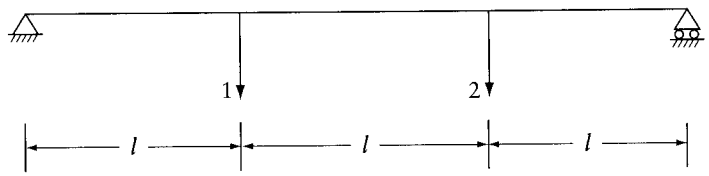

Prob. A.6

A.7 The stiffness matrix of the beam shown in part (a) of the figure is

$$[S] = \frac{4EI_0}{l}\left[\begin{array}{cc:cc} 4 & 0 & 2 & \frac{12}{l} \\ 0 & 2 & 1 & -\frac{6}{l} \\ \hdashline 2 & 1 & 6 & \frac{6}{l} \\ \frac{12}{l} & -\frac{6}{l} & \frac{6}{l} & \frac{72}{l^2} \end{array}\right] \tag{a}$$

The forces P_1, P_2, P_3, and P_4 and the corresponding displacements D_1, D_2, D_3, and D_4 along the coordinates are related as follows:

$$\begin{bmatrix} [S_{11}] & [S_{12}] \\ [S_{21}] & [S_{22}] \end{bmatrix} \begin{Bmatrix} \{D_1\} \\ \{D_2\} \end{Bmatrix} = \begin{Bmatrix} \{F_1\} \\ \{F_2\} \end{Bmatrix} \tag{b}$$

where $[S_{11}]$, $[S_{12}]$ etc., refer to the partitioned matrices in $[S]$ and

$$\{D_1\} = \begin{Bmatrix} D_1 \\ D_2 \end{Bmatrix}; \quad \{D_2\} = \begin{Bmatrix} D_3 \\ D_4 \end{Bmatrix}; \quad \{F_1\} = \begin{Bmatrix} P_1 \\ P_2 \end{Bmatrix}; \quad \{F_2\} = \begin{Bmatrix} P_3 \\ P_4 \end{Bmatrix}$$

By putting $\{F_2\} = \{0\}$ in Eq. (b), find a matrix $[S^*]$ relating the forces to the displacements along the coordinates indicated in Prob. A.7(b), such that

$$[S^*]\{D_1\} = \{F_1\} \tag{c}$$

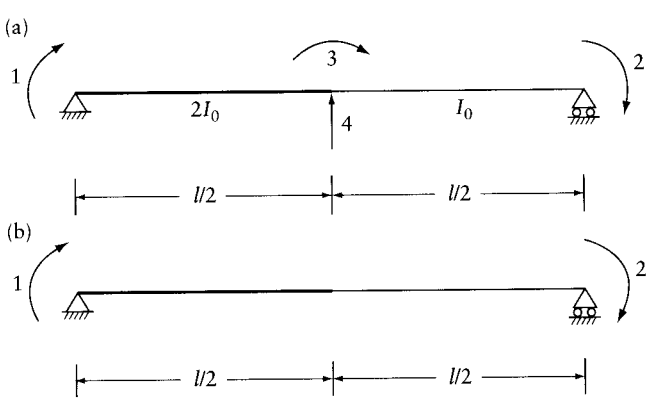

Prob. A.7

A.8 Solve the following simultaneous equations:

$$\begin{bmatrix} 8 & -2 \\ -3 & 11 \end{bmatrix} \begin{Bmatrix} x_1 \\ x_2 \end{Bmatrix} = \begin{Bmatrix} 18 \\ -17 \end{Bmatrix} \tag{a}$$

$$\begin{bmatrix} 4 & -2 & 1 \\ -3 & 8 & -2 \\ 2 & -5 & 10 \end{bmatrix} \begin{Bmatrix} x_1 \\ x_2 \\ x_3 \end{Bmatrix} = \begin{Bmatrix} 2 \\ 13 \\ 27 \end{Bmatrix} \tag{b}$$

$$\begin{bmatrix} 2 & 1 & 0 \\ 1 & 2 & 1 \\ 0 & 1 & 2 \end{bmatrix} \begin{Bmatrix} x_1 \\ x_2 \\ x_3 \end{Bmatrix} = \begin{Bmatrix} 1 \\ 1 \\ 1 \end{Bmatrix} \tag{c}$$

$$\frac{EI}{l} \begin{bmatrix} \frac{108}{l^2} & -\frac{6}{l} & -\frac{24}{l} \\ -\frac{6}{l} & 8 & 2 \\ -\frac{24}{l} & 2 & 12 \end{bmatrix} \begin{Bmatrix} D_1 \\ D_2 \\ D_3 \end{Bmatrix} = P \begin{Bmatrix} 0.5 \\ l \\ -\frac{l}{8} \end{Bmatrix} \tag{d}$$

$$\frac{l}{6EI} \begin{bmatrix} 4 & 1 & 0 \\ 1 & 4 & 1 \\ 0 & 1 & 4 \end{bmatrix} \begin{Bmatrix} F_1 \\ F_2 \\ F_3 \end{Bmatrix} = \begin{bmatrix} \frac{1}{l} \\ 0 \\ 0 \end{bmatrix} \tag{e}$$

A.9 Find the eigenvalues for the matrices in Prob. A.4 (a) and (c). Calculate the eigenvector corresponding to the highest eigenvalue.

A.10 Using iteration, evaluate the smallest eigenvalue of the matrix

$$[a] = \begin{bmatrix} 2 & -1 & 0.5 \\ -1 & 2 & 0 \\ -1 & -1 & 3.5 \end{bmatrix}$$

The eigenvalues of $[a]^{-1}$ are the reciprocals of those for $[a]$. To find by iteration the largest eigenvalue of $[a]^{-1}$, assume that the eigenvector represents the buckling mode of a strut hinged at one end and encastré at the other. The elements of the eigenvector are proportional to the deflections at equally-spaced points on the axis of the strut. (See Figure 14.8b.)

Appendix B

Displacements of prismatic members

The following table gives the displacements in beams of constant flexural rigidity EI and constant torsional rigidity GJ, subjected to the loading shown on each beam. The positive directions of the displacements are downward for translation, clockwise for rotation. The deformations due to shearing forces are neglected.

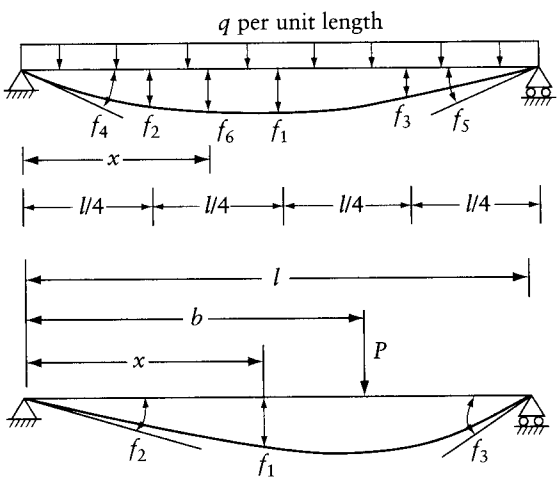

$$f_1 = \frac{5}{384}\frac{ql^4}{EI} \tag{B.1}$$

$$f_2 = f_3 = \frac{19}{2048}\frac{ql^4}{EI} \tag{B.2}$$

$$f_4 = -f_5 = \frac{ql^3}{24EI} \tag{B.3}$$

$$f_6 = \frac{qx}{24EI}(l^3 - 2lx^2 + x^3) \tag{B.4}$$

$$f_1 = \frac{P(l-b)x}{6lEI}(2lb - b^2 - x^2) \quad \text{when } x \leqslant b \tag{B.5}$$

$$f_1 = \frac{Pb(l-x)}{6lEI}(2lx - x^2 - b^2) \quad \text{when } x \geqslant b \tag{B.6}$$

$$f_2 = \frac{Pb(l-b)}{6lEI}(2l - b) \quad f_3 = -\frac{Pb}{6lEI}(l^2 - b^2) \tag{B.7}$$

When $b = l/2$, $f_2 = -f_3 = Pl^2/(16EI)$, and $f_1 = Pl^3/48EI$ at $x = l/2$ (B.8)

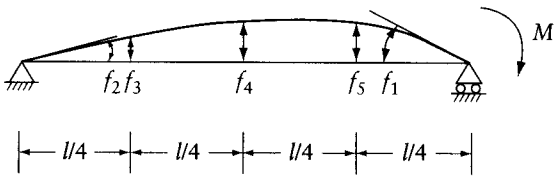

$$f_1 = \frac{Ml}{3EI} \tag{B.9}$$

$$f_2 = -\frac{Ml}{6EI} \tag{B.10}$$

$$f_3 = -\frac{15Ml^2}{384EI} \tag{B.11}$$

$$f_4 = \frac{Ml^2}{16EI} \tag{B.12}$$

$$f_5 = -\frac{21Ml^2}{384EI} \tag{B.13}$$

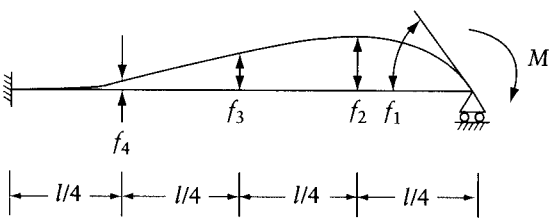

$$f_1 = \frac{Ml}{4EI} \tag{B.14}$$

$$f_2 = -\frac{9Ml^2}{256EI} \tag{B.15}$$

$$f_3 = -\frac{Ml^2}{32EI} \tag{B.16}$$

$$f_4 = -\frac{3Ml^2}{256EI} \tag{B.17}$$

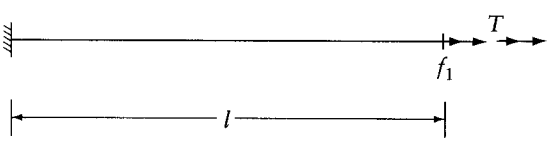

$$f_1 = \frac{Tl}{GJ} \tag{B.18}$$

(Effect of warping ignored)

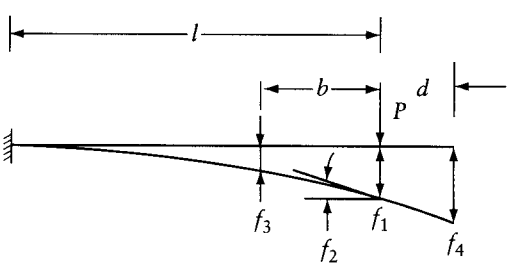

$$f_1 = \frac{Pl^3}{3EI} \tag{B.19}$$

$$f_2 = Pl^2/2EI \tag{B.20}$$

$$f_4 = f_1 + df_2 \tag{B.21}$$

$$f_3 = \frac{Pl^3}{3EI}\left(1 - \frac{3b}{2l} + \frac{b^3}{2l^3}\right)$$

for $0 \leqslant b \leqslant l$ (B.22)

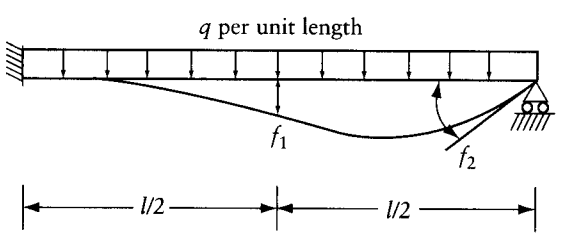

$$f_1 = \frac{ql^4}{192EI} \tag{B.23}$$

$$f_2 = -\frac{ql^3}{48EI} \tag{B.24}$$

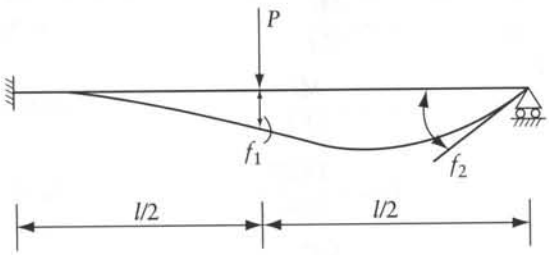

$$f_1 = \frac{7Pl^3}{768EI} \tag{B.25}$$

$$f_2 = -\frac{Pl^2}{32EI} \tag{B.26}$$

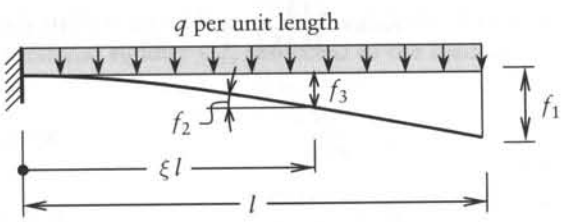

$$f_1 = \frac{ql^4}{8EI} \tag{B.27}$$

$$f_2 = \frac{ql^3}{6EI}(3\xi - 3\xi^2 + \xi^3) \tag{B.28}$$

$$f_3 = \frac{ql^4}{24EI}(6\xi^2 - 4\xi^3 + \xi^4) \tag{B.29}$$

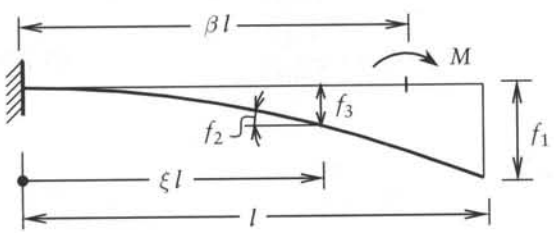

$$f_1 = \frac{Ml^2}{EI}\beta(1 - 0.5\beta) \tag{B.30}$$

$$f_2 = \begin{cases} Ml\xi/(EI) \text{ with } \xi \le \beta \\ Ml\beta/(EI) \text{ with } \beta < \xi \le 1 \end{cases} \tag{B.31}$$

$$f_3 = \begin{cases} M(\xi l)^2/(2EI) \text{ with } \xi \le \beta \\ Ml^2\beta(\xi - 0.5\beta)/(EI) \\ \quad \text{with } \beta < \xi \le 1 \end{cases} \tag{B.32}$$

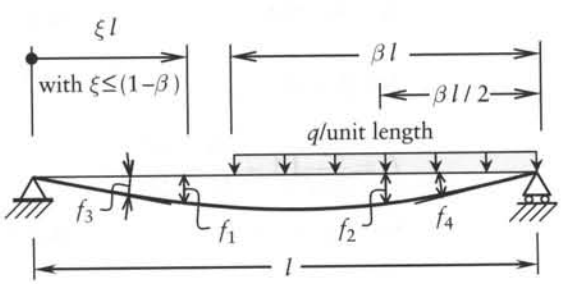

$$f_1 = \frac{ql^2}{24EI}\beta^2\xi(2 - \beta^2 - 2\xi^2) \tag{B.33}$$

$$f_2 = \frac{ql^4}{384EI}\beta^3(32 - 39\beta + 12\beta^2) \tag{B.34}$$

$$f_3 = \frac{ql^3}{24EI}\beta^2(2 - \beta^2) \tag{B.35}$$

$$f_4 = -\frac{ql^3}{24EI}\beta^2(4 - 4\beta + \beta^2) \tag{B.36}$$

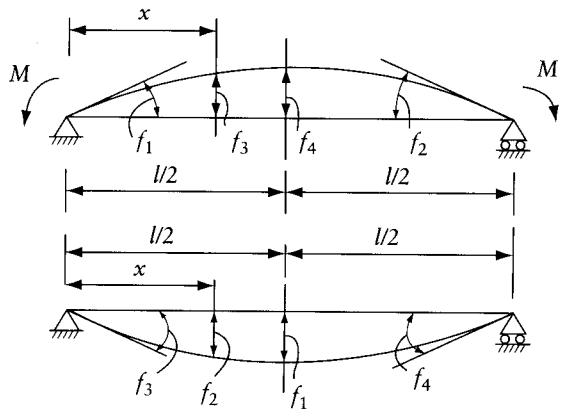

$$f_1 = -f_2 = -\frac{Ml}{2EI} \tag{B.37}$$

$$f_3 = -\frac{Mx(l-x)}{2EI} \qquad f_4 = -\frac{Ml^2}{8EI} \tag{B.38}$$

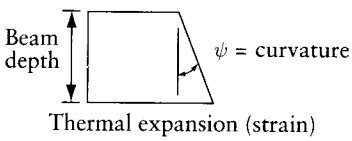

$$f_1 = \psi l^2/8 \tag{B.39}$$

$$f_2 = \frac{\psi x(l-x)}{2} \tag{B.40}$$

$$f_3 = -f_4 = \frac{\psi l}{2} \tag{B.41}$$

Appendix C

Fixed-end forces of prismatic members

The following table gives the fixed-end forces in beams of constant flexural rigidity and constant torsional rigidity due to applied loads. The forces are considered positive if upward or in the clockwise direction. A twisting couple is positive if it acts in the direction of rotation of a right-hand screw progressing to the right. When the end-forces are used in the displacement method, appropriate signs have to be assigned according to the chosen coordinate system.

	Fixed-End Force	
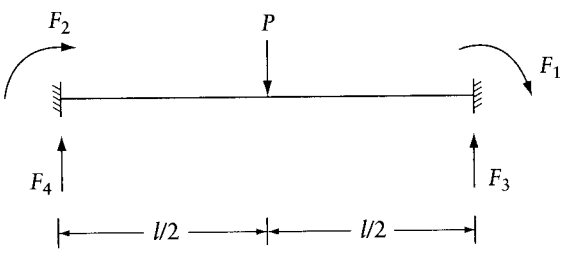	$F_1 = -F_2 = \frac{Pl}{8}$	(C.1)
	$F_3 = F_4 = \frac{P}{2}$	(C.2)
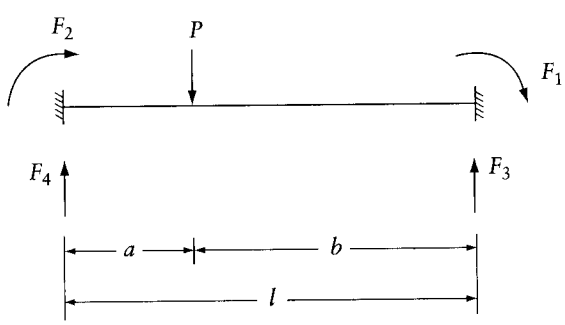	$F_1 = \frac{Pa^2b}{l^2}$	(C.3)
	$F_2 = -\frac{Pab^2}{l^2}$	(C.4)
	$F_3 = P\left(\frac{a}{l} + \frac{a^2b}{l^3} - \frac{ab^2}{l^3}\right)$	(C.5)
	$F_4 = P\left(\frac{b}{l} - \frac{a^2b}{l^3} + \frac{ab^2}{l^3}\right)$	(C.6)
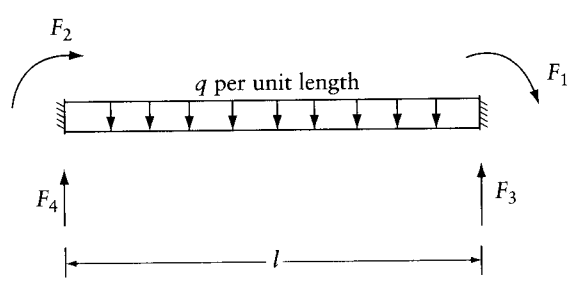	$F_1 = -F_2 = \frac{ql^2}{12}$	(C.7)
	$F_3 = F_4 = \frac{ql}{2}$	(C.8)

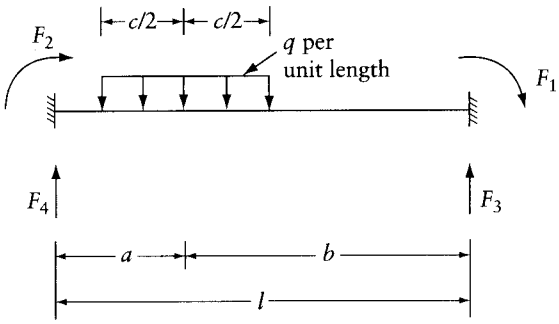

Fixed-End Force

$$F_1 = \frac{qc}{12l^2}[12a^2b + c^2(l - 3a)]$$

$$F_2 = -\frac{qc}{12l^2}[12ab^2 + c^2(l - 3b)]$$

$$F_3 = \frac{qca}{l} + \frac{(F_1 + F_2)}{l}$$

$$F_4 = \frac{qcb}{l} - \frac{(F_2 + F_1)}{l}$$

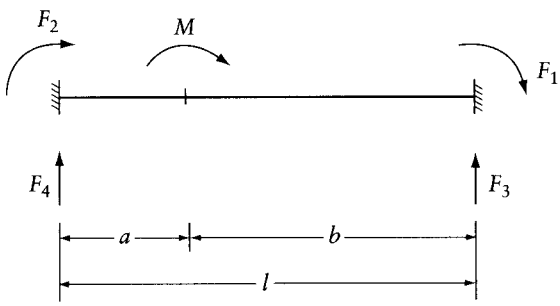

$$F_1 = \frac{Ma}{l}\left(2 - \frac{3a}{l}\right)$$

$$F_2 = \frac{Mb}{l}\left(2 - \frac{3b}{l}\right)$$

$$F_3 = -F_4 = \frac{6Mab}{l^3}$$

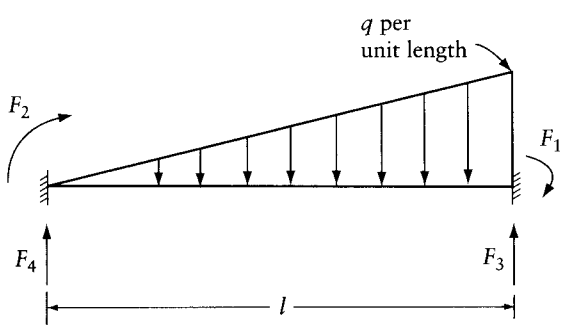

$$F_1 = \frac{ql^2}{20}$$

$$F_2 = -\frac{ql^2}{30}$$

$$F_3 = \frac{7}{20}ql$$

$$F_4 = \frac{3}{20}ql$$

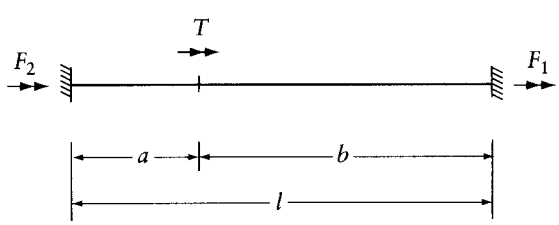

$$F_1 = -\frac{Ta}{l}$$

$$F_2 = -\frac{Tb}{l}$$

If the totally fixed support in any of the above cases, except the last, is changed to a hinge or a roller, the fixed-end moment at the other end can be calculated using the equations of this appendix and Eq. 11.46. Examples are as follows:

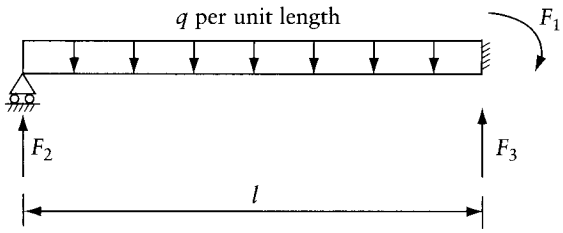

$$F_1 = \frac{ql^2}{8} \tag{C.9}$$

$$F_2 = \frac{3ql}{8} \tag{C.10}$$

$$F_3 = \frac{5ql}{8} \tag{C.11}$$

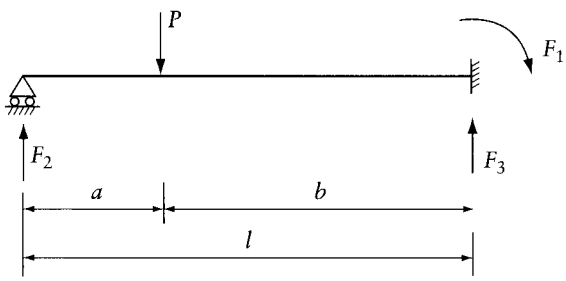

$$F_1 = \frac{Pab}{l^2}\left(a + \frac{b}{2}\right) \tag{C.12}$$

$$F_2 = P\left[\frac{b}{l} - \frac{ab}{l^3}\left(a + \frac{b}{2}\right)\right] \tag{C.13}$$

$$F_3 = P\left[\frac{a}{l} + \frac{ab}{l^3}\left(a + \frac{b}{2}\right)\right] \tag{C.14}$$

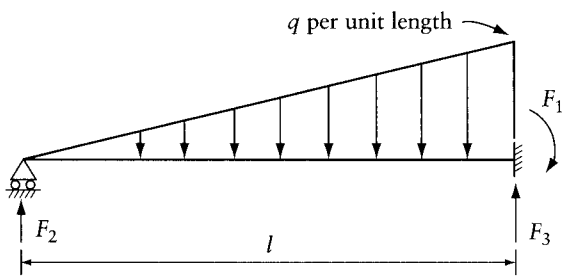

$$F_1 = \frac{ql^2}{15} \tag{C.15}$$

$$F_2 = \frac{ql}{10} \tag{C.16}$$

$$F_3 = \frac{2ql}{5} \tag{C.17}$$

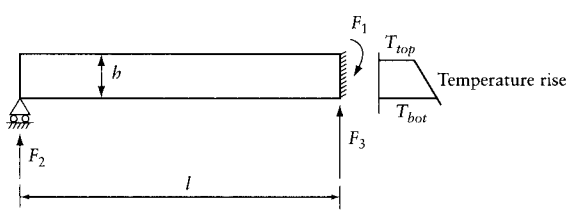

$$F_1 = \frac{3EI\alpha}{2h}(T_{bot} - T_{top}) \tag{C.18}$$

$$F_2 = -F_3 = -\frac{3EI}{2hl}\alpha(T_{bot} - T_{top}) \tag{C.19}$$

α = coefficient of thermal expansion

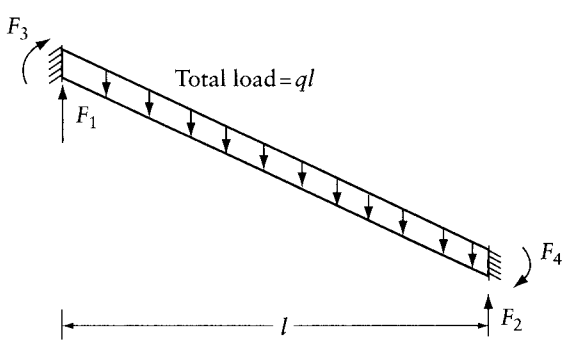

$$F_1 = F_2 = ql/2 \tag{C.20}$$

$$F_3 = -F_4 = -ql^2/12 \tag{C.21}$$

End-forces caused by end-displacements of prismatic members

The following table gives the forces at the ends of beams due to a unit translation or unit rotation of one end. The positive directions for the forces are upward and clockwise. The effect of the deformation caused by the shearing forces is neglected; this topic is considered in Section 15.2. Moreover, the equations do not account for the bending moment due to axial forces; if a member is subjected to a large axial force, its effect may be included using Table 13.2 instead of this appendix. The beams have a constant flexural rigidity EI and a constant torsional rigidity GJ.

Beam	Force
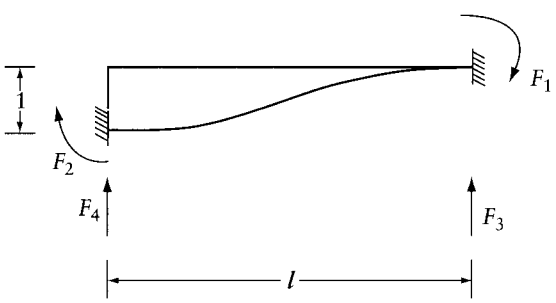	$F_1 = F_2 = \frac{6EI}{l^2}$ (D.1) $F_3 = -F_4 = \frac{12EI}{l^3}$ (D.2)
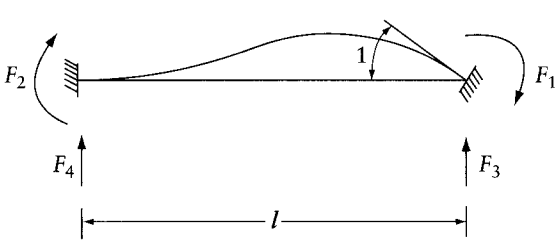	$F_1 = \frac{4EI}{l}$ (D.3) $F_2 = \frac{2EI}{l}$ (D.4) $F_3 = -F_4 = \frac{6EI}{l^2}$ (D.5)
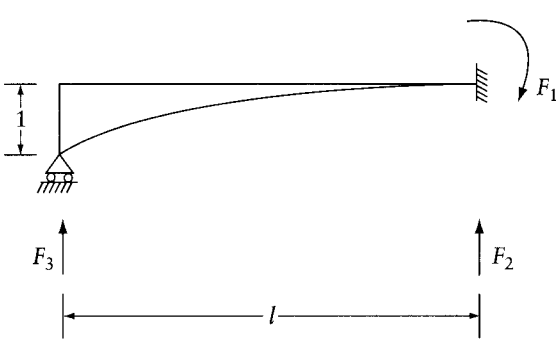	$F_1 = \frac{3EI}{l^2}$ (D.6) $F_2 = -F_3 = \frac{3EI}{l^3}$ (D.7)

Beam

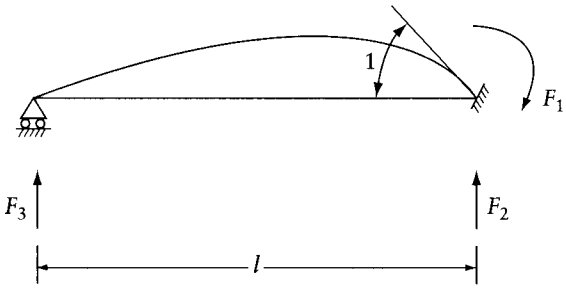

Force

$$F_1 = \frac{3EI}{l} \qquad \text{(D.8)}$$

$$F_2 = -F_3 = \frac{3EI}{l^2} \qquad \text{(D.9)}$$

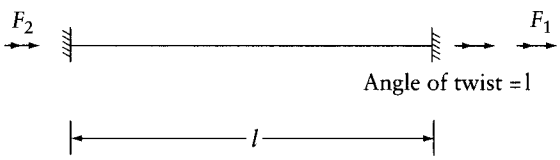

$$F_1 = -F_2 = \frac{GJ}{l} \qquad \text{(D.10)}$$

(Effect of warping ignored)

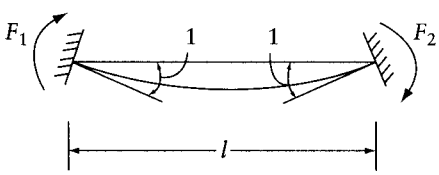

$$F_1 = -F_2 = \frac{2EI}{l} \qquad \text{(D.11)}$$

Appendix E

Reactions and bending moments at supports of continuous beams due to unit displacement of supports

The following tables give the reactions and the bending moments at the supports of a continuous beam due to a unit downward translation of each of the supports separately. All spans are of equal length l and have a constant flexural rigidity EI. The number of spans is 2 (or 1) to 5. The end supports are hinged (Table E.1), fixed (Table E.2), and fixed at the left-hand end and hinged at the right-hand end (Table E.3). The bending moment at the hinged end is known to be zero and is not listed in the tables.

Table E.1 Effect of a Unit Downward Displacement of One Support of Continuous Beams. End Supports Hinged, EI Constant, All Spans are of Equal Length l

Number of spans = 2
Support moments in terms of EI/l^2

−1.50000
3.00000
−1.50000

Reactions in terms of EI/l^3

−1.50000	3.00000	−1.50000
3.00000	−6.00000	3.00000
−1.50000	3.00000	−1.50000

Number of spans = 3
Support moments in terms of EI/l^2

−1.60000	0.40000
3.60000	−2.40000
−2.40000	3.60000
0.40000	−1.60000

Reactions in terms of EI/l^3

−1.60000	3.60000	−2.40000	0.40000
3.60000	−9.60000	8.40000	−2.40000
−2.40000	8.40000	−9.60000	3.60000
0.40000	−2.40000	3.60000	−1.60000

Number of spans = 4
Support moments in terms of EI/l^2

−1.60714	0.42857	−0.10714
3.64286	−2.57143	0.64286
−2.57143	4.28571	−2.57143
0.64286	−2.57143	3.64286
−0.10714	0.42857	−1.60714

Table E.1 (Continued)

Reactions in terms of EI/l^3

−1.60714	3.64286	−2.57143	0.64286	−0.10714	
3.64286	−9.85714	9.42857	−3.85714	0.64286	
−2.57143	9.42857	−13.71428	9.42857	−2.57143	
0.64286	−3.85714	9.42857	−9.85714	3.64286	
−0.10714	0.64286	−2.57143	3.64286	−1.60714	

Number of spans = 5

Support moments in terms of EI/l^2

−1.60765	0.43062	−0.11483	0.02871	
3.64593	−2.58373	0.68900	−0.17225	
−2.58373	4.33493	−2.75598	0.68900	
0.68900	−2.75598	4.33493	−2.58373	
−0.17225	0.68900	−2.58373	3.64593	
0.02871	−0.11483	0.43062	−1.60765	

Reactions in terms of EI/l^3

−1.60765	3.64593	−2.58373	0.68900	−0.17225	0.02871
3.64593	−9.87560	9.50239	−4.13397	1.03349	−0.17225
−2.58373	9.50239	−14.00956	10.53588	−4.13397	0.68900
0.68900	−4.13397	10.53588	−14.00957	9.50239	−2.58373
−0.17225	1.03349	−4.13397	9.50239	−9.87560	3.64593
0.02871	−0.17225	0.68900	−2.58373	3.64593	−1.60765

Table E.2 Effect of a Unit Downward Displacement of One Support of Continuous Beams. Two End Supports Fixed, *EI* Constant, All Spans of Equal Length *l*

Number of spans = 1

Support moments in terms of EI/l^2

6.00000	−6.00000
−6.00000	6.00000

Reactions in terms of EI/l^3

−12.00000	12.00000
12.00000	−12.00000

Number of spans = 2

Support moments in terms of EI/l^2

4.50000	−3.00000	1.50000
−6.00000	6.00000	−6.00000
1.50000	−3.00000	4.50000

Reactions in terms of EI/l^3

−7.50000	12.00000	−4.50000
12.00000	−24.00000	12.00000
−4.50000	12.00000	−7.50000

Number of spans = 3

Support moments in terms of EI/l^2

4.40000	−2.80000	0.80000	−0.40000
−5.60000	5.20000	−3.20000	1.60000
1.60000	−3.20000	5.20000	−5.60000
−0.40000	0.80000	−2.80000	4.40000

Reactions in terms of EI/l^3

−7.20000	10.80000	−4.80000	1.20000	
10.80000	−19.20000	13.20000	−4.80000	
−4.80000	13.20000	−19.20000	10.80000	
1.20000	−4.80000	10.80000	−7.20000	

Number of spans = 4

Support moments in terms of EI/l^2

4.39286	−2.78571	0.75000	−0.21429	0.10714
−5.57143	5.14286	−3.00000	0.85714	−0.42857
1.50000	−3.00000	4.50000	−3.00000	1.50000
−0.42857	0.85714	−3.00000	5.14286	−5.57143
0.10714	−0.21429	0.75000	−2.78571	4.39286

Reactions in terms of EI/l^3

−7.17857	10.71428	−4.50000	1.28571	−0.32143
10.71428	−18.85713	12.00000	−5.14285	1.28571
−4.50000	12.00000	−15.00000	12.00000	−4.50000
1.28571	−5.14285	12.00000	−18.85713	10.71428
−0.32143	1.28571	−4.50000	10.71428	−7.17857

Number of spans = 5

Support moments in terms of EI/l^2

4.39235	−2.78469	0.74641	−0.20096	0.05742	−0.02871
−5.56938	5.13875	−2.98564	0.80383	−0.22966	0.11483
1.49282	−2.98564	4.44976	−2.81340	0.80383	−0.40191
−0.40191	0.80383	−2.81339	4.44976	−2.98564	1.49282
0.11483	−0.22966	0.80383	−2.98564	5.13875	−5.56938
−0.02871	0.05742	−0.20096	0.74641	−2.78469	4.39235

Reactions in terms of EI/l^3

−7.17703	10.70813	−4.47847	1.20574	−0.34450	0.08612
10.70813	−18.83252	11.91387	−4.82296	1.37799	−0.34450
−4.47847	11.91387	−14.69856	10.88038	−4.82296	1.20574
1.20574	−4.82296	10.88038	−14.69856	11.91387	−4.47847
−0.34450	1.37799	−4.82296	11.91387	−18.83252	10.70813
0.08612	−0.34450	1.20574	−4.47847	10.70813	−7.17703

Table E.3 Effect of a Unit Downward Displacement of One Support of Continuous Beams. Support at Left End Fixed, Hinged at Right End, *EI* Constant, All Spans of Equal Length *l*

Number of spans = 1

Support moments in terms of EI/l^2

3.00000

−3.00000

Reactions in terms of EI/l^3

−3.00000	3.00000
3.00000	−3.00000

Number of spans = 2

Support moments in terms of EI/l^2

4.28571	−2.57143
−5.14286	4.28571
0.85714	−1.71428

Table E.3 (Continued)

Reactions in terms of EI/l^3

−6.85714	9.42857	−2.57143
9.42857	−13.71428	4.28571
−2.57143	4.28571	−1.71428

Number of spans = 3

Support moments in terms of EI/l^2

4.38462	−2.76923	0.69231	
−5.53846	5.07692	−2.76923	
1.38461	−2.76923	3.69231	
−0.23077	0.46154	−1.61538	

Reactions in terms of EI/l^3

−7.15385	10.61538	−4.15384	0.69231
10.61539	−18.46153	10.61538	−2.76923
−4.15384	10.61538	−10.15384	3.69231
0.69231	−2.76923	3.69230	−1.61538

Number of spans = 4

Support moments in terms of EI/l^2

4.39175	−2.78350	0.74227	−0.18557	
−5.56701	5.13402	−2.96907	0.74227	
1.48454	−2.96907	4.39175	−2.59794	
−0.37113	0.74227	−2.59794	3.64948	
0.06186	−0.12371	0.43299	−1.60825	

Reactions in terms of EI/l^3

−7.17526	10.70103	−4.45361	1.11340	−0.18557
10.70103	−18.80411	11.81443	−4.45361	0.74227
−4.45361	11.81443	−14.35051	9.58763	−2.59794
1.11340	−4.45361	9.58763	−9.89690	3.64948
−0.18557	0.74227	−2.59794	3.64948	−1.60825

Number of spans = 5

Support moments in terms of EI/l^2

4.39227	−2.78453	0.74586	−0.19889	0.04972	
−5.56906	5.13812	−2.98342	0.79558	−0.19889	
1.49171	−2.98342	4.44199	−2.78453	0.69613	
−0.39779	0.79558	−2.78453	4.34254	−2.58563	
0.09945	−0.19889	0.69613	−2.58563	3.64641	
−0.01657	0.03315	−0.11602	0.43094	−1.60773	

Reactions in terms of EI/l^3

−7.17680	10.70718	−4.47513	1.19337	−0.29834	0.04972
10.70718	−18.82872	11.90055	−4.77348	1.19337	−0.19889
−4.47513	11.90055	−14.65193	10.70718	−4.17679	0.69613
1.19337	−4.77348	10.70718	−14.05524	9.51381	−2.58563
−0.29834	1.19337	−4.17679	9.51381	−9.87845	3.64641
0.04972	−0.19889	0.69613	−2.58563	3.64641	−1.60773

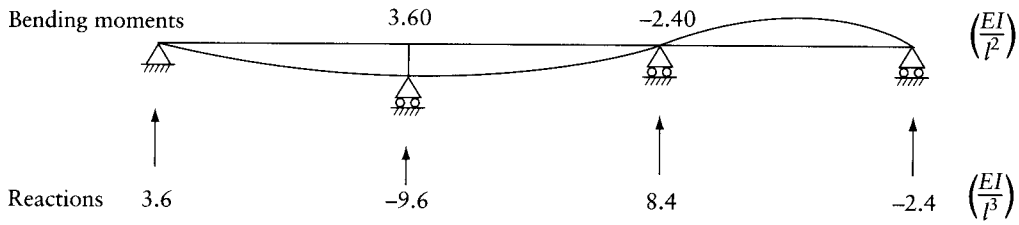

Figure E.1 Illustration of the use of tables of Appendix E.

The values given in each row are the bending moments or the reactions at consecutive supports starting from the left-hand end. The first row after the heading gives the effect of the settlement of the first support from the left, the second row gives the effect of the settlement of the second support from the left, and so on.

Figure E.1 shows an example of the use of the tables: the number of spans is 3, the second support from left settles a unit distance and the values are taken from the second row of the appropriate table.

In these tables, the reaction is considered positive when acting upward, and the bending moment is positive if it causes tension in the bottom fiber of the beam. When the reactions are used to generate a stiffness matrix, appropriate signs should be given according to the chosen coordinate system.

The effect of deformation caused by the shearing forces is neglected.

Properties of geometrical figures

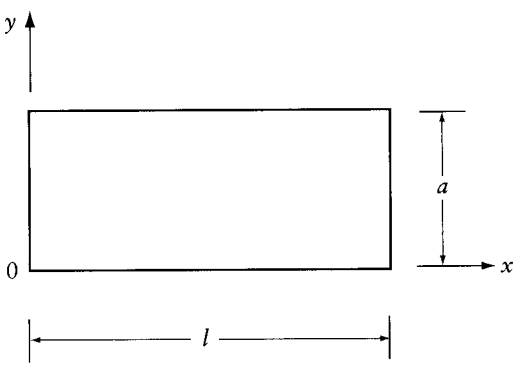

Area: $a \times l$

$\bar{x}$ and $\bar{y}$ coordinates of centroid:

$$\bar{x} = \frac{l}{2}$$

$$\bar{y} = \frac{a}{2}$$

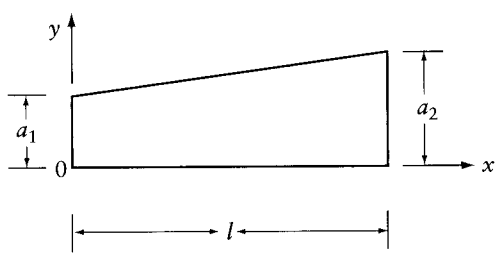

Area: $\dfrac{(a_1 + a_2)}{2} \times l$

$$\bar{x} = \frac{1}{3}\frac{(a_1 + 2a_2)}{(a_1 + a_2)}$$

$$\bar{y} = \frac{(a_1^2 + a_1 a_2 + a_2^2)}{3(a_1 + a_2)}$$

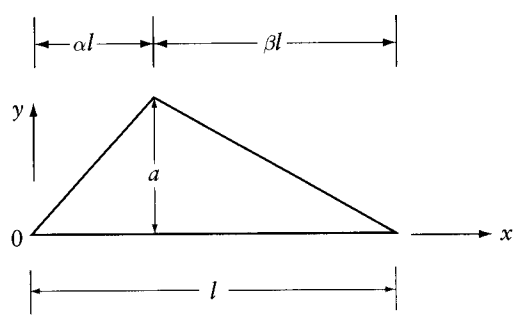

Area: $\dfrac{a \times l}{2}$

$$\bar{x} = \frac{1}{3}(\alpha l + l)$$

$$\bar{y} = \frac{a}{3}$$

Second-degree parabola

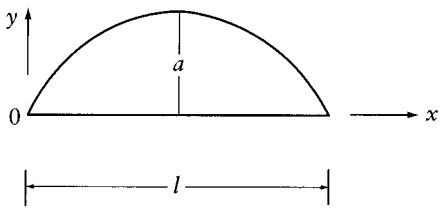

Area	Centroid
$\frac{2}{3}a \times l$	$\bar{x} = \frac{l}{2}$ $\bar{y} = \frac{2}{5}a$

Second-degree parabola

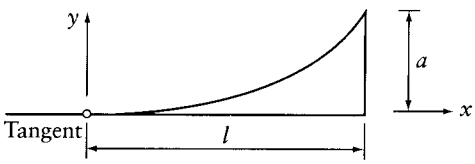

Area	Centroid
$\frac{1}{3}a \times l$	$\bar{x} = \frac{3}{4} \times l$ $\bar{y} = \frac{3}{10} \times a$

Second-degree parabola

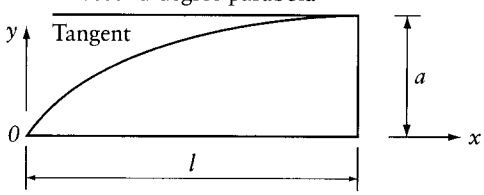

Area	Centroid
$\frac{2}{3}a \times l$	$\bar{x} = \frac{5}{8} \times l$ $\bar{y} = \frac{2}{5} \times a$

Third-degree parabola

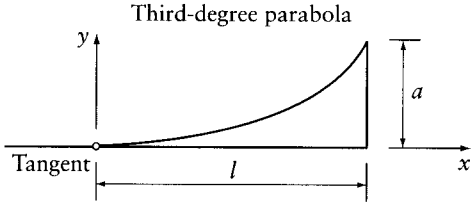

Area	Centroid
$\frac{1}{4}a \times l$	$\bar{x} = \frac{4}{5} \times l$ $\bar{y} = \frac{2}{7} \times a$

Construction of tangents of a second-degree parabola:

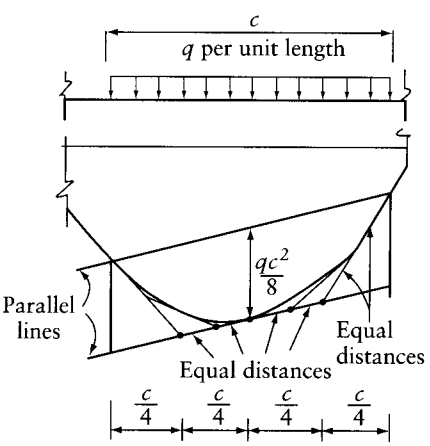

Bending moment diagram for a part of a member subjected to a uniform load

Appendix G

Torsional constant J

If a circular bar of constant cross section and of length l is subjected to a constant torque T, the angle of twist between the two bar ends is

$$\theta = \frac{Tl}{GJ}$$

where G is the shear modulus and J the polar moment of inertia.

When the cross section of the bar is noncircular, plane cross sections do not remain plane after deformation, and warping will occur caused by longitudinal displacements of points in the cross section. Nevertheless, the above equation can be used with good accuracy for noncircular cross sections, but J should be taken as the appropriate torsion constant. The torsional constants for several shapes of cross sections are listed below.

Section	*Torsional Constant J*
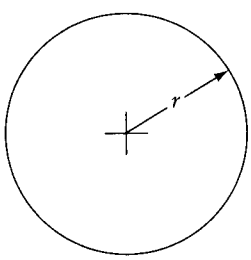	$J = \frac{\pi r^4}{2}$
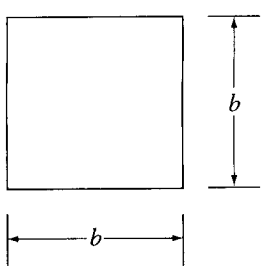	$J = 0.1406b^4$

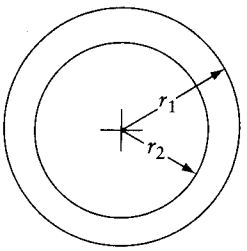	$J = \dfrac{\pi(r_1^4 - r_2^4)}{2}$
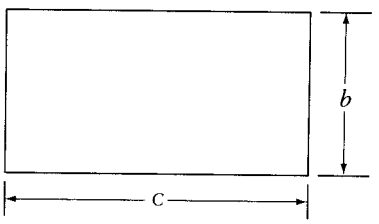	$J = cb^3\left[\dfrac{1}{3} - 0.21\dfrac{b}{c}\left(1 - \dfrac{b^4}{12c^4}\right)\right]$
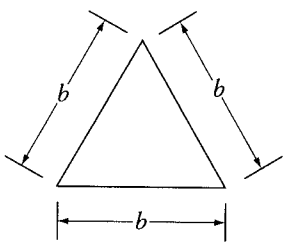	$J = \dfrac{b^4\sqrt{3}}{80}$
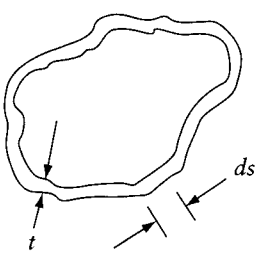	Closed section $J = \dfrac{4a^2}{\int \dfrac{ds}{t}}$ where a = area enclosed by a line through the center of the thickness and the integral is carried out over the circumference
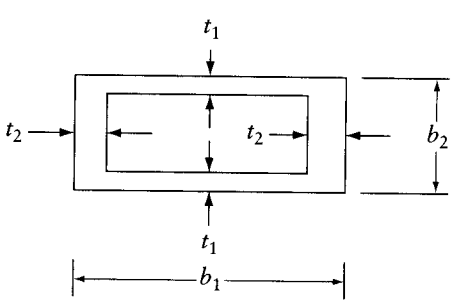	$J = \dfrac{2t_1t_2(b_1 - t_2)^2(b_2 - t_1)^2}{b_1t_2 + b_2t_1 - t_2^2 - t_1^2}$

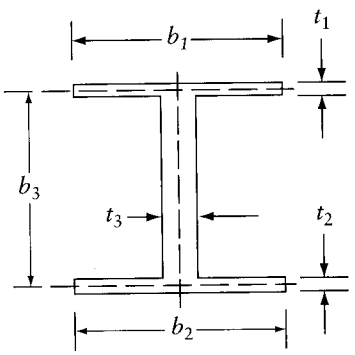

$$J = \frac{b_1 t_1^3 + b_2 t_2^3 + b_3 t_3^3}{3}$$

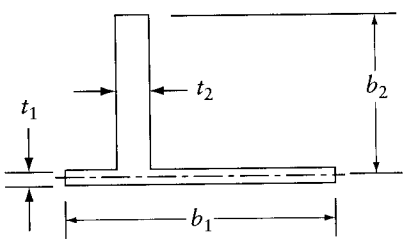

$$J = \frac{b_1 t_1^3 + b_2 t_2^3}{3}$$

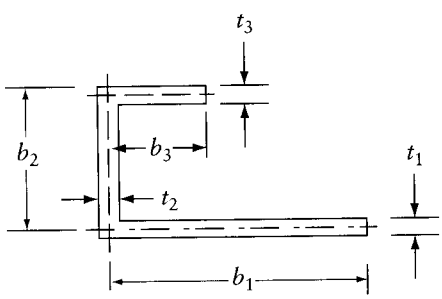

Open section composed of rectangles

$$J = \frac{1}{3} \Sigma b_i t_i^3$$

Appendix H

Values of the integral $\int_l M_u M\,dl$

The following table gives the values of the integral $\int_l M_u M\,dl$, needed in the calculation of displacement of framed structures by virtual work (Eq. 8.2). The same table can be used for the evaluation of the integrals $\int_l N_u N\,dl$, $\int_l V_u V\,dl$, $\int_l T_u T\,dl$, or for the integral over a length l of the product of any two functions which vary in the manner indicated in the diagrams at the top and at the left-hand edge of the table.

M \ M_M	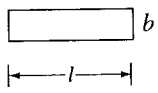	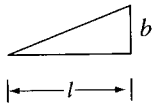	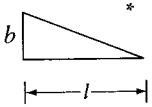 *	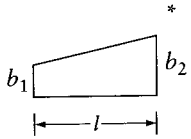 *	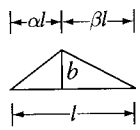 *
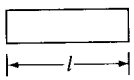	abl	$\frac{1}{2}abl$	$\frac{1}{2}abl$	$\frac{al}{2}(b_1+b_2)$	$\frac{1}{2}abl$
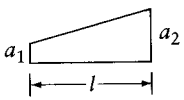	$\frac{bl}{2}(a_1+a_2)$	$\frac{bl}{6}(a_1+2a_2)$	$\frac{bl}{6}(2a_1+a_2)$	$\frac{1}{6}(2a_1b_1+a_1b_2+a_2b_1+2a_2b_2)$	$\frac{bl}{6}[(1+\beta)a_1+(1+\alpha)a_2]$
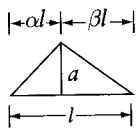	$\frac{1}{2}abl$	$\frac{abl}{6}(1+\alpha)$	$\frac{abl}{6}(1+\beta)$	$\frac{al}{6}[(1+\beta)b_1+(1+\alpha)b_2]$	$\frac{1}{3}abl$
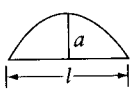	$\frac{2}{3}abl$	$\frac{1}{3}abl$	$\frac{1}{3}abl$	$\frac{1}{3}al(b_1+b_2)$	$\frac{abl}{3}(1+\alpha\beta)$
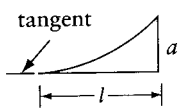	$\frac{1}{3}abl$	$\frac{1}{4}abl$	$\frac{1}{12}abl$	$\frac{al}{12}(b_1+3b_2)$	$\frac{abl}{12}(1+\alpha+\alpha^2)$
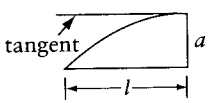	$\frac{2}{3}abl$	$\frac{5}{12}abl$	$\frac{1}{4}abl$	$\frac{al}{12}(3b_1+5b_2)$	$\frac{abl}{12}(5-\beta-\beta^2)$

* Second-degree parabola.

Deflection of a simple beam of constant *EI* subjected to unit end-moments

The values of the deflection given below are helpful in the calculation of ordinates of influence lines (see Section 12.5). The deflection y due to end-moments $M_{AB} = 1$ and $M_{BA} = 0$ (Figure I.1a) is given from Eq. 12.5 by

$$y = \frac{l^2}{6EI}(2\xi - 3\xi^2 + \xi^3) \tag{I.1}$$

where $\xi = x/l$, x is the distance from the left-hand end, and l is the member length. The values of the deflections at different values of x/l are given in Table I.1.

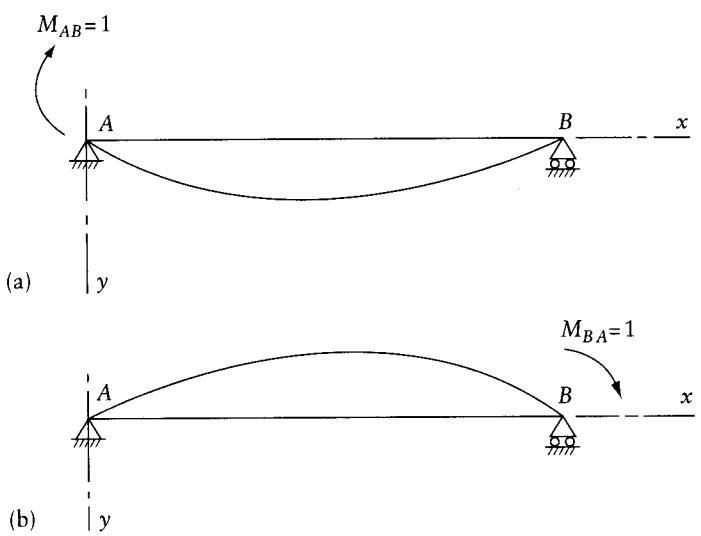

Figure I.1 Deflection of a simple beam due to unit end-moments.

Table I.1 Deflections Due to Unit Clockwise Moment at Left-Hand End

$\xi = \frac{x}{l}$	0	0.1	0.2	0.3	0.4	0.5	0.6	0.7	0.8	0.9	1.0	*Multiplier*
y	0	285	480	595	640	625	560	455	320	165	0	$10^{-4}\frac{l^2}{EI}$

Table I.2 Deflections Due to Unit Clockwise Moment at Right-Hand End

$\xi = \frac{x}{l}$	0	0.1	0.2	0.3	0.4	0.5	0.6	0.7	0.8	0.9	1.0	*Multiplier*
y	0	−165	−320	−455	−560	−625	−640	−595	−480	−285	0	$10^{-4}\frac{l^2}{EI}$

The deflection y due to $M_{BA} = 1$ and $M_{AB} = 0$ (Figure I.1b) is given by

$$y = -\frac{l^2}{6EI}(\xi - \xi^3) \tag{I.2}$$

The values of the deflection at different values of $\xi = x/l$ are given in Table I.2.

Geometrical properties of some plane areas commonly used in the method of column analogy

Property	*Figure Representing Analogous Column*
$Area = a = l/EI$ $I_{xy} = \frac{l}{6EI}(2x_A y_A + 2x_B y_B + x_A y_B + x_B y_A)$ $I_x = \frac{I}{3EI}(y_A^2 + y_B^2 + y_A y_B)$ $I_y = \frac{I}{3EI}(x_A^2 + x_B^2 + x_A x_B)$	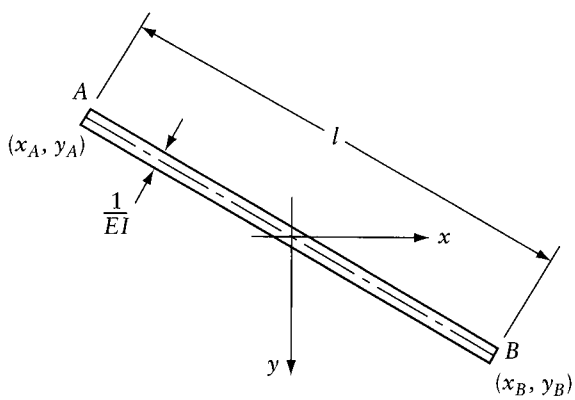 Straight member of constant EI
θ *is measured in radians* $Area = a = \frac{2\theta r}{EI}$ $\bar{y} = \frac{r\sin\theta}{\theta}$ $I_{x1} = \frac{r^3(\theta + \sin\theta\cos\theta)}{EI}$ $I_y = \frac{r^3(\theta - \sin\theta\cos\theta)}{EI}$ $r = \frac{4b^2 + l^2}{8b}$ $y = -b + r - \sqrt{r^2 - x^2}$	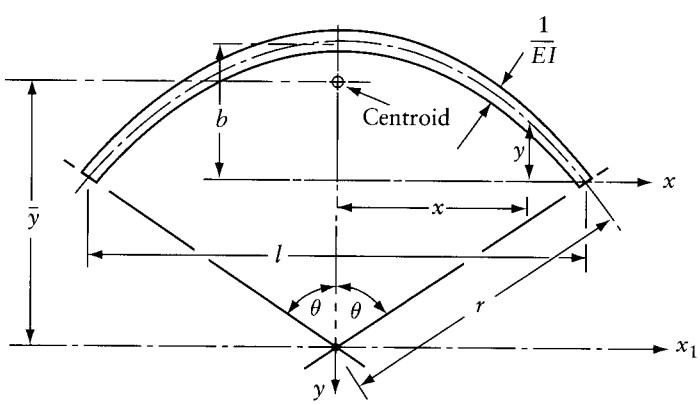 Circular arch of constant EI

Property	*Figure Representing Analogous Column*
$Area = a = \frac{l}{EI_0}$ $I_x = \frac{4b^2 l}{45EI_0}$ $I_y = \frac{l^3}{12EI_0}$	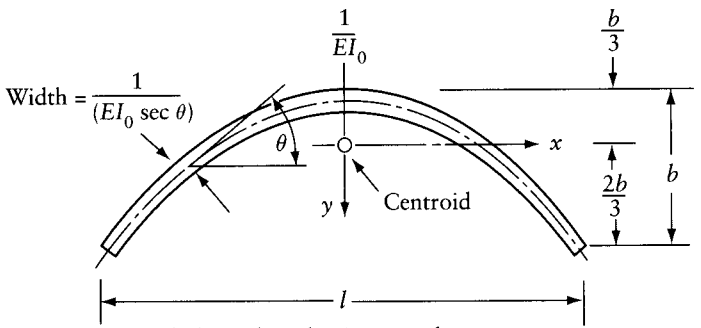 Parabolic arch with EI assumed to vary as the secant of the inclination of the arch axis, EI_0 is the flexural rigidity at the crown

Forces due to prestressing of concrete members

The figures below show sets of forces in equilibrium representing the forces that prestressed tendons exert on the concrete. The tendon profiles shown are composed of one or more straight lines or of second-degree parabolas. The symbol P represents the absolute value of the prestressing force which is assumed constant, and y represents the vertical distance between the tendon and the centroidal axis of the member. θ represents the angle between a tangent to the tendon and the horizontal; θ is assumed small so that $\theta \simeq \tan\theta \simeq \sin\theta$ and $\cos\theta \simeq 1$.

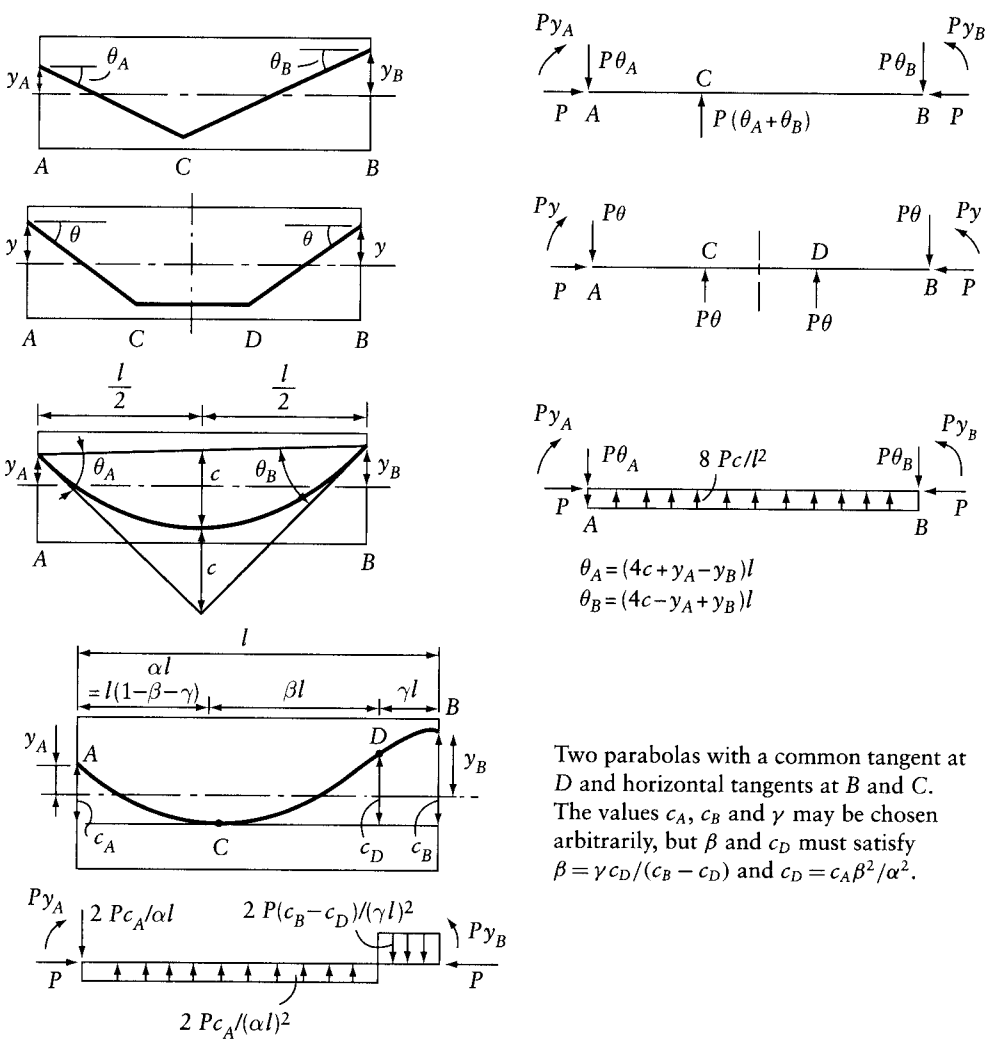

Two parabolas with a common tangent at D and horizontal tangents at B and C. The values c_A, c_B and γ may be chosen arbitrarily, but β and c_D must satisfy $\beta = \gamma c_D/(c_B - c_D)$ and $c_D = c_A\beta^2/\alpha^2$.

Appendix L

Structural analysis computer programs

L.1 Introduction

A series of microcomputer programs is available for use as a companion to this book. The programs can be employed in practical applications, involving the solution of large problems. They are also written as a learning tool. FORTRAN-language source codes are provided with extensive comments, such that the steps of the analysis can be followed. Reference is made to the various sections and equations on which the computer programs are based. Modifications of the programs to perform additional tasks can be done without difficulty, and can prove to be an efficient means of fully understanding the analysis techniques. The comments at the beginning of the source code include definitions of the symbols employed and instructions for input data preparation.

L.2 Computer programs provided at:

http://www.routledge.com/books/Structural-Analysis-isbn9780415774338

The following password will be required to access the site:

STRUCTURES

(NB: The password needs to be in capital letters.)

In Section L.4 the computer programs are divided into three groups: (A) Linear analysis programs. (B) Nonlinear analysis programs. (C) Matrix algebra. Three files described in the following section can be obtained for each program. For the computer programs in groups A and C, the files can be unloaded from the Internet at the web site address given above. The files for the computer programs of group B can be ordered using the form at end of book.

L.3 Files for each program

Three files are provided for each program:

1. The source code in FORTRAN
2. Executable file
3. Input file

Each file has a name composed of up to eight letters descriptive of the program, followed by a dot and two to three letters. For example, the three files for the program PLANEF which analyzes plane frames have, respectively, the names: PLANEF.FOR, PLANEF.EXE, and PLANEF.IN.

Typing the letters PLANEF and pressing "Enter" will execute the program, generate a file named PLANEF.OUT and – if running the program is with DOS command – cause the words "Program terminated" to appear on the screen. The file PLANEF. OUT echoes the input data and gives the results of the analysis of the problem whose data are given in PLANEF.IN.

The input files provided on the disks are for simple example problems selected from the book. Typically, an input data line contains numbers on the left-hand side and symbols or words on the right-hand side, indicating what are the parameters given on the line. Figure L.1 shows, as an example, the contents of the file PLANEF.IN, giving the input data for the plane frame of Example 21.2 (Figure 21.5 and Table 21.2). To analyze a new structure, it is proposed to revise the example input file by changing the values of the parameters, rather than creating a new file. Thus, any input file example provided on the disks should be copied in a back-up file before it is revised. Preparing an input file for a new problem in this way is similar to completing a form giving the data required on the right-hand side of the form.

As mentioned above, all symbols used are defined at the beginning of the source code of each program. We give below definition of the symbols in Figure L.1: NJ, NM, NSJ, NLC are numbers of joints, members, supported joints, and load cases respectively; JS and JE are start node and end node of an individual member. The remaining symbols and the restraint indicators are explained in Section 21.4. Program PLANEF accepts two types of loading, entered as nodal-force components $\{F_x, F_y, M_z\}$ on individual nodes, or as six fixed-end forces $\{A_r\}$ for individual members. Only the nodes subjected to nodal forces and only the members having fixed-end forces need to be listed. A dummy data line indicates the end of data for each of the two types of loadings. The dummy lines start with any integer greater than NLC (number of load cases).

Figure L.2 is part of the file PLANEF.OUT, showing the input and the results of case loading 1.

```
Plane frame Example 21.2, Figure 21.5.
4    3    2    2                          NJ, NM, NSJ, NLC
30000.      0.                             Elasticity modulus, Poisson's ratio
1        0.0    300.0                      Node number, x and y coordinates
2        0.0      0.0
3      300.0    150.0
4      300.0    300.0
1    1    2     30.0   3000.0   1.e6       Member number, JS, JE, cross-sec. a, I, ar
2    2    3     40.0   5000.0   1.e6
3    3    4     30.0   3000.0   1.e6
1    3*0       3*0.0                      Node, restraint indicators, prsc. displs.
4    0    0     1    3*0.0
1    2    4.0      0.0  0.0                Load case, node, Fx, Fy, Mz
1    3    2.0    0.0    0.0
10   0      3*0.0                          Dummy, end of forces applied at nodes
1    2    -13.42    -26.83   -1500.   -13.42   -26.83   1500.  Ld. Case, member, {Ar}
2    1    -1500.     8.    1200.    1500.   -8    1200.
10   0    6*0.                           Dummy, end of data of member loads
```

Figure L.1 Image of file PLANEF.IN containing input data for the plane frame of Example 21.2.

Plane frame Example 21.2, Figure 21.5.
Number of joints = 4
Number of members = 3.
Number of joints with prescribed displacement(s) = 2
Number of Load cases = 2
Elasticity modulus = .30000E+05; Poisson's ratio = .0000

Nodal coordinates

Node	*x*	*y*
1	.000	300.000
2	.000	.000
3	300.000	150.000
4	300.000	300.000

Element information

Element	1st node	2nd node	a	I	ar
1	1	2	.30000E+02	.30000E+04	.10000E+07
2	2	3	.40000E+02	.50000E+04	.10000E+07
3	3	4	.30000E+02	.30000E+04	.10000E+07

Support conditions

Node	Restraint indicators			Prescribed displacements		
	u	v	theta	u	v	theta
1	0	0	0	.00000E+00	.00000E+00	.00000E+00
4	0	0	1	.00000E+00	.00000E+00	.00000E+00

Forces applied at the nodes

Load case	Node	Fx	Fy	Mz
1	2	.40000E+01	.00000E+00	.00000E+00
1	3	.20000E+01	.00000E+00	.00000E+00
10	0	.00000E+00	.00000E+00	.00000E+00

Member end forces with nodal displacement restrained

Ld. case	Member	Ar1	Ar2	Ar3	Ar4	Ar5	Ar6
1	2	–.1342E+02	–.2683E+02	–.1500E+04	–.1342E+02	–.2683E+02	.1500E+04
2	1	–.1500E+04	.8000E+01	.1200E+04	.1500E+04	–.8000E+01	.1200E+04
10	0	.0000E+00	.0000E+00	.0000E+00	.0000E+00	.0000E+00	.0000E+00

Analysis results

Load case no.1

Nodal displacements

Node	u	v	theta
1	–.68055E–07	.81171E–08	–.16029E–09
2	.39935E–01	.81171E–02	.71994E–03
3	.38354E–01	.59412E–02	–.47191E–03
4	.27285E–07	.59412E–08	.61949E–03

Figure L.2 Image of the file PLANEF.OUT (see Figure L.1 for corresponding input data file). Results of case of loading 2 are omitted. This figure is continued on the next page.

Forces at the supported nodes

Node	Fx	Fy	Mz
1	.27222E+01	–.24351E+02	.19235E+03
4	–.87311E+01	–.35647E+02	.00000E+00

Member end forces

Member	F1	F2	F3	F4	F5	F6
1	.24351E+02	.27222E+01	.19235E+03	–.24351E+02	–.27222E+01	.62431E+03
2	–.48777E+01	–.24787E+02	–.62431E+03	–.21962E+02	–.28873E+02	.13097E+04
3	.35647E+02	–.87311E+01	–.13097E+04	–.35647E+02	.87311E+01	–.67057E–13

Figure L.2 (Continued)

L.4 Computer program descriptions

In the following, the available computer programs are mentioned by name and by a short description. The programs are divided into three groups:

A. Linear analysis programs (basis: Chapter 21)

- **PLANEF** (plane frame)
- **SPACEF** (space frame)
- **PLANET** (plane truss)
- **SPACET** (space truss)
- **PLANEG** (plane grid)

These five programs are, respectively, for the linear analysis of plane frames, space frames, plane trusses, space trusses, and grids.

B. Nonlinear analysis programs

- **PDELTA** (basis: Chapter 13)
- **PLASTICF** (basis: Section 22.7)
- **NLST** (basis: Chapter 23)
- **NLPF** (basis: Chapter 23)

The program PDELTA performs quasi-linear analysis of plane frames, considering the effect of axial forces on the stiffness matrix of individual members (Eqs. 13.19 and 13.23).

Analysis of collapse loads of plane frames due to the development of plastic hinges (Section 22.7) can be performed with the program PLASTICF. The program increases the values of the loads gradually and indicates the load levels at which the plastic hinges are developed, the corresponding nodal displacements and member end-forces.

The program NLST performs nonlinear analysis of space trusses, employing Newton-Raphson's technique. Cable nets can be analyzed by the same program. Cable nets with membrane triangular elements can also be analyzed.

Nonlinear analysis of plane frames can be performed by the program NLPF. Similar to the program PDELTA, the program NLPF calculates the stiffness of the members accounting for the magnitude of the axial forces. But, in addition, NLPF considers the equilibrium of the nodes in their displaced positions. The change in length of members is not ignored in determining the

geometry of the deformed structure. NLPF can be employed to indicate the nonlinear buckling loads.

C. Matrix algebra (basis: Appendix A)

To enhance the study of this book, the web site provides the following simple programs which can perform frequently needed matrix operations:

- ADD
- MULTIPLY
- INVERT
- SOLVE
- DETERM
- EIGEN

The program ADD calculates the sum: $[C] = \alpha[A] + \gamma[B]$, where $[A]$ and $[B]$ are the given matrices; α and γ are the given multipliers. The program MULTIPLY determines the product of two given matrices. The program INVERT calculates the inverse of nonsingular matrices. The program SOLVE gives the matrix $[X]$ in the simultaneous linear equations $[A]\ [X] = [B]$, when $[A]$ and $[B]$ are given. The program DETERM calculates the determinant of a given square matrix. EIGEN solves the equation: $[S]\{D\} = \lambda[m]\{D\}$; where $[S]$ and $[m]$ are square matrices; the solution gives eigenvalues, λ and the corresponding eigenvectors (see Section 20.6).

Appendix M

Basic probability theory[1]

For more comprehensive presentation of probability theory, refer to specialized texts.[2]

M.1 Basic definitions

Consider the outcome of an experiment; the experiment can be testing the strength of a material, measuring a beam depth, or the occurrence of a truck on a bridge in a specified period of time. Any outcome of the experiment is called an *event*. All possible events of an experiment comprise a *sample space*.

Example M.1: Results of compressive strength tests of concrete

Let $x_1, x_2, \ldots, x_n$ be the measured compressive strength (outcome) of n concrete cylinders. The actual compressive strength, f'_c, varies randomly, and n test results provide only limited information about its variation. For this experiment, the result f'_c can take any positive value. Theoretically, even $f'_c = 0$ is possible, but it is unlikely (when the mix is made without any cement). Events $E_1, E_2, \ldots, E_n$ can be defined as intervals; for example, E_1 occurs when the outcome of cylinder test falls within the interval (0, 10 MPa), E_2 occurs when the outcome of cylinder test falls within the interval (10, 20 MPa), and so on. The defined sample space for concrete cylinder tests is called a *continuous sample space*. A *certain* event is equal to the sample space. An example of this, using the compressive strength data, is: certain event = all positive real numbers, $0 \leq f'_c < \infty$. An *impossible* event is a set with no sample points in it, such as $f'_c < 0$.

Example M.2: Mode of flexural failure of a reinforced concrete beam

Two possible modes of flexural failure of a reinforced concrete beam are: mode 1, failure by crushing of concrete; and mode 2, failure by yielding of steel. In this example, the sample space consists of two elements, mode 1 and mode 2. This sample space has a finite number of elements (two) and it is called a *discrete sample space*.

1 This appendix was written in collaboration with the authors by Professor Andrzej S. Nowak, University of Nebraska, Lincoln, USA.

2 See the references given in Chapter 24.

M.2 Axioms of probability

Define: E = event; Ω = sample space; $P(\,)$ = probability function of events in a sample space.

Axiom 1: For any event $E, 0 \le P(E) \le 1$; where $P(E)$ = probability of event E.
Axiom 2: $P(\Omega) = 1$. This means that the probability of the sample space = 1.
Axiom 3: Consider n mutually exclusive events $E_1, E_2, \ldots, E_n$, then

$$P\left(\bigcup_{i=1}^{n} E_i\right) = \sum_{i=1}^{n} P(E_i) = 1 \tag{M.1}$$

where $\bigcup_{i=1}^{n} E_i$ = union of all events $E_1, E_2, \ldots, E_n$.

Mutually exclusive events exist when the occurrence of any one member in a set excludes the occurrence of the others. For concrete compressive strength, f'_c, examples are: $E_1 = (0 \le f'_c < 10\,\text{MPa})$; $E_2 = (10 \le f'_c < 20\,\text{MPa})$; $E_3 = (20 \le f'_c < 30\,\text{MPa})$; $E_4 = (f'_c \ge 30\,\text{MPa})$.

$$\bigcup_{i=1}^{4} E_i = (0 \le f'_c < \infty) \tag{M.2}$$

M.3 Random variable

In the example of concrete strength, f'_c is a *random variable*. A random variable X can be *continuous* or *discrete*. Examples of continuous random variables are: if $f'_c = 31.5\,\text{MPa}$, then $X(f'_c) = 31.5$ (no units, a real number), or if $X(f'_c) = \{(\text{value in MPa})/10\} - 2.0$ and $f'_c = 31.5\,\text{MPa}$, then $X(f'_c) = 1.15$.

An example of a discrete random variable is:

$$X(f'_c) = \begin{Bmatrix} 1 \text{ if } & 0 \le f'_c < 10\,\text{MPa} \\ 2 \text{ if } & 10 \le f'_c < 20\,\text{MPa} \\ 3 \text{ if } & 20 \le f'_c < 30\,\text{MPa} \\ 4 \text{ if } & f'_c \ge 30\,\text{MPa} \end{Bmatrix} \tag{M.3}$$

M.4 Basic functions of a random variable

The *probability mass function* is defined as: $p_X(x)$ = probability that a *discrete* random variable $X = x$, where x is a real number and is written as:

$$p_X(x) = P(X = x) \tag{M.4}$$

As an example, for the discrete random variable X defined in Eq. M.3, we can write:

$$p_X(1) = P(X = 1);\ p_X(2) = P(X = 2);\ p_X(3) = P(X = 3);\ p_X(4) = P(X = 4) \tag{M.5}$$

The *cumulative distribution function* (CDF) is defined as: the total accumulation of all probability distribution functions (continuous and discrete), smaller than the upper bound of a given value.

$$F_X(x) = P(X \le x) = \sum p_X(x_i) \text{ with } x_i \le x \tag{M.6}$$

For the f_c' intervals defined in Eq. M.3, assume the probability mass function as:

$$p_X(1) = 0.05;\ p_X(2) = 0.20;\ p_X(3) = 0.65;\ p_X(4) = 0.10;\ \text{Total} = 1.00 \tag{M.7}$$

From Eq. M.7, we can write the following CDF examples:

$$F_X(0.5) = P(X \le 0.5) = 0.00;\ F_X(1) = P(X \le 1) = 0.05;\ F_X(1.5) = P(X \le 1.5) = 0.05$$
$$F_X(2) = P(X \le 2) = 0.25;\ F_X(3.2) = P(X \le 3.2) = 0.90 \tag{M.8}$$

The first derivative of $F_X(x)$is called a *probability density function* (PDF), and is defined only for *continuous* random variables. Most practical engineering problems deal with continuous random variables.

$$f_X(x) = \frac{\mathrm{d}F_X(x)}{\mathrm{d}x} \tag{M.9}$$

where $f_X(x)$is used for continuous random variables to mean the same as $p_X(x)$ for discrete random variables.

M.5 Parameters of a random variable

The *mean value* of a random variable X is denoted by $\bar{x}$. For a continuous random variable or discrete random variable, respectively:

$$\bar{x} = \int_{-\infty}^{\infty} x\, f_X(x)\, \mathrm{d}x;\ \ \bar{x} = \sum_{\text{all}\, x_i} x_i\, p_X(x_i) \tag{M.10}$$

The *expected value* of X is equal to the mean value of X,

$$E(X) = \bar{x} \tag{M.11}$$

The expected value of X^n is called the *nth moment* of X. For a continuous random variable or discrete random variable, respectively:

$$E(X^n) = \int_{-\infty}^{\infty} x^n f_X(x)\, dx;\ \ E(X^n) = \sum_{\text{all}\, x_i} x_i^n\, p_X(x_i) \tag{M.12}$$

The *variance* of X, denoted σ_X^2, is defined as the expected value of $(X - \bar{x})^2$:

$$\sigma_X^2 = E\left[(X - \bar{x})^2\right] \tag{M.13}$$

$$\sigma_X^2 = E\left[\left(X^2 - 2X\bar{x} + \bar{x}^2\right)\right] = E\left(X^2\right) - 2\bar{x}\,E(X) + \bar{x}^2 = E\left(X^2\right) - 2\bar{x}^2 + \bar{x}^2$$

$$\sigma_X^2 = E\left(X^2\right) - \bar{x}^2 \tag{M.14}$$

For a continuous random variable or a discrete random variable, the *variance* is, respectively:

$$\sigma_X^2 = \int_{-\infty}^{\infty} x^2 f_X(x)\mathrm{d}x - \bar{x}^2;\ \ \sigma_X^2 = \sum_{\text{all}\, x_i} \left[x_i^2 p\,(x_i)\right] - \bar{x}^2 \tag{M.15}$$

The *standard deviation* of X is defined:

$$\sigma_X = \sqrt{\sigma_X^2} \tag{M.16}$$

The non-dimensional *coefficient of variation*, V_X, is the standard deviation divided by the mean; by convention $V_X > 0$, even though the mean may be negative.

$$V_X = \frac{\sigma_X}{|\bar{x}|} \tag{M.17}$$

Example M.3: Calculation of $\bar{x}$, $E(X^2)$, σ_X^2, and V_X

For the discrete random variable X, whose probability mass function is given by Eq. M.7, calculate: the mean value $\bar{x}$, the second moment $E(X^2)$, the variance σ_X^2, the standard deviation σ_X and the coefficient of variation V_X.

Equations M.10, M.12, M.14, M.16 and M.17 give, respectively:

$$\bar{x} = 1(0.05) + 2(0.2) + 3(0.65) + 4(0.1) \qquad = 2.8$$

$$E(X^2) = 1^2(0.05) + 2^2(0.2) + 3^2(0.65) + 4^2(0.1) = 8.3$$

$$\sigma_X^2 = 8.3 - (2.8)^2 \qquad = 0.46$$

$$\sigma_X = \sqrt{0.46} \qquad = 0.6782$$

$$V_X = 0.6782/2.8 \qquad = 0.2422$$

M.6 Sample parameters

If X is analyzed on the basis of test data: $x_1, x_2, \ldots, x_n$, then the mean can be approximated by the *sample mean*, and the standard deviation can be approximated by the *sample standard deviation*.

The sample mean (approximating mean) is:

$$\bar{x} \cong \frac{1}{n}\sum_{i=1}^{n} x_i \tag{M.18}$$

The sample standard deviation (approximating standard deviation) is:

$$\sigma_X \cong \sqrt{\frac{\sum_{i=1}^{n} x_i^2 - n\bar{x}^2}{n-1}} \tag{M.19}$$

M.7 Standardized form of a random variable

Let X be a random variable. Z is called a *standardized form* of X, and is defined as,

$$Z = \frac{X - \bar{x}}{\sigma_X} \tag{M.20}$$

The mean of Z is zero: $\bar{z} = 0$. The variance of $Z = 1$ is $\sigma_Z^2 = 1$.

M.8 Types of random variables used in reliability of structures

The most important variables used in structural reliability analysis are:

1. Uniform
2. Normal
3. Log-normal
4. Extreme type I and extreme type II

M.9 Uniform random variable

Uniform random variable means that all numbers are equally likely to appear.

$$\text{PDF} = f_X(x) = \begin{cases} \dfrac{1}{b-a} & \text{for } a \le x \le b \\ 0 & \text{otherwise} \end{cases} \tag{M.21}$$

The mean, variance, and standard deviation are,

$$\bar{x} = \frac{a+b}{2} \tag{M.22}$$

$$\sigma_X^2 = \frac{(b-a)^2}{12};\ \sigma_X = \frac{b-a}{2\sqrt{3}} \tag{M.23}$$

M.10 Normal random variable

The PDF of a normal (or Gaussian) random variable is:

$$f_X(x) = \frac{1}{\sigma_X\sqrt{2\pi}} e^{\frac{-(x-\bar{x})^2}{2\sigma_X^2}} \tag{M.24}$$

There is no closed-form solution for the CDF of the normal random variable,

$$F_X(x) = \int_{-\infty}^{x} f_X(x)\,dx \tag{M.25}$$

Properties of $F_X(x)$ and $f_X(x)$ for a normal random variable include:

1. $f_X(x)$ is symmetrical about the mean $\bar{x}$; $f_X(x+\bar{x}) = f_X(-x+\bar{x})$.
2. Sum of $F_X(x)$ calculated for $(x+\bar{x})$ and $(-x+\bar{x})$ is equal to 1; $F_X(x+\bar{x}) = 1 - F_X(-x+\bar{x})$.

The probability density function (PDF) for a *standard normal random variable* can be obtained from Eq. M.24 by substituting $\bar{x} = 0$ and $\sigma = 1$. The resulting equation is (Figure M.1a):

$$f_X(z) = \phi(z) = \frac{1}{\sqrt{2\pi}} e^{\frac{-z^2}{2}} \tag{M.26}$$

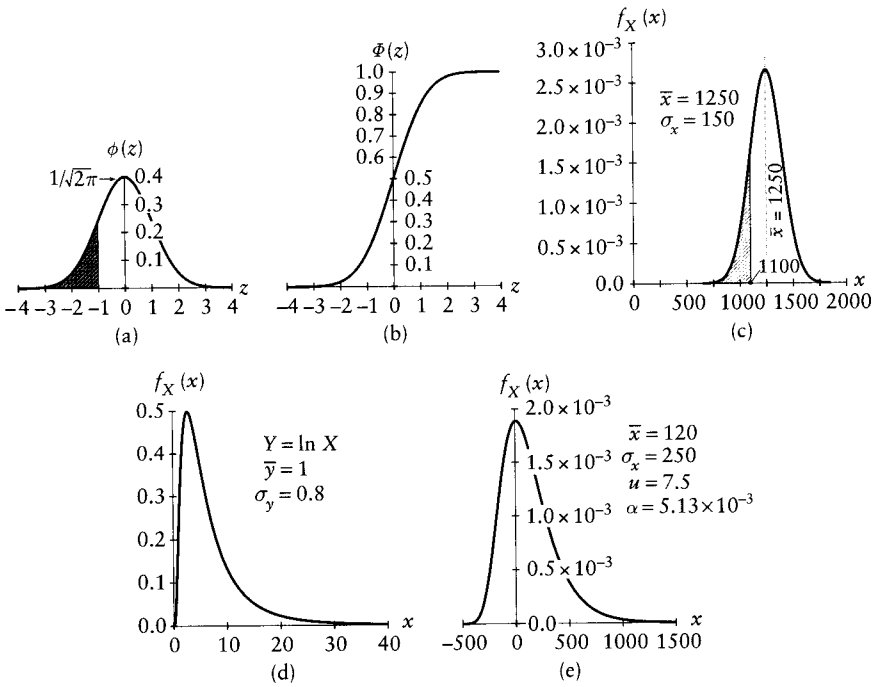

Figure M.1 Probability Density Function (PDF) and Cumulative Distribution Function (CDF). (a) PDF, $\phi\phi(z)$ for standard normal random variable (Eq. M.26). (b) CDF, $\Phi(z)$ of standard normal random variable (Table M.1). (c) PDF of a normal random variable, Example M.4. (d) PDF of a log-normal random variable (Eq. M.36). (e) PDF of an Extreme Type I random variable.

Equation M.24 can be rewritten as:

$$f_X(x) = \frac{1}{\sigma_X}\phi(z) \text{ with } z = \frac{1}{\sigma_X}(x - \bar{x}) \tag{M.27}$$

Let X be a normal random variable, and Z is its standardized form. Then, from Eq. M.20,

$$X = \bar{x} + Z\sigma_X \tag{M.28}$$

$$F_X(x) = P(X \le x) = P(\bar{x} + Z\sigma_X \le x) \tag{M.29}$$

$$F_X(x) = P\left(Z \le \frac{x - \bar{x}}{\sigma_X}\right) = F_Z\left(\frac{x - \bar{x}}{\sigma_X}\right) = \Phi\left(\frac{x - \bar{x}}{\sigma_X}\right) \tag{M.30}$$

The CDF for standard normal random variable is (Figure M.1b):

$$F_X(x) = \Phi\left(\frac{x - \bar{x}}{\sigma_X}\right) = \Phi(z) \tag{M.31}$$

where $\Phi(z)$ is equal to the value of the CDF of standard normal random variable; $\Phi(z)$ is equal to the area below the curve of $\phi(z)$ in Figure M.1a between $-\infty$ and the given value of z. The value of the CDF of a normal random variable at a given x is equal to the value of its standardized random variable at $z = (x - \bar{x})/\sigma_X$; e.g. the shaded areas in Figures M.1a and c are equal.

The area below the curve in Figure M.1a or c is equal to 1.0; from Eqs. M.10, M.15, and M.16 we can see that the mean is the x coordinate of a vertical line through the centroid; the variance is the second moment of the area about this line, and the standard deviation is its radius of gyration.

The standard normal cumulative distribution function (CDF), $\Phi(z)$, is widely available in tables, such as Table M.1, which gives values of CDF for $z = 0$ to -7.0. To find $\Phi(z)$ for positive z, use:

$$\Phi(z) = 1 - \Phi(-z) \tag{M.32}$$

Table M.1 Cumulative Distribution Function (CDF), $\Phi(z)$, of a Standard Normal Random Variable*

z	$\Phi(z)$									
	0	0.01	0.02	0.03	0.04	0.05	0.06	0.07	0.08	0.09
0	500E-3	496E-3	492E-3	488E-3	484E-3	480E-3	476E-3	472E-3	468E-3	464E-3
−0.1	460E-3	456E-3	452E-3	448E-3	444E-3	440E-3	436E-3	433E-3	429E-3	425E-3
−0.2	421E-3	417E-3	413E-3	409E-3	405E-3	401E-3	397E-3	394E-3	390E-3	386E-3
−0.3	382E-3	378E-3	374E-3	371E-3	367E-3	363E-3	359E-3	356E-3	352E-3	348E-3
−0.4	345E-3	341E-3	337E-3	334E-3	330E-3	326E-3	323E-3	319E-3	316E-3	312E-3
−0.5	309E-3	305E-3	302E-3	298E-3	295E-3	291E-3	288E-3	284E-3	281E-3	278E-3
−0.6	274E-3	271E-3	268E-3	264E-3	261E-3	258E-3	255E-3	251E-3	248E-3	245E-3
−0.7	242E-3	239E-3	236E-3	233E-3	230E-3	227E-3	224E-3	221E-3	218E-3	215E-3
−0.8	212E-3	209E-3	206E-3	203E-3	200E-3	198E-3	195E-3	192E-3	189E-3	187E-3
−0.9	184E-3	181E-3	179E-3	176E-3	174E-3	171E-3	169E-3	166E-3	164E-3	161E-3
−1.0	159E-3	156E-3	154E-3	152E-3	149E-3	147E-3	145E-3	142E-3	140E-3	138E-3
−1.1	136E-3	133E-3	131E-3	129E-3	127E-3	125E-3	123E-3	121E-3	119E-3	117E-3
−1.2	115E-3	113E-3	111E-3	109E-3	107E-3	106E-3	104E-3	102E-3	100E-3	98.5E-3
−1.3	96.8E-3	95.1E-3	93.4E-3	91.8E-3	90.1E-3	88.5E-3	86.9E-3	85.3E-3	83.8E-3	82.3E-3
−1.4	80.8E-3	79.3E-3	77.8E-3	76.4E-3	74.9E-3	73.5E-3	72.1E-3	70.8E-3	69.4E-3	68.1E-3
−1.5	66.8E-3	65.5E-3	64.3E-3	63.0E-3	61.8E-3	60.6E-3	59.4E-3	58.2E-3	57.1E-3	55.9E-3
−1.6	54.8E-3	53.7E-3	52.6E-3	51.6E-3	50.5E-3	49.5E-3	48.5E-3	47.5E-3	46.5E-3	45.5E-3
−1.7	44.6E-3	43.6E-3	42.7E-3	41.8E-3	40.9E-3	40.1E-3	39.2E-3	38.4E-3	37.5E-3	36.7E-3
−1.8	35.9E-3	35.1E-3	34.4E-3	33.6E-3	32.9E-3	32.2E-3	31.4E-3	30.7E-3	30.1E-3	29.4E-3
−1.9	28.7E-3	28.1E-3	27.4E-3	26.8E-3	26.2E-3	25.6E-3	25.0E-3	24.4E-3	23.9E-3	23.3E-3
−2.0	22.8E-3	22.2E-3	21.7E-3	21.2E-3	20.7E-3	20.2E-3	19.7E-3	19.2E-3	18.8E-3	18.3E-3
−2.1	17.9E-3	17.4E-3	17.0E-3	16.6E-3	16.2E-3	15.8E-3	15.4E-3	15.0E-3	14.6E-3	14.3E-3
−2.2	13.9E-3	13.6E-3	13.2E-3	12.9E-3	12.5E-3	12.2E-3	11.9E-3	11.6E-3	11.3E-3	11.0E-3
−2.3	10.7E-3	10.4E-3	10.2E-3	9.90E-3	9.64E-3	9.39E-3	9.14E-3	8.89E-3	8.66E-3	8.42E-3
−2.4	8.20E-3	7.98E-3	7.76E-3	7.55E-3	7.34E-3	7.14E-3	6.95E-3	6.76E-3	6.57E-3	6.39E-3
−2.5	6.21E-3	6.04E-3	5.87E-3	5.70E-3	5.54E-3	5.39E-3	5.23E-3	5.08E-3	4.94E-3	4.80E-3
−2.6	4.66E-3	4.53E-3	4.40E-3	4.27E-3	4.15E-3	4.02E-3	3.91E-3	3.79E-3	3.68E-3	3.57E-3
−2.7	3.47E-3	3.36E-3	3.26E-3	3.17E-3	3.07E-3	2.98E-3	2.89E-3	2.80E-3	2.72E-3	2.64E-3
−2.8	2.56E-3	2.48E-3	2.40E-3	2.33E-3	2.26E-3	2.19E-3	2.12E-3	2.05E-3	1.99E-3	1.93E-3
−2.9	1.87E-3	1.81E-3	1.75E-3	1.69E-3	1.64E-3	1.59E-3	1.54E-3	1.49E-3	1.44E-3	1.39E-3
−3.0	1.35E-3	1.31E-3	1.26E-3	1.22E-3	1.18E-3	1.14E-3	1.11E-3	1.07E-3	1.04E-3	1.00E-3
−3.1	9.68E-4	9.35E-4	9.04E-4	8.74E-4	8.45E-4	8.16E-4	7.89E-4	7.62E-4	7.36E-4	7.11E-4
−3.2	6.87E-4	6.64E-4	6.41E-4	6.19E-4	5.98E-4	5.77E-4	5.57E-4	5.38E-4	5.19E-4	5.01E-4
−3.3	4.83E-4	4.66E-4	4.50E-4	4.34E-4	4.19E-4	4.04E-4	3.90E-4	3.76E-4	3.62E-4	3.49E-4

Table M.1 (Continued)

z	$\Phi(z)$									
	0	0.01	0.02	0.03	0.04	0.05	0.06	0.07	0.08	0.09
−3.4	3.37E−4	3.25E−4	3.13E−4	3.02E−4	2.91E−4	2.80E−4	2.70E−4	2.60E−4	2.51E−4	2.42E−4
−3.5	2.33E−4	2.24E−4	2.16E−4	2.08E−4	2.00E−4	1.93E−4	1.85E−4	1.78E−4	1.72E−4	1.65E−4
−3.6	1.59E−4	1.53E−4	1.47E−4	1.42E−4	1.36E−4	1.31E−4	1.26E−4	1.21E−4	1.17E−4	1.12E−4
−3.7	1.08E−4	1.04E−4	9.96E−5	9.57E−5	9.20E−5	8.84E−5	8.50E−5	8.16E−5	7.84E−5	7.53E−5
−3.8	7.23E−5	6.95E−5	6.67E−5	6.41E−5	6.15E−5	5.91E−5	5.67E−5	5.44E−5	5.22E−5	5.01E−5
−3.9	4.81E−5	4.61E−5	4.43E−5	4.25E−5	4.07E−5	3.91E−5	3.75E−5	3.59E−5	3.45E−5	3.30E−5
−4.0	3.17E−5	3.04E−5	2.91E−5	2.79E−5	2.67E−5	2.56E−5	2.45E−5	2.35E−5	2.25E−5	2.16E−5
−4.1	2.07E−5	1.98E−5	1.89E−5	1.81E−5	1.74E−5	1.66E−5	1.59E−5	1.52E−5	1.46E−5	1.39E−5
−4.2	1.33E−5	1.28E−5	1.22E−5	1.17E−5	1.12E−5	1.07E−5	1.02E−5	9.77E−6	9.34E−6	8.93E−6
−4.3	8.54E−6	8.16E−6	7.80E−6	7.46E−6	7.12E−6	6.81E−6	6.50E−6	6.21E−6	5.93E−6	5.67E−6
−4.4	5.41E−6	5.17E−6	4.94E−6	4.71E−6	4.50E−6	4.29E−6	4.10E−6	3.91E−6	3.73E−6	3.56E−6
−4.5	3.40E−6	3.24E−6	3.09E−6	2.95E−6	2.81E−6	2.68E−6	2.56E−6	2.44E−6	2.32E−6	2.22E−6
−4.6	2.11E−6	2.01E−6	1.92E−6	1.83E−6	1.74E−6	1.66E−6	1.58E−6	1.51E−6	1.43E−6	1.37E−6
−4.7	1.30E−6	1.24E−6	1.18E−6	1.12E−6	1.07E−6	1.02E−6	9.68E−7	9.21E−7	8.76E−7	8.34E−7
−4.8	7.93E−7	7.55E−7	7.18E−7	6.83E−7	6.49E−7	6.17E−7	5.87E−7	5.58E−7	5.30E−7	5.04E−7
−4.9	4.79E−7	4.55E−7	4.33E−7	4.11E−7	3.91E−7	3.71E−7	3.52E−7	3.35E−7	3.18E−7	3.02E−7
−5.0	2.87E−7	2.72E−7	2.58E−7	2.45E−7	2.33E−7	2.21E−7	2.10E−7	1.99E−7	1.89E−7	1.79E−7
−5.1	1.70E−7	1.61E−7	1.53E−7	1.45E−7	1.37E−7	1.30E−7	1.23E−7	1.17E−7	1.11E−7	1.05E−7
−5.2	9.96E−8	9.44E−8	8.95E−8	8.48E−8	8.03E−8	7.60E−8	7.20E−8	6.82E−8	6.46E−8	6.12E−8
−5.3	5.79E−8	5.48E−8	5.19E−8	4.91E−8	4.65E−8	4.40E−8	4.16E−8	3.94E−8	3.72E−8	3.52E−8
−5.4	3.33E−8	3.15E−8	2.98E−8	2.82E−8	2.66E−8	2.52E−8	2.38E−8	2.25E−8	2.13E−8	2.01E−8
−5.5	1.90E−8	1.79E−8	1.69E−8	1.60E−8	1.51E−8	1.43E−8	1.35E−8	1.27E−8	1.20E−8	1.14E−8
−5.6	1.07E−8	1.01E−8	9.55E−9	9.01E−9	8.50E−9	8.02E−9	7.57E−9	7.14E−9	6.73E−9	6.35E−9
−5.7	5.99E−9	5.65E−9	5.33E−9	5.02E−9	4.73E−9	4.46E−9	4.21E−9	3.96E−9	3.74E−9	3.52E−9
−5.8	3.32E−9	3.12E−9	2.94E−9	2.77E−9	2.61E−9	2.46E−9	2.31E−9	2.18E−9	2.05E−9	1.93E−9
−5.9	1.82E−9	1.71E−9	1.61E−9	1.51E−9	1.43E−9	1.34E−9	1.26E−9	1.19E−9	1.12E−9	1.05E−9
−6.0	9.87E−10	9.28E−10	8.72E−10	8.20E−10	7.71E−10	7.24E−10	6.81E−10	6.40E−10	6.01E−10	5.65E−10
−6.1	5.30E−10	4.98E−10	4.68E−10	4.39E−10	4.13E−10	3.87E−10	3.64E−10	3.41E−10	3.21E−10	3.01E−10
−6.2	2.82E−10	2.65E−10	2.49E−10	2.33E−10	2.19E−10	2.05E−10	1.92E−10	1.81E−10	1.69E−10	1.59E−10
−6.3	1.49E−10	1.40E−10	1.31E−10	1.23E−10	1.15E−10	1.08E−10	1.01E−10	9.45E−11	8.85E−11	8.29E−11
−6.4	7.77E−11	7.28E−11	6.81E−11	6.38E−11	5.97E−11	5.59E−11	5.24E−11	4.90E−11	4.59E−11	4.29E−11
−6.5	4.02E−11	3.76E−11	3.52E−11	3.29E−11	3.08E−11	2.88E−11	2.69E−11	2.52E−11	2.35E−11	2.20E−11
−6.6	2.06E−11	1.92E−11	1.80E−11	1.68E−11	1.57E−11	1.47E−11	1.37E−11	1.28E−11	1.19E−11	1.12E−11
−6.7	1.04E−11	9.73E−12	9.09E−12	8.48E−12	7.92E−12	7.39E−12	6.90E−12	6.44E−12	6.01E−12	5.61E−12
−6.8	5.23E−12	4.88E−12	4.55E−12	4.25E−12	3.96E−12	3.69E−12	3.44E−12	3.21E−12	2.99E−12	2.79E−12
−6.9	2.60E−12	2.42E−12	2.26E−12	2.10E−12	1.96E−12	1.83E−12	1.70E−12	1.58E−12	1.48E−12	1.37E−12
−7.0	1.28E−12	1.19E−12	1.11E−12	1.03E−12	9.61E−13	8.95E−13	8.33E−13	7.75E−13	7.21E−13	6.71E−13

* For positive z values, use this table in conjunction with Eq. M.32.

The relationship for the PDF of any normal random variable, $f_X(x)$, and the PDF of its standardized normal variable, $\phi(z)$, is:

$$f_X(x) = \phi\left(\frac{x-\bar{x}}{\sigma_X}\right)\frac{1}{\sigma_X} \tag{M.33}$$

Most practical applications require the *inverse* Φ^{-1} *of the standard normal cumulative distribution function* $\Phi(z)$. Let $p = \Phi(z)$; the value of z can be accurately calculated by the approximation Eq. M.34, which is adopted in most computer procedures.

$$z = \Phi^{-1}(p) = -t + \frac{c_0 + c_1 t + c_2 t^2}{1 + d_1 t + d_2 t^2 + d_3 t^3} \text{ with } p \leq 0.5 \tag{M.34}$$

where $c_0 = 2.515517$; $c_1 = 0.802853$; $c_2 = 0.010328$; $d_1 = 1.432788$; $d_2 = 0.189269$; $d_3 = 0.001308$; $t = \sqrt{-\ln p^2}$.

For $p > 0.5$, calculate $\Phi^{-1}(1-p)$, and use Eq. M.32, which is equivalent to:

$$\Phi^{-1}(p) = -\Phi^{-1}(1-p) \tag{M.35}$$

Example M.4: Normal random variable

A normal random variable, X has $\bar{x} = 1250$ and $\sigma_X = 150$. Find: $F_X(1100), F_X(1550)$, $F_X(1400)$, $f_X(1100)$, and $f_X(1250)$.

Equations M.31 and M.32 and Table M.1 give:

$$F_X(1100) = \Phi\left(\frac{1100 - 1250}{150}\right) = \Phi(-1.0) = 0.159$$

$$F_X(1550) = \Phi\left(\frac{1550 - 1250}{150}\right) = \Phi(2.0) = 1 - \Phi(-2.0) = 1 - 0.0228 = 0.9772$$

$$F_X(1400) = \Phi\left(\frac{1400 - 1250}{150}\right) = \Phi(1.0) = 1 - \Phi(-1.0) = 1 - 0.159 = 0.841$$

Equations M.26 and M.27 give:

$$f_X(1100) = \frac{1}{150}\phi\left(\frac{1100 - 1250}{150}\right) = \frac{1}{150}\phi(-1.0) = 1.613 \times 10^{-3}$$

$$f_X(1250) = \frac{1}{150}\phi\left(\frac{1250 - 1250}{150}\right) = \frac{1}{150}\phi(0.0) = 2.660 \times 10^{-3}$$

The probability density function of this random variable is shown in Figure M.1c.

M.11 Log-normal random variable

A random variable X has a *log-normal distribution* when the random variable Y has a normal distribution; where $Y = \ln X$ (i.e. $X = e^Y$). With a mean value $\bar{y}$ and a standard deviation σ_Y, the density function $f_X(x)$ is given by Eq. M.24 substituting $e^{\frac{-(x-\bar{x})^2}{2\sigma_X^2}}$ by $e^{\frac{-(y-\bar{y})^2}{2\sigma_Y^2}}$:

$$f_X(x) = \frac{1}{\sigma_Y\sqrt{2\pi}} e^{\frac{-(y-\bar{y})^2}{2\sigma_Y^2}} \tag{M.36}$$

The cumulative distribution function, CDF, can be calculated using the standard normal values (Table M.1).

$$F_X(x) = P(X \le x) = P(\ln X \le \ln x) = F_Y(y) = \Phi\left(\frac{y - \bar{y}}{\sigma_Y}\right) \tag{M.37}$$

where σ_Y and $\bar{y}$ can be expressed in terms of V_X (defined by Eq. M.17):

$$\sigma_Y^2 = \ln\left(V_X^2 + 1\right) \approx V_X^2 \tag{M.38}$$

$$\bar{y} = \ln \bar{x} - \frac{1}{2}\sigma_Y^2 \approx \ln \bar{x} \tag{M.39}$$

The above approximations are accurate for $V_X < (\sim 0.20)$.

Example M.5: Log-normal distribution for test results of concrete strength

A test series on the strength, X, of the concrete to be used in a major project exhibits a log-normal distribution. The tests give a sample mean, $\bar{x} = 50$ MPa and a sample standard deviation, $\sigma_X = 6$ MPa. What is the probability that the concrete strength does not exceed 40 MPa? What is the characteristic concrete strength, defined as the strength below which 5 percent of random X values may fall? What is the characteristic concrete strength if the PDF is considered normal instead of log-normal?

The coefficient of variation (Eq. M.17):

$$V_X = 6/50 = 0.12$$

The variance, the standard deviation and the mean of $Y(=\ln X)$ are (Eqs. M.38 and M.39):

$$\sigma_Y^2 = \ln\left(V_X^2 + 1\right) = 0.0143;\ \sigma_Y = \sqrt{0.0143} = 0.1196;\ \bar{y} = \ln \bar{x} - \frac{1}{2}\sigma_Y^2 = 3.905$$

The probability that the concrete strength does not exceed 40 MPa is (Eq. M.37 and Table M.1):

$$F_X(40) = P(X \le 40) = \Phi\left(\frac{y - \bar{y}}{\sigma_Y}\right) = \Phi\left(\frac{\ln 40 - 3.905}{0.1196}\right) = \Phi(-1.81) = 0.035$$

$$(y - \bar{y})/\sigma_Y = \Phi^{-1}(0.05) \quad ; \quad x = e^y$$

$$(y - 3.905)/0.1196 = -1.645 \quad ; \quad y = 3.708$$

The characteristic strength, $x = e^{3.708} = 40.8$ MPa.

With normal PDF, solve for x in: $(x - \bar{x})/\sigma_X = \Phi^{-1}(0.05)$.

$$(x - 50)/6 = -1.645 \quad ; \quad x = 40.1 \text{ MPa}$$

M.12 Extreme type I (or Gumbel distribution)

The maximum or the minimum value, X, of certain events follow an extreme type I distribution (e.g. the largest wind pressure over a structure in a specified period or the lowest strength of a certain type of beam). Let $x_1, x_2, \ldots, x_n$ be values of these events in the lifetime of the considered structure or beam. The CDF and the PDF for extreme type I are:

$$F_X(x) = e^{-\left(e^{-\alpha(x-u)}\right)} \text{ for } -\infty \le x \le \infty \tag{M.40}$$

$$f_X(x) = \alpha\, e^{-\left(e^{-\alpha(x-u)}\right)} e^{-\alpha(x-u)} \tag{M.41}$$

The parameters α and u are related to the mean $\bar{x}$ and the standard deviation σ_X by the approximations:[3]

$$x \cong u + \frac{0.577}{\alpha};\ \sigma_X \cong \frac{1.282}{\alpha};\ u \cong \bar{x} - 0.45\sigma_X$$

The extreme type II distribution gives the best approximation for seismic load.[3]

M.13 Normal probability paper

The graph in Figure M.2 has two vertical axes: the first represents $\Phi^{-1}(z)$ with a linear scale from -3 to $+3$; the second represents the corresponding values of $\Phi(z)$ with a scale from 1.35×10^{-3} to $(1\text{–}1.35 \times 10^{-3}) = 0.99865$. We can use Table M.1 to compare any value on the first scale with the opposite value on the second scale: e.g. at $\Phi^{-1}(z) = -1$ and 1, the Φ scale reads 0.159 and $(1 - 0.159) = 0.841$ respectively. As another example, we can use Eq. M.34 to verify that at $\Phi(z) = 0.3$ and 0.7, the opposite values on the $\Phi^{-1}(z)$ scale are -0.524 and $+0.524$ respectively. The horizontal x axis in the graph represents a random value with a linear scale. Commercially available probability paper can be used to plot graphs similar to the one in Figure M.2. The inclined straight line in the figure represents the CDF of a normal random variable with a mean value $\bar{x} = 6.0$ and a standard deviation $\sigma_X = 1.5$. The slope of the line $= 1/\sigma_X$ and it intersects the horizontal axis at $x = \bar{x}$. The CDF of any normal random variable appears as a straight line when plotted with reference to the axes x and $\Phi(z)$ in Figure M.2, with $z = (x - \bar{x})/\sigma_X$. The rationale behind the normal probability paper is explained by considering the standardized form, z, of a normal random variable X; for any value x, the z value is:

$$z = \frac{x - \bar{x}}{\sigma_X} = \frac{1}{\sigma_X} x - \frac{\bar{x}}{\sigma_X} \tag{M.42}$$

$$\Phi^{-1}(p) = z = \frac{1}{\sigma_X} x - \frac{\bar{x}}{\sigma_X} \tag{M.43}$$

This is the equation of the inclined straight line in Figure M.2. The normal probability paper can be used to determine whether a set of data has a normal distribution or not. The inclined line in Figure M.2 intersects the $\Phi(z)$ axis at $\Phi^{-1}(p) = -\bar{x}/\sigma_X$, where $p =$ the probability of X being less than 0. The opposite value on the Φ^{-1} scale is $(-\beta)$; the parameter β, which is called the *reliability index*, is given by:

$$\beta = \bar{x}/\sigma_X \tag{M.44}$$

3 See references in Chapter 24.

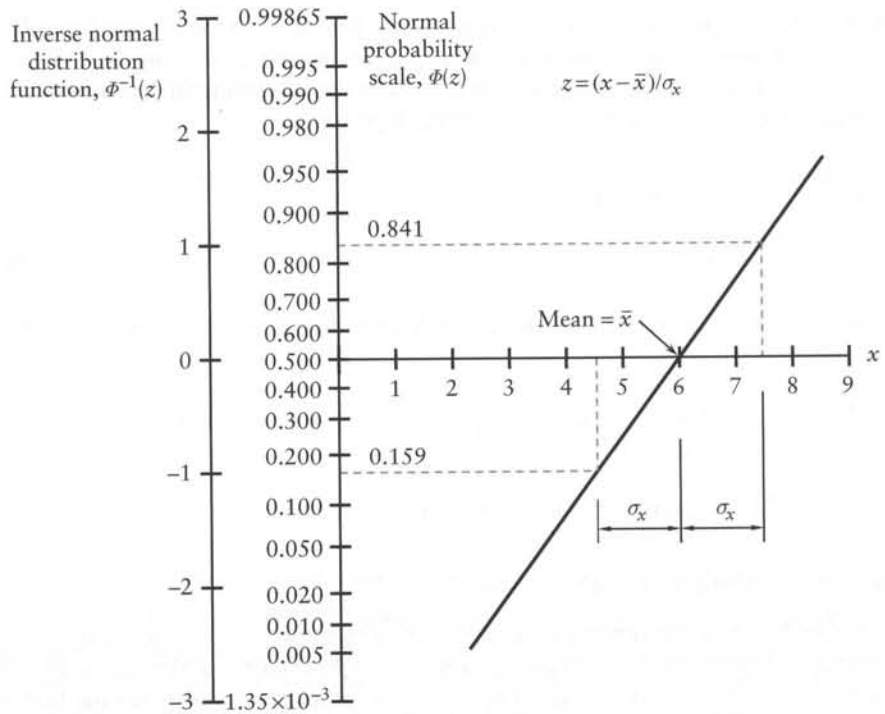

Figure M.2 Mean value and standard deviation on the normal probability paper.

In practice, in structural reliability analysis, β is positive. A negative β corresponds to a probability of failure larger than 0.5.

Wood is an example of material having a correlation coefficient (≈0.8) between its flexural strength and modulus of elasticity; it also has a smaller correlation coefficient (≈0.4 between flexural strength and weight per unit volume). The higher coefficient indicates a better correlation.

Example M.6: Use of normal probability paper

Consider a test giving $n(=9)$ data values $x_i (i=1 \text{ to } 9)$ for a random variable X; the values of x_i arranged in ascending order are given in the table. Can X be treated as a normal random variable? Find its mean value, $\bar{x}$, and standard deviation, σ_X.

Number	1	2	3	4	5	6	7	8	9
Test result value probability	5.3	5.5	5.9	5.9	6.4	6.5	6.5	6.8	7.2
$P(x \le x_i) = x_i/(1+n)$	0.1	0.2	0.3	0.4	0.5	0.6	0.7	0.8	0.9

The plot of the data on normal probability paper is shown in Figure M.3. Because the graph is approximately a straight line, we conclude that the data follow a normal distribution. A straight line fitting the graph intersects the horizontal axis at $\bar{x}=6.2$ and has a slope $1/\sigma_X = 1.55$; thus, $\sigma_X = 0.65$.

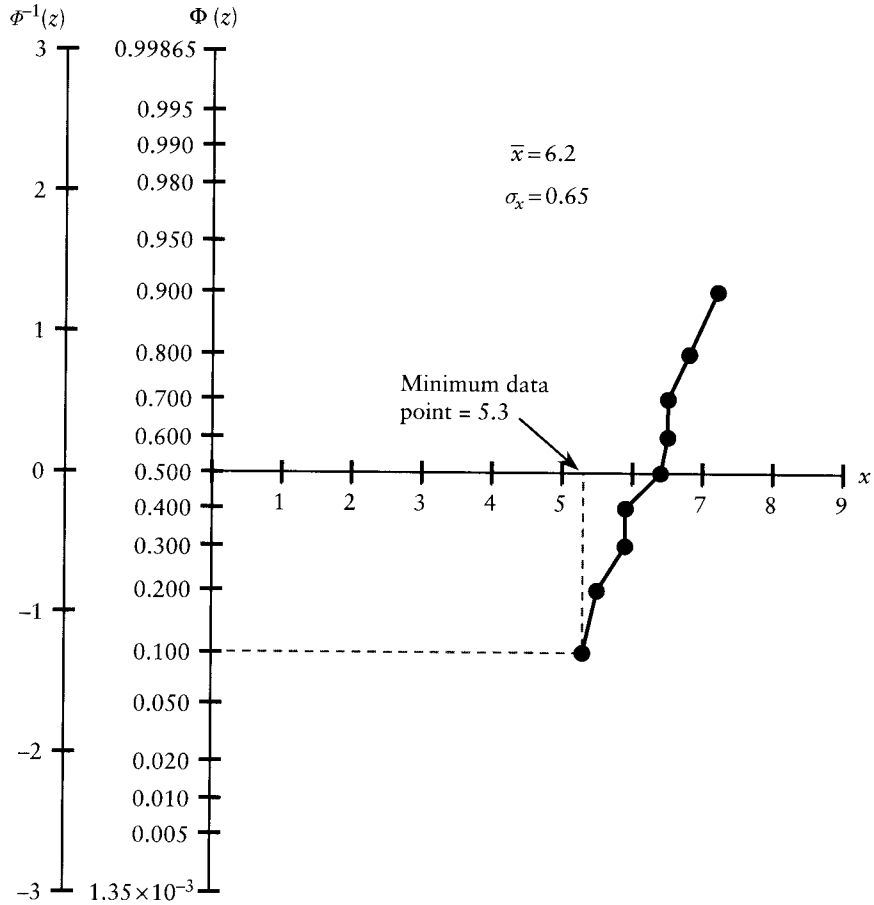

Figure M.3 CDF of the test results in Example M.6.

M.14 Covariance of two random variables

Consider a vector $\{X\}_{n\times 1}$ of n random variables. A pair of dependent (correlated) variables X_i and X_j has a *covariance*, $COV(X_i, X_j)$, a positive or negative value, defined as:

$$COV(X_i, X_j) = E\left[(X_i - \overline{x_i})(X_j - \overline{x_j})\right] = E(X_i X_j) - \overline{x_i}\,\overline{x_j} \tag{M.45}$$

The covariance of the two variables is equal to the mean of their product minus the product of their mean values. Equation M.14 is a special case of Eq. M.45 when X_i and X_j are the same. The *correlation coefficient* between X_i and X_j is defined as:

$$\rho_{X_i X_j} = \frac{COV(X_i, X_j)}{\sigma_{X_i}\sigma_{X_j}} \tag{M.46}$$

It can be shown that: $-1 \le \rho_{X_i X_j} \le 1$. The value of $\rho_{X_i X_j}$ is indicative of the degree of *linear* dependence between X_i and X_j. When $\left|\rho_{X_i X_j}\right|$ is close to one, the two variables are linearly correlated. When $\left|\rho_{X_i X_j}\right|$ is close to zero, the two variables may have a nonlinear relationship.

The *covariance matrix*, $[C]_{n\times n}$, is a square symmetrical matrix whose general element $C_{ij} = COV(X_i, X_j)$; and any diagonal element, $C_{ii} = \sigma^2_{X_i}$ (always positive). When X_i and X_j are uncorrelated, the element $C_{ij} = 0$. Similarly, the matrix of correlation coefficients, $[\rho]_{n\times n}$ is defined as:

$$[\rho] = \begin{bmatrix} \rho_{11} & \rho_{12} & \cdots & \rho_{1n} \\ \rho_{21} & \rho_{22} & \cdots & \rho_{2n} \\ \vdots & \vdots & \ddots & \vdots \\ \rho_{n1} & \rho_{n2} & \cdots & \rho_{nn} \end{bmatrix} \tag{M.47}$$

where $\rho_{ij} = \rho_{X_i X_j}$; any diagonal element $\rho_{ii} = 1$; $\rho_{ij} = 0$ when X_i and X_j are uncorrelated.

M.15 Mean and variance of linear combinations of random variables

This section gives some properties of a random variable Y, which is a linear combination of random variables $X_1, X_2, \ldots, X_n$. We can prove Eqs. M.48 to M.53, in which $a_0, a_1, \ldots, a_n$ are constants. If $Y = aX$, the mean and the variance of Y are:

$$\overline{y} = a\overline{x}; \quad \sigma^2_y = a^2\sigma^2_X \tag{M.48}$$

If $Y = a_1X_1 + a_2X_2$, the mean and the variance of Y are:

$$\overline{y} = a_1\overline{x_1} + a_2\overline{x_2} \tag{M.49}$$

$$\sigma^2_Y = a_1^2\,\sigma^2_{X_1} + a_2^2\,\sigma^2_{X_2} + 2a_1a_2COV(X_1, X_2) \tag{M.50}$$

If $Y = a_0 + a_1X_1 + a_2X_2 + \ldots + a_nX_n = \{a\}^T\{X\}$, the mean and the variance of Y are:

$$\overline{y} = a_0 + \sum_{i=1}^{n} (a_i\,\overline{x_i}) \tag{M.51}$$

$$\sigma^2_Y = \{a\}^T[C]\{a\} \tag{M.52}$$

where $[C]$ is the covariance matrix, whose general element $C_{ij} = COV(X_i, X_j)$. Equations M.49 and M.50 are for a special case of Eqs. M.51 and M.52 respectively. When the variables in $\{X\}$ are uncorrelated, the non-diagonal elements of $[C]$ are nil and Eq. M.52 becomes:

$$\sigma^2_Y = \sum_{i=1}^{n} (a_i\,\sigma_{X_i})^2 \tag{M.53}$$

The coefficient of variation of Y is:

$$V_Y = \sigma^2_Y / |\overline{y}| \tag{M.54}$$

The covariance of correlated random variables X_i and X_j,

$$COV(a\,X_i, X_j) = a\,COV(X_i, X_j) \tag{M.55}$$

Equations M.48 to M.54 give the mean, the variance, and the coefficient of variation for linear combinations of random variables, whose distributions are arbitrary. When the random variables $X_1, X_2, \ldots, X_n$ are uncorrelated and normally distributed, Y is also a normal random variable. Examples of the use of the equations in this section are given in Chapter 24.

M.16 Product of log-normal random variables

Consider a random variable Y expressed in terms of *independent* log-normal random variables X_1, X_2, and X_3, and a constant a:

$$X_0 = a\frac{X_1 X_3}{X_2} \tag{M.56}$$

$$\ln X_0 = \ln a + \ln X_1 + \ln X_3 - \ln X_2 \tag{M.57}$$

Equation M.57 is a linear combination of the normally distributed uncorrelated random variables: $Y = \ln X_0$; $Y_1 = \ln X_1$; $Y_2 = \ln X_2$ and $Y_3 = \ln X_3$. Equations M.51 and M.53 can give the mean and the variance of Y:

$$\bar{y} = \ln a + \overline{y_1} + \overline{y_3} - \overline{y_2} \tag{M.58}$$

$$\sigma_Y^2 = \sigma_{Y_1}^2 + \sigma_{Y_2}^2 + \sigma_{Y_3}^2 \tag{M.59}$$

Equations M.58 and M.59 apply to all X_i. If not all X_1, X_2, and X_3 are log-normal, Eqs. M.58 and M.59 can still apply, but we cannot say that the probability distribution of X_0 is log-normal. The use of the equations in this section is demonstrated in Example 24.2, Chapter 24.

Problems

M.1 Imperial units. The values of stress at the extreme fibers in flexural tests of 2 in. × 10 in. timber beams are given in the table below. Calculate the mean and standard deviation.

Test data (psi)								
4677	4741	4020	5436	5897	4758	3874	5023	5085
4212	5123	3845	5088	4830	7130	3966	5702	4310
4327	4930	5772	4724	6408	4667	5332	3973	5631

M.2 SI units. The values of stress at the extreme fibers in flexural tests of 38 mm × 241 mm timber beams are given in the table below. Calculate the mean and standard deviation.

Test data (MPa)								
32.3	32.7	27.7	37.5	40.7	32.8	26.7	34.6	35.1
29.0	35.3	26.5	35.1	33.3	49.2	27.4	39.3	29.7
29.8	34.0	39.8	32.6	44.2	32.2	36.8	27.4	38.8

M.3 A normal random variable, X, has the mean value, $\bar{x} = 142$, and standard deviation, $\sigma_X = 21$. Calculate the probability: (a) $X < 100$; (b) $X \geq 187$.

M.4 A log-normal random variable, X, has the mean value, $\bar{x} = 3000$, and $\sigma_X = 700$. Calculate the probability: (a) $X \leq 2500$; (b) $2800 \leq X \leq 3200$.

M.5 The CDFs of dead load, live load, and resistance are plotted on the normal probability paper, as shown. Determine the mean and standard deviation for the dead load, live load, and resistance.

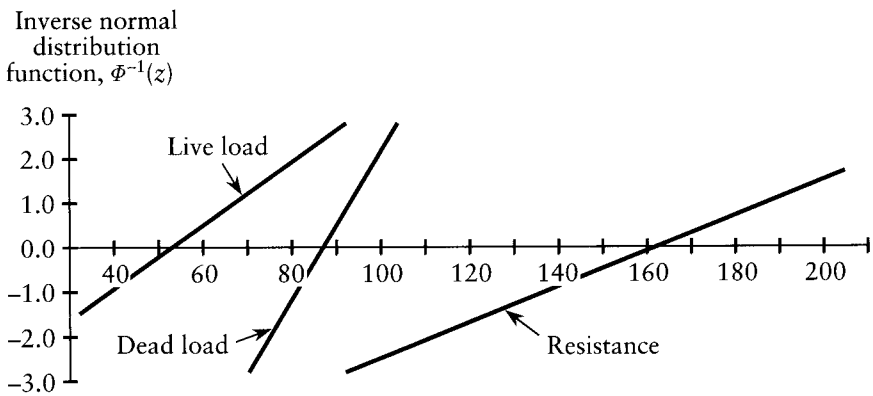

Prob. M.5

M.6 The load-carrying capacity of a structural member from 19 randomly selected samples are: {3.92, 4.62, 4.03, 3.89, 4.51, 4.39, 4.21, 3.90, 3.78, 4.53, 3.40, 4.44, 4.16, 4.31, 4.22, 4.07, 3.97, 4.12, 4.38}. Plot the test data on normal probability paper; from the plot, find the mean and the standard deviation.

Answers to problems

Chapter 1

1.1 (a) $\{\theta_A, \theta_B, \theta_C, \theta_D,\} = \{13.5, -9.4, 2.3, -1.2\} \cdot 10^{-3} ql^3/EI$
Bending moments at supports (positive moment produces tension at bottom face): $\{M_B, M_C\} = \{-32.8, 9.4\} \cdot 10^{-3} ql^2$.

(b) $\{\theta_A, \theta_B, \theta_C, \theta_D,\} = \{-7.0, 13.9, -13.9, 7.0\} \cdot 10^{-3} ql^3/EI$
Bending moments at supports (positive moment produces tension at bottom face): $\{M_B, M_C\} = \{-55.6, -55.6\} \cdot 10^{-3} ql^2$.

(c) $\{\theta_B, \theta_C\} = \{2.4, 2.4\} \cdot 10^{-3}\ Pl^2/EI$
Member end moments: $\{M_{AB}, M_{BA}, M_{CB}, M_{DC}\} = \{-0.11, -0.09, 0.07, -0.07\} \cdot$ Pl.

(d) $\{\theta_A, \theta_B, \theta_C, \theta_D\} = \{66.7, -8.3, 91.7, 16.7\} \cdot 10^{-3}\ Pl^2/EI$
$\{M_{BA}, M_{BC}, M_{CB}, M_{CD}\} = \{-0.15, 0.15, 0.35, 0.15\} \cdot Pl.$

(e) $\{\theta_A, \theta_B, \theta_C, \theta_D\} = \{225.0, 29.2, 54.2, 191.7\} \cdot 10^{-3}\ Pl^2/EI$
$\{M_{BA}, M_{BC}, M_{CB}, M_{CD}\} = \{-0.22, 0.22, 0.27, -0.27\} \cdot Pl.$

(f) $\{\theta_B, \theta_c\} = \{28.0, 14.8\} \cdot 10^{-3}\ Pl^2/EI$
$\{M_{AB}, M_{BA}, M_{BC}, M_{BE}, M_{CB}, M_{CD}\} = \{-0.24, -0.13, -0.04, 0.17, -0.09, 0.09\} \cdot$ Pl.

1.2 $\{\theta_B, \theta_C\} = \{-0.86, -0.86\} \cdot \delta/l$; $\{u_B, v_B, u_C, v_C\} = \{0.429, 0, 0.429, 1\} \cdot \delta$; $\{M_{AB}, M_{BA}, M_{BC}, M_{CD}, M_{DC}\} = \{-0.86, 0.86, -0.86, -0.86, 0.86, -0.86\} \cdot EI\delta/l^2$.

1.3 $\{\sigma_{top}, \sigma_{bottom}\} = [N/(bh)] \cdot \{4, -2\}$.

1.4 Vertical members: $\{N_{AB}, N_{BC}, N_{CD}, N_{HG}, N_{GF}, N_{FE}\} = (H/8) \cdot \{9, 5, 1, -13, -9, -5\}$; Horizontal members: $\{N_{BG}, N_{CF}\} = (H/2) \cdot \{-1, -1\}$); Inclined members: $\{N_{AG}, N_{BF}, N_{CE}\} = (H/\sqrt{2}) \cdot \{1, 1, 1\}$.

1.6 $R = (3EI/l)\psi_{free}$ (down).

1.7 $h_1 = 8l/27$; $h_2 = 10l/27$.

1.8 $M_{x=l/4} = 3Pl/32$; $M_{x=3l/4} = -3Pl/32$; positive moment produces tension at bottom face. Shear just to the right and just to the left of the applied load are $0.474P$ and $-0.474P$ respectively.

1.9 Horizontal component in all four segments $= Pl/(2h_C)$; vertical components in AB and $BC = 3Pl/(2h_C)$ and $Pl/(2h_C)$ respectively.

1.11

	Horizontal translation at B	M_{AB}	M_{BA}
Without bracing	$27.3 \times 10^{-3}\ Pl^3/(EI)_{AB}$	$-0.223\ Pl$	$-0.154\ Pl$
With bracing as shown in part (b)	$0.968 \times 10^{-3}\ Pl^3/(EI)_{AB}$	$-7.47 \times 10^{-3}\ Pl$	$-4.51 \times 10^{-3}\ Pl$
With bracing as shown in part (c)	$1.36 \times 10^{-3}\ Pl^3/(EI)_{AB}$	$-11.2 \times 10^{-3}\ Pl$	$-7.96 \times 10^{-3}\ Pl$

1.12

	Horizontal translation at B	M_{AB}	M_{BA}
Without bracing	5.91×10^{-3} m	−64.1 kN.m	−44.2 kN.m
With bracing as shown in part (b)	0.210×10^{-3} m	−2.15 kN.m	−1.33 kN.m
With bracing as shown in part (c)	0.294×10^{-3} m	−3.23 kN.m	−2.29 kN.m

1.13

	Horizontal translation at B	M_{AB}	M_{BA}
Without bracing	0.219 in.	-570×10^3 lb.in	-393×10^3 lb.in
With bracing as shown in part (b)	7.75×10^{-3} in.	-19.1×10^3 lb.in	-11.8×10^3 lb.in
With bracing as shown in part (c)	10.9×10^{-3} in.	-28.7×10^3 lb.in	-20.4×10^3 lb.in

1.14 Using computer program PLANET, horizontal translation at $B = 0.994 \times 10^{-3} Pl^3/(EI)_{AB}$; $\{N_{AB},\ N_{BC},\ N_{CD},\ N_{AC},\ N_{BD}\} = P \cdot \{0.414,\ -0.448,\ -0.336,\ 0.560,\ -0.690\}$.

1.15

Member	AG	BH	CI	AB	BC	CD	AH
Force in terms of P	−0.500	1.500	0.500	2.500	4.000	4.500	−3.536
Member	BI	CJ	HN	NO	IO	NI	OJ
Force in terms of P	−2.121	−0.707	−1.398	−1.250	−0.839	0.625	0.750

1.16

Member	AG	AB	BC	CD	AH	BI	CJ	BH
Force in terms of P	−0.500	2.500	4.000	4.500	−3.536	−2.121	−0.707	1.500
Member	CI	HN	NO	IO	NI	OJ	HI	IJ
Force in terms of P	0.500	−0.699	−0.625	−0.419	0.313	0.375	−1.250	−2.000

Chapter 2

2.1 (a) Reactions: $R_{Dx} = -0.2P$; $R_{Dy} = -0.8P$; $R_{cy} = -1.2P$. Member forces: $\{AB,\ BC,\ CD,\ DA,\ AC\} = P\{-0.200,\ -1.020,\ 0.360,\ -0.816,\ -0.256\}$.

(b) Reactions: $R_{Dy} = -2P/3$; $R_{cx} = -P/2$; $R_{cy} = -4P/3$. Member forces: $\{AB,\ BC,\ CE,\ ED,\ DA,\ AE,\ EB\} = P\{-0.25,\ -1.33,\ -0.50,\ 0,\ -0.67,\ -0.42,\ 0.42\}$.

(c) Reactions: $R_{Hy} = -P$, $R_{Ky} = -4P$; $R_{Ny} = -P$. Selected member forces: $\{BC,\ IJ,\ BJ,\ BI\} = P\{0,\ 0.5,\ -0.707,\ -0.5\}$.

(d) Forces in members: $\{AB,\ AC,\ AD\} = P\{1.166,\ -6.319,\ -0.574\}$. Reactions: $\{R_x,\ R_y,\ R_z\}_B = P\{0,\ -0.6,\ 1.0\}$; $\{R_x,\ R_y,\ R_z\}_c = P\{-2.2,\ -2.2,\ -5.5\}$; $\{R_x,\ R_y,\ R_z\}_D = P\{0.2,\ -0.2,\ -0.5\}$.

2.3 $\{R_1, R_3, R_4, R_5, R_6, R_7\} = P\{-1.833, -2.75, -2.917, -3.0, -0.625, -1.375\}$.

2.4 (a) $R_A = 0.68ql$; $R_c = 1.42ql$; $M_B = 0.272\,ql^2$; $M_c = -0.1\,ql^2$.

(b) $R_A = 1.207P$ down and $1.207P$ to the left; $R_D = 0.5P$ up and $0.5P$ to the left; $M_B = 1.207Pl$, tension side inside frame; $M_A = M_C = M_D = 0$.

(c) $R_A = 0.57ql$; $R_B = 1.23ql$; $R_C = 1.08ql$; $R_D = 0.42ql$; $M_G = 0.16ql^2$; $M_B = M_C = -0.08ql^2$.

(d) $R_A = 0.661ql$ up; $R_C = 0.489ql$ up. Member end-moments: $M_{BD} = 0.03125qb^2$; $M_{BA} = -0.06610qb^2$; $M_{BC} = 0.03485qb^2$.

(e) $R_F = 0.75ql$ up and $0.0857ql$ to the right. Member end-moments: $M_{BF} = 0.0429ql^2$; $M_{BA} = 0.05ql^2$; $M_{BC} = -0.0929ql^2$.

(f) $RA = 0.6ql$ up and $0.2ql$ to the right; $R_B = ql/\sqrt{5}$; $V_A = -V_B = ql/\sqrt{5}$; $M = 0$ at two ends and at center $M = ql^2/8$.

(g) $R_A = 2.375P$; $R_G = 1.625P$ up and $2P$ to the right. Nonzero member end-moments: $M_{FG} = -M_{FE} = 1.5Pl$; $M_{EF} = -M_{ED} = 2.625Pl$; $M_{DE} = -M_{DC} = 2.75Pl$; $M_{CD} = -M_{CB} = 1.875Pl$. $V_{Br} = 1.68P$; $V_{Dl} = 0.78P$.

(h) Considering M positive producing tension at bottom fiber, $M_{Ar} = -2.18ql^2$; $M_{Bl} = -0.56ql^2$; $M_{Br} = -0.625ql^2$. Torsion in $AB = 0.28ql^2$.

(i) $R_A = 0.4ql$; $R_B = 0.98ql$; $R_C = 0.42ql$; $M_E = 0.16ql^2$; $M_B = -0.08ql^2$.

(j) $R_A = 0.4ql$; $R_C = 0.745ql$; $R_E = 0.755ql$; $R_H = 0.4ql$; M at middle of $AB = 0.08ql^2$; $M_C = -0.1ql^2$; $M_E = -0.08ql^2$; $M_G = 0.16ql^2$.

(k) $R_B = 0.62ql$; $R_C = 1.18ql$; $R_E = 0.4ql$; $M_B = -0.02ql^2$; $M_C = -0.1ql^2$; M at middle of $DE = 0.08ql^2$.

(l) $R_1 = 0.125ql$; $R_2 = 0.8125ql$; $R_3 = 0.375ql$; $R_4 = 1.6875ql$; $M_B = 0.125ql^2$, tension side outside the frame; end moments $\{M_{DC}, M_{DF}, M_{DE}\} = ql^2\ \{0.6875, -0.1250, -0.5625\}$.

(m) $R_1 = -0.375ql$; $R_2 = 0.25ql$; $R_3 = 0.625ql$; $R_4 = 0.375ql^2$; $M_B = 0.375ql^2$, tension side inside the frame; $M_D = 0.625\ ql^2$, tension side outside the frame.

(n) $R_1 = 0.158ql$; $R_2 = 0.421ql$; $R_3 = 0.158ql$; $R_4 = 0.579ql$; $M_B = 0.0395ql^2$; $M_D = 0.0789ql^2$, tension side outside frame at B and D.

2.5 (a) $M_{\max+} = 0.405Wl$, at $0.05l$ on either side of mid-span.

(b) $M_{\max+} = 0.476Wl$, at $0.02l$ on either side of mid-span (assuming reversible loading).

(c) $M_{\max+} = 0.2628Wl$, at $0.3625l$ from the left support (when one of the two loads is at this section and the other is at $0.9125l$ from the same support).

2.6 $M_{\max+} = 0.352Wl$, at $l/30$ on either side of mid-span. $V_{\max+} = -V_{\max-} = 1.56W$ at the supports.

2.8 The maximum bending moment diagrams are symmetrical about the center line of the beam. The ordinates for the left half are as follows:

(a) $M_{\max+}$ is zero for the overhang and is the same as in Fig. 2.8a for the remaining part. M_{max-} is $0, -0.3Pl, -0.39Pl$ and $-0.195Pl$ at distances $0, 0.3l, 0.35l$ and $0.85l$ from the left end; join the ordinates by straight lines.

(b) $M_{\max+}$ is zero for the overhang; between the support and the center, M_{max+} is $Pl(1.32\xi - 1.8\xi^2)$, where ξ is the distance from the support divided by l. $M_{\max-}$ is $0, -0.35Pl$ and $-0.175Pl$ at distances $0, 0.35l$ and $0.85l$ from the left-hand end; join ordinates by straight lines.

2.9 (a) $M_{n\ \max+} = 0.2775Pl$; $M_{n\ \max-} = -0.2925Pl$; $V_{n\ \max+} = 1.11P$.

(b) $M_{n\ \max+} = 93.75 \times 10^{-3}ql^2$; $M_{n\ \max-} = -61.25 \times 10^{-3}ql^2$; $V_{n\ \max+} = 0.3425ql$.

2.10 (a) The maximum positive bending moment is $0.395Pl$; it occurs at distance from A of $0.439l$. The maximum negative bending moment is $-0.210Pl$; it occurs at C. (b) The maximum positive bending moment is $0.394Pl$; it occurs at distance from A of $0.556l$. The maximum negative bending moment is $-0.210Pl$, and occurs at C.

2.11 The maximum positive bending moment diagram has zero ordinates between D and B. Between B and C, the maximum positive bending moment diagram is the same as that in Figure 2.13a. The maximum negative bending moment diagram has the ordinates 0, $-0.285Pl$, and 0 at D, B, and C respectively; the diagram is linear between D and B and between B and C. The influence line for M_n is composed of straight lines with the ordinates: $\eta_A = 0$; $\eta_D = -0.1133l$; $\eta_B = 0$; $\eta_n = 0.2456l$; $\eta_C = 0$. The maximum positive and negative bending moments at n are $0.3380Pl$ and $-0.1615Pl$.

2.12 The force in each member running in the x, y, or z direction is $0.5T/l$ (tension). The force in each diagonal member is $-0.7071T/l$ (compression). The reaction components are nil, except: $(R_y)_I = -(R_y)_K = 0.5T/l$; $(R_z)_J = -(R_z)_L = 0.5T/l$.

Chapter 3

3.1 $i = 1$. Introduce a hinge in the beam at B.
3.2 $i = 1$. Delete members CF or ED.
3.3 $i = 3$. Make A a free end.
3.4 $i = 2$. Introduce hinges in the beam at B and D.
3.5 $i = 4$. Change support B to a roller and cut member DE at any section.
3.6 $i = 5$. Remove support B and delete members AE, IF, FJ, and GC.
3.7 $i = 3$.
3.8 (a) $i = 15$. (b) $i = 7$.
3.9 $i = 2$. Delete members IJ and EG.
3.10 5 degrees and 3 degrees when axial deformation is ignored.
3.11 14 degrees and 8 degrees when axial deformation is ignored.
3.12 9 degrees.
3.13 Cut member BC at any section. The member end-moments in the released structure are: $M_{AD} = -M_{AB} = Pb$, all other end-moments are zero. A positive end-moment acts in a clockwise direction on the member end.
3.14 Cut six members: AC, BD, AH, DG, CF, and BE. Forces in members of the released structure: $AD = -P$; $AE = P$; $DE = P\sqrt{2}$; $AF = -P\sqrt{2}$; $DH = -P$; forces in other members are zero.
3.15 (a) Cut EF and CD; each results in three releases.
(b) Member end-moments: $M_{AC} = M_{CA} = M_{BD} = M_{DB} = -Pl/2$; $M_{CE} = M_{EC} = M_{DF} = M_{FD} = -Pl/4$; $M_{EF} = M_{FE} = Pl/4$; $M_{CD} = M_{DC} = 3Pl/4$.
3.16

Member	AB	AC	BC	AD	BE	CF	BD	CD	BF	CE
Force in terms of $P/1000$	-577	-577	0	0	-577	-577	817	817	0	0

The nonzero reaction components are: $(R_y)_D = -P$; $(R_z)_D = 1.155P$; $(R_z)_E = (R_z)_F = -0.577P$.

Chapter 4

4.1 (a) $[f] = \dfrac{l}{6EI}\begin{bmatrix} 4 & 1 \\ 1 & 2 \end{bmatrix}$.

(b) $[f] = \dfrac{l^3}{6EI}\begin{bmatrix} 16 & 5 \\ 5 & 2 \end{bmatrix}$.

4.2 (a) $\{F\} = -ql^2\left\{\frac{3}{28}, \frac{1}{14}\right\}$. (b) $\{F\} = ql\left\{\frac{11}{28}, \frac{8}{7}\right\}$.

4.3 $M_B = 0.0106ql^2$, and $M_C = -0.0385ql^2$.

4.4 $M_B = 0.00380\frac{EI}{l}$, and $M_c = -0.00245\frac{EI}{l}$.

4.5 $M_B = -0.0377\,ql^2 = M_C$.

4.6 Forces in the springs:

(a) $\{F_A, F_B, F_C\} = -P\{0.209, 0.139, 0.039\}$.
Reactions:
$\{R_D, R_E, R_F, R_G\} = P\{0.51, 0.10, 0.24, 0.15\}$.

(b) $\{F_A, F_B, F_C\} = P\{0.5, 0, 0\}$; $R_D = R_F = 0.375P$; $R_E = R_G = 0.125P$.

4.7 Forces in the springs:
$\{F_A, F_B\} = P\left\{-\frac{9}{400}, \frac{9}{400}\right\}$.

4.8 or 4.9 Forces in the cables: $\{F_C, F_D\} = \{0.427, 4.658\}$ k or $\{2.12, 23.29\}$ kN.
$M_D = 1.28$ k ft or 1.96 kN m.

4.10 $M_C = -0.075ql^2$.

4.11 $\{M_B, M_C\} = ql^2\{-0.158, -0.128\}$.

4.12 The answers are in terms of $\alpha EI(T_t - T_b)/h$. Bending moments: $M_B = 9/7$; $M_c = 6/7$. Reaction components: at A, $9/7l$ up; at B, $12/7l$ down; and at C, $3/7l$ up with an anticlockwise couple of 6/7.

4.13 $M_A = -0.0556ql^2$; $M_B = -0.1032ql^2$, $M_C = -0.1151ql^2$. Upward reactions at A, B, and C are $0.785ql$, $1.036ql$, and $0.512ql$.

4.14 At end of stage 1: $M_A = M_D = 0$; $M_B = -20 \times 10^{-3}\,ql^2$; $R_A = 0.480ql$; $R_B = 0.720ql$. At end of stage 2: $M_A = M_C = 0$; $M_B = -74.4 \times 10^{-3}\,ql^2$; $M_D = 20.5 \times 10^{-3}\,ql^2$. $R_A = 0.426ql$; $R_B = 1.148ql$; $R_C = 0.426ql$.

4.16 Maximum negative bending moment at each of the two interior supports is $-0.2176ql^2$. Maximum positive bending moment at the center of each exterior span is $0.175ql^2$, and at the center of the interior span is $0.100ql^2$. Maximum reaction at an interior support is $2.300ql$. Absolute maximum shear is $1.2167ql$ at the section which is at a distance l from the ends, just before reaching the interior supports.

4.18 $M_B = -0.096ql^2$; $M_C = -0.066ql^2$; $R_B = 0.926ql$; deflection at center of $BC = 2.88 \times 10^{-3}ql^4/(EI)$.

4.19 $M_B = -1.167qb^2$; $M_C = -1.417qb^2$; $R_B = 3.326qb$; deflection at $D = 0.75qb^4/(EI)$. The reaction at B due to the settlement $= -0.298EI\delta/b^3$.

4.20 $M_{B\ \max -} = -3.952qb^2$; $M_{E\ \max +} = 2.427qb^2$; $R_{C\ \max +} = 5.546qb$.

4.21 The deflection at the middle of AD, at D, and at middle of BC is $10^{-3}\psi_{free}l^2\{45.0, -70.0, 31.3\}$. With ψ_{free} having a negative value given by Eq. 1.7, the deflections are downward at D and upward at the middle of AD and BC.

4.22 $\{M_{AB}, M_{BA}, M_{BC}, M_{CB}\} = \{0, 0.0899, -0.0899, 0\}ql^2$. Force in tie$= 0.7304ql$, tension.

4.23 Three loading cases are needed with q on all spans, combined with $0.75q$ on: (1) BC; (2) AB, and CD; (3) AB and BC. The bending moments in the three cases at B and C are:

$$\begin{bmatrix} M_B \\ M_C \end{bmatrix} = -\frac{ql^2}{1000}\begin{bmatrix} 234 & 181 & 277 \\ 234 & 181 & 222 \end{bmatrix}$$

The maximum bending moment diagram is obtained by drawing M for the three cases on the same figure. The maximum ordinates at B and C are $-0.277ql^2$; the maximum ordinates at the middle of AB, BC, and CD are $10^{-3}ql^2\{128, 195, 128\}$. Maximum $R_B = 2.416ql$; $|V_{\max}|$ at B_r is $1.264ql$.

Chapter 5

5.1 Forces in members AB, AC, AD, and AE are:
$\{A\} = P\{-0.33, 0.15, 0.58, 0.91\}$.

5.2 $A_i = PH(x_i \sin\theta_i / \sum_{i=1}^{n} x_i^2 \sin^2\theta_i)$.

5.3 See answers to Prob. 3.7.

5.4 $$[S] = \frac{Ea}{b}\begin{bmatrix} 1.707 & & \text{symmetrical} & \\ 0 & 2.707 & & \\ -1.000 & 0 & 1.707 & \\ 0 & 0 & 0 & 2.707 \end{bmatrix}.$$

5.5 Force in the vertical member $= 0.369P$. Force in each of the inclined members meeting at the point of application of $P = 0.446P$. Force at each of the other two inclined members $= -0.261P$.

5.6 Bending moment at $B = 0.298Pl$. Changes in the axial forces in AC and AD are, respectively, $0.496P$ and $-0.496P$.

5.7 Bending moment at $B = 0.202Pl$. Changes in the axial forces in AE, AG, AF and AH are, respectively, $0.299P$, $0.299P$, $-0.299P$ and $-0.299P$.

5.8 $\{M_{BC}, M_{CF}\} = Pl\{-0.0393, 0.0071\}$.

5.9 $$\{M_{BC}, M_{CF}\} = \frac{EI}{l^2}\Delta\left\{\frac{186}{35}, -\frac{72}{35}\right\}.$$

5.10 $$[S] = \frac{EI}{l}\begin{bmatrix} 8 & 2 \\ 2 & 12 \end{bmatrix}, \quad M_{BC} = -0.0507ql^2, \text{ and } M_{CB} = 0.0725ql^2.$$

Reaction at A: $0.478ql$ upward, $0.076ql$ to the right, and a couple of $0.0254ql^2$ clockwise.

5.11 or 5.12 $\{M_{BC}, M_{CB}\} = \{-0.704, -0.415\}$ k ft or $\{-0.722, -0.426\}$ kN m.

5.13 The first column of $[S]$ is $$\left\{\left(\frac{12EI_2}{l_2^3} + \frac{Ea_1}{l_1}\right), 0, -\frac{6EI_2}{l_2^2}, -\frac{Ea_1}{l_1}, 0, 0\right\}.$$

5.14 $$S_{11} = \frac{4EI_2}{l_2} + \frac{4EI_1}{l_1}, \quad S_{12} = \frac{2EI_1}{l_1}, \quad S_{13} = -\frac{6EI_2}{l_2^2}.$$
$$S_{22} = \frac{4EI_2}{l_2} + \frac{4EI_1}{l_1}, \quad S_{32} = -\frac{6EI_2}{l_2^2}, \quad S_{33} = -\frac{24EI_2}{l_2^3}.$$

5.15 The end-moments for the members are (in terms of Pl_1):
$M_{AB} = -0.010$, $M_{BA} = 0.135$, $M_{BC} = -0.135$, $M_{CB} = -0.366$, $M_{CD} = -0.366$, $M_{DC} = -0.260$.

5.16 The end-moments for the members are (in terms of Pl):
$M_{AB} = -0.123$, $M_{BA} = 0.133$, $M_{BC} = -0.133$, $M_{CB} = 0.090$. $M_{CD} = -0.090$, $M_{DC} = -0.051$.

5.17 $\{D\} = \frac{Pl^2}{EI}\{0.038l, 0.022, -0.048\}$. D_1 is a downward deflection, D_2 and D_3 are rotations represented by vectors in the positive x and z directions.

5.18 The first column of $[S]$ is
$$\left\{\frac{48EI}{l^3}, 0, 0, -\frac{12EI}{l^3}, 0, \frac{6EI}{l^2}, -\frac{12EI}{l^3}, \frac{6EI}{l^2}, 0, 0, 0, 0\right\}$$
and the second column is
$$\left\{0, \left(\frac{8EI}{l} + \frac{2GJ}{l}\right), 0, 0, -\frac{GJ}{l}, 0, -\frac{6EI}{l^2}, \frac{2EI}{l}, 0, 0, 0, 0\right\}.$$

5.19 See answers to Prob. 3.5.

5.20 Girder BE:

$\{M_B, M_I, M_J, M_E\} = Pl\{-0.184, 0.142, -0.032, -0.035\}$.

Girder AF:

$\{(M_A, M_K, M_L, M_F)\} = Pl\{-0.077, 0.051, 0.006, -0.038\}$.

5.21 $$[S] = \sum_{i=1}^{n} \begin{bmatrix} 12\dfrac{EI_i}{l_i^3} & & \text{symmetrical} \\ -6s\dfrac{EI_i}{l_i^3} & 4s^2\dfrac{EI_i}{l_i} + c^2\dfrac{GJ}{l_i} & \\ 6c\dfrac{EI_i}{l_i^2} & -sc\left(\dfrac{4EI_i}{l_i} - \dfrac{GJ_i}{l_i}\right) & 4c^2\dfrac{EI_i}{l_i} + s^2\dfrac{GJ_i}{l_i} \end{bmatrix}$$

where $s = \sin\alpha_i$ and $c = \cos\alpha_i$.

5.23 $\{D\} = (Pl^2/EI)\ \{0.0498l, 0.1504, 0.0172\}$

$\{A\} = Pl\{0, 049, 0.51, 0.49, -0.49, 0\}$.

5.24 $\{D\} = \dfrac{Pl^2}{EI}\ \{0.0572, -0.0399, 0.0730l\}$

$\{A\} = \dfrac{pl}{1000}\ \{0, 23, -23, 783, -783, -884\}$.

Chapter 6

6.1 $\{D\} = \dfrac{pl^3}{384EI}\{21, 21, 11, 11\}$. The values of the bending moments at four sections of DG are:

$\{M_D, M_J, M_L, M_G\} = \dfrac{Pl}{384}\ \{-100, 74, -10, -28\}$.

6.2 The bending moment values at four sections of beam AD are:

$M_A = M_D = 0$, $M_B = M_C = 4Pl/13$,

and for beam BF:

$M_B = 0$, and $M_F = -18Pl/13$.

6.3 (a) $$[S] = \begin{bmatrix} \dfrac{24EI}{l^3} & & \text{symmetrical} & \\ 0 & \dfrac{8EI}{l} & & \\ -\dfrac{12EI}{l^3} & -\dfrac{6EI}{l^2} & \dfrac{24EI}{l^3} & \\ \dfrac{6EI}{l^2} & \dfrac{2EI}{l} & 0 & \dfrac{8EI}{l} \end{bmatrix}.$$

(b) $$[S] = \begin{bmatrix} \dfrac{12EI}{l^3} & \text{symmetrical} & \\ 0 & \dfrac{8EI}{l} & \\ \dfrac{6EI}{l^2} & \dfrac{2EI}{l} & \dfrac{8EI}{l} \end{bmatrix}.$$

(c) $$[S] = \frac{EI}{l^3}\begin{bmatrix} 19.2 & -13.2 \\ -13.2 & 19.2 \end{bmatrix}.$$

6.4 (a) $$[S]=\begin{bmatrix} \frac{24EI}{l^3} & & \text{symmetrical} & \\ 0 & \frac{8EI}{l} & & \\ -\frac{12EI}{l^3} & -\frac{6EI}{l^2} & \frac{12EI}{l^3} & \\ \frac{6EI}{l^2} & \frac{2EI}{l} & -\frac{6EI}{l^2} & \frac{4EI}{l} \end{bmatrix}.$$

(b) $$[S]=\begin{bmatrix} \frac{24EI}{l^3} & \text{symmetrical} & \\ 0 & \frac{8EI}{l} & \\ \frac{6EI}{l^2} & \frac{2EI}{l} & \frac{4EI}{l} \end{bmatrix}.$$

(c) $$[S]=\frac{EI}{l^3}\begin{bmatrix} 13.71 & -4.29 \\ -4.29 & 1.71 \end{bmatrix}.$$

6.5 $$[S]=\frac{EI}{l^3}\begin{bmatrix} 2.5 & \text{symmetrical} & \\ -3.0 & 7.0 & \\ 1.5 & -3.0 & 2.5 \end{bmatrix} \quad \{D\}=\frac{Pl^3}{EI}\{2.85,\ 1.30,\ -0.15\}.$$

6.7 $$[S]=\begin{bmatrix} \frac{24EI}{l^3} & & \text{symmetrical} & \\ 0 & \frac{12EI}{l} & & \\ -\frac{12EI}{l^3} & -\frac{6EI}{l^2} & \frac{12EI}{l^3} & \\ \frac{6EI}{l^2} & \frac{2EI}{l} & -\frac{6EI}{l^2} & \frac{8EI}{l} \end{bmatrix} \quad [S^*]=\frac{EI}{l^3}\begin{bmatrix} 19.304 & -8.087 \\ -8.087 & 5.743 \end{bmatrix}.$$

6.8 $$S_{11}^*=S_{33}-\frac{S_{31}^2S_{22}-2S_{31}\,S_{32}S_{21}+S_{32}^2S_{11}}{S_{11}S_{22}-S_{21}^2}.$$

6.9 The value of P which makes the structure unstable is $P=\frac{EI}{2l^2}$.

6.10 The smallest value of P for the instability of the system is $P=\frac{Kl}{3}$.

6.11 Bending moment ordinates: $M_A=Pl/24$; $M_B=-Pl/12$; $M_E=Pl/6$. Reactions: $R_A=P/8$ down; $R_B=5P/8$ up.

6.13 Bending moment ordinates: $M_A=M_B=-Pl/9$; $M_C=Pl/9$. Shearing force ordinates: for AC, $V=2P/3$; for CB, $V=-P/3$. Reactions: $R_A=R_B=P$.

6.14 $M_A=-2Pl/27$; $M_B=-Pl/27$; $V_{Ar}=(19/27)P$; $V_{Al}=-(l/27)P$; $V_{Bl}=-(8/27)P$; $V_{Br}=-(1/27)P$.

6.15 $M_A=M_B=-ql^2/24$; $V_{Ar}=-V_{Bl}=ql/2$; $V_{Al}=V_{Br}=0$.

6.16 Member end-moments: $M_{AB}=0.0703qb^2$; $M_{BA}=0.1406qb^2$; $M_{BC}=-0.1406qb^2$. Reactions at A: $0.75qb$ up, $0.211qb$ horizontal to the right, and a clockwise couple $0.070qb^2$.

6.17 Member end-moments: $M_{AB}=ql^2/48$; $M_{BA}=ql^2/24$; $M_{BD}=-ql^2/24$; $M_{DB}=5ql^2/48$. Reactions at A: $7ql/16$ up, $ql/16$ to the right, and $ql^2/48$ clockwise. Reaction at $C=9ql/8$ up.

6.18 Member end-moments: $M_{AB} = -M_{BA} = -ql^2/12$ $V_A = -V_B = 0.5ql\cos\theta$.

6.19 $\{D\} = 10^{-3}\dfrac{Pl^3}{EI}(92.01l,\ -145.8,\ -76.39,\ 149.3l,\ -208.3)$.

6.20 $\{D\} = 10^{-3}\dfrac{ql^4}{EI}\left\{11.11,\ \dfrac{22.22}{l},\ 19.44\right\}$.

6.21 Stresses at top, mid-height, and bottom, in terms of αET, are -0.25, 0.25, and -0.25 respectively. The variation between these values is linear. The change in length of centroidal axis is $0.25\alpha Tl$. The deflection at mid-span is $\alpha Tl^2/8d$ upward.

6.22 At the central support, $M = 1.5EI\alpha T/d$. The stresses at top, mid-height, and bottom are, in terms of αET, -1.00, 0.25, and 0.50 respectively. Reactions at outer supports are $1.5EI\alpha T/dl$ up, and at interior support $3EI\alpha T/dl$ down.

6.23 Member end-moments in terms of $EI\alpha T/d$: $M_{AB} = -0.234$; $M_{BA} = -M_{BC} = -0.694$. Reactions at A: horizontal outward component is $0.928EI\alpha T/d^2$, and anticlockwise couple is $0.234EI\alpha T/d$.

6.24 Answers in terms of $|P|$: $\{M_A,\ M_E,\ M_B,\ M_F\} = h\{0.15,\ -0.239,\ 0.522,\ -0.278\}$; $R_A = 0.0174h/b$ up $= -R_B$; deflection at center of $AB = 0.877hb^2/EI$ up; $V_{Ar} = -0.276h/b$; $V_{Bl} = 0.382h/b$; $V_{Br} = -0.356h/b$; $V_{Cl} = 0.356h/b$; $V_{Cr} = -0.382$h/b; $V_{Dl} = 0.276$h/b.

6.25 Answers in terms of $|P|$: $\{M_A,\ M_E,\ M_B,\ M_F\} = h\{0,\ -0.3043,\ 0.3915,\ -0.4085\}$; $R_A = 0.0012$ down $= -R_B$; deflection at $E = 0.843hb^2/(EI)$ up; $V_{Ar} = -0.0869h/b$; $V_{Bl} = 0.1988h/b$; $V_{Br} = -0.1778h/b$; $V_{Cl} = 0.1778h/b$; $V_{Cr} = -0.1988h/b$; $V_{Dl} = 0.0869h/b$.

6.26 $\sigma = E\alpha T_{top}[0.167 + 0.357\,\mu - (0.5 - \mu)^5]$; extreme tension at bottom fiber $= 3.1$ MPa (or 0.45 ksi).

6.27 $M_{BA} = -M_{BC} = -M_{DE} = M_{DC} = 0.038ql^2$; $M_{CB} = -M_{BC} = 0.106ql^2$. The force in the tie $= 1.098ql$.

6.28 $M_{BA} = -M_{BC} = -M_{DE} = M_{DC} = 0.0810ql^2$; $M_{CB} = -M_{BC} = 0.0492ql^2$. The force in the tie $= 0.8555ql$.

6.29 Forces in members OA, OB, OC, and OD are, respectively, in terms of P: 0.919, -0.306, -2.756, and -1.531. $\{R_x, R_y, R_z\}_A = P\{-0.375, -0.375, 0.750\}$; $\{R_x, R_y, R_z\}_B = P\{-0.125, 0.125, -0.250\}$; $\{R_x, R_y, R_z\}_C = P\{-1.125, -1.125, -2.250\}$; $\{R_x, R_y, R_z\}_D = P\{0.625, -0.625, -1.250\}$.

Chapter 8

8.1 $D_1 = 0.248$, $D_2 = 0.228$ (inch or cm).

8.2 $D_1 = 2.121PB$. Forces in members of the indeterminate truss are (in terms of P): $CB = -0.53$, $AD = 0.88$, $AC = 0.38$, $CD = 0.38$, $DB = -0.62$, $BA = 0.38$.

8.3 $D = 3.73\dfrac{hP}{Ea}$.

8.4 Downward deflection at E in cases (a) and (b) $= b\left\{9.84\dfrac{P}{Ea},\ -0.22\times10^{-3}\right\}$.
Forces in members in case (c) are (in terms of P):
$AE = 1.78$, $EF = 1.46$, $FB = 1.56$, $AC = -2.22$, $CD = -1.88$, $DB = -1.94$, $CE = 1.26$, $DF = 0.93$, $DE = 0.40$, and $CF = 0.12$.

8.5 Vertical deflection at C in cases (a) and (b) $= \{0.11,\ -0.34\}$ in. Forces in members in case (c) are (kip):
$AB = -18.9$, $BC = -15.0$, $DE = 26.1$, $EC = 25.0$, $EA = -18.5$, $EB = -5.2$, and $BD = 6.5$.

8.6 Vertical deflection at C in cases (a) and (b) $= \{3.3,\ -8.3\}$ mm. Forces in members in case (c) are (kN):

$AB = -94.5$, $BC = -75.0$, $DE = 130.5$, $EC = 125.0$, $EA = -92.5$, $EB = -26.0$ and $BD = 32.5$.

8.7 Forces in members are (in terms of P):
$AB = -1.95$, $BC = -0.38$, $CD = -0.38$, $DE = -0.62$, $EF = 2.06$, $BE = -0.33$, $CE = 0.54$, $DB = -0.88$, $BF = 1.34$, and $EA = -1.49$.

8.8 $\{D_1, D_2, D_3\} = [Pl/(aE)]\ \{20.46, -0.09541, 3.588\}$.

8.9 $\{D_1, D_2\} = [Pl/aE)]\ \{3.828, 4.828\}$. $f_{11} = 10.07l(aE)$.

8.10 $\{N\} = P\{-0.180, 0.320, -0.180, 0.254, -0.453, 0.641\}$.

8.11 Forces in members: $\{AB, BC, AD, BE, BD, BF\} = P\{-0.577, 0.133, 0, -0.444, 0.817, -0.189\}$; the remaining forces can be determined from symmetry. The required displacement $= 3.065Pl/(aE)$.

8.12 $M_{AB} = -0.056ql^2$, $M_{BA} = 0.043ql^2$.

8.13 $M_{AB} = -0.057ql^2$, $M_{BA} = 0.130ql^2$.

8.14 $[f] = \dfrac{l}{24EI}\begin{bmatrix} 4.5 & -3 \\ -3 & 7.5 \end{bmatrix}$.

8.16 Force in tie $= 2.34P$. Bending moment values (in terms of Pb):
$M_A = 0$, $M_B = M_D = 0.099$, and $M_c = 0.132$.

8.17 Force in tie $= 25.6$ kip. Horizontal reaction component at $A = 2.44$ kN (inward). Bending moment values (kip ft): $M_A = M_E = 0$, $M_B = M_D = -73.2$, $M_C = -43.8$.

8.18 Force in tie $= 7.68$ kN. Horizontal reaction component at $A = 0.73$ kN (inward). Bending moment values (kN m):
$M_A = M_E = 0$, $M_B = M_D = -6.59$, $M_C = -3.94$.

8.19 and 8.20 Downward deflection at $A = 0.104l^3/(EI)$ and $0.0774l^3/(EI)$ respectively.

8.21 Downward deflection at $D = 0.015Pl^3/(EI)$, and rotation at $A = 0.047Pl^2/(EI)$ (clockwise).

8.22 Points E and C move away from each other a distance $= 0.0142Pl^3/EI$.

8.23 and 8.24 $[f] = \begin{bmatrix} 1.093 & 1.320 \\ 1.320 & 1.947 \end{bmatrix}$ in./kip, and $10^{-6}\begin{bmatrix} 6.402 & 7.734 \\ 7.734 & 11.400 \end{bmatrix}$ m/N.

8.27 $\{D_1, D_2, D_3\} = \{2.331, 2.992, 1.278\}\ Pl^3/(1000EI)$, in case (a); $\{D_1, D_2, D_3\} = \{353.3, -25.47, 102.7\}\ Pl^3/(1000EI)$, in case (b).

8.28 $M_A = -0.167ql^2$; $M_B = -0.080ql^2$; $M_D = 0.022ql^2$; R_A $0.0673ql$ (up).

8.29 $M_{BC} = 0.3915ql^2$; $R_B = 0.8115ql$ (up); deflection at $A = 0.1663ql^4/(EI)$.

8.30 $M_{\text{center}} = 39.83 \times l0^{-3}qr^2$ (producing tension at bottom fiber). The fixed-end forces are: $\{F^*\} = qr\{-0.5, -1.48 \times 10^{-3}r, -87.46 \times 10^{-3}r, -0.5, -1.48 \times 10^{-3}r, 87.46 \times 10^{-3}r\}$.

8.31 Redundant forces (Figure 6.6d), $\{F\} = ql(0.4012,\ 0.2495,\ 0.0358l)$. $\{M_{BA}, M_{BF}, M_{FB}, M_{BC}, M_{CB}\} = \dfrac{ql^2}{1000}\{98.8,\ 116.0,\ 133.5,\ -214.8,\ -35.8\}$.

8.32 Chosen redundants: $R_A = 0.3471ql$ (up); $N_{AD} = 0.5362ql$; $N_{ED} = 0.5134ql$. Member end-moments: $\{M_{BA}, M_{BE}, M_{EB}, M_{EC}, M_{CE}, M_{BD}\} = (ql^2/1000)\ \{8.44, -13.00, 4.58, -4.58, -9.31, 4.56\}$.

8.33 The nonzero reaction components at A are: $F_x = 0.189P$ and $M_y = 0.405Pl$. Displacement at C in the x direction is $0.2095Pl^3/(EI)$.

8.34 The influence line for M_{Br} is composed of straight segments; the ordinates are: $\{\eta_F, \eta_B, \eta_C, \eta_D, \eta_G\} = b\{-0.4, 0.4, -2.0, -0.4, 0.4\}$.
The influence line for V_{Br} is composed of straight segments; the ordinates are: $\{\eta_F, \eta_{Bl}, \eta_{Br}, \eta_D, \eta_G\} = \{0.1, -0.1, 0.9, 0.1, -0.1\}$.

8.35 $M_{BA} = -M_{BC} = M_{DC} = -M_{DE} = 0.045ql^2$. At the middle of BC, $M = 0.103ql^2$ (tension face at bottom). $M_A = M_C = M_E = 0$. Force in tie$= 0.365ql$.

8.36 Forces in members in terms of $10^{-3}P$: $AB = 2042$; $CD = -2591$; DE $= -2020$; $AH = -2152$; $HI = 439$; $CA = -1319$; $DH = -819$; $EI = 278$; $CH = 2458$; $DI = -542$. Use symmetry for the remaining members.

Chapter 9

9.1 $$[B]=\begin{bmatrix} 0.8 & -0.6 & 0 \\ 0.6 & 0.8 & 0 \\ 0 & 0 & 1 \\ -0.8 & 0.6 & 0 \\ -0.6 & -0.8 & 0 \\ 0.6l & 0.8l & -1 \\ 0.8 & 0.6 & 0 \\ -0.6 & 0.8 & 0 \\ -0.6l & -0.8l & 1 \\ -0.8 & -0.6 & 0 \\ 0.6 & -0.8 & 0 \\ 0 & 1.6l & -1 \end{bmatrix}.$$

9.2 $$[f]=\frac{1}{EI}\begin{bmatrix} 0.24l^3 & \text{symmetrical} & \\ 0.48l^3 & 1.707l^3 & \\ -0.6l^2 & -1.6l^2 & 2l \end{bmatrix}.$$

9.3 $$[f]=\frac{1}{6EI}\begin{bmatrix} 2 & \text{symmetrical} & \\ 1 & 4 & \\ 0 & -1 & 2 \end{bmatrix}.$$

9.4 $$[f]=\frac{1}{24EI}\begin{bmatrix} 9l^3 & \text{symmetrical} & \\ -15l^3 & 60l & \\ -12l^3 & 36l^2 & 32l^3 \end{bmatrix}.$$

9.5 $$[C]^T=\begin{bmatrix} 0 & 1 & 0 & 1 & 0 & 0 & 0 & 0 \\ 0 & 0 & 0 & 0 & 0 & 1 & 0 & 1 \\ 1.155 & 0 & 1 & 0 & 1 & 0 & 1.155 & 0 \end{bmatrix}.$$

$$[S]=\frac{EI}{l}\begin{bmatrix} 12 & \text{symmetrical} & \\ 4 & 12 & \\ -6.93/l & 6.93/l & 32/l^2 \end{bmatrix}.$$

9.6 $\{F\}=q\{0.041l^2,\ -0.014l^2,\ -1.366l^2\}$.
For any member i.

9.8 $$[S_m]_i=\begin{bmatrix} 12EI/l^3 & & & \text{symmetrical} & & \\ 0 & GJ/l & & & & \\ 6EI/l^2 & 0 & 4EI/l & & & \\ -12EI/l^3 & 0 & -6EI/l^3 & 12EI/l^3 & & \\ 0 & -GJ/l & 0 & 0 & GJ/l & \\ 6EI/l^2 & 0 & 2EI/l & -6EI/l^2 & 0 & 4EI/l \end{bmatrix}_i.$$

The displacements $\{D^*\}_i$ at the coordinates of the ith member are related to the displacements $\{D\}$ at the structure coordinates by the equation $\{D^*\}_i=[C]_i\{D\}$ where

$$[C]_i=\begin{bmatrix} [0] & [0] \\ [t]_i & [0] \end{bmatrix}\ (i=1,\ 2),\ [C]_3=[I].$$

$$[C]_i=\begin{bmatrix} [0] & [t]_i \\ [0] & [0] \end{bmatrix}\ (i=4,\ 5),\ [t]_i=\begin{bmatrix} 1 & 0 & 0 \\ 0 & \cos\alpha_i & \sin\alpha_i \\ 0 & -\sin\alpha_i & \cos\alpha_i \end{bmatrix}.$$

9.9 $$[S]=\begin{bmatrix} \frac{Ea}{l} & \text{symmetrical} & \\ 0 & \frac{12EI}{l^3} & \\ 0 & \frac{6EI}{l^3} & \frac{4EI}{l} \end{bmatrix}.$$

$$[S^*]=\begin{bmatrix} \frac{12EI}{l^3} & \text{symmetrical} & \\ \frac{6EI}{bl^2} & \frac{Ea}{4l}+\frac{4EI}{b^2l} & \\ \frac{6EI}{bl^2} & -\frac{Ea}{4l}+\frac{4EI}{b^2l} & \frac{Ea}{4l}+\frac{4EI}{b^2l} \end{bmatrix}.$$

9.10 $$[f]=\begin{bmatrix} \frac{l}{Ea} & \text{symmetrical} & \\ 0 & \frac{l^3}{3El} & \\ 0 & -\frac{l^2}{2El} & \frac{l}{El} \end{bmatrix}.$$

$$[f^*]=\begin{bmatrix} \frac{l^3}{3EI} & & \text{symmetrical} \\ -\frac{bl^2}{4El} & \frac{l}{aE}+\frac{b^2l}{4El} & \\ -\frac{bl^2}{4El} & -\frac{l}{aE}+\frac{b^2l}{4El} & \frac{l}{aE}+\frac{b^2l}{4El} \end{bmatrix}.$$

9.11 $$[S]=EI\begin{bmatrix} \frac{4}{l} & \text{symmetrical} & & \\ 0 & \frac{4}{l} & & \\ \frac{2}{l} & \frac{2}{l} & \frac{8}{l} & \\ -\frac{6}{l^2} & \frac{6}{l^2} & 0 & \frac{24}{l^3} \end{bmatrix}.$$

$$[S^*]=EI\begin{bmatrix} \frac{16}{b^2l} & \text{symmetrical} & & \\ -\frac{12}{b^2l} & \frac{16}{b^2l} & & \\ -\frac{16}{b^2l} & \frac{8}{b^2l} & \frac{32}{b^2l} & \\ -\frac{12}{bl^2} & \frac{12}{bl^2} & 0 & \frac{24}{l^3} \end{bmatrix}.$$

9.12 $F_1=\dfrac{\pi^4 EI}{8\,l^3}D_1.$

9.13 $F_1=D_1\left(\dfrac{\pi^4}{8}-\dfrac{\pi^2}{2}\right)\dfrac{EI}{l_3}.$

9.15 Forces in members AB, AC, AD, and AE are (in terms of P): $\{-0.3544,\ 0.1530,\ 0.6003,\ 0.885\}$.

9.16 $[S_m]$ = the 3×3 matrix in Eq. 22.25. Forces in members AB, AC, AD, and AE are (in terms of P): $\{-0.3118, -4.0535, -2.1826, 1.5590\}$.

Chapter 10

10.3 Deflection at $C = 0.197$ in. downward. Rotation at $C = 0.00413$ rad clockwise.

10.4 Deflection at $C = 5.59$ mm downward. Rotation at $C = 0.00469$ rad clockwise.

10.5 Deflection at $D = 2.40Pb^3/EI_0$. Deflection at $C = Pb^3/EI_0$ (both downward).

10.7 Vertical deflections are: at C or E, $1.212\dfrac{Hl^3}{EI}$ and at D, $1.687\dfrac{Hl^3}{EI}$, both upward.

10.8 or 10.9 $[S] = \dfrac{EI_0}{l}\begin{bmatrix} 6.59 & 2.92 \\ 2.92 & 4.35 \end{bmatrix}$.

10.10 $M = \dfrac{3}{16}\dfrac{EI}{l}$. Deflection at $D = (13/32)\ l$ downward and at $E = (3/32)\ l$ upward.

10.11 (a) Deflection at $D = -0.0070qb^4/(EI)$.
(b) The settlement $= 0.0790qb^4/(EI)$ and the rotation $= 0.1267qb^3/(EI)$.

10.12 $\{y_1, y_2, y_3\} = [10^{-3}Pl^3/(EI_0)]\ \{3.06,\ 4.98,\ 3.79\}$; rotation at $A = 12.3\ [10^{-3}Pl^2/(E1_0)]$.

10.13 $y = [10^{-3}Pl^3/(EI_0)]\ [4.478\ \sin(\pi x/l) - 0.323\ \sin(2\pi x/l)]$. $\{y_1, y_2, y_3\} = [10^{-3}Pl^3/(EI_0)]\ \{2.84,\ 4.48,\ 3.49\}$; rotation at $A = 12.0\ [10^{-3}Pl^2/(EI_0)]$.

10.14 $y = \dfrac{4ql^4}{\pi^5 EI}\sum_{n=1,3,\ldots}^{\infty}\dfrac{\sin(n\pi x/l)}{n^3[n^2 - Pl^2/(\pi^2 EI)]}$.

10.15 $a_1 = 0.02511ql^4/EI$, $a_2 = 0$, and $a_3 = 0.0000569ql^4/EI$.

10.16 $y = \dfrac{4Pl^3}{\pi^4 EI}\sum_{n=1,2,\ldots}^{\infty}\dfrac{[1 - \cos(2n\pi c/l)]\ [1 - \cos(2n\pi x/l)]}{16n^4 + 3k\ l^4/(\pi^4 EI)}$.

10.17 $D_1 = (l/192)\ [22\ \ 36\ \ 24\ \ 12\ \ 2]\ \{\Psi\}$; $D_2 = -(l/192)\ [2\ \ 12\ \ 24\ \ 36\ \ 22]\ \{\Psi\}$; $D_3 = (l^2/192)\ [1\ 6\ 10\ 6\ 1]\ \{\Psi\}$.
For the beam of Prob. 10.12; rotation at the left-hand end $= 12.2 \times 10^{-3}Pl^2/(EI_0)$; deflection at mid-length $= 4.46 \times 10^{-3}Pl^3/(EI_0)$.

Chapter 11

11.1 The member end-moments are (in terms of Pb):
$M_{AB} = -0.54$, $M_{BA} = -M_{BC} = -0.09$, $M_{CB} = -M_{CD} = -0.70$, $M_{DC} = -M_{DE} = 1.11$, $M_{ED} = -1.27$.
Reaction components at A are $0.7P$ (upward), $0.21P$ (to the left) and $0.535Pb$ (anticlockwise). Reaction components at E are: $1.3P$ (upward), 0.79 (to the left) and $1.265Pb$ (anticlockwise).

11.2 The member end-moments are (in terms of Pb):
$M_{AB} = -M_{AF} = -0.461$, $M_{BA} = -M_{BC} = M_{CB} = -M_{CD} = -0.149$.
Use symmetry to find the moments in the other half of the frame.

11.3 The member end-moments in terms of $(Pb/24)$ are: $M_{BC} = 5$, $M_{CB} = -M_{CD} = 1$, $M_{DC} = 7$.
Use symmetry about vertical and horizontal axes to find the remaining moments.

11.4 The member end-moments are (in terms of $qb^2/100$):
$M_{AB} = -188.9$, $M_{BA} = -M_{BC} = -45.7$, $M_{CB} = 111.8$, $M_{CE} = -40.0$, $M_{CD} = -71.8$.
The reaction components at A are: $0.79qb$ (downward), $2.28qb$ (to the left) and $-1.89qb^2$ (anticlockwise). The reaction components at D are $1.79qb$ (upward) and $0.72qb$ (to the left).

11.5 The member end-moments in terms of Pb:
$M_{CA} = -0.500$, $M_{CD} = 0.249$, $M_{CG} = 0.251$, $M_{DC} = -M_{DE} = -M_{DE} = 0.215$, and $M_{ED} = -0.535$.
Use symmetry to find the moments in the other half of the frame.

11.6 The forces at end A are: $1.6qb$ (upward), $1.07qb$ (to the right) and $0.213qb^2$ (anti-clockwise). Use the symmetry of the frame to find the forces at end B.

11.7 $S_{AB} = 7.272EI_0/l$, $S_{BA} = 4.364EI_0/l$, $C_{AB} = 2/5$, and $C_{BA} = 2/3$.

11.8 $S_{AB} = 9.12EI_B/l$, $S_{BA} = 4.75EI_B/l$, $C_{AB} = 0.428$, and $C_{BA} = 0.824$, where EI_B is the flexural rigidity at B.

11.9 $M_{AB} = -0.0966wl^2$, and $M_{BA} = 0.0739wl^2$.

11.10 $M_{AB} = -0.2171Pl$, and $M_{BA} = 0.0866Pl$.

11.11 The end-moments on the members are (in terms of $ql^2/1000$):
M_{AB}=25.3, M_{BA}=−M_{BC}=50.7, M_{CB}=72.5, M_{CD}=−36.3, M_{DC}=−18.1, M_{CE}=−36.3.
Reaction components at A: $0.479ql$ upward, $0.077ql$ to the right and $0.025ql^2$ clockwise.

11.12 The end-moments on the members are (in terms of $ql^2/1000$):
M_{AB}=19.6, M_{BA}=− M_{BC}=46.6, M_{CB}=75.9, M_{CD}=− 41.7, M_{DC}=− 24.5, M_{CE}=− 34.3.
Reaction components at A: $0.471ql$ upward, $0.067ql$ to the right and $0.020ql^2$ clockwise.

11.13 The member end-moments are (in terms of $ql^2/1000$):
$M_{BA} = 93.7$, $M_{BE} = 6.1$, $M_{BC} = -99.8$, and $M_{EB} = 3.1$.
The end-moments in the right-hand half of the frame are equal and opposite in sign.

11.14 The member end-moments are (in terms of $Hl/100$):
$M_{BA} = -3.39$, $M_{BE} = 7.92$, $M_{BC} = -4.53$, and $M_{EB} = 8.73$.
Because of antisymmetry the end-moments in the right-hand half are equal.

11.15 The member end-moments in terms of EI_A/l^2 are:
$M_{BA} = 10.2$, $M_{BE} = 3.5$, $M_{BC} = -13.8$, $M_{ED} = 1.2$, $M_{CB} = -17.1$, $M_{CF} = -2.7$, $M_{CD} = 19.8$, $M_{FC} = -2.0$.

11.16 The values of the bending moment at support B for the four cases of loading are: ql^2 {−0.2422, −0.3672, −0.2422, −0.1016}.

11.17 The member end-moments are (in terms of $qb^2/100$):
$M_{AB} = 2.62$, $M_{BA} = -M_{BC} = 7.95$, $M_{CB} = 24.15$, $M_{CD} = -6.15$, $M_{CE} = -18.00$, $M_{DC} = -4.42$.

11.18 (a) The member end-moments are (k ft):
$M_{AB} = 122$, $M_{BA} = -M_{BC} = 126$.
Because of symmetry, the end-moments in the right-hand half of the frame are equal and opposite.
(b) The reaction components at A are: 0.782 k to the right and 27.4 k ft clockwise, and the vertical component is zero.

11.19 (a) The member end-moments are (kN m):
$M_{AB} = 10.94$, $M_{BA} = -M_{BC} = 11.38$.
(b) The reaction components at A are: 3.62 kN to the right and 38.0 kN m clockwise, and the vertical component is zero.

11.20 The required values of the bending moments are (kip ft):

(a) $M_A = M_B = -20.7$, and $M_C = M_D = -8.3$.
(b) $M_A = -M_B = 27.8$, and $M_C = -M_D = 27.8$.
(c) $M_A = -111.5$, $M_B = -251.2$, and $M_C = -2.7$, $M_D = -142.4$.
As usual, a positive bending moment causes tensile stress in the inner fiber of the frame.

11.21 The required values of the bending moments are (kN m):

(a) $M_A = M_B = -27.1$, and $M_C = M_D = -10.8$.
(b) $M_A = -M_B = 28.5$, and $M_C = -M_D = 28.5$.
(c) $M_A = -145.2$, $M_B = -327.1$, $M_C = -3.5$ and $M = -185.4$.

As usual, a positive bending moment causes tensile stress in the inner fiber of the frame.

11.22 (a) The end-moment at the top or bottom of any of the three piers is $Pl/12$.
(b) Shear at F or H is $P/6$ and shear at G is $2P/3$.

11.23 The member end-moments in the left-hand half of the frame are: $\{M_{AB}, M_{BA}, M_{BC}, M_{CB}, M_{CD}, M_{DC}\} = Pl\{0.178, 0.150, -0.150, -0.121, 0.121, 0.116\}$; member DE has zero moment.

11.24 The member end-moments in the left-hand half of the frame are: $\{M_{AB}, M_{BA}, M_{BC}, M_{CD}\} = Pl\{0.140, 0.143, -0.143, -0.145\}$.

11.25 The member end-moments in the left-hand half of the frame are (in terms of Pb): $M_{AB} = -1.19$, $M_{BA} = -0.31$, $M_{BG} = 0.89$, $M_{BC} = -0.58$, $M_{CB} = -0.68$, $M_{CF} = 0.79$, $M_{CD} = -0.11$, and $M_{DC} = -0.89$.
The corresponding end-moments in the right-hand half are equal.

11.26 The member end-moments in the left-hand half of the frame are (in terms of Pb/10): $M_{AB} = M_{FG} = -5.71$, $M_{BA} = M_{GF} = -5.54$, $M_{BC} = M_{GH} = -1.41$, $M_{CB} = M_{HG} = -2.34$, $M_{AF} = M_{FA} = 5.71$, $M_{BG} = M_{GB} = 6.95$, $M_{CH} = M_{HC} = 0$.
The end-moments in the right-hand half are equal and opposite.

11.27 The member end-moments in the left-hand half of the frame (in terms of Pl) are: $M_{AB} = -1.545$, $M_{BA} = -0.455$, $M_{BE} = 0.614$, $M_{BC} = -0.159$, $M_{CB} = -M_{CD} = -0.341$.
The corresponding end-moments in the right-hand half are equal.

Chapter 12

12.1 The influence lines are composed of straight segments joining the following ordinates:
Reaction at B: $\eta_A = 0$, $\eta_D = 1.2$, and $\eta_C = 0$.
Bending moment at $E(l)$: $\eta_A = 0$, $\eta_E = 0.234$, $\eta_D = -0.075$, and $\eta_C = 0$.
Shear at E: $\eta_A = 0$, $\eta_{E\ \text{left}} = -\frac{3}{8}$, $\eta_{E\ \text{right}} = \frac{5}{8}$, $\eta_D = \frac{1}{5}$, and $\eta_C = 0$.

12.2 The influence lines are composed of straight segments joining the following ordinates:
Force in member Z_1: $\eta_A = 0$, $\eta_C = \frac{3}{4}$, and $\eta_B = 0$.
Force in member Z_2: $\eta_A = 0$, $\eta_C = -0.354$, $\eta_D = 0.707$, and $\eta_B = 0$.

12.3 With the line AB as a datum, the influence line is composed of straight segments joining the following ordinates:
Horizontal component of the reaction at A (inward):

$$\eta_A = \eta_B = 0, \text{ and } \eta_C = \frac{l}{4h}.$$

Bending moment at D:

$$\eta_A = \eta_B = 0, \ \eta_D = \frac{3l}{32}, \text{ and } \eta_C = -\frac{l}{16}.$$

12.4 The three required ordinates in the spans are
Bending moment at n:
Span AB: $\{-89, -123, -117\}\ l/1000$.
Span BC: $\{-62, -65, -47\}\ l/1000$.
Bending moment at center of AB:
Span AB: $\{105, 189, 92\}\ l/1000$.
Span BC: $\{-31, -33, -24\}\ l/1000$.
Shearing force at n:
Span AB: $\{-0.389, -0.623, -0.817\}$.
Span BC: $\{-0.062, -0.065, -0.047\}$.

12.5 Influence ordinates of R_A:
$\{\eta_A, \eta_D, \eta_B, \eta_E, \eta_C\} = \{1.0, 0.902, 0.677, 0.404, 0.119\}$.

Influence ordinates of R_B:
$\{\eta_A, \eta_D, \eta_B, \eta_E, \eta_C\} = \{0, 0.046, 0.126, 0.175, 0.199\}$.
Influence ordinates of the end-moment at A:
$\{\eta_A, \eta_D, \eta_B, \eta_E, \eta_C\} = l\{0, -0.350, -0.480, -0.483, -0.437\}$.

12.6 The three required ordinates in the spans are
Span AB: $\{1.36, 1.88, 1.79\}\, l/100$.
Span BC: $\{-1.79, -1.88, -1.36\}\, l/100$.

12.7 $\eta_G = 0.132l$, $\eta_H = 0.236l$, and $\eta_I = 0.132l$.

12.8 $\eta_G = 0.125l$, $\eta_H = 0.250l$, $\eta_I = 0.125l$, and $\eta_K = 0.078l$.

12.11 The influence lines are composed of straight segments joining the following ordinates:
For X_A: $\{\eta_A, \eta_B, \eta_C, \eta_D, \eta_E\} = \{0, 0.535, 0.931, 0.535, 0\}$.
For Y_A: $\{\eta_A, \eta_B, \eta_C, \eta_D, \eta_E\} = \{1.0, 0.840, 0.500, 0.160, 0\}$.
For M_{AB}: $\{\eta_A, \eta_B, \eta_C, \eta_D, \eta_E\} = b\{0, -0.222, 0.084, 0.139, 0\}$.

12.12 The influence lines are composed of straight segments joining the following ordinates:
For X_A: $\{\eta_C, \eta_D, \eta_E, \eta_F, \eta_G\} = \{0.036, 0.427, 0.643, 0.427, 0.036\}$.
For the force in DE: $\{\eta_C, \eta_D, \eta_E, \eta_F, \eta_G\} = \{0.072, -0.146, -0.714, -0.146, 0.072\}$.

12.13 The influence lines are composed of straight segments joining the following ordinates:
For the force in Z_1: $\{\eta_A, \eta_D, \eta_E, \eta_F, \eta_B\} = \{0, -0.333, -0.632, -0.860, 0\}$ and the line is symmetrical about B.
For the force in Z_2, the ordinates in the spans are
Span AB: $\{\eta_A, \eta_D, \eta_E, \eta_F, \eta_B\} = \{0, -0.125, -0.197, -0.164, 0\}$.
Span BC: $\{\eta_B, \eta_G, \eta_H, \eta_I, \eta_C\} = \{0, 0.586, 0.303, 0.125, 0\}$.

Chapter 13

13.1 $M_{BC} = -M_{BA} = 246.0$ k ft; $M_{AB} = -165.6$ k ft.

13.2 $M_{BC} = -M_{BA} = 329.6$ kN m; $M_{AB} = -226.1$ kN m.

13.3 $\{M_{BA}, M_{BC}, M_{BD}, M_{DB}\} = \{28.1, -25.8, -2.27, -11.7\}$ k ft.

13.4 $\{M_{BA}, M_{BC}, M_{BD}, M_{DB}\} = \{38.6, -34.6, -3.99, -16.5\}$ kN m.

13.5 $\{M_{AB}, M_{BA}, M_{BC}, M_{CB}\} = \{-0.589, -0.726, 0.726, 0.985\}\, EI/(10^3 l)$.

13.8 $\{M_{AB}, M_{BA}, M_{BC}, M_{CB}\} = ql^2\{-0.665, -0.366, 0.366, 0\}$.

13.9 Buckling occurs when $Q = 1.82EI/b^2$.

13.10 $Q = 93.2EI_{BC}/l^2$.

13.11 $Q = 6.02EI/l^2$.

13.14 $Q = 20.8EI/l^2$.

13.15 $Q = 3.275EI/l^2$.

Chapter 14

14.2 The required matrices are:

$$[S_{11}]_r = \begin{bmatrix} \frac{2(S_1+t_1)}{h_1^2} & & & & \text{symmetrical} \\ \frac{-2(S_1+t_1)}{h_1^2} & \frac{2(S_1+t_1)}{h_1^2}+\frac{2(S_2+t_2)}{h_2^2} & & & \\ & -\frac{2(S_2+t_2)}{h_2^2} & \frac{2(S_2+t_2)}{h_2^2}+\frac{2(S_3+t_3)}{h_3^2} & & \\ \text{elements not shown} & & \cdots\ \cdots & & \\ \text{are zero} & & \cdots & & \\ & & & -\frac{2(S_{n-1}+t_{n-1})}{h_{n-1}^2} & [2(S_{n-1}+t_{n-1})/h_{n-1}^2 + \\ & & & & +2(S_n+t_n)/h_n^2] \end{bmatrix}$$

$$[S_{21}]_r = [S_{12}]_r^T = \begin{bmatrix} -\frac{(S_1+t_1)}{h_1} & \frac{(S_1+t_1)}{h_1} & & & & & \\ -\frac{(S_1+t_1)}{h_1} & \frac{(S_1+t_1)}{h_1} - \frac{(S_2+t_2)}{h_2} & \frac{(S_2+t_2)}{h_2} & & & & \\ & -\frac{(S_2+t_2)}{h_2} & \frac{(S_2+t_2)}{h_2} - \frac{(S_3+t_3)}{h_3} & \frac{(S_3+t_3)}{h_3} & & & \\ \text{elements not} & & \cdots & \cdots & \cdots & & \\ \text{shown are zero} & & & \cdots & \cdots & \cdots & \\ & & & & \frac{(S_{n-1}+t_{n-1})}{h_{n-1}} & [(S_{n-1}+t_{n-1})/h_{n-1} & \\ & & & & & -(S_n+t_n)/h] & \end{bmatrix}$$

$$[S_{22}]_r = \begin{bmatrix} S_1 + 3(I/l)_{b1} & & & & \text{symmetrical} & \\ t_1 & S_1 + S_2 + 3E(I/l)_{b2} & & & & \\ & t_2 & S_2 + S_3 + 3E(I/l)_{b3} & & & \\ \text{elements not} & & & & t_{n-1} & [S_{n-1} + S_n + 3E(I/l)_{bn}] \\ \text{shown are zero} & & & & & \end{bmatrix}$$

where

$$S_i = \frac{(4+\alpha_i)}{(1+\alpha_i)} \frac{EI_{ci}}{h_i}$$

$$t_i = \frac{(2-\alpha_i)}{(1+\alpha_i)} \frac{EI_{ci}}{h_i}$$

$$\alpha_i = \frac{12EI_{ci}}{h_i^2 G a_{rci}}$$

The subscripts i of S, t, h, T_c, α, and a_{rc} in the above equations refer to the storey number starting from the top storey. The subscript i in $(I/l)_{bi}$ refers to the floor number starting from the roof.

14.3 The sums of moments in walls are (refer to Figure 15.7)

$\{M_A, M_B, M_C, M_D, M_E,\} = \frac{Ph}{10}\{0, 4.41, 18.80, 43.27, 77.82\}$.

The sums of moments in columns are (in terms of $Ph/10$):

$M_{FG} = -0.318$, $M_{GF} = -0.271$, $M_{GH} = -0.287$, $M_{HG} = -0.316$. $M_{HI} = -0.260$, $M_{IH} = -0.275$, $M_{IJ} = -0.196$, $M_{JI} = -0.262$.

14.4 Bending moment at Section A.A is 6.07 Ph. The moment on each end of the lower beam (at its intersection with the wall) is 0.295 Ph.

14.6 Forces on the walls are:

$\{F_1, F_2, F_3\}_A = P\{0.0003, -0.1050, -0.03272b\}$

$\{F_1, F_2, F_3\}_B = P\{-0.0003, -0.3150, -0.00027b\}$

$\{F_1, F_2, F_3\}_C = P\{0, -0.5800, -0.00027b\}$

where F_1, F_2 are components in the x and y directions respectively, and F_3 is a clockwise couple.

14.7 Forces on the walls are:

$\{F_1, F_2, F_3\}_A = P\{0.1183, 0.2739, 0.00072b\}$

$\{F_1, F_2, F_3\}_B = P\{0.0008, 0.4603, 0.00036b\}$

$\{F_1, F_2, F_3\}_C = P\{-0.1176, 0.0047, 0.00036b\}$

$\{F_1, F_2, F_3\}_D = P\{-0.0015, 0.2611, 0.00036b\}$

where F_1, F_2 are components in the x and y directions respectively, and F_3 is a clockwise couple.

14.8 The translation of point B in the x and y directions and the rotation of the deck in the clockwise direction are (kip, ft units):
$10^{-6}P\{330.68, -2.51, -1.29\}$.
The forces on the supporting elements are (kip, ft units):
$\{F_1, F_2, F_3\}_A = P\{0.4571, 0.0748, -0.0002\}$
$\{F_1, F_2, F_3\}_B = P\{0.0475, -0.0056, -0.1448\}$
$\{F_1, F_2, F_3\}_C = P\{0.1207, 0.1194, -0.1448\}$
$\{F_1, F_2, F_3\}_D = P\{0.3747, -0.1886, -0.0002\}$
where F_1, F_2 are components in the x and y directions respectively, and F_3 is a clockwise couple.

14.9 The translation of point B in the x and y directions and the rotation of the deck in the clockwise direction are (N, m units):
$10^{-6}\ P\{0.02315, -0.00019, -0.000302\}$
The forces on the supporting elements are (N, m units):
$\{F_1, F_2, F_3\}_A = P\{0.4557, 0.0747, 0.0000\}$
$\{F_1, F_2, F_3\}_B = P\{0.0485, -0.0062, 0.0446\}$
$\{F_1, F_2, F_3\}_C = P\{0.1226, 0.1207, -0.0446\}$
$\{F_1, F_2, F_3\}_D = P\{0.3732, -0.1892, 0,0000\}$.

14.11 For $I_o/I = 0.2$, $D_{top} = 38 \times 10^{-3}\, ql^4/EI$; $\{M_{CE}, M_{EC}, M_{ED}, M_{DE}\} = -10^{-3}ql^2\{45, 80, 93, 282\}$. For $I_o/I = 2.0$, $D_{top} = 34 \times 10^{-3}\, ql^4/EI$; $\{M_{CE}, M_{EC}, M_{ED}, M_{DE}\} = -10^{-3}ql^2\{35, 90, 107, 268\}$.

Chapter 15

15.1 $\{y_1, y_2, y_3\} = \dfrac{ql^4}{384EI_A}\{2.1, 2.7, 1.8\}$.

15.2 $\{y_1, y_2, y_2\} = (ql^4/1000EI)\ \{0.698, 0.843, 0.566\}$. $\{M_1, M_2, M_3\} = (ql^2/100)\ \{0.885, 0.675, 0.462\}$. $M_B = -1.811$, $R_A = 0.160ql$ and $R_B = 0.432ql$.

15.3 Rotation at A is $l/(3.882EI)$.

15.4 $[f] = \begin{bmatrix} \dfrac{l^3}{2.842EI} & -\dfrac{l^2}{2EI} \\ -\dfrac{l^2}{2EI} & \dfrac{l}{EI} \end{bmatrix}$.

15.5 End-rotational stiffness $S = 2.102EI/l$. Carryover moment $t = 2.008EI/l$. From Table 14.1, we have:
$S = 2.624EI/l$, and $t = 2.411EI/l$.

15.6 $M_B = -0.324Ql$.

15.7 $\{y_1, y_2, y_3\} = 10^{-3}\dfrac{\gamma l^5}{EI}\{0.571, 0.480, 0.469\}$.

15.8 Radial outward deflections at nodes 1, 2, ..., 5 are:
$\dfrac{\gamma H^2}{10E}\{15.853, 43.974, 72.552, 83.022, 54.410\}$.
The hoop forces per unit height at the nodes are:
$10^{-2} \times \gamma H^2\{6.605, 21.987, 42.322, 55.348, 40.807\}$.
The bending moments in the vertical direction at the nodes are:
$10^{-3} \times \gamma H^3\ \{0, -0.01, 0.77, 2.48, 2.32\}$.
The radial reaction at the bottom $= 0.172\gamma H^2$ (inward). The fixing moment at the base $= 0.013\gamma H^3$ (producing tensile stress at inner face). With $\lambda = H/20$, the solution

gives the following values at the nodes at fifth points of the height. Radial outward deflections at nodes 1, 2, ..., 5 are:

$\frac{\gamma H^2}{10^3 E}\{4.284, 43.109, 74.776, 81.176, 43.749\}$.

The hoop forces per unit height at the nodes are:

$10^{-2} \times \gamma H^2$ {1.758, 21, 554, 43.619, 54.117, 32.811}.

The bending moments in the vertical direction at the nodes are:

$10^{-3} \times \gamma H^3$ {0, 0.17, 1.05, 3.03, 1.62}.

The radial reaction at the bottom $= 0.190\gamma H^2$ and the fixing moment $= 0.019\gamma H^3$.

15.9 $\{w\} = \frac{q\lambda^4}{N}\{1.2950, 0.8456, 0.6918, 0.4586\}$.

$(M_y)_1 = 0.0241qb^2$, and $(M_y)_2 = 0.0155qb^2$.

15.10 $\{w\} = \frac{qb^4}{N}$ {0.00305, 0.00235, 0.00155, 0.00122}.

$(M_y)_1 = 0.0375qb^2$, and $(M_y)_2 = 0.0283qb^2$.

15.11 $\{w\} = \frac{M\lambda^2}{N}\{0.4494, 0.3962, 0.2332, 0.2254\}$.

$(M_y)_1 = 0.2162M$ and $(M_y)_2 = 0.1708M$.

15.12 $\{w\} = \frac{q\lambda^4}{N}$ {1.0614, 0.6764, 0.5894, 0.3869}.

$(M_y)_1 = 0.0189qb^2$, $(M_y)_2 = 0.0116qb^2$.

Bending moment in beam EF:

$M_1 = 0.00616qb^3$.

15.13 $\{w\} = \frac{p\lambda^2}{N}$ {0.2981, 0.2506, 0.2006, 0.8871, 0.7423, 0.6281}.

M_y at A, B, and C are:

$\{M_y\} = P\{-0.5962, -0.5012, -0.4012\}$

15.14 $\{w\} = \frac{p\lambda^2}{N}$ {0.2740, 0.2525, 0.2211, 0.8159, 0.7531, 0.6780}.

M_y at A, B and C are:

$\{M_y\} = -P\{0.5480, 0.5050, 0.4422\}$.

15.15 $\{w\} = \frac{pb^2}{N}\{0.0143, 0.0095, 0.0047\}$.

Reaction $R_A = 0.1039qb^2$.

Chapter 16

16.1 $$[S^*] = \frac{EI_0}{l^3}\begin{bmatrix} 18 & & & \text{symmetrical} \\ 8l & 5l^2 & & \\ -18 & -8l & 18 & \\ 10l & 3l^2 & -10l & 7l^2 \end{bmatrix}$$

$$[S^*] = \frac{EI_0}{l^3}\begin{bmatrix} 17.45 & & & \text{symmetrical} \\ 7.72l & 4.86l^2 & & \\ -17.45 & -7.72l & 17.45 & \\ 9.72l & 2.86l^2 & -9.72l & 6.86l^2 \end{bmatrix}.$$

16.2 Deflection by finite-element method is $0.1923Pl^3/EI_0$. Exact answer is $0.1928Pl^3/EI_0$.

16.3 $[S]=\dfrac{Ea}{3l}\begin{bmatrix}7 & 1 & -8\\ 1 & 7 & -8\\ -8 & -8 & 16\end{bmatrix}$, $[S^*]=\dfrac{Ea}{l}\begin{bmatrix}1 & -1\\ -1 & 1\end{bmatrix}$.

16.4 $D_2=0.375\alpha T_0 l$; $D_3=0.0625\alpha T_0 l$; $\sigma=-0.125E\alpha T_0$.

16.5 $S^*_{11}=Eh\left(0.347\dfrac{c}{b}+0.139\dfrac{b}{c}\right)$; $S^*_{21}=0.156Eh$;

$S^*_{31}=Eh\left(-0.347\dfrac{c}{b}+0.069\dfrac{b}{c}\right)$; $S^*_{41}=-0.52Eh$;

$S^*_{51}=Eh\left(-0.174\dfrac{c}{b}-0.069\dfrac{b}{c}\right)$.

16.6 $\{F_b\}=0.625\alpha TEh\{c,\ b,\ -c,\ b,\ -c,\ -b,\ c,\ -b\}$.

16.7 $[S^*]=\dfrac{Eh}{1000}\begin{bmatrix}
486 & & & & \text{symmetrical} & & & \\
156 & 486 & & & & & & \\
-278 & 52 & 486 & & & & & \\
-52 & 35 & -156 & 486 & & & & \\
-243 & -156 & 35 & 52 & 486 & & & \\
-156 & -243 & -52 & -278 & 156 & 486 & & \\
35 & -52 & -243 & 156 & -278 & 52 & 486 & \\
52 & -278 & 156 & -243 & -52 & 35 & -156 & 486
\end{bmatrix}$.

16.8 Deflection by finite-element method is $1.202Pb/Ehc$; deflection by beam theory is $(P/Eh)\,[0.5(b/c)^3+1.44(b/c)]$.

16.9 $\{\sigma\}=\{0,0,-0.5P/hc\}$.

16.10 $\{F^*_b\}=\dfrac{\alpha EhT}{1-\nu}\left\{\dfrac{c}{2},\ \dfrac{b}{2},\ \dfrac{b^2}{12},\ -\dfrac{c}{2},\ \dfrac{b}{2},\ -\dfrac{b^2}{12},\ -\dfrac{c}{2},\ -\dfrac{b}{2},\ \dfrac{b^2}{12},\ \dfrac{c}{2},\ -\dfrac{b}{2},\ -\dfrac{b^2}{12}\right\}$.

16.11 $[S^*_{11}]=\dfrac{Eh^3}{(1-\nu^2)cb}\left[\dfrac{1}{3}\left(\dfrac{b^2}{c^2}+\dfrac{c^2}{b^2}\right)-\dfrac{\nu}{15}+\dfrac{7}{30}\right]$.

Deflection at center of rectangular clamped plate $D^*_1=(S^*_{11})^{-1}(P/4)$. M_x at node 2 is $-[Eh^3/2(1-\nu^2)b^2]D^*_1$.

16.12 $[S^*]=\dfrac{Eh}{4}\begin{bmatrix}
3 & & & \text{symmetrical} & & \\
-1 & 3 & & & & \\
-1 & 1 & 1 & & & \\
0 & -2 & 0 & 2 & & \\
-2 & 0 & 0 & 0 & 2 & \\
1 & -1 & -1 & 0 & 0 & 1
\end{bmatrix}$; $[T]=\begin{bmatrix}[t] & [0] & [0]\\ [0] & [t] & [0]\\ [0] & [0] & [t]\end{bmatrix}$;

$[t]=\begin{bmatrix}c & s\\ -s & c\end{bmatrix}$ where cos α and s = sin α.

For the system in (b), $[S]=[T]^T\,[S^*]\,[T]$. For the system in (c), substitute $\alpha=180°$; thus, $[t]=-[I]$ and $[\bar{S}]=[S^*]$.

16.13 The nonzero nodal displacements are

$\{v_1, v_2, v_3, u_4, v_4, u_5, v_5, u_6, v_6\}$

$=\dfrac{P}{Eh}\{2.68, 2.21, 2.57, -0.44, 1.16, 0.03, 1.19, 0.39, 1.28\}$.

Stresses in element 2.6.3 are

$\{\sigma_x, \sigma_y, \tau_{xy}\}=\dfrac{P}{bh}\{0.392, 0.358, -0.642\}$.

16.14 $[\{B\}_1\ \{B\}_2\ \{B\}_3]=\begin{bmatrix}-(1-\eta)/b & 0 & 0\\ 0 & -(1-3\xi^2+2\xi^3)/c & -\xi(\xi-1)^2b/c\\ -(1-\xi)/c & (-6\xi+6\xi^2)(1-\eta)/b & (3\xi^2-4\xi+1)(1-\eta)\end{bmatrix}$

16.15

$$[S^*] = (Eb/1000) \times$$

$$\begin{bmatrix}
486 & & & & & & & & & & & \\
156 & 552 & & & & & & & & & & \\
-8.7b & 68b & 28b^2 & & & & & & & & & \\
-278 & 52 & 8.7b & 486 & & & & & & & & \\
-52 & -31 & 19b & -156 & 552 & & & & & & & \\
8.68b & -19b & -12b^2 & -8.7b & -68b & 28b^2 & & & & & & \\
-243 & -156 & -26b & 35 & 52 & 26b & 486 & & & & & \\
-156 & -219 & -40b & -52 & -302 & 47b & 156 & 552 & & & & \\
26b & 40b & 5.5b^2 & -26b & 47b & -0.3b^2 & 8.7b & -68b & 28b^2 & & & \\
35 & -52 & 26b & -243 & 156 & -26b & -278 & 52 & -8.7b & 486 & & \\
52 & -302 & -47b & 156 & -219 & 40b & -52 & -31 & -19b & 156 & 552 & \\
-26b & -47b & -0.3b^2 & 26b & -40b & 5.5b^2 & -8.7b & 19b & -12b^2 & 8.7b & 68b & 28b^2
\end{bmatrix}$$

Chapter 17

17.1 $$[S] = \frac{Ea_0}{l}\begin{bmatrix} 3.775 & & \text{symmetrical} \\ 0.442 & 2.443 & \\ -4.221 & -2.889 & 7.110 \end{bmatrix}$$

The function integrated is quartic; three sampling points are sufficient for exact integration.

17.2 When both q and the displacement are quadratic, the consistent restraining forces are: $F_{b1} = -(b/30)\ (4q_1 + 2q_2 - q_3)$; $F_{b2} = -(b/30)\ (2q_1 + 16q_2 + 2q_3)$; $F_{b3} = -(b/30)\ (-q_1 + 2q_2 + 4q_3)$. When q is constant and the displacement is quadratic, substitute q for q_1, q_2 and q_3, giving $\{F_b\} = -qb\ \{1/6, 2/3, 1/6\}$.

17.4 $$L_1 = \frac{1}{32}\eta(1-\eta)(3\xi+1)(3\xi-1)(\xi-1);\ L_2 = -\frac{9}{32}\eta(1-\eta)(\xi+1)(3\xi-1)(\xi-1);$$

$$L_{10} = -\frac{1}{16}(1-\eta^2)(3\xi+1)(3\xi-1)(\xi-1);\ L_{11} = \frac{9}{16}(1-\eta^2)(\xi+1)(3\xi-1)(\xi-1).$$

Consistent restraining forces in the y direction at the nodes 1 to 12 are

$$-q_y bch\left\{\frac{1}{48}, \frac{1}{16}, \frac{1}{16}, \frac{1}{48}, \frac{1}{12}, \frac{1}{48}, \frac{1}{16}, \frac{1}{16}, \frac{1}{48}, \frac{1}{12}, \frac{1}{4}, \frac{1}{4}\right\}.$$

17.5 $$\begin{Bmatrix} \{\epsilon\}_1 \\ \{\epsilon\}_2 \\ \{\epsilon\}_3 \end{Bmatrix} = [G]\begin{Bmatrix} D_1^* \\ D_2^* \end{Bmatrix};$$

$$[G]^T = \frac{1}{2\Delta}\begin{bmatrix} 3b_1 & 0 & 3c_1 & -b_1 & 0 & -c_1 & -b_1 & 0 & -c_1 \\ 0 & 3c_1 & 3b_1 & 0 & -c_1 & -b_1 & 0 & -c_1 & -b_1 \end{bmatrix}.$$

17.6 $$[\{B\}_1\ \{B\}_2] = \frac{1}{2\Delta}\begin{bmatrix} 3b_1\alpha_1 & -b_1\alpha_2 & -b_1\alpha_3 & 0 \\ & 0 & & 3c_1\alpha_1 - c_1\alpha_2 - c_1\alpha_3 \\ 3c_1\alpha_1 & -c_1\alpha_2 & -c_1\alpha_3 & 3b_1\alpha_1 - b_1\alpha_2 - b_1\alpha_3 \end{bmatrix}.$$

17.7 $$S_{11}^* = \frac{h}{4\Delta}(d_{11}d_1^2 + d_{33}c_1^2);\quad S_{12}^* = (c_1 b_1 h/4\Delta)\ (d_{12} + d_{33}).$$

17.8 $$[B] = \frac{1}{l}\begin{bmatrix} -1/l & 2/l & -1/l & -1.732 & -1.732 & 0 \\ 1/l & -2/l & 1/l & -0.577 & -0.577 & 2.309 \\ -3.464/l & 0 & 3.464l & 2 & -2 & 0 \end{bmatrix}.$$

$$[S^*] = \frac{\Delta E h^3}{1000 l^4} \begin{bmatrix} 513 & & & & & \text{symmetrical} \\ -256 & 513 & & & & \\ -256 & -256 & 513 & & & \\ -148l & -148l & 295l & 488l^2 & & \\ 296l & -148l & -148l & 232l^2 & 488l^2 & \\ 148l & -296l & 148l & -232l^2 & -232l^2 & 488l^2 \end{bmatrix}.$$

17.9 Deflection at center $= 1.154\ (Pl^2/Eh^3)$; $\{M_x,\ M_y,\ M_{xy}\}_A = (P/1000)\ \{192, 0, 0\}$.

17.10 No deflection. $\{M_x, M_y, M_{xy}\}_A = \alpha E h^2 T(0.119, 0.119, 0)$.

17.11 Deflection at $A = 0.381 qb^4/Eh^3$; $M_{xB} = -0.200 qb^2$.

17.12 Deflection at $A = 0.1536 pb^3/Eh^3$; $M_{xB} = -0.074 pb$.

17.13 Because of symmetry, one strip only needs to be considered. The nodal displacement parameters are: $\theta_{\text{at support}} = -0.1515 ql^3/Eh^3$; $w_{\text{at center}} = 0.0452 ql^4/Eh^3$.

17.14 Deflection along center line $= 10^{-3} q_o (c^4/Eh^3)\ [58 \sin(\pi y/l) - 11 \sin(2\pi y/l) + 2.8 \sin(3\pi y/l)]$.

17.15 Beam flexural stiffness $= (EIl/2)\,(k\pi/l)^4$; beam torsional stiffness $= (GJl/2)(k\pi/l)^2$. Deflection at center $= 0.204 Pl^2/Eh^3$; bending moment in an edge beam at midspan $= 0.045 Pl$.

17.16
$$S^*_{11} = \frac{Eh}{1-\nu^2}\left[\frac{c}{12b}(4-\nu^2) + \frac{b}{8c}(1-\nu)\right]; \quad S^*_{21} = \frac{Eh}{8(1-\nu)};$$

$$S^*_{31} = \frac{Eh}{1-\nu^2}\left[-\frac{c}{12b}(4-\nu^2) + \frac{b}{8c}(1-\nu)\right]; \quad S^*_{41} = \frac{Eh(3\nu-1)}{8(1-\nu^2)};$$

$$S^*_{51} = -\frac{Eh}{(1-\nu^2)}\left[\frac{c}{12b}(2+\nu^2) + \frac{b}{8c}(1-\nu)\right].$$

17.17
$$[S^*] = \frac{Eh}{1000} \begin{bmatrix} 448 & & & & & & & \\ 156 & 448 & & \text{symmetrical} & & & & \\ -240 & 52 & 448 & & & & & \\ -52 & 73 & -156 & 448 & & & & \\ -281 & -156 & 73 & 52 & 448 & & & \\ -156 & -281 & -52 & -240 & 156 & 448 & & \\ 73 & -52 & -281 & 156 & -240 & 52 & 448 & \\ 52 & -240 & 156 & -281 & -52 & 73 & -156 & 448 \end{bmatrix}.$$

Chapter 18

18.1 (a) $M_p = 0.1458 ql^2$. (b) For AC, $M_p = 0.0996 ql^2$. For CD, $M_p = 0.1656 ql^2$.

18.2 (a) $M_p = 0.29 Pb$. (b) $M_p = 0.1875 Pl$.
(c) $M_p = 1.2 Pb$. (d) $M_P = 1.59 qb^2$.
(e) $M_p = 0.11 Wl$.

18.3 $M_p = 0.1884 Pl$.

18.4 $M_p = 0.1461 ql^2$.

Chapter 19

19.1 (a) $m = 0.090 W$. (b) $m = W/18$.
(c) $m = W/6$. (d) $m = W/14.14$.
(e) $m = 0.0637 ql^2$. (f) $m = 0.0262 ql^2$.

19.2 (a) $m = 0.00961ql^2$. (b) $m = 0.299ql^2$.
(c) $m = 0.113ql^2$. (d) $m = 25P/72$.
(e) $m = 0.1902qb^2$.

Chapter 20

20.1 $\omega = 7.0$ rad/sec, $T = 0.898$ sec. The amplitude $= 1.745$ in., and $D_{t=1} = 1.692$ in.
20.2 $\omega = 7.103$ rad/sec, $T = 0.885$ sec. The amplitude $= 43.2$ mm, and $D_{t=1} = 42.8$ mm.
20.3 $\omega = 5.714$ rad/sec, $T = 1.09$ sec. The amplitude $= 2.02$ in., and $D_{t=1} = -0.101$ in.
20.4 $\omega = 5.777$ rad/sec, $T = 1.088$ sec. The amplitude $= 50.0$ mm, and $D_{t=1} = 0.9$ mm.

20.5 $$\omega_1 = \frac{3.53}{l^2}\sqrt{\frac{EIl}{ml}}; \{D^{(1)}\} = \left\{1.00, -\frac{1.38}{l}\right\}.$$

20.6 The consistent mass matrix is

$$m = \frac{\gamma l}{840}\begin{bmatrix} (240a_1 + 72a_2) & & \text{symmetrical} & & \\ (30a_1 + 14a_2)l & (5a_1 + 3a_2)l^2 & & & \\ (54a_1 + 54a_2) & (-93a_1 + 119a_2)l & (72a_1 + 240a_2) & & \\ -(14a_1 + 12a_2)l & -(3a_1 + 3a_2)l^2 & -(14a_1 + 30a_2)l & (3a_1 + 5a_2)l^2 & \end{bmatrix}.$$

20.7 $D_{\tau=T/2} = 2.107$in., $D_{\tau=T/2} = 0$, and $D_{\tau=11T/8} = 1.488$ in.
20.8 $D_{\tau=T/2} = 51.9$ mm, $D_{\tau=T/2} = 0$ and $D_{\tau=11T/8} = 36.7$ mm.
20.9 $D_{\tau=T/2} = 1.342$ in., $D_{\tau=T/2} = 0$, and $D_{\tau=11T/8} = 0.95$ in.
20.10 $D_{\tau=T/2} = 33.0$ mm, $D_{\tau=T/2} = 0$, and $D_{\tau=11T/8} = 23.3$ mm.
20.11 $\omega_d = 6.964$ rad/sec, $T_d = 0.902$ sec, $D_{t=1} = 0.866$ in.
20.12 $\omega_d = 7.067$ rad/sec, $T_d = 0.889$ sec, $D_{t=1} = 21.9$ mm.
20.13 $\xi = 0.0368$.
20.14 (a) $D_{\max} = 0.176$ in. (b) $D_{\max} = 0.174$ in.
20.15 (a) $D_{\max} = 4.49$ mm. (b) $D_{\max} = 4.45$ mm.
20.16 $D_{\tau=T_d/2} = 1.953$ in., and $D_{\tau=11T_d/8} = 0.995$ m.
20.17 $D_{\tau=T_d/2} = 48.1$ mm, and $D_{\tau=11T_d/8} = 24.5$ mm.

20.18 $$\omega_1^2 = 1.2\frac{EI}{ml^3}, \{D^{(1)}\} = \{1, 1\}.$$

$$\omega_2^2 = 18.0\frac{EI}{ml^3}, \text{and } \{D^{(2)}\} = \{1, -1\}.$$

20.19 $$\omega_1^2 = 0.341\frac{EI}{ml^3}, \{D^{(1)}\} = \{1, 0.32\}.$$

$$\omega_2^2 = 15.088\frac{EI}{ml^3}, \text{and } \{D^{(2)}\} = \{1, -3.12\}.$$

20.20 Equations of motion in the $\{\eta\}$ coordinates:

$$\ddot{\eta} + 0.34\frac{EI}{ml^3}\eta = 0.906P_1/m.$$

$$\ddot{\eta} + 15.09\frac{EI}{ml^3}\eta = 0.103P_1/m.$$

$$\eta_1 = \frac{P_1}{0.3758}\frac{l^3}{EI}\left[1 - \cos\left(\tau\sqrt{0.341\frac{EI}{ml^3}}\right)\right].$$

$$\eta_2 = \frac{P_1}{131.78}\frac{l^3}{EI}\left[1 - \cos\left(\tau\sqrt{15.09\frac{EI}{ml^3}}\right)\right].$$

$D_1 = \eta_1 + \eta_2$, $D_2 = 0.32\eta_1 - 3.12\eta_2$.

20.21 Amplitude of $m_1 = \dfrac{P_0}{0.3758\dfrac{EI}{l^3} - 1.1024\, m\Omega^2}$.

20.22 Maximum displacement of BC relative to the support = 2.01 in.

21.23 Maximum displacement of BC relative to the support = 49.5 mm.

21.24 Maximum displacement of mass m_1 relative to the support $= \dfrac{(g/4)}{1.2EI/(ml^3) - \Omega^2}$.

20.25 $V_{base} = 236.4$ kN; $M_{base} = 1728$ kN-m.

20.26 $[S] = 10^6 \begin{bmatrix} 7.935 & -11.45 \\ -11.45 & 27.69 \end{bmatrix}$ N/m; $\{\omega_1^2, \omega_2^2\} = \{94.3, 1154\}$ s^{-2}; $V_{base} = 145.9$ kN; $M_{base} = 816.7$ kN-m.

Chapter 22

22.1 $[t]_{AC} = \begin{bmatrix} 0.707 & 0.707 & 0 \\ 0 & 0 & 1 \\ 0.707 & -0.707 & 0 \end{bmatrix}$, $[t]_{DG} = \begin{bmatrix} 0.707 & 0 & 0.707 \\ 0 & 1 & 0 \\ -0.707 & 0 & 0.707 \end{bmatrix}$.

22.2 $[G]^T = E \begin{bmatrix} -ac/l & 12Is/l^3 & 6Is/l^2 & ac/l & -12Is/l^3 & 6Is/l^2 \\ -as/l & -12Ic/l^3 & -6Ic/l^2 & as/l & 12Ic/l^3 & -6Ic/l^2 \\ 0 & 6I/l^2 & 2I/l & 0 & -6I/l^2 & 4I/l \end{bmatrix}$

where $c = \cos\alpha$ and $s = \sin\alpha$.

22.3 $\{A_r\} = E\left\{-0.894\dfrac{a}{l}, -5.367\dfrac{I}{l^3}, -2.683\dfrac{I}{l^2}, 0.894\dfrac{a}{l}, 5.367\dfrac{I}{l^3}, 2.683\dfrac{I}{l^2}\right\}_{CD}$.

Matrix [G] given in the answer to Prob. 22.2 may be used in this problem.

22.6 Member end-forces at nodes 5 and 3 are $\{A\} = \{8597, -8597\}$ N.

22.7 Reactions at node 1 are: $R_1 = 2.73P$; $R_2 = -24.4P$; $R_3 = 193Pb$. Forces at the ends of member 2 are $\{A\} = \{-4.89, -24.8, -625, -22.0, -28.9, 1310\}$.

22.8 $[S^*] = \dfrac{Ebh}{l} \begin{bmatrix} 1.12 & & & & \text{symmetrical} & \\ 0 & 1.81h^2/l^2 & & & & \\ 0 & 1.09h^2/l & 0.762h^2 & & & \\ -1.12 & 0 & 0 & 1.120 & & \\ 0 & -1.81h^2/l & -1.09h^2/l & 0 & 1.81h^2/l^2 & \\ 0 & 0.722h^2/l & 0.326h^2 & 0 & -0.722h^2/l & 0.396h^2 \end{bmatrix}$.

22.9 The stiffness matrix elements on and below the diagonal are: six elements on the first three rows in Eq. 21.12 unchanged; $S_{41} = -12EI/l^3$; $S_{42} = 0$; $S_{43} = -6EI/l^2$; $S_{44} = 12EI/l^3$; $S_{51} = -6EIs/l^2$; $S_{52} = -GJc/l$; $S_{53} = -2EIs/l$; $S_{54} = 6EIs/l^2$; $S_{55} = GJc^2/l + 4EIs^2/l$; $S_{61} = 6EIc/l^2$; $S_{62} = -GJs/l$; $S_{63} = 2EIc/l$; $S_{64} = -6EIc/l^2$; $S_{65} = GJcs/l - 4EIcs/l$; $S_{66} = 4EIc^2/l + GJs^2/l$; where $s = \sin\gamma$, $c = \cos\gamma$.

22.10 The elements of [S] on and below the diagonal are (in terms of Ea/l): $S_{11} = c_1^2$; $S_{21} = c_1 s_1$; $S_{31} = -c_1 c_2$; $S_{41} = -c_1 s_2$; $S_{22} = s_1^2$; $S_{32} = -c_2 s_1$; $S_{42} = -s_1 s_2$; $S_{33} = c_2^2$; $S_{43} = c_2 s_2$; $S_{44} = s_2^2$; where $c_1 = \cos\alpha_1$, $s_1 = \sin\alpha_1$, $c_2 = \cos\alpha_2$, $s_2 = \sin\alpha_2$.

22.11 Rotations at B: $\theta_2 = -0.00658qb^3/EI$; $\theta_x = 0.09186qb^3/EI$. Bending and torsional moments in terms of $10^{-3}qb^2$; in member EB, $M_E = 181.8$, $M_B = -68.2$ and $T_E = T_B = 68.2$; in member BC, $M_B = -96.5$, $M_H = 28.5$ and $T_B = T_H = 0$. Positive bending moment produces tension in bottom fiber; twisting moment is given as an absolute value.

22.12 Member end-moments in terms of $EI\alpha T/b$: $M_{EB} = 0$; $M_{BE} = -M_{BH} = M_{HB} = 2.59$. No torsion.

22.13 Bending and twisting moments are given in terms of ql^2 and reactions in terms of ql. Positive bending moment produces tension in bottom fiber; twisting moment is given as an absolute value; upward reaction is positive. $M_E = M_F = -13.9 \times 10^{-3}$; $T_E = T_F = 24.1 \times 10^{-3}$; $R_A = R_D = 0.370$; $R_B = R_C = 0.130$.

22.14 Bending and twisting moments are given in terms of $10^{-3}ql^2$ and reactions in terms of ql. $M_E = M_F = -4.0$; $M_o = -123.0$; $T = 6.9 =$ constant over whole length; $R_A = R_D = 0.225$; $R_B = R_C = 0.156$; $R_G = R_H = 0.619$. Positive bending moment produces tension in bottom fiber; twisting moment is given as an absolute value.

22.15 Displacement components at B: $\{D\} = (qb^3/EI)\ \{0.187b,\ 0.0235,\ 0.209\}$.

22.16 Due to $P/2$ at each of B, C, G, and F, the displacements at B are $\{D\} = (Pb^2/EI)\ \{0.0544b,\ 0.00608,\ 0.0635\}$. Due to $P/2$ at each of B and C and $-P/2$ at F and G, the displacements at B are $\{D\} = (Pb^2/EI)\ \{0.0172b,\ -0.0493,\ 0.0206\}$. Due to actual loading, the displacements are $\{D\}_B = (Pb^2/EI)\ \{0.0716b,\ -0.0432,\ 0.0841\}$, $\{D\}_F = (Pb^2/EI)\ \{0.0372b,\ -0.0554,\ 0.0429\}$.

22.17 Displacements at E: downward deflection is $0.256ql^4/(EI)$; rotation vector perpendicular to AE is $0.262ql^3/(EI)$.

22.18 Deflection at O is $7ql^4/(48EI)$. Bending moments in terms of ql^2: $M_1 = 0.125$; $M_2 = -0.125$; $M_3 = 0.375$. Positive bending moment produces tension in bottom fiber.

Chapter 23

23.2 $\{D_x,\ D_y\}_B = 10^{-3}\{-0.604,\ 30.4\}$ m; $\{D_x,\ D_y\}_C = 10^{-3}b\{0.110,\ 24.3\}$ m. $\{N_{AB},\ N_{BC},\ N_{CD}\} = \{146.8,\ 146.2,\ 146.5\}$ kN.

23.3 $\{D_x,\ D_y\}_B = \{-25.0 \times 10^{-3},\ 1.23\}$ in.; $\{D_x,\ D_y\}_C = \{4.52 \times 10^{-3},\ 0.988\}$*in.*; $\{N_{AB},\ N_{BC},\ N_{CD}\} = \{32.50,\ 32.37,\ 32.45\}$ kip.

23.4 The value of F at which snap through occurs is 908.3.

23.5 $D_B = 0.0605$ m. Tensions in AB and BC are 198.4 and 198.2 kN.

23.6 $D_B = 2.67$ in. Tensions in AB and BC are 45.01 and 44.98 kip.

23.7 $D_A = 0.483$; force in any member $= 190.1$.

23.8 $P_{er} = 21.86$ (upward), corresponding to upward displacement of node A, $D_{Acr} = -0.42$.

23.9 The displacements in x, y, and z directions are: $\{\{D_5\},\ \{D_6\},\ \{D_7\},\ \{D_{11}\}\} = 10^{-3}l$ $\{\{2.50,\ 2.50,\ 21.17\},\ \{3.30,\ -0.16,\ 26.84\},\ \{2.68,\ -2.68,\ 20.93\},\ \{0,\ 0,\ 34.65\}\}$. Forces in the cables $\{F_{5-6},\ F_{6-7},\ F_{1-5},\ F_{2-6},\ F_{6-11}\ F_{3-7}\} = \{31.1,\ 31.3,\ 30.9,\ 32.0,\ 32.0,\ 31.6\}$ Q.

23.10 $\{D_x,\ D_y,\ \theta\}_B = \{1.94 \times 10^{-3},\ 0.317,\ 3.724 \times 10^{-3}\}$; forces in $AB = \{38.9,\ -0.146,\ -9.73,\ -38.9,\ 0.146,\ -4.86\}$; forces in $BC = \{38.9,\ 0,4.86,\ -38.9,\ 0,\ -4.86\}$.

23.11 Displacements and member end-forces are (units: c, F, or cF):
$\{D_x,\ D_y,\ \theta\}_B = \{0.3645,\ 0.0311,\ 0.1451\}$; $\{D_x,\ D_y,\ \theta\}_c = \{0.3647,\ 0.0317,\ 0.1459\}$.
$\{F^*\}_{AB} = 10^3\ \{1341.0,\ -379.2,\ -558.3,\ -1341.0,\ 379.2,\ -350.5\}$.
$\{F^*\}_{BC} = 10^3\ \{-20.80,\ 116.9,\ 350.5,\ 20.80,\ -116.9,\ 351.2\}$.
$\{F^*\}_{CD} = 10^3\ \{1578.4,\ -373.8,\ -351.2,\ -1578.4,\ 373.8,\ -544.5\}$.

23.12 Iteration 1: $D = 0.7l$; out-of-balance force $= 0.123Ca$. Iteration 2: $D = 0.889l$; out-of-balance force $= 0.009Ca$. The exact answer: $D = 0.905l$.

23.13 $D = 0.0075l$; $F_{AB} = 600a$; $F_{BC} = 400a$.

23.14 Nodal displacements at A: $\{D_x,\ D_y\} = 10^{-3}l\{3.017,\ 2.300\}$. Forces in the members AB, AC, AD, and AE are: $a\{-292.6,\ 96.6,\ 460.0,\ 525.3\}$.

Chapter 24

24.1 $P(M > 4300\text{ kN-m}) = 0.2$; $P(V > 1200\text{ kN}) = 0.131$.

24.2 $P(M > 3170\text{ kip-ft}) = 0.2$; $P(V > 270\text{ kips}) = 0.131$.

24.3 $P_{fM} = 242 \times 10^{-3}$; $P_{fV} = 345 \times 10^{-3}$.

24.4 Same as Prob. 24.3.
24.5 $P_f = 3.53 \times 10^{-3}$.
24.6 $P_f = 4.04 \times 10^{-4}$.
24.7 and 24.8 $P_f = 4.43 \times 10^{-3}$.
24.9 $P_f = 0.728 \times 10^{-6}$.

Appendix A

A.1 (a) $[A][B]$: not possible.

(b) $[A]^T[B] = \begin{bmatrix} 10 & 11 \\ 2 & 3 \\ 10 & 7 \end{bmatrix}$.

(c) $[A]^T\,[B]\,[A] = \begin{bmatrix} 43 & 11 & 31 \\ 11 & 3 & 7 \\ 31 & 7 & 27 \end{bmatrix}$.

(d) $[A]\,[B]^T\,[A]^T$: not possible.

A.2 (a) $[B]\,[A+C] = \begin{bmatrix} 24 & 10 & 14 \\ 20 & 7 & 13 \end{bmatrix}$.

(b) $[B]\,[A] + [B]\,[C] = \begin{bmatrix} 24 & 10 & 14 \\ 20 & 7 & 13 \end{bmatrix}$.

A.4 (a) $\frac{1}{11}\begin{bmatrix} 3 & 2 \\ 2 & 5 \end{bmatrix}$.

(b) $\begin{bmatrix} 0.750 & \text{symmetrical} & \\ 0.500 & 1.000 & \\ 0.250 & 0.500 & 0.750 \end{bmatrix}$.

(c) $\begin{bmatrix} 0.591 & \text{symmetrical} & \\ 0.545 & 0.773 & \\ 0.227 & 0.364 & 0.318 \end{bmatrix}$.

A.5 (a) $\{D\} = \left\{0,\ \frac{pl^2}{12EI}\right\}$.

(b) $S_{11} = \frac{4EI}{l}$, and $S_{21} = \frac{6EI}{l^2}$.

(c) $S_{12} = \frac{6EI}{l^2}$, $S_{22} = \frac{12EI}{l^3}$.

A.6 $[S]^{-1} = \frac{l^3}{18EI}\begin{bmatrix} 8 & 7 \\ 7 & 8 \end{bmatrix}$.

A.7 (a) $[S^*] = \frac{EI_0}{l}\begin{bmatrix} 7.272 & 2.909 \\ 2.909 & 4.364 \end{bmatrix}$.

A.8 (a) $\{x\} = \{2, -1\}$; (b) $\{x\} = \{1, 3, 4\}$; (c) $\{x\} = \{0.5, 0, 0.5\}$; (d) $\{D\} = [10^{-3}Pl^2/(EI)]$ $\{8.681\,l, 135.4, -15.63\}$; (e) $\{F\} = (EI/l^2)$ $\{1.6071, -0.4286, 0.1071\}$.

A.9 (a) $\lambda = 12.372,\ 6.628$. The required vector is $\{1.0, -2.186\}$.
(c) $\lambda = 3.414,\ 2.000,\ 0.586$. The required vector is $\{1.0, 1.414, 1.0\}$.

A.10 $\lambda = 1.111$.

Appendix M

M.1 $\bar{x} = 4944$ psi, $\sigma_X = 787$ psi.

M.2 $\bar{x} = 34.1$ MPa, $\sigma_X = 5.44$ MPa.

M.3 (a) $P(X < 100) = 22.8 \times 10^{-3}$; (b) $P(X \geq 187) = 16.2 \times 10^{-3}$.

M.4 $\sigma_Y = 0.2302$; $\bar{y} = 7.980$; (a) $P(X \leq 2500) = 249 \times 10^{-3}$; (b) $P(2800 \leq X \leq 3200) = 227 \times 10^{-3}$.

M.5 Dead load: $\bar{x} = 87$, $\sigma_X = 6$; live load: $\bar{x} = 53$, $\sigma_X = 14$; resistance: $\bar{x} = 162$, $\sigma_X = 25$.

M.6 The straight line, best fitting the data on normal probability paper, has the equation: $y = 2.820x - 11.71$. Its intersection with the x axis is the mean load-carrying capacity: $\bar{x} = 4.153$; its slope $= 1/\sigma_X = 2.820$; $\sigma_X = 0.355$.

References

1. Arbali, F., *Structural Analysis and Behavior*, McGraw-Hill, New York, 1991.
2. Argyris, J. H. and Kelsey, S., *Energy Theorems and Structural Analysis*, Butterworth, London, 1960.
3. Au, T. and Christiano, P., *Structural Analysis*, Prentice-Hall, Englewood Cliffs, NJ, 1987.
4. Bathe, K. J., *Finite Element Procedures*, Prentice-Hall, Englewood Cliffs, NJ, 1982.
5. Beaufait, F. W., *Basic Concepts of Structural Analysis*, Prentice-Hall, Englewood Cliffs, NJ, 1977.
6. Cook, R. D., Malkus, D. S. and Plesha, M. E., *Concepts and Applications of Finite Element Analysis*, Wiley, New York, 1981.
7. Crisfield, M. A., *Non-linear Finite Element Analysis of Solids and Structures*, Wiley, Chichester, England, 1991 vol. 1.
8. Gallagher, R., *Finite Element Analysis Fundamentals*, Prentice-Hall, Englewood Cliffs, NJ, 1975.
9. Gere, J. M., *Moment Distribution*, Van Nostrand, New York, 1963.
10. Ghali, A., Favre, R. and Elbadry, M., *Concrete Structures: Stresses and Deformations*, 3rd ed., Spon Press, London, New York, 1986.
11. Holzer, S. M., *Computer Analysis of Structures*, Elsevier, New York, 1985.
12. Irons, B. M. and Ahmad, S., *Techniques of Finite Elements*, Ellis Horwood, Chichester, England, 1980.
13. Irons, B. M. and Shrive, N. G., *Finite Element Primer*, Ellis Horwood, Chichester, England, 1983.
14. Jirousek, J., *Calcul des Structures par Ordinateur*, Swiss Federal Institute of Technology, Lausanne, Switzerland, 1982.
15. Kassimali, A., *Structural Analysis*, PWS-Kent Publishing Co., Boston, 1993.
16. Lightfoot, E., *Moment Distribution*, Spon, London, 1961.
17. Livesley, R. K., *Matrix Methods of Structural Analysis*, Macmillan, New York, 1964.
18. Martin, H. C., *Introduction to Matrix Methods of Structural Analysis*, McGraw-Hill, New York, 1966.
19. Neal, B. G., *Structural Theorems and Their Applications*, Macmillan, New York, 1964.
20. Paz, M., *Structural Dynamics: Theory and Computation*, Van Nostrand, New York, 1991.
21. Przemieniecki, J. S., *Theory of Matrix Structural Analysis*, McGraw-Hill, New York, 1968.
22. Rubenstein, M. F., *Matrix Computer Analysis of Structures*, Prentice-Hall, Englewood Cliffs, NJ, 1966.
23. Rumman, W. S., *Statically Indeterminate Structures*, Wiley, New York, 1991.
24. Sack, R. L., *Structural Analysis*, McGraw-Hill, New York, 1984.
25. Shames, I. R. and Dym, C. L., *Energy and Finite Element Methods in Structural Mechanics*, McGraw-Hill, New York, 1985.
26. Tartaglione, L. C., *Structural Analysis*, McGraw-Hill, New York, 1991.
27. Wang, C. K., *Intermediate Structural Analysis*, McGraw-Hill, New York, 1983.
28. Wang, P. C., *Numerical and Matrix Methods in Structural Mechanics*, Wiley, New York, 1960.
29. Weaver, W. Jr and Gere, J. M., *Matrix Analysis of Framed Structures*, Van Nostrand, New York, 1980.
30. West, H. H., *Analysis of Structures*, Wiley, New York, 1980.
31. Willems, N. and Lucas, W. M. Jr, *Matrix Analysis for Engineers*, McGraw-Hill, New York, 1978.
32. Zienkiewicz, O. C. and Taylor, R. L., *The Finite Element Method*, McGraw-Hill, London, 1989.

Index

T

861007

ADVERTISEMENT

Computer Programs for the Analysis of Framed Structures

Based on A. Ghali, A.M. Neville and T.G. Brown, *Structural Analysis: a unified classical and matrix approach (Taylor & Francis) 6th ed, 2009*

Nonlinear analysis programs

PDELTA
PLASTICF
NLST
NLPF

The above computer programs, described in Appendix L of this book, are all sold together as a set. They are available on disc, containing the following files for each program: (1) The source code in FORTRAN. (2) An executable file, for use on IBM personal computers or compatibles. (3) An input-file example. The comments, which are given at the beginning of the source code for each program, include simple instructions for input data preparation. No printed manual is needed.

Disclaimer of Warranties and Order Form

The above computer programs are sold without warranty of any kind, either expressed or implied, including but not limited to implied warranties of merchantability and fitness for any particular purpose. The seller and the author are not responsible for any damage whatsoever which may be incurred by the purchaser or any other person by reason of any defect in the software. The author reserves the right to revise the software without obligation to notify any person of revisions or changes. I hereby accept the conditions of the disclaimer.

Please send me _____ sets of the software and invoice me for the sum of $120 Canadian per set, plus a small mailing and handling charge.

Name: _____

Address: _____

_____

Signature: _____ Date: _____

Please photocopy the above order form and disclaimer, fill in the form and sign the disclaimer as acceptance of its terms and conditions, then mail to Mrs Liliane Ghali, 3911 Vincent Drive N.W., Calgary, Alberta, T3A OG9, Canada, to whom all enquiries should be sent. Please make payment by money order in Canadian dollars after receipt of an invoice.

STRUCTURAL ANALYSIS

This comprehensive textbook, now in its sixth edition, combines classical and matrix-based methods of structural analysis and develops them concurrently. New solved examples and problems have been added, giving over 140 worked examples and more than 400 problems with answers.

The introductory chapter on structural analysis modeling gives a good grounding to the beginner, showing how structures can be modeled as beams, plane or space frames and trusses, plane grids or assemblages of finite elements. Idealization of loads, anticipated deformations, deflected shapes and bending moment diagrams are presented. Readers are also shown how to idealize real three-dimensional structures into simplified models that can be analyzed with little or no calculation, or by more involved calculations using computers. Dynamic analysis, essential for structures subject to seismic ground motion, is further developed in this edition and in a code-neutral manner. The topic of structural reliability analysis is discussed in a new chapter.

Translated into six languages, this textbook is of considerable international renown, and is widely recommended by many civil and structural engineering lecturers to their students because of its clear and thorough style and content.

Amin Ghali is Fellow of the Canadian Academy of Engineering and Professor Emeritus in the Civil Engineering Department of the University of Calgary, Canada.

Adam Neville is former Vice President of the Royal Academy of Engineering and former Principal and Vice Chancellor of the University of Dundee, Scotland.

Tom G. Brown is Professor and Head of the Civil Engineering Department of the University of Calgary, Canada.

STRUCTURAL ENGINEERING

Spon Press
an imprint of Taylor & Francis
www.sponpress.com

an informa business

ISBN 978-0-415-77433-8

9 780415 774338

The cover image shows the pedestrian bridge over the Rhine River near Weil um Rhein, Germany. Courtesy of Leonhardt Andrä and Partners, Berlin.